













FUNDAMENTAL PROCESSES OF  
ELECTRICAL DISCHARGE IN GASES

By LEONARD B. LOEB

FUNDAMENTAL PROCESSES OF ELECTRICAL DISCHARGE IN GASES

717 pages, 6 by 9. 297 figures. Cloth.

ATOMIC STRUCTURE

426 pages, 6 by 9. 111 figures. Cloth.

THE NATURE OF A GAS

The first of a series of monographs published under the auspices of the Committee on Electrical Insulation of the Division of Engineering and Industrial Research of the National Research Council. 153 pages, 6 by 9. 11 figures. Cloth.

FUNDAMENTALS OF ELECTRICITY AND MAGNETISM. Third Edition.

669 pages, 6 by 9. 272 figures. Cloth.

By LEONARD B. LOEB AND ARTHUR S. ADAMS

THE DEVELOPMENT OF PHYSICAL THOUGHT

648 pages, 6 by 9. 120 figures. Cloth.

PUBLISHED BY

JOHN WILEY & SONS, INC.

**FUNDAMENTAL PROCESSES  
OF  
ELECTRICAL DISCHARGE IN GASES**

**BY  
LEONARD B. LOEB**

*Professor of Physics  
University of California*

**NEW YORK  
JOHN WILEY & SONS, INC.  
LONDON: CHAPMAN & HALL, LIMITED**

COPYRIGHT, 1939  
BY  
LEONARD B. LOEB

---

*All Rights Reserved*

*This book or any part thereof must not  
be reproduced in any form without  
the written permission of the publisher*

SECOND PRINTING, DECEMBER 1947

PRINTED IN U. S. A.

## DEDICATION

To the brilliant group of young investigators, including their master, working in the Cavendish Laboratory under the leadership of Sir J. J. Thomson in the late nineties and early nineteen hundreds, following the discovery of the electron, whose pioneering investigations did so much to establish the principles of conduction of electricity in gases, namely: Ernest Rutherford, J. S. Townsend, Paul Langevin, J. A. McClelland, H. A. Wilson, R. J. Strutt, O. W. Richardson, J. Zeleny, C. G. Barkla, N. R. Campbell, T. Lyman, R. K. McClung, G. Jaffe, J. E. Almy, R. S. Willows, A. Wood, G. Monckman, J. Henry, W. C. Baker, J. A. Cunningham, J. J. E. Durack, and J. Patterson, this book is humbly dedicated.





## PREFACE

The field of study of electrical discharge in gases has had a historical development quite unique in some respects. Actually beginning in the days of the discovery of X-rays, 1895, and of the electron, 1896, it developed with amazing rapidity in the ensuing fifteen years as a result of the studies of one of the most able group; of scientific investigators ever active in a given field at one time. As a consequence, by 1911 and 1914 J. J. Thomson and J. S. Townsend were able individually to coordinate and correlate the many studies in their two classics, the *Conduction of Electricity through Gases* and *Electricity in Gases*. In these books are presented the qualitative and in some cases the quantitative results good to better than the first-order accuracy.

Owing to two circumstances the research activity in this field gradually subsided, and much of the further progress was left to the engineers in the applied fields. The circumstances influencing this decline were the rapid advance of the more exciting fields of atomic theory, X-rays, ionizing impacts, radioactivity, spectroscopy, etc., and the increasing difficulty of further more accurate advance using the then existing techniques.

With the great clarification of atomic theory following on the wave mechanics in 1926-28, together with the remarkable improvements in laboratory technique coming from Pyrex glass, better pumps, induction furnaces, electron tubes, and oscillographs available in all laboratories, conditions have improved in the last ten or fifteen years to such a point that new advances can be made. Thus it is not surprising that we see activity in this field reviving in increasing measure, stimulated in part by the new focus of interest on electronics in response to industrial needs. In this gradual revival many workers have quietly been contributing significant results which are *buried* in the volumes of scientific literature annually published. As a result the modern physicist or engineer faced with the necessity of understanding the processes involved in some case of gaseous discharge finds himself in a peculiar situation. There is a mass of material conveniently arranged and summarized in books, or handbooks of various vintages, which in a large measure can be traced to, or will be found to be based on, the original data and theories set forth in the classical books of Thomson and Townsend. In addition there exists a welter of scientific papers running through many journals dealing with one or another aspect of a problem bearing on the question at issue. Unfortunately, with the lack of space for publication in journals, these papers cannot go far

towards correlating these particular contributions with the rest of the field. Therefore, what is seriously needed at this time is a *book based on the knowledge which modern atomic physics gives us but which picks up the broken threads connecting the classical discharge theory of the textbooks and monographs with recent experimental developments.*

Attempts have been made in the past ten years in this direction. Some of them have consisted in the inadequate rewriting or modernizing of the classics, in one fashion or another. Other textbooks have been merely summaries of literature written by men who are not familiar with the fields of research through their own or their students' researches and who therefore quite correctly refused to decide on the relative merits of the many conflicting theories and results. Finally there has appeared in German one excellent textbook, that of v. Engel and Steenbeck, which, though quite modern and in some fields authoritative, suffers from one great drawback. It presents the author's own interpretations, based on modern atomic physics, of the many conflicting views, without directly indicating the reason for the choice and without mentioning the workers involved, in many cases even failing to cite references.

Were the subject of discharge through gases a field so completely developed that controversies no longer existed, the procedure would be permissible. Such, however, is not the case. Furthermore, it is the present author's feeling that, with the advent of wave mechanics and the curtailment of space for publication, physics is tending to become too *dogmatic* and that the physical public in consequence is becoming too gullible. It is urgent that in a book of this nature one figuratively lay the cards on the table, *presenting the reader with the facts and conflicting views, and that thereafter the author throw the weight of his authority in whatever direction it should, in his opinion, go, giving his reasons in each instance.*

With this situation in mind it has long been the author's desire to write the much-needed book. In doing so it has been his intention briefly to introduce the subjects in general from the classical point of view as far as the earlier work suffices and from there on to trace, in many cases historically, the subsequent advance in terms of the experimental and theoretical considerations leading thereto, culminating in the present-day interpretation of the facts. In doing this it will be necessary clearly to point out the errors in the accepted classical concepts and to indicate how the concepts are to be modified. It will be further essential to omit certain interesting but not cogent studies and to regard others critically. Some readers will not agree in the choice of inclusions and omissions nor in many points with the criticisms. The author has attempted impartially but frankly and in a forthright fashion to pass judgment to the limit of his ability. In many of the fields studied the author and his students have been engaged in experimental investigations over periods of many years. He therefore feels

justified in exerting critical judgment. In Chapters III, V, and XI, the author makes no pretense of authority based on direct experience, since he has not been directly connected with researches on these subjects, although he has the background to understand and comment thereon. It is believed, however, that even in these cases the material not only will prove of value but also will lay a foundation for the orientation of future investigations.

Needless to say, with the present status of the subjects discussed, one can expect neither a unity of method of presentation nor uniformity in length of chapters. On some topics there is a continuity of development so that a sequential story can be told, e.g., in Chapter VI on negative ions. In other subject matter there is an enormous duplication, or better multiplication, of effort, with little development until at a single recent epoch new techniques made satisfactory progress possible. This is shown in Chapter I, where experimental methods are discussed, and again where the theory still most satisfactory with slight modifications had already been published in 1905. It is again clear that the subjects of mobilities and especially recombination, in which there is much literature and more confusion, will require much space in comparison with the subject of diffusion, as such, in which practically no work has been done in thirty years and where the only direct interest lies in the solution of the Fourier heat equation for special problems, while the information to be gained from diffusion studies is better given by mobilities both in theory and experiment.

The topics chosen, aside from the chapters dealing with discharges themselves, are designed to present the fundamental processes active in all discharge phenomena in the *evolutionary and present-day stages*. These comprise ionic mobilities, ionic and electronic recombination processes, diffusion of ions and electrons, electron mobilities, energy distribution functions of electrons in gases, electron attachment and negative-ion formation, conduction currents in gases, the first Townsend coefficient for ionization by electron impact, and the second Townsend coefficient. With these subjects presented, their application to the problems of spark discharge, the glow, and the arc makes a satisfactory conclusion to a book of the title of this one in that they illustrate the practical operation of the principles presented.

The state of knowledge in this field is obviously such that it is *not amenable to presentation in textbook form*, except at the price of being a mere dogmatic expression of opinion perhaps seriously in error. Accordingly this book is *primarily a monograph* and source book of recent coordinated information. It is, however, suitable for use in the instruction of courses in discharge through gases. Thus there is included ample material such that by judicious choice the elementary sections can be utilized for upper-division and graduate students in physics or engineering electronics. It had been the original intention of the author to include an introductory chapter on the structure of

the atom and electronic reactions to furnish under one cover all the information that the reader could want. Such a chapter was, in fact, written. As the book developed it became clear that the scope of the subject precluded its inclusion owing to lack of space. There is included for reference in the Appendix, however, a small section on elementary kinetic theory indispensable for an understanding of the material presented.

It would be desirable to present tables of essential data giving recent values of such quantities as mobilities of ions, recombination coefficients, etc. Wherever the values have any significance whatsoever, they have been included. But for ionic mobilities no values given in the literature have any general significance. Enough data on actually observed values are provided to orient the reader, but since there are no such things as standard values of mobilities no table is given.

In closing, a word must be said about the origin of this book. The need for a book of this nature has been indicated in the first part of the preface. Until recently, however, the subject has been in such a chaotic state that the writing of a book was futile. In 1937 the author gave a course on discharge phenomena to his upper-division students at the University of California. As the course developed, the lecture notes were prepared in mimeographed form at the request of the class. This survey of the status of the subject indicated the time to be ripe for the presentation of the material in book form. In the summer of 1937 the content of the mimeographed text was presented in abridged form before the Electronics Institute at the University of Michigan in a series of lectures during the month of August. In the course of these lectures the urgent need for a book of this sort became so clear that the author began writing this text in the Fall of 1937 on his return to Berkeley. It had been hoped to use the rewritten class notes of 1937. This proved to be impracticable, and the text was in a large measure rewritten de novo, following the earlier notes as outline.

In writing a book of this scope it is obvious that too much emphasis cannot be spared for style or for a detailed consideration as to the best organization in presenting the material. The need is for a critical compilation of the state of physical knowledge in the various fields today. It is the author's hope that the book will be found interesting, useful, and stimulating to further study to all those students and investigators whose problems bring them in contact with this field.

LEONARD B. LOEB

*Berkeley, California*  
*July 8, 1939*

## ACKNOWLEDGMENTS

The author wishes to acknowledge his indebtedness to the admirable book of v. Engel and Steenbeck, *Elektrische Gasentladungen*, for the lucid treatment of the elementary theory of probes and for the theory of the cathode fall and the positive column in glow discharges which have been followed in outline in the presentation of this book. He is also indebted for source material and references to the excellent articles of R. Bär and A. Hagenbach in the Geiger and Scheel *Handbuch der Physik*, Vol. 14, on glow discharge and arcs. Needless to say, the classical texts on the conduction of electricity in gases of J. J. Thomson and J. S. Townsend have come in for their share of use in the preparation of this book.

The author is much indebted to Professor Norris Bradbury, to Professor Robert N. Varney, and to Dr. Wm. R. Haseltine for their many valuable discussions on various sections of the text. He is especially indebted to Dr. Haseltine for his solution of the problem of the geometrically conditioned saturation current and for his assistance in the solution of the problem of initial recombination as well as for his aid in reading sections of the galley proof. He is also indebted to Mr. J. M. Meek of the Metropolitan Vickers Corporation for his data on long sparks in air and his valuable discussions on the theory of propagation of lightning discharge and the mechanism of breakdown of air gaps at atmospheric pressure in air. His thanks are likewise due to Dr. A. F. Kip for his assistance in reading galley proof and to both Dr. Kip and Dr. G. W. Trichel (Captain, Ordnance Corps, U. S. Army) for the many valuable discussions on the mechanism of corona discharge.

The author wishes to express his thanks to Dr. F. M. Penning and Dr. M. J. Druyvesteyn not only for placing complete files of their important contributions at his disposal but also for their valuable comments on various points embodied in his correspondence with them. He is also grateful to Professor W. S. Huxford and Dr. R. W. Engstrom for placing their interesting material on Townsend coefficients at his disposal before publication. He is grateful to Professor Wm. G. Dow for his work in editing the chapter on energy distribution laws when it appeared as a special mimeographed article promulgated by the Electronics Institute of the University of Michigan in 1938.

In the preparation and publication of the text the author's sincere thanks for valuable assistance must be recorded as follows. To

Mr. Walter Gruenig, senior student in engineering, for his computations on N.Y.A. time of the data on initial recombination, and to Mr. Leslie Cook, graduate student in physics, for his computation of the data on geometrically conditioned saturation currents, also on N.Y.A. time. To Mr. Wm. E. Norris, N.Y.A. stenographer, for much of the typing of the manuscript, as well as to Miss Wilma Belt, also for typing of the manuscript. To Messrs. Charles Kemp, Neil J. Cummings, Donald F. Biles, and Wm. E. Norris the author is indebted for many of the illustrations. To Messrs. Foster Elton, G. Jacobie, and especially to Mr. F. T. Bogard in succession, draftsmen on W.P.A. for the Physics Department, the author is indebted for the balance of the drawings. In this connection the author wishes to emphasize his gratitude to N.Y.A. and to W.P.A. (Project number 65—08—3—174 W. P.—10695), without whose help as specified this monograph could hardly have been prepared.

For the preparation of the subject and author index and the reading of page proof the author wishes to acknowledge his thanks to Miss Lanng Beran, Mrs. Elinor M. Cherry, Mr. Leon Fisher, Dr. R. N. Varney, and Lora L. Loeb.

LEONARD B. LOEB

BERKELEY, CALIFORNIA  
*September 29, 1939*

# CONTENTS

|   | PAGE  |
|---|-------|
| DEDICATION.....   | v     |
| PREFACE.....  | vii   |
| ACKNOWLEDGMENTS.....  | xi    |
| CHAPTER   |       |
| I. IONIC MOBILITIES   |       |
| PART A. MEASUREMENTS  |       |
| 1. Introduction.....  | 1     |
| 2. Air-Blast Method.....  | 3     |
| a. Zeleny Air-Blast Method.....   | 3     |
| b. The Method of Erickson.....  | 5     |
| 3. Alternating-Current Methods.....                                     | 7     |
| a. The Rutherford Method.....   | 7     |
| b. The Franck Modification of the A-C Method.....                       | 11    |
| c. The Bradbury Modification of the Tyndall and Grindley<br>Method..... | 14    |
| 4. Electrical Shutter Methods.....                                      | 19    |
| a. Tyndall and Powell Four-Gauze Method.....                            | 20    |
| b. The Bradbury-Nielsen Shutter Method.....                             | 23    |
| 5. The Townsend Magnetic Deflection Method.....                         | 26    |
| 6. The Chattock Electrical Wind Method.....                             | 28    |
| 7. References.....  | 30-31 |
| PART B. THE EXPERIMENTAL DATA ON IONIC MOBILITIES                       |       |
| 1. Introduction.....  | 32    |
| 2. Mobility and Field Strength.....                                     | 32    |
| 3. Absolute Values of Mobilities.....                                   | 33    |
| 4. Pressure Variation of Mobility.....                                  | 34    |
| 5. Temperature Variation of Mobility.....                               | 36    |
| 6. Variation of Mobility with Mass and Dielectric Constant.....         | 37    |
| 7. The Difference in Mobility of Positive and Negative Ions.....        | 38    |
| 8. Aging Effects with Ions.....   | 40    |
| 9. Mobilities in Gaseous Mixtures.....                                  | 42    |
| 10. Langevin and Intermediate Large Ions.....                           | 45    |
| 11. Groups of Ions.....   | 47    |
| 12. Difficulty in the Study of Known Ions.....                          | 48    |
| 13. Effect of Ionic Charge on Mobility.....                             | 48    |
| 14. References.....   | 49-51 |



## PART C. THE THEORY OF IONIC MOBILITIES

|  |    |
|--|----|
| 1. Introduction.....   | 52 |
| 2. The Elementary Theory of Ionic Mobility.....              | 54 |
| 3. Forces between Ions and Molecules.....                    | 56 |
| 4. The Small-Ion Theory.....                                 | 58 |
| 5. The More Exact Theories.....                              | 65 |
| 6. Mobilities at Low Pressures and in High Fields.....       | 71 |
| 7. Mobility Equations over an Extended Range of Ion Size.... | 83 |
| 8. References.....   | 85 |

## II. RECOMBINATION OF IONS

|  |         |
|--|---------|
| 1. Introduction.....   | 86      |
| 2. Types of Recombination.....   | 86      |
| 3. Definition of Coefficient of Recombination and Its Fundamental Relations.....                                     | 88      |
| 4. Methods of Measurement of $\alpha$ .....  | 91      |
| 5. Results of Earlier Work.....  | 101     |
| 6. The Langevin Theory of Recombination of Ions.....   | 103     |
| 7. The Motion of Brownian Particles Attracting Each Other in a Gas   | 108     |
| 8. The Thomson Theory of Volume Recombination.....   | 112     |
| 9. Experimental Test of the Volume Recombination Theory.....   | 120     |
| 10. Preferential Recombination.....  | 125     |
| 11. Recombination at Very Low Pressures.....   | 130     |
| 12. Initial Recombination.....   | 131     |
| 13. Columnar Ionization and Recombination.....   | 139     |
| 14. The Values of the Coefficient of Recombination and Their Interpretation.....                                     | 143     |
| 15. The Coefficient of Recombination of Large Ions in Air; The Charges Acquired by Suspended Particles in Gases..... | 148     |
| 16. Electron Recombination.....  | 149     |
| 17. References.....  | 159-160 |

## III. THE DIFFUSION OF IONS

|   |     |
|---|-----|
| 1. Introduction.....  | 161 |
| 2. Fundamental Concepts.....  | 161 |
| 3. The Early Measurements of Diffusion.....   | 164 |
| 4. Relation between Mobility and Diffusion.....   | 166 |
| 5. The Role of Diffusion in Discharge and Conduction Phenomena; The Value of the Coefficient of Diffusion and Its Variation.... | 170 |
| 6. References.....  | 176 |

## IV. ELECTRON MOBILITY

|  |     |
|--|-----|
| 1. Introduction.....                                 | 177 |
| 2. The Early Measurement of Electron Mobilities..... | 178 |

# CONTENTS

xv

## CHAPTER

PAGE

|   |         |
|---|---------|
| 3. Further Theoretical Developments . . . . .   | 182     |
| 4. Comparison of Theory and Experiment . . . . .  | 188     |
| 5. References . . . . .   | 198-199 |
| V. PART A. THE DISTRIBUTION OF ELECTRON ENERGIES IN A GAS IN AN ELECTRICAL FIELD  |         |
| 1. Introduction . . . . .   | 200     |
| 2. The Hertz Derivation . . . . .   | 202     |
| 3. The Druyvesteyn Derivation . . . . .   | 203     |
| 4. Later Derivations . . . . .  | 209     |
| 5. The Morse, Allis, and Lamar Derivation . . . . .   | 211     |
| 6. Derivations Including Inelastic Impacts . . . . .  | 215     |
| 7. The Smit Derivation . . . . .  | 221     |
| 8. The Studies of Allis, Allen, and Tonks . . . . .   | 228     |
| 9. References . . . . .   | 231     |
| PART B. THE THEORY OF PROBES AND THE INFLUENCE OF THE DISTRIBUTION OF ELECTRON ENERGIES ON THE INTERPRETATION OF PROBE MEASUREMENTS |         |
| 1. Introduction . . . . .   | 232     |
| 2. General Assumptions . . . . .  | 235     |
| 3. The Nature of a Probe Measurement . . . . .  | 236     |
| 4. The Theory of the Probe . . . . .  | 237     |
| a. The Strongly Negative Probe . . . . .  | 237     |
| b. Energy Distribution and Electron Temperature . . . . .   | 239     |
| c. The Wall Potential . . . . .   | 241     |
| d. The Plasma or Space Potential . . . . .  | 242     |
| e. Positive Probes and Plasma Potential . . . . .   | 243     |
| 5. Probe Measurements and the Determination of the Distribution Law . . . . .   | 246     |
| 6. Sources of Error in Probe Measurements . . . . .   | 251     |
| 7. References . . . . .   | 256-257 |
| VI. THE FORMATION OF NEGATIVE IONS  |         |
| 1. Introduction . . . . .   | 258     |
| 2. The Theory of J. J. Thomson . . . . .  | 261     |
| 3. The More Accurate Evaluations of the Attachment Probabilities . . . . .  | 267     |
| 4. The Method of Bailey . . . . .   | 268     |
| 5. The Introduction of the Electron Filter . . . . .  | 272     |
| 6. The Method and Results of Bradbury . . . . .   | 276     |
| 7. Atomic and Molecular Structure and Electron Attachment . . . . .   | 288     |
| 8. The Energy and Character of the Attachment Process in $O_2$ . . . . .  | 291     |
| 9. The Formation of Negative Atomic Ions . . . . .  | 296     |
| 10. References . . . . .  | 304     |

## VII. IONIZATION CURRENTS IN GASES IN FIELDS BELOW IONIZATION BY COLLISION

|   |     |
|---|-----|
| 1. Introduction.....  | 305 |
| 2. <i>Case 1.</i> The Geometrically Conditioned Saturation Current.....           | 306 |
| 3. <i>Case 2.</i> Photoelectric Currents of Low Density in Gases.....             | 310 |
| 4. <i>Case 3.</i> The Space Charge Limited Current in Vacuum.....                 | 317 |
| 5. The Effect of Positive Ions on an Electron Space-Charge-Limited Current.....   | 325 |
| 6. <i>Case 4.</i> Volume Ionization with Positive and Negative Ions in a Gas..... | 328 |
| 7. References.....  | 335 |

## VIII. IONIZATION BY COLLISION BY ELECTRONS IN A GAS

|   |         |
|---|---------|
| 1. Introduction.....  | 336     |
| 2. Experimental Procedure.....  | 337     |
| 3. Experimental Results.....  | 342     |
| 4. Theoretical Evaluation of $\alpha/p$ as a $f(X/p)$ .....                       | 358     |
| 5. v. Engel and Steenbeck's Theoretical Approximation to Townsend's Equation..... | 367     |
| 6. References.....  | 369-370 |

## IX. THE SECOND TOWNSEND COEFFICIENT

|  |         |
|--|---------|
| 1. Introduction.....   | 371     |
| 2. The Townsend Theory of Ionization by Positive Ions .....                        | 372     |
| 3. The Problem of Ionization by Positive Ions.....                                 | 374     |
| 4. The Alternatives to the Ionization by Positive Ions.....                        | 377     |
| a. Secondary Electron Emission by Positive-Ion Bombardment..                       | 377     |
| b. Photoelectric Processes at the Cathode.....                                     | 379     |
| 5. Experimental Data on the Interpretation of the Second Townsend Coefficient..... | 381     |
| 6. Falsification of Data on Second Townsend Coefficient by Space Charge.....       | 386     |
| 7. Studies of $\gamma$ on Mercury-Free Surfaces.....                               | 392     |
| 8. Summary of Secondary Mechanisms Known to be Active and Their Occurrence.....    | 402     |
| 9. References.....   | 406-407 |

## X. DISRUPTIVE DISCHARGE IN GASES; SPARKS

### PART A. THE THEORY OF SPARKING

|  |     |
|--|-----|
| 1. The Definition of a Spark.....                    | 408 |
| 2. The Townsend Sparking Criterion.....              | 409 |
| 3. Paschen's Law.....                                | 410 |
| 4. The Characteristic Curve for Spark Discharge..... | 412 |
| 5. The Minimum Sparking Potential.....               | 413 |
| 6. Cathode Surface and Sparking Potential.....       | 415 |

# CONTENTS

xvii

PAGE

|  |         |
|--|---------|
| 7. The Experimental Test of Townsend's Sparking Criterion.....   | 416     |
| 8. A Further Consideration of the Sparking Criterion: The Influence of the Initial Current .....             | 420     |
| 9. The Condition for the Self-Sustaining Discharge and Sparking Threshold.....                               | 423     |
| 10. Sparking Threshold and Spark Breakdown of a Gap. ....  | 425     |
| 11. The Mechanism of the Spark.. ....  | 426     |
| 12. The Experimental or Observed Sparking Potential.....   | 432     |
| 13. Further Consideration of the Mechanism of Spark Breakdown ..   | 433     |
| 14. A Brief Summary of the Development of the Understanding of Spark Breakdown at Atmospheric Pressure ..... | 440     |
| 15. The Time Lag of Spark Breakdown .....  | 441     |
| 16. References.....  | 448-450 |

## PART B. ESSENTIAL TECHNIQUES IN THE STUDY OF SPARK DISCHARGE<sup>A</sup>

|  |     |
|--|-----|
| 1. Introduction.....   | 451 |
| 2. The Spark Gap; Electrodes—Shape and Material .....                          | 451 |
| 3. Gaseous Purity.....   | 460 |
| 4. Power Sources and Techniques in Sparking-Potential Measurement. ....        | 462 |
| 5. The Detection of Breakdown and the Procedure of Breakdown Measurements..... | 463 |
| 6. References.....   | 470 |

## PART C. SPECIAL TYPES OF BREAKDOWN

|   |         |
|---|---------|
| 1. Introduction.....  | 471     |
| 2. Vacuum Sparks. ....  | 471     |
| 3. References for Sec. 2, Part C, Chapter X.....                                    | 476     |
| 4. Sparks at Low Pressure.....  | 476     |
| 5. References for Sec. 4, Part C, Chapter X.....                                    | 484     |
| 6. Discharges from Points and Wires... ..   | 485     |
| a. The Positive Wire Corona-Geiger Counters .....                                   | 486     |
| b. The Negative Wire Corona.....  | 504     |
| c. The Starting Potential of Corona and Pressure.....                               | 507     |
| 7. References for Section 6, Part C, Chapter X.....                                 | 513-514 |
| 8. Positive and Negative Point to Plane Coronas in Air at Atmospheric Pressure..... | 514     |
| a. Negative Point Corona.....   | 515     |
| b. Positive Point Corona.....   | 520     |
| 9. The Effect of Temperature on Sparking Potentials.....                            | 534     |
| 10. References for Sections 8 and 9, Part C, Chapter X .....                        | 535-536 |
| 11. Sparking Phenomena for Very Long Gaps and High Pressures... ..                  | 536     |
| 12. Lightning Discharge.....  | 540     |
| 13. Spark Breakdown with Alternating Current.....                                   | 550     |
| 14. References for Sections 11 to 13, Part C, Chapter X.....                        | 558-559 |

## XI. THE ARC AND GLOW DISCHARGES

## PART A. THE GLOW DISCHARGE

|  |         |
|--|---------|
| 1. The Glow Discharge as a Function of Pressure. . . . .   | 560     |
| 2. Certain Characteristic Structural Features of the Glow Discharge                              | 563     |
| 3. Potential, Field Strength, and Density Distribution in a Conventional Glow Discharge. . . . . | 565     |
| 4. Measurements of Field Strength. . . . .   | 567     |
| 5. General Mechanism of the Glow Discharge . . . . .   | 568     |
| 6. The Crookes Dark Space and the Cathode Fall of Potential. . . . .                             | 574     |
| 7. The Positive Column. . . . .  | 585     |
| 8. The Anode Fall of Potential. . . . .  | 596     |
| 9. The Energy Balance at the Cathode . . . . .   | 598     |
| 10. Sputtering at the Cathode. . . . .   | 599     |
| 11. Hollow Cathodes. . . . .   | 601     |
| 12. Plasma Oscillations. . . . .   | 601     |
| 13. References for Part A, Chapter XI. . . . .   | 602-604 |

## PART B. THE ARC DISCHARGE

|   |         |
|---|---------|
| 1. The Definition of an Arc. . . . .                            | 605     |
| 2. The Transition from a Glow to an Arc. . . . .                | 606     |
| 3. Characteristic Potential Curve of an Arc . . . . .           | 608     |
| 4. The Cathode Fall in an Arc. . . . .                          | 609     |
| 5. Cathode Temperature. . . . .                                 | 613     |
| 6. Potential Fall Measurements with Probes. . . . .             | 613     |
| 7. The Anode Fall. . . . .                                      | 615     |
| 8. The Positive Column. . . . .                                 | 616     |
| 9. Experimental Data. . . . .                                   | 622     |
| 10. Negative Characteristic and Oscillations. . . . .           | 624     |
| 11. The Arc Resistance. . . . .                                 | 626     |
| 12. Other Arc Properties. . . . .                               | 628     |
| 13. The Cathode Mechanism of Low-Boiling-Point Metal-Vapor Arcs | 629     |
| 14. The Low-Voltage Arc. . . . .                                | 636     |
| 15. References for Part B, Chapter XI. . . . .                  | 639-641 |

## APPENDIX I

|   |     |
|---|-----|
| 1. The Kinetic Nature of a Gas. . . . . | 643 |
| a. The Pressure of a Gas. . . . .       | 643 |
| b. Molecular Free Paths. . . . .        | 644 |
| c. Distribution of Velocities. . . . .  | 650 |

## APPENDIX II

|   |     |
|---|-----|
| Tables of Critical Potentials in Volts. . . . . | 656 |
|---|-----|

## APPENDIX III

|                                      |     |
|--------------------------------------|-----|
| Table of Physical Constants. . . . . | 657 |
|--------------------------------------|-----|

|                       |     |
|-----------------------|-----|
| AUTHOR INDEX. . . . . | 663 |
|-----------------------|-----|

|                        |     |
|------------------------|-----|
| SUBJECT INDEX. . . . . | 671 |
|------------------------|-----|

## CHAPTER I

### IONIC MOBILITIES

#### PART A. MEASUREMENTS\*

##### 1. INTRODUCTION

Although it may be a truism, it is nevertheless essential to point out that, when one sees the literature of a field of physics filled with *methods* of measurement, the measurements of that period are not satisfactory. This is precisely the situation in the domain of mobility measurements in the period extending for thirty years from 1896 to 1926. The unsatisfactory status of measurement in this period cannot be ascribed to a lack of ability on the part of the workers of that time. In fact, many of the most brilliant experimental physicists of the atomic epoch have been among those contributing to the scores of determinations and experimental methods developed. The difficulty must largely be ascribed to the many factors unknown at that time, to which the results are especially sensitive. One of these factors is the requirement of *sharply* defined points of origin and reception of the ions which determine the resolving power. A second and perhaps the more important factor lies in the change of ionic nature with time and the predominant role of traces of impurities, which can be avoided only with the present high-vacuum techniques.

It must be clear then that, in treating the subject as part of a chapter of a book when a complete discussion in itself might form a whole book, one must pass over a large number of excellent methods and investigations. Adequate descriptions of all the methods of measurement up to the time of publication can be found in Przibram's admirable summary in Geiger and Scheel's *Handbuch der Physik*, Volume 22, Part I, pages 345-355, Julius Springer, Berlin, 1933, and Volume 1 of the third edition of J. J. Thomson's *Conduction of Electricity through Gases*. Neither of these texts is critical, and significant advances have occurred since their preparation. It is not the purpose of this book to present a compilation of past methods and results. Its aim is to present on the basis of the author's own extensive and recent experience in the field what appear to be the best and most useful methods at the present time for the various types of measurement which are likely to be required. It is hoped that such a *critical* survey, at a time when the achievement of adequate methods makes the development of further methods in the immediate future unlikely,

\* References for Part A of Chapter I will be found on page 30.

will serve the purpose of orienting future workers and students and thus aid in avoiding waste of time and duplication of effort. It will, therefore, be possible to give only the relatively few accurate and significant modern methods and to discuss such others as have important historical significance because of their implications, or which have some value as techniques in certain special aspects of the problem. The methods which will be discussed may be listed as follows:

1. Air-blast methods.
  - a. Zeleny air-blast method, of historical importance.
  - b. Erikson parallel-plate method, useful in certain modern problems.
2. Alternating-current methods.
  - a. Rutherford a-c method, an accurate absolute method of limited applicability (applicable to negative ions in some gases only).
  - b. Franck modification of the Rutherford method, of historical importance.
  - c. Tyndall and Grindley a-c method as modified by Bradbury, one of the absolute methods of high resolving power, for ions older than  $10^{-8}$  second.
3. Electrical shutter methods.
  - a. Tyndall and Powell four gauze a-c method. Absolute, accurate, and of high resolving power, for ions of all ages, especially those from  $10^{-8}$  to  $10^{-3}$  second old.
  - b. The electrical shutter method of Bradbury for electrons, using the Loeb electron filter.
4. The Townsend deflection method in crossed magnetic and electrical fields. Applicable to rapidly moving ions or electrons at lower pressures. It is not especially accurate.
5. Electrical wind methods, of historical interest.

In the years immediately following the discovery of X-rays, J. J. Thomson<sup>1</sup> and E. Rutherford, then a student at the Cavendish Laboratory, studied the properties of the conductivity produced in air by X-rays. They quickly showed that it was due to positively and negatively charged carriers of a molecular nature which moved in gases with a velocity  $v$  proportional to the field strength  $X$  such that the ratio  $v/X = k$ , a constant, called the mobility. The carriers they termed *ions* in analogy to the terminology current in regard to aqueous solutions. The value of  $k$  observed in gases varied from about 1 to 10 cm/sec per volt/cm and was dependent on the nature of the gas. Rutherford<sup>2</sup> also developed his alternating-current method for negative ions in this early period. The difference in mobility of positive and negative ions was not known at this time, and John Zeleny, then a student at the Cavendish Laboratory, was assigned the problem of measuring mobilities of ions of both signs accurately, using an air-blast method. This pioneer investigation, which was carried out with great skill and care, was completed in 1899.<sup>3</sup> The values there obtained for air were accordingly taken as *standard* for most subsequent studies until 1923. Since these values constituted the basis of

the arbitrary calibration of many later methods, they appear in most books and tables as the standard values today. They are thus still widely used as correct in present-day calculations. Unfortunately, through uncontrollable factors, which in no way discredit the excellent early work of Zeleny, these values are wrong, being low by a factor of about 1.21. Hence, where precision is required, in using values of the mobility, one must even today carefully regard the method of measurement in order to ascertain whether the apparatus was calibrated on the Zeleny scale or whether the method was absolute. If the value is based on the Zeleny standard, multiplication by 1.21 will in general give a fairly close approximation to a proper value. It is thus essential briefly to study the Zeleny method.

## 2. AIR-BLAST METHODS

**a. The Zeleny Air-Blast Method.** A blast of air of constant velocity was blown down the cylindrical metal tube *C* of radius *b*,

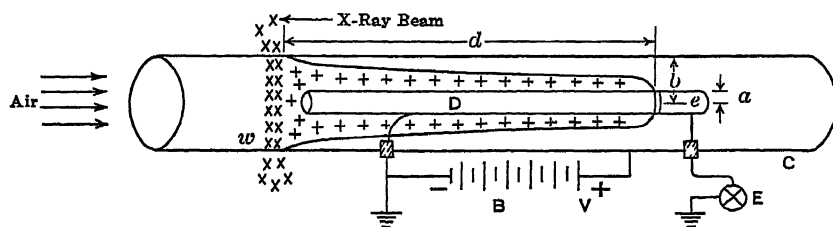


FIG. 1.—The Original Zeleny Method.

Fig. 1. This was provided with a central coaxial electrode *D* at whose end there was a small insulated electrode *e* connected to an electrometer *E*. *D* had a radius *a* and extended nearly from the window *w* through which the X-ray beam passed to the insulated segment. From the edge of the X-ray beam to *e* is a distance of *d* cm. *D* was grounded. The cylinder *C* was raised to a positive or negative potential *V* above or below ground by means of a battery *B*. This drove the ions generated by the X-rays moving down the tube along *D* with a velocity *u* radially towards *D*—positive ions when *C* was positive and negative ions when it was negative. The envelope of the mass of positive ions blown down the tube and just reaching *d* is shown by the curved line. The air velocity *u* is low at both electrodes while the field increases from *C* to *D*. Now an ion at *r* cm from the axis will have a radial velocity

$$v_r = X_r k = \frac{V k}{r \log b/a},$$

where *X<sub>r</sub>* is the field strength at *r*. Since *u<sub>r</sub>* is the velocity of the gas, along *x*, down the tube at *r*,  $dx/dr = u_r/v_r = (u_r/Vk) \log b/a$ .



The ions which cross from the surface of the tube  $C$  to  $D$ , and just reach the electrometer segment  $e$  at  $d$  cm down the tube from the X-ray beam, are the first ions detected as  $u$  is increased or  $V$  is decreased. The condition for the appearance of a current at  $E$  is then

$$\int_0^d dx = \frac{\log \frac{b}{a}}{Vk} \int_a^b u_r r dr.$$

Now

$$2\pi \int_a^b u_r r dr = Q,$$

the volume of gas flowing through the tube per second. Thus

$$d = \frac{Q}{2\pi Vk} \log \frac{b}{a} \quad \text{and} \quad k = \frac{Q \log b/a}{2\pi Vd}.$$

Accordingly, with  $Q$  constant,  $V$  is varied until a current is just recorded at  $E$ . Since the current was not observed to rise abruptly, Zeleny plotted the current  $i$  as a function of  $V$ , obtaining a curve of

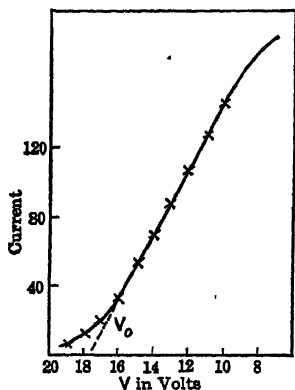


FIG. 2.

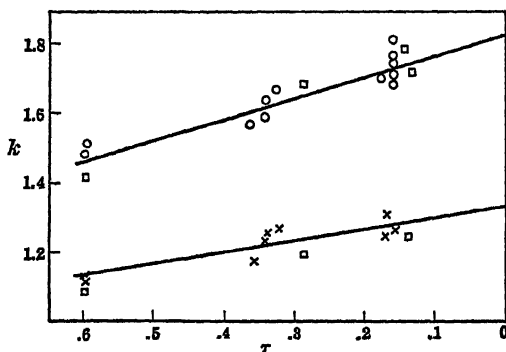


FIG. 3.

the form shown in Fig. 2. The steep part of the curve was extrapolated to an intercept  $V_0$ , and this value was used in place of the asymptotic foot which Zeleny rightfully attributed to diffusion, though turbulence may also have entered. The values of  $k$  observed at different values of  $Q$  were not constant, being higher the larger  $Q$ . Zeleny again attributed this to the diffusion. Diffusion will cause the ions to advance beyond the edge of the original beam and thus cause a greater error the smaller  $Q$  and hence the longer  $\tau$ , the time of ion transit to  $E$ . To correct for diffusion, he measured the values of  $k$  at increasing values of  $Q$ , i.e., decreasing values of  $\tau$ , and plotted the values for  $k$  against  $\tau$  for both ions as shown in Fig. 3. He observed a linear

increase of  $k$  with decrease in  $\tau$  and extrapolated his values back to  $\tau = 0$ . This gave  $k_- = 1.8$  cm/sec per volt/cm and  $k_+ = 1.4$  cm/sec per volt/cm for relatively dry room air from a gasometer. The accepted values today for pure dry air from the work of Loeb,<sup>4</sup> Tyndall and Grindley,<sup>5</sup> and Bradbury<sup>6</sup> and Varney<sup>11</sup> are  $k_- = 2.20$ ,  $k_+ = 1.6$ .

In 1929, Zeleny<sup>7</sup> repeated his measurements, using essentially the same arrangement as that above except that  $e$  was a narrow segment on  $D$  and the ions entered through a series of circular holes around the circumference of  $C$ . Carefully dried air was used. This method is in reality an adaptation of the Erikson method to the cylindrical electrode system. It has a high resolving power. In this work, turbulence was avoided, and diffusion was corrected for by theory. The results were not so consistent as those of the other workers but agree in magnitude with the accepted values, being  $k_- = 2.2$ – $2.4$  and  $k_+ = 1.7$ – $1.9$ .

The original method suffered from: (1) inaccuracies due to turbulence; (2) Poor definition of the edge of the ionized region (common to all X-ray ionization); (3) impossibility of control of the purity of the air; (4) difficulties in correcting for diffusion.

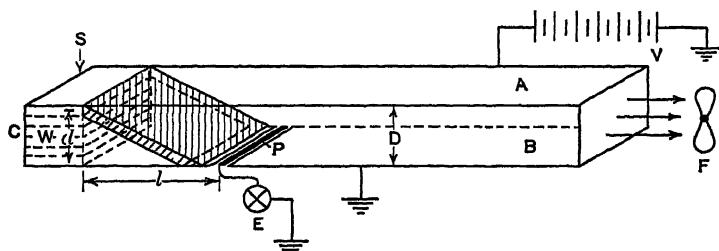


FIG. 4.—The Erikson Method.

It is impossible to arrive at the cause of the early low values of  $k$ . It is probable that items 1 and 2 advanced the edge of the ionized gas mass so far beyond the geometrical edge of the beam that ions were observed at values of  $V$  which were too high. The careful nature of this study, which for the first time gave the difference between  $k_+$  and  $k_-$ , established the values cited above as the absolute standard air values until 1926.

**b. The Air-Blast Method of Erikson.**<sup>8</sup> This is shown schematically in Fig. 4. A square rectangular tube the top and bottom of which constitute two plates of a plane parallel plate condenser system of plates  $A$  and  $B$ ,  $D$  cm apart, has a blast of air entering at  $C$ . This is drawn through the tube by means of the fan  $F$  at the other end. A narrow insulated section  $P$  of plate  $B$  is separated from it by thin slots and connected to an electrometer  $E$ .  $B$  is grounded. The strip can be made very narrow and as long as  $B$  is wide.  $P$  can be moved up or

down the gas stream by having the whole plate  $B$  movable.<sup>9</sup> At the end  $C$ , there may be a group of vanes  $W$  to insure a uniform flow of gas. In the upper segment of  $W$ , whose center is at  $d$  cm above  $B$ , the top vane, only a millimeter or two below  $A$ , may have the space ionized by some radioactive source. Ions may also be admitted from a space above through a slot in  $A$ . Between  $A$  and  $B$  there is a field  $X = V/D$ , produced by a potential  $V$  applied by the battery  $V$  whose other side is grounded. Call  $l$  the distance from the forward edge of the upper vane  $W$  to the center of  $P$ . Then as the air carries the ions along the tube the field carries them downward from  $A$  to  $B$ . If the current  $i$  to the electrometer is measured as a function of  $V$  at constant  $l$  and velocity  $u$  of the stream, the current observed if ions of three different

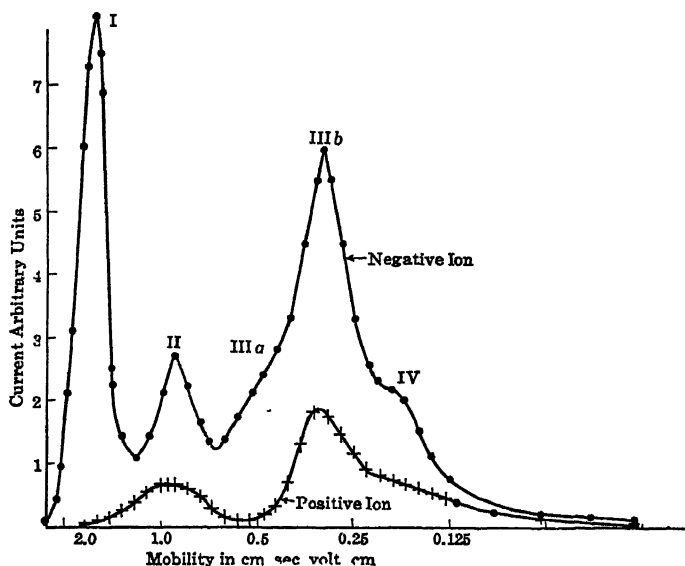


FIG. 5.—Chapman's Curves with Erickson's Method.

negative mobilities are present will have the appearance shown in Fig. 5.

These are curves taken from Chapman's studies of electrification by bubbling of water. The ions, the center of whose peak is at a potential  $V_{01}$ , traverse a distance  $d$  in the field  $X_{01} = V_{01}/D$  with a velocity  $v = k V_{01}/D = d/\tau$ , where  $\tau$  is the time of crossing. In the same time  $\tau$  the ions traverse a distance  $l$  related to  $\tau$  by  $l/\tau = u$  downstream. Thus one may write

$$\frac{l}{u} = \frac{d}{k} \frac{D}{V_{01}} \quad \text{and} \quad k = \frac{d}{l} u \frac{D}{V_{01}}.$$

The method can be made to have a high resolving power if  $D$  and  $W$  are narrow. It can cover enormous ranges of values of  $k$ . Chapman has measured values from 1.5 to  $10^{-5}$  cm/sec per volt/cm, by moving  $D$ , changing  $u$  and  $V$ . Turbulence can be eliminated by using a smoke and observing the blast in the absence of the field. The method is *incapable of giving accurate absolute* values, chiefly as  $u$  cannot be accurately evaluated over the tube. It can be used for studying aging of ions where the *gas purity* is not vital. By creating ions farther and farther up the tube from  $W$  the aging can be introduced without changing  $X$  or pressure. It was with this method that Erikson<sup>8</sup> first noted the aging of ions in air. It is to be noted that the peaks broaden as one goes down stream, owing to the increasing obliquity of the stream as well as to diffusion. If *not* regarded as an *absolute* method, it can and will be very useful for studies at atmospheric pressure of mobilities of *any* type of carrier. Its characteristics are:

1. It is subject to inaccuracies due to turbulence unless great care is taken. It is *always* disturbed by turbulence for higher gas velocities such as Erikson used.
2. The origin of the ions is *not* sharply defined; distances  $d$  and  $l$  are uncertain.
3. Diffusion corrections must be applied for low-velocity streams.
4. The velocity  $u$  cannot surely and accurately be determined and is not constant over the cross section of the tube.
5. The purity of the gases cannot be controlled.
6. It has a very high resolving power (as good as 10 per cent in Chapman's work).
7. It is useful in studies of aging.
8. It is exceptionally useful for mobility studies over large ranges of values.
9. The uniformity of fields and gas stream velocities makes it far superior to either of the cylindrical electrode techniques.

### 3. ALTERNATING-CURRENT METHODS

**a. Rutherford Method.<sup>2,4</sup>** One plate  $A$  of a parallel-plate condenser system  $AB$ , with plates  $d$  (1 to 4) cm apart, is connected to an electrometer  $E$  as shown in Fig. 6.  $E$  may be shunted by an auxiliary capacity  $C_1$  to ground. The plate  $B$  is illuminated by ultraviolet light and thus emits photoelectrons.  $B$  is connected to a collector brush  $C$  which alternately picks up a positive potential  $V_+$  and a negative potential  $V_-$ , giving a square-wave alternating current shown in Fig. 7. The potentials come from a battery whose center is grounded, but  $V_+$  is always kept about 10 per cent greater than  $V_-$ . With  $E$  disconnected but  $C_1$  in, the alternating potential is placed on  $B$  for a measured time  $t$ . It is then disconnected and  $B$  is grounded. The charge  $Q$ , due to photoelectrically formed ions from  $B$ , that has accumulated on  $A$  and  $C_1$  is then measured by  $E$ . It is usual to measure  $Q$  for a series of different values of  $V_-$  and  $V_+$  and to plot the resultant curve. It is best to have  $C_1$  some 100 times the capacity of the plate system  $AB$  and to correct  $V_-$  for the fall of potential across  $C_1$ . This pro-

cedure is necessitated if  $V_-$  is less than  $V_+$ , as electrometers are sensitive to alternating current. As a useful check on the measurement, one may make a series of measurements of  $Q = Q_0$ , using a steady potential  $V_-$  for a time  $t/2$  and the same values of  $V_-$  as used with

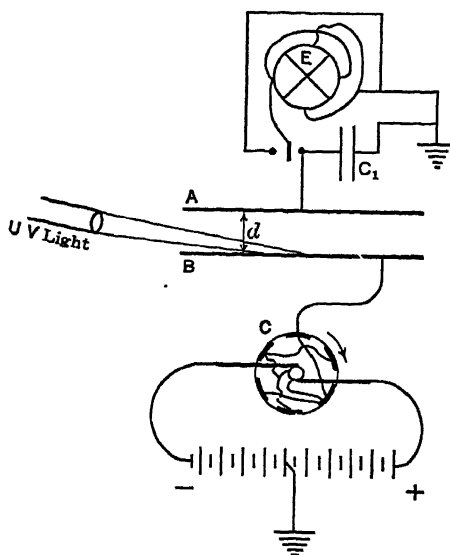


FIG. 6.—The Rutherford a-c Method.

either  $d$  or  $T$  could have been varied, keeping  $V_-$  and  $T$  or  $V_-$  and  $d$  constant, respectively. At various times, for reasons of experimental expediency, each of these variables has been used. In general,  $V_-$  is the easiest to vary. Very many determinations of mobility have also been made with this principle, using the Franck modification of the apparatus but otherwise the same technique, and evaluating  $k_-$  from  $V_{0-}$ . It is always better, however, to plot the whole curve and test the result by the curve shape. Consider the current  $Q_0$  as a function of  $V_-$  with no alternating current. Owing to the presence of gas, as  $V_-$  increases, the photoelectric current  $i_0$  and thus  $Q_0$  increase with  $V_-$ . That is, as will later be seen, photoelectric currents in gases are rarely "saturated."<sup>13</sup>  $Q/Q_0$ , the ratio of current collected with alternating current to the photo current which would have been collected in the same total time with direct current, represents the *fraction* of the carriers that reach  $A$  and hence  $E$ . Below  $V_{0-}$ , at  $k_- X_- t \leq d$ , no

alternating current. If the light source is steady, one can then plot  $Q/Q_0$  as a function of  $V_-$ , instead of  $Q$  as a function of  $V_-$ . The reason for this will become clear presently.

Call the time of one-half cycle  $T$ . At the instant when  $V_-$  is applied, the current of negative ions flows from  $B$ , and the ions formed at  $B$  move towards  $A$  at a velocity  $v = k_- X_- = k_- V_-/d$ . The ions are emitted throughout the negative phase of  $T$ . If in a time  $t = T$  the ions emitted just as  $V_-$  comes on just cross from  $A$  to  $B$ , a current should begin to be detected at  $E$ . Then at a potential  $V_{0-}$  such that  $k_-(V_{0-}/d) T = d$  the ions just cross. At this point  $k_- = d^2/(V_{0-}T)$ . If one had chosen,

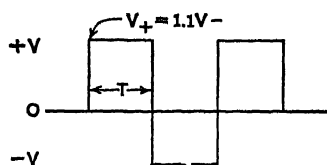


FIG. 7.

current reaches  $A$ . Above  $V_{0-}$  the current increases and  $Q/Q_0$  rises. For, as  $V_-$  increases above  $V_{0-}$ , ions liberated later in the phase than at the beginning of the  $V_-$  phase,  $T$  seconds long, can cross. At a given value of  $V_-$ , say  $V'_- > V_{0-}$ , ions liberated as late as  $t'$  seconds given by  $k_- V'_- t' = d$  can reach  $A$ . Thus, if we have a steady photo current at a potential  $V'$  of  $i_0$ ,

$$Q = i_0(T - t') = i_0 \left( T - \frac{d^2}{k_- V'_-} \right).$$

Accordingly,

$$i = \frac{Q}{T} = i_0 \left( 1 - \frac{d^2}{V'_- k_- T} \right),$$

and, as

$$T = \frac{d^2}{k_- V_{0-}}, \quad i = i_0 \left( 1 - \frac{V_{0-}}{V'_-} \right).$$

Therefore, more generally,

$$\frac{i}{i_0} = \frac{Q}{Q_0} = \frac{V_- - V_{0-}}{V_-},$$

since  $V'_-$  is any value of  $V_- > V_{0-}$ . It is thus seen that from the  $Q/Q_0 - V_-$  curve one can evaluate  $V_{0-}$  without recourse to a sharp intercept. Measurements made under proper conditions completely verify the theory.<sup>4</sup>

For values of  $T$  from seconds to  $10^{-3}$  second square-wave commutators are ideal. For higher frequencies, sinusoidal oscillations must be used. If the value of  $k_-$  is *constant*,<sup>12</sup> independent of  $V_-$  or  $X_-$ , one may use a sinusoidal alternating current of the form  $V = V_0 \sin \omega t$ , where  $\omega = 2\pi/T$ ,  $T$  being the *whole* period. In this case  $k_-$  is given by  $k_- = \frac{\pi}{\sqrt{2}} \frac{d^2}{E_{00} T}$ . Here  $E_{00}$  is the rms value corresponding to the

peak voltage  $V_0$  at intercept,  $E_{0-}$  is  $V_{0-}/d$  and the  $T$  is the *period, not* half period, of the alternating emf. The curve for  $i/i_0$  is then

$$\frac{i}{i_0} = \frac{Q}{Q_0} = 1 - \frac{1}{\pi} \cos^{-1} \left( \frac{2E_{00-}}{E_{0-}} - 1 \right).$$

With a sinusoidal alternating current, however,  $E_+$  and  $E_-$  are equal. Hence, owing to diffusion, ions cross from  $A$  to  $B$  over a series of cycles. This gives asymptotic intercepts near  $V_0$ , which make the evaluation of  $E_{00-}$  difficult. In this case a positive direct-current bias  $V_B$  can be placed on the plate  $B$ .<sup>10</sup> Then referring to Fig. 8 one sees that the condition for the rise of the electrometer current is that

$$\int_0^d dx = \int_{t_1}^{t_2} k_- X \sin \omega t dt,$$

where  $X = V_0/d$ , since the *negative phase* is acting on the ions only between  $t_1$  and  $t_2$  instead of from 0 to  $T/2$ . The values of  $t_1$  and  $t_2$  can at once be found from the ratio of  $V_B/V_0$ , where  $V_0$  is the *peak* value of the emf. What is then done is to measure  $i$  as a function of  $V_0$  with a fixed  $V_B$  and locate  $V_{00}$  the value of  $V_0$  at the intercept. Now we can calculate the value of the integral

$$\frac{d^2}{k - V_{00}} = \int_{t_1}^{t_2} \sin \omega t \, dt$$

as a function of  $V_B/V_0$  and plot a curve. Thus since

$$\frac{\pi d^2}{T k - V_{00}} = f\left(\frac{V_B}{V_{00}}\right),$$

$$k_- = \frac{\pi}{T} \frac{d^2}{V_{00} f\left(\frac{V_B}{V_{00}}\right)} = k_0 F\left(\frac{V_{00}}{V_B}\right),$$

with  $k_0 = (\pi/T) (d^2/V_{00})$ . From the values of  $V_{00}$ ,  $V_B$ ,  $d$ , and  $T$  we can at once calculate  $k_-$ .

The general method is applicable only to conditions where photoelectrons can form negative ions in the immediate neighborhood of  $B$ .

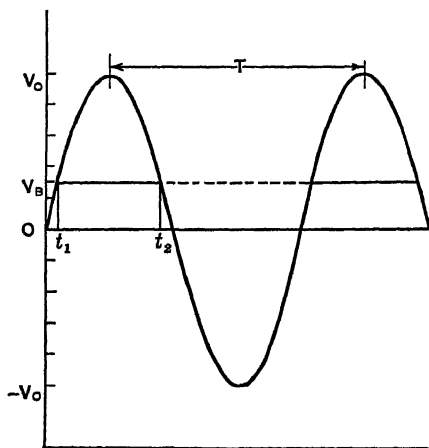


FIG. 8.

That is, the method is valid only where the distance that carriers can go in the electronic state before making ions is very small (about  $0.01 d$  or less). This occurs only for a few gases such as  $O_2$ ,  $SO_2$ ,  $HCl$ ,  $NO$  above 100 mm pressure, when  $T$  is not too short or  $V_{00}$  too high. The presence of electronic carriers is at once indicated by asymptotic intercepts and values of  $i/i_0$  in excess of those computed on any reasonable value of  $V_0$ . The method can also be used for positive ions liberated by a hot source, such as the alkali ions  $Na^+$ ,  $K^+$ , etc., from the Kuns-

man catalysts.<sup>10</sup> In that case correction must be made for the non-uniform temperatures and hence gas densities between the plates. If the ions start from  $B$  at  $T = 0$  as ions the values of  $k_-$  should be as accurate as  $T$ ,  $d$ , and  $V_0$  can be evaluated. That is, the method is absolute. *Its resolving power is very low.* Carriers of two mobilities within 20 per cent of each other, if present in the ratio of at least 15 to

100, would sufficiently distort the curves to yield a break point. Careful analysis of curves might reveal two ions within such limits. The presence of a spread of mobilities ranging 10 per cent on either side of  $V_0$  probably could not be detected in curves of the type possible.<sup>14</sup> To increase the resolving power, Varney<sup>11</sup> used intermittent ultraviolet illumination. He cut off the light of his ultraviolet source by a slot in the commutator at a time  $\tau$  seconds after the beginning of the negative phase. In this way the  $i/i_0$  curves go to *saturation* for moderate values of  $V_0$ . By differentiation, the  $i/i_0$  curves reveal the presence of other mobilities and the range of values over which the mobilities extend. He again checked the Loeb, Tyndall and Grindley, and Bradbury values for  $k_-$  in pure dry air. Air that had been irradiated for some hours with ultraviolet light showed a heterogeneous band of mobilities extending from 1.86 to 2.4.

The characteristics of this method are:

1. It is an absolute and accurate method when properly used.
2. It can be applied to gases of the highest purity.
3. It is restricted to gases that form negative ions by electron attachment close to the photoelectric source. This limits it to higher pressures and a few gases.
4. It can be used on positive ions from hot oxide sources. This introduces an uncertain temperature correction for gas density.
5. It can be applied to ions of ages ranging from  $10^{-8}$  second down, once they are formed.
6. It has a low resolving power unless used with intermittent ionization.

**b. The Franck Modification of the A-C Method.** In 1909, Franck<sup>15</sup> introduced a modification to the Rutherford method which enables both positive and negative ions to be studied.

In this modification, the ultraviolet source was replaced by a gauze or grid between  $A$  and  $B$  and fairly close to  $B$  as in Fig. 9. The alternating potential was connected to the gauze  $G$ , and a battery  $E'$ , giving an auxiliary potential  $V_a$ , was placed between  $B$  and  $G$ . By means of a commutator the gauze  $G$  could be made either positive or negative to  $B$ , thus driving

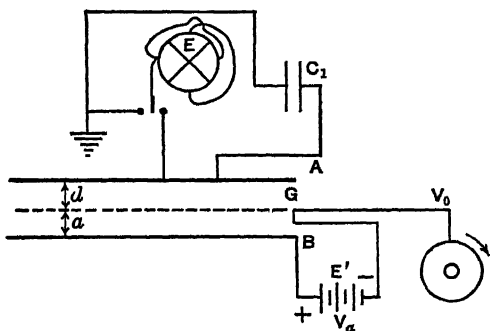


FIG. 9.—The Franck Modification of the Rutherford a-c Method.

respectively negative or positive ions into the region  $GA$ . In the space  $GB$  the gas is ionized by any convenient agent, usually a deposit of  $Po$  giving  $\alpha$  particles. It was assumed that the auxiliary



field  $X_a = V_a/a$ , where  $a$  is the distance from  $B$  to  $G$ , drove ions to the meshes of the gauze where they remained until  $G$  took on the potential to drive them to  $A$ . At this instant the ions were *assumed* to start from the plane of  $G$  distant  $d$  cm from  $A$ . From the value of the alternating potential  $V_0$  needed to drive the ions to  $A$  in the time  $T$  across  $d$ , the mobility was then calculated to be  $k = d^2/(V_0 T)$ . When Franck tested his apparatus in air it happened that the value of  $V_a$  used gave him the Zeleny values for  $k_+$  and  $k_-$ . With later workers, the choice of  $V_a$  was not always so fortunate. But it was found that, by adjusting  $V_a$  slightly, the apparatus could be "standardized" to the Zeleny air values. This was done consistently by workers using this method, including the author, until 1923.<sup>4</sup> At that time Loeb<sup>4</sup> noted that Kovarick's values for  $k_-$  with ultraviolet light using the Rutherford method were consistently around 2.1 and that, on repeating Kovarick's measurements, he also obtained Kovarick's values. On the other hand, using a gauze in the same chamber, Loeb obtained, as had others, the Zeleny value of 1.8. The difficulty was at once clarified when  $V_a$  was varied, for by increasing  $V_a$  one got higher values of  $k_-$  which could even be made to exceed those of Kovarick. As at this time the function of grid electrodes in vacuum tubes was well recognized, the explanation was simple. The gauze  $G$  especially if it has a high transmitting power for ions is *not a good screen*. Thus, first the field in  $GA$  is not  $X_0 = V_0/d$  but  $X'_0 = X_0 + \mu X_a$ , where  $X_a = V_a/a$ , and  $\mu$  is the reciprocal of the amplification factor, a small fraction for most gauzes. This correction is thus *not* important but should be made.

There is, however, a much more serious difficulty. If one regards the enlarged section of the gauzes, during the retard phase of  $V_0$  as in Fig. 10A and 10B, one will see that the fields take on very different aspects according as  $X_a$  is less or greater than  $X_0$ . Where  $X_a$  is less than  $X_0$ , Fig. 10A, the lines of force penetrate into the region  $GB$  so that the envelope of the lines is indicated by the heavy loops  $L$  connecting two adjacent grid wires. In this region just as the field reverses there are no positive ions, for all positive ions have followed the force lines and lie between the wires  $G$  and  $B$ , but not above  $L$ . Hence, at the beginning of the accelerative phase  $T$  the ions *do not start at the plane of the gauze* but from a distance  $l$  below it. Thus  $k$  is actually given by  $k = d(d + l)/(TV_0)$ . If one uses the theoretical equation  $k' = d^2/(TV_0)$ , the value  $k'$  computed is low and in error by the ratio of  $k' = k d/(d + l)$ . If on the other hand  $X_a$  is greater than  $X_0$ , the conditions of Fig. 10B obtain. Here the envelope  $L$  is  $l$  cm above the plane of  $G$  and one has  $k = d(d - l)/(TV_0)$ , which is high and in error by the ratio  $k' = k d/(d - l)$ . When  $X_0 = X_a$ , the value of  $k$  should be about correct. The fact that some of the lines of force from  $B$  reach  $A$  will result in ions of the opposite sign reaching  $A$  during the *retard phase* if  $X_0$  is greater than  $X_a$ , and some ions of the same

sign getting to  $A$  *against* the retard field if  $X_a$  is greater than  $X_0$ . Thus, interpenetration effects of the auxiliary field in mobility measurements with this method are always characterized by negative currents at  $V$  less than  $V_0$  if  $X_a < X_0$  and positive currents at  $V < V_0$  if  $X_a > X_0$

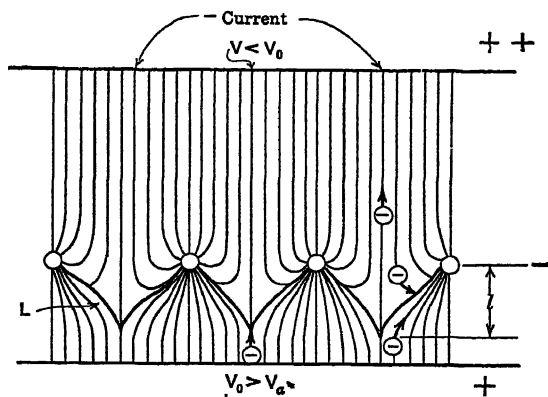


FIG. 10A.

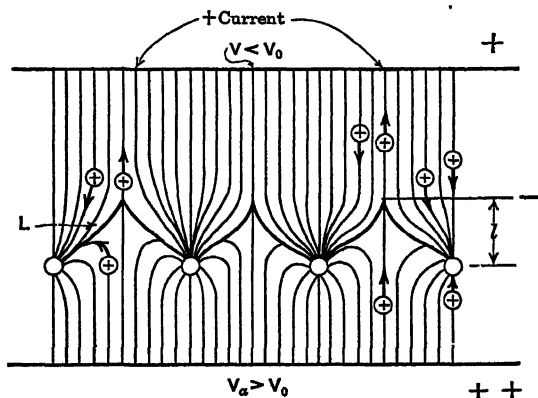


FIG. 10B.

as shown in Figs. 11A and 11B, respectively. The fact that the spaces  $L$  do not have the ions *all* starting from a common distance above or below  $G$  leads to asymptotic feet. At  $X_0 = X_a$  there are not any. Hence the Franck modification of the a-c method of measuring  $k$  is fraught with considerable uncertainty. If  $X_a = X_0$  throughout the measurements, or if  $X_a$  is adjusted to be equal to  $X_0$  at the point  $X_0$  where ions just cross, the values *should* be reliable. If one tries to vary  $V_a$  so as to keep  $X_a = X_0$  the currents  $i_0$  vary rather badly, and the method is uncertain. The  $i/i_0$  curves should be reliable. At  $X_a = X_0$

it has been shown<sup>4</sup> that the currents *approach* the ideal equation  $i/i_0 = (V - V_0)/V$  in form. Thus this method is not absolute, and though very convenient it must be used with considerable care.

The difficulty introduced by the gauze, however, is *not confined to this method*. Very many other perfectly splendid methods are rendered completely valueless as *absolute* methods by interpenetration effects through gauzes. Wherever the method requires change of fields on two sides of a gauze element to make the measurement, the same problem occurs. This vitiates most of the early electrical shutter methods, as well as mechanical shutter methods involving gauzes. In only two methods using gauzes these effects do not occur. One is the abso-

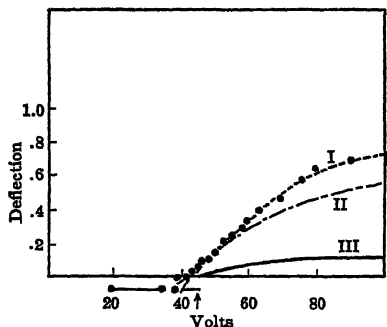


FIG. 11A.

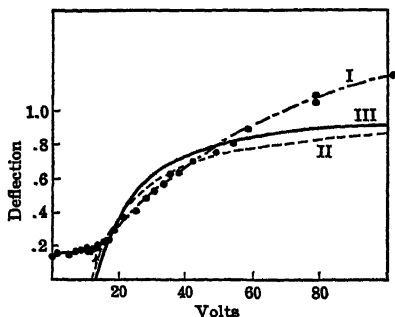


FIG. 11B.

lute use of the Tyndall and Powell four-gauze shutter method, where the influence of the symmetrical placement of gauzes somewhat reduces the magnitude of the effects. In some uses of the method, the fields can be left constant and frequency or distance changed. The uncertainty of the fields is present even here, and absolute values can be had only by changing  $d$ , as will be seen. The other case is that of parallel grid wire gauzes with high-frequency alternating current between alternate wires in the Loeb electron filters as used by Bradbury for shutters in electron mobility work. Here the lateral fields cause no difficulty as far as interpenetration goes.

It seems perhaps unnecessary to allot so much space to a useful but unsatisfactory method. The use of grids and gauzes has been and still is so frequent and the errors introduced by them lead to such serious contradictions that one cannot but feel justified in clearly pointing out their weaknesses, especially since many workers appear ignorant of these facts.

c. **The Bradbury Modification of the Tyndall and Grindley Method.** In the very early days of mobility study Langevin<sup>18</sup> in 1903 developed an ingenious method of flash X-ray ionization followed by the application of a field and its reversal using a pendulum which enabled mobilities to be measured with the existing variable X-ray

sources. He balanced out irregularities in X-ray intensities by a cleverly arranged control chamber. The method is basically an a-c one in that the same cycle could today be arranged by a commutator and flash segment with a steady source of X-rays. The method because of the usually diffuse nature of the edge of the X-ray beam did not and would not today give sharply defined break points, nor has it a high resolving power. It was in its day an original and excellent method. The results obtained by it, however, are no more reliable

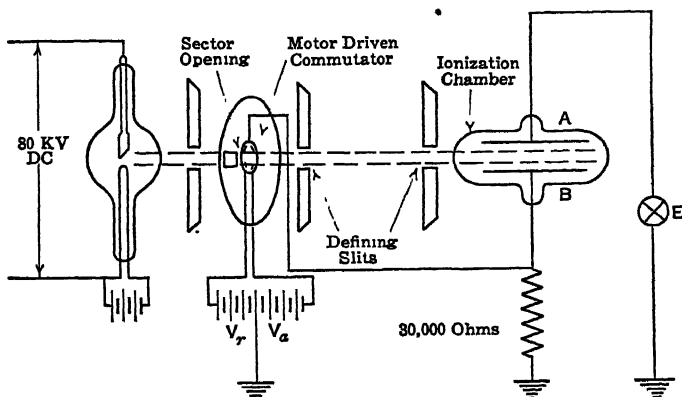


FIG. 12A.—The Bradbury Modification of the Tyndall and Grindley Method.

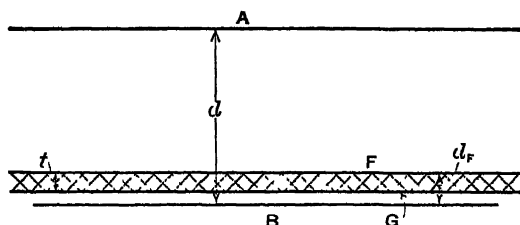


FIG. 12B.

than the earlier Zeleny results. It is not surprising that the principle of this method should later have been developed by others to a modified alternating-potential method when better sources of ionization became available. The method was first developed and applied by Tyndall and Grindley<sup>17</sup> in 1926, and its possibilities were recognized. These workers used a commutator, and as an ionizing source they used  $\alpha$  rays from a polonium segment placed on the rim of the commutator. This restricted their work to air at atmospheric pressure and precluded much purity. It further introduced difficulties in the curve shapes obtained owing to the non-uniform ionization across the ionized slab of gas given by the  $\alpha$  particles near the end of their range.

The availability of a 100,000-volt constant-potential X-ray source for ionic studies at the University of California in the hands of Bradbury<sup>13</sup> resulted in modifications of the Tyndall and Grindley method which make it a clean-cut, absolute precision method of high resolving power. The discussion of the method will accordingly be confined to the later Bradbury modification.

In a parallel-plate condenser  $AB$  with a uniform field and a plate distance  $d$  of some 4 to 10 cm a thin, uniform, well-collimated beam of X-rays is allowed to pass close to the plate  $B$  of Fig. 12A, but separated from it by a finite distance (at least 1 mm). The slab of ionized gas is  $t$  thick where  $t$  is small (1 to 4 mm) compared to  $d$ ; it is designated  $FG$  in Fig. 12B. The plate  $A$  was connected to an electrometer  $E$ . An alternating potential was supplied to  $B$  by means of a commutator,  $B$  being grounded by 30,000 ohms except when the commutator made contact with the batteries  $V$ . The commutator had a lead facing to cut off the X-ray beam. An open sector of variable size and location relative to the commutator brushes allowed the X-ray beam to be flashed into or cut off from the chamber at any desired time relative to the electrical cycle. The cycle is a rather unusual sequence of the X-ray flash followed by reverse and accelerating fields which will be discussed in detail. The procedure is to fix the potentials and relative setting of the flash and commutator segments and then to plot electrometer current as a function of the frequency or period  $T$  of revolution.

The cycle used is illustrated in Fig. 13. Beginning with an X-ray flash lasting  $\beta T$  seconds while the commutator and  $B$  are grounded, there is a period of time  $\gamma T$  during which the potential applied is  $V_r$  in such a sense that the ions of interest are dragged away from  $A$  toward  $B$ . Subsequent to  $\gamma T$  the potential reverses and a potential  $V_a$  less than  $V_r$

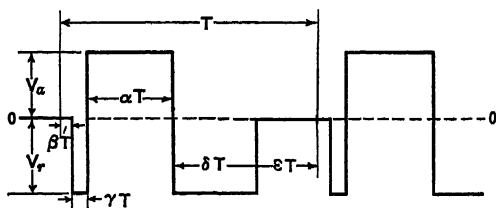


FIG. 13.

driving the ions of interest to  $A$  and thus to  $E$  is applied. This potential lasts a time  $\alpha T$ . At the end of  $\alpha T$  the potential drops to  $V_r$ , which lasts a time  $\delta T$ . This is long enough to remove all the remaining ions from the gap. Then the system is grounded for a time  $\epsilon T$  until the cycle repeats with the beginning of a new X-ray flash  $\beta T$ . In some cases where free electrons are present which could complicate the readings, Bradbury had a very small sweeping potential so as to sweep electrons to  $B$ , applied just after  $\beta T$ , and before  $\gamma T$ , which is of very short duration. Both potential and duration of this flash are so small as not to derange the rest of the cycle. The important parameters  $\beta$ ,  $\gamma$ , and  $\alpha$  are fractions,  $\beta$  and  $\gamma$  being nearly equal and of the order

of  $0.04 T$ , while  $\alpha$ ,  $\delta$ , and  $\delta$  are equal and of about  $0.32 T$  each.  $V_r$  is some 10 to 20 per cent greater than  $V_a$ . The relative values will vary somewhat in order to obtain the best results but can be estimated in advance from a knowledge of the conditions to be met.

Call the plate separation  $d$ . During  $\gamma T$  the field is  $X_r = V_r/d$ , and during  $\alpha T$  the field is  $X_a = V_a/d$ . During the flash of X-rays in  $\beta T$  the ions accumulate in the slab  $FG$ , and as a result of diffusion, etc., they are at the beginning of  $\gamma T$  in a fairly uniform distribution lying between the lines  $F$  and  $G$  of Fig. 12B. Let us disregard the ions of opposite sign from those of interest. The ions of interest,  $N$ , either positive or negative, will be drawn out of  $FG$  towards  $B$  for a time  $\gamma T$ . This time must be such that *some but not all* of the  $N$  ions in  $FG$  will reach  $B$  from  $G$  for the essential part of the measurement. The group of  $N$  ions are at the end of  $\gamma T$  in contact with  $B$  and some have been lost. On reversal, the field  $X_a$  pulls these ions to  $A$ , and if  $\alpha T$  is long and  $V_a$  great enough a current of ions from the top part of the slab then touching  $B$  will reach  $A$ . Beginning with the value of  $T$  when  $k_N X_r \gamma T \leq FB$ , as  $T$  increases this current will increase until the end of the slab which was touching  $B$  just reaches  $A$ . Thereafter, the current decreases with increasing  $T$  as the survivors from  $FG$  as  $T$ , and hence  $\gamma T$ , increases become fewer. If ionization is uniform throughout  $FG$ , the rise of current at  $A$  to a peak and the decline will be linear. The *peak* of the curve measures the point at which  $k_N X_a \alpha T_0 = d$ . The sequence of events beginning with large values of  $T$  and decreasing them is then as follows. For large  $T$ , all the ions in  $FG$  are removed during  $\gamma T$ . The current to  $A$  is zero. As  $T$  decreases some ions will not be caught by  $B$  and for a sufficiently long  $T$  will just reach  $A$ . As  $T$  gets less the survival group from  $FG$  increases linearly as  $T$  decreases. That is, if we call the distance  $FB = d_F$ , then no current will be observed until  $k_N X_r \gamma T_F \leq d_F$  and  $k_N X_a \alpha T_F > d - FG$ . From then on if we have  $n$  ions per square centimeter of plate area in  $FG$ , the quantity received by  $A$  per square centimeter at a time  $T$  greater than  $T_F$  as defined above is

$$Q = ne(d_F - k_N X_r \gamma T). \quad (1)$$

Let us call  $GF = t$ . If  $\alpha T_0$  was chosen so that when  $k_N X_a \alpha T_0 = d$ , the relation between  $d_F$ ,  $t$ ,  $X_r$ ,  $\gamma$ , and  $T_0$  is given by  $d_F - (t/2) = k_N X_r \gamma T_0$ , then at  $T = T_0$  half the ions in  $FG$  reach  $A$  and the current is a maximum, of magnitude  $Q_0 = ne t/2$ . In general, if the adjustment is not exact, the quantity  $Q$  at  $T_0$  is given by the equation above with  $T$  replaced by  $T_0$ . From  $T_0$  on as  $T$  gets shorter, the ions captured are only those of the survivors which can reach  $A$  in  $\alpha T$ . At any time  $T_a < T_0$  ions are collected from a distance  $d_a = k_N X_a \alpha T_a$  and

$$\begin{aligned} Q &= ne[(d_F - k_N X_r \gamma T_a) - (d - d_a)] \\ &= ne[d_F + k_N (X_a \alpha - X_r \gamma) T_a - d]. \end{aligned} \quad (2)$$

At and beyond values of  $T_\alpha = T_2$  where  $d \geq d_F + k_N(X_{\alpha\alpha} - X_r\gamma)T_2$  the current is zero. It is seen that, in equations 1 and 2,  $Q$  is a linear function of  $T$ .

The resulting curves should then show the form indicated in Fig. 14.

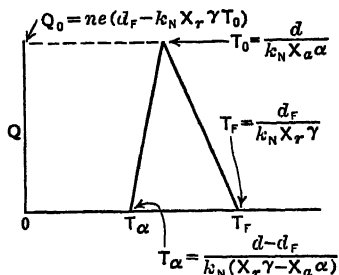


FIG. 14.

The resolving power depends on the width of the strip  $GF$  and on the conditions which will bring  $T_F$  and  $T_2$  closer together. These are limited by the sensitivity of the electrometer system, the width of the beam, and the distance  $FB$  relative to  $d$ . It is probable that the resolving power could be increased to at least five times that used by Bradbury. In Figs. 15A and 15B we see curves taken by Bradbury,

one for positive ions in pure  $N_2$ , ions of only one mobility being present, and one in tank  $H_2$ , with ions of two mobilities present. The peaks at 8.2 and 13.1 are clearly resolved.

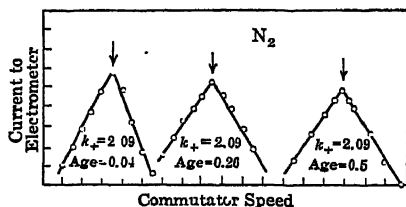


FIG. 15A.

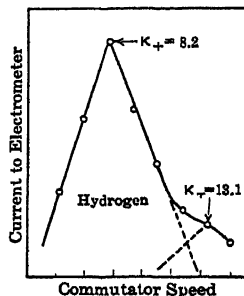


FIG. 15B.

Fig. 16 shows the mobilities in  $N_2$  and  $NH_3-N_2$  mixtures during a fixed time interval of measurement. The predominance of the ion  $N_2 NH_3^+$  over the  $N_2$  ion in the same time with increasing amounts of  $NH_3$  is seen. It is possible that more than one type of  $NH_3 + N_2^+$  ion is present, e.g.,  $N_2 NH_3^+$  and  $(NH_3)_2 N_2^+$ , at the higher concentrations. This method has the high-

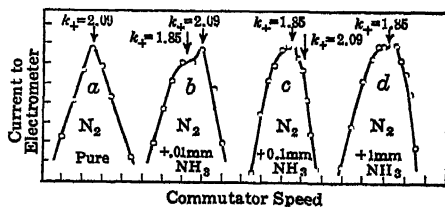


FIG. 16.

est resolving power of any except the Tyndall and Powell method.

The characteristics of this method are:

1. It is an absolute method giving sharp and accurate values of mobility. Its

accuracy is as great as the accuracy of measurement of  $T$ ,  $\alpha$ ,  $\gamma$ ,  $X_r$ , and  $\dot{X}_a$  and the uniformity of the ion density permit.

2. It can be used in a completely outgassed chamber on any and all gases, and can be applied to gases of the greatest purity.

3. It has an exceedingly high resolving power and is capable of giving accurate values of mobilities by ions separated by 10 per cent in mobility if properly used.

4. It depends on a steady and uniform X-ray source of considerable power. It does not require internal ionizing sources.

5. It is limited in its scope to ions of  $10^{-3}$  second in age on up to seconds in age.

#### 4. ELECTRICAL SHUTTER METHODS

Although some of the electrical shutter methods involve alternating currents, they really belong in a class by themselves. Their development began relatively late in the history of mobility measurement, and strangely enough practically all the shutter methods arose independently and nearly simultaneously in the period 1927 to 1929.

In 1927, M. La Porte<sup>20</sup> developed a *mechanical* shutter system for measuring mobilities. It consisted in an adaptation of the Fizeau toothed wheel method for determining the velocity of light to the study of ions. Ions originating in a chamber  $A$  were sent by means of an auxiliary field through a gauze to another chamber  $B$ . Here the ions traversed an accurately measured distance between gauzes in a constant field. From chamber  $B$  they again went through a third and fourth gauze to be collected in a chamber  $C$  and the current measured. Between gauzes 1 and 2 of chambers  $A$  and  $B$ , and between gauzes 3 and 4 of chambers  $B$  and  $C$ , there revolved two slotted *ebonite* discs. The slot on one disc could be displaced relative to that on the other. Hence, except during transits of the slots opposite the gauzes 1 and 2, or 3 and 4, ions could not get through from chamber  $A$  to  $B$ , or from  $B$  to  $C$ . By changing the frequency of revolution and observing the currents, it was possible to measure the time of transit of ions through chamber  $B$ . The method was used largely for rather aged ions in air. The results were affected by diffusion, by the contamination of the gas by the ebonite discs, by the turbulence of the air caused by the discs, and by the interpenetration of fields in the gauzes. As a result, despite claims to the contrary, the method is neither absolute nor particularly satisfactory. It is possible that with modifications it could be adapted to the study of very slow ions.

The following year, and apparently quite independently, Tyndall, Starr, and Powell,<sup>17</sup> and R. J. Van de Graaf<sup>22</sup> in England devised means for measuring mobilities which replaced the mechanical shutter of La Porte by the more flexible, cleaner, and effective electrical shutters. Both methods were similar in principle and at that time suffered from the effect of interpenetration of fields. The results were thus not of particular significance. Van de Graaf left the problem for other fields of work. Tyndall and Powell persisted, and over a period of



years developed the method into one of the most outstanding in mobility measurement. The results of these measurements were published under the name of Tyndall and Powell, and Powell<sup>18,19</sup> and Brata.<sup>23</sup> The method was later extended to the measurement of mobility as a function of temperature and at high fields by Mitchell and Ridler<sup>24</sup> and by Tyndall and Pearce.<sup>25</sup> In 1929, Hamshire<sup>21</sup> developed another electrical shutter employing gauzes. He, however, employed only a single shutter so that in a sense his method was more like that of Varney using the Rutherford method or like that of Fontell.<sup>26</sup> Hamshire's work was good, and he recognized the difficulties introduced by the gauzes. Despite the fact that he applied the criterion that the ratio  $V_0/V_a$  should be unity, the results obtained are not entirely clear and some interpenetration effect of fields must have taken place.

**a. The Tyndall and Powell Four-Gauze Method.** The ultimate success of the method of Tyndall and Powell merits a detailed discussion.

The principle is exceedingly simple. An arrangement of fields of which one is an alternating field admits ions of one sign to a gas space of constant and uniform field strength extending over an accurately known distance. At the other end of this distance, an alternating field synchronized with the first field admits ions to a collector from the measured gas space at regular intervals after the first impulse started the ions on their way. By varying the frequency of oscillation, i.e., time to cross the measured distance between successive pulses, or by changing this measured distance so that the ions that were caught on the successive openings of the collector are with increased distance caught on the second succeeding opening of the shutter, the mobility can be measured.

The electrode arrangement of the elaborate apparatus evolved is shown in Fig. 17 as used for positive ions.  $F$  is a filament giving electrons accelerated over a long gap by the field set up by a gauze  $I$  at a potential  $V_F$  positive to  $F$ . The electrons ionize the gas in the space between gauze  $I$  and gauze  $G_1$ , whose potential is such as to keep *electrons* from going beyond  $G_1$ . It also pulls the positive ions from the space  $IG_1$  through  $G_1$ . If it is desired,  $F$  and  $I$  may be replaced by a Kunsman catalyst filament, giving  $\text{Na}^+$ ,  $\text{K}^+$ , and  $\text{Cs}^+$  ions. In both cases the source is placed sufficiently far down the tube so that the density of the gas is not affected by the heat from the filament and the Kunsman source region can be water cooled. A pair of electrodes with a high-frequency high-voltage source could be substituted for  $F$  to give ions by a glow discharge. All these sources have been used. The gauzes  $G_1$  and  $G_2$  constitute the first shutter. They are constantly biased by a field of the order of 10 volts extending over 2 mm in such a sense as to oppose positive ions. Superposed on this field called  $X_B$  is an a-c field of appropriate and variable frequency and constant

amplitude established between  $G_1$  and  $G_2$ . This field  $X_{ACB}$  is such that during the positive swing of its alternation it is slightly larger than  $X_B$ . During the interval when  $X_{ACB} > X_B$  the positive ions enter as a burst into the measuring space  $G_2G_3$ . This space has a length  $d$  with a constant potential  $V_d$  imposed on it, so directed that positive ions move to  $G_3$ . Coupled to the same master oscillator as the a-c field on  $G_1G_2$ , is an a-c field  $X_{ACC}$  maintained between gauzes  $G_3$  and  $G_4$  which constitute the second shutter. This shutter also has a d-c field  $X_C$  identical to that in  $G_1G_2$  opposing the positive ions and is similar in every way. The coupling of the oscillators to the master oscillator for  $X_{ACB}$  and  $X_{ACC}$  was accomplished by inductive coupling in Tyndall and Powell's

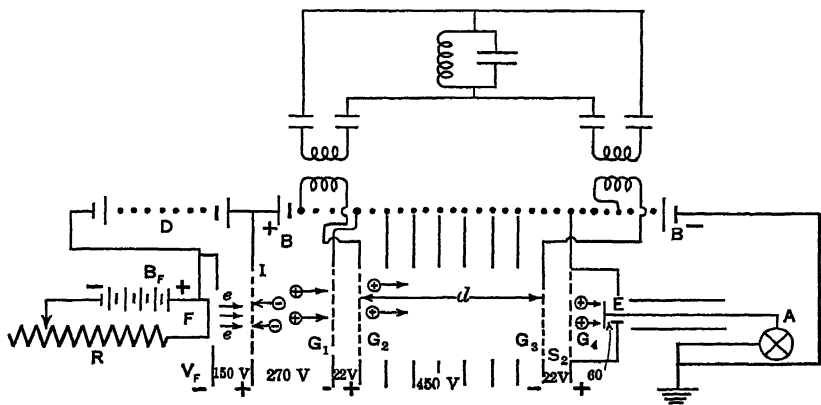


FIG. 17.—The Tyndall and Powell Four Gauze Method.

apparatus. For frequencies of several hundred cycles or more, capacity coupling has certain advantages. Back of  $G_4$  is a Faraday cage for catching the ions with a small driving potential to the electrometer plate  $E$ . The field between  $G_2$  and  $G_3$ , i.e.,  $X_d$ , is kept constant over a length of  $d$  centimeters by means of equipotential vanes connected to regular points on a high resistor.

The source assembly  $FIG_1G_2$  can, if desired, be placed on a single support and moved relative to  $G_3G_4$  by means of an electromagnet from outside. The whole assembly with connections as shown in Fig. 17 can be sealed into a chamber. With monel metal electrodes, outgassing by heating, etc., the purity of the gases can readily be controlled. The distance  $d$  can be read by cathetometer. The measurement can be made by setting the frequency  $N = 1/T$  at about the right value with properly chosen potentials and fields, and varying either  $d$  or  $T$  until a series of maxima of current are obtained representing ions that reached  $E$  during a time of transit  $T_1$  corresponding to the first opening of  $G_1G_2$  and the next opening of  $G_1G_2$  and  $G_3G_4$ , or the time  $T_2$  corresponding to the passage of two periods  $T_1$  before the ions crossed  $d$ , and

so on for  $T_3$ ,  $T_4$ . Then, as for all such a-c methods, we measure the  $\Delta d$  between any two peaks if  $d$  is varied or the  $\Delta T$  between any two peaks if  $T$  is varied and at once get  $k$  from  $k = (\Delta d)^2/(VT)$  or  $k = d^2/(V\Delta T)$ . The use of the variable  $\Delta d$  gives absolute values. The interpenetrating fields  $X_{rG_1}$ ,  $X_{G_1G_2}$ ,  $X_d$  and  $X_d$ ,  $X_{G_3G_4}$ , and  $X_E$ , while giving false values for  $k$  at a fixed  $d$ , since  $d$  can not be known (see page 12), are independent of this if  $d$  is varied and  $\Delta d$  is used, for subtracting the values of  $d_1$ ,  $d_2$ ,  $d_3$ , etc., eliminates the errors at the gauzes. Again it appears that, if the fields are kept constant and  $T$  alone is varied, the errors caused by interpenetration introduced by  $X_d$  and  $X_{G_1G_2}$  should be largely compensated for by the error introduced by  $X_d$  and  $X_{G_3G_4}$ . The field  $X_d$ , however, is still uncertain according to Tyndall and Powell. They accordingly used the work in He performed by varying  $d$  to

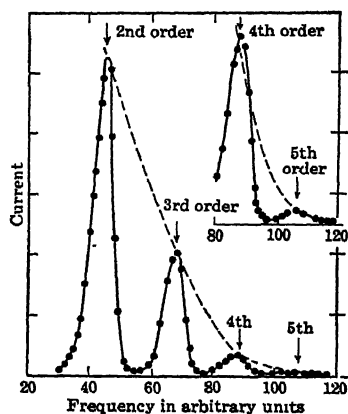


FIG. 18.

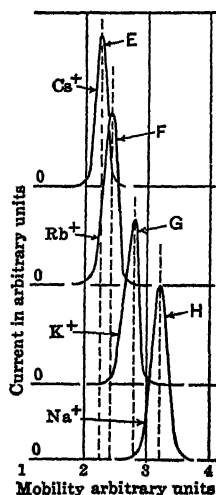


FIG. 19.

obtain a calibration of the apparatus, and the absolute values of all other ions are determined by them on the basis of He. It is not to be expected that under similar conditions the interpenetration would change the relative values of  $k$ , so that one may accept these values as essentially correct.

Some of the curves observed by Tyndall and Powell are shown in Figs. 18 and 19. Fig. 18 shows  $\text{Na}^+$  in A at about 10 mm, using a Kunsman source with  $X_{G_1G_2}$  and  $X_{G_3G_4}$  about 10 volts/cm, with  $X_{ACI}$  and  $X_{ACG}$  about 4.75 volts/cm,  $X_d$  about 100 volts/cm,  $X_E$  about 10 volts/cm. It gives five orders for the variation of current with  $T$ . The intensity decreases rapidly with the order, owing to losses by diffusion to the vanes. Fig. 20 shows the current as a function of the change in distance  $d$ . This is one of the calibrating runs in He, pressure about

40 mm, field about 32 volts/cm, frequency 24,000. Fig. 19 shows curves for the alkali ions in argon giving the approximate resolving power of the method. The resolving power depends on the frequency of the alternating current that is used, which is a disadvantage for low mobilities. The higher  $N$  the sharper the peaks and the narrower the burst of ions getting through the shutters. Of course, diffusion in long periods of transit across  $d$  reduces the resolving power. It is probable that the method has a resolving power slightly better than that obtained by Bradbury. Actually it is possible that Bradbury's method can be improved in resolving power well beyond this method for low speeds. This method, however, can be carried from ion ages of  $10^{-5}$  second on up. It has the following characteristics:

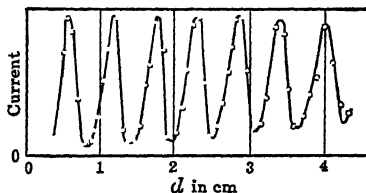


FIG. 20.

1. It is absolute and accurate to about 1 per cent or better.
2. It can be used on the purest gases and with the greatest modern refinements.
3. It can be used for ions from all sources. It has not been, but could be, used on negative ions.
4. Its range of applicability is very large as regards ion ages, going on up from  $10^{-5}$  second.
5. It has so far the record for the highest resolving power. This decreases with the slower ions which limits its usefulness.
6. However, not only is it tedious to operate but also it requires very complex gas-tight glass apparatus with a great many glass-to-metal seals. This makes the avoidance of leaks very trying. In order to set up such a device and to get it operating properly requires at least six months with ideal laboratory facilities.

**b. The Bradbury-Nielsen Shutter Method.** Bradbury and Nielsen developed a type of shutter, invented by Loeb for a different purpose, to measure the mobilities of electrons. The Loeb electron filter<sup>28</sup> consists of a grid of fine parallel wires separated by a distance of the order of 1 mm and insulated from one another. Alternate wires are connected to the opposite terminals of a high frequency oscillator giving from  $10^4$  to  $10^7$  cycles per second. A potential difference of some tens of volts applied to such a pair of wires makes them able to catch all the free electrons in their neighborhood or between them. For electrons have a velocity of  $10^4$  to  $10^6$  cm/sec per volt/cm in the range of fields and pressures usually studied. Hence, such a grid is "transparent" to electrons for a very short time only when it is passing through zero potential difference. With *weak* fields normal to such a grid the electrons are effectively caught by the grid, while the massive gaseous ions passing between the wires in the transverse field are not seriously disturbed by the high-frequency field, i.e., they make oscillations of minute amplitude as they go through the grid. Thus, the grid

with weak fields normal to it is an effective electron "trap" and was designed by Loeb as a means of filtering unattached electrons out of a mixture of ions and electrons in the study of negative-ion formation by electron attachment. The device was first tested by Lusk as a master's thesis at the University of California in 1926. It was later used by Cravath<sup>28</sup> for studies of electron attachment. It was finally successfully applied by Bradbury<sup>29</sup> to studies of electron attachment in gases, in 1933-34. Later Bradbury<sup>27</sup> conceived the idea of increasing the transverse or normal field, thus permitting the passage of electrons as a sort of burst during instants of zero high-frequency field. Since such grids can be made equipotential with any section of the gas, and since the electrons getting through are only those just within a minute layer *in the plane of the grids* at the time of zero field, there are no interpenetration effects. Thus, two such grids separated by a distance  $d$  in a uniform field perform the same function as the gauzes  $G_1G_2$  and  $G_3G_4$

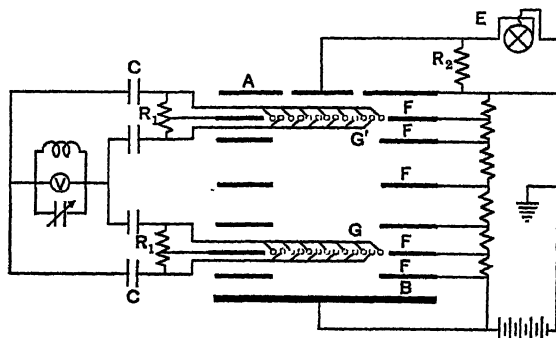


Fig. 21.—The Bradbury-Nielsen Shutter Method.

in the four-gauze method. There is no reason why the method could not be applied equally well to the study of ionic mobilities, using lower frequencies. Since the other methods proved satisfactory, however, at the time this method was developed no need existed for its application to ions. But there was a great need for a method of study of electron mobilities. These require high frequencies ( $10^4$  to  $10^6$  cycles per second) when a-c methods are used, and sinusoidal oscillations cannot be used without corrections, as  $k_e$  for electrons is a function of the field strength  $X$ .<sup>12</sup>

Fig. 21 shows the apparatus used by Bradbury for electrons. Photoelectrons from a plate  $B$  moved in a field  $X$  kept uniform by guard rings to a collector plate  $A$ ,  $d = 5.93$  mm distant, which was connected to an electrometer  $E$ . The electrical oscillator giving  $10^4$  to  $10^7$  cycles acted on the alternate grid wires of the two grid systems  $G$  and  $G'$ , through capacity-coupled systems. The mean potential of the grids was equal to that of the equipotential plane in which they lay, and the a-c

potential fluctuated by  $\pm V_G$  on either side of the potential of the plane by connecting the guard ring at that position to the center of the high resistances  $R_1$  across the condenser outputs. The wires were number 40 copper, spaced 1 mm apart on mica frames. The electrodes could be placed in all glass system capable of outgassing at  $300^\circ \text{C}$ . The frequency used in one experiment for which curves are given was  $2.205 \times 10^6$  cycles/sec. The potential between grid wires was about 40 volts. This curve shown in Fig. 22 is not particularly sharp, being a sample taken at random to show the type of peaks. Maxima were observed at 6.8 mm pressure in  $\text{H}_2$  gas at 390, 119, and 62 volts corresponding to electrons in peaks A, B, and C which crossed in  $\frac{1}{2}$ ,  $\frac{2}{3}$  and  $\frac{5}{6}$  of a cycle. The velocities were  $26.5$ ,  $13.2$ , and  $8.84 \times 10^5$  cm/sec. A study of the theory of operation of the shutters gives the agreement between theoretical and experimental curves shown in Fig. 23. It is seen that for electrons where the mobility, or drift velocity,

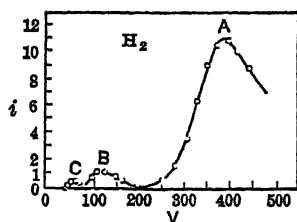


FIG. 22.

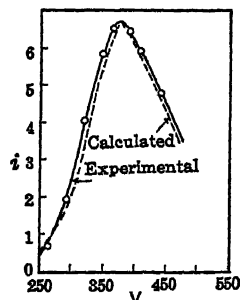


FIG. 23.

is unique the method is highly satisfactory since the peaks can be located with at least 2 per cent accuracy. For ions where more than one species may be present the resolving power may be inadequate. The mobility is computed as with the other shutter methods from  $k = 2d^2/V_0T$ , where  $T$  is the whole period and  $V_0$  is the potential at a peak.

The characteristics of this method are:

1. It is absolute and accurate for electrons and probably for ions to about 2 per cent.
2. It is applicable to all very pure gases, though the mica insulation of the grids precludes baking out above  $300^\circ \text{C}$ .
3. It has a relatively poor resolving power since the curves are not narrow, though the peaks can accurately be determined.
4. It is probably the most accurate method of electron mobility measurement.
5. It has not been applied to ions but should be applicable.
6. It can be used with any source of electrons or ions.

## 5. THE TOWNSEND MAGNETIC DEFLECTION METHOD

In 1914, Townsend<sup>30</sup> proposed a method for the study of ion mobilities at low pressures. At that time, the present high-frequency sources were not available, and experiments by Todd<sup>29</sup> indicated that low-pressure mobility measurements of ions should be of some interest. Actually, with the magnetic fields then available Townsend<sup>29</sup> found that the method was *not* applicable to ionic mobilities. However, he made his famous electron mobility measurements by this method. The method was fairly accurate, and for a long time (twenty years or more) the values yielded by this method were the only ones available for pressures below 50 mm. At higher pressure corrected Rutherford a-c measurements of Loeb<sup>12</sup> from 1922 on, and recently the measurements of Bradbury and Nielsen,<sup>27</sup> respectively supplement and supersede the Townsend method. In the urgent need for knowledge concerning ion mobilities in the pressure region extending from 5 mm to about 0.1 mm and from ratios of field strength to pressure  $X/p$  ( $X$  in volts per centimeter,  $p$  pressure in millimeters of mercury) from 3 to 100, the Townsend method has recently been applied by Hershey<sup>31</sup> to  $K^+$  ions from Kuns-

man catalysts in  $H_2$ ,  $N_2$ , He, and A. In this method it is possible to be sure of the *initial* nature of the ion since the apparatus when evacuated can be used as a mass spectrograph.

The device is extremely simple. It consists of a hot filament or photoelectric source of electrons or ions  $F$  opposite a slit  $S$ , as seen in Fig. 24. The ions then pass downward a distance  $d$  from the axially placed slit  $S$  perpendicular to the plane of the figure to three insulated plates  $C_1$ ,  $C_2$ , and  $C_3$  separated by a small fraction of a millimeter and in the plane of the plate  $B$  of zero potential. The field is kept uniform by the guard rings. The distance  $d$  is of the order of 10 cm. The plates

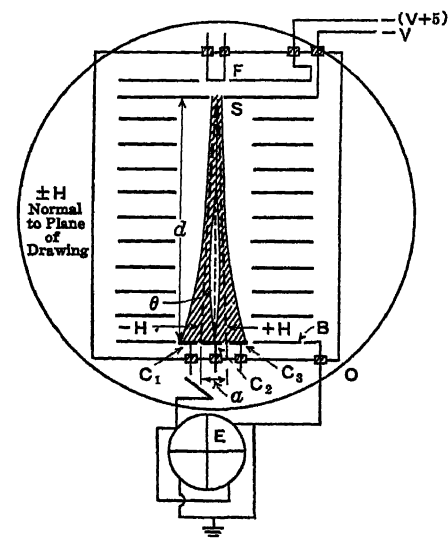


FIG. 24.—The Townsend Magnetic Deflection Method.

$C_1$ ,  $C_2$ , and  $C_3$  can in turn be connected to an electrometer  $E$  and their currents measured.  $C_1$  and  $C_3$  are 1.5 cm and  $C_2$  about 0.5 to 1 cm wide. The field  $X$  applied between the slit  $S$  and  $C_1$ ,  $C_2$ , and  $C_3$  which are essentially at ground potential drives the ions to the plates. In a gas on the way to  $C_2$ , owing to diffusion and self-repulsion, the

beam which is a narrow ribbon in vacuum spreads so that some charge is received on  $C_1$  and  $C_3$  as well as on  $C_2$ . If the apparatus is symmetrical the amounts on  $C_1$  and  $C_3$  are equal. If now a uniform magnetic field  $\pm H$  is placed perpendicular to the plane of the figure, the beam of ions or electrons has its axis shifted to the right or left of the axis of the center of the undisplaced beam through  $F$ . The deflection is *small for ions* even at 5000 gauss on account of the mass of the ions. For electrons the deflection is conveniently large. It is small compared to  $d$ , however. If, for given  $p$  and  $X$ , the field  $+H$  is varied so that the current to  $C_3$  equals the combined current to  $C_1$  and  $C_2$ , and on reversal  $-H$  is adjusted so that the current on  $C_1$  is equal to the combined current to  $C_2$  and  $C_3$ , we eliminate all lack of symmetry in the field and apparatus. We also know that the center of the beam has been displaced the width of  $C_2$  by the sum of the two fields. Then, if the distance from the center of the slit between  $C_1$  and  $C_2$  and that between  $C_2$  and  $C_3$  is  $a$ , we can write that for a field  $\bar{H} = \frac{|+H| + |-H|}{2}$  the beam was deflected  $a/2$  cm.

With the small curvatures involved, we can with little error write that  $\theta$ , the angle of deflection, is related to the fields and mobilities as follows:

$$\tan \theta = \frac{a}{2d} = \frac{f_a}{f_d} = \frac{\bar{H}ev}{Xe}$$

Here  $e$  is the ionic or electronic charge and  $v$  is the drift velocity in the field. Since for ions  $v = kX$ , and for electrons we have  $v = k_e X$ , where  $k_e$  is *not* independent of  $X$  but can be called the "electron mobility," we have  $a/(2d) = \bar{H}k$ , and  $k = a/(2d\bar{H})$ . Thus, by evaluating  $k$ , we can see directly whether it is a function of  $X$  or not, for, were  $k$  independent of  $X$ , it would be constant irrespective of  $X$ . In the case of electrons at all fields and of ions at higher  $X/p$ , we find that  $k$  is a function of  $X$ , or better  $X/p$ . The results of Hershey on ions, shown in Figs. 34 to 37, page 76, give a good idea of the applicability of the method. Its usefulness for electrons has been sufficiently demonstrated by Townsend's studies. That the method is of limited use for ions can be seen from the following considerations. It happens that, until  $X/p$  becomes high,  $k = K 760/p$ . This permits us to compute the maximum pressure which can be used for a given set of values of  $H$ ,  $k$ ,  $a$ , and  $d$ . It is given by  $p = \frac{2 \times 760 K d H}{10^8 a}$ . The factor  $10^8$

results from the conversion of  $k$  in volts per centimeter to emu. Choosing a maximum field of  $H = 5000$  gauss, over a value of  $d = 10$  cm, and  $a/2 = 0.5$  cm, we get for  $K = 2$  as found in air,  $p$  about 1.52 mm, and for  $K = 13$  as found in  $H_2$  nearly 10 mm pressure. Hence, the method is good only at very low pressures. Using one of the early cyclotron magnets with 30-cm pole faces, Hershey obtained a constant field



steady and uniform to better than 1 per cent over his apparatus. The method is limited at low pressures to values of  $X/p$  at which electrons begin to multiply by collision and discharges set in. Furthermore, when the pressure gets too low, one can no longer speak of "mobilities," for the ions make so few impacts that they do not acquire steady drift velocities.

The characteristics of this method are:

1. It is absolute and accurate to 2 per cent.
2. It can be used on the purest gases.
3. It is applicable to free electrons and to newly created positive ions only.
4. It is applicable to ions and electrons only below certain pressures, electrons below about 50 mm, ions below 10 to 0.5 mm.
5. There is no resolving power to speak of, for only an average mobility is evaluated.
6. It is very useful for pressure regions and mobilities where  $k$  varies with  $X$  and where velocities are greater than about  $5 \times 10^4$  cm/sec, in other words, where a-c methods begin to fail.

#### 6. CHATTOCK ELECTRICAL WIND METHOD

Relatively early in the investigation of ionic mobilities, Chattock<sup>32</sup> arrived at a rather novel way of measuring mobilities. This was based on the following reasoning. The field  $X$  exerts a total force  $F = AXend$  on the  $n$  ions per cubic centimeter of charge  $e$  confined in a volume of base area  $A$  and length  $d$ , parallel to the field. This force acts on each ion between its  $10^9$  collisions with molecules per second to give it momentum in the field direction. At each of the  $10^9$  impacts, some of this momentum is yielded to the neutral molecules with which the ion collided. As a result, the molecules are set into a mass motion along  $X$ . This produces the well-known phenomenon of the "electrical wind" which is so nicely demonstrated when the discharge from a needle point blows out a candle flame.

This wind exerts a mechanical pressure which can be measured. From the third law of motion, it is clear that the force exerted on the ions by the field  $F_x$  must just balance the force exerted on the molecules and hence the force of the wind  $F_w$ . Thus  $F_x = AXend = -F_w$ . But  $F_x/A = Xend = -F_w/A = -p$ , where  $p$  is the wind pressure, so that  $-p = Xend$ . Now the current  $i$  flowing in the same area is  $i = Anev = AnekX$ , where the ion velocity  $v = kX$ . Whence,

$$ne = \frac{i}{A k X}, \text{ so that } p = Xend = \frac{i X d}{A k X} = \frac{id}{A k}.$$

It is now merely a question of devising a means of measuring  $p$  and  $i$  for evaluating  $k$ . In Fig. 25,  $N$  is an insulated electrified needle point charged to some thousands of volts by a battery or generator  $B$ , producing a corona discharge within a few tenths of a centimeter from the

point and launching a mass of positive or negative ions down the glass tube  $T$ , depending on the sign of the charge put onto  $N$ . At a considerable distance down the tube there is a collector ring, or gauze,  $R$ , connected to the grounded end of the battery  $B$  through a galvanometer  $G$ . The ions are practically all picked up by the ring (a gauze can be used if desired). A sensitive manometer  $M$  is placed with openings separated  $d$  centimeters, far enough from  $N$  so as to be beyond the active breakdown zone of the needle and extending just beyond  $R$ . The pressure difference  $p$  is read on  $M$ . The distance  $d$  is the distance between

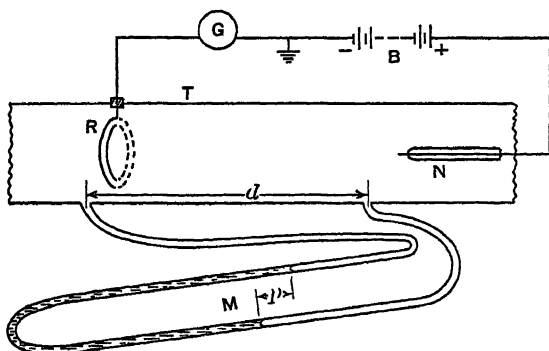


FIG. 25.—Chattock Electrical Wind Method.

the centers of the manometer orifices. It must, however, be noted that, while  $p$  is the pressure difference read, part of the force  $F$  is borne by the ring or the gauze. The force  $F$  is then not  $F = pA = id/k$ , as the simple equation implies, but the effective force  $F_1 = (id/k) - f$ , where  $f$  is the force borne by the ring. Hence the pressure difference observed is

$$P = \frac{F_1}{A} = \frac{id}{Ak} - \frac{f}{A} = \frac{id}{Ak} - p'.$$

Now  $p'$  or  $f$  is hard to estimate. Experiment showed that in moderate limits  $f$  or  $p'$  was independent of  $d$ . Hence, to eliminate  $f$  or  $p'$ , two measurements of  $p_1$ ,  $p_2$ , and  $i_1$ ,  $i_2$  should be made at  $d_1$  and  $d_2$ . Then

$$P_1 = \frac{i_1 d_1}{Ak} - \frac{f}{A}, \quad P_2 = \frac{i_2 d_2}{Ak} - \frac{f}{A}.$$

whence  $P_1 - P_2 = \frac{1}{Ak} (i_1 d_1 - i_2 d_2)$ , and, if  $i_1 = i_2$ ,

$$P_1 - P_2 = \frac{i}{Ak} (d_1 - d_2) \text{ or } k = \frac{i}{A} \frac{d_1 - d_2}{P_1 - P_2}.$$

The greatest of care on the part of Chattock and later Chattock and Tyndall<sup>32</sup> did not suffice to eliminate minor inaccuracies due to loss of

ions, etc. Hence, the method is not one of high accuracy. It has historical significance since by it Chattock and Tyndall were believed to have shown that the high fields at the point do not effectively and permanently break up the ion cluster, for they observed perfectly normal mobilities at these high fields. The argument is not conclusive today, since the high fields are now known to exist only near the points, and the ions have ample time to reform down the tube did they really initially smash up. Actually how much smashing occurs remains to be seen at a later point.

A variant of this was developed by Ratner<sup>33</sup> as a relative method. Ratner blew his wind through a gauze which collected the electrical current. The wind pressure was measured on a vane manometer on the far side of the gauze from the point. As may readily be seen, this has not much value except in relative measurement. The method in general has the following characteristics:

1. It is absolute but relatively inaccurate, good to about 5 per cent at best and probably poorer.
2. It can be performed under fairly clean conditions as regards purity if the chamber is closed off and turbulence can be avoided.
3. It requires high fields and large ion currents to produce much of a pressure. It is thus confined to needle-point or analogous discharges.
4. It has very little resolving power, if any, since it gives only an average value of the mobilities.
5. It is purely of historical and academic interest in view of the very accurate modern methods.

## 7. REFERENCES FOR PART A, CHAPTER I

1. THOMSON and RUTHERFORD, *Phil. Mag.*, **42**, 392, 1896.
2. E. RUTHERFORD, *Phil. Mag.*, **44**, 422, 1897.
3. J. ZELENY, *Phil. Trans. Roy. Soc.*, **195**, 193, 1900.
4. L. B. LOEB, *J. Franklin Inst.*, **196**, 537, 771, 1923.
5. TYNDALL and GRINDLEY, *Proc. Roy. Soc.*, **A 110**, 341, 1936.
6. N. E. BRADBURY, *Phys. Rev.*, **40**, 508, 524, 1932.
7. J. ZELENY, *Phys. Rev.*, **34**, 310, 1924; **36**, 35, 1930; **35**, 1441, 1930; **38**, 2239, 1931.
8. H. A. ERIKSON, *Phys. Rev.*, **17**, 400, 1921; **18**, 100, 1921; **19**, 275, 1922; **23**, 110, 1924; **24**, 502, 1924.
9. S. CHAPMAN, *Phys. Rev.*, **52**, 184, 1937.
10. L. B. LOEB, *Phys. Rev.*, **38**, 549, 1931.
11. R. N. VARNEY, *Phys. Rev.*, **42**, 547, 1932.
12. L. B. LOEB, *Phys. Rev.*, **23**, 163, 1924.
13. N. E. BRADBURY, *Phys. Rev.*, **40**, 980, 1932.
14. LOEB and BRADBURY, *Phys. Rev.*, **38**, 1722, 1931.
15. J. FRANCK, *Ann. Physik*, **21**, 972, 1906; FRANCK and POHL, *Verhandl. deut. physik. Ges.*, **9**, 62, 1907.
16. P. LANGEVIN, *Ann. chim. phys.*, **28**, 289, 1903.
17. TYNDALL, STARR and POWELL, *Proc. Roy. Soc.*, **A 121**, 172, 1928.
18. TYNDALL and POWELL, *Proc. Roy. Soc.*, **A 134**, 125, 1931.
19. TYNDALL and POWELL, *Proc. Roy. Soc.*, **A 136**, 145, 1932.
20. M. LA PORTE, *Ann. phys.*, **8**, 466, 1927.

21. J. L. HAMSHERE, *Proc. Camb. Phil. Soc.*, **25**, 205, 1929; *Proc. Roy. Soc.*, **A 127**, 298, 1930.
22. R. J. VAN DE GRAAF, *Phil. Mag.*, **6**, 210, 1928.
23. POWELL and BRATA, *Proc. Roy. Soc.*, **A 138**, 117, 1932.
24. MITCHELL and RIDLER, *Proc. Roy. Soc.*, **A 146**, 911, 1934.
25. TYNDALL and PEARCE, *Proc. Roy. Soc.*, **A 149**, 426, 1935; A. F. PEARCE, *Proc. Roy. Soc.*, **A 155**, 490, 1936.
26. N. FONTELL, *Soc. Sci. Fenn. Comm. Phys. Math.*, **6**, 6, 1932; **5**, No. 23, 1931; **6**, 17, 1932.
27. BRADBURY and NIELSEN, *Phys. Rev.*, **49**, 388, 1936.
28. For data on the electron filter: H. F. LUSK, master's thesis, University of California, 1926; A. M. CRAVATH, *Phys. Rev.*, **33**, 605, 1929; N. E. BRADBURY, *Phys. Rev.*, **44**, 883, 1933; L. B. LOEB, *Phys. Rev.*, **48**, 684, 1935.
29. TODD, *Phil. Mag.*, **22**, 791, 1911; **25**, 163, 1913.
30. TOWNSEND and TIZARD, *Proc. Roy. Soc.*, **A 88**, 336, 1913.
31. A. V. HERSHEY, *Phys. Rev.*, **51**, 146, 1937; **54**, 237, 1938; **56**, 1939.
32. A. P. CHATTOCK, *Phil. Mag.*, **48**, 401, 1899; **1**, 79, 1901; CHATTOCK and TYN-DALL, *Phil. Mag.*, **19**, 543, 1909.
33. S. RATNER, *Phil. Mag.*, **32**, 442, 1916.

## *PART B. THE EXPERIMENTAL DATA ON IONIC MOBILITIES \**

### **1. INTRODUCTION**

It is next necessary to present in a clear and orderly fashion the results of the hundreds of studies of ionic mobilities in the literature.<sup>34</sup> Needless to say, a complete list of the results achieved in such a large number of investigations cannot be given in this book. Furthermore, although many excellent investigations gave important results valuable in their time, later knowledge and developments render their inclusion unnecessary today. Finally, in the enormous mass of data accumulated by the most diverse techniques and under widely differing conditions, the apparently contradictory and conflicting nature of the results requires great care in selection and analysis in order that a clear picture of the effects be available to the reader. Such a critical analysis of the data in the light of the more recent knowledge does not exist today. It is the aim of this book to furnish such information. Unfortunately, here again the reader must rely on the judgment and experience of the author. In what follows, the conclusions of the author will be presented in a terse, categorical, and at times seemingly dogmatic fashion. Much of the reasoning by which the choice of data or conclusions was arrived at must needs be left out, as will be a large proportion of the references. In all cases the latest and apparently the most cogent references will be given. Where past beliefs, or the present views of a school or group of investigators, are at variance with conclusions given, this fact will be clearly stated and the reason for the discrepancy will be indicated if this can be done briefly. With this foreword, one may proceed to discuss ionic behavior.

### **2. MOBILITY AND FIELD STRENGTH**

The mobility is a constant independent of field strength  $X$  for completely formed stable ions from the smallest fields of fractions of a volt per centimeter to fields up to 16,000 volts/cm in air and 20,000 volts/cm in  $H_2$  at atmospheric pressure.<sup>35</sup> Since not field strength alone but rather the ratio of field strength  $X$  to pressure  $p$  is the essential criterion for the energy of the ions acquired between impacts in an electrical field at constant temperature (most ion studies have been made at about room temperature), it is better to describe this phe-

\* References for Part B of Chapter I will be found on page 49

nomenon in terms of  $X/p$  expressed in volts per centimeter per millimeter pressure. Thus, for positive and negative ions in air and  $H_2$ ,  $k$  is constant independent of  $X$  for ranges of  $X/p$  from less than  $10^{-3}$  to 20. Negative ions in  $O_2$  can be expected to show deviations above  $X/p = 80$ , where the ions shed their electrons, if not before.<sup>36</sup> Mitchell and Ridler,<sup>37</sup> working with  $N_2$ , and Hershey<sup>38</sup> with  $H_2$ ,  $N_2$ , He, and A, have observed  $k$  to increase for ions of the alkalis above certain values of  $X/p$ . In  $N_2$ , Mitchell and Ridler observed  $k$  to be constant for the monatomic ions  $Li^+$ ,  $Na^+$ ,  $K^+$ , and  $Rb^+$  up to  $X/p = 55, 17, 10$ , and 5 respectively. In  $H_2$  and  $N_2$  Hershey found that  $K^+$  is constant up to  $X/p \sim 10$ , while in He and A it is constant to  $X/p \sim 5$ . Above these values, the values of  $k$  increase. In Hershey's work the mobilities increase to a maximum and ultimately decrease monotonously along a hyperbola-like curve. According to Mitchell and Ridler, the beginning of the rise of  $k$  in  $N_2$  decreases linearly with the value of  $1/M$ , where  $M$  is the molecular weight. On theory,  $k$  should be constant with  $X$  as long as the energy gain per free path is not comparable with the energy of agitation. While the theory for the variation of  $k$  with electron energy has been developed when the gain per free path is comparable with the energy of agitation the theory has not been developed successfully for ions. Thus, there is no quantitative theory for the results of Mitchell and Ridler and Hershey in regions where ions gain of the order of hundredths of volts and more between impacts, although the behavior is qualitatively explicable, as will be seen.

### 3. ABSOLUTE VALUES OF MOBILITIES

Could an *absolutely pure* gas be obtained, there would be an ion of unique mobility which is constant with time extending onward from  $10^{-6}$  second after formation. Since at atmospheric pressure ions make of the order of  $10^9$  impacts per second it becomes practically impossible to obtain gases of such purity that after  $10^{-3}$  second the ions have not encountered molecules of some impurity. Since such traces of impurity are beyond the possibility of any control, it is not unexpected to find that the mobilities are observed to vary with time (or age) and to differ in the samples of gas used by different observers. It appears that in the more modern techniques ions of the same age and in gases of the same relative degree of purity as studied by different methods are found to have the same mobilities. In general, however, the diversities of the methods used with inherent instrumental errors of at least 20 per cent, together with the widely differing techniques of preparation, purification, and contamination from the measuring chamber, as well as the different ages of the ions observed, have led to the utmost confusion and diversity in the experimental values. Thus little confidence is to be placed in the various tables of ionic mobilities as given by Przibram,<sup>34</sup> by J. J. Thomson,<sup>39</sup> or by Loeb<sup>40</sup> in the *Inter-*

*national Critical Tables.* Averaging the results of various observers is of absolutely no value since the differences are *not due to chance errors but are definitely different values due to differences in method, ion age, and purity.* Thus, averaging the Kovarick and Loeb values using an absolute method with the values from the old Zeleny and Franck methods, which are on the Zeleny scale, improves nothing. Such averages merely give incorrect values.

A survey of one of the more recent tables of mobilities shows inclusion of a most varied assortment of values. Some of these values due to Loeb were never intended for more than comparison purposes in mixture work where they were used. These were included in the tables without a notation as to Loeb's specific designation as to whether the values were absolute or on the Zeleny scale.<sup>45</sup> As pointed out by Loeb,<sup>40</sup> most values in these tables (except those in his table specifically exempted) should be multiplied by 1.22 to change them from the old Zeleny scale (see page 5) to the present absolute standard in air obtained by Loeb,<sup>41</sup> Tyndall and Grindley,<sup>42</sup> Bradbury,<sup>43</sup> and Varney.<sup>44</sup> As rough average values for computations these corrected values may suffice.

Accurate absolute values for known ions in pure gases, when freshly formed, have been obtained by Tyndall and Powell,<sup>46</sup> by Hershey,<sup>38</sup> and possibly by Loeb.<sup>47</sup> Bradbury<sup>48</sup> has also obtained accurate absolute values. His values, however, have no *general* significance, for they apply to ions of *specific ages* and in gases prepared according to certain techniques. It is probable that in the more accurate results of the future the mobilities at ages  $> 10^{-4}$  second will be specified in terms of age and nature of the purification process.

From what has gone before, it must be clear that there are no reliable or significant values of ionic mobilities of general applicability. Any attempt to give such a table of values at this time would be futile and, what is worse, misleading. In general, for ions more than  $10^{-3}$  second old, even when determined by more modern methods, any value in the table when on an absolute scale is as likely to be reliable for a given gas as any other, unless the conditions in question closely parallel those in a particular measurement. For gases such as Bradbury<sup>48</sup> used, the results are significant *under the same conditions.* It is for only a few ions in carefully purified gases measured  $10^{-4}$  second or earlier after formation that any data can be given concerning specific mobilities in specific gases. Since these are the mobilities on which to test our theories, these values will be reserved for later discussion.

#### 4. PRESSURE VARIATION OF MOBILITY

According to all theories, the mobility  $k$  should vary inversely as the number of molecules of gas per unit volume, i.e.,  $k$  should be inversely proportional to gas density. Thus, one should write that

$k = K \rho_0 / \rho$ , where the *mobility constant*  $K$  is the mobility at the gas density  $\rho_0$  at  $0^\circ \text{C}$  and 760 mm pressure, and  $\rho$  is any density corresponding to  $k$ . At constant temperature  $\rho$  is proportional to the pressure  $p$ , and thus for most mobility work which is carried out at constant temperature one can write  $k = \left[ K \frac{760}{p} \right]_T$ , where  $p$  is expressed in millimeters of mercury.

This law has been observed to hold for pressures extending from about 0.1 mm up to about 60 atmospheres. Above 60 atmospheres, the results in one laboratory<sup>49</sup> show that  $k$  decreases slightly more slowly than  $p$  increases, i.e.,  $K$  appears to increase with  $p$ . Though the result could be ascribed to inaccuracies in the gauges at the higher pressures, the care with which the work was done makes it possible that the variation is real. Theory is unable to account for such an increase if real. Below 0.1 mm pressure, if  $X/p$  becomes high, the effects discussed under section 2 may occur. Again, at such pressures, unless the distances become large, the ions may not make enough collisions to reach a terminal velocity. In this case, one could hardly speak of a mobility, and the observed values of  $K$  might show a variation with  $p$ .

At pressures below 10 cm in air, and at various pressures in other gases depending on purity and gaseous character, spuriously high negative ion mobilities have sometimes been observed.<sup>50</sup> That is,  $K$  as computed from the curves *appears to increase* rapidly to electronic magnitudes below 100 mm in air. This was taken as a deviation from the pressure law just enunciated and was ascribed to the "breaking up" of the *supposed* "ion cluster."<sup>51</sup> Positive ions show no such effect. The studies of Wellisch,<sup>52</sup> Thomson,<sup>53</sup> Loeb,<sup>54</sup> Wahlin,<sup>55</sup> Bailey,<sup>56</sup> and later Bradbury<sup>57</sup> showed that the effect was of a different sort. If one measures  $k$  on negative carriers which are generated as electrons, these, at low pressures, may not have had opportunity to attach to molecules to give ions. The value of  $K$  for electrons is of the order of 10,000 times  $K$  for ions. Hence such low-pressure measurements are made on electronic carriers which are just attaching in the measuring field to give ions. The mobilities measured are those of ions which have not formed at their supposed origin. They formed between the plates at points which the electrons reach in very short intervals of time. As the distance of electron travel before attachment varies very rapidly with  $p$ , it is clear that the residual distance of ion travel will likewise vary with  $p$  and hence  $K$  will *appear* to vary with  $p$ .<sup>52, 54</sup> It has been shown by Wellisch,<sup>52</sup> Loeb,<sup>53</sup> Tyndall and Powell,<sup>58</sup> and Nielsen and Bradbury<sup>59</sup> that negative ions once formed have  $K$  independent of pressure. Hence, within the wide pressure ranges given,  $K$  is constant for any given species of ion, positive or negative, once it is formed, irrespective of  $p$ .



## 5. TEMPERATURE VARIATION OF MOBILITY

The earlier investigations on the temperature variation of  $K$ , which were all too few in number, leave much to be desired as regards reliability of method, purity of gases, and the constancy of the gaseous constitution with temperature.<sup>34</sup> The early results of Phillips<sup>60</sup> indicating a variation of  $K$  with temperature following Sutherland's equation for viscosity were not substantiated by Kovarick<sup>61</sup> and Erikson.<sup>62</sup> Later work of Schilling<sup>63</sup> purporting to prove the Sutherland law was carried out under cleaner conditions but used the Franck modification of the Rutherford a-c method. The range of temperature, 60° C, over which the Sutherland law was tested by him is entirely inadequate for testing any particular equation. Erikson's results appear to be about the best of the older studies. They covered a range from 400° K down to liquid-air temperatures.  $K$  changed relatively little except at the lowest temperatures where it decreased about 10 per cent. Recently,

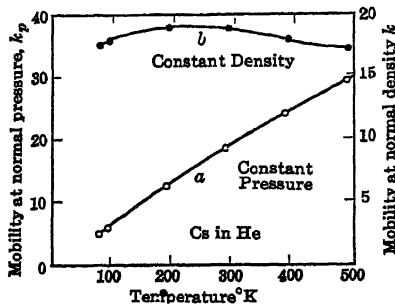


FIG. 26A.

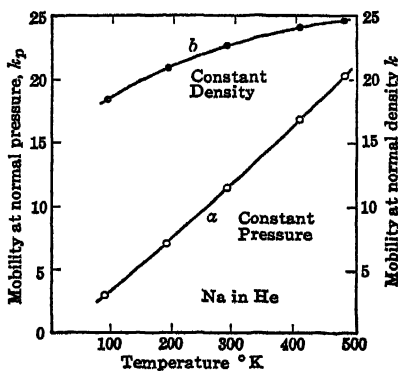


FIG. 26B.

using the four-gauze method, Tyndall and Pearce and Pearce<sup>64</sup> measured the variation of  $K$  for  $\text{N}_2^+$  in  $\text{N}_2$  gas and for  $\text{Na}^+$  and  $\text{Cs}^+$  in He. The results on  $\text{N}_2^+$  in  $\text{N}_2$  are of less interest owing to change of charge (Kallmann-Rosen effect). The results for  $K$  in He are shown in Figs. 26A and 26B. The insensitivity to change in  $T$  is noticed, and the results are in general agreement with the trend of the values observed by Erikson. The results are compared to the theory assuming the ions to be attractive and repulsive force centers interacting with the molecules. Curves  $a$  of Figs. 27A and 27B assume elastic solid impacts with dielectric attractive forces of the inverse fifth power type. Curves  $b$  assume the same attractive forces and repulsive forces of a low order of magnitude (i.e.,  $1/r^9$ ). It is seen that the experimental curves  $c$  fall between the two theoretical curves. That is, the repulsive force laws are of the order of an inverse eleventh to fourteenth power instead of

the inverse ninth postulated in *b*. This is in general agreement with the kinetic theory data on He.<sup>65</sup> These results do much to establish the nature of the laws governing ionic mobilities and, after many years of controversy, settle quite clearly the question of ionic mobility. In essence, they are of the type postulated by Sutherland, but the modern kinetic-theory methods of Chapman and Lennard-Jones now enable

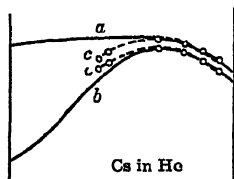


FIG. 27A.

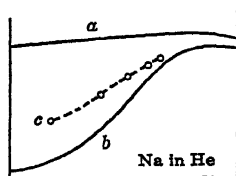


FIG. 27B.

us to go much further in evaluating the force laws than did the simple Sutherland theory.<sup>65</sup>

## 6. VARIATION OF MOBILITY WITH MASS AND DIELECTRIC CONSTANT

Early in the history of mobility measurement, Kaufmann<sup>66</sup> stated that in simple permanent gases  $K$  appeared to vary as  $1/\sqrt{M_0}$ , where  $M_0$  was the molecular weight of the gas molecules. Later, Loeb<sup>67</sup> pointed out that the law could be extended further if the dielectric constant  $D$  was included in the form  $K \propto \frac{1}{\sqrt{(D-1)}\sqrt{M_0}}$ . Theoretically, Langevin<sup>68</sup> in 1905, as a special case of a solid elastic mobility equation with an inverse fifth power law of dielectric attraction, had derived the equation for point centers of force as

$$k = \frac{A \sqrt{\frac{M+m}{m}}}{\rho/\rho_0 \sqrt{(D-1)_0 M_0}}.$$

Here  $m$  is the mass of the ion,  $A$  is a constant,  $M_0$  is the molecular weight of the gas molecules,  $M$  is the mass of the gas molecule, and  $(D-1)_0$  refers to the value of  $(D-1)$  at  $0^\circ \text{C}$  and 760 mm pressure. Loeb<sup>69</sup> independently, in 1924, arrived at practically the same equation, except for the value of the constant  $A$ , by applying an inverse fifth power attractive force expression for momentum loss of ions to molecules in a gas previously developed by J. J. Thomson.<sup>70</sup> The value of Loeb's constant  $A = 0.104$ , is less accurate than that of Langevin, which is 0.235. With the rough mobility data of 1924, the equation was found to fit distinctly better than the empirical equation of 1917.

It is, in fact, surprising that the equation should fit as well as it does, which obviously cannot be much closer than within 20 per cent of any particular value. The conditions underlying its deduction enable one to predict that the theory should hold for known alkali ions in the pure polarizable gases A, Kr, Xe. In that case, the agreement is striking, the observed constant  $A$  being 0.23, 0.24, and 0.245 respectively<sup>71</sup> while theory gave 0.235. In some cases of pure simple gases, the equation is so sensitive to ionic mass that Brata<sup>71</sup> used it in a search for the undiscovered alkali atom  $Z = 87$  by a mass determination of  $K$  in a known gas. In less pure gases where  $m$  is not known or where the kinetic-theory radius (solid elastic radius) is comparable to the effective radius produced by the dielectric polarizability, the law should fail. This it does for alkali ions in Ne and He. Further discussion of the equation must be left for the section on mobility theory. It thus is seen that under some conditions  $K$  depends primarily on  $D$  and  $M_0$ .

## 7. THE DIFFERENCE IN MOBILITY OF POSITIVE AND NEGATIVE IONS

One reason for the failure to obtain a closer agreement between the Langevin theory and experiment for aged ions in common polarizable gases at atmospheric pressure is that it is impossible to decide whether to use the positive or the negative ion to test the theory, for, in general,  $K_+$  and  $K_-$  differ. This fact was early discovered by Zeleny,<sup>3</sup> and later experiment has borne out the differences in all but the heavier organic vapors where  $K$  is low and  $K_+$  and  $K_-$  are *nearly* the same.<sup>72</sup> In general,  $K_-$  is larger than  $K_+$ , but this is not true in the gases  $\text{Cl}_2$ ,  $\text{HCl}$ , and  $\text{SO}_2$ , or in the alcohols, where  $K_+$  is greater than  $K_-$ .<sup>72</sup> Erikson<sup>8</sup> in 1921 showed that, in air which is slightly moist, the newly formed ions had  $K_+$  nearly equal to  $K_-$  while after some  $10^{-2}$  second  $K_+$  had dropped to the conventional value,  $K_-$  remaining constant. Loeb<sup>73</sup> in 1926 showed that the minutest traces of  $\text{NH}_3$  in  $\text{H}_2$  *increased*  $K_+$  from the lower value of about 8 in  $\text{H}_2$  to the higher value of 10 characteristic of the negative ion. On the other hand, traces of the amine  $\text{CH}_3\text{NH}_2$  were shown by Loeb and Dyk<sup>74</sup> in 1929 not to affect  $K_+$  or  $K_-$ , while minute traces of  $\text{CH}_3\text{CH}_2\text{CH}_2\text{NH}_2$  left  $K_-$  unchanged but *lowered*  $K_+$  to very low values. Analogous results were observed in a number of gaseous mixtures, especially for the alcohols and negative ions, by Tyndall and Phillips,<sup>75</sup> for positive ions with ethyl ether by Loeb,<sup>77</sup> and for negative ions with  $\text{HCl}$  and  $\text{Cl}_2$  by Loeb<sup>77</sup> and Mayer<sup>78</sup>. The changes are produced by quantities less than 0.01 per cent of these active impurities. The magnitudes of the changes in  $K$  are of the order of some tens of per cent except where the impurity is a very bulky organic molecule. Another cause for the difference in mobilities of positive and negative ions must be ascribed to the change of charge. Positive ions will undergo change of charge with atoms of lower ionization potential, e.g., Hg. These give  $\text{Hg}^+$

ions of low  $K$ . Hg does not usually give a negative ion. The presence of  $10^{-3}$  mm pressure of Hg in most measurements will give many  $\text{Hg}^+$  ions.<sup>107</sup>

The interpretation of these differences is obvious. The dielectric term in the mobility equations is *not charge sensitive*, and, though it accounts for the order of magnitude of the mobility, it cannot account for differences in  $K_+$  and  $K_-$ . The very specific charge sensitivity of  $K$  to certain molecules indicates that the charge causes complex-ion formation by addition of certain specific molecules present as impurities or otherwise in a gas.<sup>72</sup> Thus aged positive ions in air (more than 0.01 second old) pick up some specific but more bulky molecule than does the negative ion.<sup>74,78</sup> This picking up is aided by intense activation of the air by  $\alpha$  rays or by ultraviolet light but is hindered by the presence of moisture.<sup>78</sup> Adding a trace of  $\text{NH}_3$  replaces this bulky companion of the positive ion by the less bulky  $\text{NH}_3$  molecule.<sup>74</sup> Such complex-ion formation with  $\text{NH}_3$  molecules has been observed by Powell and Brata<sup>79</sup> in  $\text{N}_2$  through the mass determination of the ion from its mobility. The  $\text{CH}_3\text{NH}_2$  molecule also adds to positive ions in air, replacing some other molecules, but its complex ion is now as bulky as the previous companion of the ion, so that  $K_+$  is not changed. When the large  $\text{CH}_3\text{CH}_2\text{CH}_2\text{NH}_2$  molecule adds to positive ions it lowers  $K_+$  materially.<sup>74</sup> The negative ion is not affected. On the other hand,  $\text{H}_2\text{O}$  and especially alcohols are readily picked up by the negative ions.<sup>75</sup> Evidence is at hand that  $\text{HCN}$  and ethyl ether are also picked up by the positive ions.<sup>72</sup> The nature of the ion complexes for positive ions has been observed by Luhr<sup>80</sup> for newly formed ions ( $10^{-5}$  second old), using the mass spectrograph on ions in a molecular beam.

The sign preferences for molecules in gases are not materially different from those long known for ions of the same sign in solutions. Thus, the union of positive ions to form complex ammonium and cyanide ions hardly needs to be recalled. We can thus confidently assert that the deviations of the mobilities in gases from the values predicted by the Langevin and later theories of force centers, *and* the differences between positive and negative ions, are due to the formation of definite stoichiometrical complex ions of a specific sign-dependent kind.<sup>72</sup> It must also not be forgotten that, in purer gases, some atoms and molecules do not form negative ions, and change of charge may alter the initial positive carrier. Hence, it is not strange owing to mass factor alone that  $k_+$  and  $k_-$  in the same gas may differ aside from complex-ion formation.<sup>107</sup> The complex ions are analogous to the complex solution ions containing at most a few molecules. They are in no sense to be confused with the indefinite cluster ions in the past frequently invoked in ion theory.

## 8. AGING EFFECTS WITH IONS

The specific charge affinity of certain molecular species at once leads one to expect another phenomenon first discovered in 1921 by Erikson<sup>8</sup> in air, that is, the change of ionic mobility with time. An ion at 760 mm pressure makes some  $10^9$  impacts per second with gas molecules. If then an impurity present to 1 part in  $10^6$  for which the ion has an affinity is encountered, the ion forms an attachment product. It then changes its mobility at least by the change in  $m$  if not by its increase in solid elastic radius. Similar changes of mobility in very short time intervals can also be produced by charge transfer where  $E_i$  of one constituent of the gas is lower than  $E_a$  for the ionized atom or molecule.<sup>107</sup> Since the work of Erikson in air, similar effects have been observed by Tyndall and Grindley,<sup>81</sup> by Bradbury<sup>6</sup> in several gases, by Loeb<sup>10</sup> and by Tyndall<sup>18,19,123</sup> and Powell<sup>79</sup> in other gases. Analogous effects of a more complex sort have also been observed by Zeleny,<sup>7</sup> Hamshire,<sup>21</sup> Bradbury,<sup>6</sup> Fontell,<sup>28</sup> Varney,<sup>11</sup> and Luhr<sup>80</sup> on ions of greater ages in air. Here the single sharp mobility at  $10^{-2}$  second age went to a "mobility spectrum" in the form of a broadened peak or band with a range of values of about 10 per cent on either side of the peak. In the case of  $\text{Na}^+$  in  $\text{H}_2$ , Loeb<sup>10</sup> observed two distinct changes from a value of  $K = 17$  to  $K = 13$  and from  $K = 13$  to  $K = 8.6$ , which is the normal mobility.

Practically all the workers are unanimous in observing the change of mobility to take place in a single step.<sup>123</sup> *At a given age either one form of ion or the other is present.* As the age of the ion reaches the value where attachment is probable, the *changed mobility appears at once as a separate peak* (if the resolving power of the method is good). This peak is small in size compared to that caused by the mobility existing at the earlier age. As age increases, the original group declines in size and the new group increases until a time is reached at which the original peak has disappeared and the altered ion group is the only one noted. *There is no evidence so far of intermediate steps in the formation of the new ion.*<sup>123</sup> All the transformations observed so far in pure gases in times of the order of  $10^{-2}$  second or less are due to the addition of a *single molecule of some active impurity*. The absence of intermediate ions, and the simultaneous existence of only two ions in different relative amounts over a relatively short time interval, indicate the process to be a single step addition of a molecule. With the aging times observed, the chance of two molecules being added in one step is remote. The nature of the products formed is indicated by the compounds mentioned in the last section. In the case of  $\text{Na}^+$  in  $\text{H}_2$ , it is suspected that the first molecule attached was an  $\text{H}_2\text{O}$  molecule. This was probably later replaced by one of several organic molecules coming from stopcock grease vapors or whatnot. The extent of the purity needed for ions  $10^{-3}$  second old or older transcends the usual chemical

techniques. Thus, Bradbury<sup>6</sup> generated  $O_2$  by heating  $KClO_3$  and found his mobilities affected presumably by oxides of Cl, or by Cl. Yet this is essentially the method followed in preparing  $O_2$  for atomic-weight determinations.  $O_2$  prepared by heating  $KMnO_4$  as well as tank  $O_2$  showed none of these mobilities.

As stated, no more than two mobilities and usually only one mobility appear for ions in a *pure gas at any one age* below  $10^{-2}$  second.<sup>83</sup> It appears likely that many of the molecular species which attach to ions do so in their first kinetic impact. One might thus expect that ions that are more than  $10^{-1}$  second old and have experienced  $10^8$  impacts with molecules would have had a good chance to pick up one of several different possible companions present in the order of 1 part in  $10^8$ . This would obviously be true in heterogeneous gases, such as air, especially if the air is subjected to the action of ionizing radiations for some time. Hence, aside from the broadening of mobility peaks due to diffusion in longer time intervals, it should not be surprising to find that Bradbury's<sup>6</sup> curves in air become broad at the top owing to the presence of ions of several mobilities not widely different in different proportions after 0.5 second of age. This is seen in the curves of Fig. 28, due to Bradbury. The existence of such a "mobility spectrum" in air has been observed by Luhr,<sup>80</sup> using conditions which resemble the gas

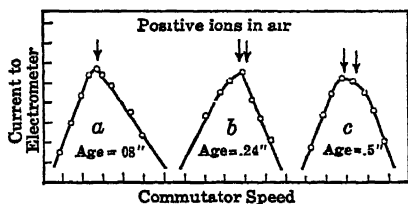


FIG. 28.

conditions in a metal mobility chamber, and a mass spectrograph, on fairly young positive ions. He found quite an assortment of ions ranging from the mass 14 for  $N^+$  up to 200 for  $Hg^+$ .  $Hg^+$  ions were also observed by Mitchell and Ridler.<sup>107</sup> In the oldest gas, Luhr found  $N^+$ ,  $O^+$ ,  $N_2^+$ ,  $O_2^+$ , and ions of mass 42, 48, 56, 60, 64, 76, 82, 96, 108, 160. These are doubtless ions due to oxides of nitrogen, nitric acid, and perhaps some organic vapors, etc. That such aging occurs is shown nicely by measurements of the coefficient of recombination.<sup>83</sup> The coefficient depends primarily on the thermal velocity and hence mass of the ion. The faster ions in air recombine rapidly, leaving only the slower ions. As time and ion age increase, the residual ions after 1 second are only those of greater mass and smaller  $K$ . Thus, while the band of mobilities of positive ions, not recombining, in air at 1 second age covers roughly an average 10 per cent change in mobility, the recombination coefficient where faster ions are removed is in 1 second reduced to  $\frac{1}{3}$  its value at 0.02 second of age. In pure  $O_2$ , in an out-gassed chamber, where as Luhr shows aging does not alter the mobilities, Gardner finds the coefficient of recombination constant.

As detailed above, the recent clean-cut and cogent data give a con-

sistent picture of the aging and mobility spectrum phenomena. The isolated claims to the *more universal* existence of such spectra in gases and the more extensive ranges <sup>7,20,21,26</sup> of values reported by investigators working largely with impure gases and air at ages of the order of 0.1 second or more are *not* warranted.<sup>6,11,14</sup> In some cases the appearance of such spectra of mobility can be laid directly to neglect of instrumental factors such as the cosine law in the Erikson tube, the neglect of turbulence, or *failure to correct for diffusion*, which in 1 second cannot be neglected. These matters have been discussed by Loeb and Bradbury<sup>88</sup> in detail. In these discussions, mobility spectra due to chemical action, spray electrification, etc., have not been considered. These form an entirely different problem.

### 9. MOBILITIES IN GASEOUS MIXTURES

Mobilities of ions in gaseous mixtures were first studied by Blanc<sup>84</sup> in 1908. Blanc worked in mixtures of gases such as H<sub>2</sub> and air, air and CO<sub>2</sub>, and H<sub>2</sub> and CO<sub>2</sub>. In these gases the ions were of ages where they had reached stability, and the impurities effecting attachment were common to all gases, presumably the same contaminants, e.g., water vapor, stopcock grease vapor, Hg, etc.<sup>107</sup> As a result, his investigations substantiated a simple law which follows from the concept of mobility.

If we have a mass of gas of base area  $A$  with  $n$  ions per cm<sup>3</sup> of charge  $e$  and mobility  $k$  in it, the current  $i$  is given by  $i = Anev = AnekX = AnekV/d$ , where  $V$  is the potential difference over a length of gas column  $d$ . The gap has an effective resistance  $R = V/i = (d/A)(1/nek)$ . Thus, the specific resistance of the gas  $R_s$  as given by  $R = R_s(d/A)$ , is  $R_s = 1/(nek)$  and  $nek = \sigma$ , the specific conductivity of the gas. It is thus seen that  $R_s$  is proportional to  $1/k$  for constant ion density. One may now consider a unit volume of gas  $a$  at 760 mm pressure with  $n$  ions of mobility constant  $K_a$ . It will have a specific resistance  $R_a = 1/(neK_a)$ . Another gas in unit volume has a mobility constant  $K_b$  and a resistance  $R_b = 1/(neK_b)$ . At a pressure  $p_a$  of gas  $a$  the value of  $R_a$  is

$$R_a = \frac{1}{neK_a \frac{760}{p_a}} = A \frac{p_a}{K_a},$$

and likewise at a pressure  $p_b$  of the gas  $b$ ,

$$R_b = \frac{Ap_b}{K_b}, \text{ with } A = \frac{1}{760ne}.$$

In a mixture of gases  $a$  and  $b$  of partial pressures  $p_a$  and  $p_b$  the total specific electrical resistance  $R_{ab}$  is given by

$$R_{ab} = R_a + R_b = A \left( \frac{p_b}{K_b} + \frac{p_a}{K_a} \right).$$

If we call  $p_b/760 = f_b$  and  $p_a/760 = 1 - f_b$ , where  $f_b$  is the mole fraction of gas  $b$ , then

$$R_{ab} = A' \left( \frac{f_b}{K_b} + \frac{(1 - f_b)}{K_a} \right),$$

the mixture being at 760 mm, with  $A' = 1/ne$ . Hence

$$R_{ab} = A' \frac{f_b K_a + (1 - f_b) K_b}{K_a K_b},$$

so that

$$K_{ab} = \frac{A'}{R_{ab}} = \frac{K_a K_b}{f_b K_a + (1 - f_b) K_b}.$$

It is at once seen that, while  $R_{ab} = f_b R_b + (1 - f_b) R_a$  is a linear function of  $f_b$ , to wit,  $R_{ab} = (R_b - R_a) f_b + R_a$ ,  $K_{ab}$  is a hyperbolic function of  $f_b$ . Blanc's<sup>84</sup> experiments bore out the law very nicely. In 1909, Przibram<sup>85</sup> and later Bělár also did some work. The effects studied by Przibram concerned themselves with only values of constituent  $b$ . It was the need of more extensive data over the whole range that prompted Loeb to undertake his intensive studies in 1924.

If the addition of gas  $b$  to gas  $a$  changes the nature of the ion in gas  $a$  either by forming a  $b$  complex with the positive or negative ion which replaces the normal ion in  $a$ , or by introducing some impurity characteristic of its preparation which is not in  $a$ , the law might be expected to be modified. Loeb was the first to study the complete behavior in gases of vastly different kinds, i.e., in mixtures of  $\text{NH}_3$  and air,  $\text{NH}_3$  and  $\text{H}_2$ , and  $\text{HCl}$  and  $\text{H}_2$ .<sup>72</sup> This was at once followed by other studies on mixtures of this sort, notably by Tyndall and Phillips<sup>75</sup> and Mayer.<sup>76</sup> It was as a result of these studies that the alteration of the ionic mobility by complex-ion formation was observed. In general, it was found that the smallest traces, 0.1 to 0.01 per cent or less, of the active substance  $b$  in the gas  $a$  sufficed to cause abrupt changes in the value of  $K$ . From the *changed* value  $R'_a$  of  $R_a$  on to the resistance of the pure gas  $R_b$ , the value of  $R'_{ab}$  changed in a linear fashion with  $f_b$ , irrespective of the attachment, with the exception of certain effects produced by gases of *high dielectric constants*, to be discussed. In other words, all that the gas  $b$  did was, in minute traces, to alter all the ions in the gas  $a$  to values  $R'_a$  or  $K'_a$ , that is, new values of  $R_a$  or  $K_a$ , and thereafter to alter  $R_{ab}$  in conformity to Blanc's law. It is possible that, where gas  $b$  has present some impurity in small amounts that can alter  $K_a$ , *methods of low resolving power* will show departures from the Blanc law in the regions of small concentrations of  $b$  while the ions are in part of mobility  $K_a$  and in part of mobility  $K'_a$ . A *method of high resolving power*, however, would not indicate any departures from linearity of  $R'_{ab}$ , for  $R'_a$  would be distinct and could be followed. The Franck modification of the a-c method used by Loeb for convenience in these studies has little resolving power and should not be used in future for this work.



It was early found by Loeb<sup>86</sup> that when a gas  $b$  with a high dielectric constant  $D$  was mixed with a gas like  $H_2$  or air, aside from the initial change due to changes in the ion  $a$ , and for ions which were not changed (e.g., the negative ion in  $NH_3$ ), the curves of  $R_{ab}$  as a function of  $f_b$  were bowed upwards concave to the axis of abscissas instead of being a straight line as Blanc's law demands. This effect is such as would be expected if  $R_{ab}$  was increased more rapidly by small concentrations  $f_b$  of gas  $b$  than in direct proportion. P. Debye<sup>87</sup> pointed out at the time that the effect was what one would expect if, owing to dielectric forces, the molecules  $b$  were much more strongly attracted to the ion than were molecules  $a$ . This happens to be true in gases of differing  $D$ , for the force  $F$  between ions and molecules has the form  $F = (D - 1)e^2/2\pi Nr^5$ , where  $D$  is the dielectric constant of the molecules,  $N$  the number of molecules per cubic centimeter, and  $r$  the distance between ion and molecule. Since, for example,  $D - 1$  for  $H_2$  is 0.00026 and  $D - 1$  for  $NH_3$  gas is 0.0072, it is seen that  $F$  for  $NH_3$  is 27 times as strong as for  $H_2$ . Accordingly, the concentration of the  $b$  molecules about the ion will be greater than that expected for a uniform distribution of  $b$  molecules in the gas  $a$ . Hence the ion will move in a region of space with a relatively greater number of  $b$  molecules than called for by  $f_b$ . The effect of this will be to *increase the resistance*  $R_{ab}$  above that due to  $f_b$ , which is normally proportional to  $f_b$ . Condon has shown that, as a result of the Boltzmann equation for the potential energy of a particle in a field of force in a gas, the relative

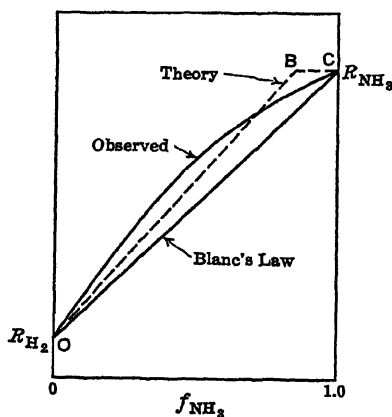


FIG. 29.

increase in concentration of molecules  $b$  at any distance  $r$  from the ion over the concentration due to  $f_b$  will be

$$f_{br} = f_b e^{\frac{(Da - Db)e^2}{8\pi Nr^4 kT}}.$$

The net effect of the increase in concentration at all values of  $r$  requires an averaging process. Its result is that we must replace  $f_b$  by  $f_{br}$ . This produces an increase in slope of the line  $R_{ab}$  for a region from  $f_b = 0$  to  $f_{br} = (f_{br}/f_b)f_b = 1$ , which will now occur at value of  $f_b = f_b/f_{br}$ , and not at  $f_b = 1$ . From then on to  $f_b = 1$  the value of  $R_{ab}$  should be

constant. Actually the effect is not quite so simply expressed, and the theoretical curve of Fig. 29 which is the broken line  $O - B - C$  is replaced by the smooth curve shown. Hence, owing to wide diversity in the attractive forces of ions for different molecular species of differing dielectric constants, the concentrations of molecules  $b$  acting on

$R_{ab}$  may be greater than anticipated. The ion then moves in a sort of a cloud of greater density of molecules  $b$  than exist in free space. The effect is usually small. Such an increased density of molecules constitutes a sort of *statistical cluster*. It is *not* to be confused with the *old cluster ion* at one time postulated where an ion is composed of an aggregate of the *same ten to thirty permanent molecules* as it moves through the gas. The statistical cluster is made of molecules of  $b$  that are never closely linked to the ion, but are slightly thicker about the ion than they would be were the ion absent.

# 10. LANGEVIN AND INTERMEDIATE LARGE IONS

So far the discussion has been entirely focused on the so-called *normal* gaseous ions, also called the small ions. Larger charged aggregates have long been known. Thus, in free air, carriers of both signs of two more or less distinct classes have been observed. The slowest class are the ions discovered by Langevin<sup>88,89</sup> in air having a mobility of 0.0005 cm/sec per volt/cm. They are now called Langevin ions. In addition, there exist quite a number of ions of both signs of mobility 0.07 cm/sec per volt/cm.<sup>89</sup> These are called intermediate ions as they are intermediate in size between normal ions and the Langevin ions. Little is known about these ions, and little work has been done on them. Pollock<sup>89</sup> believed he had shown that *no large ions exist in carefully filtered air*; this is probably correct. He further believed that he had found a difference in the intermediate and Langevin ions based on their mobility as affected by the aqueous content of the air. According to him,  $K_L$  for the Langevin ions decreases nearly linearly with the *relative humidity* of the atmosphere, while  $K_I$ , the mobility constant of the intermediate ions, depends on the *vapor pressure* of the water vapor. He found further that the small ions varied in inverse number with the classes of large ions. He concluded that large ions were due to *solid* particles and on thermodynamic grounds that the Langevin ion represented a liquid sheath about a solid nucleus and the intermediate ion a gaseous envelope about a solid nucleus. He found *no evidence that these ions grew by accretion of water molecules about a normal ion, as was currently supposed*. Later work reported by Wait of the Department of Terrestrial Magnetism indicated that the Langevin ions do not change their mobility with relative humidity.<sup>91</sup> Careful studies of numerous investigators<sup>90</sup> have also *ruled out solid dust particles as the basis of these ions*. These investigators have *confirmed* the observations of Pollock that the small ions disappear to give large ions,<sup>92</sup> that small ions disappear to give intermediate ions<sup>108</sup> and that these in turn disappear to give Langevin ions. Torreson, as well as others, has shown that the large ions are definitely related to the *neutral nuclei* of cloudy condensation in the atmosphere.<sup>93</sup> These are produced by any sort of chemical action, e.g., combustion. In the Berkeley labora-

tory neutral nuclei have also been produced by a cloudy condensation and a subsequent evaporation of the clouds as well as by spraying of water. These nuclei can be detected by the Aitken counter, and their relation to the number of large and intermediate ions can be determined. From the evidence it seems quite clear that the Langevin and probably the intermediate ions are produced by nuclei of condensation which pick up charges by capturing the normal ions in the atmosphere. It is also probable that large solid dust particles can pick up charges, especially in turbulent air as in dust storms.<sup>132</sup> Normally these *do not figure in the large ion content of the air*. As to the nature of the nuclei giving rise to these ions, little is known. Recent work in the author's laboratory<sup>94</sup> seems to give some indication. In the C. T. R. Wilson cloud chamber condensation studies, one is forced to conclude that with most liquids there are two kinds of embryonic molecular groupings that lead to visible drop formation on supersaturation. The ones whose nature offers the least trouble are the condensation nuclei that have once formed drops and that re-evaporate to an invisible stable form. They are liquid and are large enough to have a well-developed surface-tension layer. They correspond to the minimum in J. J. Thomson's<sup>95</sup> radius-vapor-tension curve. These can pick up charges by capturing normal ions. Their mobility when charged assigns to them a radius of about  $3 \times 10^{-6}$  cm, with number of molecules of the order of  $3 \times 10^6$ . The other class of water particles are possibly pseudo-crystalline with no surface in the liquid sense and are in general very small. With moderate supersaturation they cannot condense vapor unless charged. In some cases the orientation of the molecules in these charged droplets and their dipole moments in the vapor lead to sign preference in condensation which is unrelated to the sign preference in complex-ion formation.<sup>94</sup> Studies of spray electrification and electrification of water by bubbling indicate the transitory existence (of the order of a second) even in ordinary air of a number of different carriers.<sup>96</sup> In pure water are observed normal *negative* ions due to evaporated droplets with one excess electron of mobility about 2. There are also positive and negative ions, whose mobilities may differ slightly, of value about 0.8, and positive and negative ions of mobility about 0.3, as well as at least two groups of less importance. If salts or sugar are added to the water, the faster groups disappear and give place to ions of mobility of the order of 0.125 to 0.06, and somewhat less, which appear fairly stable. These ions increase in number with the vapor pressure of the water vapor present. They appear to be closely analogous to the intermediate ions in air.

Whether spraying leads to the formation of intermediate ions as observed in free air is doubtful,<sup>108</sup> but they can be generated in this fashion. The intermediate ions produced by spraying occur at concentrations where the droplets of mobility 0.063 which have a radius of the order of  $3.3 \times 10^{-7}$  cm with about 4000 molecules of water can

acquire one molecule of salt or sugar. The work on bubbling, therefore, definitely indicates a number of structure-sensitive aggregations beyond the normal positive and negative gaseous ion found in air. These appear to be small aggregates containing an  $\text{OH}^-$  group or an  $\text{H}^+$  ( $K \sim 0.8$ ) or containing ions of the salt such as  $\text{Na}^+$  or  $\text{Cl}^-$  or sugar ( $K \sim 0.3$ ), etc. How stable they are is not at present known. With growing concentrations of salt or sugar and increasing humidity and age, the many smaller and faster ions disappear and only ions of the mobility of the intermediate ions in air persist. It is suspected that the smaller ions at  $K = 0.3, 0.5$ , etc., represent the hydrated ion groups about the  $\text{OH}^-$ ,  $\text{H}^+$ ,  $\text{Na}^+$ ,  $\text{Cl}^-$ , etc., if such exist in the solutions. It is probable that eventually these disappear in favor of the larger ions by capture. In agreement with Wait the writer believes that they cannot *grow* to Langevin ions except by drastic supersaturation. Large uncharged nuclei can capture such ions and yield Langevin ions.

One may then conclude that the large ions of the atmosphere, aside from the ultra large ions such as solid dust particles, consist of the following: (1) stable nuclei of condensation such as the invisible liquid droplets which are found after condensation and re-evaporation of a cloud, charged or uncharged, or which are produced by spraying, *without necessary impurities*, of the order of  $10^6$  to  $10^7$  molecules—the Langevin ions; (2) intermediate ions probably of the order of 4000 molecules which are probably not stable unless charged and contain some one molecule of dissolved substance whose size varies, within limits, with the vapor pressure of the liquid. These ions usually acquire charges by picking up normal air ions or in the process of generation as in the spraying or bubbling of liquids. The Langevin ions require supersaturation, condensation, and re-evaporation for the formation of nuclei. They must then acquire charges. The intermediate ions must form by charge acquisition by a growing pseudo-crystalline drop at a condition of supersaturation of the gas. The intermediate ions recombine rapidly, according to Wait. *There is at present no evidence for the progressive growth of a normal ion in free air by gradual successive condensation through a continuous train of different sizes to nuclei or visible droplets.* This is in conformity with cloud-chamber studies as well as ion mobilities. With adequate sudden supersaturation such an ion will *rapidly* increase to a visible size or to the size of a Langevin ion. The time taken for this process is of the order of  $10^{-2}$  second.

## 11. GROUPS OF IONS

At times claims have been made for the discovery of the simultaneous existence of groups of normal ions,<sup>97</sup> and of ion groups produced in spraying, chemical action, etc. Many of these claims came before the advent and use of mobility-measuring methods of high resolving

power. They were made on the basis of "breaks" in curves, probably in many cases ascribable to instrumental difficulties. Where methods of high resolving power have been used, so far no more than two and usually only one mobility was present at a given age of ion.<sup>98</sup> With spray electrification at larger ages in saturated air, no *groups* have been observed, despite claims to the contrary.<sup>98</sup> In dry air (50 per cent humidity at 22° C) with high resolving power and in short time intervals very definite groups whose nature has been discussed<sup>96</sup> do appear, on spraying and especially on bubbling water. They are, however, only transitory.

## 12. DIFFICULTY IN THE STUDY OF KNOWN IONS

Early workers attempted to study the effect of the initial nature of the ionized molecule on the mobility. Several such studies were made on radioactive ions and on ordinary ions.<sup>99</sup> usually the results of these studies were completely negative. The reason for this was not clear until after the Kallmann-Rosen effect was discovered in 1929.<sup>137</sup> In the time consumed in these measurements, the ions can change their character many times by change of charge. Again, complex-ion formation by addition of active molecules at these ages is practically certain in the work cited. Thus, one never measures a mobility under ordinary conditions on an unmodified ion. It was Loeb<sup>100</sup> who in 1930 pointed out that it is only when the alkali atom ions in *pure* gases are studied in intervals of less than  $10^{-4}$  second after formation that we can be sure of the nature of the ion. Subsequent studies have borne this out, as seen by the work of Tyndall and Powell and Powell and Brata.<sup>94</sup>

An exception could be made as regards *change of charge where radioactive ions radioactively detected have been used*. Here, however, changes in ionic radius due to complex-ion formation cannot be ruled out. Furthermore, the measurement of mobilities of such radioactive ions in the ways possible in the earlier days left much to be desired as regards precision. It is now known that mass and sometimes radius and mass determine the mobility of the ion.

## 13. EFFECT OF IONIC CHARGE ON THE MOBILITY

At various times, the question as to the value of the ionic charge  $e$  and its influence on mobilities has been raised.<sup>101</sup> In fact, it has been claimed that certain high mobilities observed may be explained by assuming *multiple* charges on ions.<sup>101, 104, 105</sup> In one case, such a claim has been shown to be due to unexpected sources of error in technique.<sup>102</sup> It is probable from theory that the size of the charge exerts little effect on the mobility of the normal ion obeying the Langevin equation of page 63, as will be shown later. If the solid elastic radius becomes

large compared to the apparent radius produced by polarization forces, then  $K$  will depend largely on  $e$ . Hence,  $K$  depends slightly on  $e$  in He and Ne for alkali ions, while in A, Kr, and Xe it does not depend on  $e$  at all. In the large ions and in oil drops  $K$  is proportional to  $e$ . With the conditions existing under ordinary circumstances, owing to the Kallmann-Rosen effect,<sup>137</sup> multiple charged ions will not persist for any length of time in a gas.<sup>104</sup> Thus, Millikan<sup>108</sup> was able by the oil-drop method to detect double charged ions in He produced by  $\alpha$  particles in times of  $10^{-3}$  second after formation.<sup>104</sup> The later work of Townsend which tests this directly on ordinary ions is in agreement with the statement in showing only singly charged positive ions after  $10^{-2}$  second, as will be seen on page 169. Hence, it is only under unusual circumstances that we can expect to find multiple charged ions in gases.<sup>104, 105</sup> Where they do appear, the effect of the multiple charge will probably not seriously alter  $K$ , as later theory will show. This appears further borne out by the results of Brata<sup>106</sup> on ions, of Ga, In and Tl as emitted from a hot filament. These ions might be doubly charged. In  $N_2$  Brata's ions were definitely singly charged, whereas in He there were indications that they were possibly multiple charged with a resultant slight increase in  $K$ .

#### 14. REFERENCES FOR PART B, CHAPTER I

34. K. PRZIBRAM, "Ions in Gases," GEIGER and SCHEEL, *Handbuch der Physik*, Vol. 22 Part I, Chap. 4, pp. 343-423, Julius Springer, 1933.
35. L. B. LOEB, *Phys. Rev.*, **8**, 633, 1916; K. L. YEN, *Phys. Rev.*, **11**, 337, 1918; *Proc. Natl. Acad. Sci.*, **4**, 91, 1918.
36. L. B. LOEB, *Phys. Rev.*, **48**, 684, 1935.
37. MITCHELL and RIDLER, *Proc. Roy. Soc.*, A **146**, 911, 1934.
38. A. V. HERSEY, *Phys. Rev.*, **56**, 1939.
39. J. J. THOMSON, *Conduction of Electricity through Gases*, 3d Edition, Cambridge Press, 1931, Vol. 1.
40. L. B. LOEB, *International Critical Tables*, Vol. VI, pp. 111, 112, McGraw-Hill, New York, 1929.
41. L. B. LOEB, *J. Franklin Inst.*, **196**, 4, 537, 1923.
42. TYNDALL and GRINDLEY, *Proc. Roy. Soc.*, A **110**, 341, 1926.
43. N. E. BRADBURY, *Phys. Rev.*, **37**, 1311, 1931.
44. R. N. VARNEY, *Phys. Rev.*, **42**, 547, 1932.
45. LOEB and ASHELEY, *Proc. Natl. Acad. Sci.*, **10**, 351, 1924; LOEB and DU SAULT, *Proc. Natl. Acad. Sci.*, **14**, 384, 1928.
46. TYNDALL and POWELL, *Proc. Roy. Soc.*, A **134**, 125, 1930; A **136**, 145, 1932.
47. L. B. LOEB, *Phys. Rev.*, **38**, 549, 1931.
48. N. E. BRADBURY, *Phys. Rev.*, **40**, 508, 1932; **37**, 1311, 1931; **40**, 524, 1932.
49. A. J. DEMPSTER, *Phys. Rev.*, **34**, 53, 1912; MCLENNAN and KEYES, *Phil. Mag.*, **30**, 484, 1915.
50. A. F. KOVARICK, *Phys. Rev.*, **30**, 415, 1910.
51. J. S. TOWNSEND, *Electricity in Gases*, Oxford, 1914, Chap IV, Secs. 102 and 103.
52. E. M. WELLISCH, *Am. J. Sci.*, **39**, 583, 1915; **44**, 1, 1917; *Phil. Mag.*, **31**, 186, 1916; **34**, 33, 1917.
53. J. J. THOMSON, *Phil. Mag.*, **30**, 321, 1915.
54. L. B. LOEB, *Phys. Rev.*, **17**, 89, 1921; *Phil. Mag.*, **43**, 230, 1922.

55. H. B. WAHLIN, *Phys. Rev.*, **23**, 169, 1924.
56. V. A. BAILEY, *Phil. Mag.*, **50**, 843, 1925.
57. N. E. BRADBURY, *Phys. Rev.*, **44**, 883, 1933; *J. Chem. Phys.* **2**, 827, 835, 840, 1934.
58. TYNDALL and POWELL, *Proc. Roy. Soc.*, A **129**, 173, 1930.
59. NIELSEN and BRADBURY, *Phys. Rev.*, **51**, 69, 1937.
60. P. PHILLIPS, *Proc. Roy. Soc.*, A **78**, 167, 1906.
61. A. F. KOVARICK, *Phys. Rev.*, **30**, 415, 1910.
62. H. A. ERIKSON, *Phys. Rev.*, **3**, 151, 1914; **6**, 345, 1915.
63. H. SCHILLING, *Ann. Physik*, **83**, 23, 1927; L. B. LOEB, *Ann. Physik*, **84**, 689, 1927.
64. TYNDALL and PEARCE, *Proc. Roy. Soc.*, A **149**, 426, 1935; A. F. PEARCE, *Proc. Roy. Soc.*, A **155**, 490, 1936.
65. L. B. LOEB, *Kinetic Theory of Gases*, 2nd Edition, McGraw-Hill, New York, 1934, pp. 198, 199, also Secs. 63 and 64.
66. W. KAUFMANN, *Physik. Z.*, **1**, 22, 1899.
67. L. B. LOEB, *J. Franklin Inst.*, **182**, 786, 1917.
68. P. LANGEVIN, *Ann. chim. phys.*, **8**, 238, 1905.
69. L. B. LOEB, *Phil. Mag.*, **48**, 446, 1924; **49**, 517, 1925.
70. J. J. THOMSON, *Phil. Mag.*, **47**, 337, 1924.
71. POWELL and BRATA, *Proc. Roy. Soc.*, A **138**, 117, 1932.
72. L. B. LOEB, *Phys. Rev.*, **32**, 81, 1928; also *Z. physik*, **75**, 555, 1932.
73. L. B. LOEB, *Proc. Natl. Acad. Sci.*, **12**, 677, 1926.
74. LOEB and DYK, *Proc. Natl. Acad. Sci.*, **15**, 146, 1929.
75. TYNDALL and PHILLIPS, *Proc. Roy. Soc.*, A **111**, 577, 1926.
76. H. F. MAYER, *Physik. Z.*, **27**, 513, 1926; **28**, 637, 1926.
77. L. B. LOEB, *Phys. Rev.*, **35**, 184, 1930; *Proc. Natl. Acad. Sci.*, **12**, 35, 42, 1926.
78. R. N. VARNEY, *Phys. Rev.*, **42**, 547, 1932; H. A. ERIKSON, *Phys. Rev.*, **33**, 403, 1929; J. J. MAHONEY, *Phys. Rev.*, **33**, 217, 1929; TYNDALL and GRINDLEY, *Proc. Roy. Soc.*, A **110**, 364, 1926.
79. POWELL and BRATA, *Proc. Roy. Soc.*, A **138**, 129, 1932.
80. O. LUHR, *Phys. Rev.*, **38**, 1730, 1931; **44**, 459, 1933.
81. TYNDALL and GRINDLEY, *Proc. Roy. Soc.*, A **110**, 341, 1926; TYNDALL, GRINDLEY and SHEPPARD, *Proc. Roy. Soc.*, A **121**, 172, 1928.
82. K. PRZIBRAM, *Handbuch der Phys.*, loc. cit., p. 365.
83. LOEB and BRADBURY, *Phys. Rev.*, **38**, 1716, 1931; M. E. GARDNER, *Phys. Rev.*, **53**, 75, 1938; O. LUHR, *Phys. Rev.*, **35**, 1394, 1930.
84. A. BLANC, *J. phys.*, **7**, 825, 1908.
85. K. PRZIBRAM, *Wien. Ber.*, Ila, **118**, 1419, 1909; M. BĚLĀR, *Wien. Ber.*, Ila, **130**, 373, 1921.
86. LOEB and ASHELEY, *Proc. Natl. Acad. Sci.*, **10**, 351, 1924; L. B. LOEB, *Proc. Natl. Acad. Sci.*, **12**, 35, 42, 677, 1926.
87. L. B. LOEB, *Kinetic Theory of Gases*, 2nd Edition, p. 572 ff.
88. P. LANGEVIN, *Compt. rend.*, **61**, 232, 1905; *Le radium*, **4**, 218, 1907; MCLELLAND and KENNEDY, *Proc. Roy. Irish Acad.*, **30**, 71, 1912; J. A. POLLOCK, *Proc. Roy. Soc. N. S. Wales*, **43**, 198, 1909.
89. J. A. POLLOCK, *Phil. Mag.*, **29**, 514, 617, 1915.
90. Communicated in letter from G. R. WAIT, Dec. 27, 1934.
91. WIGAND, *Met. Z.*, **30**, 10, 1913; BAYLAN, *Proc. Roy. Irish Acad.*, **37**, 58, 1926.
92. WAIT and TORRESON, *Terrest. Mag. and Ats. Elect.*, **39**, 111, 1934.
93. O. W. TORRESON, *Terrest. Mag. and Ats. Elect.*, **39**, 65, 1934; NOLAN, BOYLAN and DESACHY, *Proc. Roy. Irish Acad. Sci.*, A **37**, 1, 1925.
94. LOEB, KIP, and EINARSSON, *J. Chem. Phys.*, **6**, 264, 1938.
95. J. J. THOMSON, *Conduction of Electricity through Gases*, 3d Edition, Vol. 1 pp. 320-333.
96. S. CHAPMAN, *Phys. Rev.*, **52**, 184, 1937; **54**, 520, 528, 1938.

97. W. B. HAINES, *Phil. Mag.*, **30**, 503, 1915; **31**, 339, 1916; J. J. NOLAN, *Proc. Roy. Irish Acad.*, **36**, 31, 1922; *Phys. Rev.*, **24**, 16, 1924; H. B. WAHLIN, *Phys. Rev.*, **25**, 630, 1925; NOLAN and NEVIN, *Proc. Roy. Soc.*, **A 127**, 155, 1930.
98. O. BLACKWOOD, *Phys. Rev.*, **19**, 281, 1922; **20**, 999, 1922; L. B. LOEB, *Phys. Rev.*, **25**, 101, 1925; K. PRZIBRAM, *Handbuch der Physik*, Vol. 22, Part 1, Chap. 4, pp. 363, 365.
99. A. BLANC, *J. phys.*, **7**, 825, 1908; E. M. WELLISCH, *Proc. Roy. Soc.*, **A 82**, 500, 1909; TYNDALL and GRINDLEY, *Phil. Mag.*, **48**, 711, 1924; E. RUTHERFORD, *Phil. Mag.*, **5**, 95, 1903; J. FRANCK, *Ber. deutsch. physik. Ges.*, **11**, 397, 1909; FRANCK and MEITNER, *Ber. deutsch. physik. Ges.*, **13**, 671, 1911; H. A. ERIKSON, *Phys. Rev.*, **24**, 622, 1924; **26**, 465, 1925.
100. L. B. LOEB, *Phys. Rev.*, **36**, 152, 1930.
101. H. A. ERIKSON, *Phys. Rev.*, **24**, 622, 1924; **26**, 465, 1925.
102. LOEB and LOEB, *Proc. Natl. Acad. Sci.*, **15**, 305, 1929.
103. R. A. MILLIKAN, *Phys. Rev.*, **18**, 456, 1921.
104. L. B. LOEB, *Science*, **67**, 468, 1928.
105. L. B. LOEB, *Proc. Natl. Sci.*, **13**, 703, 1927.
106. L. BRATA, *Proc. Roy. Soc.*, **A 141**, 454, 1933.
107. MITCHELL and RIDLER, *Proc. Roy. Soc.*, **A 146**, 911, 1934.
108. G. R. WAIT, *Phys. Rev.*, **48**, 383, 1935.



## PART C. THE THEORY OF IONIC MOBILITIES \*

### 1. INTRODUCTION †

Almost as soon as the mobilities of ions were measured, attempts were made to derive theoretical equations using the kinetic theory of gases which was then rapidly gaining acceptance. The analyses at once indicated that the ions were of the order of magnitude of molecular dimensions.<sup>110</sup> The values calculated for the mobilities assuming monomolecular ions whose charges did not affect their motion were in general about five times the observed values. This could be ascribed to only one term in the theory, namely, the ionic mean free path. The free path in order to give agreement had therefore to be about one-fifth that assumed for the forceless molecules. Since the mean free path depends characteristically only upon the sum of the apparent ionic and molecular radii, the radii of the ions has to be assumed about twice as large as those of single molecules. The obvious interpretation in the period before 1909, except for those really schooled in kinetic theory, as was Langevin, was that the ion was a *cluster* of molecules of appropriate size about the charged molecule. The nature of the forces exerted between ions and molecules was then known. It should thus have been clear that the forces must extend well beyond the  $8 \times 10^{-8}$  cm characterizing the size of the cluster. Accordingly,

\* References for Part C of Chapter I will be found on page 85.

† The theories of ionic mobility have not in recent years been treated critically in any textbook except in Loeb's *Kinetic Theory* and Przibram's summary. Przibram<sup>109</sup> presents all theories with some discussion. In this treatment somewhat more critical choice will be made from the viewpoint of recent results and of kinetic theory. We need not thus be surprised to see many earlier good but not entirely satisfactory treatments such as those of Wellisch, Sutherland, and Lenard omitted in favor of the more adequate kinetic-theory treatments. Since the reader may question the author's choice of what is a more-satisfactory theory, his criterion will be given. When a theory is developed on the basis of adequate assumptions as closely as possible similar to actual conditions, it can be considered as having a satisfactory basis. Thus a mobility derivation for normal ions that omits the action of forces except in cluster formation is physically unreal and *can never be accepted*; similarly, an equation neglecting solid elastic impacts or their equivalent will, in general, not have an adequate basis. In addition the derivation of the equation should involve acceptable and legitimate methods of procedure, especially in regard to the methods of averaging, etc. Finally, when the result based on sound assumptions has been checked more or less independently by one or more workers using accepted or, better, differing procedures, one can have confidence in the result. This situation applies to the ion mobility equation of Langevin assuming inverse fifth power attraction and to the Druyvesteyn equation for the energy of electrons in a field in a gas.

it should have been clear that  $K$  depended on the action of such forces as well as on the cluster size. Until 1909 this was recognized by very few and utilized by Langevin<sup>111</sup> only. In 1909, Sutherland and independently Wellisch<sup>112</sup> recognized the situation and tried to account for  $K$  *entirely on the basis of the forces without clustering*. This led to the so-called *small-ion* theory as opposed to the *cluster-ion* theory. The controversy was prolonged and at times far from objective. It was largely prolonged by the conflicting and inadequate experimental data.

With the development of modern physics, a more widespread appreciation and understanding of kinetic theory among physicists, and adequate methods of measurement, the controversy among the present generation of physicists should be relegated to the limbo of forgotten things. Unfortunately, most books on the subject make available to the non-specialist only the earlier work. Thus the errors of the past are passed on to the present day. As in all such controversies, neither party was entirely right. Clustering in the form of complex-ion formation does occur under the proper conditions and *in an unpredictable fashion*. It is *charge sensitive* and *is not due to inverse fifth power attraction*. *The greater portion of the decrease in free path or apparent increase in the ionic radius is due to attractive forces of the Sutherland type and not to a cluster*. In some gases the small-ion theory is almost accurately applicable; in others, not. The theory of Langevin<sup>111</sup> developed thirty years before the field was ready to adopt it is in general nearly correct. Greater accuracy can be obtained only by applying inverse fifth power attractive force fields and the appropriate repulsive force fields to the particular molecules and ion in question.<sup>113</sup> These are not known with sufficient accuracy to give much better agreement than the Langevin equation gives. Wave-mechanical<sup>114</sup> treatment suffers from the same deficiencies as the force law equation: to wit, lack of adequate data about interaction terms and force fields. It is perhaps at present somewhat less applicable, as the nature of all the interactions is not known. In any case, to any one conversant with modern kinetic theory and sympathetic to the wave-mechanical approach, it is clear that the theoretical aspect of the mobility problem is solved in as satisfactory a fashion as experimental data warrant. For ions older than  $10^{-4}$  second where the nature of the complex-ion formation is not known with precision, no theory is accurately applicable. Once the characteristics of the ion are known, the theories above will suffice.

In order to discuss the theory adequately, it will be necessary to lead up to the more elaborate equations gradually. There is no space for a complete derivation of such an equation as Langevin's, nor would the inclusion of the lengthy derivation be warranted from an illustrative point of view. It is best to introduce the concepts by a most elementary and simple deduction of the mobility equation. This

gives the essential nature of all other equations except for certain refinements. Some of these can be found in Loeb's *Kinetic Theory of Gases*.<sup>109</sup> For the rest the reader must go to the original literature. With the simple equation as a background, it is then possible to develop all the necessary concepts so that when the full theory of Langevin is discussed its nature will be understood and the reader will be able to accept the correctness of the introductory statement just given.

## 2. THE ELEMENTARY THEORY OF IONIC MOBILITY

Assume the ion to be a molecule of the solid spherical elastic type with a mass  $m$  and a charge  $e$  moving in a gas composed of similar molecules, all having the radius  $\sigma/2$ . Assume that the ions exert no force on each other except on impact when their centers are  $\sigma$  cm apart. The molecules and ions in the absence of the field move around with a root mean square velocity of agitation  $C$  and an energy of agitation  $\frac{1}{2} mC^2$ . The average velocity is  $\bar{c}$ . The free path of the ion is as for molecules  $L = 1/(\pi\sqrt{2} N\sigma^2)$ . Assume that the force on the ion due to the field  $X$  acting is  $Xe$ .  $X$  is the field strength and is to be taken so low that the energy  $XeL$  gained by the ion in a mean free path is small compared to  $\frac{1}{2} mC^2$ . This means that the path of the ion between impacts is not seriously curved, a condition which generally holds in experimental study. The result is that each free path suffers a very slight distortion in the field direction, and the ion in its zigzag heat motion slowly drifts in the field direction. The value  $S_t$  of this drift over one free path lasting  $t$  seconds will be  $S_t = \frac{1}{2} at^2$ , where the acceleration  $a$  of the ion is  $a = Xe/m$ . The time  $t$  between impacts is then  $t = L/\bar{c}$ . Hence

$$S_t = \frac{1}{2} \frac{Xe}{m} \left( \frac{L}{\bar{c}} \right)^2.$$

Now we are interested in the average velocity of drift  $\bar{v}$  in the field direction, which is given by,

$$\bar{v} = \frac{S_t}{t} = \frac{1}{2} \frac{XeL}{m\bar{c}}.$$

The mobility  $k$  is then at once found to be

$$k = \frac{\bar{v}}{X} = \frac{1}{2} \frac{eL}{m\bar{c}}.$$

This equation is only a rough approximation to the mobility. For one thing,  $L$  is not really a constant value but ranges from short to long paths. Hence, the longer paths will yield a larger  $S_t$  as  $S_t$  depends on  $(L/\bar{c})^2$ . Also, the velocities of the molecules are not all equal and equal to  $\bar{c}$ , and this introduces errors. Finally, in the more

general case where the ion has a mass  $m$  while the molecules have a mass  $M$ , the persistence of velocity requires correction. Using classical but fairly rigorous kinetic-theory methods, Langevin<sup>110</sup> solved this problem about as accurately as it can be solved on a solid elastic theory with the assumptions made. The resulting equation even though criticized by Lenard's school is the best equation that can be derived on this basis, and because of the general faulty nature of the forceless solid elastic theories in general it will suffice. It reads,

$$k = 0.815 \frac{e}{M} \frac{L}{C} \sqrt{\frac{m+M}{m}},$$

where  $C$  is the root mean square velocity  $\sqrt{\bar{c}^2}$  of the gas molecules and not the average velocity  $\bar{c}$  used heretofore. The constant 0.815 takes care of the result of the variation of the free paths and velocities in the averaging process. In the simple derivation  $m$  was assumed equal to  $M$ . If this is no longer so,  $C$  will designate the rms velocity of the gas molecules and  $C_m$  the rms velocity of thermal agitation of the ions. Since by kinetic theory (page 644)  $C/C_m = \sqrt{m/M}$ , the equation can be transformed to the form

$$k = 0.815 \frac{e}{m} \frac{L}{C_m} \sqrt{\frac{M+m}{M}}.$$

In this form it has its use in discussing electron velocities but is of no interest in the present discussion. In the expression

$$k = 0.815 \frac{e}{M} \frac{L}{C} \sqrt{\frac{M+m}{m}}$$

it is seen that, if  $m = M$ ,  $k = 1.154 \frac{e}{M} \frac{L}{C}$ , with the radical

$$\sqrt{\frac{(m+M)}{m}} = \sqrt{2}.$$

It should at once be possible to test this equation, since  $e$  was early found to be one electron,  $M$  is the mass of a gas molecule,  $C$  is the root mean square velocity of the gas molecules, and  $L$  is the molecular free path.

Putting in the values for  $L$  in air, the value of  $k$  is 7.62 cm/sec per volt/cm, while the observed value is close to 2.18 cm/sec. In addition, this theory makes  $k \propto e$ ,  $k \propto 1/\sqrt{M}$ , since  $C \propto 1/\sqrt{M}$ ,  $k \propto L$  and  $k \propto 1/\sqrt{T}$ , since  $C \propto \sqrt{T}$ , with no variation of  $k$  with the dielectric constant  $D$ . Hence the theory fails in that

$k$  as observed is *not*  $\propto 1/\sqrt{T}$ ,  
 $k$  as observed is *not* independent of  $D$ ,  
 $k$  as observed is *not*  $\propto L$ .

However, both by theory and by experiment  $k$  is  $\propto 1/\rho$ , since  $L \propto 1/\rho$ , where  $\rho$  is the density. Finally, the theory gives a computed value of  $k$  three times the observed value. The order of magnitude of numerical disagreement for this theory is more or less universal for most ions. The ratio of the absolute value of  $k$  computed and observed is also checked by the fact that molecules in  $O_2$  diffuse about three times as fast in  $O_2$  as do ions of  $O_2$  moving in  $O_2$ , and diffusion is closely related to mobility.

As stated, the physicists engaged in these studies about 1905 did not have the knowledge which we have today. The important item to them was the fact that  $k$  computed was three to five times  $k$  observed.\* Now the only uncertain factor in the equation is  $L$ . It was obvious that  $L$  for ions must be about one-fifth that for molecules. From the nature of  $L$ , this can happen only if for an ion the effective collision radius  $\sigma_m/2$  is greater than  $\sigma_M/2$  for the molecule. Hence by observing  $k$  and solving the equation for  $L$ , one can place  $L = 1/(\sqrt{2} \pi \sigma^2 N)$  and evaluate  $\sigma$ , i.e., the average *effective* value of the sum of the radii of ion and molecule in impact. Hence at that time the discrepancy merely meant that the sum of the radii of ion and molecule was  $\sqrt{5}$ , or about 2.2, times the diameter of a molecule, or that the ion had an average diameter 1.7 times that of a molecule. Thus, it was natural to assume that the ion was not a single molecule with a charge but a *cluster* of several molecules about the charged molecule. This conclusion was borne out by certain other considerations to follow. As a result today a diminishing number of physicists still assert that the deviation of the mobility value from the theory for a monatomic carrier is due to the "cluster-ion" formation. They then calculate the ion radius from the "apparent" value of  $L$  inferred from one of the solid elastic equations. Now *it is true that  $L$  is less than the kinetic theory value for an uncharged molecule*, but *it is not true that this is all due to cluster formation*, for the results already given, many of recent date, preclude this explanation.

### 3. FORCES BETWEEN IONS AND MOLECULES

We must next regard the forces between ions and neutral molecules before we can understand the problem further. Now an ion at a distance  $r$  has an electric field about it given by  $X = e/r^2$ , where  $e$  is the charge. At  $10^{-8}$  cm,  $X$  is of the order of  $10^8$  volts/cm, and even at  $10^{-6}$  cm it is of the order of  $10^4$  volts/cm, which is a high field. The outer shells of electrons in molecules and atoms are not rigid. In an electric field the electron shells are urged towards the positive pole, the nuclei are urged towards the negative pole, and the

\* The earlier values of  $k$  observed and  $k$  computed gave a ratio of five rather than three, and this will be used from now on in discussion.

atom becomes an *induced dipole*, i.e., the plus and minus charge centers are separated a distance  $l_1$  and the atom or molecule has an electric moment  $\mu = el_1$ . If the molecule is already a dipole such as HCl the molecule acts to align its moment in the field with its positive end towards the minus charge and its negative end towards the plus charge. Since the dipole is continually being disoriented by heat impacts it is partly oriented in the field in proportion to the field strength and has thus an average moment parallel to the field axis proportional to  $X$ . In this orientation the dipole of moment  $\mu$  induced or oriented is attracted to the charge  $e$ , causing the field  $X = e/r^2$ , with a force  $f$  proportional to  $\mu e/r^3$ , where  $r$  is the distance between the molecule and the ion. (This case is analogous to the force between a bar magnet and a pole on its axis.) Thus, since  $\mu$  is proportional to  $X = e/r^2$ ,  $f \propto Ae^2/r^5$ . The force can be accurately calculated as follows. If we have a block of dielectric material in an electric field  $X$  the material due to its polarization has a flux of electrical lines of force per square centimeter given by  $F = X + 4\pi\Sigma$ , where  $\Sigma$  is the number of charges per square centimeter produced by induction on the face of the block. But  $F = XD$ , where  $D$  is the dielectric constant of the material. Hence,  $XD = X + 4\pi\Sigma$  and  $\Sigma = \frac{X(D-1)}{4\pi}$ . But  $(\Sigma A)l = \Sigma V$  is the total electrical moment  $\mu_T$  of the block, for if  $A$  is its area  $\Sigma A$  is the total charge  $q$ , and  $ql = \mu_T$ , while  $Al = V$ , the volume. Hence

$$\mu_T = \Sigma V, \Sigma = \frac{\mu_T}{V}, \text{ and } \frac{\mu_T}{V} = \frac{X(D-1)}{4\pi}.$$

Now,  $\mu_T/NV = \mu$ , the moment of a single molecule for  $N$  is the number of molecules per unit volume and  $\mu_T/V$  is the moment per unit volume. Thus,

$$\mu = \frac{X(D-1)}{4\pi N}.$$

But  $X = e/r^2$ , so that

$$\mu = \frac{e(D-1)}{4\pi Nr^2},$$

and if  $r$  is large compared with  $\mu/e$ , then the force  $f$  on the molecule of moment  $\mu$  due to polarization is

$$f = \frac{2\mu e}{r^3} = \frac{(D-1)e^2}{2\pi Nr^5}.$$

The potential energy between ion and molecule is then

$$w = \int_{-\infty}^{\infty} f dr = -\frac{(D-1)e^2}{8\pi Nr^4}.$$

One can at once apply this evaluation of the force to the question of the stability of the ion cluster, for, if the potential energy is equal to or greater than the kinetic energy of heat motion, then the ion begins to be stable as a cluster. Hence, if  $r$  represents the distance between ion center and the center of a molecule of the cluster, then the cluster will be stable if with the given values of  $r$  and  $D$   $W/KE \geq 1$ . Now  $KE = \frac{1}{2} m C_m^2 = \frac{1}{2} M C^2$ , and

$$\frac{W}{KE} = \frac{(D-1)e^2}{4\pi N M r^4 C^2} = \frac{(D-1)e^2}{12\pi p r^4},$$

where  $p$  is the gas pressure. If we use  $O_2$  and insert the value of  $\sigma = r$  for  $O_2$ ,  $W/KE = 3.1$  at N.T.P. and it looks as if the cluster would be stable with one layer of 12 spherical  $O_2$  molecules about the  $O_2^+$  ion. For 12 spheres is the largest number of spheres one can build in a monomolecular layer around an equal sphere. With  $r = 2\sigma$ ,  $W/KE = 0.19$  and a larger cluster would be unstable. Thus, for gases of large  $D$ , it seemed likely that ions could be clusters of up to 30 molecules about a charge. Hence, there was justification at that time in assuming ions to be clusters. There is, however, one doubt in all this reasoning. For matter in bulk and in weak fields one can write that

$$f = \frac{(D-1)e^2}{2\pi N r^5}. \quad \text{When fields reach values of the order of } 10^8 \text{ volts/cm}$$

at values of  $\sigma$  such as are considered in clustering, with highly divergent fields over a single atom, i.e., changing by a factor of nearly ninefold across a molecule in the cluster, it is dangerous to assume with certainty that  $f$  is that given by theory. Again, the values of  $\sigma$  are not known with any certainty, and the whole reasoning hinges critically on the value of  $\sigma$ , so that again one should proceed with caution. Thus it is just in the clustering region of values of  $r$  that the theory is unreliable. At distances  $3\sigma/2$  or more it is not badly off. In this region while the forces are insufficient for cluster formation they can alter ion free paths materially.

#### 4. THE SMALL-ION THEORY

It was with this matter in mind that Sutherland and Wellisch<sup>112</sup> independently in 1909 suggested that while  $L$  was reduced by a factor of 5 this need not be due to a cluster formation and a change in the real ionic diameter  $\sigma$ , but that, since forces of the general type,  $f = \frac{(D-1)e^2}{2\pi N r^5}$  existed, these must also cause the ionic free paths to

be altered and curved towards the molecules, thus bringing on collisions which would *not* occur with forceless molecules, and shortening  $L$ . *This action must and does take place appreciably well before cluster formation occurs, and whether it precludes cluster formation or not,*

it must be considered. Sutherland<sup>115</sup> had shown that from such a viewpoint we could explain the change in *viscosity* with temperature in gases. He made an unsuccessful attempt to carry his law over to the calculation of gas ion mobilities.<sup>112</sup> Wellisch did the same, using approximate and somewhat inaccurate reasoning inherent in the free path concept. Thus, whether cluster formation takes place or not, these forces are active, and it is *erroneous to ascribe all shortening of  $L$  to cluster formation alone*. It is at this point that the cluster-theory school are in the wrong in their procedure. Until later experiment or theory aided us it could be said that the proportion of the lowering of  $L$  and hence  $k$  ascribable to clustering and the proportion ascribable to the distortion of free paths by the forces were indistinguishable. One must then at this point say that all that was known was that  $L$  is decreased by two types of action and that one could but speculate on how much it was decreased by either factor.

Fortunately, there are now more data on hand when proper analyses are made. In 1905 Langevin<sup>111</sup> had extended his solid elastic theory to apply to solid elastic ions of radius  $\sigma$  that attracted gas molecules according to a law of force  $f = \frac{(D-1)e^2}{2\pi Nr^5}$ . As has been stated, the very beautiful and elaborate calculation was buried in an obscure French journal and was promptly forgotten for nearly twenty years. In 1924 J. J. Thomson<sup>116</sup> published a theory of ionic behavior in which the ions acted essentially as point centers of force attracting molecules according to the law above. Using the equation of Thomson for momentum loss, Loeb<sup>117</sup> arrived at an equation for ionic mobility which had the exceedingly simple and interesting form

$$k = \frac{0.104 \sqrt{\frac{M+m}{m}}}{\frac{\rho}{\rho_0} \sqrt{(D-1)_0 M_0}},$$

which it will be recalled strikingly well represents the behavior of the gaseous ions as it was then known and is much more successful with the present-day knowledge.

It was subsequently pointed out by H. R. Hassé,<sup>118</sup> at that time engaged in working out the mathematical theory of ion mobilities, that the equation of Loeb was a rediscovery, in inexact form as regards the numerical value of the constant, of a special case of Langevin's equation of nearly twenty years before. Hassé<sup>118</sup> had been checking the equation of Langevin and was thus familiar with the case in question. Langevin's full theory to be discussed later permitted of a simplification when one could assume that a quantity  $1/\lambda$  became very small.  $\lambda$  is proportional to the square root of the ratio of dielectric attractive potential energy to the relative kinetic energy of ion



and molecule at a distance  $S = (\sigma_m/2) + (\sigma_M/2)$ . Here  $\sigma_m$  and  $\sigma_M$  are the diameters of ion and molecule respectively. The quantity  $\lambda$  is given by

$$\lambda = \sqrt{\frac{3(D-1)_0 e^2}{8\pi N_0 S^4 M C^2}}.$$

When  $\lambda$  becomes large,  $S$  small,  $MC^2$  small, and  $(D-1)_0$  large,  $1/\lambda$  approaches zero, and a quantity  $0.462 (3/16Y)$ , which depends on  $1/\lambda$ , becomes constant and equal to 0.235. Hence the general Langevin equation

$$k = \frac{3}{16Y} \frac{0.462 \sqrt{\frac{M+m}{m}}}{\frac{\rho}{\rho_0} \sqrt{(D-1)_0 M_0}}$$

becomes

$$k = \frac{0.235 \sqrt{\frac{M+m}{m}}}{\frac{\rho}{\rho_0} \sqrt{(D-1)_0 M_0}}.$$

This is identical with the Loeb-Thomson equation, except that 0.235 replaces 0.104. As usually found in the literature, the equation of Langevin is written

$$k = \frac{3}{16Y} \frac{\sqrt{\frac{M+m}{m}}}{\sqrt{(D-1)_\rho}}.$$

The equations are the same except that  $(D-1)$  is not reduced to standard density, and the density enters in absolute fashion, concealing the molecular weight.

Making  $\lambda$  large is essentially making  $S$  approach zero, i.e., making the ion a point charge. This neglects the solid elastic collisions due to the real dimensions of the ion and atom in comparison to those conditioned by the attractive force and is in essence a true "small-ion" theory. Since the successes and failures of this theory are of great value in understanding the problem we must consider the equations somewhat more closely.

The manner in which equations of this type are derived follows from the mechanical principle that the force exerted by the field on the ion in equilibrium  $Xe$ , is just equal to the rate of momentum loss to the molecules in impacts. What is required then is merely that we calculate the momentum loss of an ion in a molecular encounter for a given velocity of ion and molecule, multiply this by the chances of the velocities showing these values and by the number of encounters per second of this type, and integrate over all values of the velocities.

This procedure is justified since the number of losses per second for an ion is so large that it comprises all sorts of velocities in encounters. For elastic spherical ions of mass  $m$  and molecules of mass  $M$ , with a collision radius  $S$  between centers, and velocity components  $u$  and  $U$  in the field direction respectively and of relative velocity  $C$ , we can write

$$Xe = \frac{mM}{m+M} \iint (u - U) N \pi S^2 C df dF,$$

where  $df$  and  $dF$  represent the velocity distribution functions for ion and molecule, i.e.,  $f$  is Maxwell's law with the average ionic drift velocity  $\omega$  in the field included,

$$df = \left(\frac{hm}{\pi}\right)^{3/2} e^{-hm[(u-\omega)^2 + v^2 + w^2]} du dv dw.$$

If now we admit of attractive forces between ions and molecules, the problem is more complicated.<sup>119,116</sup> Momentum transfer does not occur only on impact between elastic spheres. Instead we have in general the ions and molecules undergoing momentum exchanges in describing orbits about their common center of mass. On an inverse fifth power law, various types of orbits are possible, somewhat similar to the orbits on an inverse square law. Every slight deflection of the ion by the molecule in such encounters, conditioned by attractive forces only, is associated with a momentum change. The momentum exchange can be described in terms of the perpendicular  $p$  of the position of the molecule onto the initial relative path of the ion, the angle through which deflection takes place, and the velocities and masses of the ion and molecule. These involve the kinetic energy of the ion and molecules and the attractive forces. For a point ion, such as is assumed in the equations of page 60, it appears that, if  $p$  has a value  $p_0$  given by

$$p_0^4 \leq \frac{(D-1)e^2}{2\pi N \left(\frac{mV^2}{2}\right)},$$

there will be no completed orbit with momentum change, but the ion and molecule will collide physically. The velocity  $V$  is in this case the total relative velocity of the ion and molecule. The loss of momentum of the ion in such an impact will be that caused by a central impact for the point ion.

The losses of the ion to momentum exchange in impacts where ion and molecule do not collide, i.e., where the ion orbit about the molecule has an apse, can be computed. This is done by taking the

chance that the ion and molecule will pass at a distance  $p$  (between  $p$  and  $p + dp$ ) of each other with

$$p^4 > p_0^4 = \frac{(D-1)e^2}{2\pi N \left( \frac{mV^2}{2} \right)}$$

and extending to infinity, multiplying it by the momentum loss for an encounter at  $p$  and integrating over all values of  $p$ , and of the velocities. For the collisions at values of  $p$  within  $p_0$ , one sums up the losses for all velocities at central impact for all possible collisions between  $p = 0$  and the critical value of  $p_0$ . It was in this way that Thomson calculated the average momentum loss and thus enabled Loeb<sup>119,117</sup> to calculate the mobility. In Langevin's complete derivation the impacts at larger values of  $p$ ,  $p > p_0$  were calculated essentially as outlined.\* Langevin, however, took into account the fact that the ions were not point charges. Then, while the collision condition remains unaltered if  $p_0$  is greater than the collision radius  $S$ , the collision takes place between spherical surfaces whose centers are executing inverse fifth power law orbits. The impacts will usually not be central as Thomson assumed them to be.† Hence the momentum losses on the average will be less than Thomson collisions lead one to predict. The inclusion of the characteristics of these impacts in the integration process, therefore, probably makes the constant in Langevin's expression somewhat more accurate and gave him a variation of the value of the constant with  $\lambda$  which does not occur in Thomson's equation. If the attractive term is much greater than the energy so that  $\lambda$  is large, i.e., values of  $S$  vanishingly small, the equation of Langevin becomes identical with Thomson's in form and the constants differ by a factor of 2.26. Both these special-case equations are in the truest sense of the word small-ion theories.

Since this type of theory has proved remarkably successful in many ways, and is particularly serviceable because of its simplicity, it is of importance to discuss it. From its weaknesses, one can then with a clearer understanding pass to a discussion of the more esoteric equations of Langevin and of Hassé and Cook. From the equation

$$k = \frac{0.235 \sqrt{\frac{m+M}{m}}}{\frac{\rho}{\rho_0} \sqrt{(D-1)_0 M_0}}$$

it is seen that  $k$  depends on the relative masses of ion  $m$  and molecule  $M$ , on the dielectric constant  $D$  evaluated at  $0^\circ \text{C}$  and 760 mm, on the molecular weight  $M_0$  of the gas molecules, and on the density  $\rho$  of

\* This can apply only if  $S$  is less than  $p_0$ . If not, integration must be carried on from  $S$  to infinity for apsidal energy losses.

† In Langevin's theory he actually treated  $S > p_0$  and calculated the impacts from  $p = 0$  to  $p = S$  on the basis of solid elastic impacts with due regard for the orbit shapes.

the gas relative to  $\rho_0$  at standard conditions. These are all easily determinable quantities. Thus, under conditions where theory makes the equation applicable, we can say the following things:

1. It gives mobilities directly and in absolute measure with *no arbitrary assumptions* if  $m$  is known.

2.  $k$  is independent of  $X$  as it is by the elementary theory except at high values of  $X/p$ , whose effect has not been included in theory so far.

3.  $k$  is proportional to  $1/\rho$ , and at constant  $T$  it is proportional to  $1/p$ , as has been observed in experiment and as elementary theory predicts.

4.  $k$  is independent of temperature for constant  $\rho$ . This is *nearly* in conformity with experimental observation in some cases. This is contrary to elementary theory where  $k \propto 1/\sqrt{T}$ . The reason for this is as follows: While as in the elementary equation the random velocity  $C$  and in consequence  $T$  decreases  $k$ , the *energy loss in collisions caused by attractive forces* also is reduced in direct proportion to  $C$ . Thus, the effect of  $C$  and hence of temperature is canceled out. That such a cancelation is possible arises through the neglect of the elastic solid impacts. When the quantity  $\lambda$  is very large, then we are justified in neglecting the effects of  $S$ . This is true in A, Kr, and Xe, and we can expect to find  $k$  at constant density independent of  $T$  until  $\lambda$  becomes too small. In He, where  $(D - 1)$  is small and  $S$  is relatively larger, we can expect some deviation, especially at lower temperatures. Through any extended range of temperatures, however, we cannot neglect  $S$ , and to this extent the theory is faulty. It is corrected for by using  $3/16Y$  as a function of  $1/\lambda$  in the full theory.

5.  $k$  is proportional to  $\frac{\sqrt{(M+m)/m}}{\sqrt{(D-1)_0 M_0}}$  when  $\lambda$  is large. This equation has been experimentally tested and found accurate for alkali and other ions in  $N_2$ , A, Kr, and Xe. It fails for He and Ne as shown in Part B of this chapter. It also fails where  $m$  is not certainly known and in gases where the change of charge alters momentum exchange, i.e., for  $N_2^+$  ions in  $N_2$ ,  $He^+$  ions in He, etc.<sup>120</sup>

6.  $k$  appears independent of the charge  $e$  on the ion, an apparent paradox. This is ascribable to the same effect as the independence of temperature. The force of the field  $X$  on the ion is  $Xe$  and is directly proportional to  $e$ . When the momentum loss in impacts is entirely due to the attractive forces as with vanishingly small  $S$  and large  $(D - 1)_0$ , then the retarding force on the ion due to momentum loss varies as  $0.98 \left\{ \frac{(D - 1)e^2}{\pi N S^4 M C^2} \right\}^{1/2}$  and

$$k = \frac{0.815e}{MCS^2\pi N} \frac{\sqrt{(M+m)/m}}{0.98 \left\{ \frac{(D-1)e^2}{\pi N S^4 M C^2} \right\}^{1/2}},$$

so that  $k$  is independent of  $e$ . When, however, real physical radii are involved and  $\lambda$  is small, some of the momentum loss is independent of  $e$ , and  $k$  is a complex but slowly changing function of  $e$ . For large particles  $k$  is proportional to  $e$ . No data on the variation of  $k$  with  $e$

are on hand. There is a bare chance that some results of Brata on Ga, In, and Tl ions in He and N<sub>2</sub> can be interpreted on the basis of the double charge in conformity with the theory.

The agreement obtained between theory and experiment is nicely illustrated by the curves in A and He shown in Figs. 30 A, B. In these the atomic weights of the ions Na<sup>+</sup>, K<sup>+</sup>, Rb<sup>+</sup>, Cs<sup>+</sup> are shown plotted against the mobility. In A a polarizable gas, the predicted variation is exceptionally good. In He, which has the lowest polarizability of

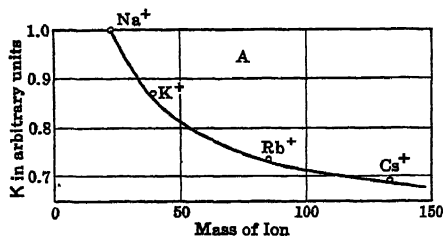


FIG. 30A.

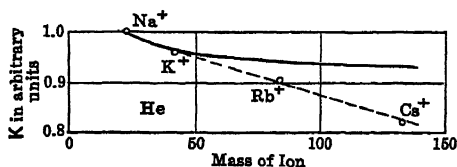


FIG. 30B.

any gas, the deviations from the simple equation are obvious. An analogous curve in N<sub>2</sub> for a number of different ions is shown in Fig. 31. N<sub>2</sub> is also polarizable and seems well suited for these experiments. Ne is less polarizable, and the equation fails but not so badly

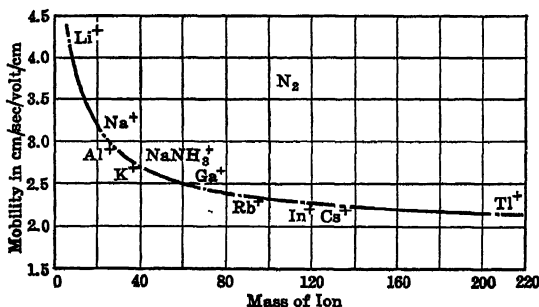


FIG. 31.

as in He. Kr and Xe are the best. It is possible that owing to the divergent character and the high values of the fields near ions we cannot properly apply the value of  $D - 1$  from low uniform field data. The evidence above and that from absolute values of the constant 0.235 for different gases shows that for polarizable gases the

effects at larger values of  $S$  predominate and the correction is small. Some data on  $K$  as computed from the full Langevin theory for  $\text{Li}^+$  in He and for  $\text{Na}^+$  in  $\text{H}_2$  and  $\text{N}_2$  indicate that  $D - 1$  in the high fields near ions is some 10 to 20 per cent less than the value one would expect from  $D$  under normal conditions. The effect can be likened to a saturation effect of the polarization, i.e., as fields increase, the displacement increases more gradually than proportional to  $X$ , and hence the constant  $D$ , assuming proportionality, appears to decrease at high fields.

### 5. THE MORE EXACT THEORIES

In general, then, it is clear that we must use the complete equation of Langevin. Before discussing it, we must clearly recognize what it purports to cover. It assumes spherical elastic molecules and ions.

These attract each other at a distance  $r$  with a force  $f_a = \frac{(D-1)e^2}{2\pi N r^5}$ .

They exert no repulsive forces at  $r > S = (\sigma_m/2) + (\sigma_M/2)$  and a very large force at  $r = S$ ,  $f_r = 1/r^n$ , with  $n = \infty$ . The equation is completely solved for ions of any mass  $m$  and molecules of any mass  $M$ . It is only solved for the case where the energy gained between impacts in the field is small compared to the energy of agitation, and where the ions on the average have an energy  $\frac{3}{2} kT$ . This suffices for ordinary ion studies. The equation as derived does not suffice for studies where  $X/p$  becomes so large that the conditions above no longer hold. It has been shown by Compton that in the equation for ion mobilities neglecting attractive forces under conditions where the terminal energy of the ion  $eU_T > \frac{3}{2} kT$  the mass term  $\sqrt{(M+m)/m}$  must be replaced by a term involving the energies as well as masses. Compton's equation, however, is not satisfactory, as Hershey has shown, and further study is needed as will later be seen.

We may now turn to the discussion of the more complete Langevin<sup>11</sup> equation. The equation reads

$$k = \frac{3}{16Y} \frac{0.462 \sqrt{(M+m)/m}}{\frac{\rho}{\rho_0} \sqrt{(D-1)_0 M_0}} = \frac{3}{16Y} \frac{\sqrt{(M+m)/m}}{\sqrt{(D-1)_\rho}}$$

The quantity  $3/16Y$  is a function of the variable

$$\lambda = \sqrt{\frac{3(D-1)_0 e^2}{8\pi N_0 S^4 M C^2}} = \sqrt{\frac{(D-1)_0 e^2}{8\pi p_0 S^4}},$$

$p_0$  being  $\frac{1}{3} N_0 M C^2$ , the pressure of the gas at N.T.P. This assumes that the terminal energy of the ions  $U_{Te} = \frac{1}{2} M C^2 = \frac{3}{2} kT$ , where  $U_T$  is the terminal energy of the ion in equivalent volts of potential energy.  $M C^2 = U_{Te} + \frac{1}{2} M C^2$  then represents the relative kinetic

energy of ion and molecules. The relation between  $3/16Y$  and  $1/\lambda$  is given in the form of a curve taken from the integrals of Langevin as corrected by Hasse.<sup>118</sup> These are shown in Figs. 32A and 32B.

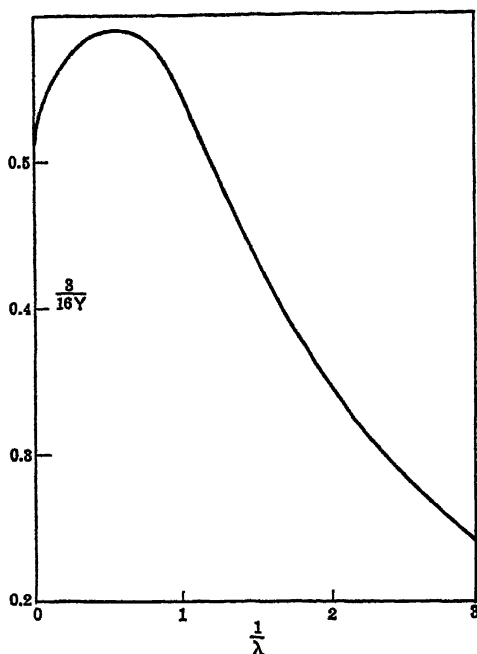


FIG. 32A.

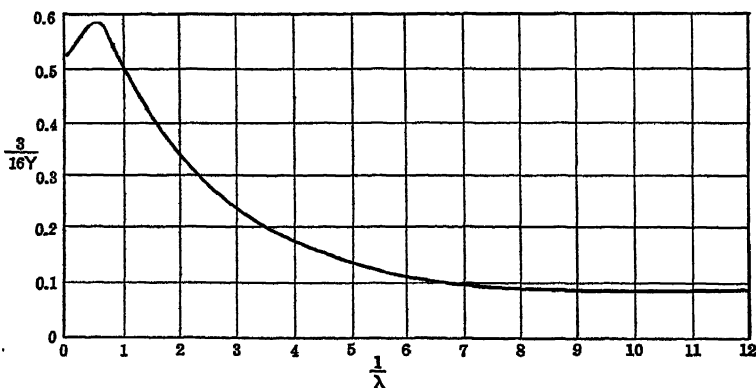


FIG. 32B.

Since this equation is the only one assuming attractive forces which is nearly correct and which enables nearly accurate computations of

mobilities to be made, the curves are given in some detail. It is seen that the value of  $\lambda$  and of  $k$  depends quite critically on the value of  $S$  chosen. It is here that one encounters trouble. Unless the nature of the ion is definitely known, e.g.,  $K^+$  ions,  $He^+$  ions, etc., one cannot but speculate as to  $S$ . For such cases as  $K^+$  ions in A, perhaps the best one can do is to go to the charge density distribution functions, wave mechanically calculated, and choose  $\sigma_m/2$  and  $\sigma_M/2$  as the distance from the nucleus to the point where the charge density becomes sensibly zero. For the gases A, Ne, etc., one could use  $\sigma$  as determined from viscosity or the closest packing in liquids. The value of  $\sigma_m$  for the alkali ions can then be assumed as very close to the value for the nearest inert gas. The values of  $\sigma$  from viscosity as determined by the evaluation of  $L$  using Jeans's<sup>123</sup> equation will be too large on account of the attractive van der Waals forces. The data on temperature variation of viscosity yield values of the diameter  $\sigma$ , assuming a solid elastic type of impact, which are quite good.<sup>124</sup> Similar results are obtained from the constants of the equation of state.<sup>125</sup> Since the values of  $\sigma$  are in some doubt, the results must be discounted in the appropriate amount. Actually, the solid elastic evaluations of  $\sigma$  are incorrect, for  $\sigma$  is due to repulsive force laws and hence will vary slightly with the energy of impact and will be different from the solid elastic values. For some gases the repulsive force laws between atoms are known from viscosity data and data from the equation of state. In general,  $f_r \propto 1/r^n$  with  $n$  equal to 14 for He; 11 for Ne, Xe, and  $H_2$ ; 9 for A; and 10 for Kr. For  $N_2$ , one power appears to be as good as another.<sup>126</sup> With these laws the values of the diameters computed differ from the values on the solid elastic impacts with  $n = \infty$ . The values of  $\sigma$  so computed are in general from 1.5 to 2 times larger than  $\sigma$  when  $n = \infty$ , the discrepancy being less the higher  $n$ .

One procedure that can be resorted to is to use the Langevin equation for computing  $\sigma$  assuming  $D = 1$  as given in tables. Since the value of  $D = 1$  is as uncertain as  $\sigma$  (although its effects are less emphasized since  $\sigma$  is raised to the fourth power), one had best be content with both values as given in reliable and appropriate tables.

As regards the attractive force, many workers<sup>127</sup> including the author<sup>128,129</sup> have considered the *addition* of the *van der Waals* attractive forces to the  $\frac{(D-1)e^2}{2\pi N r^5}$  attractive force term. After considerable thought, the author believes that *the high fields will so distort the atoms that the ordinary van der Waals attractive forces cannot develop*. Additional forces of a character analogous to the van der Waals type must, of course, be active, but these cannot be estimated. Since we are probably already *overestimating* the attractive inverse fifth power law forces and do not know the other forces, it is best to accept what data we have with a due acknowledgment of their weaknesses. This same ignorance as to basic data applies to any theory, be it a force field or



wave-mechanical theory. Were experimental measurement more accurate and data more extensive, possibly the situation would not be so unsatisfactory. Unless more work is done, then we shall have to content ourselves with the present data.

TABLE I

| <i>s</i> | <i>I(s)</i> | <i>s</i> | <i>I(s)</i> | <i>s</i> | <i>I(s)</i> | <i>s</i> | <i>I(s)</i> |
|----------|-------------|----------|-------------|----------|-------------|----------|-------------|
| 0.05     | 2.2584      | 0.55     | 0.3747      | 1.1      | 0.2866      | 2.2      | 0.2867      |
| 0.10     | 1.5619      | 0.60     | 0.3515      | 1.2      | 0.2848      | 2.4      | 0.2878      |
| 0.15     | 1.2496      | 0.65     | 0.3343      | 1.3      | 0.2839      | 2.6      | 0.2888      |
| 0.20     | 1.0431      | 0.70     | 0.3216      | 1.4      | 0.2836      | 2.8      | 0.2897      |
| 0.25     | 0.8634      | 0.75     | 0.3121      | 1.5      | 0.2836      | 3.0      | 0.2905      |
| 0.30     | 0.7129      | 0.80     | 0.3049      | 1.6      | 0.2838      | 3.2      | 0.2913      |
| 0.35     | 0.5971      | 0.85     | 0.2995      | 1.7      | 0.2842      | 3.4      | 0.2920      |
| 0.40     | 0.5121      | 0.90     | 0.2953      | 1.8      | 0.2846      | 3.6      | 0.2927      |
| 0.45     | 0.4508      | 0.95     | 0.2922      | 1.9      | 0.2852      | 3.8      | 0.2933      |
| 0.50     | 0.4067      | 1.00     | 0.2898      | 2.0      | 0.2857      | 4.0      | 0.2938      |

In 1931, Hassé and Cook<sup>127</sup> applied a rigorous kinetic-theory analysis of the type used by Chapman and Lennard-Jones in viscosity problems, to the study of ionic mobility in gases. They had previously analyzed the viscosity of gases by this means, assuming an inverse fifth power attractive van der Waals force law and an inverse ninth power repulsive law.<sup>128</sup> The attractive force for the ions was an inverse fifth power law, the coefficient of which  $\mu'$  was the sum of the force constants of van der Waals and the  $\frac{(D-1)e^2}{2\pi N}$  coefficient. The repulsive law had a coefficient  $\lambda'$ . Hence,  $f = +\mu'r^{-5} - \lambda'r^{-9}$ . The equation derived is as follows:

$$k = \frac{3}{16} \frac{e}{2\sqrt{\pi RT}} \left[ \frac{M+m}{Mm} 2RT \right]^{\frac{3}{4}} \frac{(1+\delta)}{N_0 I(s) (\lambda')^{\frac{3}{4}}}.$$

If  $m = M$ , as for a monomolecular ion,

$$k = \frac{3e}{16} \left( \frac{2}{\pi M} \right)^{\frac{3}{4}} \frac{1}{(2RT\lambda')^{\frac{3}{4}}} \frac{(1+\delta)}{N_0 I(s)}.$$

Here  $\lambda'_1 = \lambda' \frac{M+m}{Mm}$ , and  $\lambda'$  is the repulsive force coefficient. The quantity  $s$  is given by  $s^2 = 2RT\lambda' / (\mu')^2$ , where  $\mu'$  is the attractive force coefficient;  $1+\delta$  is a correction factor for elastic spheres which lies between 1 and 1.015;  $I(s)$  is an integral which is given for various values of  $s$  in Table I. On this basis, Hassé and Cook calculated a

number of ionic mobilities. In this they were no more successful than Hassé with the Langevin equation. The reason for this is simple. First, except for argon the inverse ninth power repulsive law is incorrect. Again, they added to  $\frac{(D-1)e^2}{2\pi N}$  the value of the van der Waals constant. For  $H_2$  this added quantity increased the  $(D-1)$  term by only 10 per cent, and the error is not serious. The constants for the repulsive forces came from viscosity studies. If we could develop the theory for repulsive forces of the power 9, 10, 11, and 14, it is probable that with the present knowledge we could get results slightly superior to those given by the Langevin theory.

Massey and Mohr<sup>114</sup> in 1934 calculated the mobility for  $He^+$  ions in He on the basis of wave mechanics. The problem here is complex because of change of charge in the  $He^+$  ion (Kallmann-Rosen effect). They used the Majorana and Pauling interaction energy for  $He^+$  ions in He. The mobility deduced was 12, whereas the observed value is 21.4. Mott suggests that this low result may be due to an overestimate of the effect of exchange forces. In any case, it is seen that the state of knowledge as to the wave-mechanical interactions in the case of ions and molecules is at present, and perhaps will be for some time to come, *not* so satisfactory for calculations as the present kinetic theory in its more esoteric forms.

The character of the agreements may be best seen from the tables shown. Table II, taken from Powell and Brata,<sup>79</sup> gives the agreement

TABLE II

|          | Li <sup>+</sup> |       | Na <sup>+</sup> |       | K <sup>+</sup> |       | Rb <sup>+</sup> |       | Cs <sup>+</sup> |       |
|----------|-----------------|-------|-----------------|-------|----------------|-------|-----------------|-------|-----------------|-------|
|          | Obs.            | Calc. | Obs.            | Calc. | Obs.           | Calc. | Obs.            | Calc. | Obs.            | Calc. |
| Kr.....  | 4.03            | 4.03  | 2.34            | 2.42  | 1.98           | 1.98  | 1.61            | 1.58  | 1.44            | 1.47  |
| Xe. .... | .....           | 3.22  | .....           | 1.80  | 1.50           | 1.50  | 1.12            | 1.19  | 0.99            | 1.01  |

shown by the special case of the Langevin theory for point-charge alkali ions in the polarizable gases Kr and Xe. The agreement as noted before is excellent.

Table IIIA gives the mobilities observed and computed for  $Na^+$  ions in  $H_2$  and  $N_2$ . The experimental values are those of Loeb and of Tyndall and Powell.<sup>120</sup> Loeb's values are not so reliable as those of Tyndall and Powell in view of an unknown correction factor for the density changes in the gas produced by the Kunsman filament. It is seen that the solid elastic equation, assuming no attractive forces, gives a value of  $K$  between three and five times the observed. Langevin's full equation and the equation of Hassé and Cook are

equally good. The values of  $K$  are low, doubtless owing to the use of a  $D - 1$  which is too high.

TABLE IIIA

| Gas            | Observed |                           | Calculated                      |  |  |
|----------------|----------|---------------------------|---------------------------------|--|--|
|                | Loeb     | Tyndall, Probably Correct | Solid Elastic Theory, No Forces | Point Centers of Force, Hassé and Cook | Full Langevin Theory, Elastic Solid with Attractive Forces |
| H <sub>2</sub> | 17.5     | 13.6                      | 48.7                            | 10.2                                   | 10.25  |
| N <sub>2</sub> | 3.75     | 3.04                      | 14.9                            | 2.22                                   | 2.72   |

For monomolecular ions in their own gases, or as near this as possible, we have Table IIIB. Where A<sup>+</sup> in A and H<sub>2</sub><sup>+</sup> in H<sub>2</sub> could

TABLE IIIB

| Gas            | Observed                               | Calculated                          |  |
|----------------|--|-------------------------------------|--|
|                |  | Langevin                            | Hassé and Cook                                   |
| A              | K <sup>+</sup> in A 2.78               | 2.95                                | 2.68   |
| He             | 21.4                                   | 26.3                                | 29.97  |
|                |  | 21.0 corrected for change of charge | } Observed results low owing to change of charge |
| N <sub>2</sub> | 2.67                                   | 3.44                                |  |
|                |  | 2.89 corrected for change of charge |  |
| H <sub>2</sub> | Li <sup>+</sup> in H <sub>2</sub> 13.3 | 19.0                                | 18.2   |

not be given, the values K<sup>+</sup> in A and Li<sup>+</sup> in H<sub>2</sub> are given. In these two cases *no change of charge* occurs and the agreement is not bad, except for Li<sup>+</sup> in H<sub>2</sub> which is not a good substitute for H<sub>2</sub><sup>+</sup> in H<sub>2</sub> because of the mass factor. For He<sup>+</sup> in He and N<sub>2</sub><sup>+</sup> in N<sub>2</sub> the Hassé and Cook equation and Langevin's full equation are not seriously different *but both are high*. Neither theory envisages the Kallmann-Rosen effect.<sup>139</sup> This allows large momentum losses in change of charge. If the *probability* of change of charge in a kinetic gas collision is one-half, the Langevin equation value for He reduces to 21.0 in *good* agreement with observation. This probability may be too high, but it indicates that the effect produces changes of the correct order of

magnitude. Wave mechanics allows one to include the effect of change of charge, but the inadequate data as to exchange forces made this method yield unsatisfactory results. These results indicate fairly well how successful the theoretical development today is. It can be seen that it is no longer a question of cluster ion or small ion. The kinetic theory as classically developed on either one of two approximations (Langevin or Hassé and Cook) is capable of giving the mobilities within the accuracy of knowledge of the necessary gaseous and ionic parameters and within the accuracy of experiment.

Before we leave this subject, it must again be urged that for older ions the formation of complex ions, change of charge, etc., complicate the interpretation. How important these complications are is best illustrated by the results of Mitchell and Ridler<sup>120</sup> in  $N_2$ . Here the presence of Hg vapor at its normal pressure at room temperatures is able completely to "wipe out" the  $N_2^+$  ions and replace them by  $Hg^+$  ions. With the additions of Kr, Xe, or Hg in hundredths of a per cent, appreciable numbers of  $Kr^+$ ,  $Xe^+$ , and  $Hg^+$  ions appear. In this case, it is not the formation of an addition product which is active in producing the change but the ionization of Kr, Xe, and Hg (ionization potentials, 13.9, 12.1, and 10.4 volts), at the expense of  $N_2^+$  ions at 15.5 volts. The Hg present will also replace ions due to Kr and Xe, for it has the lowest ionization potential and is thus more stable. In  $N_2$ ,  $Kr^+$  are removed by Xe without removal of the  $N_2^+$ . As the ions in  $N_2$  were generated by glow discharge, in part the suppression of  $N_2^+$  ions with Hg and the other gases may also have been due to the discharge being carried largely by the atoms of lower ionization potential since these would tend to keep the electrons from getting the necessary 15.5 volts to make  $N_2^+$  ions. However, change of charge is probably as much at fault as the other action.

## 6. MOBILITIES AT LOW PRESSURES AND IN HIGH FIELDS

It is now essential to consider the question of mobilities of ions in fields where the pressure is low so that the average energy of the ions is well above the energy of the molecules of the gas. Such conditions are met with in glow-discharge plasma and in discharge tubes in general. Under such conditions the positive ions have some tenths of a volt of energy and both complex-ion formation and forces on molecules become negligible so that we can again consider a simple problem. The ions are monomolecular and sensibly forceless.  $L$  is conditioned primarily by solid elastic impacts. The mobilities may thus be derived in a fashion analogous to that used for electrons with an energy  $eU_T > MC^2/2$ , which will be discussed in a later chapter. If we assume an energy distribution which is *not widely different from the Maxwellian type*, a condition which is probably fulfilled in plasma, the solution given by Compton<sup>122</sup> suffices. This requirement is not

precisely fulfilled for the electrons, and, as will later be seen, the Compton equation is not exact for electrons. The equation deduced by Compton for ions is given in his article in the *Reviews of Modern Physics*.<sup>122</sup> In our terminology, the equation reads

$$k = \frac{0.921e\lambda_0}{(2em)^{1/2}} \left[ \frac{\Omega}{2} + \left( \frac{\Omega^2}{4} + \frac{\lambda_0^2 X^2 (M+m)^2}{5.32 Mm} \right)^{1/2} \right]^{-1/2} \\ \left[ 1 + \frac{m}{M} \frac{1}{\frac{1}{2} + \left( \frac{1}{4} + \frac{\lambda_0^2 X^2 (M+m)^2}{5.32 Mm \Omega^2} \right)^{1/2}} \right]^{1/2} . *$$

Here  $\lambda_0 = 1/\pi\sigma^2 N$  and is  $\sqrt{2} L$ , where  $L$  is the mean free path of the monomolecular forceless ion in the gas. The quantity  $\Omega$  is the thermal energy of the molecules expressed in electron volts, i.e.,  $e\Omega = \frac{3}{2} kT = \frac{1}{2} MC^2$ . When it is noted that the term

$$\frac{\Omega}{2} + \left[ \frac{\Omega^2}{4} + \frac{\lambda_0^2 X^2 (M+m)^2}{5.32 Mm} \right]^{1/2} = U_T ,$$

where  $U_T$  is the terminal energy of the ions in the gas, it is seen that the equation is not different from the Langevin<sup>110</sup> solid elastic equation for forceless ions

$$k = \frac{0.815eL}{mC} \sqrt{\frac{M+m}{M}}$$

of page 55, with the 0.815 replaced by 0.912, with  $\sqrt{eU_T} = \sqrt{m/2} C$ , and with  $\sqrt{(M+m)/M}$  replaced by the bracket

$$\left[ 1 + \frac{m}{M} \frac{1}{\frac{1}{2} + \left( \frac{1}{4} + \frac{\lambda_0^2 X^2 (M+m)^2}{5.32 Mm \Omega^2} \right)^{1/2}} \right]^{1/2} .$$

This last term is Compton's special contribution and is more accurate than the Langevin factor  $\sqrt{(M+m)/M}$  as it takes care of the "persistence of velocities." There is no reason why the equation should not be quite successful where it is supposed to apply unless the distribution law changes. It was the only equation deduced to fit these conditions until the work of Hershey, to be presented.

For the intermediate regime in which  $X/p$  becomes so large that the forces of the ions on the molecules just begin to decrease there is as yet no adequate theory. The Langevin equation with forces active is applicable just before this point. In high fields the only alteration is to increase  $U_T$  so as to make the force term negligible and to replace

\* There is a slip in Compton's equation given in his article in which  $\Omega^2$  was omitted in the denominator of the second bracket. This oversight was kindly pointed out by W. R. Haseltine.

$\sqrt{(M+m)/M}$  by the bracketed term of Compton above. In fact, the full Langevin equation goes over to a solid elastic equation when  $\lambda$  is about 3 and the equation is essentially a solid elastic equation above  $\lambda = 3$ . Thus keeping the Langevin equation as it is and including the change in  $\lambda$  due to the field  $X$  is quite legitimate. At low fields the Compton mass factor is identical with the factor,  $\sqrt{(M+m)/M}$ . We can, therefore, estimate that the general behavior of  $k$  in this region will be given approximately by

$$k = \frac{3}{16 Y_1} \frac{0.462 \sqrt{1 + \frac{m}{M} \frac{1}{2 + \left\{ \frac{1}{4} + \frac{\lambda_0^2 X^2 (M+m)^2}{5.32 M m \Omega^2} \right\}^{1/2}}}}{\frac{\rho}{\rho_0} \sqrt{(D-1)_0 m_0}}$$

Here  $m_0$  is the molecular weight of the ion, and  $3/16 Y_1$  takes its value from Langevin's curve for the argument  $\lambda_1$  given by

$$\lambda_1 = \sqrt{\frac{(D-1)_0 e^2}{8\pi p_1 S^4}} = \sqrt{\frac{3(D-1)_0 e^2}{8\pi N_0 S^4 (U_i) e}}$$

The reason for this change is that, while at low energies  $MC^2 = (2\Omega)e$  was taken for the relative kinetic energy of ion and molecule, the relative energy in higher fields is the sum of the terminal energy of the ion plus the energy of agitation of the molecules. The value of  $U_i$  is determined by the field and reads

$$U_i = \frac{\Omega}{2} + \left[ \frac{\Omega^2}{4} + \frac{\lambda_0^2 X^2 (M+m)^2}{5.32 M m} \right]^{1/2}.$$

It is seen that the effect of these changes is to keep  $k$  constant at low values of  $X\lambda_0$ , i.e.,  $X/p$ . When, however, the terms in  $X\lambda_0$  approach the point where they become comparable with  $\Omega$  then the quantity  $\lambda_1$  increases.  $3/16 Y_1$  at first increases, increasing  $k$ , and then eventually the term  $3/16 Y_1$  and the term in brackets cause the value of  $k$  to decrease. Thus far the increase only has been noted by Mitchell and Ridler and both increase and decrease in  $H_2$ ,  $N_2$ , He, and A with  $K^+$  ions by Hershey.

The urgent need for experimental data in the regions of high  $X/p$  induced the author in 1932 to initiate experiments in this direction. A canvass of existing methods of mobility measurement indicated that for the high velocities of the ions at high  $X/p$  there were at the time no satisfactory methods. The experiments of Mitchell and Ridler<sup>120</sup> have since shown the limitations of the Tyndall and Powell method. Square-wave alternating potentials of adequate frequency,  $\sim 10^6$  cycles, were not available, although, thanks to new tube techniques, we are likely to realize them in the near future. The

only hope lay in the use of the Townsend deflection method which had proved so useful for electrons; see page 26 and Fig. 24. To this end a large water-cooled solenoid was built and the work was initiated by Dr. Gladys Finney. Circumstances having forced her to abandon this work, it was subsequently undertaken by Dr. A. V. Hershey. Preliminary results were obtained with the coil and reported by Hershey.<sup>134</sup> When the coil eventually burned out the whole apparatus was reconstructed by Hershey.

The magnetic field was obtained from the discarded core of the first million-volt cyclotron of Professor Lawrence. It had pole pieces 28 cm in diameter with a 10-cm gap. The current from an 800-ampere 6-volt generator was run through eight coils of  $\frac{3}{4}$ -inch copper tubing which were water cooled. The generator was controlled by a specially designed thyatron regulator devised by Hershey, which reduced the field fluctuations to less than 0.1 per cent. The field was calibrated by a specially constructed flip coil. The field was uniform at the center to better than 0.2 per cent over the whole length of the gap. It was constant within 2 per cent at 8 cm radially from the center

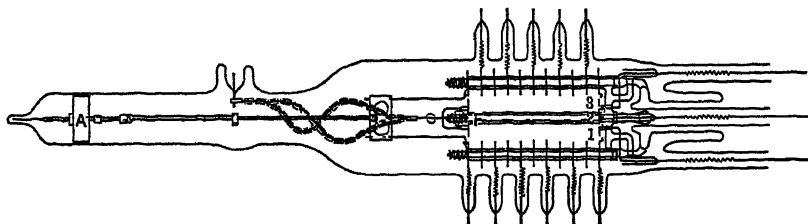


FIG. 33.—Hershey's Mobility Chamber.

at all distances from the pole pieces. The electrical accelerating field was maintained constant in the apparatus to 0.1 per cent by means of a modified Evans voltage stabilizer. The chamber used was constructed with extreme care and was housed in an all-glass system shown in Fig. 33. The  $K^+$  ions were generated by means of a heated filament coated with a Kunsman catalyst prepared from the purest chemicals by Hershey.<sup>135</sup> They emerged through a slit *F* in their housing chamber, which could be raised or lowered by electromagnetic control operating on the lug *A* from the outside. The field was maintained uniform by means of brass guard rings. The carefully spaced receiving electrodes are numbered 1, 2, and 3. The metal used was largely brass. The whole chamber and the purifying and vacuum system could be moved about. The chamber was removed from the region of the pole pieces, introduced into a furnace outgassed at 400°, filled with gas, and then reinserted into the magnet.

The filament was 1 cm long and 1 mm wide. The guard rings were 0.065 cm thick had a diameter of 7.87 cm and a hole of 3.55-cm diam-

eter inside. They were spaced about 0.92 cm apart. The center collecting plate was 1.0161 cm wide with slits 0.043 cm wide. The distance from the collecting plate to the farthest guard ring, indicated as flush with the source  $F$  in the figure, was 9.867 cm. Calculations of the field distortions due to the finite distance between guard rings showed that the error in the regions traversed by the beam were negligible. Corrections were made for the finite width of the slits between collectors 1, 2, and 3. The gases used were prepared by the best standard techniques available today. The nature of the ions could be determined by evacuating the chamber and making an  $e/m$  determination on the ions. The molecular weight showed the ions to be the ions  $K^+$  with less than 1 per cent of contamination. An elaborate study was made of the effect of the filament on the gas temperatures in the chamber. The result gave the difference in temperature between the guard rings and the gas along the axis as  $2.5^\circ C$  in  $H_2$  at the highest pressure 2.75 mm and  $3.5^\circ$  in He at 3.9 mm pressure at 5 cm from the filament. In  $N_2$  and Ar it was about  $1^\circ$ . The total correction for the change in density of the gas was thus at most of the order of 1 per cent.

The theory of the Townsend deflection method discussed on page 27 gives  $\tan \theta = Hk/C$ , where  $\theta$  is the angle of deflection and  $C$  is  $10^8$  if  $H$  is the average magnetic field in gauss and  $k$  is the mobility in cm/sec per volt/cm. An analysis of the path of the ions indicated that near their source the path is cycloidal before they reach their terminal velocity. As they acquire a terminal velocity the path becomes a straight line whose slope defines  $\tan \theta$ . The straight line thus does not intercept the source, and the two lines from the slit defining  $2\theta$  then intercept the axis above the source. The distance between intercept and source is  $y_0$ . The true value of  $\tan \theta$  is then  $(a/2)/(y - y_0) = Hk/C$ , where  $y$  is the length of the line from the collector to the intersection of the line defining  $\tan \theta$  with the axis of the tube, and  $a$  is the distance between the slits. If  $H$  is measured for two values of  $y$ ,  $y_1$ , and  $y_2$ , then  $y_0$  can be solved for and eliminated. Hence we have the mobility given by

$$k = \frac{\frac{a}{2} C (H_1 - H_2)}{(y_2 - y_1) H_1 H_2}.$$

On this basis, with all the corrections included, the values of the mobility constant  $K$ , derived from  $k$  and corrected for density, are plotted against  $X/p$  in Figs. 34, 35, 36, and 37, which were obtained for the gases  $H_2$ ,  $N_2$ , He and A respectively.<sup>135,38</sup> The values are indicated as crosses, dots, and circled points connected by full lines for various pressures within the limits to be achieved with the apparatus. In A and  $N_2$  the highest pressures achieved were 0.7 mm, and in  $H_2$



and He they were 2.7 and 3.8 mm respectively. These limits are set by the values of  $k$ , the geometry of the apparatus, and the field.

It is at once seen that, contrary to expectation, while  $K$  was a function of  $X/p$  it appeared to vary with  $p$  at the lower pressures. The values at higher pressures,  $p$ , appear to approach a common limit which is fairly high. The curves for lower values of  $p$  all fall short of

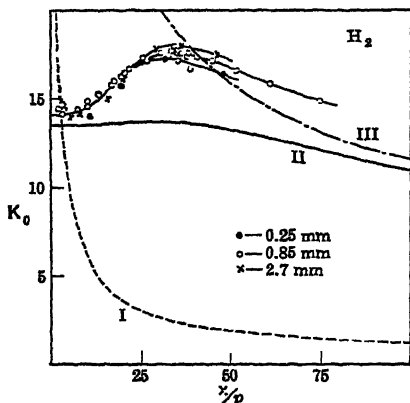


FIG. 34.

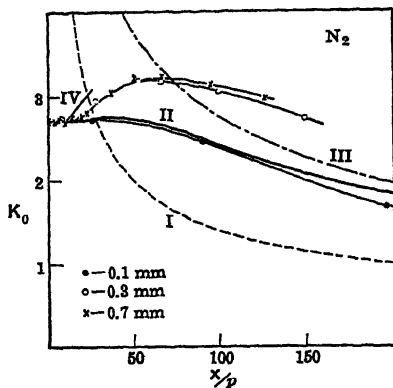


FIG. 35.

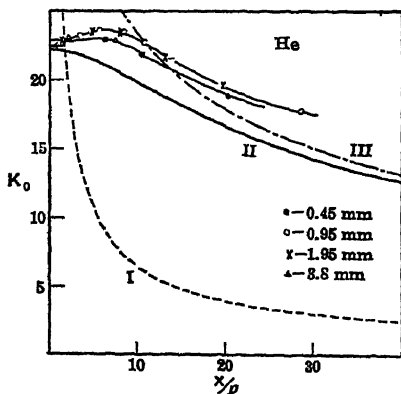


FIG. 36.

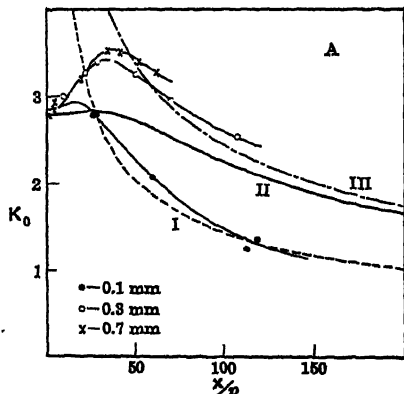


FIG. 37.

the upper limit and do so increasingly rapidly as  $p$  decreases. On the basis of all theory the mobility constant  $K$  should be a function of  $X/p$  and should be *independent* of  $p$ . It should thus be the same for all pressures. The observed spread of values with  $p$  is greatest for the gases of higher molecular weight. It is in general to be expected that at low pressures the term mobility will become meaningless since the ions do not acquire their terminal velocities in a sufficiently short

distance. At 0.1-mm pressure the ionic free paths begin to approach values between 0.1 and 1 mm in length. Hence it is not inconceivable that the terminal velocities may not be reached in the 10–100 collisions made in their first centimeter or two of path. It is improbable, however, that this effect is very serious at the higher pressures of about 1 mm in the apparatus used. The fact that the pressure variation observed at lower pressures is of an instrumental nature is indicated by the effect of moving the source nearer the collectors. Thus in moving the filament from 10 cm to within 5 cm of the collector the value of  $H$  required should be about twice as great. It was, in fact, observed to be much less at low pressures. For example, in one experiment in A at 0.096 mm pressure it was 1.53 times as great. This discrepancy disappears at higher pressures. The conclusion is that, for some reason connected with ionic behavior, when the free paths are long the measurement of  $k$  at too low pressures in this apparatus is meaningless, since the basic assumptions made in the deduction do not apply.

The results at the higher pressures are probably nearly correct, being *slightly* too low if anything at the higher  $X/p$ . At the lower values of  $X/p$ , however, the values of  $K$  for all gases are remarkably close to the values observed by Tyndall<sup>133, 38, 46</sup> and Powell, Powell and Brata,<sup>79</sup> and Mitchell and Ridler<sup>120</sup> for  $K^+$  in these gases. These values are indicated by the arrows at the left of the figures in all cases. This agreement should give us confidence in the method as regards yielding approximately proper values of the mobility at higher pressures. In fact, the great care used by Hershey has resulted in showing that the deflection method is capable of giving results for ions good to 1 or 2 per cent in the higher pressure range. It is now essential to compare the observed variation with theory. The theory of Compton<sup>122</sup> just given with slightly altered constants to be discussed leads in each case to the dashed curves marked I in each figure. It shows neither the rise observed by Mitchell and Ridler in the case of  $K^+$  in  $N_2$  indicated by the full line marked IV nor the more gradual rise indicated by Hershey's results. The modification of the Compton equation suggested by the writer on page 73, showed a slight rise near the origin but was not much more successful than Compton's equation on which it was built. Accordingly Hershey investigated the problem anew. As a result he developed a more satisfactory approximate theory which merits being given since it goes about as far as one can go with our present knowledge in the face of nearly insuperable mathematical difficulties. The detailed mathematical steps will be omitted, but a summary of Hershey's<sup>88</sup> work as presented in his thesis will be reproduced, with his permission. His statement is as terse as it can be made. His symbols are modified to agree with the notation in this book as far as possible.

The variation of mobility with increasing  $X/p$  may be explained

qualitatively in terms of the forces acting between the ions and molecules. Were the ions and molecules simple elastic spheres, the mobility would be two or three times higher than that observed. The mean free path, and hence also the mobility, is lowered by forces of attraction arising from polarization of the molecules by the charged ions, and from van der Waals forces. As the ions are speeded up, the attractive forces become less effective, and the ions smash into the molecules as though they were solid elastic spheres. The initial rise in mobility may be interpreted as the result of a decrease in the effectiveness of the attractive forces. The presence of peaks in the curves of  $H_2$ ,  $N_2$ , and A may be associated with the greater polarizability of these gases.

The subsequent decrease in mobility occurs when the drift velocity possessed by the ions is greatly in excess of the thermal velocities of the molecules. The rate at which the ions lose momentum is proportional to the product of their momentum, the fractional loss of momentum on collision, and the frequency of collision. Since they act essentially as solid elastic spheres, the collision cross section is essentially constant. The collision frequency is proportional to the product of the collision cross section and the velocity. The rate of loss of momentum is therefore proportional to the square of the velocity, and the mobility varies inversely as the square root of  $X/p$ . At low field intensities the collision frequency is determined primarily by the temperature, and is therefore independent of drift velocity. The rate of loss of momentum is directly proportional to the velocity, and the mobility is independent of  $X/p$ .

The equation of Compton<sup>122</sup> which was discussed on page 72 may be derived on the same basis as Langevin's solid elastic equation, and it takes the form

$$k = \frac{0.815\lambda_0 e}{(2em)^{1/2}} \frac{\left[ 1 + \left( \frac{m}{M} \right) \frac{1}{\frac{1}{2} + \left\{ \frac{1}{4} + \frac{\lambda_0^2 X^2 (M+m)^2}{6.02 \Omega^2 M m} \right\}^{1/2}} \right]^{1/2}}{\left[ \frac{\Omega}{2} + \left\{ \frac{\Omega^2}{4} + \frac{\lambda_0^2 X^2 (M+m)^2}{6.02 M m} \right\}^{1/2} \right]^{1/2}}.$$

Here the constant 0.912 given by Compton is replaced by 0.815, and the constant 5.32 is replaced by 6.02. It is not applicable to potassium ions in light gases, however, since it is based on the assumption that the ion random energy far exceeds the drift energy. On the contrary, the random energy is less than the drift energy. The formula gives too low a mobility, since it assumes too high a collision frequency. In Figs. 34 to 37 the curves labeled I are a plot of the formula of Compton. The discrepancy between the theory and experiment amounts to nearly a factor of 10 in  $H_2$ , but diminishes as the molecular weight of the gas is increased.

An ideal theoretical treatment of the problem of ion mobility would consist of the direct solution of Boltzmann's equation, which applies the laws of continuity to the motion of ions in momentum and coordinate space. This may some day be accomplished through the equations published by Pidduck in 1915. He was able to effect one of the five integrations involved, and transformed the Boltzmann equation into another integral equation of a more tractable form. The problem is exceedingly complex. In the absence of a direct solution of Boltzmann's equation, a simple approximate distribution function may be selected, and the parameters contained in it may be so adjusted that the equation is satisfied in the mean. For example, let the ions have a Maxwellian distribution about the drift velocity. Such a distribution is expressed by the equation

$$f_1 = \frac{n_1}{(2\pi m_1 k T_1)^{3/2}} e^{-\frac{(p_1 - m_1 v)^2}{2m_1 k T_1}}, \quad (1)$$

in which  $f_1$  is the number of ions per unit volume of momentum space,  $m_1$  is the ionic mass,  $n_1$  is the number of ions per unit volume of coordinate space, and  $p_1$  is the vector momentum. In the distribution function,  $f_1$ , there are two parameters, the drift velocity  $v$  and the ion temperature  $T_1$ . These may be evaluated by a momentum balance and by an energy balance. The distribution function of the molecules is expressed by the equation

$$f_2 = \frac{n_2}{(2\pi m_2 k T)^{3/2}} e^{-\frac{p_2^2}{2m_2 k T}}, \quad (2)$$

in which  $f_2$  is the number of molecules per unit volume of momentum space,  $m_2$  is the molecular mass,  $n_2$  is the number of molecules per unit volume of coordinate space, and  $p_2$  is the vector momentum.

Substitution of the distribution functions into the balance equations, and performance of five of the six integrations, lead to the rate of gain of momentum by an ion,  $\partial p_1 / \partial t$ , and to the rate of gain of energy,  $\partial w_1 / \partial t$ . They are expressed by the equations

$$\frac{\partial p_1}{\partial t} = -\frac{8}{\sqrt{\pi}} \frac{m_1 k T + m_2 k T}{m_1 + m_2} n_1 n_2 \Sigma_1 + n_1 e X = 0 \quad (3)$$

and

$$\begin{aligned} \frac{\partial w_1}{\partial t} = & -\frac{8}{\sqrt{\pi}} \frac{n_1 n_2 v}{m_1 + m_2} \left\{ \frac{m_1 m_2}{m_1 + m_2} k(T_1 - T) \Sigma_2 + m_1 k T \Sigma_1 \right\} \\ & + n_1 e v X = 0 \quad (4) \end{aligned}$$

The first term of each represents the contribution from impacts between ions and molecules, and the second term represents the con-

tribution from the field.  $\Sigma_1$  and  $\Sigma_2$  are integrals. They are expressed by the equations

$$\Sigma_1 = \int_0^\infty e^{-\xi^2 - \lambda^2} \frac{1}{2\lambda\xi} (\cosh 2\lambda\xi - \frac{1}{2\lambda\xi} \sinh 2\lambda\xi) Q(\lambda) \lambda^4 d\lambda \quad (5)$$

and

$$\Sigma_2 = \int_0^\infty e^{-\xi^2 - \lambda^2} \frac{1}{(2\lambda\xi)^2} \sinh 2\lambda\xi Q(\lambda) \lambda^6 d\lambda. \quad (6)$$

$Q(\lambda)$  is the collision cross section for the transfer of momentum.  $\xi$  and  $\lambda$  are defined by the equations

$$\xi^2 = \frac{m_1 m_2 v^2}{2(m_1 kT + m_2 kT_1)}$$

and

$$\lambda^2 = \frac{m_1 m_2 v_{12}^2}{2(m_1 kT + m_2 kT_1)}.$$

$v_{12}$  is the relative velocity between an ion and a molecule.

If  $\xi$  is made very small, equations 3 and 4 are reduced to the equation

$$v = \frac{Xe \sqrt{\frac{m_1 + m_2}{m_1 m_2}}}{\frac{4}{3} \sqrt{2\pi kT} \frac{2}{\pi} \int_0^\infty Q(\lambda) e^{-\lambda^2} \lambda^5 d\lambda}.$$

An equivalent equation was published by Langevin.<sup>111</sup> In fact, his theory is a special case. He proceeded to evaluate  $Q$  for a model consisting of elastic spheres attracting with a force which varies inversely as the fifth power of the distance of separation. Assuming that the force arose solely from polarization, he expressed it in terms of the dielectric constant  $D$  of the gas. He gave another equation for the drift velocity, which was equivalent to the equation

$$v = \frac{XA \sqrt{\frac{m_1 + m_2}{m_1}}}{\sqrt{\rho} \sqrt{D - 1}} \quad (\text{see page 65}),$$

in which  $\rho$  is the density of the gas. He plotted the coefficient  $A$  as a function of a parameter  $\frac{1}{\lambda_1}$  which was defined by the equation \*

$$\frac{1}{\lambda_1} = S^2 \sqrt{\frac{8\pi p}{(D - 1)e^2}} \quad (\text{see page 65}),$$

\*  $\lambda_1$  is not to be confused with the  $\lambda$  above.

in which  $S$  is the sum of the radii of ion and molecule. Langevin's theory was checked, and accurate values of  $Q$  and  $A$  were later computed by Hassé.<sup>118</sup>

The general theory may be made into an extension of Langevin's theory by redefining  $1/\lambda_1$  by the general equation

$$\frac{1}{\lambda_1} = S^2 \sqrt{\frac{8\pi p}{(D-1)e^2}} \sqrt{\frac{m_1 kT + m_2 kT_1}{kT(m_1 + m_2)}}. \quad (7)$$

Equations 3 and 4 are then transformed into the three equations

$$A = \frac{\frac{1}{2}\pi S^2 \lambda_1 \xi}{\Sigma_1} = \frac{v}{X} \sqrt{\rho} \sqrt{D-1} \sqrt{\frac{m_1}{m_1 + m_2}}, \quad (8)$$

$$\frac{\Sigma_1}{\Sigma_2 - \Sigma_1} = \frac{m_1 k(T_1 - T)}{m_1 kT + m_2 kT_1}, \quad (9)$$

and

$$B = \frac{\frac{1}{(\xi)^2} \Sigma_1}{\Sigma_2 - \Sigma_1} = \frac{2k(T_1 - T)}{m_2 v^2}. \quad (10)$$

$A$  and  $B$  are plotted in Figs. 38 and 39 as functions of  $\frac{m_1 k(T_1 - T)}{m_1 kT + m_2 kT_1}$ .

To obtain them it was necessary to calculate  $\Sigma_1$  and  $\Sigma_2$  by numerical integration. Hassé's values were used for the collision cross section  $Q$ .

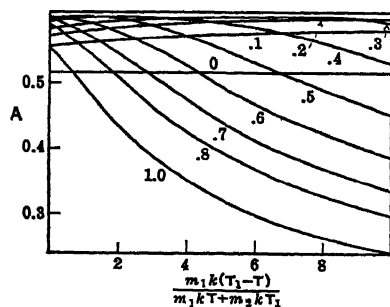


FIG. 38.

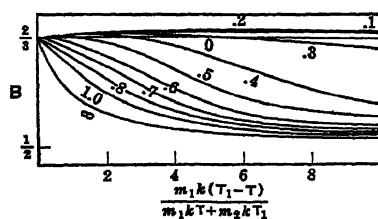


FIG. 39.

Before the theory can be compared with experiment, values of  $S$  and  $D$  must be selected. They should not be taken from measurements of diffusion, viscosity, or the dielectric constant of the gas. Van der Waals' forces and limitations on the polarizability of the molecules may be expected to make  $S$  and  $D$  differ materially from their field-free values. In the absence of more accurate knowledge of the law of force, the mobility itself may be used as a source of information. Those values of  $S$  and  $D$  were found by trial, which brought Langevin's theory into the closest agreement with the measurements by the

Tyndall and Powell method. The theory and experiment are compared in Figs. 40 and 41.

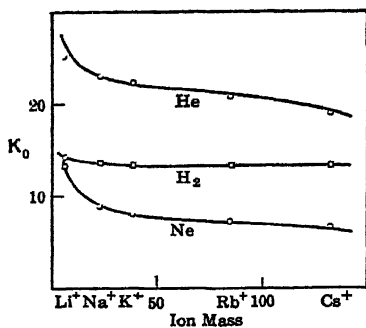


FIG. 40.

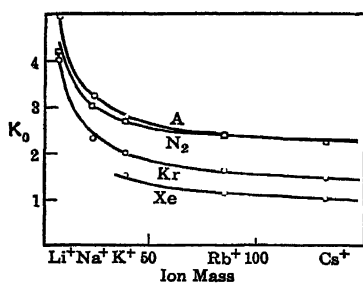


FIG. 41.

The chosen radii in Å are:

TABLE IVA

| He              | Ne              | A              | Kr              | Xe              | H <sub>2</sub> | N <sub>2</sub> |
|-----------------|-----------------|----------------|-----------------|-----------------|----------------|----------------|
| 1.00            | 1.50            | 1.55           | 1.60            | 1.85            | 1.05           | 1.65           |
| Li <sup>+</sup> | Na <sup>+</sup> | K <sup>+</sup> | Rb <sup>+</sup> | Cs <sup>+</sup> |                |                |
| 0.45            | 1.35            | 1.40           | 1.50            | 1.80            |                |                |

The values of  $D$  at 0° C are:

TABLE IVB

|              | He        | Ne       | A        | Kr       | Xe      | H <sub>2</sub> | N <sub>2</sub> |
|--------------|-----------|----------|----------|----------|---------|----------------|----------------|
| Computed $D$ | 1.000052  | 1.000106 | 1.00063  | 1.00091  | 1.00148 | 1.00028        | 1.00082        |
| Observed $D$ | 1.0000665 | 1.000123 | 1.000504 | 1.000768 | 1.00124 | 1.000252       | 1.000589       |

In He, the value of  $D$  is smaller than the dielectric constant, and in A and N<sub>2</sub> it is larger. The polarizability of the He atom is probably limited as a result of its small size, and the polarization forces in A and N<sub>2</sub> are likely augmented by van der Waals forces.

Values of the mobility were calculated by the extended Langevin theory. They are represented in Figs. 34 to 37 by the curves labeled II. Values of the mobility were also calculated on the assumption that there were no attractive forces by setting  $Q$  equal to  $\pi S^2$ . They are represented by the curves labeled III. The effect of attractive forces may be seen by a comparison between curves II and III.

Subsequent analysis by Hershey using the Hassé and Cook procedure with attractive forces of the inverse fifth power type and repulsive forces of the inverse ninth power type has shown that one gets curves analogous to those obtained above except that the curves have maxima that are higher than those observed. Thus the observed curves are bracketed between the theory of Langevin assuming solid elastic impacts and those assuming an inverse ninth power repulsive law in analogy to the variation of  $k$  with temperature. The deviations from the inverse ninth power law mobility curve were greatest for He and least for A, as they should be. Here again we see that within the limitations of our knowledge of the actually existing force laws in individual gases the theory is adequate to explain the results. It is not unreasonable to suppose that with a better choice of the distribution function and the use of proper force laws the theory can be made to fit within experimental error.

## 7. MOBILITY EQUATIONS OVER AN EXTENDED RANGE OF ION SIZE

Before leaving the subject of mobilities one may answer a question that is frequently raised. How do the ions which are created by capture of charges by droplets and particles move in an electrical field. This problem is one of increasingly great industrial application in air conditioning, dust and fume removal, oil cleansing, and ore recovery by electrical processes. Millikan<sup>131</sup> long ago showed that small charged particles (preferably spherical) moving in a gas under a field or under gravity obey Stokes's law. This says that the force required to give a particle a constant velocity  $v$  in the presence of the viscous drag is  $F = 6\pi\eta av$ , where  $a$  is its radius and  $\eta$  is the coefficient of viscosity. If  $F = Xe$  due to the field  $X$  acting on the charge  $e$ , then  $Xe = 6\pi\eta av$ , and  $k = v/X = e/(6\pi\eta a)$ . This mobility equation makes  $k$  proportional to  $e$ , to  $1/\eta$ , and to  $1/a$ . The equation holds until  $a$  becomes so small that it is comparable with the ionic free path. At this point, a semi-empirical correction due to Cunningham must be used. It has been verified by Millikan<sup>131</sup> and others. This says that  $F = 6\pi\eta av / \left(1 + A \frac{L}{a}\right)$ , where  $L$  is the mean free path and  $A$  from Millikan's work is a constant of value 0.874. The correction is due to the fact that for a fraction of its path the particle is moving freely. Therefore,

$$k = \frac{e}{6\pi\eta a} \left(1 + A \frac{L}{a}\right).$$

For particles whose dimensions begin to be of the order of  $10^{-5}$  cm at N.T.P.,  $L/a$  can no longer be neglected. As the particles get still smaller,  $AL/a$  becomes much greater than 1 and the expression for  $k$



becomes  $k = AeL/6\pi\eta a^2$ . Now from kinetic theory  $\eta = 0.5 NM\bar{c}L$  and

$$k = \frac{AeL}{3\pi NM a^2 \bar{c}L} = A \frac{e}{M\bar{c}} \frac{1}{3\pi Na^2}.$$

Since  $A = 0.874$  and  $\bar{c} = 0.922 C$ ,

$$k = 0.95 \frac{e}{MC} \frac{1}{3\pi Na^2}.$$

If the droplet is large compared to the molecule but small compared to the free path,  $a$  is equivalent to the mean collision distance  $S$ . Hence, since for such large particles  $L = 1/(\pi S^2 N)$ ,  $1/(3\pi Na^2)$  is equivalent to  $L/3$ , and  $k = 0.32 eL/(MC)$ . It is seen that this, except for the mass factor  $\sqrt{(M+m)/m}$ , which for large  $m$  is about 1, and a different constant, is the solid elastic mobility equation with no forces acting. Had the equation been deduced directly, as was Langevin's, instead of from Stokes's law, the constant would have been different. The significance of the terms appearing in these equations changes under different conditions such as collision radius, and the correction for the relative velocity of the ion and molecules. Thus if  $a \gg \sigma_M/2$  we can set  $1/(3\pi Na^2) = L/3$ , for then  $S = a + \sigma_M/2$  is not very different from  $a$  and the  $\sqrt{2}$  can be omitted from  $L$  as the relative velocity correction is absent. When  $a = \sigma_M/2$ ,  $S = 2a = \sigma_M$ ,  $1/(3\pi Na^2) = (4\sqrt{2}/3)L$ , and the factor  $\sqrt{(M+m)/m}$  becomes greater than 1. If then attractive forces begin to be active,  $L$  must again be re-interpreted in terms of the forces instead of the solid elastic  $L = 1/(\sqrt{2}\pi S^2 N)$  and its assumed momentum loss by impact only. The result of this is an equation of the type

$$k = \frac{0.815e}{MC} \frac{1}{\sqrt{2}\pi S^2 N} \frac{\sqrt{(M+m)/m}}{0.98 \left\{ \frac{(D-1)e^2}{\pi NS^4 MC^2} \right\}^{1/2}} = \frac{0.235 \sqrt{(M+m)/m}}{\rho_0 \sqrt{(D-1)_0 M_0}},$$

the "small-ion" form of Langevin's equation. It is thus seen that essentially physically, and therefore dimensionally, the mobility equation is consistently the same sort of equation for particles extending from macroscopic to atomic dimensions. All that changes in these equations is the precise interpretation of such concepts as viscous drag, the mean free path, factors involved in the persistence of velocities, and numerical coefficients obtained by averaging. These change with changing conditions modifying the equations in detail. The equations are not contradictory or inconsistent. Each applies to its own regime with transition forms from one regime to the other. Some of these must be empirical or semi-empirical because of the involved character of the interactions. As in nature these conditions merge continuously into each other, accordingly the relations express-

ing the changes must also merge. This is nicely exemplified above. With this understanding of the problem of the ionic mobility, we can leave this subject secure in the knowledge that it is basically clear though requiring much more work for accuracy in detail.

### 8. REFERENCES FOR PART C, CHAPTER I

109. L. B. LOEB, *Kinetic Theory of Gases*, 2nd Edition, sections 103–106 incl.; K. PRZIBRAM, *Handbuch der Physik*, sections 38 to 46 incl.; J. J. THOMSON, *Conduction of Electricity in Gases*, 3d. Edition, pp. 165–189.
110. P. LANGEVIN, *Ann. chim. phys.*, 28, 317, 495, 1903; 5, 245, 1905; H. F. MAYER, *Ann. Physik*, 62, 358, 1920; K. T. COMPTON, *Rev. Modern Phys.*, 2, 210–218, 1930.
111. P. LANGEVIN, *Ann. chim. phys.*, 8, 238, 1905.
112. SUTHERLAND, *Phil. Mag.*, 18, 341, 1909; E. M. WELLISCH, *Phil. Trans.*, A 209, 249, 1909.
113. HASSÉ and COOK, *Phil. Mag.*, 12, 554, 1931.
114. MASSEY and MOHR, *Proc. Roy. Soc.*, A 144, 188, 1934.
115. L. B. LOEB, *Kinetic Theory*, 2nd Edition, p. 221 ff.
116. J. J. THOMSON, *Phil. Mag.*, 47, 337, 1924.
117. L. B. LOEB, *Phil. Mag.*, 48, 446, 1924; 49, 517, 1925.
118. H. R. HASSÉ, *Phil. Mag.*, 1, 139, 1926.
119. L. B. LOEB, *Kinetic Theory*, 1st Edition, section 108, p. 460.
120. MITCHELL and RIDLER, *Proc. Roy. Soc.*, A 146, 916, 1934; A 134, 135, 1931.
121. L. BRATA, *Proc. Roy. Soc.*, A 141, 454, 1933.
122. K. T. COMPTON, *Rev. Modern Phys.*, 2, 210–218, 1930.
123. L. B. LOEB, *Kinetic Theory of Gases*, 2nd Edition, p. 214.
124. L. B. LOEB, *Kinetic Theory of Gases*, 2nd Edition, p. 228.
125. L. B. LOEB, *Kinetic Theory of Gases*, 2nd Edition, pp. 198–199.
126. L. B. LOEB, *Kinetic Theory of Gases*, 2nd Edition, p. 578.
127. HASSÉ and COOK, *Phil. Mag.*, 12, 554, 1931.
128. A. P. ALEXIEVSKY, *Phys. Rev.*, 27, 811, 1926.
129. HASSÉ and COOK, *Proc. Roy. Soc.*, A 125, 196, 1929.
130. TYNDALL and POWELL, *Proc. Roy. Soc.*, A 136, 145, 1932; L. B. LOEB, *Phys. Rev.*, 38, 549, 1931.
131. R. A. MILLIKAN, *The Electron*, Chicago, 1917, p. 95 ff. See also *Electrons (+ and -), Protons, Photons, Neutrons, and Cosmic Rays*, Chicago, 1936, Chap. V.
132. P. E. SHAW, *Proc. Roy. Soc.*, A 122, 49, 1928.
133. A. M. TYNDALL, *Mobility of Positive Ions in Gases*, Cambridge Physical Tracts, Cambridge Press, Cambridge, 1938, p. 72.
134. A. V. HERSHEY, *Phys. Rev.*, 51, 146, 1937.
135. A. V. HERSHEY, *Phys. Rev.*, 54, 237, 1938.
136. PIDDUCK, *Proc. London Math. Soc.*, 15, 89, 1915.
137. See Loeb, *Atomic Structure*, John Wiley and Sons, New York, 1938, pp. 287 and 324.

## CHAPTER II\*

### RECOMBINATION OF IONS

#### 1. INTRODUCTION

In 1896 J. J. Thomson and Rutherford<sup>1</sup> observed that a gas ionized by X-rays, if left to itself, lost its charge with time. Part of this loss of charge was known to be due to diffusion of the ions to the walls, but the larger proportion appeared to be due to a recombination of positive and negative charges in the body of the gas. In 1897 Rutherford<sup>2</sup> confirmed this belief by measuring the disappearance of ions due to recombination in a stream of gas ionized at one point by X-rays. By measurement of the loss of ions at various points downstream the time rate of recombination was determined. The air-blast method was later used by McClelland<sup>3</sup> and Townsend.<sup>4</sup> The method, however, is not satisfactory, as will later be seen, and much more accurate measurements are now available. It nevertheless sufficed to indicate that the initial inferences of Rutherford and Thomson were correct. As the subject developed, it appeared that the phenomenon of recombination presented an exceedingly complex and very troublesome problem requiring refinements of measurement even beyond modern techniques. The general problem has now reached a stage in its development where its fundamental nature is becoming fairly clear.

#### 2. TYPES OF RECOMBINATION

Before attempting to consider the methods of measurement and the results achieved, one must arrive at a clear understanding of what is implied by the term recombination. The term ion being used in the broadest sense of the word to designate an electrical carrier, be it an electron or a massive charged droplet or particle, recombination implies the combination of negative and positive ions present in a mass of gas to give neutral particles. The significance of the prefix "re" comes from the fact that, in the case of ions of both signs in gases, the charges initially are produced by the ionization of neutral molecules, the union of the ions of opposite sign constituting a *recombination* of the carriers to the original neutral particles.

The term as used in this general fashion leads to some difficulties, inasmuch as it implies by its definition and basic equation a similarity

\* References for Chapter II will be found on page 159.

of the recombination processes under various conditions whereas in reality the processes involved differ materially. That this must be so follows at once from the wide difference in nature of the carriers and the conditions in which ion formation leaves them. Thus it must be at once clear that the process by which a free electron combines with either its parent positive ion or another positive ion will differ radically from the process by which a charge transfers from a normal negative gaseous ion to a normal positive gaseous ion. This process may again be different from the contact process by which two Langevin ions neutralize their charges. This, however, is not all. Conditions of ionization, electron attachment, etc., produce very diverse situations in which an electron may recombine *preferentially with its own positive ion*, or where it will usually *combine only with some other positive ion*. Again, ionization does not result in a uniform distribution of ions of both signs; at times the ions *are created in adjoining pairs*; at other times they *may be distributed along paths or columns*. Each of these varied distributions of different types of carriers ultimately results in recombination. The mechanism and characteristic constants of the process are, however, in each case different and require separate treatment. Hence today we may under the general process of recombination refer to *electron recombination, initial recombination, preferential recombination, columnar recombination, and volume recombination*. It is possible that eventually one may have to distinguish between preferential electron recombination and volume electron recombination, the preferential being recombination where the electron returns to its parent positive ion and volume where it returns to some other positive ion.

The *electron recombination* occurs usually only at *lower pressures* and at *high ion densities*, such as in arcs and in the plasma of discharge tubes. It is an improbable process and apparently does not account for much loss of ions. The *volume recombination* between ions is the normal process and occurs for *ions randomly distributed in space* appearing usually in equal numbers. It is the type usually assumed but actually observed only under special conditions, hence many of the discordant interpretations of results. *Initial recombination* occurs when ionization by X-rays or other agents takes place at *atmospheric pressures in gases forming negative ions readily*. It is due to the *initial creation of ions in pairs of opposite sign so far apart that preferential recombination does not occur* but sufficiently close that the distribution is not random. It goes over to volume recombination by diffusion some time after the ionizing act. *It becomes preferential recombination at very high pressures*. *Columnar ionization* such as in the dense tracks of  $\alpha$  particles also leads to a special type of recombination process. Where *electrons form ions so close to the parent atom that the ion and electron ultimately recombine*, one has *preferential recombination*. Finally, it may be possible that the recombination of large Langevin ions so differs from

that of normal ions in volume recombination that it constitutes a further mechanism. This, however, does not appear to be the fact.

### 3. DEFINITION OF THE COEFFICIENT OF RECOMBINATION AND ITS FUNDAMENTAL RELATIONS

For quantitative study, the process of recombination of ions is described by a constant characteristic of the process called the *coefficient of recombination*. The experimental evaluation of this constant and its theoretical interpretation form the basis of this chapter. For the sake of simplicity in its study and in the analysis of the problem, the definition of the coefficient of recombination was made on the assumption of an *idealized recombination process* characteristic of simple volume recombination. Thus, recombination has been studied experimentally and theoretically in terms of this natural but idealized concept. Since the various factors entering into recombination in general are usually not in conformity with this idealized process, the *rather surprising behavior of the idealized coefficient* inferred from experiment has led to considerable confusion.

Actually the basic equation defining recombination is the same, irrespective of the process. *It is thus always possible to evaluate a coefficient of recombination.* This coefficient one unsuspectingly treats as the idealized concept only to discover that it does not conform to such a concept. At this point a careful study must be made to interpret the observed coefficient properly in terms of the existing conditions. It is here that we have in the last fifteen years learned to distinguish the widely different coefficients, preferential, initial, columnar, volume, electron.

Let us consider a gas which is ionized with  $n_+$  positive ions of one species and  $n_-$  negative ions of one species per cubic centimeter. It must be assumed that  $n_+$  and  $n_-$  are concentrations which are fairly constant over the volume considered. It is next obvious that ions can recombine only if ions of one sign *encounter* ions of the opposite sign. What we mean by *encounter* is left completely undefined. If ions disappear by encounters of ions of the opposite sign, it is perfectly clear that  $dn$ , the loss of the number of ions by recombination in a time  $dt$ , must be proportional to  $n_+$ , to  $n_-$ , and to  $dt$ . For the chance of encounter depends on  $n_+$ , on  $n_-$ , and on  $dt$ , irrespective of how they arrive at an encounter. We then write this in equation form as

$$dn = -\alpha n_+ n_- dt,$$

where  $\alpha$  is a characteristic of the process, being independent of  $n_+$ ,  $n_-$ , and assumedly of  $t$ , but dependent on the nature of the carriers. It is called the *coefficient of recombination*. It is to be noted that the negative sign means that  $dn/dt$  is negative, i.e., that  $n$  decreases as  $t$  increases. It should be noted also that, for integration in the above form, this equa-

tion implies that  $n_+$  and  $n_-$  are constant in any interval  $dt$  and that  $n_+$  and  $n_-$  do not change with  $t$  except by recombination. If  $n_+$  and  $n_-$  or  $\alpha$  are functions of  $t$  other than as specified, these functions must be inserted before integration. It is the failure to recognize this fact that has led to confusion. It is further to be understood that, when one implies that  $dn \propto n_+ n_-$ , it is assumed that  $n_+$  and  $n_-$  are uniform concentrations over the volume considered. In experimental measurement  $n_+$  and  $n_-$  are never measured. One measures  $q_+$  and  $q_-$ , the charges, in a volume  $V$ , and sets  $n_+ = q_+/V$  and  $n_- = q_-/V$ . If, however, by the process of ion formation the ions are initially grouped in pairs or along dense tracks of small volume,  $n_+$  and  $n_-$  are not  $q_+/V$  and  $q_-/V$ . Furthermore, as time progresses and diffusion disorients and distributes the ions, a change of  $n_+$  and  $n_-$  occurs in time with no change in  $q_+$  and  $q_-$ .

As a result, if the implied conditions are not fulfilled as regards  $n_+$  and  $n_-$ , the substitution of values for  $n_+$  and  $n_-$  computed from  $q_+$ ,  $q_-$ , and  $V$  will give values of  $\alpha$  which apparently vary with time and which are incorrect in absolute value.

It must also be borne in mind that  $\alpha$  is a constant characteristic of a process. In transition regions, where one mechanism replaces another, the behavior of  $\alpha$  may be strange. Finally,  $\alpha$  may depend on the nature of the ion or carrier, and, as this changes with time, or if several carriers of different  $\alpha$  occur together, the average value of  $\alpha$  will appear to vary with time as one group of ions disappears and the other predominates. In order to simplify calculations, it is usually arranged to have conditions in the gas such that  $n_+ = n_-$ . This is achieved by *ionizing only the body of the gas by radiations* such as X-rays or  $\alpha$ -rays. If radiations strike the metal walls, an excess of negative carriers is usually produced. If the gas is one in which electronic carriers persist for some time, the diffusion coefficient of these, which is of the order of  $10^4$  times that of ions, causes a loss of negative carriers by diffusion so that  $n_+ > n_-$ . If these conditions are avoided, one can usually set  $n_+ = n_- = n$ . The equation then becomes  $dn = -\alpha n^2 dt$ . Integration, assuming the absence of the factors above, is then simple. To obtain  $n$  as a function of  $t$ , we must integrate  $n$  from  $n = n_0$  at  $t = 0$  to  $n = n$  at  $t = t$ .

$$\begin{aligned} \frac{dn}{n^2} &= -\alpha dt, & \int_{n_0}^n \frac{dn}{n^2} &= -\alpha \int_0^t dt. \\ \left(-\frac{1}{n}\right)_{n_0}^n &= -\alpha t, & \alpha t &= \frac{1}{n} - \frac{1}{n_0}. \\ \alpha &= \frac{1}{t} \left(\frac{1}{n} - \frac{1}{n_0}\right), \\ n &= \frac{n_0}{1 + n_0 \alpha t}. \end{aligned}$$

It is seen that  $n/n_0$  decreases hyperbolically from  $n_0$  with  $t$  at a rate which depends on  $n_0\alpha$  and is 0 at  $t = \infty$ , as shown in Fig. 42. Furthermore, one can evaluate  $\alpha$  by observing  $n$  and  $n_0$  as a function of  $t$ , so that the analysis indicates an experimental method for evaluating  $\alpha$ .

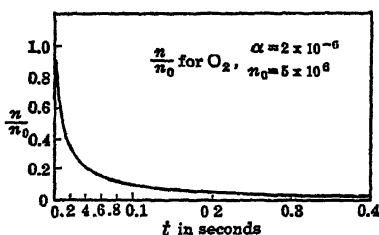


FIG. 42.

If  $\alpha$  should by any chance be a function of  $t$ , it is not proper to integrate from  $t = 0$  to  $t = t$ , for then the  $\alpha$  computed from data represents a meaningless average value. Should  $\alpha$  indicate a variation with  $t$ , one must define a value of  $\alpha_t$  measured over an interval  $\Delta t = t_2 - t_1$  so short that  $\alpha$  has not materially changed. This has not been possible until the availability of new precision

techniques dependent on vacuum-tube control of the X-ray sources, etc. Under these circumstances we integrate from  $n = n_1$  at  $t = t_1$  to  $n = n_2$  at  $t = t_2$ , whence one has

$$\alpha_t = \frac{1}{t_2 - t_1} \left( \frac{1}{n_2} - \frac{1}{n_1} \right),$$

which for a small  $t_2 - t_1$  gives  $\alpha_t$  at a value of  $t = (t_1 + t_2)/2$ . How important this is can be seen in Fig. 58, page 137, for air, given by Luhr, where the upper curve uses  $t_0$  and  $t$  while the lower one is for  $t_1$  and  $t_2$ .

We must next consider another case: Assume that in a space  $n = 0$  at  $t = 0$ , and beginning with  $t = 0$  a constant source of ionization acts for a time  $t$ . If this source produces new ions at the rate of  $q$  ions per cubic centimeter per second, then  $n$  increases on account of this factor but decreases owing to the loss of ions by recombination. Eventually  $n$  increases to a point where production is just equaled by loss and we have  $n_\infty$ , the *equilibrium* ion concentration. Now in unit volume  $q dt$  ions are produced in  $dt$ , while  $\alpha n^2 dt$  are lost by recombination. Hence we can state this in symbolic form as  $dn = q dt - \alpha n^2 dt$ , so that  $dn/dt = q - \alpha n^2$ . For constant  $\alpha$  and the ideal conditions assumed above, this must be integrated from  $n = 0$  at  $t = 0$  to  $n = n$  at  $t = t$ . Let us call  $k^2 = q/\alpha$ , then

$$\frac{1}{\alpha} \frac{dn}{dt} = k^2 - n^2, \quad \frac{dn}{k^2 - n^2} = \alpha dt,$$

$$\int_0^n \frac{dn}{k^2 - n^2} = \int_0^t \alpha dt, \quad \left[ \frac{1}{2k} \log \frac{k+n}{k-n} \right]_0^n = \alpha t.$$

$$\log \frac{k+n}{k-n} - \log 1 = 2k\alpha t,$$

$$\frac{k+n}{k-n} = e^{2k\alpha t}, \quad k+n = (k-n)e^{2k\alpha t},$$

$$n = k \frac{e^{2k\alpha t} - 1}{e^{2k\alpha t} + 1}.$$

At  $t = 0$ ,  $n = 0$ , and at  $t = \infty$ ,  $n_{\infty} = k = \sqrt{q/\alpha}$ . The curve for  $n/n_{\infty}$  as a function of time is shown in Fig. 43. It rises linearly with  $t$  for low values and then approaches the limit  $n_{\infty}$  asymptotically. Again, it is seen that, if  $q$  is measured, we can determine  $\alpha$  from  $n_{\infty}$  or from the ratio of  $n/n_{\infty}$  as a function of  $t$ . This again allows us to devise experiments for determining  $\alpha$  and testing the law. Either the growth or decay of  $n$  with  $t$ , it is seen, furnishes a test of the law. Although the growth method has certain advantages in the direction of eliminating errors and difficulties in measurement, the complicated form of the equation makes interpretation of deviations difficult. On the basis of this theory, one may consider the various methods for evaluating  $\alpha$  that have been used in the past, for it is only by a study of  $\alpha$  that one gains an insight into the nature of the process.

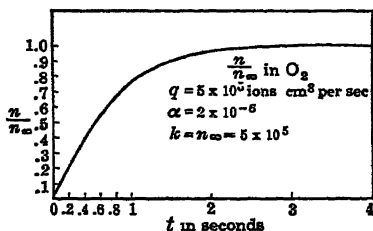


FIG. 43.

#### 4. METHODS OF MEASUREMENT OF $\alpha$

As seen from the theory just given, there are three ways in which  $\alpha$  may be determined. The first is by measuring the disappearance of the ions with time owing to recombination; the second the growth of the number of ions in a volume with time where ions are created at a constant rate and are recombining simultaneously; the third comes from a knowledge of the rate of ion production and the equilibrium number of ions after equilibrium between recombination and ionization has been reached. All three methods have been utilized. The last method appears by all odds to be the most simple since it involves only the measurement of the rate of ion production and the measurement of the equilibrium number of ions. Measurements of this character are not simple, nor are they accurate, especially in view of difficulties in measuring the small equilibrium number relative to the rate of production which can be determined by the "saturation" current due to ionization. Actually the rate of "production" of ions as interpreted by the recombination process is not independent of the sweeping field required to measure the current, and difficulties ensue. There is also quite a disparity in the quantities measured when the equilibrium number is contrasted with the rate of production. This was especially serious as a source of error in the early days when inconstant and non-uniform X-ray sources were available, or when  $\alpha$ -ray ionization was resorted to. Similar criticism must be made of the earlier determinations by the second method before the use of commutators and constant ionization as from  $\gamma$  rays or from Coolidge X-ray tubes. The greatest difficulty, however, with the second method, even at the



present day, lies in the fact that the complexity of the equations, and the presence of two processes simultaneously which preclude the separation of initial from volume recombination, make the analysis of the results difficult. The first method appears from the somewhat extensive studies of the group at California to be the most amenable to giving clean-cut results. The price one pays for analytical simplicity, however, is the complexity of the techniques required to avoid the innumerable sources of error in measurement. To set up and operate the apparatus successfully for a reproducible and consistent set of data requires such refinements that even in a well-equipped laboratory with a good background of experience a full two years' research program is entailed.

As regards sources of ionization that have been used, it may be said that  $\alpha$ -particle ionization introduces difficulties of a special kind in interpretation and that the results of early experiments in which sources were utilized in ignorance of the situation are unacceptable as giving information concerning the mechanism of volume recombination. In general, ionization by X-rays and perhaps the less satisfactory  $\gamma$ -rays for studies after 0.10 second of age may be considered the more satisfactory sources.

It is thus clear that most of the measurements that were made before the availability of Coolidge X-ray tubes, high-vacuum technique, and high-tension rectifier systems devoid of fluctuations, original and meritorious though they may be, cannot be of much assistance in the analysis of the complicated phenomena existing. The early work will therefore largely be listed and described in principle, details being given only where the results have a bearing on the development of our understanding. The methods used are:

Class 1.

- a. Air-blast methods.
- b. Pendulum interrupter.
- c. Commutator.

Class 2.

- a. Commutator.

Class 3.

- a. Measurement of a saturation current with the source on, and then a measurement of the equilibrium number of ions produced with no field on but with the source on, sweeping out the ions after equilibrium had been reached and measuring their charge.

In what follows, the various types of measurement will not be listed in order. The methods which have yielded unsuccessful or dubious results as regards the study of volume recombination will be listed first, with the references and a statement why from our modern standpoint the results are not of great contemporary significance. In doing

this, it must be repeated that some of the ablest investigators of their time were engaged in these studies. That their results do not stand as significant for all time reflects on them no more than the accurate measurements of Regnault on gases reflect on the epoch-making pioneer investigations of Robert Boyle and others. For it must be clear that the technical and scientific advance in the last thirty years probably many times transcends the advances along similar lines between the time of Boyle and that of Regnault. It is essential, however, to recognize that the data in these highly complex phenomena recorded three decades ago, and still appearing as the correct solution today in practically *all* books, are no longer completely reliable and that the interpretation of results must be made on the more refined methods of the present day.

1. Methods involving air or gas streams. These were among the earliest methods and were utilized by none less than Rutherford,<sup>2</sup> Townsend,<sup>4</sup> and McClelland.<sup>3</sup> The methods are merely applications of the equation

$$\alpha = \frac{1}{t_2 - t_1} \left( \frac{1}{n_2} - \frac{1}{n_1} \right).$$

In this case  $n_1$  and  $n_2$  were measured at various downstream points in the gas where  $t$  could be calculated from the velocity of the gas stream and the distances between the points where  $n_1$  and  $n_2$  were determined. They suffer from the usual difficulties of air-blast methods such as turbulence, non-uniform flow, and lack of purity. In addition one must note that the various collectors at which  $n_1$ ,  $n_2$ ,  $n_3$ , etc., are measured modify the concentrations by abstracting ions by diffusion or attraction so that  $n_2$  and  $n_3$  are concentrations which are changed by a diffusion or current loss as well as by recombination.

2. The measurement of the equilibrium concentration of ions  $n_\infty$  and of the rate of ion production in unit volume. This method employs the equation  $n_\infty = \sqrt{q/\alpha}$ . It was early followed by McClung,<sup>5</sup> Erikson,<sup>6</sup> and Hendren,<sup>7</sup> some of these workers using  $\alpha$ -particle ionization. In the attempt to collect more of the ions (no true saturation currents can be observed with  $\alpha$ -particle ionization), the conditions were such in one instance as to introduce serious losses by diffusion to the walls.

3. The method using the rate of increase of ionization with time was employed extensively only by one observer, Rümelin,<sup>8</sup> in an excellent piece of work utilizing  $\gamma$ -ray ionization and a commutator. Marshall<sup>9</sup> in his initial survey also investigated the use of this method with X-ray flashes and a commutator, verifying the equations. For the evaluation of  $\alpha$ , however, it was found convenient to utilize the rate of decay. The method was also tried by Sayers<sup>10</sup> but later discarded.

4. Rutherford and Thomson<sup>1</sup> in 1896 first measured  $\alpha$  by means of the variation of the current as a function of the clearing field  $X$ , using a constant rate of ion production of  $q$  ions per cubic centimeter per

second. The volume  $V$  between two plates of a parallel-plate condenser of area  $A$  and plate separation  $l$  is ionized by the X-rays. At equilibrium the rate of production  $q$  per unit volume must just equal the rate of loss by recombination plus the loss by current flow  $i$ . Hence  $q = \alpha n^2 + (A/v)(i/e)$ , where  $e$  is the ionic charge. Since the current is due to the motion of the ions,  $i = ne(k_+ + k_-)X$ , where  $n$  is the ion concentration and  $k_+$  and  $k_-$  are the mobilities of positive and negative ions. Since  $V/A = l$ , and if  $I$  is the saturation current when  $X$  is very large, one can write

$$\frac{\alpha}{e} = \frac{(I - i)(k_+ + k_-)^2 X^2}{i^2 l}.$$

The method requires some corrections, which were made by Riecke and Mie.<sup>10</sup> It suffers from the inconvenience that "saturation" is never exactly achieved, and the importance of initial and preferential recombination in such considerations obscures the results. To get accurate results  $X$  must be small so that  $i$  will differ appreciably from  $I$ .

5. Rutherford<sup>11</sup> was the first to attempt the measurement of  $\alpha$  by measuring the disappearance of ions by recombination at an interval  $t$  after an ionizing X-ray flash, sweeping the ions out electrically by a high field  $X$ . The operation was accomplished by a pendulum which closed and opened the circuit to an induction coil flashing the X-rays, and then after a variable time  $t$  applied a high sweeping field  $X$  to the plates collecting the ions remaining. The method was not very successful at that time since the X-ray flashes were not reproducible or of equal intensity. This method was later employed by Plimpton<sup>12</sup> in obtaining results of considerable theoretical significance. In Plimpton's work the X-ray flash was also used, but apparently the improvements in X-ray tubes by that time had somewhat overcome the earlier difficulties.

Langevin<sup>13</sup> ingeniously developed a modification of this method, using two ionizing chambers each in the form of a parallel-plate condenser. Ionization came from the same flash of the X-ray tube in both chambers. In these the charge collected corresponded to a different degree of aging, i.e., a different equivalent time  $t$  for each chamber. In this way the quantities  $q_1$  and  $q_2$  collected after different equivalent times  $t_1$  and  $t_2$  were directly compared for the same X-ray flash. Actually Langevin did not vary  $t$ . He excited the *weak* sweeping fields  $X$  and  $X_1$  immediately the flash was over.  $t$  and  $t_1$  were then determined by the time the ions were together before the fields  $X$  and  $X_1$  pulled the positive and negative ions apart. The method aside from giving excellent results in its time has an important theoretical interest since it evaluates a quantity  $\epsilon = \alpha/[4\pi(k_+ + k_-)]$  directly. This quantity was believed by Langevin to be of great theoretical significance. In view of the later theoretical analysis and the fact that the results it

has yielded in the past have been quite concordant, it is of interest to present the principles involved in the method.

The principle is as follows. Two plates  $A$  and  $B$  forming a parallel-plate condenser were used in each chamber, Fig. 44.  $B$  went to an electrometer  $E$  which could be grounded and whose potential was that of ground.  $A$  went to the pendulum interrupter. The plate  $A$  was initially grounded. The pendulum first sent a flash of X-rays

through the system by closing the circuit through the primary of an induction coil, activating an X-ray tube, which is not shown. The beam of X-rays  $ab$ ,  $l$  cm wide, entered through the slit in the lead screen  $S$ . The distance  $l$  was of the order of half the distance  $d$  between  $A$  and  $B$ . Immediately after the flash of X-rays a field  $X$  was placed on  $A$  such that the positive ions moved towards  $A$  while the negative ions moved towards  $B$ . If  $X$  is very high the positive ions go to  $A$  and the negative ions go to  $B$  so rapidly that no ions get a chance to recombine and the total ion quantity in  $ab$  at the end of the flash of X-rays contributes to the current.

If, however,  $X$  is not so strong, then positive ions move away from  $a$  with a velocity  $Xk_+$ , and negative ions move away from  $b$  with a velocity  $Xk_-$ , and these ions are no longer able to recombine. It is only the ions left in a zone  $l - (k_+ + k_-)Xt$  thick that are recombining after a time  $t$ .

In this region the number of ions on simple theory diminishes according to  $n = n_0/(1 + \alpha n_0 t)$ , if  $n = n_0$  was the number at a time  $t = 0$  after the flash. Thus, in  $dt$ ,  $X(k_+ + k_-)dt$  represents the width of the zone of ions escaping recombination, and the number escaping recombination per unit area of  $A$  or  $B$  is then  $nX(k_+ + k_-)dt$ . This drift apart will continue from  $t = 0$  to  $t = l/[X(k_+ + k_-)]$ . Hence the number of ions escaping recombination per square centimeter of  $A$  or  $B$  and giving a current to  $E$  in  $dt$  is found to be

$$nX(k_+ + k_-)dt = \frac{n_0X(k_+ + k_-)dt}{1 + n_0\alpha t}.$$

In the interval from  $t = 0$  to  $t = l/[X(k_+ + k_-)]$ , the number of ions escaping is  $N$  and the quantity of charge measured by  $E$  is

$$Q = Ne = \int_{t=0}^{t=\frac{l}{X(k_+ + k_-)}} enX(k_+ + k_-)dt$$

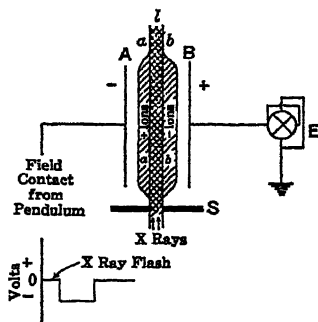


FIG. 44.—Langevin's Method for Measuring Recombination.

$$\begin{aligned}
 &= \int_0^{\frac{l}{X(k_+ + k_-)}} \frac{en_0 X(k_+ + k_-)}{1 + n_0 \alpha t} dt \\
 &= \frac{eX(k_+ + k_-)}{\alpha} \log \left( 1 + \frac{n_0 \alpha l}{X(k_+ + k_-)} \right).
 \end{aligned}$$

One may designate  $\alpha/[4\pi e(k_+ + k_-)]$  by the letter  $\epsilon$  and call  $n_0 l \epsilon = Q_0$ , where  $n_0$  is the number of ions per cubic centimeter at  $t = 0$ , and  $Q_0$  is the charge per square centimeter which the plates will receive if  $t = 0$  and  $X$  is large. Then we have at once

$$Q = Ne = \frac{X}{4\pi\epsilon} \log \left( 1 + \frac{Q_0 4\pi\epsilon}{X} \right).$$

Now  $Q_0$  could be found by making  $X$  very large in the second condenser and measuring  $Q_0 A$ , where  $A$  is the area of the plates. It is just as simple to make  $X = X$  in one condenser and to make  $X = X_1$  in the other. The charges collected will then be

$$Q_1 = \frac{X_1}{4\pi\epsilon} \log \left( 1 + \frac{4\pi\epsilon Q_0}{X_1} \right).$$

By solving the equations for  $Q$  and  $Q_1$ , one finds

$$\frac{4\pi\epsilon}{X} Q_0 = e^{\frac{4\pi\epsilon Q}{X}} - 1$$

and

$$\frac{4\pi\epsilon}{X_1} Q_0 = e^{\frac{4\pi\epsilon Q}{X_1}} - 1$$

so that

$$X_1 e^{\frac{4\pi\epsilon Q_1}{X_1}} = X e^{\frac{4\pi\epsilon Q}{X}} + X_1 - X.$$

From the observed values of  $X$ ,  $X_1$ ,  $Q$ , and  $Q_1$ ,  $\epsilon$  can be evaluated. Then, from  $\alpha = 4\pi e(k_+ + k_-)\epsilon$ , one can evaluate  $\alpha$ . Langevin contented himself with the evaluation of  $\epsilon$ , which was near 1 at atmospheric pressure and above, but fell rapidly to small values below. At this time  $e$  was not known, and the observed  $\epsilon$  served to show the ratio between  $\alpha$  and the theoretical expression  $\alpha = 4\pi e(k_+ + k_-)$ . The method has one feature in common with the current flow methods. It applies a field separating ion pairs at once. Hence, the influence of initial recombination will be less in the results from this method. However, the field variation in the presence of preferential and initial recombination will cause a variation in the degree to which these effects are decreased that may make results difficult to interpret.

6. The more modern methods. In 1914, Rümelin had used a rotating shutter and commutator with  $\gamma$ -ray ionization in measuring  $\alpha$  by means of the rate of growth of ionization indicated on page 91. Without knowledge of Rümelin's<sup>14</sup> work, the author in 1924 suggested

to L. C. Marshall that the commutator which was so useful in studying ion mobilities might, together with the Coolidge X-ray tube, be adapted to an improvement of the Rutherford<sup>11</sup> rate of disappearance method of measuring  $\alpha$ . The idea at that time was to apply this method to the study of  $\alpha$  in gases where electrons were permanently free, such as pure  $H_2$  or  $N_2$ . The task of building up a suitable high-voltage X-ray source, so that uniform constant ionization could be obtained over a sufficiently large volume, proved to be a much more difficult task than anticipated. It became essential to use 100-kv X-rays and to place the focus of the tube about 2 to 3 meters from the tube. By 1928 Marshall began to obtain results for the coefficient of recombination in air which called forth a careful analysis of both the method and later the theory of the recombination process. The results completed in 1929 were carried further by O. Luhr, who still further perfected the technique. Luhr's excellent work completed in 1931 left much to be desired as regards the final absolute determination of a volume coefficient of recombination for ions in a single pure gas which could be compared with theory. Since at this time the technique for achieving the required gas purity was not developed, the problem was abandoned for two years, while the X-ray source was being applied by Bradbury to the successful absolute determination of ionic mobilities in pure gases. This work terminated in 1932. It laid the foundation for a resumption of Luhr's studies by M. E. Gardner, who applied the technique of Bradbury for handling pure gases to the recombination problem. In this phase of the work the steadiness of the X-ray voltage was much improved through the development of high-capacity condensers, vacuum-tube control of the motor-generator output, and the use of an auxiliary ionization chamber and a compensating chamber for induction effects. Finally, Loeb designed a commutator which eliminated practically all static charging of the lower plate during the recombination period. With these improvements, Gardner by 1937 succeeded in achieving an accurate absolute evaluation of  $\alpha$  in  $O_2$  and in determining the variation of  $\alpha$  with pressure and temperature.

The device as developed by Gardner is shown in detail in Figs. 45 and 46. The X-ray tube was of the Coolidge type with a broad focal spot. For prolonged usage as in these measurements a 200-kv tube is best. The potential used was 80 to 100 kv smoothed by means of heavy choke coils and a 0.125 microfarad capacity. The power came

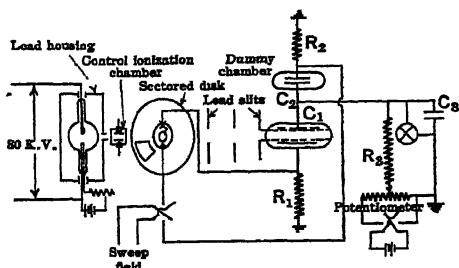


FIG. 45.—Gardner's Method for Measurement of Recombination.

from a motor-generator set giving 500 cycles and was controlled by a tube circuit and saturable core reactor. The tube was in a heavy lead case, and the X-ray beam passed through an ionization chamber on its way to the sectored disc of the commutator, *com.* This chamber gave a continuous reading of the X-ray intensity on a scale. The intensity could be controlled by control of either filament current or the applied potential. After passing the sectored disc, the beam was limited by slits and entered the chamber  $C_1$  roughly 2.5 meters away from the tube. In this way a slightly divergent beam of nearly uniform intensity was available. The chamber consisted of a pair of plane parallel electrodes with guard rings and mid potential vanes. The field distribution was determined electrolytically by cross-section models. The plates

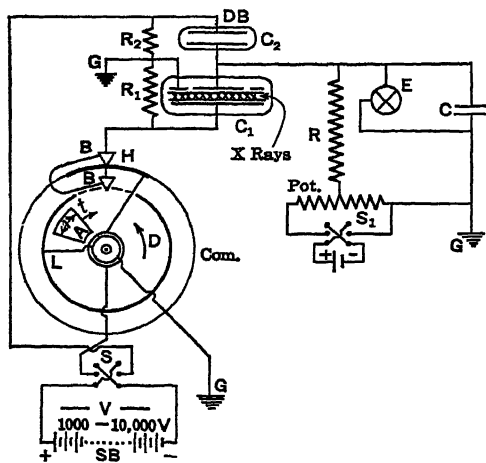


FIG. 46.—Detail of Gardner's Arrangements.

were some 10 cm apart, and the ionized volume was 700  $\text{cm}^3$ . The X-ray beam was kept about 2 cm from the collecting plates but extended laterally well beyond the edge of the plates. These measures reduced diffusion loss to a minimum. The chamber was shielded with Monel metal screening, and contact potentials were reduced to a minimum by careful choice of metals. The apparatus could be outgassed at 400° C. Referring to Fig. 46,  $C_1$  is the ionization chamber with its guard rings.  $C_2$  is a dummy balance chamber containing a pair of plates analogous to  $C_1$  with capacities in the ratio  $C_1$  to  $C_2$ . The lead goes from between  $C_1$  and  $C_2$  to the electrometer  $E$  and to a condenser  $C$  in parallel with  $E$ .  $R$  is a resistance of  $10^{10}$  ohms which allows the charge on the upper plate of  $C_1$  to leak to ground very slowly. *Pot.* is a potentiometer and commutator switch to raise the potential of the lower end of  $R$  to any potential above the ground  $G$ .  $R_1$  and  $R_2$  are two high resistances in the same ratio as the capacities  $C_1$  and  $C_2$ . The ground at  $G$  between  $R_1$  and  $R_2$  serves effectively to keep the  $iR$  drops consistent with the drops through the capacities. The commutator, *com.*, devised by Loeb, is arranged as follows. The two collector brushes  $B$   $B'$  pick off high potential at segment  $H$ , or zero potential at segment  $L$ . The segments are separated on *two levels* so that the instant  $B$  loses contact with  $H$  it makes contact with  $L$ , with, however, no short insulator surface between  $B$  and  $L$ , which may have 10,000 volts difference of potential. The rotation is counterclockwise

along the arrow  $D$ . Thus a flash of X-rays enters  $C_1$  through sector  $A$  whose displacement  $t$  from the end of  $L$  and the beginning of  $H$  can be varied by moving the lead disc with the sector  $A$  cut out about the axis and clamping it in position. The high potential came from the sweeping battery  $SB$  of 1000 to 10,000 volts. This sweep potential may also be given by a kenotron rectifier. By means of the commutator switch  $S$ , either positive or negative potential could be placed on segment  $H$ , the opposite pole going to the other end of  $R_1$ . Thus, the cycle was as depicted in Fig. 47. The X-ray flash was followed by the recombination period  $t$  and then by a strong field to sweep residual charges to the electrodes. By making sector  $A$  variable and  $t = 0$ , one can evaluate  $Q/e$ , the number of ions formed as a function of time with recombination taking place and constant ionization acting. The method can then be used for an evaluation of  $\alpha$  by the growth of ionization. In using the apparatus with  $A$  fixed in size but  $t$  varied, the rate of disappearance

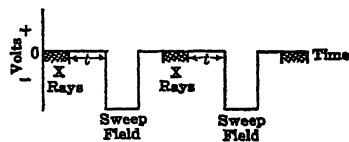


FIG. 47.

method can be used. If we make  $t = 0$ , we get  $Q_0/e$ , the number of ions formed initially by the flash. When the sweep field is applied the ratio  $R_2/R_1 = C_1/C_2$  insures that the induced potential on the electrometer  $V_1$  due to the lower part of  $C_1$  is just canceled by that induced due to  $V_2$  on the upper part of  $C_2$ . As charge accumulates on  $E$  owing to the  $iR$  drop across  $R$ , the potentiometer  $Pot.$  applies a potential of appropriate sign through  $S_1$  to neutralize the charge at  $E$ , the current still flowing in  $R$ . Thus,  $E$  and the upper plate of  $C_1$  remain at ground potential, a most important circumstance, since during  $t$  there must be no field in  $C_1$  to drive out ions. Actually contact potentials of some tenths of a volt are always unavoidably present in the chamber. These make measurement of electron recombination and work at low pressures impossible. They are not serious in their effects on ordinary ions at 760 mm. To use the method in application to the equation  $\alpha = \left(\frac{1}{t}\right)\left(\frac{1}{n} - \frac{1}{n_0}\right)$  all that need be done

is to determine the current  $i$  from the measured value of the potentiometer reading  $E$  and the value of  $R$  and divide this by the volume  $V$  between the plates of  $C_1$  that is ionized, first when  $t = 0$  and then when  $t = t$ . This follows, since we assume that  $n = Q/(eV)$ , where  $Q$  is the quantity in volume  $V$  and  $e$  is the electron. Now  $Q = iT$ , where  $T$  is the time of one complete revolution over which the current thrust due to ions is being collected. Hence,  $i = Q/T = E/R$ , so that  $n = Q/(eV) = ET/(eRV)$ . Then in general changing  $t$  from 0 with  $n_0 = E_0T/(eRV)$  to  $t = t$  with  $n = ET/(eRV)$  we have

$$\alpha = \frac{RV}{etT} \left( \frac{1}{E} - \frac{1}{E_0} \right).$$



If  $\alpha$  is to be in absolute units,  $R/(eE)$  must be expressed in absolute units; if  $e$  is in esu then  $R/E$  must also be in esu. Instead of  $T$ , the frequency  $N = 1/T$  is used directly, and  $t = (\theta/2\pi)T$ , where  $\theta$  is the angular displacement of  $A$  from  $II$  in radians. Thus

$$\alpha = \frac{2\pi VRN^2}{e\theta} \left( \frac{1}{E} - \frac{1}{E_0} \right),$$

so that, as  $\theta$  varies,  $E$  and  $\theta$  give  $\alpha$ . If  $\alpha$  varies with  $t$ , it has been shown by Luhr<sup>14</sup> to be desirable to measure  $E_1$  at  $\theta_1$  and  $E_2$  at  $\theta_2$  instead of  $E_0$  and  $E$ . Then by varying the value of  $(\theta_1 + \theta_2)/2$  one gets values of  $\alpha$  as a  $f(t)$ .

Sayers<sup>62</sup> raises a question concerning the size of the ionized volume. After careful study of the ionization in *C. T. R. Wilson cloud track pictures of X-ray beams*, Marshall<sup>9</sup> concluded that the secondary electron tracks extending beyond the geometrical edges of the beam in air at atmospheric pressure introduced an uncertainty of less than 1 per cent in the estimated volume. It was on the basis of this careful investigation that all the studies made in the author's laboratory on recombination used the geometrical volume of the X-ray beam as delineated by photographs at both ends of the chamber. Sayers asserts that this procedure is in error. He used instead ionization that nearly filled the chamber and assumed the ionized volume to be defined by the plates. In the effort to avoid diffusive losses and to prevent *ionization by photoelectric liberation from the plates by the X-rays*, which introduce serious inhomogeneities into the density of volume ionization near the plates, the technique used in the Berkeley laboratory was the questionable technique alluded to by Sayers. It is probable that the errors inherent in Sayers' technique by *overestimate* of the volume, diffusive loss, or else inhomogeneity of ionization were as bad as the volume errors of Gardner, Luhr, and Marshall. The errors would have been such as to *decrease* Gardner's  $\alpha$  below the true value by 1 or 2 per cent at most. By the like token Sayers' results were probably increased above the true value by a fractional amount of nearly the ratio of the difference between volume of the geometrical beam and the volume between the plates to the volume between the plates. If Sayers' X-rays struck the plates, the enormous photoelectric liberation from the plates, relative to the gas, produced intense inhomogeneities in his ion densities whose effect would have been to increase the observed value of  $\alpha$ . At the lowest pressure used by Gardener, viz., 50 mm, the error due to underestimate of the volume ionized could have been of the order of 10 per cent. At 400 mm pressure the error relative to that at 760 mm from Gardner's observed points as compared to theory could not have been in excess of 5 per cent.

As regards the question of the ionized volume in future work, neither procedure is accurate. The ideal procedure would be to make

cloud track pictures of the beam used, in the gas used, at various pressures, and from them to correct the geometrical volumes as utilized by Gardner.

## 5. RESULTS OF EARLIER WORK

As stated in the introduction, the problem of recombination is exceedingly complex. As a result of this complexity, which was not recognized, together with the inadequacy of the technical development when most of the earlier work was done, the results are not of great significance in the present-day interpretation of the recombination process. Specifically, it must be recognized that until the last ten years the studies of recombination suffered from one or several of the deficiencies listed below, despite the fact that they were ingeniously conceived and skillfully carried out in their time.

1. The exact nature of the recombination *processes* was not recognized. Hence, no differentiation was made between volume, initial, columnar, and preferential recombination. Measurements were interpreted as giving coefficients for volume recombination although initial or columnar effects were present in larger or smaller measure. Thus it is only by a recognition of the existence of the different forms of recombination and a proper choice of conditions involving the recombination period, and a recognition of the effect of external fields, of the nature of the ionizing agency, and of pressures on recombination, that a technique can be selected to give values of  $\alpha$  from the equations which are significant as regards interpretation.

2. The range in time intervals over which recombination was studied was limited. Measurable recombination requires considerable changes in concentration to be accurately evaluated, especially with unsteady ion sources. Thus, early measurements were limited to a range consistent with measurable changes of concentration. Hence  $\alpha$  was usually measured between  $t = 0$  and  $t = t$  and over limited ranges chiefly from 0.01 to 0.2 second.

3. The necessity of *extreme* purity in the gases studied was not recognized until after 1932. The failure to recognize this factor is especially serious for the following reasons.

- a. Accurate measurements require that  $t_2 - t_1$  for concentrations of  $10^7$  ions/cm<sup>3</sup> down be more than  $10^{-3}$  and more nearly  $10^{-1}$  sec.

- b. In these time intervals ions make  $10^6$  to  $10^8$  collisions with gas molecules.

- c. Impurities present to 1 part in  $10^6$  or less will then interact with the ions either to load them down by forming complex ions or by exchanging charge.

- d. Increasing the mass of an ion from  $m_1$  to  $m_2$  changes  $\alpha$  roughly in proportion to  $\sqrt{m_1/m_2}$ .

- e. As  $\alpha$  decreases, the recombination decreases. Hence, as time goes on, the ions of greater  $m$  will survive and  $\alpha$  will change. Changes

in  $\alpha$  due to aging are for this reason much more pronounced than changes in the mobility. Thus Luhr<sup>16</sup> observed changes in  $\alpha$  from 0.1 to 1 second in air by a factor of 3 while  $k$  changed by an average value of 10 per cent. As ions of one sign only are used in mobility measurement, faster ions are not eliminated.

Hence, up to the present, the results of Gardner on  $O_2$  are the only values of  $\alpha$  obtained on a really pure gas of a single molecular species. It must be pointed out that the only other *pure* gases in which true values of  $\alpha$  of any significance can be obtained are the few gases in which electron attachment when pure readily takes place. Aside from  $SO_2$  and the halogens this represents a very limited number of gases. In other *pure* gases the presence of free electrons seriously complicates the results.

4. In relatively few of the earlier researches were great precautions taken to eliminate ion loss by diffusion. It was always endeavored to make the volume as large as possible compared to the diffusion surfaces. In addition the supposed diffusion losses were increased by the presence of uncompensated potentials of small amount and by contact potential differences. It is only by keeping the ionized beam far from the collecting electrodes, using very broad sources of ionization, ample guard rings, and field distribution of known form that losses of ions giving erroneous values of tens of per cent can be avoided. If free electrons are present in any number (most gases used prior to 1928, however, were not pure enough for this), owing to diffusive losses measurement becomes virtually impossible. Luhr<sup>14</sup> and Marshall,<sup>9</sup> with some precautions, sought mathematically to correct for diffusion with no great success. In Gardner's work it was experimentally reduced to a minimum in oxygen.

5. None of the earlier methods using  $\alpha$ -ray sources of ionization can furnish results of any great significance *except* when the times are of the order of 0.1 to 1 second and fields are present. Otherwise, the recombination coefficient is that characteristic of columnar ionization discovered by Bragg and successfully treated theoretically by Jaffé.

6. The earlier methods using X-ray flashes in gas-filled tubes, except the compensating method of Langevin, suffered by the lack of steadiness of the X-ray source.

7. In some cases the liberation of excess electrons and hence negative ions when the X-ray beams struck the plates or parts of the chamber contiguous to the recombination volume caused serious errors.

8. Air-blast methods have other disadvantages already listed.

Taking into account these difficulties, it will not be profitable to list the discordant values of  $\alpha$  or to discuss the very discordant observations of the variation of  $\alpha$  with pressure and temperature. The more significant investigations as regards these variables will be given in their proper place.

In view of the earlier results, and of an *erroneous theory* as to the process of "volume" recombination at atmospheric pressure which was blindly accepted by physicists including the author for nearly twenty years, it becomes necessary to present the development of the present understanding in a more or less historical form. Even though the presentation in this fashion has the disadvantage of losing compactness, it is still very essential, owing to the conflicting views exhibited in books and current periodicals. Thus, theory and experimental result will be woven together in a more readable but somewhat more extensive story. This must follow in a field which is relatively far less clarified than that of ionic mobilities.

## 6. THE LANGEVIN THEORY OF RECOMBINATION OF IONS

The early results obtained gave values of  $\alpha$  of the order of  $1.5 \times 10^{-6}$  for air, while for other gases the values, which differ considerably among the various observers, lay within 20 per cent of the value for air. This circumstance in itself should have given rise to some suspicion that was all not well with the results. The pioneer investigation of Langevin furthermore added interesting information as to the pressure variation of  $\alpha$ . For pressures well below atmospheric,  $\alpha$  appeared to decrease as  $p$  decreased, while above 1 atmosphere and up to 5 atmospheres in air  $\alpha$  increased to a maximum and then began to decline. The decline in  $\alpha$  above 3 atmospheres<sup>17,18</sup> has been confirmed more recently, in none too clean air, and tends towards a linear decrease with pressure near 20 atmospheres. This behavior has not been clearly interpreted until very recently.<sup>19,22</sup> In what was essentially his thesis, Langevin<sup>13</sup> gave an exhaustive analysis of ionic behavior. In Part III of the thesis Langevin analyzed the process of recombination. He was aware that for ions on the average  $10^{-2}$  cm apart the attractive forces must be minute indeed and that diffusion must play an important role. When, however, he computed the rate at which kinetically conceived oppositely charged gas ions several times larger than molecules could, as a result of heat motion, collide with each other so as to neutralize, he obtained a value for  $\alpha$  of the order of  $0.75 \times 10^{-9}$  instead of  $10^{-6}$ . He thus logically concluded that the *attractive forces must be active* in causing ions to drift together.

He then made the following assumption. The ions attract each other according to the Coulomb law, which says that  $f = e^2/r^2$ . If now we regard one ion as *fixed* relative to the other ion, then the field  $X$  of the fixed ion at a distance  $r$  is  $X = e/r^2$ . The fixed ion accordingly attracts the mobile ion, and the mobile ion drifts towards the fixed ion with a velocity  $v = X(k_+ + k_-)$ , where  $k_+$  and  $k_-$  are the mobilities of positive and negative ions respectively. If now we draw about the fixed ion a sphere of radius  $S$ , where  $S$  is large compared to the ionic free path (he placed  $S$  as about 0.1 the average distance of ionic separa-

tion), the rate at which the ions of opposite sign move through the surfaces  $S$  about all the fixed ions of one sign per cubic centimeter is  $dn/dt = n_+n_-4\pi S^2v$ , since there are  $n_+$  ions per cubic centimeter and  $n_-$  ions per cubic centimeter available. Hence  $dn = n_+n_-4\pi S^2 e/S^2 (k_+ + k_-)dt = n_+n_-4\pi e(k_+ + k_-)dt$ . Since  $\alpha$  is defined by  $dn = -\alpha n_+n_-dt$ ,  $\alpha = 4\pi e(k_+ + k_-)$ .

This theory involves the assumptions (1) that the drift from the average distance of ionic separation to  $S$  does not occupy appreciable time, and (2) that the *opposite ions represent an isolated dynamical system moving in what is virtually a continuous resistant medium*. This assumption is clearly indicated in specifying  $S$  as greater than the free path, and in adding the mobilities.

The assumptions are actually only partially justified, and the error contained in them was not clearly pointed out until 1929.<sup>20</sup> However, before this, without discussing the difficulties in Langevin's procedure, J. J. Thomson<sup>21</sup> recognized the proper procedure needed in reconciling the low value for  $\alpha$  yielded by a pure diffusion theory with the basic attractive mechanism which Langevin correctly divined must play an important part in recombination. These considerations will receive full discussion in their proper place.

Using the expression for  $\alpha$  deduced above, Langevin calculated that  $\alpha$  for air would be about  $0.75 \times 10^{-5}$  instead of the value  $\alpha = 0.75 \times 10^{-9}$  given by diffusion. This value, as is seen, is of the correct order of magnitude. It is, however, some four to five times higher than the value of  $\alpha$  at atmospheric pressure. This discrepancy, Langevin pointed out, could be explained by the assumption that the *neutralization did not take place at every encounter between ions of opposite sign*. He therefore wrote that  $\alpha = 4\pi e(k_+ + k_-)\epsilon$ , where  $\epsilon$  is a factor less than unity which may vary with pressure. It must now be recalled that the Langevin method of mobility measurement directly evaluated the quantity  $\epsilon = \alpha/[4\pi e(k_+ + k_-)]$ . Langevin attempted to find a theoretical basis for  $\epsilon$  but did not succeed. In 1905 Richardson<sup>22</sup> derived a theoretical expression for  $\epsilon$ . It is precisely the same expression for the *correction factor*  $\epsilon$  independently arrived at by J. J. Thomson in 1924 in order to correct his diffusion equation for recombination. Both the expressions of Richardson and Thomson as originally deduced contained a slight blunder in the deduction which has since then been corrected by Cravath<sup>23</sup> and by Thomson himself.<sup>24</sup> Richardson's correction factor  $\epsilon$  was conceived on a sound physical basis and one *which is consistent with the proper recombination mechanism as envisaged by Thomson*. Richardson's  $\epsilon$  is thus based on principles which are logically contradictory to the mechanism assumed by Langevin. In ignorance of this inconsistency, it was used to attempt to account for the values of  $\epsilon = \alpha/[4\pi e(k_+ + k_-)]$  as observed by Langevin. Since *below 3 atmospheres' pressure in air Langevin's theory is definitely wrong*, and since Richardson's factor  $\alpha$  is based on principles logically

contradictory to that theory, it must not be used with it. It is therefore not surprising that the value of  $\epsilon$  from Richardson's theory did not agree with  $\epsilon$  as evaluated experimentally by Langevin from  $\epsilon = \alpha/[4\pi e(k_+ + k_-)]$ . The quantity  $\alpha$  deduced by Langevin's measurements as  $\alpha = 4\pi e(k_+ + k_-)\epsilon$  will be a *true observed value of  $\alpha$*  as yielded by the conditions of this experimental method. The Richardson-Thomson  $\epsilon$ , then, will give *correct* values of  $\alpha$  only when combined with Thomson's diffusion theory of recombination and is *not related in any way to Langevin's  $\epsilon$* . This will become clear later.

For *high* pressures it will be seen that  $\epsilon$  becomes approximately unity. In this region the mechanics of ion formation results in ion distributions and densities which begin to approach the conditions assumed to exist by Langevin. Hence at high pressures Langevin's theory is applicable. As will later be seen, the mechanism of recombination is then no longer a *volume* recombination but is *preferential* recombination.

The experimental results following the development of Langevin's theory, however, were not such as to raise any doubts about the theory. The theory accordingly has been accepted as correct and is *today taught as the appropriate theory* despite the fact that nearly ten years have elapsed since the error was pointed out, and the error was rediscovered in 1932 independently by Harper.<sup>25</sup>

The next significant advances in the study of recombination occurred in the years 1913 and 1914 through the work of Plimpton<sup>12</sup> and Rümelin.<sup>8</sup> Rümelin in 1914 used the rate of growth method with  $\beta$ -ray and  $\gamma$ -ray ionization for which a revolving shutter was required. This gave Rümelin a chance to measure  $\alpha$  over relatively greater ranges of time and at relatively short ages,  $10^{-3}$  second. To his surprise, Rümelin found that  $\alpha$  was quite high at shorter time intervals and that it fell to more normal values with time. Since Rümelin was working with fairly clean gases he explained his result as being caused by the early existence of *mobile free electrons*, which he believed would recombine much more *rapidly* with ions than would the slow negative ions. At that time the existence of electronic carriers in gases at early ages was just being recognized. In the assumption of possible free electrons in the initial periods after ionization, Rümelin was therefore justified. However, he did not know what is known today, namely, that electron recombination is an *unlikely* process and that  $\alpha$  for *electrons* is of the order of  $10^{-10}$ .

Plimpton<sup>12</sup> in 1913 under the direction of Wellisch used the Rutherford rate of disappearance method for measuring  $\alpha$ . A flash of X-rays of very short duration ionized the gas, and after a time  $t$ , determined by pendulum, the ions were collected by a strong sweeping field and measured. Plimpton plotted  $1/n$ , the reciprocal of the observed ion concentrations  $n$ , as a function of time  $t$  from 0.025 to 0.3 second with values for  $1/n$  at  $t = 0$  also recorded. The concentration  $n$  was the

collected ion quantity  $Q$  divided by the ionized volume  $V$ . The flash time was always very short compared to  $t$ . As these curves showed  $n$  to vary with  $t$  he evaluated  $\alpha$  from the slope of the curves according to the equation  $\alpha = d(1/n)/dt$ . This was done for several gases at pressures ranging from 37 to 355 mm in  $\text{SO}_2$ , and over less extended ranges in other gases. In all gases  $\alpha$  was less at lower pressures than at higher. In all gases  $\alpha$  was high at very short time intervals, and decreased rapidly at first, later decreasing less rapidly. In no gas, however, had  $\alpha$  become constant at 0.3 second. In air the value of  $\alpha$  changed by a factor of 2.5 in the range of time intervals covered. The increase in  $\alpha$  with decreasing age of the ions was ascribed by Plimpton to an initial non-random distribution of the ions in space shortly after the short ionizing flash of the X-rays which gave densities differing from his assumed density  $n = Q/V$ . As time went on, the ions diffused to a random distribution and  $\alpha$  fell. This excellent piece of work and the correct explanation of the phenomenon, however, appear to have been overlooked, and its full implications were not then realized.

During the years 1926 to 1928, while Marshall was developing his apparatus, Loeb and later in discussions Loeb with A. Joffé had arrived at the conclusion that the theory of Langevin was inconsistent with that of Thomson in principle and that an  $\epsilon$  could not be worked out in theory that would justify Langevin's proposed mechanism. It was further borne in on Loeb<sup>27</sup> that the fact that  $\text{H}_2$  gas with its high values of the ionic mobility  $k$  had an  $\alpha$  of the same magnitude, or even less, than  $\alpha$  for air was highly inconsistent with Langevin's theory. This and other factors seemed to favor Thomson's theory of recombination as against Langevin's. There was no convincing experimental evidence of a definite sort, however, since Plimpton's results were not then known to Loeb or apparently any other workers in the field. As soon as Marshall began to obtain results with the commutator method, the curves of  $n$  as a  $f(t)$  quickly convinced Loeb and Marshall that  $\alpha$  was not constant, especially at short time intervals. The work of Plimpton and of Rümelin was thus confirmed. In the ignorance of Plimpton's work, Loeb and Marshall thus independently had arrived at the same explanation as had Plimpton, viz., that the initial non-random distribution of ions gave high values of  $\alpha$ . At greater ages the value of  $\alpha$  fell as ions drifted or diffused apart to a more random distribution as time went on. This conclusion was tested, far more extensively than was Plimpton's, in various ways, such as varying the flash period and the density of ionization by varying the intensity of the X-ray beam by a known amount. Increasing the density of ionization, as Cravath pointed out, should decrease the abnormally high value of  $\alpha$  found at a given value of  $t$ . Later this was proved more extensively by Gardner.

As soon as it was clear that the ions were diffusing apart in time, it was quite clear to Loeb that the necessary experimental data were at hand to establish definitely the validity of Thomson's theory and the

failure of Langevin's theory for air at atmospheric pressure. *Langevin's theory does not permit of a drift apart of the ions*, i.e., diffusion. The ions *must drift together* at all times. It then became necessary to discover the source of error in Langevin's reasoning. The error, once it was sought, became obvious. At  $10^{-2}$  cm apart and even down to  $10^{-3}$  cm apart gaseous ions at atmospheric pressure exert very feeble forces on each other. This fact would be immaterial were the ions immersed in a continuous fluid. They are, however, executing heat motions in equilibrium with gas molecules that are not many times less massive than the ions. Thus each of the ions is being knocked hither and thither randomly by molecular impacts, *whose impact forces are larger than the attractive forces*. The two ions, therefore, cannot be treated as an *isolated system* subject only to their mutual attractive forces. Thus actually, as Richardson and J. J. Thomson had tacitly assumed, the ions undergo random heat motions and *nearly* pure diffusion until they are within a distance  $r_0$  of each other such that the Coulomb potential energy  $e^2/r_0$  equals or exceeds the average energy of translation  $\frac{3}{2} kT$ . Inside this region,  $r_0$ , the ions are actively drawn together somewhat as Langevin had predicted. Outside the sphere of radius  $r_0$  the ions separate by diffusion at first much more slowly than usual, later more normally.

At this time Loeb had the opportunity of discussing the problem with Sommerfeld, who confirmed Loeb's reasoning and developed the Brownian-movement theory of the process.<sup>20</sup> The same general conclusion was arrived at independently and somewhat later by W. R. Harper<sup>25</sup> working with the Tyndall group in the Bristol laboratory. Although the treatment of Harper differs from that of Sommerfeld, and the constants of the derived expressions differ, the two men are in general agreement as to the process, whose mathematical difficulties are nearly insuperable.<sup>68</sup> At the request of the author, R. H. Fowler reviewed both derivations. He stated that neither of the treatments was more rigorous than the other and that they represented the situation about as well as approaches of this type permit since more rigorous ones seem at present to be impossibly difficult. As will be seen, however, there is urgent need for an accurate study of the diffusion equation for two particles attracting each other on a Coulomb law in a gas in the proximity of the region where kinetic and potential energies begin to equalize.

It can therefore be accepted without question that in part the Langevin theory *is incorrect* under ordinary circumstances in air. The error comes essentially in Langevin's neglecting the high value of the kinetic energy and thus making  $S$  thousands of times  $r_0$ . As a consequence of this, Langevin naturally also neglected to include in his value of  $\alpha$  the time taken for diffusion down to the sphere of active attraction. It is in this respect that Thomson has achieved the proper approach. Where the gaseous density becomes so high and  $T$  so low that all the



ions are generated *within*  $r_0$ , however, the Langevin theory can be expected to hold.

In air at atmospheric pressure and below the gaseous density is too low, and Plimpton's results indicate that this condition applies equally to the other gases. It thus becomes essential first to consider the nature of the ionic diffusion for ions of opposite signs in a gas as a function of the distance, and second to derive the Thomson theory of *ionic volume recombination*.

## 7. THE MOTION OF BROWNIAN PARTICLES ATTRACTING EACH OTHER IN A GAS

Consider two particles 1 and 2 in a three-dimensional coordinate system subjected to the unbalanced impact forces  $X_1$  and  $X_2$  caused by unequal bombardment of gas molecules.

Let  $u_1$  = vector velocity of 1 =  $\dot{\omega}_1$ .

Let  $u_2$  = vector velocity of 2 =  $\dot{\omega}_2$ .

Let  $\omega_1$  = position vector of 1.

Let  $\omega_2$  = position vector of 2.

Let  $B$  = coefficient of viscous drag in the gas.

Let  $e$  = charge on ion.

Let  $r$  = scalar distance between ions.

Then we have from the laws of motion

$$m\dot{u}_1 = -Bu_1 + X_1 + \frac{e^2}{r^2} \left( \frac{\omega_2 - \omega_1}{r} \right), \quad (1)$$

$$m\dot{u}_2 = -Bu_2 + X_2 + \frac{e^2}{r^2} \left( \frac{\omega_1 - \omega_2}{r} \right). \quad (2)$$

Multiply 1 by  $\omega_1$  and 2 by  $\omega_2$ ; then, since

$$\omega_1 u_1 = \frac{1}{2} d(\omega_1^2),$$

$$\omega_1 \dot{u}_1 = \frac{d}{dt} (\omega_1 u_1) - u_1^2,$$

it follows that

$$m \left[ \frac{d}{dt} (\omega_1 u_1 + \omega_2 u_2) - (u_1^2 + u_2^2) \right] = -\frac{B}{2} \frac{d}{dt} (\omega_1^2 + \omega_2^2) \\ + X_1 \omega_1 + X_2 \omega_2 + \frac{e^2}{r^3} [(\omega_2 - \omega_1)\omega_1 + (\omega_1 - \omega_2)\omega_2].$$

Now

$$[(\omega_2 - \omega_1)\omega_1 + (\omega_1 - \omega_2)\omega_2] = [(\omega_2 - \omega_1)(\omega_1 - \omega_2)] = -r^2.$$

If times are sufficiently large, the displacements are as often positive as negative so that  $X_1\omega_1$  and  $X_2\omega_2$  become sensibly zero.\* Also

$$m(u_1^2 + u_2^2) = 2(KE_1 + KE_2) = 2(\frac{3}{2}kT + \frac{3}{2}kT) = 6kT,$$

where  $k$  is the Boltzmann constant. Hence

$$m \frac{d}{dt} (\omega_1 u_1 + \omega_2 u_2) = -\frac{B}{2} \frac{d}{dt} (\omega_1^2 + \omega_2^2) + 6kT - \frac{e^2}{r}. \quad (3)$$

It is now necessary to find the time average of the integral of this equation over an interval  $\tau$  such that  $\tau$  does not vary by too large an amount, i.e., it is required to know the average velocity of diffusion for a given value of  $r$ . This is found as follows:

$$\begin{aligned} \frac{m}{\tau} \int d(\omega_1 u_1 + \omega_2 u_2) &= -\frac{B}{2\tau} \int d(\omega_1^2 + \omega_2^2) \\ &+ \frac{6kT}{\tau} \int_0^\tau dt - \frac{1}{\tau} \int_0^\tau \frac{e^2}{r} dt. \end{aligned} \quad (4)$$

The  $\int d(\omega_1 u_1 + \omega_2 u_2)$  vanishes for time intervals of the order of  $\tau$  used in this discussion since it is responsible for a transient term which in more than  $10^{-5}$  second for ions ceases to exert an influence. We can then set  $\Delta_1 = \omega_1^2 - \omega_0^2$  and  $\Delta_2 = \omega_2^2 - \omega_0^2$ , where  $\Delta_1$  and  $\Delta_2$  are the squared displacements from the initial value  $\omega_0$  of the particles in the time  $\tau$ . Then

$$\Delta_1 + \Delta_2 = \omega_1^2 + \omega_2^2 - 2\omega_0^2$$

and

$$d(\Delta_1 + \Delta_2) = d(\omega_1^2 + \omega_2^2).$$

One must next evaluate  $r$  as a  $f(t)$ . Since at large distances from the opposite ion the movement is a diffusion phenomenon,  $r$  may be expressed to a rough approximation as  $r = r_0 + a\sqrt{t}$ , where  $a$  is a constant.†

\* This deduction follows the procedure of the Langevin derivation of the Einstein Brownian-movement equation. In that, the error made by assuming that  $X_1\omega_1$  and  $X_2\omega_2$  when averaged over many impacts are zero appears not to be serious. The present derivation has been considered by Dr. Robert Serber, who points out that in the potential field of the ions the dropping of the terms  $X_1\omega_1$  and  $X_2\omega_2$  for the molecular impacts may not be warranted. The neglect of these terms while they will not alter the resultant expression in order of magnitude might well alter the numerical values of the constant terms obtained by amounts equal in magnitude to those found.

† This assumption is an approximation made in order to understand how the motion will be altered. It is not valid near the opposite ion and thus holds for large values of  $d$  only. The numerical values resulting from its use are not to be considered significant.

To a rough approximation it can then be shown by expansion in series and choosing the first two terms that

$$\int_0^{\tau} \frac{dt}{r_0 + a\sqrt{t}} = \frac{\tau}{r_0}.$$

This yields the result that

$$\frac{B}{2\tau} (\Delta_1 + \Delta_2) = 6kT - \frac{e^2}{r_0},$$

whence

$$\Delta_1 + \Delta_2 = \frac{2\tau}{B} \left( 6kT - \frac{e^2}{r_0} \right) = 2 \frac{6kT\tau}{B} \left( 1 - \frac{e^2}{6r_0kT} \right).$$

Now  $B = e'K$ , where  $K$  is the ionic mobility. Multiply top and bottom of the term  $2kT\tau K/e$  by the Avogadro number  $N_A$ . Then since  $N_A k = R$ , as  $RT = PV$ , as  $N_A e/V =$  the Faraday constant  $Ne$  per cubic centimeter, and since  $K/D = Ne/P$ , where  $D$  is the coefficient of diffusion, we have

$$\Delta_1 + \Delta_2 = 2 \left\{ 6D\tau \left( 1 - \frac{e^2}{6r_0kT} \right) \right\}.$$

This represents the rate of *diffusion apart* of the *two* ions in three dimensions. If  $r_0$  is large then  $\Delta = 2\Delta_1 = \Delta_1 + \Delta_2 = 2\{6D\tau\}$ . This is just twice the Brownian displacement equation for a single particle in three dimensions, as deduced by Einstein and V. Smoluchowski. We see then that the equation represents a diffusion *apart* of the ions beyond a distance  $r_0 = e^2/(6kT)$ . Beyond but near this value of  $r_0$  there is a *retarded diffusion apart* whose numerical value is probably not properly represented by the equation. Inside  $r_0 = e^2/(6kT)$  the equation is meaningless and the value of  $\Delta$  is not correctly given. Physically, however, we know that inside  $r_0$  the motion is at first a *retarded drift of the ions together* which well inside  $r_0$  becomes the type of motion assumed by Langevin.

In 1932 W. R. Harper<sup>25</sup> independently deduced an analogous equation by a somewhat different but equally loose reasoning process. In his original paper Harper made the mistake of using  $2Dt$  for the square of the diffusion displacement in three dimensions in a time  $t$  instead of  $6Dt$ . This was later corrected.<sup>28</sup> Neglecting charges, Harper arrived at an expression for the square of the separation  $r$  of the ions in a time  $t$  due to diffusion alone, which reads

$$r^2 = 6(D_1 + D_2)t + \bar{R}_0^2.$$

This expression Harper differentiated to get the rate of radial diffusion apart  $dr/dt$ . Hence he finds  $dr/dt = 3(D_1 + D_2)/r$ . From this quantity Harper deducts the relative drift velocity of the ions, which is  $(k_+ + k_-)e/r^2$ .

Harper then assumes that the value of  $dr/dt$  when attractive forces act is given by

$$\frac{dr}{dt} = \frac{3(D_1 + D_2)}{r} - \frac{(k_+ + k_-)e}{r^2}.$$

This expression as rewritten below is then equivalent to equation 3, page 109, of the Sommerfeld derivation after omitting the transient term and  $X_1\omega_1$  and  $X_2\omega_2$  but before integration. This can be seen as follows: Since

$$\begin{aligned} r \frac{dr}{dt} &= \frac{1}{2} \frac{d(r^2)}{dt} \\ \frac{d(r^2)}{dt} &= 6(D_1 + D_2) + \frac{2(k_+ + k_-)e}{r}. \end{aligned}$$

Equation 3, omitting  $X_1\omega_1$  and  $X_2\omega_2$  and the transient term, yields the equivalent expression as

$$\frac{d(r^2)}{dt} = \frac{d(\omega_1^2 + \omega_2^2)}{dt} = \frac{2}{B} 6kT - \frac{2e^2}{Br}.$$

Since for practical purposes one may set  $D_1 = D_2 = D$  and  $k_1 = k_2 = K$  to a sufficient degree of approximation with  $B = e/K$  the transformations above applied to Harper's equation give

$$\frac{d(r^2)}{dt} = 2(6D) - \frac{4Ke}{r},$$

while equation 3 yields

$$\frac{d(r^2)}{dt} = 2(6D) - \frac{2Ke}{r}.$$

The difference of the differential equations before integrating lies only in the factor 2 in the second term  $Ke/r$ . It can be ascribed to the difference in the process of setting up the equations. Harper evaluates what he calls the radial velocities of diffusion and ionic attraction separately and adds them as scalars. In the derivation above, the velocities are added by solution of the equations of motion. Both derivations neglect the  $X_1\omega_1$  terms. Hence both equations may well be numerically inexact. Whether Harper's addition of diffusion and mobility is better justified than the procedure using the equation of motion it is hard to state. Though both equations may be inexact, the question is not entirely trivial inasmuch as the condition  $d(r^2)/dt = 0$  gives the value of  $r_0 = d_0$  at which diffusion just equals attraction. According to equation 3 this occurs at  $6D = Ke/d_0$ ; according to Harper it occurs at  $6D = 2Ke/d_0$ . Bearing in mind the transformations, equation 3 gives  $d_0 = e^2/(6kT)$  while the other equation yields  $d_0 = e^2/(3kT)$ . In deriving his equation of recombination, J. J. Thomson set as the limiting radius of his sphere of active attraction the condition that the

potential energy  $e^2/d_0$  of the ions just equal the average molecular energy of translation  $\frac{3}{2}kT$ . This has been used by most of the experimentalists interested in testing Thomson's theory, including Gardner. Thus, Thomson sets  $e^2/d_0 = \frac{3}{2}kT$ , or  $d_0 = e^2/(\frac{3}{2}kT)$ .

The reason why one uses  $\frac{3}{2}kT$  when each ion has independently  $\frac{3}{2}kT$  is that the ions form a system, and it is the "relative" kinetic energy of the ions in the system that is of consequence. In the system the center of mass has an energy of  $\frac{3}{2}kT$ . The rest of the 2 ( $\frac{3}{2}kT$ ) in the system, namely,  $\frac{3}{2}kT$ , is available to the motion of the ions relative to the center of mass. It can be seen that this is correct when one considers that the relative energy when both ions move in the same sense is zero and in opposite senses it is  $2(\frac{3}{2}kT)$ . Thus for all possible motions the average value will be  $\frac{3}{2}kT$ . One is thus bound to set  $e^2/d_0 = \frac{3}{2}kT$  as the limiting condition from open orbits to closed "capture" orbits. This criterion, according to several mathematical physicists recently consulted, appears to give the most nearly correct value of  $d_0$  in the absence of any precise and rigorous theory. Until the difficult rigorous theory is at hand we will therefore use the criterion of Thomson, which gives excellent agreement with experiment at the present state, in place of either Harper's or Sommerfeld's theory. The reason why both Harper's and the Sommerfeld's treatments lead to an incorrect criterion for attraction doubtless lies in the neglect of the  $X_1\omega_1$  and  $X_2\omega_2$  terms since, in the field near  $d_0$ ,  $\omega_1$  and  $\omega_2$  are functions of  $e^2/r$  and not randomly independent. In what follows, then, Thomson's and not Harper's or Sommerfeld's condition for  $d_0$  will be used.

It is at once seen that for a given value of  $T$  the value of the radius  $d$  of the sphere of active attraction  $d_0$  is fixed, since it depends only on  $e$ ,  $k$ , and  $T$ . For  $0^\circ \text{C}$  it is  $4.051 \times 10^{-6} \text{ cm}$ , on the basis of Thomson's condition. On the criteria of Harper and of the Sommerfeld theory, it is one-half or one-fourth as large, respectively.  $d_0$  varies as  $273/T$ . In a gas at N.T.P. it is of the order of twelve times the average molecular distance and is about one-half of a molecular mean free path, or of the order of about twice an ordinary ionic free path. It is 100 to 200 times the average molecular radius. *The quantity  $d_0$  is the basic parameter which distinguishes between the processes of recombination and determines whether recombination will be of the preferential or Langevin type or whether it will be of the volume or J. J. Thomson type.* The physical order of magnitude of  $d_0$ , it is seen, places conditions in most gases at N.T.P. near the point of transition from one type of mechanism to the other. One is now in a position to consider the theory of J. J. Thomson.

## 8. THE THOMSON<sup>21,24</sup> THEORY OF VOLUME RECOMBINATION

Let it be assumed that the ionizing act and the process of electron attachment to molecules to give negative ions in a given volume have resulted as follows:

1. All the negative ions are separated from their parent positive ions by distances larger than  $d = e^2/(\frac{3}{2}kT)$ .\*

2. That the ions of both signs are isotropically distributed but with a random space distribution of positive ions relative to negative ions.

3. That there are  $n_+$  positive ions and  $n_-$  negative ions per cubic centimeter. That the ions are moving with an average thermal velocity  $\bar{c}_+$  and  $\bar{c}_-$ , where these are related to the average root mean square velocities  $C_+$  and  $C_-$  in the usual manner and  $\frac{1}{2}m_+C_+^2 = \frac{1}{2}m_-C_-^2 = \frac{3}{2}kT$ . The average relative velocity is then  $\sqrt{\bar{c}_+^2 + \bar{c}_-^2}$ , which for  $\bar{c}_+ = \bar{c}_- = \bar{c}$  becomes merely  $\sqrt{2}\bar{c}$ .

4. That when an ion of one sign reaches the surface of a sphere of radius  $d$  of opposite sign in which active attraction occurs the ions recombine.

Then, if one considers the ions of one sign as fixed and those of the opposite sign as moving in a random fashion with the relative velocity among them, the moving ions each sweep out a volume  $\pi d^2 \sqrt{\bar{c}_+^2 + \bar{c}_-^2}$  per second within which any opposite ion will be expected to combine with that ion. Hence in a time  $dt$ , in 1 cm<sup>3</sup> of volume,  $dn$  such combining encounters will occur as given by

$$dn = n_+ n_- \pi d^2 \sqrt{\bar{c}_+^2 + \bar{c}_-^2} dt.$$

If we count these combinations as decreasing the number of ions present, the expression requires a negative sign in front of the  $n$ . Now the coefficient of recombination is defined by  $dn = -\alpha n_+ n_- dt$ , whence we see that on this basis  $\alpha = \pi d^2 \sqrt{\bar{c}_+^2 + \bar{c}_-^2}$ . This is precisely the equation used in Langevin's first attempt at a diffusion theory of recombination. It failed only because in place of  $d$ , the radius of the sphere of active attraction, Langevin placed the ionic collision radii.†

\* From now on it will not be necessary to place the subscript 0 after the  $d$  as heretofore; the latter  $d$  will signify  $d_0$ .

† In the third edition of his *Conduction of Electricity through Gases*, Thomson points out that one can try to use the Langevin expression replacing the ionic diameter  $\sigma$  by a quantity  $b$  defined by  $b^2 = \sigma^2 \left( 1 + 2 \frac{m_+ + m_-}{m_+ m_- C^2} \frac{e^2}{\sigma} \right)$ . Here  $m_+$  and  $m_-$  are the ionic masses and  $C^2$  is the averaged square of the relative thermal velocity  $\bar{c}_+^2 + \bar{c}_-^2$ . This term virtually represents the apparent increase in the ionic diameter owing to the free interaction of the ionic forces during the last mean free path.  $b$  is the increased collision diameter caused by attractive Coulomb forces. For  $\sigma = 2.95 \times 10^{-8}$  at 0° C the added term gives  $b^2/\sigma^2 = 140$ . Hence, the  $\alpha$  calculated by Langevin from  $\alpha = \pi \sigma^2 \sqrt{\bar{c}_+^2 + \bar{c}_-^2}$  is to be increased 140 fold. However, this factor is still inadequate to account for  $\alpha$ , as it raises  $\alpha$  from  $7.5 \times 10^{-10}$  to  $1.05 \times 10^{-7}$  only, instead of to  $1.5 \times 10^{-6}$ . It is clear that this factor again is not adequate and that a strict "collision" theory of recombination will not suffice. For this reason Thomson developed the present theory based on the sphere of attraction, whose coefficient has just been derived.

Again, however, while this expression gives approximately the right magnitude for  $\alpha$  its values as estimated from Thomson's  $d$  are *too high*. This can be seen as follows. Assume  $\bar{c}_+ = \bar{c}_-$ .  $C_r^2 = 6kT/m$ , where  $C_r = 2C_+$  and  $C_+$  is the rms velocity. For  $O_2$ ,  $m = 2M$ , where  $M$  is the molecular weight. This gives  $\bar{c}_r = 5.2 \times 10^4$  cm/sec. Hence  $\alpha = \pi \times 6.6 \times 10^{-12} \times 5.2 \times 10^4 = 2.7 \times 10^{-6}$ , which is higher than Gardner's observed value of  $2.0 \times 10^{-6}$ . It is therefore essential to see what happens inside the distance  $d$ . This obviously depends on pressure and on the dimensions of  $d$ . If  $d$  is large compared to the free path of the ions entering, then a modified diffusion equivalent to a gradual drift together will begin. If  $d$  is small compared to the free path, the ions entering  $d$  will rapidly accelerate towards each other. They may then undergo a collision (see footnote), or more frequently they will separate on open orbits. Some of the ions may suffer molecular collisions within  $d$  and form closed orbits. Eventually, in either event, the ions will attract each other with no intervening impacts and end either by having neutralizing impacts or by executing the appropriate inverse square attractive force law orbits about their common center of mass. Depending on whether the energy of the ions at the last encounter is less than, equal to, or greater than that gained in a free fall from infinity under the attractive forces, the orbits will be closed ellipses, parabolas, or hyperbolas. If the value of  $d$  is of the order of a free path or less the ions will in general come together with energies which are the heat energies plus the energy gained in the field, and the orbits will be open. Thus, in this case, the ions have a good chance of separating after passing each other. If, however, they make kinetic impacts with neutral molecules inside  $d$  they have a fair chance of losing part of the energy gained in the field and thus have a fair chance of being "captured" into elliptical orbits.

It was assumed by both Richardson and Thomson that capture into such an orbit meant neutralization of charge. This will receive discussion later. J. J. Thomson postulated that one impact of one of the ions inside  $d$  would in general serve to reduce the energy sufficiently to close the orbit. Richardson, in his attempt to arrive at Langevin's observed value of  $\epsilon$  (which is impossible as Langevin's  $\epsilon$  is not physically consistent with Richardson's calculation), considered the effect of two or more collisions within  $d$ . Inasmuch as there was a slight error in the original solution of the theory, the equations for double and triple impacts are not available for test without recalculation. As will later be seen, the criterion of a single impact suffices for Thomson's theory, while more were required to give the numerical values of Langevin's observed  $\epsilon$ .

Before proceeding to the calculation of the correction to the coefficient  $\alpha$  it is necessary to consider further the actual recombination as a fundamental process. The positive ion consists of a molecule or perhaps two or three molecules lacking an electron and having a net posi-

tive Coulomb field which acts to an electron as a potential trough having various vacant low-lying levels. How the virtual energy levels of an ion complex would look, one cannot say. They would be of the nature of molecular levels. The negative ion in general consists of a similar aggregate of perhaps one or two molecules with the extra electron sitting in a small potential trough in the ion. In  $O_2^-$  the depth of this trough is estimated to be less than 0.2 volt; in  $Cl^-$  it is more nearly 5.1 volts.

As the ions approach, the Coulomb potential trough of the positive ion lowers the barrier of the negative electron trough in the negative ion, as shown in Fig. 48. If the ions approach sufficiently closely so that the barrier is obliterated, the electron will roll into one of the vacant energy levels in the positive ion. This condition should be achieved for oxygen ions at a distance of some  $7 \times 10^{-7}$  cm, provided that the a priori probability for the transition from the ionic state to a vacant level in the positive ion in the absence of a barrier will permit transfer in the time during which the ions are at this distance. In the case of  $Cl^-$  the approach would have to be of the order of  $3 \times 10^{-8}$  cm, or virtually that involved in a kinetic-theory impact. There is also some chance in both cases, however, that the electron will diffract over the potential hill and thus neutralize the ion. This chance can be expressed in the form  $W_{tr} = ae^{-1/\tau}$ , where  $a$  is the a priori probability of the transition and  $\tau$  is a characteristic time interval which decreases rapidly as  $r$ , the interionic distance, decreases. Thus, if the ions approach to within  $r$  of each other for a time greater than  $\tau$ , or better yet to within  $r_1$  for a time  $\tau_1$  characteristic of  $a$  alone, the transfer will be relatively likely. As the more likely form of recombination process is non-radiative, it is conceivable that  $a$  may be very small until the ions approach to distances  $r \sim \sigma$ , where  $\sigma$  is of the order of the kinetic-theory collision radius at which the ions can take up the energy of neutralization in recoil. It is likely that adequate data on  $a$  in different gases in which the collision probability can be eliminated by calculation would aid in answering the questions raised. No such data exist today.

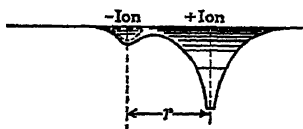


FIG. 48.

In the absence of further knowledge, it is, therefore, proper in discussing gases at N.T.P. to assume with Thomson that once two opposite ions approach to within  $d$  of each other one impact of either ion with a neutral molecule will on the average suffice to give orbits of such a nature that the time spent in close approach permits neutralization. The ions which do not suffer such impacts then escape recombination and must in general await encounters with *other* ionic partners before being neutralized. Further justification of this assumption is furnished by the agreement of the meager data on hand with Thomson's theory.



Thus we must multiply the value of  $\alpha$  inferred above,

$$\alpha = \pi d^2 \sqrt{\bar{c}_+^2 + \bar{c}_-^2},$$

by the fraction  $\epsilon$ , which we may compute with Thomson from the chance that an ion encounters a molecule when the ions are within  $d$  of each other.

Consider an ion path  $AB$ , of a negative ion headed through a sphere of radius  $d$  drawn about a positive ion assumed at rest as shown in Fig. 49. The assumption of the fixed positive ion is here permissible, as we are dealing with ions in their last free paths and the ions are interacting on a Coulomb law for the time being without outside interference. The path would cross the sphere and enter it at a point making an angle  $\psi$  with the line drawn from the positive ion. For simplicity it will be assumed that the path  $AB$  is straight, which is certainly incorrect, as the ion path will be deflected by the attractive forces. This

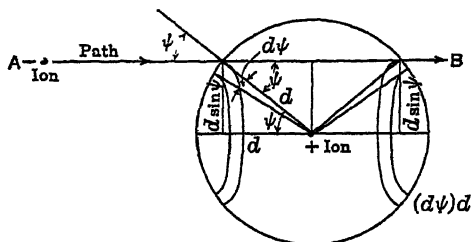


FIG. 49.

assumption which is contrary to fact could introduce an error of perhaps as much as 50 per cent in the value of the path. The error will be serious for those paths so directed or associated with such energy that recombination is certain (see footnote, page 113). They would thus not influence the result, as they would merely make

assurance more sure. For other paths the error will not be serious. The effect on the paths that would alter the number of ions recombining will be such as to increase the value over what is calculated. Hence neglect of path curvature will lead to a calculated  $\alpha$  which may be at most some ten per cent too low. In view of the uncertainty in the values of the physical parameters required the error is not serious. Curvature being neglected, the length of path inside  $d$  is  $x = 2d \cos \psi$ , as can readily be seen from Fig. 49.

The chance of escaping an impact in the path  $x$  is given by  $e^{-x/L_-}$  (see page 647), where  $L_-$  is the mean free path of the negative ion. Now the chance of an ion striking the surface of  $d$  at an angle  $\psi$  with the normal to the surface is not equally probable over the surface (it is here that Thomson and Richardson made their original error, since corrected). The chance depends on the area of the zone between  $\psi$  and  $\psi + d\psi$  and on the base of the hemisphere of radius  $d$  about the positive ion perpendicular to the direction of motion. The relative area of the zone is

$$\frac{2\pi d^2 \sin \psi d\psi}{\pi d^2} = 2 \sin \psi d\psi,$$

and this must be multiplied by  $\cos \psi$  to give the area projected on the normal to the direction of motion of the negative ion. Thus the chance of *escaping* collision with a neutral molecule in  $d$  for all angles  $\psi$  is the integral of the quantity

$$2e^{-\frac{2d}{L_-} \cos \psi} \sin \psi \cos \psi d\psi$$

from 0 to  $\pi/2$ . Since  $d(\cos \psi) = -\sin \psi d\psi$ , this gives the chance of *escaping* collision in  $d$  as

$$-2 \int_0^{\pi/2} e^{-\frac{2d}{L_-} \cos \psi} \cos \psi d(\cos \psi) = \frac{2L_-}{2d} \left[ \frac{L_-}{2d} (1 - e^{-\frac{2d}{L_-}}) - e^{-\frac{2d}{L_-}} \right].$$

Thus the chance that the negative ion collides and hence recombines is

$$\omega_- = 1 - \frac{2L_-^2}{4d^2} \left[ 1 - e^{-\frac{2d}{L_-}} \left( \frac{2d}{L_-} + 1 \right) \right].$$

For the chance of a positive ion experiencing a collision near a negative ion we have

$$\omega_+ = 1 - \frac{2L_+^2}{4d^2} \left[ 1 - e^{-\frac{2d}{L_+}} \left( \frac{2d}{L_+} + 1 \right) \right].$$

The chance that *both* ions suffer a collision within  $d$  is then  $\omega_+ \omega_-$ . Thus the probability of impacts in  $d$  ending in recombination  $\epsilon$  becomes  $\epsilon = \omega_+ + \omega_- - \omega_+ \omega_-$ . The reason for subtracting  $\omega_+ \omega_-$  is that in adding  $\omega_+$  and  $\omega_-$  we have counted the simultaneous impacts twice. Thus we can write that  $\alpha$  is given by

$$\alpha = \pi d^2 \sqrt{\bar{c}_+^2 + \bar{c}_-^2} (\omega_+ + \omega_- - \omega_+ \omega_-).$$

For purposes of computation one can, without serious error, use a mean value of  $L$  given by  $(L_+ + L_-)/2 = L$ . By a similar token one can in our present inexact knowledge in most gases set  $\sqrt{\bar{c}_+^2 + \bar{c}_-^2} = \sqrt{2} \bar{c}$ , where  $\bar{c}$  is an average value of  $c$ . If the ions are known to be very diverse in mass, this procedure is incorrect. Under the conditions assumed,  $\alpha$  becomes

$$\alpha = \pi \sqrt{2} d^2 \bar{c} (2\omega - \omega^2)$$

with

$$\omega = \left[ 1 - \frac{L^2}{2d^2} \left\{ 1 - e^{-\frac{2d}{L}} \left( \frac{2d}{L} + 1 \right) \right\} \right].$$

Loeb attempted to calculate a value of  $\alpha$  using  $\epsilon_L = \omega^2$  in place of  $(2\omega - \omega^2)$  for  $\epsilon$ . This makes recombination depend on simultaneous collisions of molecules with both positive and negative ions within  $d$  of each other. The curve for  $\epsilon_L$  is shown as curve II in Fig. 50. The present data on hand for  $O_2$ , however, do not warrant such a stringent condition for energy loss and insuring recombination. It is possible that in gases like  $Cl_2$  where ions are more stable  $\epsilon_L$  should be used.

In order to apply the equation for  $\alpha$  to practical problems, one can call the ratio  $2d/L = x$ . Then one has

$$d = \frac{e^2}{\frac{2}{3}kT} = 4.05 \times 10^{-8} \frac{273}{T}.$$

To facilitate solution one can set

$$L = 1 \times 10^{-5} \frac{760}{p} \frac{L}{L_A},$$

where  $L/L_A$  is the ratio of the mean free path of the ion to that of a molecule in air at N.T.P. This ratio can be found by evaluating  $L$  from the solid elastic mobility equation

$$k = 0.815 \frac{e}{M} \frac{L}{C} \sqrt{\frac{M+m}{m}}.$$

It has a value of the order of  $\frac{1}{3}$  in air and ranges from  $\frac{1}{3}$  to  $\frac{1}{2}$  in most gases. Under these conditions

$$x = 0.81 \frac{273}{T} \frac{p}{760} \frac{L_A}{L},$$

for a gas at *constant density* with  $p$  in millimeters of mercury and  $T$  in degrees Kelvin. Since  $L = L_0 \frac{760}{p} \frac{T}{273}$ , when the *density is not constant*

$$x = 0.81 \left( \frac{273}{T} \right)^2 \frac{p}{760} \frac{L_A}{L}.$$

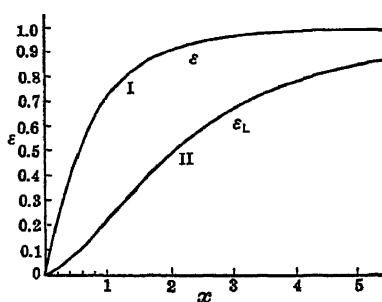


FIG. 50.

The values for  $\epsilon = 2\omega - \omega^2 = 2f(x) - f(x)^2$ , curve I, and for  $\epsilon_L = f(x)^2 = \omega^2$ , curve II, as a function of  $x$  for a range of  $x$  covering ordinary experimental measurements are shown in Fig. 50. For convenience a table of values of  $\omega$  and  $\omega^2$  for values of  $x$  ranging from 0.2 to 10.0 is also included as compiled by Gardner. It should be noted that great care must be used in computing  $\omega$  at small values of  $x = 2d/L$ , since the differences encountered

require *extensive expansion* of the exponential term.

If one set  $\bar{c}_+ = \bar{c}_- = \bar{c}$ , one can for purposes of computation make  $\sqrt{\bar{c}_+^2 + \bar{c}_-^2} = \sqrt{2}\bar{c} = 0.922 \sqrt{2} \sqrt{2/M} 1.84 \times 10^5 \sqrt{T/273}$ , where  $M$  is the molecular weight of the gas and  $1.84 \times 10^5$  is the root mean square velocity of agitation of the  $H_2$  molecule at 273° absolute.

TABLE V  
PROBABILITY FUNCTION FOR RECOMBINATION

$$\epsilon = f(x) = \omega = 1 - \frac{2}{x^2} [1 - e^{-x}(x+1)], \text{ where } x = 2d/L$$

| $x$  | $2/x^2$  | $e^{-x}$ | $\frac{f(x)}{\omega}$ | $\frac{\epsilon_L}{\omega^2} \{f(x)\}^2$ | $2\omega - \omega^2$ |
|------|----------|----------|-----------------------|--|----------------------|
| 0.2  | 50.00000 | 0.818731 | 0.12385               | 0.01534                                  | 0.23236              |
| 0.4  | 12.50000 | 0.670320 | 0.23070               | 0.05322                                  | 0.40818              |
| 0.6  | 5.55556  | 0.548812 | 0.32277               | 0.10418                                  | 0.54136              |
| 0.8  | 3.12500  | 0.449329 | 0.40248               | 0.16199                                  | 0.64297              |
| 1.0  | 2.00000  | 0.367879 | 0.47152               | 0.22233                                  | 0.72071              |
| 1.2  | 1.38889  | 0.301194 | 0.53143               | 0.28242                                  | 0.78044              |
| 1.4  | 1.02041  | 0.246597 | 0.58350               | 0.34047                                  | 0.82653              |
| 1.6  | 0.78125  | 0.201897 | 0.62885               | 0.39545                                  | 0.86225              |
| 1.8  | 0.61729  | 0.165299 | 0.66840               | 0.44676                                  | 0.89004              |
| 2.0  | 0.50000  | 0.135335 | 0.70300               | 0.49421                                  | 0.91179              |
| 2.2  | 0.41322  | 0.110803 | 0.73330               | 0.53773                                  | 0.92887              |
| 2.4  | 0.34722  | 0.090718 | 0.75988               | 0.57742                                  | 0.94234              |
| 2.6  | 0.29586  | 0.074274 | 0.78325               | 0.61348                                  | 0.95302              |
| 2.8  | 0.25510  | 0.060810 | 0.80385               | 0.64619                                  | 0.96151              |
| 3.0  | 0.22222  | 0.049787 | 0.82203               | 0.67573                                  | 0.96833              |
| 3.5  | 0.16327  | 0.030197 | 0.85892               | 0.73774                                  | 0.98010              |
| 4.0  | 0.12500  | 0.018316 | 0.88645               | 0.78579                                  | 0.98711              |
| 4.5  | 0.09876  | 0.011109 | 0.90728               | 0.82316                                  | 0.99140              |
| 5.0  | 0.08000  | 0.006738 | 0.92350               | 0.85285                                  | 0.99415              |
| 5.5  | 0.06612  | 0.004087 | 0.93664               | 0.87730                                  | 0.99598              |
| 6.0  | 0.05556  | 0.002479 | 0.94541               | 0.89380                                  | 0.99702              |
| 6.5  | 0.04734  | 0.001503 | 0.95319               | 0.90838                                  | 0.99800              |
| 7.0  | 0.04082  | 0.000912 | 0.95948               | 0.92060                                  | 0.99836              |
| 7.5  | 0.03556  | 0.000553 |                       |  |                      |
| 8.0  | 0.03125  | 0.000335 | 0.96884               | 0.93865                                  | 0.99903              |
| 9.0  | 0.02470  | 0.000123 |                       |  |                      |
| 10.0 | 0.02000  | 0.000050 | 0.98001               | 0.96042                                  | 0.99960              |

Thus, using Thomson's value for  $d$ ,  $\alpha$  becomes

$$\alpha = 1.73 \times 10^{-5} \left( \frac{273}{T} \right)^{3/2} \left( \frac{1}{M} \right)^{1/2}$$

$$\left[ 2f \left\{ 0.81 \left( \frac{273}{T} \right) \left( \frac{p}{760} \right) \left( \frac{L_A}{L} \right) \right\} - f^2 \left\{ 0.81 \left( \frac{273}{T} \right) \left( \frac{p}{760} \right) \frac{L_A}{L} \right\} \right],$$

when  $\alpha$  is measured at constant density starting at N.T.P. When the density is varied, i.e., at constant pressure, the  $(273/T)$  in the two  $f$  terms must be squared. If we use the Harper criterion for  $d$ , the absolute value for  $\alpha$  would have to be divided by 4, making the constant  $0.43 \times 10^{-5}$ , and the 0.81 in  $f$  would become 0.405; if the  $d$  which is inferred from the Brownian movement equation is used, the constant  $1.73 \times 10^{-5}$  becomes  $1.08 \times 10^{-5}$ , and the 0.81 in  $f$  becomes 0.205.

It is seen that the value of  $d$  is exceedingly important and that the whole phenomenon shifts to a different pressure range quite critically with the value of  $d$  chosen.

## 9. EXPERIMENTAL TEST OF THE VOLUME RECOMBINATION THEORY

It is clear that the final test of the recombination theory just developed must come by comparison with experiment. The Thomson

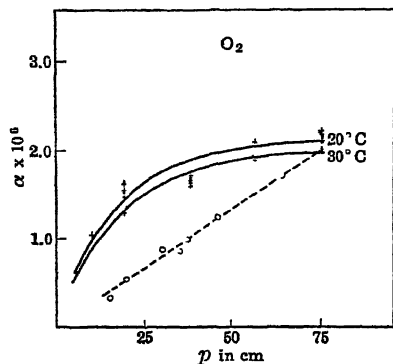


FIG. 51.

theory indicates a variation of  $\alpha$  with pressure which differs radically from that of the Langevin theory, and a similar striking difference applies to the temperature variation. Since the complicated form of the Thomson equation for  $\alpha$  does not permit of a visual picture of the variations, the curves calculated for  $O_2$  by Gardner will be given. For these the values chosen were  $d = 4.05 \times 10^{-6}$  cm,  $L_A/L = 5$ ,  $M = 64$ . These values are all more or less in agreement with our knowledge about the sizes and free paths of ions in pure  $O_2$ . See Chapter I. Prob-

ably the masses of positive and negative ions differ, and  $L_A/L$  may be more nearly 3.5 than 5; still the approximations are about as good as one can make, and  $2\omega - \omega^2$  is rather insensitive to small changes. For the variation of  $\alpha$  with pressure shown by the full curves of Fig. 51,  $T$  was chosen as  $293^\circ$  K and  $303^\circ$  K. For the variation of  $\alpha$  with temperature at constant pressure the full curve of Fig. 52 was computed for  $p = 760$  mm. It is to be noted that, near atmospheric pressure in  $O_2$ ,  $\alpha$  is nearly constant. It decreases as  $p$  decreases, at first slowly and then more rapidly, becoming very small at low values of  $p$ . In  $O_2$  and in air  $\alpha$  decreases somewhat hyperbolically as  $T$  increases.

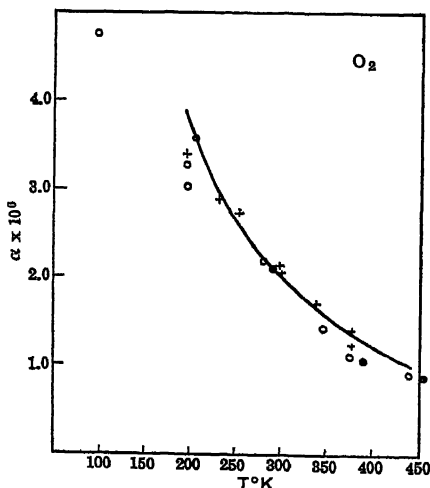


FIG. 52.

The Langevin theory with  $\epsilon$  constant makes  $\alpha$  inversely proportional

to pressure and at constant pressure demands that  $\alpha$  be nearly proportional to  $T$  as density, and hence  $1/k$ , the mobility, vary inversely with  $T$ . At constant density Langevin's  $\alpha$  should change little with  $T$ , as the mobility constant changes very little with  $T$  as shown on page 36. The factor  $\epsilon$  cannot be computed on Langevin's theory, but it must undergo a very rapid and complex change with  $p$  near atmospheric pressure to give the behavior such as predicted by Thomson's theory. Thomson's theory gives  $\epsilon = 1$  at higher pressures (above 5 atmospheres in air), and it will be shown that conditions there begin to favor preferential recombination, which obeys Langevin's law.

The older experimental data on which to test Thomson's theory are most unsatisfactory. Several measurements of  $\alpha$  as a function of  $p$  have been made. Most of the earlier measurements excepting those of Langevin,<sup>13</sup> Plimpton,<sup>12</sup> and Thirkill<sup>30</sup> followed uncertain methods, including  $\alpha$ -particle ionization. Of those observers mentioned, Langevin and Thirkill used Langevin's method, while Plimpton followed the original Rutherford method.<sup>11</sup> Plimpton's results were falsified by initial recombination to an unknown amount, and this factor was also present in the work of the other two observers. How change in pressure will affect the values obtained with initial recombination in time intervals of 0.05 to 0.3 second is not known. All results of these workers in air have been adjusted to a single point on Gardner's computed curve for  $O_2$  in Fig. 51, and the relative variation of  $\alpha$  with  $p$  can be seen from the circled points to be nearly linear. Except for Plimpton's one high value the observations of the various observers with this method lie quite well along the same curve. Their actual values, however, did not agree. In the case of the temperature variation we have merely the results of Phillips<sup>31</sup> at constant pressure and those of Erikson<sup>29</sup> at constant density to go on. Phillips<sup>31</sup> used Langevin's method while Erikson used the equilibrium value method in his second paper.

This method is definitely affected by initial recombination as seen on page 123. The results with changing temperature, however, are not nearly so adversely affected by initial recombination as are the results with pressure variation. Gardner has found that the form of the curve given by theory is very little changed in the range of temperatures from those of solid  $CO_2$  to  $100^\circ C$  by measuring at constant density or constant pressure. Accordingly, the relative results of Erikson and of Phillips in air adjusted to fit Gardner's theoretical curve at  $293^\circ C$  can be plotted as circles and circled crosses on the curve of Fig. 52 without serious error.

It is seen that the deviation from theory even in these early results is not serious and that Erikson's results taken at constant density, which should be slightly above the points (crosses), actually nearly coincide with them. The one significant feature of the results is the

single point of Erikson's (circle) at liquid-air temperatures which lies well below the theoretical extrapolated curve. Thus the earlier work essentially confirms the temperature variation but deviates somewhat from the expected pressure variation of the Thomson theory. These results are in any case not in accord with Langevin's theory unless one does considerable violence to that theory. More precise results in a known *pure* gas with only volume recombination and elimination of initial recombination and diffusion are required.

The only recent investigations in this region made with the greatest of care to eliminate all disturbing variables are those of Gardner<sup>15</sup> and Sayers.<sup>62</sup> Gardner's experimental points are plotted as crosses in Fig. 51 and Fig. 52. In the study of pressure variation his temperatures could not well be controlled in the twelve-hour runs of the experiment and one has them bracketed between two curves at 20° and 30°. Two different ionization chambers of volume 200 and 700 cm<sup>3</sup> were used, and values of  $\alpha$  were chosen only for intervals of 1 and 2 seconds when  $\alpha$  *had apparently reached a steady value* free from initial recombination. In such intervals the loss of electrons by diffusion at low pressures made study below 100 mm impossible. The losses of this sort raise the value of  $\alpha$  measured as the method can detect only a loss of ions and cannot distinguish the cause. In the case of the temperature variation, the conditions are much more uniform. It is seen that both Erikson's circled points and Gardner's crosses follow theory fairly well. Gardner observed in pure O<sub>2</sub> a falling off from the theoretical increase in  $\alpha$  at -79° C. A similar falling off in Erikson's values is observed in air with its lower O<sub>2</sub> content at liquid-air temperatures. This may be ascribable to a tendency of O<sub>2</sub> to form complexes at appropriate partial pressures as  $T$  decreases. Gardner showed that, if  $M = 96$  at -79° C, one gets his observed value. Pure O<sub>2</sub> condenses at liquid-air temperature, and such an hypothesis is consistent with the results observed. Thus, using the Thomson value of  $d$ , Gardner got (1) numerical agreement with his computed value of  $\alpha$ ; (2) acceptable agreement as to pressure variation in a limited region, and (3) encouragingly good agreement as regards temperature variation. One can thus confidently assert that the Thomson mechanism for recombination has been demonstrated for O<sub>2</sub> below 1 atmosphere to be in approximate agreement with experiment. This observation, taken together with the observed diffusion of ions apart, at and below 1 atmosphere, and the theoretical inadmissibility of Langevin's deduction in this range as well as the signal disagreement of his theory with experiment, establishes beyond a doubt the general validity of Thomson's procedure.

Some months after the publication of Gardner's work on O<sub>2</sub>, J. Sayers<sup>62</sup> published a paper on ionic recombination in air. This investigation was done with the same care and by essentially the same techniques as Gardner's. Sayers was able to measure and balance out his contact potentials by small bias batteries. His beam occupied the

whole volume between the plates while Gardner's did not. Sayers thus had to correct for diffusion. The correction was significant at low ion concentrations, otherwise not (see page 100). He measured  $\alpha$  using the rate of disappearance of ions as did Gardner. He did not measure  $\alpha$  for short intervals of time but used the slope of the reciprocal of concentration plotted against time as did Plimpton. From 0.05 to 0.5 second these were in general straight lines, that is,  $\alpha$  was constant. He also measured the *equilibrium ion* concentration and used the equation  $N_{\infty} = \sqrt{q/\alpha}$  for measuring  $\alpha$ , which he mistakenly calls "Rümelin's method." The method was *first* used by McClung in 1902. Rümelin used the rate of growth method in some of his work but found the equation  $N_{\infty} = \sqrt{q/\alpha}$  convenient for evaluating  $\alpha$ . In conformity with Plimpton, Marshall, and others Sayers observed initial recombination. In his work  $\alpha$  varied from about  $6 \times 10^{-6}$  to  $3 \times 10^{-6}$  in the time interval from  $10^{-3}$  to  $10^{-1}$  second. By the equilibrium concentration method of McClung under otherwise the same conditions the value of  $\alpha$  observed was  $5.2 \times 10^{-6}$  which is near the highest of the erroneous values observed at short time intervals due to initial recombination. This indicates that the methods where  $\alpha$  is measured with the generating source of ions acting continuously give fictitiously high values of  $\alpha$  due to initial recombination, as one could have suspected. It is seen, however, that the method gives an observed value of  $\alpha$  as indicated by the actual disappearance of ions *under those conditions*, which is double the equilibrium value of  $\alpha$  due to a real volume recombination process. This beautifully illustrates the statements made on page 91 concerning recombination coefficients in general.

Sayers also observed a decrease in  $\alpha$  with ion concentration varying from  $2.65 \times 10^{-6}$  with  $1.5 \times 10^6$  ions per  $\text{cm}^3$  down to  $2.3 \times 10^{-6}$  at  $4.4 \times 10^6$  ions per  $\text{cm}^3$ . This change in  $\alpha$  with ion concentration Sayers attributed to the formation of chemical substances, notably  $\text{O}_3$ , by the rays. Using softer X-rays, Sayers observed values of  $\alpha$  as low as  $1.65 \times 10^{-6}$ . Since between 0.1 and 0.5 second Sayers' curves for  $\alpha$  appeared constant, Sayers assumed that initial recombination was over after 0.1 second. This assumption is *not unreasonable*, and it was the hope of Gardner and the author in the course of Gardner's work to find this to be an experimental fact. In consequence Sayers logically ascribed the ion concentration effects mentioned to chemical changes of the gas and subsequent changes in the nature of the ions instead of to initial recombination. Such chemical changes undoubtedly take place, especially in air where oxides of nitrogen having a strong ion affinity are forming. Ozone is less likely to be an agent than nitric oxides, since unpublished results of Miss E. A. Higley in the author's laboratory showed that ion mobilities were little affected by  $\text{O}_3$ .

However, the facts are that Gardner, who was working with pure  $\text{O}_2$  where *much chemical change cannot take place* under X-ray ionization, observed the same sort of action, though perhaps to a lesser



degree. He investigated these phenomena over *much larger ranges of time intervals, concentration changes, etc.*, than did Sayers. He found that the *variation of the flash time* produced rather important changes in the  $\alpha_i - t$  curves. His conclusion was that in general the *appearance of constancy* in the values of  $\alpha$  between intervals from 0.1 to 0.5 second was largely illusory, the values continually changing with time, albeit slowly. As the later discussion of Gardner's results in this regard will show, the effect observed by both Sayers and Gardner is very complex, being due in part to initial recombination and in part to chemical changes. It is quite certain that if Sayers had extended his investigations over longer flash times and recombination periods as did Gardner

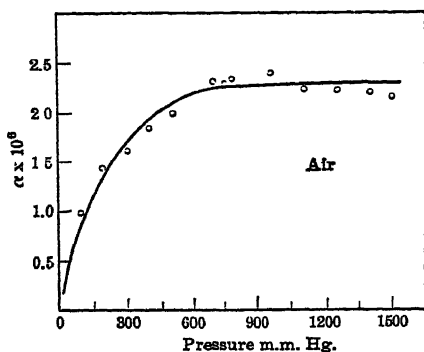


FIG. 53.

he would have been forced to the same conclusions. The author has hopefully looked for data indicating that the initial recombination period was short, but results appear to indicate a more complex mechanism. Sayers investigated the pressure variation of  $\alpha$  from 50 up to 1500 mm Hg in air. The points obtained lie closely along the curve of Thomson's theory, as shown in Fig. 53, where the full line is the theoretical curve. It is likely that the deviations at 1500 mm are real. In Fig. 54 we see Sayers' curve from 50 mm to 2 atmospheres combined with that of Mächler's data going from 5 atmospheres upward. The decline in Sayers' value of  $\alpha$  in *pure air* above 1 atmosphere seems to fit comfortably onto the prolongation of Mächler's curve in *impure air* above 5 atmospheres. Hence one may assume the decline to be real. It occurs, however, at a surprisingly low pressure. Thus again the Thomson theory seems to be established for *air from low pressures up to atmospheric pressure*. The decline of the curves above 1 atmosphere must be ascribed to a change in the

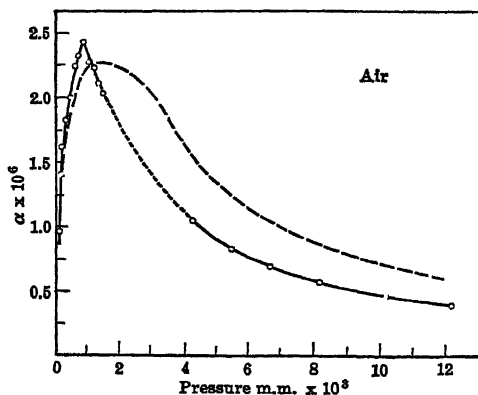


FIG. 54.

mechanism of recombination at higher pressures, which will presently be discussed.

#### 10. PREFERENTIAL RECOMBINATION

The analysis instituted by Thomson can be made to show that a mechanism akin to the *Langevin type of recombination must occur at very high pressures*. For if  $p$  becomes such that many molecules are moving within the sphere  $d$ : (1) the electrons will attach to form ions within  $d$ , and (2) the quantity  $\epsilon$  will automatically become unity. In this case the *electron or its ultimate negative ion never gets out of the sphere of influence of its parent atom*. It will then eventually literally recombine with it. If electrical fields are absent, the gas would essentially be un-ionized. Externally applied fields of sufficient magnitude, however, will be able to *pull the ions apart* and give rise to the measurement of *some* of the surviving ions. The number of these that are counted or measured will depend on the field strengths used.

In air, fields at atmospheric pressure up to 15,000 volts per cm may be used, and at higher pressures they can reach 15,000  $p/760$  volts per cm. These could separate ionic partners that are no closer than  $3.1 \times 10^{-6} \sqrt{760/p}$  cm apart if the heat motions were absent. With the energy of motion added it is probable that ions a bit inside the sphere of radius  $d$  can be separated even at 1 atmosphere. At 36 atmospheres, ions  $5.02 \times 10^{-7}$  cm apart can be separated without heat motions aiding. It is clear, however, that many of the ions, i.e., those that are close together, cannot be separated by the imposed outer field, and hence where preferential recombination is measured only a fraction of the ionized pairs are ever counted. In time, in the absence of fields, the ions within  $d$  that are available for count at higher fields will decrease in number and at the rate predicted by Langevin's theory. Hence in this region we have a new process of recombination, which has been called *preferential recombination*. It is in a class by itself, obeying a different law from that of the volume recombination. It will always appear where ion pairs are formed within the radius  $d$ . Owing to the slow rate of electron attachment this can occur only in gases where negative-ion formation readily takes place. Thus, *in the pure inert gases*, He, Ne, Ar, etc., *preferential recombination would not be expected to occur* at pressures usually attainable. It will probably not occur readily in *pure*  $H_2$  or  $N_2$  gases. It will occur readily in  $O_2$ ,  $Cl_2$ ,  $SO_2$ ,  $CO_2$  and in relatively impure gases above 5 to 10 atmospheres. It will also be of importance relative to volume recombination when ion densities become so low that volume recombination is rare. This has been observed in some cosmic-ray experiments.

It was clearly indicated that the presence of preferential recombination demanded electron attachment to form negative ions inside of  $d$ . By using the equation for electron attachment, one should be able to

account for the resultant observed coefficient of recombination in the pressure transition region between that where pure volume and pure preferential recombination occur. This was attempted by Loeb<sup>19</sup> in the following fashion. At any given pressure the number of electrons which have gone a distance greater than  $d$  before attaching should be capable of evaluation from the attachment law; see page 261. If a fraction  $f$  of the electrons goes the distance  $d$  or more from the positive ion before attaching, then these negative ions will in theory at least be in a condition to undergo volume recombination. Those that attach within  $d$ , i.e.,  $1 - f$ , will undergo preferential or Langevin recombination. Then if  $\alpha_T = 4\pi d^2 \sqrt{\bar{c}_+^2 + \bar{c}_-^2} (2\omega + \omega^2)$  represents the value of  $\alpha$  for the Thomson mechanism and  $\alpha_L$  represents the coefficient  $\alpha_L = 4\pi e(k_+ + k_-)$  for the preferential recombination, we can write  $\alpha = \alpha_T f + \alpha_L (1 - f)$ . To evaluate  $f$  one may proceed as follows.

If there were no field about the positive ion, the electron would diffuse a distance  $d$  in a time  $t$  given by  $d = \sqrt{(12/\pi)Dt}$ , where  $D$  is the coefficient of diffusion of the electron. This quantity  $D$  is roughly  $D = \frac{1}{3}\lambda\bar{c}_e$ , where  $\lambda$  is the electron free path and  $\bar{c}_e$  is the average electronic velocity. The electrical field reduces the diffusion away from the positive ion inside of  $d$ , and we must diminish  $D$  by a numerical factor  $\eta$  which up to the present has not been open to evaluation. Hence  $d = \sqrt{(12/\pi)(Dt/\eta)}$ . If  $n$  is the number of electrons per cubic centimeter, the number  $dn$  attaching in a time  $dt$  is  $dn = hn\bar{c}_e dt/\lambda$ . Here  $h$  is the probability of attachment, as will be shown in Chapter VI, and  $\bar{c}_e/\lambda$  is the electron collision frequency. If  $n$  is the number of electrons out of  $n_0$  electrons at  $t = 0$  which at a time  $t$  have not attached,  $f = n/n_0 = e^{-\frac{h\bar{c}_e t}{\lambda}}$ . Substituting  $\pi d^2 \eta / 12D = t$  and  $D = \frac{1}{3}\lambda\bar{c}_e$  into the equation, one has  $f = e^{-\frac{\pi h d^2 \eta}{4\lambda^2}}$ , which, neglecting the variation of  $\lambda$  and  $h$  with electron energy, can be written as  $f = e^{-a(\frac{p}{760})^2}$ . Again  $4\pi e(k_+ + k_-) = b/760/p$ . This gives the value for  $\alpha$  as

$$\alpha = \alpha_T e^{-a(\frac{p}{760})^2} + [1 - e^{-a(\frac{p}{760})^2}] b \frac{760}{p}.$$

Here  $p$  is the pressure in millimeters of mercury,  $a = (\pi/4)(hd^2\eta/\lambda_0^2)$ , where  $\lambda_0$  is the mean free path at 760 mm, and  $b = 4\pi e(K_0 + + K_0 -) = \alpha_L p/760$ .

The data available on which to check the theory are very poor. However, the work of Mächler<sup>17</sup> at high pressures, and of Langevin<sup>18</sup> up to 5 atmospheres and less, allows one to estimate that the theory becomes valid if  $\eta$  is taken as  $10^6$  for air. That the diffusion rate in the sphere  $d$  must be diminished by a factor of  $10^6$  in order to make the equation which is basically physically justified and of the right form fit the observed data, such as the data are, is rather surprising.

However, nothing whatever is known of the behavior of an electron or an ion when it is in the neighborhood of  $d$ , especially inside of  $d$ . Judging from the average energy with which electrons are removed from atoms or molecules and the low value of  $h$ , the author had for years contended that below 100 atmospheres preferential recombination was impossible. Since preferential recombination definitely appears to occur around 10 atmospheres in air, the required high value of  $\eta$  must be ascribed to either a decreased diffusion or an increased  $h$ . There is no doubt about the decreased diffusion inside  $d$ . The decrease is doubtless large, but the factor cannot be  $10^6$ . There is a distinct possibility that the presence of the ionic field inside of  $d$  and the initial high energies of the escaping electrons,  $\sim 1 - 7$  volts at  $10^{-7}$  cm from the positive ion, may facilitate electron attachment by perturbing the molecule. Bradbury has shown very rapid increases in the value of  $h$  above energies causing inelastic impacts or dissociation, as seen in Chapter VI. In this case with a 10 to 100 fold reduction of the diffusion and a  $10^5$  or  $10^4$  fold increase in  $h$ , the factor  $10^6$  could be explained. The relation given by the theory for the transition from volume to preferential recombination around 10 atmospheres in air with the observed values of  $\alpha_L$  and  $\alpha_T$  for  $O_2$  using  $\eta = 10^6$  is shown in Fig. 55. It is in agreement, such as the data warrant, with Langevin and Mächler's observations. This same value for  $\alpha$  is compared with Sayers' <sup>68</sup> curve for air as the dashed curve of Fig. 54. It should be pointed out that there is no adjustment of an empirical nature in the form of this relation. It is a direct and logical deduction from well-known physical facts. The only arbitrary factor involved is the numerical value of  $\eta$ , which can in part be accounted for on retarded diffusion and on increases of  $h$  with electron energy shown by Bradbury to occur in gases like  $O_2$ .

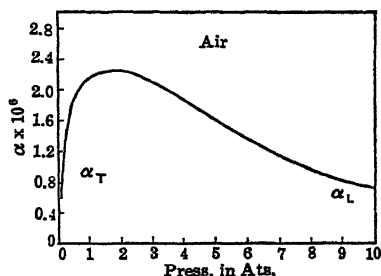


FIG. 55.

Unfortunately one cannot say as much for the general theory of recombination covering the same range deduced by Harper.<sup>25</sup> The theory has been proposed to supplant Thomson's theory at lower pressures and Langevin's theory at higher pressures. Harper, on the basis of physical reasoning, with no great mathematical precision, has derived what he believes are expressions for  $\alpha$  when the quantity  $d \doteq e^2/(3kT)$  is greater than  $L$ , the free path, and when  $d$  is less than  $L$ . These he believes are more accurate than Thomson's or Langevin's expressions. Although this view is not necessarily shared by others the equations deserve discussion. Starting with these expressions, Harper then devises an *empirical mathematical transition equation* giv-

ing the Langevin and Thomson expressions in the limit and passing smoothly from one to the other. There is no *physical justification* for the equation used except that it does its duty fairly well.

In the higher pressure region Harper calculates  $\alpha$  assuming that the ions *diffuse* to the sphere of attraction  $d_0 = e^2/(3kT)$ , and with  $d_0 > L$  he sets  $\epsilon$  as unity. It must be noted that Harper uses the factor  $3kT$  in the denominator instead of the *more correct Thomson factor*  $\frac{2}{3}kT$  (see page 112). Harper points out that a correction factor must be included for the curvature of the paths caused by the attractive forces. As a result of reasoning which is far from clear, owing to his failure to define his terms clearly before he uses them, Harper arrives at what he calls an attraction factor  $f(d)$  which reads

$$f(d) = 1 + \frac{d_0}{d} \log \frac{(n_+ + n_-)^{-1/2}}{2(d + d_0)}.$$

Here  $d$  is any value of the "collision" radius active in recombination which circumstances require. At high pressures it is virtually  $d_0$ .  $n_+$  and  $n_-$  are the average *initial* concentrations of the positive and negative ions respectively. This expression gives the value of  $\alpha$  for high pressures, essentially preferential recombination, in the Langevin regime as

$$\alpha = 3\pi d_0(D_+ + D_-) \left\{ 1 + \log \frac{(2n)^{-1/2}}{4d_0} \right\},$$

where  $2n = n_+ + n_-$ , and  $d = d_0$ . If one recalls that, when diffusion apart and drift together are equal,  $(D_+ + D_-) = (k_+ + k_-)e/d_0$ , the equation above becomes

$$\alpha = 3\pi e(k_+ + k_-) \left\{ 1 + \log \frac{(2n)^{-1/2}}{4d_0} \right\}.$$

This equation deduced on entirely different reasoning with admittedly uncertain numerical factors, however, differs from the Langevin expression only in replacing a 4 by a 3 and in including the factor  $1 + \log \frac{(2n)^{-1/2}}{4d_0}$  which corrects for the curvature of the paths caused by

attractive forces. For  $10^6$  ions per  $\text{cm}^3$  the logarithm term amounts at  $0^\circ \text{C}$  to about 6.9. If  $10^9$  ions per  $\text{cm}^3$  are produced the expression is 4.6. To date, the impurity of the gases used in the high-pressure region makes the observed values of  $\alpha$  meaningless for comparison with theory, for  $D$  and  $k$  depend on the nature of the ion, which in the work to date is much in doubt. The existing data show that, in air,  $\alpha$  at high pressures obeys Langevin's equation. Since Harper's theory makes  $\alpha$  a slowly changing function of  $n$  and since  $n$  with a constant ionizing agent is proportional to  $p$ ,  $\alpha$  should appear to decrease more slowly with  $p$  than inversely as  $p$ . It is doubtful, however, if the accuracy of the present data is sufficient to test this feature of Harper's theory.

Doubtless the curvature of the paths requires correction in the Langevin region while it is difficult to determine whether Harper's factor is adequate.

At the other extreme when  $L > d$  and pressures are low Harper agrees that one should use the *basic* Thomson equation  $\alpha = \pi d^2 \sqrt{c_+^2 + c_-^2} = \pi d^2 U$ , where  $U = \sqrt{c_+^2 + c_-^2}$ . Here again  $d$  is left undefined, but Harper assumes that we must correct for the attractive forces between the ions. To this end he invokes the increase of the ionic recombination radius  $d$  by attractive forces earlier tried out by Thomson and found inadequate (see footnote, page 113). This factor replaces  $d^2$  by

$$b^2 = d^2 \left( 1 + \frac{2(m_+ + m_-)e^2}{(m_+ m_-) U^2 d} \right).$$

Hence in the low-pressure regime one has  $\alpha = \pi b^2 U$ , where the  $d$  involved in  $b$  may be the kinetic-theory radius of the ion or some appropriate value. In going from high to low pressures there must be an expression which takes  $\alpha$  smoothly from the Langevin expression to what Harper *wrongly* calls the Thomson expression. Thomson's expression is the one deduced assuming a collision with a neutral molecule inside of  $d_0$ .

The relation straddling both regions which Harper uses is

$$\alpha = 3\pi d(D_+ + D_-) \left[ 1 - e^{-\frac{Ud}{3(D_+ + D_-)}} \right].$$

This can at once be seen if one recalls that from elementary kinetic theory  $D = \frac{1}{3}L\bar{c}$ . Harper on this basis sets  $D_+ + D_- = \frac{2}{3}LU$ . The numerical validity of the  $\frac{2}{3}$  can be questioned since  $U$  is *already* the *relative* velocity. Assuming, however, that exact numerical agreement is unimportant in the rough equation, it can be seen that the expression for  $\alpha$  becomes

$$\alpha = 3\pi d(D_+ + D_-) \left[ 1 - e^{-\frac{d}{2L}} \right].$$

When  $d \gg L$ ,  $\alpha$  is of the Langevin form, and when  $L \gg d$  the expression for  $e^{-d/(2L)}$  expanded in series in its first two terms becomes

$$\alpha = 3\pi d^2 \frac{(D_+ + D_-)}{2L} = \pi d^2 u.$$

In order, however, to make the relations exact, one must now introduce the attractive force factors

$$1 + \frac{d_0}{d} \log \frac{(n_+ + n_-)^{-1/2}}{2(d + d_0)} \quad \text{and} \quad 1 + \frac{2(m_+ + m_-) e^2}{m_+ m_- u^2} \frac{e^2}{d},$$

in such a fashion that the appropriate terms will appear and/or vanish in the two extremes. This is accomplished by multiplying the logarithm-

mic factor by  $1 - e^{-\xi L}$ , where  $\xi$  is a numerical factor greater than unity and  $\xi L$  represents *several* mean free paths. Thus  $\alpha$  as determined by Harper becomes

$$\alpha = 3\pi d(D_+ + D_-)[1 - e^{-\frac{vd}{3(D_+ + D_-)}}] \\ \left[1 + \frac{d_0}{d} \{1 - e^{-\frac{d}{\xi L}}\} \log \frac{(2\pi)^{-1/2}}{2(d + d_0)}\right] \\ \left[1 + \left\{\frac{2(m_+ + m_-)e^2}{m_+ m_- U^2} \left(\frac{1}{d} - \frac{1}{L}\right) \text{ or } 0\right\}\right].$$

This holds for all values except where  $d_0 > L$ , for which impact on  $d_0$  is sure to give recombination since  $\epsilon$  is 1. The  $d$  used in each case of application requires interpretation in terms of the recombination criterion. Harper applies it to the charging of large neutral particles or nuclei. In this case he makes  $d$  equal the radius of the particle. In the absence of other theoretical and experimental data the theory would be a satisfactory semi-empirical expression. However, the Thomson expression for recombination based on a molecular impact within  $d_0$  for  $L \geq d_0$  despite the neglect of path curvature appears to be theoretically and experimentally more nearly justified than Harper's use of Thomson's first tentative expression. The equation of Harper in what has been called the preferential regime, though perhaps more logically deduced, has as yet not been established as superior to Langevin's equation. The transition from one regime to the other suggested by the author on the basis of ion formation by electron attachment is definitely based on processes known to take place instead of being purely empirical and is thus superior to Harper's treatment. Finally, the uncertainty of the values of the constant terms used by Harper in the equation makes it quantitatively no better than the other equations derived. Thus it is quite doubtful that today one should replace the equations earlier deduced by the theory of Harper.

L. Onsager<sup>63</sup> has more recently considered the problem of preferential recombination, which he *misnames* "initial" recombination. He shows that some equations deduced by himself which are applicable to ions in solutions may well be applied to gases. As the distribution of the attached electrons at  $t = 0$  is not known the problem cannot be solved completely. However, he points out the importance of preferential recombination at high pressures.

## 11. RECOMBINATION AT VERY LOW PRESSURES

The problem of initial and preferential recombination at very low pressures need not be considered. We deal merely with a true volume recombination for which, except in the limit of lowest pressures (less than 0.1 mm), the Thomson theory should suffice. It is essential, how-

ever, to discuss the value of  $\alpha$  at the very low pressures which one encounters in the ionosphere and in discharge tubes. The process is a pure volume recombination and should be governed by the Thomson theory unless diffusion loss to the walls of the container becomes too great. In the free upper atmosphere, diffusion loss does not occur. Here then the Thomson theory should be applicable. In this case  $\alpha = \pi d^2 \epsilon \sqrt{c_+^2 + c_-^2}$ , in which  $d$  will alter slightly with temperature as will the velocities. The large effect will come from  $\epsilon$ . This depends on one ion colliding with a molecule within  $d$  cm of the opposite partner, and as  $p$  decreases  $\epsilon$  rapidly decreases.\*

It is then clear that  $\epsilon$  and hence  $\alpha$  will decrease with  $p$  to a value where the chance of two ions of radius  $r_0$  colliding directly so as certainly to produce recombination will be greater than the chance of a Thomson process. Under these conditions  $\alpha$  will be given by  $\alpha = \pi r_0^2 \sqrt{c_+^2 + c_-^2}$  in place of  $\alpha = \pi d^2 \epsilon \sqrt{c_+^2 + c_-^2}$ . Strictly speaking, the Thomson theory should include an added term for such ions as make direct encounters without molecular collision. These will be relatively negligible until we get to pressures of 0.01 mm, at which point they will become comparable with the Thomson process. The value of  $\alpha$  assuming  $r_0 = 4 \times 10^{-8}$  cm is on direct impact recombination  $\alpha_r = 2 \times 10^{-10}$ , while at 0.0067 mm pressure  $\alpha_T$  on Thomson's theory is  $\alpha_T = 1.68 \times 10^{-10}$ . The value of  $\alpha_r$  is independent of pressure and depends only on the relative ionic velocities and  $r_0$  for neutralization by impact. It should be noted that estimates made by Kenty and by Mohler<sup>28</sup> place  $\alpha$  for *free electron* recombination with positive ions at this same order of magnitude, viz.,  $\alpha_r \sim 8.8 \times 10^{-10}$  for  $\text{Cs}^+$  ions in a glow discharge. Calculations of Bradbury<sup>24</sup> on the *E* and *F* layers in the ionosphere using Thomson's  $\alpha$  give sensible results. Calculations of Sayers<sup>22</sup> as to the conductivity of the lower atmosphere using Thomson's theory of  $\alpha$  also lead to excellent agreement with observation.

## 12. INITIAL RECOMBINATION

We must now return to measurements made by Plimpton,<sup>12</sup> Rümelin,<sup>8</sup> Marshall,<sup>9</sup> Luhr,<sup>14</sup> Gardner,<sup>15</sup> and Sayers<sup>22</sup> on the apparent variation of  $\alpha$  with time. As stated, both Plimpton, and Loeb and Marshall independently came to the conclusion that the initial high value of  $\alpha$  came from the improper estimate of the *concentrations* of the ions at  $t_0$ ,  $t_1$ ,  $t_2$ , etc., from the measured quantities  $q_0$ ,  $q_1$ ,  $q_2$  found after the elapsed times. As stated in section 1 of this chapter, it was assumed that the ions were randomly distributed in space. Then it is justifiable

\* Great care must be exercised in calculating  $\epsilon$  below 0.1 mm pressure since the expansion of the quantities used requires a sufficient number of terms to make  $\epsilon$  reliable. Thus, the use of two terms in expansion gave a value of  $\alpha$  of  $10^{-8}$  when the correct expansion to three terms at 0.0067 mm gave a value of  $10^{-10}$ .



to write  $n_+ = n_- = n = q/V$ , where  $V$  is the gross volume of gas ionized and  $q$  is the number of ions measured.

In fact, however, the process of ionization proceeds as follows. In the case of  $\alpha$  particles the ions are distributed along the paths of the particles, which are 3 to 7 cm long and, probably  $10^{-6}$  second after the  $\alpha$  particle passed (i.e., before much diffusion takes place), some  $10^{-4}$  to  $10^{-3}$  cm in radius. In 1-cm length of such a path there are roughly about 20,000 to 30,000 ion pairs, that is,  $n$  is of the order of  $10^{10}$  to  $10^8$  ions per  $\text{cm}^3$ . Owing to electron diffusion and later the ion diffusion, the concentration decreases.

In the case of  $\beta$  rays or fast electrons produced by X-rays, the ion density along the path is much less, in the neighborhood of 100 to 1000 ion pairs per cm being observed. For electrons of 60,000 volts' energy, the density is 200 ion pairs per cm length of path. This reduces the initial concentration to values ranging between  $3 \times 10^8$  to  $3 \times 10^6$  ions per  $\text{cm}^3$ . In the  $\alpha$ -ray column not only are the ions close together radially but also the average separation *along* the column is of the order of  $10^{-3}$  or  $10^{-4}$  cm, while in  $\beta$ -ray and X-ray ionization the ions are distinctly more widely spaced *along* the path and tend to form tracks which are even visually perceptibly composed of isolated ion groups. The straight columnar character and the high density of  $\alpha$ -particle ionization make the problem mathematically more tractable, and a partial solution of the question of columnar ionization has been achieved by Jaffé.<sup>32</sup> This will be discussed later.

In the case of  $\beta$ - and X-ray ionization the situation is somewhat different. The secondary electron is knocked out of the parent atom with an energy which varies from just that to escape to infinity to an energy of several volts exceeding that energy. What the average excess is it is hard to state. It could well be of the order of 1 volt, which is 30 times the energy of thermal agitation. This energy the electron gradually dissipates in collisions with molecules or atoms. In the inert gases and Hg, the electron makes elastic impacts losing a fraction, roughly  $2m/M$ , of its energy per impact. In molecular gases the loss of energy appears to be greater when electron energies are of the order of 1 volt or more. Thus endowed with the energy of escape to infinity plus extra energy, the electron moves about in the gas and dissipates its energy. If the pressure is high, the dissipation may well occur inside the sphere of radius  $d$ , the electron diffusion being much retarded by the field, or the electron may attach to form a negative ion owing to *an increased probability of attachment at high energies*. If it has not attached at an early date, once the electron has an appropriately low energy, it will ultimately attach to certain molecules or atoms and will form a negative ion. Depending on the rate of energy dissipation and the probability of attachment  $h$ , the electron will or will not form an ion inside the sphere of attraction  $d$ . If the electrons attach outside of  $d$ , the ions will be statistically distributed in their distance from the parent atom since

attachment is a chance phenomenon. Hence, the distribution of the number of ions that exceed a distance greater than  $x$  from their parent atoms will be much like the distribution function for free paths, as will later be seen. If now the average distance  $S$  which the ions have gone before attachment is less than the average distance required for a random distribution, the ion distribution will as a whole be far from random. Hence, most of the ions will be arranged in pairs of opposite charge, at distances less than the normal recombination with random distribution warrants.

The question of the effect of such a distribution of ions on the measurement of  $\alpha$  can now be answered as follows. We observe two quantities of charge  $q_1$  and  $q_2$  in an ionized volume  $V$  after times  $t_1$  and  $t_2$ . We evaluate  $\alpha$  in the simplest case from

$$\alpha_t = \frac{1}{t_2 - t_1} \left( \frac{1}{n_2} - \frac{1}{n_1} \right),$$

where  $n_1$  and  $n_2$  are respectively  $q_1/V$  and  $q_2/V$ ,  $V$  being the gross ionized volume. But  $n_1$  and  $n_2$  are in reality  $q_1/V'_1$  and  $q_2/V'_2$ , where  $V'_1$  and  $V'_2$  are special volume assignments due to a non-random distribution of ions. These volumes  $V'_1$  and  $V'_2$  increase with  $|t|$  and strive towards  $V$  as a limit. This increase in  $V'_1$  and  $V'_2$  is ascribed to the diffusion of ions apart, which was noted by all later workers investigating initial and columnar recombination. Hence, in reality, since we observe  $q_1$  and  $q_2$  at  $t_1$  and  $t_2$ , we calculate a fictitious value of  $\alpha$ ,  $\alpha'$  given by

$$\alpha' = \frac{V}{t_2 - t_1} \left( \frac{1}{q_2} - \frac{1}{q_1} \right)$$

instead of the true  $\alpha$  given by

$$\alpha = \frac{1}{t_2 - t_1} \left( \frac{V'_2}{q_2} - \frac{V'_1}{q_1} \right).$$

For our purposes we can assume  $V'_2$  and  $V'_1$  essentially equal if  $t_2 - t_1$  is not too great an interval of time. Thus, if we set  $V'_2 = V'_1 = V'$ , we can compare

$$\alpha = \frac{V'}{t_2 - t_1} \left( \frac{1}{q_2} - \frac{1}{q_1} \right)$$

with the  $\alpha'$  evaluated. This at once yields the relation  $\alpha'/\alpha = V/V'$ . Thus  $\alpha' = (V/V')\alpha$ .

Since  $V'$  is a function of  $t$  which as a result of diffusion continually moves towards the value  $V$  as  $t$  increases,  $\alpha'$  will be observed to decrease in time from a value which may at  $t = 10^{-8}$  second in air be as high as  $\alpha' = 8\alpha$  towards  $\alpha' = \alpha$  at values of  $t = 1$  second. Such results have been repeatedly observed by Marshall, Luhr, and Gardner. Owing to disturbing influences such as diffusion, and in mixed or impure gases

like air to the progressive aging of the ions, the later and slow disappearance of the initial recombination could not be followed with certainty. In Gardner's work elimination of aging in  $O_2$  and the use of large guard rings resulted in a constancy of  $\alpha$  such that at atmospheric pressure the slow decrease of  $\alpha'$  could be followed to 0.5 second and at low pressures to 1 second. The persistence of this effect for such long time intervals cannot be discussed until the attempt is made to evolve a theory of the phenomenon. So far no one has developed anything approaching a theory. In what follows, such an attempt will be made.

Let us assume a flash of X-ray ionization creating  $n_0$  ions in a volume  $V$ . This flash lasts some  $10^{-5}$  second, and then, some  $10^{-6}$  second later, before much diffusion has taken place but most of the electrons have attached, one regards the gas. If the pressure is atmospheric and the gas is oxygen, the ions are distributed about as follows. Inside the spheres of radius  $d$ , about each positive ion there will in some few cases be a negative ion. If attachment occurs freely for electrons of high energy, there may be many more. Inside  $d$  the distribution of ions cannot even be estimated, and actually it is of no consequence. Those ions are destined to preferential recombination and contribute practically nothing to the value of  $\alpha$  in volume recombination. Well outside of  $d \sim 4 \times 10^{-6}$  cm, there is the usual exponential distribution of attached electrons as a function of  $x$ , the distance from the parent atom. This distribution neglecting the ions inside  $d$  can be represented by  $q = q_0 e^{-x/s}$ , where  $q$  represents the number of negative ions formed at more than  $x$  cm from the parent atom. The average distance of separation  $S$  for this curve at the beginning of our time measurement after attachment represents a scale factor which depends on the attachment coefficient  $h$ , the pressure, the mean free path  $L$ , etc.

Let us assume that, at  $t = 0$ ,  $S = r_0$ . From cloud track pictures, etc., one can estimate that  $S$  at the time in question may lie at  $10^{-4}$  or  $10^{-3}$  cm. By observation, however,  $S$  is distinctly less than  $r_r$ , the *average distance between* ions in a random distribution given by  $r_r = \sqrt[3]{V/q_0}$ . Owing to diffusion, as time goes on  $S$  increases. It increases following a diffusion equation of the form  $S = r_0 + \sqrt{(6D/\eta)t}$ , where  $D$  is the coefficient of diffusion for normal ions and  $\eta$  may be a diminishing factor ascribable to the attractive force. Thus, one can picture the situation after  $t = 0$  as shown by the curve *a* of Fig. 56 A. At a time  $t = t_1$  later, the distribution will be more as shown in curve *b*. Now the  $q_r$  ions in the distribution under the curve from  $x = r_r$  to  $x = \infty$  are all at random distribution and undergo a normal recombination,  $(dn/dt)_n = -\alpha (q_r/V)^2$ . But

$$q_r = q_0 \int_{r_r}^{\infty} \frac{1}{S} e^{-\frac{x}{s}} dx.$$

Between  $x = d$  and  $x = r_r$ , the ions recombine according to an expres-

sion  $dn_x/dt = -\alpha(q_x/V'_x)^2$ , where  $q_x$  is the number between  $x$  and  $x+dx$ , and  $V'_x$  is the volume appropriate to them. Since

$$r_r = \sqrt[3]{V/q_0}, \quad \frac{V'_x}{V} = \frac{4\pi x^2 dx}{\frac{4}{3}\pi r_r^3} = \frac{3x^2 dx}{r_r^3}, \quad \text{and} \quad q_x = \frac{q_0}{S} e^{-x'/S} dx,$$

we may proceed as follows:

$$\frac{dn_x}{dt} = -\alpha \left( \frac{q_x}{V'_x} \right)^2,$$

$$\frac{dq_x}{dt} = -\alpha \left( \frac{q_x}{V'_x} \right)^2 V'_x = -\frac{\alpha(q_x)^2}{V'_x} = -\frac{\alpha q_0^2 r_r^3}{3S^2 V} \frac{e^{-2x/S}}{x^2} dx.$$

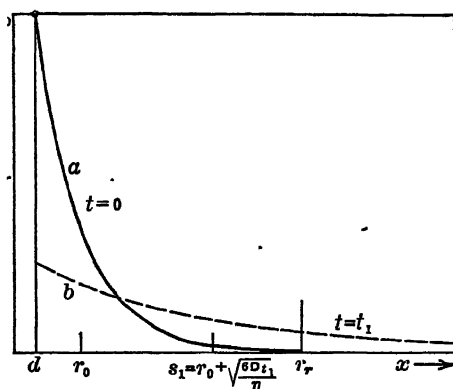


FIG. 56A.

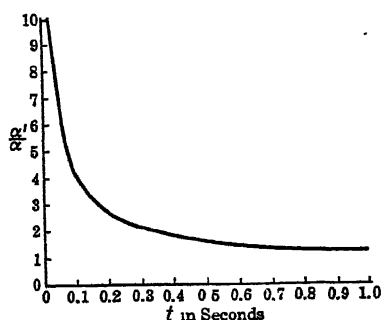


FIG. 56B.

Thus, combining the recombination beyond  $r_r$  and that between  $r_r$  and  $d$ , and integrating, one has:

$$\begin{aligned} \frac{dn}{dt} &= \frac{1}{V} \frac{dq}{dt} = -\alpha \frac{q_0^2}{V^2} \left[ \int_d^{r_r} \frac{r_r^3}{3S^2 x^2} e^{-\frac{2x}{S}} dx + \left\{ \int_{r_r}^{\infty} \frac{e^{-\frac{x}{S}}}{S} dx \right\}^2 \right] \\ &= -\alpha n^2 \left[ \frac{r_r^3}{3S^2} \left\{ \int_d^{r_r} \frac{e^{-\frac{2x}{S}}}{x^2} dx \right\} + e^{-\frac{2r_r}{S}} \right]. \end{aligned}$$

Thus,

$$\begin{aligned} \frac{dn}{dt} &= -\alpha n^2 \left[ \frac{2r_r^3}{3S^3} \left\{ \frac{e^{-\frac{2d}{S}}}{2d/S} - \frac{e^{-\frac{2r_r}{S}}}{2r_r/S} \right\} \right. \\ &\quad - \frac{2r_r^3}{3S^3} \left\{ \log r_r - \log d - \frac{2}{S} (r_r - d) + \frac{4}{2.2! S^2} (r_r^2 - d^2) \right. \\ &\quad \left. \left. - \frac{8}{3.3! S^3} (r_r^3 - d^3) + \dots \right\} + e^{-\frac{2r_r}{S}} \right]. \end{aligned}$$

Now we may assign the following values for the various quantities on the basis of experiments such as Gardner performed.  $n = 10^6$  ions per  $\text{cm}^3$ , so that  $r_e = 10^{-2}$  cm. Take  $\alpha = 2 \times 10^{-6}$  and  $d = 4 \times 10^{-6}$ . Choose  $D$ , the diffusion coefficient, which is the sum of the coefficients of both ions, as  $D = 4 \times 10^{-2}$ , and  $\eta = 1$ .  $r_0$ , the initial distance of separation of the ions, can be chosen as  $2 \times 10^{-5}$  cm, i.e., outside the region of retarded diffusion. In the time intervals involved, i.e.,  $t > 10^{-3}$  sec,  $r_0$  is of no importance in calculation. Thus since  $S = r_0 + \sqrt{6Dt/\eta}$ , with  $\eta = 1$ , we note that  $S$  lies between the values  $1.58 \times 10^{-2}$  and  $5.0 \times 10^{-1}$  in the time interval between  $10^{-3}$  and 1 sec. Accordingly  $S$  is of the order of magnitude and greater than  $r_e$ . As a result we may ignore all but the first and last terms in the bracket of the expression for  $dn/dt$  above, so that

$$\frac{dn}{dt} \simeq -\alpha n^2 \left[ \frac{r_e^3 e^{-\frac{2d}{S}}}{3S^2 d} + e^{-\frac{2r_e}{S}} \right].$$

Putting  $S^2 \simeq 0.24t$ , since  $r_0$  can be neglected, one can separate variables and solve for  $n$  as a  $f(t)$ .

For our purposes it suffices to remember that we defined  $n$  as  $q/V$ , where  $V$  is the volume of ionized gas, and that therefore

$$-\frac{1}{n^2} \frac{dn}{dt} = \alpha',$$

the fictitious but observed value of  $\alpha$ . Hence

$$-\frac{1}{n^2} \frac{dn}{dt} = \alpha' = \alpha \left[ \frac{r_e^3 e^{-\frac{2d}{\sqrt{0.24t}}}}{0.72td} + e^{-\frac{2r_e}{\sqrt{0.24t}}} \right],$$

so that

$$\frac{\alpha'}{\alpha} = \frac{0.347}{t} e^{-\frac{1.63 \times 10^{-5}}{\sqrt{t}}} + e^{-\frac{0.041}{\sqrt{t}}}.$$

The character of the curve for  $\alpha'/\alpha$  as a  $f(t)$  is seen in Fig 56B, from 0.01 to 1.0 sec. From 0.001 to 0.01 the curve falls from  $\alpha'/\alpha = 347$  to 7.76.

The curves obtained by Gardner in  $\text{O}_2$  at low pressures in the same region of time intervals are shown in Fig. 57. The character of the curves for the variation of  $\alpha'/\alpha$  with time are seen to be similar. It must be recognized that experimental curves are limited to finite flash times. Hence only sections of curves can be obtained at any single commutator speed. One must thus compare the section of the curve at 4 rps with the analogous section of the theoretical curve. There is, however, the striking difference to be observed, namely, that, Gardner's curves, while covering the same *range of changes* of  $\alpha'/\alpha$ , *change*

*much more slowly* than the theoretical curves. The reason for this is clear. Gardner did not generate his ions over a short time interval and then measure

$$\alpha'_i = \frac{1}{t_2 - t_1} \left( \frac{V}{q_2} - \frac{V}{q_1} \right).$$

Instead he generated his ions in a finite flash interval which compared in magnitude with recombination time. Furthermore, each curve taken at a higher frequency had a higher commutator speed so that the flash time was reduced. Thus for his flash time at  $T = 0.25$  second the distribution of the ions was more nearly the exponential attachment distribution envisaged by theory than the curves at  $T = 0.5, 1$ , and 2 seconds. For all these intervals, however, the distribution of ions is far from the exponential fall assumed in theory, the distribution being in those times certainly more hyperbola-like in form and of milder slope than the exponential functions used. Again, Gardner measured not  $\alpha'_i/\alpha$  but

$$\frac{\alpha'}{\alpha} = \frac{1}{t} \left( \frac{V}{q} - \frac{V}{q_0} \right),$$

and, in plotting  $\alpha'/\alpha$  as a function of time,  $t$  was used instead of  $t/2$ , which is the more nearly representative time in his study. Hence, as  $\alpha'_i/\alpha$  is a function of  $t$ , using  $q_0$  and  $q$  gave higher values of  $\alpha'/\alpha$  at a given  $t$  than corresponds to the true value. Such curves also mask the more rapid true fall of  $\alpha'/\alpha$  as indicated by Luhr's curves in air, shown

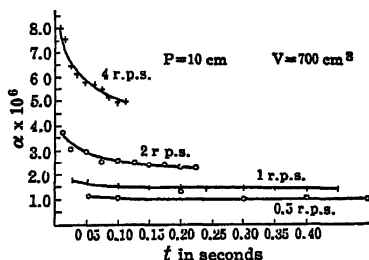


FIG. 57.

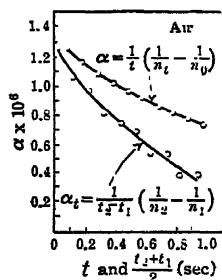


FIG. 58.

in Fig. 58. All these factors cause Gardner's curves of  $\alpha'/\alpha$  to *appear to fall more gradually with  $t$  than they do for the rigorous theory.*

The equation shows that  $\alpha'/\alpha$  varies as  $r_r^2$  in shorter time intervals. Since  $r_r^2 = V/q_0$ ,  $\alpha'/\alpha$  should be proportional to  $1/q_0$ . Since in shorter time intervals  $\alpha'/\alpha$  is nearly proportional to  $1/t$ , we have  $\alpha'/\alpha$  proportional roughly to  $1/tq_0$ . Thus if we reduce  $q_0$  by a factor of 10 by using copper filters on the X-rays, the same value of  $\alpha'/\alpha$  for the same flash time should occur at a  $t$  ten times as great. Using flash times

which varied with  $t$ , Gardner observed the same values of  $\alpha'/\alpha$  occurring at values of  $t$  fifty times longer with the filters than without.

With pressure  $r^3$  varies as  $1/p$  since  $q_0$  is proportional to  $p$ . On the other hand,  $D$  varies as  $1/p$  so that  $\alpha'/\alpha$  should be independent of  $p$  at the shorter time intervals open to study. Gardner's curves at 76, 38, and 10 cm pressure shown in Figs. 60, 59, and 57 are not suitable to use in verification of this prediction since the flash times are not the same. In those curves at lower pressures,  $\alpha'/\alpha$  appears higher at the same ages but decreases more rapidly with  $t$  than at higher pressures. There is thus no apparent agreement.

The experiment and theory are, however, hardly in a condition to yield other than very rough agreement. Experimental data are needed taking a uniform short flash period and measuring  $\alpha'_t$  using values of  $t_2$  and  $t_1$  which do not differ radically. The theory is weak in that it

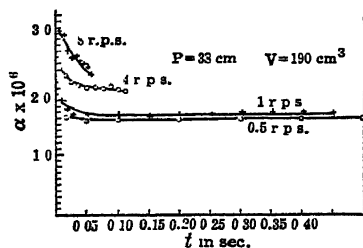


FIG. 59.

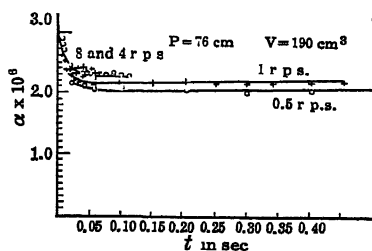


FIG. 60.

utilizes a faulty point of departure. This arises from the choice of the expression for the concentration produced by non-random distribution. The ions were assumed *randomly* distributed in a volume  $V'$  instead of the volume  $V$  ionized, where  $V'$  was taken as  $q/n'$ . The value of  $n'$  is then determined from  $x$ , the distance of separation of positive and negative ions in pairs. The ion *pairs* themselves are randomly distributed in  $V$ , but ions of opposite signs are related to each other in space such that they are in pairs at an average distance  $x$  corresponding to  $n'$  and  $V'$ . If the ions of opposite sign so arranged in pairs all recombined as if the density were really  $n'$ , the value of  $V'$  would be correctly chosen and  $\alpha'/\alpha$  would be correctly computed. This would give the high value of  $\alpha'/\alpha$  of 347 computed above at  $t = 10^{-3}$  sec. However, the ions arranged in pairs of opposite sign corresponding to  $V'$  are not in the same situation as ions of both signs initially randomly placed in a volume  $V'$ , for each pair has a fairly good chance of drifting apart. Hence the choice of a value of  $V'$  is quite optimistic and only a small fraction of the ions in the fictitious density  $n'$ , or volume  $V'$ , recombine at the increased rate. This fraction will vary with the spatial distribution of the ions in pairs. It is not clear physically how it can be computed. This circumstance accounts for the low value of  $\alpha'/\alpha$  observed in  $10^{-3}$  sec compared to the computed value above.

Even though this theory is not satisfactory, enough has been gained by its derivation to indicate that the observed variation of  $\alpha$  in recent studies in time intervals of  $10^{-3}$  to 1 sec may in general be adequately accounted for by some such process and thus to classify initial recombination as a distinct phenomenon. At the Pacific Coast meetings of the American Physical Society, June 29, 1939, N. E. Bradbury presented a solution of this problem giving approximate agreement with Gardner's data. Owing to the brevity of the presented papers, details of the solution are not available at this date. With the assurance that the solution of the problem is near, one may leave the subject and turn to the more easily formulated problem of columnar ionization which is closely akin to the process of initial recombination.

### 13. COLUMNAR IONIZATION AND RECOMBINATION

Bragg<sup>34</sup> and Kleeman in 1906 in their studies in radioactivity were the first to call attention to the fact that it was much more difficult to obtain saturation currents with  $\alpha$ -ray ionization than with other sources. They attempted to explain the phenomenon on the basis of what we today call preferential recombination. Moulin<sup>35</sup> in 1910 showed that the phenomenon was *not preferential* but was to be ascribed to the non-uniform distribution of the ions in space along the  $\alpha$ -ray paths. In 1913 as a result of studies in the conduction currents produced by the ionization of liquids, Jaffé<sup>36</sup> was led to the same conclusion. He then developed the first part of his theory of columnar ionization.<sup>32</sup> He assumed the ions to be distributed radially about the axis of the  $\alpha$ -ray tracks according to a Gaussian error curve, from a maximum at the center decreasing in density outward.\* Diffusion causes these columns to expand outward in time. In the meanwhile, the ions are recombining. Jaffé for the purposes of theoretical study makes the same simplifying assumption made in the previous analysis of *initial* recombination, namely, that the recombination does not change the *form* of the initially assumed Gaussian distribution curve. The analytical procedure is essentially the same as that used before and gives as a solution

$$n = \frac{N_0}{1 + \frac{\alpha N_0}{8\pi D} \log \left( \frac{4Dt + b^2}{b^2} \right)} \frac{e^{-\frac{r^2}{4Dt + b^2}}}{\pi(4Dt + b^2)},$$

with  $D$  the coefficient of diffusion, and  $b$  a constant related to the average displacement  $\bar{r}_0 = b\sqrt{\pi/4}$  of the Gaussian curve from the columnar axis. At  $t = 0$ ,  $n = N_0 e^{-r^2/b^2}/(\pi b^2)$ ,  $r$  being the distance of the ion from the axis of the column.

\* Note that this differs from the form of the distribution of ions in pairs in initial recombination assumed in section 12 of this chapter.



The diffusion of the columns can eventually (for very large values of  $t$ ) lead to a random distribution. Before this occurs in the dense ionization usually studied, the columns swell to a point where they touch each other. This then yields about a normal distribution of ions in the volume. At this point a certain fraction of the ions have escaped columnar recombination and are available for volume recombination. Both Moulin and Jaffé have shown how the number of these escaped ions can be determined. For liquids the estimate can be quite accurate, although only  $10^{-3}$  of the ions escape. Each column is then considered as being surrounded by a coaxial cylindrical surface of radius  $R$  which is equal to the mean separation of two columns. Every ion going beyond this radius can be said to have escaped. This diffusion loss, or escape fraction, from a column can be computed. The fraction is given by

$$\frac{N_1}{N_0} = - \int_{\xi_0}^0 \frac{e^{-\xi} d\xi}{1 + \frac{\alpha N_0}{8\pi D} \log \frac{\xi_0}{\xi}},$$

where  $\xi_0 = R^2/b^2$  and  $\xi = R^2/(4Dt + b^2)$ . The quantity  $R^2/b^2$  is a ratio which is not particularly critical in its effect on  $N_1/N_0$ . Though it does vary with the density of the columns, these are in the measurable range usually so nearly the same in order of magnitude that they can be taken as constant. Jaffé shows that by using  $\xi = 550$  as estimated from experiments his results in liquids and those of Moulin in gases agree quite satisfactorily in the values of  $N_1/N_0$  which the theory yields. The character of the diffusion process is seen in Fig. 61. The upper curve labeled  $N$  gives the decline of ionization with time. The lower curves with Roman numerals give the distribution of ions relative to the column axis at different times corresponding to the Roman numerals on the lower curves and on the upper curve.

Jaffé then considered the theory of the column in an electrical field. Here the angle of the column axes with the field must be considered. The extreme cases are for the columns parallel or perpendicular to the field. For the perpendicular case one finds that  $(N_\infty/N_0)_x$ , where  $N_\infty$  is the number of ions escaping recombination as a function of the electric field  $X$ , is given by

$$\left(\frac{N_\infty}{N_0}\right)_x = \frac{1}{1 + \frac{\alpha N_0}{8\pi D} \sqrt{\frac{\pi}{z}} S(z)},$$

with  $z = b^2 k^2 X^2 / (2D^2)$ , where  $k$  is the ion mobility and  $X$  is the field strength.

$$S(z) = \frac{1}{\sqrt{\pi}} \int_0^\infty \frac{e^{-s} dS}{\sqrt{S \left(1 + \frac{S}{z}\right)}}.$$

If the columns make an angle  $\phi$  with the field, the equations become

$$F(X) = \frac{1}{1 + \frac{\alpha N_0}{8\pi D} \sqrt{\frac{\pi}{z'}} S(z')}, \quad z' = \frac{b^2 k^2 X^2 \sin^2 \phi}{2D^2},$$

which holds for most cases where  $X$  and  $\phi$  are not too small. The curves for air of 750 mm pressure obtained by Moulin with columns perpendicular (I) at  $45^\circ$  (II), and parallel (III), to the field are compared with theory in Fig. 62. The curves for the value of  $F(X)$  *parallel* to the field, III, deviate badly owing to the impossibility of obtaining strict parallelism in practice. These equations neglect normal recombination

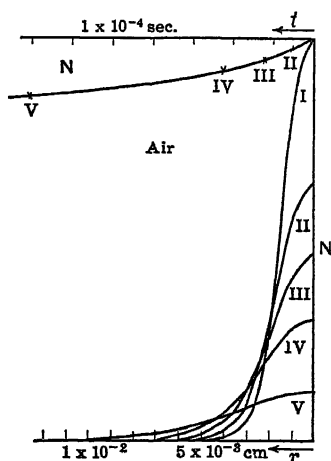


FIG. 61.

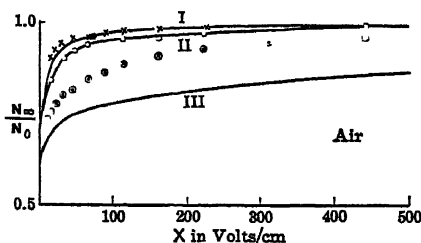
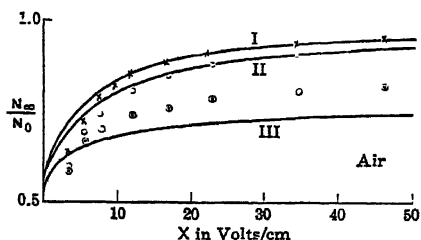


FIG. 62.

during the times of measurement. At  $X = 1$  volt/cm it can be estimated that only 4 per cent of the ions undergo normal recombination, and at  $X = 5$  volts/cm the loss is only 0.3 per cent. Jaffé attempted to carry the solution over to  $\beta$ - or  $\gamma$ -ray ionization. His experimental data were meager and apply only to pressures above 8 atmospheres. The method is hardly applicable to the problem of initial recombination as envisaged today, which has been treated from the more modern point of view.

The theory remained in this status for some sixteen years. In 1928, J. Schemel<sup>33</sup> carried on an investigation with  $\alpha$ -particles. His results are not of particular significance except that in general he confirmed the findings of Jaffé. His methods of study of  $\alpha$  comprised all

three of the methods outlined in this text, the rate of growth, the rate of disappearance, and the equilibrium measurement. In an article in 1929 Jaffé considered the effect of higher pressures on the phenomenon.

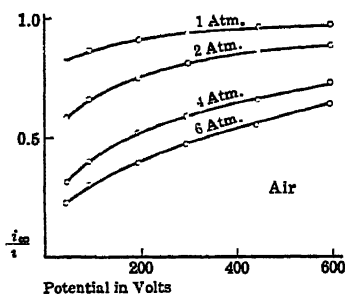


FIG. 63.

He carried out measurements in air,  $\text{CO}_2$ ,  $\text{H}_2$ , and  $\text{O}_2$  from 1 to 6 atmospheres and up to 600 volts with fields nearly parallel to the  $\alpha$ -particles. His gases were not particularly pure, but the results agree excellently with theory as shown in the curves of Fig. 63. In a final article Jaffé derived a more exact expression for the columnar ionization by  $\alpha$ -particles in the absence of a field. He derived the expressions for two possible arrangements of the columns.

The calculations are carried out for comparison with Schemel's work on  $\alpha$ -particles. The curves for the apparent value of  $\alpha$ ,  $\alpha'$ , relative to the true  $\alpha$ , are plotted on theory, using constants taken from Schemel for different recombination times and for different ionization times. A satisfactory qualitative agreement

with Schemel's observed curves for  $\alpha'/\alpha$  as a  $f(t)$  is obtained. The comparison is shown in Fig. 64. The upper set of curves are from Jaffé's theory for  $\alpha'/\alpha$  as a  $f(t)$  for different flash or ionizing periods. The lower set of curves are Schemel's observed curves for the same times. The constants required by Jaffé's theory were evaluated in part from Schemel's curves. Note the analogy both in form and in the difference between theory and experiment between these curves and analogous curves for *initial* recombination. Thus one can assert that the phenomenon of columnar recom-

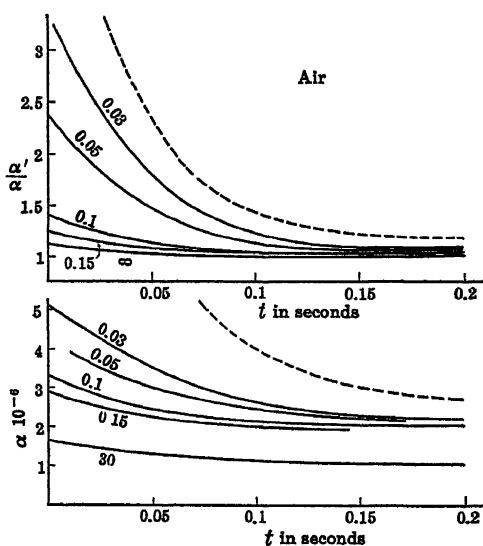


FIG. 64.

bination in  $\alpha$ -particle ionization has been successfully solved in a semi-quantitative fashion and that it no longer presents any fundamental mysteries.

## 14. THE VALUES OF THE COEFFICIENT OF RECOMBINATION AND THEIR INTERPRETATION

In what has been presented above we have followed the development of our understanding of the process of recombination of ions and have given what theoretical inferences we have been so far able to deduce. These inferences have been compared with experiment to the extent to which cogent data were at hand. In this treatment it was seen that, depending on conditions, one did not have a single recombination mechanism with but one coefficient for each gas. Instead, we have so far recognized five such processes. The processes, the conditions under which they occur, and the order of magnitude of their values are given in Table VI. With such a table before one, and the realization that in the intermediate ranges, values of  $\alpha$  are in transition, it is clear that tables of values of  $\alpha$  lose much significance, except under exactly specified conditions where only one mechanism is active. The value of  $\alpha$  for preferential recombination should have perfectly defined values for pure gases. Since, however, the mobilities are most sensitive to impurities, one can say about  $\alpha_L$  what was said about mobilities. The values have a meaning only in terms of a specified vessel cleaned in a specified way with gas prepared in a clearly defined and repeatable manner. *No such measurements exist to date.* In the absence of such data, if the mobility is known, we can more safely take  $\alpha_L = 4\pi e(k_+ + k_-)$  than any existing data.

As regards electron recombination only two measurements have been made.<sup>26</sup> These are approximate, owing to the great difficulty of eliminating electron loss by diffusion, etc. Theoretically the process depends on the approach of an electron close enough to a positive ion to come under its influence and then on the a priori chance of capture to a vacant orbit which should be calculable from wave mechanics if the electron energy is known. The work of Mohler is outstanding, but more satisfactory results require further technical advances before greater accuracy can be obtained.

The value of  $\alpha$  for what was assumed to be volume recombination has often been measured in diverse ways and for various gases. Many of these earlier values have been falsified by diffusion, initial recombination, and probably most seriously by aging and lack of adequate purity. Despite great precautions on this score, the results neither of Marshall nor of Luhr for the various gases have much significance except in terms of an apparatus such as they used for ions of the age of theirs. This is especially true for air. Here Luhr could find absolutely no constant value.  $\alpha$  when measured for times  $t_2$  and  $t_1$  varied with the age  $\tau = (t_2 + t_1)/2$ , decreasing continuously. This is shown very nicely in the curves of Fig. 58, where  $\alpha$  is plotted against  $\tau$ . The upper curve shows the same effect when  $t = 0$  and  $t_\infty$  are used when  $\alpha$  is plotted against  $\tau$ . This proceeding, as stated, averages  $\alpha$  over the

TABLE

| Name and Character     |                                  |  |  |
|------------------------|----------------------------------|--|--|
| Carrier                | Type                             | Approximate Value of $\alpha$ and Theory if any  | Gas Type   |
| Electronic             | Volume                           | $\alpha \sim 10^{-10}$<br>Wave mechanics   | Inert gases<br>Possibly H <sub>2</sub> , N <sub>2</sub> , alkalis  |
| Electronic             | Preferential                     | Probably much higher<br>than $10^{-10}$  | Inert gases<br>Alkali vapors   |
| Electronic<br>or ionic | Wall<br>recombination            | No value can be com-<br>puted  | All gases with free elec-<br>trons. Other gases with<br>ions near walls.   |
| Ionic                  | Preferential                     | $\alpha \sim 10^{-6}$<br>Langevin equation   | Only gases <i>readily</i> attach-<br>ing electrons, O <sub>2</sub> , SO <sub>2</sub> ,<br>Cl <sub>2</sub> , etc. |
| Ionic                  | Columnar                         | $\alpha' \sim 10^{-8}$ to $10^{-6}$<br>From $t = 10^{-8}$ to $t = 1$<br>Jaffé theory   | All gases forming nega-<br>tive ions, O <sub>2</sub> , SO <sub>2</sub> , Cl <sub>2</sub> ,<br>etc.               |
| Ionic                  | Initial                          | $\alpha' \sim 10^{-4}$ to $10^{-6}$<br>From $t = 10^{-8}$ to $t = 1$<br>Loeb theory  | All gases forming nega-<br>tive ions, O <sub>2</sub> , SO <sub>2</sub> , Cl <sub>2</sub><br>etc.                 |
| Ionic                  | Volume                           | $\alpha \sim 10^{-6}$<br>Thomson theory<br>Drift together by ther-<br>mal velocities. Requires<br>a 3-body impact at a<br>critical distance with<br>neutral molecule | All gases forming nega-<br>tive ions, O <sub>2</sub> , SO <sub>2</sub> , Cl <sub>2</sub> ,<br>etc.               |
| Ionic                  | Volume<br>Very low pres-<br>sure | $\alpha \sim 10^{-10}$<br>Ions collide in kinetic<br>theory impact to change<br>charge   | All gases forming nega-<br>tive ions   |

## VI

## Conditions of Occurrence

| Pressures                            | Carrier Density<br>No. per cm <sup>3</sup>                      | Age Range  | Special Conditions  |
|--------------------------------------|---|--|---|
| All                                  | $> 10^9$  | Most likely<br>$< 10^{-2}$ sec.                        | Discharge tube plasma, arc plasma, decreases as $1/T_e^{3/2}$   |
| $< 10^{-1}$ mm                       | Not important   | $< 10^{-3}$ sec.                                       | In absence of external fields   |
| All; most important at low pressures | All. Great when concentrations are great                        | Best at longer times. Depends on carriers and pressure | Occurs wherever ions can diffuse to walls. Where volume recombination is small it becomes very important. It is facilitated by fast free electrons that diffuse to walls and draw the positive ions after them. Ambipolar diffusion |
| Usually $> 10$ atm                   | All. Important relative to volume recombination when $n < 10^2$ | All  | $\alpha \propto 1/p$ . At constant $p$ independent of $T$ . Important in cosmic-ray studies at high pressures, or at very low ion densities   |
| All pressures<br>$> 10$ mm           | Density $> 10^6$ along tracks                                   | All $< 10$ sec.  | Proton or $\alpha$ -particle tracks, $\alpha'$ varies with $t$ of formation and recombination   |
| All pressures<br>$> 10$ mm           | Ions in pairs. Small for $10^9$ or more ions cm <sup>3</sup>    | Down to 1 sec  | $\gamma$ -ray, $\beta$ -ray, or X-ray ionization. $\alpha'$ depends on $t$ of ionization and recombination, on ion density, on pressure   |
| From about 1 atm, down to 0.01 mm    | $10^9$ to $10^2$  | All ages   | $\alpha$ decreases rapidly with increase in $T$ . $\alpha$ constant at 1 atm. Decreases rapidly below 100 mm  |
| From about 0.01 mm down              | All   | All  | Need large volume. Confined to ionosphere. $\alpha$ independent of $p$ . $\alpha \propto \sqrt{T}$ .  |

interval  $\tau/2$  and reveals less change. This result of Luhr's is characteristic of practically all evaluations of  $\alpha$  over any range of time. All other values of other observers fell off with  $t$  where variation with  $t$  was measured.

Gardner could *not* measure  $\alpha$  in  $N_2$  and  $H_2$  owing to loss of free electrons by diffusion. In this case the electrons were doubtless free in much larger numbers than in Luhr's experiments. Luhr did find  $\alpha$  in  $H_2$  constant with time and very low. This result is rather remarkable since one would not have expected to find negative ions in  $H_2$  gas. It may be that some electron diffusion and some recombination of electrons attached to impurities in  $H_2$  occurred, and that the loss of ions measured was caused largely by diffusion of electrons. Otherwise pure  $H_2$  should show *electron recombination* only, and this is assumed to have a low value of  $\alpha$ . Initial recombination was also notoriously absent in  $H_2$  in Luhr's study. The addition of  $O_2$  or air up to 5 per cent in  $H_2$  did slightly *raise*  $\alpha$ , and the curves showed signs of initial recombination. The best guess one can make concerning Luhr's data in  $H_2$  was that the electrons were picked up by heavy molecules of impurity after diffusing considerable distances to random distribution. These ions and the low value of  $\alpha$  in electron recombination gave low values of  $\alpha$ . Introduction of  $O_2$  produced some faster negative ions and the conditions more as in air. The work of Gardner in pure  $O_2$  is the only study of volume recombination in a pure gas where  $\alpha$  was observed to remain constant over any extended intervals of  $t$ . In this case a pure gas was carefully selected in which early electron attachment occurred and contamination was reduced to a minimum. In a small chamber with inadequate guard rings and a small contact potential,  $\alpha$  actually *increased* slowly with time owing to a loss of ions by diffusion. In the larger chamber after 1 second  $\alpha$  was constant. No other results have shown constancy of the same order. Gardner's values in  $O_2$  were materially *higher* than those of Luhr. This can be ascribed only to the greater purity of the  $O_2$  in the outgassed chamber.

The reason for the unsatisfactory nature of the values of  $\alpha$  in volume recombination, once one has eradicated diffusion and initial recombination, must be ascribed to the effect of impurities and aging in changing the ionic characters.

Initial recombination precludes measuring  $\alpha$  at times less than  $10^{-1}$  second even in  $O_2$ . Thus, the ions make some  $10^8$  impacts with gas molecules before study. The initially ionized atoms change charge, and/or add impurities in complex-ion formation. The negative ions may change charge, e.g.,  $O_2^-$  may react with  $Cl_2$  to give  $Cl^-$ ,  $Cl$ , and  $O_2$ , but are more likely to form complex ions. These complexes in a metal chamber with grease seals can and will undergo on the order of 1 to 3 changes in 0.10 second, getting progressively larger. Again, selective recombination of the lighter and thus faster complexes will lead to a more pronounced change in the measured value of  $\alpha$  with

time, as it will give a larger proportion of heavier ions with time. Thus  $\alpha$  should show marked changes in time on aging.

In contrast to this, the mobility  $k$  is affected only slightly on aging, for the increased mass of the ion, which changes velocity and hence recombination so much, changes mobility little, for this varies as  $\sqrt{(m + M)/m}$ . Again, in many gases the changes in physical radius of the ions are not significant, since the mobility is conditioned by polarization forces. Thus, aging in most cases changes  $k$  for ions only some tens of per cent. On the other hand,  $\alpha$  is proportional to  $\sqrt{\bar{e}_+^2 + \bar{e}_-^2}$  or  $\sqrt{1/m_+ + 1/m_-}$ . Thus, the change of mass from  $H^+$  ions and  $H_2O^-$  ions which one might expect in soiled  $H_2$  gas to two ions of mass 64, or one ion of mass 200,  $Hg^+$ , and the other of mass 64, would decrease  $\alpha$  by factors of 4.22 and 5.22 respectively.\* Thus the changes observed by Luhr in air by a factor of 3 are not surprising since, in addition to air, Hg and organic vapors were present. Luhr<sup>38</sup> later studied ions produced by a glow discharge  $10^{-5}$  second after ionization in a chamber with waxed joints, using molecular beams and a mass spectrograph. In a later study air was used in an outgassed chamber. In the waxed-joint chamber the oldest ions showed values of the mass ranging from 14 to 200 for positive ions. In the clean chamber the range was restricted to oxygen and nitrogen ions of various types and to oxides of nitrogen. The molecular weight of the ions all lay below 60.  $H_2O^+$  was a prevailing ion in a chamber that was not baked out but was otherwise clean.

This result clearly defines the type of difficulties and shows why tables of values for  $\alpha$  are more or less meaningless. For purposes of orientation the results of Luhr<sup>14</sup> in a large metal chamber with stop-cock grease seals and *some* waxed joints in reasonably pure gases are given. They have significance only as regards the apparatus in which studied, witness Gardner's probably more accurate value in  $O_2$  which is included for comparison. With this one can leave the problem of the recombination of normal ions in gases.

TABLE VII

| Gas   | Observer | Volume Coefficient<br>$\times 10^6$ |
|-------|----------|-------------------------------------|
| $O_2$ | Gardner  | $2.05 \pm 0.05$                     |
| $O_2$ | Luhr     | $1.32 \pm 0.1$                      |
| $N_2$ | Luhr     | $1.06 \pm 0.1$                      |
| $H_2$ | Luhr     | $0.28 \pm 0.05$                     |
| Air   | Luhr     | $1.23 \pm 0.1$                      |
| Air   | Sayers   | 2.65                                |

\* These changes just computed do not include the changes in  $\alpha$  produced by changes in  $L$ , the ionic free path, which are relatively small at N. T. P. since  $\epsilon$  is nearly unity.



# 15. THE COEFFICIENT OF RECOMBINATION OF LARGE IONS IN AIR: THE CHARGES ACQUIRED BY SUSPENDED PARTICLES IN GASES

The problem of the coefficient of recombination of large ions has been studied with relatively little success. Some measurements have been made in air for the large ions<sup>41,42</sup> and the intermediate ions<sup>40</sup> as normally observed. The values found are very uncertain. For example, P. J. Nolan and O'Brolchain deduced a value of  $5.7 \times 10^{-6}$  in 1925. In 1933 Nolan reinterpreted his data and found  $1.9 \times 10^{-6}$ . Wait found  $7.1 \times 10^{-7}$  for the intermediate ion in air.<sup>40,48</sup> J. J. Nolan, Boylan, and de Sachy found  $8.7 \times 10^{-6}$ . Whipple<sup>89</sup> and Harper<sup>26</sup> treated the question theoretically. Harper used the theory presented in section 10. In form it is not essentially different from Langevin's equation. Calculating the theoretical value of the attraction factor in his theory for these ions, Harper arrives at a value of 8.7 which is twice the value of the attraction factor commonly observed and three to four times the attraction factor obtained on the more recent interpretation of results. This is not surprising in view of the doubts expressed in section 10 concerning the validity of the *large* attraction factor in Harper's equation for normal ions at high pressures. It must clearly be pointed out that the theory used does not apply to  $\alpha$  for *two large ions*. Two large ions of the order of  $10^{-6}$  cm radius have an  $\alpha$  which is so small that it cannot be measured experimentally. In all large-ion recombinations we deal with the value of  $\alpha$  for a combination of a *small and fast ion with a large and slow Langevin or intermediate ion*. Thus, the values of  $\alpha$  and the nature of the problem are largely concerned with the recombination of small ions. There seems to be, and should be, no serious difficulty in this problem except as Harper's theory makes it. The theory should not differ from that for ordinary ions until the radius of the ions reaches values larger than  $4 \times 10^{-6}$  cm. From there on, the collision radius for recombination is larger than  $d$  and the direct impact theory should hold. The problem has one great drawback, and that lies in the difficulty of measurement and the interpretation of the measurements. On the other hand, it is greatly simplified by the fact that for all but the small or ordinary air ions the radius of the large ion, which is the important factor, is easily determined from the ionic mobility.

Another complication which one meets in the study of large ions and charged particles lies in the existence of multiple charges on ions. As will be seen, ions of about  $10^{-6}$  cm radius are quite likely to be multiply charged. The problem of the rate of charging of fumes, dusts, and smokes in ionized air, as well as the size of charges observed, etc., has been extensively studied by those interested in electrical precipitation. Studies of the charges on droplets and particles in electrical smoke precipitation and on charged particles produced by spraying show an

almost linear increase of charge with drop size.<sup>44,47</sup> This increase in magnitude of charge in an atmosphere of ions of one sign has been theoretically calculated and observed by Arendt and Kallmann.<sup>47</sup> Rohmann<sup>46</sup> and Deutsch<sup>48</sup> have also independently studied the acquisition of charges by large particles in dense clouds of ions of one sign. Arendt and Kallmann<sup>47</sup> have shown that the particles acquire charges largely by diffusion of ions to the particles. Hence the charging depends on the energy of thermal agitation in carrying the ions to the charged particles against the field of the charge. The gain of charge is slightly aided by the attractive image forces of the ion on the particle. The effect of the conductivity of the particle has also been studied. At first the uncharged particles charge rapidly, but as they increase their potential, the rate of charging decreases until the particles tend towards a limiting value. This value depends on the radius of the particle. Thereafter the charge fluctuates about the limiting value. In densely ionized gases the rate of charging is surprisingly rapid for particles of the order of  $10^{-5}$  cm radius. If the ions are moving in an electrical field relative to the particles, the ion stream also plays a role in charging as shown by Rohmann. Thus, since  $k$  for normal ions is larger than for the large particles, the field sweeps the ions against the droplets. The *mobility* of all these larger ions appears to be nearly constant irrespective of particle size. This has been shown by Rohmann and by Arendt and Kallmann to be caused by the proportionality of charge magnitude and particle size. All workers agree in ascribing to ions of radius below  $10^{-6}$  cm charges of the order of a single electron.

The fact that the results using diffusion equations for the charging of particles by ions in a gas agree so well with experiment leads one to believe that the problem of charging of neutral particles by ions and of recombination of large ions with ambient ions does not present serious theoretical difficulties. Obviously the intermediate ions and those for which the radius  $\sigma$  is less than  $d$  will require treatment such as that given the problem by Thomson rather than the diffusion type of approach alluded to for larger ions.

## 16. ELECTRON RECOMBINATION

On the basis of very recent advances, it is not amiss at this point briefly to treat the problem of electron recombination. According to the original Bohr theory, the lines emitted in a line spectrum are to be ascribed to electron transitions between excited or occupied outer levels and unoccupied inner levels of lower potential energy. The energy difference  $\Delta E$  is related to the frequency  $\nu$  of the line by the well-known relation  $\Delta E = h\nu$ . If the energy change  $\Delta E$  of the electron just amounts to the energy required to take an electron from a given inner level,  $s$ , to infinity, the frequency  $\Delta E_{\infty} = h\nu_{\infty}$ , corresponds to the *ionizing*

energy of the electron from that orbit. See Loeb, *Atomic Structure*, Chapters VI part 7, XIII, and XIV. The wavelength of the line emitted when the electron falls to the orbit from infinity then represents the *short-wavelength limit* of the series of lines which are permitted by selection rules through fall to the level  $s$  from outer levels. It was always assumed that electrons having energies greater than  $\Delta E_\infty$ , did not belong to the particular atom and came from the surrounding plasma. Such electrons then had kinetic energies at infinity given by  $\frac{1}{2}mv^2$ , where  $v$  was their velocity. When such electrons fall into the level  $s$ , the energy radiated is  $\Delta E_\infty + \frac{1}{2}mv^2 = h\nu$ , leading to the frequency  $\nu$  in the spectrum. Since such electrons of all values of  $\frac{1}{2}mv^2$  exist in quantity in discharge plasma, it was believed that there would be a continuous spectrum beyond  $\nu_\infty$ , which decreased in intensity toward higher values of  $\nu$  since the high-energy electrons are usually present in decreasing numbers and since capture of these is a less likely phenomenon.

Bartels<sup>49</sup> has recently shown that the neglect of a fraction of the electron wave packets in the wave-mechanical analysis of the process of ionization in the past was not justified. This neglected incoming wave train must be interpreted physically as the return of electrons raised to higher virtual energy levels in the continuum beyond  $\Delta E_\infty$  to their normal levels  $s$  in the same excited atom. That is, an electron removed from the level  $s$  in an atom to an outer level of energy greater than  $\Delta E_\infty$ , above  $s$  in the continuum *must be regarded as an excited state of the atom* just as much as the states below  $\Delta E_\infty$ . In the absence of external disturbances such as impacts and superposed fields, these electrons remain in an excited state and return to one of the  $s$  lower levels emitting wavelengths  $\nu$  in the continuum. Under certain conditions such "*self*" recombination, especially in certain series of the alkalis and alkaline earths, is, according to Bartels, responsible for a great portion of the continuum. The variation of the intensities in such continuous spectra with current density, pressure, excitation conditions, and the intensities of the subjacent lines is radically different from that to be expected in a real electron recombination spectrum. Thus the Bartels phenomenon, which is essentially a *preferential* electron recombination, can readily be distinguished spectroscopically from the phenomenon of true or volume electron recombination with which we shall deal.

The study of the rate of recombination ascribable to electrons in discharge was initiated by Kenty<sup>50</sup> in 1928. Kenty studied the afterglow in an A discharge at 0.8 mm, using positive probe wires, and at electron temperatures of 3100° K he obtained a coefficient of value  $2 \times 10^{-10}$ , with possible errors of the order of a factor of 5 caused by inadequate data. The problem was taken up in 1929 by Mohler and Boeckner,<sup>51</sup> Boeckner,<sup>52</sup> and later again by Mohler<sup>53, 54, 55</sup> for the case of Cs vapor both in the arc and in the afterglow. After these years of

study, the theory and technique of the investigations have reached such a stage that they merit discussion.

The work of Hayner<sup>56</sup> and Kenty<sup>50</sup> had indicated that, in a discharge plasma, the loss of electrons to the walls by diffusion was negligible since the positive space charge inhibits a diffusion of too many electrons. Thus, diffusion corrections give losses comparable only to the loss of positive and negative ions to the walls at the rate of motion of the positive ions. This was small compared to the loss of charges in the volume of the gas caused by recombination of electrons and atoms. Hence measurements of loss of charge should be significant in giving information as to electron recombination. Mohler<sup>54, 55</sup> in his studies attempted by means of photometric methods to avoid probes as far as possible, inasmuch as these could give false results. In the end, after obtaining concordant results with photometer and probe, he used both negative and positive probes.

The method first used was a spectrophotometric study of the intensity of the glow discharge light in the continuous spectrum emitted at various times after the arc was cut off. A commutator interrupted the Cs arc in a specially designed bulb by short-circuiting the potential supply operating the arc. This caused a sharp cut-off of the arc, for no arc is drawn out at the contacts as would happen on interrupting a 6-ampere current by a breaker. The commutator also made contacts to probes, one a large-area negative wall probe giving the current to the wall, and the other a large negative wire probe in the volume of the gas. Slots in the disc enabled the central portion of the afterglow to be viewed at appropriate times after cut-off. The light was photometered and compared with filtered light from an incandescent filament diffused over a paper surface. The motor ran the commutator at appropriate speeds, the arc at 1200 rpm, being on for 0.0007 second, with the probes on for 0.001 second at various times after cut-off, which could be adjusted by moving the contacts and viewing slits relative to the shorting contacts. When photographic measurements were required, the comparison was with a calibrated series of steps made by a lamp back of the sectorized disc. The measurement of  $\alpha$  involves an evaluation of the intensity,  $j$ , of the afterglow as a function of time as well as the point and wall probe currents.

The theory was developed over a series of years of study and may be found only by reading the collected papers.<sup>51, 52, 53, 54, 55</sup> Basically it is as follows. If the intensity in the yellow afterglow is entirely due to recombination,  $j$ , the intensity must be proportional to  $n^2$ , the square of the number of ions and electrons per cubic centimeter. The assumption that  $n_e n_+ = n_e^2 = n_+^2$  is justified by the earlier work of Kenty<sup>50</sup> and Hayner.<sup>56</sup> Hence we can set  $j \propto n^2$  or  $n = Kj^{1/2}$ .  $K$  is a constant that changes slowly with electron energy. With this limitation, Mohler says that  $j^{1/2}$  is a measure of electron concentration without any assumption that the change in  $n$  comes entirely from spontaneous volume

recombination. If it does come entirely from recombination, integration of the equation  $dn = -\alpha n^2 dt$  gives

$$\frac{1}{n_2} - \frac{1}{n_1} = \alpha(t_2 - t_1) \quad \text{and} \quad \frac{1}{j_2^{1/2}} - \frac{1}{j_1^{1/2}} = K\alpha(t_2 - t_1).$$

If *volume* recombination predominates, a plot of  $j^{-1/2}$  against time will be linear. Diffusion to the walls and subsequent recombination at the walls make the curves steeper and concave upwards. The extent to which these conditions are fulfilled is shown in Fig. 65 for various

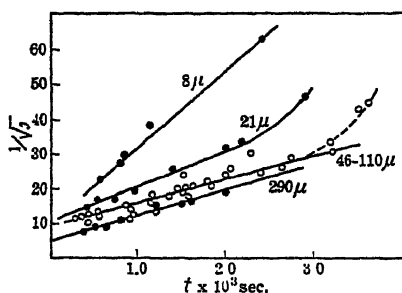


Fig. 65.

pressures in microns,  $\mu$ , of mercury. To determine  $\alpha$  from the straight portions of the curves,  $K$  must be evaluated. If, at  $t = 0$ ,  $n = n_0$ , then if  $n_0$  can be determined we can obtain  $K$  from  $n_0 = Kj_0^{1/2}$ , where  $j_0$  is the extrapolated value of  $j$  at  $t = 0$ . To get  $n_0$  a probe is placed in the center of a bulb operated under identical conditions with the current running. In the pressure

range from 46 to 110  $\times 10^{-3}$  mm of Hg the mean value of  $n_0$  was  $1.9 \times 10^{12}$ . Then the intercept of the  $j^{1/2} - t$  curves at  $t = 0$  gives  $K$ , and the slope of the curve gives  $\alpha = 3.5 \times 10^{-10}$ , neglecting diffusion to the walls.

If  $n_e = n_+$  is directly determinable as a function of  $t$ , one can evaluate  $\alpha$  from the expression  $(1/n_{e2}) - (1/n_{e1}) = \alpha(t_2 - t_1)$ . Now Mohler has shown that we can estimate both  $n_e$  and  $T_e$ , the electron temperature, from measurements of  $j$  at different wavelengths. The theory of the process is as follows:

When the electron of velocity  $v$  recombines with an atom into a level of limiting frequency  $\nu_1$ , the frequency  $\nu$  radiated is given by  $h\nu = h\nu_1 + \frac{1}{2}mv^2$ . The intensity  $j(\nu)$  of light radiated at this frequency depends on the concentration of electrons of speed  $v$ ,  $N^-(v)$ , on the concentration of positive ions,  $N^+$ , and on the velocity  $v$  of the electrons that are sweeping out a recombination volume  $vq(v, \nu_1)$  within which the electrons of velocity  $v$  are captured by the ions into the level of limiting frequency  $\nu_1$ .  $q(v, \nu_1)$  is the ionic absorbing cross section for recombination under these conditions. Thus the number of quanta radiated between  $\nu$  and  $\nu + d\nu$  is

$$\frac{j(\nu)d\nu}{h\nu} = \sum N^-(v)N^+vq(v, \nu_1)d\nu.$$

Now, to a sufficient approximation, for purposes other than excitation

and ionization efficiency studies the quantity  $N^-(v)$  is given by the Maxwellian law as

$$\frac{4N_e}{\alpha^3\sqrt{\pi}} v^2 e^{-\frac{v^2}{\alpha^2}} dv^* \quad (\text{see pages 652 and 654}),$$

so that

$$\frac{j(v)dv}{h\nu} = q(v, \nu) n_e^2 4\pi^{-\frac{1}{2}} \frac{v^3}{\alpha^3} e^{-\frac{v^2}{\alpha^2}} dv,$$

with  $N^+ = N_e = n_e$ . Expressing  $v$  in terms of electron volts,  $\frac{1}{2}mv^2 = Ve$ , and  $\frac{1}{2}m\alpha^2 = V_0e = kT_e$ , where  $T_e$  is the electron "temperature" (see page 235), and  $V_0$  is the most probable electron energy, we can write

$$\frac{j(v)dv}{h\nu} = vq(v, \nu) n_e^2 \frac{4\pi^{-\frac{1}{2}}h}{\sqrt{2me}} \frac{V}{V_0^{\frac{3}{2}}} e^{-\frac{v}{V_0}} dv.$$

From the condition of detailed balance there is a general relation between the probability of recombination  $vq(v, \nu_1)$  into the state  $\nu_1$  and absorption  $B(\nu, \nu_1)$  at an incident frequency  $\nu$  corresponding to  $v$  or a potential  $V$  such that

$$vq(v, \nu_1) = K'B \frac{v^3}{\sqrt{\nu - \nu_1}}.$$

(See Loeb, *Atomic Structure*, page 266.)  $B$  applies to electrons initially in the state  $\nu_1$  and can be measured only where this is the normal state. In X-ray work,  $B$  is proportional to  $\nu^{-4}$ . Quantum-mechanical theory shows that for hydrogen-like atoms it will approximate the same law. Oppenheimer<sup>57</sup> finds it to vary from  $-4.3$  to a minimum of  $-3.5$  at the normal level. Thus one can write that approximately

$$vq(v, \nu_1) = \frac{K_1}{v\sqrt{\nu - \nu_1}}.$$

Near the series limit the value according to Oppenheimer is  $(\nu - \nu_1)^{-\frac{3}{2}}$ . Intensity measurements of Mohler and Boeckner<sup>51</sup> give a very close fit for the relative probability of recombination into the  $2P$  state of Cs against wavelength with the equation

$$vq(v, 2P) = \frac{K_2}{v^2\sqrt{\nu - \nu_1}}.$$

\* Note that the  $\alpha$  used here is the most probable molecular speed and *not* the coefficient of recombination  $\alpha$ .

This is shown in Fig. 66. This relation makes  $B$  proportional to  $\nu^{-5}$ . A curve for this relation for the  $1S$  state derived from the evaluation of

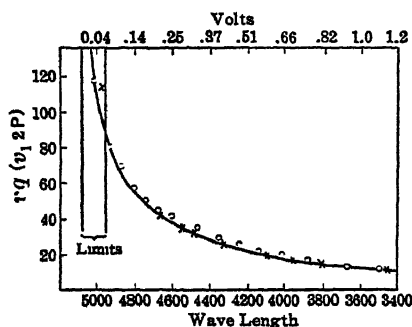


FIG. 66.

$B$  from photoionization measurements of Mohler, Foote, and Chenault and of Little<sup>58</sup> does not fit this variation very well. From these data, whose absolute values are in doubt (see reference 54, page 772), the effective value of  $q(v, 2P)$  for 0.2 volt electron into the  $2P$  state of Cs is  $2 \times 10^{-19} \text{ cm}^2$ . This means that one collision in 5000 kinetic-theory impacts would result in recombination. The chance would be four times as great at 0.05 volt, and a third as great at 0.5 volt.

Since  $\frac{1}{2}mv^2 = h(\nu - \nu_1)$ , the equation above yields

$$vq(v, \nu) = \frac{K_2}{v\nu^2}.$$

This is in agreement with the results of a later paper of Stueckelberg and Morse,<sup>59</sup> who showed on quantum theory that  $vq(v, \nu) = k/(v\nu^s)$ , where  $s$  is undefined but can be of the order of 2 as observed by Mohler. Hence, one can safely write that

$$\frac{j(\nu)d\nu}{h\nu} = \frac{vK_2n_e^2}{v\nu^2} \frac{4\pi^{-1/2}h}{\sqrt{2me}} \frac{V}{V_0^{3/2}} e^{-\frac{\nu}{V_0}} d\nu.$$

so that, with  $Ve = h\nu$ , and  $\nu = c/\lambda$ ,

$$\lambda j(\lambda) = K_3 \frac{n_e^2}{V_0^{3/2}} e^{-\frac{\nu}{V_0}}$$

Mohler previously had evaluated  $q(\nu, v)$  for  $V = V_0 = 0.3$  volt as  $1.7 \times 10^{-21} \text{ cm}^2$ . The equation just given then becomes

$$\lambda j(\lambda) = 0.51 \times 10^{-21} \frac{4\pi^{-1/2}hcn_e^2}{\sqrt{2meV_0^{3/2}}} e^{-\frac{\nu}{V_0}} = 4.26 \times 10^{-13} \frac{n_e^2}{V_0^{3/2}} e^{-\frac{\nu}{V_0}},$$

with  $j(\lambda)$  in ergs and  $\lambda$  in centimeters. Again

$$\log \lambda_1 j(\lambda_1) - \log \frac{K_3 n_e^2}{V_0^{3/2}} = -\frac{V_1}{V_0}$$

and

$$\log \lambda_2 j(\lambda_2) - \log \frac{K_3 n_e^2}{V_0^{3/2}} = -\frac{V_2}{V_0},$$

where  $V_1$  and  $V_2$  are voltages corresponding to  $\lambda_1$  and  $\lambda_2$  through  $\nu_1$  and  $\nu_2$ . Thus

$$\frac{V_2 - V_1}{V_0} = \log \lambda_1 j(\lambda_1) - \log \lambda_2 j(\lambda_2),$$

and, since  $eV_0 = \frac{1}{2}m\alpha^2 = kT_e$ , we have

$$T_e = 5040 \frac{V_2 - V_1}{\log \lambda_1 j(\lambda_1) - \log \lambda_2 j(\lambda_2)}.$$

Thus we can evaluate  $T_e$  and hence  $V_0^{3/2}$ , that is, the probable electron energy or "temperature" at any time during the arc or after the arc is out. On this basis Mohler<sup>54</sup> found, at  $t = 0.9 \times 10^{-3}$  and  $1.8 \times 10^{-3}$  second after a 5.8-ampere arc at 68 microns pressure was cut off, that the plots of  $\log \lambda j(\lambda)$  gave values of  $T_e$  of 1350 and 1200° K. During discharge the electron temperature was 2700° K. At 85 microns the temperatures at  $0.87 \times 10^{-3}$  and  $1.63 \times 10^{-3}$  second were 1360 and 1200° K. From the absolute intensity  $j(\lambda)$  at the series limit,  $V_0$  and the equation  $\lambda j(\lambda) = 4.26 \times 10^{-13} (n_e^2/V_0^{3/2})e^{-V/V_0}$  being known, it is possible to evaluate  $n_e$ . Under the two pressures and the two time intervals the values of  $j(\lambda)$  and  $T_e$  gave

$$n_e = 1.78 \times 10^{12} \quad \text{and} \quad 0.95 \times 10^{12}$$

and

$$n_e = 1.45 \times 10^{12} \quad \text{and} \quad 0.98 \times 10^{12}.$$

When these were placed in the recombination equation, loss of ions to the walls, being neglected, they gave

$$\alpha = 5.5 \times 10^{-10} \quad \text{and} \quad 4.3 \times 10^{-10}.$$

These values could be quite badly in error on account of inaccuracies in the interpretation of the absolute intensity measurements.

Finally the recombination was studied by means of positive probes.<sup>60,61</sup> In the bulb of radius  $r$  the rate of loss of ions  $\Delta n$  in a time  $\Delta t$  by wall current and volume recombination is given by

$$\frac{4\pi}{3} r^3 \frac{\Delta n}{\Delta t} = \frac{4\pi r^2 i_w}{e} + \frac{4}{3} \pi r^3 \alpha n^2.$$

Here  $i_w$  is the wall current per square centimeter, and  $e$  is the electron. The current density to the walls is determined by the large negative wall probe. Negative probes were not used in measuring positive-ion currents, since extensive experiments with electron current probes in Cs had shown such measurements to be possibly inaccurate. Now in measuring  $\Delta n$  and solving for  $\alpha$  it is necessary to evaluate  $n$  from the currents. Thus, it is assumed that  $n = Ki_+$ , where  $K$  is a factor of



proportionality which must be determined at each pressure. Putting this into the equation above, one has

$$\frac{4}{3} \pi r^3 K \frac{\Delta i_+}{\Delta t} = \frac{4 \pi r^2 i_w}{e} + \frac{4}{3} \pi r^3 \alpha K^2 i_+^2.$$

The data are taken from the probe wire curves at constant pressure but different times. From two pairs of measurements one can solve for both  $K$  and  $\alpha$ . In actual practice,  $K$  was evaluated at low  $i_+$ . From the value of  $K$  the mean value of  $n$  at various time intervals could be calculated. With these data, curves for  $\Delta n / \Delta t$  could be plotted against  $n$  for the different pressures used. To get  $K$ , one uses small values of  $i_+$ , and to get  $\alpha$ , large values of  $i_+$ , since in the former case recombination is small while in the latter it is relatively larger. Thus, by measuring the wall current to the flat probe and the current to the wire probe in the volume of the gas, we can obtain values of  $\Delta n / \Delta t$  and  $i_w$  at various times, as a function of probe potential. These curves give the quantities needed in the equation as well as the space and wall potential for wire and disc. In all cases the space current to the wire

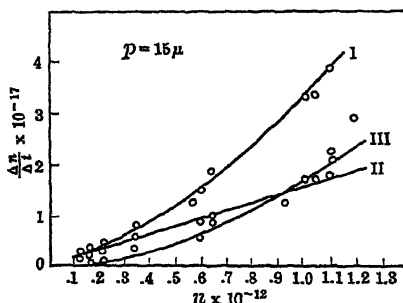


FIG. 67.

probe is greater than the current to the disc, in the ratio of about 2.5 or 3 to 1. This was done for four different pressures from 10 to 70 microns for times from  $1.5 \times 10^{-3}$  to  $2.5 \times 10^{-3}$  second. Fig. 67 shows the curves at 15 microns. Curve I is the total  $\Delta n / \Delta t$ , curve II gives the wall current, and curve III is the difference. From curve III, one then can derive the value of  $\alpha$ . Below 30 microns pressure, the value of  $\alpha$  is  $\alpha = 3.4 \times 10^{-10}$ .

Measurements for times from 0.7 to  $1.5 \times 10^{-3}$  second give similar values but larger errors. Thus  $\alpha = (3.4 \pm 0.5) \times 10^{-10}$  is the best value. In the optical measurements where values of  $5.5 \times 10^{-10}$  and  $4.3 \times 10^{-10}$  were observed, the volume recombination from 46 to 110 microns pressure accounts for 0.6 to 0.7 of the total change in  $n$ . Thus the optically determined values must be multiplied by 0.6 or 0.7, which gives  $\alpha = 3.6 \times 10^{-10}$ . One is therefore in a position to assert that for Cs vapor in discharges of the type above and with electron temperatures between 1500 and 1000°K the value of  $\alpha$  is closely  $3.4 \times 10^{-10}$ , as given by three nearly independent methods of study. This is in agreement with Kenty's result of  $2 \times 10^{-10}$  in A well within Kenty's limits of error.

In the discussion of his paper, Mohler makes the assertion that

the quantity  $\alpha$  probably varies as the inverse first or higher power of the electron temperature,  $T_e$ . He gives no experimental evidence for this. However, in theory  $q(r, v) = K_2/(v^2 v^2)$ , so that, while the rate of recombination due to electron motion varies as  $\sqrt{T_e}$ , it is probable that  $\alpha \propto 1/T_e^{3/2}$ . Hence Mohler estimates an  $\alpha$  of  $2 \times 10^{-10}$  or less in the Cs arc at a value of  $T_e = 2700^\circ \text{C}$ . A comparison of electronic volume recombination and wall current in the discharge with a positive column, which is of some interest, is given in Table VIII. At low pressures, as has been stated before, volume recombination accounts for only a small portion of the ion loss in the positive column, the wall current and hence recombination at the walls being mostly responsible. At 100 to 300 microns the two may become comparable, depending on the variation of  $\alpha$  with pressure and temperature.

TABLE VIII

| Current | Pressure  | Tube Diameter | Electronic Volume Recombination Loss | Wall Current Loss Per Cm Length of Tube |
|---------|-----------|---------------|--------------------------------------|---|
| 4 amp   | 15 $\mu$  | 1.8 cm        | $1 \times 10^{17}$                   | $10^{18}$                               |
| 4 amp   | 290 $\mu$ | 1.8 cm        | $5 \times 10^{17}$                   | $5 \times 10^{17}$                      |

In a still later paper Mohler<sup>55</sup> gives the result of a study of a 6-ampere Hg arc at 270 microns pressure. In this investigation the afterglow was studied by probes only. An added small positive wire probe was inserted into the center of the bulb near the large negative wire probe used for Cs. In this way both electron and ion concentrations could be measured. The arc studied was short-circuited, but an arc was kept burning in a region below the observation space at all times to facilitate re-ignition. This introduced the possibility of constant ion production in the observation space following cut-off. The ion current at the space potential was computed from the measured current at various negative potentials for cylindrical collectors.<sup>60, 61</sup> The electron temperatures given by the small positive<sup>60</sup> probe agreed well with those observed by Randall and Webb in a Hg jet at 390 microns pressure at corresponding times after cut-off. From the electron current density  $n_e$ , the electron concentration could be determined, from  $n_e = 4.03 \times 10^{13} i_e/T_e^{1/2}$ . This relation comes from the fact that  $en_e v \times 1 \text{ cm}^2 = i_e$ , and that  $v \propto T_e^{1/2}$ . Thus, electron energy or temperature  $T_e$  and density  $n_e$  are measured as a function of time after cut-off. The positive-ion current density  $i_+$  was measured by the negative probe. From this it could be shown that, if  $n_e = n_+$ , except for the 0.001-second measurement,  $n_e = 1.18 \times 10^{15} i_+$ , with an uncertainty of the order of 10 per cent, probably to be ascribed to the electron current measurements giving  $n_e$ . If the gas were at  $400^\circ \text{K}$

the positive ions in equilibrium would *diffuse* to the probe if their concentration  $n_+$  were equal to that of the electrons so as to give a current of  $n_+ = 1.22 \times 10^{15} i_+$ . This agrees well with the value observed above, so that the ion "temperature" may be assumed to be about that of the gas. At *lower* pressures diffusion does *not* account for the currents. Thus, while the electron temperature drops from 2960° K at 0.001 second to 1600° K at 0.006 second after cut-off, the positive-ion temperature of a higher value drops to 400° K, the gas temperature, within less than  $10^{-3}$  second, and the equation above is then constant.

$$\text{The equation} \quad \frac{\Delta n}{\Delta t} = A \frac{i_+}{e} + V \alpha n^2$$

can be used as before, where  $A$  is wall area and  $V$  is the volume. Curves analogous to those in Cs for 270 microns pressure yield  $\alpha = (2.3 \pm 0.4) \times 10^{-10}$ . However, the auxiliary discharge for re-ignition of the arc may make this value for  $\alpha$  incorrect, for, if the auxiliary arc is producing ions *after cut-off*, then the rate of decay from which  $\alpha$  is inferred does not represent the true  $\alpha$ . Considering the possibility of errors we can compare the values of  $\alpha_e$  for three gases. These can be compared with the theory of electron recombination for the H atom.<sup>57,69</sup> There are two cases:

TABLE IX

| Gas | Pressure<br>in Microns | Electron<br>Temperature<br>in Degrees K | $\alpha_e$            | Observer |
|-----|------------------------|---|-----------------------|----------|
| A   | 800                    | 3100°                                   | $2 \times 10^{-10}$   | Kenty    |
| Cs  | 10-30                  | 1200°                                   | $3.4 \times 10^{-10}$ | Mohler   |
| Hg  | 270                    | 2000°                                   | $2.3 \times 10^{-10}$ | Mohler   |

1. The electron energy is small compared to the energy of the quantized level  $n$ .
2. The energy is much greater than that for the quantized level  $n$ .

For a given quantum level  $n$  the equations for cases 1 and 2 are:

1.  $\alpha_n = 5.94 \times 10^{-13} A_n V^{-1/2}$ . Here  $A_n = 0.326/n$  for values of  $n$ , the quantum level, greater than 3, and  $V$  is the electron energy in volts.

2.  $\alpha_n = 6.3 \times 10^{-11}/V^2 n^3$ .

For the experimental cases studied in the alkalis,  $\alpha_n$  is the sum of all these for the different quantum values of  $n$ , assuming that the case of the alkalis is analogous to that of the H atom. This gives the theoretical values for H under conditions 1 and 2 as approximately

1.  $\alpha_n = 1.7 \times 10^{-12}$  at 0.1 volt.
2.  $\alpha_n = 2.3 \times 10^{-12}/V$  at higher energies.

These should represent about the values found in Cs and Hg. Actually, they are about one-hundredth of the values found. The difficulty in applying the hydrogenic theory to the atoms Cs and Hg above is that the high quantum values are involved and important. These are, however, seriously perturbed by discharge conditions in the plasma. Mohler further points out that there is some pressure dependence of  $\alpha$  even at a pressure as low as 10 microns in Cs, so that the recombination cannot be the simple process envisaged in theory.\* This view is strengthened by the fact that pressure increase increases the observed  $\alpha$ . The value of  $\alpha$  experimentally determined also includes the increase of ion concentrations caused by the reionization of excited states which may or may not be negligible. *It is possible that perturbation may so distort the levels as to facilitate capture.* Hence  $\alpha$  would be materially higher than that for simple theory. Increase in pressure would increase perturbation. It is not a cause of great concern that elementary theory does not agree with observation. However, whether the observed value of  $\alpha$ , is that occasioned by the simple theoretically considered process or not is entirely irrelevant. *For practical purposes the values of  $\alpha$ , given suffice to enable one to account for the ion balance in a gas under the reported conditions,* assuming that it is the coefficient of electron recombination.

## 17. REFERENCES FOR CHAPTER II

1. THOMSON and RUTHERFORD, *Phil. Mag.*, **42**, 392, 1896.
2. E. RUTHERFORD, *Phil. Mag.*, **44**, 422, 1897.
3. J. A. McCLELLAND, *Phil. Mag.*, **46**, 29, 1898.
4. J. S. TOWNSEND, *Trans. Roy. Soc.*, A **193**, 144, 1899.
5. R. K. MCCLUNG, *Phil. Mag.*, **3**, 283, 1902.
6. H. A. ERIKSON, *Phys. Rev.*, **27**, 473, 1908.
7. L. L. HENDREN, *Phys. Rev.*, **21**, 314, 1905.
8. G. RUMELIN, *Physik. Z.*, **9**, 657, 1908; *Ann. Physik*, **43**, 821, 1914.
9. L. C. MARSHALL, *Phys. Rev.*, **34**, 618, 1929.
10. E. RIECKE, *Ann. Physik*, **12**, 814, 1903; G. MIE, *Ann. Physik*, **13**, 857, 1904.
11. E. RUTHERFORD, *Phil. Mag.*, **47**, 109, 1899.
12. S. J. PLIMPTON, *Phil. Mag.*, **25**, 65, 1913.
13. P. LANGEVIN, *Ann. chim. Phys.*, **28**, 289, 433, 1903.
14. O. LUHR, *Phys. Rev.*, **35**, 1394, 1930; **36**, 24, 1930; **37**, 998, 1931.
15. M. E. GARDNER, *Phys. Rev.*, **53**, 75, 1938.
16. LUHR and BRADBURY, *Phys. Rev.*, **36**, 1394, 1930; N. E. BRADBURY, *Phys. Rev.*, **37**, 1311, 1931.
17. W. MÄCHLER, *Z. Physik*, **104**, 1, 1936.
18. P. KRAUS, *Ann. Physik*, **29**, 449, 1937.
19. L. B. LOEB, *Phys. Rev.*, **51**, 1110, 1937.
20. LOEB and MARSHALL, *J. Franklin Inst.*, **208**, 371, 1929.
21. J. J. THOMSON, *Phil. Mag.*, **47**, 337, 1924.

\* The probability of an electron combining with a positive ion may be greatly increased by a 3-body process involving a neutral molecule. In this process the conditions of conservation of momentum and energy are much more easily met. This would result in a pronounced pressure variation of  $\alpha$ .

22. O. W. RICHARDSON, *Phil. Mag.*, 10, 242, 1905.
23. L. B. LOEB, *Kinetic Theory of Gases*, 2nd Edition, p. 593, McGraw-Hill, New York, 1934.
24. J. J. THOMSON, *Conduction of Electricity through Gases*, 3rd Edition, Vol. 1, p. 46, Cambridge, 1928.
25. W. R. HARPER, *Proc. Camb. Phil. Soc.*, 28, 219, 1932; 31, 430, 1935; *Phil. Mag.*, 18, 97, 1934; 20, 740, 1935.
26. C. KENTY, *Phys. Rev.*, 34, 624, 1928; F. L. MOHLER, *Bu. Standards J. Research*, 19, 447, 1937.
27. L. B. LOEB, *Kinetic Theory of Gases*, 1st Edition, p. 490, McGraw-Hill, New York, 1927.
28. W. R. HARPER, *Proc. Camb. Phil. Soc.*, 31, 430, 1935.
29. H. A. ERIKSON, *Phil. Mag.*, 18, 328, 1909; 23, 747, 1912.
30. H. THIRKILL, *Proc. Roy. Soc.*, A 88, 490, 1913.
31. P. PHILLIPS, *Proc. Roy. Soc.*, A 33, 246, 1910.
32. G. JAFFÉ, *Ann. Physik*, 42, 303, 1913; 1, 977, 1929; *Physik Z.*, 30, 849, 1929.
33. J. SCHEMEL, *Ann. Physik*, 85, 137, 1928.
34. BRAGG and KLEEMAN, *Phil. Mag.*, 11, 466, 1906; R. D. KLEEMAN, 12, 273, 1906.
35. M. MOULIN, *Ann. chim. phys.*, 21, 550, 1910; 22, 26, 1911.
36. G. JAFFÉ, *Le Radium*, 10, 126, 1913.
37. G. JAFFÉ, *Ann. Physik*, 1, 977, 1929.
38. O. LUHR, *Phys. Rev.*, 38, 1730, 1931; 44, 459, 1933.
39. E. J. W. WHIPPLE, *Proc. Phys. Soc. London*, 45, 367, 1933.
40. G. R. WAIT, *Phys. Rev.*, 48, 383, 1935.
41. ISRAEL, *Gerland's Beiträge*, 40, 29, 1933.
42. P. J. NOLAN, *Proc. Roy. Irish Acad.*, 41, 61, 1933; 37, 1, 1925; and J. J. NOLAN, BOYLAN, and DESACHY, *Proc. Roy. Irish Acad.*, 37, 71, 1927.
43. WAIT and TORRESON, Congrès internationale d'électricité, Paris, 1932.
44. S. CHAPMAN, *Physics*, 5, 150, 1934.
45. W. DEUTSCH, *Ann. Physik*, 68, 335, 1922.
46. H. ROHMANN, *Z. Physik*, 17, 253, 1923.
47. ARENDT and KALLMANN, *Z. Physik*, 35, 421, 1925.
48. PAUTHENIER and MOREAU-HANOT, *J. phys.*, 3, 590, 1932.
49. H. BARTELS, *Z. Physik*, 105, 704, 1937.
50. C. KENTY, *Phys. Rev.*, 32, 624, 1928.
51. MOHLER and BOECKNER, *Bur. Standards J. Research*, 2, 489, 1929.
52. C. BOECKNER, *Bur. Standards J. Research*, 6, 277, 1931.
53. F. L. MOHLER, *Bur. Standards J. Research*, 10, 771, 1933.
54. F. L. MOHLER, *Bur. Standards J. Research*, 19, 447, 1937.
55. F. L. MOHLER, *Bur. Standards J. Research*, 19, 559, 1937.
56. L. HAYNER, *Z. Physik*, 35, 365, 1925.
57. J. OPPENHEIMER, *Z. Physik*, 41, 268, 1927; *Phys. Rev.*, 31, 349, 1928.
58. MOHLER, FOOTE, and CHENAULT, *Phys. Rev.*, 28, 37, 1926; E. M. LITTLE, *Phys. Rev.*, 30, 109, 1927.
59. STUECKELBERG and MORSE, *Phys. Rev.*, 36, 16, 1930.
60. MOHLER and BOECKNER, *Bur. Standards J. Research*, 2, 491, 1929.
61. MOTT-SMITH and LANGMUIR, *Phys. Rev.*, 28, 727, 1928; LANGMUIR and BLODGETT, *Phys. Rev.*, 22, 347, 1923.
62. J. SAYERS, *Proc. Roy. Soc.*, A 169, 83, 1938.
63. L. ONSAGER, *Phys. Rev.*, 54, 554, 1938.
64. N. E. BRADBURY, *Terrestrial Mag. and Ats. Elect.*, 43, 55, 1938.

## CHAPTER III\*

### THE DIFFUSION OF IONS

#### 1. INTRODUCTION

The distribution of ions or electrons in a gas in space and time as a result of their random thermal agitation, which we call diffusion, is ever present to complicate experimental study. Essentially a study of diffusion for itself today presents little of interest since the important coefficient to be derived from its study can be evaluated more accurately by studies of the mobility. Historically the early studies of diffusion were of great significance, and much credit goes to J. S. Townsend for his skill and imagination in overcoming considerable mathematical and experimental difficulties in clarifying the field. The mathematical complexity involved in solving even the simpler problems of diffusion has further discouraged quantitative study of diffusion processes in discharge problems where it might well have been done, and where it would still be of great value in experimental interpretation. Even though at present little active study of this feature of the behavior of gaseous ions is in progress, because of the important influence of diffusion in the study of ionic behavior, especially in the case of the plasma of discharge tubes, it is necessary that the student of this field should have a clear concept of the phenomenon. Consequently an elementary description of the character of diffusion will be given. This will be followed by the fundamental classical researches of Townsend on the diffusion of ions and a discussion of their implications. A final section will present a survey of one or two problems showing qualitatively how ionic diffusion operates in a gas.

#### 2. FUNDAMENTAL CONCEPTS

Let us consider a mass of ions all of one sign existing in a gas. These could be negative ions produced by photoelectrically or thermionically generated electrons or positive ions from a Kunsman catalyst. These ions are a group of separate entities differing from the gas molecules in being complexes of one to several molecules carrying a charge. With the densities of ions which can usually be attained in gases, these ions are on the average quite far apart. In

\* References for Chapter III will be found on page 176.

solutions, the completely dissociated molar solution, a mole of ions in 1000 cm<sup>3</sup> of liquid, has some  $6 \times 10^{23}$  ions. This gives  $6 \times 10^{20}$  ions/cm<sup>3</sup> with an average distance of  $1/\sqrt[3]{6 \times 10^{20}} = 1/(0.85)10^7 = 1.15 \times 10^{-7}$  cm between ions. In gases the average distance with intense ionization is of the order of  $1/\sqrt[3]{10^7} = 4.7 \times 10^{-8}$  cm. In sparks after  $10^{-7}$  second and in arcs and glow discharge plasma larger concentrations occur. Except in sparks and some arcs the concentrations are less than  $10^{12}$  ions/cm<sup>3</sup> with distances of  $10^{-4}$  cm. Thus, electrostatic forces between ions in molar solutions in liquids are appreciable and important whereas in gaseous discharge they are usually negligible.

Accordingly, under ordinary conditions gaseous ions in a gas act merely as a type of foreign molecule and exert their own partial pressure as do all foreign molecules in a gas in accord with Dalton's law. This partial pressure of ions is merely an expression of the natural tendency of the random heat motions of the ions to carry them to a completely random or (better on a larger scale) to a more uniform distribution in a given volume from one in which there was a greater concentration at some point relative to another. In the random thermal wandering of the ions, the tendency will obviously be for more ions to move from a high concentration to a lower one than in the reverse sense. Thus, in time the regions of high concentrations will lose molecules to the regions of lower concentration and equalization will occur. The net mass motion of ions towards lower concentrations is called *diffusion*, and the fact that a certain net number of such ions move across a boundary in the gas in a given time gives us a *velocity of diffusion*. From the point of view of the gas laws the diffusion is ascribed to a force per unit area, or a pressure difference. This is in value  $p_1 - p_2 = \frac{1}{3} N_1 m u^2 - \frac{1}{3} N_2 m u^2 = \frac{1}{3} m u^2 (N_1 - N_2)$ , where  $N_1$  and  $N_2$  are the numbers of ions per unit volume at the two points 1 and 2 causing the pressures  $p_1$  and  $p_2$  and hence the diffusion. It is clear that one might expect that, the greater the force difference per unit area causing the flow, i.e., the greater  $p_1 - p_2 = dp$  over a given distance  $dx$  between points 1 and 2, the faster the flow or net transfer. Again, the flow should be proportional to the time  $dt$  when conditions are steady, and finally it should be proportional to the area  $A$  across which a flow takes place.

Hence it is not surprising that under the simple conditions for a steady flow of molecules along one axis experiments on the diffusive flow of gases showed that the net number of ions or molecules flowing by diffusion in a time  $dt$  is given by  $dn = -D(dp/dx)A dt$ . Since  $dp$  is proportional to the change in density ( $N_1 - N_2$ ) of the molecules or ions over  $dx$ , the expression is

$$\frac{dn}{dt} = -DA \frac{dn}{dx}.$$

Here  $D$  is a constant of dimensions  $LT^{-1}$  or velocity per unit area depending on the units used and, as we shall see, is characteristic of the resistance offered by the gas to the motion of the ions or molecules. If we note, however, that this expresses the rate of transfer in a special case of the steady-state motion it is clear that the equation will be much more complicated where the flow  $dn/dt$  and hence  $dn/dx$  is changing with time and position along the three coordinate axes,  $X$ ,  $Y$ , and  $Z$ . The general equation for this condition can be set up in analogy with the Fourier heat conduction equation, which reads

$$\frac{\partial \theta}{\partial t} = h^2 \left( \frac{\partial^2 \theta}{\partial x^2} + \frac{\partial^2 \theta}{\partial y^2} + \frac{\partial^2 \theta}{\partial z^2} \right) = h^2 \nabla^2 \theta,$$

where  $\theta$  is temperature,  $t$  is time, and  $h^2$  is called the *temperature diffusivity*. The inverted delta ( $\nabla^2$ ), called the Laplacian operator, or  $\text{del}^2$ , represents the operation indicated in the parentheses. In the case of diffusion, the general differential equation of the change in concentration in time and space is then

$$\frac{dn}{dt} = D \left( \frac{\partial^2 n}{\partial x^2} + \frac{\partial^2 n}{\partial y^2} + \frac{\partial^2 n}{\partial z^2} \right).$$

This is a linear partial differential equation of the second order. The form of the solution depends on the conditions imposed by a given problem, such as how  $n$  varies with  $t$  at some point, or how  $n$  varies with  $x$ ,  $y$ , and  $z$  at some time. That is, the character of the solution depends on the initial conditions, termed the *boundary conditions*, imposed by a given problem. The solutions of equations of this type for  $n$  as a  $f(x, y, z, t)$  are in general very complex. They are simplified by choosing for a variation of  $n$  with  $t$  a variation which can be expressed as the sum of a series of sine and cosine terms, called a Fourier series. The method of solution of diffusion and heat-conduction problems furnishes the material for the content of a book in itself. The facility in measuring temperature compared to that of evaluating concentrations, and the need of solutions of these problems in the thermal case for practical application, have resulted in the solution of many problems for the thermal case. Although boundary conditions in the two cases may differ, it is possible that the solutions of certain diffusion problems may be derived from the analogous thermal case.

It is possible in studying diffusion to use one of two procedures. The first is to utilize a simple apparatus and procedure and then apply tedious methods of calculation in the solution of the complicated equations resulting. The other is to make experimental procedures so elaborate that simple boundary conditions apply, the solution of which is easy. Practically the only work done on diffusion was the early pioneer work of J. S. Townsend at a time when elaborate techniques were not at hand. He used the simple and crude techniques



of the early period and with considerable mathematical skill solved the difficult boundary problems satisfactorily. The significance of the results in those days was very great. Today, however, though the general conclusions stand, the experimental difficulties and sources of error lie buried in a mass of complex mathematics, and accurate or improved solutions have not been attempted as the data needed can easily be obtained from mobilities.

### 3. THE EARLY MEASUREMENTS OF DIFFUSION

The first experiments involved an air-blast method.<sup>1,2,3</sup> In this study uniformly ionized air containing ions of both signs was blown down a series of cylindrical metal tubes whose diameter was small, so that the ratio of surface to volume was large. In this case, the loss of ions by diffusion to the walls is greater than the loss by volume recombination of ions. By having two sets of tubes of the same diameter but different lengths, and measuring the positive ions and the negative ions escaping diffusion to the tube walls by catching them on an electrode beyond the tubes, solution of the complicated equations enabled Townsend to evaluate  $D$ . The diagram of his apparatus is shown in Fig. 68. A gas current  $C$  of velocity  $V$  enters the tube.

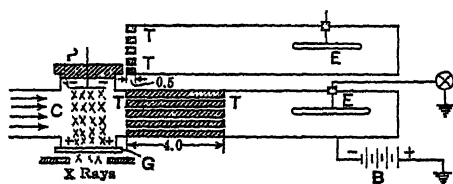


FIG. 68.—The Townsend Air-Blast Diffusion Apparatus.

When ultraviolet light is used the plate  $P$  is illuminated through gauze  $G$  and the ions are drawn off to  $G$  by the field across the gas stream. The plug and plate  $P$  are not used with X-rays, and these rays merely traverse the stream. In this case the ions of opposite sign are separated by wire gauzes having a field of appropriate sense parallel to the gas stream between the mouth of  $C$  and the tubes  $T$ . The ions pass through the tubes  $TT$ , which are either 4 cm long =  $x_1$  or 0.5 cm long =  $x_2$ . The velocity of the air blast  $V$  is kept constant by adjusting the pressure as the tubes are changed. A sort of mechanism holding the tubes like the mechanism in a revolver allows the tube sets  $T$  with lengths  $x_1$  and  $x_2$  to be interchanged during a run. The battery  $B$  forces the ions from  $TT$  and the tube walls to the collecting electrode  $E$ , after they leave the tubes. If the tube lengths in the two sets, which are interchanged at will, are  $x_1$  and  $x_2$ , while the radii  $a$  are unchanged, then the number of ions,  $n_1$  and  $n_2$ , collected on the electrodes in the two cases are given by:

$$\frac{n_1 e}{n_2 e} = \frac{0.195e^{-\frac{7.313Dx_1}{2a^2V}} + 0.0243e^{-\frac{44.5Dx_1}{2a^2V}}}{0.195e^{-\frac{7.313Dx_2}{2a^2V}} + 0.0243e^{-\frac{44.5Dx_2}{2a^2V}}}$$

In the experiments  $n_{1e}$  and  $n_{2e}$  are the currents collected by  $E$  when tubes of length  $x_1$  and  $x_2$  are used. The coefficient of diffusion is  $D$ ,  $V$  is the velocity of the gas blast, and  $a$  is the radius of the tubes. To solve such an equation for  $D$  it is merely necessary to assign  $x_1$ ,  $x_2$ ,  $a^2$ , and  $V$  the values to be used in any set of measurements and by varying the value of  $D$  within reasonable limits to compute curves for  $n_1/n_2$  as a function of the quantity  $Z$  such as shown in Fig. 69 for  $x_1/x_2 = 4$

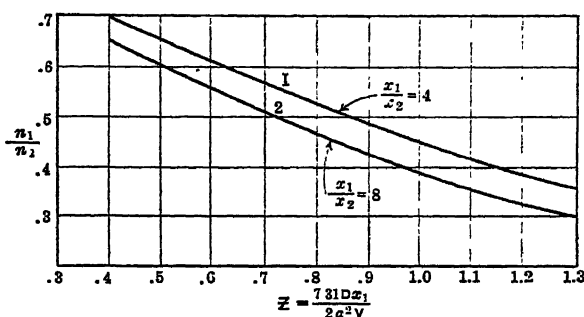


FIG. 69.

and  $x_1/x_2 = 8$  over an adequate range where  $Z = 7.313 D x_1 / (2 a^2 V)$ . The equation cited then yields

$$\frac{n_{1e}}{n_{2e}} = \frac{0.195e^{-Z} + 0.0243e^{-\frac{44.5}{7.31}Z}}{0.195e^{-Z\frac{x_2}{x_1}} + 0.0243e^{-\frac{44.5}{7.31}Z\frac{x_2}{x_1}}}$$

From such a curve with  $x_2$  and  $x_1$  known the observed ratio of  $n_1/n_2$  will at once give the value of  $Z$  and thus of  $D$ , since  $D = 2Za^2V/(7.313x_1)$ . Townsend<sup>1,2</sup> in 1899 found the value of  $D$  for gaseous ions to be as follows.\*

It is at once to be seen that  $D$  for ions is low and is about one-fourth to one-fifth the value of the  $D$  for the diffusion of *uncharged molecules*

TABLE X

|                      | $D_+$ Ions | $D_-$ Ions | $D$ for Molecules<br>Gas into Gas             |
|----------------------|------------|------------|---|
| Air .....            | 0.028      | 0.043      | O <sub>2</sub> into N <sub>2</sub> 0.171      |
| CO <sub>2</sub> .... | 0.023      | 0.026      | CO <sub>2</sub> into N <sub>2</sub> O 1.5-1.0 |
| H <sub>2</sub> ..... | 0.123      | 0.190      | H <sub>2</sub> into N <sub>2</sub> 0.739      |

\* In giving these values of  $D$  it is to be noted that they represent air-blast measurements. The values of  $D$  like those of  $k$ , the mobility in the Zeleny air-blast method, are of significance *only as orienting magnitudes*. They are not expected to be accurate or significant except in such an orienting sense.

in a closely similar gas. This is the same sort of result which was observed for the mobility of gaseous ions. In fact, a most important equation which we shall shortly derive leads us to expect that the mobility  $k$  and the diffusion coefficient  $D$  are closely related.

#### 4. RELATION BETWEEN MOBILITY AND DIFFUSION

In a gas in an electrical field  $X$  acting with a force  $Xe$  on ions of charge  $e$ , the ions move with a velocity  $kX$ . Gas ions urged by their own partial pressure have a force  $pA$  exerted on an area  $A$ , and diffuse with a velocity  $v$ . Since the velocities  $kX$  and  $v$  are caused by the forces given above acting on bodies in a medium giving the same resistance, it should be possible from the resistance to compute the relation between  $v$  and  $kX$  and hence between  $D$  and  $k$ . Assume a column of ionized gas of unit area,  $A = 1$ . The number of ions  $n$  diffusing through  $1 \text{ cm}^2$  in 1 second is  $n = D(dn'/dx)$ , where  $dn'/dx$  is the concentration gradient in the direction of diffusion. The velocity of diffusion  $v$  is then defined by writing  $n = vn'$ , where  $n'$  is the concentration. Hence  $v = (D/n')(dn'/dx)$  and as  $p$  is proportional to  $n'$ ,  $p = bn'$ ,  $dp = bdn'$ , where  $b = \frac{1}{2}mC^2$ , so that  $dn'/n' = dp/p$ . Thus we have  $v = (D/p)(dp/dx)$ . For  $1 \text{ cm}^3$  of gas, the force acting on  $1 \text{ cm}^2$  of area across  $dx = 1 \text{ cm}$  is simply  $(dp/dx)(1 \text{ cm})(1 \text{ cm}^2) = dp/dx$ . This applies to the  $n'$  ions per  $\text{cm}^3$ . Thus  $(dp/dx)(1/n')$  is the force on one ion, and since from above  $dp/dx = pv/D$ , the force on one ion is  $F_D = (pv/D)(1/n')$ . But as the result of a field  $X$  the force on an ion is  $Xe$  and the velocity produced is  $v = kX$ . Since  $X = v/k$ , the force on the ion is  $ve/k$  when it has a velocity  $v$ . Now the force on an ion causing diffusion with the velocity  $v$  is  $F_D = (pv/D)(1/n')$ , while the force of an electrical field  $F_e = ve/k$  also produces a velocity  $v$  on an ion in the same medium. Since in both cases the motion is steady and uniform the resisting viscous forces depend only on  $v$  and they are equal so that  $F_e = F_D$ . Accordingly

$$\frac{pv}{D} \frac{1}{n'} = \frac{ve}{k},$$

so that  $k/D = n'e/p$ . Now the partial pressure  $p$  of the ions corresponds to a concentration  $n'$ , and at atmospheric pressure the pressure  $P$  would correspond to  $N$ , the number of molecules per cubic centimeter at N.T.P. That is, since  $p = bn'$ ,  $p/P = n'/N$ . Hence  $k/D = Ne/P$ , where  $Ne$  is the charge on  $2.687 \times 10^{19}$  ions and  $P$  is the pressure in dynes per square centimeter at N.T.P.

The same law can at once be deduced from elementary kinetic theory.<sup>4</sup> This says that  $k$ , the mobility, is given by

$$k = 0.815 \frac{e}{M} \frac{L}{C} \sqrt{\frac{m+M}{m}};$$

see page 55. For the coefficient of diffusion computed for ions in a gas under the same assumptions as to processes of averaging<sup>16</sup>

$$D = 0.815 \frac{CL}{3} \sqrt{\frac{m+M}{m}}.$$

Thus we can write

$$\frac{k}{D} = \frac{0.815 \sqrt{\frac{m+M}{m}} 3Le}{0.815 \sqrt{\frac{m+M}{m}} LMC^2} = \frac{e}{\frac{1}{3}MC^2} = \frac{Ne}{\frac{1}{3}NMC^2} = \frac{Ne}{P}.$$

Thus the coefficient of diffusion  $D$  divided into the mobility is a constant such that  $k/D = Ne/P = 42.7$ , if  $e$  has the same value as  $e$  for monovalent ions in electrolysis and if  $k$  is in cm/sec per volt/cm. This follows since  $22,414 Ne = N_A e$ , which is the Faraday constant of 9650 absolute emu, and  $P = 1.013 \times 10^6$  dynes/cm<sup>2</sup>, and volts are  $10^8$  emu, so that

$$\frac{k}{D} = \frac{Ne}{P} = \frac{2.7 \times 10^{19} \times 4.8 \times 10^{-10}}{1.013 \times 10^8} = 12,810 \text{ per esu.}$$

Since  $1 \text{ esu} = 300 \text{ volts}$ ,  $k/D = 12,810/300 = 42.7$ , and  $D = 0.0235 k$

It is seen at once that by measuring  $k$  and  $D$  on the same ions we at once can decide whether  $e$  has the quantity of charge of the unit electrolytic  $H^+$  ion, or a larger charge. Now it happened that in 1900 it was impossible to tell with certainty whether the charge of an electron or of a positive ion that has lost an electron was the same numerically as that of the  $H^+$  ions in electrolysis. Prior to that date, the value of  $e/m$  for an electron had been determined by J. J. Thomson to be about 1836 times that for the  $H^+$  ion. Hence if  $e$  for an electron was as large as that for an  $H^+$  ion in electrolysis, the mass  $m$  of the electron had to be  $1/1836$  that of the  $H$  atom. It was, of course, of great importance at that time to prove this fact. Townsend thus in 1900 was the first to ascertain from the observed values of  $k/D$  that most of the positive and negative ions observed gave a ratio close to 0.0235 and that electrons and positive ions in gases carried the same charge as the electrolytic ions. This then fixed the mass of the electron. It was not until somewhat later that J. J. Thomson got direct evidence as to the size of the charge of the electron, and it took eleven years before Millikan had evaluated the electronic charge accurately.

The actual value of  $k/D$  observed for ions of both signs by Townsend gave a value of  $Ne$  of  $1.25$  to  $1.63 \times 10^{10}$  esu. For monovalent electrolytic ions,  $Ne$  is  $2.7 \times 10^{19} \times 4.8 \times 10^{-10}$  or  $1.30 \times 10^{10}$  esu. Thus the values of Townsend for negative ions ranged from  $1.25$  to  $1.31$  while they ranged from  $1.45$  to  $1.63$  for positive ions in  $O_2$  and  $H_2$ .

At the time the inaccuracies in the evaluation of  $k$  were not known. Again  $k$  and  $D$  were not studied in the same apparatus and in the same samples of gases. It is thus not strange that a wide diversity of results of about the right order of magnitude was observed. In fact, it is rather more surprising that the results were as close to theory as they were.

The fact that  $Ne$  from  $k/D$  for positive ions was higher than for negative ions led Franck<sup>5</sup> to propose that some 10 per cent of the positive ions might be doubly charged. In the case of doubly charged ions, the mobility  $k$  which was *assumed* proportional to the charge of the ion would be larger by a factor of 2 than  $D$ , which was *assumed* unaffected by the charge. Thus the average value of  $k$  might be expected to be higher with 10 per cent doubly charged ions and thus  $Ne$  *should* be higher. For negative ions that come from electrons double charges do not occur. Since this explanation seemed so logical

Franck<sup>5</sup> and Westphal redetermined  $k$  with this end in view and confirmed Franck's belief. The speculation of Franck led Townsend<sup>1,6</sup> to devise an exceedingly ingenious method for comparing  $k$  and  $D$  experimentally and for obtaining the ratio  $k/D$  in one apparatus at the same time. Consider the apparatus depicted in Fig. 70. An annular beam of X-rays or ultraviolet light entered a chamber through the annular slot  $SS$  and struck a plate  $PP$ . The ions made in the space between the plate  $B$  in the plane of

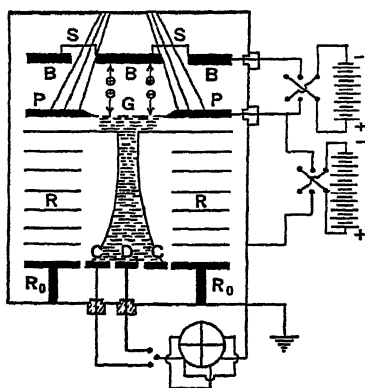


FIG. 70.—The Townsend Apparatus for Measuring the Ratio  $NeX/P$ .

long uniform electrical field  $X$  existed. The ions were carried along  $X$  by the field and reached an electrode  $CDC$  which was cut into an inner disc  $D$  and an outer annular segment  $CC$ , either of which went to an electrometer  $E$ . The guard rings  $RR$  kept the field  $X$  uniform.

In three dimensions,  $x$ ,  $y$ , and  $z$ , the field  $X$  being along  $x$ , we can write that per unit area

$$n_x = -D \frac{dn_1}{dx} + Xkn',$$

$$n_y = -D \frac{dn_1}{dy},$$

$$n_z = -D \frac{dn_1}{dz}.$$

For along  $x$  the movement is increased by the field  $X$ . This gives on rearrangement through the equation for diffusion in a steady state the differential equation

$$\frac{d^2n}{dx^2} + \frac{d^2n}{dy^2} + \frac{d^2n}{dz^2} = \nabla^2 n = \frac{NeX}{P} \frac{dn}{dz},$$

since  $k/D = Ne/P$ . This indicates that the number  $n$  of ions reaching a point depends on  $NeX$ . By converting  $y$  and  $z$  to cylindrical coordinates and inserting boundary conditions involving the length  $l = 7$  cm of the field, the radius  $a$  of the hole in the top plate  $AA$ , the radius  $b$  of the annular rings  $RR$  when the disc  $D$  has a radius  $a$  and the ring  $C$  has a radius  $b$ , one can solve the equation for the ratio of the number of ions going to  $D$  relative to those caught by  $D + C$ . The solution of the very complex equations results in the evaluation of the ratio  $R = en_D/en_{D+C}$ , of the currents to  $D$  and to  $D + C$ , as a function of  $NeX/P$ . By assuming values of  $NeX/P$  within the probable experimental range, the ratios for a given  $l$ ,  $a$ , and  $b$  can be calculated from the equation. From these values of  $R$  plotted as curves against  $NeX/P$ , see Fig. 71, any observed value of  $R$  will at once fix the value of  $NeX/P$ . Townsend<sup>6</sup> and Haselfoot<sup>7</sup> at once found that for clean dry gases  $Ne$  for positive ions was the same as for negative ions and close to the theoretical value. This method obviates any deviations due to difficulties in the absolute evaluation of  $k$  and  $D$  and differences in the purity of the gas.

When the gas was particularly dirty with hydrocarbon vapors from vaseline smeared in the chamber  $SS-PP$ , Townsend observed high values for  $Ne$  for positive ions. What this means is not clear, and it is hard to believe that results obtained when conditions are particularly bad should be significant.

Now it is true that in some cases the primary ionization act does create multiple positively charged ions. In Hg under favorable conditions as many as 10 per cent of the ions may be  $Hg^{++}$ . In He with  $\alpha$  particles at a particular velocity some 16 per cent doubly charged  $He^{++}$  are formed. In some cases X-rays giving rise to fast  $K$ ,  $L$ ,  $M$ , and  $N$  electrons from one atom through the Auger effect will liberate as many as four electrons from one atom. These cases occur very rarely. In

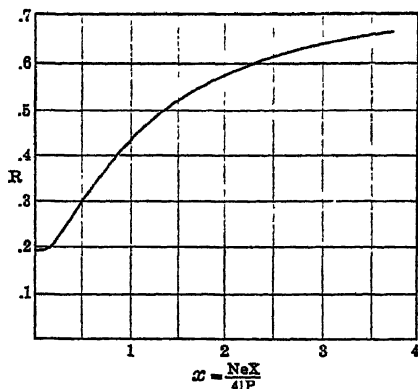


FIG. 71.

the  $10^8$  collisions of ions with gas molecules per second, the Kallmann-Rosen effect results in a rapid loss in the number of doubly charged positive ions to singly charged ions by charge transfer, so that in ordinary ion work very few doubly charged ions are observed. Thus, it is doubtful whether the value of  $Ne$  in such experiments at ages of more than  $10^{-3}$  second can be interpreted in terms of the charge  $e$  on the ion.<sup>8</sup> At high fields and at low pressures some doubly positively charged ions could be detected.

Since it has been shown that the mobility of ordinary ions is relatively insensitive to the ionic charge (see page 63), one might question the appearance of the quantity  $Ne$  in the relation  $k/D = Ne/P$ . In Chapter I it was pointed out that for small ions an equation of the

form  $k = \frac{A\sqrt{(M+m)/m}}{\rho/\rho_0\sqrt{(D-1)_0}M_0}$  holds, which contains no  $e$ . This

question requires analysis, since it was shown that the deduction of the relation  $k/D = Ne/p$  was *rigorous without the use of kinetic theory*. The answer to this question can be given in terms of the derivation of the relation  $k/D$  from kinetic theory. We had, neglecting the factor  $\sqrt{(M+m)/m}$  in both equations, written that on a *solid elastic theory*  $k = 0.815 (e/M) (L/C)$  and  $D = (0.815/3)LC$ , neglecting the fact that  $L$  might also depend on  $e$ . Now in the Langevin point charge equation for  $k$ , the  $e$  is absent since the free paths are such that  $L$  varies with  $e$  according to  $L = A/e$ , where  $A$  is some constant. But  $D$  also is *proportional to  $L$* ; thus we can write that

$$\frac{k}{D} = \frac{0.815 A}{MC} \bigg/ \frac{0.815 A}{3 e} C = \frac{e}{\frac{1}{3} MC^2} = \frac{Ne}{\frac{1}{3} NMC^2} = \frac{Ne}{P}$$

so that under any theory, as shown by simple mechanical considerations,  $k/D = Ne/P$ . Aside from permitting us to evaluate  $D$  from measurements of  $k$ , this equation is of great use in all discharge phenomena where diffusion can occur.

### 5. THE ROLE OF DIFFUSION IN DISCHARGE AND CONDUCTION PHENOMENA: THE VALUE OF THE COEFFICIENT OF DIFFUSION AND ITS VARIATION

The influence of diffusion in ionic studies may be clearly visualized in terms of the following experiment. Assume that a volume of ionization of one kind is created near a plate  $D$  of a parallel-plate condenser system  $DE$ . The cross-sectional area of this volume is represented by the rectangle  $AB$  of mid section at  $FF$ . Now let fields of four different strengths  $X_0$  be applied to  $DE$  such that the ionized volume is carried so that  $F$  coincides with  $E$  at a time  $T_0$  of respectively  $10^{-5}$ ,  $10^{-3}$ , 1, and 10 seconds after the flash creating the ions. Let it be possible to vary the field  $X$  by  $\Delta X$  below and above  $X_0$  so that  $F$

will be short of or past the plate  $E$  at the end of a time  $T_0 \pm \Delta T$ , at which  $(X_0 \pm \Delta X)$  is cut off, so that the charge on  $E$  can be measured. Such an operation was actually used by Fontell<sup>9</sup> in his mobility measurements.

Assume the ions in  $AB$  to have initially been uniformly distributed in density throughout the volume. If one regard the progress of the

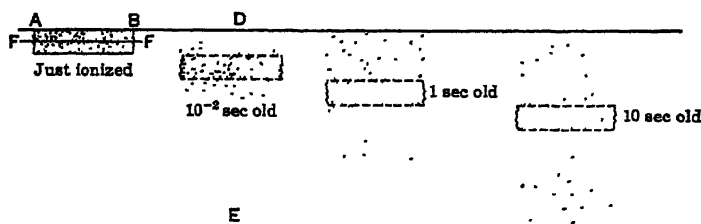


FIG. 72A.

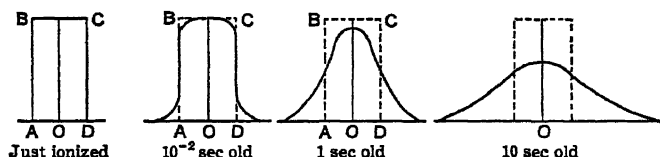


FIG. 72B.

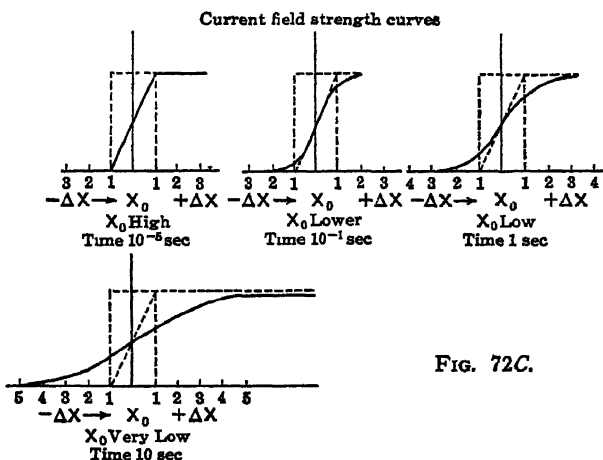


FIG. 72C.

ion distribution relative to  $AB$  at times  $T_0$  equal to  $10^{-5}$ ,  $10^{-2}$ , 1, and 10 seconds the distribution of ions will be seen as depicted in Fig. 72A. If one had counted the number of ions as a function of their displacement  $\Delta x$  from the line  $F$  or the zero line as a function of  $X_0$  on the times  $T_0$  of crossing of  $10^{-5}$ ,  $10^{-2}$ , 1, and 10 seconds, one would have plotted the distributions as shown in Fig. 72B. The initial distri-



bution is the dotted rectangle on each curve. Thus diffusion spreads the ions backwards and forwards of  $F$  as the ions move across the plates. If  $X_0$  is the field to cause the center of the group  $F$  to cross in times  $T_0$  of  $10^{-5}$ ,  $10^{-2}$ , 1, and 10 seconds, then as we begin measuring the current to  $E$  at large values of  $-\Delta X$  in  $X_0 - \Delta X$  and gradually decrease  $\Delta X$  to 0 and increase it to positive values the current measured at  $E$  will be the integral of the curves of Fig. 72B expressed as functions of  $\pm \Delta X$  instead of the distance  $\pm x$  from  $F$ , for these are related by means of the equations  $\pm \Delta X k T = \pm x$ . Such integrated curves are shown in Fig. 72C for the four cases cited. It is seen that at  $T = 10^{-5}$  second with a high value of  $X_0$ , the current rises abruptly at  $\Delta X = -1$ , below the value  $X_0$  at which the center of the volume reaches  $E$ . Here  $\Delta X = 1$  corresponds to the displacement  $\Delta x$  of the lower edge of the initially ionized beam from  $F$ . From there on, the rise  $I/I_0$  is linear to a constant value at  $\Delta X = +1$  above the value of  $X_0$ , after which the current  $I = I_0$  and is constant. At  $T = 10^{-2}$  second the curve rises asymptotically, starting somewhat below  $\Delta X = -1$ . At  $T = 1$  second the curve begins to rise asymptotically at  $\Delta X = -3$  and does not reach the maximum of  $I = I_0$  until  $\Delta X = +3$ . At  $T = 10$  seconds the situation is even more pronounced. The current  $I$  in this case never reaches its previous saturation value  $I = I_0$  since some of the ions *have diffused against* the field  $X$  and been lost to the plate  $D$ .

The phenomena pictured occur not only in such experiments as described but, depending on the values of  $X$ ,  $D$ ,  $T$  and  $k$ , they occur through the whole range of discharge conditions from thermionic emission in the presence of gas to photoelectric currents in gases and in discharge-tube plasma. Had one attempted in the case of the 10-second transit illustrated above to infer the mobility of the ions by the extrapolated slope of the curve, one would have inferred a field strength not of  $X_0 + \Delta X$  but of  $X_0 - 4\Delta X$ , which would have made a material error in the value of the mobility. Such a spread of an ion group by diffusion may also mislead one to ascribing the curve shape to a broad continuous distribution of mobilities among the ions, a circumstance which probably does not often occur. In the presence of diffusion, therefore, the correct procedure is not to use the extrapolated rise of the current as indicating the critical field strength. It is more correct to make a graphical differentiation of the curve and from this infer the location of the peak of the curve, which should remain fixed relative to the center of the ion group and thus give the distance that  $F$  has moved in the time  $T_0$ . Though some doubts may arise as to the accuracy of such graphical integration, the fact is that it gives results far more accurate than those yielded by other procedures.<sup>10</sup> One could also<sup>11</sup> compute the diffusion of the ions in the time  $T$  by means of the Einstein formula, to be given. Taking the displacements in  $\Delta X$  obtained for a fraction  $(I/I_0)_D$  of the integral

of such a computed curve, one may deduct the diffusion spreading from the observed value of  $I/I_0$ ,  $(I/I_0)_0$  for the mobility curve at the same  $\Delta X$ . This will give the real curve for the rise of the current with  $X$ . Both procedures have been resorted to at various times. In general the diffusion corrections for normal *ions* at atmospheric pressure are negligible under  $10^{-2}$  second, as will later be seen with great concentrations of electrons even at low pressures and *with free electrons in gases*, especially if any appreciable electrical fields are present, *one cannot neglect diffusion*.<sup>12</sup>

In "vacuum" tubes, especially in the presence of small gas pressures where thermionic emission takes place with low fields giving space-charge-limited currents, what is essentially a diffusion phenomenon takes place. If the electrons are emitted from the cathode with zero velocity the electrical potential gradient, i.e., the electrical field at the cathode, is virtually zero. If, however, owing to a high filament temperature, the electrons are emitted with a high energy from the cathode, the electrons will diffuse as a cloud of such density to some distance from the cathode that the applied field gradient near the cathode is *reversed* and the cathode is slightly positive to the dense electron cloud as seen on page 320. The field then passes with a negative slope through zero and becomes positive on the anode side of the cloud. Such a negative potential trough has important consequences in tube performance, and it acts as a positive ion trap for low-energy positive ions.<sup>13</sup> The effect is very pronounced when small pressures of gas are present,  $10^{-2}$  mm or more. It is this circumstance that helps to make the negative space charge especially valuable for the detection of slow positive ions, as Varney has found.<sup>13</sup>

Probably the most important cases of diffusion at low pressures in gases occur for free electrons in electrical fields. Under these conditions owing to the elasticity of electron impact the electrons gain energy in the field until they have *thermal velocities far in excess of the value  $C$*  appropriate to the temperature of the gas. Hence the quantity  $C$  in  $D = \frac{1}{2} LC$  is very much increased. In an analysis published in 1925, G. Hertz<sup>12</sup> showed that, if we assume a gas in which electrons make *perfectly elastic impacts* with molecules of relatively infinite mass, and if electrons start from the cathode with zero velocity, the *average velocity caused by diffusion is of the same order as that attained as a drift velocity in the field direction*. This indicates why, at low pressures in discharge tubes where  $L$  and  $C$  are large,  $D$  becomes so large that the discharge fills the whole tube. It also indicates that the diffusion current of electrons to the walls and the anode where field gradients are small may play an important role in the economy of the discharge and in the characteristics of the positive column. It is not proper at this place to discuss in detail the derivation of the Hertz equation. Since 1925 the problem has been extended, by Druyvesteyn and others, with inclusion of the real elasticity of electron impact to

the study of the distribution of electron energy in gases. This question will thus be extensively treated at another point and in another connection in Chapter V.

In conclusion, it is of value to give the results of Einstein's classical analysis<sup>14</sup> of the Brownian movement of a particle caused by molecular bombardment and its relation to the coefficient of diffusion. The equations are exceedingly useful in the study of any problem involving diffusion of ions or particles to which a kinetic analysis is to be applied. Examples of such an application can be seen in several places in the chapter on ionic recombination.

Einstein<sup>14</sup> has shown that, out of  $N_0$  particles or ions which are moving independently of each other with their heat motions and which were at a time  $t = 0$  at the origin  $x = 0$ , the number that are to be found at any later time with an  $x$  component of displacement between  $x$  and  $x + dx$  is given by

$$n_{dx} = \frac{N_0}{\sqrt{4\pi Dt}} e^{-\frac{x^2}{4Dt}dx}.$$

Here  $D$  is the coefficient of diffusion of the particles. The form of this curve as a function of  $x$  at any time  $t$  is that of the well-known Gaussian

error curve. As time goes on, its form remains inviolate but its scale factor  $4Dt$  increases.

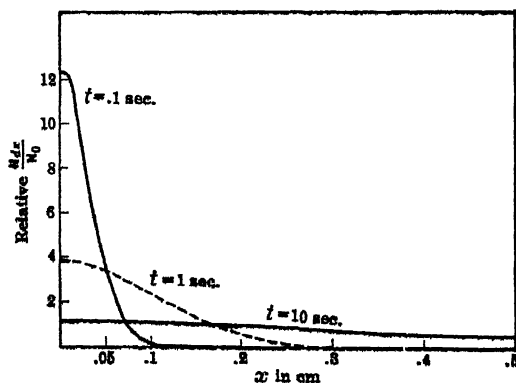


FIG. 73.

The evolution of this distribution in time and along  $x$  is shown by the three curves of Fig. 73, for negative ions in air at atmospheric pressure at 0.1, 1, and 10 seconds. These curves are analogous to those shown in Fig. 72, A, B and C, which approximately represent conditions when the equation is applied

to an initial volume distribution. The expression also yields the relation that, if  $N_0$  is the ion density in an elementary volume at  $t = 0$ , the density  $N$  at a distance  $r$  from the center of this volume at a time  $t$  produced by the diffusion of particles from the elementary volume will be given by

$$N = \frac{N_0}{(4\pi Dt)^{3/2}} e^{-\frac{r^2}{4Dt}}.$$

From the first expression it can be shown that the square root of the

average squared displacement along one axis,  $\sqrt{x^2} = \sqrt{2Dt}$ . For diffusion in three dimensions  $\sqrt{\bar{R}^2} = \sqrt{x^2 + y^2 + z^2} = \sqrt{6Dt}$ . In a distribution the *average displacement*  $\bar{x}$  is not the same as  $\sqrt{x^2}$ , for the square root of the average square favors the larger values. Hence  $\sqrt{x^2}$  is larger than  $\bar{x}$ , the relation being

$$\bar{x} = \sqrt{\frac{2}{\pi}} \sqrt{x^2} = \sqrt{\frac{4Dt}{\pi}}.$$

If a finite number  $n$  of such random displacements are observed, the probable error in the value of  $\bar{x}$  is  $(\sqrt{n}/n)\bar{x}$ . In three dimensions  $\bar{R} = \sqrt{12Dt/\pi}$ . With the evaluation of  $D$  from the approximate expression  $D = \frac{1}{3} \bar{c}L$  or from the exact expression  $D = kP/N_e = 0.0235 k$ , it is then possible to study the variation in density or displacement of the particle or ion with time. In air at N.T.P.,  $k$  for negative ions is 2.2 cm/sec per volt/cm. Thus  $D = 0.0518$ . For a free electron, for which  $k$  is of the order of  $5 \times 10^3$  times that for an ion,  $D$  becomes  $D_e = 259$ . Thus in  $t$  seconds, the average  $x$  component of the ionic displacement is  $\bar{x} = \sqrt{0.066t} = 0.257 \sqrt{t}$  cm. For an electron under the same conditions  $x = 18.2 \sqrt{t}$  cm. For most ion measurements the displacement of an ion of 0.0257 cm in  $10^{-2}$  second is negligible, while the 1.82 cm for an electron is serious. Since to observe measurable recombination accurately at ion densities usually obtainable requires of the order of  $10^{-2}$  second it can be seen why diffusion introduces serious errors in the case of free electrons.

As regards the variation of  $D$  with temperature and pressure one had best use the kinetic-theory definition of  $D$  which is

$$D = \frac{1}{3} 0.815LC \sqrt{\frac{M+m}{m}}.$$

It is clear that since  $L$  is inversely proportional to density  $\rho$  and therefore, at constant temperature, inversely proportional to pressure  $p$ , while  $C$  is constant, then  $D \propto 1/\rho$  and at constant temperature to  $1/p$ . For *molecules* in general,  $L$  changes somewhat with temperature according to  $\frac{1}{A+B/T}$  while  $C \propto \sqrt{T}$ . Hence, one would expect

$D \propto \frac{\sqrt{T}}{A+B/T}$ . In the case of gaseous ions if polarization forces are large  $L$  depends on  $C$ , and the Langevin equation (see page 63) in this case indicates that  $k$  which depends on  $L/C$  is practically independent of temperature. This condition is largely corroborated in the case of ions in polarizable gases and nearly applicable even in He. Thus,  $L$  for ions must be nearly proportional to  $C$ . Hence,  $D$  is pro-

portional to  $C^2$ , and thus  $D$  for ions should vary as the absolute temperature. This is borne out by the equation

$$D = \frac{kP}{Ne} = \frac{k\frac{1}{2}MC^2}{e}.$$

Thus except as  $k$  varies with  $T$ ,  $D$  is proportional to  $T$ . From the kinetic-theory expression for  $D$  it is at once seen that  $D$  is proportional to

$$C\sqrt{\frac{M+m}{m}} = C_0\sqrt{\frac{m_0}{m}}\sqrt{\frac{M+m}{m}}.$$

This differs somewhat from the simple classical kinetic-theory expression for self-diffusion in which  $D$  is proportional to  $1/\sqrt{m}$  owing to persistence of velocities. It is in general to be noted that ionic diffusion differs from molecular diffusion in that the free path  $L$  is very much more seriously affected by attractive forces in the case of ions than in that of molecules. Aside from this, the diffusion coefficient offers little of interest which has not been covered by ion theory. The coefficient is, of course, of great use in the solution of problems involving diffusion. The problems involving diffusion where encountered are amenable to calculation from the diffusion equation in analogy to similar calculations using the Fourier heat equation. Each study presents its own problem in the application of the boundary conditions, which it is not profitable to take up in this book.

## 6. REFERENCES FOR CHAPTER III

1. J. S. TOWNSEND, *Electricity in Gases*, Oxford Press, 1914, Chap. V.
2. J. S. TOWNSEND, *Phil. Trans. Roy. Soc.*, A 193, 129, 1899.
3. E. SALLES, Thésis Faculté des Sciences, Paris, 1913.
4. L. B. LOEB, *Kinetic Theory of Gases*, 2nd Edition, Chap. XI, p. 554, McGraw-Hill, 1934.
5. FRANCK and WESTPHAL, *Verhandl. deutsch. physik. Ges.*, 7, 146, 276, 1909.
6. J. S. TOWNSEND, *Proc. Roy. Soc.*, A 80, 207, 1908; A 81, 464, 1908; A 85, 25, 1911.
7. C. E. HASELFOOT, *Proc. Roy. Soc.*, A 82, 18, 1909; A 87, 350, 1912.
8. L. B. LOEB, *Proc. Natl. Acad. Sci.*, 13, 703, 1927; *Science*, 67, 468, 1928; L. B. and L. L. LOEB, *Proc. Natl. Acad. Sci.*, 15, 305, 1927.
9. NILS FONTELL, *Soc. Scient. Fenn. Comm. Phys. Math.*, 5, 23, 1931; 6, 6, 1932; 6, 17, 1932.
10. R. N. VARNEY, *Phys. Rev.*, 42, 547, 1932.
11. JOHN ZELENY, *Phys. Rev.*, 34, 310, 1929.
12. G. HERTZ, *Z. Physik*, 32, 298, 1925.
13. R. N. VARNEY, *Phys. Rev.*, 53, 732, 1938.
14. A. EINSTEIN, *Ann. Physik*, 17, 549, 1905.
15. L. B. LOEB, *Kinetic Theory*, 2nd Edition, pp. 266, 267.
16. L. B. LOEB, *Kinetic Theory*, 2nd Edition, p. 552.

## CHAPTER IV \*

### ELECTRON MOBILITIES

#### 1. INTRODUCTION

The problem of the velocities of electrons in gases in electrical fields is closely bound up with the conditions of the energy distribution of electrons in electrical fields. In fact, as will be seen, until these conditions are known the velocities of electrons in electrical fields cannot be computed properly. It would be logical in a theoretical text to treat the distribution of electron energies in electrical fields in gases first and from these to derive the expressions for the electron velocities or mobilities. Historically, and for the purposes of instruction, it appears to be better to present the study of electron mobilities first and from the difficulties encountered in such a study to lead up to the vastly more involved problem of the distribution of energies among electrons in a gas. For in this domain, as in all others, advances as time went on revealed more and more clearly the complex nature of the problem. It was only when really good values for the electron velocities in pure gases over extended ranges of field strength and pressure were available that it was finally found that serious deviations were produced by the non-Maxwellian distribution of the electron energies at certain values of the fields. Accordingly in the course of the discussion of the measurements and theory of electron mobilities on a historical basis we will be gradually but understandingly introduced to the very complex concepts involved in the following chapter on energy distribution.

The initial measurements were made by Townsend in the low-pressure region below 100 mm in 1912. Townsend<sup>1</sup> in developing his magnetic deflection method for a study of ion mobilities at low pressures discovered that at lower pressures  $p$  and higher values of the ratio of field strength  $X$  to pressure  $p$ ,  $X/p$ , the negative carriers were electronic and not ionic. The new deflection method proved at once to be ideally suited to the measurement of mobilities<sup>5,6,7,8,9,10</sup> under these conditions, and the results from it have remained the best results in the region of high  $X/p$ , despite inadequate gaseous purity, until the work of Bradbury and Nielsen in 1936.<sup>2,3,4</sup> In 1920-21, Loeb<sup>11</sup> discovered that electrons remain free in many purer gases at atmospheric pressure and that they moved with velocities much higher than

\* References for Chapter IV will be found on page 198.

the earlier work of Franck<sup>12</sup> had indicated. He developed a technique of measurement based on the Rutherford a-c method which sufficed for the higher-pressure region.<sup>13,14,15,16</sup> The values of Loeb<sup>13,14,15,16</sup> and Wahlén<sup>17,18</sup> in this region of  $p$  and  $X/p$  are the only ones available today. Where Bradbury and Nielsen's data on still purer gases overlap Townsend's data and Loeb's data, the agreement is as satisfactory as can be expected considering the differences in purity and techniques.

## 2. THE EARLY MEASUREMENT OF ELECTRON MOBILITIES

In order to introduce the problem of electron mobilities or velocities one had best begin with the elementary kinetic theory of the process. In the solid elastic theory for ionic mobilities of Langevin it will be recalled that the mobility  $k$  was given by

$$k = 0.815 \frac{e}{M} \frac{L}{C} \sqrt{\frac{M+m}{m}},$$

$M$  being the mass of the gas molecules,  $C$  being their root mean square velocity, and  $m$  the mass of the ion. If one wishes, however, since  $\frac{1}{2}mC_1^2 = \frac{1}{2}MC^2$ , one may transform the equation to

$$k = 0.815 \frac{e}{m} \frac{L}{C_1} \sqrt{\frac{m+M}{M}}.$$

Here  $C_1$  is the root mean square velocity of the ion. Since we must in analysis use  $\bar{c}_1$ , the average velocity, instead of  $C_1$ , the equation has the form

$$k = 0.75 \frac{e}{m} \frac{L}{\bar{c}_1} \sqrt{\frac{m+M}{M}}.$$

For free electrons  $e/m$  is the well-known ratio of J. J. Thomson for an electron expressed in esu divided by 300 if  $k$  is in volts per centimeter.  $L$  becomes  $\lambda$ , the electron free path, which classically is  $\lambda = 4\sqrt{2}L = 5.6L$ ,\* where  $L$  is the free path for molecules. Again  $M \gg m$  so that  $\sqrt{(m+M)/M} = 1$ . Whence  $k_e$ , the mobility of a free electron, should be given by

$$k_e = 0.75 \frac{e}{m} \frac{\lambda}{\bar{c}_1},$$

\* In practice one cannot accurately call  $\sqrt{(m+M)/M} = 1$ , and the velocity of the molecules cannot be neglected. In this case kinetic theory<sup>21</sup> sets

$$\lambda = \frac{1}{\pi N \left(\frac{\sigma}{2}\right)^2 \sqrt{1 + \frac{\bar{c}^2}{\bar{c}_1^2}}} = \frac{4\sqrt{2}}{\sqrt{1 + \frac{\bar{c}^2}{\bar{c}_1^2}}} L.$$

with  $\bar{c}_1$  the *average electron velocity*. Such a value of  $k_e$  was anticipated by Townsend when he measured the value of  $k_e$  for free electrons in gases at low pressures.

For this study of electron velocities in gases, Townsend and Tizard<sup>1</sup> in 1912 used the magnetic deflection method, the principle of which has already been presented (see page 26). From this method it will be recalled one obtains

$$\tan \theta = \frac{a}{2l} = \frac{Hev}{Xe}, \quad \text{or} \quad v = \frac{Xa}{H2l},$$

where  $v$  is the electron velocity. *If the ion or electron has a mobility*  $v = k_e X$ , and if  $k_e$  is constant, we would expect  $k_e = (1/H)(a/2l)$  to be constant irrespective of the field strength  $X$ . Townsend *observed that  $k_e$  was not constant* even when corrected for pressure,  $p$ . That is,

he found that the mobility constant,  $k_e$ , defined by  $K_e = k_e \frac{p}{760}$ , was not a constant but varied with both  $X$  and  $p$ . Townsend at once divined the reason why the electron velocity per unit field reduced to standard pressure was not constant as  $X/p$  was varied. If one looks at the equation

$$k_e = 0.75 \frac{e \lambda}{m \bar{c}_1},$$

one realizes that  $k_e$  will be constant only if  $\lambda$  and  $\bar{c}_1$  are constant. Now, were electrons in thermal equilibrium in an electrical field with the gas molecules  $\bar{c}_1 = 0.922 C_1$ ,  $C_1$  would be calculable at once from  $\frac{1}{2} m C_1^2 = \frac{1}{2} M C^2 = \frac{3}{2} kT$ , where  $k$  is the Boltzmann constant. However, electrons have a small mass and as we know today make quite elastic impacts with molecules below energies leading to excitation or ionization (see Loeb, *Atomic Structure*, page 273). Thus the electrons retain a good share of the energy  $Xe\lambda$  which they gain from the field  $X$  between collisions. Hence, their energy might be well above that given by  $C_1 = \sqrt{3kT/m}$  and will depend on  $X$  and on  $p$  since the pressure  $p$  changes  $\lambda$  and hence the rate of gain or loss of energy. Townsend accordingly set the electron energy as being  $\eta(\frac{3}{2}kT) = \frac{1}{2} m C_1^2$ ; such that for  $\bar{c}_1$  one should write  $\bar{c}_1 \sqrt{\eta}$ . Townsend next set out to evaluate the quantity  $\eta$ . To do this it is essential *to measure the energy of agitation of the electrons directly*. Now it was stated under the discussion of diffusion that the velocity of diffusion was the greater the greater the velocity of agitation of the ion, and that the ratio of  $k/D = Ne/P$  was altered if, for constant  $N$ ,  $P$  was changed by changing  $T$ . Thus,  $P$  is changed at constant  $N$  in the proportion that  $\frac{1}{2} m C_1^2$  is changed, i.e., by  $\eta$ , so that the quantity  $k_e/D = Ne/P$  must be changed to read,  $k_e/D = Ne/\eta P$ , for electrons in an electrical field. Accordingly Townsend and Tizard<sup>1</sup> proceeded to evaluate  $k_e/D =$



$Ne/\eta P$  experimentally for electrons. The apparatus was precisely the one used for the evaluation of the ratio  $Ne/P$  for ions in a gas except that it was used at such pressures that the electrons were free (see page 168). The basic equation for the solution of the problem in this case was

$$\nabla^2 n = \frac{NeX}{\eta P} \frac{dn}{dz},$$

instead of that on page 168. Solution gave, for a known distance  $l$  and an aperture of radius  $a$ , a curve between  $X/\eta$  and the ratio  $R$  of the currents to the electrodes, from which  $X/\eta$  could at once be evaluated for an observed  $R$ . In this case the ratio  $Ne/P$  is known and is a constant. Thus Townsend, simultaneously using the magnetic deflection method, see page 26, and the diffusion method, see page 168, on electrons at low pressures, was able to evaluate the velocity of the electron  $v$  from  $v = (X/\bar{H}) (a/2l)$  and the value of  $\eta$  from the value of  $X/\eta$  through the diffusion method. One may, from these data at once construct a table such as Table XI for electrons in  $O_2$  as given by Brose<sup>8</sup> in a later and improved investigation.

TABLE XI

## OXYGEN GAS AT 1 MM. PRESSURE

| $X/p$ in volts/cm(mm)   | 0.4  | 0.6  | 1    | 2    | 5    | 10   | 15   | 20   | 30   | 40   | 50   |
|---|------|------|------|------|------|------|------|------|------|------|------|
| $p$ in mm.....  | 1    | 1    | 1    | 1    | 1    | 1    | 1    | 1    | 1    | 1    | 1    |
| $v = Xk_e$ in cm/sec $\times 10^{-6}$ .....                               | 1    | 1.6  | 2.2  | 3.0  | 4.3  | 6.0  | 7.8  | 9.8  | 13.6 | 17.2 | 20.5 |
| $k_e$ cm/sec per volt/cm $\times 10^{-6}$ .....                           | 2.5  | 2.67 | 2.2  | 1.5  | 0.86 | 0.60 | 0.52 | 0.49 | 0.45 | 0.43 | 0.41 |
| $\eta$ .....  | 6    | 8.4  | 13   | 24   | 47   | 64   | 77   | 90   | 113  | 133  | 150  |
| $\sqrt{\eta} \bar{c}_1$ in cm/sec $\times 10^{-6}$ .....                  | 28.2 | 33.4 | 41.3 | 56.3 | 78.8 | 92.0 | 101  | 109  | 123  | 133  | 141  |
| $\lambda = \frac{m}{0.75 e} \sqrt{\eta} \bar{c}_1$<br>$\times 10^2$ ..... | 4.93 | 6.22 | 6.39 | 5.91 | 4.89 | 3.86 | 3.67 | 3.74 | 3.87 | 3.99 | 4.05 |

At the time Townsend did not realize the full significance of his results. He noted that, if  $e/m$  was constant, on putting the observed values of  $\eta$  into the equation,  $\lambda$ , the computed electron free path, varied with velocity as is seen in the table. Now in  $O_2$  at 760 mm  $L = 9.95 \times 10^{-6}$ , whence classically  $\lambda$  at 1 mm should be  $4\sqrt{2} \times 9.95 \times 10^{-6} \times 760 = 4.27 \times 10^{-2}$  cm. Thus his values approximately agreed with classical theory in order of magnitude but varied with  $\eta$ . The surprising fact, however, was the variation of  $\lambda$  with  $\eta$ . It was not until 1921 when Ramsauer by direct measurement of electron scattering found a real variation of  $\lambda$  with velocity that Townsend realized the significance of these results and his pupils began to insist

on his priority. The values of Townsend agree with Ramsauer's in general magnitude and trend of the velocity-free-path curves. Some curves as given by the later work of Brose and Sayman<sup>33</sup> are shown in Fig. 74. The agreement is not and cannot be exact since Ramsauer and others use electrons of a nearly unique and clearly defined velocity or energy while  $\sqrt{\eta \bar{e}_1}$  is some sort of an *average* velocity representing electrons of all velocities in a distribution. For *low* values of  $X/p$ , Townsend can get values of  $\lambda$  in this fashion which are not open to study by Ramsauer's method. Townsend, with his method, however, cannot go much below an  $X/p$  of 0.5 where the energy is of the order of 0.2 volt. The measurements of  $v$  and  $\eta$ , furthermore, suffer from this circumstance that they are not made in the same gas samples and that the gases except in the later work of Brose<sup>8</sup> were not at all pure since adequate purity has been attainable only in very recent years. Since the effects of traces of impurity materially alter the elasticity of impact and  $\lambda$  it is clear particularly in inert gases that these early determinations must be quite unsatisfactory. However, they yield the only available data on  $\eta$  to date. For, although the values of  $v$  of Bradbury and Nielsen,<sup>2,3,4</sup> are unquestionably more accurate than the values of  $v$  of Townsend's group, their work does not give  $\eta$ . It is urgent that better evaluations of  $\eta$  be made under modern conditions of purity. In a measure this has been accomplished by Brose and Sayman,<sup>33</sup> and an excellent summary of the work of the Townsend school as of 1930 is given in this paper.

In 1921 Loeb<sup>11</sup> discovered that the value of  $k_e$  for electrons in  $N_2$  at N.T.P. was far greater than the value 200 cm/sec per volt/cm ascribed to it by Franck.<sup>12</sup> Loeb then set to work to measure the electron mobility  $k_e$  at pressures from 760 to about 50 mm and values of  $X$  of the order of 10 volts/cm upward. He followed the Rutherford a-c method on photoelectrons (see pages 7 and 10), using high-frequency oscillations from the newly developed three-electrode vacuum-tube oscillators.<sup>13,14,15,16</sup> At that time oscillator tubes could not even be bought on the market but were loaned by the Western Electric Company. Now the velocity  $v$ , or better the mobility  $k_e$ , is not constant with field strength. Hence the use of a sine-wave oscillation was not justified without correction. Loeb<sup>16</sup> used the sine-wave oscillation to get the general shape of the curve of variation of  $k_e$  with  $X$ . He then used this approximate form of the equation for the variation to introduce it into the integrand, giving the mobility with an alternating current of sine-wave form. The introduction of the

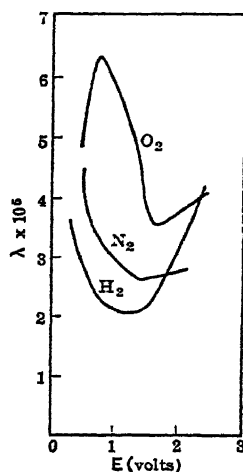


FIG. 74.

form of variation observed into the integrand did not materially change the form of the variation of  $k_e$  with  $X/p$ , but it indicated corrections to be applied to constant terms in the resulting observed  $k_e - X/p$  curves in order to obtain the true values of  $k_e$ . The values of  $k_e$  as a  $f(X/p)$  were determined with considerable care in *carefully purified*  $H_2$ ,  $N_2$ , and He in *metal chambers free from all greases and organic vapors*. The gas He was studied in an all-glass vessel with He circulating over charcoal cooled in liquid air. Outgassing was not possible until ten years later. The results have since been checked by Bradbury at the higher end of the  $X/p$  range and are fairly good. At low  $X/p$  they are the only values available today. H. B. Wahlin<sup>17, 18</sup> in 1923 carried the results in  $N_2$  gas to still lower values of  $X/p$  and discovered a peculiar shape to his curve. This shape near the axis of  $X/p$  was just of the form predicted by the theory of K. T. Compton,<sup>19</sup> which was then being derived.

### 3. FURTHER THEORETICAL DEVELOPMENTS

On the discovery that even high pressures gave values of  $k_e$  for electrons that varied with  $X/p$ , Loeb<sup>13</sup> studied the expression of Townsend  $k_e = 0.75 (e/m) (\lambda/\sqrt{\eta \bar{c}_1})$ , and attempted to derive an expression for  $\eta$ . An evaluation of the energy of an electron in a field in a gas had previously been deduced by Pidduck<sup>20</sup> and was later deduced by Compton.<sup>22</sup> Pidduck's<sup>20</sup> expression was formulated on an analysis of the distribution of energy among electrons as calculated by Lorentz in the electron theory of metals. Although quite advanced for its time and proceeding in a proper direction it ran into difficulties which were not recognized until 1936. It was in agreement with the later expression of Compton.<sup>22</sup> Loeb used Compton's equation in an attempt to evaluate  $\eta$ . His expression for  $\eta$  was not rigorously deduced. It indicated, however, the general form of the variation of  $k_e$  with  $X/p$  and helped to guide Loeb in developing the corrections for the sinusoidally observed value of  $k_e$  using the a-c method. It also served to indicate the role played by the inelasticity of electron impact and the variations of the mean free paths with velocity that were being published at that time. It marked the first attempt of a direct theoretical evaluation of  $\eta$  for inclusion in the mobility equation and prompted Compton again to study the question. As Compton<sup>19</sup> subsequently pointed out, the method of averaging the thermal velocity with that gained in the field to give  $\eta$  as carried out by Loeb was not quite justified. Thus Compton<sup>19</sup> in 1923 developed the theory in a more accurate form.

Compton assumed that the electron mobility was given by  $k_e = 0.75(e/m) (\lambda/\bar{c}_1)$ , where  $\bar{c}_1$  is the average value of the electron velocity, for the present undefined. Now  $\bar{c}_1/\lambda$  is the average number of electron collisions per second with molecules, and  $\lambda/\bar{c}_1$  is the time between

impacts. The average advances of an electron in the field direction between impacts is then  $s = k_e X \lambda / \bar{e}_1 = 0.75 \lambda^2 e X / m \bar{e}_1^2$ . It will now be convenient to express  $\bar{e}_1$  in terms of the equivalent energy in electron volts.\* Thus the electronic charge  $e$  multiplied by the equivalent energy in volts  $u$ ,  $eu = \frac{1}{2} m C_1^2$ , and  $u = 1.18 m \bar{e}_1^2 / 2e$ . Whence  $s = 0.441 \lambda^2 X / u$  is the average advance in the field direction. Now Cravath<sup>21</sup> and Compton have shown that the average energy lost by an electron of mass  $m$ , in an elastic impact with a spherical molecule of mass  $M$ , is a fraction  $f$  of its energy given by  $f = (8/3) [Mm/(m + M)^2] [1 - (\Omega/u)]$ , as long as the energy of the electron is low enough to give no excitation. See Loeb, *Atomic Structure*, page 273. Here  $\Omega e$  is the average energy of the gas molecule expressed in terms of electron volts, i.e.,  $\frac{1}{2} m C_1^2 = e \Omega = (\frac{3}{2}) kT$ . At  $X/p \gg 0.1$  or more,  $\Omega \ll u$ , and the term can be neglected. For low values of  $X/p$  it must be retained. Again  $mM/(m + M)^2$  is essentially  $m/M$ , so that for most purposes  $f = 2.66 m/M$ . We can then write that the change  $edu$  of the energy  $eu$  of an electron in a field of strength  $X$  in advancing a distance  $x$  is given by  $edu = eXdx - feu dx/s$ , for the electron gains  $eXdx$  in  $dx$  cm in the field and loses in each of the  $dx/s$  impacts a fraction  $f$ , or  $feu dx/s$  equivalent volts. Inserting the values for  $f$  and  $s$  we get

$$\frac{du}{dx} = X - 6.02 \frac{m}{M} u \frac{u - \Omega}{\lambda^2 X} \cdot \dagger$$

This equation is of some importance, for it tells us that the electron gains in energy from the initial value of  $\Omega e$  until at some point in the gas  $du/dx = 0$ , when  $X = 6.02 mu_T (u_T - \Omega) / \lambda^2 M X$ . At this point  $u$  has a value  $u_T$ , or the terminal energy, and on the average the electron neither gains nor loses energy. Hence electrons pick up energy at first rapidly then more and more slowly until the rate of loss in impact equals the rate of gain and the electron has its terminal energy  $\frac{1}{2} m C_1^2 = eu_T$ , and hence a terminal velocity  $C_1$ . It is seen that this value  $u_T$  is given by

$$u_T = \frac{1}{2} \Omega + \sqrt{\frac{\Omega^2}{4} + \frac{\lambda^2 M X^2}{6.02 m}}$$

It depends on  $X$ , on  $\lambda$ , and on  $M/m$ , increasing as these increase.

\* What is meant by equivalent volts in reference to electron energy is merely the potential difference in volts through which an electron would have to be freely accelerated in vacuum to acquire the energy  $\frac{1}{2} m C_1^2$ . Since the potential difference  $u$  multiplied by the charge  $e$  of an electron,  $eu = \frac{1}{2} m C_1^2$ ,  $u$  is the electron energy in equivalent volts. See also Loeb, *Atomic Structure*, pages 14 and 160.

† Note that here again we differ from Compton's earlier and later<sup>22</sup> values. His earlier values set  $f = 2 m/M$  instead of  $2.66 m/M$ . Since in the present case Cravath's<sup>21</sup> value for  $f$  is used while it appears not to be used by Compton. The later values of Compton are deduced using the constant 0.921 instead of 0.815 in the mobility equation. It is believed that Langevin's rigorous deduction of the mobility equation is more accurate in its averaging than Compton's recent deduction from a composite of diffusion and free path equations.

This assumes that the energy loss  $f$  is purely elastic. If  $X$ ,  $\lambda$ , and  $M$  are such that  $u_T \geq E_s$ ,  $E_v$ , or  $E_i$  for the gas present,\* the rate of gain will no longer hold. For impacts at  $E_s$ ,  $E_v$ , and  $E_i$  lead to a loss of all the energy, or a large fraction, in one impact out of several, and the average  $u_T$  will be lowered. See Loeb, *Atomic Structure*, Chapter XIV. There is also the assumption that  $\lambda$  is independent of  $u$ . Now actually, as Ramsauer showed (page 648), this is not the case, and the equation is distinctly more involved. Finally the deduction of the expression for  $s$  in the use of  $k_s = 0.75(e/m)(\lambda/\bar{e}_1)$  involves the assumption of the Maxwellian distribution of velocities. This holds for molecules and is also supposed to hold for electrons with the average energy  $\bar{e}_1$ . Actually this is not correct, and the wider the variation of  $\lambda$  with  $u$  the more does the distribution deviate from the Maxwellian. Recognizing that the assumptions are not exact, one nevertheless can assume the equation for  $u_T$  to be exact in order of magnitude and thus to see where it leads.

Before doing this it must be recognized that the integration of the expression

$$du = Xdx - 6.02 \frac{m}{M} \frac{u(u - \Omega)}{\lambda^2 X} dx$$

will enable us to determine the value of the distance  $x$  which an electron requires to acquire a given fraction, e.g., 0.9, 0.99, etc., of its terminal velocity. Call  $6.02(m/M)(1/\lambda^2) = a^2$ . Then integration from  $u = 0$  at  $x = 0$  to  $u = u$  at  $x = x$  gives

$$u = \frac{1}{2}\Omega + X \sqrt{\frac{1}{a^2} + \frac{\Omega^2}{4X}} \frac{e^{2a^2 \sqrt{\frac{1}{a^2} + \frac{\Omega^2}{4X}}} - 1}{e^{2a^2 \sqrt{\frac{1}{a^2} + \frac{\Omega^2}{4X}}} + 1}.$$

If  $X = 0$ ,  $u = \Omega$ . If  $X$  is very large, so that  $\Omega$  may be neglected,

$$u = \frac{X}{a} \frac{e^{2ax} - 1}{e^{2ax} + 1}.$$

$$\text{When } x \rightarrow \infty, u \rightarrow u_T = \frac{X}{a}; \quad u_T = \sqrt{\frac{\lambda^2 M X^2}{6.02 m}} = \frac{\lambda X}{2.45} \sqrt{\frac{M}{m}}.$$

The average number of collisions in going  $x$  cm from the cathode is given by

$$\bar{n} = \int_0^x \frac{dx}{s} = \int_0^x \frac{u}{0.441\lambda^2 X} dx.$$

\* Note that in what follows  $E_s$  represents the excitation potential or energy,  $E_v$  that for excitation of vibrations and  $E_i$  the ionization potential. These are the energies in electron volts required to excite or ionize the atom. For details see, for example, Loeb's *Atomic Structure*, page 254 and Chapter XIV.

Inserting the approximate value of  $u$  when  $u \gg \Omega$  above, and integrating, one finds  $\bar{n} = (M/4m) [\log_e (2 + e^{2ax} + e^{-2ax}) - \log_e 4] = (M/2m) \log_e \cosh ax$ . The value of  $\bar{n} = 0$  as  $x = 0$ , and if  $x$  is large  $\bar{n}$  approaches  $x/1/s_T$ . Here  $s_T = 0.441 \lambda^2 X/u_T$ , and the average number of impacts made per centimeter advance is given by  $1/s_T = (0.925/\lambda) \sqrt{M/m}$ . If we call  $u/u_T = \phi$  the fraction of the terminal energy gained, then from the values of  $u$  and  $u_T$ , neglecting  $\Omega$ , one can evaluate the distance  $x = d$  required to achieve the fraction  $\phi$  of their terminal energy. This gives

$$d = \left( \frac{1}{2a} \right) \log \frac{1 + \phi}{1 - \phi},$$

and the average number of collisions made in gaining  $\phi$  is

$$\bar{n}_\phi = \left( \frac{M}{4m} \right) \log \frac{1}{1 - \phi^2}.$$

It is seen that both  $d$  and  $\bar{n}_\phi$  depend critically on the value of  $f$  and  $\lambda$  but not on  $X$ .

In view of these conditions it is clear that calculations of  $d$ , etc., based on these equations are of little better than orienting magnitudes since  $f$  for all but the monoatomic gases is far from the value given and in all cases  $\lambda$  is a function of  $X$  as the Ramsauer free paths show.

From what has gone before it is clear that we can at once evaluate  $C_1$  and hence  $k_e$  from  $u_T$ . If we remember that for low fields and higher pressures  $u_T$  is comparable with  $\Omega$ ,

$$u_T = \frac{\Omega}{2} + \sqrt{\frac{\Omega^2}{4} + \frac{X^2 \lambda^2 M}{6.02 m}}.$$

For fields and pressures where  $u_T \gg \Omega$ ,

$$u_T = \frac{\lambda X}{2.45} \sqrt{\frac{M}{m}}.$$

Since  $\frac{1}{2} m C_1^2 = e u_T$ , while  $e \Omega = (\frac{2}{3}) k T = \alpha T$ , we can write

$$C_1 = \sqrt{\frac{2e u_T}{m}} = \left[ \frac{2e}{m} \left\{ \frac{\Omega}{2} + \sqrt{\frac{\Omega^2}{4} + \frac{X^2 \lambda^2 M}{6.02 m}} \right\} \right]^{1/2},$$

or at high fields

$$C_1 = \left[ \frac{2e \lambda X}{m 2.45} \sqrt{\frac{M}{m}} \right]^{1/2}.$$

The quantity  $C_1$  can also be expressed as

$$C_1 = \frac{1}{\sqrt{m}} \left[ \alpha T + \left( \alpha^2 T^2 + \frac{X^2 \lambda^2 e^2 M}{1.50 m} \right)^{1/2} \right]^{1/2},$$

Where  $\alpha = \frac{2}{3} k$ ,  $k$  being Boltzmann's constant; see page 644.

This equation gives us  $k_e$  as

$$k_e = \frac{0.815e\lambda}{mC_1} = \frac{0.815e\lambda}{\sqrt{m} \left[ \alpha T + \left( \alpha^2 T^2 + \frac{\lambda^2 X^2 e^2}{1.50} \frac{M}{m} \right)^{1/2} \right]^{1/2}}.$$

It is to be noted here that  $\lambda = 1/[\pi(\sigma/2)^2 N]$ , where  $\sigma$  is the molecular diameter.

As will later be seen, it will be desirable not to restrict the value of  $f$  to the classically deduced expression of Cravath.<sup>21</sup> In the case of collisions at energies greater than excitation or ionization energies in all gases, and in molecular gases such as  $H_2$  and  $N_2$  well below  $E$ , or  $E_e$ , it is essential to remove such restrictions. If we desire to do this we must write

$$du = Xdx - fu \frac{dx}{0.441\lambda^2 X/u}.$$

At  $u_T$ ,  $du/dx = 0$ , and we have  $X - fu_T^2/0.441\lambda^2 X = 0$ . Hence

$$u_T = \sqrt{\frac{0.441X^2\lambda^2}{f}} = \frac{0.664X\lambda}{\sqrt{f}},$$

where  $f$  may be a function of  $u_T$  and will depend on  $m$  and  $M$  and  $u$  and  $\Omega$ . In this case observed values of  $f$  as a function of  $M$ ,  $m$ ,  $u$ , and  $\Omega$  must be derived from experiment and inserted in the equation. Accordingly

$$C_1 = \left( \frac{1.328eX\lambda}{m\sqrt{f}} \right)^{1/2}$$

and

$$k_e = \frac{0.815e\lambda}{mC_1} = \frac{0.815e\lambda}{\left( \frac{1.33emX\lambda}{\sqrt{f}} \right)^{1/2}} = 0.705 \sqrt{\frac{e\lambda}{mX}} \sqrt{f}.$$

The equation may be rearranged for application to computation by the following procedure. The quantity  $\lambda$  is given by  $\lambda = \lambda_0(760/p)$  ( $T/273$ ), where  $\lambda_0$  is the free path at 760 mm pressure. Let us divide the expression for  $k_e$  by  $\sqrt{\alpha T}$  and substitute the values of the constants. We then have

$$k_e = \frac{1.825 \times 10^8 \lambda_0 \frac{760}{p} \left( \frac{T}{273} \right)^{1/2}}{\left[ 1 + \left\{ 1 + 5.71 \times 10^{11} M_0 \lambda_0^2 \left( \frac{X}{p} \right)^2 \right\}^{1/2} \right]^{1/2}} \quad (1)$$

in cm/sec per volt/cm, with  $M_0$  the molecular weight of the gas. If

$\lambda$  is expressed as  $\lambda_1$  for 1-mm pressure instead of at 760 mm, we have

$$k_e = \frac{1.825 \times 10^8 \lambda_1 \left(\frac{1}{p}\right) \left(\frac{T}{273}\right)^{3/2}}{\left[1 + \left\{1 + 0.988 \times 10^8 M_0 \lambda_1^2 \left(\frac{X}{p}\right)^2\right\}^{1/2}\right]^{3/2}} \frac{\text{cm}^2}{\text{volt sec}}. \quad (1a)$$

In actually using this equation in computing the theoretical value of  $k_e$  for comparison with his results, Bradbury<sup>2</sup> again modified it so as to introduce needed corrections. He replaced  $\lambda$  by  $\lambda = 1/\pi N \sigma_1^2$  where  $\sigma_1$  is the collision radius  $\sigma_1 = \sigma/2$ , and  $N$  the number of molecules per cubic centimeter. Bradbury at the time used Compton's<sup>22</sup> revised equation with the constant 0.921 in the ion mobility equation instead of 0.815, which probably is the more correct constant. He used  $f = 2 m/M$  in conformity with Compton's<sup>22</sup> practice in order to replace the ratio  $2 m/M$  of Compton's equation by  $f$  so that he could try different values of  $f$  in fitting theory and observation. In doing this Bradbury was somewhat inconsistent. For  $u_T$  was computed using  $f = 2 (m/M) (1 - \Omega/u)$  to get the average energy. However, the error is slight since only a small change in  $f$  is produced by the omission, while  $f$  is known to be much greater than  $2 m/M$  in molecular gases and to vary with  $u$ . The modified experimental values of  $f$  can then be introduced into the equation for  $k_e$  in order to seek agreement. Under these conditions he obtained for  $k_e$  the value

$$k_e = \frac{1.115 \times 10^{-10} \left(\frac{1}{p}\right) \left(\frac{1}{\sigma_1^2}\right) T^{3/2}}{\left[1 + \left\{1 + 1.265 \times 10^{-31} \left(\frac{X}{p}\right)^2 \left(\frac{1}{\sigma_1^4 f}\right)\right\}^{1/2}\right]^{3/2}} \frac{\text{cm}^2}{\text{volt sec}}. \quad (2)$$

In view of what has been said about using the value of 0.815 instead of 0.921, and the constant 6.02 in place of 5.32 in the denominator of the second term under the radical in the expression for  $u_T$ , the equation of Bradbury reads more properly

$$k_e = \frac{1.00 \times 10^{-10} \left(\frac{1}{p}\right) \left(\frac{1}{\sigma_1^2}\right) T^{3/2}}{\left[1 + \left\{1 + 1.15 \times 10^{-31} \left(\frac{X}{p}\right)^2 \left(\frac{1}{\sigma_1^4 f}\right)\right\}^{1/2}\right]^{3/2}} \quad (2a)$$

with  $k_e$  in cm/sec per volt/cm,  $X$  in volts/cm, and  $p$  in millimeters of mercury. This last equation is properly the equation to apply for the computation of  $k_e$  at all low values of  $X/p$ . At high values of  $X/p$  one may properly use

$$k_e = 5.38 \times 10^{-3} \left(\frac{1}{p}\right) \sqrt{\frac{T \sqrt{f}}{\sigma_1^2 X/p}}, \text{ in } \frac{\text{cm}^2}{\text{volt sec}}. \quad (3)$$

\* Nielsen and Bradbury's paper gives an erroneous exponent in the denominator of 32 instead of 31, owing to typographical error.



It should be noted that equations 1 and 1a are applicable only to gases where  $f = 2.66 m/M$ , that is, the atomic gases. In the molecular gases  $f$  is no longer so simply conditioned. In the forms 2a and 3 one can insert the values of  $f$  and of  $\sigma_1$  at any given  $X/p$  as taken from collision studies and Ramsauer cross sections if  $u_T$  is known or can be estimated from the distribution law in order to give us the values of  $\sigma_1$  and  $f$  at the appropriate  $u_T$ .

#### 4. COMPARISON OF THEORY AND EXPERIMENT

While the theory of Compton was in press Wahlin<sup>17</sup> measured  $k_e$  in  $N_2$ , using an improvement of Loeb's technique at very low  $X/p$ . His results indicated that below  $X/p = 0.01$  the curves instead of continuing upward as  $X/p$  decreased underwent an inflection and

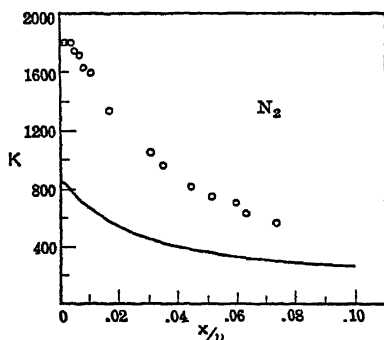


FIG. 75.

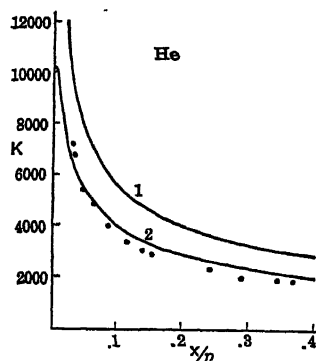


FIG. 76.

intercepted the  $y$  axis at a definite value. This behavior was not expected on Loeb's<sup>13</sup> modified theory nor from his data at higher  $X/p$ . It was, however, in striking agreement with the form of the curve predicted by Compton's<sup>19</sup> new theory. The agreement between the curve computed for  $N_2$  using  $f = m/M$  and  $\sigma_1$  as one-half the kinetic-theory collision diameter for  $N_2$  molecules is shown in Fig. 75. Here  $K_e = k_e (p/760) (273/T)$  is plotted against  $X/p$ . Now Loeb's<sup>13</sup> results had shown that the theory for  $N_2$  required higher values for  $L$  and smaller values for  $\sigma_1$ , than given by kinetic theory in keeping with Ramsauer's work. However, Wahlin's<sup>17</sup> results showed that not only did agreement between theory and experiment require the use of Ramsauer cross sections but in addition the value of  $f$  in  $N_2$  had to be considerably larger than that given by  $f = 2.66 m/M$ . At that time no definite evidence was at hand to justify the failure of the law for energy loss in electron impact,  $f = 2.66 m/M$ , which seemed so firmly established by quantum principles and the Franck and Hertz experiments (see Loeb, *Atomic Structure*, page 249). It is true that Franck and Hertz had observed greater losses in  $He$  and  $N_2$

than in the inert gases, but the data were not adequate and the gases were assumed impure. Later, Baerwald<sup>23</sup> indicated the inelasticity of impacts in  $H_2$ . It was not until the work of Harries<sup>24</sup> and of Ramien,<sup>25</sup> however, that this fact was clearly established. Its explanation on the basis of the Franck Condon principle was not at hand until 1928 (see Loeb, *Atomic Structure*, page 316).

Similar differences were observed in other gases. Loeb's results in He, where  $f = 2.66 m/M$  from an  $X/p$  of 0.05 to 0.4, could be fitted fairly well using  $f = 2.66 m/M$ , by adjusting the mean free path as would be expected. In  $O_2$  the observed mobilities were very much greater than the theoretical values, indicating a relatively high energy loss in impacts. These results are compared with theory in the curves of Figs. 76, 77A, and 77B. Curve 2 agreeing with experimental points in

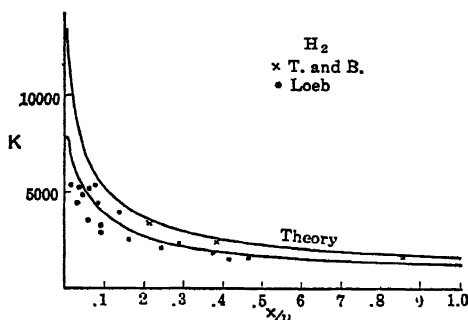


FIG. 77A.

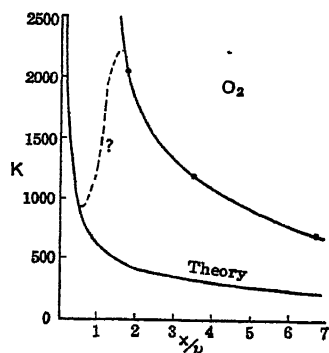


FIG. 77B.

Fig. 76 for He uses 0.5 the kinetic theory free path while curve 1 uses a free path of the kinetic-theory value. In  $O_2$  no fit is possible and  $f$  appears to be very much greater than  $2.66 m/M$ . No more intensive work was done on electron velocities, especially of such character as to encourage the investigators to put them to the test of the Compton theory, from about 1925 until 1936. At this time Bradbury<sup>2,3,4</sup> and Nielsen undertook to measure electron velocities by a direct method using electrical shutters of the Loeb electron filter type.

The method has been described in detail on page 23. With it Bradbury and Nielsen<sup>2,4</sup> and later Nielsen<sup>3</sup> were able to evaluate the drift velocity  $k_e X = v$  for a number of different gases to a fairly high degree of precision. In  $H_2$ ,  $N_2$ ,  $O_2$ , and air, results extended from  $X/p = 0.05$  to  $X/p = 20$ , while in He, Ne, and A they extended from 0.02 to between 2 and 5, depending on the breakdown value for the gas. The results obtained by Bradbury and Nielsen for  $H_2$ ,  $N_2$ ,  $O_2$ , air, He, Ne, and A are shown in Figs. 78 to 84, in which  $v = k_e X$  multiplied by  $10^{-5}$  is plotted against  $X/p$ ,  $X$  in volts per centimeter,  $p$  in millimeters. In  $H_2$  the value of  $v$  as computed from Bradbury's

version of Compton's equation using kinetic-theory constants is shown as the dashed curve *A*, while the full curve of Fig. 85 gives the observed results. When the Ramsauer values for  $\sigma_1$  are inserted in place of the constant value of  $\sigma_1$  from kinetic theory one gets the dot-dashed

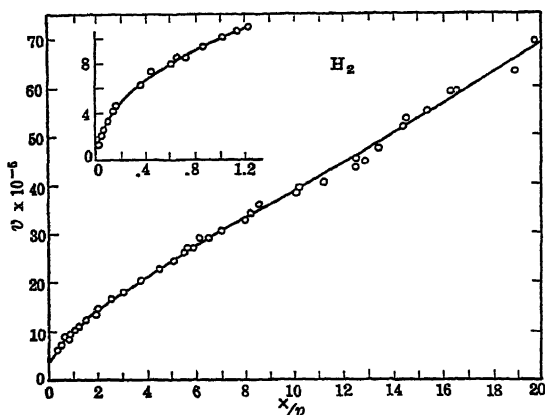


FIG. 78.

curve *B*. To get the Ramsauer values for  $\sigma_1$  one takes the observed values of  $\sigma_1$  given by Normand<sup>26</sup> for different values of the electron energies. To convert the values of  $\sigma_1$  to correspond to the values of  $X/p$  for insertion into equation 2*b* one must take the *Townsend*<sup>5,6,7,8,9,10</sup>

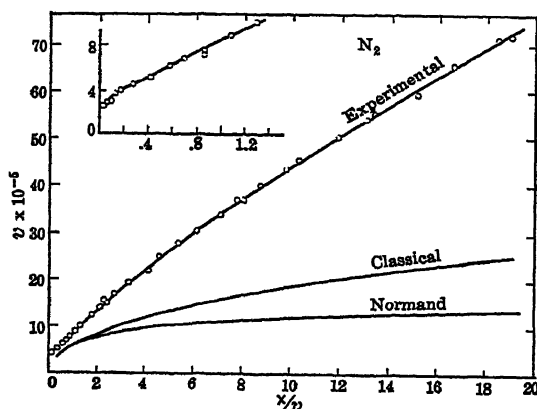


FIG. 79.

*data* on the value of  $\eta$  for given values of  $X/p$  observed in the gas and convert  $\frac{2}{3}\eta kT$  to volts of average electron energy. With this correction, curve *B* of Fig. 85 resembles the observed curve in form but departs badly in magnitude. Hence we must conclude that  $f$  is not

2.66  $m/M$ . Ramien has data on  $f$  in  $H_2$ , and finds that *on the average* a 4.15-volt electron loses 0.02 volt of energy per impact. Actually it loses about 1 or 2 volts, to the vibrational excitation of an  $H_2$  molecule after some 50 or perhaps 100 impacts. However, in the many impacts, we can consider its average energy loss as 0.02 volt. This makes  $f$  at  $X/p = 20$  in  $H_2$  twelve times the quantity  $f = 2.66 m/M$  given by theory. If in addition this value of  $f$  decreases linearly as  $X/p$ , and hence energy decreases, one can compute the double dot-dashed curve  $C$  by introducing this variation into the equation. On making this correction the observed curve is seen to be in good agreement with theory. Thus it is clear that fairly good agreement can be obtained by using even the approximate values

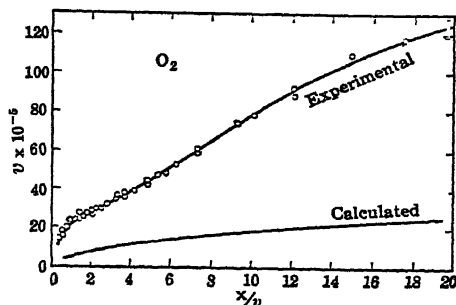


FIG. 80.

of  $f$  and  $\sigma_1$ . A more accurate evaluation of  $k_0$  requires detailed allowance for variation of the cross section, scattering angle, and inelasticity of electron impact, for which adequate data are not at hand. In  $N_2$  the curves for the kinetic-theory value of  $\sigma$  and the Normand values are shown relative to experiment. No data on  $f$  which could be of use in this matter are available. However, it is

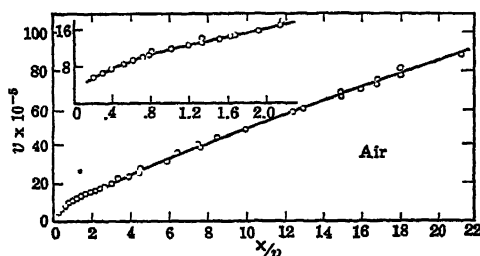


FIG. 81.

clear that  $f > 2.66 m/M$  in considerable measure and probably varies with  $X/p$ .

In the inert gases He, Ne, and A, the inelasticity of impact, below values of  $X/p$  at which excitation or ionization occur, is ruled out. Hence one can use  $f = 2.66 m/M$ , and insertion of the Normand values for  $\sigma_1$

in place of the constant kinetic-theory value should give good agreement. The agreement is, in fact, seen to be fairly good *in all cases at low values of  $X/p$*  and up to certain critical values. In He this holds up to  $X/p = 2.25$ , in Ne to about 0.40, and in A to 1.75. Above these values of  $X/p$ , *inelastic impacts should appear* due to excitation and at higher energy values even to ionization. The rise of the observed curves above the theoretically computed ones bears out this conjecture. It is next essential that this be confirmed by

determining whether electrons at  $X/p$  of 2.25 in He, 0.4 in Ne, and 1.75 in A correspond to electrons having energies at which a few electrons (some per cent in the distribution), can experience exciting impacts, so that the average  $f$  ceases to be given by  $f = 2.66 m/M$  and becomes materially greater. With larger  $f$  it is seen from theory that  $k_e$  and  $v$  increase. As increasing  $X/p$  increases the energy  $u_T$  above

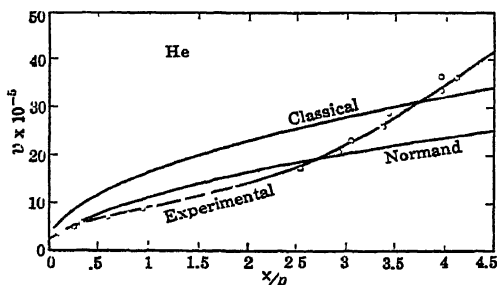


FIG. 82.

the critical values, more and more electrons in the distribution are able to excite, and hence the average value of  $k_e$  increases as the average value of  $f$  increases.

Now again the need of accurate values of what Townsend called  $\eta$  determined as a function of  $X/p$  are very much apparent. For from  $(\frac{2}{3})kT\eta = eu_T$  we get the average terminal energy  $eu_T$  of the electrons as a function of  $X/p$ . We have, of course, the data of the Townsend<sup>5,6,7,8,9,10</sup> school which were largely obtained before modern techniques of purity were available. These can therefore give but orienting magnitudes. Furthermore, we have no idea exactly what sort of an average  $(\frac{2}{3})kT\eta$  gives over the distribution of velocities, as the *exact form of the distribution law is not known*. Since  $\eta$  is derived from an effective pressure it would be natural to assume that the energy represents that corresponding to the root mean square average of the velocities in a Maxwellian velocity distribution. Then  $\eta kT$  is the most probable energy. If the distribution is not Maxwellian the position of such an average relative to the most probable velocity or peak in the distribution curve will, of course, vary with the form of the distribution law and will not be in the ratio  $\sqrt{3}/2$  to 1. The distribution law as we shall see is not the same in the three gases considered. Hence again difficulties will be encountered in the interpretation of the results.

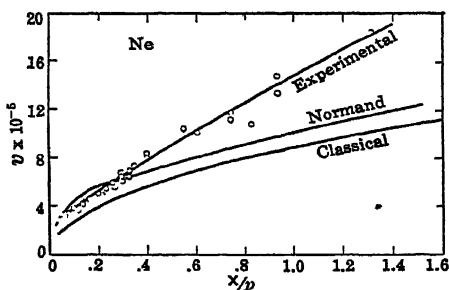


FIG. 83.

The difficulties encountered by Nielsen in interpreting the results obtained in these three gases from the bend in the curves can be seen in Table XII. In this table are the values of the observed energies

at  $X/p = 2.25, 0.4$ , and  $1.75$  in He, Ne, and A, i. e., the corresponding energies equivalent to the root mean square velocity as given by Townsend's  $\eta$ . The values of the energies corresponding to the most probable velocities on a Maxwellian distribution are also given. These

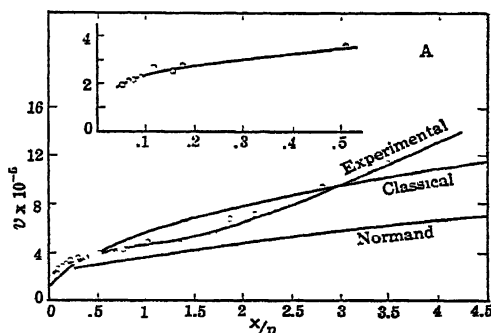


FIG. 84.

quantities can be visualized in the energy distribution diagram for a Maxwellian energy distribution shown in Fig. 293A, whose equation is

$$N_{dE} = \frac{2N_0}{\pi^{1/2}} \sqrt{\frac{E}{kT}} e^{-\frac{E}{kT}} \frac{dE}{kT}.$$

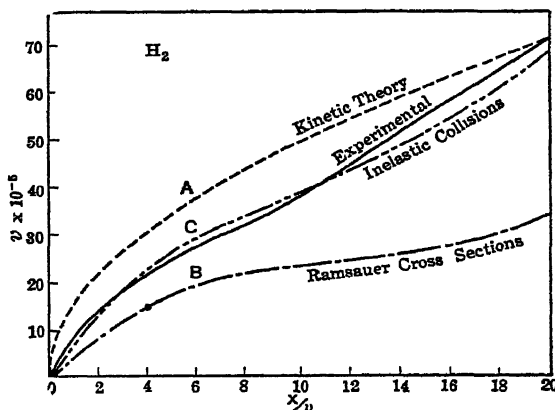


FIG. 85.

Finally there is given the value of the energy which is exceeded by 0.05 of the electrons. The number of the electrons under the distribution curve to the right of this value comprise only some 5 per cent of the total electrons. If, as a result of the inelastic impacts, 5 per cent of

the electrons suffer a material loss in energy, then the average should be affected and the velocity curve might be expected to show a break.

TABLE XII

| Gas | Deviation Observed at $X/p$ | Electron Energy in Volts Corresponding to r m s Velocity | Electron Energy in Volts Corresponding to Most Probable Velocity | Energy Which is Exceeded by Fastest 5% of Electrons | First Excitation Potential |
|-----|-----------------------------|--|--|---|----------------------------|
| He  | 2.25                        | 4.25   | 2.83   | 16-17   | 19.77                      |
| Ne  | 0.4                         | 4.3  | 2.86   | 16-17   | 16.58                      |
| A   | 1.75                        | 11.1   | 2.33   | 41  | 11.57                      |

On the basis of the Maxwellian law one thus sees that we should hardly be getting a departure of the curve from that for elastic impacts in He at  $X/p = 2.25$ . In Ne at  $X/p = 0.4$  the upward trend might just be beginning, and in A at  $X/p = 1.75$  the greater proportion of the electrons should be making inelastic impacts and the departure from the curves *should have occurred at a much lower  $X/p$* . Hence the assumption of the Maxwell distribution law leads to incorrect results. A similar result is obtained when the more legitimate distribution law of Druyvesteyn,<sup>27</sup> later rediscovered by Morse, Allis, and Lamar,<sup>28</sup> is used. This law determines the distribution for electrons at equilibrium in an electrical field *when  $\sigma$  is independent of  $u$  or  $X/p$  and  $f = 2.66 m/M$* . The law is not seriously different from Maxwell's. This difficulty with Druyvesteyn's law was pointed out by Nielsen and Bradbury.<sup>3,3,4</sup> The effect of the Ramsauer cross sections which are functions of the electron energy on the Druyvesteyn distribution cannot easily be evaluated accurately. Qualitatively Bradbury was able to show that if the value of the free path decreases as the energy increases, as is the case with A in this energy range, *the distribution curve has its most probable energy (as well as the average energy) shifted to higher values*, but the curve drops off very sharply to few electrons at energies much above the most probable. In such a distribution the most probable energy will be near the maximum energy in the distribution so that the rms energy can be well below it. Hence, while appreciable electrons would have an energy of 40 volts on the basis of the laws mentioned using constant free paths, in A where  $\lambda$  decreases with  $E$  we must have relatively few electrons with energy more than 12 volts, otherwise the curve would have shown a break at an  $X/p$  of much less than 1.75. In He *the free paths increase with increase in energy* in the region studied. This has the effect of emphasizing the energy of the few faster electrons. Thus the higher-energy portion of the Druyvesteyn<sup>27</sup> law is prolonged beyond its normal position

relative to the most probable and average energies. Thus more electrons of very high energy relative to the average should appear in He, and hence even at an  $X/p$  of 2.25 we can expect an increase of the mobility caused by an average increase in  $f$ . In Ne, as  $\lambda$  is nearly constant in the range of observation, the law is approximately the Druyvesteyn law and we get a rough agreement with the onset of increased mobilities at an  $X/p$  of 0.4.

Nielsen<sup>3</sup> tested this question in another way. He took some point beyond the onset of the increased mobility in each of the gases, e.g., at an  $X/p$  of 1.2 in Ne. From these data the mobility equation gives the value of  $\epsilon f$ , or the factor  $\epsilon$ , by which  $f$  must be increased to give the observed value of  $v = k_e X$ , at the value of the energy  $E$  (e.g., 8.75 volts in Ne) which the Townsend data give as corresponding to a given  $X/p$ . Now since  $f = 2 m/M$ , as used by Nielsen, is known, we can compute the average energy loss per electron per impact as  $(\epsilon - 1)f$  caused by excitation. It must be remembered that in so doing, however, the energy is not lost in the impacts between 0 and 16.58 volts, but an electron in the distribution of 16.58 volts or over loses 16.58 volts at one impact. If now  $K$  is the fraction of electrons having an energy of more than 16.58 volts in the distribution and if  $\omega$  is the probability of an excitation at impact, then  $\omega K = (\epsilon - 1)f$ . Since from the Druyvesteyn law one can estimate  $K$  one can set up Table XIII for evaluating  $\omega$  for the three gases. Values of  $\omega$  can be estimated from observed excitation function curves in these gases.

TABLE XIII

| Gas | $X/p$ | $E$<br>Volts | $\epsilon$<br>from<br>Devia-<br>tion<br>Observed | $E f$<br>Volts           | $(\epsilon - 1)$<br>$E f$<br>Volts | $K$<br>from<br>Druy-<br>vesteyn | $\omega$ calc. | Magnitude<br>of $\omega$<br>Relative to<br>Values<br>Observed |
|-----|-------|--------------|--|--------------------------|------------------------------------|---------------------------------|----------------|---|
| He  | 4.5   | 6.1          | 7.35   | 1.66<br>$\times 10^{-3}$ | 1.05<br>$\times 10^{-2}$           | 0.003                           | 0.09<br>0.58   | Too high  |
| Ne  | 1.2   | 8.75         | 5.7  | 4.8<br>$\times 10^{-4}$  | 22.6<br>$\times 10^{-4}$           | 0.11                            | 0.002          | About<br>right  |
| A   | 4     | 11.5         | 16   | 3.13<br>$\times 10^{-4}$ | 4.7<br>$\times 10^{-3}$            | 0.5                             | 0.001          | Much too<br>low   |

It is again clear from this table that, for He,  $K$  taken from the Druyvesteyn<sup>27,28,3</sup> distribution is too small and hence makes  $\omega$  appear too large. For A it is clear that with  $K$  taken as 0.5 all the higher states of A above 11.57 volts must be excited. Hence the value of  $\omega = 1 \times 10^{-3}$  is far too small for the process. Thus in A we can



expect that  $K$  must be much less, perhaps of the order of 0.05, making  $\omega = 10^{-2}$ . These results are in agreement with the predictions of Bradbury<sup>3</sup> as to the effect of a variable  $\lambda$  on the form of the distribution laws.

More recently Allen<sup>30</sup> in collaboration with Allis has made a study of the effect of inelastic impacts due to excitation on the form of the distribution law, as well as a study of the effect of variable cross section. An even more accurate study has been made by Smit<sup>29</sup> for the case of the distribution law in He at values of  $X/p$  ranging from 3 to 10. Smit's curves will be shown elsewhere. The curves for the energy distribution for He, Ne, and A taken from Allen's paper are shown in

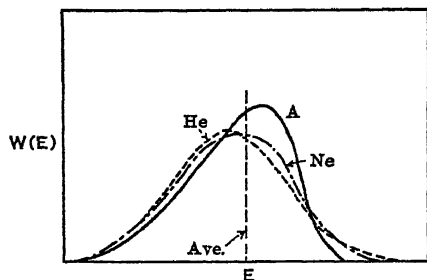


FIG. 86.

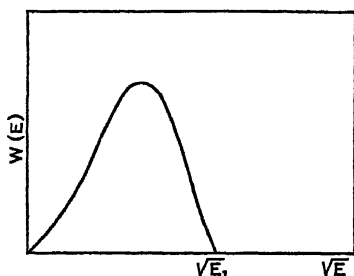


FIG. 87.

Fig. 86. Their abscissas are chosen so as to give the same mean energy. These curves are given for *average energies* well below the excitation energy and would be applicable to the studies of these inert gases at values of  $X/p$  up to energies where appreciable excitation begins. At values of  $X/p$  such that inelastic impacts become frequent the curve is modified by these impacts and is shown, in a very approximate form only, in Fig. 87. In this curve Allen arbitrarily cuts off the function at an energy  $E_1$ , lying between the first excitation potential and the ionization potential. This is probably not justified, as can be seen from Smit's curve in He at  $X/p = 10$ , page 228.

The application of the results of Allen's theory with  $E_1$  arbitrarily chosen to agree with mobility measurements is shown in the curves of Figs. 88 to 90 for He, Ne, and A. The full curves are the theoretical curves, the circles are the results from the Townsend<sup>5,6,7,8,9,10</sup> method, and the crosses are Nielsen's values. Using the average energy of the electrons as given by  $\eta$  from measurements of the Townsend group, Allen was enabled from the theory, which also gives the electron energy in terms of  $E_1$ , to make a more successful *guess* as to the value of  $E_1$ . For He, if  $E_1$  is put equal to 19.7, the first excitation potential, it gives a curve of electron energies agreeing exactly with the data of Townsend and Bailey.<sup>11</sup> The drift velocity curves for  $v = k_e X$  as a function of  $X/p$  in general agree quite well with the Townsend and the

Nielsen data in He. The calculated curves for  $k_e X = v$  surprisingly appeared the *same* irrespective of whether  $E_1$  was taken as 19.7 volts or at infinity. This strange circumstance is caused by fortuitous compensating factors.  $k_e$  increases with decreasing *average* energy of the electrons. The energy depends on  $Xe\lambda$ , which determines the advance in the field direction but which is diminished owing to the decrease in  $\lambda$

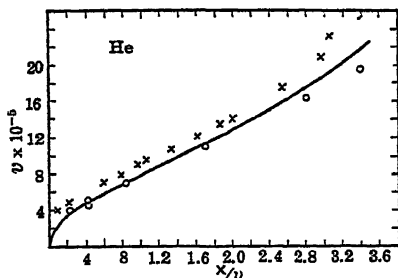


FIG. 88.

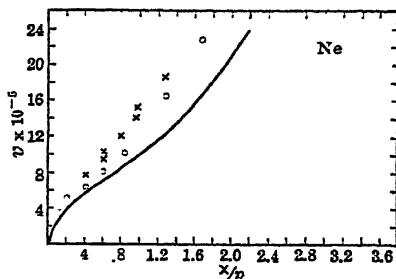


FIG. 89.

with decreasing average  $E$  in about the same measure. In Ne the electron energies gave a good fit if  $E_1$  was chosen as 21.5 volts, the ionization potential, while  $k_e$  required a lower value. Hence the curve for  $k_e$  in Ne, computed in this case with  $E_1 = 21.5$ , using a constant cross section and the Druyvesteyn distribution, which Ne exhibits below 16.75 volts energy, departs from the observed points. In A the average energy is nearly double that computed in a Maxwellian distribution. In this case agreement for *electron energies* is obtained at high  $X/p$  by choosing  $E_1 = 15.6$ , the ionization potential. For the evaluation of  $k_e X = v$ ,  $E_1$  must be chosen as 11.57 the first critical or excitation potential. For A under these conditions fair agreement is found with Nielsen's values. Townsend's velocities do not agree with Nielsen's above  $X/p = 0.6$ . In this case Nielsen's data are to be preferred on the basis of the greater gas purities which are now possible.

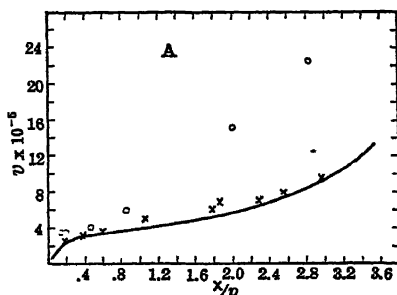


FIG. 90.

In general, then, it can be seen that a mobility equation of the Compton type, or the more esoteric electron drift velocity equations to be deduced simultaneously with the energy distribution laws, are capable of giving good values of the electron drift velocities *provided that one takes into account variable Ramsauer collision cross sections, and energy losses due to inelasticities of electron impact produced by molecular*

*excitation or electronic excitation and ionization.* In order to evaluate and correct for these properly it is necessary to know the distribution of electron energies in a given gas at the existing pressure and at the existing field strength. This factor again depends on the electron free paths and the elasticity of impact. Thus some study of the electron energy distribution in gases must be made in order to facilitate such analysis as is needed. Both mathematical computation and experimental study of this question present formidable difficulties. The methods for the mathematical evaluation of the energy distribution functions have recently been clearly formulated. The solution of the complicated differential equations, however, presents difficulties which can be overcome only by the most tedious and elaborate calculations. Since up to the present, the experimental determinations giving the energy distribution with any certainty have completely failed, the theoretical calculation is at present our only solution. The study of both the theoretical and experimental phases of this problem, the latter by means of probes, will constitute the body of Chapter V.

As regards the accuracy of the theoretical evaluation of electron drift velocities or mobilities, one can say that at present the theory is such that, given the energy distribution function, we can make as accurate an evaluation as time, our mathematical skill, the accuracy of supplementary data such as the Ramsauer curves, and our patience will permit. With this statement one may leave drift velocities and turn to the study of energy distribution among electrons in an electrical field.

## 5. REFERENCES FOR CHAPTER IV

1. TOWNSEND and TIZARD, *Proc. Roy. Soc.*, A 87, 357, 1912; A 88, 336, 1913; also J. S. TOWNSEND, *Electricity in Gases*, Oxford, 1914, p. 122 ff.
2. NIELSEN and BRADBURY, *Phys. Rev.*, 49, 338, 1936.
3. R. A. NIELSEN, *Phys. Rev.*, 50, 950, 1936.
4. NIELSEN and BRADBURY, *Phys. Rev.*, 51, 69, 1937.
5. TOWNSEND and BAILEY, *Phil. Mag.*, 42, 873, 1921; 43, 594, 1922.
6. TOWNSEND and BAILEY, *Phil. Mag.*, 44, 1033, 1922.
7. TOWNSEND and BAILEY, *Phil. Mag.*, 46, 657, 1923.
8. H. L. BROSE, *Phil. Mag.*, 1, 536, 1925.
9. SKINKER and WHITE, *Phil. Mag.*, 46, 630, 1923; M. F. SKINKER, *Phil. Mag.*, 44, 924, 1922.
10. MCGEE and JAEGER, *Phil. Mag.*, 6, 1107, 1928.
11. L. B. LOEB, *Proc. Natl. Acad. Sci.*, 7, 307, 1921.
12. J. FRANCK, *Verhandl. deut. physik. Ges.*, 12, 613, 1910.
13. L. B. LOEB, *Phys. Rev.*, 19, 24, 1922.
14. L. B. LOEB, *Phys. Rev.*, 20, 397, 1922.
15. L. B. LOEB, *Proc. Natl. Acad. Sci.*, 9, 335, 1923.
16. L. B. LOEB, *Phys. Rev.*, 23, 157, 1924.
17. H. B. WAHLIN, *Phys. Rev.*, 23, 169, 1924.
18. H. B. WAHLIN, *Phys. Rev.*, 21, 517, 1923.
19. K. T. COMPTON, *Phys. Rev.*, 22, 333, 432, 1923.
20. F. B. PIDDUCK, *Proc. Roy. Soc.*, A 88, 296, 1913.

21. A. M. CRAVATH, *Phys. Rev.*, **36**, 248, 1930.
22. COMPTON and LANGMUIR, *Rev. Modern Phys.*, **2**, 219, 1930.
23. H. BAERWALD, *Ann. Physik*, **76**, 829, 1925.
24. W. HARRIES, *Z. Physik*, **42**, 26, 1927.
25. H. RAMIEN, *Z. Physik*, **70**, 351, 1931.
26. C. E. NORMAND, *Phys. Rev.*, **35**, 1217, 1930.
27. M. J. DRUYVESTEYN, *Physica*, **10**, 69, 1930.
28. MORSE, ALLIS, and LAMAR, *Phys. Rev.*, **48**, 412, 1935.
29. J. A. SMIT, *Physica*, **3**, 543, 1937.
30. H. W. ALLEN, *Phys. Rev.*, **50**, 707, 1937.
31. L. B. LOEB, *Kinetic Theory of Gases*, 2nd Edition, McGraw-Hill, New York, 1934, p 99.
32. K. T. COMPTON, *Phys. Rev.*, **7**, 489, 501, 509, 1916; **9**, 234, 1918.
33. BROSE and SAYMAN, *Ann. Physik*, **5**, 747, 1930.

## CHAPTER V

### PART A. THE DISTRIBUTION OF ELECTRON ENERGIES IN A GAS IN AN ELECTRICAL FIELD \*

#### 1. INTRODUCTION

Probably the most important single function for the study and analysis of electrical discharges, ionization coefficients, electron mobilities, etc., is the energy distribution law for the electrons in an electrical field as a function of the distance traversed in the field, the field strength and gas pressure, and characteristics of the gas molecules. As is well known, electrons make nearly elastic impacts with gas atoms in atomic gases up to the excitation energy  $E_e$ , or the ionization energy  $E_i$ . (See Loeb, *Atomic Structure*, Chapter XIV.) In molecular gases the excitation energy is expended in excitation of electronic levels at the relatively high values of  $E_e$ . Owing, however, to the Franck-Condon principle, the energy losses in molecular gases set in at energy values  $E_v$ , where  $E_v$  represents the excitation energy of the lowest vibrational level of the molecule. Since for a gas like  $N_2$ ,  $E_i \sim 15.5$  volts,  $E_e \sim 6.14$  volts, and  $E_v > 1.0$  volt, it is seen that even for low electron energies the molecular gases already have inelastic impacts.<sup>1,2</sup> Below  $E_e$  for such gases and  $E_i$  for atomic gases the electrons *lose on the average* in impact a fraction  $f$  of their energy, which is roughly  $2m/M$  and more accurately  $2.66m/M$ , where  $M$  is the mass of the molecules or atoms and  $m$  is the mass of the electron.

Hence, it is clear that in an electrical field an electron gains energy between impacts at the rate of  $XeS$  from the field, where  $S$  is the average advance in the field direction between impacts,  $X$  is the field strength, and  $e$  the electronic charge. It loses in elastic impacts energy at the rate of  $fE$ , where  $f$  is the fraction referred to above and  $E$  is the energy. Above  $E_e$ ,  $E_v$ , or  $E_i$ , the energy lost by the electron is anywhere from  $E$ , its whole energy for  $E_i$ , to  $E - E_v$ ,  $-E_e$ , or  $-E_i$ . In order to simplify calculations, it is usually advisable to assume that the loss is complete and that the electron departs from rest. Actually, this is not correct, and the effect of the neglect of this fact is seen in the relatively diffusely defined boundaries of excitation and ionization regions in gases observed in the dark and luminous portions of discharges and in probe studies. The problem is further complicated by the fact that, when an electron has achieved the energy  $E_v$ ,  $E_e$ , or  $E_i$ ,

\* References for Part A of Chapter V will be found on page 231.

it does not lose it at the first impact, but the loss is accompanied by a certain chance or probability  $P_v$ ,  $P_e$ , or  $P_i$ . These probabilities  $P_e$  and  $P_i$  have been observed experimentally and are roughly given by curves such as the Compton-Van Voorhis curves for  $P_i$  (see Loeb, *Atomic Structure*, page 281). Later studies show that these curves are somewhat complicated integrals of a sum of individual happenings for which the probability is likely a maximum at  $E_e$  or  $E_i$  and decreases. This was shown for Hg by Lawrence, Haupt, and Nottingham<sup>23</sup> as seen on page 284 of the *Atomic Structure*. However, for the purposes of the distribution law, the more recent curves of Smith are satisfactory for  $E_i$ . For  $E_e$  the shape of the functions has been measured by H. Sponer and R. Seiler<sup>2</sup> for Hg, and by Maier-Leibnitz<sup>4</sup> for Ne and He. For the region of energies usually studied, it suffices to use for these curves linear elements in which  $P_i = \beta_1(E - E_i)$ ,  $P_e = \beta_2(E - E_e)$ . The probabilities can and perhaps should be more conveniently expressed in terms of absorbing cross sections  $Q_v$ ,  $Q_e$ , and  $Q_i$  for the process. These are defined by the number  $n$  of electrons out of  $n_0$  initial electrons experiencing these events which can happen to an electron of appropriate energy, per centimeter advance in the field per millimeter of gas pressure, given by  $n = n_0 e^{-N_1 Q_i p x}$ , where  $p$  is the pressure in millimeters and  $x$  is distance in the field direction in centimeters. Here  $Q_i = \pi \sigma_1^2$ , and  $\sigma_1$  represents the cross section of a single atom for the process, with  $N_1$  atoms per  $\text{cm}^3$  at 1 mm pressure.

A final complication which is usually not included in derived equations for the sake of simplicity, but which must be introduced as far as possible into the calculations in its specific form for each kind of gaseous species, is the fact that the electron free path  $\lambda$ , defined in terms of energy loss or small deviations in direction due to encounters, is also a function of  $E$ . That is, we must correct for the Ramsauer free paths  $\lambda$  of electrons; see pages 648–650. These are defined again in terms of an “absorbing” cross section for deflection, in angle, momentum transfer, etc., given by  $n = n_0 e^{-N_1 Q p x}$ , where  $Q = \pi \sigma^2$  is in the present work the collision cross section leading to the average energy loss  $E$  by momentum transfer and is related to the *electron free path*  $\lambda$  by

$$\lambda = \frac{1}{\pi N_1 \sigma^2} = \frac{1}{N_1 Q}.$$

From what has gone before, it is seen at once that, owing to the continual gain and loss of energy in the field, electrons, in virtue of elastic impacts, are *not* in thermal equilibrium with gas molecules or atoms. Hence their average energy and their distribution of energies cannot be of the Maxwellian form. Where densities of electrons are so high that they interact among themselves through their fields, the law may again become Maxwellian.\* Although sometimes the use of the

\* See Part B of this chapter.

Maxwellian distribution function in equations involving the application of the energy distribution has led to results in fair agreement with observation, this application is incorrect and may be seriously in error in many applications such as those involved in the calculation of the Townsend coefficients.

It is necessary, therefore, to attempt to study the distribution law utilizing the above data as far as our mathematical patience and skill permit us. It will be seen that since 1930 correct and fairly satisfactory laws have been deduced for certain simplified cases. More adequate laws can be derived in only a general and usually very complicated form requiring specific variations of  $Q$ , and  $Q_i$ ,  $Q_e$ , and  $Q_s$ , to be introduced for the more exact evaluation of the distribution law in each particular gas and energy regime.

Probably the first attempt at a derivation of the law for electrons in a gas must be credited to Pidduck<sup>6</sup> as early as 1913. The law deduced has since been shown by Morse, Allis, and Lamar to be faulty, leading to erroneous results. The derivation is based on the classical study of H. A. Lorentz in evaluating the energy distribution of free electrons in a metal lattice, which is, of course, now superseded by the Fermi distribution for metals but is still applicable to gases. The calculation based on classical kinetic-theory considerations concerning equilibrium is published in *The Theory of Electrons*, second edition, p. 267, Teubner, Leipzig, 1916, and Pidduck's deduction followed along the lines laid down by Lorentz, but applied to a gas where free electrons had energies greater than molecules as shown by Townsend and Pidduck. This method of Lorentz also later formed the starting point of a rigorous deduction by Morse, Allis, and Lamar.

In the period 1916 to 1918, K. T. Compton<sup>6</sup> attempted on the basis of the then new Franck and Hertz experiments to arrive at an energy distribution law for electrons in a field and to evaluate the Townsend coefficient for ionization by collision on the basis of such a law. The first papers assuming perfectly elastic impacts against infinitely massive molecules yielded a Maxwellian type of law which is obviously incorrect. The later paper introduced corrections into the theory for the Townsend coefficient in He occasioned by the neglect of the fractional energy loss  $f$ , in impact, the distribution law previously deduced remaining essentially unaltered. The law deduced suffered chiefly by being attempted prematurely before the adequate data on mechanisms were at hand.

## 2. THE HERTZ DERIVATION

In 1925, G. Hertz<sup>7</sup> deduced a rigorous expression for the diffusion of electrons between parallel plates in a gas with an electrical field acting. In this deduction he assumed elastic electron impacts with *no* momentum transfer in impact and electrons leaving the cathode with zero velocity. The equation deduced showed the importance of

diffusion in gaseous conduction problems. It enabled Hertz to calculate the velocity of drift of electrons in a gas and the *average* collision frequency  $\nu$  of electrons, in a gap of length  $a$  in terms of a mean free path  $\lambda$  assumed constant, as  $\nu = (3/4)a^2/\lambda^2$ . This theory was applied to the calculation of the number of exciting impacts of electrons in Hg in a region from  $x = x_1$  to  $x = a$ , in a gap of length  $a$  used by H. Sponer,<sup>8</sup> and it showed the need for a radical correction of the interpretation of the results. In a later article, W. Harries and G. Hertz<sup>9</sup> extended the theory of Hertz to the case where electrons are emitted with an initial velocity which is greater than 0, and for the case of a radial diffusion in a cylindrical condenser in the absence of a field. They showed that the mean collision frequency is

$$\bar{\nu} = \frac{a^2}{\lambda^2} F\left(\frac{E_a}{E_0}\right) = \frac{a^2}{\lambda^2} F(Z),$$

where  $E_a$  is the energy of the electrons at the plate and  $E_0$  is the initial energy.  $F(Z) = F(E_a/E_0)$  is given by

$$F(Z) = \frac{3}{4} \frac{1}{(Z-1)^2} \left( Z^2 + 1 - \frac{Z^2 - 1}{\log Z} \right)$$

and varies from 0.5 to 0.75. The actual collision frequency at any point, however, is a rapidly varying function of the electrical field, though the average is not very different for different fields. These authors discuss the effect of Ramsauer free paths on the problem, and indicate how these enter into the calculations (page 186). The paper by Hertz, however, is of far greater importance historically than in the immediate results yielded, which are of limited applicability. Hertz in deriving his equation developed a new method of approach, subsequently applied in many of these studies, which probably affords the easiest approach to the solution of these problems.

### 3. THE DRUYVESTEYN DERIVATION

Basing his procedure on the analysis of Hertz, M. J. Druyvesteyn<sup>10</sup> made the first successful attempt to derive a law of energy (or velocity) distribution for electrons in an electrical field in a gas. This followed an earlier attempt by Penning and Druyvesteyn<sup>11</sup> to calculate the ionization by electrons near the anode of a Hertz condenser system. In view of the fact that Druyvesteyn arrived at the correct law and that his method has been carried further in the solution of distribution law problems than nearly any other, it will be given here. The deduction of Druyvesteyn made the following assumptions:

1. The electrons leave the cathode with a velocity zero, and all reach the anode.
2. The *gain* in speed per free path is small compared to the velocity in the path. This requires the free path  $\lambda$  to conform to the condition that the plate distance  $d \gg \lambda$ .



3. The direction of motion of the electron after impact is independent of the direction before impact.

4. The electrons lose at each impact an *average* energy  $fE$ , where  $f = 2m/M$  and  $E$  is their energy. Then, from the assumptions of the small loss of energy in impact combined with  $d \gg \lambda$ , we must not accept as did Hertz the postulate that  $\frac{1}{2}mv^2 = X\epsilon x$ , where  $x$  is the distance covered in the field direction. This expression in the equations of Hertz says that  $v^2 = 2\gamma x$ , where  $\gamma = Xe/m$ . Hereafter,  $\gamma$  will be used for the electron acceleration in the field according to  $\gamma = Xe/m$ .

5. The free path of the electrons is independent of  $v$ .

6. The electron density at the anode is zero, i.e., there is no electron reflection or secondary emission.

The derivation, based on a classical kinetic-theory foundation, is as follows.

Imagine a small pillbox of base area  $dA$  and height  $dh$ , placed with  $dA$  normal to a uniform electrical field at a distance  $x$  from the cathode as shown in Fig. 91. In order that an electron of velocity  $v$  arrive in the box it must have collided in a volume element  $d\sigma$  with a gas atom, and its velocity before impact must have been  $v^*$ . After impact it moves in a path that is parabolic from  $d\sigma$  to  $dA$ . The number of electrons of velocity  $v^*$  which in  $d\sigma$  have impacts with gas atoms per second is

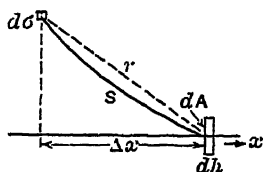


FIG. 91.

$$\rho(x + \Delta x, v^*) \frac{v^*}{\lambda} dv^* d\sigma.$$

$\rho(x + \Delta x, v^*) dv^*$  is the function giving the density of electrons of velocity  $v^*$  at the distance  $\Delta x$  from the point  $x$  where the pillbox is placed.  $v^*/\lambda$  is the collision frequency for the electrons of velocity  $v^*$ , their free path being  $\lambda$ .  $d\sigma$  is the volume from which the electrons start.

The chance that after an impact in  $d\sigma$  an electron goes through  $dA$  is given by  $e^{-S/\lambda} d\omega/4\pi$ . Here  $S$  is the length of the parabolic path between  $d\sigma$  and  $dA$ .  $d\omega$  is closely related to the solid angle subtended by  $dA$  at  $d\sigma$ . Now the electrons going through  $dA$  at an angle  $\phi$  with the normal to  $dA$  at the velocity  $v$  with which they reach  $dA$  spend a time  $dh/(v \cos \phi)$  in the pillbox. Thus the density of electrons from  $d\sigma$  which reach  $dA$  in the volume of the pillbox is the number arriving per unit time multiplied by the time spent in the volume. This at once gives the equation for the density  $\rho(v, x) = \text{number}/(dA dh)$  as

$$\rho(v, x) = \int \frac{\rho(x + \Delta x, v^*) v^* e^{-S/\lambda} dh d\omega dv^* d\sigma}{4\pi \lambda v \cos \phi dA dh dv}. \quad (1)$$

This equation may be simplified by relating  $v$  and  $v^*$ . Since the field  $X$  acts on positive charges in the positive  $x$  direction, it will act on elec-

trons to cause them to gain energy in going from  $d\sigma$  to  $dA$ . In the absence of elastic impacts we can write that  $(mv^2/2) + Xe\Delta x = (mv^{*2}/2)$ , and, calling  $\gamma = Xe/m$ , that  $v^{*2} = 2\gamma\Delta x + v^2$  (note that  $Xe$  is negative, because  $e$  is negative, so that  $v^2 < v^{*2}$ ). If the impacts in  $d\sigma$  are elastic, the average loss being  $fE = (2m/M)E$ , we must write  $v^{*2} = 2\gamma\Delta x + v^2 + f(2\gamma\Delta x + v^2)$ . Now  $d\sigma$  for purposes of integration may be set as  $2\pi r dr d(\Delta x)$ , i.e., an annular volume  $2\pi\sqrt{r^2 - \Delta x^2}$  long,  $(\partial/\partial r)(\sqrt{r^2 - \Delta x^2})dr$  deep, and  $d(\Delta x)$  high. Calling  $\delta = \gamma/2v^2$ , the length of parabolic arc can be expanded in terms of a series in  $r$ ,  $\Delta x$ , and  $\delta$  as

$$S = r \left\{ 1 - \frac{1}{8}\delta^2(\Delta x)^2 + \frac{1}{8}\delta^2 r^2 \right\},$$

$$d\omega = dA \frac{\Delta x}{r^3} \left\{ 1 - \delta\Delta x - \delta \frac{r^2}{\Delta x} + \frac{7}{2}\delta^2(\Delta x)^2 + \frac{7}{2}\delta^2 r^2 \right\},$$

$$\frac{1}{\cos \phi} = \frac{r}{\Delta x} \left\{ 1 - \delta\Delta x + \delta \frac{r^2}{\Delta x} + \frac{3}{2}\delta^2(\Delta x)^2 - \frac{5}{2}\delta^2 r^2 + \delta^2 \frac{r^4}{(\Delta x)^2} \right\}.$$

Thus the various elements of equation 1 are now expressed in terms of series expansions in which  $\Delta x$  and  $v^* - v$  are carried to the second order, while terms in  $f$  are of the first order.

To integrate the resulting equation we find, in neglecting  $f$  and  $\lambda$  compared to unity but retaining the terms with  $f/\lambda^2$ , that

$$\rho''_{xx} + 4v\delta\rho''_{xv} + 4v^2\delta^2\rho''_{vv} - 4\delta\rho'_x - 12v\delta^2\rho'_v + 16\delta^2\rho + \frac{3f}{2\lambda^2}(2\rho + v\rho'_v) = 0, \quad (2)$$

and replacing  $v$  by  $\eta = v^2/2\gamma$  we have

$$\rho''_{xx} + 2\rho''_{x\eta} + \rho''_{\eta\eta} - \frac{1}{\eta\rho'_x} - \frac{1}{\eta\rho'_\eta} + \frac{\rho}{\eta^2} + \frac{3f}{\lambda^2}(\rho + \eta\rho'_\eta) = 0. \quad (3)$$

The integration of this equation presents considerable difficulty, and Druyvesteyn limits his solution to two cases.

*Case a.* Assuming that the energy loss per free path is very small, then  $\eta = v^2/2\gamma$  is distinctly smaller than  $x$ . Then not only are  $1 \gg \lambda$ ,  $1 \gg f$ , but also  $1 \gg f/\lambda^2$ . Introducing  $y = x - \eta$  as a new variable and calling the electron density, as a function of  $x$  and  $y$ ,  $V_{x,y}$ , we have

$$V''_{xx} - \frac{1}{x-y} V'_x + \frac{V}{(x-y)^2} + \frac{3f}{\lambda^2} \{ V - (x-y)V'_y \} = 0. \quad (4)$$

In a first approximation we can neglect  $y$  relative to  $x$  since  $xV'_y \gg V$ . Thus one has

$$V''_{xx} - \frac{1}{x} V'_x + \frac{V}{x^2} - \frac{3f}{\lambda^2} x V'_y = 0. \quad (5)$$

This equation is now open to solution as the variables are separable. One finds

$$V_{(x,v)} = \sum_n A_n \left( e^{-\frac{C_n \lambda v^2}{3J}} \right) x J_0 \left( \frac{2}{3} \sqrt{C_n} X^{3/2} \right) \quad (6)$$

Here  $A_n$  and  $C_n$  are constants, and  $J_0$  is a Bessel function of the first kind of zero order.  $C_n$  comes from the condition that, at the anode,  $x = 1$ ,  $V = 0$ . If  $\epsilon_n$  is the  $n$ th root when  $J_0 = 0$ , then  $\frac{2}{3} \sqrt{C_n} = \epsilon_n$ . To get  $A_n$  one must evaluate  $N_0 dA$ , the part of the electrons  $N_0 dA = dA \int N(x, v) dv$  that go through a surface  $dA$  normal to the field between  $x = 0$  and  $x = 1$ .  $N_0$  is independent of  $x$ , since these  $N_0$  are the initially created electrons. Druyvesteyn, following Hertz in his calculation of the number of electrons crossing  $dA$  in unit time, calculates this integral from  $d\sigma$  in the absence of energy loss in impact. The equation integrated by Druyvesteyn is equation 1, divided by  $dn/(v \cos \phi dA dh)$ , i.e., it is

$$N_{(v,x)} dv dA = \int \frac{\rho(x + \Delta x, v^*) v^* e^{-s/\lambda}}{4\pi\lambda} d\omega d\sigma dv^*. \quad (1a)$$

This, just as in Hertz's case, integrates to a form for the number per unit volume,

$$N(v, x) = -\frac{\rho v \lambda}{3} (q - 4\delta)$$

where  $q$  is now given by

$$q = \frac{1}{\rho} \frac{\partial \rho}{\partial x} - \frac{\gamma}{v\rho} \frac{\partial \rho}{\partial v}$$

instead of

$$q = \frac{1}{\rho} \frac{\partial \rho}{\partial x} - \frac{\gamma}{v^2},$$

as in Hertz's case of perfectly elastic impacts against atoms of infinite mass. The solution is then

$$N_{(v,x)} = \frac{\lambda \gamma}{3} \left( -\frac{\partial \rho}{\partial x} - 2v\delta \frac{\partial \rho}{\partial v} + 4\delta\rho \right), \quad \text{with} \quad \delta = \frac{\gamma}{2v^2}. \quad (6a)$$

From the condition  $N_0 dA = dA \int N(v, x) dv$  we obtain

$$N_0 = \frac{f\gamma}{\lambda} x^{3/2} \sum \frac{A_n}{\sqrt{C_n}} J_1 \left( \frac{2}{3} \sqrt{C_n} x^{3/2} \right). \quad (6b)$$

In order to evaluate  $A_n$  from this one must test for convergence possibilities which exist when, for  $x = 0$ , the number  $N_0$  is 0 at  $x = 0$  and

$N_0$  at  $x = 1$ . If we call  $N = \int N(v, x) dx$ , and set, from  $0 < x < \theta^{2/3}$ ,  $N = N_0(x^3/\theta^2)$ , and from  $\theta^{2/3} < x < 1$  (assuming the anode at  $x = 1$ ), that  $N = N_0$ , we can get convergence if  $\theta$  is small. This means that the electrons are *not generated* at  $x = 0$  but between  $x = 0$  and  $x = \theta^{2/3}$ . At  $x > \theta^{2/3}$  equation 6 holds. We can assume it to hold for  $x < \theta^{2/3}$ . From this  $A_n$  becomes

$$A_n = \frac{6N_0\lambda}{f\gamma} \frac{J_1(\epsilon_n, \theta)}{\epsilon_n \theta J_1^2(\epsilon_n)}, \quad (6c)$$

and thus we get

$$V_{(x, y)} = \frac{6N_0\lambda x}{f\gamma} \sum_n e^{-\frac{3\lambda^2}{4f}\epsilon_n^2 y} \frac{J_1(\epsilon_n, \theta)}{\epsilon_n \theta J_1^2(\epsilon_n)} J_0(\epsilon_n, x^{3/2}), \quad (7a)$$

$$\rho(x) = \int \rho(v, x) dv = \frac{8N_0\sqrt{x}}{\lambda\sqrt{2\gamma}} \sum_n \frac{J_1(\epsilon_n, \theta)}{\epsilon_n^3 \theta J_1^2(\epsilon_n)} J_0(\epsilon_n, x^{3/2}). \quad (7b)$$

If  $\theta$  is small,  $\theta = 0.01$ , equation 7b is closely similar to the equation of Hertz, to wit,

$$\rho(x) = \frac{3N_0\sqrt{x}}{\lambda\sqrt{2\gamma}} \log \frac{1}{x},$$

for the case of no energy losses; i.e., the average charge distribution is not seriously affected by elastic impacts. Equation 7a becomes at once the velocity distribution in terms of  $y = x - \eta = x - (v^2/2\gamma)$ , if we substitute the value of  $x$  at which the velocity distribution is desired to be known. At the anode  $x = 1$ , we then have at once

$$V_{(1, y)} = B \sum_n e^{-\frac{3\lambda^2}{4f}\epsilon_n^2 y} \frac{J_1(\epsilon_n, \theta)}{\theta J_1(\epsilon_n)}.$$

It is seen that  $V$  is directly determined by  $(\lambda^2/f)y$ . The shape of the function  $V_{(1, y)}$  as a function of  $(3\lambda^2/4f)y$  is shown in Fig. 92. It must be noted that this relation applies to any point in the path of the electrons, i.e., before they have reached their terminal velocities. Hence the energy is a function of  $x$ .

*Case b.* If, however, we have  $x \gg \lambda$ , so that the electrons can reach their terminal velocity, we can at once evaluate  $V_{(0)}$  and hence the velocity distribution as case *b*. This condition is termed by Druyvesteyn the "stationary" state. It will be termed steady state in what follows.

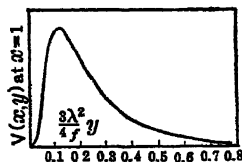


FIG. 92.

To arrive at the solution for the steady state, we need to know the solution of equa-

tion 2, which is independent of  $x$ . If we drop out variation with  $x$  and confine ourselves to  $v$  only, equation 2 becomes

$$\rho''_{vv} - \frac{\rho'_v}{v} \left( 3 - \frac{3f}{2\lambda^2\gamma^2} v^4 \right) + \frac{\rho_v}{v^2} \left( 4 + \frac{3f}{\lambda^2\gamma^2} v^4 \right) = 0. \quad (8)$$

This yields as a solution

$$\rho_v = cv^2 e^{-\frac{3f}{8\lambda^2\gamma^2} v^4}, \quad (9)$$

which is the steady-state energy distribution for a swarm of electrons in a field  $X$  making elastic impacts at which a fraction  $f$  of the energy gained in the field is lost per impact, beyond the point where the electrons have their terminal velocity.

Druyvesteyn has deduced this equation 9 very simply, using the condition of equilibrium in the field between loss and gain of energy. In 1 second the average energy loss of the electrons of velocity  $v$  and present in a number  $\rho(v) dv$  per unit volume is  $\rho(v) dv (v/\lambda) f (\frac{1}{2}mv^2)$ . In the same time the number of electrons of velocity  $v$ , equal to  $i(v)dv$ , flowing past a point per unit area per second, has been given the energy  $Xei(v)dv = i(v)\gamma m dv$ . This follows since current density is the density of electrons  $i$  that pass unit area at a point per second times the distance  $x$  traversed in that second. Now  $i(v)dv = Nxe$  in 1 second. But  $NexX$  is the work done in 1 second on those electrons by the field and  $\gamma = Xe/m$ . Thus the work is  $Nxm\gamma = i(v)dv m\gamma$  (which in the steady state equals the loss due to collisions). We have accordingly

$$i(v)dv\gamma m = \frac{\rho(v)dv}{\lambda} 2 \frac{m}{M} \frac{m}{2} v^2 \quad \text{or} \quad i(v)\gamma = \frac{v^3}{\lambda} \frac{m}{M} \rho(v), \quad (10)$$

with  $i(v)$  taken from equation 6a as equation 11.

$$i(v) = -\frac{\gamma\lambda}{3} \frac{d\rho(v)}{dv} + \frac{2\gamma\lambda\rho(v)}{3v}. \quad (11)$$

The term  $-(\lambda v/3)[\partial\rho(v, x)/\partial x]$  in equation 6a is zero, as at equilibrium the density is constant with  $x$ . Elimination of  $i(v)$  from equations 10 and 11 gives a simple differential equation of the first order in  $\rho(v)$  the number of electrons of velocity  $v$  per cubic centimeter.

$$\frac{d\rho(v)}{dv} + \left( \frac{3v^3 m}{\gamma^2 \lambda M} - \frac{2}{v} \right) \rho(v) = 0. \quad (12)$$

This integrates at once into equation 9.

In an article, Druyvesteyn<sup>13</sup> attempts to calculate the energy distribution for electrons in Ne gas at values of field strength and pressure such as occur in the positive column of a Geissler tube. In doing this, losses of energy due to inelastic impacts only are counted. That is, he

neglects the small loss of energy  $fE$  at the high  $X/p$  but considers losses of energy to ionization and excitation. The absorbing cross section for excitation of Ne is taken as constant (its value was not known at that time), which is, of course, incorrect, while the absorbing cross section for ionization follows the approximate form indicated in the introduction. As a result an energy distribution law obtained by setting  $E_e/E_i$  for Ne as 0.8 is found with an arbitrary constant for the absorbing cross section for excitation of Ne. By comparing the value of the Townsend coefficient derived on the basis of his distribution law with experiment, the value of the constant is obtained. The resulting equations combined with Langmuir and Tonk's equation for the wall current in discharge tubes enable the ionization in the positive column to be computed. Since the equations are not complete or accurate they will not be given. However, they mark the first attempt at an appropriate theory of the Townsend coefficient.

#### 4. LATER DERIVATIONS

In 1930-33, Didlauskis<sup>14</sup> derived a distribution law for electrons in an electrical field in a gas using statistical considerations of time fluctuations of energy. The laws deduced were at marked variance with other laws and were so unusual and so at variance with Druyvesteyn that Cravath<sup>15</sup> undertook to check the results of Didlauskis. This he failed to do, and, at a Physical Society meeting in 1934, he presented his analysis of the problem. Unfortunately his full paper was never published, and all that exists is the abstract, which is given here in toto because of its value. It is probably one of the more complete studies of the problem in its scope. It is to be found in abstract form. Cravath states:

"Didlauskis found that the energy distribution was less than  $1/20$  as wide as Maxwell's unless the free path increased rapidly with the speed. Didlauskis' term  $D + E$  should have contained the *mean square* of the component of the velocity in the direction of the field *instead* of the *square of the mean component*. With this correction a number of distributions have been calculated. Let  $W(E)dE$  equal the fraction of electrons having energy  $E$  in the interval  $dE$ , and  $fE$  the energy lost in a collision.

"1. If  $f = 0$  when  $E < E_e$  and  $f = 1$  when  $E > E_e$ ,

$$W(E) = 2.25E_e^{-3/2}E^{1/2} \log \frac{E_e}{E}, \quad \bar{E} \text{ the average energy is } \frac{9}{25} E_e.$$

"2. If  $|f| \ll 1$  for all collisions (not merely for the average) and if  $\bar{E}$  is very much greater than the average energy of the molecules

$$W(E) = aE^{1/2}e^{-3 \int_0^E (1-f)E_e dE / X^2 e^2},$$

where  $a$  is a constant,  $X$  is the field strength,  $q$  is the number of collisions per centimeter,  $P$  is the average cosine of the angle of scattering, all for electrons of energy  $E$ .

"3. If  $q^2(1 - P)f = q_0^2 f_0 E^h$ ,  $q_0^2 f_0$  being constant

$$W(E) = aE^{1/2}e^{-3q_0^2 f_0 E^{(2h+2)}} / (2h+2) X^2 e^2.$$

Unless  $h$  is greater than  $-1$ , there is no terminal or steady state.

"4. If the mean free path is proportional to velocity, and  $P$  and  $f$  are constant,  $h = -\frac{1}{2}$  and the distribution is Maxwellian.

"5. If mean free path,  $P$ , and  $f$  are all constant,  $h = 0$ ,

$$W(E) = 1.038 \frac{E^{1/2}}{\bar{E}^{3/2}} e^{-0.547(\bar{E}/E)^2},$$

and

$$\bar{E} = \frac{0.604Xe}{q(1-P)^{1/2}f^{1/2}}.$$

"6. For elastic spheres  $P = 0$ ,  $f = 2m/M$ , and the above becomes Druyvesteyn's distribution" in the form

$$\begin{aligned} W(E) &= 1.038 \left\{ \frac{(2m/M)^{1/2}}{0.604Xe\lambda} \right\}^{3/2} E^{1/2} e^{-0.547 \left( \frac{E^2(2m/M)}{0.604Xe\lambda} \right)} \\ &= 2.17 \left[ \frac{(2m/M)^{1/2}}{Xe\lambda} \right]^{3/2} E^{1/2} e^{-1.49 \frac{E^2(2m/M)}{\lambda^2 e^2 X^2}}, \end{aligned} \quad (13)$$

which is just Druyvesteyn's law, with the constants evaluated in the energy form.

In 1930 Townsend<sup>16</sup> in a very involved analysis making certain approximate assumptions concerning the distribution of energies about a mean value  $E_1$  arrived at an expression for the energy distribution of the electrons about the mean energy  $E_1$  given by

$$W(E) = \frac{N}{E_1 \sqrt{\pi}} e^{-\left(\frac{E}{E_1} - 0.85\right)^2}.$$

Here the value of  $E_1$  is not determined by theory but assumedly can be evaluated experimentally from Townsend's well-known diffusion measurements for a group of electrons in a beam in an electrical field in the gas. Since the deduction is an exceedingly rough approximation, and since it fails to use the correct Hertz expression for the velocity of diffusion of electrons in an electrical field, it is not surprising that it is in disagreement with the correct expression of Druyvesteyn, Cravath, and Morse, Allis, and Lamar. It is applicable to the higher end of the distribution law only. It is, like these equations, confined to energies below excitation and ionization. It also gives very much poorer fits

with observation when used in the calculation of Townsend's  $\alpha$  by Emmeléus, Lunt, and Meek<sup>17</sup> than does Maxwell's law, and should not have been used for this calculation.

### 5. THE MORSE, ALLIS, AND LAMAR DERIVATION

Finally in 1935 Morse, Allis, and Lamar,<sup>18</sup> inspired by K. T. Compton, formally derived a distribution for electrons making elastic impacts with atoms (the loss per impact being that previously given) in an electrical field. In this treatment they in essence follow the procedure of Lorentz in his study of the motion of the electron atmosphere in a metal. The analysis is precisely the same in computing the loss of electrons in a volume in phase space due to the field and to diffusion as well as to collisions. It departs from Lorentz in including the electrons scattered into the volume as a result of the loss of energy due to impacts. Lorentz assumed his atoms to be of infinite mass, while in this deduction electrons lose an energy

$$\Delta E = fE = \frac{2m}{M} E(1 - \cos \theta)$$

as the result of a finite atomic mass  $M$ , where  $\theta$  is the angle of electron scattering. The inclusion of this condition adds another term to the energy balance equation. By equating corresponding terms of the resulting equation of balance, two equations are obtained. One of these enables the balance between gain of *momentum* due to diffusion and drift down the field and the loss of *momentum* in collisions to be computed, a relation which Lorentz also found in his study of electrons in metals. Such an equation leads to an evaluation of the electron drift velocity or mobility if the distribution law is known. As Lorentz did not have this, he assumed Maxwell's law.

As a result of the added term, Morse, Allis, and Lamar obtained the second equation giving the balance of *energy* caused by the gain from the field due to diffusion and drift and loss by collisions. Lorentz did not have the *energy* balance equation and as a result was forced arbitrarily to assume a Maxwellian form. Pidduck in his derivation equated the *total* energy gain in the field to the *total* loss in collisions and used this to determine the temperature of the *assumed* Maxwell distribution, in order to calculate the drift velocity. This procedure resulted in entirely too many high-energy electrons to agree with theory. The two correct equations of Morse, Allis, and Lamar permit of a solution for the energy distribution law without further assumptions as to the form of the law, as the second equation gives the form of the law. Thus, assuming a stationary or steady state with the energy gain from the field equal to the loss to collisions *for each velocity range*, assuming a terminal energy distribution in which the distribution is



independent of the position of the electron in the field,  $x$ , and assuming a constant Ramsauer free path or cross section independent of energy  $E$ , the law arrived at becomes

$$\rho(v)dv = NW(v)dv = 4\pi Av^2 e^{-h^4 v^4} dv \quad (14)$$

with

$$h^4 = \frac{3m}{M} \left( \frac{m NQ}{2 eX} \right)^2, \quad Q = \pi\sigma^2, \quad \frac{1}{2}mv^2 = E$$

and  $N$ , the number of electrons per cubic centimeter,  $NQ$  being the absorbing cross section. Here

$$A = \frac{N}{\int_0^\infty 4\pi v^2 \phi(v) dv} = \frac{Nh^3}{\pi \Gamma_{\frac{3}{4}}^2},$$

$$\frac{1}{2}mv^2 = E, \quad dv = \frac{dE}{\sqrt{2Em}}, \quad \lambda = \frac{1}{\pi N \sigma^2}.$$

The average energy  $E_A$  is

$$E_A = \frac{\Gamma_{\frac{5}{4}}}{\Gamma_{\frac{3}{4}}} \left( \frac{M}{3m} \right)^{\frac{1}{2}} \frac{Xe}{NQ} = 0.427 \frac{eX M^{\frac{1}{2}}}{\pi N \sigma^2 m^{\frac{1}{2}}}$$

$$= 0.427 X e \lambda \left( \frac{M}{m} \right)^{\frac{1}{2}}.$$

Thus

$$\rho(v)dv = NW(v)dv = \frac{4N}{\Gamma_{\frac{3}{4}}^2} \left[ \frac{3m}{4M} \left( \frac{m}{Xe\lambda} \right)^2 \right]^{\frac{3}{4}} v^2 e^{-\frac{3}{4} \frac{m}{M} \left( \frac{m}{Xe\lambda} \right)^2 v^4} dv, \quad (15)$$

or, since  $\frac{Xe}{NQ} = E_A \frac{\Gamma_{\frac{3}{4}}}{\Gamma_{\frac{5}{4}}} \left( \frac{3m}{M} \right)^{\frac{1}{2}}$ ,  $h^4 = \frac{m^2}{4E_A^2} \left( \frac{\Gamma_{\frac{5}{4}}}{\Gamma_{\frac{3}{4}}} \right)^2$ ,

$$NW(E)dE = 2N \frac{(\Gamma_{\frac{5}{4}})^{\frac{3}{4}}}{(\Gamma_{\frac{3}{4}})^{\frac{3}{4}}} \frac{E^{\frac{1}{2}}}{E_A^{\frac{3}{2}}} e^{-\frac{E^2}{E_A^2} \left( \frac{\Gamma_{\frac{5}{4}}}{\Gamma_{\frac{3}{4}}} \right)^2} dE \quad (16)$$

Here,  $\Gamma_{\frac{5}{4}} = 0.9064$  and  $\Gamma_{\frac{3}{4}} = 1.2254$ .

For comparison, Maxwell's equation in the same form is given as

$$NW_M(E)dE = 2\pi N \left( \frac{3}{2\pi E_A} \right)^{\frac{3}{2}} E^{\frac{1}{2}} e^{-\frac{3}{2} \frac{E}{E_A}} dE, \quad (17)$$

with  $E_A = \lambda eX M^{\frac{1}{2}} / (2.31 m^{\frac{1}{2}})$  and with  $1/2.31 = 0.433$  in comparison to 0.427 with the Morse, Allis, and Lamar equation. The equation may also be expressed in the notation of Druyvesteyn as follows: Since  $\gamma = Xe/m$ ,  $2m/M = f$ , we have in Druyvesteyn's notation

$$\rho(v)dv = NW(v)dv = \frac{4N}{\Gamma_{\frac{3}{4}}^2} \left( \frac{3}{8} f \frac{1}{\gamma^2 \lambda^2} \right)^{\frac{3}{4}} v^2 e^{-\frac{3}{8} \frac{f}{\lambda^2 \gamma^2} v^4} dv. \quad (18)$$

This is identical with Druyvesteyn's and Cravath's equations. The solution of the first Lorentz equation together with this equation gives the average drift velocity  $u$  as

$$u = \frac{\pi^{1/2}}{3\Gamma_{3/2}} \left(\frac{3m}{M}\right)^{1/2} \left(\frac{2Xe}{mNQ}\right)^{1/2} = 0.6345 \left(\frac{m}{M}\right)^{1/2} \left(\frac{2Xe}{mNQ}\right)^{1/2} \\ = 0.756 \left(\frac{e}{m} \lambda X \sqrt{f}\right)^{1/2}.$$

It is thus seen that, by their three different derivations, Druyvesteyn, Cravath using the corrected Didlauskis method, and Morse, Allis and Lamar with the amplified Lorentz procedure, arrive at the same distribution law for electrons in a gas in a field making elastic impacts but losing a fraction of energy  $f$  at each impact,  $f$  being relatively small. It is seen that this equation differs very little from the equivalent equation of Compton assuming a Maxwellian distribution of velocities which reads

$$u = k_e X = 0.705 \left(\frac{e}{m} \lambda X \sqrt{f}\right)^{1/2};$$

see page 186.

Assuming constant Ramsauer cross sections, this equation is certainly applicable to restricted regions in some of the inert gases where  $Q$  is nearly constant, Ne and He. Whether it holds in molecular gases is doubtful, although it could hold in  $H_2$ . In  $N_2$  and also in  $A$  the Ramsauer cross section varies too rapidly. In these gases Nielsen<sup>20</sup> and Bradbury have shown that we must correct for the Ramsauer cross section. This is done by writing,  $Q \neq \pi\sigma^2$ , but  $Q$  is a function of  $E$ ,  $Q(E)$  or of  $v$ ,  $Q(v)$ . In this case, Morse, Allis, and Lamar find

$$W(v) = A e^{-\frac{3N^2m^2}{(Xe)^2 M} \int^v Q^2(v) dv}, \quad (19)$$

$$W(E) = A e^{-6 \left(\frac{N}{Xe}\right)^2 \frac{m}{M} \int^E E Q^2(E) dE} \quad (20)$$

(20 is corrected by Bradbury owing to a misprint in the original paper), with  $A$  determined by

$$N = 4\pi A \int_0^\infty v^2 W(v) dv,$$

where, since  $W(v)$  is now different,  $A$  will be different and determined by the form  $Q(v)$  or  $Q(E)$ .

The effect of  $Q(E)$  can be seen at once by assuming a linear change of  $Q(E)$ , with  $E$ , i.e.,  $Q(E) = Q_0 \pm bE$ , where the plus sign indicates that  $Q$  is increasing ( $\lambda$  decreasing) with increasing  $E$ , and the minus sign means that  $Q$  is decreasing ( $\lambda$  increasing) with  $E$ . If, then,  $b$  is small,  $Q^2(E) = Q_0^2 \pm 2bEQ_0$ . Integration gives then a  $W(v)$  or  $W(E)$  cor-

responding to constant cross section  $Q_0$  multiplied by an exponential obtained from  $\int^E \pm E(2bEQ_0)dE = \pm bQ_0E^3 = \pm \Omega$ . Hence the distribution becomes

$$NW(E_QE)dE = NW(E_{Q_0})dEe^{\pm (\frac{3}{2}bQ_0E^3)}, \quad (21)$$

with  $e^{+\Omega}$  for the case of increasing  $Q$  (decreasing  $\lambda$ ), and  $e^{-\Omega}$  for the case of decreasing  $Q$  (increasing  $\lambda$ ), and  $NW(E_{Q_0})dE$  given by equation 16. As  $E$  increases, the  $e^{+\Omega}$  emphasizes the higher values in equation 16, while with  $e^{-\Omega}$  the high  $E$  emphasizes the lower values of  $E$  in the normal distribution of equation 16. Hence, where  $Q$  increases with  $E$  ( $\lambda$  decreases), there will be relatively more fast electrons, while where  $Q$  decreases with  $E$  ( $\lambda$  increases) there will be relatively more slow electrons. This allows us to plot the equations for comparison in Fig. 93. The effect is as follows. The increase of  $Q$  (decrease of  $\lambda$ ) with  $E$  gives

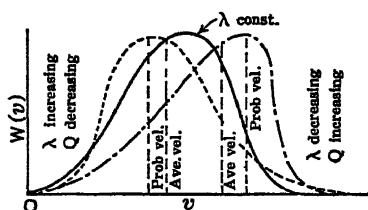


FIG. 93.

relatively few electrons beyond the most probable value, owing to the rapid fall of  $W(E_{Q_0})$  despite  $e^{\Omega}$ . Higher energies are emphasized, but the change in the average is not indicated, by this procedure. It can be found only if the constant  $A$  is evaluated for a given set of conditions. The curve has a most probable velocity at a higher energy than the

Maxwellian, a sharp decline to low values, and a gradual decline to low energies. If one measures the average energy value as one would in a Townsend study of the spreading of an electron beam in a field, then the number of electrons say at twice or three times the average measured energy is less in percentage than in a Maxwellian or a Druyvesteyn distribution of about the same average. This is actually observed for electrons in A. The decrease of  $Q$  or increase of  $\lambda$  with  $E$  gives a probable energy displaced to lower values of  $E$ . The relative number of electrons of energy well beyond the probable value is now very much increased compared to a Druyvesteyn distribution, while the decline of the curve toward low energies is much steeper. This emphasis on the higher energy well beyond the average value has been observed for electrons in He to a slight extent. It is not immediately clear physically, however, how much and why the probable energy is reduced by increasing  $\lambda$  as  $E$  increases, nor how a decreasing  $\lambda$  as  $E$  increases produces an increase in the probable energy at a steady state. On the other hand, it is clear how the percentage of fast electrons relative to the most probable value is greater with a  $\lambda$  increasing with  $E$ , and vice versa. For those electrons having longer paths get more energy and hence can gain more energy than those with shorter paths, giving a greater spread to the high energy electrons when  $\lambda$  increases with  $E$ .

Proceeding in much the same way as Morse, Allis, and Lamar, B. Davydov<sup>21</sup> in Russia independently arrived at the same equation as that of Druyvesteyn and Morse, Allis, and Lamar, using a constant absorbing cross section. His analysis is quite clearly carried out, most of the steps being included, which is not true of other derivations owing to lack of space in the journals. He includes, however, the effect of *atomic velocities* on  $f$  in impact, which gives the solution for cases where the fields are quite low. The correct solution of the equilibrium condition thus gives a more accurate expression for the drift velocity, at low  $X/p$  than does Compton's equation.

## 6. DERIVATIONS INCLUDING INELASTIC IMPACTS

For most problems of interest in electronics other than the evaluation of electron mobilities, e.g. the first Townsend coefficient at low fields, it is important to have the distribution law in such form that for  $X/p$  high enough to cause inelastic impacts to excitation and ionization we can calculate  $NW(v)dv$ . This problem has been attacked by Druyvesteyn<sup>22</sup> for only one gas viz., pure Ne. It has in part been solved for Ne with small admixtures of A by Druyvesteyn and Kruit-hof.<sup>23</sup> It is thus of value to reproduce this analysis somewhat in detail as it indicates the approach to the solution of the problem.

Druyvesteyn assumes that we are dealing with electrons in a field in a gas where the distance traversed from the origin is such that Townsend's  $\alpha$ , and hence  $W(v)$ , is no longer a  $f(x)$ , the distance traversed. He terms this a stationary energy distribution. It is obviously what we term a steady state in which the electrons have reached their terminal drift velocity. He assumes on an average that the gain of energy of electrons in the field will equal the loss of energy in impacts. An "elastic" collision is defined as one in which the average energy loss is  $fE = (2m/M)E$ . This implies that the energy of the electrons is much greater than that of the atoms, and that the loss is  $fE$  per collision, which is not true for an individual collision but is true on the average.

In conformity with the introductory statement, Druyvesteyn assumes much higher energy losses for excitation and ionization and assumes for simplicity only *one* excitation and *one* ionization potential to exist. It is necessary for solution of the equations to assume simple functions for the probabilities of these events as a function of electron energy. It has in the past been customary to accept Maxwell's law, which is correct for high current densities such as in arcs and discharge plasma where electrons interact with each other. At lower current densities, equilibrium comes from the field and interaction with atoms alone, as was seen for elastic impacts. However, the distribution which we have studied is not applicable since the probabilities of excitation and ionization play an important role. An earlier attempt has been made by Druyvesteyn in the case of Ne, keeping the excitation

for Ne a constant independent of  $E$ . With the work of Maier-Leibnitz, Ramsauer, and others there are now available for Ne values of  $P_e$ ,  $P_i$ , and  $Q$  so that an exact calculation without assumptions is possible. Druyvesteyn then proceeds as follows. Equation 6a reads

$$N(v, x) = \frac{\lambda v}{3} \left( -\frac{\partial \rho(v)}{\partial x} - 2v\delta \frac{\partial \rho(v)}{\partial v} + 4\delta \rho(v) \right). \quad (6a)$$

This may be rewritten in the newer notation of Druyvesteyn's

$$i(x, w) = -\frac{\lambda}{3} \left( \sqrt{w} \frac{\partial \rho(w)}{\partial x} + 2\gamma \sqrt{w} \frac{\partial \rho(w)}{\partial w} - \frac{2\gamma}{\sqrt{w}} \rho(w) \right), \quad (22)$$

where  $i(x, w)$  is the net number of electrons passing 1 cm<sup>2</sup> area placed perpendicular to the field in the direction of increasing,  $x$ ,  $i$  and  $\rho(w)$  being constant in time, and writing  $w = v^2$ ,  $dw = 2v dv$ ,  $\gamma/2v^2 = \delta$ . Now in equation 10 it was seen that, for elastic collisions, equilibrium and the stationary state demand that

$$i(v)\gamma = \rho(v) \frac{v^3}{\lambda} \frac{m}{M} \quad (10)$$

This can be translated into the relation

$$2\gamma i(w) = \rho(w) \frac{w^{3/2}}{\lambda} f, \quad (23)$$

and as was seen when combined with 22 gives the distribution law, if one sets  $\partial \rho(w)/\partial x = 0$ . This yields equation 12 in the new notation as

$$2\gamma \left[ -\frac{2\gamma\lambda\sqrt{w}}{3} \frac{\partial \rho(w)}{\partial w} + \frac{2\gamma\lambda}{3\sqrt{w}} \rho(w) \right] = \frac{fw^{3/2}\rho(w)}{\lambda}. \quad (24)$$

This represents the equilibrium and defines Druyvesteyn's law for elastic impacts.

One may now apply the conditions that inelastic impacts due to excitation take place at a value of  $w$  equal to  $w_s$ , and ionizing impacts take place at a value of  $w$  equal to  $w_i$ . In addition call  $A(w)$  and  $I(w)$  the probabilities of excitation and ionization respectively. In this case the steady state will not be given by the condition that the number of electrons with  $w$  passing through a value  $w$  from both directions must be equal, but that the number of electrons entering the interval between  $w$  and  $w + dw$  must be equal to the number of electrons leaving the interval. The number of electrons with a definite value of  $w$ ,  $w > w_s$ , will be reduced by an amount  $\rho(w)\sqrt{w}A(w)/\lambda$  by excitation and  $\rho(w)I(w)\sqrt{w}/\lambda$  by ionization. For  $w > w_i$ , the steady state from equation 24 must be replaced by the differential equation correspond-

ing to the new conditions set. In the absence of inelastic impacts the new steady state would be expressed by the differential equation,

$$-\frac{\partial i(w)}{\partial x} - 2\gamma \frac{\partial i(w)}{\partial w} = -\frac{\partial}{\partial w} \left\{ \frac{\rho(w)w^{3/2}f}{\lambda} \right\}$$

instead of by condition 23. To this expression one must add the inelastic losses, whence one obtains for a steady state, when  $w > w_i$ ,

$$-\frac{\partial i}{\partial x} - 2\gamma \frac{\partial i}{\partial w} = \frac{\rho(w)\sqrt{w}A(w)}{\lambda} + \frac{\rho(w)\sqrt{w}I(w)}{\lambda} - \frac{\partial}{\partial w} \left( \frac{f\rho(w)w^{3/2}}{\lambda} \right). \quad (25)$$

In this equation the number of electrons *entering* the range by loss of energy to very fast electrons has been omitted, i.e., it is assumed that  $\rho(2w_a)$  is negligible. If  $w_a < w < w_i$ , the equation is the same as 25 with  $I(w) = 0$ . For  $w < w_a$ , the electrons increase as a consequence of loss of energy to excitation from electrons with an energy  $w + w_a$ , and by ionization from electrons of an energy  $2w + w_i$ , assuming that both electrons on the average get  $w$  after ionization.

For  $w < w_a$  one has

$$\begin{aligned} \frac{\partial i}{\partial x} + 2\gamma \frac{\partial i}{\partial w} = & \frac{\rho(w + w_a)\sqrt{w + w_a}A(w + w_a)}{\lambda} \\ & + \frac{[4\rho(2w + w_i)\sqrt{2w + w_i}I(2w + w_i)]}{\lambda} + \frac{\partial}{\partial w} \left( \frac{\rho(w)f w^{3/2}}{\lambda} \right). \end{aligned} \quad (26)$$

The factor 4 in the ionization term comes from the fact that, for each electron of energy  $2w + w_i$ , two electrons of energy  $w$  are produced. If we set

$$\rho(x, w) = e^{\alpha x} \rho(w), \quad (27)$$

$$i(x, w) = e^{\alpha x} i(w), \quad (28)$$

as a result of ionization by collision, where  $\alpha$  is Townsend's coefficient, and eliminate  $i$  from 22 with the aid of 27 and 28, we find equations 29, 30, and 31 for  $w > w_i$ ,  $w_i > w > w_a$  and  $w_a > w$  respectively.

$$\begin{aligned} \frac{\partial^2 \rho(w)}{\partial w^2} + \frac{\partial \rho(w)}{\partial w} \left( \frac{\alpha}{\gamma} + \frac{3fw}{4\gamma^2\lambda^2} \right) \\ + \rho(w) \left\{ \frac{\alpha^2}{4\gamma^2} + \frac{1}{4w^2} + \frac{9f}{8\gamma^2\lambda^2} - \frac{3}{4\gamma^2\lambda^2} (A(w) + I(w)) \right\} = 0, \end{aligned} \quad (29)$$

$$\begin{aligned} \frac{\partial^2 \rho(w)}{\partial w^2} + \frac{\partial \rho(w)}{\partial w} \left( \frac{\alpha}{\gamma} + \frac{3fw}{4\gamma^2\lambda^2} \right) \\ + \rho(w) \left\{ \frac{\alpha^2}{4\gamma^2} + \frac{1}{4w^2} + \frac{9f}{8\gamma^2\lambda^2} - \frac{3A(w)}{4\gamma^2\lambda^2} \right\} = 0, \end{aligned} \quad (30)$$

$$\begin{aligned} \frac{\partial^2 \rho(w)}{\partial w^2} + \frac{\partial \rho(w)}{\partial w} \left( \frac{\alpha}{\gamma} + \frac{3fw}{4\gamma^2\lambda^2} \right) + \rho(w) \left[ \frac{\alpha^2}{4\gamma^2} + \frac{1}{4w^2} + \frac{9f}{8\gamma^2\lambda^2} \right] \\ = - \frac{3}{4\gamma^2\lambda^2\sqrt{w}} \{ \rho(w + w_a)\sqrt{w + w_a}A(w + w_a) \\ + 4\rho(2w + w_i)\sqrt{2w + w_i}I(2w + w_i) \}. \end{aligned} \quad (31)$$

Inserting  $\rho(w) = ye^{\left[\frac{-3fw^2}{16\lambda^2\gamma^2} - \frac{\alpha w}{2\gamma}\right]}$  in 29 and 30 and integrating 31, neglecting  $\alpha$  the equations below are found. If  $\alpha$  cannot be neglected in 31, then  $\alpha$  must be assumed and the velocity distribution calculated, finding  $\alpha$  from equations 42 and 45 and repeating the process until the same value of  $\alpha$  is found for 45 as was used in the distribution.

$$\begin{aligned} \frac{\partial^2 y}{\partial w^2} + \frac{\partial y}{\partial w} \left[ \frac{1}{4w^2} + \frac{3f}{4\gamma^2\lambda^2} - \frac{9f^2w^2}{64\gamma^4\lambda^4} - \frac{3\alpha fw}{8\lambda^2\gamma^3} \right. \\ \left. - \frac{3}{4\gamma^2\lambda^2} (A(w) + I(w)) \right] = 0. \end{aligned} \quad (32)$$

$$\frac{\partial^2 y}{\partial w^2} + \frac{\partial y}{\partial w} \left[ \frac{1}{4w^2} + \frac{3f}{4\gamma^2\lambda^2} - \frac{9f^2w^2}{64\gamma^4\lambda^4} - \frac{3\alpha fw}{8\gamma^3\lambda^2} - \frac{3A(w)}{4\gamma^2\lambda^2} \right] = 0. \quad (33)$$

$$\begin{aligned} \frac{\partial \rho(w)}{\partial w} - \frac{1}{2w} \rho(w) + \frac{3fw}{4\gamma^2\lambda^2} \rho(w) = - \frac{3}{4\gamma^2\lambda^2\sqrt{w}} \left\{ \int_{w_a}^{w+w_a} \rho(w)\sqrt{w}A(w)dw \right. \\ \left. + 2 \int_{w_i}^{2w+w_i} \rho(w)\sqrt{w}I(w)dw \right\}. \end{aligned} \quad (34)$$

If  $A(w)$  and  $I(w)$  are known and  $\alpha$  may be neglected,  $y$  or  $\rho(w)$  can be found from 32 and 33 for  $w > w_a$ , whereas from 34 for  $w < w_a$  one finds

$$\begin{aligned} \rho(w) = D\sqrt{we}^{-\frac{3fw^2}{8\gamma^2\lambda^2}} + \frac{3}{4}\frac{\sqrt{w}}{\gamma^2\lambda^2} e^{-\frac{3fw^2}{8\gamma^2\lambda^2}} \int_w^{w_a} \frac{e^{\frac{3fw^2}{8\gamma^2\lambda^2}}}{w} dw \\ \times \left\{ \int_{w_a}^{w+w_a} A(w)\rho(w)\sqrt{w}dw + 2 \int_{w_i}^{2w+w_i} \rho(w)\sqrt{w}I(w)dw \right\}. \end{aligned} \quad (35)$$

Putting into 35 the values of  $\rho(w)$  for  $w > w_a$ , one obtains  $\rho(w)$  for  $w < w_a$ . In most cases the last terms of 32 and 33 are by far the most important, so that one may write

$$\frac{\partial^2 y}{\partial w^2} - \frac{3y}{4\gamma^2\lambda^2} \{A(w) + I(w)\} = 0, \quad w > w_i; \quad (36)$$

$$\frac{\partial^2 y}{\partial w^2} - \frac{3yA(w)}{4\gamma^2\lambda^2} = 0, \quad w_i > w > w_a. \quad (37)$$

One can assume that

$$I(w) = \frac{C(w - w_i)}{w_i} \quad \text{and} \quad A(w) = b \left( \frac{w - w_a}{w_a} \right),$$

whence

$$\frac{\partial^2 y}{\partial w^2} - sy(w - w_i) = 0, \quad w > w_i; \quad (38)$$

$$\frac{\partial^2 y}{\partial w^2} - ry(w - w_a) = 0, \quad w_i > w > w_a, \quad (39)$$

$s$  and  $r$  being constants. These yield as solutions

$$y = \sqrt{w - w_i} A' iH_{\frac{1}{2}}^{(1)} \left\{ \frac{2i\sqrt{s}}{3} (w - w_i)^{\frac{3}{2}} \right\} \quad \text{for } w > w_i; \quad (40)$$

$$y = \sqrt{w - w_a} BiJ_{\frac{1}{2}} \left\{ \frac{2i\sqrt{r}}{3} (w - w_a)^{\frac{3}{2}} \right\} \\ + \sqrt{w - w_a} CiJ_{-\frac{1}{2}} \left\{ \frac{2i\sqrt{r}}{3} (w - w_a)^{\frac{3}{2}} \right\} \quad (41)$$

for  $w_i > w > w_a$ .  $H_{\frac{1}{2}}^{(1)}$  is a Hankel function of the order  $\frac{1}{2}$ , and  $J_{\frac{1}{2}}$  and  $J_{-\frac{1}{2}}$  are the Bessel functions of the order  $\frac{1}{2}$  and  $-\frac{1}{2}$ .

The constants  $A'$ ,  $B$ ,  $C$ , and  $D$  are to be determined in such a way that  $w$  is continuous for  $w = w_a$ , and  $w = w_i$ , and  $\partial \rho(w)/\partial w$  for  $w = w_i$ . The steady-state velocity distribution has thus been obtained, but its properties can be determined only when numerical values are inserted, because of its complicated form.

The equations can be used for various purposes. The electron mobility  $k_e$  in the field can be found by integrating 22 with

$$k_e = \frac{\int i(w)dw}{\int \rho(w)dw} = \frac{2\lambda e}{3m} \frac{\int \frac{\rho(w)}{\sqrt{w}} dw}{\int \rho(w)dw}.$$

The evaluation of these integrals is very difficult, however.

Townsend's  $\alpha$  can be calculated as follows. Call  $q = N_i W_i / N_{a1} W_{a1}$  the ratio of energy lost by electrons in ionization to that lost in excitation, the number of electrons exciting atoms being  $N_{a1}$  and those ionizing atoms being  $N_i$ :

$$q = \frac{N_i W_i}{N_{a1} W_{a1}} = \frac{C \int_{w_i}^{\infty} w_i \rho(w) \sqrt{w} (w - w_i) dw}{\frac{w_{a1}}{w_a} b \int_{w_a}^{\infty} \rho(w) \sqrt{w} (w - w_a) dw}. \quad (42)$$



Assuming that the loss of energy  $wf$  can be neglected compared to  $w_i$  and  $w_a$ , one can then compute Townsend's  $\alpha$ . In a distance  $dx$  in the field the electrons gain  $ieXd$  from the field, they lose  $\frac{1}{2}N_a mw_a dx$  by excitation and  $\frac{1}{2}N_i mw_i dx$  by ionization, when  $i$  electrons enter  $dx$  and  $i + di$  leave  $dx$ , with an average kinetic energy  $\frac{1}{2}mw_m$ . Hence

$$\frac{2ieX}{m} dx = N_a w_a dx + N_i w_i dx + w_m di. \quad (43)$$

Now  $N_i dx = \alpha i dx$ ,

$$q = \frac{N_i w_i}{N_a w_a} \text{ from equation (42), } \frac{di}{dx} = N_i.$$

$$\frac{2Xe}{m} = w_a \alpha \left( 1 + \frac{1}{q} \right) + \alpha w_m. \quad (44)$$

Solving for  $\alpha$  and dividing by  $p$ , we have, since  $mw_i/2e = V_i$ , the ionizing potential,

$$\frac{\alpha}{p} = \frac{q}{1 + q + \frac{w_m}{w_i} q} \frac{X}{p V_i}. \quad (45)$$

If  $q = N_i w_i / N_a w_a$  is small,  $\alpha$  is not very dependent on the value of  $w_m$ . If one put  $w_m = \frac{1}{2}w_i$ , which is not badly off,

$$\frac{\alpha}{p} = \frac{q}{1 + 1.5q} \frac{X}{p V_i}. \quad (46)$$

Thus if one can calculate  $q$  from  $A(w)$ , and  $I(w)$ ,  $w_a$ ,  $w_i$ ,  $\gamma$ ,  $\lambda$ , etc. (assuming  $\lambda$  constant),  $\alpha/p$  may be found from equation 42 in the restricted regions over which the simplified values of  $A(w)$  and  $I(w)$  hold. For Ne this is possible for  $X/p$  from 5 to 30. Here the constant  $B$  is nearly equal to  $C$  in equation 41. The numerical calculations for Ne made  $\rho(w) = \gamma$ , which is allowable, and  $q$  was evaluated "in a numerical way." The results agree with those of Townsend and McCallum quite well as shown by the points of Fig. 94. This is most strange since the Townsend gases all had Hg contamination and the values of  $\alpha/p$  can be tens of per cent off. For  $X/p > 30$ , the error in the assumption that  $w_m = \frac{1}{2}w_i$  may become too serious.

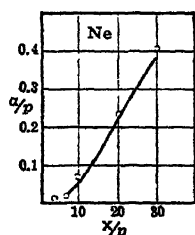


FIG. 94.

Penning showed the losses of energy to elastic collisions at  $X/p = 5$  to be 4 per cent of those for inelastic impacts, so that neglect of these was justified. It is perhaps as much as can be said that the calculations give the correct order of magnitude for  $\alpha/p$  in view of the mathematical complexity and the simplifying assumptions made.

## 7. THE SMIT DERIVATION

J. A. Smit<sup>24</sup> presents by far the most complete calculation of energy distribution for various cases. After setting up the general equations on a principle of detailed balancing for a variety of cases, and including actions neglected by Druyvesteyn for the sake of simplicity, the distribution is actually worked out in He for  $X/p$  from 3 to 10, assuming ionization, excitation, and variable free paths. In Smit's discussion it is pointed out that the problem has been solved for elastic impacts by Druyvesteyn, Morse, Allis, and Lamar and by Davydov, with the added fact that the last deduction includes the assumption of the energy of agitation of the gas atoms, allowing therefore an extension to lower ranges of electron energy.

In this study Smit, as did Davydov, allows for the energy  $E_a$  of the atoms and adds the effect of the variation of  $\lambda$  with  $E$ . He, like the others, assumes isotropy of electron distribution in direction after impact, which appears justified from scattering data at these energies. Since the more complete analyses to be given require a deviation from the analytical procedure of Druyvesteyn, Smit initiates his analysis de novo, arriving as special cases at the solutions of Davydov and Druyvesteyn.

He begins by establishing the following criterion for the stationary or steady state. Electrons alter their energy continually by: (1) Exchange of energy with other electrons. This is later shown to be very complicated and can be neglected for lower densities. For electron densities of the order of 1/1000 that of the atoms, the condition leads to a Maxwellian form of law. At very high electron densities such as those in metals we have the Fermi distribution. At intermediate values the qualitative character of the correction only is found. (2) Movement in the electrical field. (3) Elastic impacts with atoms. (4) Inelastic impacts with atoms. The stationary state is then defined by saying that per cubic centimeter per second the number  $n'$  of electrons passing through a state of energy  $E$  to one of higher energy must be equal to the number  $n''$  of electrons that pass the value  $E$  in the opposite direction. Hence the condition for a steady state is that  $n' - n'' = 0$ , which will in turn define the distribution function  $W(E)$ . For process 1, the energy exchange depends on the electron density. For processes 2, 3, and 4 it does not so depend. Below a certain density of electrons the action of process 1 may be neglected. This will be assumed in what follows.

The energy of an electron passes through  $E$  only in jumps as a result of a collision. This occurs for electrons per cubic centimeter per second ( $n'$ ) or ( $n''$ ) times for elastic collisions and ( $n'$ )<sub>inel.</sub> or ( $n''$ )<sub>inel.</sub> for inelastic collisions, and continuously in traversing a free path  $\lambda$  in the field  $X$ : to wit ( $n'$ )<sub>x</sub> and ( $n''$ )<sub>x</sub> times. From what has been said, balance exists when

$$(n' - n'')_{el.} + (n' - n'')_x = (n'' - n')_{inel.} \quad (47)$$

To see how Smit proceeds, one may evaluate  $(n' - n'')_{\text{el.}}$  with him as follows. In an elastic impact where the energy increases by  $\Delta$  and passes  $E$ , the initial energy lies between  $E - \Delta$  and  $E$ . In this we exclude the condition  $E - \Delta < 0$ , since  $\bar{\Delta} \ll \bar{E}$ , so that  $E - \Delta \geq 0$ . Call  $[n'(\xi, \Delta)]_{\text{el.}} d\Delta d\xi$  the number of impacts per cubic centimeter per second with increase between  $\Delta$  and  $\Delta + d\Delta$  in which the initial energy is between  $\xi$  and  $\xi + d\xi$ . Then it follows that

$$\begin{aligned} (n' - n'')_{\text{el.}} &= \int_0^\infty d\Delta \int_{E-\Delta}^E d\xi [n'(\xi, \Delta) - n''(\xi + \Delta, \Delta)]_{\text{el.}} \\ &\approx \int_0^\infty d\Delta [n'(\eta, \Delta) - n''(\eta + \Delta, \Delta)]_{\text{el.}} \Delta. \end{aligned} \quad (48)$$

Here  $\eta$  is a definite energy value between  $E - \Delta$  and  $E$ . This approximation is permissible because  $\bar{\Delta} \ll \bar{E}$ . In elastic exchange between electrons of energy  $E$  and atoms  $E_A$   $\bar{\Delta}$  is of the order of  $\sqrt{E_A E (m/M)}$ , where  $m$  and  $M$  are the masses of electrons and atoms respectively. In general, one may write

$$[n'(E, \Delta)]_{\text{el.}} = NW(E) [k'(E, \Delta)]_{\text{el.}}$$

Here  $NW(E)dE$  is the number of electrons per cubic centimeter per second with energy between  $E$  and  $E + dE$ .  $k'(E, \Delta)d\Delta$  is the chance per second that an electron of kinetic energy  $E$  will increase its energy by an amount between  $\Delta$  and  $\Delta + d\Delta$ . In this expression  $k'$  is independent of  $W(E)$  but depends on the average atomic energy  $E_a$ . The ratio  $[k'(E, \Delta)] / [k''(E + \Delta, \Delta)]_{\text{el.}}$  can be found since free electrons in the absence of a field  $X$  share in the Maxwellian distribution of gas atoms. Even for electrons one may apply the principle of detailed balancing, under these circumstances, which says that

$$n'(E, \Delta) dE d\Delta = n''(E + \Delta, \Delta) dE d\Delta,$$

in which only elastic impacts with gas atoms are to be regarded. If  $L(E)$  is the Maxwellian distribution of electron and gas atom energies, one may write

$$NL(E)[k'(E, \Delta)]_{\text{el.}} = NL(E + \Delta)[k''(E + \Delta, \Delta)]_{\text{el.}},$$

whence the ratio 49 becomes

$$\left[ \frac{k'(E, \Delta)}{k''(E + \Delta, \Delta)} \right]_{\text{el.}} = \frac{L(E + \Delta)}{L(E)}. \quad (49)$$

This can be introduced into the calculation of  $(n' - n'')_{\text{el.}}$  in equation 48, which gives as an approximation for the expression in 48 under the integral sign

$$\left[ -\Delta \frac{d}{dE} \frac{W(E)}{L(E)} / 2 \frac{W(E)}{L(E)} \right] [n(E, \Delta)]_{\text{el.}}. \quad (50)$$

Here  $n(E, \Delta) Ed\Delta$  is the number of electrons per cubic centimeter per second which by a jump in energy of  $\Delta$  to  $\Delta + d\Delta$  leave the energy interval  $(E, E + \Delta)$ . The approximation given in expression 50 is again allowable since  $\bar{\Delta} \ll \bar{E}$ . Substitution gives the equation

$$(n' - n'')_{el.} = \frac{1}{2} \left[ \int_0^\infty n(E, \Delta) \Delta^2 d\Delta \right]_{el.} \frac{d}{dE} \left( \log \frac{L(E)}{W(E)} \right). \quad (51)$$

A simple kinetic-theory consideration, in which  $\Delta^2$  is averaged over the various possible collision processes, yields

$$\bar{\Delta}^2 = \frac{8}{3} \frac{m}{M} \left( \bar{E}_a + 2 \frac{m}{M} E \right),$$

in which, in the more important applications,  $\bar{E}_a \gg (2m/M)E$ . On the basis of kinetic theory this then leads to the evaluation

$$\left[ \int_0^\infty n(E, \Delta) \Delta^2 d\Delta \right]_{el.} = N \sqrt{\frac{2}{m}} \frac{8}{3} \frac{m}{M} \frac{1}{\lambda} \bar{E}_a E^{3/2} W(E), \quad (52)$$

$$(n' - n'')_{el.} = N \sqrt{\frac{2}{m}} \frac{4}{3} \frac{m}{M} \frac{1}{\lambda} \bar{E}_a E^{3/2} \left\{ W(E) \frac{d}{dE} \log L(E) - \frac{dW(E)}{dE} \right\}, \quad (53)$$

in which

$$\frac{d}{dE} \log L(E) = \frac{1}{2E} - \frac{3}{2\bar{E}_a}.$$

A similar procedure is next used to calculate  $(n' - n'')_x$ . In this calculation the number of electrons passing  $E$  due to gain from the field is first computed from

$$[n'(E, \Delta)]_x dE d\Delta = N W(E) [k'(E, \Delta)]_x dE d\Delta,$$

assuming that the paths are not bent by the field. After setting up and determining the integrals equivalent to 48 for this case, the correction for the curvature of the paths is computed by means of the mobility equation and introduced, leading to the expression

$$(n' - n'')_x = N \sqrt{\frac{2}{m}} \left( \frac{1}{6} X^2 e^2 \lambda E^{-1/2} W(E) - \frac{1}{3} X^2 e^2 \lambda E^{1/2} \frac{dW(E)}{dE} \right). \quad (54)$$

To calculate  $(n'' - n')_{inel.}$  it is to be noted that all collisions have been included in the *elastic* impact losses. The number of collisions of an electron per centimeter is  $1/\lambda$ .  $(n'' - n')_{inel.}$  now tells us how many electrons as a result of *inelastic* impacts pass through the energy value  $E$ . Since the higher electronic states are normally absent, one need regard only excitation and ionization of the ground state. That is, only one potential for each is needed. The absorbing cross section  $Q_i$  or  $Q_e$  is also in general an increasing function of  $E$ . Hence, with the large

cross-sections encountered, it is clear that in general the electrons making inelastic impacts at  $E$ , or  $E_e$  will have low values  $E_2$  of its residual energy. Thus without much inaccuracy one may assume that each inelastic impact results in an electron going from above  $E$  downward, at least for energies above  $E > 1$  volt. Hence one can write that  $(n'' - n')_{\text{inel.}} = (n'')_{\text{inel.}}$  such that

$$(n'')_{\text{inel.}} = N \sqrt{\frac{2}{m}} N_a \int_E^\infty \alpha(\xi) \xi^{1/2} W(\xi) d\xi. \quad (55)$$

Here  $N_a$  is the number of atoms per cubic centimeter;  $\alpha(\xi)$  is the sum of all the absorbing cross sections of all excitation and ionization levels.

Therefore, introducing expressions 53, 54, and 55 into 47, one obtains

$$\begin{aligned} \frac{2}{3} \frac{m}{M} \frac{1}{\lambda} \bar{E}_a E^{1/2} W(E) - 2 \frac{m}{M} \frac{1}{\lambda} E^{3/2} W(E) - \frac{4}{3} \frac{m}{M} \bar{E}_a \frac{1}{\lambda} E^{3/2} \frac{dW(E)}{dE} \\ + \frac{1}{6} X^2 e^2 \lambda E^{-1/2} W(E) - \frac{1}{3} X^2 e^2 \lambda E^{1/2} \frac{dW(E)}{dE} \\ = N_a \int_E^\infty \alpha(\xi) \xi^{1/2} W(\xi) d\xi, \end{aligned} \quad (56)$$

so that

$$F_0 W(E) + F_1 \frac{dW(E)}{dE} + r = 0, \quad (57)$$

$$F_0 = -\frac{F_1}{2E} + \frac{2m}{M} \frac{1}{\lambda} E^{3/2}, \quad (58)$$

$$F_1 = \frac{4}{3} \frac{m}{M} \frac{1}{\lambda} \bar{E}_a E^{3/2} + \frac{1}{3} X^2 e^2 \lambda E^{1/2}, \quad (59)$$

$$r = N_a \int_E^\infty \alpha(\xi) (\xi)^{1/2} W(\xi) d\xi, \quad (60)$$

which is a constant for  $E < E_e$ . The equation does not hold for  $E < 1$  volt. This general solution may now be applied to special cases.

A. No inelastic impacts.  $\lambda$  independent of  $E$ . Then

$$r = 0, \quad \frac{dW(E)}{dE} = -W(E) \frac{F_0}{F_1}.$$

This yields at once

$$W(E) = C_3 E^{1/2} \left[ \left( 1 + \frac{E}{\Omega} \right)^\Omega \right]^{\frac{1}{kT}} = C_2 E^{1/2} (E + \Omega)^{\frac{\Omega}{kT}} e^{-\frac{E}{kT}}, \quad (61)$$

with

$$\Omega = \frac{1}{4} X^2 e^2 \lambda^2 \frac{m}{M} \frac{1}{\bar{E}_a}, \quad \bar{E}_a = \frac{3}{2} kT.$$

The equation starred is Davydov's equation.

1. If  $\frac{1}{2} X e \lambda \sqrt{M/m} \ll \bar{E}_a$ ,  $\Omega \ll \bar{E}_a$ ,  $\bar{E} \approx \bar{E}_a$ . In this case

$$W(E) = C_4 E^{3/2} e^{\frac{\Omega}{kT}} e^{-\frac{E}{kT}}, \quad (62)$$

with

$$\frac{1}{C_4} = (kT)^{\frac{\Omega}{kT} + \frac{3}{2}} \Gamma\left(\frac{\Omega}{kT} + \frac{3}{2}\right).$$

For  $\frac{1}{2} X e \lambda \sqrt{M/m} / \bar{E}_a \rightarrow 0$ , the limit of  $W(E)$  is

$$W(E) = \frac{2}{\sqrt{\pi}} \frac{E^{3/2}}{(kT)^{3/2}} e^{-\frac{E}{kT}}, \quad (63)$$

which is Maxwell's law with  $\bar{E} = \bar{E}_a$ . Hence the deviation from Maxwell's law due to the field in 62 is given by

$$\left(\frac{E}{kT}\right)^{\frac{\Omega}{kT}} \bigg/ \left[ \frac{2}{\sqrt{\pi}} \Gamma\left(\frac{\Omega}{kT} + \frac{3}{2}\right) \right].$$

2. If  $\frac{1}{2} X e \lambda \sqrt{M/m} \gg \bar{E}_a$ , and  $\bar{E} \ll \Omega$ ,

$$W(E) = C_3 E^{3/2} e^{-\left(\frac{E}{kT}\right) + \frac{\Omega}{kT} \log\left(1 + \frac{E}{\Omega}\right)}. \quad (64)$$

Development in series then yields:

$$W(E) = C_5 E^{3/2} \left(1 + \frac{E^2}{3 \Omega^2 kT}\right) e^{-\frac{E^2}{2 \Omega kT}}, \quad (65)$$

with

$$\frac{1}{C_5} = \frac{1}{2} (2 \Omega kT)^{3/2} \Gamma\left(\frac{3}{2}\right) + \frac{1}{3} (2 kT)^{3/2} \Omega^{3/2} \Gamma\left(\frac{9}{4}\right).$$

In the case of

$$\frac{1}{2} X e \lambda \sqrt{\frac{M}{m}} / \bar{E}_a \rightarrow \infty$$

the limit of  $W(E)$  is

$$W(E) = \left(\frac{2}{2 \Omega kT}\right)^{3/2} \Gamma\left(\frac{3}{2}\right) E^{3/2} e^{-\frac{E^2}{2 \Omega kT}}, \quad (66)$$

with

$$\bar{E} = \frac{4}{\pi \sqrt{6}} X e \lambda \sqrt{\frac{M}{m}} \Gamma^2\left(\frac{5}{4}\right),$$

which is Druyvesteyn's equation. Thus an exchange of energy with atoms in a Maxwellian distribution produces a change in Druyvesteyn's expression by a factor

$$\left(1 + \frac{E^3}{3\Omega^2 kT}\right) / \left\{1 + \frac{5}{3\sqrt{2}} \left(\frac{kT}{\Omega}\right)^{1/2} \frac{\Gamma_2^1}{\Gamma_2^2}\right\}.$$

B. For inelastic impacts.

1. For energies less than  $E_e$ . This applies to the positive column in Ne at low electron densities. Here

$$\frac{4}{3} \frac{m}{M} \frac{1}{\lambda} \bar{E}_a E^{3/2} \ll \frac{1}{3} X^2 e^2 \lambda E^{1/2}.$$

The energy is less than 20 volts but  $> 1$  volt, and  $\bar{E} > 1$  volt. Thus one has

$$\frac{dW(E)}{dE} + \left(2g_1 E - \frac{1}{2} E^{-1}\right) W(E) + 2g_2 E^{-1/2} = 0, \quad (67)$$

with

$$g_1^{-1} = \frac{1}{3} X^2 e^2 \lambda^2 \frac{M}{m}, \quad \text{and} \quad g_2 = \frac{3r}{2X^2 e^2 \lambda^2}.$$

If  $\lambda$  is constant,

$$W(E) = C \eta^{1/2} e^{-\eta^2} - g_1^{1/2} g_2 \eta^{1/2} e^{-\eta^2} \bar{E} i(\eta)^2, \quad (68)$$

where

$$\eta = g_1^{1/2} E, \quad \text{and} \quad \int_a^b \frac{e^{-x} dx}{x} = \bar{E} i(x) \Big|_a^b.$$

2. Above  $E > E_e$ , i.e., above excitation, the equation one has for the stationary state

$$-F_0 W(E) - F_1 \frac{dW(E)}{dE} = N_a \int_E^\infty \xi^{1/2} \alpha(\xi) W(\xi) d\xi,$$

so that

$$\begin{aligned} -F_0 \frac{dW(E)}{dE} - \frac{dF_0}{dE} W(E) - F_1 \frac{d^2 W(E)}{dE^2} - \frac{dF_1}{dE} \frac{dW(E)}{dE} \\ = -N_a E^{1/2} \alpha(E) W(E). \end{aligned} \quad (69)$$

In general, however,

$$\left| \frac{dF_0}{dE} W(E) + \frac{dF_1}{dE} \frac{dW(E)}{dE} \right| \ll \left| F_0 \frac{dW(E)}{dE} + F_1 \frac{d^2 W(E)}{dE^2} \right|,$$

whence to a good approximation

$$F_1 \frac{d^2 W(E)}{dE^2} + F_0 \frac{dW(E)}{dE} = N_a E^{1/2} \alpha(E) W(E), \quad (70)$$

in which  $F_1$  and  $F_0$  can be regarded as constants. In addition, experiment shows that to a good approximation  $E^{1/2}\alpha(E) = \beta(E - E_0)$ . The equation then becomes

$$\frac{d^2 W(E)}{dE^2} + 2F_2 \frac{dW(E)}{dE} = F_3(E - E_0)W(E), \quad (71)$$

with

$$F_2 = \frac{F_0}{2F_1}, \quad F_3 = \frac{N_a\beta}{F_1}.$$

The general solution is

$$W(E) = x^{1/2} e^{-F_2(E-E_0)} [A_1^{1/2} J_{-1/2}(\frac{2}{3}ix^{3/2}) - Bi^{-1/2} J_{1/2}(\frac{2}{3}ix^{3/2})], \quad (72)$$

where  $J_{\pm 1/2}$  is a Bessel function and  $x = F_3^{1/2}(E - E_0) + F_2^2 F_3^{-3/2}$ .

The theory is next utilized for evaluation of  $W(E)$  for He. In this calculation the variation of  $\lambda$  with  $E$ , i.e.,  $Q(E)$ , as well as  $Q_a$  and  $Q_i$  from Maier-Leibnitz for He, are used.

The experimental variations and the analytical forms of these functions as used are given in Figs. 95A and 95B. The full curve is the

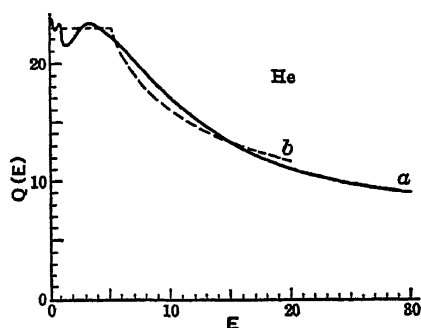


FIG. 95A.

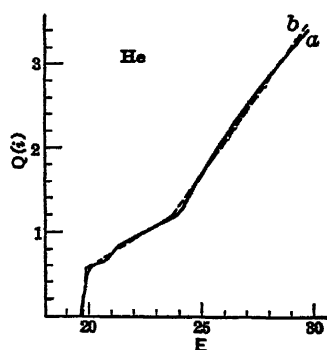


FIG. 95B.

curve for  $Q(E)$ ; the dotted curve is the assumed curve for which  $0 \leq E \leq 5$  and  $\lambda = 1/(23p)$ ,  $5 \leq E \leq 19.8$ ,  $\lambda = (1/23\sqrt{5}p)E^{1/2}$ ,  $19.8 \leq E$ ,  $1/\lambda (d\lambda/dE) = 0.02$ . For the excitation and ionization function, Maier-Leibnitz data corrected for 1 volt breadth of energy distribution were used idealized, following  $b$ .

$$19.8 \leq E \leq 23.6, E^{1/2}Q(i) = 0.16(E - 16.5);$$

$$E_0 = 16.5 \quad \text{and} \quad N_a\beta = 0.16p,$$

$$23.6 \leq E, E^{1/2}Q(i) = 0.37(E - 20.5),$$

$$E_0 = 20.5, N_a\beta = 0.37p.$$



Solution of the very complicated equations, in some regions resorting to graphical integrations, gave the curves of Fig. 96 for electrons in He at values of  $X/p$  of 3, 4, 6, and 10. Finally it was possible to calculate the fraction of the energy gained by electrons which was lost to elastic

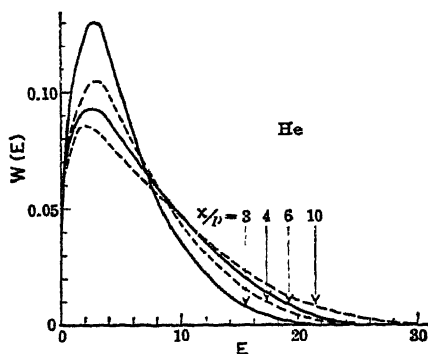


FIG. 96.

collisions. This is shown in Table XIV as the number of inelastic and elastic collisions divided by  $pN\sqrt{2/m}$ , where  $N$  is the number of free electrons per cubic centimeter, and  $p$  is the pressure in millimeters of mercury.

TABLE XIV

| $X/p$ | $\bar{E}$ | $E_{el.}$            | $E_{inel.}$ | $E_{total}$ |
|-------|-----------|----------------------|-------------|-------------|
| 3     | 5.55      | 0.0735               | 0.0195      | 0.094       |
| 4     | 6.4       | 0.087                | 0.081       | 0.165       |
| 6     | 7.0       | 0.095                | 0.28        | 0.37        |
| 10    | 7.7       | 0.11                 | 0.87        | 1.0         |
|       |           | times $pN\sqrt{2/m}$ |             |             |

### 8. THE STUDIES OF ALLIS, ALLEN, AND TONKS

In a series of recent articles, Allis and Allen,<sup>25</sup> Allen,<sup>26</sup> and Tonks and Allis<sup>27</sup> apply the method of Morse, Allis, and Lamar to several important cases. The first article deals with a study of the significance of the Townsend estimate of the average electron energy in a field and the electron mobility, using the lateral diffusion and magnetic deflection methods. As will be recalled, Townsend measured the factor  $\eta$  by which the electron energies exceeded the atomic energies from his study of the ratio of diffusion to mobility as given by the lateral spreading of a beam of electrons in a vertical field  $X$  in a gas. The ratio of currents received by concentric circular electrodes could be related to the expression  $N_e X / \eta P$  between the Faraday constant for an elec-

tron, the field strength  $X$ , the gas pressure at N.T.P.,  $P$ , and the factor  $\eta$ . Since, however, the coefficient of diffusion  $D$  and mobility  $K$  for electrons are related to the quantity  $N_e, \eta P$  by the relation  $K/D = N_e/\eta P$ , and since  $P = \frac{1}{3} N M C_M^2$ , and  $KX = v_e$ , where  $v_e$  is the drift velocity, and as  $\frac{1}{2} m C_e^2 = \frac{3}{2} k T_e$ , where  $C_e$  is the rms random velocity of the electrons and  $T_e$  the equivalent electron "temperature," we have  $T_e = eXD/kv_e$ . This would be the electron temperature if the distribution of the electron velocities were Maxwellian. This temperature is measured by Townsend. The drift velocity was measured by a deflection of the beam of electrons by a magnetic field  $H$  while the electrons are moving in an electrical field  $X$  in the gas. The angle of deflection  $\theta$  of the beam on an assumed Maxwellian distribution is then  $\tan \theta = H v_e / X$ . It is necessary to study the effect of the non-Maxwellian distribution on these essential measurements. The first paper proceeds to deduce the drift velocities  $v_e$  and diffusion coefficients with the Druyvesteyn distribution, assuming constant Ramsauer cross sections. This gives the values of  $v_e$  and  $D$  as

$$v_e = \frac{\left(\frac{3m}{M}\right)^{1/4}}{3\Gamma_{\frac{3}{4}}} \left(\frac{2\pi X e \lambda}{m}\right)^{1/2}, \quad (73)$$

$$D = \frac{\lambda}{3\Gamma_{\frac{3}{4}} \left(\frac{3m}{M}\right)^{1/4}} \left(\frac{2X e \lambda}{m}\right)^{1/2}. \quad (74)$$

Further analysis indicates how the energy distribution differs from the one assumed, and how it changes from point to point. The magnetic field changes the energy distribution as well as the direction of drift by reducing the number of high velocity electrons. It is shown that for the average deflection,  $\tan \theta$  differs from  $H v_e / X$  in the amount  $\tan \theta = 1.06 H v_e / X$ . The correction, it is seen, is of the order of 6 per cent. It is thus evident that the determinations of the various quantities given on page 180 by Townsend's measurements are somewhat uncertain but not seriously so.

The second paper is of interest in that it evaluates the change in the distribution law for elastic collisions introduced by the variable Ramsauer free paths or cross sections in He, A, and Ne. This is an accurate solution of the Morse, Allis, and Lamar distribution in the sense indicated by Bradbury. The values used for the cross sections are those of Ramsauer and Kollath and Normand. The Ramsauer cross sections  $Q$  divided by  $\sqrt{M}$ , the atomic weight, and multiplied by  $10^{-12}$  are plotted against  $X/p$  in Fig. 97. The resulting distributions are plotted as  $E f_0$ , where  $E$  is the energy and  $f_0$  the probability, against  $\sqrt{E}$  in Fig. 86. The average energy is indicated by  $\bar{E}$ , and the curves are computed for the same energy. The curve for Ne with nearly con-

stant cross section is close to the normal Druyvesteyn or Morse, Allis, and Lamar distribution. The curve for A is, as was shown by Brad-

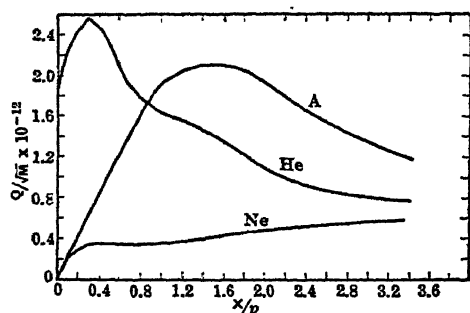


FIG. 97.

bury, steeper on the high energy side, but is adjusted to have the rms velocity *the same average value as the others*. The most probable velocity is higher in this case than the rms velocity. This indicates that the number of fast electrons is fostered by  $\lambda$  decreasing with increasing  $E$ . However, there are far fewer *very* fast electrons, as Bradbury and Nielsen's work indicated.

In He the effect is the reverse of that for A, and is much smaller as predicted by the previous analysis.

A very rough approximation for the distribution with *inelastic* impacts was attempted. The calculation is not comparable in rigor with Smits for He. Miss Allen concludes that "This distribution function (obtained with reasonably constant cross section) should hold up to the first resonance potential where it should be joined by some other function whose form will depend on the total inelastic cross section at all energies above the resonance potential. As this is an unknown quantity, some simpler assumption must be made. The simplest is to keep the above function up to some point where it crosses the axis for  $E = E_1$ , leaving  $E_1$  as an *adjustable* parameter which should, however, fall between the first resonance potential and the ionization potential. There is some justification for assuming that there are practically no electrons above a certain energy in the measurements of Kelly (Doctor's Thesis, Massachusetts Institute of Technology, June, 1936) who finds that in He the distribution follows a smooth curve attaining the axis about the second resonance potential." Such a distribution is shown in Fig. 87. With the data at hand the theory was checked against the electron drift velocity data of Townsend and Bailey, Bailey, and of Nielsen for He, Ne, and A. The agreement is fairly good in some cases, as shown in Chapter IV. In general the rather incomplete theory is not satisfactory, inasmuch as there is an arbitrary choice as to the intercept  $E_1$ . The values for the electron "temperatures"  $T_e = XeD/kv_e$  from Townsend's data do not agree with the value of  $E_1$  needed to fit the curves for  $v_e$ , the drift velocity, with observation.

This means that, if Townsend's method evaluates the *average* energy (i.e.,  $T_e$ ), then, using  $E_1 = 15.6$  volts in the case of A as the intercept for the curve, we can get agreement between average energy

and the point where the curve strikes the axis. But this estimate of  $E_1$  is *not in agreement with the velocity curve*. If Townsend's measurement gives the most probable velocity,  $\alpha_e$ , instead of  $\sqrt{c^2}$ , then the estimate of  $T$  from  $v_e$  is consistent with the use of  $E_1 = 11.57$  volts and with the mobility. It is impossible to decide whether the difficulty lies in the impure Hg-contaminated A used by Townsend in measuring  $T_e$ , or at any rate the difference in purity of Townsend's A and that used by Nielsen in measuring  $v_e$ , or whether this result indicates that Townsend's measurements yield an average that does not correspond to  $\sqrt{c^2}$ .

It is seen from the foregoing that the developments in recent years have clarified the questions of energy distribution and mobilities immeasurably. They have yielded several procedures which are applicable to individual problems. In the absence of any good experimental data they furnish the only source of information. The results to be achieved can be made as rigorous as the data on hand and the pains taken in mathematical manipulation allow. The chief difficulty is that, owing to the wide variation of parameters for different gases, together with the many such parameters needed, no general solution is of any immediate value. Thus long, intricate, and tedious procedures are required for the solution in any one particular case.

#### 9. REFERENCES FOR PART A, CHAPTER V

1. W. HARRIES, *Z. Physik*, **42**, 26, 1927.
2. H. RAMIEN, *Z. Physik*, **70**, 353, 1931.
3. R. SEILER, *Z. Physik*, **83**, 789, 1933.
4. MAIER-LEIBNITZ, *Z. Physik*, **95**, 499, 1935.
5. B. F. PIDDUCK, *Proc. Roy. Soc., A* **88**, 296, 1913.
6. K. T. COMPTON, *Phys. Rev.*, **7**, 489, 501, 509, 1916; **9**, 234, 1918.
7. G. HERTZ, *Z. Physik*, **32**, 298, 1925.
8. H. SPONER, *Z. Physik*, **7**, 185, 1921.
9. HARRIES and HERTZ, *Z. Physik*, **46**, 177, 1928.
10. M. J. DRUYVESTEYN, *Physica*, **10**, 69, 1930.
11. PENNING and DRUYVESTEYN, *Z. Physik*, **52**, 197, 1928.
12. G. HERTZ, *Z. Physik*, **32**, 302, 1925.
13. M. J. DRUYVESTEYN, *Physik. Z.*, **33**, 836, 1932.
14. DIDLAUKIS, *Ann. Physik*, **5**, 221, 1930; *Z. Physik*, **82**, 709, 1933.
15. A. M. CRAYATH, *Phys. Rev.*, **46**, 332, 1934.
16. J. S. TOWNSEND, *Phil. Mag.*, **9**, 1158, 1930.
17. EMMELÉUS, LUNT, and MEEK, *Proc. Roy. Soc., A* **156**, 394, 1936.
18. MORSE, ALLIS, and LAMAR, *Phys. Rev.*, **48**, 412, 1935.
19. H. A. LORENTZ, *The Theory of Electrons*, 2nd Edition, p. 267, Teubner, Leipzig, 1916.
20. R. A. NIELSEN, *Phys. Rev.*, **50**, 950, 1936.
21. B. DAVYDOV, *Physik. Z. der Sowjetunion*, **8**, 59, 1935.
22. M. J. DRUYVESTEYN, *Physica*, **3**, 65, 1936.
23. DRUYVESTEYN and KRUTHOF, *Physica*, **4**, 440, 1937.
24. J. A. SMIT, *Physica*, **3**, 543, 1937.
25. ALLIS and ALLEN, *Phys. Rev.*, **52**, 703, 1937.
26. HARRIET W. ALLEN, *Phys. Rev.*, **52**, 707, 1937.
27. TONES and ALLIS, *Phys. Rev.*, **52**, 710, 1937.
28. W. B. NOTTINGHAM, *Phys. Rev.*, **55**, 203, 1939.

## PART B. THE THEORY AND USE OF PROBES AND THE INFLUENCE OF THE DISTRIBUTION OF ELECTRON ENERGIES ON THE INTERPRETATION OF PROBE MEASUREMENTS \*

### 1. INTRODUCTION

The problem of determining the energy distribution of electrons in an electrical field experimentally under the various conditions where this is desirable has never been successfully solved.

For a beam of electrons in a gas Townsend has shown that, by observing the velocity of lateral diffusion of the electrons relative to their drift velocity parallel to a uniform field, one could evaluate the average terminal energy  $\frac{1}{2}\eta mC^2$  of the electrons. This method is applicable only as long as electrons do not ionize atoms by impact in the field. Though possible if the ionization probabilities are known, it is unlikely that the theory can be modified when ionization by impact becomes considerable. Since the studies of the Townsend group extend slightly into a range of  $X/p$  in most gases where ionization by collision has begun, one cannot place too much emphasis on their values of  $\eta$  and  $\lambda$  in that region. Furthermore, their method of study tells us nothing of the form of the distribution law and hence of the relation of the most probable and average velocities to the high energy value beyond which there are relatively negligible numbers of electrons. Thus in the region of low energies only part of the problem is solved, and that rather incompletely.

There is, however, another important set of conditions in discharge phenomena from which can be gained some knowledge concerning not only the average energies of the electrons but perhaps also the energy distribution of electrons. The method applicable to these conditions is that of the electrical probe initiated and developed in a large measure by Langmuir and H. Mott-Smith, Jr.,<sup>1</sup> in 1923, and later by Langmuir<sup>2</sup> and his other associates. Subsequently the development has been carried on by many other workers as well, and the probe has become one of the valuable instruments of the physicist working on discharge tubes.<sup>3,4,5</sup> The probes are primarily applicable to discharge phenomena giving high ion densities of both signs, such as one observes in the luminous positive column in discharge tubes. This region of the discharge, or the state of the gas, has aptly been termed plasma by Langmuir. Its prime requisite is a high conductivity caused by a high

\* References for Part B of Chapter V will be found on page 256.

density of ionization. In principle the electrical probe is not new, for elementary students in physics in studying and mapping the potential field about conducting surfaces use a good conducting electrolytic bath and a probe of high resistance drawing little current with an instrument showing zero current. The primary requisite of a probe is that it must not alter the field and that therefore its effective resistance must be large compared to that of the medium in which it is to be used. This condition happens to exist in the plasma of discharge tubes.

Another circumstance facilitating such studies happens to follow from the character of the energy distribution in many discharges. At *very low* fields the electron and ion energy distributions are not far from Maxwellian. Owing to free paths that vary with energy and to an energy loss which is a function of energy, the electrons at higher fields, however, depart radically from the Maxwellian energy distribution and even from the Druyvesteyn distribution. The latter distribution for constant free paths and a fractional electron energy loss  $f = 2.66 m/M$  is a consequence of the very low value of  $f$  for electrons in many gases. As has been seen, these deviations are most important, especially in the high-energy end of the distribution. In the case of the positive and negative *ions* the fractional loss of energy at impact is large. While there is some variation of angle of scattering in collisions with energy and with changing masses which follows quantum-mechanical rather than classical scattering laws, especially at low energies and for larger angles, the deviations are not serious. It is thus doubtful whether the distribution of energies among the *ions* in a gas of molecules of nearly the same mass is ever very far from Maxwellian even at higher positive-ion energies. At very high densities of ionization, i.e., of the order of  $10^{12}$  ions/cm<sup>3</sup>, the average distance between electrons is  $10^{-4}$  cm. At this distance the field of one electron is of the order of 10 volts/cm., and the potential energy of one electron in the field of the other is of the order of one-fifth the energy of thermal agitation. Thus the electrons are exchanging energy rather frequently with one another. As a result, theory indicates that the electrons redistribute their energy among themselves, and the energy distribution is again Maxwellian. Thus in the plasma of gaseous discharges at high ion densities the electrons are again in a condition approaching a Maxwellian energy distribution. At much smaller densities, i.e., of the order of  $10^9$  ions/cm<sup>3</sup>, even despite an inadequate explanation the Maxwellian distribution still appears to hold.<sup>37</sup> This fortunate condition not only makes it possible to use the probe measurements to determine the energy distribution of the electrons, assuming other disturbing factors non-operative, but also permits one to apply the analysis derived from an assumed Maxwellian distribution of electrons and positive ions to evaluate certain important parameters of the gaseous discharge from the measurements. These parameters are the average energy of the electrons and positive ions, the densities of

the electrons and positive ions, and the plasma potential of an isolated electrode under the influence of positive ion and electron bombardment in contact with the plasma. This latter potential relative to the plasma potential determines the wall current, i.e., carrier loss to the walls of the discharge tube, at the point in question. The energies of the electrons and positive ions under these conditions are usually expressed in terms of the electron "temperature"  $T_-$  or the ion "temperature"  $T_+$  which are derived from the average energies assuming a Maxwellian energy distribution on the usual kinetic-theory basis. If the energy distribution is not Maxwellian the quantities  $T_-$  and  $T_+$  denote an energy on the assumed Maxwellian distribution which, though not a true temperature, gives a convenient measure of the electron energy. Again, fortunately as we shall see, the derivation of the electron energy, or  $T_-$ , from the experimental data gives a criterion, on the basis of the linearity of a plotted curve, for the existence of a closely Maxwellian distribution. Thus even if the only slightly different Druyvesteyn energy distribution existed, the fact that probe measurements single out the sensitive asymptotic high-energy portion of the distribution law would lead to a marked departure from the linear relation. The departure of the positive-ion distribution from the Maxwellian form, however, is not indicated from the data, but it is hardly likely that the deviations are serious. Hence with the linearity of the electronic curves the legitimacy of the temperature measurement is assured. Where deviations are indicated the possibility of the departure being ascribed to disturbing agents probably in most cases precludes a direct determination of the correct distribution law by this means.

Finally it also fortunately happens that the disturbance of the plasma by the presence of the probe is usually largely prevented by the action of the space-charge sheath which separates the electrode surface with its complicating actions sufficiently from the plasma to reduce its alterations on the plasma to a minimum. The precision of the quantities evaluated by probe measurements varies rather widely with the quantities measured. For plane probes the electron temperatures may be evaluated to perhaps 1 per cent. The evaluation of the electron and ion densities is not nearly so reliable; neither is that of positive-ion temperatures. Under some circumstances the evaluations are good in order of magnitude only.

The theory of probe measurements is in the main scattered through the hundred or more original papers on various applications and studies of probe measurements. Darrow in his book *Electrical Phenomena in Gases*, Williams and Wilkins, Baltimore, 1932, page 344 and following, gives a rather complete list of papers and a detailed critical account of the work. An exceptionally clear condensed presentation of probe theory with unfortunately only too meager a bibliography is given by v. Engel and Steenbeck in their book *Elektrische Gasentladungen*, Springer, Berlin, 1934, Vol. II, §14-16. Their general approach in

the presentation of the subject will largely be followed in this section, as it seems to be the only direct and logical treatment of the subject and in principle cannot be improved upon. A few of the principal earlier articles will be cited, as will a few of the later papers written subsequent to 1934 which appear to be of importance. In making this presentation it must be emphasized that this represents the *idealized theory* of what occurs in a probe analysis. The vital simplifying assumptions will be clearly pointed out. In actual practice many deviations from the ideal will be encountered. At the end of the presentation some of these complications will be indicated together with their causes. Since this discussion can in no sense be considered exhaustive, the details will be left to be found by the reader in the references given. It is believed that the theory here given will suffice to afford the reader a clear notion of the principles and operation of a probe, as to what can be learned from it under ideal conditions, and to place him in a position intelligently to follow further more detailed studies or allusions to probe measurements in the literature. The references given here cover the high points of the earlier literature.

## 2. GENERAL ASSUMPTIONS

In a plasma where electrons do not attach to make ions one may assume  $N_-$  electrons per cubic centimeter and  $N_+$  positive ions per cubic centimeter and that  $N_+ = N_-$ . The last assumption arises from the circumstance that one assumes the ions to be created in the volume of the plasma from neutral molecules and that, except near walls or electrodes or in the dark spaces of the discharge, the action of space charges in the dense ionization would preclude any great disparity in numbers in the weak fields existing in plasma. If electrons attach to form negative ions  $N_+ = N_- + N_{i-}$ , where  $N_{i-}$  is the concentration of negative ions. The presence of negative ions in appreciable quantities would very much complicate the interpretation and will not be considered as in most discharge tubes they do not occur.

In a Maxwellian distribution of energies  $\frac{1}{2}m_-C_-^2 = \frac{1}{2}MC^2\eta = \frac{3}{2}\eta kT = \frac{3}{2}kT_- = eu_-$ , where  $m_-$  is the mass of the electron;  $M$  that of a molecule;  $C_-$  is the root mean square velocity of the electrons;  $C$  that of the gas molecules;  $\eta$  is the Townsend factor, see page 179;  $T$  is the gas temperature;  $T_-$  the electron temperature;  $k$  the Boltzmann constant, see page 644; and  $u_-$  is the average electron energy expressed in volts, see page 183. For the positive ions the average energy may be above that of the molecules, and with a Maxwellian energy distribution one may also write

$$\frac{1}{2}M_+C_+^2 = \frac{1}{2}MC^2\eta' = \frac{3}{2}\eta'kT = \frac{3}{2}kT_+ = eu_+.$$

Here  $M_+$  is the mass of the positive ions (usually equal to  $M$ ),  $C_+$  is the root mean square velocity of the ions,  $\eta'$  the ionic analog of Townsend's



$\eta$  for electrons (usually  $\eta' \ll \eta$ ),  $T_+$  the temperature of the positive ions, and  $u_+$  is the average energy in equivalent volts. Again it should be recalled that simple kinetic theory gives the number of molecules  $\nu$  of average velocity  $\bar{c}$  striking unit area per second from a space where there are  $N$  molecules per cubic centimeter, as  $\nu = N\bar{c}/4 = NC/\sqrt{6\pi}$ .<sup>38</sup> Here the quantity  $\bar{c}$  is the average velocity while  $C$  is the rms value. Finally the Maxwellian distribution of velocities gives the number of molecules having a component of velocity along the  $x$  axis as

$$N_x = \frac{N}{\alpha\sqrt{\pi}} e^{-\frac{c_x^2}{\alpha^2}} dc_x,$$

as shown on page 654. Here  $\alpha^2 = 2kT/M$ , and  $\alpha$ ,  $\bar{c}$ , and  $C$  are in the ratios  $1:2/\sqrt{\pi}:\sqrt{3/2}$ . These equations can be carried over to electrons and ions with appropriate changes in subscript.

### 3. NATURE OF A PROBE MEASUREMENT

When a probe is used it usually is inserted into the plasma existing between two electrodes which are maintaining the discharge. There is thus a fall of potential down the tube from the anode to the cathode, and each point of the plasma has its appropriate value of the potential.

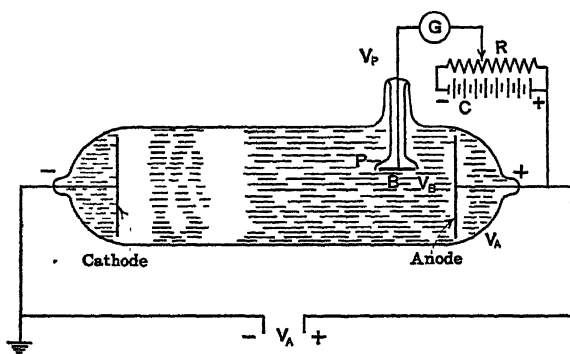


FIG. 98.—Probe Arrangement in a Glow Discharge.

Let us now assume such a discharge and place a plane parallel probe electrode,  $P$ , with its surface parallel to the axis of the tube and its center at some point  $B$  in the plasma, of potential  $V_B$ , whose characteristics we desire to determine; see Fig. 98. Assume the cathode grounded and the anode at a potential  $V_A$  to maintain the discharge. By means of the cells  $C$  and the potential divider  $R$  the probe can be made negative to the anode by an amount  $V_A - V_P$  and such that the potential  $V = V_P - V_B$  can be made positive or negative by several tens of volts if desired. A galvanometer or microammeter  $G$  inserted

in the probe circuit enables one to measure the probe current  $i$  as the potential  $V$  is altered. From the variation of the current  $i$  as a function of  $V$  the various desired quantities can be determined. In some cases the *current density*  $j$  is more useful and will be used. Since the theory of the plane probe is devoid of certain complicating geometrical factors it is best to use this probe for the analysis of the problem. Such a probe in theory should have a fairly large surface and should be shielded on the back and sides. Owing to its space extension it is not local in its indications, but it is in general more accurate except where rapid changes in discharge conditions with distance down the column occur. The alterations produced on theory when small spherical or cylindrical probes are used will be indicated at each point.

#### 4. THE THEORY OF THE PROBE

a. **The Strongly Negative Probe.** One may begin with the probe potential  $V_P$  quite negative to  $V_B$ , i.e., with  $V_B > V_P$  and  $V = V_P - V_B$  strongly negative. Under these conditions the electrons of the plasma are repelled by  $P$  and a positive-ion space-charge-limited current  $i_+$  flows to  $P$ . This follows since with  $V$  some tens of volts negative even the fastest electrons of the distribution directed towards the probe cannot reach the probe against the high field. Since in plasma positive-ion densities well in excess of  $10^8$  ions/cm<sup>3</sup> exist, any current of positive ions to the probe will be *space-charge-limited*; see page 317. Thus the probe will be surrounded by a *positive-ion space-charge sheath*. The thickness  $d$  of this sheath will depend largely on the ratio of the negative potential of the probe  $V$  to the average density and energy of the electrons, for the energy of the electrons determines how close to the probe they can penetrate before reversing their velocities on repulsion. Owing to the distribution of electron energies there will be a zone at the outside edge of the sheath into which the electrons penetrate. If  $V$  is large and the electron energy is normal the width of this zone will be small compared to  $d$ . Hence for practical purposes we can choose the outer surface of area  $F$  of the space-charge sheath as the effective electrode area into which positive ions diffuse and which marks the boundary of interaction of the undisturbed plasma and the probe. As the field due to  $V$  is large and  $d$  is small all the positive ions entering this area eventually are dragged to the probe by the field. Hence outside of  $F$  the positive-ion density is  $N_+$ , and the probe current  $i_p$  equals the positive-ion current  $i_+$  to  $F$ , provided that no ionization by impact occurs within  $d$  and no electrons are liberated by any action from  $P$ .<sup>3,5,6,7</sup> That such a sheath actually exists can clearly be seen in the case of a luminous plasma when  $V$  is high. Under these circumstances the probe surface is separated from the plasma by a dark band of thickness  $d$  with slightly diffuse outer edge. The dark space is only relatively dark and represents a region where the positive

ions in the space charge are not recombining nor are the atoms excited to radiation in the absence of electron impacts. The dimensions of  $d$  visually observed agree with those calculated from theory. The existence of the positive sheath then enables us to investigate the conditions in the relatively undisturbed plasma beyond  $F$ .

Owing to their diffusive heat motions, the positive ions diffuse into the sheath across the area  $F$  giving a positive probe current  $i_+ = +nFv_+e = +FeN_+\bar{c}_+/4$ . The corresponding *current density* is then  $j_+ = i_+/F = eN_+\bar{c}_+/4$ . The space-charge limitation inside of the sheath also gives a value for  $j_+$  in terms of  $V$  and  $d$  as shown on page 319.

$$j_+ = \frac{1}{9\pi} \sqrt{\frac{2e}{M_+}} \frac{V^{3/2}}{d^2} = \frac{eN_+\bar{c}_+}{4}. \quad (1)$$

Since  $V$  does not alter the plasma outside of the surface  $F$ ,  $N_+$ , and  $\bar{c}_+$  are constant and altering  $V$  does not alter either  $j_+$  or  $N_+\bar{c}_+$ . Thus, with the strongly negative values of  $V$ ,  $j_+$  is constant and  $d$  varies as  $V^{1/2}$ . Hence by measuring  $j_+$  and knowing  $V$ ,  $d$  can be calculated, and vice versa, from  $V$  and  $d$ ,  $j_+$  can be calculated. To get an idea of the magnitude of  $d$  assume  $N_+ = 10^{12}$  ions/cm<sup>3</sup>, with  $\frac{1}{2}m_+C_+^2$  about 0.1 volt, i.e., three times the energy of thermal agitation at room temperature, a not unlikely value. For an Hg<sup>+</sup> ion this gives  $\bar{c}_+ = 3 \times 10^4$  cm/sec. Then  $d = 1.04 \times 10^{-2} V^{1/2}$ , so that, at  $V = -81$  volts,  $d = 2.8$  mm. This is clearly visible in a discharge tube. The theory has been verified by direct measurement of  $d$  and is found to hold.

If in place of a plane probe we use a small spherical probe the equation above is not altered in principle. The surface  $F$  is now replaced by  $4\pi r_F^2$ , where  $r_F$  is the radius of the outer edge of the space-charge sheath. The space-charge-limited current for concentric spherical electrodes of radii  $r_p$  and  $r_F$  must be used in place of the one for plane parallel electrodes. Hence equation 1 becomes

$$i_+ = 4\pi r_F^2 \frac{e\bar{c}_+N_+}{4} = \frac{4}{9} \sqrt{\frac{2e}{M_+}} \frac{V^{3/2}}{A_s}. \quad (2)$$

In this equation  $A_s$  is a correction factor depending on the ratio of  $r_F/r_p$ , where  $r_p$  is the probe radius.<sup>12</sup> v. Engel and Steenbeck give a plot of  $A_s$  as a function of  $(r_F/r_p) - 1$  which is shown in Fig. 99 as the full curve. In the case of the cylindrical probe analogous charges give the equations per unit length of cylinder as

$$i_+ = 2\pi r_F \frac{eN_+\bar{c}_+}{4} = \frac{2}{9} \sqrt{\frac{2e}{M_+}} \frac{V^{3/2}}{r_c A_c}, \quad (3)$$

with  $r_F$  the radius of the cylindrical space charge sheath,  $r_c$  that of the cylinder, and  $A_c$  taken from the dashed curve in the plot of Fig. 99 as a function of  $(r_F/r_c) - 1$ .

**b. Energy Distribution and Electron Temperature.** As one reduces the negative value of  $V$ , i.e., as  $V_p$  becomes less negative towards  $V_B$ , at first, as seen above,  $i_-$  or  $j_-$  is constant and no change is noted, except the decrease in the value of  $d$ . When, however,  $V$  becomes sufficiently low so that the faster electrons in the distribution directed towards the surfaces can penetrate the distance  $d$  and reach the probe surface the electron current  $i_-$  reduces the observed positive ion current  $i_p = i_+$  to a value  $i_p = i_+ - i_-$ , where  $i_-$  is the electron current reaching  $P$ . For convenience it is assumed that the molecules inside  $F$  do not influence these electrons, and we have the electron current reaching the probe electrode surface *against the retarding potential*  $V$  exactly as if the current of electrons were a thermionically emitted current moving in an opposing field in vacuum. Under these conditions the change of electron current with a decrease in  $V$  would give us a clear picture of the energy distribution of the electrons. Thus as the negative values of  $V$  decrease one must subtract an increasing negative electron current  $i_-$  from the constant space-charge-limited positive current  $i_+$ , so that the resultant current is  $i_p = i_+ - i_-$ . Since  $i_+$  is measured for a large negative  $V$  we get  $i_-$  from  $i_+$  and  $i_p$ . This idealized picture assumes that the electrons will not change their energy distribution in impact with neutral molecules in the sheath and that the very few electrons do not materially alter the positive-ion space charge. Under some circumstances these conditions are met fairly well, under others not, but usually the long electron free paths aid in meeting these conditions.

The magnitude of  $i_-$  can be calculated by a summation of all the plasma electrons in the distribution of energies which have an energy such that the directed component of velocity  $c_x$  normal to the plane probe surface fulfills the condition  $\frac{1}{2}m_-c_x^2 \geq Ve$ , and which strike the surface per second. Since out of the  $N_-$  electrons per cubic centimeter in the plasma the number  $N_x$  given by

$$N_x = \frac{N_-}{\alpha\sqrt{\pi}} e^{-\frac{c_x^2}{\alpha^2}} dc_x$$

have a velocity component normal to the probe between  $c_x$  and  $c_x + dc_x$ ,

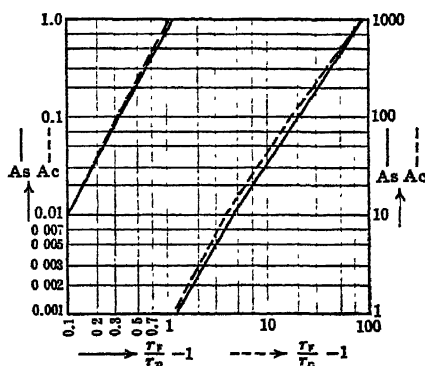


FIG. 99.

and since of this number  $AN_x c_x/4$  strike an area  $A$  of the probe per second, we can write

$$i_- = \frac{1}{4} \frac{A e N_-}{\sqrt{\pi}} \int_{c_x}^{\infty} \frac{c_x}{\alpha} e^{-\frac{c_x^2}{\alpha^2}} d c_x = \frac{A}{4} e N_- \bar{c}_- e^{-\frac{c_x^2}{\alpha^2}}.$$

Now  $\alpha^2 = 2kT_-/m_-$ , where  $T_-$  is the electron temperature in degrees K, and  $m_-$  is the electron mass, while  $V_e = \frac{1}{2} m C_x^2$ . Thus we can write

$$i_- = e A N_- \sqrt{\frac{k T_-}{2 \pi m_-}} e^{-\frac{V_e}{k T_-}}, \quad (4)$$

and

$$j_- = \frac{i_-}{A} = e N_- \sqrt{\frac{k T_-}{2 \pi m_-}} e^{-\frac{V_e}{k T_-}}. \quad (5)$$

For non-Maxwellian velocity distributions the quantity  $N_x$  equals  $N_- f(c_x) d c_x$  and the quantity  $(1/\alpha \sqrt{\pi}) e^{-\frac{c_x^2}{\alpha^2}}$  must be replaced by  $f'(c_x)$  as it conforms to the existing distribution. It is seen that even the Druyvesteyn distribution would profoundly influence the variation of current with  $V$ .

Assuming that  $T_-$  and  $N_-$  are constant independent of  $V$  as has been assumed it follows from equation 5 that  $\log j_- = B - (Ve/kT_-)$ , where  $B$  is a constant depending on  $N_-$ ,  $T_-$ , and  $e$ ,  $k$ , and  $m_-$ . Thus the  $\log j_- - V$  curve is linear, its slope giving the value of  $Ve/kT_-$  and its intercept with the  $j$  axis evaluating  $B$ . The slope of the line is given by

$$\frac{d(\log j_-)}{dV} = \frac{d(\log j_-)}{dV_p} = -\frac{e}{kT_-}. \quad (6)$$

This relation permits us at once to evaluate  $T_-$ . In the case of the Druyvesteyn distribution the integral would contain  $e^{-\left(\frac{eV}{kT}\right)^2}$ , and the relation would yield as its most important term depending on  $V$  the form  $\log j_- = B' - (eV/kT)^2$ , which is *not linear*, in place of equation 6. For the even more complicated forms existing at lower ion densities even wider deviations can be expected. Could one be sure that under the conditions of appearance of non-linear  $\log j_- - V$  curves no other factors were operative, the form of the energy distribution law could thus be found.

Assuming the Maxwellian form which is indicated by the linear character of the  $\log j_- - V$  curves, the equations can be simplified for a quick evaluation of  $T_-$  in the form

$$\frac{d(\log j_-)}{dV_p} = -\frac{1.17 \times 10^4}{T_-}, \quad (7)$$

when  $V$  is measured in volts and  $j_-$  is measured in amperes per square centimeter. One need not even measure the slope directly to obtain  $T_-$ . If we designate as  $\Delta V_p$  the difference in potential for two values of  $V_P$ ,  $V_{P_1}$  and  $V_{P_2}$ , at which  $j_{-1}$  and  $j_{-2}$  are in the ratio 1: 2.718, then

$$T_- = 1.17 \times 10^4 \Delta V_p. \quad (8)$$

If spherical or cylindrical electrodes are used the equations evaluating  $T_-$  are not in the least changed. In these cases, however, we measure  $i_-$ , the *current*, instead of  $j_-$ , the *current density*. Since the ratios are used this makes no difference at all.

This procedure for determining the *electron* temperature is the first step in evaluating the important variables in the discharge as its value is required in subsequent calculations. If the method fails at this point the results must be interpreted with the greatest caution.

**c. The Wall Potential.** As the negative potential  $V$  or the negative value of  $V_P - V_B$  still further decreases, a point will soon be reached at which the positive probe current  $i_p$  becomes 0. At this point  $i_p = 0 = i_+ - i_-$  and  $i_+ = i_-$ . Let us designate this value of  $V$  as  $V_w$ . At this point the negative electron current due to diffusion just equals the positive space-charge-limited ion current drawn in by the potential  $V_w$ . It is seen at once that  $V_w$  is still negative to  $V_B$ . It is not equal to  $V_B$ . This potential  $V_w$  is the potential which an *isolated* probe drawing no current would assume. Since positive ions and electrons are reaching the probe it represents what is known as the "*wall current*" and can be made to give the loss of carriers caused by *recombination* at the walls per unit area. It is the potential which an insulating discharge tube wall would acquire at the point. The mechanism of this current is simple. As electrons diffuse very much faster than the ions, owing to their mass difference alone,  $\bar{e}_- \gg \bar{e}_+$ , and as, in addition,  $T_-$ , because of the low value of  $f$  for electron impact, is greater than  $T_+$  for the ions for which  $f \sim 0.3$  it is clear that the electrons will charge the wall to a negative potential. This potential reaches such a value that at equilibrium the field produced draws in positive ions as fast as electrons diffuse in. Potential differences of this sort produced by differences in diffusion velocities are not confined to plasma alone. They are universal, appearing at the surfaces of contact of liquids and liquids, solids and liquids, and solids and solids. These effects are especially pronounced in electrolytic solutions.

The magnitude of the wall potential  $V_w$  can at once be computed on the basis of the theoretical considerations so far given. At  $V = V_w$  we can write

$$i_+ = \frac{eN_+\bar{e}_+}{4} = \frac{eN_-\bar{e}_-}{4} e^{-\frac{V_w}{kT_-}} = i_- \quad (9)$$

If as is frequently the case in undisturbed plasma  $N_+ = N_-$ , we can at once write

$$V_w = \frac{kT_-}{e} \log \left( \frac{\bar{c}_-}{\bar{c}_+} \right) = \frac{kT_-}{2e} \log \frac{T_- M_+}{T_+ M_-}. \quad (10)$$

Even when the fields are so low that  $T_- = T_+$  it is seen that, since  $M_-, m_- = 1836 A^-$ , where  $A^-$  is the atomic weight of  $M_+$ , the logarithmic term is positive. Thus, since  $e$  is negative,  $V_w$  will be negative. In a mercury discharge plasma with  $T_- = 2000^\circ \text{K}$  and  $T_+ = 400^\circ \text{K}$ , which is not unusual, we have  $M_+, m_- = 1836 \times 200$ , so that the value of  $V_w$  is given at once as  $V_w = -2.46$  volts. The use of spherical and cylindrical probes does not materially alter the balance at  $i_p = 0$  since the electrode area cancels out and the probes are still negative.

**d. The Plasma or Space Potential.** As the potential  $V$  is still further reduced we approach the point where  $V = 0$  and  $V_P = V_B$ . At this point the value of  $V_P$  gives us  $V_B$ , the plasma potential. When  $V_P = V_B$  no counter potential  $V$  opposes the electron current or urges positive ions to the probe. Hence at this value of  $V$  both signs of ion reach  $P$  in *proportion to their normal rates of diffusion*, and the field relative to the plasma is 0. Here also  $d$  is initially zero. In this case the  $V$  in the exponential for the electron current  $e^{-Ve/kT_-}$  is zero and  $e^{-Ve/kT_-} = 1$ . Hence the electron current density is

$$j_{-V_B} = eN_- \sqrt{\frac{kT_-}{2\pi m_-}}. \quad (11)$$

Beyond this current the increase in  $j_-$  ceases, for, as  $V = V_P - V_B$  becomes positive, the positive ions are repelled, electrons are attracted, and a negative space-charge sheath builds up. The electron current, assuming that all electrons striking the surface of the space-charge sheath  $F$  reach the plane probe area  $A$ , becomes  $i_- = eFN_- \sqrt{kT_-/2\pi m_-}$ , and the density as computed for the probe of area  $A$  is  $j_- = i_-/A$  and remains constant as  $V$  increases. The positive-ion current  $i_+$  is rapidly reduced to zero at a very low positive value of  $V_+$  as  $T_+$  is usually low. This means that at  $V = 0$  and  $V_P = V_B$  the  $\log j_- - V$  curve undergoes a sudden change in slope. This kink in the curve at once fixes the point  $V = 0$ . The value of  $V$  can be determined quite accurately by the intersection of the two straight-line elements passing through the straight  $\log j_-$  sections adjacent. Hence, having located the point  $V = 0$ , we can at this point assert that

$$j_{-V_B} = eN_- \sqrt{\frac{kT_-}{2\pi m_-}} \quad (11)$$

and that, since

$$\bar{c}_+ = \sqrt{\frac{8kT_+}{\pi m_+}}, \quad j_{+V_B} = \frac{eN_+ \bar{c}_+}{4} = eN_+ \sqrt{\frac{kT_+}{2\pi m_+}}; \quad (12)$$

as the positive ion current is produced by diffusion and no field exists. Now we can evaluate  $T_-$  from the slope of the  $\log j_- - V$  curve. Again from  $i_{pV_B}$  at  $V_B$  and thus from  $i_{-V_B} = i_- - i_+$ , knowing  $A$  and  $i_+$  and  $F$  from measurements at large negative  $V$ , we have  $j_{pV_B} - j_+ = j_{-V_B}$ . Then from  $j_{-V_B}$  and our value of  $T_-$  we can get  $N_-$ . If now as in normal plasma we assume  $N_- = N_+$  we can, from  $j_{-V_B}$  and  $N_- = N_+$ , evaluate  $T_+$ . In evaluating  $i_{pV_B}$  from the measured  $i_p$  the area is no longer  $F$  but the probe area  $A$  for  $d$  is zero. It must be noted that many circumstances can act to make the break point at  $V_B$  far from sharp. Thus electron emission from the probe surface which changes rapidly with negative  $V$  near  $V_B$ , ionization by electrons in the area near the probe as  $V$  becomes positive, electron reflection at the probe, etc., will all act to make a more gradual change in the  $\log j_- - V$  curve, which makes the choice of  $V_B$  difficult.

When one considers the small spherical probe or the cylindrical probe at  $V = 0$  and  $V_P = V_B$ , the current

$$i_{-V_{BS}} = 4\pi r_p^2 e N_- \sqrt{\frac{kT_-}{2\pi m_-}} \quad (13)$$

for the spherical electrode, and

$$i_{-V_{Bc}} = 2\pi l r_p e N_- \sqrt{\frac{kT_-}{2\pi m_-}} \quad (14)$$

for the cylindrical probe of length  $l$ . With such probes, however, the breakpoint at  $V = 0$  and  $V_P = V_B$  is not nearly so sharp as for the plane probe. The cause for this effect is that as we pass into the region of positive values of  $V$  the large negative sheath thickness for small spheres and cylinders causes rapid alterations in the values of  $j_-$  with  $V$ , of a purely geometrical nature, which superpose themselves on the transition indicated by theory and prolong it well into the positive values of  $V$ . This circumstance forces us to a new procedure for evaluating  $V_B$  or  $V = 0$ .

**e. Positive Probes and Plasma Potential.**<sup>10,11</sup> If one makes the probe still more positive,  $V_P > V_B$ , all that is done is to introduce a space-charge-limited electron current, with  $i_+ = 0$ , such that conditions for electrons are very much like those for positive ions with a *strongly* negative probe. Thus for the plane probe

$$i_- = \frac{eFN_- \bar{e}_-}{4} = eFN_- \sqrt{\frac{kT_-}{2\pi m_-}} = \frac{1}{9\pi} F \sqrt{\frac{2e}{m_-}} \frac{V^{3/2}}{d^2} \quad (15)$$

and

$$j_- = eN_- \sqrt{\frac{kT_-}{2\pi m_-}} = \frac{1}{9\pi} \sqrt{\frac{2e}{m_-}} \frac{V^{3/2}}{d^2} \quad (16)$$



In this case, however,  $d_-$  for a given  $j_-$  is *very much larger than the value of  $d$  for the positive space-charge sheath* in view of the fact that  $m_-$  for electrons is very much less than for ions. For a large plane probe this causes relatively little difficulty.<sup>15</sup> In the case of the small positive spherical or cylindrical wire probe the large value of the radius  $r_F$  of the space-charge sheath does introduce complications. For the positive space-charge sheath with  $r_F \sim r_p$  the field is so strong that *all the positive ions* entering the surfaces  $F$ ,  $4\pi r_F^2$ , or  $2\pi r_F l$  per cm reached the probe. With the small probe radii  $r_s$  (sphere) or  $r_c$  (cylinder), and the large values of  $r_F$ , the radius of the negative space-charge sheath, especially with small  $V$  such that  $eV/kT_-$  is very small, *not all the electrons* entering the surfaces  $4\pi r_F^2$  or  $2\pi r_F l$  per cm *will reach the probe surface*. If the electrons from the sheath all reach the probe surface the current to the probe is  $i_{-s \max} = j_- 4\pi r_F^2$  for the sphere and  $i_{-c \max} = j_- 2\pi r_F l$  for the cylinder, where  $l$  is the length of the cylinder. The current densities measured at the probe surface are then  $\frac{i_{-s \max}}{4\pi r_F^2} = j_-$  and  $\frac{i_{-c \max}}{2\pi r_F l} = j_-$ .

If the field did *not* draw in *any* electrons from the sheath surface then the current would be just the diffusion current density multiplied by the area of the probe itself, viz.,  $i_{-s0} = 4\pi r_s^2 j_-$  and  $i_{-c0} = 2\pi r_c l j_-$ . Hence it is seen that  $i_{-s \max} = i_{-s0} (r_F/r_s)^2$ , and  $i_{-c \max} = i_{-c0} (r_F/r_c)^2$ .

For a given ratio of  $r_F/r_s$  or  $r_F/r_c$  it is possible to calculate the factor by which  $i_{-s0}$  or  $i_{-c0}$  must be multiplied to give  $i_{-s \max}$  or  $i_{-c \max}$ . This fraction  $f_s$  or  $f_c$  is a function of  $eV/kT_-$  and can be computed from the amount that the orbit of the electron entering with an average energy  $kT_-$  at  $r_F$  will be bent by the field due to the potential  $V$  on the wire. At high values of  $eV/kT_-$  and for reasonable ratios of  $r_F/r_s$  or  $r_F/r_c$  the quantities  $f_s$  and  $f_c$  by which  $i_{-s0}$  and  $i_{-c0}$  must be multiplied to give  $i_{-s \max}$  and  $i_{-c \max}$  are merely  $(r_F/r_s)^2$  and  $r_F/r_c$ , i.e., all electrons reach the probe. For  $r_F/r_s$  or  $r_F/r_c$  approaching infinity, or for small values of  $eV/kT_-$ , the quantity  $f_s = 1 + eV/kT_-$ , and  $f_c = (2/\sqrt{\pi}) \sqrt{1 + (eV/kT_-)}$ . The quantities  $f_s - 1$  and  $f_c - 1$  as plotted against  $eV/kT_-$  for various values of  $r_F/r_s$  and  $r_F/r_c$  are shown in Figs. 100 and 101 as given by v. Engel and Steenbeck. Hence from a measured current  $i_{-s0}$  or  $i_{-c0}$  as given by the probe for a given ratio of  $r_F/r_s$  or  $r_F/r_c$  and a given value of  $V$  and  $T_-$ , we can at once find  $f_s$  or  $f_c$  and hence  $i_{-s \max}$  or  $i_{-c \max}$  for the probe. Since these currents are in any case about the same as the currents evaluated at or near  $V = 0$ , this correction is not vital for we can get  $i_-$  if  $V_B$  is known. It is useful at times to obtain the values of  $i_{-s \max}$  good to 1 or 2 per cent in this way. The currents observed as  $i_{-s0}$  and  $i_{-c0}$  differ from the maximum probe currents  $i_{-s \max}$  and  $i_{-c \max}$  when  $eV/kT_- > 3[(r_F^2 - r_s^2)/r_s^2]$  and  $eV/kT_- > 3[(r_F^2 - r_c^2)/r_c^2]$  by very small amounts (under 5 per cent in the first case and by even less in the second). Since for larger values of  $r_F/r_s$  and  $r_F/r_c$  and small values of  $eV/kT_-$  we have  $f_s = 1 + eV/kT_-$  and

$f_c = (2/\sqrt{\pi}) \sqrt{1 + (eV/kT_-)}$ , we will observe experimentally in this region that, as  $V_p$  and hence  $V$  is increased in positive values from near  $V_B$ , or  $V = 0$ , the currents  $i_{-s0}$  and  $i_{-c0}$  received by the probe appear to increase as

$$i_{-s0} = B \left( 1 + \frac{eV}{kT_-} \right) = B \left[ 1 + \frac{e}{kT_-} (V_{Ps} - V_B) \right]$$

and

$$i_{-c0} = B' \sqrt{1 + \frac{eV}{kT_-}} = B' \sqrt{1 + e \frac{(V_{Pc} - V_B)}{kT_-}},$$

where  $B$  and  $B'$  are constants. Hence plots of  $i_{s0}$  and  $i_{c0}$  for small  $eV/kT_-$  and larger ratios of  $r_F/r_s$  or  $r_F/r_c$  will be linear with  $V_p$ . If

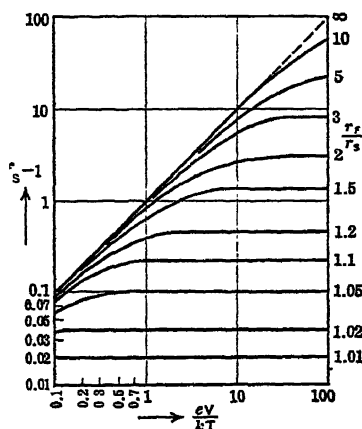


FIG. 100.

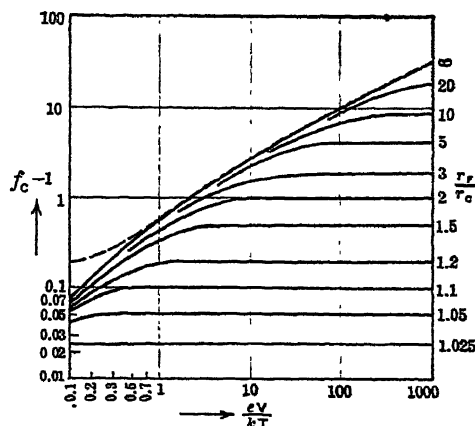


FIG. 101.

these lines are extrapolated down to  $i_{-s0} = 0$  and  $i_{-c0} = 0$ , we can write at once that

$$0 = 1 + \frac{e}{kT_-} (V_{Pos} - V_B)$$

or

$$0 = 1 + \frac{e}{kT_-} (V_{Poc} - V_B).$$

Hence

$$V_B = V_{Pos} - \frac{kT_-}{e} \quad (17)$$

or

$$V_B = V_{Poc} - \frac{kT_-}{e}. \quad (18)$$

Since  $V_{Pos}$  and  $V_{Poc}$  are obtained by extrapolation of the linear curves, and since  $T_-$  is determined from the slope of the  $j_- - V$  curves with  $V$  negative, we can locate  $V_B$ . Then, from  $V_B$ ,  $i_-$ , and  $i_+$ ,  $N_-$  can be found. If we assume that  $N_+ = N_-$ , then from  $i_+$  we can evaluate  $T_+$ . Thus in the event that Maxwell's law holds and that our primary assumptions hold without disturbing factors quite a bit can be learned about the discharge plasma.

## 5. PROBE MEASUREMENTS AND THE DETERMINATION OF THE DISTRIBUTION LAW

In the event that Maxwell's law does not hold, one may legitimately inquire whether any information concerning the plasma can be obtained by probes. Obviously, as indicated at the appropriate place in equation 6, one would have to modify the equations to conform to the new law. The law, however, would have to be known. Since it is unlikely that the complicated equations in the theoretical calculations can be solved for the case of discharge plasma as met in the laboratory, the information must come from direct measurement. After 1930 the first steps in this direction were taken, and by 1934 an adequate technique had been developed for the study. Before attempting to discuss this work it must be pointed out that, when such conditions exist, the concept of the electron "temperature" must be abolished. Temperature determined by the processes above derives its meaning in analogy to the molecular definition *on the basis of the applicability of Maxwell's law*. Thus for non-Maxwellian energy distributions the quantity  $kT_-$  will have to be abandoned as a mode of expression and a velocity or energy representing a specified sort of average in the new law must be used to avoid confusion and error. It must also be recognized that the laws experimentally derived will in rare cases only have the simple analytical form such as Maxwell's. Hence in the derivation of the analog of equation 3 using the new form the integrations will have to be done graphically, and in general it will not surprise us to see graphical procedures more frequently required. With adequate correction for the form of the law the general procedures outlined will still enable one to gain useful information. All this, however, presupposes that the apparent deviations from Maxwell's law as indicated by the non-linearity of the  $\log j_- - V$  curves are not caused by one of the very many disturbing factors to be discussed later. Only a knowledge of the existing conditions in a given case can allow us to rule out the different disturbing factors and thus permit us to interpret the observed results as a true change in form of the distribution law.

In view of his pioneer work on non-Maxwellian energy distribution among electrons it is not surprising that to M. J. Druyvesteyn should go the credit for initiating the application of the probe measurements to studies in the non-Maxwellian case. In an article on the low-voltage

arc, Druyvesteyn<sup>16</sup> turns to a study of the energy distribution by means of probes. He starts with the electron current  $i_-$  in the negative probe voltage region below the break point  $V_0$  as given by Langmuir and Mott-Smith, assuming a Maxwellian energy distribution, viz.,

$$i_- = eFN_- \sqrt{\frac{eV_-}{3\pi m_-}} e^{-\frac{3}{2} \frac{V_B - V_P}{V_-}}, \quad (19)$$

where  $eV_-$  is the average energy of the electrons expressed in volts instead of as  $kT_-$ , and  $F$  is the electrode area. For the Maxwellian distribution,  $\log i_-$  plotted against  $V_P$  should be linear. This was not found to be so under some conditions in the low-voltage arc. This is shown in the curves *c* and *d* of Fig. 102, where the  $\log i - V_P$  curves

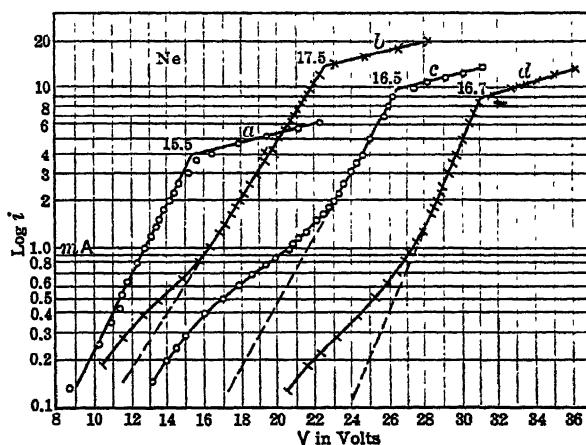


FIG. 102.

are *not linear* in contrast to the linear curve *a* and the less linear one *b*. The former were taken with a barium oxide coated cathode, and the other two were taken with a pure tungsten cathode. The equation applicable to this case for the plane probe can be deduced as follows. Let us assume that outside of the space-charge sheath surface  $F$  at the distance  $d$  from the probe the energy distribution  $f(c)dc$  exists, and call  $V = V_B - V_P$ . Then in accord with the theory given earlier

$$\frac{i_-}{eF} = \frac{1}{2} \int_{\sqrt{\frac{2eV}{m_-}}}^{\infty} f(c)dc \int_0^{\theta} c \cos \alpha \sin \alpha d\alpha, \quad (20)$$

where  $\alpha$  is the angle with the normal to the surface. The limit of integration,  $\theta$ , is given by  $\frac{1}{2}mc^2\cos^2\theta = eV$ . This is merely a different

manner of applying the criterion that the velocity component *normal* to the surface must exceed  $V$  in order to register as current. Then

$$i_- = \frac{eF}{4} \int_{\sqrt{\frac{2eV}{m_-}}}^{\infty} cf(c)dc \left(1 - \frac{1}{c^2} \frac{2eV}{m_-}\right). \quad (21)$$

If now we differentiate this expression twice with respect to  $V$  we get

$$f \left\{ \sqrt{\frac{2e}{m_-} (V_B - V_P)} \right\} = f \left\{ \sqrt{\frac{2eV}{m_-}} \right\} = \frac{4m_-}{e^2 F} V \frac{d^2 i_-}{dV_P^2}. \quad (22)$$

It is seen that by multiplying  $d^2 i_- / dV_P^2$  by  $4m_- V / Fe^2$  we at once get the distribution curve of energies in terms of the value of  $\sqrt{2eV/m_-}$ , and hence of the  $V$  applied.

For the cylindrical probe the velocity distribution must be introduced along three perpendicular coordinate axes,  $F(u, v, w) du dv dw$ , where  $w$  is parallel to the axis of the cylinder, and  $v$  radial from the center of the probe. Call  $r$  the radius and  $l$  the length of the probe while  $R$  is the radius of the space-charge sheath. We then have,

$$i = 2\pi R l e \int_{-\infty}^{+\infty} dw \int_{-\infty}^{+\infty} du \int_{\sqrt{u^2 \frac{R^2 - r^2}{r^2} + \frac{2eV}{m_-}}}^{+\infty} F_1(u, v, w) v dv, \quad (23)$$

the limits for  $v$  coming from the conservation of the moment of momentum about the probe axis. If we differentiate (23)

$$\frac{di}{dV} = -\frac{e^2 F}{m_-} \int_{-\infty}^{+\infty} dw \int_{-\infty}^{+\infty} dz f_1 \left( z \frac{r}{R}, \sqrt{z^2 \frac{R^2 - r^2}{R^2} + \frac{2eV}{m_-}}, w \right),$$

where  $z = Ru/v$ , and  $F = 2\pi r l$ . Inserting  $f(c)dc$  with

$$c = \sqrt{z^2 + w^2 + \frac{2eV}{m_-}},$$

we find

$$\frac{di}{dV} = -\frac{e^2 F}{2m_-} \int_{\sqrt{\frac{2eV}{m_-}}}^{\infty} \frac{1}{c} f(c) dc.$$

A second differentiation again gives equation 22. A similar deduction for the spherical probe leads to the same form as 22. Thus the equation for deriving the distribution law from probe measurements is *not* affected by probe form. The result of the application of this procedure by graphic differentiation, following equation 22 in the case of curve  $c$  of Fig. 102 is shown by the curve with crosses of Fig. 103. It is seen that the electrons of between 4 and 9 volts energy are distinctly fewer

in this curve than the Maxwell law, shown by the curve with circles in Fig. 103, requires. This is contrary to the expectation of an excess of such electrons from the circumstance that  $\log i_-$  is larger than the value that the linear relation requires at 4 volts below the break point. The absence of these electrons of 4 to 9 volts energy is ascribed to the ionization and excitation of the Ba and Sr atoms evaporating from the oxide coating of the filament. These ions have ionization potentials of 5.2 and 5.7 volts respectively.

The practical difficulty with the proposed method of Druyvesteyn lies in the considerable error involved in the double graphical differentiation of the  $i_- - V$  curve. The second derivative curve can be *measured directly* by an exceedingly ingenious method proposed by Emmeléus and developed by Sloane and McGregor.<sup>18</sup> It was later used by Van Gorcum, who clearly described its operation.<sup>19</sup> The principle of the method is as follows. A current-voltage curve free from discontinuities such as the probe measurements yield for  $V \geq 0$  may be represented by an equation  $i = f(V)$ , where  $f(V)$  is an infinite series in  $V$  of the form  $i = \alpha + \beta V + \gamma V^2 + \delta V^3 + \eta V^4 + \dots$ . If, at any point  $V$  on the curve, one superposes a small alternating potential  $E = A \sin pt$ , Landale<sup>28</sup> has shown by an expansion of  $i = f(V + E)$  by Taylor's theorem that the current is given by

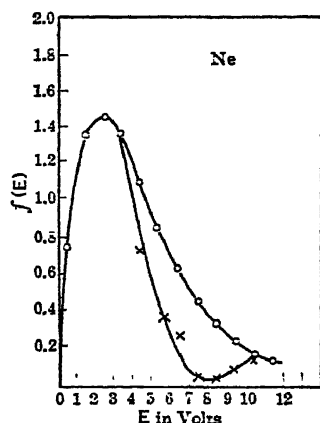


FIG. 103.

$$\begin{aligned}
 i = f(V) &+ \frac{A^2}{4} f''(V) + \frac{A^4}{64} f''''(V) + \dots \\
 &+ \left[ A f'(V) + \frac{A^3}{8} f'''(V) + \dots \right] \sin pt \\
 &- \left[ \frac{A^2}{4} f''(V) + \frac{A^4}{48} f''''(V) + \dots \right] \cos pt \\
 &- \left[ \frac{A^3}{24} f'''(V) \dots \right] \sin 3pt \\
 &+ \left[ \frac{A^4}{192} f''''(V) \dots \right] \cos 4pt + \dots
 \end{aligned}$$

Here  $f', f'', f'''$ , are first, second, third derivatives respectively of  $i$  with respect to  $V$ . The alternating emf has thus led to two new d-c

terms besides  $f(V)$  coming from the constant potential  $V$  alone, which depend on the second and fourth derivatives. It has given rise to an infinite number of new harmonic terms. If the value of  $A$  is sufficiently small we can neglect the fourth derivative and set  $\Delta i$ , the *increase in current above  $i = f(V)$* , as

$$\Delta i = \frac{A^2}{4} f''(V),$$

with a fair degree of approximation. Thus  $\Delta i$  is the *change of the current above the d-c value* on imposing the small a-c component at a potential  $V$ . Thus, by keeping  $A$  constant and small,  $\Delta i$ , the change in current on superposing the alternating current, gives a direct measure of the second derivative, i.e., of  $(A/4)f''(V)$ . Hence, by changing  $V$  and reading  $i$  for direct current and  $i + \Delta i$  for the direct plus the superimposed alternating current, a plot of  $f''(V)$  is obtained as a function of  $V$ . This is the rectified current. If  $A$  is kept small and the *alternating*

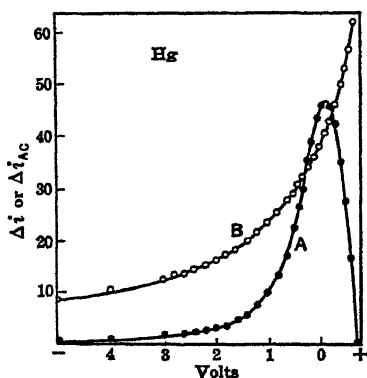


FIG. 104.

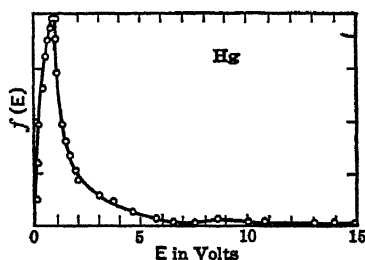


FIG. 105.

potential is measured it is chiefly  $\Delta i_{ac} = Af'(V) \sin pt$ . Thus by measuring  $\Delta i_{ac}$  one can obtain  $Af'(V)$ , the *first* derivative of  $i$  with respect to  $V$ . The curves of Fig. 104B and 104A are the first and second derivative curves measured in a low-voltage mercury arc by means of this method by Sloane and McGregor. The electron energy distribution curve derived from Fig. 104 is shown in Fig. 105 as given by Sloane and McGregor.

The current and potential actually measured in such procedures with probes are  $i_p = i_+ - i_-$ , and  $V_p$ . Since  $i_+$  is either constant or a linear function of  $V$ ,

$$\frac{d^2 i_+}{dV_p^2} = 0 \quad \text{and} \quad \frac{d^2 i_p}{dV_p^2} = \frac{d^2 i_-}{dV_p^2}.$$

In any case, at very negative probes  $i_- = 0$  and  $d^2 i_+/dV^2$  can be

measured and corrected for. In measurement we vary  $V_p$ , the probe potential. We require for plotting the law of  $\Delta i$  as a  $f(V)$ , which is given as  $\Delta i = d^2 i_- / dV^2$ , the value  $V$ , the probe potential, relative to the space potential  $V_B$ , i.e.,  $V = V_B - V_p$ . We can evaluate the space potential  $V_B$  quite accurately for Maxwellian distribution. For non-Maxwellian distribution this is difficult. Sloane and McGregor<sup>18</sup> discuss the evaluation of the space potential  $V_B$  when Maxwell's law holds and when it fails. It is recommended that  $V_B$  in the present method be chosen as the value of  $V_p$  at which the second derivative current difference  $\Delta i$  vanishes. The character of the failure of the Maxwellian law near the cathode of a neon discharge tube is beautifully illustrated by Van Gorcum.<sup>19</sup> Emmeléus and Ballantine report analogous deviations where the ion densities in discharges are low.<sup>21</sup> A recent extensive study of probe action and probe failure has been made by Greeves and Johnston<sup>23</sup> for a glow discharge in  $O_2$ . Further tests of the applicability of probes to various parts of the discharge, at low pressures and currents, and of the effect of positive space charges on probe measurements are given in the recent work of the Belfast group associated with Emmeléus.<sup>23, 24, 25, 26, 27</sup> These measurements orient one as to the present status of the subject about as well as possible. It is now essential that we discuss the sources of error in the measurements by means of probes.

## 6. SOURCES OF ERROR IN PROBE MEASUREMENTS

1. It is a primary assumption in all probe measurements that the presence of the probe does not alter either the potential distribution or the charge distribution in the region to be studied. Since probes operate near the space-charge potential they should not seriously disturb the charge. In regions where fields and conditions alter rapidly with distance the larger probes and above all the probe leads and their shields will produce serious distortions. This among other factors makes probe measurements in the cathode dark space and near corona points practically valueless. Unless the ion densities are rather high the current requirements for a probe measurement may be inadequate. This circumstance has limited the use of probes to studies where ion densities are greater than  $10^8$  ions/cm<sup>3</sup>, for by then the maximum values of  $j_-$  are of the order of  $10^{-14}$  amp/cm<sup>2</sup>. In the case of discharge plasma, however, the density of carriers is well in excess of this figure, so that the methods are applicable with little correction. When conditions such as those observed with probes are studied the probe is furthermore protected from the plasma by the positive or negative space-charge sheath. Thus the direct disturbing action of the metal surface on the discharge plasma is eliminated. Hence if the current drawn by the probe is small the conditions leading to the current in the plasma are relatively little disturbed, for diffusion into the space-charge



sheath is not complicated by the disturbing reflections and emissions of a metal surface, and *all* ions and electrons entering the sheath are in general little disturbed by the sheath, thus eventually reaching the probe. It must be recognized, however, that there is *always some disturbance* of the *plasma by the probe*.<sup>18,22</sup> At larger negative probe potentials the reversal of the repelled electron paths does change the electron density at the outside of the sheath. Such disturbances are recognized in the interactions of one probe on the readings of an adjacent second probe relative to those in the absence of the second probe. The effects show some disturbance which appears not to affect the temperature  $T_-$  but does introduce uncertainty into the values of  $N_-$  and  $N_+$  which may reach 5 fold in value.

2. In the derivation of the theory it is assumed that all the carriers that strike the space-charge sheath reach the probe. Corrections of a geometrical nature are introduced for the spherical and cylindrical probes, to which we shall later refer. Aside from deviations calling for such corrections it is assumed that electrons do not collide with molecules in the sheath. If they do collide this fact will have two consequences. First, it will divert or dissipate a small fraction of the probe current by means of reflection. Druyvesteyn<sup>17</sup> shows how this can be corrected for in the case of the electron current where the effect is not very large.

Secondly, the energy distribution of electrons and of positive ions can be materially altered by molecular impacts. This is especially true for electrons with energies above the critical values  $E_c$ ,  $E_a$ , and  $E_i$  characteristic of the gas, if many impacts occur in the space-charge sheath. Fortunately in the critical region of probe measurement near  $V_B$  where  $V = 0$  the sheath is *thin* and few impacts will occur. The effects of collisions will also be especially bad in discharges at higher pressures with strongly negative probes where the gaseous mean free path is small and  $d$  is large. It is for this reason that we cannot apply the probe to measurements of the electronic energy distribution in gases at low values of  $X/p$  such as were studied by Loeb, Wahlin, and Nielsen and Bradbury. Thus probe measurements at higher values of negative probe potentials in gases at pressures above a centimeter of mercury must be regarded as of doubtful value. Finally, above the excitation and ionizing energies  $E_a$  or  $E_i$  characteristic of the gas, the collisions of electrons with molecules or atoms produce excited atoms or *new* ions. These excited atoms or ions can act to alter the interpretation of conditions existing *outside* the sheath by giving false contributions to  $i_-$  or  $i_+$  directly by the ions and electrons created or by photoelectric action which liberates electrons from the cathode. Thus both the  $i_+$  and  $i_-$  observed for strongly negative probes can be larger than the real currents  $i_+$  and  $i_-$  coming from the plasma and so completely falsify the results obtained from theory which assumes such effects non-existent.

In the positive columns of many discharges the numbers of electrons with  $E$  much greater than  $E_i$  or  $E_i$  is small, and  $P_e$  and  $P_i$ , the total excitation and ionization probabilities, are in general small near  $E_i$ . Hence, especially near  $V_p = V_D$ , where the sheath is thin, disturbances of this sort are negligible. In outer parts of the discharge, i.e., in the cathode dark space, this is not true, and probe currents can give false results. These ionizing effects are most serious at large positive and particularly intermediate negative values of  $V$ .<sup>6,7</sup>

3. Metastable atoms, positive ions, and photons from the plasma induce secondary electron emission from negative probes. Although, because of low efficiencies, the photoelectric effects are in general less important as is also the case with some of the slower positive ions (especially where the work function of the surface  $\phi_e > E_i$ ), the metastable atoms and some positive ions have been assumed to produce serious disturbances at times. In fact, secondary electron emission in some cases is claimed to have completely masked the real course of the  $i_- - V$  curves which are conditioned by the energy distribution. These disturbing effects are reduced by using probe surfaces that are poor secondary emitters.<sup>30</sup> These are usually degassed surfaces such as Mg. They are reduced by higher gas pressures and by relatively lower negative probe potentials. The metastable atoms are present only in certain gases. The effects of metastable atoms should not be serious in Hg vapor with metals of high work function because of the low energy of the Hg metastable atoms. In He and Ne the effects should be more serious.<sup>29</sup>

There seems to be some difference of opinion as to how important the effects of metastable atoms are. According to Uyterhoeven they cause serious difficulties.<sup>7</sup> Kenty is inclined to consider their effectiveness overrated.<sup>29</sup> These disturbing factors are also assumed to alter the temperature equilibrium.<sup>20</sup> How serious all these effects are is really not known. The repeated observations of linear  $\log j_- - V$  curves in many discharges denoting undisturbed Maxwellian distributions indicate that the effects of this type are not serious in many cases. No accurate data are available as to electron liberation by positive ions or metastable atoms at metal surfaces under the conditions at probe surfaces. Discharge studies indicate that at low energies (of the order of 1 volt) perhaps a positive ion in one hundred or less will liberate an electron. The efficiency cannot be very much greater with metastable atoms.<sup>20</sup> Photons are ever so much less efficient but will reach the probe in larger amounts. Kenty estimates that photoelectric currents are of the order of 2 to 10 times those caused by metastable atoms on W electrodes in Ne, He, and A discharges. Kenty finds that for short-wavelength ultraviolet radiation from He, Ne, and A the yields range from 11 to 0.6 electrons per 100 photons from 584 Å to 1060 Å respectively at 0.12 mm pressure. Helium gives most secondaries. Outgassing the cathode reduces the yields materially. The pres-

ence of gaseous molecules reduces all these emissions in a considerable measure by reflection back to the surface.

If impurities of ionizing energy  $E_i$ , less than  $E_m$ , the energy of the metastable state, are present, considerable ion currents from the impurities in the gas ionized by metastable atoms are encountered. These influence the space-charge sheath, as discussed in the preceding section. They may be quite effective under some conditions. Unless exceptionally heavy photon and metastable atom production gives many of these agents striking the cathode, relative to the number of electrons from the plasma, they will not mask the electron energy distribution seriously. The disturbance will be the most serious in the part of the distribution involving the faster electrons, where the results can be seriously distorted by relatively few secondaries, which give a positive charge of decreasing magnitude to the probe as the negative value of  $V$  decreases.

The peculiar actions giving rise to self counting in Geiger counters discussed on page 498 may also be a source of trouble in some discharges.

4. Both electrons and positive ions suffer reflection at metal surfaces.<sup>18</sup> This is stated in another way by saying that the *accommodation coefficient* of electrons and ions is less than unity. Fast electrons, furthermore, will often knock other electrons out of a surface. Such losses of electrons result in the measurement of a smaller current  $i_+$  or  $i_-$  than is characteristic of the plasma. The losses of current on this basis, however, are quite small. They are again greater for the faster electrons at the higher negative probe potentials. For positive ions with negative probe and electrons with positive probe the error is probably negligible for the plane parallel probe and is essentially included in the correction factors  $f_s$  and  $f_c$  for the sphere and cylinder. Here again, as with the secondary electron emission, the error will be most serious at the high-velocity end of the distribution law and will become less as  $V_p = V_B$ . Increased gas pressure helps to reduce such losses.

5. It must be constantly borne in mind that the applied probe potentials  $V_p$  as given by the potentiometer may not be the true potential differences active. Since after all  $V_p$  is the *probe potential relative to the anode, cathode, or some other electrode* it must be remembered that *contact potential differences* may and do occur. This is especially likely in discharge plasma even with electrodes of the same metal where surface layers of gases of varying nature may alter the contact potential. For example, a *cathode* of Pt bombarded by high-energy ions and a Pt probe in the positive column can be in quite different states as regards their Volta potentials. Hence for accurate and absolute work in determining  $V_w$ ,  $V_B$ , etc., it is essential to ascertain the contact potential between probe and reference electrode by any one of the convenient methods under as near the operating conditions of the

surfaces as possible. Since  $V_B$  and  $V_P$  are *both* measured relative to the anode or cathode the important quantity  $V = V_B - V_P$  will, however, not be affected by contact potentials.

6. Early in his study of energy distributions in plasma, Langmuir<sup>22,31</sup> and his associates found that, besides the electrons and ions with energy distributions appropriate to the average energies which one might expect in the discharge, there were present groups of ions and electrons having distributions of energies about very much higher values. In some discharges these high-energy ion groups had energies as much as five times the energies given by the temperature  $T_-$  of the electron group.<sup>22</sup> In other discharges electrons were found that could reach a probe with  $V = V_B - V_P = -40$  volts. These odd groups even occurred in low-voltage arcs and in low-pressure plasma where the electronic mean free path was of the order of the electrode distance. Attempts to explain the fast electron groups on the basis of inelastic impacts of the second class failed at the low pressures. No mechanism could be invoked to explain the behavior in the case of positive ions.

An exhaustive study by Langmuir, Tonks,<sup>22,31</sup> and others<sup>32,33,34,35,36</sup> ultimately revealed the fact that plasma provided with electrodes has electrical properties which make it particularly subject to the creation and maintenance of electrical oscillations, see page 601. The frequencies depend on the conditions in the plasma such as ion densities and temperatures, and on boundary conditions imposed by the form of the discharge. Both high- and low-frequency oscillations occur and may reach considerable amplitudes. The occurrence of oscillations of potential in the plasma makes the space potential at the probe oscillate about  $V_B$  by amounts  $\Delta V_B$ . Hence when measurements of currents  $i_p$ ,  $i_-$ , and  $i_+$  are made, the probe potential being  $V_p$ , the value of the important potential in these studies is not  $V = V_B - V_p$  but  $V = V_B \pm \Delta V_B - V_p$ . Hence the currents will correspond to potentials  $V \pm \Delta V_B$ , which can be as much as 40 volts positive or negative to an assumed value  $V = V_B - V_p$ . If the plasma potential had been assumed as  $V_B$ , and  $V = V_B - V_p$  were made  $-40$  volts, then during the positive peak phase of an oscillation the value of  $V$  would be  $V = V_B + 40 - 40 = V_B$ . An electron current  $i_-$  would flow to the probe for a short time. In ignorance of oscillations one would then record the presence of electrons which could reach the probe at an assumed potential of  $V$  given by  $V = -40$ . Thus plasma oscillation will seriously impair the validity of the interpretation of any probe measurement, and when unusual distributions of this kind are observed the results should be regarded with suspicion.

7. The correction factors for spherical and cylindrical probes as given are highly idealized and are not accurate. Furthermore, the existence of these correction factors imposes conditions on the measured current-voltage characteristics of the probes which are not included in the theory developed. This difficulty can be overcome only

by a tedious series of successive graphical correction approximations which are hardly worth the effort. This is especially true since the corrections achieved by this means are small compared to the inherent uncertainties in the probe method caused by secondary electron liberation, etc.

8. Finally underlying most of the theory outlined we have assumed the existence of the Maxwellian distribution of energies. As has been amply shown this condition is not frequently encountered. Where one is certain of the absence of other disturbing agents, such as those listed under 1, 2, 3, 4, and 5, one may then by the procedures outlined in section  $e^{16, 18, 19, 21}$  determine  $f(c)dc$ , the new distribution, and proceed with the analysis. In many cases, however, the lack of linearity in the  $\log j_- - V$  curves cannot surely be ascribed to a failure of Maxwell's law. One must then proceed with circumspection in interpreting the results of probe studies. With these restrictions it is seen that probe theory has given us in the method of probe measurement a most useful tool in ascertaining the essential parameters  $N_+$ ,  $N_-$ ,  $T_+$ , and  $T_-$  of certain forms of discharge and in giving us the electron energy distribution in some cases where this is unknown. For many cases of interest, however, there is no experimental means as yet of determining the energy distribution of electrons in electrical fields in gases.

## 7. REFERENCES FOR PART B, CHAPTER V

1. LANGMUIR and MOTT-SMITH, *Gen. Elec. Rev.*, **26**, 731, 1923; **27**, 449, 583, 616, 726, 810, 1924; *J. Franklin Inst.*, **196**, 751, 1923; *Phys. Rev.*, **28**, 727, 1928.
2. I. LANGMUIR, *Phys. Rev.*, **26**, 585, 1925; TONKS, MOTT-SMITH, and LANGMUIR, *Phys. Rev.*, **28**, 104, 1926; I. LANGMUIR, *Phys. Rev.*, **31**, 357, 1928; **33**, 954, 1929; **33**, 195, 990, 1929; TONKS or TONKS and LANGMUIR, *Phys. Rev.*, **33**, 239, 1929; **34**, 876, 1929; **37**, 1458, 1931; T. J. KILLIAN, *Phys. Rev.*, **35**, 1238, 1925.
3. SCHOTTKY and ISSENDORFF, *Z. Physik*, **25**, 342, 1924; **26**, 85, 1924; **31**, 163, 1925.
4. R. SEELIGER, *Physik. Z.*, **30**, 527, 1929; SEELIGER and STRAEHLER, *Physik. Z.*, **30**, 929, 1929.
5. COMPTON and ECKART, *Phys. Rev.*, **25**, 139, 1925.
6. H. GÜNTHERSCHULTZE, *Z. Physik*, **62**, 619, 1930.
7. MORSE and UYTERHOEVEN, *Phys. Rev.*, **31**, 827, 1928; W. UYTERHOEVEN, *Proc. Natl. Acad. Sci.*, **15**, 32, 1929; UYTERHOEVEN and HARRINGTON, *Phys. Rev.*, **35**, 438, 1930; **36**, 709, 1930.
8. LANGMUIR and TONKS, *Phys. Rev.*, **33**, 195, 1929.
9. V. ISSENDORFF, *Wiss. Veröffent. Siemens-Konzern*, **4**, 124, 1929.
10. MOTT-SMITH and LANGMUIR, *Phys. Rev.*, **28**, 728, 1926.
11. K. K. DARROW, *Electrical Phenomena in Gases*, William and Wilkins, Baltimore, 1932, p. 366 ff.
12. LANGMUIR and BLODGETT, *Phys. Rev.*, **22**, 347, 1923.
13. F. L. MOHLER, *Bur. Standards J. Research*, **2**, 492, 1929.
14. C. BOECKNER, *Bur. Standards J. Research*, **6**, 280, 1931.
15. F. L. MOHLER, *Bur. Standards J. Research*, **19**, 561, 1937.
16. M. J. DRUYVESTEYN, *Z. Physik*, **64**, 790, 1930.

17. M. J. DRUYVESTEYN, *Z. Physik*, **64**, 793, 1930.
18. SLOANE and MCGREGOR, *Phil. Mag.*, **18**, 193, 1934.
19. A. H. VAN GORCUM, *Physica*, **3**, 207, 1936.
20. SPIWAK and REICHRUDEL, *Physica*, **3**, 304, 1936; *Ann. Physik*, **17**, 65, 1933.
21. EMMELÉUS and BALLANTINE, *Phys. Rev.*, **50**, 672, 1936.
22. TONKS and LANGMUIR, *Phys. Rev.*, **34**, 876, 1929.
23. GREEVES and JOHNSTON, *Phil. Mag.*, **21**, 659, 1936.
24. SLOANE and EMMELÉUS, *Phys. Rev.*, **44**, 333, 1933.
25. EMMELÉUS, GREEVES and MONTGOMERY, *Proc. Roy. Irish Acad.*, **43**, 35, 1936.
26. EMMELÉUS, BROWN, and MCGOWAN, *Phil. Mag.*, **17**, 136, 1934.
27. EMMELÉUS and BROWN, *Phil. Mag.*, **22**, 898, 1936.
28. S. E. A. LANDALE, *Proc. Camb. Phil. Soc.*, **25**, 355, 1929.
29. CARL KENTY, *Phys. Rev.*, **38**, 377, 1931; **43**, 181, 776, 1933.
30. CARL KENTY, *Phys. Rev.*, **44**, 891, 1933.
31. LANGMUIR and JONES, *Phys. Rev.*, **31**, 357, 1928; LANGMUIR and TONKS, *Phys. Rev.*, **33**, 195, 990, 1929.
32. A. F. DITTMER, *Phys. Rev.*, **28**, 507, 1926.
33. F. M. PENNING, *Physica*, **6**, 241, 1926.
34. C. T. CHOW, *Phys. Rev.*, **37**, 574, 1931.
35. G. W. FOX, *Phys. Rev.*, **37**, 815, 1931.
36. BROWN and COMAN, *Phys. Rev.*, **38**, 376, 1931.
37. W. R. HASELTINE, *J. Math. and Physics*, **18**, 174, 1939.
38. L. B. LOEB, *Kinetic Theory of Gases*, 2nd Edition, p. 104 ff. McGraw-Hill, New York, 1934.

## CHAPTER VI \*

### THE FORMATION OF NEGATIVE IONS

#### 1. INTRODUCTION

In 1910 Franck<sup>1</sup> studied the mobility of ions in He and N<sub>2</sub>, using the Franck modification of the Rutherford a-c method. He found a mobility of negative ions in N<sub>2</sub> and He of 200 and 500 to 1000 cm/sec per volt/cm for these gases, respectively. These he believed to be *free* electron mobilities in these gases, since normal *positive* ions in these gases had mobilities lying between 2 and 6. These gases he designated as *free electron gases* in which electrons do not attach to atoms or molecules to form ions. Franck further postulated that there were molecular gases, that could be called "electronegative" in the chemical sense, and that would pick up electrons to make negative *molecular* ions. Such gases he identified with the electronegative atoms in columns six and seven of the periodic table. The identification of *molecular* affinities with *atomic* affinities for negative charges are as we know today theoretically not justified. In fact, while *atoms* are electronegative in the sense used we should hardly expect stable molecules to be so, and it is especially wrong to correlate such *molecular* behavior with atomic behavior. In general, however, Franck concluded that electrons will not attach to He, Ne, N<sub>2</sub>, or H<sub>2</sub> gases *if pure* but they will do so in O<sub>2</sub>, SO<sub>2</sub>, HCl, and Cl<sub>2</sub>. Almost simultaneously Townsend<sup>2</sup> and his students were discovering that in many gases at sufficiently low pressures the electrons appeared to remain free.

In 1910, Kovarick,<sup>3</sup> using the Rutherford a-c method in air at various pressures, had observed a sequence of transitions of the mobility curves for negative ions in air as one went to lower pressures as shown in Fig. 106. In this case the frequencies have been adjusted so that for normal negative ions all curves should coincide with the curve having an intercept at  $X = 20$ . It is seen that the negative-ion group appears to have some few faster ions at 7.5 cm, many faster ions at 5.5 cm, and an apparent mobility at least 10 times that of the normal ion at 3.75 cm. A similar behavior was observed by Ratner<sup>4</sup> with an electrical wind method as well as by others. This behavior of negative ions was ascribed to a *progressive break-up of the ion cluster* beginning at a ratio of field strength to pressure  $X/p = 10/760 = 0.015$ . Meanwhile Loeb<sup>5</sup> had been studying the *supposed break-up of normal ions* as a

\* References to Chapter VI will be found on page 304.

function of  $(X/p)$  and had in 1916 shown that the positive and negative ion mobilities  $k_+$  and  $k_-$  were independent of  $X/p$  and of  $X$  up to values of  $X/p = 16$  in  $H_2$  and 12 in air at 360 mm. This result did not seem consistent with the postulated low-pressure break-up of negative ions.

In 1915 Wellisch<sup>6</sup> had studied the change in mobility with pressure using the *Franck modification* of the Rutherford a-c method in air; see page 11. His curves were unlike those of Kovarik; they are

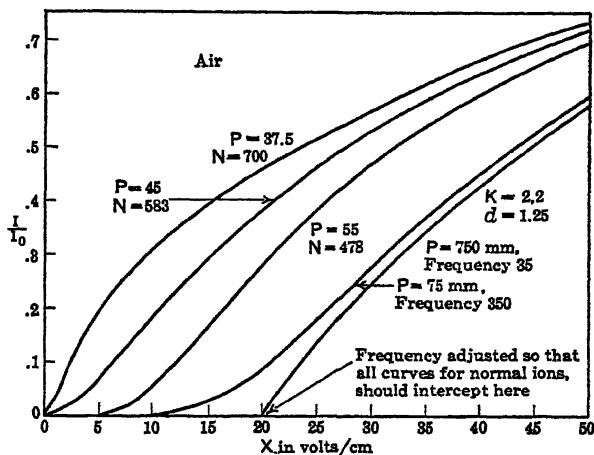


FIG. 106.

shown in Figs. 107 and 108. In Fig. 107 the field strength of the auxiliary field is constant and the pressure is varied for each curve, as is true of Kovarik's curves, the frequency being so chosen as to bring in normal ions at a value of 40 volts. In Fig. 108 the pressure is held constant at 56 mm and the frequency is 710, while the field strength of the auxiliary field is varied for each curve. These curves were taken from Loeb's<sup>7</sup> studies to be discussed later. It is seen that in a narrow range of pressure the curves are dual, showing *unmistakable evidence* of a *negative* ion of normal mobility. In addition, parts of curves that resembled Kovarik's lower-pressure curves were present. Finally the important role of the auxiliary field at low pressure and high frequency is to be noted.

On the basis of his observations Wellisch concluded that the negative ion did *not break up at low pressures* but that the appearance of the dual curves must be ascribed to the *process of ion formation*. He accordingly postulated that if, at the instant of creation, electrons had a high enough energy they could stick to molecules and form ions; otherwise they remained free. He next assumed that as the electron receded from the parent atom it lost kinetic energy to potential energy



of separation, and if it did not collide with a molecule within a distance  $d$  of the ion so that its energy exceed that required for attachment the electron remained free. Thus he assumed that *either electrons would stick to molecules or escape capture and remain free*. On this view, as

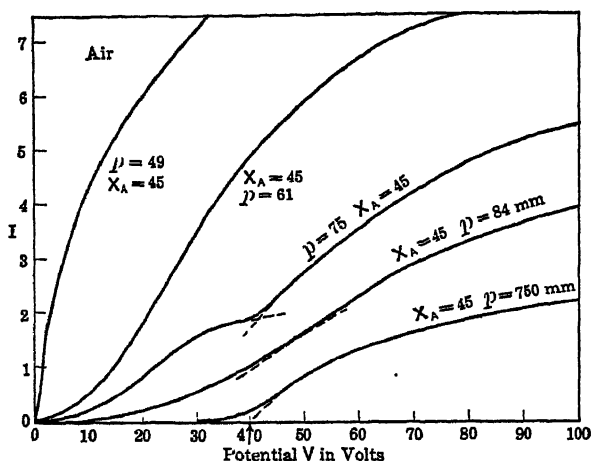


FIG. 107.

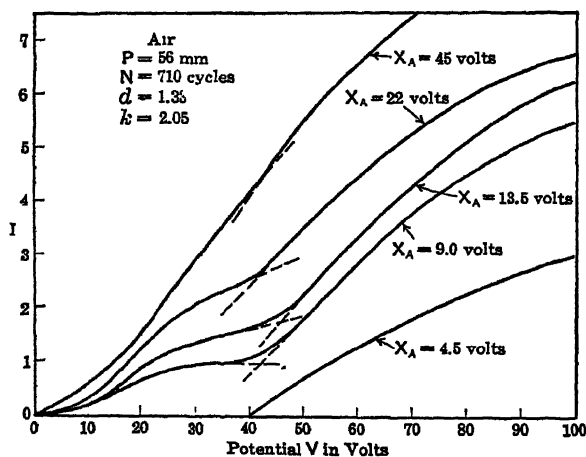


FIG. 108.

pressure decreases the chance of an impact within  $d$  decreases, and unattached electrons increase in number as  $p$  decreases. This rather original concept was interesting, but it was *faulty* for it did *not* explain the difference between the Wellisch and Kovarick curves nor the move-

ment of the foot of the faster electron curves in both investigations. It was further *incorrect since most electrons are liberated with more than just the energy of escape* and since it is at present apparent that the faster the electrons go the *less* easily they attach, because the probability of the loss of energy in radiation is the less likely the more there is to radiate.

## 2. THE THEORY OF J. J. THOMSON

In 1915 J. J. Thomson<sup>3</sup> proposed a theory to explain Kovarič's results. In this he also attributed the observed results to *ion formation* rather than ion break-up. He assumed that *electrons do not readily attach to molecules* and that *irrespective of energy* there is a certain chance  $h = 1/n$  of its making an attachment in one impact. For *simplicity* he assumed  $h$  to be a function of the character of the molecule only, irrespective of energy. Thus he assumed that an electron will on the average take  $n = 1/h$  impacts to attach to a molecule, where  $n$  is a characteristic property of the gas. For the inert gases and  $N_2$  and  $H_2$ , if pure, he assumed  $n = \infty$  and  $1/n = h = 0$ . For  $O_2$  or air he assumed  $n$  fairly large. On this basis he derived the following theory.

Let the average velocity of agitation of the electron be  $\bar{c}_1$  and its free path  $\lambda$ . It will then make  $\bar{c}_1/\lambda$  impacts per second. In a field  $X$  the electron moves  $k_e X$  cm/sec in the field direction, where  $k_e$  is the electron mobility, see page 178. Hence it takes the electron  $1/k_e X$  sec to go 1 cm, and in this time it makes  $(\bar{c}_1/\lambda)(1/k_e X)$  impacts. Thus, in advancing  $x$  cm from one electrode to the next, it makes  $x(\bar{c}_1/\lambda)(1/k_e X)$  impacts. Hence if we start with  $y$  electrons the number  $dy$  out of  $y$  which attach in going  $dx$  cm will depend on  $y$ , on  $\bar{c}_1/k_e \lambda X$ , and on  $dx$ . If  $\alpha$  is a constant of proportionality we can then write

$$dy = -\alpha y \frac{\bar{c}_1}{\lambda k_e X} dx.$$

If  $y = N_0$  at  $x = 0$ , and  $y = y$  at  $x = x$ , integration at once gives  $y = N_0 e^{-\frac{\alpha \bar{c}_1}{\lambda k_e X} x}$ . Thus out of  $N_0$  electrons the number that progress a distance  $x$  *without* attachment is given above as  $y$ . To get  $\bar{x}$ , the average distance gone by electrons before attachment, we must merely write

$$\bar{x} = \frac{\int_0^{N_0} x dy}{\int_0^{N_0} dy} = \frac{\lambda k_e X}{\alpha \bar{c}_1}.$$

Since an electron makes  $\bar{x}\bar{c}_1/\lambda k_e X$  impacts in going  $\bar{x}$  cm, the *average number of impacts to attach* will be

$$n = \frac{1}{h} = \frac{\lambda k_e X}{\alpha \bar{c}_1} \frac{\bar{c}_1}{\lambda k_e X} = \frac{1}{\alpha}.$$

Thus the average number of impacts to attach is  $1/\alpha$ , and the probability of attachment is  $h = \alpha$ . We can thus write

$$y = N_0 e^{-\frac{\bar{c}_1 h}{\lambda k_e X} x}.$$

Now, as shown by Loeb,  $\bar{c}_1/\lambda$  is not easy to evaluate directly. Since on Langevin's theory for electron mobility, see Chapter IV, irrespective of the values of  $\bar{c}_1$  and  $\lambda$ , we have

$$k_e = 0.815 \frac{e}{m} \frac{\lambda}{C_1} = 0.75 \frac{e}{m} \frac{\lambda}{\bar{c}_1}, \quad \frac{\lambda}{\bar{c}_1} = \frac{mk_e}{0.75e},$$

and we can write

$$y = N_0 e^{-\frac{0.75exh}{mk_e^2 X}} = N_0 e^{-\frac{1.35 \times 10^{15} hx}{(k_e)^2 X}},$$

with

$$dy = -\frac{0.75eh}{mk_e^2 X} N_0 e^{-\frac{0.75exh}{mk_e^2 X}} dx.$$

This equation enables one to account for some of the phenomena described, in semi-quantitative fashion. To gain an idea of the effect of such an attachment process let us assume  $h$  to be constant and about  $2.5 \times 10^{-5}$ , as it is in  $O_2$ . At  $X = 10$  volts/cm at 750 mm pressure,  $k_e$  is of the order of  $10^4$  cm/sec and increases as  $\sqrt{X/p}$ , the square root of the field strength in volts per centimeter divided by the pressure. This gives one  $y = N_0 e^{-34x}$ , so that  $y/N_0$  becomes equal to  $1/e = 0.36$  at a value of  $x = \bar{x}$  such that  $34\bar{x} = 1$ , or  $\bar{x} = 0.029$  cm. Hence at atmospheric pressure in  $O_2$  the *average* electron at  $X = 10$  volts/cm attaches within 0.3 mm of the point of origin. About this distance as a mean, electrons are attaching along an exponential curve. If  $h$  remained constant with  $X/p$ , the average electron would be expected to advance  $100 \times 0.03$  or 3 cm before forming an ion at 7.5 mm pressure. Thus the mobility curves taken with the Rutherford a-c method and analogous to Kovarick's<sup>3</sup> curves would show normal negative-ion mobilities at 750 mm with plates 1 cm apart even for values of  $N \sim 500$ . At 75 mm the curves would show a distinct asymptotic foot caused by the electrons that attached on the average 3 mm from the origin. and the mobilities computed from the shape of the curve might appear 10 to 30 per cent high. At 7.5 mm pressure, only electronic carriers of high mobility should be obtained. The curves of Fig. 109 illustrate this behavior very well. They are plots of  $y/N_0$  for  $X = 10$  at various

values of  $p$  plotted against  $x$ . The average distance  $\bar{x}$  is the distance corresponding to an ordinate  $1/e = 0.36$ . In these curves  $\bar{h}$  is assumed constant.

The effect of such behavior on mobility curves of the Kovarick type is shown in the curve computed from these data for  $p = 76$  mm,  $d = 1$  cm, and a frequency of 200 cycles. The basis of computation is simple. It assumes that the electrons attach at various distances  $x$  from the cathode given by  $y/N_0$ . They traverse  $x$  in a time very short compared to the time of ion transit. From  $x$  to the plate separation  $d$  they move as ions with a mobility  $k = 20$  cm/sec per volt/cm. From the distribution of the electrons along  $d - x$  gleaned from  $y/N_0$  one

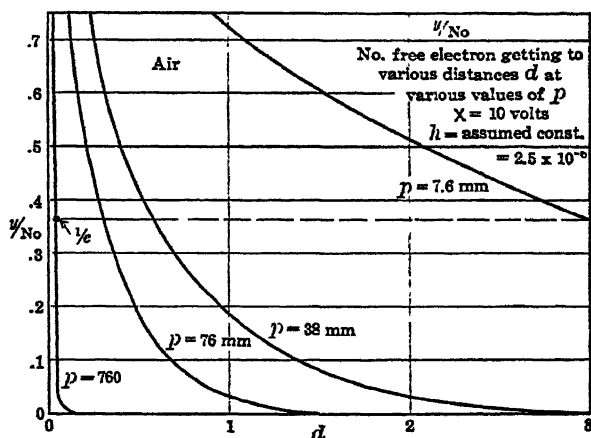


FIG. 109.

can estimate the contribution to the current at values of  $X$  below  $X_0$  for normal ions. At and above  $X_0$  the residual ions and attaching electrons reach the plate along approximately a normal mobility curve. This computed curve assuming  $\bar{h}$  constant is not accurate, since it does not take into account ions and electrons liberated later in the cycle. Such a neglect will decrease the asymptotic foot in relative value. The type of error made is shown by comparing the curve of Fig. 106 at 350 cycles and 76 mm with that computed as shown in Fig. 110.

An attempt to correlate the lower-pressure curves computed in this fashion with the Kovarick curves shows one marked deviation which was not explained until later. Although the computed curves do follow the evolution of the observed curves with pressure in general form, the observed curves complete their evolution in a very much narrower range of pressure than those given by theory, i.e., between 37.5 and 100 mm, whereas theory requires a range of 10 mm to 100 mm. The cause of this lies in the fact that, as  $X/p$  increases with decreasing

$p$ ,  $h$  is not constant.  $h$  decreases as the electron energy and hence  $X/p$  increases. With the change in  $h$ , accurate agreement between theory and experiment can be achieved.

From the Kovarick curves an approximate evaluation of  $h$  can be obtained, as Loeb<sup>7</sup> has shown. The mobility equation for the Rutherford method with a square-wave alternating current places the condition for the rise in ion current as  $d = (V/d)k_i T$ , where  $V$  is the potential,  $d$  the plate separation,  $k_i$  the normal ionic mobility, and  $T$  the time of a half cycle. Now with attachment the average ion goes a distance  $\bar{x}$  as an electron, before attaching, at a very high speed. The average ion starts from  $d - \bar{x}$  instead of  $d$ . Hence, if one extra-

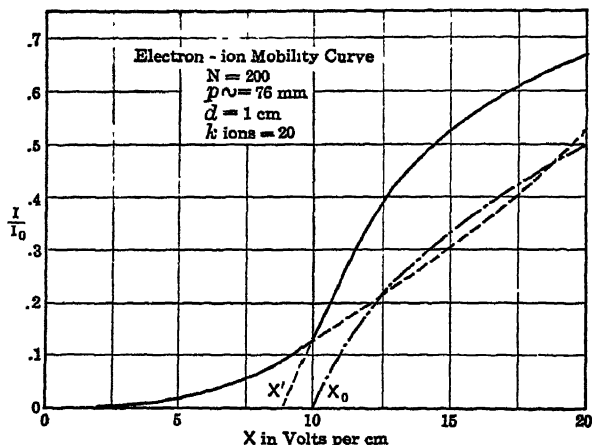


FIG. 110.

polates the steep portion of the curve, see Fig. 110, to the potential axis, it will make an intercept not at  $V_0$ , or  $X_0 = V_0/d$ , but at a point  $V'$ , or  $X' = V'/d$ , of lower potential or field strength. Hence ignoring the asymptotic foot in Kovarick's curves an estimate of  $V'$  will lead to a fictitious and high value of  $k_i$  given by  $d = (V'/d)(k_i)T$  if we use  $d$ . Actually one should use  $d - \bar{x} = (V'/d)(k_i)T$  as a more correct approximation. Since  $d = (V_0/d)(k_i)T$ , where  $V_0$  is the value of  $V$  at which normal ions cross with  $k_i$ ,  $d$ , and  $T$ , we have

$$k_i = \frac{d^2}{V_0 T} \quad \text{and} \quad \frac{T d(d - \bar{x})}{d^2 T} = \frac{V'}{V_0}, \quad d - \bar{x} = d \frac{V'}{V_0},$$

which from  $V'$  and  $V_0$  yields the value of  $\bar{x}$ . From  $\bar{x}$  one may then roughly evaluate  $h$  from  $(0.75 eh\bar{x}/mk_e^2 X) = 1$  if  $k_e$  is known. This was achieved by Loeb<sup>7</sup> when he undertook a study of this problem in 1920.

In 1915, however, neither adequate experimental curves nor a knowledge of  $k_e$  were at hand with which Thomson<sup>8</sup> could test his

theory. His attempts therefore to correlate his theory with observation were at that time not quite convincing or satisfactory. The war precluded further work on this problem. It was not until 1919 that, stimulated by Thomson's theory and the dilemma of ionic stability at high pressures at high  $X/p$ , Loeb<sup>7</sup> undertook the test of the theory. In order to clarify the question, both curves of the type of Kovarick<sup>3</sup> and Wellisch<sup>6</sup> were obtained by Loeb, samples of which are given in Figs. 106, 107, and 108. These results and their interpretation as given above on the basis of Thomson's theory strongly pointed to the correctness of Thomson's general viewpoint as opposed to the theory of the break-up of the negative ion or the theory of Wellisch.

The plausibility of Thomson's picture was still further enhanced by the effect of the gauze and auxiliary field in the Wellisch experiments. In Kovarick's method the curves result from the hybrid character of the carrier in its progress across the plates, the carriers being electrons part of the way and ions the rest. The distance at which attachment occurs is then given by a continuous probability distribution. In the Wellisch experiments the electronic carriers spend some time in a weak constant auxiliary field, before they cross the plates, in which some will attach. Hence a certain fraction of them will *always start as ions* while the electrons passing through the gauze will behave precisely like Kovarick's carriers. Hence one can with a low auxiliary field expect the dual curves observed by Wellisch in a limited pressure range as seen in Fig. 107. The effect is still more striking if conditions are left constant at an appropriate pressure and frequency, only the auxiliary field being varied as in Fig. 108. Here even at 56 mm with an auxiliary field of 4.5 volts/cm only normal carriers were observed, while at 45 volts/cm more than half the carriers started across the field as electrons.

On the theory of Wellisch the attachment is a process that depends on pressure only and should be independent of the auxiliary fields for the weak fields used. Hence the curves of Fig. 108 speak strongly against the Wellisch theory. In 1921 Wahlin further disproved the Wellisch theory by putting on auxiliary fields of such magnitudes that the electron energies below the gauze approached those causing ionization by electron impact. These auxiliary fields did not increase or alter the amount of attachment below the gauze. If the Wellisch concept of a minimum energy of attachment had been correct, the number of *ions* observed emerging through the gauze, which was zero at an  $X/p$  for the auxiliary field of 2.5, would have increased perceptibly as the value of  $X/p$  in the auxiliary field increased to nearly 25, which is close to the measurable onset of ionization by collision of electrons in air. This increase in ions at the expense of the electrons was not observed. Hence in air the mechanism proposed by Wellisch appeared definitely disproved, while the Thomson mechanism was at least qualitatively substantiated.

In the interests of accuracy it must be stated that some gases, such as  $\text{NH}_3$ , for example, do *require an adequate electron energy for attachment*, but in an essentially different sense, as we shall learn. In these gases the energy required is not that for attachment, but that for the dissociation or alteration of the molecule *from a type incapable of attaching electrons to an atom or molecule with electron affinity*. Again in  $\text{O}_2$  electrons of about 1.62 volts energy *also appear* to show an increase in the value of  $h$ , as will be seen. This also is not explicable on the theory of Wellisch, for electrons of higher energy do not attach. However, such electrons in a field with 1.62 volts can and do *suddenly lose all their energy* in inelastic impacts, producing excitation in the  $\text{O}_2$  molecule. These electrons in the fields existing are the only electrons of low enough energy to permit of attachment, while in *low* fields all electrons have a good chance of attaching, as will later be seen.

The evidence from the studies of Loeb, while favoring the Thomson mechanism and eliminating the Wellisch picture, was not contrary to the theory of the negative-ion break-up first proposed to explain the high mobilities. This interpretation, however, was completely ruled out in that the experiments of Loeb <sup>6</sup> and of Yen <sup>10</sup> had shown that at atmospheric pressure neither for  $\text{H}_2$  nor for air is there any change in the mobility for negative or positive ions at  $X/p$  values as high as 20 or 16. On the other hand, at an  $X/p$  as low as 0.2 at 10 cm pressure the *negative ion only shows the beginning of an anomalous behavior* while the positive ion is normal at all pressures. Since theoretically a *breaking up* of the negative ion is inconceivable as caused by *pressure alone*, the break-up hypothesis can, under no conditions, be retained. It may be added in passing that the negative ion in  $\text{O}_2$  has been observed to *lose its electron* at an  $X/p = 90$ . This is a different type of break-up which occurs at a value of  $X/p$  of an entirely different order from that applied in the earlier experiments.

With these facts established, Loeb <sup>11</sup> and later Wahlin <sup>9</sup> in Loeb's laboratory used the rough equations and the mobility method outlined for evaluating the probability of attachment  $h$ , or better its reciprocal  $n$ , the average number of impacts required to attach. These values were calculated in rough order of magnitude only, assuming for the electron mobility  $k_e$  in these gases the observed negative-ion mobility multiplied by the ratio between the observed electron and ion mobilities in  $\text{N}_2$ . In default of all knowledge of electron mobilities near atmospheric pressures in these gases, this was the best that could be done. Even though these quantities are seriously in error, the enormous range in the variation of  $h$  or  $n$  with the molecular species obtained, as shown in Table XV, minimized the importance of the error and somewhat justified the procedure. It was, in fact, the first attempt at even a semi-quantitative expression of molecular electron affinities, and the surprisingly great range discovered in the values of these quantities in a large measure justified the faulty procedure.

Since the results were impaired by the uncertainty in the value of  $k$ , Loeb<sup>11</sup> left the further evaluations of  $\bar{x}$  for various substances to Wahlin<sup>9</sup> and turned to a study of electron mobilities  $k_e$  in the higher-pressure ranges needed in these studies.

TABLE XV

| Gas                           | $n$               | Gas                              | $n$                 |
|-------------------------------|-------------------|----------------------------------|---------------------|
| N <sub>2</sub>                | $\infty$          | N <sub>2</sub> O                 | $6 \times 10^5$     |
| H <sub>2</sub>                | $\infty$          | C <sub>2</sub> H <sub>5</sub> Cl | $3.7 \times 10^5$   |
| CO                            | $1.6 \times 10^3$ | Air                              | $4.3 \times 10^4$   |
| NH <sub>3</sub>               | $9.9 \times 10^7$ | O <sub>2</sub>                   | $8.7 \times 10^3$   |
| C <sub>2</sub> H <sub>4</sub> | $4.7 \times 10^7$ | Cl <sub>2</sub>                  | $< 2.1 \times 10^3$ |
| C <sub>2</sub> H <sub>2</sub> | $7.8 \times 10^6$ |                                  |                     |
| C <sub>2</sub> H <sub>6</sub> | $2.5 \times 10^6$ |                                  |                     |

The method of evaluating  $k_e$  used by Loeb is given on pages 177 and 181. It was not particularly amenable to use in gases where  $h$  is large and  $n$  is small. It was possible, however, to measure  $k_e$  in air as a function of  $X/p$  in a range from 40 mm to 90 mm.

### 3. THE MORE ACCURATE EVALUATION OF THE ATTACHMENT PROBABILITY

In the meantime, Dr. Melvin Mooney<sup>12</sup> applied the Thomson theory in a rigorous mathematical fashion to the Rutherford a-c method. In consequence he was able to derive the equation for the current  $i$  as a  $f(X, T)$  for a square-wave form Rutherford a-c method with electrons having a constant  $h$ . These equations permit a rigorous test of the theory. The equations of Mooney for  $i$  as a  $f(T, V)$  read as follows: From  $V = 0$  to  $V = V_0$ , where  $d^2/V_0 = k_i T$ , with  $k_i$  the ion mobility, the ratio of the alternating current to saturation current with no alternating current for half a period (see page 9) is:

$$\frac{i}{i_0} = \frac{1}{hATk_i} \left[ e^{-Ah \left( \frac{d^2}{V} - k_i T \right)} - e^{-Ah \frac{d^2}{V}} \right],$$

with  $A = 0.75e/mk_e^2$ . At  $V = V_0$  for ions

$$\left( \frac{i}{i_0} \right)_{V_0} = \frac{1}{hATk_i} \left[ 1 - e^{-Ah \frac{d^2}{V_0}} \right].$$

Above  $V_0$  where both ions and electrons cross

$$\left( \frac{i}{i_0} \right)_{>V_0} = \frac{V - V_0}{V} + \frac{1}{hATk_i} \left[ 1 - e^{-Ah \frac{d^2}{V}} \right].$$



From  $(i/i_0)_r$ , if  $A$ ,  $T$ ,  $k_e$ , and  $V_0$  are known, we get  $h$  at once. From his directly observed value of  $k_e$  for air<sup>13</sup> and this equation, Loeb<sup>12</sup> was able to show that  $n = 2 \times 10^5$  for air,  $h = 5 \times 10^{-6}$ . Putting  $h$  into the equations and assuming  $h$  constant with  $X/p$ , Loeb<sup>12</sup> obtained a very satisfactory variation of  $i/i_0$  as a function of  $X/p$ ,  $p$ , etc., for numerous curves.<sup>14</sup> However, at this time H. A. Wilson had shown that a correction should be applied to the directly observed values of  $k_e$  due to the use of a sine-wave a-c method when  $k_e$  is a  $f(X/p)$ . Such a correction was made, and the use of the corrected  $k_e$  in the attachment work was logically essential. With the correction, what had been a good agreement between theory and experiment ceased being more than an agreement in a qualitative sense as regards the changes in curves with  $p$  and  $T$ . The original agreement using the directly observed values was, as we know today, fortuitous. Loeb<sup>12</sup> at that time concluded that the phenomenon was qualitatively correctly explained but that quantitatively agreement was not satisfactory.

With the elaborate equations above existing it was impossible to see how to correct the failure. Later it will be found that the failure was due to the fact that  $h$  or  $n$  is a *function of electron energy*, and it is certain that correct values of  $h$  as a  $f(X/p)$  will give good agreement. The publication of these findings in the years 1920 to 1923 and the establishment of the Thomson theory as being correct as a guiding principle stimulated Townsend and his pupils to undertake an investigation of the problem with their own methods. There are in general two methods by which problems of this sort can be solved. One of these employs simple and direct theoretical considerations but much more elaborate experimental technique. The other employs simple experimental technique but requires elaborate mathematical treatment. It is this second procedure that characterizes the method of Townsend and Bailey<sup>15</sup> in contradistinction to those of Cravath<sup>16</sup> and Bradbury.<sup>17</sup>

#### 4. THE METHOD OF BAILEY

Bailey<sup>15</sup> began his analysis with the attachment equation of J. J. Thomson, viz., that the number of electrons  $n$  out of  $n_0$  starting that go a distance  $x$  without attaching is  $n = n_0 e^{-\alpha x}$ , and thus that the number of ions formed in  $x$  is  $n_0(1 - e^{-\alpha x})$ , where  $\alpha = h\bar{c}\sqrt{\eta}/\lambda X k_e$ ; see page 262. Here  $h$  is the probability of attachment;  $\bar{c}\sqrt{\eta}$  is the average electronic velocity of agitation,  $\eta$  being the Townsend factor given on page 179;  $\lambda$  is the electron free path; and  $X$  is the field strength acting along  $x$ , while  $k_e$  is the electron mobility. The apparatus shown in Fig 111 in principle consists of a plate  $P$  which is a photoelectric source of electrons in a gas at a pressure  $p$ . Below  $P$ , in Fig. 112, which is schematic are a series of plates labeled 0, 1, 2, and 3, with rectangular slots perpendicular to the plane of the paper which are aligned along the vertical  $x$  axis. The plates 0, 1, and 2

are  $c$  cm apart. Thus photoelectrons liberated from  $P$  are drawn downward in the field  $X$  and attaching along the way arrive at plate 0 with  $n_0$  electrons and  $N_0$  ions passing per second through the slit in 0.

Now in the distance  $c$  between 0 and 1 the ion and electron beams spread laterally by diffusion and electrons attach to make ions on the way. Since electrons diffuse much more rapidly than ions, more electrons than ions will be caught by 1. For this reason, and also by virtue of attachment, relatively more ions  $N_1$  pass through 1 than passed through 0. Similar events occur between plates 1 and 2, so that  $n_2$  electrons and  $N_2$  ions pass through the slit in 2 and are received by plate 3. The ratio  $\xi$  of the currents received by plates 2 and 1 and the ratio  $\zeta$  of the currents received by plates 3 and 2 respectively can be measured, for various values of the field strength  $X$  and the pressure  $p$ . From  $\xi$  and  $\zeta$  the ratio  $S$  may be calculated for each plate, where  $S$  is the ratio of the current passing through the slit to the total current arriving on the plane of the opening. Thus one can evaluate  $S_1$  at plate 1 and  $S_2$  at plate 2 as

$$S_1 = \frac{\xi(1 + \zeta)}{1 + \xi(1 + \zeta)} \quad \text{and} \quad S_2 = \frac{\zeta}{1 + \zeta}.$$

If now  $n_0$  electrons and  $N_0$  ions pass through 0, then  $n_0 e^{-\alpha c}$  electrons reach the plane of plate 1 with a distribution ratio between capture at the plate and transmission  $R_e$ , which is a determinable function  $\phi(Q_e)$ , where  $Q_e$  is  $N_e X / 2\eta P$ . Here  $N$  is the number of molecules per cubic centimeter at

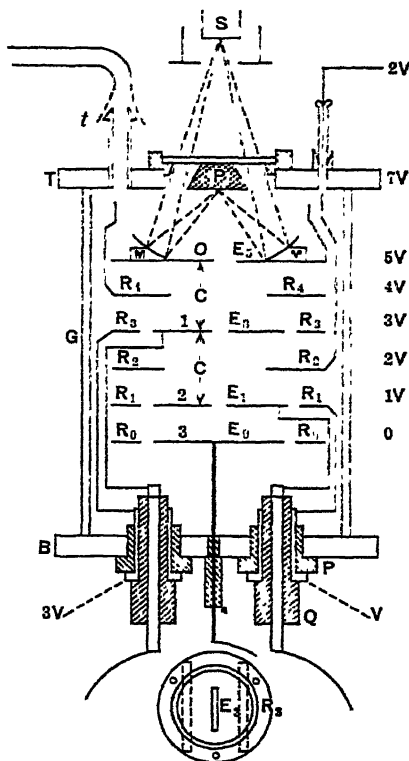


FIG. 111.—Bailey's Arrangements for Studying Attachment.

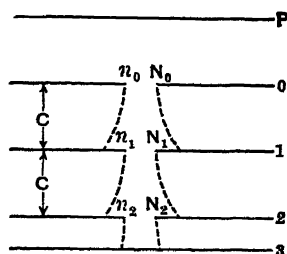


FIG. 112.

760 cm and  $15^\circ$  C,  $e$  the electron,  $X$  the field strength,  $\eta$  the

Townsend factor, and  $P$  the pressure 760 mm, as has been indicated on pages 179 and 180. Thus  $n_1 = n_0 R_e e^{-\alpha c}$ , and similarly  $n_2 = n_0 R_e^2 e^{-2\alpha c}$ . The  $n_0/(1 - e^{-\alpha c})$  electrons which attached between plates 0 and 1 formed ions and arrived at plane 1 with an unknown distribution  $r$ , while the  $N_0$  ions arrived at the same plane with the known ratio  $R = \phi(Q)$ , where  $Q = NeX/2P$ . Hence  $N_1 = RN_0 + r(1 - e^{-\alpha c})n_0$  or  $N_1 = RN_0 + bn_0$ , and similarly  $N_2 = RN_1 + bn_1 = R^2N_0 + (Rb + bR_e e^{-\alpha c})n_0$ . But  $S_1 = (n_1 + N_1)/(n_0 + N_0)$  and  $S_1S_2 = (n_2 + N_2)/(n_0 + N_0)$ , so that we have

$$S_1 = [R_e e^{-\alpha c} + r(1 - e^{-\alpha c}) - R] \frac{n_0}{n_0 + N_0} + R,$$

$$S_1S_2 = [R_e e^{-\alpha c} + r(1 - e^{-\alpha c}) - R] \frac{n_0}{n_0 + N_0} + (R_e e^{-\alpha c} + R) + R^2,$$

whence

$$S_1S_2 - R^2 = (S_1 - R)(R_e e^{-\alpha c} + R),$$

so that

$$R_e e^{-\alpha c} = \frac{S_1(R - S_2)}{R - S_1}.$$

Now, from the observed values of  $\xi$  and  $\zeta$ ,  $S_1$  and  $S_2$  can be evaluated. Again from  $Q = NeX/2P$  for ions,  $R = \phi(Q)$  can be evaluated. Thus a numerical expression for

$$R_e e^{-\alpha c} = \phi\left(\frac{NeX}{2\eta P}\right) e^{-\alpha c} = a_1$$

is obtained. However, both  $\alpha$  and  $NeX/2\eta P$  are unknown. If, however,  $X$  and  $p$  are changed, by a factor  $n$ , to  $X/n$  and  $p/n$ , then  $\phi(Ne(X/n)/2\eta P) e^{-\alpha c/n}$  is altered in value to  $a_n$ , and  $Q_e$  goes to  $Q_e/n$  while  $\alpha$  goes to  $\alpha/n$ . For  $\alpha$  is changed to  $\alpha/n$  by the increase in  $\lambda$ , the values of  $c\sqrt{\eta}$  and  $Xk_e$  being unchanged since  $X/p$  is constant, while in  $Q_e$ ,  $X$  is changed to  $X/n$ . Hence, with  $a_1$  and  $a_n$  experimentally given,

$$\phi\left(\frac{Ne \frac{n}{X}}{2\eta P}\right) e^{-\frac{\alpha}{n}c} = a_n$$

$$\phi\left(\frac{NeX}{2\eta P}\right) e^{-\alpha c} = a_1,$$

can be solved simultaneously for  $\alpha$  and  $NeX/2\eta P$ . Then from

$$\alpha = \frac{hc\sqrt{\eta}}{\lambda X k_e}$$

one can evaluate  $h$  if  $\eta$ ,  $Xk_e$ , and  $\lambda$  are known.

Bailey<sup>15</sup> used an apparatus illustrated in Fig. 111, which is largely self-explanatory. An attempt was made in the construction of the

apparatus to avoid sources of contamination of the gas. However, some ebonite surfaces were still exposed in the chamber, and these are notoriously effective in contaminating gases. The photoelectric source of electrons could be replaced by a thermionic source. The slits were rectangular, and  $c$  was 4 cm. The electron densities were assumed to be uniform over the first slit. This assumption enables  $R_s$  to be calculated as a function of  $Q_s$ , which is then plotted as a function of  $X/\eta$ . The calculation of  $R_s$  was not accurate, as the distribution over the slit was not uniform and because of diffusion to the edge of the slit. Certain assumptions as to the distribution at the second slit must be made, but these can be justified below values of 2.6 for a certain parameter  $v$ ,  $v = \sqrt{2\phi_s a^2/c}$ , where the slit width  $2a = 0.4$  cm. This assumption as to distribution and the amount of loss by diffusion could be tested on the *free* electrons in  $H_2$  for which  $\eta$ ,  $k_s$ , etc., are known. In this case  $S_2$  and  $R_s$  should be the same. They were found to be so for values of  $R > 0.36$ , but below this  $S_2$  was appreciably less. This was ascribed to the slit edges. It was then decided that, below values of  $X/\eta$  of 1.2,  $S_2$  represents the correct distribution ratio.  $S_1$  and  $S_2$  were nearly equal in  $H_2$ , but  $S_1$  was about 6 per cent less than  $S_2$ . They should have been equal below values of 0.55. The discrepancy was ascribed to inaccuracies in mechanical or electrical construction. One discrepancy was corrected for by an extension of the theory to include the difference.

Air stored over KOH for six weeks was used in a chamber that had not been baked out. Measurements extended over a range of pressures from 8 to 22.6 mm and of  $X$  ranging from 5 to 20 volts/cm. Losses at low  $X/p$  and high  $p$  were in a great measure due to ions, and self-repulsion became nearly as important as diffusion under these conditions. Thus the measurements were confined to higher values of  $X/p$ . The results obtained enable one to evaluate  $\eta$  as well as the quantity  $\alpha$  as a function of  $X/p$ . The values of  $\eta$  for air when compared with Townsend and Tizard's results made in 1913 show fair agreement, considering that Bailey's air was considerably cleaner. The values of Bailey obtained for  $h \times 10^6$  as a function of  $X/p$  are shown as crosses in Fig. 121. Then, since  $\alpha = h\bar{e}\sqrt{\eta}/\lambda X k_s$ , if values of  $k_s$  and  $\lambda$  are taken from the data of Townsend and Tizard, one can evaluate  $h$ . Since the gas of Townsend and Tizard<sup>22</sup> differed in purity from that of Bailey, producing changes in  $\alpha$  of the order 15 to 20 per cent, one must infer some uncertainty in the values of  $k_s$  and  $\lambda$ , so that the evaluation of  $h$  may be in doubt by some percent. The values of  $h$  obtained for three values of  $X/p$  were:

TABLE XVI

| $X/p$ | $h$                  |
|-------|----------------------|
| 0.5   | $3.3 \times 10^{-6}$ |
| 1.0   | $2.0 \times 10^{-6}$ |
| 2.0   | $0.7 \times 10^{-6}$ |

It is seen at once that Bailey's results show  $h$  to decrease as  $X/p$  increases. This is a result unsuspected by either Thomson or Loeb but one which need not surprise one today. Whatever the attachment process, we know now that energy must be dissipated in attachment. Whether this dissipation is as radiation or kinetic energy, the probability of dissipation must be the greater the less energy there is to dissipate. Had this knowledge which is common today been available at the time Loeb<sup>12</sup> made his study in air, he could have determined the form of the variation of  $h$  with electron energy, or better  $X/p$ , in order to make the observed and theoretical curves for ion currents made with the square-wave-form alternating current agree. It is seen, however, that, in general, the value of Loeb  $h = 5 \times 10^{-6}$  found at lower values of  $X/p$  is of the same order of magnitude as that of Bailey.

### 5. THE INTRODUCTION OF THE ELECTRON FILTER

The next advance in this field came with the work of Cravath<sup>16</sup> in Loeb's laboratory. In an endeavor to devise a scheme to measure electron attachment directly, Loeb in 1926 assigned to H. F. Lusk,<sup>18</sup> as a master's thesis, the task of testing out a newly devised "electron filter." This thesis was completed in 1927 and is on file in the archives of the University of California Library. It is entitled "An Attempt to Measure the Attachment Coefficient of Electrons to Molecules in Air Using a Combination of Alternating and Steady Fields Adapted to Galvanometric Measurement."

This scheme consisted of a group of parallel insulated wires of small diameter spaced 1 or 2 mm apart. Alternate wires were connected to one terminal of a radio-frequency oscillator, the other wires being connected to the other terminal of the oscillator. This plane grid of wires was placed at a convenient point in a parallel-plate condenser in which electrons and ions were moving from one plate to the other, the plane of the grid being parallel to the plates. Its potential was adjusted to equal that appropriate to the plane of the condenser at which it lay. The frequency of the alternating potential varied between  $5 \times 10^5$  and  $5 \times 10^7$  cycles per second depending on the gas pressure. The potential  $V_g$  could be varied at will. If now electrons start at the electrode  $A$  of the condenser and form ions between  $A$  and the plane of the grid  $C$ , then, in the absence of an alternating field between the wires of  $C$ , the current will flow to the plate  $E$  connected to an electrometer, except for the ions and electrons caught by the wires as a result of their area and diffusion. If now a high-frequency alternating potential is placed between wires of the grid, so that with the field midway between wires large enough to capture electrons during the greater portion of the cycle in a time relatively short compared to the cycle, the *electrons* will be captured by the grid.

This occurs provided that the field between  $A$  and  $E$  is sufficiently weak to make the transit of electrons over a distance equal to the separation of grid wires occur in a period several times the period of the alternating current.

It was found by Lusk<sup>18</sup> that such a device will transmit the ions with some loss, and with appropriate conditions it will also capture *all* electrons. The device is thus useful in various applications. In an endeavor to insure the transmission of *all* ions and the capture of *all* electrons, subsequent investigations have shown that one cannot increase the frequency and hence  $V_g$  beyond certain limits, and that the grid wires cannot be too fine. For at low pressures, if the fields about the wires are too high, in the attempt to use a high-frequency alternating potential, the fields at the wires can cause excitation and ionization of the gas by electron impact in the grid meshes. This would obviously falsify the results. To this end the grid wires must *not* be made too fine. On the other hand, large grid wires increase the loss of ions and electrons by "absorption" as a result of diffusion. This loss can be corrected for or eliminated in some measurements if the wires are not too large.

The effect of the action of high fields about grid wires that are too small may explain a phenomenon observed by Cravath<sup>18</sup> and termed by him the "hump effect." This is the appearance of a sudden *increase* in ion current, or in electrons escaping capture, as the grid potentials  $V_g$  are increased, giving maxima in the current transmitted by the gauze. These maxima just precede sharp declines due to *detachment* of the electron from the negative ion by impacts with molecules. The phenomenon occurs at high frequencies only. The humps of Cravath, who used fine wires, appeared at electron energies of about those needed for excitation of radiations capable of liberating photoelectrons from the grid. The hump must thus have been due to production of photoelectrons from the grid wires, and Loeb<sup>19</sup> has given evidence in this direction. At fields above those for excitation at 8 volts but below fields where the electrons ionize gas molecules by impact at 16 volts the fields are great enough to cause the *negative ions* to break up and give electrons, which are then captured. This causes the decline on the high field side of the hump. All these effects confuse and complicate the interpretation of the results obtained with the filters, especially if improperly used with fine wires and high frequencies. The filters, however, work quite successfully if alternating fields are maintained low and as nearly uniform as possible, while the frequencies used are not too high.

With the pioneering data of Lusk<sup>18</sup> on the usefulness of the filters for evaluating  $h$ , Cravath set out to use the filter to measure the fraction of electrons  $n$  out of a total  $n_0$  that had escaped capture after traversing a distance  $x$  in a gas at a given field  $X$  and pressure  $p$ . The ratio of  $n/n_0$  then at once makes possible the evaluation of  $h$  directly

if  $k_e$  is known. The apparatus used is shown diagrammatically in

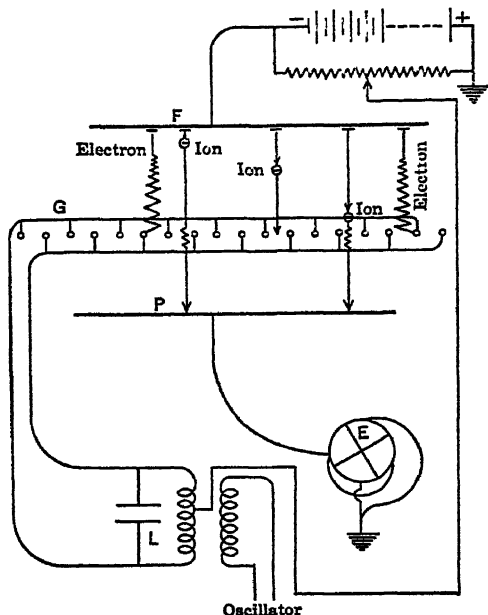


FIG. 113.—The Loeb Electron Filter Applied to Attachment Studies.

Fig. 113.  $F$  was an oxide-coated hot-filament electron source operating at as low a temperature as possible.  $G$  was the grid, and  $P$  the collecting plate. The grid wires had a diameter of 0.008 cm and were 1 mm apart. The coil  $L$  applied the alternating potential of value  $V_g$  to the grid wires. The electrons pass through the gas the distance  $x$  cm from  $F$  to  $G$  and attach on the way. Then if the filter is effective the electrons that remain unattached after going  $x$  cm are caught.

By measuring the current  $I_0$  to  $P$  with  $V_g = 0$  and the current  $I$  with  $V_g$  acting, one can evaluate the ratio  $R$  of ion current to total current  $I/I_0$  as a function of  $V_g$ . If all the electrons are caught, then

$$(1 - R) = \frac{y}{N_0} = e^{-\frac{1.35 \times 10^{15} h \nu}{(k_e)^2 x^2}}$$

Actually, the grid wires will capture ions, electrons will escape capture in the field, and electrons diffuse to the grid rapidly when  $V_g = 0$ . Hence  $R$  as observed may not give an accurate evaluation of  $y/N_0$ . It was in an endeavor to find the optimum values of  $V_g$  and frequency  $\nu$  that Cravath observed the "hump" effect and electron detachment. By choosing the flat portions of the  $R - V_g$  curves, Cravath was able to get reasonably correct values of  $R$ . Some typical curves obtained by Cravath for  $R$  as a function of  $V_g$  are shown in Fig. 114 *a*,

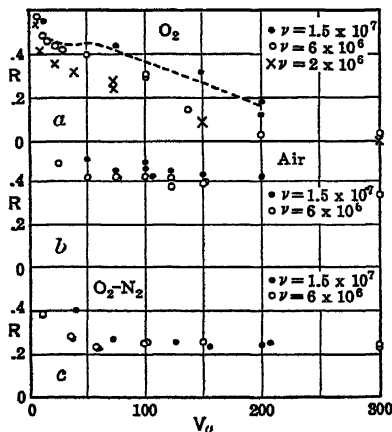


FIG. 114.

$b$ , and  $c$ . The data pertaining to the curves are given in Table XVII. The values of  $x$  used were 5.51 and 2.80 cm.  $X/p$  applies to the field between  $F$  and  $P$  only. The alternating fields at the wire surfaces as a result of  $V_g$  are much greater. The frequencies applied are indi-

TABLE XVII

|                  | $a$<br>O <sub>2</sub> | $b$<br>Air | $c$<br>1.3% O <sub>2</sub> , 98.7% N <sub>2</sub> |
|------------------|-----------------------|------------|---|
| $\phi$ in mm.... | 15                    | 60         | 100   |
| $X/p$ . . .      | 1.05                  | 0.89       | 0.12  |
| $R$ . . .        | 0.42                  | 0.42       | 0.26  |

cated as  $\nu$  for the points, circles, and crosses. It is seen that higher pressures give curves that are more nearly constant. The initial decrease in  $R$  near the axis as  $V_g$  increases is due to the failure of the grid to capture all electrons at low fields. The decline of the curves at low pressure for high values of  $V_g$  are due to *detachment* of electrons from ions in the high fields about grid wires. This phenomenon will be discussed in more detail at a later point. To evaluate  $h$  the value of  $k_s$  for the various gases was taken from the data of Townsend and

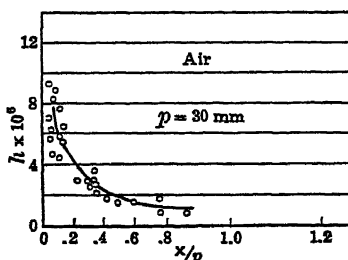


FIG. 115.

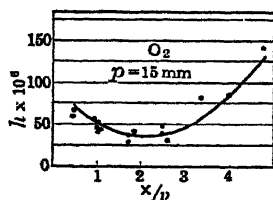


FIG. 116.

Tizard<sup>22</sup> and of Brose.<sup>21</sup> These data cannot be considered too accurate, since the purity of the gases used by Townsend and Tizard leaves much to be desired.

With this data Cravath computed  $h$  for air and O<sub>2</sub> at various pressures. His results all showed  $h$  to decrease with increasing  $X/p$  from a value of about 0.1 to 1.2, asymptotically approaching a constant value. A curve, at 30 mm pressure in air, is shown in Fig. 115. The values in O<sub>2</sub> at 15 mm pressure are shown in Fig. 116. Unfortunately, the results of Cravath in air varied somewhat with pressure, the curve at 15 mm showing lower values of  $h$  than that at higher pressure and thus relatively less change. The results of Bailey fell fairly closely on the Cravath curve for 15-mm pressure. In O<sub>2</sub> the results of *all* pressures lay fairly evenly about the



full curve of Fig. 116. As there is no reason why  $h$  should vary with pressure alone in air, while it might be expected to vary with  $X/p$  in all gases, one could not consider Cravath's results in air satisfactory. It must be remembered, however, (1) that Cravath used Townsend and Tizard's value of  $k_e$  for air, (2) that he used a metal housing on his chamber and that the hot filament may have caused the liberation of impurities with time so that his gas may not always have been pure. In addition, the hot filament changed the gas density over part of the electron path, and this change is different at different pressures. Thus some of Cravath's pressure variation may have been of instrumental origin. Why oxygen did not show this behavior, if it is of instrumental origin, is not clear.

Cravath also investigated artificial mixtures of  $O_2$  and  $N_2$ , as well as the effect of  $H_2O$  on air. These results were not extensive enough to be satisfactory. It was found that the value of  $h$  in air was not at once calculable from the percentage of  $O_2$  present if one used the values for  $h$  in  $O_2$ . The work of Cravath, however, was as good as one might have expected with a new method and the existing techniques. It must thus not surprise one to observe that the important features of Cravath's work were sustained and the discrepancies disappeared as the result of a new attack on the problem by Bradbury,<sup>17</sup> who had available the newer facilities of outgassed apparatus and improved electrical techniques.

## 6. THE METHOD AND RESULTS OF BRADBURY

Bradbury<sup>17</sup> began his investigations at the Massachusetts Institute of Technology after having developed at the University of California the technique of purifying gases and using outgassed glass systems for ion studies. In the author's laboratory he had also developed a new simple method of measuring  $k_e$ , the electron mobility.<sup>20</sup> This method will be discussed in detail in Chapter VII and is mentioned on page 277 as well.

In essence he used for his attachment study an all-glass chamber, capable of being baked out to  $200^\circ C$ , with Monel metal parts. Instead of the single electron filter of Cravath, Bradbury used two filters which could be inserted by magnetic control at two planes  $E$  and  $D$  in the field of the parallel-plate condenser  $PA$  of Figs. 117  $A$  and  $B$ , which represent front and side views respectively. The lower zinc plate  $A$  was a photoelectric source of electrons, thus avoiding the bad effects of the hot filament of Cravath. Plate  $P$  was the electrometer plate. In addition the arrangement allowed both filters to be removed so that the electron current could be measured from  $P$  to  $A$  as a function of field strength  $X$  and the pressure  $p$ . From such a measurement, as will elsewhere be shown (see page 315), we can evaluate  $k_e$  as a function of  $X/p$  provided that the mean energy of photoelectric emission from the zinc plate is known. This was determined in the classical

fashion by concentrating the ultraviolet light used onto the central zinc electrode  $Z$  of a spherical condenser  $S$  through a slit  $H$  and measuring the currents to the sphere with retarding fields as seen in Fig. 117B. Under these circumstances the currents to  $P$ ,  $I_0$ ,  $I_0$ ,  $I'_1$ , and  $I'_2$ , were measured with  $G_1$  and  $G_2$  alternating in place, with and without an alternating potential.  $I_0$  was measured with  $G_1$  in place and no alternating potential  $V_g$  on the grids, and  $I'_1$  was measured with an alternating potential  $V_g$  on the plates. Similarly  $I_0$  and  $I'_2$  were observed for gauze  $G_2$ . Then the electron currents surviving

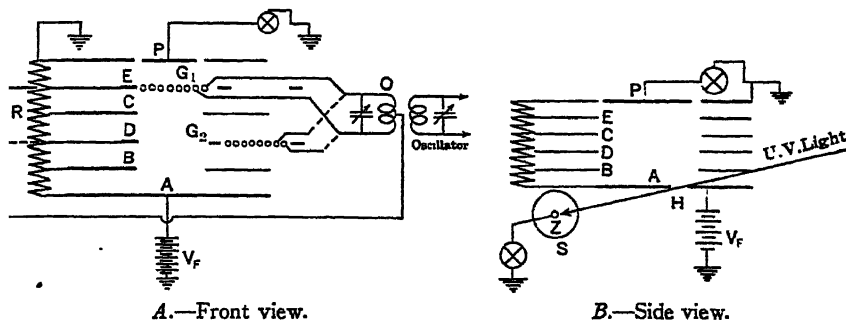


FIG. 117.—The Bradbury Apparatus for Attachment Studies.

ion formation at  $G_1$  and  $G_2$  are  $I_1 = I_0 - I'_1$  and  $I_2 = I_0 - I'_2$ , respectively. From the theory previously given, it at once follows that

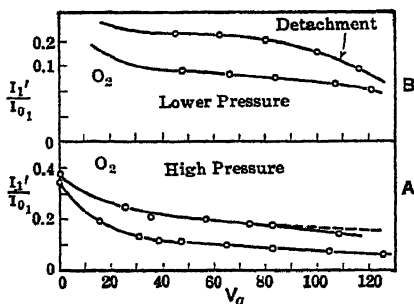
$$\frac{I_2}{I_1} = e^{-\frac{1.35 \times 10^{15} h}{k_e X}},$$

with  $x$ , the distance between the two gauzes, given as 2.40 cm. The value of  $k_e$  is computed from the ratio of the photocurrents from  $A$  with the gauzes removed at the pressure and field strength used for measuring  $I_2$  and  $I_1$  (current  $i$ ), and at 0 pressure (current  $I_0$ ) by the relation<sup>20</sup>

$$\frac{i}{I_0} = \frac{\sqrt{6\pi k_e X}}{c_0 + \sqrt{6\pi k_e X}}.$$

Here  $c_0$  is the probable velocity of escape of the photoelectrons evaluated by means of the zinc sphere, which was about 0.7 electron volt. By the use of two gauzes the loss of electrons to the grid wires by diffusion at  $V_g = 0$  and by capture of ions by the wires is in a large measure eliminated as a serious source of error, which was not the case with Cravath's treatment. If calculations are made by measuring  $I'_1$  and  $I'_2$  at the same value of  $V_g$ , the loss of ions is fairly well corrected for. The distance from  $A$  to  $P$  was 7 cm, and the area was 10 cm<sup>2</sup>. Mercury vapor and grease were eliminated by liquid-air

traps. The tube was baked out at 200° C, higher temperatures distorting the zinc plates. O<sub>2</sub> gas was first used, the formation of O<sub>3</sub>



FIGS. 118A-118B.

being prevented by a 12-cm-long filter of Cl<sub>2</sub> gas. The gas was circulated through the apparatus at 5-10 cm<sup>3</sup>/sec to maintain purity.

The curves for  $I_1'/I_{01}$  and  $I_2'/I_{02}$  in O<sub>2</sub> as a function of  $V_g$  at two pressures are shown in Figs. 118A and 118B. Fig. 118A shows the two curves at higher pressures with a normal ratio. The curves are like those of Cravath. The curves of Fig. 118B

represent those taken at a lower pressure, indicating an increase in the electron current caused presumably by the break-up of attached O<sub>2</sub><sup>-</sup> ions in the high field of the grid, due to  $V_g$ . This phenomenon

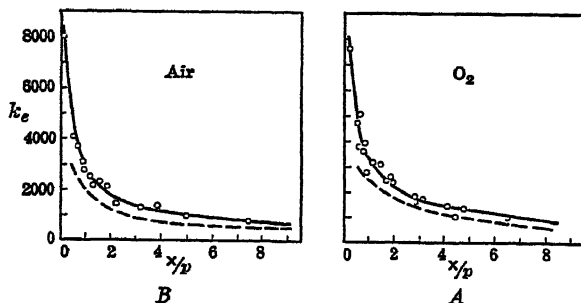


FIG. 119.

was also observed by Cravath<sup>11</sup> and was later studied by Loeb.<sup>19</sup> The electron mobilities  $k_e$  observed in O<sub>2</sub> and air are plotted as functions of  $X/p$  in Fig. 119A and B. The values of Townsend are given by

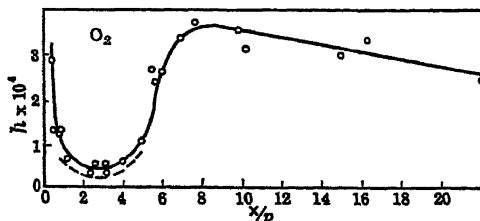


FIG. 120.

the dashed lines. It is seen that they agree within the limits of accuracy of both experiments.

With these data the value of  $h$  in  $O_2$  was determined as a function of  $X/p$  as shown in Fig. 120. The values at different pressures  $p$  from 18.5 to 3.5 mm are all included in the points and, it is seen, consistently delineate a single curve. Cravath's<sup>16</sup> results in  $O_2$  are shown by the dashed curve. The agreement is not at all bad, since Bradbury and Cravath used slightly different values of  $k_e$ . The results obtained in air are shown in Fig. 121, for pressures from 77 to 4.2 mm. These again delineate a single curve and show *no variation of  $h$  with pressure*. The crosses in Fig. 121 represent Bailey's results in air. Cravath's results at 120 mm fall slightly above Bradbury's curve, and at 15 mm they fall close to Bailey's. The previous results thus bracket Bradbury's curve. The discrepancies can readily be ascribed to impurities and inadequate values of  $k_e$  in the earlier work. The curves for  $O_2$  and air show a rapid decrease of  $h$  with  $X/p$  followed by a subse-

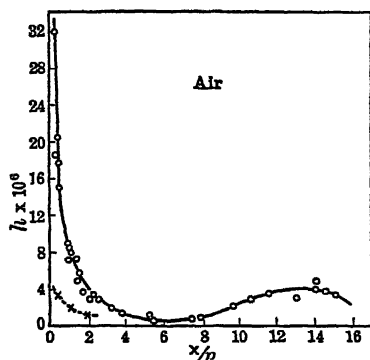


FIG. 121.

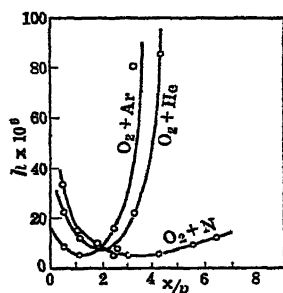


FIG. 122.

quent rise to a maximum value and thence a slow decline. The rise begins in  $O_2$  at an  $X/p$  of about 3 and in air at about 6. The maxima appear in  $O_2$  and air at an  $X/p$  of approximately 8 and 14 respectively. Fig. 122 shows curves for  $h$  in equal-volume mixtures of  $O_2$  and He,  $O_2$  and Ar, and  $O_2$  and  $N_2$ . The minimum appears in all curves but is much less pronounced in  $N_2$  than in  $O_2$ . In the inert-gas mixtures the rise of  $h$  following the minimum is most pronounced. In order to understand and interpret this remarkable behavior it is necessary to evaluate the *average electron energy* and study  $h$  as a function of electron energy instead of as a function of  $X/p$ . The reason for this is that, though the average energy is a function of  $X/p$ , this function differs radically in different gases and is not linear.

Although it should be possible to calculate the average energy as a function of  $X/p$  from the terminal energy of the electrons in a field from Compton's theory (see Chapter IV), or better still from the theory of Druyvesteyn (see Chapter V), this becomes impossible in gases

like  $O_2$  and  $N_2$ . The reason for this lies in the nature and extent of the inelasticity of electron impacts in molecular gases as indicated by observations on electron mobilities. Bradbury therefore had to make rough evaluations of electron energies in air and  $O_2$  as a function of  $X/p$  from the data of Townsend and Tizard<sup>20</sup> and Brose.<sup>21</sup> With these data he plotted  $h$  as a function of  $E_e$ , the average electron energy

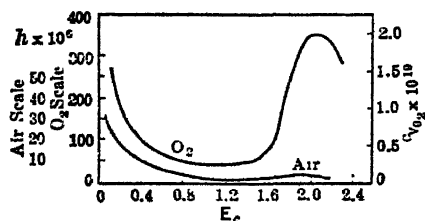


FIG. 123.

as shown in Fig. 123. The upper curve is for  $O_2$  and the lower one for air. It is seen at once that in both gases  $h$  decreases rapidly at first and then asymptotically approaches a constant value. Between  $E_e = 1.2$  and  $1.6$  volts this decrease ceases and the curve rises slowly. At about  $1.6$  volts *both* curves rise sharply to a peak at about  $2$  volts energy.

Thereafter they fall. It is to be noted that on an energy scale the rise of the curves occurs at the *same energy in  $O_2$  and air* and is quite pronounced.

The explanation is simple. Electrons in  $O_2$  at  $1.62$  volts excite the lowest *electronic* level in the  $O_2$  molecule, the  ${}^3\Sigma_g^-$  state, which is a metastable level. The probability of excitation to this state is relatively high. As a result, electrons in a group of an average energy near but below  $1.62$  volts begin to have inelastic impacts. At  $1.62$  volts average energy, *many electrons have impacts losing their whole energy to excitation*. Such electrons with residual energies near that of thermal agitation have a high value of  $h$ . Thus the *average observed value of  $h$  rises abruptly* near  $1.62$  volts electron energy. Accordingly, whereas on theory  $h$  should decrease roughly as  $1/\sqrt{E_e}$ , where  $E_e$  is the energy of the electron, when the *average* electron energy reaches such values that electrons in the distribution can lose  $1.62$  volts and thus be reduced to thermal energies  $h$  should begin to increase. As the average energy goes very slightly above  $1.62$  volts, more and more electrons in the distribution suffer inelastic impacts and the *average value of  $h$  rapidly increases*. When, however,  $E_e$  gets materially above  $1.62$  volts the electrons colliding at  $1.62$  volts and losing *only*  $1.62$  volts will have *more and more residual energy*. For these,  $h$  decreases as before. Hence the value of  $h$  should again decrease after the value of  $E_e$  appreciably exceeds  $1.62$  volts.

These conclusions are substantiated by the observations in  $O_2$ -He and  $O_2$ -A mixtures. Here unfortunately one does not have a scale for  $E_e$  as a function of  $X/p$ . But, as the elasticity of electron impact decreases in the order A, He,  $N_2$ , it would be expected that  $E_e$  should reach  $1.62$  volts in  $O_2$ -A mixtures at a lower  $X/p$  and that one should see the rise due to inelastic impacts occurring in the order A, He, and

$N_2$ , which is observed in Fig. 122.  $N_2$ , giving very inelastic electron impacts compared to He and A, should and does show a rise at much higher values of  $X/p$ .

Bradbury next attempted to calculate the value of  $h$  in air from that in  $O_2$ : For since electrons attach only to  $O_2$  molecules one might expect the chance in air to be in direct proportion to the mole fraction of  $O_2$  present in air. This should make the value of  $h$  in pure  $O_2$ ,  $h_{O_2}$ , equal to 5 times the value in air,  $h_a$ . However, the electron free paths  $\lambda_{O_2}$  and  $\lambda_{N_2}$  are different in  $O_2$  and  $N_2$  and vary with  $X/p$ . Hence one must compute the relative numbers of impacts between  $O_2$  molecules and electrons in  $O_2$  and in air. The collision frequencies of electrons in  $O_2$  and air as given by kinetic theory are as follows:

$$z_{O_2} = \frac{c}{\pi N_0 f_{O_2} \sigma_{O_2}^2}$$

and

$$z_a = \frac{c}{\pi f_{O_2} N_0 \sigma_{O_2}^2 + \pi f_{N_2} N_0 \sigma_{N_2}^2} = \frac{c}{\pi N_0 [f_{O_2} \sigma_{O_2}^2 + (1 - f_{O_2}) \sigma_{N_2}^2]}.$$

Here  $f_{O_2}$  is the mole fraction of  $O_2$  present in the binary mixture with  $N_2$ , and  $f_{N_2} = 1 - f_{O_2}$ . Accordingly we can write for the ratios of  $h$  that

$$\begin{aligned} \frac{h_{O_2}}{h_a} &= \frac{z_{O_2}}{f_{O_2} z_a} = \frac{f_{O_2} \sigma_{O_2}^2 + (1 - f_{O_2}) \sigma_{N_2}^2}{f_{O_2} \sigma_{O_2}^2} \\ &= 1 + \frac{(1 - f_{O_2})}{f_{O_2}} \frac{\sigma_{N_2}^2}{\sigma_{O_2}^2} = 1 + \frac{(1 - f_{O_2})}{f_{O_2}} \frac{\lambda_{O_2}}{\lambda_{N_2}}. \end{aligned}$$

This is analogous to the equation deduced by Cravath.

Now at 0.8 volt electron energy in which the values of  $h$  in  $O_2$  and air flatten out we have no good values of  $\lambda_{O_2}/\lambda_{N_2}$  from Ramsauer cross sections. Townsend and Tizard<sup>22</sup> evaluate  $\lambda_{O_2}/\lambda_{N_2}$  in this region as roughly 2. Inserting this value and  $f_{O_2} = 0.2$ , the value in air, into the equation above we observe that  $h_{O_2}/h_a$  is roughly 9. The observed value in the region 0-10 volts is of the order of 10 or 13. Obviously one can hardly expect the values of  $h$  to be in this ratio at energies approaching those of inelastic impacts at 1.62 volts. At 1.8 volts  $h_{O_2}$  is 50 times the value of  $h_a$ , while  $\lambda_{N_2}/\lambda_{O_2}$  is only about twice as great as at 0.8 volt. This, however, is easily explained. Even at very low electron energies  $h_{O_2}$  is small. Thus, immediately after an impact, when the electron energy is reduced to near thermal values by the loss of 1.62 volts, it must make *several impacts with*  $O_2$  molecules before it can attach. Between each two of these impacts it is *gaining some energy from the field*. If, now, it is in air or  $O_2$ -He mixtures, in which it makes relatively elastic impacts with  $N_2$  molecules and He atoms, *the energy gain is rapid and it will gain roughly 9 to 18 times as much*

energy in air between potential attacking impacts with  $O_2$  molecules as in pure  $O_2$ . Hence the chance of gaining energy and lowering  $h_a$  on the average after the inelastic impacts at 1.62 volts is far greater than in pure  $O_2$ . This mechanism thus readily accounts for the discrepancy in the values of  $h_{O_2}/h_a$  at values of the electron energy above 1.62 volts. It is accordingly seen not only that these experiments afford good values of  $h_{O_2}$  and  $h_a$  over a considerable range of electron energies, but also that with them we clarify all the discrepancies in the work of Cravath<sup>16</sup> and the earlier investigators. It is interesting to note that the true electronic behavior is remarkably more complex than the simple theory of Thomson envisaged. How much more complex it is will become clear when the attachment observed in other gases is discussed.

In their original work on electron attachment in gases, Loeb<sup>7</sup> and Wahlin<sup>9</sup> had found that, at atmospheric pressures and with values of fields up to some 60 volts/cm, electrons remained quite free in pure, dry  $NH_3$  gas. They estimated  $h$  as of the order of  $10^{-9}$  and designated  $NH_3$  as virtually a free electron gas. V. A. Bailey carried out an investigation<sup>23</sup> following along the lines of his original investigation on  $NH_3$  gas under exceedingly adverse laboratory conditions at Sydney. With his experimental conditions (so bad that  $NH_3$  had to be dried over  $P_2O_5$ ), he observed electron attachment in  $NH_3$  gas and evaluated  $h$ . Bailey apparently did not note that he had studied  $h$  in  $NH_3$  at values of  $X/p$  of the order of 160 times as high as those of Loeb and Wahlin. He further failed to realize that with his techniques of purification of  $NH_3$ , enforced by inadequate facilities, the burden of proof in clarifying the apparent discrepancy lay on him, for his  $NH_3$  showed attachment while Wahlin's did not. He accordingly launched an unnecessarily savage attack<sup>23</sup> on the work of Loeb<sup>7</sup> and Wahlin.<sup>9</sup> The attack was sufficiently unfair to require a repetition of the measurements by Loeb and a reply<sup>24</sup> to Bailey pointing out Loeb's confirmation of the previous results as well as the difference in conditions under which the measurements of Bailey were made.

In order to clarify the question, Bradbury<sup>25</sup> undertook a study of  $NH_3$  gas using the method already outlined for  $O_2$ . This study was followed by that of many other gases and vapors,<sup>26,27</sup> with the results to be presented. In what follows no details as to the process of purification will be given. It can be assumed that Bradbury achieved the greatest chemical purity that could be obtained with modern techniques on the quantities of gas required.

The results observed in  $NH_3$  are shown in Fig. 124. There it is seen that, up to  $X/p = 9$ , far above Wahlin and Loeb's values,  $h$  in  $NH_3$  is 0. Above  $X/p = 9$ ,  $h$  rises abruptly and rapidly. This agrees with Bailey's work at high  $X/p$ . Bradbury at once interpreted this by assuming that some change occurred in  $NH_3$  when hit by electrons with an energy above that corresponding to an  $X/p = 9$ , with the

result that the electron stuck to the product. It was next shown experimentally by Bradbury that under electron bombardment at an  $X/p$  of about 10 the  $\text{NH}_3$  was decomposed into  $\text{H}_2$  and  $\text{NH}$  in measurable amounts, as seen in Fig. 125. Bailey<sup>13</sup> had also noted that his  $\text{NH}_3$  after use could be sparked with  $\text{O}_2$ , but he could not interpret

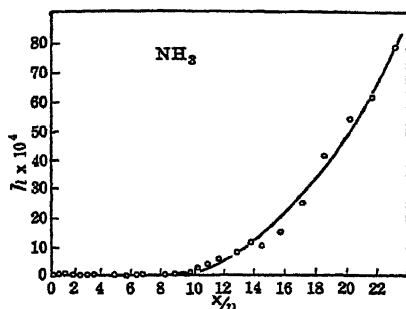


FIG. 124.

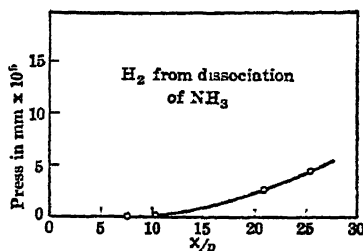


FIG. 125.

this fact. The reaction presumably then follows an equation of the form



Here  $E_{\text{NH}^-}$  is the energy of formation of  $\text{NH}^-$ . The value of the energy of 3 volts needed is that to be expected from photochemical studies of the decomposition of  $\text{NH}_3$  into  $\text{NH}$  and  $\text{H}_2$ . This reaction forming  $\text{NH}^-$  probably occurs in a single impact, since then the products  $\text{H}_2$  and  $\text{NH}^-$  can carry off the extra electron energy. Furthermore, if the formation of  $\text{NH}$  went in two steps to wit:



the attachment to  $\text{NH}$  would require that  $h = 1$  in order to occur at all. The study of the values of  $h$ , in mixtures of  $\text{NH}_3$  with  $\text{N}_2$ ,  $\text{A}$ , and  $\text{He}$ , as a function of  $X/p$ , indicated in Fig. 126, furthermore showed that the value of  $X/p$  at which the electron gave  $\text{NH}_3$  the dissociating energy corresponded to an electron energy of the order of 4 electron volts, which is as close to the photochemical value as these data can yield.

Studies in  $\text{CO}$  by Bradbury<sup>28</sup> gave  $h$  as  $10^{-8}$  or less, in agreement with Wahlin,<sup>9</sup> who believed  $h$  to be about zero in  $\text{CO}$ . The Bradbury apparatus is incapable of measuring values of  $h$  less than  $10^{-8}$ , so that Bradbury set  $h$  as zero from  $X/p = 0.25$  to  $X/p = 20$ . To

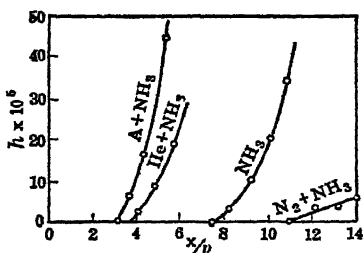


FIG. 126.



dissociate CO requires 9 volts of energy. Thus the electrons did not get energy enough to dissociate CO and form  $O^-$  up to  $X/p = 20$ . Measurements of Townsend<sup>45</sup> in CO at  $X/p = 20$  actually indicate the electron energy as about 2 volts, so that attachment should not have been observed. CO incidentally has closely the electronic structure of  $N_2$ , which has no electron affinity.

For NO, Bradbury found the probability  $h$  to be a function of pressure as well as a function decreasing monotonically with increasing  $X/p$ . The results for  $h$  as a function of  $X/p$  are shown in Fig. 127. The results

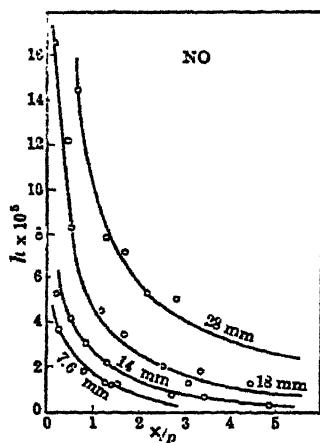


FIG. 127.

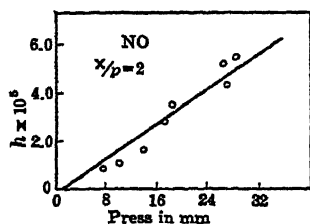
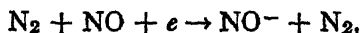
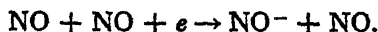


FIG. 128.

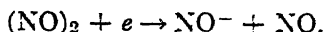
for  $h$  at a given  $X/p$  as a function of the pressure  $p$  are shown in Fig. 128. They show  $h$  to be a linear function of the pressure. This indicates that attachment depends on some property of NO that has to do with pressure and suggests the probability of a multi-body impact reaction. Using mixtures of equal parts of NO and  $N_2$  it was found that  $h$  was one-third of that for pure NO. Hence, of the three types of possible three-body impacts needed to give attachment and take away the energy of formation of  $NO^-$ , which is only reluctantly radiated, only one is possible. The three types of impacts possible in  $N_2$ -NO mixtures are:



It is clear that the only possible one of the three reactions is



Now NO tends to form  $(\text{NO})_2$  with about 0.05 volt energy. The existence of  $(\text{NO})_2$  depends on pressure, as the 0.03 volt average molecular energy molecules of  $(\text{NO})_2$  do not let molecules of  $(\text{NO})_2$  last long. Thus the process active probably is



Perhaps the most interesting molecules to study are those of the truly electronegative gases  $\text{Cl}_2$  and  $\text{HCl}$ . Except for its low heat of dissociation, 1.5 volts,  $\text{Cl}_2$  is *inert* chemically. It should have no electron affinity. James Franck, when he was in California in 1928, in a conversation with the author on the question of electron attachment, stated it as his opinion that in these gases one would find that attachment proceeded as follows: The formation of  $\text{Cl}^-$  gives 4.1 electron volts of energy while the heat of dissociation of  $\text{Cl}_2$  requires but 1.5 volts. Thus it is probable that the attachment in  $\text{Cl}_2$  and probably even in  $\text{HCl}$  proceeds through the attachment of an electron to a  $\text{Cl}_2$  or  $\text{HCl}$  molecule followed immediately by the dissociation of

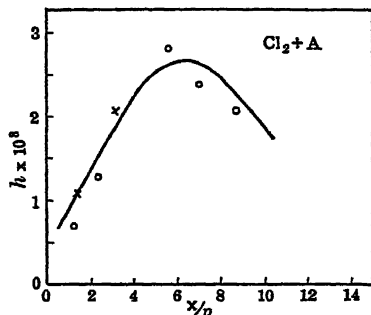


FIG. 129.

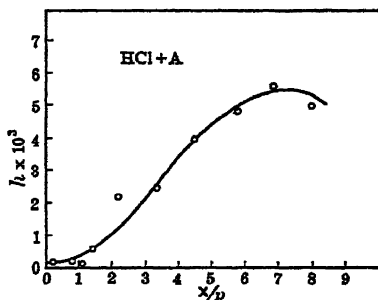
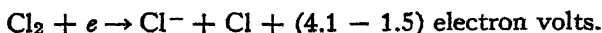


FIG. 130.

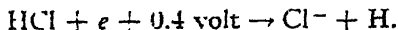
$\text{Cl}_2^-$  into  $\text{Cl}$  and  $\text{Cl}^-$  or  $\text{H}$  and  $\text{Cl}^-$ . Now Wahlin had found that  $h$  in  $\text{Cl}_2$  was too low to measure and appeared to be less than  $10^{-3}$ . In order to measure  $h$  in  $\text{Cl}_2$  as a function of  $X/p$ , Bradbury therefore diluted his  $\text{Cl}_2$  with A. The curve observed in an A- $\text{Cl}_2$  mixture by Bradbury is shown in Fig. 129. The reaction appears to go according to the equation



Mass spectrographic studies of Hogness and Lunn<sup>29</sup> some years before had indicated the existence of only  $\text{I}^-$  ions and never  $\text{I}_2^-$ . This is in excellent agreement with the proposed mechanism which is common to all the halogens.

In  $\text{HCl}$  as in  $\text{Cl}_2$  attachment was very rapid. Bradbury thus again used A- $\text{HCl}$  mixtures. With these he obtained the curve for  $h$  as a function of  $X/p$  given in Fig. 130. The curve is interesting in

that it resembles slightly the curve observed in  $\text{NH}_3$ . Attachment sets in only when electron energy reaches a certain value. Below  $X/p = 1$  the value of  $h$  is relatively low. It rises rapidly above this value. Now the heat of formation of  $\text{Cl}^-$  is 4.1 volts, while the heat of dissociation of  $\text{HCl}$  is 4.5 volts. Thus to get  $\text{Cl}^-$  from  $\text{HCl}$  an added energy of 0.4 volt is needed. The equation then is



This explains the rise of  $h$  in  $\text{A}$  at low values of  $X/p$ , for until the average energy of the electrons approaches 0.4 volt the reaction cannot take place. This work is also borne out by mass spectra of Barton in  $\text{HCl}$ , who found only  $\text{Cl}^-$  ions and no ions of  $\text{HCl}^-$ .

Wahlin<sup>9</sup> had studied laughing gas,  $\text{N}_2\text{O}$ , and estimated  $h \sim 10^{-6}$ . The results of Bradbury and Tatel<sup>22</sup> in  $\text{N}_2\text{O}$  and  $\text{N}_2\text{O-A}$  mixtures are shown in the curves of Fig. 131 and Fig. 132. It is clearly seen

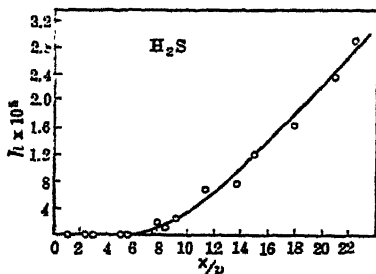


FIG. 131.

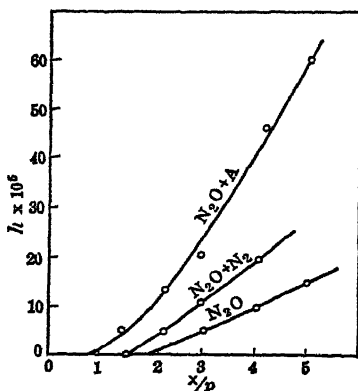
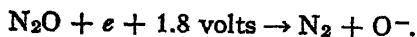
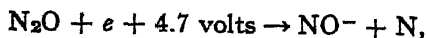


FIG. 132.

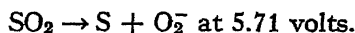
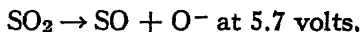
that  $\text{N}_2\text{O}$  has a value of  $h$  of the order of zero below  $X/p = 2$ , and that as in  $\text{NH}_3$  it rises beyond this critical value. It is further seen that the value of  $h$  is independent of pressure above  $X/p = 2$  for the circled points over values in pressure ranging from 3 mm to 21 mm. The gain of energy of electrons in  $\text{N}_2$  is much the same as in  $\text{N}_2\text{O}$ , as shown by the curves of Fig. 132. Thus from Townsend and Tizard's<sup>22</sup> data on  $\text{N}_2$  it is possible to place the rise of the curves at  $X/p = 2$  as corresponding to an energy of 1.7 volts. This at once identifies the reaction taking place as the second one of the two possible reactions considered below, to wit



These possible reactions are the result of photo and thermochemical studies. The absence of a pressure variation of  $h$  indicates that the  $O^-$  is formed simultaneously with the process of attachment.

$CO_2$  had been studied by Loeb<sup>7</sup> and by Wahlin.<sup>9</sup> Loeb generated his  $CO_2$  from marble acted on by  $HCl$ . His values varied from  $10^{-7}$  upward and indicated some form of contamination from the chamber. Bradbury and Tatel<sup>26</sup> used tank  $CO_2$  adequately purified by fractionation. They found  $h$  equal to zero up to the highest  $X/p$ . Since  $CO_2$  does not dissociate into  $CO + O$  below 5.5 volts it must be concluded that  $CO_2$  has a value of  $h = 0$  up to high values of  $X/p$  and energies below 5.5 electron volts.

The only gas besides  $O_2$  to show a real electron attachment without a secondary process is  $SO_2$ . The curves for  $SO_2$  and a mixture of equal parts  $SO_2$  and A are shown in Fig. 133. The value of  $h$ , as in  $O_2$ , decreases rapidly with the increase in  $X/p$  and hence energy. It reaches a minimum at  $X/p = 12$  which corresponds to about 4–6 electron volts. It then increases. This increase may be due to a dissociation and the beginning of a new attachment process. At 5.7 and 5.71 volts two processes of dissociation on electron impact are possible, to wit



It is impossible to decide which reaction occurs.

$H_2S$  was very difficult to purify.

The curve for  $h$  in  $H_2S$  is shown in Fig. 134. It is seen that  $H_2S$  shows no electron attachment until an  $X/p = 6$  is reached. It then has an  $h$  increasing with electron energy. Here again we have dissociation and attachment. There are, from photochemical data, two possible reactions; they are:

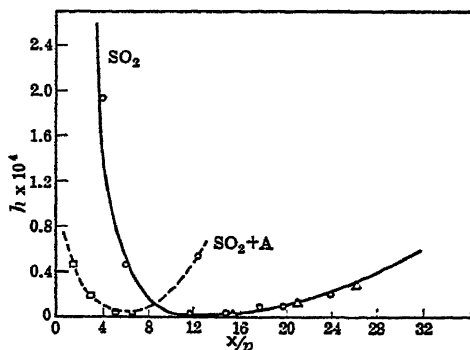


FIG. 133.

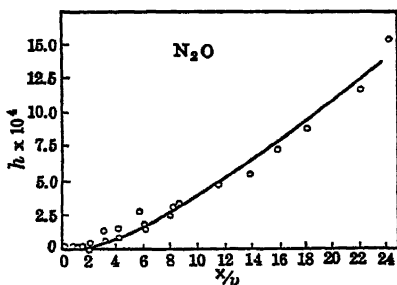


FIG. 134.

Argon mixture studies indicated that the second reaction is the more probable.

Water vapor yielded very interesting effects, as shown in Fig. 135. At low pressures  $H_2O$  acted like  $H_2S$ . No attachment occurred up to  $X/p = 8$ , and then attachment occurred. Argon mixtures showed that at  $X/p = 8$  the energy was about 5 volts. For the dissociation  $H_2O \rightarrow H + OH$  to occur requires 5.4 volts. Thus the curves giving

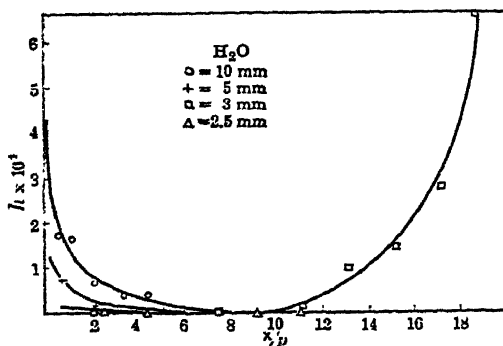
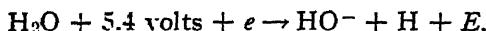
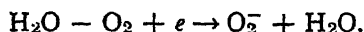


FIG. 135.

$h$  increasing with  $X/p$  above  $X/p = 8$  at low pressure are due to the reaction



The high-pressure attachment is easily explained. At room temperatures at pressures of 10 mm the  $H_2O$  is near saturation, and nuclei of condensation occur that give negative ions. Dissolved gases, e.g.,  $CO_2$  and  $O_2$ , that react with water aid this effect. A and  $N_2$  do not react to increase the effect. On the other hand,  $O_2$  and  $CO_2$  dissolving in water or reacting with it form



This is then in its action like  $NO$ , only with reactions between two molecules of a different sort instead of two of the same sort.

## 7. ATOMIC AND MOLECULAR STRUCTURE AND ELECTRON ATTACHMENT

The gases considered cover the list studied by Bradbury.<sup>20, 25, 26</sup> It is seen that the attachment of electrons and the formation of negative ions take place by one of several processes. On the basis of the results presented, Bradbury<sup>27</sup> was able to summarize or classify the different types of reactions in tabular form. In addition, for diatomic molecules the generalizations enabled Bradbury<sup>27</sup> to associate electron attachment with the spectroscopic classification of the molecular states

TABLE XVIII

| Molecule or Atom   | Ground State  | Negative Ions Form | Electron Energy at Which Attachment Begins                     | Reaction Accompanying Attachment   | Classification of Process   |
|--|---|--------------------|--|--|---|
| He, Ne, Ar, Kr, Xe<br>H <sub>2</sub> , N <sub>2</sub> , CO<br>Cl <sub>2</sub> , Br <sub>2</sub> , I <sub>2</sub> | <sup>1</sup> S <sub>0</sub><br><sup>1</sup> Σ<br><sup>1</sup> Σ | No<br>No<br>No     | .....<br>.....<br>Attaches spontaneously at all energies to Cl | .....<br>.....<br>.....  | .....<br>.....<br>.....   |
| HCl, HBr, HI   | <sup>1</sup> Σ  | No                 | In HCl above 0.4 volt  | Cl <sub>2</sub> + e → Cl <sup>-</sup> + Cl + (4.1 - 1.5) volts<br>HCl + e + (4.5 - 4.1) volts → H + Cl <sup>-</sup>                                | Attachment to one atom and spontaneous dissociation<br>With adequate energy to dissociate, attachment to one atom and dissociation<br>Dissociation by impact with attachment to one constituent |
| NH <sub>3</sub>  | .....   | No                 | Above 3 volts  | NH <sub>3</sub> + e + 3 volts → NH <sup>-</sup> + H <sub>2</sub>   | Dissociation by impact with attachment to one constituent   |
| N <sub>2</sub> O   | <sup>1</sup> Σ  | No                 | Above 1.7 volts  | N <sub>2</sub> O + e + 1.7 volts → O <sup>-</sup> + N <sub>2</sub>   | Dissociation by impact with attachment to one constituent   |
| CO <sub>2</sub>  | <sup>1</sup> Σ  | No                 | .....  | .....  | .....   |
| H <sub>2</sub> S   | .....   | No                 | Above 3.7 volts  | .....  | .....   |
| H <sub>2</sub> O   | .....   | No                 | Above 5.4 volts  | .....  | .....   |
| O <sub>2</sub>   | <sup>3</sup> Σ  | Yes                | All energies, <i>h</i> decreases as energy increases           | H <sub>2</sub> O + e + 5.4 volts → H <sub>2</sub> O <sup>-</sup> + H <sub>2</sub><br>O <sub>2</sub> + e → O <sub>2</sub> <sup>-</sup>              | Dissociation by impact with attachment to one constituent<br>Dissociation by impact with attachment to one constituent<br>Direct attachment, energy goes to vibration, lost in impact later     |
| NH   | <sup>3</sup> Σ  | Yes                | In NH <sub>3</sub> above 3 volts                               | NH + e → NH <sup>-</sup>   | .....   |
| SO   | <sup>3</sup> Σ  | Yes                | In SO <sub>2</sub> above 5.7 volts                             | SO + e → SO <sup>-</sup>   | .....   |
| SO <sub>2</sub>  | .....   | Yes                | All energies, <i>h</i> decreases as energy increases           | SO <sub>2</sub> + e → SO <sub>2</sub> <sup>-</sup>   | Direct attachment, energy goes to vibration, lost in impact later   |
| CN   | <sup>2</sup> Σ  | Yes                | .....  | .....  | .....   |
| NO   | <sup>2</sup> π  | Yes                | All energies   | .....<br>2NO → (NO) <sub>2</sub><br>(NO) <sub>2</sub> + e → NO <sup>-</sup> + NO   | Pressure dependent. Depends on complex formation to take off energy   |
| OH   | <sup>4</sup> π  | Yes                | In H <sub>2</sub> O above 5.7 volts                            | OH + e → OH <sup>-</sup>   | .....   |
| H <sub>2</sub> O   | .....   | No                 | All energies   | (2H <sub>2</sub> O) + e → 2(H <sub>2</sub> O) <sup>-</sup><br>H <sub>2</sub> O + CO <sub>2</sub> + e → H <sub>2</sub> CO <sub>2</sub> <sup>-</sup> | Pressure dependent. Requires formation of complexes to attach to  |
| Cl   | <sup>3</sup> P <sub>3/2</sub>                                   | Yes                | All energies   | Cl + e → Cl <sup>-</sup>   | Direct attachment if energy can be carried off by another atom  |
| O  | <sup>3</sup> P <sub>2</sub>                                     | Yes                | All energies   | O + e → O <sup>-</sup>   | Direct attachment if energy can be carried off by another atom  |

or types. This showed that the spectral classification of molecular species has a close correlation with attachment behavior. The table also contains the dissociation reaction or the ion-forming reaction involved.

From the table it is clear that *neither* the  $^1S_0$  atomic nor the  $^1\Sigma$  molecular electronic configurations will normally attach electrons to make negative ions. Thus, unless the electron attachment or the kinetic energy of the electron itself can furnish adequate energy to *dissociate* the molecule no attachment can take place. In the halogens, where the energy of ion formation exceeds dissociation, *spontaneous attachment* at once occurs, the ions, however, being composed of dissociation products. For all other substances the added energy for dissociation must be supplied by the kinetic energy of the electrons. Such molecular states are characterized by absolutely free electrons or else by the appearance of ions only above a certain critical electron energy or above an equivalent value of  $X/p$ .

On the other hand, it is seen that the  $^3\Sigma$ , possibly the  $^2\Sigma$ , and the  $^2\pi$  and  $^2P$  and  $^3P$  states of molecules and atoms can attach electrons. The attachment will take place at all energies of the electrons but is always more probable the lower the electron energy. Although in general the ion formation is possible, the chief difficulty lies in the dissipation of the energy of ion formation plus the kinetic energy of the electron. For electrons at rest the energy to be dissipated ranges from a few tenths of a volt for  $O_2$  to as much as 4.1 volts for  $Cl^-$ . As a means of dissipation, radiation is an improbable mechanism. Hence such reactions are always facilitated by the presence of other molecules, so that it can be dissipated as kinetic energy of separation. Hence, where a dissociable molecule occurs, the process takes place readily, accompanied by dissociation, with kinetic energy given the constituent atoms. In other cases the existence of polymers permits of attachment followed by dissociation. In two substances, however, direct attachment occurs,  $O_2$  and  $SO_2$ . The exact mechanism is unknown for  $SO_2$  but is interesting for  $O_2$ . It appears that for  $O_2$  the energy of attachment is taken up into vibrational states of the molecule without dissociation and is dissipated in subsequent impacts. For such processes to occur, however, the *energy of ion formation must be small*.

Where energy is dissipated as kinetic energy the probability of attachment may or may not increase with energy at first. Where energy is needed to start dissociation the reaction is characterized by a small or zero value of  $h$  until a threshold is reached. Thereafter  $h$  increases with  $X/p$  as more and more electrons in the distribution acquire the attachment energy. Thereafter  $h$  may decrease.

Where polymer formation must take place to facilitate attachment and energy dissipation, the value of  $h$  will be pressure dependent. Finally, where attachment takes place directly, the value of  $h$  decreases

monotonically and approximately proportional to  $1/\sqrt{E}$ , where  $E$  is the electron energy. It will thus also decrease as  $X/p$  increases. Where inelastic impacts at higher values of  $X/p$  occur which give electrons of low residual energy it is clear that  $h$  may again *appear* to increase with  $X/p$ .

So far no cases of radiative electron capture have been observed. Where large amounts of energy are liberated, as in Cl<sup>-</sup> ion formation, an *ion spectrum* might be expected. These have been looked for in the halogens with no success.<sup>31,32</sup> In O<sub>2</sub>, radiations would be in the extreme infrared and could not be detected.<sup>19,20</sup> From what has gone before, it is likely that the chance of ion formation by processes which do not give rise to radiation is so much more probable than the radiative processes that the radiative processes cannot readily be observed. A detailed wave-mechanical analysis of negative-ion formation is to be found in a recent booklet by Massey.<sup>40</sup>

#### 8. THE ENERGY AND CHARACTER OF THE ATTACHMENT PROCESS IN O<sub>2</sub>

The foregoing summary which appropriately follows the table of attachment processes anticipates in a measure some of the later work in O<sub>2</sub>. In view of the character of the attachment process in O<sub>2</sub> and SO<sub>2</sub>, it became imperative to study the energy of negative-ion formation for O<sub>2</sub><sup>-</sup> in order to see in what measure electrons are bound to the O<sub>2</sub> molecule. This energy is not amenable to calculation, though, from its order of magnitude, wave mechanics enables one to interpret the character of the attachment process. As any attempt to determine the energy spectroscopically seemed out of the question, the only hope lay in a study of the energy required to detach the electron from the negative ion. That this could be done in moderate fields was indicated from the studies of Cravath<sup>16</sup> and of Bradbury,<sup>20</sup> using the electron filters. Here it was observed that the ratio of the transmitted current to the total current at higher values of  $V_g$  began to decrease. The decrease indicated that less ions were getting through, or more ions were being captured. As these decreases were observed at such high-frequency alternating fields that ions could not be captured in appreciable numbers, both Bradbury and Cravath believed that the *ions must be losing their electrons in view* of the violent impacts with neutral molecules in the high grid fields. In fact, Bradbury went so far as to estimate that this break-up occurred at an  $X/p$  of 110 in O<sub>2</sub>.

The problem was studied in detail by Loeb.<sup>19</sup> Electrons and ions from a high-frequency glow discharge in O<sub>2</sub> were driven through a gauze to an electron filter. There the majority of the electrons were removed and the ions passed to a second filter with large wires, thus having a nearly uniform field between the wires. This was called the "smasher" field. The alternating potential  $V_g$  applied to these



wires was such as to remove the electrons and to accelerate the negative ions so as to cause them to shed their electrons in collisions with  $O_2$  molecules. The apparatus is shown in Fig. 136. What was then measured was the negative ion current to plate  $P$  with filter  $S_1$  active as the potential  $V_g$  to  $S_2$  was increased. On occasion the current to  $S_2$  could also be measured. The field  $X_g$  in the smasher varied from  $1.318 V_g/d$  at the surface of the wire to  $0.879 V_g/d$  in the center. A decrease in the current through  $G_2$  with an increase in the current through  $G_1$  indicates a capture of electrons or of ions by the smasher. An increase in both currents denotes a production of electrons in the smasher field. The pressures varied from 2 to 60 mm of  $O_2$ , and frequencies of  $10^6$ ,  $3 \times 10^6$ , and  $10^7$  cycles were used.

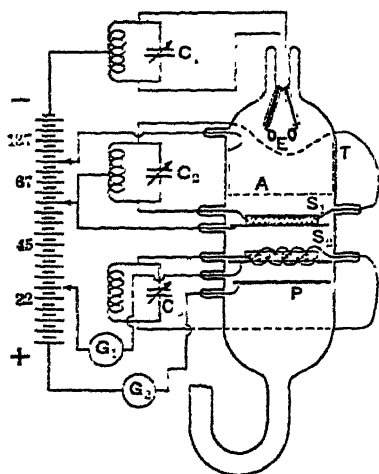


FIG. 136.—Loeb's Device for Detecting Electron Detachment.

comparing the currents in  $G_1$ , dashed, and those in  $G_2$ , full. The portion of the curves marked  $D$  represent a capture of a few stray electrons by the smasher as  $V_g$  was increased. The sharp declines marked  $B$  are observed only at the lower frequencies. At  $9.1 \times 10^6$  cycles  $B$  is marked by hump or rise  $H$ , the "hump effect" of Cravath,<sup>18</sup> which also ultimately declines owing to the "smashing" of negative ions which characterizes  $B$  at lower frequencies. The sharp peaks marked  $R$  occur at all frequencies. They are due to the production of new electrons in the smasher field by electrons liberated. At higher potentials these suffer increased capture and the current declines. Finally the current increase reaches such proportions that an arc breaks at the points  $A$ . It can be seen from Fig. 137C that the cause of the hump is associated with a simultaneous increase in currents in  $G_1$  and  $G_2$  indicating an electron production. This is presumably due to photoelectron liberation from the smasher wires due to exciting impacts of electrons in the smasher field.

The same figure shows the increase in the current in  $G_1$  when the current in  $G_2$  declines owing to the action designated as  $B$ . This indicates that the decline labeled  $B$  is due to loss of ions to the smasher, presumably caused by ion break-up in the smasher field. A plot of the values of  $V_g$  at which  $B$  occurs at different pressures is shown in Fig. 138. It is a linear relation which enables the value of  $X/p$  for

ion break-up to be calculated. The break-up value of  $X/p$  may be set as closely 90 volts per cm per mm pressure. At this  $X/p$  the extrapolated data of Brose<sup>21</sup> on electrons in O<sub>2</sub> permit us to estimate the *electron* energy at 7.8 volts. Where  $R$  begins the average electron energy is of the order of 10 volts, while at the beginning of the hump effect the electron energy is close to 8 volts. What the energy of the

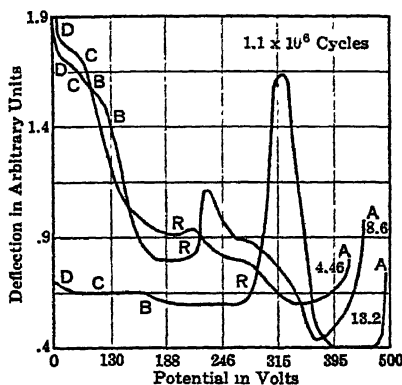


FIG. 137A.

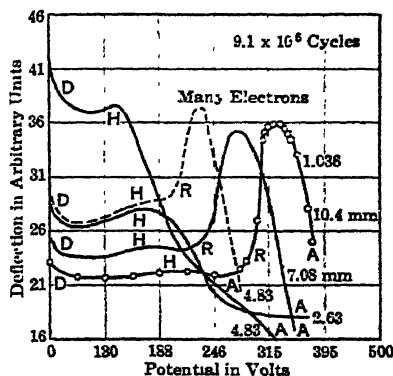


FIG. 137B.

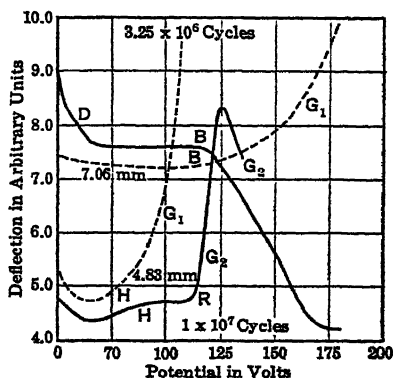


FIG. 137C.

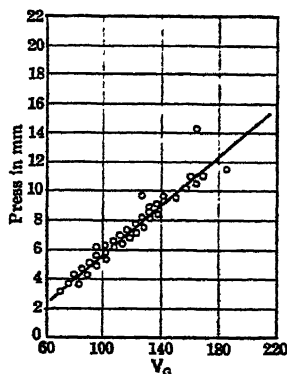


FIG. 138.

*negative ions* at an  $X/p$  of 90 is one cannot accurately say. It can be estimated as of the order of the energy that an ion would acquire over two free paths in this field. The uncertainty in the value of the free path of an ion at the energy which it has at an  $X/p = 90$  makes the evaluation of the ion energy still more uncertain. The result of the uncertainties places the energy of detachment of the electron from the negative O<sub>2</sub><sup>-</sup> ion as lying between the limits of 0.136 and 0.68 electron volt. Of this energy only half is available for the

work of detachment. Hence one can estimate the heat of formation of  $O_2^-$  as lying between 0.068 and 0.34 electron volt.

Further light on the attachment process in  $O_2$  was shed by a theoretical discussion of Bloch and Bradbury<sup>37</sup> which was being undertaken at the same time as Loeb's<sup>19</sup> experiments were under way. In earlier papers Jen<sup>34</sup> and later Massey and Smith<sup>35, 40</sup> had studied the question of the formation of negative atomic ions of  $H^-$ ,  $Cl^-$ , and  $Hg^-$ , using wave mechanical considerations. Of this work more will be said later. It appeared from these studies, however, that the cross section for radiative capture in the formation of  $H^-$  was of the order of  $10^{-22}$  cm<sup>2</sup>, which would make  $h$  in  $H$  of the order of  $10^{-7}$ . In no case was the value of  $h$  as a function of electron energy greater than  $10^{-6}$  as a result of these investigations, and it is possible from experimental data that these estimates were too high. In any event it was quite clear that in the capture of electrons by  $O_2$  molecules the observed value of  $h \sim 10^{-4}$  could not be accounted for by a radiative process. Since a capture occurs for which  $h$  is large and decreases with energy, and since in some cases capture was observed to occur by dissociation and attachment of the electron to a constituent molecule, it was not illogical to imagine a different mechanism. The mechanism proposed considered the attachment of the electron to the molecule without radiation but with an absorption of the energy of ion formation by the vibrational system of the molecule. Thus the relatively small energy of  $O_2^-$  ion formation is not sufficient to cause  $O_2$  to dissociate but is able to cause it to increase its energy of vibration. If this increased energy of vibration can then be lost to other molecules before the attachment process reverses itself the electron will stay attached and the  $O_2^-$  ion will be stable. It is also clear that if in an impact the  $O_2^-$  ion receives the energy of electron attachment as vibrational energy it will stand a finite chance of having its electron detached as has been observed at  $X/p = 90$ .

On this basis Bloch and Bradbury<sup>38</sup> proceeded to calculate the probability of the capture of an electron by an  $O_2$  molecule into a stable orbit with the additional absorption of the energy of attachment into a change in vibrational state on the basis of wave mechanics. This quantity having been calculated, it was next essential to calculate from the average lifetime  $\theta$  in this state the chance that such an excited ion would lose the vibrational energy to a neutral molecule. If the average collision cross section for a transfer of vibrational energy is designated by  $s$  it is at once possible to calculate the average time  $\tau$  between transfers of vibrational energy to molecules. Unless  $\theta \gg \tau$  the capture process above cannot lead to a finite value of  $h$ . On the basis of their analysis Bloch and Bradbury set  $h$  as given by

$$h = \beta \frac{m}{M} \frac{2A^2a}{hv_0} f(E^*) \frac{p}{p+p'}$$

Here  $\beta$  is a numerical constant of the order of magnitude of 1.  $p$  is the pressure of O<sub>2</sub>, and  $p'$  is a "critical pressure" for which  $\theta = \tau$ . At very low values of  $p$ ,  $\tau$  which is proportional to  $1/p$  becomes so large that  $h$  is a function of  $p$ . At large values of  $p$  such that impacts insure attachment whenever capture takes place  $h$  is independent of  $p$ .  $m$  and  $M$  are the masses of electron and molecule.  $v_0$  is the average speed of the electron directly derivable from  $E_0$ , the average energy. The quantity  $A$  is the binding energy of the electron, or the electron affinity, and  $a$  is given by  $(h, 2\pi)^2 / (2ma^2) = A$ .  $a$  is of the order of magnitude of the orbital dimensions of the electron in the bound state. The quantity  $E^* + A$  is the total energy lost by the electron in the capture process and must equal the increased vibrational energy. Hence  $E^* = n'\hbar\omega - A$ , with  $\omega$  the circular frequency of oscillation.  $n'$  is the quantum number of the state of capture and is found to be unity. Thus  $E^*$  is the kinetic energy of the free electron. Using the Druyvesteyn or the Morse, Allis, and Lamar energy distribution function (see Chapter V) for  $f(E^*)$ , we have

$$f(E^*) = \text{const.} \left( \frac{E^{*1/2}}{E_0^{3/2}} \right) e^{-b \left( \frac{E^*}{E_0} \right)^2}, \text{ with } b = 0.847.$$

Here  $E_0$  is the mean electron energy. Putting  $v_0$  into the energy form as  $\propto \sqrt{E_0}$ , Bloch and Bradbury show that

$$h \propto \left( \frac{1}{E_0^3} \right) e^{-b \left( \frac{E^*}{E_0} \right)^2}.$$

On this basis, Bloch and Bradbury have calculated the curve of Fig. 139 for  $h$  in arbitrary units as a function of  $E_0$ , the average electron energy.

In this calculation the electron affinity  $A$  is taken as 0.11 volt, so that  $E^* = 0.08$  volt. The circles are the experimentally observed points of Bradbury for O<sub>2</sub> in this range. The value of the theoretical curve has been adjusted to fit experiment at  $E_0 = 0.3$ . The theoretical rise at low values of  $E_0$  is too rapid. This they ascribe to having chosen

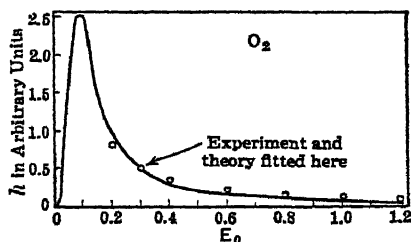


FIG. 139.

for the Ramsauer cross section and capture cross section a behavior which they would show in the *limit of small velocities* and which may not be correct at higher velocities. Since experimentally  $h$  does not appear to approach a maximum even for the smallest values of  $E_0$  one is forced to the conclusion that  $E^*$  cannot be bigger than 0.12 volt. This enables one to place the electron affinity  $A$  between

the limits  $0.07 < A < 0.19$  electron volt. These values are not in disagreement with Loeb's<sup>19</sup> observations.

That even at 3 mm pressure the value of  $h$  is independent of pressure merits discussion. For  $n = 1$  the value of  $\theta$  is  $\theta \sim 10^{-10}$  sec. For  $s$  we can use the value of the cross section as observed in ion mobilities. This gives  $\tau \sim 10^{-9}$  second. Thus to make  $\theta \gg \tau$ ,  $s$  must be 10 to 100 times the collision cross section for unexcited ions. Such a value is not inconsistent with the consideration that vibrational energy transfer will occur by resonance even if the molecules are separated by distances considerably greater than their linear dimensions. At very low pressures in  $O_2$ , however, there is qualitative evidence of a pressure variation of  $h$ . It is thus seen that while we have no accurate data on the attachment process in  $O_2$  we have a fairly good general idea of the process as described by wave mechanics.

## 9. THE FORMATION OF NEGATIVE ATOMIC IONS

Despite the satisfactory description of the behavior of  $O_2$  there is again a rather remarkable discrepancy between the conclusions reached in what has preceded and certain other experimental observations. Ever since the early studies of J. J. Thomson with the mass spectrograph, observers have repeatedly reported the presence of negative ions  $H^-$  and  $N^-$  in canal rays of the gases  $H_2$  and  $N_2$ . Neither of the molecules  $H_2$  nor  $N_2$  has an electron affinity, and negative-ion formation had not under normal conditions of X-ray ionization been reported for these molecules. The *atoms*, however, have not been available for study of attachment under simple conditions so that little is known about their reaction with electrons.

Perhaps one of the latest reports on this subject comes in the work of Tüxen,<sup>36</sup> which gives recent data. He drew the negative ions out of a glow discharge tube and ran them through a mass spectrograph of the J. J. Thomson type. In  $H_2$  he observed  $H^+$ ,  $H_2^+$ , and  $H_3^+$ . When the fields were reversed he observed  $H^-$  and proved that it came directly from  $H$  molecules or ions and *not* from  $OH$  or other bodies. In air he found the positive ions  $N^+$ ,  $O^+$ ,  $N_2^+$ ,  $NO^+$ ,  $O_2^+$ , and the negative ions  $O^-$ ,  $OH^-$  (impurity),  $O_2^-$ ,  $NO_2^-$ ,  $NO_3^-$ . The  $NO_2^-$  and  $NO_3^-$  he believed were readily formed. In  $N_2$  no  $N^-$  ions were found, though Thomson has reported them as being observed infrequently. In  $He$ ,  $Ne$ , and  $A$  he observed not only  $He^+$ ,  $Ne^+$ , and  $A^+$  but molecules of  $He_2^+$ ,  $Ne_2^+$ , and  $A_2^+$  as well. He found *no negative ions of inert gases*. These results are typical and such as to leave no doubt about the facts. Massey<sup>40</sup> showed that the ions  $H^-$  and  $N^-$  were stable while  $He^-$  and  $A^-$  were not. Table XIX shows electron affinities of some of the atoms. Negative values of the energy indicate unstable ions.

The question of the formation of negative ions in gases by different processes had before the time of the work of Bradbury and Bloch been discussed rather extensively from the wave-mechanical aspect by Massey and Smith<sup>35</sup> as regards atomic ions. There it was shown that He and Ne would not be expected to form negative ions while H and Cl might be expected to do so. They calculated the cross section of the atom for *radiative* capture in H and found it to be of the order of  $10^{-22}$  cm<sup>2</sup> compared to  $10^{-16}$  cm<sup>2</sup> for a collision between an H atom

TABLE XIX

VALUES OF THE ELECTRON AFFINITIES OF THE ELEMENTS IN ELECTRON VOLTS  
AS GIVEN BY MASSEY<sup>40</sup>

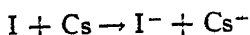
| Atom     | A   | B    |      | C    |      | D     | E      |
|----------|-----|------|------|------|------|-------|--------|
|          |     | 1    | 2    | 1    | 2    |       |        |
| H. ....  |     |      |      |      |      | 0.700 | 0.76   |
| He. .... |     |      |      |      |      | 0     | -0.53  |
| Li. .... |     |      |      |      |      | 0.54  | 0.34   |
| C. ....  |     |      |      |      |      |       | 1.37   |
| N. ....  |     |      |      |      |      |       | 0.04   |
| O. ....  | 2.2 |      |      |      |      |       | 3.80   |
| F. ....  |     |      |      |      | 4.13 |       | 3.94   |
| Ne. .... |     |      |      |      |      |       | -1.20  |
| Na. .... |     |      |      |      |      |       | 0.08   |
| Mg. .... |     |      |      |      |      |       | -0.87  |
| Al. .... |     |      |      |      |      |       | -0.16  |
| S. ....  |     |      |      |      |      |       | 2.06   |
| Cl. .... |     |      |      | 3.83 | 3.75 |       | 3.70   |
| A. ....  |     |      |      |      |      |       | (-1.0) |
| Br. .... |     |      | 3.82 | 3.65 | 3.54 |       |        |
| I. ....  |     | 3.14 | 3.24 | 3.15 | 3.22 |       |        |
| Hg. .... |     |      |      |      |      |       | 1.79   |

A, from collisions; B, from equilibrium constants of attachment reactions; C, from energy cycles—1, from experiments only, 2, using calculated values of crystal energies; D, calculated values; E, empirical extrapolated values.

and electron. Analogous calculations for Na, Hg, and Cl resulted in the curves between energy and capture cross section shown in Fig. 140. The cross sections are large enough so that  $h$  in Hg should be of the order of  $10^{-6}$ . This ready capture in Hg vapor was *not* observed, and it must be concluded that the assumptions underlying the calculation are not accurate.

The possibility of negative-ion formation by electron capture by molecules accompanied by dissociation was shown by Massey and Smith to be feasible and was justified on the Franck-Condon principle. This process, as has been seen, has since been amply established by

Bradbury. A third possibility considered was that attachment occurs as a result of the collision of heavy atoms. Thus they suggested that the reaction



could occur, for the formation of  $\text{Cs}^+$  requires 3.87 volts while that of  $\text{I}^-$  gives up 3.3 volts, the reaction thus requiring only 0.6 volt. Such reactions are akin to molecule formation and separation, provided that the energies of  $\text{I}^-$  and  $\text{Cs}^+$  are great enough to carry the ions apart from the  $\text{CsI}$  molecule after formation, i.e., provided that the energies are above 10 volts. They finally considered a possibility suggested by K. G. Emmeléus that a slow atom of electron affinity  $A$  striking a metal surface of work function  $\phi_s$ , where  $A > \phi_s$ , could rebound from

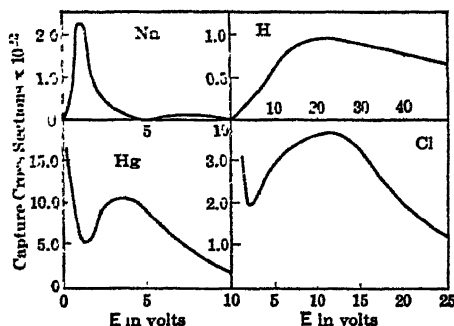


FIG. 140.

the surface as a negative ion. Whether one of the last two processes could account for the appearance of the negative ions in canal-ray studies demands further experimental study. In what follows it will be seen that, in fact, negative ions are formed by a modification of the process of Emmeléus. Massey<sup>40</sup> further shows that, where negative ions are stable, when an electron strikes a molecule during

a polar phase in its vibration the molecule can dissociate into a positive and a negative atom ion. Such ion production has been observed in the case of CO by Lozier and Tate and Lozier.<sup>33</sup>

In 1936 Arnot and Milligan<sup>37</sup> were engaged in a study of the formation of diatomic Hg molecules by the attachment of excited Hg atoms to normal atoms. They used for this purpose an ionization chamber and a magnetic analyzer of special design. In the course of the experiments Arnot and Milligan observed the presence of a *considerable number of negative ions of Hg*. This observation surprised them, for the electron affinity of Hg, according to Glockler, is 1.79 volts, which is less than the work function  $\phi_s$  of the tungsten filament which is 4.52 volts. The filament, however, was unquestionably the source of some of these  $\text{Hg}^-$  ions. Hence the process suggested by Massey and Smith<sup>35</sup> for neutral Hg atoms in this case seems improbable. The process was further tested by using an oxide-coated filament, testing for  $\text{Hg}^-$ , and then flashing the filament and again testing for  $\text{Hg}^-$ . The intensities of the peaks were not changed by changing the value of  $\phi_s$  with the oxide coating.

A diagram of the apparatus is shown in Fig. 141. Here  $F$  is the tungsten filament.  $E_1$  is a grid to accelerate the electrons so as to ionize the Hg vapor coming from Hg. The potential  $V_0$  from  $F$  to  $E_1$  is positive when it accelerates electrons. From  $E_1$  to  $E_2$  the field can retard electrons and accelerate positive ions, or vice versa. Its poten-

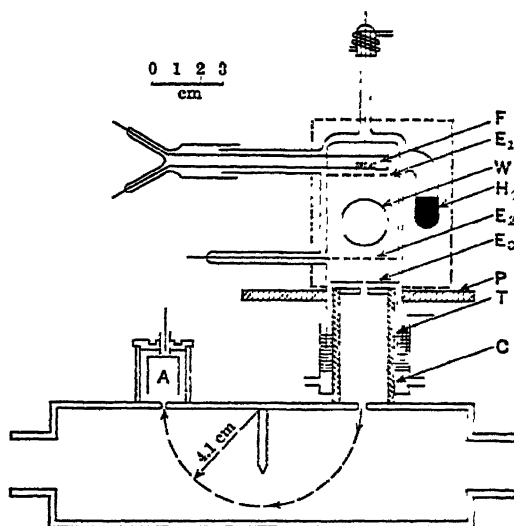


FIG. 141.—Arnot's Apparatus for the Study of Negative Ion Production at Surfaces.

tial is called  $V_1$  and is negative when arranged for positive ions. Between  $E_2$  and the iron cylinder  $T$  (or  $E_3$  if it was used) the potential is called  $V_2$ . Since  $V_0$  is taken as positive,  $V_1$  and  $V_2$  are *negative* in sign if they act to *retard electrons*.  $\text{Hg}^-$  ions appear when  $V_0 + V_1 + V_2$  are all of the same sign.

Keeping the *sum* of the values constant at 204 volts while varying  $V_0$ ,  $V_1$ , and  $V_2$ , the other potentials *always gave one  $\text{Hg}^-$  peak corresponding to closely 204 volts*. Thus the formation of some of the ions must be *on the filament or near it*. No  $\text{Hg}^-$  ions were formed between  $E_1$  and  $E_2$ , and no  $\text{Hg}_2^-$  ions could be detected. The formation of both  $\text{Hg}^+$  and  $\text{Hg}^-$  was *directly* proportional to the electron emission from the filament. To see whether the  $\text{Hg}^-$  ions originated from the dissociation of diatomic molecules the variation of  $\text{Hg}^-$ ,  $\text{Hg}^+$ , and  $\text{Hg}_2^+$  currents with pressure was taken. The  $\text{Hg}^+$  and  $\text{Hg}^-$  curves showed an initial rapid increase with pressure of Hg. They then fell to low values,  $\text{Hg}^-$  falling somewhat *more* rapidly than  $\text{Hg}^+$ .  $\text{Hg}_2^+$  increased linearly with pressure at first and then increased more slowly. The  $\text{Hg}^-$  is seen to be proportional to  $\text{Hg}^+$  throughout, except that its more rapid decline with pressure may be ascribed to destruction of  $\text{Hg}^-$  by impact with neutral molecules as pressure increases.  $\text{Hg}_2^+$



formation, and hence molecule formation, does not influence  $\text{Hg}^-$  production in the least. Stille<sup>39</sup> had suggested that  $\text{HgH}^-$  was being observed and not  $\text{Hg}^-$ . Introduction of H in no way affected the  $\text{Hg}^-$  curves except to decrease their intensity. The energy distribution of the  $\text{Hg}^-$  ions indicated that the  $\text{Hg}^-$  ions had *quite high energies*, having a larger spread of energies than the positive ions or the electrons. Some of the  $\text{Hg}^-$  ions had an excess energy of 20 volts above the main energy of acceleration of 200 volts to which they were accelerated. This is a far greater spread to high energies than the positive ions possess, for their spread is about 2 volts only. The *deficit* of energy of the  $\text{Hg}^-$  and  $\text{Hg}^+$  ions is accounted for by impacts with Hg atoms in the fields.

The only logical explanation of these phenomena consistent with the data is that the  $\text{Hg}^+$  striking the filament and rebounding with an energy of from 0 to 20 volts not only neutralize themselves *but in addition add a second electron giving  $\text{Hg}^-$* . By using two filaments  $F$  instead of one and measuring the current peaks with one filament 200 volts negative to  $E_1$  and the other only 150 volts negative, the origin of the  $\text{Hg}^-$  ions could be distinguished by the value of the magnetic field required to bring in the 150- and 200-volt peaks. The space-charge sheath about the filaments precluded their interfering with each other. It was at once found that, irrespective of whether the 150-volt filament was cold or hot, 150-volt  $\text{Hg}^-$  ions appeared, and vice versa, 200-volt  $\text{Hg}^-$  ions came from the hot or cold 200-volt filament *when* the 150-volt filament alone furnished the ions. Further control experiments also established the formation of  $\text{Hg}^-$  from the *underside* of gauze  $E_2$  at  $V_0 = 50$  volts,  $V_1 = -100$  volts, and  $V_2 = 200$  volts. This gave 200-volt  $\text{Hg}^-$  from  $\text{Hg}^+$  which had been striking the gauze  $E_2$  on their back-and-forth motion in the opposing fields. Finally, keeping the  $\text{Hg}^+$  ion current constant the current of  $\text{Hg}^-$  from  $E_2$  was tested as a function of pressure. This remained constant. Hence the formation of  $\text{Hg}^-$  was not due to the attachment of electrons from  $E_2$  to Hg atoms.

On this basis one must conclude that when a  $\text{Hg}^+$  ion strikes a surface of W above some critical energy a certain fraction of the  $\text{Hg}^+$  ions rebound from the metal surface in the form of  $\text{Hg}^-$  ions. This is analogous to the Emmeléus mechanism but applied to  $\text{Hg}^+$  and not Hg. They then gather their quota of energy from the field between  $F$  and  $E_2$  or  $T$  and may *retain* as well some of the energy with which  $\text{Hg}^+$  struck the filament. The condition under which such a reaction can occur is that  $V_i$ , the ionization potential of the atom, plus  $V_f$ , the electron affinity of the atom, is related to the work function of the surface by  $V_i + V_f > 2\phi_s$ . Now  $V_i$  for Hg is  $V_i = 10.39$  volts.  $V_f = 1.79$  volts.  $\phi_s = 4.52$  volts for W and 5.02 volts for the Ni gauze  $E_2$ . Hence there is 3.14 and 2.12 volts, respectively, excess energy for W and Ni surfaces. The chance of this excess energy being

absorbed in the metal depends on the depth of penetration and hence on the energy of the  $\text{Hg}^-$  ion. At about 10 diameters from the surface the  $\text{Hg}^-$  has a field powerful enough to extract one electron from the surface. In  $10^{-12}$  second the atom is at this surface so that the first electron does not radiate. The excited atom of Hg is then reflected from the surface, giving  $V_i + V_f - 2\phi$  to an electron or

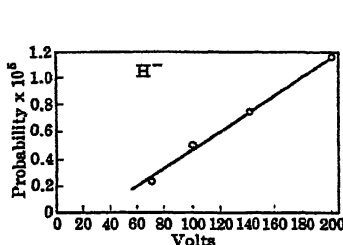


FIG. 142A.

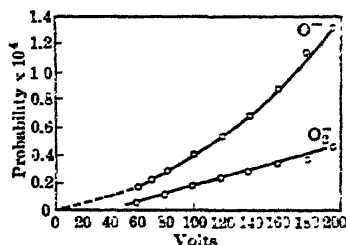


FIG. 142B.

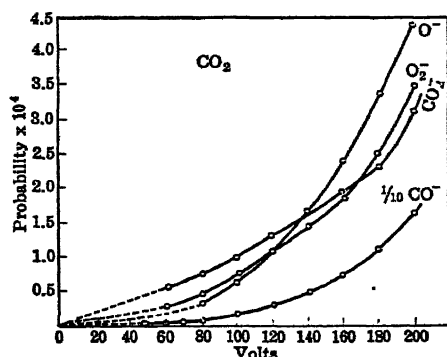


FIG. 142C.

atom in the surface. There is thus negative ion formation *without radiation*. The *accommodation coefficient* of the surface for the  $\text{Hg}^+$  ion is defined by

$$\alpha = \frac{E_i - E_r}{E_i - E_s},$$

where  $E_i$ ,  $E_r$ , and  $E_s$  are the incident kinetic energy, the reflected kinetic energy, and the energy corresponding to the temperature of the surface. If energy is *not* lost on reflection,  $\alpha = 0$ ; and if all the energy is absorbed,  $\alpha = 1$ . In these experiments  $E_s = 0.285$  volt. For 200-volt ions  $\alpha$  is less than 0.9, for there are  $\text{Hg}^-$  ions of more than 20 volts energy beyond that obtained from the field.

On the basis of this result in Hg, Arnot<sup>28</sup> carried out investigations in a number of other gases showing atomic negative ions. The results are shown in the curves given in Figs. 142A, B, and C. Before dis-

cusssing these it must be added that studies of pressure variation of the currents for the positive as well as negative peaks established conclusively as in the case of Hg that *all these ions came by direct impact of the positive ion on a metal surface*. Only  $O^-$  and  $H^-$  were produced with  $N_2$  and  $H_2$  gases, although  $N^-$ ,  $N_2^-$ , and  $H^-$ , and  $H_2^-$  were detected.  $O_2$  gas gave  $O^-$  and  $O_2^-$ , while  $CO_2$  gave  $CO_2^-$ ,  $CO^-$ ,  $O_2^-$ , and a small amount of  $C^-$ . These results are consistent with the previous attachment findings of Bradbury.<sup>27</sup>  $N_2$  and  $H_2$  do *not give negative ions*. Under proper conditions H may do so. These conclusions thus also account at least for some of the negative atomic ions found in canal-ray studies.

The curves show the probability of conversion of positive ions into negative ions in  $O_2$ ,  $H_2$ , and  $CO_2$  as a function of the energy of the impinging positive ions on Ni surfaces. Table XX also gives the values of the probabilities for various positive ions at 180 volts energy on Ni.

TABLE XX

PROBABILITY OF CONVERSION OF 180-VOLT POSITIVE IONS INTO NEGATIVE IONS ON A NICKEL SURFACE

| Negative Ion | Positive Ion from Which Formed  | Probability of Formation. Units of $10^{-4}$ |
|--------------|---------------------------------|--|
| $Hg^-$       | $Hg^+$                          | 5.4  |
| $H^-$        | $H_2^+$                         | 0.104  |
| $O^-$        | $O_2^+$                         | 1.10   |
| $O_2^-$      | $O_2^+$                         | 0.42   |
| $CO_2^-$     | $CO_2^+$                        | 2.31   |
| $CO^-$       | $CO_2^+$                        | 2.51   |
| $O^-$        | 77.4% $CO_2^+$<br>+22.6% $CO^+$ | 10.8   |
| $C^-$        |                                 | 3.37<br>(0.1)                                |

There is little comment to be made on these data except to point out that the probability of formation is in all cases quite small. It appears especially large in the case of  $Hg^-$  and  $CO^-$  and  $O^-$  from  $CO_2$ . Further search was made for negative-ion production either by dissociation on electron impact or by radiative processes. There was no evidence for any such action. Table XXI gives data as to the excess energy of the ions.

In a final study Arnot evaluated the energy distribution of the negative ions formed by the process just considered. The curves of Figs. 143A and B show the energy distribution among the negative ions formed by 140-volt positive ions of H and O. It is seen that in  $O_2$  there are some  $O^-$  ions with as much as 55 volts energy in excess of the energy coming from the field in which they were accelerated.

This energy comes as residual energy from the 140-volt positive ions which generated them. The values of the negative energy spread observed (i.e., energy less than the accelerating energy) come from collisions with the gas molecules in the chamber.

TABLE XXI

| Negative Ion    | Positive Ion from Which Formed | $V_i$ volts | $V_f$ volts | Excess Energy<br>$V_i - V_f - 2\phi_e$ volts |
|-----------------|--------------------------------|-------------|-------------|--|
| Hg <sup>-</sup> | Hg <sup>+</sup>                | 10.39       | 1.79        | 2.12   |
| H <sup>-</sup>  | H <sup>+</sup>                 | 13.5        | 0.76        | 4.20   |
| H <sup>-</sup>  | H <sub>2</sub> <sup>+</sup>    | 15.5        | 0.76        | 6.20   |
| O <sup>-</sup>  | O <sup>+</sup>                 | 13.5        | 3.80        | 7.24   |
| O <sup>-</sup>  | O <sub>2</sub> <sup>+</sup>    | 13.0        | 3.80        | 6.74   |
| O <sup>-</sup>  | CO <sup>+</sup>                | 14.1        | 3.80        | 7.84   |
| O <sup>-</sup>  | CO <sub>2</sub> <sup>+</sup>   | 14.4        | 3.80        | 8.14   |
| C <sup>-</sup>  | CO <sup>+</sup>                | 14.1        | 1.37        | 5.41   |
| C <sup>-</sup>  | CO <sub>2</sub> <sup>+</sup>   | 14.4        | 1.37        | 5.71   |

In a more recent note Arnot and Beckett<sup>41</sup> report that negative ions of masses 16, 24, 32, 37, and 44 are emitted when A<sup>+</sup>, N<sub>2</sub><sup>+</sup>, or Hg<sup>+</sup> strike a filament that has not been degassed. The 16 and 32 ions are doubtless O<sup>-</sup> and O<sub>2</sub><sup>-</sup>, while 24 may be C<sub>2</sub>H<sup>-</sup>. These were produced

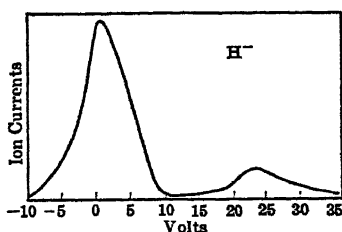


FIG. 143A.

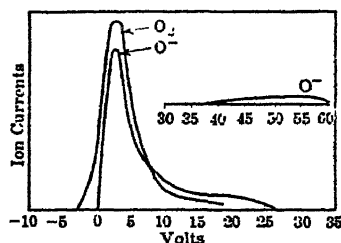


FIG. 143B.

from gases occluded on the surfaces on bombardment by foreign ions of adequate energy. Outgassing the filament removed these peaks. Flushing the chamber with O<sub>2</sub> gave merely peaks of O<sup>-</sup> and O<sub>2</sub><sup>-</sup> that were very intense. The N<sup>-</sup> peaks previously reported were doubtless O<sup>-</sup> knocked out by N<sub>2</sub><sup>+</sup> and not resolved in the mass spectrograph. These results have been confirmed independently by Sloane and Press.<sup>42</sup> The theory has recently been worked out by R. A. Smith.<sup>43</sup>

It can be seen from the foregoing material that, between the initial recognition of the existence of negative molecular or atomic ions, the assumption of ion break-up at low pressures, and the later analysis of

the phenomena, we have progressed a great deal in an understanding of the subject. In any event, the character of the electron attachment and in general of the formation of negative ions is far more complicated than we had anticipated. The processes, once understood, however, appear quite consistent with our later knowledge of electronic behavior.

#### 10. REFERENCES FOR CHAPTER VI

1. FRANCK and POHL, *Verhandl. deut. physik. Ges.*, 12, 291, 613, 1910.
2. TOWNSEND and TIZARD, *Proc. Roy. Soc., A* 87, 357, 1912; *A* 88, 336, 1913.
3. A. F. KOVARICK, *Phys. Rev.*, 30, 415, 1910.
4. S. RATNER, *Phil. Mag.*, 32, 442, 1916.
5. L. B. LOEB, *Phys. Rev.*, 8, 633, 1916; *J. Franklin Inst.*, 184, 755, 1917.
6. E. M. WELLISCH, *Am. J. Sci.*, 39, 583, 1915; 44, 1, 1917; *Phil. Mag.*, 31, 186, 1916; 34, 33, 1917.
7. L. B. LOEB, *Phys. Rev.*, 17, 84, 1921; *Proc. Natl. Acad. Sci.*, 7, 5, 1921.
8. J. J. THOMSON, *Phil. Mag.*, 30, 321, 1916.
9. H. B. WAHLIN, *Phys. Rev.*, 19, 173, 1922.
10. KIA-LOK, YEN, *Phys. Rev.*, 11, 337, 1918.
11. L. B. LOEB, *Phil. Mag.*, 43, 229, 1922.
12. L. B. LOEB, *J. Franklin Inst.*, 195, 45, 1924.
13. L. B. LOEB, *Proc. Natl. Acad. Sci.*, 9, 335, 1923.
14. L. B. LOEB, *Phys. Rev.*, 23, 163, 1924.
15. V. A. BAILEY, *Phil. Mag.*, 22, 825, 1925.
16. A. M. CRAVATH, *Phys. Rev.*, 34, 605, 1929.
17. N. E. BRADBURY, *Phys. Rev.*, 44, 883, 1933.
18. H. F. LUSK, Thesis, Univ. of California, May, 1927.
19. L. B. LOEB, *Phys. Rev.*, 48, 684, 1935.
20. N. E. BRADBURY, *Phys. Rev.*, 40, 980, 1932.
21. H. L. BROSE, *Phil. Mag.*, 50, 536, 1925.
22. TOWNSEND and TIZARD, *Proc. Roy. Soc., A* 88, 336, 1913.
23. V. A. BAILEY, *Phil. Mag.*, 6, 1073, 1928.
24. L. B. LOEB, *Phil. Mag.*, 8, 98, 1929.
25. N. E. BRADBURY, *J. Chem. Phys.*, 2, 827, 1934.
26. BRADBURY and TATEL, *J. Chem. Phys.*, 2, 835, 1934.
27. N. E. BRADBURY, *J. Chem. Phys.*, 2, 840, 1934.
28. J. S. TOWNSEND, *J. Franklin Inst.*, 200, 563, 1925.
29. HOGNESS and LUNN, *Phys. Rev.*, 30, 26, 1927.
30. F. A. BARTON, *Phys. Rev.*, 30, 614, 1927.
31. O. OLDENBURG, *Phys. Rev.*, 43, 534, 1933.
32. HOGNESS and HARKNESS, *Phys. Rev.*, 32, 784, 1928; TATE and LOZIER, *Phys. Rev.*, 39, 254, 1932; W. W. LOZIER, *Phys. Rev.*, 42, 8, 1934.
33. BLOCH and BRADBURY, *Phys. Rev.*, 48, 689, 1935.
34. JEN, *Phys. Rev.*, 43, 540, 1933.
35. MASSEY and SMITH, *Proc. Roy. Soc., A* 155, 472, 1936.
36. O. TÜXEN, *Z. Physik*, 103, 463, 1936.
37. ARNOT and MILLIGAN, *Proc. Roy. Soc., A* 156, 538, 1936.
38. F. L. ARNOT, *Proc. Roy. Soc., A* 158, 137, 1937.
39. STILLE, *Ann. Physik*, 17, 635, 1933.
40. H. S. W. MASSEY, *Negative Ions*, Cambridge Physical Tracts, Cambridge Press, 1938.
41. ARNOT and BECKETT, *Nature*, 141, 1011, 1938.
42. SLOANE and PRESS, *Nature*, 141, 872, 1938.
43. R. A. SMITH, *Proc. Roy. Soc., A* 168, 19, 1938.

## CHAPTER VII \*

### IONIZATION CURRENTS IN GASES IN FIELDS BELOW IONIZATION BY ELECTRON IMPACT

#### 1. INTRODUCTION

In order to understand and to appreciate the much more complicated phenomena occurring in gaseous discharges the characteristics of ordinary currents in gases must be understood in principle. From such studies the important factors active in discharges, such as geometrical, diffusion, space charge, and other influences, may be understood. In introducing this material it will therefore be presented in terms of four typical cases illustrating these important factors. They are as follows: We consider first electrons or ions emitted isotropically at a uniform rate from the surface of one of a pair of equal circular plates forming a plane parallel plate condenser of plate distance  $d$  and radius  $R$ . The plates are placed in a vacuum, and the current density is so small that space-charge effects do not occur. It is required to find the current  $i$  as a function of field strength, initial velocity, and geometry of the plate system. The current must start at a finite value for zero field strength, approaching but never reaching a constant saturation value. The rate of rise depends on the ratio of  $d/R$  and on the initial velocity of emission. In this case the character of the current is limited by geometrical factors, and the loss of carriers is due to such factors. Although in practice serious disturbance by geometrical factors can be avoided in a measure by suitable guard rings, these are never completely effective and frequently cannot be applied. The effect of such factors on the current-voltage characteristic is thus of some interest but not of vital importance.

The second case is the emission of electrons or ions of one sign from one of a pair of parallel plates of a condenser in the presence of a gas. Here space charges and the geometrical loss are neglected by limiting the ionization to a small area at the center of the system. The variation of the current with field strength and pressure in this case therefore depends primarily on the initial velocity of the ions or electrons and the loss by diffusion. No exact solution has been achieved, but an approximate equation of Thomson will be derived. The case is one of practical importance in ionic studies and leads to a fairly

\* References for Chapter VII will be found on page 335.

good evaluation of electronic mobilities. It further clearly indicates the conditions under which loss of carriers by diffusion is of importance.

The third case is that of the space-charge-limited current between parallel-plate electrodes in vacuum resulting from the emission of high current densities. The effect of the energy of emission will be briefly considered, and some data on the effect of positive ions on the space-charge-limited current in a cylindrical condenser will be given. The practical application of the principles illustrated in this case need hardly be called to mind.

In the fourth case the ionization currents in a gas with a volume ionization of positive and negative ions will be sketched and treated in brief for positive and negative ions of equal mobility. The ions are assumed to be produced at a constant rate throughout the volume, and are lost by recombination. The losses by recombination and by the current are considered large relative to diffusion, which is neglected. From the character of the space charge or potential distribution curves, as well as of the field strengths as functions of the distance from the electrodes, a good picture is obtained of the conditions existing in discharge tubes but brought about by a simpler mechanism amenable to computation. This is especially true for the extension of the considerations to the case where the mobility of one carrier is far greater than that of the other.

It will thus be seen that by presenting a number of easily realized examples separately under idealized simple conditions the important effects of gap geometry, diffusion, space-charge limitation, and field distortion produced by difference in mobilities can be demonstrated.

## 2. CASE 1. THE GEOMETRICALLY CONDITIONED SATURATION CURRENT

Consider a pair of circular plane parallel electrodes of radius  $R$  separated by a distance  $d$  as shown in Fig. 144. From plate  $A$  there are liberated at a uniform rate over the whole surface photoelectrons at a uniform velocity  $v_0$ . This is actually not realized in practice, for such electrons are usually liberated with a distribution about a probable velocity near 0.6 the maximum velocity of emission. The assumption of a uniform velocity, however, simplifies calculation and does not alter the problem in any essential point. It is next assumed that the electrons are emitted isotropically in azimuth and in all directions vertically. The space between the plates is devoid of any gas. The electrons are accelerated freely between the plate  $A$  and the electrometer plate  $E$  by an appropriate potential  $V$  applied to  $A$ , giving a field of strength  $X$ . The field between  $A$  and  $E$  is assumed uniform up to the edge of the plates and is then set as zero. An electron liberated from some point  $D$  on  $A$  at an angle  $\theta$  with the vertical will be accelerated in the amount  $a = Xe/m$  towards  $E$  by this field. It

will describe a parabolic path until it strikes the bounding cylindrical plane about the plates. From then on it ideally continues along the tangent to the parabolic orbit. If the ratio of the velocity of emission  $v_0$  and the acceleration  $a$  are appropriate for a given angle  $\theta$ , and point  $D$ , the electrons projected within certain azimuthal angles about  $OD$  will describe trajectories so as to reach  $E$  under a given ratio of  $R/d$ . Thus, given a fixed set of conditions such as the ratio  $R/d$ ,  $OD$ , angle  $\theta$ , and velocity  $v_0$ , the electrons between a given limiting pair of azimuthal angles will all be captured for a given value of field strength  $X$ . By evaluating these limits for different values of  $X$  and all values of  $OD$  from zero to  $R$  we can plot the fraction  $f = i/i_\infty$  of the emission current  $i_\infty$  from  $A$  that reaches  $E$  as a function of  $X$ . It is quite clear physically that at all times there will be some electrons from the plate  $A$  reaching  $E$  even in the absence of a field. Hence one can expect the current to start at  $X = 0$  from some *finite* value. At very high values of  $X$  there must be in the limit a current  $i_\infty$  caught. For low values of  $v_0$ , lower values of  $X$  will be required to reach a given value of  $f$  than with high values of  $v_0$ . The problem was kindly set up by Dr. W. R. Haseltine, and the integrations were carried out by Mr. Leslie Cook, an N. Y. A. computer. It will suffice at this point to indicate how the problem was set up and to discuss the resulting curve

Let us call  $R$  the radius of the plates and  $d$  the distance of separation. Consider an element of area  $d\sigma$  of the plate  $A$  located at a point  $D$ , distant  $r$  from the center  $O$ . At  $D$  set up a system of polar coordinates. Let  $\theta$  be the angle between the velocity  $v_0$  and the perpendicular to the plates, measured from the vertical down. Let  $\phi$  be an azimuthal angle with respect to a line through  $OD$  measured counterclockwise from  $OD$  about  $D$  as shown in Fig. 144. Call  $x_0$  the distance from  $D$  to any point on the edge of the plate. Then  $R^2 = r^2 + x_0^2 - 2rx_0 \cos \phi$ . Let an electron start from  $D$  in a direction  $\theta, \phi$ , with an initial velocity  $v_0$ . If the field strength is  $X$ , the time taken to cross the distance  $d$  between the plates is  $t$ , given by

$$d = \frac{1}{2} \frac{Xe}{m} t^2 + v_0 t \cos \theta.$$

In this time  $t$  the electron traverses a distance  $x = v_0 t \sin \theta$  horizontally along  $x_0$ . By eliminating  $t$  from these equations we find  $x$ , the hori-

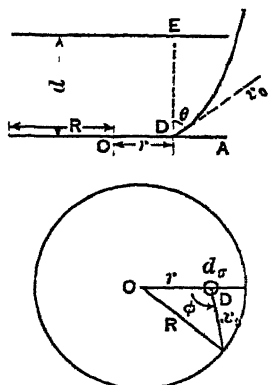


FIG. 144.



zontal distance along  $x_0$  covered before striking  $E$  as a function of  $d$ ,  $X$ ,  $v_0$ , and  $\theta$ . Call  $a = Xe, 2m$ ; then we have

$$x = v_0 \sin \theta \left[ -\frac{v_0 \cos \theta}{2a} + \sqrt{\frac{v_0^2 \cos^2 \theta}{4a^2} + \frac{d}{a}} \right],$$

and

$$R^2 = x_0^2 + r^2 - 2rx_0 \cos \phi,$$

which gives

$$x_0 = r \cos \phi - \sqrt{r^2 \cos^2 \phi + (R^2 - r^2)}.$$

Now if  $\theta$  is less than some limiting value  $\theta_c$ , all electrons projected at angles less than  $\theta_c$  along  $x_0$  will reach the upper plate  $E$ . All electrons projected at angles greater than  $\theta_c$  will escape capture by the upper plate. If the distance  $x$  which the particles move horizontally along  $x_0$  between the plates in  $t$  is less than  $x_0$  for the given element  $d\sigma$  chosen, these particles will be captured by  $E$ . If it is greater, the particles will escape. Hence the critical angle  $\theta_c$  is found by setting  $x = x_0$ . Accordingly  $\theta_c$  is given by

$$v_0 \sin \theta_c \left( -\frac{v_0 \cos \theta_c}{2a} + \sqrt{\frac{v_0^2 \cos^2 \theta_c}{4a^2} + \frac{d}{a}} \right) = r \cos \phi - \sqrt{r^2 \cos^2 \phi + (R^2 - r^2)}.$$

Let us now simplify by setting up a number of dimensionless constants, calling  $r/R = \rho$ ,  $\gamma = aR^2/dv_0^2$ , and  $\delta = d/R$ , whence  $v_0^2/2aR = 1/2\gamma\delta$ . Then

$$-\frac{\sin \theta_c \cos \theta_c}{2\gamma\delta} + \sqrt{\frac{\cos^2 \theta_c \sin^2 \theta_c}{4\gamma^2\delta^2} + \frac{\sin^2 \theta_c}{\gamma}} = \rho \cos \phi + \sqrt{\rho^2 \cos^2 \phi + 1 - \rho^2}.$$

From this  $\theta_c$  can be evaluated, albeit in a troublesome form.

To find the number of electrons leaving the plate  $A$  which reach  $E$  we must integrate over all values of  $\theta$  from  $\theta = 0$  to  $\theta = \theta_c$ , assuming that the number emitted as a function of  $\theta$  is known. This expression must next be integrated over all values of  $\phi$  from 0 to  $2\pi$ , which is complicated by the fact that  $\phi$  is a function of  $\theta_c$ . Finally we must integrate over the area of the plates. Calling  $j$  the normal current per unit area per unit solid angle, the current emitted at an angle  $\theta$  is  $j \cos \theta$ . Thus the total current is given by

$$\begin{aligned} i &= 2\pi j \int_0^R r dr \int_0^{2\pi} d\phi \int_0^{\theta_c} \cos \theta \sin \theta d\theta \\ &= 2\pi j \int_0^R r dr \int_0^{2\pi} d\phi \left[ \frac{\sin^2 \theta_c}{2} \right]. \end{aligned}$$

If all the ions are to be caught,  $\theta_c = \pi/2$ , so that the maximum possible current is  $i_\infty$ , which is given by  $i_\infty = j\pi^2 R^2$ . Hence, as  $\rho = r/R$ , the fraction of the total emission captured is at once

$$\begin{aligned} f = \frac{i}{i_\infty} &= \frac{2}{\pi} \int_0^1 \rho d\rho \int_0^\pi d\phi [\sin^2 \theta_c] \\ &= \frac{2}{\pi} \int_0^1 \rho d\rho \int_0^\pi d\phi \Psi(\rho, \phi, \delta). \end{aligned}$$

The solution of the equation for  $\theta_c$  under different circumstances is a tedious and troublesome affair. It can be solved for under three different cases, to wit:

1. For small fields  $4R^2 < dv_0^2/a$  or  $\gamma < \frac{1}{4}$ , when

$$\frac{i}{i_\infty} = \frac{2}{\pi} \int_0^1 \rho d\rho \int_0^\pi \Psi(\rho, \phi, \delta) d\phi,$$

with

$$\begin{aligned} \Psi(\rho, \delta, \phi) &= \frac{1 + \rho^2 \cos^2 2\phi + 2\rho \cos \phi \sqrt{1 - \rho^2 \sin^2 \phi}}{2(\delta^2 + 1 + \rho^2 \cos 2\phi + 2\rho \cos \phi \sqrt{1 - \rho^2 \sin^2 \phi})} \left\{ (2\delta^2 \gamma + 1) \right. \\ &\quad \left. + \sqrt{1 + 4\delta^2 \gamma - 4\delta^2 \gamma^2 (1 + \rho^2 \cos 2\phi + 2\rho \cos \phi \sqrt{1 - \rho^2 \sin^2 \phi})} \right\} \end{aligned}$$

II.  $4R^2 > dv_0^2/a$  or  $1 > \gamma > \frac{1}{4}$ .

$$\frac{i}{i_\infty} = \frac{2}{\pi} \int_0^{-1+\frac{1}{\sqrt{\gamma}}} \rho d\rho \int_0^\pi \Psi(\rho, \phi) d\phi + \frac{2}{\pi} \int_{-1+\frac{1}{\sqrt{\gamma}}}^1 \rho d\rho \left\{ \phi_0 + \int_{\phi_0}^\pi \Psi(\rho, \phi) d\phi \right\},$$

where

$$\cos \phi_0 = \frac{1 - \gamma(1 - \rho^2)}{2\rho\sqrt{\gamma}}.$$

III. For large fields  $R^2 > dv_0^2/a$  or  $\gamma > 1$ .

$$\frac{i}{i_\infty} = (1 - \gamma^{-1/2})^2 + \frac{2}{\pi} \left\{ \int_{1-\frac{1}{\sqrt{\gamma}}}^1 \rho d\rho \left[ \phi_0 \int_{\phi_0}^\pi \Psi(\rho, \phi) d\phi \right] \right\}.$$

These integrations were carried out graphically by Mr. Leslie Cook on N.Y.A. time for two cases:  $\delta = d/R = 0.1$ , and  $\delta = 1$ . They were evaluated for the values of  $\gamma = aR^2/dv_0^2 = (Xe/2m) R^2/dv_0^2 = (Xe/2m) R/dv_0^2$ , equal to 0, 0.25, 0.5, 1, 9, 100. The results are plotted in the curves of Fig. 145, which give  $f = i/i_\infty$  as a function of  $\gamma$  and of a corresponding  $X$  in the two cases. If we had used photoelectrons of 1-volt energy,  $v_0 \sim 6 \times 10^7$  cm/sec. If  $R = 5$  cm and  $\delta = 1$ , then  $\gamma = 1.22X$ , where  $X$  is in volts per centimeter. The values of  $X$  needed for the

values of  $\gamma$  plotted in this case are 0, 0.308, 0.616, 1.22, 11.0, and 122 volts/cm. In the case where  $\delta = 0.1$ , the fields needed are 0, 0.031, 0.062, 0.12, 1.1, and 12.2 volts/cm. It is seen that, while the currents never completely saturate, the error caused by lack of saturation

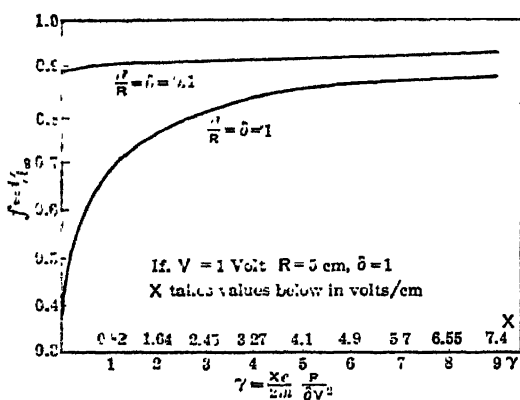


FIG. 145.

produced by the geometrical factor under these conditions is relatively small when  $\delta = 0.1$  if fields of 10 to 12 volts/cm are used.

### 3. CASE 2. PHOTOELECTRIC CURRENTS OF LOW DENSITY IN GASES

Consider a current of photoelectrons or carriers all of one sign liberated from the plate  $A$  of the parallel-plate condenser shown in Fig. 146. They are uniformly liberated from a small area  $A$  in the

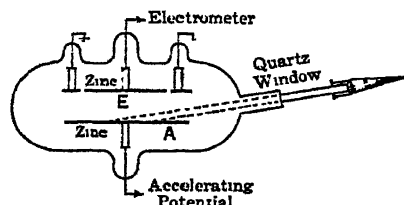


FIG. 146.

uniform field portion, and we neglect loss due to lateral motion. They have an *average* velocity on liberation designated by  $C$ . The space between the plates is filled with a gas at a pressure  $p$ . For simplicity this gas can be considered one in which electrons do not attach to form ions. The calculation is modified in details only if we use a gas

like air where the electrons attach after some  $10^5$  impacts. We are interested in knowing the current received by plate  $E$  as a function of the uniform field  $X$  applied to the plates and the pressure  $p$ . In varying the pressure we must assume that the initial photoelectric current  $i_0$  set free by the light is not affected by gas pressure. Although it is true that the photoelectric work function, threshold, and thus current

are very much influenced by adsorbed gas layers, it appears that pressures of the order of a millimeter of mercury and more do not alter these quantities or  $i_0$ . The reason probably lies in the fact that, while adsorbed gas films change rapidly with degassed surfaces and surfaces subjected to very low gas pressures, at such pressures as we are to deal with the change of pressure cannot alter the established monomolecular films that affect  $i_0$ . Analogous reasoning will hold if instead of photoelectrons we use a thermionic source of electrons or positive ions. Unless gases oxidizing or altering the filament, such as  $O_2$  on W, are used the effect of change in  $p$  will be negligible. Hot sources, however, do introduce another difficulty in that they reduce the density of the gas in their neighborhood in an incalculable fashion and to an extent which may vary with  $p$  and alter  $i$ . Hence for this reason they are not so satisfactory as the photoelectrons in such a study as we wish to make.

The introduction of a gas changes the conditions which were considered in case 1 independently of the altered geometrical assumptions. The electrons no longer are freely accelerated towards the plate  $E$ , but, starting with their original velocity of emission  $C$  which owing to collisions with gas molecules quickly becomes random, they are accelerated towards the plate  $E$  and rapidly reach a steady-state drift velocity in the field direction. This means that after a short distance in the gas they move with a drift velocity  $v = k_e X$  in the field direction, where  $k_e$  is the electron mobility and  $X$  is the field strength assumed uniform and undistorted by the few electrons present. In the neighborhood of the plate  $A$  from which they are emitted, however, the accumulation of electrons due to the retarding effect of molecular impacts and high random velocities will result in a diffusion of the electrons *back* to plate  $A$ . Diffusion also takes place in the field direction towards  $E$  but does not seriously concern us. The diffusion back to plate  $A$ , however, is more important, for it results in most of the electrons which diffuse back to  $A$  being captured by  $A$  and being thus lost to the current. Hence, of the current  $j_0$  per square centimeter of surface emitted by the light, the current  $j$  collected by  $E$  will be less by the diffusion loss. That the diffusion loss may not be small in the case of electrons was indicated in Chapter V in the calculations of G. Hertz.<sup>1</sup> The importance of this loss, however, was not at first recognized, as will be seen.

The problem of calculating the currents under these conditions was first undertaken by J. J. Thomson<sup>2</sup> as far back as 1906. With simplifying assumptions he arrived at an approximate but basically sound equation. Experimental tests, even with the improved techniques, using free electron gases, did not seem to confirm the theory. In fact, the pressure variation of the currents observed was radically different from that yielded by the theory, as shown by Woolsey.<sup>3</sup> This problem was temporarily abandoned until the appearance of a

paper on the subject by Langmuir.<sup>4</sup> Langmuir had derived a new theory applicable to *low* pressures only on the basis of the Hertz<sup>1</sup> equation cited. He extrapolated the theory to higher pressures a procedure which led to unjustified predictions. Stimulated by this article and in order to correct the error in extrapolation Loeb and Bradbury again considered the problem. Bradbury<sup>5</sup> proceeded to get some current-potential curves using the highly improved techniques which he had developed. In the meanwhile Loeb discovered that the difficulty with Thomson's equation was caused by the misinterpretation of the velocity  $C$  used in the equation. With a proper interpretation of the meaning of  $C$  and the new data, Bradbury<sup>6</sup> was able to verify Thomson's theory and to use the measurements as a new approximate method for evaluating electron mobilities. Subsequently Young and Bradbury<sup>6</sup> attempted to derive a more correct equation using wave-mechanical procedures. As Cravath<sup>7</sup> pointed out, however, the problem is essentially a purely classical diffusion problem of a very complicated sort and is not amenable to wave-mechanical treatment. After spending some months endeavoring to achieve an accurate and satisfactory solution to the problem, Cravath abandoned the effort as unprofitable. Despite the doubtful assumptions, the Thomson theory, which accounts for the observations within some 10 per cent, is the only practical solution available. Thus, even though it is not accurate, it allows us a fairly clear understanding of the processes active. Furthermore, it yields useful information concerning electron mobilities that is otherwise difficult to achieve.

Consider  $n_0$  electrons of charge  $e$  emitted per square centimeter per second from the electrode  $A$ . As a result of impacts of these electrons with the gas molecules this emission results in a density of  $n$  electrons per cubic centimeter in the neighborhood of the electrode  $A$ . Unquestionably the density  $n$  of electrons is *not* constant with distance as we recede from  $A$  towards  $E$ . The nature of the agreement between theory and experiment indicates, however, that the error of assuming  $n$  constant from the electrode  $A$  to the electrode  $E$  is not very serious, although the reason for such close agreement, under the circumstances, is quite obscure. Thus one may assume with J. J. Thomson that as a result of the emission of the  $n_0$  electrons per square centimeter per second there are in the gas between  $A$  and  $E$   $n$  electrons per cubic centimeter. These start out with a velocity distribution dependent on photoelectric emission. The maximum value of the velocity can be estimated from the Einstein photoelectric law, which says that  $\frac{1}{2}mv^2 = h\nu - \phi_0$ , where  $\phi_0$  is the work function of the surface and  $\nu$  is the frequency of the incident light. Since several frequencies are present in the light source, and the velocities are altered to some extent by energy losses in the surface, the probable energy of emission can be determined by using a spherical condenser with central electrode of the same material as  $A$  and running retarding potential curves

on the current emitted. In general, the energy for zinc electrodes and light from a quartz mercury arc will be in the vicinity of 2 electron volts.

In virtue of electron collisions with gas molecules the average energy of the electrons will decrease to the equilibrium value for electrons in a gas at the existing field  $X$  and pressure  $p$  (see Chapter V). Let us designate the average *random* electron velocity to be  $\bar{c}$  and assume that this is the velocity *near* the electrode  $A$ . From the kinetic theory of gases<sup>31</sup> we can then at once write that the number of electrons striking  $A$  per square centimeter per second as a result of heat motions (i.e., diffusion) will be  $n_1 = n\bar{c}/4 = nC\sqrt{6\pi}$ , where  $\bar{c}$  is the *average* velocity and  $C$  is the root mean square velocity. Hence the electron current  $j$  per square centimeter reaching  $E$  will be  $j = n_0e - n_1e = n_0e - nCe/\sqrt{6\pi}$ , for  $n_1e$  electrons per square centimeter per second return to  $A$  by diffusion despite the field. On the other hand, since the  $n$  electrons per square centimeter are uniformly distributed along the gap from  $A$  to  $E$ , the current density received by  $E$  is  $j = neXk_e$ , where  $X$  is the field,  $k_e$  is the electron mobility, and  $n$  is the number of electrons per cubic centimeter. Thus since

$$n = \frac{j}{eXk_e}, \quad j = n_0e - \frac{jC}{\sqrt{6\pi}Xk_e},$$

so that

$$j = n_0ek_eX \frac{\sqrt{6\pi}}{C + \sqrt{6\pi}Xk_e}.$$

Now  $k_e = (760/p)K_e$ , where  $K_e$  is the reduced mobility, so that

$$j = \frac{760\sqrt{6\pi}n_0eK_eX/p}{C + 760\sqrt{6\pi}K_eX/p}.$$

Remembering that  $K_e$  is itself a function of  $X/p$  which can be obtained for some gases from the data of Bradbury and Nielsen<sup>8</sup> or of Townsend, Townsend and Tizard, Bailey, Brose,<sup>9</sup> and others, we can evaluate  $j$  if  $n_0$  and  $C$  can be evaluated. Now  $n_0e = j_0$  can at once be measured, as  $j_0$  is the *vacuum* photoelectric current per square centimeter of electrode  $A$ . Hence the evaluation of  $j$  and the comparison of  $j/j_0$  with experiment depends critically on the proper evaluation of  $C$ , the root mean square electron energy assumed. If  $C \gg 760\sqrt{6\pi}XK_e/p$ , then  $j/j_0$  is proportional to  $(X/p)K_e$ , and for *negative ions* where  $K_e$  is constant  $j/j_0$  is a linear function of  $X/p$ . If  $760\sqrt{6\pi}K_eX/p \gg C$ ,  $j/j_0 = 1$ , and we have a "*saturation*" current. Thus, since for electrons  $K_e$  is roughly  $\propto 1/\sqrt{X/p}$ , the current ratio  $j/j_0$  initially rises roughly as  $\sqrt{X/p}$  and gradually approaches a saturation value as  $K_eX/p$  becomes much larger than  $C$ . It is seen however, that the region of  $X/p$  at which saturation is reached depends on the value of  $C$ .

Now experiments made at various times failed to confirm the theory.<sup>8,10</sup> Perhaps the best example of this disagreement can be taken from later studies of Woolsey,<sup>9</sup> who worked under more favorable conditions than Partzsch and Varley.  $j_0$  being assumed constant independent of pressure, and  $C$  being assumed about the *velocity of thermal agitation* in the gas, the family of curves of  $j/j_0$  as a function of  $p$  at various pressures should reach "saturation" at much lower values of  $X/p$  than was observed. Again as plotted the curves at higher pressures *appeared* to reach saturation at values far below the values for *apparent* saturation at low pressures. Hence it at first appeared that  $j_0$  was decreasing with pressure, and an attempt was made to ascribe the decrease in  $j_0$  to a "reflection" of emitted electrons back to  $A$  after the first few impacts in the gas.<sup>3</sup> Woolsey<sup>3</sup> insisted that the curves he obtained at the higher pressures were *not* showing any *real* "saturation," and that the apparent flattening of his curves was an illusion due to the scale of plotting. In this conclusion he was correct, and a *general warning* may be issued at this point concerning conclusions as to "saturation" currents arrived at by inspection. Time and again serious mistakes have been made by assuming *apparent* "saturation" to be real. Perhaps the worst errors in recent times came in the cosmic-ray studies antedating 1928, in which conclusions were drawn from *apparent* saturation curves in ionization. From the studies on recombination of ions it will be seen that real saturation is only an ideal which can never be achieved. It is probable that with few exceptions the same holds for the majority of cases dealing with measurements of ion and electron currents in practice. The errors introduced may vary all the way from errors of hundreds of per cent. as above to negligible amounts.

When Bradbury<sup>5</sup> repeated the measurements of Woolsey with the improved techniques available the correctness of Woolsey's contention was obvious. Loeb<sup>6</sup> in studying the problem anew then recognized that the error in applying Thomson's equation had lain in the interpretation as to the value of  $C$ . Near the cathode  $A$  the electrons *have an energy corresponding closely to the neighborhood of the values of the probable velocity of electron emission*. Hence the diffusive loss (not a real reflection) is dependent on the *high* values of  $C$  near the cathode  $A$  and not on the low values in the body of the gas at the existing  $X/p$ . The reason for this is obvious, since diffusive loss of electrons at the cathode is largely due to electrons not more than 10 free paths away, and the electrons emitted with energies of volts lose only a small fraction of energy, ( $f = 2m/M$ ), in atomic gases and not more than a per cent per impact in molecular gases. That this is true can be beautifully shown in the curves of Woolsey for  $O_2$ , where electrons attach in  $10^5$  impacts. Even there it is seen that the electron diffusion results in large losses at 715 mm pressure. In Figs. 147*A* and *B* are shown Woolsey's curves for  $O_2$  and  $N_2$ . One should in passing also note the

illusion of "saturation" in the case of  $N_2$  at 71.3 cm pressure. Figs. 148A, B, and C show Bradbury's <sup>5</sup> curves in  $H_2$ . Fig. 148A, curve *a*, shows the photoelectric current  $I_0$  as a function of potential for plates of 20.9 cm<sup>2</sup> area, 3.00 cm apart. This curve in vacuum requires fields of the order of 50 volts/cm to collect nearly all the ions owing to the geometrical factor discussed in case 1. It is seen that even here complete saturation is not achieved. The ratio of  $i/I_0$  for each of

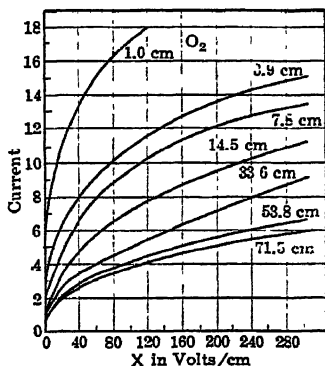


FIG. 147A.

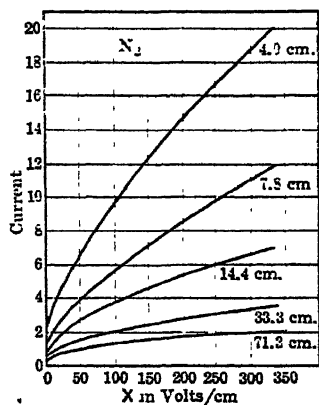


FIG. 147B.

the curves of Figs. 148A, B, and C can be inferred from the values of  $I_0$  and  $V$  given with electrode distance  $d = 3$  cm.

With the suggestion of Loeb as to the value of  $C$  and Bradbury's <sup>5</sup> data it was at once possible to establish the theory. The work function of zinc was taken as 3.57 volts, and the dominant wavelength of the mercury arc was 2537 Å at 4.9 volts. The maximum energy of emission was taken as 1.29 volts, giving a most *probable* energy of 0.77 volt. This being put in terms of velocity in place of  $C$ , and the values of  $i/I_0$  observed as a function of  $X/p$  being inserted, the data were then used to evaluate  $K_e$  as a function of  $X/p$ . The results are shown in the curves of Fig. 149 and Fig. 150 for  $H_2$  and  $N_2$ . The circles correspond to different pressures from 9.5 to 67 mm. Had the work function of zinc been chosen as 3.87 instead of 3.57 volts, the curves would have given accurate agreement with the observed values of  $K_e$  of Loeb <sup>11</sup> and Townsend and Bailey.<sup>9</sup>

Later experiments on electron attachment to molecules by Bradbury <sup>12</sup> utilized this method for evaluating  $K_e$ , as seen in Chapter VI. In that case Bradbury measured the probable energy of electron emission directly. In view of later accurate measurements of electron velocities using the electron filters, see Chapter IV, Bradbury and Nielsen <sup>8</sup> were able to check the accuracy of the evalua-



tions of  $K_e$  by the method outlined. The agreement was satisfactory well within 20 per cent. The theory, weak as it is, thus appears to have been substantiated to a surprising degree.

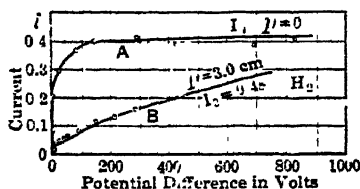


FIG. 148A.

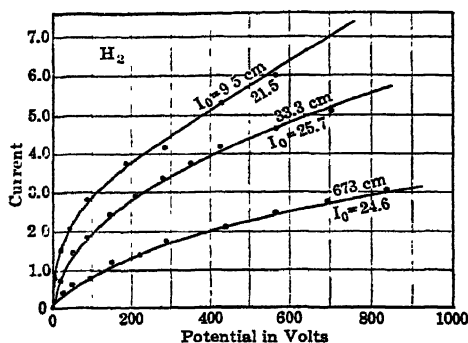


FIG. 148B.

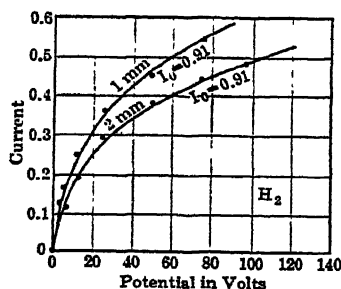


FIG. 148C.

The problem studied is of particular value in that it illustrates the importance of diffusion loss of electrons *even* in the presence of fields, especially *when the electronic energy is large*, as it frequently is. It must be noted that for thermoelectric electrons and positive thermions

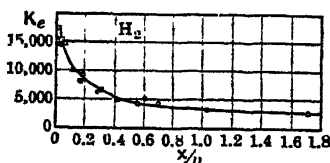


FIG. 149.

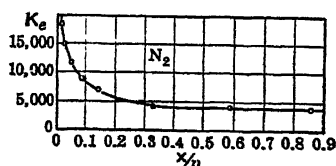


FIG. 150.

$C$  would be far smaller and saturation could be more readily achieved. It is further seen that, even with  $X/p$  as high as 20, where in  $N_2$  detectable ionization by electron impact begins and the average

energy of the electrons is not more than 2 volts, the current ratio  $j/j_0$  is still far from unity. Hence sparking potentials may be reached before one achieves saturation even in this single case.

As previously stated, the problem has been attacked by Bradbury and Young<sup>6</sup> and by Langmuir with no better success. The equation of Langmuir<sup>4</sup> neglects energy losses of electrons to elastic impacts, as did the Hertz<sup>1</sup> equation on which it is based. As a result, though it is not far in error below 1 mm pressure the theory is seriously in error at more than 100 mm. In view of later failures to derive a more exact equation accounting for the changes in electron concentration near the cathode and in the gap the Thomson equation must suffice. Added support for this equation also comes from measurements in Ne and Ne-A mixtures by Kruithoff and Penning.<sup>30</sup>

#### 4. CASE 3. SPACE-CHARGE-LIMITED CURRENTS IN VACUUM

Consider now a source of electrons emitted between two plane parallel electrodes  $CA$  in vacuum. In this case the velocity of emission may, to begin with, be considered as 0.

The geometrical factors of case 1 are eliminated by limiting the emission to a region near the center of the cathode plate  $C$  whose linear dimensions are large compared to the plate separation  $d$ . The electrons, however, are to be emitted in such numbers as to achieve considerable current densities, say of the order of  $10^{-10}$  amp/cm<sup>2</sup> or larger. Let us place the cathode  $C$  at 0 potential and apply at the electrometer plate  $A$  a potential of  $+E$  volts. In the absence of the electrons there exists between the plates  $A$  and  $C$  a uniform fall of potential as indicated by the line  $AO$ ,

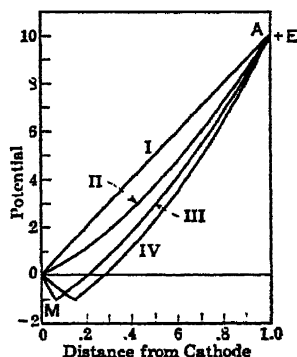


FIG. 151.

curve I, of Fig. 151, which is taken from Langmuir and Compton's<sup>13</sup> paper. There the potential is plotted in terms of the distance  $x$  from the cathode  $C$ . If now as a result of electron emission from  $C$  there are at any instant  $N$  electrons per cubic centimeter giving a volume space charge of density  $\rho = Ne/\text{cm}^3$  there will emerge from this unit volume  $4\pi\rho$  lines of force. If the plane parallel condenser  $CA$  is effectively of infinite extent compared to  $d$ , these lines of force will run *normally* through 1 cm<sup>2</sup> of surface parallel to the plane of the electrodes. Hence as a result of these  $N$  electrons per cubic centimeter there will be a change  $dX/dx$  in the field intensity  $X$  along the  $x$  axis normal to the plates. Since  $X$  changes by  $4\pi\rho$  lines in 1 cm of length along  $x$ , the value of  $dX/dx = 4\pi\rho$ . But again by definition the field strength  $X = dV/dx$ , where  $dV/dx$  is the rate of change of potential. Hence

we can write  $d^2V/dx^2 = 4\pi\rho$ . This is an elementary derivation of Poisson's equation applicable to the simple case above. Thus a space charge due to accumulated electrons will alter the field  $X$  and hence the potential distribution.

Let us now assume that at a given potential across the plates the resultant current density is  $j$  amp/cm<sup>2</sup>. Thus if at any point the electrons have a velocity  $v$  cm/sec the current density will be given by  $j = v\rho$ . Now in vacuum at any point  $x$  the velocity  $v$  is determined by the potential  $V$  through which the electrons have fallen such that  $\frac{1}{2}mv^2 = Ve$ , where  $e$  is the electronic charge and  $m$  is the electronic mass. Thus

$$v = \sqrt{\frac{2Ve}{m}} \quad \text{and} \quad \rho = \frac{j}{\sqrt{\frac{2Ve}{m}}}.$$

Accordingly

$$\frac{d^2V}{dx^2} = 4\pi j \sqrt{\frac{m}{2Ve}}.$$

In order to integrate this differential equation and thus to evaluate  $j$  as a function of  $V$  and  $d$ , we may multiply both sides of the equation by the integrating factor  $2 dV/dx$ . Hence

$$2 \frac{dV}{dx} \left( \frac{d^2V}{dx^2} \right) = 8\pi j \sqrt{\frac{m}{2e}} \frac{dV}{V^{3/2} dx}.$$

This equation may now be integrated between the limits  $(dV/dx)_0$  at  $x = 0$  where  $V = 0$ , and  $dV/dx$  at  $x = x$  where  $V = V$ . This yields

$$\left[ \left( \frac{dV}{dx} \right)^2 \right]_{\left( \frac{dV}{dx} \right)_0}^{\frac{dV}{dx}} = 8\pi j \sqrt{\frac{2m}{e}} [V^{1/2}]_0^V.$$

Since the potential  $V$  at  $x = 0$  is 0, and since with electrons at rest the force and hence the field acting must be zero, we may set  $(dV/dx)_0 = 0$ .\* We may therefore write

$$\left( \frac{dV}{dx} \right)^2 = 8\pi j \sqrt{\frac{2m}{e}} V^{3/2}$$

Thus we have

$$\frac{dV}{V^{3/2}} = \sqrt{8\pi j} \sqrt{\frac{2m}{e}} dx,$$

\* The question as to the value of  $(dV/dx)_0$  at  $x = 0$  is controversial in this form of derivation, for it is said that if the velocity  $v$  and field  $(dV/dx)_0$  at  $C$  are 0 no current could flow. The difficulty is basically formal as we are at a limiting case in which the current  $j = \rho v$  with  $\rho = \infty$  and  $v = 0$ . That the assumption is justified follows from the more rigorous derivations which in the limit give the same result.

which must now be integrated from  $V = 0$  at  $x = 0$  to  $V = E$  at  $X = d$ . This yields

$$\frac{4}{3} E^{3/2} = \sqrt{8\pi j} \sqrt{\frac{2m}{e}} d \quad \text{or} \quad \frac{16}{9} E^{3/2} = 8\pi j \sqrt{\frac{2m}{e}} d^2$$

with

$$j = \frac{1}{9\pi} \sqrt{\frac{2e}{m}} \frac{E^{3/2}}{d^2}.$$

Inserting numerical values for the constants we have the simple equation deduced by Child <sup>14</sup> in 1911 for ions in arcs in the form

$$j = 2.334 \times 10^{-6} \frac{E^{3/2}}{d^2} \text{ amp./cm}^2.$$

The equation was independently derived for electron currents in vacuum by Langmuir in 1913. It is thus seen that the effect of the *space charge is to retard the flow of current* causing it to rise as the  $\frac{3}{2}$  power of the potential applied. Thus the *space-charge-limited current* is proportional to  $E^{3/2}$  and to  $1/d^2$ . If  $j$  is constant it is seen that  $E$  varies as  $d^{4/3}$ .

The effect of the space charge on the potential distribution is shown in curve II of Fig. 151, where the potential  $V$  is plotted as a function of the distance  $x$  from  $C$ . There the straight line  $AO$ , curve I, showing the potential fall in the absence of space charge is changed to the form shown in curve II. It is seen that in this case for zero initial velocity of electrons the slope of the  $V$ - $x$  curve at  $x = 0$  is 0, and that the space charge increases the slope  $dV/dx$  at  $x = d$ . The value of the slope represents the field strength  $X = dV/dx$ . It can be computed at once for any value of  $V$ , or of  $x$  corresponding to that value of  $V$ , for a fixed value of  $j$  by the expression

$$X_V = \left( \frac{dV}{dx} \right)_V = 8\pi j \sqrt{\frac{2m}{e}} V^{1/4}.$$

The gradient increases with  $j$  and is steeper the larger  $V$ . Since for constant  $j$ ,  $V$  is proportional to  $d^{4/3}$ , i.e.,  $x^{4/3}$ , it is seen that the field  $X$  is proportional to  $x^{1/3}$ .

The equation for the space-charge-limited current is not, however, confined to electron emission alone. From certain heated salts, from the Kunsman catalysts, and from hot surfaces of certain elements exposed to alkali atom vapors we can achieve considerable current densities of positive ions. In this case the equations deduced still hold except that we must replace  $e/m$  for an electron by  $\bar{v}e/M$  for the positive ion so that such currents are also space-charge-limited.<sup>15</sup> Here  $\bar{v}$  is the valence of the ion, i.e., the number of charges  $e$  which it carries, and  $M$  is the mass of the ion. Since we can express  $M$  in

terms of a multiple of the atomic weight  $M_1$  of the ion (taking O as 16), the equation for space-charge-limited ion currents becomes

$$j_i = 5.462 \times 10^{-8} \sqrt{\frac{\bar{v}}{M_1}} \frac{E^{3/2}}{d^2} \text{ amp./cm}^2.$$

This equation places a definite limit to the positive ion currents which can be obtained at a given energy.

When for a given thermionic source and value of  $d$  at a given temperature one raises  $E$  indefinitely, the current density  $j$  increases according to the law for the space-charge-limited equation *until the electrons are removed as fast as they are thermionically emitted*. This for electrons occurs at a current density  $j_s$  given by the wave-mechanical equation

$$j_s = \frac{4\pi me k^2}{h^3} DT^2 e^{-\frac{b}{T}} = AT^2 e^{-\frac{b}{T}},$$

with  $A$  for most metals lying between 60.2 and 120.4 amp/cm<sup>2</sup>/degree<sup>2</sup>,  $b$  the work function of the surface divided by the Boltzmann constant,

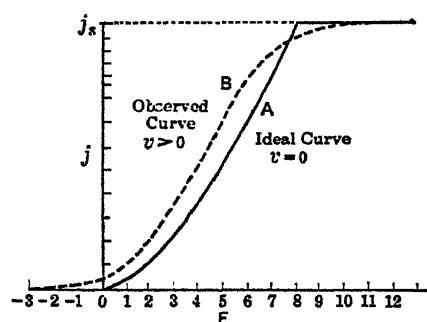


FIG. 152.

and  $T$  the absolute temperature. When  $j = j_s$ , the value of the current density depends only on  $T$  and no longer on  $E$  or  $V$  and  $d$ . This current is called the *saturation current*. Ideally the curve for  $j$  as a function of  $E$  should rise as indicated by the equation and as shown in Fig. 152, curve A, until  $j_s$  is reached; thereafter it should remain at  $j_s$ . In practice, however, the curve starts at slightly negative values of  $E$ , parallels the ideal curve more or less at lower values of  $j$

and fairly well towards  $j_s$ , but eventually it falls below the theoretical curve and rises asymptotically to  $j_s$  following the smooth dashed curve B. This behavior must be largely ascribed to the fact that *the electrons are not emitted with zero velocity* but emerge with a velocity distribution. This circumstance also profoundly alters the shape of the potential distribution curve near  $x = 0$ . The solution of this problem is due to the efforts of Langmuir,<sup>18,17</sup> Schottky,<sup>18</sup> Epstein,<sup>19</sup> Fry,<sup>20</sup> and many others at later times. It is discussed in an excellent fashion in Langmuir and Compton's<sup>13</sup> article on electrical discharges in gases in the *Reviews of Modern Physics*, 1931. At this point we will present merely the elementary treatment of the effect of velocities on the space-charge problem.

Let us assume that *all the electrons are emitted with a definite velocity component  $v_0$  normal to the surface*. The lateral components do not play any role in the present discussion. Now space-charge limitation of current means that, because of the retarding action of the accumulated charges in the space, the current is reduced below  $j_s$ , owing to the *return of emitted electrons to the cathode*. This can occur only if there exists at some point distant from the cathode  $x_0$  a *negative potential* of such magnitude as to reduce the normal velocity component  $v_0$  to zero. That is, owing to the accumulation of electrons in the space  $CA$  there must be a point at some distance  $x_0$  from  $C$  at a potential  $-V_0$ , defined by  $V_0e = \frac{1}{2}mv_0^2$ . At  $x_0$  the electrons start for  $A$  with 0 velocity. Hence we can again apply our equations and reasoning, previously applied to the cathode, to a *new plane parallel to the cathode at  $x_0$  cm from it*. Thus we must measure  $V$  and  $x$  from the minimum  $V_0$  and from  $x_0$  and set  $(dV/dx)_0 = 0$  at  $x_0$ . Then the equations above apply. Between the minimum and  $C$ , the electron current  $j_s$  is flowing towards  $A$ , while a return current  $j_s - j$  is flowing toward  $C$  repelled by the minimum.  $j$  is the current received by  $A$ . As a result of these two opposite electron currents the density of space charge is the same as if it were produced by a current  $2j_s - j$  in one direction. Hence between the cathode and the minimum the potential distribution is given by

$$2j_s - j = 2.334 \times 10^{-6} \frac{V_0^{3/2}}{x^2},$$

while between the minimum and the anode, calling  $V_a = E + V_0$ , and  $x = x_0 + x_a$ , we can write

$$j = 2.334 \times 10^{-6} \frac{V_a^{3/2}}{x_a^2}.$$

Combining these two equations and inserting the values for  $V_a$  and  $x_a$ , one arrives at the solution

$$x_0 = \frac{x}{\left[ 1 + \left\{ 1 + \frac{V}{V_0} \right\}^{3/2} \left\{ 2 \frac{j_s}{j} - 1 \right\}^{1/2} \right]},$$

or if  $V \gg V_0$ ,

$$\frac{x_0}{x} = \left( \frac{V_0}{V} \right)^{3/2} \left\{ \frac{j}{(2j_s - j)} \right\}^{1/2}.$$

From these equations Langmuir<sup>12</sup> has calculated curves III and IV of Fig. 151, using  $V = 10$  volts,  $V_0 = 1$  volt,  $x = 1$  cm, and  $j_s/j$  being taken as 5 for curve 3 and 1 for curve IV.

It is seen at once that the potential at the minimum *falls* to values  $-V_0$  which are respectively at about 0.07 and 0.14 of the distance to

the anode in the two cases. It then rises more steeply than before to the value  $E$  at the anode. The more interesting thing to note, however, is that the plane parallel to  $A$  and  $C$  at the minimum at  $x_0$  acts just like a new cathode source, giving a current  $j$  starting with  $v = 0$  at  $x = 0$  and sending a current  $j_s - j$  back to the true cathode.

In practice the electrons are never emitted with a uniform normal component  $v_0$  from the cathode. They are emitted from the cathode with the Maxwellian distribution of velocities. The electrons in this distribution that are effective are those emitted with the directed Maxwellian distribution normal to the cathode. The problem is presented in a simplified form in Langmuir's article.<sup>13</sup> Only a few points taken from Langmuir's article will here be given. Call  $V_1$ ,  $V_2$ , and  $V_0$  the potentials at cathode, anode, and minimum corresponding to the coordinates  $x_1$ ,  $x_2$ , and  $x_0$  for these. There is a well-known relation of Boltzmann that gives the relative numbers of particles  $n$  and  $n_s$  in a heat motion at equilibrium on two sides of a potential field of value  $W$  as  $n/n_s = e^{-W/kT}$ , see page 654. In the case of electrons moving through the region  $V_1 - V_0$  we can replace  $W$  by  $e(V_1 - V_0)$  and  $n/n_s$  by  $j/j_s$  and evaluate the constants. This gives  $V_1 - V_0 = (T/5040) \log_{10} j_s/j$  in volts. With this equation we can calculate  $j$  from

$$j = 2.334 \times 10^{-6} \frac{(V - V_0)^{3/2}}{(x - x_0)^2} \left[ 1 + 0.0247 \frac{T^{1/2}}{V - V_0} \right].$$

If we measure potentials from the cathode we must set  $V_1 = 0$  in the expression relating  $V_0$  and  $j_s/j$ . The value of  $x_0$  may be calculated from an equation

$$x_0 = 1.090 \times 10^{-6} (-\xi_1) \frac{T^{3/4}}{j^{3/4}} \text{ in cm.}$$

Here  $-\xi_1$  can be evaluated from the curve of Fig. 153, given by Langmuir,<sup>13</sup> from the value of  $\eta = e(V - V_0)/kT = (11,606/T)(V - V_0)$  which at the cathode is  $\eta_1 = 2.303 \log_{10}(j_s/j)$ , which will give a negative value of  $\xi_1$  in Fig. 153. Then substitute  $\xi_1$ ,  $T$ , and  $j$  in  $\xi = 9.174 \times 10^5 T^{-3/4} j^{3/4} (x - x_0)$  which gives  $x_0 - x_1$  the distance from the cathode. This allows  $\xi$  to be found for any other  $x$  and from this  $\eta$  can be found for the point, and thus  $V - V_0$  is obtained. Hence for plane parallel electrodes the  $j$ - $V$  curve can be plotted.

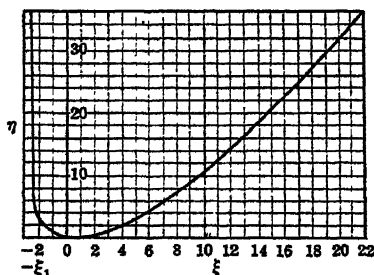


FIG. 153.

For concentric cylinders, assuming negligible velocities of emission, we have the current  $i$  given by

$$i = \left(\frac{2}{9}\right) \sqrt{\frac{2e}{m}} \frac{L V^{3/2}}{r \beta^2},$$

which for electrons is

$$i = 14.66 \times 10^{-6} \frac{L V^{3/2}}{r \beta^2} \text{ amperes}$$

and for ions of molecular weight  $M_1$  ( $O = 16$ ) with a single charge

$$i = 3.432 \times 10^{-7} \sqrt{\frac{1}{M_1}} \frac{L V^{3/2}}{r \beta^2} \text{ amperes.}$$

Here  $L$  is the length of the cylinder,  $r$  is the radius of the collecting cylinder (anode for electrons), and  $\beta^2$  is a coefficient to be taken from

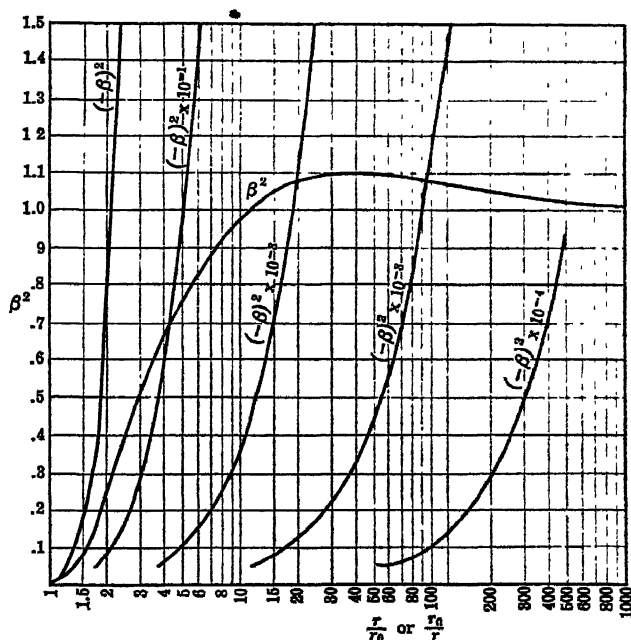


FIG. 154.

the curve of Fig. 154 from Langmuir.<sup>12</sup>  $r_0$  is the radius of the emitter (cathode for electrons) and  $r$  that of the collector. For  $r > r_0$ , which is the usual case, the curve of  $\beta^2$  applies. For  $r_0 > r$  the curves for



$(-\beta^2)$  should be used. For  $r/r_0$  near unity the curve of Fig. 155 must be used.

In the case of discharges in plasma in cylindrical condensers the collector of radius  $r$  is surrounded by a space-charge sheath within which the current due to ions or electrons is carried (see Chapter V).

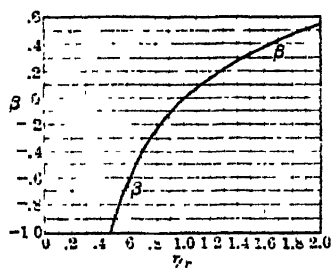


FIG. 155.

The radius of this sheath is  $r_0$ . The outer surface of the sheath then constitutes a source or emitter of ions or electrons as seen in Chapter V, and the equations above are directly applicable. As the applied voltage  $V$  changes, the current density  $j_0$  to the outer sheath remains constant, so that the collector current  $i$  varies as  $i = 2\pi r_0 L j_0$ . If we measure  $i$  at a given potential  $V$  the value of  $r_0$  can be determined by finding  $\beta^2$  from  $i$ ,  $L$ ,  $V$ , and  $r$ , and then from  $\beta^2$  evaluating  $r_0/r$ .

For the case where the initial velocity of emission is not zero, Schottky<sup>13</sup> has shown that the space charge at every point is approximately reduced in the ratio of  $\sqrt{V/(V+V_a)}$ , where  $V_a$  is the equivalent average initial energy in a radial direction of the electrons expressed in volts. This requires that, in the equations for the cylindrical condensers above with an internal emitter of radius  $r_0$  small compared to  $r$  the radius of the external collector, we replace  $V$  by a value  $V_s$  given by

$$V_s = V - V_0 + \frac{V_a}{4} \left( \log_e \frac{V}{\lambda V_0} \right)^2.$$

Here  $V_0$  is the potential at the minimum obtained above for plane electrodes with  $V_1 = 0$ ,  $\lambda$  is a numerical factor of about 1.5, and  $V_a = \frac{3}{2} kT/e = T/7733$  volts. The calculation of the radius  $r_m$  for the minimum for the cylindrical case can be found in Langmuir and Compton. Beyond  $r = r_m$  the electrons are accelerated and the case of an external collector is applicable. This gives

$$2 \left( \frac{i_s}{i} \right) - 1 = \left[ \frac{(V_a - V_0)}{(V - V_0)} \right]^{3/4} \left( \frac{r}{r_0} \right) \left( \frac{\beta}{\beta_0} \right)^2.$$

$\beta_0$  and  $\beta$  are functions of  $(r_m/r_0)$  and of  $(r/r_m)$ . Since  $r/r_m$  is large,  $\beta$  will be close to unity and its value will be nearly independent of  $r/r_m$ . If  $V$  is large we may neglect  $V_0$  compared to  $V$ , and if the potential of the emitter is 0 we have

$$\beta_0^2 = \beta^2 \frac{\left( \frac{r}{r_0} \right) \left( -\frac{V_a}{V} \right)^{3/4}}{\left[ 2 \left( \frac{i_s}{i} \right) - 1 \right]}.$$

From this  $r_m/r_0$  can be obtained from the curve for 3 in Fig. 154.  $\beta_0$  refers to the half of the curve where  $\beta$  has negative values and  $r_m/r_0$  is equivalent to  $1/(r'/r_0)$  for this curve.

## 5. THE EFFECT OF POSITIVE IONS ON AN ELECTRON SPACE-CHARGE-LIMITED CURRENT

In the study of space-charge-limited currents so far, only the currents in vacua have been considered. In the presence of a gas, however, as in many discharges and under other circumstances, *positive* ions as well as *electrons* may occur. The effect of positive ions on a electronic space-charge-limited current has been treated by Langmuir<sup>22</sup> for plane parallel electrodes and by Kingdon<sup>23</sup> for concentric cylinders. It is clear that the effect of *positive ions* in the electronic space charge is to *reduce the effective space-charge density*. These ions will thus act to increase the current. For plane parallel electrodes in the absence of gas molecules the effect of a positive ion will be in the inverse ratio of its velocity to that of the electron, for the time spent by the ion in the field will be in inverse proportion to its velocity. Hence the effectiveness of an ion will be about in the ratio of  $\sqrt{1836M_1} : 1$ , where  $M_1$  is the molecular weight of the ion ( $H = 1$ ). This makes an A ion equivalent to some 270 electrons, while for He the ratio is 85.

With the cylindrical electrodes the effect is even more pronounced, as was indicated by Kingdon. Assume relatively little gas present and consider the ion liberated near the anode as outer electrode. The positive ion starting from rest at a radius  $R$  of the outer tube is attracted towards the filament by the field and will obviously strike the filament of radius  $r$  and in this case the effectiveness of the positive ions will as above be in the ratio  $\sqrt{1836M_1}$  to 1. Actually positive ions are never at rest but have energies of thermal magnitudes or more. If for this reason the positive ion has an initial thermal velocity component  $v_0$  transverse to the radius it will describe an orbit about the filament. In most cases this orbit will take it *past* the filament and carry it to some point of positive potential beyond the filament equal to that from which it departed. It will then start anew for the filament with the same transverse velocity component but reversed in sense unless it collides with gas molecules.

The conditions to be fulfilled in order that the ion miss the filament have been determined by Hull. The effect of the magnetic field of the filament current will obviously alter these relations, but these alterations will not be serious in weak fields and in the absence of a gas. For simplicity, however, since the fields involved are usually weak except very near a filament, the magnetic fields will be neglected. The condition that the ion should miss the filament is that the potential  $V$  be less than  $eV_0 = \frac{1}{2}mv_0^2(R/r)^2$ . Here  $V_0$  is the potential of the point

of origin of the positive ion,  $m$  is its mass, and  $R/r$  is the ratio of the radii of the cylinder and filament. It is seen that the value of  $V_0$  depends on  $v_0$ , on the ratio  $R/r$ , and on  $m$ . Thus the greater  $\frac{1}{2}mv_0^2$  and the greater  $R/r$  the greater will be  $V_0$  and hence the greater the chance that the ion will not be caught, for, the greater  $V_0$ , the larger will be the volume from which positive ions can come ( $\pi R_0^2 L$ ) and miss the electrode. That is, all ions of a given  $v_0$  lying inside the  $R_0$  for which the potential is  $V_0$  will miss the filament. Hence, at appropriately high values of  $v_0$  and  $R/r$ , the many positive ions can move around in the cylinder and neutralize the negative space charge. Of the *electrons* in the space charge, all cross the cylinders directly, and all except a few which are reflected from the anode are caught in one transit from cathode to anode. Thus, in time of passage, owing to their low velocities and the number of trips before capture by the cathode, the positive ions will be much more effective than the electrons. It can thus happen that one positive ion may effectively neutralize  $10^4$  or more of the space-charge electrons. Hence by the use of positive ions the space-charge limitation of currents in tubes may be very much reduced. This in effect is the nature of the action of the gas-filled tubes such as the thyratrons of commerce.

There is another very important application of this property of positive ions in space charges. This lies in the use of the space-charge-limited electron current as a *detector* for positive ions. In this case a gas in which positive ions may be created by photoeffect or positive-ion or neutral-atom impact *in the gas* is placed in the detector. Positive ions produced by these processes will then effectively change the space charge, and consequently  $j$  or  $i$  will be changed.<sup>22,23</sup> By balancing the space-charge current in such a cylinder against that in an identical one where *no* positive ionization is produced the change due to a few positive ions can be detected by a sensitive bridge circuit.<sup>24</sup> The importance of this device and its potential uses merit a brief discussion of the problem. It is desired to detect positive ions created by the change of the space-charge-limited current in a cylindrical condenser with a gas present and to make the ions as effective in neutralizing the space charge as possible. The positive ions created in such a system may be lost from the space charge as follows:

1. By absorption at the small cathode wire.
2. By escape from the ends of the cylinder.
3. By recombination with electrons.
4. By the effect of collisions with gas molecules which ultimately leads to mechanism 1.

By covering the cylinder ends with caps provided with small holes for the filament wires, loss 2 becomes a negligible factor. Item 3 is usually small and cannot be avoided. It depends on electron energy and concentration. Item 4 is the cause of a serious loss. Collisions

of ions with atoms always result in a loss of energy by the positive ions and hence in a reduction of the velocity component  $v_0$ . (The energy loss on such impacts is relatively great and on the average of the order of 20 per cent of the energy of the ion.) Owing to the energy loss, the ions will not penetrate as far toward the anode after a trip, thus shortening the time of a trip. The first few collisions will reduce the length of path and the energy. They will, however, in general increase  $v_0$ . It is therefore evident that collisions must ultimately make capture certain and thus reduce the effectiveness of the neutralization. On the other hand, the process will be such that quite a few impacts are required to insure capture. The pressure of the gas does increase loss by capture materially. Kingdon, from measurements in tubes with various gases, was able roughly to determine the quantity  $\alpha$  which represents the increase in current per positive ion. The value of  $\alpha$  for ions in He at various pressures using a K-27 tube with 35 volts on the anode is given in Fig. 156. The pressure is in  $10^{-3}$  mm, and the plot is logarithmic. The quantity  $\alpha$  increases with  $1/p$ , and the slope of

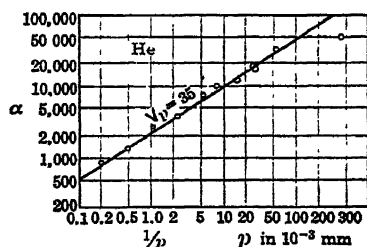


FIG. 156.

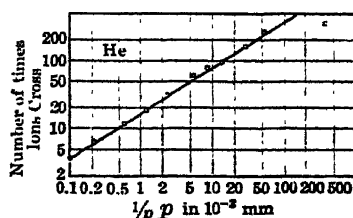


FIG. 157.

the line is  $\frac{2}{3}$ . If the free path alone were responsible for the effect this slope should be 1. The deviation may be due to the loss of ions through the holes for the filament in the caps which is greater at lower values of  $p$ . The measurements, however, were incomplete, for they did not include the ions discharged to the cathode which at lower pressure must have had a considerable effect. From the ratio of the time  $T_+$  for a positive ion to cross from anode to cathode directly, and  $T_-$ , the time for an electron to go from cathode to anode, we are able from  $\alpha$  to calculate roughly the number of trips made per positive ion as  $N = \alpha/(T_+/T_-)$ . For He in the K-27 tube,  $T_+ \sim 1.4 \times 10^{-6}$  second and  $T_- = 1.08 \times 10^{-8}$  second, with  $V = 35$  volts. Thus  $T_+/T_- = 130$ ; which is larger than the ratio of the square roots of the masses (85) as a result of the potential distribution between the electrodes. Hence, with an  $\alpha$  of the order of 26,000, it is apparent that some 200 trips occurred at a pressure of  $2 \times 10^{-4}$  mm, as seen in Fig. 157. The test with different gases indicated that the slow Hg<sup>+</sup> ions were, as expected, much more effective than the He<sup>+</sup>

ions. The effectiveness is roughly proportional to the reciprocal of the ion velocity and to its mean free path. Fig. 158 shows the result of a calculation for the trajectory of an  $\text{Hg}^+$  ion in a cylinder of  $R = 1$  at 35 volts with  $v_0$  equal to the average energy at  $300^\circ \text{K}$ .

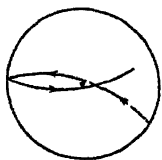


FIG. 158.

It has been observed by Varney<sup>26,27</sup> that, in using the balanced space-charge method for detecting ionization by rapidly moving alkali atoms or by neutral atoms, the effectiveness was much increased at high filament temperatures. Loeb<sup>28</sup> suggested that in this case the negative potential trough about the filament was effective in trapping the slower positive ions and thus increasing their neutralizing activity. Considerable more work remains to be done in the study of the phenomena in the space-charge detectors and in further developing the usefulness of the balanced space-charge detector.

#### 6. CASE 4. VOLUME IONIZATION WITH POSITIVE AND NEGATIVE IONS IN A GAS

This case presents a particularly important example of a gaseous current in that under the relatively simple assumptions analysis is possible and allows one to see what in general will happen in the more complex cases. The problem was set up and solved by J. J. Thomson<sup>28</sup> and can be found in extenso in the first volume of the third edition of his classic *Conduction of Electricity through Gases*. It is reproduced in brief here only in order to have available in one book a more complete discussion of the various aspects of the problem of gaseous currents.

Let us assume a parallel-plate condenser such that loss of carriers by lateral diffusion is precluded. This could be achieved by means of a large parallel-plate condenser with the collecting plate a small circular section concentric with the axis, the whole volume between the plates being uniformly ionized by an agent such as X-rays at a constant rate. Under these conditions the measured current would be little affected by loss through diffusion. The ionization could be created by X-rays, care being taken not to have the rays strike the plates. In this way  $q$  ions per cubic centimeter per second are created. The diffusion of the ions is slow in a gas, and furthermore the volume ionization decreases the abnormally high diffusion loss at the electrode studied in Case 2. Under such conditions the large loss of ions will be through the current and by recombination. Hence, to simplify the considerations, diffusion will be neglected.

The ions while being created are continually being lost by two processes. The first is a movement to the two electrodes, as a result of the electrical field  $X = dV/dx$ , parallel to the axis of the condenser plates along the  $x$  axis. The second source of loss is by volume recom-

bination in the body of the gas (see Chapter II). This loss is not usually very large. However, in such practical applications as to the positive column of discharge tubes, analogous processes occur, like loss by recombination at the walls, which is large. This takes the place of the volume recombination in the case to be studied.

One can now discuss the equilibrium case of constant current. Let us call  $n_+$  and  $n_-$  the number of positive and negative ions per cubic centimeter at any coordinate  $x$ . The positive and negative ions move with velocities  $v_+ = k_+X$  and  $v_- = k_-X$  at points in the field where the strength is  $X$ . Here  $k_+$  and  $k_-$  are the mobilities of the positive and negative ions respectively. Let  $q$  be the number of ions produced per cubic centimeter per second. If we assume  $n_+$  and  $n_-$  ions per cubic centimeter in any volume, the net volume density of electrification  $\rho$  is  $(n_+ - n_-)e = \rho$ . From Poisson's equation deduced in Case 3 it then follows that

$$\frac{d^2V}{dx^2} = \frac{dX}{dx} = 4\pi(n_+ - n_-)e.$$

The current density  $j$  is  $n_+ek_+X + n_-ek_-X = j$ . One may then write

$$n_+e = \frac{1}{k_+ + k_-} \left\{ \frac{j}{X} + \frac{k_- dX}{4\pi dx} \right\},$$

$$n_-e = \frac{1}{k_+ + k_-} \left\{ \frac{j}{X} - \frac{k_+ dX}{4\pi dx} \right\}.$$

Neglecting loss of ions by diffusion and taking into account only the production and the loss by recombination, we find that in the stationary state in a cubic centimeter the increase in ions leaving over that which entered through 1 cm<sup>2</sup> perpendicular to  $X$  by the current just equals the production of new ions and loss by recombination in that volume. Hence one must write

$$\frac{d(n_+k_+X)}{dx} = q - \alpha n_+n_-,$$

$$- \frac{d(n_-k_-X)}{dx} = q - \alpha n_+n_-,$$

where  $\alpha$  is the coefficient of recombination; see Chapter II. It then follows that

$$\frac{d^2X^2}{dx^2} = 8\pi e(q - \alpha n_+n_-) \left( \frac{1}{k_+} + \frac{1}{k_-} \right).$$

From this equation one may obtain some information as to the field distribution between the plates. If  $q - \alpha n_+n_-$  is positive so that

$d^2X^2/dx^2$  is positive, the curve of  $X^2$  as a function of  $x$  is convex to the axis of  $x$ . If it is negative, recombination in excess of ionization, it is negative in sign, and  $X^2$  is concave to the axis of  $x$ . Inserting into the equation above the values of  $n_+e$  and  $n_-e$  from the preceding equations, we have

$$\frac{d^2X^2}{dx^2} = 8\pi e \left( \frac{1}{k_+} + \frac{1}{k_-} \right) \left\{ q - \frac{\alpha}{e^2 X^2 (k_+ + k_-)^2} \left( j + \frac{k_-}{8\pi} \frac{dX^2}{dx} \right) \left( j - \frac{k_+}{8\pi} \frac{dX^2}{dx} \right) \right\}.$$

For a constant value of  $q$  and with  $k_- = k_+$  the equation has a general solution which can be found by changing variables. Call  $X^2 = y$  and  $dy/dx = p$ , and let  $k_+ = k_- = k$ . Then

$$p \frac{dp}{dy} = \frac{16\pi e}{k} \left\{ q - \frac{\alpha}{4e^2 k^2 y} \left( j^2 - \frac{k^2 p^2}{64\pi^2} \right) \right\}.$$

Integration yields

$$\frac{k^2 p^2}{64\pi^2} - j^2 = \frac{qek}{2\pi \left( 1 - \frac{\alpha}{8\pi ek} \right)} y + C y^{\frac{\alpha}{8\pi ek}},$$

where  $C$  is a constant of integration.

This relation enables one to evaluate the ratio of the field midway between the plates  $X_0$  to that near the plates  $X_1$ , for, since  $k_+ = k_-$ , the field is symmetrical and  $dX/dx$  and  $p$  are zero. If the net space charge between the plates is zero in the center, which is likely when  $k_+ = k_-$ ,  $d^2X/dx^2 = 0$ . Thus

$$X_0^2 = \frac{\alpha j^2}{4e^2 k^2 q},$$

and

$$\frac{-X_0^2 \frac{4k^2 e^2 q}{\alpha}}{1 - \frac{\alpha}{8\pi ek}} = C X_0^{\frac{\alpha}{4\pi ek}}.$$

At the anode, i.e., positive plate,  $n_+ = 0$  as the ions are repelled, and at the negative plate, i.e., the cathode,  $n_- = 0$ . Hence at both plates  $n_+ n_- = 0$ . But inasmuch as

$$n_+ n_- = \frac{1}{4k^2 e^2 X^2} \left( j^2 - \frac{k^2 p^2}{64\pi^2} \right)$$

we can evaluate  $X_1$ , the field at either plate, as

$$\frac{-X_1^2 \frac{qek}{2\pi}}{1 - \frac{\alpha}{8\pi ek}} = CX_1^{\frac{\alpha}{4+\alpha}}.$$

Thus one evaluates the ratio  $X_0/X_1$  as

$$\frac{8\pi ke}{\alpha} = \left(\frac{X_0}{X_1}\right)^{\frac{\alpha}{4+\alpha}-2},$$

and if one calls

$$\frac{8\pi ke}{\alpha} = \beta, \quad \frac{X_0^2}{X_1^2} = \beta^{1-\beta}.$$

Now  $\beta^{\beta(1-\beta)}$  decreases from 1 to zero as  $\beta$  increases from  $\beta = 0$  to  $\beta = \infty$ . Hence  $X_0/X_1$  is never greater than unity. That is,  $X_1$  is always greater than or equal to  $X_0$ . Again  $\beta$  does not depend on  $q$  or  $j$ . It does depend on  $k/\alpha$ , so that the ratio  $X_0/X_1$  depends only on  $k$  and  $\alpha$  but not on  $j$  or  $q$ . Since  $k$  in esu is about 520 and  $\alpha$  is  $1.6 \times 10^{-6}$ , while  $e = 4.77 \times 10^{-10}$  esu, we find  $\beta$  at atmospheric pressure and  $0^\circ \text{C}$  to be about 3.9 for air. Again  $k \propto 1/P$ , where  $P$  is the pressure, while  $\alpha$  is directly proportional to  $P$  (this is not always accurate, as seen in Chapter II). Thus  $\beta \propto 1/P^2$ , so that  $\beta$  becomes quite large at a few millimeters of mercury. If  $\beta = 4$ ,  $X_1/X_0 = 4^{2/3} = 2.51$ . At lower pressures,  $X_1/X_0 = \beta^{1/2}$ , so that  $X_1/X_0$  varies approximately as  $1/P$ . This enables one to plot the value of  $X$  as a function of  $x$  approximately as shown in Fig. 159. This plot indicates that there are three regions in the gap, one at each electrode where the field strength is high and of value  $X_1$ , and one in the center where the field strength is nearly constant, uniform, and of a lower value  $X_0$ .

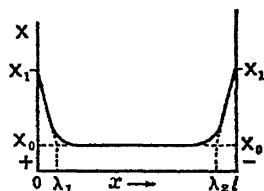


Fig. 159.

To obtain the fall of potential  $V$  as a function of  $X$  we must evaluate  $\int X dx$  from these equations from  $x = 0$  at the anode to  $x = l$  at the cathode distant  $l$  centimeters. The performance of the integration over the whole region is complicated and tedious. The essential features can be determined if for convenience the field is broken up into three parts as follows. First one has the drop of the field from  $X_1$  at the anode to  $X_0$ , in going from  $x = 0$  to a point  $x = \lambda_1$ ; next there is the region of constant field strength  $X_0$  going from  $x = \lambda_1$  to  $x = l - \lambda_2$ ; and finally there is rise in field to  $X_1$  at



the cathode going from  $X = X_0$  at  $x = l - \lambda_2$  to  $X = X_1$  at  $x = l$ . For simplicity these changes of  $X$  may be assumed linear. The physical cause for the existence of these regions is as follows: In the region near the anode the negative ions are being rapidly removed so that at the anode no negative ions exist and at short distances the negative ions are being withdrawn as rapidly as created out to a distance  $\lambda_1$ . Analogous reasoning applies to positive ions at the cathode, the distance being  $\lambda_2$ . The values of  $\lambda_1$  and  $\lambda_2$  may readily be roughly computed. The current density at any point is due to the positive and negative ions going through a square centimeter in opposite directions. At the anode it is due to negative ions only, and at the cathode to positive ions only. Thus at the anode  $(j/e)k_-/(k_+ + k_-)$  negative ions arrive per square centimeter per second, and at the cathode  $(j/e)k_+/(k_+ + k_-)$  positive ions arrive per second per square centimeter. Where  $k_- = k_+$  at the anode  $(j/e)(k/2k)$  ions arrive per second, and this number comes from the quantity  $q$  created in the volume  $\lambda_1$  long and 1 cm<sup>2</sup> in area which is  $q\lambda_1 = (j/e)(k/2k) = j/2e$ . Hence  $\lambda_1 = j/2qe$ , and similarly  $\lambda_2 = j/2qe$ . In these regions, owing to the zero value of  $n_+n_-$ , no recombination occurs, so that  $X_1$  and  $X_2$  are produced by the space charges of positive ions at the anode and negative ions at the cathode. Between  $\lambda_1$  and  $\lambda_2$  where the field is  $X_0$ , the positive and negative ions are moving through each other and recombination occurs as  $n_+n_-$  has a finite value, the field being nearly constant. Actually the field is constant at  $X_0$  for only a small distance and rises gradually to the values at  $\lambda_1$  and  $\lambda_2$ . For convenience and illustration the curve with linear elements assumed above will suffice. As a result we can picture the fall of potential  $V$  from anode to cathode as a function of  $X$  as follows: The total potential  $V$  applied is roughly given by

$$\lambda_1 X_1 + [l - (\lambda_1 + \lambda_2)]X_0 + \lambda_2 X_2 = V = V_1 + V_0 + V_2.$$

With  $k_+ = k_- = k$ ,  $V_1 = V_2$  and  $\lambda_1 = \lambda_2$ . Hence

$$\begin{aligned} V &= 2\lambda_1 X_1 + (l - 2\lambda_1)X_0 = \frac{j}{qe} X_0 \frac{1}{\sqrt{\beta^{1-\beta}}} + \left(l - \frac{j}{qe}\right) X_0 \\ &= X_0 \frac{j}{qe} \left( \frac{1}{\sqrt{\beta^{1-\beta}}} - 1 \right) + X_0 l. \end{aligned}$$

If  $\beta$  is large,  $\beta^{1-\beta} = 1/\beta$  with  $\beta = 8\pi ke/\alpha$ . Thus, inserting the value of  $X_0$ , we have

$$V = \frac{j^2 \sqrt{\alpha}}{2e^2 k q^{\frac{3}{2}}} \left( \sqrt{\frac{8\pi ke}{\alpha}} - 1 \right) + \frac{j \sqrt{\alpha}}{2ek q^{\frac{1}{2}}} l = Aj^2 + Bj.$$

This gives the current density increasing parabolically with the potential as shown by the curve of Fig. 160. This curve has in general the shape of the so-called current-potential curves observed in such cases. It is clear that there is no real saturation current although the rise of current with potential eventually becomes small for equal increments of potential. The rise is the faster the larger  $q$  and  $k$  and the smaller  $\alpha$ . From the values of  $V_1$ ,  $V_0$ , and  $V_2$ , one may plot the fall of potential between the plates as a function of  $x$ . This is shown schematically in Fig. 161A. In this figure the sharp discontinuities at  $\lambda_1$  and  $\lambda_2$  have been replaced by smooth curves and the straight lines have been replaced by curved lines such as are observed.

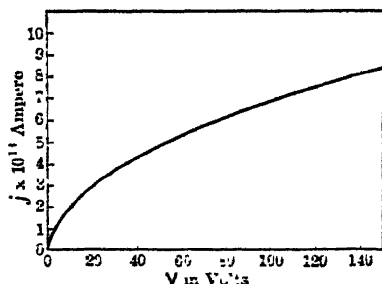


FIG. 160.

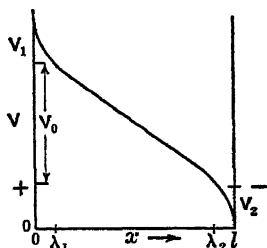


FIG. 161A.

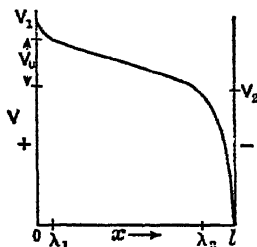


FIG. 161B.

In the Third Edition of his *Conduction of Electricity through Gases*, J. J. Thomson has solved the problem where  $k_+$  and  $k_-$  are different. Here analogous reasoning leads to the expressions

$$X_1 = X_0 \left\{ 1 + \frac{4\pi e k_+}{\alpha k_-} (k_+ + k_-) \right\}^{\frac{1}{2}},$$

$$X_2 = X_0 \left\{ 1 + \frac{4\pi e k_-}{\alpha k_+} (k_+ + k_-) \right\}^{\frac{1}{2}}.$$

Calling

$$\beta_+ = \frac{4\pi e k_+}{\alpha k_-} (k_+ + k_-) \quad \text{and} \quad \beta_- = \frac{4\pi e k_-}{\alpha k_+} (k_+ + k_-),$$

one has

$$X_1 = X_0(1 + \beta_+)^{\frac{1}{2}},$$

$$X_2 = X_0(1 + \beta_-)^{\frac{1}{2}}.$$

And for large  $\beta_+$  and  $\beta_-$  we get approximately

$$X_1 = X_0 \beta_+^2, \quad X_2 = X_0 \beta_-^2, \quad X_0 = \sqrt{\frac{q}{\alpha e(k_+ + k_-)}}, \quad \lambda_- = \frac{k_+}{k_+ + k_-} \frac{j}{qe},$$

so that

$$V_1 = \frac{1}{2} \frac{\alpha^2}{e^2 q^2} \frac{j^2 k_-}{(k_+ + k_-)^2} \left\{ (1 + \beta_-)^{1/2} + \frac{1}{\sqrt{\beta_-}} \log(\sqrt{\beta_-} + \sqrt{1 + \beta_+}) \right\},$$

$$V_2 = \frac{1}{2} \frac{\alpha^2}{e^2 q^2} \frac{j^2 k_-}{(k_+ + k_-)^2} \left\{ (1 + \beta_-)^{1/2} + \frac{1}{\sqrt{\beta_-}} \log(\sqrt{\beta_-} + \sqrt{1 + \beta_-}) \right\}.$$

For large  $\beta_+$  and  $\beta_-$  we get approximately

$$V_1 = \frac{\sqrt{\pi} j^2}{k_-^2} \left\{ \frac{k_- k_-}{qe(k_+ + k_-)} \right\}^{3/2},$$

$$V_2 = \frac{\sqrt{\pi} j^2}{k_+^2} \left\{ \frac{k_- k_-}{qe(k_+ + k_-)} \right\}^{3/2}.$$

This makes  $V_1/V_2 = k_+^2/k_-^2$ . It can be shown that, since  $k_+$  and  $k_-$  are inversely proportional to pressure while  $q$  varies directly as pressure,  $V_1$  and  $V_2$  will vary inversely as the pressure. The current will obviously vary with  $V$  in the same general fashion as in the simple case. The effect of a difference in the values of  $k_+$  and  $k_-$  is to alter the magnitudes of the potential falls  $V_1$  and  $V_2$ . This is illustrated in Fig. 161B, where the mobility of the ions  $k_- \gg k_+$ . Thus where electrons are the negative carriers we would expect the chief potential fall to be caused by the positive space charge at the cathode with a relatively small fall at the anode. In practical cases the approximate theory has been tested by Seeman<sup>29</sup> and is in agreement with observation. In most discharge tubes it will be seen that, in fact, we have distributions closely analogous to those indicated here. The fall of potential at the cathode,  $V_2$ , is of the order of hundreds of volts; that in the positive column,  $V_0$ , is some volts per centimeter length; and that at the anode,  $V_1$ , due to electron space charge, is perhaps 2 to 10 volts. The anode fall would be much less were it not for the fact that here the random electronic velocities are high and electron diffusion has the effect of lowering  $k_-$  and increasing the space charge.

With these four general cases one is now in a position to consider further extensions of the problem of currents in gases to fields so high that electrons produce new carriers by impact. In these applications we will in part deal with conduction cases which at lower fields correspond to Cases 2 and 4 presented here. In the analysis of the ionization by collision studies of Townsend we shall in fact begin with precisely the currents discussed in Case 2. In the study of the principles

of glow discharges, etc., the currents will bear a close resemblance to the currents investigated in Case 4. Case 1 is merely of academic interest, while Case 3 is of great importance in the study of certain hot-filament-source discharge tubes, as well as in the theory of probes; see Chapter V.

## 7. REFERENCES FOR CHAPTER VII

1. G. HERTZ, *Z. Physik*, **32**, 298, 1925.
2. J. J. THOMSON, *Conduction of Electricity through Gases*, 3d Edition, Vol. 1, Cambridge University Press, Cambridge, 1928, p. 466.
3. R. E. WOOLSEY, master's thesis, University of California, 1926.
4. I. LANGMUIR, *Phys. Rev.*, **38**, 1656, 1931.
5. N. E. BRADBURY, *Phys. Rev.*, **40**, 980, 1932.
6. YOUNG and BRADBURY, *Phys. Rev.*, **43**, 34, 1933.
7. A. M. CRAVATE, in private correspondence with Loeb and Bradbury.
8. BRADBURY and NIELSEN, *Phys. Rev.*, **49**, 388, 1935.
9. J. S. TOWNSEND, *J. Franklin Inst.*, **200**, 563, 1925; TOWNSEND and TIZARD, *Proc. Roy. Soc.*, **A 88**, 386, 1913; TOWNSEND and BAILEY, *Proc. Roy. Soc.*, **A 87**, 357, 1912; *Phil. Mag.*, **42**, 873, 1921; **44**, 1033, 1922; H. L. BROSE, *Phil. Mag.*, **1**, 536, 1925.
10. STOLETOW, *J. phys.*, **9**, 468, 1890; E. SCHWEIDLER, *Compt. rend.*, **127**, 224, 1898; P. LENARD, *Ann. Physik*, **2**, 359, 1900; VARLEY, *Phil. Trans. Roy. Soc.*, **A 202**, 439, 1904; PARTZSCH, *Ann. Physik*, **44**, 556, 1914.
11. L. B. LOEB, *Kinetic Theory of Gases*, 1st Edition, p. 504, McGraw-Hill, New York, 1927; *Phys. Rev.*, **19**, 24, 1922.
12. N. E. BRADBURY, *Phys. Rev.*, **44**, 883, 1933; *J. Chem. Phys.*, **2**, 827, 1934.
13. LANGMUIR and COMPTON, *Rev. Modern Phys.*, **3**, 191, 1931.
14. C. D. CHILD, *Phys. Rev.*, **32**, 492, 1911.
15. I. LANGMUIR, *Phys. Rev.*, **2**, 450, 1913.
16. P. KECK and L. B. LOEB, *Rev. Sci. Instruments*, **4**, 486, 1933.
17. I. LANGMUIR, *Phys. Rev.*, **21**, 419, 1923.
18. W. SCHOTTKY, *Physik. Z.*, **15**, 526, 624, 1914.
19. P. S. EPSTEIN, *Verhandl. deut. physik. Ges.*, **21**, 85, 1919.
20. P. C. FRY, **17**, 441, 1921; **22**, 445, 1923.
21. I. LANGMUIR, *Phys. Rev.*, **33**, 954, 1929.
22. K. H. KINGDON, *Phys. Rev.*, **21**, 408, 1923.
23. MOHLER and CHENAULT, *Phys. Rev.*, **27**, 30, 1927; FOOTE and MOHLER, *Phys. Rev.*, **26**, 195, 1925.
24. LAWRENCE and EDLEFSEN, *Phys. Rev.*, **34**, 233, 1929.
25. ROSTAGNI, *Phys. Rev.*, **53**, 729, 1938.
26. R. N. VARNEY, *Phys. Rev.*, **53**, 732, 1938.
27. R. N. VARNEY, *Phys. Rev.*, **47**, 483, 1935; **50**, 159, 1936.
28. J. J. THOMSON, *Conduction of Electricity through Gases*, 3d Edition, Vol. I, p. 193 ff; Cambridge University Press, Cambridge, 1928.
29. SEEMAN, *Ann. Physik*, **38**, 781, 1912.
30. KRUITHOFF and PENNING, *Physica*, **4**, 434, 1936.
31. L. B. LOEB, *Kinetic Theory of Gases*, 2nd Edition, p. 104, McGraw-Hill, New York, 1934.

## CHAPTER VIII\*

### IONIZATION BY COLLISION BY ELECTRONS IN A GAS

#### 1. INTRODUCTION

In Chapter VII when currents in gases were studied care was taken to restrict the fields to values in which the energy of electrons was not high enough to enable new electrons to be produced by impact with atoms or molecules. It was shown in Chapter V, however, that, in virtue of the elasticity of electron impact, in many gases the electron energy in fields could reach values at which excitation and ionization of the gas would occur on impact. In fact, on the basis of the energy distribution among electrons in a field it was shown in outline how various workers had attempted to and in part succeeded in calculating the ionization produced. In a sense, the introduction of this subject in an early chapter of the book was premature, for it puts interpretation of early experimental results, which had been sought for some forty years of intensive research, as the result of a much later esoteric and complicated theoretical development without laying a proper foundation. It will thus be necessary to refer back to Chapter V for the later more rigorous interpretation of what is detailed here.

The studies leading to a development of the problem of ionization by electron impact began with Townsend<sup>1</sup> in 1900. His remarkable results and his brilliant interpretation of them have for all time associated his name with the field of ionization by collision and its coefficients. The vital importance of the phenomenon for all types of electrical discharge or breakdown at high fields has therefore fittingly made the Townsend concepts and mechanisms pre-eminent in the explanation of practically all phenomena of this type. The ingenuity and boldness of the concepts as well as their generality have created for them a prestige which dominates and has guided the whole field of thought. Unfortunately, as physicists have learned to their sorrow in recent years, nature in its action does not always follow the simplest and seemingly the most logical procedures. It is thus not surprising that with the newer understanding of atomic structure and the development of techniques many of the broader generalizations should begin to show themselves as unsatisfactory when studied in detail. The contradictions observed should then make us skeptical of the general applicability of many of the broader concepts and conclusions in par-

\* References for Chapter VIII will be found on page 369.

ticular cases *where they occur*. The prestige of tradition and certain amazingly fortuitous agreements between theory and data over limited ranges have, however, militated against the necessary skepticism and have thus impeded advance. It is now necessary in the light of modern advance to accept what is stimulating and to correct and question the rest. In what follows, the subject will be presented as it developed from the experimental data. Townsend's results and conclusions will be given and evaluated in terms of modern facts. The sources and nature of the erroneous conclusions, where met with, will be clearly pointed out. On the other hand, it must be clearly understood that in so proceeding there is no intent other than to establish the important bases of discharge theory on a firm foundation of fact. The writer and all those who read these pages cannot help but stand in admiration of the foundations of discharge theory as conceived by Townsend, whose importance and value are in no sense dimmed by the fact that after forty years it is found in some points to be inadequate.

## 2. EXPERIMENTAL PROCEDURE

In order to introduce the subject one may conceive of the following experiment. Imagine a plane parallel-plate condenser with a uniform field isolated and immersed in a gas. It is placed in a glass system which is capable of being baked out, and the glass walls of the tube are screened with grounded Monel metal screenings to prevent accumulations of charges on the glass, as shown in Fig. 162. Through a quartz window sealed by a graded quartz to Pyrex seal, not shown, ultraviolet light from a steady quartz arc can be focused on a spot in the center of the negative plate B of the system, giving a uniform constant source of photoelectrons of limited area in the field. The photoelectric current density is kept in the order of  $10^{-14}$  amp/cm<sup>2</sup> so as to avoid space-charge effects. The cathode with its incident light is kept fixed while the upper plate D can be moved parallel to itself by means of a rotating nut A and the screw thread on its supporting shaft. The nut is rotated by means of an electromagnet placed outside the chamber in virtue of the iron lug F fastened to the nut. The distance of travel of the upper or electrometer plate is as large as it can be without distorting the field between the plates in the neighborhood of the photoelectric emission. For plates 8 cm in diameter this distance can be from 1 to 3 cm, and for plates 30 cm in diameter it can be from 1 to 10 cm. The distortion of the field can readily be determined by electrolytic cross-sectional model studies of the potential

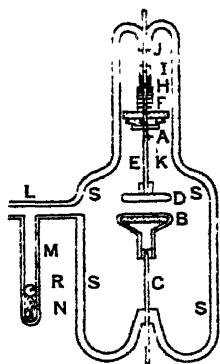


FIG. 162.—Bowls' Chamber for the Measurement of  $\alpha$ .

distribution. The plate distance can be read accurately by cathetometer. The chamber and metal parts can be chemically cleaned and the system baked out under vacuum at  $400^{\circ}\text{C}$ . In modern work great precautions must be used to exclude Hg vapor. If it once gets in from the pressure gauges, nothing short of a chemical treatment can remove it. Liquid-air traps of long path length are the only effective agents for removing Hg. To the lower plate B a constant negative potential whose value  $V$  can be chosen at will is applied, giving a field strength  $X = V/x$  across the plates separated  $x$  centimeters. The current to the anode which is at ground potential through a high resistance can be measured by an electrometer capable of giving a large range of currents by varying the high resistance. With this arrangement one is in a position to measure the current  $i$  to the anode as a function of  $X$  at a given pressure  $p$ . This constitutes a modern modification of the historically famous scheme used by Townsend in his early studies. A sketch of the tube used recently in studies by Bowls<sup>2</sup> and Hale<sup>3</sup> in the author's laboratory is shown in Fig. 162. The side tube  $M$  was an arrangement for admitting Na vapor from the capsule  $N$ , by breaking the tube by means of the ball-bearing dropped on it from above.

It was found by Townsend that at low values of  $X/p$  the current increased as the field strength  $X$  increased in essentially the manner exhibited by the photoelectric currents of Case 2 in Chapter VII. The current at first increased rapidly, and eventually more slowly, appearing to attain a saturation value which we now know it never attained (see Chapter VII, section 2). Above a value of  $X/p$  which was characteristic of the gas the currents began to rise at first slowly and then exponentially or faster, passing rapidly to an unstable state called the spark as shown in Fig. 163. This rise had been observed by the earlier workers.<sup>4</sup> It was studied in detail by Townsend. The region of values of the  $X$  at which the rise begins depends on the pressure  $p$  such that the value of the ratio  $X/p$  is a characteristic ratio marking this point for each gas. It will be seen in what follows that the ratio  $X/p$  will become the most important parameter in most of the phenomena to be discussed. In common practice,  $X$  is the field strength in volts per centimeter and  $p$  is the pressure in millimeters of mercury. Thus the rise of the current curves for pure inert gases begins at ratios ranging from  $X/p = 2$  to  $X/p = 5$ . In  $\text{H}_2$  it begins near  $X/p = 10$ , and in  $\text{N}_2$  and air at  $X/p = 20$ , but becomes pronounced only at the higher pressures if  $x$  is small.

Townsend<sup>1</sup> studied the process by choosing a value of  $X/p$  near the rise of the current indicated by the region  $AB$  of Fig. 163, and, holding  $p$  and  $X$  constant, he varied the plate separation  $x$ . As a result he found that once in region  $AB$  the current  $i$  for a given  $X$  and  $p$  rose *exponentially*, with  $x$  according to  $i = i_0 e^{\alpha x}$ , as shown by the curve of Fig. 164 taken by Sanders for air. Thus he found that, by plotting

the logarithm of  $i/i_0$ , where  $i_0$  was the current for zero plate separation, against  $x$ , he obtained a straight line of slope  $\alpha$ . The value of  $\alpha$  he found to vary with the field  $X$  and with  $p$  and to be greater the greater  $X$  and smaller  $p$ . Actually a careful analysis indicated that

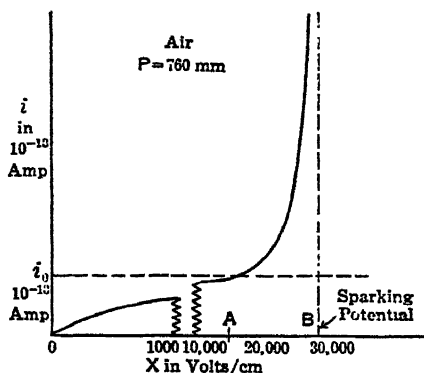


FIG. 163.

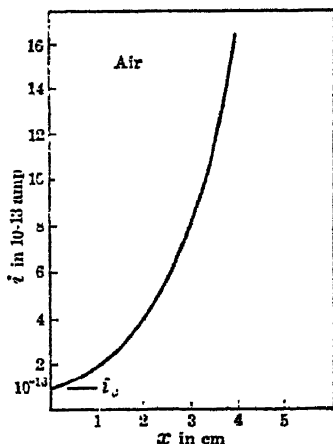


FIG. 164.

$\alpha/p$  was a continuous function of  $X$ ,  $p$ . In Fig. 165 is shown a series of curves of  $\log i/i_0$  plotted against  $X$  for air contaminated by Hg at  $10^{-3}$  mm pressure as observed by Sanders.<sup>6</sup> In this case a special metal chamber with insulation for 30,000 volts was used, capable of giving values of  $x = 10$  cm. The chamber is shown in diagrammatic form in Fig. 166, while the power source is shown in Fig. 167. It is seen that the lines are beautifully straight if  $x$  is not too great and that they all pass through the origin. In practice it is not convenient to evaluate  $i_0$ , the current at  $x = 0$ , directly. Instead, the equations

$$\frac{\log i_1 - \log i_0}{x_1} = \alpha = \frac{\log i_2 - \log i_0}{x_2}$$

allow one to evaluate  $i_0$  from  $i_1$ ,  $i_2$ ,  $x_1$ , and  $x_2$ . From this value the slopes  $\alpha$  are computed from plotted points by a least-square reduction.

When Townsend did his original work the refinements of today did not exist. The potentials  $V$  could be obtained only from sets of batteries, so that high values of  $X$  could be obtained only for small values of  $x$ . Again, small values of  $x$  mean that accurate measurements of  $i/i_0$  can be made only for values of  $x$  and  $X/p$  such that appreciable changes in  $i$  can be obtained relative to fluctuations in  $i_0$ . Hence values of  $x$  lying between 2 and 12 mm preclude measurements of small values of  $\alpha$ . Thus Townsend's measurements were



limited to values of  $X/p$  in all but the inert gases, which were well above 40 and chiefly covered the range from  $X/p = 100$  to  $X/p = 800$ . Hence the measurements of Townsend<sup>6</sup> were confined to lower pressures and high  $X/p$ . Since in most gases sparking at atmospheric

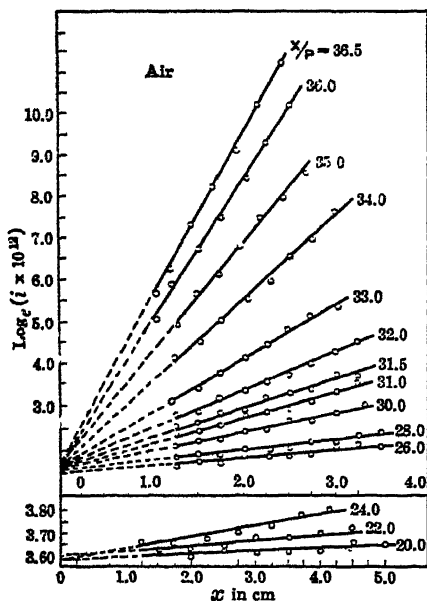


FIG. 165.

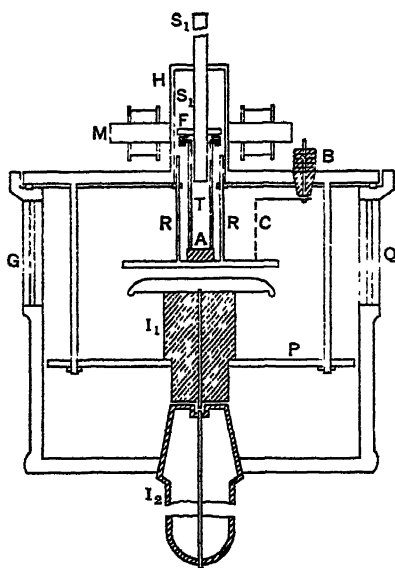
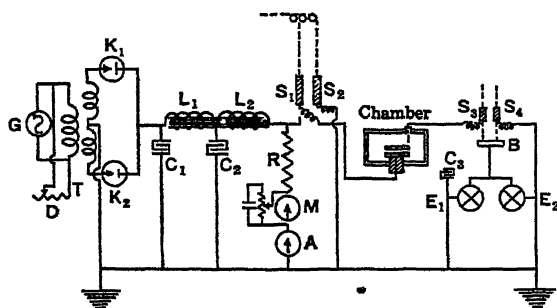
FIG. 166.—Sanders' and Posin's Chamber for the Measurement of  $\alpha$ .

FIG. 167.—Sanders' High Tension Set and Connections.

pressure sets in below the lower values of  $X/p$  achieved by Townsend, many of his data are applicable only to phenomena at lower pressures and higher  $X/p$ . This to some extent determined the later development of Townsend's theories. In order to obtain data for sparking in

air, Sanders<sup>5</sup> used larger values of  $x$ , so that with values of  $x$  up to 5 cm he was able to measure  $\alpha$  in air down to an  $X/p = 20$  at atmospheric pressure. Owing to the limited values of  $x$  used Townsend and others after him used a source of ultraviolet light that penetrated a grid anode and struck the metal cathode normally.

The use of large values of  $x$  was not available to Townsend's group, and neither Paavola nor Masch as late as 1932 using  $x$  less than 1 cm was able to measure  $\alpha$  below an  $X/p = 30$  in air. Thus even these measurements made in 1932 presented difficulties in achieving really steady high-tension sources for such work. Today (1939), thanks to the development in tube design, fluctuations of high-tension sources due to line fluctuations can be reduced by saturable-core reactors to hundredths of a per cent. It is essential in what follows to bear in mind the limitations imposed on Townsend in his earlier measurements, and the type of technique required by inadequately controlled high-tension sources.

From the increase of the current with  $x$ , Townsend<sup>1</sup> at once inferred what was taking place. He believed that at sufficiently high values of  $X/p$  the "negative ions" received enough energy from the field  $X$  so that they could ionize neutral atoms or molecules on impact. Thus he argued that, if the negative ion could create  $\alpha$  new ions in a path of 1 cm in the field direction, the increase in number of ions  $dn$  produced by  $n$  ions in a distance  $dx$  in the field could be written as  $dn = \alpha ndx$ . Here  $\alpha$  was assumed to depend on the nature of the ions and the ratio  $X/p$ . If we start with  $n_0$  ions at  $x = 0$ , and at  $x = x$  have  $n$  ions, we may integrate the expression  $dn = \alpha ndx$  between these limits and get

$$\int_{n_0}^n \frac{dn}{n} = \alpha \int_0^x dx.$$

Whence  $n = n_0 e^{\alpha x}$ , and, since with an ionic charge  $e$  the currents  $i = ne$  and  $i_0 = n_0 e$ , we at once obtain Townsend's equation  $i = i_0 e^{\alpha x}$ . Thus Townsend ascribed the increase of current to *the creation of new ions by the impact of existing "negative ions" with neutral molecules*. He called the process "ionization by collision by negative ions," and the term "ionization by collision" remains today. It was not many years after the initial work that the mobility studies showed Townsend<sup>9</sup> that under the conditions of these experiments he was not dealing with "negative ions" but with free electrons instead. He therefore later adapted the term to the "ionization by collision" by electrons. The recognition of this fact, however, came some time *after* he had derived an expression for  $\alpha$  as a function of  $X/p$  which depended on the ionization being caused by ions, as we shall see. This circumstance, however, had a profound effect on Townsend's later interpretations, as it led to an erroneous theory which appeared to fit the limited range of the data on hand.

It is seen at once that the coefficient  $\alpha$  represents the number of new electrons created per centimeter of path along the x direction. It will hereafter be designated as the "first Townsend coefficient." When Townsend first plotted his values of  $\alpha$  as a function of  $X/p$  he was not able to get a continuous curve. If, however,  $\alpha/p$  was plotted as a function of  $X/p$ , then all Townsend's results could be expressed by plotting  $\alpha/p$  as a function of  $X/p$  in a single curve. It is thus the

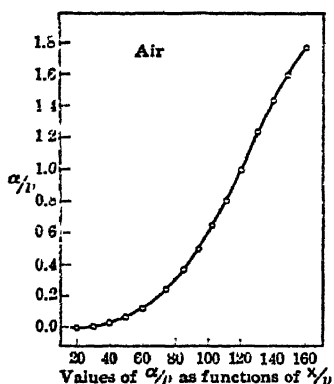


FIG. 168.

practice today to evaluate  $\alpha$  and from this to plot  $\alpha/p$  as a function of  $X/p$ . A characteristic curve of this type is shown in Fig. 168, which gives Sanders' <sup>5</sup> more recent results in air from  $X/p = 20$  up to  $X/p = 160$  instead of giving the earlier curves of Townsend. It may be remarked in passing that, in the region of values above an  $X/p$  of 40, Sanders' values were not materially different from Townsend's, although because of higher resolving power they are a bit more accurate.

In general it may also be said that within limits of 20 per cent or so at lower pressures the recent repetitions of the measurements of  $\alpha$  in Hg-contaminated gases, in all but the inert gases, have not been seriously different from the early measurements of Townsend and his students.

### 3. EXPERIMENTAL RESULTS

Townsend's original measurements of 1902, 1903, and 1904 on air,  $O_2$ , and  $H_2$  were extended to include  $N_2$  and  $CO_2$  by Hurst <sup>10</sup> in 1906. In 1908 and 1912 Gill and Pidduck <sup>11</sup> carried over the measurements to a study of the inert gases A and He. In all these studies, evaluations of the sparking potentials as well as the quantity  $\alpha/p$  and a coefficient  $\beta/p$ , to be considered later, were made. The Townsend theories of sparking and ionization by collision were thus tested on the combined data furnished over limited pressure ranges. As a result of the general agitation for the use of purer gases following the development and extended use of the mercury diffusion pumps in 1917, Townsend and his group realized the importance of impurities in gases for such critical phenomena as ionization by collision. Ayers <sup>12</sup> therefore undertook a redetermination of the coefficients  $\alpha/p$  and  $\beta/p$  as a function of pressure in distinctly purer samples of  $H_2$ ,  $N_2$ , and A than had previously been used. He was further stimulated to this study by the work of Townsend and Bailey <sup>13</sup> which had indicated that electrons had rela-

tively high energies in gases at values of  $X/p$  well below 40, which were the lower limits of Townsend's work. The results of Ayers, despite precautions, showed anomalies which it is hard to explain. He observed a measurable  $\alpha/p$  at values of  $X/p$  in  $N_2$  far lower than any other workers. His experiments in the upper ranges of  $X/p$  agreed fairly well with those of Townsend and the earlier workers except where their purity was to be seriously questioned, as in A.

With equipment many times more sensitive because of the large plate distance to be achieved, and using  $N_2$  distinctly purer in view of the improvements in technique, Posin was unable to duplicate the very high values of  $\alpha/p$  found in  $N_2$  by Ayers at low values of  $X/p$ . Posin used tank  $N_2$  made from the evaporation of liquid air and carefully purified. Ion studies of Bradbury<sup>15</sup> had shown this to be the purest form of  $N_2$  obtainable. Masch<sup>8</sup> also used tank  $N_2$ , and his results agree with Posin's within reasonable limits but lie far below Ayers' values at low  $X/p$ . The same applies to Bowls'<sup>2</sup> results in still purer tank  $N_2$  devoid of Hg. In pure Hg-free  $H_2$ , however, the values of Hale<sup>3</sup> lie very close to Ayers' values except at high  $X/p$  and low  $p$ , where Hg contamination in Ayers' work alters the results. The causes for the striking difference in results in  $N_2$  must probably be ascribed to questions of purity. The work of Bowls and Hale as well as that of Penning and Kruithoff<sup>16,17</sup> in inert gases have shown the striking effects on the coefficients due to traces of A in Ne or He or of Hg in A down to 0.0001 per cent and in the work of Bowls and Hale of traces of Hg and Na near the threshold of spectroscopic detection. The chemical method of preparation of the  $N_2$  in Ayers' experiments could easily have caused such effects since other nitrogen compounds produced in the reaction are not all excluded. The results of Ayers in A on the basis of later work also definitely indicate contamination, as shown by Kruithoff and Penning.

When the studies on the influence of cathode material at low pressures in inert gases in the laboratory of Holst and Oosterhuis<sup>18</sup> revealed the importance of the cathode material, doubts began to be cast on the validity of the mechanism proposed by Townsend to account for his second coefficient  $\beta$  and interest focused on the role of space-charge distortion. In order to make calculations utilizing space charges at atmospheric pressure, the low values of  $X/p$  at which sparking set in made a knowledge of the Townsend coefficients in gases at values of  $X/p$  below 40 imperative. Accordingly, in different laboratories, beginning in about 1928-1930, redeterminations of  $\alpha$  as a function of  $X/p$  with emphasis on low values of  $X/p$  were undertaken. Independently Rogowski at Aachen and Loeb at California put their students to work on the problem. The work at first was done on air and later extended to other gases.

Simultaneously Paavola at Aachen and Sanders<sup>9</sup> at Berkeley studied the coefficients in air. Paavola used more or less standard equipment

like that of Townsend. His plate distances  $x$ , however, were small, so that he could not get down to lower values of  $X/p$  in air than 30. Sanders, with a grant in aid from the National Research Council, built up a high-tension set for a d-c potential supply and used a very large ionization chamber of cast brass coated inside with pure tin. The plates were large and so arranged that values of  $x$  up to 10 cm could be used. The design of the high-tension set and the chamber used are shown in Figs. 166 and 167. The scale of the apparatus can be judged when the diameter of the cylinder is given as 50 cm. The insulator for introducing the high potential consisted of a hollow glass Pyrex plug filled with transformer oil and sealed off. The IV lead was sealed into the Pyrex, and the plug was ground to fit into the brass base of the box. It was sealed from the outside with sealing wax.

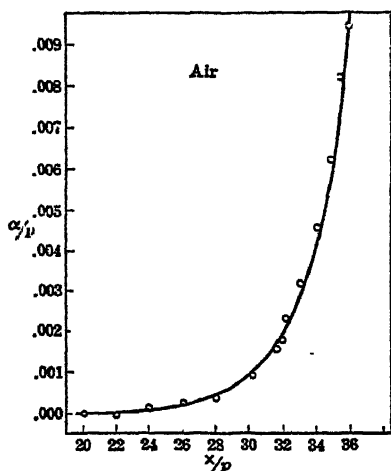


FIG. 169.

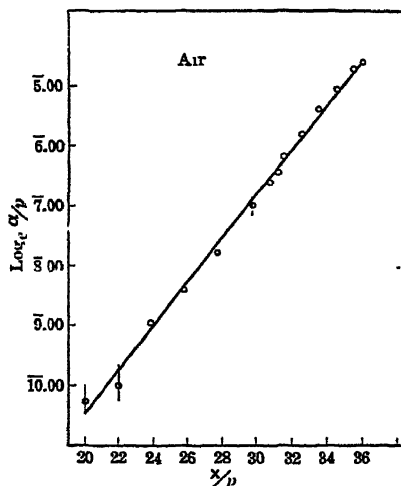


FIG. 170.

The contact between the insulators  $I_1$  and  $I_2$  was made by a small pool of Hg. The chamber was thus at all times contaminated with  $10^{-3}$  mm of Hg vapor. At this time the importance of the effect of Hg was not known.

Sanders' measurements were conducted with great care at all points of the investigation, and the success of his studies can be seen in the excellent curves which he obtained for  $\log i/i_0 - x$  and for  $\alpha/p$  as a  $f(X/p)$  shown in Figs. 165 and 168. In Fig. 169 the plot of Sanders' values for  $\log \alpha/p$  against  $X/p$  for  $X/p = 20$  to  $X/p = 36$  is shown. The values are expressed by the equation  $\alpha/p = 2.67 \times 10^{-8} e^{0.35X/p}$ , as shown by Fig. 170 with probable error. Sanders' results were in fair, but not good, agreement with Paavola's in the region above  $X/p = 30$ . Below  $X/p = 30$  Paavola could not

go. In 1933 Sanders<sup>5</sup> reported further measurements in air going up to an  $X/p$  of 160. At the same time Masch<sup>8</sup> in Rogowski's laboratory had improved on and extended Paavola's measurements to  $N_2$ ,  $O_2$ , and air. He also used relatively small values of  $x$  so that he could not go below an  $X/p = 30$  in air. The results of Masch and Sanders agreed very well except that the greater resolving power given by a larger  $x$  gave Sanders somewhat higher precision. Sanders' curve of  $\alpha/p$  as a  $f(X/p)$  is given in Fig. 168. Sanders attempted to evaluate  $\beta/p$ , the second Townsend coefficient, which put in appearance at an  $X/p$  of 120 instead of at 160 as found by Townsend. Paavola had observed values of  $\beta/p$  at even lower values of  $X/p$ , which, however, were not consistent among themselves.

Sanders next undertook the study of  $N_2$  but was unable to complete the work before he left. In the meanwhile he had trained Posin<sup>14</sup> to carry on the measurements in  $N_2$ . The apparatus and procedure of Posin were essentially the same as those of Sanders. The results of Posin for  $\alpha/p$  as a  $f(X/p)$  in  $N_2$  from an  $X/p$  ranging from 20 to

TABLE XXII  
VALUES OF  $X/p$ ,  $p$ , AND  $\alpha/p$

| $X/p$<br>(V/cm, mm) | $p$<br>(mm) | $\alpha/p$ | Probable<br>Error | $\alpha/p$<br>(Masch) |
|---------------------|-------------|------------|-------------------|-----------------------|
| 20.0                | 380.0       | 0.000034   | $\pm 0.00004$     |                       |
| 22.0                | 380.0       | 0.000052   | 0.000011          |                       |
| 24.0                | 380.0       | 0.000134   | 0.000001          |                       |
| 26.0                | 380.0       | 0.000234   | 0.000028          |                       |
| 28.0                | 380.0       | 0.000430   | 0.000015          |                       |
| 30.0                | 380.0       | 0.000910   | 0.000019          |                       |
| 31.0                | 380.0       | 0.00136    | 0.00002           | 0.00152               |
| 32.0                | 380.0       | 0.00201    | 0.00002           | 0.00204               |
| 33.0                | 380.0       | 0.00305    | 0.00003           | 0.00309               |
| 34.0                | 380.0       | 0.00459    | 0.00005           | 0.0044                |
| 35.0                | 380.0       | 0.00605    | 0.00008           | 0.0059                |
| 36.0                | 380.0       | 0.00820    | 0.00005           | 0.0076                |
| 40.0                | 25.00       | 0.0167     | 0.0001            | 0.0168                |
| 50.0                | 9.95        | 0.0554     | 0.0006            | 0.057                 |
| 60.0                | 4.90        | 0.127      | 0.001             | 0.130                 |
| 70.0                | 1.000       | 0.224      | 0.005             | 0.235                 |
| 80.0                | 0.980       | 0.340      | 0.003             | 0.365                 |
| 90.0                | 0.970       | 0.491      | 0.003             | 0.51                  |
| 100.0               | 0.960       | 0.637      | 0.006             | 0.68                  |
| 110.0               | 0.975       | 0.806      | 0.004             | 0.85                  |
| 120.0               | 0.975       | 1.007      | 0.006             | 1.05                  |
| 130.0               | 0.973       | 1.236      | 0.019             | 1.23                  |
| 140.0               | 0.950       | 1.477      | 0.019             | 1.40                  |
| 150.0               | 0.990       | 1.602      | 0.017             | 1.60                  |
| 160.0               | 1.000       | 1.758      | 0.038             | 1.83                  |

TABLE XXIII

VALUES OF  $\alpha/p$  FOR NITROGEN(
 $\alpha$  is the number of new pairs of ions created by one electron in advancing 1 cm in the direction of the field)

| $X/p$ | $\alpha/p$ |         |         |         | $X/p$ | $\alpha/p$ |       |         |        | Probable Error in $\alpha/p$ | Pressure Used |
|-------|------------|---------|---------|---------|-------|------------|-------|---------|--------|------------------------------|---------------|
|       | Ayers      | Masch   | Posin   | Posin   |       | Ayers      | Masch | Posin   | Posin  |                              |               |
| 10    | 0.6110     |         |         |         | 120   |            | 80    | 95000   | 007000 |                              | 1.000         |
| 15    | 0.179      |         |         |         | 125   | 850        |       |         |        |                              |               |
| 20    | 0.234      |         |         |         | 127   |            |       | 1.13500 | 102000 |                              | 0.490         |
| 25    | 0.305      | 0.00009 | 0.00007 | 0.00002 | 130   |            | 98    |         |        |                              |               |
| 26    |            | 0.0022  | 0.00258 | 0.0002  | 137   |            |       | 1.272   | .0160  |                              | .425          |
| 27    |            | 0.0011  |         |         | 140   |            | 1.15  | 1.400   | .0140  |                              | .720          |
| 28    |            | 0.0060  | 0.00156 | 0.00036 | 142   |            |       | 1.451   | .0145  |                              | .345          |
| 29    |            | 0.0081  |         |         | 150   | 1.32       | 1.32  |         |        |                              |               |
| 30    | .0362      | 0.0112  | .000911 | .000040 | 156   |            |       | 1.635   | .0170  |                              | .420          |
| 31    |            | .00150  |         |         | 160   |            | 1.50  |         |        |                              |               |
| 32    |            | 0.0190  | .00199  | .000048 | 166   |            |       | 2.020   | .0241  |                              | .290          |
| 33    |            | 0.0245  |         |         | 175   | 1.84       |       |         |        |                              |               |
| 34    |            | 0.0315  | 0.0281  | 0.00108 | 176   |            |       | 2.350   | 1500   |                              | .425          |
| 35    |            | 0.0385  | 0.0305  | 0.00076 | 180   |            | 1.95  |         |        |                              |               |
| 36    |            | 0.0475  | 0.0441  | 0.00160 | 196   |            |       | 2.522   | .0304  |                              | .230          |
| 38    |            | 0.071   | .00521  | .000120 | 200   | 2.50       | 2.25  |         |        |                              |               |
| 40    | .0350      | 0.1(4)  | .00734  | .000330 | 215   |            |       | 3.07    |        |                              | .330          |
| 44    |            |         | .01670  | .001100 | 230   |            |       | 3.20    |        |                              | .25           |
| 45    |            | .0208   | .01353  | .000900 | 250   |            | 3.15  | 3.50    |        |                              | .25           |
| 50    | .0820      | .0373   |         |         | 270   |            |       | 4.00    |        |                              | .25           |
| 59    |            |         | .09340  | .007110 | 300   | 4.10       | 3.90  |         |        |                              |               |
| 60    | .121       | .087    |         |         | 310   |            |       | 4.40    |        |                              | .18           |
| 68    |            |         | 14500   | .007110 | 350   |            | 4.55  | 4.93    |        |                              | .18           |
| 70    |            | .162    |         |         | 400   | 5.43       | 5.2   | 5.50    |        |                              | .14           |
| 78    |            |         | 28300   | .009450 | 450   |            | 5.7   | 6.00    |        |                              | .125          |
| 80    | .257       | .260    |         |         | 500   | 6.29       | 6.1   | 6.23    |        |                              | .125          |
| 88    |            |         | 41200   | .025200 | 750   | 7.91       |       | 8.78    |        |                              | .075          |
| 90    |            | .375    |         |         | 1000  | 9.02       |       | 10.8    |        |                              | .075          |
| 100   | .471       | .505    | .70000  |         | 2000  | 11.24      |       |         |        |                              |               |
| 108   |            |         | 72900   | .053500 | 3000  | 12.10      |       |         |        |                              |               |
| 110   |            | .65     | 73000   |         |       |            |       |         |        |                              |               |

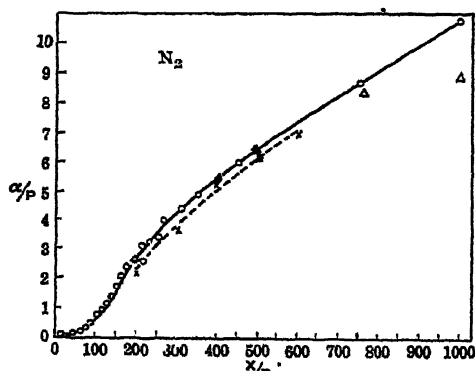


FIG. 171.

1000 are shown in Fig. 171. In this figure the circled points and the full line are Posin's, the dot-dashed curve is Townsend's,<sup>6</sup> the crosses are Masch's<sup>8</sup> data, and the triangles are Ayers' <sup>12</sup> values. The deviations of Ayers' values at low  $X/p$  are not clear on the curve. They are shown clearly in the tables of values. Table XXII gives Sanders and Masch's data for air, both mercury contaminated, and Table XXIII gives Posin's, Ayers', and Masch's data

in  $N_2$  all contaminated with Hg. It will be seen in Figs. 172, 173, and 174 that Posin's values of  $\alpha/p$  can be expressed by three distinct empirical equations as a function of  $X/p$ . These equations are:

TABLE XXIV

|       |          |   |
|-------|----------|---|
| $X/p$ | 20-38    | $\alpha/p = 5.75 \times 10^{-5} p^{2.45 X/p}$   |
| $X/p$ | 44-176   | $\alpha/p = 1.17 \times 10^{-4} (X/p - 32.2)^2$ |
| $X/p$ | 200-1000 | $(\alpha/p - 3.65)^2 = 0.21 X/p$                |

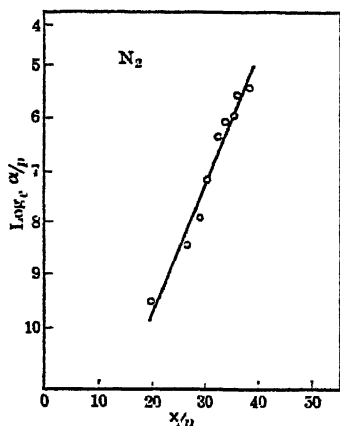


FIG. 172.

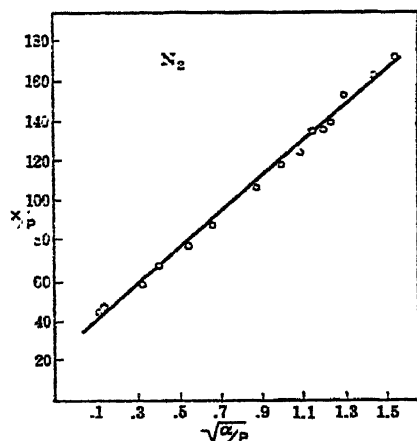


FIG. 173.

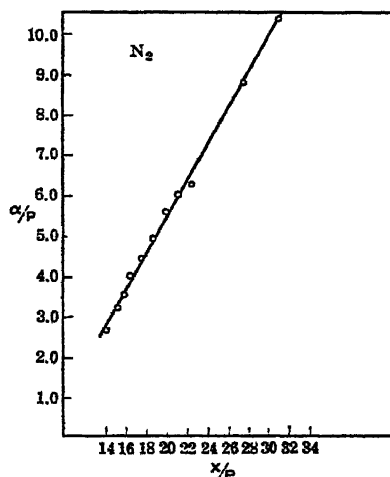


FIG. 174.

The fit of these equations within the limits given is shown in Figs. 172, 173, and 174. This indicates that the function expressing  $\alpha/p$



as a function of  $X/p$  is exceedingly complicated. The cause for this will be seen later to lie in the change of the *form* of the electron energy distribution function in the gas as the value of  $X/p$  changes, together with the complex variation of electron drift velocities and ionization probabilities, all of which enter into a product to be integrated in evaluating  $\alpha/p$ .

One particularly important point was brought out in Posin's work. In evaluating  $\beta/p$  from the curves, his values of  $\beta/p$  even for one curve were not consistent. A study of this problem led to the conclusion that these deviations were caused by space-charge distortion produced by large values of the photoelectric emission current density over large values of  $x$ . An investigation by Varney, White, Loeb, and Posin<sup>19</sup> showed that, unless current densities in  $i_0$  are kept below  $10^{-14}$  amp/cm<sup>2</sup>, space charges would distort the curves for  $\log i/i_0$  at larger plate separations  $x$  and produce fictitious values of  $\beta$ . This probably explains why Sanders and Paavola observed values of  $\beta$  which were not consistent. There is little doubt that the earlier studies of  $\alpha/p$  in general avoided this source of error in part unquestionably because of small values of  $x$  and feeble light sources.

Townsend<sup>20</sup> had early derived the fundamental equations governing the characteristics of corona discharges at low pressures, which are roughly correct. However, he pushed the interpretation of his data beyond the theory and as will later be seen drew unwarranted conclusions. His work was extended by Huxley<sup>21</sup> and later also by Boulind.<sup>22</sup> The peculiar pressure variation of the starting potential for positive and negative wires had arrested the interest of Penning,<sup>23</sup> working in the Phillips Company Research Laboratories at Eindhoven. In a series of brilliant investigations Penning showed that the peculiar characteristics were caused by the admixture of gases (i.e., presence of impurities). The importance of impurities, especially such as had ionization potentials less than the energy of metastable states of the gas used, had impressed itself on Penning. Accordingly in 1934 he and his assistants<sup>24</sup> undertook a study of the starting potential of a glow discharge between parallel-plate electrodes in pure inert gases and mixtures of these. With these, using Townsend's theory of spark breakdown, they attempted to calculate the values of the Townsend coefficients  $\alpha_1/p$  and  $\alpha_2/p$  or rather  $\eta_1 = \alpha_1/X$  and  $\eta_2 = \alpha_2/X$  for Ne and A in Ne-A mixtures. In calculating these coefficients they used the  $\beta/p$  or better  $\beta/\alpha$  values given by Townsend and McCallum.

The general procedure of attempting to evaluate the Townsend coefficients from the starting or sparking potential is the inverse of the procedure of Townsend and his group, who measured  $\alpha/p$  and  $\beta/p$  and from these calculated the starting or sparking potential. This procedure of Penning and Addink,<sup>24</sup> first used by Klemperer,<sup>50</sup> has been more recently resorted to<sup>25,26</sup> and in the author's opinion constitutes a questionable practice, a fact which was definitely recognized by

Penning, as later events show. The reason for the undesirability of this procedure is twofold. First, as will be seen under the theory of sparking in Chapter X, despite the apparent validity of the theory at lower pressures it is very doubtful whether the theory is in principle really applicable to many sparking conditions. Secondly, even at low pressures where the theory is more likely to be applicable it is doubtful whether it gives any values of  $\alpha/p$  and  $\beta/p$  that are accurate or significant. The reason for this is that a considerable latitude of values of  $\alpha/p$  and  $\beta/p$ —and worse, different pairs of values of these—will lead to nearly the same value of  $V_s$ , the sparking potential. Finally,  $V_s$  is *not accurately determinable*, as it is a disruptive non-equilibrium phenomenon and very difficult to measure.

TABLE XXV  
MEAN VALUES OF  $\alpha/p$  FOR ARGON

| $X/p$ | $\alpha/p$           | $X/p$ | $\alpha/p$ | $X/p$ | $\alpha/p$ |
|-------|----------------------|-------|------------|-------|------------|
| 5     | $2.4 \times 10^{-4}$ | 20    | 0.766      | 90    | 1.714      |
| 5.5   | $3.7 \times 10^{-4}$ | 22    | 0.1000     | 100   | 1.986      |
| 6     | $5.6 \times 10^{-4}$ | 25    | 0.1405     | 120   | 2.508      |
| 7     | 0.00113              | 28    | 0.1886     | 140   | 3.019      |
| 8     | 0.00207              | 32    | 0.262      | 160   | 3.520      |
| 9     | 0.00346              | 36    | 0.340      | 180   | 4.003      |
| 10    | 0.00576              | 40    | 0.433      | 200   | 4.466      |
| 11    | 0.00885              | 45    | 0.553      | 240   | 5.30       |
| 12    | 0.0129               | 50    | 0.677      | 280   | 6.06       |
| 14    | 0.0240               | 60    | 0.935      | 320   | 6.73       |
| 16    | 0.0384               | 70    | 1.195      | 360   | 7.35       |
| 18    | 0.0551               | 80    | 1.453      | 400   | 7.87       |

TABLE XXVI  
MEAN VALUES OF  $\alpha/p$  FOR NEON

| $X/p$ | $\alpha/p$           | $X/p$ | $\alpha/p$ | $X/p$ | $\alpha/p$ |
|-------|----------------------|-------|------------|-------|------------|
| 2.0   | $6.5 \times 10^{-4}$ | 11    | 0.0522     | 70    | 1.037      |
| 2.2   | $7.9 \times 10^{-4}$ | 12    | 0.0748     | 80    | 1.198      |
| 2.5   | 0.00115              | 14    | 0.1016     | 90    | 1.348      |
| 2.8   | 0.00157              | 16    | 0.1302     | 100   | 1.493      |
| 3.2   | 0.0023               | 18    | 0.1607     | 120   | 1.757      |
| 3.6   | 0.0032               | 20    | 0.1924     | 140   | 1.999      |
| 4.0   | 0.0042               | 22    | 0.225      | 160   | 2.219      |
| 4.5   | 0.0059               | 25    | 0.276      | 180   | 2.453      |
| 5.0   | 0.0080               | 28    | 0.328      | 200   | 2.596      |
| 5.5   | 0.0104               | 32    | 0.398      | 240   | 2.890      |
| 6     | 0.0133               | 36    | 0.469      | 280   | 3.156      |
| 7     | 0.0204               | 40    | 0.540      | 320   | 3.309      |
| 8     | 0.0290               | 45    | 0.620      | 360   | 3.452      |
| 9     | 0.0389               | 50    | 0.715      | 400   | 3.560      |
| 10    | 0.0501               | 60    | 0.882      |       |            |

It is not surprising then that Penning was dissatisfied with his results obtained in this fashion. Ultimately Kruithoff and Penning<sup>16,17</sup> undertook a series of measurements of  $\alpha/p$  and also  $\beta/p$  in A-Ne mixtures. The method was in essence the classical one of Townsend and of Paavola<sup>7</sup> and Masch.<sup>8</sup> The electrodes were copper, and plate distance was changed by a siphon bellows system from outside. The cathode was illuminated by holes in the anode. All the plate distances were small (under 1 cm). Photoelectric currents densities were high, of the order of  $10^{-9}$  amp/cm<sup>2</sup>. This does not seem seriously to have distorted the curves for  $\alpha/p$  and to have given fictitious values of  $\beta/p$  or  $\beta/\alpha$ . Such distortions were observed when  $i_0 \sim 10^{-7}$  amp/cm<sup>2</sup>. The reason for this must lie in the use of very short gaps, although errors of this character are not precluded. In the case of inert gases the values of  $X/p$  used were quite low. As a consequence, the photoelectric current-potential curve was far from saturation, and a correction for  $i_0$  was required. In view of the short gaps, corrections were also made for the distance traversed before the terminal velocities were acquired in low fields and at lower pressures.

It is in all such procedures a question whether ultraviolet illumination from the side as carried out by the Berkeley group and the use of values of  $x$  from 0.5 cm to greater values or the Townsend method of illumination through the anode is better. Both have good features and also drawbacks. With good high-potential sources the Berkeley method may ultimately prove to be better.

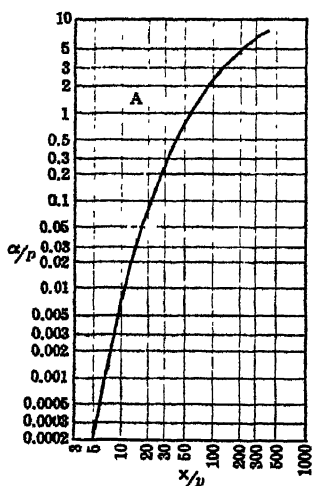


FIG. 175.

Mean values of  $\alpha/p$  obtained for A are given in Table XXV. These are plotted in Fig. 175. The values deviated considerably from those of Townsend and McCallum,<sup>26</sup> falling 20 per cent below the latter's. The reason for this difference must be ascribed to contamination by Hg vapor in Townsend and McCallum's work. The avoidance of Hg had not been practiced before the work of Kruithoff<sup>16,17</sup> and Penning and of Bowls,<sup>2</sup> as will be seen. It may be added that the facilities for the purification of A and its study were far better at the time of the later

work and especially in the Phillips Laboratory where the commercial use of these gases had necessitated special studies of this problem. The values of  $\alpha/p$  for Ne observed by Kruithoff and Penning are given in Table XXVI and plotted in Fig. 176. Recently Huxford and Engstrom<sup>51</sup> evaluated  $\alpha/p$  for A-filled tubes using Cs-Ag-O

and Ni-Cs electrodes in sealed-off Hg-free tubes. The results are not accurate, owing to limitations imposed by sealed-off tubes.

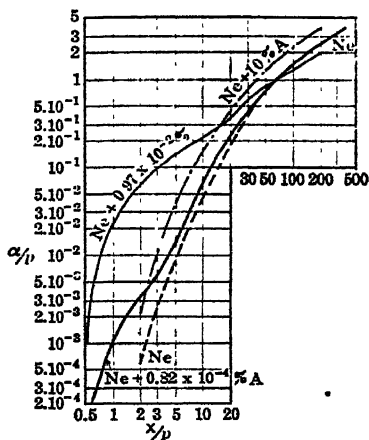


FIG. 176.

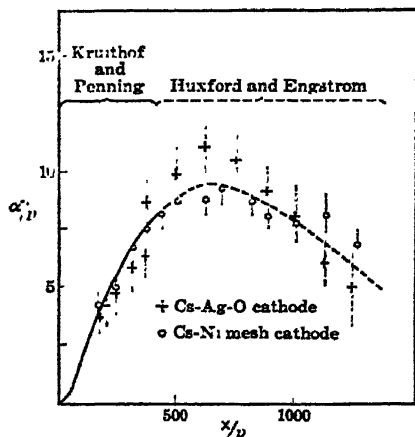


FIG. 177.

However, they checked the curves of Penning and Kruithoff but went to values of  $X/p$  up to 1250. Above an  $X/p$  of 700 the  $\alpha/p$ - $X/p$  curve rapidly declines.<sup>53</sup> This expected variation in  $\alpha/p$  with  $X/p$  had not previously been observed. The curve is shown in Fig. 177. Hale<sup>52</sup> has recently found a decline in  $H_2$  followed by a rise at an  $X/p$  around 1300.<sup>52</sup>

Probably the most interesting feature of the work of Penning and Kruithoff are the curves obtained for  $\log i/i_0$  as a function of  $x$ . These are shown in Figs. 178 and 179, giving curves of  $i$  plotted against the *potential of the anode*  $V$  instead of  $x$ . This is equivalent to plotting  $i$  against  $x$ , for the field strength  $X$  is constant and thus  $x = V_a/X$ . Fig. 178 shows the curves for a mixture of Ne with  $2 \times 10^{-3}$  per cent of A at different values of  $X/p$ . At low  $X/p$  the very wavy curve for  $i$  should be noted. It

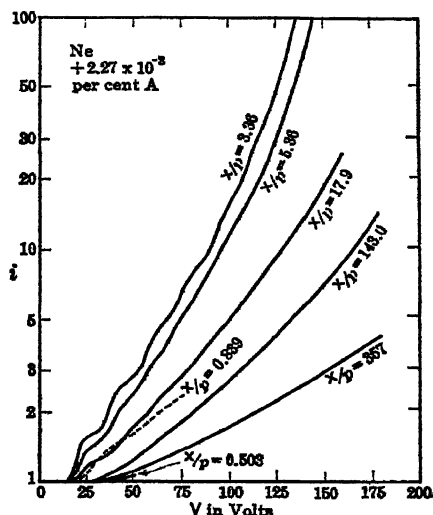


FIG. 178.

should also be noted that this steplike characteristic disappears as soon as  $X/p$  reaches higher values. That the steplike characteristic is

caused by *small* but not *very small* admixtures of A can be seen in Fig. 179, where  $X/p = 3.36$  while the percentage of A is altered.

At low values of  $X/p$  the *average* electrons get enough energy to excite but *not to ionize* Ne. Then at constant  $X/p$  but varying potential  $V$  such that  $V/xp$  remains constant one measures  $i$ . This is equivalent to increasing the distance  $x$ . Thus with a low  $X/p$  in pure Ne little if any ionization by collision should be observed and  $i$  should

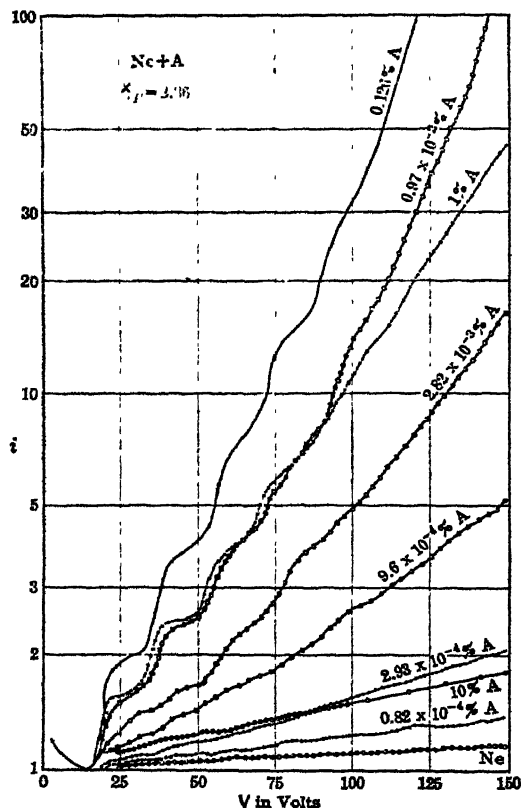


FIG. 179.

current increases correspondingly. This effect is an optimum when the Ne atoms are many and enough A is present to contribute to the current. When A increases in concentration still more, the *A atoms are directly excited* and some are ionized by electron impact at *energies lower than the metastable level for Ne*. The increase in current then is a small and continuous function of  $x$  as the probability of *excitation* is greater for A than for Ne at lower energies and the electrons in low fields do not succeed in exciting Ne, having lost their energy in excit-

remain small as  $V$  increases, for  $\alpha$  is very small. This is shown in Fig. 179 for  $X/p = 3.36$ . If now just enough A is present, which is very effectively ionized by Ne metastables, one should observe a current due to a gain of electron energy in a plate distance  $x_1$  of such length that the average electron with a total potential  $V$  acting can gain the energy to excite Ne metastables. At this value A is ionized by Ne metastables and the current increases. After the inelastic impacts of electrons giving Ne metastables occur, further increase in current ceases until  $V$  and  $x$  are such that  $x \sim 2x_1$  so that the electron group can again gain the energy to excite metastables. At this point the number of ions is suddenly increased and the

ing A. The effect of the ionization of A by metastable Ne is thus reduced, and the direct ionization of A is not large.

At high values of  $X/p$ , on the other hand, the electrons gain energy so quickly that they ionize Ne directly, as this is present in great preponderance, and the chance of excitation of Ne by high-energy electrons becomes less while direct ionization of Ne increases. At very high energies the chance of excitation is small and the chance of ionization by electron impact also decreases. We therefore at higher  $X/p$  in Fig. 178 see the current rising slowly and continuously with  $V$  since  $\alpha$  decreases as  $X/p$  increases at high  $X/p$ . It is clear, of course, that at small values of  $X/p$  the electrons will not even have enough energy appreciably to excite Ne metastables, and so the curves will be low.

In Fig. 179 the *fall* of current from  $V = 0$  to  $V = 15$ , at which little excitation of Ne occurs and only a few electrons lose energy to A, must be ascribed to another well-known phenomenon. In this region, while  $V$  is increasing  $\alpha$  is also increasing. Now at small  $\alpha$  and low pressure some of the photoelectrons emitted from the plate with high initial energies will *diffuse* across from cathode to anode and give a current. If  $X$  is constant and  $\alpha$  increases, less and less of the electrons are carried away from the cathode by the weak  $X$  and so more and more return to the cathode by diffusion as the Thomson equation of Chapter VII as interpreted by Loeb shows. When  $\alpha$  increases so that  $V > E_a$  or  $E_i$ , the excitation and ionization potentials, the electrons emitted from the cathode lose their energy to inelastic impacts and the diffusion loss is less. The situation is thus an extreme example of Case 2 of Chapter VII in which with low  $X$  and short  $\alpha$  the electrons diffuse to both electrodes at low  $p$ . At higher  $\alpha$  the loss is largely *back to the cathode*, and when  $V$  reaches a value where inelastic impacts begin the loss decreases, the field taking control.

At the inception of Posin's<sup>14</sup> work it had been the intention to vary the character of the brass cathode surface and to measure Townsend's  $\beta/p$  as a function of electrode material over an extended range of pressures and  $X/p$ . The presence of Hg in the Sn walls of the chamber and on the brass electrodes made this impossible, as all electrodes quickly became coated with monomolecular films of Hg. In order to study the effect of the nature of the surface on the value of  $\beta/p$ , Bowls<sup>2</sup> undertook a new determination of the constants in  $N_2$ , using an all-glass chamber with Pt electrodes and Monel metal screening which could be properly outgassed. Measurements were to be made in pure *Hg-free*  $N_2$  with the Pt electrode and with Na distilled in the apparatus giving a cathode with an Na coating. This was then thought to be the best way to obtain a cathode of changed work function without interfering with the gas since Na has a vapor pressure of  $10^{-10}$  mm at  $0^\circ$  C.

The results obtained by Bowls were striking. His values of  $\alpha/p$

with Hg absent did *not* in the least duplicate the values of Posin, Masch, or Townsend, which at high  $X/p$  and low  $p$  were as much as 17 per cent above Bowls' values.

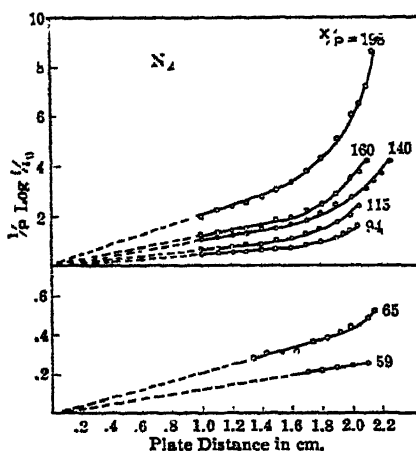


FIG. 180.

determined from the straight-line portions of the curves at the lower ends.

The results of Bowls without Hg, with Hg, and with Na in the tube are shown in Fig. 181, properly labeled. It is seen that the introduction of the Na into the tube *increased*  $\alpha/p$  above the value observed in  $N_2$  in the absence of Na, even above the value obtained with  $1.4 \times 10^{-8}$  mm of Hg present. At the highest  $X/p$  and lowest  $p$  the increase due to Na was some 25 per cent above the value for pure  $N_2$ , in contrast to 17 per cent with Hg.

The action of Hg on  $\alpha/p$  is in good accord with similar results observed by Penning and his associates in inert gases when atoms were added to the gas where

the ionization potential was less than the excitation potential of the main gas. The *percentage* of Hg present varies with the pressure of  $N_2$  and is of the order of 0.1 per cent at 1 mm pressure, while

Contaminating the chamber with a trace of Hg vapor *restored the curve to a good agreement with the values of Townsend*. Once the chamber had been contaminated, the Hg could not be removed completely by outgassing 24 hours at  $400^\circ C$ . Only dismantling and cleaning with nitric acid removed the Hg. The apparatus used by Bowls is shown in Fig. 162. It is capable of giving precision results,  $\alpha$  being variable from about 7 mm to 25 mm. Current densities of ultraviolet light were kept below  $10^{-13}$  amp/cm<sup>2</sup>. The curves for  $1/p \log i/i_0$  against  $x$  for various values of  $X/p$  are shown in Fig. 180.  $\alpha/p$  was

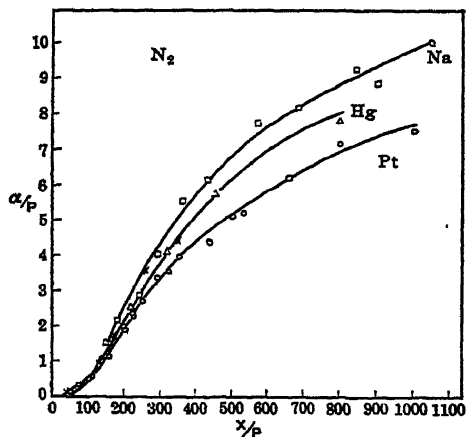


FIG. 181.

it is far less at higher pressures. The ionization potential of Hg is 10.4 volts, that of  $N_2$  is 15.5 volts, with many excited levels between 6.14 and 15.5 volts. There are metastable states of  $N_2$  at 6.14 volts, and there may be other states at 9.77 volts and perhaps higher. Mullikan<sup>27</sup> has found that 10.4 volts can be transferred by active  $N_2$ . An atom of N combining with an excited atom gives a molecule excited to 11.5 volts, which may be a metastable state. This could also ionize Hg. Kaplan<sup>47</sup> points out that there are many excited and active states of  $N_2$  of long life that could ionize Hg. Calculation shows that at  $X/p = 100$  with a Maxwellian energy distribution the direct ionization of the Hg vapor by electron impact could increase  $\alpha/p$  by 1 per cent. If the Maxwellian electron energy distribution function assumed in the computation is in error, as it may well be,

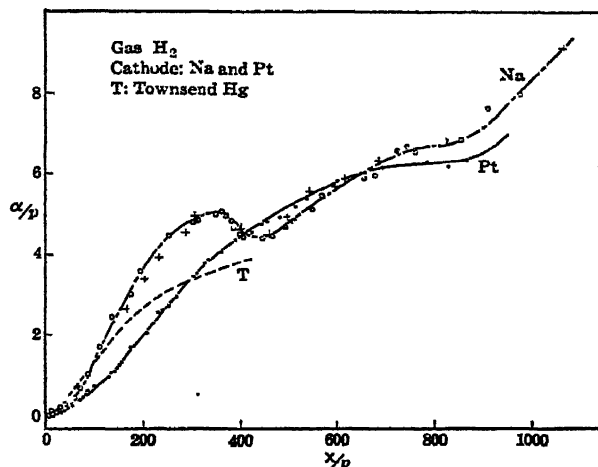


FIG. 182.

the increase of 6 per cent could easily be accounted for. Hence the effect of Hg contamination on  $\alpha/p$  in  $N_2$  is clearly explicable.

Quite analogous results have been observed by Hale<sup>3</sup> in the Berkeley laboratory for  $H_2$ . At high pressure and low  $X/p$  the values of  $\alpha/p$  of Hale in pure  $H_2$  in Bowls' apparatus fall slightly above but close to Ayers' dashed curve,  $T$ . In this region Hale's values are more accurate as his values of  $x$  are greater. These are shown in Fig. 182 for pure  $H_2$  as the full curve labeled  $Pt$ . Ayers'<sup>12</sup> curve is the dashed curve labeled  $T$ . The dot-dashed curve labeled  $Na$  is for  $H_2$  with  $Na$  present. As  $p$  decreases and  $X/p$  increases, the values of Townsend and of Ayers in  $H_2$  lie 80 per cent higher than Hale's at  $X/p = 80$  but fall below at  $X/p = 250$ . The data on  $\alpha/p$  as a function



of  $X/p$  for pure Hg-free  $N_2$  and  $H_2$  as found by Bowls and Hale are given in Tables XXVII and XXVIII.

TABLE XXVII  
BOWLS' VALUES OF  $\alpha/p$  IN PURE MERCURY-FREE  $N_2$

| $X, p$ | $\alpha, p$         | $X/p$ | $\alpha/p$        |
|--------|---------------------|-------|-------------------|
| 59     | $0.1189 \pm 0.0073$ | 250   | $2.68 \pm 0.11$   |
| 65     | $0.2128 \pm 0.0067$ | 290   | $3.378 \pm 0.068$ |
| 78     | $0.297 \pm 0.015$   | 320   | $3.58 \pm 0.11$   |
| 94     | $0.4047 \pm 0.0066$ | 350   | $3.96 \pm 0.14$   |
| 115    | $0.6120 \pm 0.013$  | 440   | $4.372 \pm 0.080$ |
| 140    | $0.961 \pm 0.032$   | 500   | $5.163 \pm 0.085$ |
| 160    | $1.196 \pm 0.072$   | 530   | $5.19 \pm 0.27$   |
| 195    | $1.898 \pm 0.059$   | 660   | $6.203 \pm 0.008$ |
| 198    | $1.993 \pm 0.093$   | 800   | $7.19 \pm 0.40$   |
| 215    | $2.215 \pm 0.30$    | 1000  | $7.58 \pm 0.18$   |

TABLE XXVIII  
HALE'S VALUES FOR  $\alpha/p$  IN PURE MERCURY-FREE HYDROGEN

| $X/p$ | $p(\text{mm})$ | $\alpha$ | $\alpha/p$ | $X/p$ | $p(\text{mm})$ | $\alpha$ | $\alpha/p$ |
|-------|----------------|----------|------------|-------|----------------|----------|------------|
| 22.7  | 17.60          | 0.715    | 0.041      | 252.6 | 0.475          | 1.310    | 2.757      |
| 24.0  | 12.50          | 0.500    | 0.040      | 271.4 | 0.468          | 1.369    | 2.928      |
| 30.6  | 8.50           | 1.045    | 0.123      | 277.9 | 0.475          | 1.459    | 3.071      |
| 32.3  | 9.30           | 1.200    | 0.129      | 299.0 | 0.475          | 1.520    | 3.200      |
| 45.5  | 7.70           | 1.320    | 0.172      | 306.4 | 0.360          | 1.177    | 3.268      |
| 52.3  | 4.20           | 1.000    | 0.238      | 328.4 | 0.335          | 1.280    | 3.820      |
| 61.9  | 3.23           | 1.076    | 0.334      | 337.4 | 0.290          | 1.120    | 3.870      |
| 68.6  | 5.10           | 2.000    | 0.392      | 362.0 | 0.335          | 1.342    | 4.010      |
| 74.7  | 1.82           | 0.809    | 0.444      | 392.6 | 0.270          | 1.160    | 4.290      |
| 85.0  | 1.13           | 0.654    | 0.578      | 424.0 | 0.283          | 1.263    | 4.463      |
| 100.0 | 1.20           | 0.943    | 0.785      | 448.0 | 0.250          | 1.184    | 4.736      |
| 130.4 | 1.15           | 1.144    | 0.995      | 452.0 | 0.270          | 1.280    | 4.750      |
| 136.2 | 0.94           | 1.020    | 1.085      | 481.0 | 0.283          | 1.378    | 4.870      |
| 144.7 | 0.76           | 0.850    | 1.119      | 516.0 | 0.283          | 1.473    | 5.210      |
| 146.0 | 1.15           | 1.411    | 1.220      | 536.0 | 0.250          | 1.323    | 5.290      |
| 153.8 | 0.91           | 1.053    | 1.157      | 600.0 | 0.190          | 1.100    | 5.810      |
| 164.7 | 0.668          | 0.907    | 1.358      | 663.5 | 0.190          | 1.149    | 6.050      |
| 175.8 | 0.910          | 1.543    | 1.690      | 694.5 | 0.190          | 1.159    | 6.120      |
| 209.6 | 0.668          | 1.374    | 2.056      | 787.8 | 0.165          | 1.032    | 6.260      |
| 219.7 | 0.910          | 2.044    | 2.245      | 833.5 | 0.120          | 0.730    | 6.180      |
| 228.0 | 0.475          | 1.193    | 2.380      | 867.0 | 0.120          | 0.757    | 6.300      |
| 240.0 | 0.450          | 1.163    | 2.540      | 916.7 | 0.120          | 0.805    | 6.700      |

The conclusion is obvious. With the exception of Hale's, Bowls', and Penning's, all previous measurements of the Townsend coefficients

have been made in gases contaminated more or less by Hg vapor. All electrodes have been covered with monomolecular or thicker films of Hg. This accounts for the uniformity of the results for  $\beta/p$  irrespective of cathode as well as the high values of  $\alpha/p$ . The source of contamination where Hg seals were not exposed to the chamber are simply divined. In all such measurements Hg manometers and McLeod gauges are used. Once the system is evacuated for filling, using Hg pumps or otherwise, Hg vapor distils from the gauges throughout the apparatus, as spectroscopic studies by Ehrenkrantz<sup>28</sup> revealed; and, in conformity with Bowls' findings, once in an apparatus, Hg can never be removed except by radical chemical treatment. In fact, the results in the presence of small traces of Hg are worse than when  $10^{-3}$  mm are present, since then capricious variations in Hg vapor content disperse the values of  $\alpha/p$  in a meaningless fashion. In a carefully conducted measurement of  $\alpha/p$ , a spread of values definitely indicates uncontrollable contamination. The variable contamination with Hg vapor quite readily explains the diversity of results between observers and scattering of points in a single curve made over an extended time period with gas leakage in between. It is clear then that we must recognize this difficulty in older work, and that standard studies of gases such as air must be repeated without contamination of this sort. It is believed that to date the values in A, Ne, N<sub>2</sub>, and H<sub>2</sub><sup>16,17,2,3</sup> here given are correct. Bowls' results in N<sub>2</sub> should be extended to lower  $X/p$ , as should Hale's results in H<sub>2</sub>.

The results with Na in N<sub>2</sub> are quite surprising. Analogous results for Na in H<sub>2</sub> are shown in Fig. 182. Here with the careful technique of Hale we see a phenomenon not so far observed, namely, a *peak* in the  $\alpha/p - X/p$  curve at an  $X/p = 300$  with the appearance of discontinuities in both the Na and Pt curves at an  $X/p$  of 900. In both N<sub>2</sub> and H<sub>2</sub> the value of  $\alpha/p$  with Na present rises well above the value when Na is absent, despite the fact that the *vapor pressure of Na is given as  $10^{-10}$  mm at 22° C.* The points with Na present scatter badly. That Na acts in this fashion is borne out by the studies of sparking potential made by Ehrenkrantz<sup>28</sup> in Hg-free gases A, N<sub>2</sub> and H<sub>2</sub> with Na present. In A the Na *decreased* the sparking potential by only 8 per cent at higher values of  $p\delta$ , the sparking distance times pressure. This amount is consistent with a lowering of the minimum sparking potential at low pressure by 50 per cent due to a change in cathode surface when the Na was distilled in. In both H<sub>2</sub> and N<sub>2</sub> the Na *decreased* the sparking potential by amounts so large at high  $p\delta$  that they can be attributed only to *changes in  $\alpha/p$  and not to changes in secondary emission* from the cathode. These observations were confirmed by very heavy predischARGE currents in sparking experiments whenever Na was in the tube with H<sub>2</sub> or N<sub>2</sub> but not with A. Conversion of Na to NaH by prolonged sparking, or by heating the cathode to 600° C and the gas in the gap to above 300° C, destroyed

the effect of Na. One must conclude then that all these peculiar phenomena with Na in the chamber must be ascribed to the presence of some unknown volatile compound easily ionized whose vapor pressure may be as high as  $10^{-3}$  mm of Hg. This compound is then ionized either directly by electron impact as with Hg or by excited molecules of  $N_2$  or  $H_2$ . It is therefore unfortunate that Na was the substance chosen to change the work function of the cathode as it complicates the studies of sparking and of  $\beta/p$  by altering  $\alpha/p$  and the nature of the gas as well as the cathode.

The decrease in  $\alpha/p$  at an  $X/p = 300$  in  $H_2$  when Na is present must indicate that above this energy the ionization of the gas by one mechanism involving Na ceases to be effective and only direct ionization of  $H_2$  by electron impact remains. The second dip in this curve at  $X/p = 900$  is unexplained at present if real.<sup>63</sup> Analogous tendencies may be noted in the Ne-A mixture curves of Kruithoff and Penning, Fig. 176.

From what has gone before concerning the experimental data on the first Townsend coefficient, one sees that in essence little is basically changed in the procedure. The greatest advance has been in the understanding of the nature of the effect of impurities, the sensitivity of  $\alpha/p$  to traces of such impurities, and the elimination of the undesirable contamination. In this direction most of the credit must go to the technical developments such as Pyrex glass, quartz-glass seals, and tungsten leads which make cleanliness possible. The desirability of having larger values of  $\alpha$  and the necessity of avoiding excessive current densities are also obvious. The possibility of the direct determination of  $\alpha/p$  with some precision makes unnecessary the other indirect evaluations of doubtful nature, such as from spark potential measurements. It is clear that, since the importance of the contamination due to Hg has been recognized, it would be desirable that new determinations for a number of gases, especially air, be made over the whole range of  $X/p$ . For practical applications the values in air from  $X/p$  of 20 to 40 are especially valuable, as are data at low and high  $X/p$  for  $N_2$  and high and low  $X/p$  for pure  $H_2$ .

#### 4. THEORETICAL EVALUATION OF $\alpha/p$ AS A $f(X/p)$

One must now consider the theory of the variation of  $\alpha/p$  as a function of  $X/p$ . The first attempt at such a theory was due to Townsend<sup>29</sup> and although erroneous must be given in some detail as its implications have colored all the subsequent writings of the Townsend school. In explaining the theory it must be recognized that most of Townsend's own data on  $\alpha/p$  as a  $f(X/p)$  as stated covered a limited range of values at the higher  $X/p$ . With such a range of data it is frequently possible to fit many relations with arbitrary constants. This in a measure explains much of what follows.

Considering, in the light of existing knowledge in the early nineteen hundreds, that the ionization was caused by the impact of *ions*, and knowing that ions making impact with molecules must sacrifice most of their energy gained from the field, Townsend assumed tentatively that ionization of a molecule could come only from the impact of an ion that had acquired its ionizing energy in its *last* free path in the field. Since in fields with a high  $X/p$  ions are accelerated largely in the field direction, thermal energy being relatively small compared to the energy gained in a free path, Townsend reasoned as follows: Assume an ionic path of length  $\lambda$  in the field direction. The ion gains an energy  $Xe\lambda$  in that free path from the field  $X$ . At the end of the impact the ion loses *all its energy* and must begin over again. This assumption is obviously not correct, for what Jeans terms the persistence of velocity must play a considerable role. However, it is not seriously wrong as an approximation. Thus unless in a free path of length  $\lambda$  an ion gains an energy  $Xe\lambda \geq E_i$ , where  $E_i$  is the ionizing energy, the ion cannot ionize. At that time the so-called *ionizing potential*, ionizing energy expressed in equivalent electron volts, was not known, but the existence of a value  $E_i$  was for the first time assumed by Townsend.

The chance that a negative ion would ionize was thus dependent on the *chance of an ionic free path*  $\lambda \geq \lambda_i = E_i/Xe$ . Now, out of  $N_0$  ions starting, the number  $N$  that have paths  $x \geq \lambda_i$  without impact is given by the well-known distribution law for free paths  $N = N_0 e^{-(\lambda_i/\bar{\lambda})}$  where  $\bar{\lambda}$  is the mean free path; see page 647. This is then the number of ions  $N$  out of  $N_0$  executing paths that are created by negative-ion impact. Now if  $N_0$  is the number of impacts an ion makes in advancing 1 cm in the direction  $x$  of the field in the gas, then  $N$  must equal  $\alpha$  in the equation interpreted as above. But  $N_0 = 1/\bar{\lambda}$  so that we may write

$$\alpha = \frac{1}{\bar{\lambda}} e^{-\frac{E_i}{X\bar{\lambda}}}.$$

Since  $\bar{\lambda} = \lambda_0(760/p)$ , where  $p$  is the pressure in millimeters of mercury, we at once have

$$\frac{\alpha}{p} = \frac{1}{760\lambda_0} e^{-\frac{E_i}{(\lambda/p)760e\lambda_0}}.$$

Thus the quantity  $\alpha/p = f(X/p)$  gives

$$f\left(\frac{X}{p}\right) = \frac{1}{760\lambda_0} e^{-\frac{E_i}{760e\lambda_0(X/p)}}.$$

Now  $\lambda_0$ , the free path of the ion in a gas at these fields, is not accurately known, and  $E_i$  was at that time completely unknown. It was therefore possible to assume  $\lambda_0$  for the ion to be that of the molecule of the gas and to evaluate  $E_i$ . This Townsend did. In doing so he

made the first evaluation of an ionizing potential for an ion or electron in a gas. When Townsend's own experiments on ion velocities at low pressures somewhat later showed him that the carrier was the free electron and not a negative ion, he did not materially alter the theory. All that was done in replacing ionization by ions with ionization by electrons was to replace  $\lambda_0$  for an ion by its value  $\lambda_e$  for an electron. This on kinetic theory is but  $4\sqrt{2}$  times as great as  $\lambda_0$ . Using this value, Townsend, from the values of  $\alpha/p$ , obtained the first estimates for the ionization potentials of the gases. These values appeared to lie between 20 and 30 electron volts in most gases and varied very little from gas to gas.

The values obtained directly by Franck and Hertz using lower pressures and electrons accelerated over only one path were materially lower than the earlier values of Townsend for most gases, the values being of the order of 10 to 16 volts for all but Ne and He.<sup>31</sup> The values obtained by these workers, furthermore, were notably more distinctive and characteristic of the gaseous behavior than the nearly uniform values of Townsend. Townsend, however, persisted for a long time in insisting that his values gave the true ionizing potential. In this he was encouraged by the fact that his values for  $\alpha/p$  as a function of  $X/p$  appeared to fit his observed curves for a considerable range in values. This same apparent coincidence forcibly impressed the author when, as late as 1923, he applied the equation to the results given by Townsend in his book. Actually the fit was *never* good over any extended range even with Townsend's own data. As will appear, however, the agreement is purely fortuitous and is not even fair except for *very* limited ranges of his curves. This is at once seen in trying to fit Townsend's equation to Sanders' data at low  $X/p$ . There is no

fit, for Sanders' data obey an empirical relation  $\alpha/p = Ae^{\frac{B-X}{p}}$  from  $X/p = 20$  to  $X/p = 38$  and thereafter as Jodelbauer<sup>32</sup> showed an equation of the form  $\alpha/p = [(X/p)A_1 - B_1]^2$  to  $X/p = 140$ , where  $A, A_1, B, B_1$  are constants. With Sanders' <sup>5</sup> equipment, Posin<sup>14</sup> later covered an extended range in  $N_2$ , going from  $X/p = 20$  to  $X/p = 1000$ . Posin's curve for Hg-contaminated ( $10^{-3}$  mm pressure)  $N_2$  is shown in Fig. 171. As was shown with such extended data, *there is no simple analytical function* empirical or otherwise that will fit the data. Closely the same equations apply to the corresponding regions of Posin's curve for  $N_2$ .<sup>33</sup> At high values of  $X/p$  after passing through a nearly linear region at the point of inflection, Posin's curve was in its higher values closely approximated by an expression proportional to  $\sqrt{X/p}$ . Since in most pure gases, even including Hg-free gases, the trend of the  $\alpha/p = f(X/p)$  curves is quite similar to those for  $N_2$ , we see that Townsend's expression does not represent the phenomenon of ionization by collision at all. The character of the agreement over a limited range is seen in a curve taken from v. Engel and Steenbeck shown in

Fig. 183. The observed agreement was therefore entirely illusory through the fortuitous agreement of the equation with a very limited stretch of curve. That the theory should not fit is not at all strange, as will be seen when the complicated nature of the processes are realized.

It is a curious anomaly, however, to find in Townsend's book two chapters<sup>34</sup> not unduly separated in which in one case he infers the theory for  $\alpha/p$  and evaluates  $E_{ii}$ , assuming that *electrons make inelastic impacts with gas molecules below the ionizing potential*, and in the second case shows that *owing to elastic electronic impacts the electrons in a gas in a field gain energy over many free paths acquiring an energy on the average  $\eta$  times the thermal energy*; see page 179. Since Townsend's measurements and analyses concerning electron energies in gases have been so amply verified in principle by widely diverse methods and are furthermore quite consistent with modern quantum theory, there can be no doubt but that Townsend in his own work has shown the fallacy of his theory of electron ionization by collision. Townsend's theory for the evaluation of  $\alpha/p$  as a function of  $X/p$  is in agreement neither with other facts concerning electronic behavior nor with experiment. Had this theory been accepted by its author as merely one of the many incorrect guesses made by all investigators when adequate knowledge is not yet at hand and then abandoned, the matter could be passed over without comment. In view of the fact that for many years<sup>36</sup> Townsend did not accept the Franck and Hertz experiments and in later writings has never clearly retracted the theory, and in view of the authoritativeness of his work and its inclusion in the old form in many current texts, it is necessary at this point once and for all clearly to indicate the fallacy.

The Franck and Hertz experiments and the evaluation of the ionization and excitation potentials by them succeeded because they worked at low pressures and studied the results of individual impacts at the requisite energy. Townsend's experiments, although correct and of significance, failed to be amenable to interpretation and to a simple evaluation of the ionizing potential for the reason that at the higher pressures the energy gain owing to elastic impacts and the probabilities of excitation and ionization loss make the evaluation of the electron energy impossible.<sup>36</sup> As seen on page 220, and as will be seen at a later point in this chapter, from an exceedingly complicated mathematical process using the true values of  $E_{ii}$ ,  $E_{ii}$ ,  $P_{ii}$ , and  $P_{ii}$ , one can evaluate  $\alpha/p$  as a function of  $X/p$  in an approximate fashion. Accordingly,

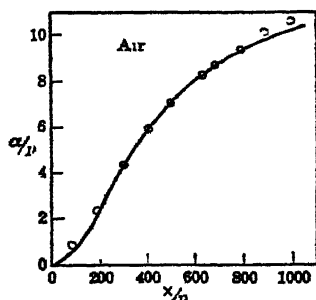


FIG. 183.

inversely,  $E_i$  can be determined from  $\alpha/p$  as a  $f(X/p)$ , and the values of  $E_i$ ,  $P_i$ , and  $P_e$  by an equally inaccurate and complicated calculation. Since it is easier to *evaluate*  $E_i$  *directly*, the former procedure is not justified. It is obvious that Townsend could not have foreseen the futility of his proposed method at the outset. The fortuitous agreement with limited data led him astray in a fashion which was natural. On the other hand, with the rest of the physical world, Townsend should have accepted the Franck and Hertz experiments and their conclusions and corrected the theory.<sup>36</sup> Since 1928 Townsend has unquestionably accepted in part these experiments and attempted in fact to develop a theory of ionization by collision in terms of it.<sup>38</sup> To this end he developed a distribution law for electron energies in a gas.<sup>35</sup> The derivation is difficult to follow and leads to an approximate law at variance with the elegant laws deduced by Druyvesteyn and Smit and one which is also experimentally less satisfactory in evaluating  $\alpha/p$  than Maxwell's law.<sup>45</sup> Thus the old expression for  $\alpha/p$  as a function of  $X/p$  has to date not been corrected by the Townsend group. It is thus necessary to use caution in applying theoretical interpretations on this question promulgated by the Townsend group especially prior to 1928. With this warning, one is in a position to review the twenty years of effort towards the deduction of an adequate theory for  $\alpha/p$  as a  $f(X/p)$  on the part of others who early accepted the significance of the Bohr theory and the Franck and Hertz experiments.<sup>54</sup>

The first one to recognize the importance of the elastic electron impacts in relation to the evaluation of  $\alpha/p$  was K. T. Compton<sup>37</sup> in 1917-18. He assumed that in He the electrons gained energy continuously in a field, losing the fraction  $f = 2m/M$  of the energy at each electronic impact as indicated on page 202. He then considered that when the electrons had gained an energy greater than  $E_i$  they had a chance of ionizing. This probability of ionization,  $P_i$ , he assumed in the absence of more definite information could be expressed as  $P_i = (E - E_i)/E$ . Here  $E$  was the energy of the electron and  $E_i$  the ionizing potential. This equation had been deduced on purely classical grounds for elastic spherical atoms some years before by Bergen Davis.<sup>38</sup> Though incorrect as applied to real atoms, it is not seriously different from the approximately correct expression when  $E \sim E_i$ , which is  $P_i = \beta(E - E_i)$ ; see page 201. The resulting expression for  $\alpha/p = f(X/p)$  computed by Compton fitted fairly well the observed values of Gill and Pidduck in what was then supposed to have been pure He. Thus the agreement was again purely fortuitous, for the He was far from pure and He is especially sensitive to impurities.

The theory of Compton<sup>37</sup> was a definite step in advance. It was defective, however, since it neglected the losses to excitation involving the probabilities of excitation  $P_e$  at the excitation potentials  $E_e$ . Finally the Ramsauer electron free paths which are functions of electron energy  $E$  were neglected, as these were unknown at the time. It

was the neglect of these factors which made the Compton investigation incomplete. The procedure instituted by Compton, however, was a big step in advance on the Townsend theory. Further direct advances in this direction were not possible until Druyvesteyn<sup>39</sup> had evaluated the energy distribution of electrons in an electrical field in a gas. The solution of this problem is treated in detail in Chapter V. In 1932, with inadequate data on Ne, Druyvesteyn<sup>40</sup> attempted to evaluate the Townsend coefficient. The unknown factor was the absorbing cross section for excitation of Ne. Taking his expression for the energy distribution with an arbitrary constant involving the unknown factor, Druyvesteyn used Townsend's  $\alpha$  for Ne to evaluate the constant. The data which this gave Druyvesteyn he then checked by applying them to Langmuir and Tonk's equation for the wall current in the positive column of a Ne glow discharge tube. This computation yielded reasonable results. This in a sense gave a more complete and successful test of the theory for  $\alpha/p$  than any previous one.

With the evaluation of the needed cross section for excitation of Ne and other gases by Maier-Leibnitz, it became possible for a complete theory to be evolved for the energy distribution of electrons in inert gases in fields of various values above that where ionization by collision begins. Druyvesteyn<sup>41</sup> in 1936 was the first one to accomplish this and to carry his calculations through to an evaluation of  $\alpha/p$  for Ne in an approximate form. With this equation he obtained fair agreement with Townsend and McCallum's<sup>28</sup> values for  $\alpha/p$  in Ne. Since later work by Kruithoff and Penning<sup>16,17</sup> cast doubts upon the purity of the gases used by Townsend and McCallum, the agreement need not be considered significant.

The electronic energy distribution at values of  $X/p$  causing ionization by collision was most completely and accurately evaluated by Smit<sup>42</sup> in 1937. From these data, accurate values of  $\alpha/p$  for He for values of  $X/p$  of 3, 4, 6, and 10 *could* be computed. This has not as yet been applied to the evaluation of  $\alpha/p$  at these values of  $X/p$  for He, as the data of Smit are relatively recent. In a later paper Miss Allen,<sup>43</sup> working with Allis, carried their computations over to inelastic impacts. The solution was only approximate, however, and not comparable with those of Druyvesteyn or Smit. It is thus clear that though no satisfactory calculations have been made as yet we are approaching a point where  $\alpha/p$  can be computed seriously as a function of  $X/p$ .

The method of computation of  $\alpha/p$  as a function of  $X/p$  is simple, once one has certain information and the patience to carry out a number of tedious integrations, most of them graphical. The procedure is as follows:  $\alpha$  represents the number of *new* electrons created per centimeter *advance* in the field direction in a gas. If in 1 second the electron advances by drift velocity  $v$  centimeters in the field direction, we can write that the number of electrons directly created *per second*



by the electron is  $\alpha v$ . Now  $v = k_e X = (760/p) K_e X$ , where  $K_e$  is the well-known mobility constant for the electron in the field  $X$  and  $v$  is the drift velocity of the electron in the field direction. This has been recently accurately evaluated by Bradbury<sup>44</sup> and Nielsen for a number of pure gases. Now this same electron in 1 second due to its random drift velocity of value  $c$  covers a zigzag path of  $c$  centimeters in the gas. On the other hand, an electron of velocity  $c$  above the velocity  $C_i$ , corresponding to that of an electron of ionizing energy  $E_i$ , will have a certain probability  $P_i$  of ionizing the gas molecules. This quantity can be evaluated as an absorbing cross section by measurements of the Compton-Van Voorhis or Smith type;<sup>56</sup> see Loeb's *Atomic Structure*, page 282. Call  $P_i(c)$  the number of such ions made per centimeter random motion in the gas at 1 mm pressure. At  $p$  mm pressure,  $p c P_i(c)$  ions will be made in 1 second by an electron of velocity  $c$ . Now the chance of an electron having a velocity  $c$  is given at once if we can calculate  $f(c)dc$ , the distribution law for the electrons in a gas at a given  $X/p$ . This has been done fairly successfully and completely by Smit<sup>42</sup> for He. With due labor it can be done for other gases. It must be noted, however, that  $f(c)dc$  is a function of  $X/p$  and varies decidedly with it. If now we integrate  $p c P_i(c) f(c)dc$  over all values of  $c$  from  $C_i$  to  $\infty$  we have the totality of new ions created in 1 second by one electron at a given  $X/p$  in the gas. This, however, must just equal  $\alpha v$ . Hence we can write:

$$\alpha v = \alpha X K_e \frac{760}{p} = p \int_{C_i}^{\infty} c P_i(c) f(c) dc,$$

so that

$$\frac{\alpha}{p} = \frac{1}{760 \frac{X}{p} K_e} \int_{C_i}^{\infty} c P_i(c) f(c) dc.$$

Since, further,  $\frac{1}{2} m c^2 = V_e/300$  if  $V$  is in volts,  $c = \sqrt{2e/300m} \sqrt{V}$ . We can also express  $P_i(c)$  as  $P(V)$  and  $f(c)dc$  as  $F(V)dV$ . Accordingly, we have at a given  $X/p$  the relation

$$\frac{\alpha}{p} = \frac{\sqrt{\frac{2e}{300m}}}{760 \frac{X}{p} K_e} \int_{E_i}^{\infty} P(V) V^{1/2} F(V) dV.$$

To evaluate this function we must know  $K_e$  as a function of  $X/p$  from Bradbury and Nielsen's<sup>44</sup> work or from the measurements of Townsend's<sup>13</sup> group on gases of more questionable purity. We must also know  $P(V)$ , which for most cases can be taken as  $P(V) = \beta(V - E_i)$  up to values of  $V = 3E_i$ , the  $\beta$  coming from Smith's curves. Then we

must know  $F(V)dV$  at the given value of  $X/p$ . To date, Smit's<sup>43</sup> calculations in He are the only ones extant for values of  $X/p$  from  $X/p = 3$  to  $X/p = 10$ . If some person cares to carry out the tedious graphical integrations we can have the first complete and fairly accurate evaluation of  $\alpha/p$  for He in a limited region. Unfortunately, there are no really good values of  $\alpha/p$  in pure, mercury-free He, for comparison (see page 342). This method was first applied by R. Holm<sup>44</sup> to air,  $N_2$  and  $H_2$  over a limited range of  $X/p$  in connection with a study of the positive column of the glow discharge. In this case the Maxwellian distribution is applicable. Failing in an accurate knowledge of the distribution laws at lower ion densities, Emmeléus, Lunt, and Meek<sup>45</sup> proceeded to compute  $\alpha/p$  for a number of gases, taking  $F(V)dV$  as expressed by Maxwell's law. They took the average energy  $kT$ , of the most probable velocity, for their evaluation of  $F(V)dV$  from the value of  $\frac{1}{2}mC_1^2 = \frac{1}{2}\eta mC^2 = \frac{3}{2}\eta kT$  for molecules by using Townsend's  $\eta$  at the appropriate  $X/p$ .<sup>30</sup> They also used 760 ( $X/p$ ) K. from the measurements of the Townsend school.<sup>12</sup> Performing the tedious integrations, using Smith's value of  $\beta$ , they evaluated  $\alpha/p$  theoretically for a number of gases including  $H_2$ ,  $N_2$ ,  $O_2$ , and A. They also used the values of  $\alpha/p$  as determined by the Townsend<sup>10, 11, 12</sup> school in Hg-contaminated gases for comparison. The agreements in the gases  $H_2$ ,  $N_2$ , and air were not seriously off except at very low and very high values of  $X/p$ . In A their calculations for  $\alpha/p$  were orders of magnitude too high as compared with observed values. The nature of the agreement is seen in Tables XXIX and XXX for  $H_2$  and air, where comparison is made with the better values of Sanders<sup>5</sup> in Hg-contaminated air and Hale's<sup>3</sup> excellent values in pure Hg-free  $H_2$ . As is seen in these tables, the value of the ratio observed to calculated, using Hale's<sup>3</sup> values in  $H_2$ , is not too bad except at lower  $X/p$ . In air, using Sanders' <sup>5</sup> values, which are probably high on account of Hg vapor, the agreement is again not bad. At high values of  $X/p$ , Emmeléus<sup>45</sup> contends that the theory is not very good as then  $v = k_e X$  becomes comparable to  $C$  or  $\frac{1}{2}mv^2$  becomes comparable to  $\bar{V}$ . This circumstance they attempt to correct in a semi-empirical fashion. The corrections, as seen, improve the fit in  $H_2$  in that they maintain the calculated values above the observed values, making the theory more consistent. The agreement in  $H_2$ , however, is not very satisfactory. It gives  $\alpha/p$  of the correct order of magnitude, but  $\alpha/p$  is too high at low  $X/p$  and unless empirically corrected too low at high  $X/p$ . It is, however, the kind of an agreement we might expect from the theory and for a *wonder* is not fortuitously accurate. In the case of Sanders' data in air the agreement is too good for the data.

One may then conclude that except at very low values of  $X/p$ , the rough theory and the use of a Maxwellian distribution give results which roughly fit experiment. The calculated values for A, assuming a Maxwellian distribution, however, gave values for  $\alpha/p$  which were

TABLE XXIX

 $H_2$ 

| $X/p$ | Townsend's<br>$\nu \times 10^{-7}$ | Calculated<br>$\alpha/p$ | Hale's<br>Observed $\alpha/p$ | Calculated $\alpha/p$<br>Corrected for Drift |
|-------|------------------------------------|--------------------------|-------------------------------|--|
| 13    | 0.47                               | 0.0004                   | 0.015 (Ayers)                 | 0.0004                                       |
| 21    | 0.73                               | 0.015                    | 0.030                         | 0.015  |
| 31.5  | 1.20                               | 0.089                    | 0.085                         | 0.089  |
| 43.5  | 1.82                               | 0.23                     | 0.162                         | 0.256  |
| 57.5  | 2.63                               | 0.40                     | 0.280                         | 0.425  |
| 72.5  | 3.62                               | 0.57                     | 0.43                          | 0.631  |
| 88    | 4.62                               | 0.77                     | 0.625                         | 0.868  |
| 105   | 5.75                               | 0.95                     | 0.72                          | 1.10   |
| 118   | 6.60                               | ...                      | 0.90                          | 1.53   |
| 123   | 6.98                               | 1.10                     | 0.95                          | 1.33   |
| 130   | 7.45                               | .....                    | 1.04                          | 1.70   |
| 155   | 9.06                               | .....                    | 1.34                          | 2.00   |
| 161   | 9.50                               | 1.33                     | 1.40                          |  |
| 203   | 12.30                              | 1.47                     | 2.00                          |  |

TABLE XXX

AIR

| $X/p$ | Townsend's<br>$\nu \times 10^{-7}$ | Calculated<br>$\alpha/p$ | Sander's *<br>Observed $\alpha/p$ |
|-------|------------------------------------|--------------------------|-----------------------------------|
| 20    | 0.9                                | 0.0002                   | 0.00034                           |
| 36    | 1.35                               | 0.011                    | 0.0082                            |
| 55    | 1.84                               | 0.074                    | 0.09                              |
| 75    | 2.25                               | 0.24                     | 0.28                              |
| 100   | 2.70                               | 0.53                     | 0.637                             |
| 130   | 3.19                               | 0.92                     | 1.236                             |
| 163   | 3.74                               | 1.39                     | 1.65                              |
| 198   | 4.23                               | 1.90                     |                                   |

\* Sander's values were obtained in Hg-contaminated air and thus high at high  $X/p$ . The agreement is fortuitously good.

finite and large at values of  $X/p$  at which *no values of  $\alpha/p$  could be observed* experimentally. They furthermore gave values of  $\alpha/p$ , throughout, which were orders of magnitude  $10^4$  to  $10^2$  too high. The cause for this deviation lies in the nature of the true energy distribution law for A, which deviates badly from the Maxwellian in having *far fewer high-energy* electrons than the Maxwellian would allow, as seen on page 194. It is in cases like these that the importance of the energy distribution law manifests itself. With the proper form of the distribution law at hand, it is probable that  $\alpha/p$  could be calculated as accurately as experimental values can be observed.

It is seen at once that the theory for  $\alpha'/p$  as a function of  $X/p$  is not impossibly difficult, although it is not simple. The chief difficulty lies in the determination of  $f(V)dV$ , which varies with  $X/p$ . For the present,  $f(V)dV$  must be calculated as it *cannot* be measured directly. In any case, however, the theory is far more involved than Townsend's original theory and is quite different in its nature. It must also be noted that, since the form of  $f(V)dV$  changes materially as  $X/p$  changes,  $\alpha'/p$  will indeed be a complicated  $f(X/p)$ .

## 5. v. ENGEL AND STEENBECK'S THEORETICAL APPROXIMATION TO TOWNSEND'S EQUATION

Using in general the method initiated by Holm and assuming a *Maxwellian* distribution law for electron energies, v. Engel and Steenbeck, in their book,<sup>48</sup> in 1932, justified the Townsend equation of  $\alpha'/p$  as a  $f(X/p)$  as an approximation to a more exact expression. It is of interest to follow the derivation given by them, as it shows the purely fortuitous nature of the agreement of Townsend's original equation.

The number of impacts per second encountered by an electron of free path  $\lambda_0$  moving with a velocity of agitation between  $c$  and  $c + dc$  is  $c/\lambda_0$ . The chance of an electronic velocity  $c$  on Maxwell's law is

$$\frac{4}{\sqrt{\pi}} \frac{c^2}{\alpha_1^3} e^{-\frac{c^2}{\alpha_1^2}} dc,$$

see page 652, where  $\frac{1}{2}m\alpha_1^2 = kT_0$ . Thus the number of collisions of one electron at a velocity between  $c$  and  $c + dc$  per second is

$$dz = \frac{4}{\sqrt{\pi}} \frac{1}{\lambda_0} \frac{c^3}{\alpha_1^3} e^{-\frac{c^2}{\alpha_1^2}} dc.$$

Now the chance that an electron of velocity above  $c_i$  can ionize, where  $\frac{1}{2}mc_i^2 = E_i = eV_i$ ,  $V_i$  being the ionizing potential expressed in volts, can at once be derived from the Smith curves and are given by  $P(V) = \beta(E - E_i) = \beta((m/2)c^2 - eV_i)$ , which may be written  $P_i(c) = a'(c^2 - c_i^2)$ . Thus the number of ions created per second by one electron will be given by

$$z' = \int_{c_i}^{\infty} P_i(c) dz = a' \frac{4\alpha_1^3}{\sqrt{\pi}\lambda_0} e^{-\frac{c_i^2}{\alpha_1^2}} \left[ 1 + \frac{1}{2} \frac{eV_i}{kT_0} \right],$$

where  $\frac{1}{2}m\alpha_1^2 = kT_0$ . If  $s$  is the number of electrons created per centimeter random path in a gas per millimeter pressure as given directly by the Smith curves, the quantity  $P(V)$  is equal to  $s$  divided by the number of impacts per centimeter random path in a gas, i.e., it is  $P(V) = s/(1/\lambda_0) = s\lambda_0$ . Hence from the Smith curves we get directly  $s = a(E - E_i)$ , and from this  $P(V) = s\lambda_0 = a\lambda_0(E - E_i)$ .

Since we express  $E$  in volts at 1 mm pressure, we may write  $a' = a\lambda_e(300/2)(m/e)p$ . This gives  $z'$  as

$$z' = 600a \frac{mp}{e\sqrt{\pi}} \alpha_1^3 e^{-\frac{eV_i}{kT_e}} \left[ 1 + \frac{1}{2} \frac{eV_i}{kT_e} \right].$$

Now the number of ions created in 1 second per electron is by the definition of  $\alpha$  merely  $\alpha v$ , where  $v$  is the electronic velocity. Hence one may set  $\alpha = z'/v$ . If we use the v. Engel and Steenbeck equation equivalent to Compton's electron mobility equation, see page 186,

$$v = \frac{\sqrt[4]{2}}{\sqrt[3]{\pi}} \sqrt{\frac{e}{m}} X\lambda_e \sqrt{f},$$

with  $f$  the fractional loss of energy on electron impact, and if we call the electron temperature

$$T_e = \frac{\sqrt[4]{\pi}}{2\sqrt{2}} \frac{eX\lambda_e}{k\sqrt{f}}^*,$$

we may, from the values of  $z'$  and  $v$  given, get an equation for  $\alpha$ . This equation reads

$$\frac{\alpha}{p} = \frac{600aV_i}{\sqrt{2}\sqrt[4]{\pi}\sqrt{f}} e^{-\frac{2\sqrt{2}}{\sqrt[4]{\pi}} \frac{\sqrt{f}V_i}{(X/p)\lambda_{e0}}} \left[ 1 + \frac{eV_i}{2kT_e} \right].$$

Here  $\lambda_{e0}$  is the mean free path at 1 mm. At very high  $X/p$  in some gases  $eV_i/2kT_e \ll 1$  when the electron energy has increased well above the ionization potential. Under these conditions we have

$\alpha/p = Ae^{-\frac{eV_i}{kT_e}}$ , which is the Townsend form. It is to be noted, however, that this equation has now been deduced on a strictly modern basis, taking into account the energy loss of the electron per impact, the probability of ionization, and the energy distribution function. It must furthermore be noted that it can hold in the Townsend form only if  $kT_e \gg eV_i$ , which applies only above  $X/p \sim 200$  or more in air. Again it must be noted that it assumes Maxwell's law. Hence it will hold roughly for air and less well for  $H_2$ , and will vary by orders of magnitude for A as we have seen in the work of Emmeléus, Lunt, and Meek. v. Engel and Steenbeck advocate its use in calculations<sup>50</sup> and themselves apply it to the derivation of their equations for the Crookes dark space in a glow discharge; see page 582. In the dark space, Maxwell's law is approached but *does not hold very accurately*, and  $X/p$  is high. The law fails completely below  $X/p = 100$  in air and does not apply at all in other gases. It is used as an empirical relation by v. Engel and Steenbeck,<sup>49</sup> and as *such the constants can be adjusted to*

\* In this equation  $T_e$  is derived from  $C$  in the denominator of an electron mobility equation of the Compton type; see page 186.

fit observations over a limited range of  $X/p$  in most gases in the region above the point of inflection of the  $\alpha/p = F(X/p)$  curve.

With this discussion we may leave the consideration of the first Townsend coefficient  $\alpha$  and proceed to consider what happens as  $x$  is further increased or when  $X/p$  becomes larger.

## 6. REFERENCES FOR CHAPTER VIII

1. J. S. TOWNSEND, *Nature*, **62**, 340, 1900; *Phil. Mag.*, **1**, 198, 1901.
2. W. E. BOWLS, *Phys. Rev.*, **53**, 293, 1938.
3. D. H. HALE, *Phys. Rev.*, **54**, 241, 1938; **56**, 815, 1939.
4. A. STOLETOW, *J. phys.*, **9**, 468, 1890; H. KREUSLER, *Verhandl. physik. Ges.*, Berlin, **17**, 86, 1898; E. VON SCHWEIDLER, *Wien. Ber.*, **18**, 273, 1899.
5. F. H. SANDERS, *Phys. Rev.*, **41**, 667, 1932; **44**, 1020, 1933.
6. J. S. TOWNSEND, *Phil. Mag.*, **3**, 557, 1902; **6**, 389, 598, 1903; **8**, 738, 1904.
7. M. PAAVOLA, *Arch. Elektrotech.*, **22**, 443, 1929.
8. K. MASCH, *Arch. Elektrotech.*, **26**, 589, 1932.
9. TOWNSEND and TIZARD, *Proc. Roy. Soc.*, **A 87**, 357, 1912; **A 88**, 336, 1913.
10. H. E. HURST, *Phil. Mag.*, **11**, 535, 1906.
11. GILL and PIDDUCK, *Phil. Mag.*, **16**, 280, 1908.
12. T. L. R. AYERS, *Phil. Mag.*, **45**, 353, 1923.
13. TOWNSEND and BAILEY, *Phil. Mag.*, **42**, 874, 1921; **43**, 593, 1922; **44**, 1033, 1922.
14. D. Q. POSIN, *Phys. Rev.*, **50**, 650, 1936.
15. N. E. BRADBURY, *Phys. Rev.*, **40**, 525, 1932.
16. KRUTHOFF and PENNING, *Physica*, **3**, 515, 1936.
17. KRUTHOFF and PENNING, *Physica*, **4**, 430, 1937.
18. HOLST and OOSTERHUIS, *Phil. Mag.*, **46**, 1117, 1923.
19. VARNEY, WHITE, LOEB and POSIN, *Phys. Rev.*, **48**, 818, 1935.
20. J. S. TOWNSEND, *Phil. Mag.*, **28**, 83, 1914; also *Electrician*, June 6, 1913.
21. L. G. H. HUXLEY, *Phil. Mag.*, **5**, 721, 1928; **8**, 128, 1929; **10**, 183, 1930; J. H. BRUCE, *Phil. Mag.*, **10**, 476, 1930.
22. BOULIND, *Phil. Mag.*, **18**, 909, 1934.
23. F. M. PENNING, *Z. Physik*, **57**, 723, 1929; *Physica*, **10**, 47, 1930; **12**, 65, 1932; *Phil. Mag.*, **11**, 979, 1931.
24. PENNING and ADDINK, *Physica*, **1**, 1007, 1934.
25. R. SCHOEFER, *Z. Physik*, **110**, 21, 1938.
26. TOWNSEND and McCALLUM, *Phil. Mag.*, **5**, 695, 1928; **6**, 857, 1928.
27. R. S. MULLIKAN, *Phys. Rev.*, **32**, 186, 1928; SAHA and MATHUR, *Proc. Natl. Acad. Sci. India*, **6**, 120, 1936.
28. F. EHRENKRANTZ, *Phys. Rev.*, **55**, 219, 1939.
29. J. S. TOWNSEND, *Electricity in Gases*, Oxford Press, 1914, Chapter VIII.
30. TOWNSEND and TIZARD, *Proc. Roy. Soc.*, **A 88**, 336, 1913.
31. L. B. LOEB, *Atomic Structure*, pp. 249 ff., John Wiley & Sons, New York, 1938.
32. JODELBAUER, *Z. Physik*, **92**, 116, 1934.
33. L. B. LOEB, *Rev. Modern Phys.*, **8**, 277, 1936.
34. J. S. TOWNSEND, *Electricity in Gases*, Chapters IV and VIII, Oxford Press, 1914.
35. J. S. TOWNSEND, *Phil. Mag.*, **9**, 1173, 1930; **20**, 242, 1935.
36. R. D'E. ATKINSON, *Proc. Roy. Soc.*, **A 119**, 325, 1935.
37. K. T. COMPTON, *Phys. Rev.*, **7**, 489, 501, 509, 1916; **8**, 449, 1917; COMPTON and BENADE, *Phys. Rev.*, **11**, 234, 1918.
38. BERGEN DAVIS, *Phys. Rev.*, **24**, 93, 1907; **5**, 118, 1915.
39. M. J. DRUYVESTEYN, *Physica*, **10**, 69, 1930.
40. M. J. DRUYVESTEYN, *Physik. Z.*, **33**, 836, 1932.
41. M. J. DRUYVESTEYN, *Physica*, **3**, 65, 1936; **4**, 440, 1937.

42. J. A. SMIT, *Physica*, **3**, 543, 1937.
43. H. W. ALLEN, *Phys. Rev.*, **52**, 710, 1937.
44. BRADBURY and NIELSEN, *Phys. Rev.*, **49**, 388, 1936; R. H. NIELSEN, *Phys. Rev.*, **50**, 950, 1936.
45. EMMELÉUS, LUNT, and MEEK, *Proc. Roy. Soc., A* **156**, 394, 1936.
46. R. HOLM, *Z. Physik*, **75**, 180, 1932.
47. J. KAPLAN, *Phys. Rev.*, **55**, 111, 1939.
48. v. ENGEL and STEENBECK, *Elektrische Gasentladungen*, Vol. I, pp. 89, 184, and 192, Julius Springer, Berlin, 1932.
49. v. ENGEL and STEENBECK, reference 48, p. 97.
50. O. KLEMPERER, *Z. Physik*, **52**, 650, 1928.
51. W. S. HUXFORD, *Phys. Rev.*, **55**, 754, 1939.
52. D. H. HALE, *Phys. Rev.*, **55**, 815, 1939.
53. The decline in the curve of Huxford as well as the declines and subsequent rises of the  $\alpha/p - X/p$  curves observed by Hale were at first attributed to the decline in ionizing efficiency of rapidly moving electrons following the Smith curves.<sup>56</sup> This occurs above 100 volts for electrons in A and above 60 volts in H<sub>2</sub>.<sup>48</sup> The energy of electrons in A at an  $X/p$  of 700 or an  $X/p$  of 1000 in H<sub>2</sub> is not known, but it is hardly likely to be as high as the 100 or the 60 volts required by this assumption. The disappearance of the rather uncertain dips of Hale's curves at  $X/p = 900$  and then reappearance at  $X/p = 1300$  when he went to a new apparatus at which  $x$  could be extended to 3 cm suggests that they are of instrumental origin. It is not at all unlikely that they are in part caused by a failure of the electrons at the low pressures of 0.1 mm used to achieve their terminal energies before reaching the cathode.
54. Townsend's derivation for evaluating  $\alpha/p$  using the mean free path equation, which he has recently carried over to the calculation for  $\beta/p$  for positive ions,<sup>55</sup> is in principle erroneous. The theory implies that the fields are such that the electron or ion-free paths will lie in the field direction. Now owing to the field the average energy of the electrons and ions is such that their random velocities or energies are greater than their drift velocities or energies in the field direction. Thus the paths resulting from collisions are such that the free paths are not laid out in the field direction. Hence, to calculate  $\alpha/p$  or  $\beta/p$  Townsend with his procedure should multiply his expression by the chance that a free path in the existing fields is sufficiently in the field direction to gain the ionizing energy. Could such a calculation be made, it would obviously reduce the values of  $\alpha/p$  or  $\beta/p$  calculated by Townsend's method by a considerable amount, and should in the end lead to equations analogous to those based on the energy distribution.
55. J. S. TOWNSEND, *Phil. Mag.*, **28**, 111, 1939.
56. P. T. SMITH, *Phys. Rev.* **36**, 1293, 1930; TATE and SMITH, *Phys. Rev.*, **39**, 270 1932.

## CHAPTER IX \*

### THE SECOND TOWNSEND COEFFICIENT

#### 1. INTRODUCTION

If in the experiments described at the beginning of Chapter VIII the field strengths, or better the ratios of  $X/p$ , are above a certain value characteristic of each gas, e.g., 120 for air and 5 for Ne, the curves for  $\log i/i_0$  plotted against  $x$  are no longer straight lines. The  $\log i/i_0 - x$  curves bend upwards at first gradually and then more sharply, terminating abruptly at values of  $x$  giving rise to a spark. Sets of such curves taken from Sanders' data<sup>1</sup> in air and Bowls' data<sup>2</sup> in  $N_2$  are shown in Figs. 184 and 185. At values of  $X/p$  below the curved portions, the linear graphs of  $\log i/i_0 - x$  also break off abruptly at certain values of  $x$  when sparking occurs.<sup>3</sup> Disregarding the appearance of the spark for the present, it appears that, if large current densities are avoided for large values of  $x$  (less than  $10^{-13}$  amp/cm<sup>2</sup> for  $x \sim 3$  cm), the curvatures of the  $\log i/i_0 - x$  graphs observed by Townsend and others may usually be closely approximated by

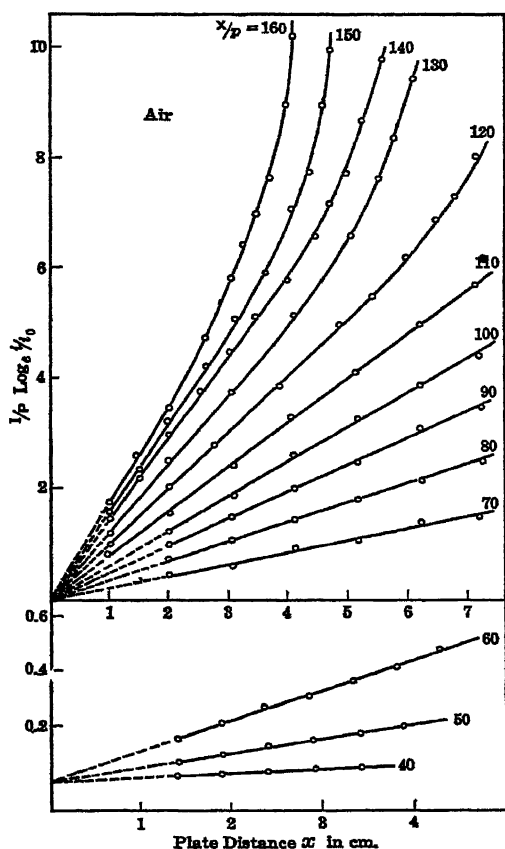


FIG. 184.

\* References for Chapter IX will be found on page 406.



equations of a definite type. With the heavier current densities and larger values of  $x$ , space-charge effects, having nothing to do with the phenomena in question, can increase  $\log i/i_0$  at a rate higher than a linear increase with  $x$ , thus causing an apparent deviation from the linear relationship. This phenomenon will therefore be left for discussion at a more opportune point. The type of equation was originally

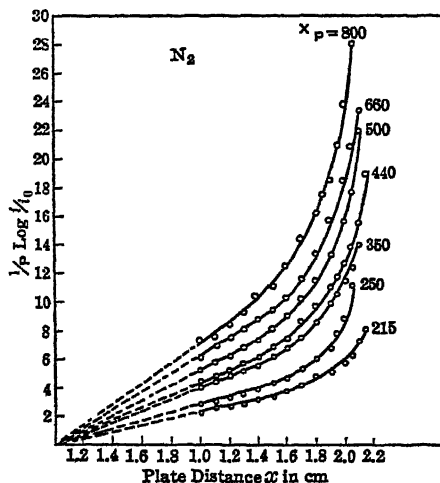


FIG. 185.

arrived at by Townsend<sup>3</sup> in terms of a single equation on the basis of a theory quite logical at the time of its deduction.

The assumption underlying the theory is the following: Since initially the ionization by collision was attributed by Townsend to the impact of *negative ions* and *not* electrons on gas molecules it was not unnatural to look upon the *positive ions* as possible ionizing agents as well. Thus Townsend logically assumed that, at somewhat higher values of  $X/p$ , positive ions could ionize molecules by impact. He accordingly postulated that each posi-

tive ion could create  $\beta$  new electrons *per centimeter path in the field direction*. This quantity  $\beta$  was termed the "coefficient of ionization by positive-ion impact." We shall henceforth refer to  $\beta$  as the *second Townsend coefficient*, leaving its nature and its interpretation open, for reasons to be discussed.

## 2. THE TOWNSEND THEORY OF IONIZATION BY POSITIVE IONS

Let us for the present assume with Townsend that each positive ion in 1 cm of its path in the field direction produces  $\beta$  new ion pairs as it moves towards the cathode. Let us further assume that  $\beta/p$ , like  $\alpha/p$ , is some function of  $X/p$ . We may now consider  $n_0$  photoelectrons liberated per square centimeter from the cathode of a plane parallel-plate condenser filled with gas, the anode being  $d$  centimeters distant. Take a slab of gas  $dx$  thick at a distance of  $x$  centimeters from the cathode and parallel to it. Let  $p$  be the number of positive ions generated per square centimeter of area parallel to the cathode between the cathode  $C$  and the slab  $dx$ , by positive *and* negative *ions*. Let  $q$  be the number of such ions generated in the distance  $d - x$  remaining between  $dx$  and the anode  $E$ . If  $n_0$  is the number of ions per square centimeter generated at

the cathode by an external source, i.e., by ultraviolet light, then there arrive at the anode  $n = n_0 + p + q$  negative ions. In the slab  $dx$  there are generated  $(n_0 + p)\alpha dx + q\beta dx$  ions. Thus  $dp$ , the increase of ions in  $dx$ , is  $dp = (n_0 + p)\alpha dx + q\beta dx$ . Inserting the value of  $q = n - n_0 - p$  from the equation above, one has

$$\frac{dp}{dx} = (n_0 + p)\alpha + \beta(n - n_0 - p) = (n_0 + p)(\alpha - \beta) + n\beta.$$

Separating variables, this relation yields

$$\frac{dp}{(n_0 + p) + \frac{n\beta}{\alpha - \beta}} = (\alpha - \beta)dx,$$

which on integration gives

$$\log \left[ (n_0 + p) + \frac{n\beta}{\alpha - \beta} \right] = x(\alpha - \beta) + \log A,$$

or

$$n_0 + p = A e^{(\alpha - \beta)x} - \frac{n\beta}{\alpha - \beta}.$$

As  $p = 0$  at  $x = 0$

$$A = n_0 + \frac{n\beta}{\alpha - \beta};$$

and as, at  $x = d$ ,  $n = n_0 + p$ , we have

$$\begin{aligned} n &= \left( n_0 + \frac{n\beta}{\alpha - \beta} \right) e^{(\alpha - \beta)d} - \frac{n\beta}{\alpha - \beta}, \\ n \left( 1 + \frac{\beta}{\alpha - \beta} - \frac{\beta}{\alpha - \beta} e^{(\alpha - \beta)d} \right) &= n_0 e^{(\alpha - \beta)d}, \\ n &= n_0 \frac{(\alpha - \beta) e^{(\alpha - \beta)d}}{\alpha - \beta e^{(\alpha - \beta)d}}. \end{aligned}$$

When  $\beta = 0$  this equation at once reduces to  $n = n_0 e^{\alpha d}$ , which yields the linear expression  $\log n/n_0 = \alpha d$  for ionization by negative ions alone. If  $n$  and  $n_0$  are multiplied by the ionic charge  $e$ , on setting  $i = ne$  and  $i_0 = n_0 e$ , one has an equation at once open to experimental test in the form

$$i = \frac{i_0(\alpha - \beta)e^{(\alpha - \beta)x}}{\alpha - \beta e^{(\alpha - \beta)x}},$$

where  $i_0$  is the photoelectric current and  $x$  is the variable plate separation. Applying this equation to the experimental values at large  $X/p$  and  $x$ , Townsend at once found that, at a given  $X/p$ , each curve for  $i/i_0$  as a function of  $x$  was satisfied by a single constant value of  $\beta$ ,

within experimental accuracy. Furthermore, if one calls  $\delta$  the value of  $d$  in the denominator  $\alpha - \beta e^{(\alpha-\beta)d}$  at the point where  $\alpha = \beta e^{(\alpha-\beta)\delta}$ , it is seen that  $i$  becomes indefinitely large irrespective of  $i_0$ . Thus at a value of  $(X/p)_s$  and  $\delta$  at which  $\alpha = \beta e^{(\alpha-\beta)\delta}$  we have an indefinitely large current  $i$  with a plate separation  $\delta$ . This Townsend *interpreted as the condition for a spark*, and  $(X/p)_s$  and  $\delta$  respectively represented the value of  $X/p$  for a spark and the sparking distance  $\delta$ . Concerning this application of the theory a great deal will be said at a later point. It may be stated now, however, that, within the rough limits of accuracy obtaining, the observed sparking data at low pressures agree with the values of  $(X/p)_s$  and  $\delta$  derived from  $\alpha$  and  $\beta$ .

Such agreement appeared to be well beyond the realms of a fortuitous coincidence, and Townsend as well as the rest of the scientific world including the author accepted the agreement as constituting not only a proof of the correct *form* of the equations but a *proof* of the *correctness of the basic assumptions as well*. Nature, however, is not so simple as man would like to have it, and as might today be suspected it appears that both the basic assumptions as to mechanism of secondary-ion production giving rise to the second Townsend coefficient and the basic assumptions as to mechanism of spark propagation are wrong in principle. Here again the error must be laid to a fortuitous agreement in the form of the equations which the inaccurate measurements in this domain make it difficult clearly to discern. Unfortunately here as elsewhere Townsend and his school have been the last to concede the errors in reasoning, and because of the plausibility of the agreements and the tremendous prestige of Townsend's achievements the errors are being perpetuated in the literature.<sup>63</sup> It is true, however, that in this case the differences are much more subtle and require far more careful modern techniques for their detection than in Townsend's *theory of  $\alpha$* . With increasing accuracy it is daily becoming clearer that the errors exist and in what direction they lie. Thus, for example, with mercury-free gases, Ehrenkrantz<sup>4</sup> found good agreement with her sparking potential data using Townsend's equation above, and Posin's<sup>5</sup> values for  $\alpha$  and  $\beta$  in  $N_2$  badly contaminated with Hg, while Bowls<sup>2</sup> values of  $\alpha$  and  $\beta$  in really pure  $N_2$  gave inferior agreement, as we shall see.

In what follows, the theoretical aspect of the errors of Townsend's interpretation of his second coefficient will first be pointed out, leaving for a later chapter a consideration of the erroneous character of the sparking equation. Following that discussion the experimental results will be interpreted in the light of theory.

### 3. THE PROBLEM OF IONIZATION BY POSITIVE IONS

With Townsend's recognition of the electron and not the negative ion as the agent in ionization by collision giving rise to the first Townsend coefficient  $\alpha$ , a difficulty inherent in his original theory was at once

removed. The coefficient  $\alpha/p$  takes on detectable magnitudes at values of  $X/p$  far lower than the second coefficient  $\beta/p$ . This is seen in the detection of an  $\alpha$  in air at  $X/p = 20$  by Sanders<sup>1</sup> whereas  $\beta/p$  can be measured only at  $X/p = 120$ . Analogously, in  $H_2$ ,  $\alpha$  takes on measurable values at  $X/p = 10$ , while in Hale's<sup>7</sup> careful work  $\beta$  does not appear measurable below  $X/p = 30$ . This is not consistent with the *relatively unimportant differences between mobilities and other properties of positive and negative ions*. Thus a difference in the ionizing agent as between electron and positive ion removed this difficulty, at least temporarily.

From the Franck and Hertz experiments the nature of ionization by electron impact is clear, and with the added knowledge of the high average electron energy in an electrical field the appearance of an  $\alpha$  at low  $X/p$  is also clear. What is now not so clear, however, is the mechanism, or the character of ionization by positive ions at the energies which these can acquire in fields where  $X/p$  is as low as 100, or 30. The theory of ionization of atoms by moving positive or negative charges has been studied by Thomson, Bohr, Henderson, Fowler,<sup>8</sup> and others. For electrons it presents no great difficulties, and for *faster* positive ions theory and experiment agree at least in order of magnitude. As Thomson<sup>8</sup> has pointed out, however, the laws of dynamics do not permit positive ions below certain characteristic energies to remove electrons from atoms. This results from the massive character of the ion compared to the electron. For atoms of ionizing energy about 10 volts, the minimum energy in the case of a  $He^{++}$  ion is 10,000 volts and of a  $H^+$  ion 3000 volts, according to Thomson. All other ions require higher energies still. Actually effective ionization by  $\alpha$  particles ceases far above 10,000 volts, though canal rays of these positive ions do show evidence of ionizing at lower values. Subsequent to his experiments on the ionization by collisions by electrons, J. Franck<sup>9</sup> postulated that positive ions could ionize atoms at an energy roughly 1.5 times  $E_i$ , the ionizing potential. This value was chosen since an electron in escaping would have to escape from the field of the positive ion as well as from its own atom with a residual positive charge.

Early experiments of Franck and v. Bahr<sup>9</sup> and Pavlow<sup>10</sup> appeared to indicate such a phenomenon. Later work by Horton and Davies<sup>11</sup> and by W. J. Hooper<sup>12</sup> indicated that this was not correct and that the electrons observed were due to secondary emission from metal surfaces on positive-ion bombardment. Loeb<sup>14</sup> in 1927 pointed out that, although on dynamical grounds classical ionization in virtue of the positive charge on the ion acting directly on electrons was ruled out, as Thomson showed, in the case of slow ions a mechanism might exist for the ionization postulated by Franck. This, it was suggested, was some sort of an interaction by *electrons* in the positive ions with *electrons* in the atom, which, if the relative energy of the ion and atom exceeded  $E_i$  plus the energy needed for conservation of momentum and

energy, would result in *squeezing out one of the atomic electrons*. In a sense it would be the inverse of dissociation by electron impact explained on the Franck-Condon principle (see Loeb, *Atomic Structure*, page 316). It was pointed out that in this event  $H^+$  and  $He^{++}$  could *not* ionize below 3000 or 10,000 volts while  $H_2^+$  or  $He^+$  or any positive ion with one or more electrons might ionize.

The subsequent work of Beeck<sup>13</sup> and Sutton<sup>15</sup> independently and later of Sutton and Mouzon, Mouzon,<sup>16</sup> Beeck, and Nordmeyer,<sup>17</sup> culminating with the work of Varney<sup>18</sup> using a balanced space-charge method for detecting the positive ions, proved this interpretation to be correct. Varney<sup>18</sup> and Rostagni, with some success, also extended the studies to the ionization of inert gas atoms by their own rapidly moving atoms. The results are highly interesting, for they definitely establish the phenomenon of ionization of atoms by positive atom ions at energies far below that to be expected on the Thomson mechanism. Positive ions of  $Na^+$ ,  $K^+$ ,  $Rb^+$ , and  $Cs^+$  ionize the inert gases Ne, A, Kr, and Xe, the lowest value of the energy being required in each case by the alkali ion having the identical electronic structure with the gas ionized. Thus, for instance,  $Na^+$  in Ne,  $K^+$  in A,  $Rb^+$  in Kr, and  $Cs^+$  in Xe give the lowest values in the different possible combinations when the results are reduced to take account of the losses to ions required by the laws of momentum and energy. The lowest actual observed potential is that for  $K^+$  in Kr, which is 69 volts. The reduced value, i.e., the *actual energy available for ionization*, is 38 volts for  $Cs^+$  in Kr, the ionization potential of Kr being 11.5 volts. He could *not* be ionized by any ion, and  $Li^+$  could *not* be observed to ionize any gas by Varney<sup>18</sup> up to 400 volts. Beeck and Mouzon<sup>16</sup> reported ionization by  $Li^+$ , but the  $Li^+$  sources are badly contaminated with  $K^+$ , and the value for  $Li^+$  in A observed by these men agreed with the value for  $K^+$  in A fairly well. The ionizations obtained by  $Na^+$  in gases other than He by Beeck and Mouzon<sup>16</sup> could not be checked by Varney, and most of them lay in the 300- to 400-volt range, where secondary emission from metal surfaces by positive-ion bombardment could seriously complicate the results. Later Varney<sup>20</sup> showed that Hg could be ionized by  $Na^+$  at 88 volts but not by  $K^+$  up to 300 volts.

The efficiencies of ionization were highest for  $Cs^+$  in Xe and  $K^+$  in A and were zero at onset, rising to perhaps 20 per cent of the kinetic-theory impacts at 500 volts. Other efficiencies are notoriously less. Excitation of atoms by positive-ion impact is observed generally in canal rays well above 1000 volts energy and in some cases at lower energies. Some of these appearances are due to the action of multiply charged positive ions and are connected with the change of charge mechanism. Tate<sup>21</sup> observed the Hg lines for  $Na^+$  ions at 40 volts. This was later confirmed by Kirchstein.<sup>22</sup> All attempts to excite or ionize molecular gases such as  $H_2$  or  $N_2$  by positive-ion impact below energies of 400 volts have failed.

Further evidence as to the very special nature of the observed ionization by positive-ion impact lies in the results of Beeck<sup>23</sup> and Wayland, Rostagni,<sup>14</sup> Wayland,<sup>19</sup> and Varney<sup>19</sup> on the ionization by neutral atoms. Varney obtained fast inert gas atoms by the Kallmann-Rosen effect (see Loeb, *Atomic Structure*, page 287) from accelerated ions of these gases and used these atoms to cause ionization in gases of their own species. In conformity with Rostagni he observed the effects in Ne and A and also found them to occur in Kr and Xe. Varney<sup>24</sup> did not observe them in He, contrary to Rostagni. The energies involved ranged between 35 and 74 volts and gave a reduced energy (available after energy going to conservation was deducted) as low as 17.5 volts for Xe in Xe, or only 6 volts above the ionization potential.

It is quite clear from this that: (1) positive ions can ionize *atoms* by impact at potentials materially below those envisaged by the Thomson mechanism; (2) this ionization is of a very specialized type, evidently depending on interactions of the wave functions of closely similar electronic configurations; (3) it requires in all cases above 60 volts of energy per positive ion; (4) at the onset at these energies the probability of ionization is small and rises only at higher energies; (5) it does not occur for most combinations of ions and gases and not for molecular gases below 500 volts of energy per ion; (6) energies involved in impact ionization by neutral atoms are somewhat less, but in no case are they less than 35 volts. Such ionization by positive ions through neutralization and ionization is most improbable, as it involves *two* processes.

In addition to the information above, one must recognize that even with a distribution of energy of positive ions in an electrical field in a gas the large energy exchanges in impact between positive ions and gas molecules *cannot allow of very many ions with even ten times the energy gained in a free path*. It therefore becomes clear that *it is physically impossible for enough positive ions to gain the 60 to 1000 volts of energy required for ionization from fields where  $X/p$  ranges in value from 0 to 200, which the observed values of  $\beta$  would require*.

#### 4. THE ALTERNATIVES TO IONIZATION BY POSITIVE IONS

##### a. Secondary Electron Emission by Positive-Ion Bombardment.

The solution to the paradox produced as a result of the impossibility of accounting for  $\beta$  in terms of ionization by positive ions, while sensible and constant values of  $\beta$  are derived from experiments in apparent agreement with the theory, must now be sought. The results indicate a correct theory and an apparently constant value of  $\beta/p$  at a given  $X/p$ . Hence we must now seek another interpretation for  $\beta$  which does not do too much violence to the form of the theory. Early in the study of the phenomenon Townsend<sup>25</sup> and J. J. Thomson<sup>26</sup> had independently considered a second process of electron production by positive

ions and one consistent with well-known phenomena. This is the secondary emission of electrons from the cathode by positive-ion impact. Concerning this process much information is at hand, though none is satisfactory owing to the impossibility of producing or studying reproducible surfaces. The phenomenon is briefly discussed in Loeb's *Atomic Structure*, pages 287 and 327.

Let us now consider a plane parallel-plate condenser as before with  $n_0$  initial photoelectrons liberated per square centimeter per second. Call the plate separation  $x$ , and assume that  $X/p$  is of such value that  $\alpha/p$  is finite and appreciable but that a fraction  $\gamma$  of *new electrons are created at the cathode by each impacting positive ion*. Let  $n$  total electrons reach the anode  $x$  centimeters distant, and let the positive ions at a given  $x$  and  $X/p$ , or  $\gamma$ , liberate  $n'_0 - n_0$  electrons *from the cathode*. That is, let  $n'_0$  be the total number of electrons per square centimeter liberated at the cathode by *positive ions and light* combined. Since  $n - n'_0$  positive ions are created in the gas, we can write

$$n'_0 = n_0 + \gamma(n - n'_0),$$

whence

$$n'_0 = \frac{n_0 + \gamma n}{1 + \gamma}.$$

Again, with  $n'_0$  electrons from the cathode, Townsend's original equations for ionization by electron impact yields  $n = n'_0 e^{\alpha x}$ , whence

$$n = \frac{n_0 + \gamma n}{1 + \gamma} e^{\alpha x},$$

or

$$n(1 + \gamma - \gamma e^{\alpha x}) = n_0 e^{\alpha x} \quad \text{and} \quad n = n_0 \frac{e^{\alpha x}}{1 - \gamma(e^{\alpha x} - 1)}.$$

If the quantities  $n$  and  $n_0$  are multiplied by the electronic charge  $e$  and by the area of electrode used, we at once find

$$\frac{i}{i_0} = \frac{e^{\alpha x}}{1 - \gamma(e^{\alpha x} - 1)}.$$

If now we set  $\gamma = \beta' / (\alpha - \beta')$ , where  $\beta'$  is a constant of appropriate value, we get

$$\frac{i}{i_0} = \frac{(\alpha - \beta') e^{\alpha x}}{\alpha - \beta' e^{\alpha x}}.$$

If  $\beta'$  is small compared to  $\alpha$ ,  $\gamma$  is practically  $\beta' / \alpha$ . This expression may at once be compared to Townsend's equation involving  $\beta$ , which is

$$\frac{i}{i_0} = \frac{(\alpha - \beta) e^{(\alpha - \beta)x}}{\alpha - \beta e^{(\alpha - \beta)x}}.$$

If now one notes that in most studies so far made  $\beta$  is small compared to  $\alpha$  it is clear that within the limits of accuracy of measurement the equation involving  $\gamma$  is indistinguishable from that involving  $\beta$ . We can thus roughly set  $\gamma = \beta'/\alpha = \beta/\alpha$  and consider the second coefficient as a secondary electron liberation due to positive-ion impact on the cathode.

Thus the apparent paradox involving the successful equation yielding a proper value of  $\beta$  and the impossibility of ionization by positive-ion impact is at once clarified. The equation is *approximately correct only since it is closely similar in form to an equation based on a possible mechanism*. Thus the  $\beta$  observed must be translated into a  $\gamma$  by proper algebraic reduction. One must at this point, however, *urge caution in jumping too quickly to conclusions* by anticipating further analysis with the statement that *the mechanism using a  $\gamma$  is only one of three and perhaps more plausible and probably active mechanisms*. These mechanisms lead to equations of types so closely similar that present experimental accuracy is incapable of differentiating between them.

**b. Photoelectric Processes at the Cathode.** In fact, in 1928, R. B. Brode and L. J. Neuman<sup>26</sup> in a seminar paper showed that on certain simplifying assumptions, for cases of electron liberation by photons in the gas or at the cathode or by impacts of metastable atoms in the gas or at the cathode, one could arrive at equations closely similar to the original Townsend equation or else to the equation just deduced. The assumptions made neglected processes by which metastable atoms or photons were removed from the gas without producing ionization and assumed the ion production as strictly proportional to the photons or metastable atoms produced. Inasmuch as none of these derivations is particularly accurate on account of the assumptions, only the derivation of the case for photons at the cathode will be considered at this point.

Let  $n_0$  electrons be liberated per second at the cathode by an outside agent. These electrons, plus the  $\eta z$  electrons liberated at the cathode by the  $z$  photons that are created in the gas by electrons and reach the cathode, constitute the total electron emission at the cathode  $n'_0$ , i.e.,  $n'_0 = n_0 + \eta z$ . Thus  $\eta$  is the fraction of the photons which produce electrons that succeed in leaving the cathode.  $dz$  is the number of photons available to the cathode produced in a distance  $dx$  of the gas in the field direction at a distance  $x$  from the cathode by electron impact. It is given by  $dz = (n'_0 + p)g\theta e^{-\mu x}dx$ . Here  $n'_0$  is the number of electrons leaving the cathode, and  $p$  is the number of new electrons created by collision in the distance from the cathode to  $x$  in the field direction.  $\theta$  is the number of photons produced by an electron in advancing 1 cm in the gas in the field direction. The quantity  $\mu$  is the absorption coefficient of the photons in the gas. These are heterogeneous in wavelength, and  $\mu$  therefore represents an average value. The factor  $g$  is a geometrical factor. It represents the fraction of the photons created in the gas that can reach the cathode. This is necessi-



tated by the fact that photons are emitted in all directions so that only a fraction can reach the cathode. It is clear that  $g$  will be less than one-half. For electrodes whose linear dimensions are small compared to the plate distance it will vary with  $x$ , and its average value will be less than  $\frac{1}{2}$ . For the sake of simplicity one can consider infinite plane parallel electrodes, where  $g$  will be 0.5 at the center, if the external ionizing agent acts uniformly over the cathode.

The generation of electrons by electron impact in the gas according to classical theory allows one to write  $dp = (n'_0 + p)\alpha dx$  in conformity with previous notation,  $\alpha$  being the number of ions created per centimeter path in the field direction by electron impact. If  $p = n'_0$  at  $x = 0$ , integration between 0 and  $x$  yields  $n'_0 + p = n'_0 e^{\alpha x}$ , whence  $p = n'_0(e^{\alpha x} - 1)$ , and  $dz = n'_0 e^{\alpha x} g \theta e^{-\mu x} dx$ . Thus

$$z = \left( \frac{n'_0 \theta}{\alpha} \right) g e^{(\alpha - \mu)x} + c \quad \text{and} \quad c = - \frac{n'_0 \theta g}{\alpha}.$$

Accordingly

$$z = \left( \frac{n'_0 \theta g}{\alpha} \right) [e^{(\alpha - \mu)x} - 1]$$

and

$$n'_0 = n_0 + n'_0 \left( \frac{\alpha \eta \theta g}{\alpha} \right) [e^{(\alpha - \mu)x} - 1],$$

yielding

$$n = \frac{n_0 e^{\alpha x}}{1 - (\theta \eta g / \alpha) (e^{(\alpha - \mu)x} - 1)}.$$

Here  $n$  is the number of electrons reaching  $x$  at a steady state, i.e.,  $n = n'_0 + p$ . The equation for the number  $n$  of electrons set free by the  $n_0$  electrons generated by an external agent at the cathode in a gap of length  $x$  is thus in this case

$$n = \frac{\alpha n_0 e^{\alpha x}}{\alpha - \theta \eta g (e^{(\alpha - \mu)x} - 1)}. \quad (6)$$

Assuming for the present that  $\alpha \gg \mu$ , which is true below 10 cm pressure, this equation has the form  $n = n_0 \alpha e^{\alpha x} / [\alpha - B(e^{\alpha x} - 1)]$ , with  $B = \theta \eta g$ . This is somewhat similar in form to Townsend's for ionization by positive ions in the gas, which reads

$$n = \frac{n_0 \alpha e^{\alpha x}}{\alpha - \beta (e^{\alpha x})},$$

when  $\alpha \gg \beta$ . It is closely similar to the equation for electron liberation at the cathode by positive ions, which reads  $n = n_0 \alpha e^{\alpha x} / (\alpha - \alpha \gamma [e^{\alpha x} - 1])$ .

The results of this analysis then again confirm the indications previously given. These are that, although the particular mechanism first assumed by Townsend was *incorrect*, the equations derived *appeared* to be verified by experiment since they were so similar in form to the equations resulting from other plausible mechanisms that experiment is not able to differentiate between the theories. There does appear to be one circumstance where one could differentiate between Townsend's theory and the last two theories. This will occur under conditions where  $\beta$  becomes comparable with  $\alpha$ , when setting  $\gamma = \beta' / (\alpha - \beta')$  will not bring agreement in form since the quantity  $\alpha - \beta$  in the exponent can differ materially from  $\alpha$  and thus alter  $i/i_0$ . To date there are no data of this sort because of the experimental inaccuracies of the data. Before leaving this question to consider the results and their interpretation one may anticipate by saying that under varying conditions all the factors mentioned leading to equations of the form above *except ionization by positive ions* have separately or in combination been observed to be active, and the second Townsend coefficient, under modern techniques, is proving to be indeed a complex quantity.

#### 5. EXPERIMENTAL DATA ON THE INTERPRETATION OF THE SECOND TOWNSEND COEFFICIENT

With these comments one must now turn to the experimental results and their interpretation, which will of necessity be presented in an historical fashion. Until 1922 the Townsend ideas had been generally accepted, and they universally formed the basis for most research investigations. In that year Holst and Oosterhuis<sup>27</sup> studied sparking potentials in *clean inert gases* using different electrode materials. Under these conditions they observed that, near the minimum, the sparking potential for the same gas varied by a factor of 2 or more, *depending on the electrode material*, the potential being found lower, the lower the work function of the cathode surface. These results have since been amply confirmed by Neuman<sup>34</sup> and by Ehrenkrantz.<sup>4</sup> Since on Townsend's general theory of sparking the value of the sparking potential in the same gas must depend on  $\beta$  (a gas dependent quantity), this meant that in these experiments  $\beta$  *appeared to be a function of the cathode material and not of the gas*.

Now previously practically all observations of sparking potentials at higher pressures had indicated that sparking potential was independent of electrode material, except in the case of oxidized or soiled surfaces and perhaps in the case of Al and Mg which are always covered with an oxide film.<sup>35</sup> This fact had strengthened Townsend in his interpretation of  $\beta$ . Actually we shall later see that the nature of Townsend's theory at atmospheric pressure and longer gaps even did it represent the true mechanism is such as to make the sparking poten-

tial *insensitive* to considerable changes in the value of  $\beta$ , so that the result above cited need not surprise us. In addition the one great difficulty today lies in getting clean reproducible surfaces of differing work function for a study of the influence of work function on sparking potentials and on  $\beta$ , whatever its interpretation. Thus it now appears nearly certain that most earlier studies at higher pressures *were not significant* because of the general incapability of detecting significant changes in  $\beta$  or  $\gamma$  with the relatively soiled surfaces, or in later work, surfaces covered with a monomolecular layer of Hg. Thus Holst and Oosterhuis, being pioneers in the use of clean unmodified electrodes, observed what had not been observed before. Their results, however, left no doubt about the fact that at the pressures and in the gases which they used the secondary mechanism for electron emission was *not a gas-controlled phenomenon*. This meant that  $\beta$  had to be interpreted as *a secondary electron emission from the cathode on positive-ion bombardment or a surface photoelectric effect and not ionization of the gas by positive ions*.

The exact nature of the mechanism giving rise to a  $\beta$  due to cathode action was not clear. Omitting the possibility of a photoelectric action *in the gas*, several explanations were put forward, to wit: (1) It was believed that positive ions might by image forces "pull electrons out of the metals." (2) It was also possible that if one considered the impact of a single positive ion on a surface the "local temperature" was raised to a value where thermionic evaporation was possible. (3) It was suggested by Taylor<sup>28</sup> in about 1927 that the action could be a photoelectric action caused by neutralization of the positive ions and the consequent emission of radiation of ultraviolet frequencies near the cathode. (4) In 1930 Oliphant and Moon<sup>29</sup> studied secondary electron emission on positive-ion bombardment and attempted to interpret their results in terms of the wave mechanics. Whether their particular interpretation is correct or not, the ultimate solution of the problem will come through a wave-mechanical analysis.<sup>64</sup>

Aside from the earlier studies on secondary electron liberation due to positive-ion bombardment, the problem has been carefully investigated by Penning,<sup>30</sup> Oliphant,<sup>29</sup> and Oliphant and Moon. From these studies and those of Jackson<sup>31</sup> and Schneider<sup>32</sup> it is clear that: (1) all positive ions of over 50 to 100 volts energy can liberate secondary electrons from a surface, the yield *increasing with the gas content of the surface* (depending on gases and surface metals) *and especially with the energy of the bombarding positive ions*. Thus the emission under these conditions must increase with increasing  $X/p$ . The researches also show that (2) if the work function of the surface is *less* than the ionization potential of the atoms there will be secondary electron emission at energies of the order of 10 volts or lower.<sup>29, 30</sup> It is not known, however, at exactly how low an energy this occurs, nor what the efficiencies under these conditions may be. Part of the difficulties lie in the vari-

abilities of the surfaces at present used. The future will probably yield both techniques and surfaces suitable for this study, and these questions can be answered. In addition to secondary electron liberation by positive-ion bombardment there still remains the possibility of photoelectric liberation at the cathode by photons from the body of the gas. This has not been directly observed or studied, but the studies of Cravath and Dechène<sup>32</sup> as well as of Kenty<sup>33</sup> and of Greiner<sup>34</sup> make this mechanism possible and likely. Hence there is no doubt but that, by at least two general known processes, secondary electron liberation at cathodes can take place. It is accordingly safe to conclude that in conformity with the results of Holst and Oosterhuis *there is a process which depends on the cathode*. Accordingly, Townsend's  $\beta$  must be interpreted in terms of a new constant,  $\gamma$ , or  $\eta\theta g$ , signifying electron liberation by positive-ion bombardment or photoelectric liberation at the cathode either in Taylor's sense or in the sense of the theory here given.

In considering the significance of their research, Holst and Oosterhuis for the first time clearly pointed out also that for ionization by positive-ion impact the values of  $X/p$  at which Townsend's  $\beta$  appeared were impossibly low if positive ions had to gain some tens of volts energy between impacts in order to ionize. If we apply Townsend's original theory for ionization by negative-ion impact, which is more applicable to the case of positive ions<sup>65</sup> if we neglect the probability of ionization  $P_i$  at  $E_i$ , the values of  $\beta/p$  as a function of  $X/p$  are given by

$$\frac{\beta}{p} = \frac{1}{760\lambda_0} e^{-\frac{E_i}{(X/p)760\lambda_0}}.$$

For  $N_2$  at  $X/p = 100$ , i.e., well above sparking potentials at 760 mm,  $X = 76,000$  volts/cm = 253 esu/cm,  $p = 760$ ,  $\lambda_0 \sim 10^{-5}$  cm,  $E_i = 1.5 \times 14$  volts =  $21 \times 1.59 \times 10^{-12} = 3.35 \times 10^{-11}$  erg,  $e = 4.8 \times 10^{-10}$ . Hence  $\beta/p = 130e^{-27.6}$ . The observed value of  $\beta/p$  in  $N_2$  near sparking according to Posin is  $1.6 \times 10^{-5}$ , which is far greater than the theoretical figure above. It is also clear that, if, as the results of Beeck,<sup>13,16</sup> Sutton,<sup>15</sup> Varney,<sup>18</sup> and others show,  $E_i$  for positive ions in molecular gases is  $\sim 300$  volts instead of 20, the positive ions just cannot ionize.

This circumstance caused Loeb<sup>35</sup> and Rogowski<sup>36</sup> independently to attempt to salvage the theory of sparking by altering it to include space-charge distortions as a result of electron ionization in order to give values of  $X$  at sparking great enough to cause ionization by positive ions. As will later be seen, the surmise as to the importance of space charges in the case of some spark propagation ultimately proved to be nearly correct, *not*, however, via ionization by positive ions, but in an exceedingly complicated and interesting fashion.<sup>66</sup> As will presently

be seen, space charges under some conditions do arise to distort the  $\log i/i_0$  curves simulating a  $\beta$ . They also occur in many discharge phenomena. However, the distortions *are never great enough to cause an ionization by positive ions, as will be seen*. The reason for this lies in the fact that, as fields of this nature increase, other secondary processes more effective than Townsend's ionization by positive ions become active.

Despite the overwhelming accumulation of information against ionization by positive ions in a gas, Townsend and his group have never been ready to concede the error in the interpretation of the second coefficient  $\beta$ .<sup>63</sup> In 1933 Townsend and Jones<sup>57</sup> actually carried on a series of measurements in which they attempted to prove the existence of ionization by positive ions. The method of investigation was not a clean cut or direct one. Evidence for the *multiplication* of ions in a complicated system of fields was definite, but the interpretation as to its origin was far from clear and the effects observed could easily have been due to secondary processes such as primarily photoelectric ionization in the gas, possibly photoelectric emission from the walls, and secondary emission from the walls on positive ion impact. In any case, no direct studies such as those of Beeck, Sutton, and Varney were made by the Townsend group.

In addition, one circumstance cited by Townsend influenced the author for years in favor of the positive-ion mechanism. This was the difficulty in explaining the ionization in the case of the positive point to plane corona and the positive wire corona at high pressures as well as in long sparks where the cathode mechanism could not play any role. Actually there was no real difficulty if one considered the possibility of *photoionization in gases*, for this is a mechanism that would be just as effective as ionization by positive ions in accounting for such occurrences, as will later be seen. At the time, however, not so much was known concerning photoionization in ordinary gases as is known today, and the experiments of Cravath and Dechène<sup>32</sup> on corona, Gorrill<sup>33</sup> and Raether<sup>57</sup> with cloud chamber, and Greiner<sup>39</sup> on Geiger counters showing such ionization had not yet been done. This eliminates the need of invoking ionization by positive ions to explain coronas and long sparks.

With the removal of that argument for the *necessity* of ionization by positive ions there remains no phenomenon for which ionization by positive ions in the gas is *the only or necessary process*. Hence, since, in addition to the above, all direct experimental evidence makes ionization by positive ions in gases physically impossible at the values of  $X/p$  under which discharges occur, there *remains no alternative but to rule out this mechanism once and for all in all ordinary discharge processes now known*. This means that when hereafter in this book the second Townsend coefficient is referred to by its initial symbol  $\beta$  it is clearly to be understood that the symbol *represents only the second*

coefficient  $\beta$  determined by experiment from an equation of the general form

$$i = i_0 \frac{(\alpha - \beta)e^{(\alpha - \beta)x}}{\alpha - \beta e^{(\alpha - \beta)x}},$$

or, where  $\alpha \gg \beta$ , of the form

$$i = i_0 \frac{\alpha e^{\alpha x}}{\alpha - \beta e^{\alpha x}}.$$

It signifies nothing as to the nature of the secondary process assumed *except that it cannot include ionization by positive-ion impact in a gas*. The reason for the retention of the symbol is that it is associated with the equation and since a general symbol is needed it should be retained for sentimental reasons. Where, however, one of the allowed processes is specifically referred to or represented analytically in a study of a discharge problem, it should be designated by an appropriate and different symbol. Thus referring to the secondary liberation of electrons by positive ions at a surface we will use  $\gamma$ , and for photoelectric liberation from the cathode by photons created in the gas we will use  $\eta\theta g$ , and so on. Accordingly, hereafter  $\beta$  will refer to any one of the *allowed* secondary processes while  $\gamma$ ,  $\eta\theta g$ , etc., will refer to specific secondary processes.

Having now clarified the situation as regards the equations used for analysis and their interpretation, one may proceed to consider the evaluations made of the second Townsend coefficient  $\beta$ . In discussing this material we must say several things. First, values of  $\beta$  have been determined for practically all gases for which  $\alpha$  has been determined, beginning with Townsend's early studies. Hence references to early measurements of  $\beta$  can be found in the literature for the evaluation of  $\alpha$  under Chapter VIII. Secondly, these values of  $\beta$  were determined under conditions of cleanliness of the metal and of gaseous purity which today we know to be such as to make their interpretation difficult if not meaningless. They were merely values of  $\beta$  of an orienting magnitude observed with a cathode composed of a given metal whose state was completely uncontrolled. Even today, when we have some control of the purity of the gas, using outgassed vessels and relatively clean metal surfaces we *cannot* reproducibly control the surfaces. Avoidance in studies of  $\alpha$  and  $\beta$  of contaminants such as stopcock greases, porous metal surfaces, amberoid, ebonite, and mercury vapor in outgassed sealed-off vessels which did not leak really began only with the work of Penning and his associates around 1934 in Europe and in 1936 in the work at California. Since, except for the orienting nature of their values, the early studies can contribute little or nothing to an understanding of the processes underlying  $\beta$  and probably are not sufficiently reproducible to apply to later analyses, it does not pay to list tables of values or to discuss the work in detail. In one or two

instances examples of the types of results obtained by later studies antedating Penning will be given for purposes of comparison. Otherwise the later results only will be given or discussed. It may be added, however, that as time went on techniques in general improved so that the values gained more significance. But, since the most vital step in the elimination of Hg vapor was not accomplished until later, the improvements were not such as to be worth noting.

#### 6. FALSIFICATION OF DATA ON SECOND TOWNSEND COEFFICIENT BY SPACE CHARGE

We may begin the discussion with some experiments by Posin conducted under somewhat unsatisfactory conditions as regards Hg contamination, because of a new element in the interpretation of upcurving  $\log i/i_0 - x$  curves which they introduced, an element which must be avoided in further researches.

Sanders in his papers on the first Townsend coefficient in air had observed that, with a large  $x$  and his relatively strong source of ultraviolet illumination giving  $i_0$ , the curved portions of the  $\log i/i_0 - x$  curves did not yield consistent values of  $\beta$ . That is, the values of  $\beta$  from different parts of the same  $\log i/i_0 - x$  curve were *in no sense*

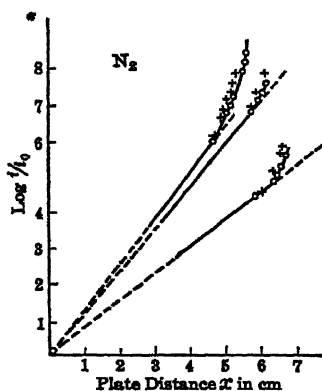


FIG. 186.

*constant*. M. Paavola<sup>40</sup> had also observed values of  $\beta$  at *very low* values of  $X/p$  (of the order of 30) which *decreased* as  $p$  decreased. This circumstance was investigated by Posin<sup>5</sup> in  $N_2$ . Posin found that unless  $i_0$  was kept at such a magnitude that the current density  $j_0$  ( $i_0/A$ , where  $A$  is the area illuminated) was less than about  $10^{-13}$  amp/cm<sup>2</sup> it was impossible to evaluate a constant  $\beta/p$  or  $\gamma$  at a given  $X/p$  from one  $\log i/i_0 - x$  curve; see the crosses of Fig. 186 compared to the circles. A theoretical study by Varney, White, Loeb, and Posin,<sup>41</sup> in which the equations for ion production and space-charge distribution were set up and integrated, showed that, above

certain values of  $j_0$ ,  $x$ , and below certain values of  $X/p$  space-charge distortions due to positive ions at the cathode, caused an apparent increase in  $\beta$ . Since the limitations can apply quite generally, it becomes worth while to give the solution of the problem so that it can be applied where needed.

Two parallel-plate electrodes enclosed in a tube are separated a distance  $d$  and are raised, respectively, to potentials 0 and  $V_a$ . The cathode is illuminated with ultraviolet light which liberates photo-

electrically a current of electrons  $i_0$ . The  $i_0$  electrons proceed through the gas toward the anode, producing by ionization further electrons and their associated positive ions. At any point in the gas a distance  $x$  from the cathode, the electron current is given by  $i_- = i_0 e^{\alpha x}$ , where  $\alpha$  is the electron ionization coefficient. The current reaching the anode is thus  $i_- = i_0 e^{\alpha d}$ . From the condition of continuity, that the total current crossing any plane parallel to the electrodes must be a constant, we get at once that  $i = i_+ + i_-$ . There are no positive ions crossing the plane of the anode, so the total current is just  $i = i_- = i_0 e^{\alpha d}$ . Substituting in  $i = i_+ + i_-$ , we have  $i_0 e^{\alpha d} = i_+ + i_0 e^{\alpha x}$ , giving  $i_+ = f(x)$

$$i_+ = i_0(e^{\alpha d} - e^{\alpha x}).$$

To determine the effect of space charge we must solve Poisson's equation for this case:  $\nabla^2 V = -4\pi\rho$ . Since the current flow is unidimensional and consists of both positive and negative charges this reduces to:  $d^2V/dx^2 = -4\pi(\rho_+ - \rho_-)$ . By using the equations  $j = \rho v$ ,  $v = kX$  ( $v$  = velocity,  $k$  = mobility), and  $X = -dV/dx$ , and inserting the values of  $i_-$  and  $i_+$ , we get

$$\frac{d(dV/dx)}{dx} = -\frac{4\pi j_0}{dV/dx} \left( \frac{e^{\alpha d} - e^{\alpha x}}{k_+} - \frac{e^{\alpha x}}{k_-} \right),$$

where  $j_0$  is the electron current density at the cathode and is used instead of  $i_0$  because Poisson's equation is expressed in terms of charge density.

Since  $k_+$  is only  $10^{-4}$  of  $k_-$ ,  $1/k_-$  may be neglected with respect to  $1/k_+$ , giving

$$\frac{dV}{dx} \cdot \frac{d(dV/dx)}{dx} = -\frac{4\pi j_0}{k_+} (e^{\alpha d} - e^{\alpha x})$$

or

$$\frac{XdX}{dx} = -\left(\frac{4\pi j_0}{k_+}\right) (e^{\alpha d} - e^{\alpha x}).$$

Now  $\alpha/p$  is a function of  $X/p$ , or, at constant pressure,  $\alpha = f(X)$ . In the derivation of the equation  $i_- = i_0 e^{\alpha x}$  it was assumed that  $X$  was uniform throughout the electrode gap, which is not the case if the field is distorted by space charge. We cannot, therefore, write  $i = i_0 e^{\alpha d}$  because  $\alpha$  is not a constant throughout  $d$ . We must write, instead of  $e^{\alpha x}$ ,  $\exp\left(\int_0^x \alpha dx\right)$ , and in place of  $e^{\alpha d}$ ,  $\exp\left(\int_0^d \alpha dx\right)$ . The equation to be solved then becomes

$$\frac{XdX}{dx} = -\left(\frac{4\pi j_0}{k_+}\right) \left( \exp\left(\int_0^d \alpha dx\right) - \exp\left(\int_0^x \alpha dx\right) \right).$$



Make two substitutions:

Let  $\int_0^x \alpha dx = u$ , then  $du/dx = \alpha$ . Replace  $j_0 \exp\left(\int_0^x \alpha dx\right)$  by its equivalent,  $j$ . Then

$$XdX = \left(\frac{4\pi}{k_+}\right)(j_0 e^u - j)dx = \left(\frac{4\pi}{k_+}\right)(j_0 e^u - j) \frac{du}{\alpha},$$

or

$$\alpha X dX = \left(\frac{4\pi}{k_+}\right)(j_0 e^u - j)du.$$

Note that, while  $j$  is dependent on  $u$  and  $X$ , in any particular experiment in which  $d$  and  $X$  are not changed,  $j$  will be a constant for it is not a function of  $x$ .

We thus get

$$\int_{x_0}^x \alpha X dX = \left(\frac{4\pi}{k_+}\right) \int_0^u (j_0 e^u - j) du.$$

In the range of values of  $X/p$  from 40 to 180 for  $N_2$  gas, where the relation of  $\alpha/p$  to  $X/p$  is parabolic, it is sufficient to make the following approximation over a small region:

$$\frac{\alpha}{p} = A' \left(\frac{X}{p}\right)^2 \quad \text{or} \quad \alpha = AX^2.$$

Inserting this value of  $\alpha$ ,

$$\int_{x_0}^x \alpha X dX = A \int_{x_0}^x X^3 dX;$$

Therefore

$$\left(\frac{A}{4}\right)(X^4 - X_0^4) = \left(\frac{4\pi}{k_+}\right)(j_0 e^u - ju - j_0).$$

We thus have an expression for  $X$  as a function of  $u$

$$X^4 = \left(\frac{16\pi}{Ak_+}\right)(j_0 e^u - ju - j_0) + X_0^4,$$

in terms of two *unknown* constants,  $j$  and  $X_0$ . We have two equations for determining them:

$$\frac{du}{dx} = \alpha = AX^2;$$

Therefore

$$\int_0^{\log(u/j_0)} \frac{du}{AX^2} = \int_0^d dx \quad (1)$$

and  $X = -dV/dx$ ; therefore

$$\int_0^d X dx = - \int_0^{V_d} dV, \quad (2)$$

and since  $dx = du/AX^2$  we have

$$\int_0^{\log(j/j_0)} \frac{du}{AX} = V_d = X_A d,$$

where  $X_A$  is the applied field. By inserting the value of  $X$  above,

$$\int_0^{\log(j/j_0)} \frac{du}{[(16\pi/Ak_+)(j_0 e^u - ju - j_0) + X_0^2]^{3/2}} = Ad,$$

$$\int_0^{\log(j/j_0)} \frac{du}{[(16\pi/Ak_+)(j_0 e^u - ju - j_0) + X_0^2]^{1/2}} = AX_A d.$$

These two equations must be solved in the following manner:

Given a value of  $j_0$ , the applied field  $X_A$ , and  $d$ ; find the corresponding values of  $j$  (or  $j/j_0$ ) and  $X_0$ . We want  $j$  as a function of  $d$ . Since the quadrature cannot be performed directly, the method of solution is one of trial and error, using numerical integration on a tried value of  $X_0$  and  $j$  and seeing whether  $X_A$  and  $d$  are obtained correctly.

Note that in these equations it is the current density and not the total current which enters. Thus a current of  $10^{-12}$  amp may leave the cathode, but if this current only comes from  $1 \text{ mm}^2$  of surface, the current density will be  $10^{-10}$  amp/cm<sup>2</sup>.

A sample calculation was made on the following assumptions:  $j_0 = 1.75 \times 10^{-11}$  amp;  $X_A = 120$  volts/cm;  $p = 1$  mm. The value of  $\alpha$  for the undistorted field was 1.00. Plotting  $\log(j/j_0)$  against  $d$  showed that, at  $d = 7.96$  cm,  $\log(j/j_0) = 8$ , and at  $d = 8.6$  cm, the slope of the  $\log(j/j_0)$  vs.  $d$  curve became infinite (a suitable condition for a spark).

As mentioned above, the increase of  $\alpha$  as the field is distorted depends on the functional relation of  $\alpha/p$  to  $X/p$ . If the function  $\alpha/p$  increases faster than  $X/p$ , ( $\alpha/p = f(X/p)$ ), then it can be shown in a simple way that  $\log(j/j_0)$  will increase above its value when the field is undistorted. Similarly, when  $\alpha/p$  increases more slowly than  $X/p$ , the space charge can no longer give an apparent large value of  $\alpha$  but must give a smaller value. This may be shown as follows (taking  $\alpha = AX^2$  first):

We had two equations to satisfy,

$$\int_0^d \alpha dx = A \int_0^d X^2 dx = \int_0^{\log(j/j_0)} du = \log \frac{j}{j_0}, \quad (3)$$

$$\int_0^d X dx = X_A d. \quad (4)$$

If there is a uniform field  $X_A$ ,  $\log(j/j_0) = \alpha_0 d$ ,  $\alpha_0$  being a constant. We must show whether the value of  $\log(j/j_0)$  obtained from the first integral is greater or less than  $\alpha_0 d$  under the condition imposed by the second integral.

Shift the  $X$  axis to  $X_A$ ; then  $\int_0^d X dx = \int_0^d (X' + X_A) dx$ , which by (2)  $= X_A d$ .

Now  $\int_0^d X_A dx = X_A d$ . Therefore  $\int_0^d X' dx = 0$ . There is thus as much area above  $X_A$  as beneath  $X_A$ ; i.e.,  $X'$  is part negative and part positive.  $\int_0^d X^2 dx$  becomes  $\int_0^d (X' + X_A)^2 dx = \int_0^d X'^2 dx + 2X_A \int_0^d X' dx + \int_0^d X_A^2 dx$ . Noting that  $\int_0^d X' dx = 0$ ,

$$A \int_0^d X^2 dx = A \int_0^d X'^2 dx + A X_A^2 d = A \int_0^d X'^2 dx + \alpha_0 d.$$

Since  $X'^2 > 0$  this shows that  $\log(j/j_0)$  will be greater than  $\alpha_0 d$ .

If  $\alpha$  should equal  $AX$ , it is obvious that  $\log(j/j_0)$  will be unchanged by space charge. If  $\alpha = AX^n$  and  $n > 1$ ,  $\log(j/j_0)$  will increase; if  $n < 1$ ,  $\log(j/j_0)$  will decrease. Since  $\alpha/p = f(X/p)$  corresponds to  $n > 1$  for  $X/p$  up to 180 in  $N_2$  and 130 in air and corresponds to  $n < 1$  above 180 and 130, respectively, space charge can explain an apparent increase in  $\alpha$  above  $\alpha_0$  only on the lower side.

The solution indicates the following facts:

Depending on the number of molecules present in a given spark gap, with sufficient illumination, a value of  $X/p$  great enough to cause ionization by collision will give rise to space-charge formation of such magnitude as materially to distort the curves of  $\log(i/i_0)$  plotted against  $d$ , and in such fashion that they resemble the curves of  $\beta$  or  $\gamma$  observed at low  $p$  by Townsend. Furthermore, this apparent space-charge distortion can lead to an ultimate breakdown of the gap without the intervention of a  $\beta$ , provided that the field distortion does not become so high as to bring  $\alpha/p$  into the third region of variation with  $X/p$ . It is probable that in the first region of variation of  $\alpha/p$  with  $X/p$ , i.e., when  $\alpha/p = Ae^{Bx/p}$ , which occurs for  $X/p$  around 40, space charges can be built up for values of  $j_0$  of an extremely low order. Hence there exists under these conditions, with sufficient gap length, an exceedingly unstable condition. With such instability it becomes practically impossible to study experimentally the curvature of the  $\log(i/i_0)$  vs.  $d$  curves before spark breakdown occurs in view of the fluctuations of the high-potential source and the extreme sensitivity to variations in  $X/p$ .<sup>23</sup>

In the lower-pressure regime, at high  $X/p$ , in which the experimental work initiating this investigation was performed and where  $\alpha/p$  varies as  $(X/p)^2$ , the equation has been completely solved. In this region measurable upward curving of  $\log(i/i_0)$  vs.  $d$  curves will occur at  $X/p = 120$  in  $N_2$  for a current density  $j_0$  of  $2 \times 10^{-11}$  amp/cm<sup>2</sup> and a plate distance of 7.5 cm, and the spark will appear at 8.1 cm. The values obtained in Posin's experiment fit these criteria. Using an estimated density of  $10^{-16}$  amp/cm<sup>2</sup>, Posin observed a true and constant  $\beta$  with no sign of space-charge distortion. With a current density estimated at about  $10^{-12}$  amp/cm<sup>2</sup> at  $X/p = 120$ , Posin observed an  $\alpha$  showing signs of space-charge distortion, i.e.,  $\beta$  was not constant. Because of the non-homogeneous nature of the focused image of the quartz mercury arc it is impossible to evaluate  $j_0$  accurately. These estimates are therefore only approximate, and to this degree of approximation appear to fit the equation. This indicates that extreme care must be exercised in this region in interpreting the experimental results obtained, and a very careful study of the conditions, using a photoelectric emission of controlled and uniform nature, is definitely required. The results of Posin indicate quite clearly that in this pressure region apparently both a real  $\beta$  or  $\gamma$  and a space-charge-distorted  $\alpha$  may occur simultaneously. Hence in this region the sparking mechanism may be exceedingly complex.<sup>62</sup> In this region, however, because of the slower variation of  $\alpha/p$  with  $X/p$ , it becomes possible experimentally to observe in more detail the deviation of the  $\log(i/i_0)$  vs.  $d$  curve from a straight line. Even here, however, when space-charge effects occur, the curvature is so sharp that a spark occurs very shortly after the initiation of the departure from linearity. When a true  $\beta$  occurs in this region one can follow the curvature over a far greater length of curve before the spark breaks. In this region of  $p$  and  $X/p$  it is doubtful whether a spark could be initiated due to space charge with inadequate illumination, and it is probable that, because of the importance of the  $\beta$  with lower illumination, both values of  $\beta$  and sparking potential will be dependent on electrode material.

In the third regime, which with few exceptions is the regime in which Townsend worked, we can expect no space-charge effects and the existence of a true  $\beta$  or  $\gamma$ . This is due to the fact that  $\alpha/p$  varies linearly with, or even more slowly than,  $X/p$ .

The theory makes it possible to calculate the amount of space-charge distortion produced at the cathode by the primary electron process for the sparking value of the current density. This is surprisingly low at higher pressures, being but 14 per cent in the case above while at  $X/p = 120$  the value of the field is 50 per cent above that for a linear fall of potential taken as  $V_0/\delta$ . This is interesting in that such distortion at the maximum point will not change  $X/p$  by a sufficient amount so as to change the form of the function  $\alpha/p = f(X/p)$  from one where  $f(X/p) = (X/p)^n$  with  $n > 1$  to one where  $n < 1$ .

From this material it is clearly seen that, even in the absence of secondary processes, space-charge formation can, under appropriate circumstances, give a *fictitious and inconstant*  $\beta$ . Care must be used then in interpreting the curvature of the  $\log i/i_0 - x$  graphs obtained. It does not seem to have been active except in the work of Paavola,<sup>40</sup> Sanders,<sup>1</sup> Posin,<sup>5</sup> and at higher currents in that of Kruithoff and Penning.<sup>42</sup>

## 7. STUDIES OF $\beta$ ON MERCURY-FREE SURFACES

When Posin<sup>5</sup> undertook this study it was his hope to vary the work function of his cathode and thus to see whether  $\beta$  could be proved to be purely a function of cathode material. Unfortunately the mercury seal in his apparatus had insured his cathode being essentially an Hg instead of a brass surface, so that it was deemed hopeless to use the large Sander's-Posin chamber for such a study. Subsequently Bowls<sup>2</sup> and later Hale<sup>7</sup> studied pure  $N_2$  and pure  $H_2$  in a chamber practically devoid of Hg. It was their intention to use a Pt surface on the cathode and then by distilling Na into the chamber to work with a Na surface: for Neuman<sup>34</sup> had shown that in some three to ten minutes in A gas the Na in a tube will condense on the electrodes to a sufficient extent to form an effective Na cathode with characteristic sparking potential. It was also considered safe to use Na since the critical tables assign to Na a vapor pressure of the order of  $10^{-10}$  mm. Actually the choice was most unfortunate, since Na in the presence of  $N_2$  and  $H_2$  appears to form some volatile compound whose vapor pressure is such as not only seriously to alter the nature of the gas but even to influence the values of  $\alpha/p$  as seen in Chapter VIII.

Bowls' results, however, were quite striking. He evaluated a  $\beta$  for each curve as follows: Five to eight values of  $\beta$  were computed from the equation

$$i = i_0 \frac{(\alpha - \beta)e^{(\alpha - \beta)x}}{\alpha - \beta e^{(\alpha - \beta)x}}.$$

The values of the average  $\beta$  which gave the best fit to the observed  $\log i/i_0 - x$  curves were used. The curves for  $\beta/p$  plotted as a function of  $X/p$  observed by Bowls for Pt and for Na cathodes are shown in Fig. 187. The dotted curve represents the values of Townsend<sup>18</sup> and also fairly closely the values of Posin in what was known to be Hg-contaminated  $N_2$  for Posin and can safely be assumed to be Hg-contaminated  $N_2$  for Townsend. The triangles represent Bowls' values of  $\beta$  when he deliberately soiled his  $N_2$  with Hg. The difference between the  $\beta/p = f(X/p)$  curves with and without Hg is striking. Bowls also found that it took very little Hg to contaminate the cathode, and once it was contaminated it could not be cleaned by baking 48 hours at  $400^\circ C$ . Only complete dismantling and chemical cleaning thereafter served successfully to free the chamber of Hg.

The results show beyond a shadow of a doubt that the *previous standard values of  $\beta/p$  in  $N_2$  at least* were due to a uniformly Hg-contaminated cathode. The comparison of Bowls' results of  $\alpha/p$  with those of the other workers quite confirms this conclusion. Since for all cases where  $\alpha/p$  and  $\beta/p$  were measured in gases such that, in filling, the apparatus was exhausted with a mercury gauge in contact with the system *without constant use of liquid air* between system and gauge, *we can be certain that there was Hg contamination.* Hence in these cases  $\beta/p$  was evaluated in each instance with an Hg surface and a gas soiled by Hg. The general agreement of the  $\beta$  values, despite the use of different cathode materials, bears this out.

The character of Bowls' curves, furthermore, indicates a definite change in behavior of  $\beta/p$  with cathode surface and gas content from that usually seen. The nature of this change indicated the possibility of more than one process at work, of which at least one was cathode surface dependent. Hence it was desirable to calculate the value of the coefficient for secondary emission from the cathode by positive bombardment or photoelectric effect from  $\beta/p$ . A study of the equations on pages 378 and 381 shows that, with a sufficient degree of approximation consistent with the accuracy of the data, we may set  $\gamma = \beta/\alpha = \theta(\eta/\alpha)g$ . Plotting  $\beta/\alpha$  against  $X/p$ , the curves of Fig. 188 were obtained for the three cases studied. Such striking results had not previously been observed in any gas. There were, however, values of Kruithoff and Penning<sup>40,43</sup> for pure A and for Ne with Cu surfaces that indicated a possible rise in  $\gamma$  at lower  $X/p$ . But in these gases it was impossible to measure  $\gamma$  much below  $X/p = 16$  in A and  $X/p = 2$  or 3 in Ne as a result of the rapid increase in  $\alpha$  at low  $X/p$ . The curves of  $\gamma$  in Ne and in Ne with A contamination are shown in Fig. 189. The curves of  $\gamma$  in pure A are not given. They were evaluated in a series of different runs with the Cu surface in different conditions having a  $\gamma$  varying widely between them. When plotted they all show an eventual rise at low  $X/p$ , in one case very pronounced, in the others less so.

The interpretation of Bowls' results can be only tentative at this time. It is clear, however, that at least two processes are active and

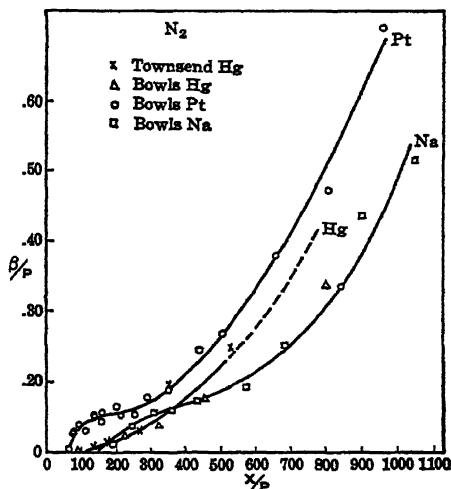


FIG. 187.

that they are in part cathode phenomena. The purity of the  $N_2$  devoid of Hg had lowered the values of  $\alpha/p$  at the lower values of  $p$  by material amounts below those observed in older measurements. This indicated that the Hg was being ionized either directly by electron impact or through photons emitted by electron impact in  $N_2$ . If the latter occurred

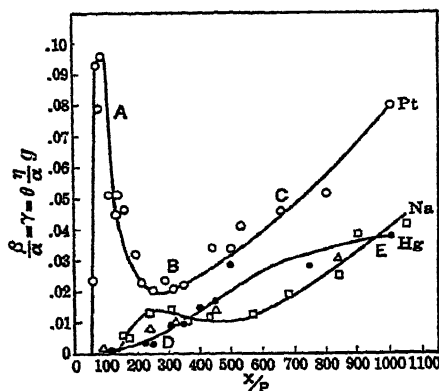


FIG. 188.

a function of electron energy, or better  $X/p$ . Unfortunately, the only data of value in these calculations come from the Townsend-group measurements of electron energy which have been discussed in Chapter IV. The general type of functions obtained easily explain the fall of the photoelectric emission at higher  $X/p$ . They do not account for the fall of Bowls' peak at the still lower values of  $X/p$  and in fact predict that it should continue high. It must be remembered, however, that we are here dealing not only with a photoelectric characteristic of the metal surface with a definite threshold but also with an excitation function of the gas with an electronic energy distribution varying with  $X/p$ . Again, most of the light emission comes largely from the anode region subject to strong absorption in various unknown spectral regions. The interaction of all these variables could adequately account for the peak in the  $\gamma$  or  $\eta\theta g$  curve for low  $X/p$ , although its sharpness and magnitude are surprising.

The destructive action of Hg vapor confirms this, as does the action of the Na. Surprisingly enough, with the high photoelectric sensitivity

to any appreciable extent it can explain the absence of the sharp peak at low  $X/p$  with Hg, for the Hg vapor was then destroying photons that normally liberate photoelectrons from the Pt cathode in the absence of Hg. This circumstance and the low value of  $X/p$  at which the peak occurs in  $N_2$  indicates rather definitely that the process is due to a photoelectric effect. In fact, in a recent article Penning<sup>48</sup> has tried to evaluate the photon and ion production in various gases, including  $H_2$  and  $N_2$ , as

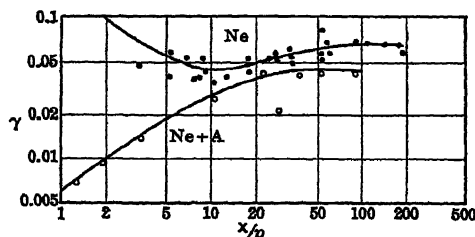


FIG. 189.

of Na one would *expect measurable values* of  $\gamma$  at far lower values of  $X/p$  and possibly of even greater amplitudes than those for Pt. The real photosensitivity of the surface is attested by the fact that, whereas the Hg arc was required to give an adequate  $i_0$  in  $N_2$  with Pt, the light of a Mazda lamp of low candlepower stopped way down sufficed for the Na surface.\* The fact is, however, that with the Na the highly ionizable vapor caused an *even greater increase in  $\alpha/p$*  than it did when Hg was present. This apparently converted most of the photons to ions (increasing  $\alpha$ ) and *did not permit the longer wavelengths* to reach the Na surface. The *shorter-wavelength* photons, however, were apparently *not absorbed* by the vapor, so that a small peak appears at the higher values of  $X/p$ . Beyond the decline of the photoelectric peaks in both curves there is a general increase in  $\gamma$  not seriously different from that with Hg which appears at an  $X/p$  of about 200 to 300. This can without much difficulty be ascribed to a liberation of electrons on positive-ion bombardment. At this value of  $X/p$  the positive ions on the average strike the cathode with an energy of the order of 2 to 4 volts.

Nothing is known about the value of  $X/p$  at which secondary emission begins. Penning<sup>30</sup> as well as Oliphant and Moon<sup>29</sup> have observed values of  $\gamma$  which amount to as much as 0.2 for positive ions of ionizing potential well above the work function of the metal at the lowest kinetic energies which they could achieve. Penning found that for ions of 500 volts energy  $\gamma$  was high for positive ions of the inert gases but fell to less than one-third of the value when much Hg was present. The Hg ions, because of the low  $E_i$ , are less efficient at the cathode even at the high values of energy used. Hence Hg apparently can lower  $\gamma$ , for being more readily ionized than He it can furnish ions of low energy which are not good secondary emitters. In  $N_2$  gas it is hard to predict what will happen on secondary emission. The Hg appears to have been more efficient on the Hg surfaces than Na on the NaH surface.

In  $H_2$  with Pt cathode and with Na and an NaH cathode, Hale's results are more fantastic but clearer than Bowls'. The Na in the chamber obviously introduces the same sort of volatile easily ionized impurity as it does in  $N_2$ . At *low  $X/p$*  and high  $p$ , Hale's values for  $\alpha$  without Na or Hg are not vastly different from Ayers' with Hg contamination, as was the case with Bowls' and Posins' values for  $\alpha$ . At higher  $X/p$  and lower  $p$  the values of  $\alpha/p$  in pure  $H_2$  were as much as 50 per cent *lower than Ayers'* values, as is to be expected. The curves of Hale for  $\beta/p$ ,  $\beta/\alpha$ , and  $\gamma$  calculated directly are shown in Figs. 190 A, B, and C, respectively.

\* The surface of the metal was supposedly Na. Actually, in Bowls' experiments some NaH or other substance appears to have been present, as judged from the low photoelectric threshold. According to Hale, Na in pure  $H_2$  was not photosensitive nor was its emissive power constant in time. He therefore deliberately made his cathode one of NaH by discharge in  $H_2$ .



The values of  $\alpha$  in pure  $H_2$  begin around an  $X/p = 10$ , and detectable values of  $\beta$  or  $\gamma$  appear at about 32.3. *There appears to be a peak of considerable amplitude at  $X/p = 140$ .* The peak falls to a minimum at about  $X/p = 200$ , to rise slowly again to  $X/p \sim 600$ . Thereafter  $\gamma$  rises more sharply and continuously to about 0.12 at an  $X/p$  of 900. In this respect it resembles  $N_2$  except that the peak appears at a higher  $X/p$ . When NaH was used on the cathode the whole picture changed. Appreciable values of  $\alpha$  were detectable at an  $X/p = 5.85$ , i.e.,  $\alpha = 0.318$ ,  $\alpha'/p = 0.155$ , and  $\beta = 0.072$ ,  $\beta/p = 0.0353$  with  $\gamma = 0.040$ .  $\gamma$  rose to a peak at  $X/p = 8.65$  of the extraordinarily high value of 0.1137. Thereafter it fell to relatively low values, showing several peaks rising as high as 0.025 but no higher at an  $X/p$  of 50, 450, and

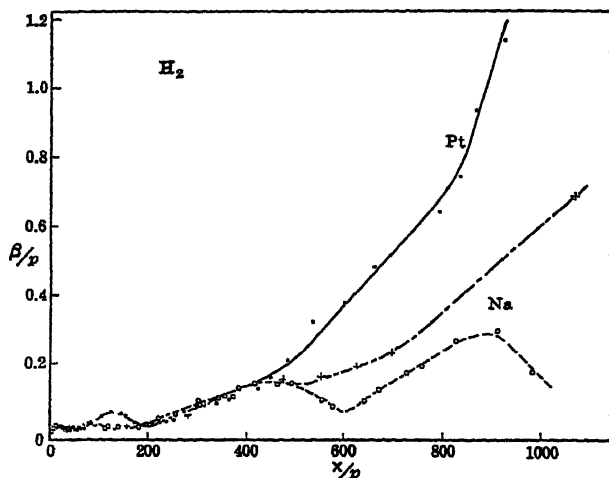


FIG. 190A.

850. It shows no general rise with increasing  $X/p$ . With a surface of Na with some NaH, the dashed curve was observed. It departed from the NaH curve in showing a gradual rise above an  $X/p$  of 600. The action on the NaH surface appears to be largely photoelectric, for high values of  $\gamma$  at low  $X/p$  signify a considerable production of secondary electrons *at the cathode per primary positive ion*, which is just what one would expect of photons as these are efficiently produced at low values of  $X/p$  before many ions are produced and  $\eta\theta g$  may not be proportional to  $\alpha$  at all. In this case the NaH surface appears to act in its proper role of being exceedingly photosensitive to radiations in  $H_2$ , especially at lower  $X/p$ . It should also be noted that with NaH the dip at an  $X/p \sim 200$  corresponds to a peak in the curve for  $\alpha/p$  on page 355, and the peak at  $X/p = 450$  corresponds to the dip in the  $\alpha/p$  curve indicating the absorption of photons to ionization at an  $X/p \sim 200$  and a

transmission of photons at an  $X/p = 450$ . NaH, however, seems to be a poor secondary emitter under bombardment either of the  $\text{Na}^+$  ions produced by ionization of the volatile compound or of the  $\text{H}^+$  ions.

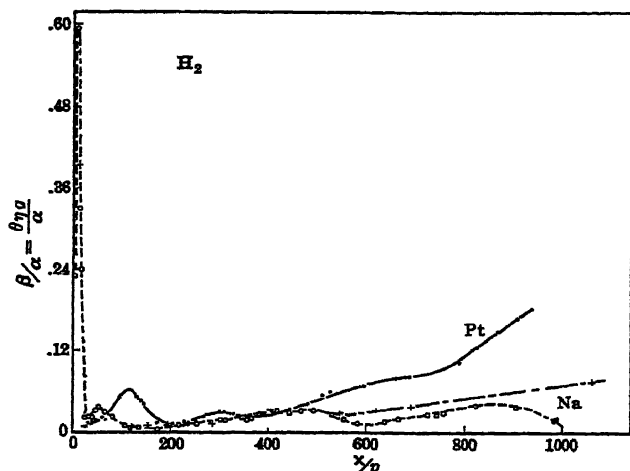


FIG. 190B.

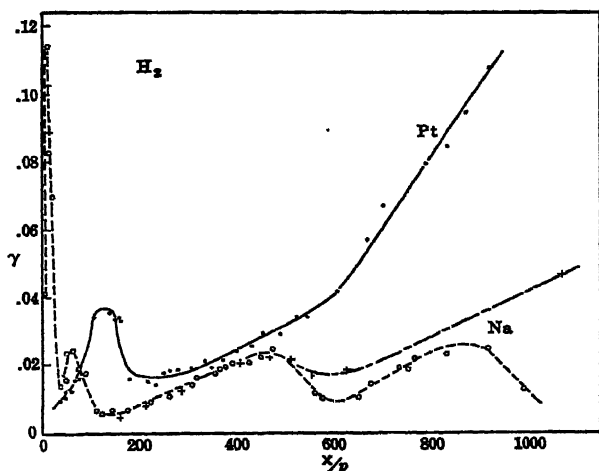


FIG. 190C.

In this case perhaps 20 to 50 per cent of the positive ions at high  $X/p$  are  $\text{Na}^+$  ions. This action is not necessarily surprising. Pt cathodes, on the other hand, show a marked photosensitivity in  $\text{H}_2$  at an  $X/p$  far higher than for the NaH surface, viz., 140 as compared to 8.6. Thus

the NaH both in low-wavelength threshold and in yield is a good photoelectric producer.

The photosensitivity of Pt to  $H_2$  radiations is less than that to  $N_2$  at an  $X/p$  of about 90. Pt may show other more doubtful photoelectric peaks in  $H_2$  but in general rises fairly monotonously, starting at an  $X/p$  between 200 and 300. It seems evident that the Pt can emit secondary electrons under bombardment of positive H ions fairly effectively. In this connection it may be recalled that Pt is definitely a catalyst for  $H_2$  reactions. That is, it adsorbs  $H_2$  on its surface in such a state that  $H_2$  is chemically very reactive, probably in the atomic state. These surfaces are known to be very good secondary electron emitters in high fields, as shown by Curtiss<sup>47</sup> studies on the negative point Geiger counter. The result, therefore, need not surprise us. However, in conjunction with earlier work on secondary emission on positive-ion bombardment and with Penning's work on the same subject, the results definitely bear out the extreme variability of surfaces as regards secondary emission.

TABLE XXXI

GAS: HYDROGEN

CATHODE: NaH

| $X/p$ | $\gamma$ | $X/p$ | $\gamma$ | $X/p$ | $\gamma$ |
|-------|----------|-------|----------|-------|----------|
| 5.85  | 0.0404   | 115.0 | 0.0055   | 445.0 | 0.0228   |
| 8.65  | 0.1137   | 138.0 | 0.0060   | 466.0 | 0.0250   |
| 10.2  | 0.0821   | 176.0 | 0.0065   | 493.0 | 0.0209   |
| 20.4  | 0.0691   | 218.0 | 0.0095   | 555.0 | 0.0115   |
| 34.1  | 0.0142   | 253.0 | 0.0104   | 571.0 | 0.0102   |
| 40.0  | 0.0161   | 302.0 | 0.0143   | 642.0 | 0.0109   |
| 47.0  | 0.0152   | 312.0 | 0.0167   | 667.0 | 0.0145   |
| 49.0  | 0.0237   | 349.0 | 0.0178   | 724.0 | 0.0196   |
| 56.2  | 0.0248   | 359.0 | 0.0194   | 760.0 | 0.0228   |
| 69.0  | 0.0185   | 369.0 | 0.0196   | 827.0 | 0.0235   |
| 84.0  | 0.0178   | 385.0 | 0.0205   | 908.0 | 0.0253   |
| 113.0 | 0.0060   | 420.0 | 0.0200   | 980.0 | 0.0127   |

Calculated from  $\delta = i_0 e^{ax} / [1 - \gamma(e^{ax} - 1)]$ .

TABLE XXXII

GAS: HYDROGEN

CATHODE: Na (Second Surface)

| $X/p$ | $\gamma$ | $X/p$  | $\gamma$ |
|-------|----------|--------|----------|
| 10.6  | 0.1058   | 461.0  | 0.0225   |
| 13.6  | 0.1107   | 505.0  | 0.0219   |
| 158.0 | 0.0043   | 545.0  | 0.0177   |
| 203.0 | 0.0077   | 620.0  | 0.0184   |
| 280.0 | 0.0123   | 690.0  | 0.0217   |
| 400.0 | 0.0204   | 1066.0 | 0.0467   |

TABLE XXXIII

GAS: HYDROGEN

CATHODE: Pt

| $X/p$ | $\gamma$ | $X/p$ | $\gamma$ | $X/p$ | $\gamma$ |
|-------|----------|-------|----------|-------|----------|
| 32.3  | 0.0095   | 209.6 | 0.0154   | 448.0 | 0.0292   |
| 39.6  | 0.0107   | 228.0 | 0.0135   | 481.0 | 0.0289   |
| 52.3  | 0.0120   | 240.0 | 0.0178   | 516.0 | 0.0340   |
| 61.9  | 0.0152   | 252.6 | 0.0180   | 536.0 | 0.0344   |
| 68.6  | 0.0158   | 271.4 | 0.0182   | 600.0 | 0.0413   |
| 100.0 | 0.0342   | 299.0 | 0.0185   | 663.5 | 0.0579   |
| 136.2 | 0.0350   | 328.4 | 0.0215   | 694.5 | 0.0672   |
| 144.7 | 0.0327   | 337.4 | 0.0178   | 787.8 | 0.0797   |
| 146.0 | 0.0342   | 362.0 | 0.0208   | 833.5 | 0.0838   |
| 153.0 | 0.0337   | 392.6 | 0.0240   | 867.0 | 0.0948   |
| 175.8 | 0.0152   | 424.0 | 0.0255   | 916.7 | 0.1068   |

It should also be pointed out that a good photoelectric emitter of low work function *need* not necessarily be a good emitter of secondary electrons on positive-ion bombardment. In fact, the Farnsworth research group in their study of high secondary electron emitters under

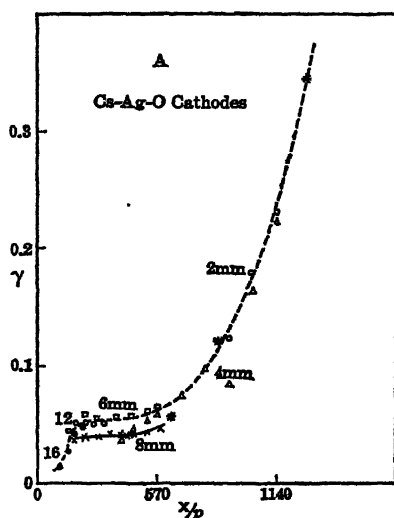


FIG. 191A.

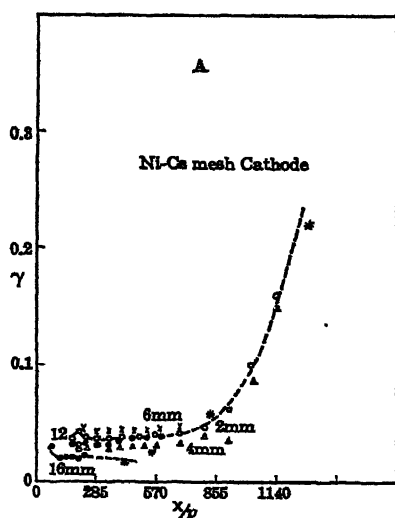


FIG. 191B.

electron bombardment with the Cs-Ag-O surfaces have found that high photoelectric emitters *were not necessarily good emitters of secondary electrons under electron bombardment*. This fact must be constantly borne in mind. The secondary-emission process under electron bom-

bardment, positive-ion bombardment of different types, and photoelectric emission are different mechanisms. It is hardly to be expected that close parallelisms may exist in these phenomena for different surfaces. Obviously a *low work function should facilitate all secondary emission, but not equally*. These data for the present comprise all the definite information which we have.

One should not leave this subject without mentioning the very recent studies of Huxford and Engstrom<sup>48</sup> on Cs-Ag-O surfaces and of Engstrom on Ba surfaces which have not yet appeared in print. They indicate interesting behavior on the part of  $\gamma$  or  $\eta\theta g$ . The curves for  $\gamma$  as a function of  $X/p$  for Cs-Ag-O surfaces and for Ni - Cs surfaces in A observed by Huxford and Engstrom are shown in Figs. 191A and B. Note the approximate agreement between the points for  $\gamma$  obtained from sparking potentials marked by crosses compared to those obtained directly. The method of observation precludes accurate curves, hence one cannot draw too many conclusions. Moreover, positive-ion bom-

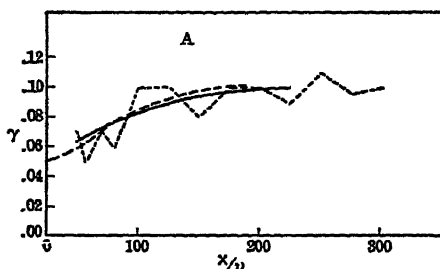


FIG. 192.

bardment itself changes  $\gamma$ , and  $\eta\theta g$  is very much influenced by the radiation of the surface by light of different wavelengths. In a later paper Engstrom<sup>48</sup> has studied the coefficients in A with a Ba cathode. The results were obtained by measuring  $i$  as a function of  $X/p$  instead of  $x$ , for various constant fields. They are thus equivalent to Penning and

Kruithoff's measurements in Ne-A mixtures. The curves for  $\log i/i_0$  as a  $f(x)$  were deduced for these by interpolation and correction. The method of illumination was that of Kruithoff and Penning, and  $x$  varied from 1 to 15 mm. Space-charge effects were avoided in the main, and pure gases were carefully striven for. The wavy lines for  $\log i/i_0$  at low values of  $x$ , however, indicate the presence of a trace of an easily ionized gas, probably Hg in *very small amounts*. The values of  $\gamma$  as calculated are seen in the broken line of Fig. 192. These are from direct measurements. The sparking potential gave the full-line curve for  $\gamma$ , and the dashed curve gives Schofer's<sup>44</sup> values for  $\gamma$  also obtained from  $V_*$ . It is not certain that the broken curve is not the *true* curve for  $\gamma$ , as the work of Hale and Bowls shows peaks for  $\gamma$  for Na, Pt, and NaH. These peaks never appear from evaluations of  $\gamma$  from  $V_*$ . The reason lies in the irregular character of individual  $V_*$  measurements, the use of average values, and the *insensitivity* of  $V_*$  to values of  $\gamma$ . It is concluded by Engstrom from time lag studies that the mechanism with Ba is a positive-ion or photon liberation at the cathode and *not one due to metastable atoms*. With Cs-Ag-O surfaces in A, time lag studies in such

cells by Engstrom showed a definite contribution to  $\gamma$  caused by metastable atoms. Their contribution to  $\gamma$  ranged from about 0.02 to 0.10 with different values of  $X/p$ . The *total* values of  $\gamma$  as shown in Figs. 191A, B rose up to 0.35 or 0.40. The difference between the contribution due to metastable atoms and the total observed  $\gamma$  can be ascribed to an electron liberation by positive-ion bombardment. Recent studies by Kruithoff<sup>60</sup> on the time lags of such cells led him to suggest that they were accounted for by the action of metastable atoms. There is no doubt but that in the next years many more data will be at hand, though the tedium and difficulty of these experiments under conditions of high purity and surface uniformity do not make the field of study attractive.

Before closing the discussion one more statement concerning the second coefficient must be made. There appears to be some question<sup>64</sup> as to whether the second coefficient, and specifically  $\gamma$ , is a function of  $X/p$ . This question is answered in part by what has gone before. Inasmuch as the second coefficient  $\gamma$  must be a composite of many different actions, of which at any  $p$  and  $X/p$  in a given gas one predominates, it is clear that  $\gamma$  in the broad sense here used must vary in a complex fashion as its mechanism changes with  $X/p$ . In general,  $\gamma$  will be small at low  $X/p$  and larger at high  $X/p$ , as active photon production (spark lines) and secondary emission by positive-ion bombardment are furthered by high  $X/p$ . However, photoelectric peaks may and do appear at certain favorable values of  $X/p$ , and the specific variation for a surface is quite unpredictable.

For secondary electron emission from the cathode by any process there is one circumstance that must not be lost sight of. Whereas peaks and special emissions at given photon wavelengths and  $X/p$  may vary rapidly with  $X/p$ , there is a universal change of  $\gamma$  or  $\eta$  which depends on the *number of electrons which succeed in leaving the cathode*. While  $\gamma$  and  $\eta$  depend on  $X/p$  through the energy of the incident photon or ion, and on the nature of the gas in the kind of ions it furnishes and its chemical effect in changing the surface work function, they also depend on  $X/p$  in another way. For, although  $\eta$  and  $\gamma$  depend on the mechanism of liberation and the number of particles liberated from the surface per incident particle, this whole number of the *liberated electrons is not available for the current owing to loss of electrons back to the cathode by diffusion*. With any appreciable gas pressure the electrons liberated by any process from the cathode diffuse in all directions. For high energies of liberation (short-wavelength photons, for example), the electrons diffuse very rapidly, and a large proportion is lost by backward diffusion to the cathode. For ultraviolet illumination in pure  $N_2$  at 760 mm, as shown on page 315, probably less than 1 per cent and perhaps only 0.1 per cent of the liberated current  $i_0$  is received by the cathode at 300 volts/cm. At 3 mm pressure the fraction of the electrons liberated by light with about 2 volts energy, under conditions where

$X/p = 100(X/p$  for a spark in  $N_2$  in a gap of 1 cm), is about 0.45. Hence, as  $X/p$  decreases, owing to this circumstance alone the secondary electron liberation  $\gamma$  or  $\eta$  goes down. The approximate variation of the fractional loss  $f_d$  as a function of  $X/p$  in  $N_2$  is shown in the curve of Fig. 193.

It is seen that at the value of  $X/p$  for most sparks it is not a serious cause of loss. However, in the case of the cathode emission in Geiger-Mueller counters at the cylindrical cathode, where  $X/p$  is of the order 1 or more, it reduces the current materially. In such counters  $\eta\theta g$  is of the order of  $10^{-4}$ .

As to the change of  $\gamma$  or  $\eta$  with the pressure of a given gas beyond the change above noted, nothing is known.

There is no reason why above  $10^{-3}$  mm or less of a given pure gas the work function should alter with pressure.

As  $\gamma$  and  $\eta\theta g$  cannot be detected much below an  $X/p$  of 50 for most molecular gases with existing techniques, little is known of the variation with pressure.<sup>62</sup> If other factors causing secondary liberation were constant, such as absorption of photons, one should reduce  $\gamma$  at pressures above 1 mm

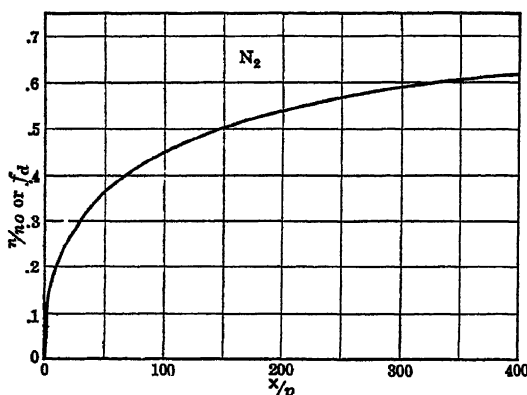


FIG. 193.

by a factor  $f_d$  such as shown for  $N_2$ . More data on  $\dot{\gamma}$  at higher pressures and lower  $X/p$  are urgently needed. In the extreme limits such as in positive corona at atmospheric pressure or for very large gaps this circumstance renders cathode processes in discharge practically inoperative and forces photoionization of the gas to become the active mechanism.<sup>62</sup>

## 8. A SUMMARY OF SECONDARY MECHANISMS KNOWN TO BE ACTIVE AND THEIR OCCURRENCE

Before concluding this chapter, some of the definite indications should be given as to the conditions under which one may find a given mechanism active in determining the nature of the second Townsend coefficient  $\beta$ . In introducing this subject a summary of the different possible interpretations to be placed upon a  $\beta$  will be presented. The second Townsend coefficient  $\beta$  can be ascribed to any one of the following mechanisms:

1. The secondary liberation of electrons at cathode by positive-ion bombardment, all positive ions reaching the cathode. This occurs for:

- a. All ions with energies greater than 50 volts.
- b. Ions for which  $E_i > \phi_s$ , where  $\phi_s$  is the work function of the surface. This occurs for energies certainly less than 10 volts.

2. A photoelectric action *at the cathode* by photons produced in the gas largely near the anode, a large fraction of potentially active photons being incapable of reaching the cathode due to absorption or loss by propagation in the wrong direction.

3. A photoelectric action *in the gas* by means of photons corresponding to *spark lines* acting on normal atoms or by photons of one gas *A* acting on a gas *B* for which  $E_{sA} > E_{sB}$ . In this process many photons otherwise active are lost through escape from active areas.

4. Metastable atoms of one gas *A* acting on a gas *B* if  $E_{mA} > E_{sB}$ . The electrons produced may be very effective and they are produced irrespective of field gradients. Except with proper values of the concentration of the atoms *B*, the production is small.

5. Metastable atoms acting on the cathode if  $E_m > \phi_s$ . This occurs under favorable conditions but is not more effective than process 1b, since metastables diffuse slowly and are readily destroyed.

6. A false coefficient appears at high current density  $j_0$  for larger values of  $x$  and for values  $\alpha/p$  which increase faster than  $(X/p)$ . For higher pressures and values of  $x$  of 4-6 cm the limit is  $10^{-12}$  amp/cm<sup>2</sup>; for the conditions used by Penning it is  $10^{-8}$  amp/cm<sup>2</sup>.

7. A false secondary emission may appear if small bits of non-conducting material on the cathode charge up by photoionization or by positive ions. These lead to local discharges. They are especially bad with Al and Mg cathodes in Ne and He, as seen on page 498.

Action 1 actually occurs in nearly all glow discharges at *lower* pressures. It is operative at higher  $X/p$  in most studies with plane parallel electrodes and is quite important at lower pressures, i.e., near the minimum sparking potential. It doubtless occurs in a greater or less degree in all gases if  $E_i > \phi_s$ , but may not be important. It is a very capricious behavior and depends on the surface condition of the electrode. Denudation of a gas film by positive-ion bombardment has been known to change  $\gamma$  materially. Curtiss has shown that certain gases "poison" surfaces and change  $\gamma$ .

Action 2 actually occurs to some degree in all gases. It is effective at low  $X/p$  for more or less transparent gases and where absorbing vapors are not present. It is the important feature in the operation of the positive wire Geiger-Mueller counter, as shown by Greiner.<sup>39</sup> Here the pressure is *low*, but the field at the negative cylinder (cathode) is exceedingly weak. If metastables are absent and if  $E_i$  is not greater than  $\phi_s$  for the surface, the action of the counter is entirely dependent on the photoelectric process at the surface.<sup>39</sup> Spark lines in air near the positive wire get to the negative cylinder, liberating on the average one electron per  $10^3$  to  $10^4$  photons. Note also that the geometrical



form factor is such as to retain photons in the cylinder so that eventual liberation is certain. It also appears as a modifying factor in positive corona in short point to plane gaps.<sup>58</sup>

Action 3 actually has been observed in corona discharge by Cravath, Raether,<sup>57</sup> and Dechène.<sup>52</sup> It is the basis of the action of the positive point to plane or positive wire corona in air and other gases at atmospheric pressure.<sup>49</sup> It is probably the basic feature in the propagation of all long sparks in air (exceeding 1-cm length and probably even less). This includes lightning discharges.<sup>50</sup> It is probably the basis of propagation of the stepped leader strokes of Schonland and Collins<sup>51</sup> and Allibone and Meek,<sup>52</sup> as Cravath and Loeb<sup>50</sup> and Meek<sup>51</sup> have indicated. It must occur wherever a cathode mechanism is lacking or ineffective. It will probably occur in all gases, since spark lines are present in all except perhaps  $H_2$ . It will be particularly effective in mixed gases.

Action 4 occurs quite definitely in certain combinations of inert gases, A or Ne in He, A or Hg in Ne, Hg in A, etc. It may occur for Hg and Na compounds in  $N_2$ . It is exceedingly effective in the case of the positive wire cylindrical cathode corona discharge whenever metastable atoms can exist with the mixtures indicated above. Penning<sup>44</sup> has shown that metastable actions of this sort account for the reversal of starting voltages for positive and negative corona with pressure. The effects are at an optimum for the proper percentage of admixture of active impurity, and the effects of as much as 0.0004 per cent of A in Ne can be detected. The metastables in a gas are *more* effective than at the surface since all electrons liberated by them in the gas count, whereas at surfaces a considerable fraction are lost by backward diffusion. It is doubtful whether this action is basically the *only* action operative in a discharge. Conditions favoring it also favor actions 1b and 5, so that it accompanies other actions. However, it is sufficiently important to alter the sparking potentials and the values of  $\alpha/p$  and  $\beta/p$  or  $\gamma$  to the extent of tens of per cent and more in some cases.

Action 5 occurs irrespective of whether action 4 does or does not, provided that metastable atoms persist long enough to reach the cathode. The yield of secondaries is no greater than that due to positive ions, if as great, for all positive ions get to the cathode, since recombination in the gas is small, while fewer metastables survive and succeed in diffusing to the cathode. Except at low  $X/p$  the metastable atoms do not necessarily outnumber the positive ions so very much. The metastable atoms, however, are more effective in liberation than the same number of positive ions.<sup>59</sup> Thus while metastable atoms do act in both mechanisms 4 and 5 and do cause effects these may never supersede action 1.

Action 6 occurs only at lower  $X/p$  with large  $i_0$  and long  $x$ . It is dependent on  $\alpha/p$  increasing as  $(X/p)^n$ , where  $n > 1$ .

When we consider the various mechanisms active and note that several are simultaneously active in greater or less measure and that most of the mechanisms are exceedingly sensitive to small changes in cathode surface or gas composition it is clear that the theory in any case must be very involved. With the present accuracy of measurement it is also clear that it is difficult to differentiate the mechanism active, through the form of the theory. For the ionization by positive ions and for the electron liberation at the cathode by positive-ion bombardment the theories deduced are relatively exact. The theory for photoelectric action at the cathode due to photons largely produced near the anode is not particularly accurate. The derivations of the expressions for photons in the gas and for the action of metastable atoms, though leading to similar expressions to those deduced, are entirely too inaccurate, owing to simplifying assumptions as to loss of metastables, etc., to warrant their being given. In view of this situation and the present inaccuracy of measurements it suffices then to take the  $i/i_0$  data as is being done and to evaluate  $\alpha$  and *either* a  $\beta$  or a  $\gamma$  directly from it. Recognizing at this juncture that  $\beta$  is *not an ionization by positive ions* in the gas we can treat  $\beta/p$  as due to metastables or photons in the gas or  $\beta/\alpha = \gamma = \eta\theta g$  as an effect of positive ions or photons at the cathode. Thus, until both more accurate theory and more accurate data are available, the evaluation of a second Townsend coefficient,  $\beta$  or  $\gamma$ , from the data suffices, due care being taken to understand and label the actual possible predominating mechanism active.

This apparent paradox that the descriptive coefficient in the equation for ion multiplication is *general* and not *selective*, while for the control of the currents and the understanding of resultant discharges the nature of the mechanism leading to the coefficient is vital, is one of the most remarkable situations in physics. The reason for this situation aside from a general similarity in the immediate multiplicative nature of different processes lies in the exponential character of ion multiplication by ionization by collision. This means that except at  $X/p$  values near the minimum sparking potential even small changes in  $i_0$  due to other factors play a relatively unimportant role compared to small changes in  $x$  or  $\alpha$ . Thus a doubling in  $i_0$  due to a secondary process will be compensated for by a relatively small increase in  $x$ . And since in turn  $\alpha/p$  is a function of  $X/p$  which in some regions varies exponentially or as the square of  $X/p$  the situation becomes still clearer. In addition, since the increase in  $i$  as  $x$  or  $X/p$  increases is relatively so rapid, leading to an unstable regime called the spark, the region of values of  $x$  or of  $X/p$  in which a value of  $\beta$  or  $\gamma$  can be observed is very short. Hence it is only in a very short range of values of  $x$  between the linear part of the  $\log i/i_0 - x$  curves and a spark that  $\beta$  can be evaluated. Finally the unsteadiness in  $i_0$ , the fluctuations of the potential source, and the unstable conditions near sparking make measurements both of  $\beta$  or  $\gamma$  and of the sparking potential highly uncertain. Any

evaluation of sparking potentials to better than 1 per cent and of values of  $\beta$  good to 5 per cent is an achievement.

With this statement as to the reasons for the incomplete development of the theory, and with hopes that the future will bring more accurate results on the basis of the analysis given, we can turn to an even more unsatisfactory and incomplete field of study—that of the theory and mechanism of the electrical spark, which will be described in Chapter X.

## 9. REFERENCES FOR CHAPTER IX

1. F. H. SANDERS, *Phys. Rev.*, **41**, 667, 1932; **44**, 1020, 1933.
2. W. E. BOWLS, *Phys. Rev.*, **53**, 293, 1938.
3. J. S. TOWNSEND, *Phil. Mag.*, **3**, 557, 1902; **6**, 389, 598, 1903.
4. F. EHRENKRANTZ, *Phys. Rev.*, **55**, 219, 1939.
5. D. Q. POSIN, *Phys. Rev.*, **50**, 650, 1936.
6. TOWNSEND and TIZARD, *Proc. Roy. Soc.*, **A 87**, 357, 1912; **A 88**, 336, 1913; T. L. R. AYERS, *Phil. Mag.*, **45**, 353, 1923.
7. D. H. HALE, *Phys. Rev.*, **55**, 815, 1939.
8. J. J. THOMSON, *Phil. Mag.*, **23**, 449, 1912; N. BOHR, *Phil. Mag.*, **25**, 19, 1913; **30**, 581, 1915; G. H. HENDERSON, *Phil. Mag.*, **44**, 680, 1922; R. H. FOWLER, *Proc. Camb. Phil. Soc.*, **21**, 521, 1923.
9. J. FRANCK, *Z. Physik*, **25**, 312, 1924; FRANCK and v. BAHR, *Verhandl. deut. physik. Ges.*, **16**, 57, 1914.
10. V. J. PAVLOW, *Proc. Roy. Soc.*, **A 90**, 398, 1914.
11. HORTON and DAVIES, *Proc. Roy. Soc.*, **A 95**, 333, 1919.
12. W. J. HOOVER, *J. Franklin Inst.*, **201**, 311, 1926.
13. O. BEECK, *Ann. Physik*, **6**, 1001, 1930; *Physik. Z.*, **35**, 36, 1934.
14. L. B. LOEB, *Science*, **66**, 627, 1927.
15. R. M. SUTTON, *Phys. Rev.*, **33**, 364, 1929; SUTTON and MOUZON, *Phys. Rev.*, **35**, 694, 1930; **37**, 310, 1931.
16. BEECK and MOUZON, *Ann. Physik*, **11**, 737, 858, 1931; J. C. MOUZON, *Phys. Rev.*, **41**, 605, 1932; BEECK, *Physik. Z.*, **35**, 36, 1934.
17. M. NORDMEYER, *Ann. Physik*, **16**, 697, 1933.
18. R. N. VARNEY, *Phys. Rev.*, **47**, 483, 1935.
19. R. N. VARNEY, *Phys. Rev.*, **50**, 159, 1936; **53**, 732, 1938; A. ROSTAGNI, *N. Cimento*, **11**, 34, 1934; *Phys. Rev.*, **53**, 729, 1938; N. WAYLAND, *Phys. Rev.*, **52**, 31, 1937.
20. VARNEY and COLE, *Phys. Rev.*, **50**, 261, 1936; VARNEY, COLE, and GARDNER, *Phys. Rev.*, **52**, 526, 1937.
21. J. T. TATE, *Phys. Rev.*, **23**, 293, 1924.
22. B. KIRCHSTEIN, *Z. Physik*, **60**, 184, 1930.
23. BEECK and WAYLAND, *Ann. Physik*, **19**, 129, 1934.
24. R. N. VARNEY, *Phys. Rev.*, **53**, 732, 1938.
25. J. J. THOMSON, *Conduction of Electricity through Gases*, 2nd Edition, p. 490 ff., Cambridge Press, 1911. J. S. TOWNSEND, *Electricity in Gases*, page 331, Oxford Press, 1915.
26. BRODE and NEUMAN, Seminar in Discharge through Gases, California, Spring, 1928.
27. HOLST and OOSTERHUIS, *Phil. Mag.*, **46**, 1117, 1923.
28. JAMES TAYLOR, *Phil. Mag.*, **3**, 753, 1927; **4**, 505, 1927; *Proc. Roy. Soc.*, **A 114**, 73, 1927; A. VON HIPPEL, *Ann. Physik*, **81**, 1043, 1926; **86**, 1006, 1928.
29. M. L. E. OLIPHANT, *Proc. Roy. Soc.*, **A 124**, 228, 1929; OLIPHANT and MOON, *Proc. Roy. Soc.*, **A 127**, 373, 1930.
30. F. M. PENNING, *Proc. Koenigl. Akad. v. Wetens. Amsterdam*, **31**, 14, 1928; **33**, 841, 1930; *Physica*, **8**, 13, 1928.
31. W. J. JACKSON, *Phys. Rev.*, **28**, 524, 1926; **30**, 473, 1927.

32. A. M. CRAVATH, *Phys. Rev.*, **47**, 254, 1935; G. DECHÈNE, *J. phys. et le radium*, **7**, 533, 1936.
33. CARL KENTY, *Phys. Rev.*, **44**, 891, 1933; CASHMAN and HUXFORD, *Phys. Rev.*, **48**, 734, 1935.
34. L. J. NEUMAN, *Proc. Natl. Acad. Sci.*, **15**, 259, 1929.
35. L. B. LOEB, *J. Franklin Inst.*, **205**, 305, 1928.
36. W. ROGOWSKI, *Arch. Elektrotech.*, **20**, 99, 1928.
37. TOWNSEND and JONES, *Phil. Mag.*, **15**, 282, 1933.
38. S. GORRILL, research in progress, University of California, 1939.
39. E. GREINER, *Z. Physik*, **81**, 543, 1933; S. WERNER, *Z. Physik*, **90**, 384, 1934; **92**, 705, 1934.
40. M. PAAVOLA, *Arch. Elektrotech.*, **22**, 443, 450, 1929.
41. VARNEY, WHITE, LOEB, and POSIN, *Phys. Rev.*, **48**, 818, 1935.
42. KRUITHOFF and PENNING, *Physica*, **3**, 515, 1936.
43. KRUITHOFF and PENNING, *Physica*, **4**, 430, 1937.
44. F. M. PENNING, *Phil. Mag.*, **11**, 976, 1931.
45. J. S. TOWNSEND, *Electricity in Gases*, pp. 281, 320, Oxford, 1915.
46. F. M. PENNING, *Physica*, **4**, 286, 1938.
47. L. F. CURTISS, *Phys. Rev.*, **31**, 1060, 1127, 1928.
48. W. S. HUXFORD, *Phys. Rev.*, **55**, 754, 1939.
49. G. W. TRICHEL, *Phys. Rev.*, **55**, 382, 1939.
50. CRAVATH and LOEB, *Physics*, **6**, 125, 1935.
51. SCHONLAND and COLLINS, *Proc. Roy. Soc.*, **A 164**, 132, 1938.
52. ALLIBONE and MEEK, *Proc. Roy. Soc.*, **A 166**, 97, 1938.
53. R. W. ENGSTROM, *Phys. Rev.*, **56**, 1939.
54. R. SCHÖFER, *Z. Physik*, **110**, 21, 1938.
55. G. SCHNEIDER, *Ann. Physik*, **11**, 357, 1931.
56. O. KLEMPERER, *Z. Physik*, **52**, 650, 1928.
57. H. RAETHER, *Z. Physik*, **110**, 611, 1938.
58. A. F. KIP, *Phys. Rev.*, **55**, 549, 1939.
59. M. L. E. OLIPHANT, *Proc. Roy. Soc.*, **A 124**, 228, 1929.
60. A. KRUITHOFF, *Phillips Tech. Rev.*, **4**, 48, 1939.
61. J. M. MEEK, *Phys. Rev.*, **55**, 972, 1939.
62. It is to be noted that the curves of  $\log i/i_0 - x$  observed for lower values of  $X/p$  are all straight and terminate at high values of  $x$  in a spark with no indications of upcurving or of a  $\gamma$ . However above a characteristic value of  $X/p$  and below certain values of  $p$  and  $x$  for each gas there abruptly appear  $\log i/i_0 - x$  curves with upcurving at higher values of  $x$  yielding a constant and finite value of  $\gamma$  in the absence of space charge distortion caused by high  $i_0$ . It is the spark occurring at high values of  $x$  with low  $X/p$  which limits the investigation and prohibits evaluation of  $\gamma$  for lower  $X/p$  and larger  $x$ . The cause for this spark has remained obscure until the recent work by Meek.<sup>66</sup> In conformity with the mechanism of the spark postulated in Chapter X at lower  $X/p$  and higher  $p$  and  $x$  the spark propagates as a positive streamer proceeding as a result of a localized space charge accumulation and photo-ionization in the gas. Thus whenever  $p$ ,  $x$ , and  $X/p$  reach values such that  $\gamma$  becomes small and adequate localized space charge densities can accumulate in an electron avalanche, breakdown proceeds by streamer mechanism before upcurving begins. The quantitative criterion for streamer propagation applied by Meek<sup>66</sup> gives correct values for the sparking potential in air at higher  $p$  and  $x$  but fails at values of  $X/p$ ,  $p$  and  $x$  at which the upcurving begins and at which  $\gamma$  is thus measured.
63. TOWNSEND, J. S., *Phil Mag.*, **28**, 111, 1939.
64. SMITH, R. A., *Proc. Roy. Soc.*, **A 168**, 19, 1939.
65. VARNEY, LOEB and HASELTINE. Paper submitted to *Phil. Mag.*, Sept. 1939. See also reference 54, Chapter VIII.
66. MEEK, J. A. Paper submitted to *Proc. Roy. Soc.*, Sept. 1939.

## CHAPTER X

### DISRUPTIVE DISCHARGE IN GASES; SPARKS

#### PART A. THE THEORY OF SPARKING \*

##### 1. THE DEFINITION OF A SPARK

Before discussing the nature and mechanism of the electrical spark it is quite important that we define it carefully. In what follows, we shall define the spark as *an unstable and discontinuous occurrence marking the transition from one more or less stable condition of current between electrodes in a gas to another one.* Thus the transitions from a conduction current in a gas to an arc or a glow discharge, or from a corona to an arc or a glow discharge, very frequently if not always are accompanied by a spark. It may also occur that the transition process may start but fall short of achieving the transition owing to circuit conditions such as power supply. Under these circumstances all the transition phenomena will appear except the stable end discharge. The phenomenon is still a spark. On the other hand, arcs or glows, for example, may originate without a spark, for arcs may be drawn out by separating electrodes in contact, and glows may continuously and smoothly go over to arcs by heating of the cathode without the discontinuous intermediary of a spark. Even with this careful definition there are cases where it becomes difficult to decide whether a process is to be termed a spark. The ignition of a stable corona is probably in no sense a spark, although under some conditions a sparklike process may initiate the corona. It is seen that this rather broader definition of the electric spark embraces phenomena ranging from the flick of a microammeter needle on the initiation of a glow discharge to the tremendous and awe-inspiring phenomenon displayed by nature in lightning discharge.

The choice of the definition above may seem somewhat unusual, since one generally associates with the word spark only that startling, luminous, and noisy phenomenon observed in the electrical breakdown of air gaps at atmospheric pressure. However, since the application of Townsend's<sup>1</sup> theory to the phenomena the word has generally taken on a much broader aspect than that which is popularly associated with it. It is seen that the above definition fittingly brings together

\* References to Part A of Chapter X will be found on page 448.

through the common elements of instability and discontinuity all the phenomena which on any basis have in the past been classed as sparks. It is in fact the discontinuous nature of the processes which result from instability that typifies sparks and at the same time makes them inaccessible to analysis, understanding, or control. Aside from the purely scientific interest in the mechanism of such phenomena, the difficulties in controlling such destructive happenings in the industrial applications of modern electricity are further demanding more complete solutions of the problems than those that sufficed in the past. It is with this need in view that a chapter in this book will be devoted to the theory and mechanism of the spark, leaving for other more specialized texts the extensive discussions of the applications of the fundamental processes to the glow discharge and arc. These will be only superficially treated in a later chapter.

## 2. THE TOWNSEND SPARKING CRITERION

Although sparking phenomena had been studied for many years previous to 1900, real progress began only under the directive action of the theory of sparking promulgated by J. S. Townsend<sup>1</sup> in 1902. This theory, in turn, was a result of the studies on the conduction of electricity in gases first made possible through the discovery of X-rays in 1895 and the consequent discovery of the electron in 1896.

As shown in Chapter IX, Townsend described the form of the rise in photoelectric currents in a plane parallel electrode gap at adequate  $X/p$  with increasing gap length  $x$  by means of an equation depending on two coefficients  $\alpha$  and  $\beta$ . These represent the number of ions created per centimeter path in the field direction by negative electrons and by positive ions. It was further shown that, while the electron mechanism was probably correct, the positive ions under normal conditions could not contribute to the current by ionization by impact *in the gas*. An alternative equation, using a coefficient  $\gamma$  representing the number of secondary electrons liberated from the cathode per positive ion incident on the cathode, led to an expression which did not differ materially in form from the first equation. It was also shown that still another equation, differing only slightly in form from Townsend's equations but dependent on a photoelectric ionization at the cathode by photons produced throughout the gap, might also be invoked. In fact, it was stated in Chapter IX that according to Brode several other mechanisms involving processes in the gas due to photons and metastable atoms or at the cathode due to metastable atoms would also lead to analogous equations. Thus, from the nature of the Townsend experiments, it appears that the currents may be accounted for by any one of three or more similar equations within the limits of experimental accuracy. Three of these equations which are relatively accurate are

given below the significance of the constants of which can be found in Chapter IX. They are:

$$i = i_0 \frac{(\alpha - \beta)e^{(\alpha - \beta)x}}{\alpha - \beta e^{(\alpha - \beta)x}},$$

$$i = i_0 \frac{e^{\alpha x}}{1 - \gamma(e^{\alpha x} - 1)},$$

$$i = i_0 \frac{\alpha e^{\alpha x}}{\alpha - \eta \theta g [e^{(\alpha - \mu)x} - 1]}.$$

Neglecting  $\beta$  and  $\mu$  in comparison to  $\alpha$ , and 1 in comparison to  $e^{\alpha x}$ , these equations become

$$i = i_0 \frac{\alpha e^{\alpha x}}{\alpha - \beta e^{\alpha x}},$$

$$i = i_0 \frac{e^{\alpha x}}{1 - \gamma e^{\alpha x}},$$

$$i = i_0 \frac{\alpha e^{\alpha x}}{\alpha - \eta \theta g e^{\alpha x}}.$$

It is at once seen that when  $x$  reaches some value  $\delta$  for which the denominator approaches 0 the currents  $i$  become indefinitely large, irrespective of the value of  $i_0$ . In respect to the first equation Townsend in 1902 *interpreted this as representing the condition for the initiation of a self-sustaining discharge, that is, the condition for a spark*. Since his assumed mechanism involving  $\beta$  is known to be improbable,  $\beta$  as derived from measurement must be interpreted more generally in terms of either a  $\gamma$ , an  $\eta \theta g$ , or some equivalent mechanism. This can be done within the limits of error by setting  $\alpha/\beta = 1/\gamma = \alpha/\eta \theta g$ . Then, on the basis of Townsend's criterion, the sparking condition results when

$$\frac{\alpha}{\beta} = e^{\alpha \delta}, \quad \text{or} \quad \frac{1}{\gamma} = e^{\alpha \delta}, \quad \text{or} \quad \frac{\alpha}{\eta \theta g} = e^{\alpha \delta}.$$

Analogous equations would represent the same criterion for other mechanisms. Neglecting, for the purpose of the present discussion, the various different mechanisms proposed, we can use the expression  $1/\gamma = e^{\alpha \delta}$  as a typical equation which does apply under some conditions, and confine our discussion to it.

### 3. PASCHEN'S LAW

Now experiment as seen in Chapter IX reveals that  $\alpha/\beta = 1/\gamma = \alpha/\eta \theta g$  is some function  $\phi(X/p)$  of  $X/p$ , while  $\alpha/p$  as shown in

Chapter VIII is also another function  $f(X/p)$  of  $X/p$ . Hence, according to Townsend and others after him, a spark occurs when

$$\frac{1}{\phi(X/p)} = e^{pf\left(\frac{X}{p}\right)\delta} \text{ or when } \log \frac{1}{\phi(X/p)} = p\delta f\left(\frac{X}{p}\right).$$

Thus

$$\log \frac{1}{\phi\left(\frac{X\delta}{p\delta}\right)} = p\delta f\left(\frac{X\delta}{p\delta}\right).$$

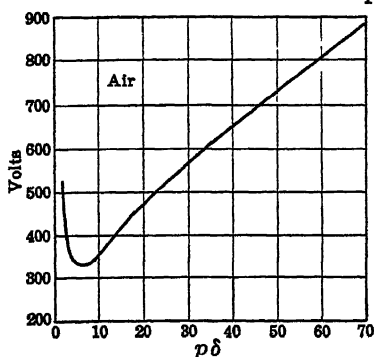


FIG. 194A.

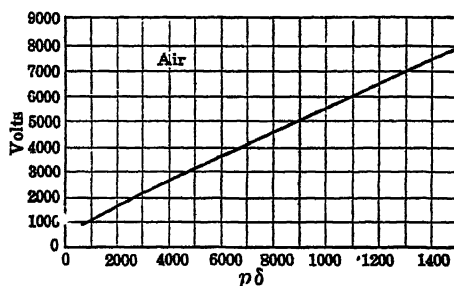


FIG. 194B.

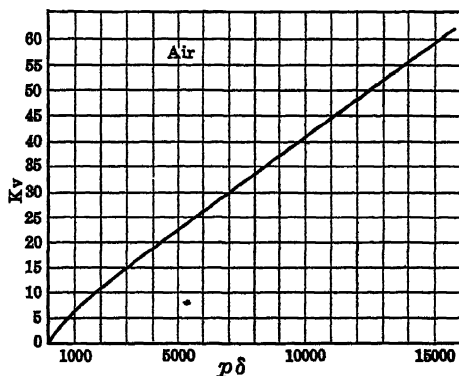


FIG. 194C.

If we are dealing with uniform fields  $X\delta = V_s$ , the sparking potential. Thus we should expect that the sparking potential could be evaluated from the functional equation

$$f\left(\frac{V_s}{p\delta}\right) = \frac{1}{p\delta} \log \frac{1}{\phi\left(\frac{V_s}{p\delta}\right)}.$$



This is known as Paschen's <sup>2,3,5,6</sup> law, and it is seen that on this basis  $V_s$ , the sparking potential, is a function of  $p\delta$ , i.e.,  $V_s = F(p\delta)$ . This has been found experimentally to be true. The law was discovered by Paschen <sup>2</sup> experimentally in 1889. It was proved theoretically correct by Townsend <sup>3</sup> and others <sup>5,6</sup> on general considerations, irrespective of the mechanism assumed. It is obvious from the deduction that it holds for uniform fields or non-uniform fields caused by gap geometry. Varney <sup>4</sup> has shown that it holds *only approximately* when the fields are distorted by space charge, as might be expected.<sup>69</sup> It has been verified experimentally over a large range of working conditions within the limits of accuracy, which in no case exceed 1 per cent. The form of  $V_s = F(p\delta)$  can be seen from the curve of Figs. 194A, B, and C, taken from Meyer <sup>7</sup> and Paschen as given by Schumann.<sup>5</sup>

The physical interpretation of this law is relatively simple. The product  $p\delta$  represents in essence the number of molecules to be encountered by an ion or electron in crossing the gap. Then the number of ions produced and the value of  $V_s$  at which enough are produced must depend only on  $p\delta$  and the values of  $\alpha$  and  $\gamma$ .

For large  $p\delta$ , small values of  $\alpha$  and  $\gamma$  or low values of  $X/p$  suffice, as the ions can build up to the number needed cumulatively.

#### 4. THE CHARACTERISTIC CURVE FOR SPARK DISCHARGE

The curve of  $V_s$  plotted against  $p\delta$  for very large values of  $p\delta$  is *nearly* a straight line of constant slope. This condition arises from the circumstance that, for low values of  $X/p$ ,  $\alpha/p$  is nearly an exponential function of  $X/p$  (see page 344). Hence, if  $\alpha/p = A_1 e^{B_1 X/p}$ , we find that

$$V_s = \frac{p\delta}{B_1} \left[ \log \left( \frac{1}{A_1 p\delta} \log \frac{1}{\gamma} \right) \right],$$

so that  $V_s$  is very little dependent on changes in  $\gamma$  and does change somewhat more slowly than proportional to  $p\delta$  since a factor  $\log 1/p\delta$  comes in.

In the region of  $X/p$  somewhat above the linear regime the increase in  $\alpha/p$  as a function of  $X/p$  is nearly parabolic for many gases (see page 347), so that  $\alpha/p = A_2(X/p - B_2)^2$ . Here then

$$V_s = B_2 p\delta + \left( \frac{1}{A_2} \log \frac{1}{\gamma} \right)^{1/2} (p\delta)^{3/2}.$$

The increase of  $V_s$  with  $p\delta$  is then somewhat more rapid than linear, or the curve for  $V_s$  falls more rapidly as  $p\delta$  decreases.

When one reaches regions where  $p\delta$  is small and where  $\alpha/p$  changes linearly, or even more slowly than  $X/p$ , the inadequacies in the values of  $\alpha$  and  $p\delta$  must be compensated by an increase in  $\gamma$ . It is therefore

not surprising to find that, since  $\gamma$  and  $\alpha$  increase but slowly with  $X/p$ , higher values of  $X/p$  and thus higher values of  $V_s$  are required to produce the spark. Thus the  $V_s - p\delta$  curve passes through a minimum to rise sharply at lower values of  $p\delta$ , as seen in Fig. 194A. The effect of this minimum is strikingly illustrated in a discharge tube with electrodes between which there are two paths which a discharge can take, a long one and a short one. At higher pressures the discharge takes the shorter path, but as the pressure goes down the discharge ceases over this path and at a suitable voltage takes place across the longer path. Thus at a certain pressure,  $p$ , the voltage given does not suffice in the short path to give an adequate  $p\delta$  but may give a spark in the longer path.

In the region near the minimum  $V_s$  in some gases, where  $\alpha/p$  is approximately given by

$$\frac{\alpha}{p} = \left( \frac{A_4 X}{p} \right)^{1/2} - B_4,$$

as seen in Chapter VIII, we have

$$V_s = \frac{B_4^2}{A_4} p\delta + \frac{2B_4}{A_4} \log \frac{1}{\gamma} + \frac{1}{p\delta} \frac{\log^2 (1/\gamma)}{A_4}.$$

Here, depending on  $\gamma$ ,  $B_4$ , and  $A_4$ , we see that the equation leads to a minimum. This must occur whenever  $\alpha/p$  varies more slowly than linearly with  $X/p$ . It is seen that in this region  $\gamma$  plays an important role, and we would expect sparking potential to be quite sensitive to  $\gamma$ .<sup>8,9</sup> At high pressures and in long gaps (large  $p\delta$ ),  $V_s$  is quite insensitive to the value of  $\gamma$ , and sparking appears to be somewhat independent of electrode material, unless extreme experimental care is taken. In certain cases it is entirely independent of  $\gamma$ .<sup>10</sup>

## 5. THE MINIMUM SPARKING POTENTIAL

The real existence of a minimum sparking potential has been observed experimentally for all gases and must probably be expected in all cases. Thus, for example, *a spark will not pass below about 275 volts in air, no matter what the conditions.* Similar values hold for other gases, being lowest for the inert ones, especially when slightly impure, such as He or Ne with A or Hg present, and for electrodes of low work function. The value of the minimum can be found by differentiating  $V_s$  with respect to  $p\delta$  and setting the derivative equal to zero. This procedure makes the minimum occur roughly at

$$\frac{dV_s}{d(p\delta)} = 0 = \frac{B_4^2}{A_4} - \frac{\log^2 (1/\gamma_m)}{A_4} \frac{1}{(p\delta_m)^2},$$

or

$$p\delta_m = \frac{\log (1/\gamma_m)}{B_4^2},$$

so that

$$V_{sm} = \frac{3B_4}{A_4} \log \frac{1}{\gamma_m} + \frac{B_4}{A_4} \frac{1}{\log (1/\gamma_m)},$$

for the gas  $N_2$  and some others. It is clear that  $V_s$  will depend on the values of  $A_4$ ,  $B_4$ , and  $\gamma_m$ , all of which are functions of the characteristics of the gas and the secondary processes in the gas or at the cathode. It can hardly be expected, then, that, except with unusual care, the values for  $V_{sm}$  and  $p\delta_m$  obtained by various observers should agree, for there is little or no control of the value of  $\gamma_m$  which can change in the process of illumination<sup>10</sup> or successive spark passage. It is *most important*, however, to realize that *the minimum sparking potential exists and that below it a spark cannot pass*. This fact is sometimes overlooked in practical application.

Values of the minimum sparking potential,  $V_{sm}$ , have been obtained for common gases in the past by many workers. For the reasons given above, the values for the same gas and electrodes of different observers agree only in order of magnitude. Such values need hardly be cited. These values and their significance can be seen in Table XXXIV compiled from recent data under *pure* gas conditions.<sup>11,12</sup>

TABLE XXXIV

| Gas              | Cathode        | $p\delta_m$<br>in mm $\times$ cm | $V_{sm}$ |
|------------------|----------------|----------------------------------|----------|
| A                | Pt (clean)     | 1.45                             | 195      |
| A                | Pt (bombarded) | .. .                             | 275      |
| A                | Na             | 1.0                              | 95       |
| A *              | Fe             | 1.45                             | 265      |
| H <sub>2</sub>   | Pt             | 1.25                             | 295      |
| H <sub>2</sub>   | Pt + NaH       | ....                             | 221      |
| H <sub>2</sub>   | Na             | 1.0                              | 175      |
| Hg <sup>61</sup> | Ni             | ...                              | 380      |
| Hg <sup>61</sup> | Fe             | ....                             | 520      |
| Hg <sup>61</sup> | Hg             | ....                             | 330      |
| N <sub>2</sub>   | Pt             | 0.75                             | 275      |
| N <sub>2</sub>   | Na             | 0.6                              | 200      |
| Ne *             | Fe             | 3.0                              | 244      |

The starred values are Penning and Addink's values in A and Ne of the same purity as the others using an Fe cathode. In A the values of  $V_s$  otherwise all agree except at the minimum. Recently Jones and Galloway and Gregorovici<sup>61</sup> have studied Hg vapor under relatively

clean conditions, giving the values shown in the table. Ehrenkrantz<sup>11</sup> has shown that the addition of Na to pure A, H<sub>2</sub>, and to N<sub>2</sub> gases with Pt cathodes changes the minimum quite markedly, as shown in the table. It must be noted that even with the non-reactive gas A the change in the surface produced by bombardment by positive ions in discharge so alters  $\gamma$  as to make  $V_s$  nearly 30 per cent higher. It is also seen how relatively little pure Ne and pure A differ for the same electrodes, while a change from Pt to Na in A changes  $V_s$  by 50 per cent.

## 6. CATHODE SURFACE AND SPARKING POTENTIAL

The question of the role of  $\gamma$  or the second Townsend coefficient in initiating sparks is nevertheless a peculiarly involved one. Experiment has shown that for longer sparks ( $> 3$  mm) in air at atmospheric pressure it is impossible to detect with any certainty the effect of cathode material on  $V_s$ . This, in fact, gave Townsend a strong argument in favor of his theory of the mechanism since his  $\beta$  as originally conceived was a *gas-dependent constant* and independent of cathode material. Holst and Oosterhuis,<sup>8</sup> however, showed that, at lower pressures (i.e., near the minimum) in pure gases where  $\gamma$  could be controlled to some extent, the value of  $\gamma$  was very important in giving a value to  $V_s$ . Neuman<sup>13</sup> in the writer's laboratory in 1927 showed that in pure A where Na produced a lowering of some 20 per cent on an Ni cathode at pressures of 1 mm the sparking potential at 20 mm pressure and above was the same for A irrespective of the presence of Na on the Ni cathode. Ehrenkrantz<sup>11</sup> tried to repeat these experiments in modified form with better conditions for the evaluation of a true  $V_s$ . She found that, although the lowering of  $V_s$  for Pt by Na in A at the minimum was 50 per cent, it was still 7.5 per cent lower at a  $p\delta$  of 240 mm  $\times$  cm or at 24-mm pressure with a 1-cm gap.

Using Posin's<sup>14</sup> data for N<sub>2</sub> with Hg contamination, the writer<sup>15</sup> showed that on theory at 1-mm pressure at 5.0-cm distance with  $X/p = 120$  the value of  $V_s$  should be 5 per cent below the value for a spark with a surface for which  $\gamma$  was half as great and 14 per cent for one for which  $\gamma$  was one-fifth as great. These facts indicate that both theory and experiment lead to a very small dependence of sparking potential on  $\gamma$  at higher values of  $p\delta$ .<sup>\*</sup> When in general we consider that the previous work was done in many cases with Hg-coated cathodes from the gauges and that the purity of the gases left much to be desired it is also probable that the conclusions drawn from previous work are relatively uncertain. In fact, up to the present no data are available for the test of this aspect of the theory. There as yet are no consistent sets of measurements of  $V_s$ ,  $p\delta$ ,  $\alpha/p$ , and  $\gamma$  over an *extended range* of

<sup>\*</sup> There is now much evidence that at least one of the mechanisms active in sparks exceeding 1-cm length in air at 760 mm is a purely gas-dependent one involving photoionization in the gas.<sup>16</sup>

$p\delta$  which enable us to test the theory properly. This is due to two circumstances. For higher values of  $p\delta$ ,  $X/p$  is low, and values of  $\gamma$  are not observed with present techniques below an  $X/p$  much less than 100.<sup>69</sup> Furthermore, the earlier results with Hg contamination and ill-defined cathodes are of little value from the present-day point of view.

## 7. THE EXPERIMENTAL TEST OF TOWNSEND'S SPARKING CRITERION

The theory given above for the curve between  $V_s$  and  $p\delta$ , however, has been frequently tested in a rough fashion and for limited regions. This has come about through the circumstance that, dating from the initiation of these investigations by Townsend, the arrangement for evaluating  $\alpha$  and  $\beta$  or  $\gamma$  permits of a simultaneous determination of  $V_s$ . Since  $V_{sm}$  is very much dependent on  $\gamma$ , which is varied by sparking, the agreement to be expected in this region is far from good. It does give a value of  $V_{sm}$  which agrees roughly with the value of  $p\delta_m$  predicted, but the value of  $V_{sm}$  computed is usually not the same as experiment by tens of per cent, as will later be seen in Hale's<sup>18</sup> results.

The tests have in general been *limited* to regions above  $p\delta_m$  but of low  $p$ , larger  $X/p$ , and large  $\alpha/p$ , since proper values of  $\gamma$  are hard to obtain at low  $X/p$ .<sup>69</sup> In this region a spark in the commonly accepted sense frequently does not occur, but a glow discharge suddenly breaks, and this circumstance has led to the rather modified definition of a spark given in section 1. In this case, as will later be seen, the criterion for a spark,  $1/\gamma = e^{\alpha\delta}$ , may more nearly be expected to apply. Hence, in some cases, above  $V_{sm}$  but at high  $X/p$  and low  $p$ , agreement may have actually been fairly good for a *limited region*. In fact, agreement between the observed  $V_s$  and that computed from  $\alpha$  and  $\gamma$  has at times appeared sufficiently good to encourage a number of workers to evaluate  $\alpha$  and  $\gamma$  from the measurements of  $V_s$  and  $p\delta$ .<sup>63, 19, 17, 18, 12</sup>

This *practice is of an exceedingly doubtful validity* for the following reasons: First, as will be seen, it is probably wrong in principle to use Townsend's criterion for a spark as being really applicable to any of the very complicated mechanisms now known to occur. Secondly,  $V_s$  is very difficult to measure, and the errors inherent in such measurements make errors in the measurements of  $\gamma$  highly uncertain and large. Third, owing to the nature of the equations,  $V_s$  is, except near the minimum, *somewhat if not very insensitive to changes in  $\gamma$* , so that a large range of values of  $\gamma$  can yield nearly the same values of  $V_s$ . Finally,  $\alpha$  and  $\gamma$  are so functionally related that if we are not sure of values of  $\alpha$  there are many combinations of  $\alpha$  and  $\gamma$  that can give closely the same value of  $V_s$ .<sup>11</sup> On this basis we can expect that the use of the  $V_s - p\delta$  curve to evaluate  $\gamma$  can give values of  $\gamma$  which are correct only in order of magnitude, and the curves for  $\gamma$  evaluated as a  $\phi(X/p)$  from the relation are *smoothed average* values of approxi-

mately the correct order of magnitude if *good values of  $\alpha$  are taken from other data*. Any finer variations of  $\gamma$  with  $X/p$  as observed by Hale and Bowls<sup>20</sup> will pretty well be wiped out or ignored in plotting the curves. This is nicely illustrated in the curves of Engstrom<sup>19</sup> and of Schoefer<sup>17</sup> for Ba in A when compared with the directly measured values of  $\gamma$ , which show fluctuations naturally interpreted by Engstrom as inherent in his measurements of  $\gamma$ , but which may be real; see Fig. 192. In A with Cs-Ag-O surfaces<sup>10</sup> the agreement between  $\gamma$  as evaluated by both methods in the same tube using independently observed values of  $\alpha$  is seen in Fig. 191.

It will not pay to present any of the earlier data to indicate the type of agreement observed between theory and experiment. There is ample material obtained more recently with better techniques for this purpose. Of these, one of the most complete sets of data over an extended range comes from Posin's rather extensive test of the theory in Hg-contaminated  $N_2$ . Using values of  $\gamma$  for three separate regions of variation of  $\alpha/p$  as a function of  $X/p$  in  $N_2$ , two values at very high values of  $X/p$ , and a value each at lower values of  $X/p$ , and employing the equations given on page 346 and 347, Posin<sup>14</sup> was able to plot the curve

for  $V_s$  as a function of  $p\delta$  in  $N_2$  up to  $p\delta = 2000$ . This is shown in Figs. 195A and B. The continuous curve in Fig. 195A is Posin's. The dotted curve gives Hurst's observed values, while the dot-dashed curve gives Strutt's<sup>21</sup> values. There are no experimental data for the higher  $p\delta$  given in Fig. 195B. The break in the curve occurs where the functional variation of  $\alpha/p$  with  $X/p$  is not known. It is seen that the trend of the curve is that predicted by theory and similar to that observed experimentally.

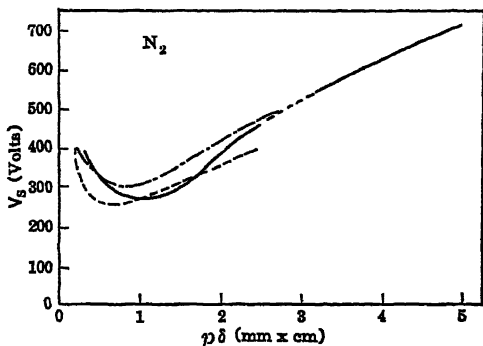


FIG. 195A.

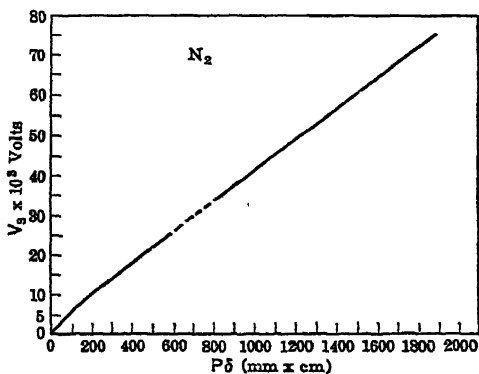


FIG. 195B.

In 1937 Ehrenkrantz<sup>11</sup> used pure  $N_2$  gas and measured  $V_s$  both for a Pt cathode and for a Pt cathode coated with Na. The results for Na were not tested by theory, since the spark in Na *was always preceded by a glow discharge and relatively heavy predischARGE currents*. When Ehrenkrantz used Bowls' data for  $\alpha$  and  $\gamma$  also taken in comparatively Hg-free  $N_2$  to compute the theoretical curve for  $V_s$  as a function of  $p\delta$ , she found it difficult to get any good agreement. In part this must be ascribed to the rather incomplete and irregular values of  $\alpha/p$  at the lower values of  $X/p$  corresponding to values of  $p\delta$  above  $p\delta_m$ . By trying various functional forms of  $\alpha/p = f(X/p)$  which would fit Bowls' observed points, the best expression which

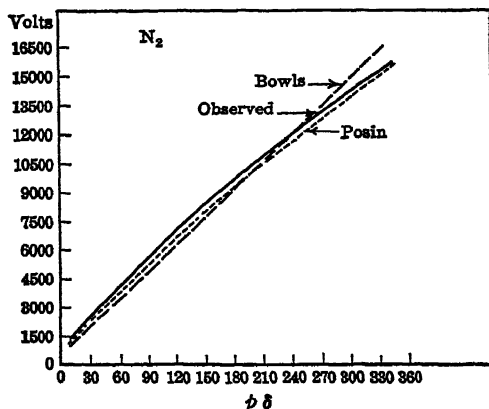


FIG. 196.

could be found for  $V_s$  as a function of  $p\delta$  was that shown by the dashed curve of Fig. 196. The observed curve is the full curve, while Posin's data with Hg-contaminated  $N_2$  gave the dotted curve. It is seen that with entirely different values of  $\gamma$  and  $\alpha/p$  produced with and without Hg contamination the curves lie surprisingly close together. It is further seen that the form of Posin's curve is closer to that of Ehren-

krantz than Bowls' is, and that the agreement is far better, even though Ehrenkrantz had entirely different gas and electrodes to deal with.

As a final example the beautiful results of Hale<sup>12</sup> may be used for computing  $V_s - p\delta$  curves in  $H_2$  both for Pt electrodes and for NaH electrodes. Hale's results also yielded values of  $V_s$  so that his values in pure  $H_2$  may be compared with those of Ehrenkrantz. Hale's values of  $V_s$  were single values taken at the end of each  $\log i/i_0$  curve. The curves are carried out only as far as  $p\delta \sim 36$  with  $p \sim 5$  mm and less. In Figs. 197A, B, and C we have the curves of Ehrenkrantz in  $H_2$  with Pt and NaH cathodes as full lines respectively. The dashed lines and crosses are Hale's observed values of  $V_s$ ; the dotted lines with circles are Hale's curves computed from his values of  $\alpha$  and  $\gamma$ . The character of the agreement obtained is clearly seen. In form, trend, and approximate values the agreement appears satisfactory. Yet at high  $X/p$ , in  $H_2$ , Ehrenkrantz' values for  $V_s$  lie 5 per cent below those of Hale. This could be ascribed to differences in gaseous purity, the gas of Ehrenkrantz being purer in a minor degree. Ehrenkrantz

obtained her points as averages over many sparks whereas Hale had only occasional points and may not have observed the minimum value. His values are too consistently high to make this likely, however. In the case of Na, Hale's NaH surface would readily account for the difference in  $V_s$  observed at lower pressures as Ehrenkrantz used a

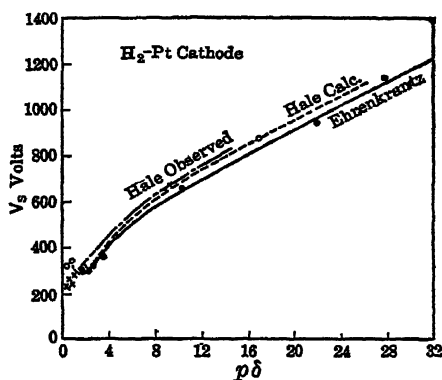


FIG. 17A.

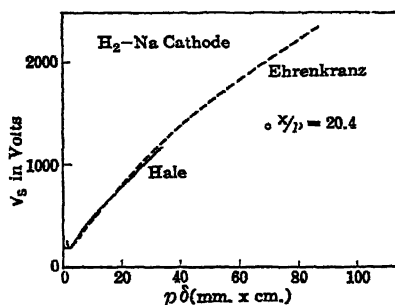


FIG. 17C.

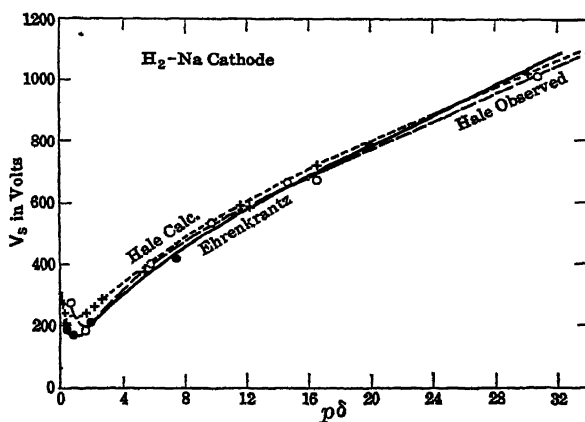


FIG. 17B.

surface with more Na and less NaH. As regards the computed values for  $V_s$  in comparison to Hale's observed values, agreement at higher  $p\delta$  is good for Pt- as well as for NaH-coated electrodes. However, the agreement becomes unsatisfactory near the minimum. There is no reason at once obvious for this difference. But in all this comparison it must be remembered that, if  $\gamma$  varies over the surface, sparks will occur most likely at the points of the lowest  $\gamma$  and thus not be consistent with the average value of  $\gamma$  measured over the whole area illuminated in



measurement. In Hale's NaH surface, this could well account for the result.

The sparking potentials observed by Hale did not show any of the peculiarities to be expected from the observed peaks of  $\gamma$  as a  $f(X/p)$ . For the smaller changes in  $\gamma$ , as with most peaks with Na, the insensitiveness of  $V_s$  to  $\gamma$  could account for this fact. For the large peak with Na at low  $X/p$ , however, the value of  $V_s$  should have been 25 per cent lower than the observed curve at  $p\delta$  about 28; see the point at  $p\delta = 60$ , Fig. 197C. However, using the average value at the base of the peak, the plotted curve was obtained. Since the peak is so very narrow it is probable that, *unless  $V_s$  were measured at just the value of  $X/p$  (20.4), where the peak occurred, its influence on the value of  $\gamma$  and of  $V_s$  might be negligible.* With such peaks there should be values of  $V_s$ , at the *correct  $X/p$* , that do not fit on the smooth curves at all and are abnormally low. It is difficult to vary conditions over such a range that  $V_s$  falls into the desired region of  $X/p$ . It may be such circumstances as these that give the occasional sparks which break at unexpectedly small potentials.

It is thus seen that, although in a limited range the Townsend sparking criterion leads to better than qualitative agreement with observation if approximate values of  $\alpha/p$  and  $\gamma$  are used, it never gives good *quantitative* agreement and should not do so. It could be argued that this is to be ascribed to the relative inaccuracies the values of  $\alpha/p$  and  $\gamma$ , the variability of  $\gamma$  over a surface, as well as the inaccuracies in the observed values of  $V_s$ . However,  $V_s$  can be measured within 1 or 2 per cent and  $\alpha/p$  and  $\gamma$ , with uniform surfaces, should, as used in the equations, give values that are fairly good. It is therefore more *probable that the theory really does not hold much more than qualitatively, except in a limited region*, and that otherwise it is applicable only in order of magnitude. It is therefore essential that one examine with greater care the sparking criterion of Townsend that has led to the theory so far discussed.

#### 8. A FURTHER CONSIDERATION OF THE SPARKING CRITERION: THE INFLUENCE OF THE INITIAL CURRENT

The expressed view as to the rather illusory and fortuitous agreement of the sparking criterion with observation as revealed by measurements in a limited range of  $p\delta$  is further borne out by a more careful scrutiny of the sparking criterion which results when one studies the influence of  $i_0$  on the value of  $V_s$ .

According to the theory of Townsend,

$$i = i_0 \frac{e^{\alpha\delta}}{1 - \gamma e^{\alpha\delta}}.$$

Now, if one sets the criterion of a spark as being the condition  $1/\gamma = e^{\alpha\delta}$ ,

this condition makes  $V_s$  independent of  $i_0$ . For a time, experiment appeared to bear out this conclusion, and  $V_s$  was found in a *limited range of values* of  $i_0$  to be independent of  $i_0$ . In 1934 H. J. White,<sup>22</sup> however, discovered that, when  $i_0$  was increased  $10^6$  times or more, by using a naked spark for an ultraviolet source instead of a quartz Hg lamp, the value of  $V_s$  was reduced by about 10 per cent. Similar results were independently obtained by Rogowski and Walraff<sup>23</sup> some months later. Now in these cases the spark breakdown occurred in  $10^{-8}$  second. Thus the phenomenon could *not be ascribed to the gradual space-charge accumulation of positive ions at the cathode* which would be required were the lowering to be ascribed to a change in  $\alpha/p$  by space charge resulting from too high a current density, as suggested by Varney, White, Loeb, and Posin.<sup>4</sup> In longer times of breakdown such an effect could be expected at high pressure. Since  $i_0$  cannot always be ignored, we are led to regard much more closely the criterion of Townsend for a spark, as Loeb<sup>15</sup> did. In so doing we shall discover one of the causes of the inadequacy of the Townsend criterion. Townsend had crassly assumed that, when  $1/\gamma = e^{\alpha\delta}$ , irrespective of  $i_0$ , a spark must ensue, for then the current

$$i = i_0 \frac{e^{\alpha\delta}}{1 - \gamma e^{\alpha\delta}}$$

becomes indefinitely great no matter how small  $i_0$ . Now such a criterion is mathematically meaningless and indeterminate. From the physical viewpoint, at least one electron is needed to initiate the discharge, but it is impossible to identify such an electron with any sensible interpretation of  $i_0$ . The reason for this difficulty is quite simple and seems to have been ignored up to the present. The equation deduced *was never intended to be a condition for a transient phenomenon such as a spark. It is a steady-state equation* for current increase by primary and secondary processes in a gap.

It is clear, of course, that for a given set of values of  $\alpha$ ,  $\gamma$ ,  $\delta$ , and  $i_0$  there will result a definite value of the current  $i$ , no matter how large. If at a certain value of  $i = \bar{i}$  the current becomes self-sustaining without any external electron current  $i_0$  as an arc or a glow, one might calculate the values of  $i_0$ ,  $\alpha$ ,  $\gamma$ , and  $\delta$  which would raise  $i$  to the value  $\bar{i}$ . In this case one *ideally would not expect a spark to occur*. All that would *ideally* ensue is that, as  $\delta$  was increased for a likely set of values of  $i_0$ ,  $\alpha$ , and  $\gamma$ , the current would increase smoothly to  $\bar{i}$ , and after removal of  $i_0$ , it would continue. In reality such an ideal sequence does not occur in nature. What does occur is that as  $\delta$  or  $V$  is increased  $i$  increases to some value  $\bar{i}$  which marks the beginning of current instability. At this current  $\bar{i}$ , *space-charge accumulations suddenly develop, or existing ones alter*, so that, for the constant potential applied,  *$i$  changes abruptly to some larger value and continues at this*

value *in the absence of*  $i_0$ . It is this abrupt transition that defines the spark in its broader aspect. At higher pressures the transition is very striking and marked. At lower pressures diffusion and the slower variation of  $\alpha/p$  with  $X/p$  make conditions such that the alteration of space-charge distribution becomes less and the transition from dark current to glow is perceptible but not striking.

Ignoring for the present the exact value or the significance of the value of the current  $\bar{i}$  which can initiate a spark, but utilizing the concept of a critical current  $\bar{i}$ , Loeb<sup>15</sup> has calculated the effect of  $i_0$  on the sparking potential. If one has two photoelectric currents  $i_0$  and  $i_{00}$  with the same gap length  $\delta$ , they will yield a gap current  $\bar{i}$  when the sparking potentials  $V_{s_0}$  and  $V_{s_{00}}$  are reached, which give values of  $\alpha$  equal to  $\alpha_0$  and  $\alpha_{00}$ . Since under these conditions

$$\bar{i} = \frac{i_0 e^{\alpha_0 \delta}}{1 - \gamma e^{\alpha_0 \delta}} = \frac{i_{00} e^{\alpha_{00} \delta}}{1 - \gamma e^{\alpha_{00} \delta}},$$

we can write that

$$\frac{1}{\delta} \log \frac{i_{00}}{i_0} = \frac{1}{\delta} \log \frac{1 - \gamma e^{\alpha_{00} \delta}}{1 - \gamma e^{\alpha_0 \delta}} + (\alpha_0 - \alpha_{00}).$$

If one for convenience assumes  $(1 - \gamma e^{\alpha_{00} \delta})/(1 - \gamma e^{\alpha_0 \delta}) \sim 1$ , the sparking values of  $\alpha_0$  and  $\alpha_{00}$  in the two gaps will be related by the simple expression  $\log i_{00}/i_0 = \delta(\alpha_0 - \alpha_{00})$ . In this event it can be shown that the resulting fractional change in sparking potential will be

$$\frac{V_{s_0} - V_{s_{00}}}{V_{s_0}} = p\delta \frac{\log(i_{00}/i_0)}{2A_2 V_{s_0}^2},$$

in the range of  $V_s$  and  $(X/p)_s$  used by White. With White's estimated value of  $i_{00}/i_0 = 10^5$  when 4 per cent lowering of  $V_s$  was observed by him, the equation above yields a lowering of 1.7 per cent. The discrepancy is surprisingly small. White also found that  $\log i_{00}/i_0$  varied linearly with  $(\alpha_0 - \alpha_{00})$ , but the observed slope was not exactly  $1/\delta$ . The calculation above, however, assumes the quantity  $(1 - \gamma e^{\alpha_{00} \delta})/(1 - \gamma e^{\alpha_0 \delta}) = 1$ , which may be far from correct. Thus the agreement need not be taken as too significant.

It is seen that, in the necessity of explaining White and Rogowski's observation concerning an effect of  $i_0$ , we have been forced to modify the rather simple condition of Townsend quite radically, for instead of attempting to use the equation as a steady-state equation, which it is, Townsend had applied it to a discontinuous process, making it impossible of interpretation. In order to arrive at the interpretation above, we have been led to *assume a value of current  $i$  as setting a limit to stability*. Under these circumstances the value of the sparking potential must depend not only on the condition that  $1/\gamma$  approach  $e^{\alpha \delta}$  in value *but on*  $i_0$  *as well*. On the other hand, the condition  $1/\gamma = e^{\alpha \delta}$  is

no longer the exact criterion for a spark, and *one expects  $V_s$  to vary continuously with  $i_0$* . This is not experimentally observed, and it is only with values of  $i_0$  of exceedingly large magnitudes that any variation is observed. In this case, however,  $\bar{i}$  being unknown and unpredictable by theory, there is no reason for the rough correspondence between the  $V_s - p\delta$  curves and theory even in a limited region.

It is quite possible that a study of  $\bar{i}$  just before the spark is reached might give us some clue in this question. It is because of the circumstance, however, that in the region of instability, which for an entirely different reason is above  $\frac{1}{\gamma} = e^{\alpha\delta}$ , the current  $i$  increases so exceedingly rapidly with  $\alpha$ , or  $V$  and  $\delta$ , that we are likely to confuse criteria or events occurring at perhaps widely different values of  $i$ . These events become experimentally indistinguishable, owing to the very small changes in  $V$  and  $\delta$  which cause them. On the other hand, as was correctly stated, the equation discussed is in no sense intended for the purpose of setting a sparking criterion, as it is a *steady-state equation*, so that it at once leads to indeterminate conditions when we try to utilize it otherwise.

## 9. THE CONDITION FOR SELF-SUSTAINING DISCHARGE AND SPARKING THRESHOLD

Another consideration has confused the issue. This is that the condition  $1/\gamma = e^{\alpha\delta}$  has an entirely different and perfectly valid significance having nothing to do with the *current* equation. The new significance results from the fact that the equation *represents the condition for a self-sustaining discharge following the spark*. For if  $1/\gamma = e^{\alpha\delta}$ , then for each ion created in the gap by ionization by electron impact there are created by a secondary process at the cathode or elsewhere enough electrons to maintain  $\gamma e^{\alpha\delta}$  at its existing value. One may see this at once if one recognizes that  $e^{\alpha\delta}$  is the multiplication of 1 electron in the gap. Hence  $1/e^{\alpha\delta}$  is the fraction of an electron,  $\gamma$ , needed to be supplied by a secondary process to keep the product of  $\gamma e^{\alpha\delta} = 1$  and *maintain the discharge*. If  $\gamma e^{\alpha\delta}$  is greater than unity, the current will increase. If it is less, the current will cease unless externally stimulated by an  $i_0$ . Since current increases when  $\gamma e^{\alpha\delta} > 1$ , space charges increase until a rearrangement at a new current regime abruptly sets in with  $\gamma_1 e^{\alpha\delta} = 1$  as a new discharge. In this readjustment one can recognize the spark. This perfectly correct interpretation of the *end result of a spark*, probably first proposed by Holst,<sup>8</sup> has been thus confused with the Townsend current equation preceding the spark and hence has led to Townsend's definition of a spark. Actually, again, this equation is probably too simple to apply to any real discharge. However, it must apply to the cathode region of a glow discharge or an arc in a rough fashion.

The circumstance that, before a stable discharge occurs, the condition  $\gamma e^{\alpha\delta} = 1$  represents the condition for the threshold of instability probably furnishes a clue to the reason for the apparent general and rough agreement between the observed sparking potential and Townsend's theory. For, since  $\alpha/p$  increases very rapidly with  $X/p$  i.e., as  $e^{B(X/p)}$  or  $(A(X/p) - B)^2$ , the quantity in the region near  $\gamma e^{\alpha\delta} = 1$  increases *exceedingly rapidly* with  $X/p$ ,  $V$ , or  $\delta$ . Hence, even though the quantity  $\gamma e^{\alpha\delta}$  may have to increase well beyond unity before a breakdown ensues, the observed change in the value of  $V$  or  $\delta$  may be indistinguishably small. This condition is thus probably the cause for the rough agreement between the observed  $V_s - p\delta$  curves and those calculated from the condition  $1/\gamma = e^{\alpha\delta}$ .

*Before a spark occurs* and space charges alter the values of the steady-state photoelectrically stimulated current, it is clear that, when values of  $\alpha$ ,  $\gamma$ , and  $\delta$  are reached which exceed  $\gamma e^{\alpha\delta} = 1$ , *one propitiously placed electron* will cause the current to grow indefinitely and thus build up the condition where transition occurs. Whether the breakdown occurs just at the point at which  $\gamma e^{\alpha\delta} = 1$  must depend largely on conditions in the gap, for if by any chance the processes of electron multiplication lead to space charges which can in any way prevent the secondary emission from reaching its expected value the spark will be choked off. Under such conditions a higher value of  $V$  than that corresponding to the condition  $\gamma e^{\alpha\delta} = 1$  will be required to overcome this difficulty. Such conditions indubitably occur under different circumstances (especially at higher pressures and in longer gaps or in distorted fields such as exist in the negative point or wire corona). At lower pressures these inhibiting conditions due to space charge are less probable. Thus, in the region where Townsend's criterion  $\gamma e^{\alpha\delta} = 1$  *appears to give approximately the observed values of the*  $V_s - p\delta$  *curve*,  $V_s$  may not have to exceed the calculated  $V$  by very much.

It is seen that, where the inhibitory effects of space charge prevent sparks at just  $\gamma e^{\alpha\delta} = 1$ , fortunate time and space sequences of electron production may occasionally produce spark transitions at values of  $V$  more nearly equal to that condition. Since such events can take place by means of any one of a large number of different possible combinations of happenings of a purely random nature, it must be clear that observed spark transitions take place over a considerable range of values of  $V$ . Some of those combinations operative at low values of  $V$  will be extremely rare, while those which will work at higher values of  $V$  are more and more frequent. By making the conditions as nearly uniform as possible, i.e., using a constant relatively weak ionization current  $i_0$ , some approach to a fairly definite mean value of  $V_s$  under operating conditions may be had. By increasing  $i_0$  to very large values the rarer happenings are more likely in reasonable time intervals and the *average* experimentally observed values of  $V_s$

may be lowered materially. This question will be considered later in more detail.

It is thus clear that *there is no single and unique value of the sparking potential  $V_s$* . Since  $\gamma$ ,  $\alpha$ , and  $1 < \gamma e^{\alpha \delta}$  vary so very rapidly with  $V_s$  and  $\delta$ , the fluctuations of  $V_s$  and  $\delta$  do not appear to be as large as they might be. This, taken together with the difficulty of experimental control, makes  $V_s$  *appear to have a definite value, and we have the illusion of a fixed sparking potential*.

We are now in a position to fix the real criterion for the lower threshold of a spark transition. Below the condition  $\gamma e^{\alpha \delta} = 1$  *no spark can occur*. At  $\gamma e^{\alpha \delta} \geq 1$  a spark may occur *provided that one electron appears in the gap to start the spark*. The observed sparking potential  $V_s$  will be determined by the values of  $\alpha$ ,  $\gamma$ , and  $\delta$  which in a given arrangement will make  $\gamma e^{\alpha \delta}$  *sufficiently greater than unity* so that with the occurrence of initiating electrons in time and space the transition has a fair chance of taking place. Sparks will occur below such a  $V_s$  more and more rarely as  $V$  decreases.

It is seen that while this condition precludes any calculation of the exact sparking potential it gives a *threshold* value in agreement with earlier studies. It is entirely free from the complications involving the significance of an  $i_0$ . It makes the sparking potential the statistically varying quantity observed in practice. It makes the spark propagation basically dependent on the propitious appearance of a single electron, thus limiting the spark path to no more than the area required by the single electron avalanche processes observed. It allows for the statistical fluctuations in time of occurrence and in frequency of occurrence as a function of  $V$  that are observed, as will later be seen. Finally, it will enable us to understand the conditions which produce gap breakdown in the very short time intervals observed. This is *not* possible under the previous interpretation.

#### 10. SPARKING THRESHOLD AND SPARK BREAKDOWN OF A GAP

Before proceeding to apply this theory to the mechanism of breakdown of the plane parallel gap, a word must be said concerning the end state of the transition given by the spark. When the value of  $V_s$  has been reached, a single electron starts its career of cumulative ionization. If, in the process, it and its progeny *cross the gap* and produce sufficient positive ions and photons so that, with the electrons and ions created, the fields are such that the secondary processes at the cathode or in the gas are adequate to sustain the discharge, the spark passes.<sup>66</sup> In general this requires that there be a *continuous conducting filament or ionized path extending from anode to cathode*. At lower pressures, owing to diffusion, the conducting path may comprise as much as the area of the electrodes.

Once the conducting path is produced *and an efficient secondary*

source is established at the cathode, one of several things can happen. If the circuit resistance is high a current will flow discharging the capacity of the plates and the filament will flash up brightly and then go out. If the resistance is not too high, current will continue to flow and the ion migration in the conducting path will build up a permanent space-charge regime with a Crookes dark space and cathode fall giving some form of a stable glow discharge. If the power supply is ample and a "hot spot" can develop at the cathode the discharge may vaporize metal and produce a vapor arc or it may just continue as a gas arc. Thus, before the spark can be said to have passed: (1) *A conducting path must have formed completely bridging the gap;* (2) *an efficient source of secondary emission must be provided at the cathode;* (3) *under these conditions the conductivity produced must have been sufficient to at least discharge the electrodes.*

It is seen therefore that the occurrence of a spark depends on a good deal more than the simple realization of  $\gamma e^{\alpha\delta} > 1$  and the appearance of a single electron in the gap. It requires that a series of events following on these conditions occur in such a way as to *bridge the gap, produce a secondary emission, and remain sufficiently conducting so as to enable the existence of an end state of higher current at least sufficient to discharge the adjacent electrical capacity.* Many avalanches occur that do not succeed in bridging the gap with a conducting filament, and many of the conducting filaments fail owing to their failure to achieve a secondary emission. Just what must actually occur in the case of the spark between plane parallel electrodes at higher pressures in order that these conditions be met, at least in part, will now be seen.

## 11. THE MECHANISM OF THE SPARK

The mechanism of the spark between plane parallel electrodes may now be analyzed under these conditions as follows: Let us assume a plane parallel-plate condenser gap with an  $X/p = 41.6$  for  $\delta = 1$  in air. The observed value of  $V_s = 31,600$  volts and  $\alpha$  is about 17 as given by Sanders. This gives  $e^{\alpha\delta} \sim 2.4 \times 10^7$ , of which the first ion pair is created at 0.0407 cm from the cathode. There are 4914 ions at 0.5 cm from the cathode,  $3.66 \times 10^5$  ions 0.75 cm from the cathode, and  $1.2 \times 10^7$  ions within 0.0407 cm, or one ionizing free path, from the anode. In order to calculate the field, let us assume that the important contribution to the space charge comes from a spherical volume of positive ions of radius  $r$ , to be evaluated later. Then the field strength  $X = 4\pi qe/4\pi r^2$ .<sup>\*</sup> Here  $e$  is the electron and  $q$  is the number of positive ions in the sphere, which is  $q = \frac{4}{3}\pi r^3 N$ ,  $N$  being

<sup>\*</sup> The author desires to call attention to a blunder in the calculation of  $X$  for this case in a paper by Loeb and Kip.<sup>40</sup> The calculation here replaces the erroneous calculation there given. The correction does not materially affect the results or conclusions there given.

the density of positive ions. Accordingly we can write  $X = \frac{4}{3}\pi r N_e$ . The ion density is found by remembering that the ions are in what is essentially a cylinder of radius  $r$  equal to the radial distance of electron diffusion in progressing the  $x$  cm from the cathode across the gap. In going the distance  $x$  the positive ions created lie largely in the last two or three ionizing free paths and in a path element  $dx$  they are  $\alpha e^{ax} dx$  in number. Hence

$$N = \frac{\alpha e^{ax} dx}{\pi r^2 dx} = \frac{\alpha e^{ax}}{\pi r^2}.$$

Thus we have  $X = \frac{4}{3}\epsilon \alpha e^{ax}/r$ . According to Raether<sup>24</sup>  $r = \sqrt{2Dt}$  where  $t$  is the time of advance of the avalanche to  $x$ , and  $D$  is the coefficient of diffusion. In the case above  $r = 0.01$  cm so that  $X = 7800$  volts per cm, which is 25 per cent of the applied field. If an overvoltage of 5 per cent or an  $X/p = 43.6$  had been applied,  $\alpha$  would have been 20 and  $X$  would have been 184,000. Thus it is seen that at the conventionally observed sparking potential space charge fields in one cm advance are appreciable, and with slight overvoltages they are such that they could materially inhibit the advance of the electron avalanche towards the anode.

The avalanche will proceed to cover this distance in the relatively short time of about  $1.5 \times 10^{-7}$  second, as estimated from the electron mobility at  $X/p = 42$ . The *first* of the *new positive ions* will reach the cathode from the 0.041-cm point above the cathode in  $1.2 \times 10^{-8}$  second. Now the light produced by the spark will not be visible in the first avalanche until somewhere well beyond the halfway mark, owing to the small ionization density below this. Thus, until the second or later avalanches of electrons take place, the luminous spark streamer should not appear all the way across the gap for intervals of the order of microseconds at least, if the process depends on positive-ion migration. But studies with the Kerr<sup>25,26,27</sup> cell shutter show luminous channels well across the gap of  $\sim 1$  cm in periods of  $10^{-8}$  second. It is thus clear that the direct simple self-sustaining mechanism resulting from  $\gamma e^{ax} = 1$  and *an orderly series of avalanches* cannot be the usual mode of spark propagation. Even with the postulated *electron* velocities at  $X/p = 42$  it is difficult to get such short times of spark development, to say nothing of positive-ion migration. Hence we can be sure that the secondary electron liberation at the cathode by positive-ion impact on the cathode is *not* the mechanism by which breakdown proceeds in this case, at least until low pressures and high values of  $X/p$  are reached.

Even if we postulate a movement of *electrons* completely across the gap the *electron* mobilities are not adequate. H. J. White<sup>28</sup> has measured these mobilities in  $H_2$  and  $N_2$ , using the Kerr cell shutter, and found them to be of the order of  $3.2 \times 10^7$  and  $1.4 \times 10^7$  cm/sec at the tips of streamers. He was also able to measure the time for the



luminosity to cross the gap as a streamer. This was  $1.8 \times 10^{-8}$  and  $2.7 \times 10^{-8}$  second, respectively, in the two gases mentioned. Using the C. T. R. Wilson cloud chamber, Raether<sup>24</sup> has measured the velocity of the electron avalanche as  $1.25 \times 10^7$  cm/sec in air at 250 mm pressure, just below sparking, while the time for the breakdown of the gap at slightly higher potentials was of the order of  $10^{-8}$  second. It is possible to explain breakdown in these cases only by assuming that *the electrons do not traverse the whole gap*. Only if we picture the process of breakdown as accomplished by several electrons, each traversing but fractions of the distance along the discharge path, can we get breakdown in about one-tenth the time taken for the single electron to cross the gap. In fact, because of this difficulty, Loeb<sup>29</sup> as early as 1929 suggested that we must consider the possibility of using a succession of electron avalanches along a breakdown path, the distance of travel in each one being but short. At that time two items of information were lacking to complete the picture; the first was the knowledge as to how such avalanches could occur simultaneously, and the second was an answer to the question as to why they should occur so as to join each other in nearly straight paths. That information is now available. To see how it operates one may assume a sparking condition and follow the events in sequence.

Assume a spark gap with plane parallel electrodes having a uniform field and let it be in a gas at atmospheric pressure. Let the potential be raised to a value above the threshold at which a spark *may* pass, and assume that an electron or a negative ion finds itself somewhere near the center of the gap at the critical moment. The reason for the choice of the center of the gap is that it permits of a somewhat more complete discussion of events. Usually the electrons are liberated from the cathode. Since they ionize cumulatively and rather slowly, as seen above, the first real field distortion will appear well into the gap. If an ion had appeared and not an electron, the ion would have had to await fields of considerably higher value than  $X/p = 42$  before it would be likely to shed its electron. Loeb<sup>30</sup> has shown that at an  $X/p = 90$  the negative ion loses its electron. Occasional impacts at an  $X/p = 60$  might liberate the electron. Flegler and Raether<sup>31</sup> in their cloud track studies have differentiated between discharges initiated by ions which must lose their electrons and the initial electrons and have observed that higher values of  $V_c$  are required in the former case.

Assuming, then, an electron in mid gap in a field sufficiently high, one can reason as follows: The electron moves toward the anode and cumulatively ionizes as it goes. In some 3 or 4 mm or less it has produced some hundreds to thousands of new electrons and ions. These are concentrated along a narrow path in the field direction. Because of the high electron mobility they move on and leave behind them a cloud of positive ions. Most of the positive ions are bunched

in a fairly dense group two or three ionizing paths long. The electrons are towards the anode and are in a somewhat spatially larger cloud as a result of diffusion. The rear of the electron cloud is being held back by the positive-ion space charge while the advance region is being drawn towards the anode. The region between electron and positive ion clouds thus forms a conducting plasma. In fact, as the electron avalanche advances, the ionizing avalanche of electrons spreads, so that the profile of the positive-ion space charge is wedge shaped with an apex towards the cathode. This phenomenon has been calculated by Slepian<sup>32</sup> and Ollendorf<sup>33</sup> and observed by Raether.<sup>24</sup> The space charges of this electron avalanche path, however, are mainly arranged along a line parallel to the field of the gap and with distinctly more space extension parallel to the field than at right angles. These space charges superpose additional potentials on the normal potentials present. Thus the potential is high in the positive space charge, and it falls off more steeply on the cathode end of the positive space charge than it would in the absence of space charge. On the anode side of the

electron cloud the potential rises more steeply than usual. Between the positive ions and electrons the fall in potential is less than in the undistorted gap. It may, in fact, even be reversed with heavy space charges. In that event some of the electron cloud may be bound by the positive field and thus temporarily prevented from advancing.\* Except in high fields (20 per cent over voltage) this will not occur. The electrical field is therefore seriously distorted along the axis of the avalanche and increased in the direction of anode and cathode. The form of the field distortion is shown in Fig. 198, part A. In these regions  $\alpha$  is therefore also increased. The possibility of such distortion was foreseen

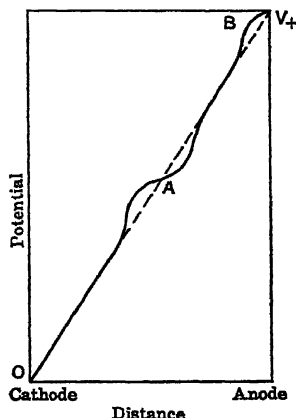


FIG. 198.

as early as 1928 by Slepian,<sup>32</sup> and calculations were made on the field distortion and electron diffusion. The results are *not* satisfactory, since the velocity of agitations of the electrons was taken as far too low. The concept was in the right direction, however, and was independently arrived at by Loeb in 1929. Further application of the concept needed more data for its proper development.

In the act of ionizing, the electron avalanche also created perhaps four or more times as many photons as it did ions. These are radiated

\* The picture of this process without the concept of photoionization has been developed following Flegler and Raether's work by Strigel,<sup>32</sup> although the present description was independently developed by the author before discovering Strigel's paper.

out in all directions during time intervals of the order of gap breakdown (i.e.,  $\tau$  for excitation is of the order of  $10^{-8}$  second). A large fraction of these are of wavelength too long to ionize *in the gas*. A fraction of the photons will certainly ionize in the gas, as shown by Cravath,<sup>34</sup> Raether,<sup>65</sup> and Dechène.<sup>34</sup> More or less all the photons can liberate electrons from the usual metal electrodes. Thus all about the avalanche photoelectric ionization will be present. Owing to attenuation by absorption and the spreading of radiation, the photoionization should be most intense near the cathode and anode ends of the avalanche. On the other hand, some of the photons will reach the cathode and liberate electrons from the cathode. The number doing so will be greater the nearer the avalanche space charge to the cathode. Though few photons reach the cathode, most of them can produce photoelectrons. Again the greatest effect produced by these will be at the intercept of the cathode with the projection of the avalanche axis. The photons travel with the speed of light. Thus *almost simultaneously with the avalanche formation new electrons are being created in the gap*. These start fresh avalanches from the cathode and from other points of the gap wherever *chance* creates a new photoelectron.

Since there is an axial field distortion parallel to the avalanche this is reflected in greater or less measure in the intensity of ionization produced at various points, for the increase in  $\alpha$  causes the points of high field strength to be favored. Thus, aside from more effective photoionization at the ends of the avalanche, a general directive action is caused by field distortion across the whole gap enhancing ionization along the axis of the initial avalanche. In consequence, the photoelectrons from the gas on the cathode side of the positive space charge will start electron avalanches towards the space charge and electrons will stream into it. This effectively extends the positive space charge towards the cathode. The new electrons created will in part neutralize the original positive space charge and allow the electron avalanche ahead to move on in case it was restrained by the heavy original positive space charge. In general, the positive end of the avalanche will advance towards the cathode rapidly and by steps as each photoelectron ahead creates a new avalanche, for the photons from the tip advancing outward with the velocity of light start new avalanches in the strong field region in advance of the tip, which ultimately send the new electrons running up the positive-space-charge column. At the anode end the *leading electrons* of the diffuse electron cloud and the photons produce ionization ahead of the avalanche tip. In the enhanced field gradient from the negative space charge the electrons so created start new avalanches, which in turn leave a positive space charge behind. This draws in the rest of the first original electron cloud that was bound by the positive space charge, and so on. Since the photons proceed with the velocity of light and bridge considerable

sections of the gap in very short time intervals, and since in so doing they produce new avalanches in increasing number and in rapid succession along the region of axial field distortion, the breakdown of the gap along a streamer crossing the plates in  $10^{-8}$  second becomes obvious. Thus breakdown proceeds essentially in the development of breakdown streamers, created very rapidly by nearly a simultaneous breakdown along the direction of field distortion by the initial avalanche, in virtue of photoionization.

In the process of breakdown it is to be noted that the electron avalanche ending at the anode surface has one advantage in that electrons are removed as rapidly as they reach the anode, see Fig. 198, part *B*. Hence the positive space charge at the anode will produce greater distortion and will progress more certainly than in the mid-gap streamers.<sup>66</sup> This action of the anode is confirmed in the observations of the streamers propagated from points in the positive point to plane corona.<sup>37,38</sup> As a consequence, whether a mid-gap streamer appears in breakdown or not, well before the end of the spark a streamer develops from the anode, moving with fair speed towards the cathode. This is shown in the Kerr cell studies of both White<sup>28</sup> and von Hamos<sup>27</sup> and in Flegler and Raether's<sup>39,67</sup> cloud pictures. The appearance later in the breakdown process is to be expected, since the electrons are initially mostly liberated from the cathode and some ionization must occur before enough photons are created to start the anode streamer. In overvolted gaps the anode or mid-gap streamer is of most frequent occurrence. At lower fields, shorter gaps, and lower pressures the discharge appears to start from the cathode with ultraviolet illumination and gradually progress across the gap. One reason for this is that at the lower fields streamers are not favored and the positive-space-charge distortion is not great enough to hamper the advance of the electron avalanche. As little as 5 per cent increase in overvoltage, however, in this region of field strengths can hamper avalanche advance towards the anode materially and favor streamer propagation towards the cathode. This action of high fields definitely appears to be the case in positive corona where streamer formation is readily studied.<sup>33,40</sup> When these streamers can develop they do so, and breakdown proceeds by the streamer process emanating from mid-gap or from the anode.<sup>66</sup> Since these streamers propagate more rapidly than the electron avalanche mechanism, it is still more likely that they will predominate at higher fields such as in overvolted gaps. The effect of changes in overvoltage of 10 per cent, both on the mode of breakdown and the time involved, has been noted by Flegler and Raether.<sup>41</sup> They observe the time of breakdown to drop from  $2 \times 10^{-8}$  to  $10^{-7}$  second for a 10 per cent decrease in overvoltage.

At lower fields with ultraviolet illumination of the cathode, avalanches start at the cathode. If an avalanche shortly after its inception can start a *photoelectron* along its axis from the cathode, or near it,

it is possible that an adequate secondary supply of electrons could be built up in a short time, causing the streamer to appear to develop outward from the cathode. This would be especially true *if a succession of such electrons is liberated*. In this case, propagation is mostly from the negative end of the avalanche until the later phases of breakdown when the anode streamer starts. It is to be noted, however, that for such a mechanism to start *requires a relatively fortunate sequence of photoelectric emissions*. Since such occurrences are rare, many and in fact most of the  $i_0$  photoelectrons liberated from the plate merely give avalanches that result in no breakdown. Hence one would expect that the statistical time lag for such low-voltage sparks would be long and that with them even breakdown would require a somewhat longer time as noted by Flegler and Raether.<sup>31</sup> By increasing  $i_0$ , as White<sup>22</sup> did, to a point where, in  $10^{-8}$  second,  $10^4$  electrons were liberated from his cathode in place of the  $10^{-2}$  observed with a quartz lamp, it is seen that what was but rarely possible from avalanche ionization might readily occur with such cathode emission. Hence the probability of achieving sparks at a lower potential becomes large enough with such illumination to lead to the evaluation of a *lower* sparking potential. To understand this statement one must analyze the meaning of the experimentally observed sparking potential.

## 12. THE EXPERIMENTAL OR OBSERVED SPARKING POTENTIAL

Experimentally the sparking potential is defined *in fact* by the potential the application of which for some fixed time, say 30 seconds, produces a spark 50 or 90 per cent of the time. The choice of the percentage, 50, 90, or 99, is at the caprice of the observer. It is at once seen that the permutations and combinations of events which can occur to the avalanches after the first electron has been liberated are unlimited, and that, at a given potential above the one required by the condition  $\gamma e^{a\delta} \geq 1$ , a certain number of combinations only will result in a spark. Hence, could one count the initial electrons liberated in the effective region of the gap yielding  $i_0$ , one would thus determine the *real probability* of the spark as a function of potential. This form of study must give a far better method for investigating and defining the sparking potential than the one now used. This sort of condition concerning spark breakdown threshold readily explains the very occasional appearance of sparks at what appear to be potentials far below the average arbitrary minimum value established by current practice, as well as explains White's lowering by  $i_0$ .

On the basis of the considerations above, with the usual gaps studied, the conventionally observed sparking potential near atmospheric pressure is well above the limiting threshold condition for which  $\gamma e^{a\delta} \geq 1$ . However, since 10 per cent change in  $X$  in this region can produce such profound changes in mechanism, the value of  $V$ , as

conventionally observed may not be more than 15 per cent above that for which  $\gamma e^{as} \geq 1$ . Such a gap set at the conventional value of  $V_s$  could be termed "*overvolted*." The term, however, is usually applied where the conventionally accepted value of the potential as determined by the rather capricious definition above is exceeded.

### 13. FURTHER CONSIDERATION OF THE MECHANISM OF SPARK BREAKDOWN

In any case, with sufficient overvoltage to form mid-gap streamers, conditions will exist under which the positive streamer tip may divide. This occurs through the following chain of circumstances. An advancing positive streamer tip producing a number of the photons about itself may produce an electron off to the side and at some small distance. This will start an avalanche which, owing to the combined action of the streamer-tip space-charge field and the imposed gap field, will move towards the main streamer tip. If this avalanche succeeds in making a junction with the main streamer, and if adequate ions are produced by it, the streamer may propagate along the new direction of the streamer axis. Hence the spark path will be bent. The chance of this occurrence will be the greater, the greater the strength of the streamer-tip field relative to the directive field gradient in the gap. Hence in the longer gaps the chance of the occurrence is facilitated. This accounts for the zigzag nature of the spark path in longer sparks.

If now two such avalanches head for the streamer tip from, say, a direction more axial and one off to the side, both avalanches may develop nearly simultaneously and reach the tip at nearly the same time. In this event the streamer branches. If abundant energy and field distortion are present, both branches will develop. The more lateral streamer, owing to the importance of the axial field distortion, will therefore have less chance of propagating across the gap than the axial streamer. If the energy in the streamer is inadequate to maintain both branches, one may cease propagating. It may also occur that several such avalanches appear nearly simultaneously. In this case the energy available will not be enough to propagate even a single streamer, the field at the tip is reduced, and the streamer extinguishes. In longer gaps, branching is frequent and is one of the striking features of lightning discharge.<sup>35, 36</sup> As the cathode is approached and the streamer has adequate energy the lateral branching is favored, especially if there are points of lower  $\gamma$  at the cathode which will stimulate the final development of the branches towards those points of the cathode. With the strong fields and heavy streamer production in the preonset region of positive corona discharge, cloud pictures show that branching is very common. This is also confirmed by visual and photographic study.

Again, in a short gap, if one streamer is developing and at the cathode end a photoelectron starts an avalanche which is laterally displaced from the streamer axis but which in the short gap is parallel to the undistorted field, the interaction of the positive end of the streamer near the anode with the electron cloud of the second streamer may effect a junction of the two. In such an event a *single* discharge



FIG. 199A.—Raether's Cloud Track Photographs of Electron Avalanches below Breakdown. Cathode at bottom.

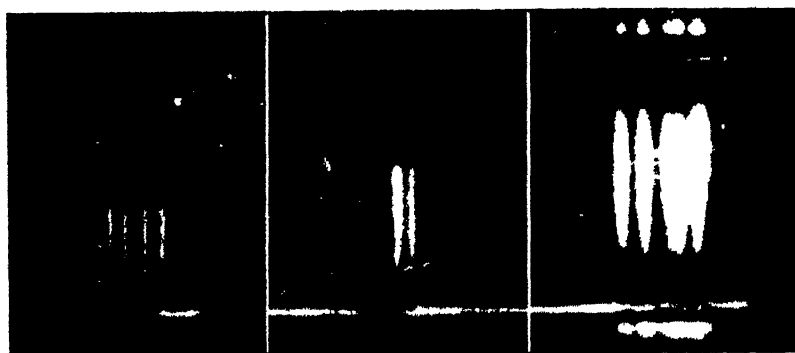


FIG. 199B.—Raether's Cloud Track Photographs of Electron Avalanches of Progressively Increasing Age. Cathode at bottom.

path may materialize with a sharp kink or bend along the combined channels. Such an occurrence is beautifully illustrated in Fig. 199A, which is one of Raether's cloud track pictures. Figs. 199B and C are Raether's cloud track pictures of avalanche breakdown below sparking. The time between the left- and right-hand tracks in 199C is  $10^{-7}$  second. Figs. 200A, B and C show avalanches above sparking produced by photoelectrons A and B and ions C. Fig. 201 shows branch-

ing in positive corona streamers taken by Gorrill. Figs. 202*A* and *B* as well as 203 show Dunnington and White's Kerr cell studies of spark development.

There is another condition which favors branching aside from the long gap as shown by Allibone and Meek's<sup>36</sup> studies. This is the reduction, in a limited measure, of the gaseous pressures. Such a reduction favors a wider dissemination of photoelectrons in the gas and on the electrodes due to the reduction of absorptions in the gas. Thus branched streamer production is favored. However, as pressures are further reduced the streamers cease to develop successfully, owing to decreased ion densities in avalanches. For diffusion, both of electron avalanches and the consequent positive space-charge channels, results in a more widespread extension of the avalanches. The single avalanches advance further before being hampered by the positive space-charge accumulations and may extend across the gap without causing breakdown. Thus branching and broadening and diffusion of the discharge path result. According to Allibone and Meek,<sup>36</sup> this change is accompanied by an initial increase and an eventual decrease in velocity of the streamers and the speed of breakdown.

As one approaches a pressure of the order of 5 mm, the diffusion is so great that virtually the whole volume between the area of the plates becomes the seat of ionization and breakdown. In this case the space-charge changes attendant on the initiation of a glow discharge are taking place over the plate area and moving somewhat rapidly during gap breakdown. The reason for this lies in the fact that at such pressures the value of  $X/p$  for the spark is relatively higher than at high pressures. Thus in  $N_2$  at 5-mm pressure with a 1-cm gap  $V_s \sim 300$  volts and  $X/p = 60$ , while at 760-mm pressure  $X/p = 39$ . Hence the ion velocity is increased.

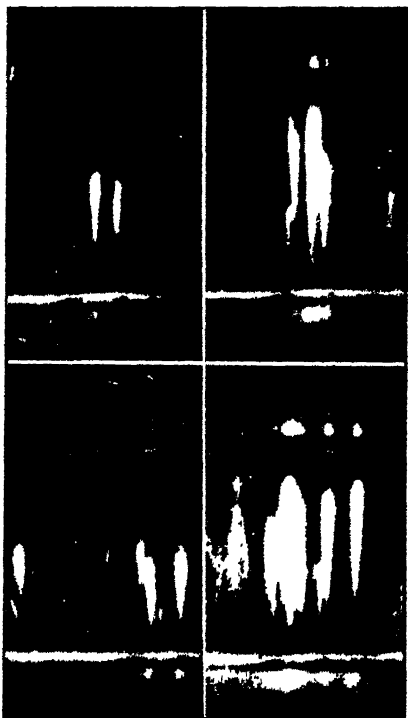


FIG. 199*C*.—Raether's Cloud Track Photographs of Electron Avalanches. Those to the right are  $10^{-7}$  sec older than those to the left. Cathode at bottom.





FIG. 200A.—Raether's Cloud Track Photographs above Sparking Potential. Note the midgap streamers. Cathode below.



FIG. 200B.—Raether's Cloud Track Photographs of Electron Avalanches above Sparking. Cathode below.

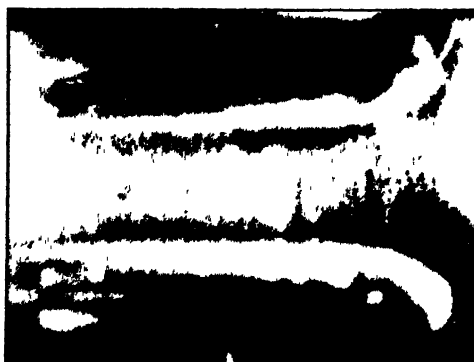


FIG. 200C.—Raether's Cloud Track Photographs of Electron Avalanches above Sparking. Produced by ions, *not* by photoelectrons from the cathode below.

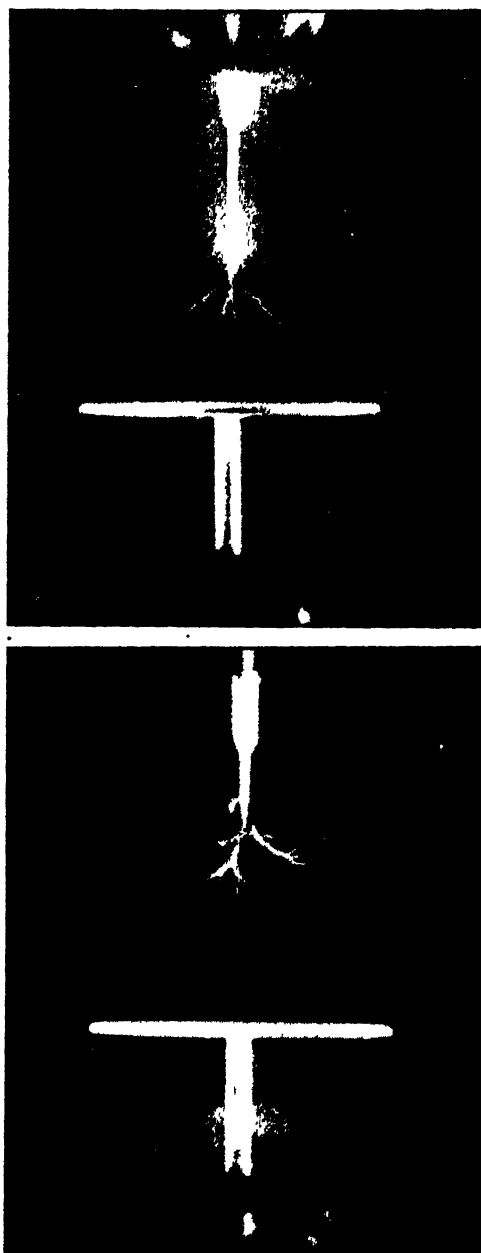


FIG. 201.—Gorrill's Cloud Track Pictures of Positive Point to Plane Corona Streamers. Those below are taken after shorter time intervals. Note branching close to anode.

With the decrease in pressure and the spread of the photons in the space, all the ionization produced by the photoelectrons liberated by the current  $i_0$  from the cathode contributes. Breakdown *ceases to depend on a single electron path, and a set of fortunate happenings, for*

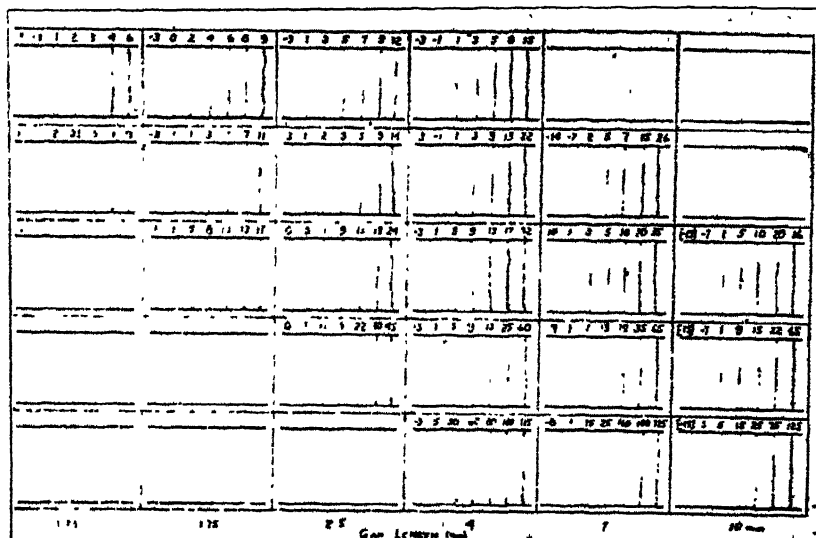


FIG. 202A.—Dunnington's Kerr Cell Studies of Sparks in Air as a Function of Time. The cathode is below. Time increases to right. Gap length in mm given below. Pressures, reading from top row down, 76, 60, 45, 30 and 20 mm respectively.

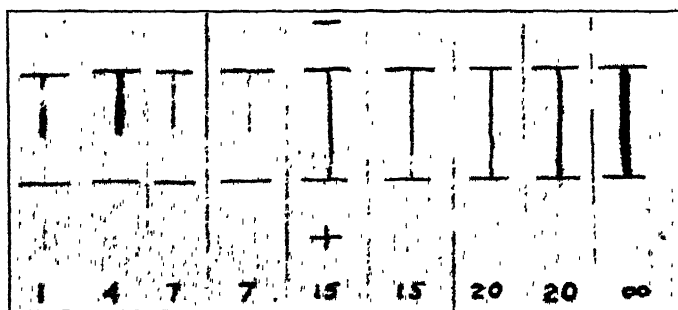


FIG. 202B.—Dunnington's Kerr Cell Photographs of Static Spark Breakdown at Atmospheric Pressure with 5 mm Gap. Path times in  $10^{-9}$  sec are indicated below.

*the density of ionization is no longer great enough to propagate streamers.* All electron avalanches pool or share their photoelectric effects in the gas. Although no time lag studies have been made for the low-

pressure region, it is clear that, since sufficient ionization in a single channel cannot take place, the breakdown must proceed by gross space-charge changes over the electrode area conditioned by repeated avalanches and space-charge movement, in agreement with the theories of Franck and von Hippel,<sup>47</sup> Sämmer,<sup>49</sup> Schumann,<sup>48</sup> Rogowski,<sup>45</sup> and Loeb.<sup>46</sup> Breakdown then approaches more nearly to the condition of instability produced when the current  $i$  for the whole electrode area becomes very large for a fixed  $i_0$  as  $\gamma e^{\alpha \delta}$  approaches

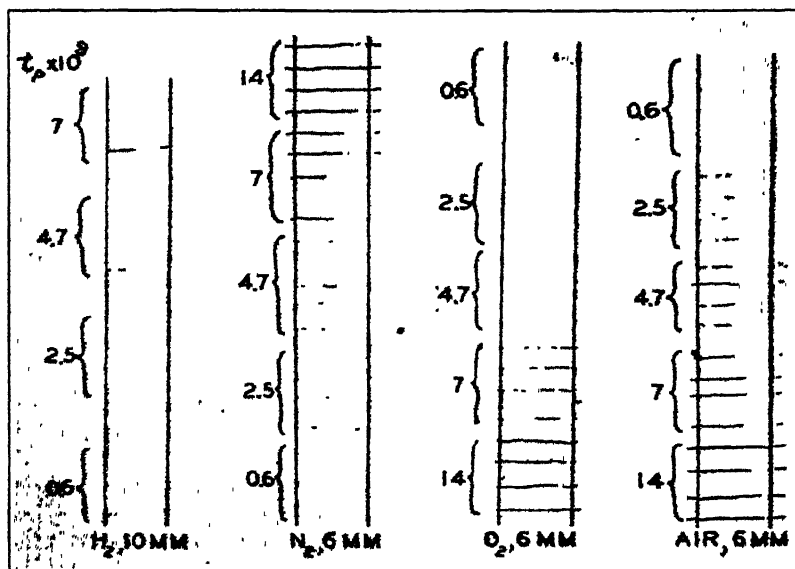


FIG. 203.—White's Kerr Cell Photographs of Static Spark Breakdown. Cathode is at left. Time scale is at left of each vertical column in  $10^{-9}$  second. Reflected light from electrodes appears to prolong path beyond vertical line electrode surfaces. Pressure is atmospheric. Gap length given at bottom in mm.

unity. Under these conditions, breakdown is approaching more nearly to the original Townsend mechanism, and the  $V_b - p\delta$  curves should be predictable from the condition  $\gamma e^{\alpha \delta} = 1$  with greater success, as appears to be the case up to about 40-mm pressure.

Furthermore, it need not surprise us to find in shorter gaps and at lower pressures, where even with the space-charge distortions produced by avalanches  $p\delta$  does not yield enough molecules for breakdown, that the mechanism is altered. Under these conditions we should expect to observe longer time lags and more dependence of  $V_b$  on  $i_0$ . Considerable work remains to be done on the study of the time lags in spark breakdown at lower pressures.

#### 14. A BRIEF SUMMARY OF THE DEVELOPMENT OF THE UNDERSTANDING OF SPARK BREAKDOWN AT ATMOSPHERIC PRESSURE

With these pictures in mind, one is now in a position to understand and analyze the time lag studies. However, before doing so, a word must be said concerning the rather new, comprehensive, and probably correct interpretation of the mechanism of the high-pressure spark.

In promulgating such a picture the author lays no claim to being the originator of the picture. Like so many clarifications of obscure phenomena this one has resulted from the cumulative efforts of many investigators. Primarily credit for the incentive to the interpretation must go to P. O. Pedersen<sup>41</sup> and the many others<sup>25, 41, 42, 43, 44, 45</sup> after him who first, in about 1923 to 1928, found the very short time required for the materialization of the spark. Slepian<sup>32</sup> first conceived of axial space-charge distortion by electron movement. The author<sup>29</sup> independently arrived at the same concept but suggested in addition *spatial successions of nearly simultaneous electron avalanches across the gap*, making the distances of electron travel millimeters instead of centimeters. In his first paper, however, the author did not have any clue to the *mechanism* of these separate short-length electron avalanches, or streamers, as he was then still striving to utilize the process of ionization by positive ions in high fields. Partly for the same reason, those who later studied the problem further from the concept of *successive avalanches in time*<sup>46, 46, 47, 49, 50</sup> missed the trail and came to mechanisms that may occur (low pressures or short gaps) but are not those for longer gaps.

Next came the important photoelectric ionization experiments of Cravath<sup>34</sup> with the corona discharge at atmospheric pressure. With them the concept of the propagation of a spark discharge by photoelectric ionization was made probable. This concept together with the velocity determinations of lightning discharge of Schonland and Collens<sup>33</sup> in 1934 led inevitably to the paper of Cravath and Loeb<sup>51</sup> showing how such velocities could be achieved by a combination of photoionization and short-path electron travel. At the same time the results of Dunnington<sup>36</sup> and afterwards especially of H. J. White<sup>23</sup> revealed the *velocity of the electrons in an avalanche* and simultaneously the short time of breakdown. In this paper the conclusions of White about the movement of the positive mid-gap streamer were a great step in advance. v. Hamos<sup>27</sup> also had observed the progress of such streamers in a careful Kerr cell study and commented thereon. Then followed the time lag studies of Zuber<sup>52</sup> and v. Laue, Tilles,<sup>53</sup> White,<sup>54</sup> and especially Wilson,<sup>55</sup> Newman,<sup>56</sup> and Strigel,<sup>56</sup> which as we shall see added much to the picture from the statistical side. Coincident with these investigations came the revealing cloud track studies of Flegler and Raether<sup>31, 39</sup> and later Raether.<sup>34</sup> Those of Raether confirmed the Kerr cell studies of White and also the velocities observed. Flegler

and Raether emphasized in their discussions the important fact that neither space-charge distortion by ion movement nor successive electron avalanches in time could account for the tracks at higher pressures and longer gaps ( $p > 100$  mm and  $\delta > 3$  mm in air). They again reiterated the importance of photoionization and the progress of positive streamer tips.

The work of Schonland and Collens<sup>35</sup> on lightning, and more recently similar studies of Allibone and Meek<sup>36</sup> on long sparks, also made necessary this interpretation and furnished valuable clues. Finally the corona discharge studies of Kip<sup>38,40</sup> and Trichel<sup>37,58</sup> in collaboration with the author<sup>40</sup> added much important information on the inhibiting effect of space charges and the nature and propagation of the streamers.<sup>66</sup> The cumulative data from these sources therefore today leave little doubt as to the mechanism active.

## 15. THE TIME LAG OF SPARK BREAKDOWN

If a sparking potential is applied to a given gap it will be observed that the spark discharge may occur at almost any interval of time after the gap has acquired the sparking potential  $V_s$ . The delay may be exceedingly short or very long ( $10^{-5}$  second to 30 minutes) provided inadequate ionization exists near the cathode. The time between the occurrence of the spark and the application of the potential is called the spark lag. In recent years this time lag has been the object of considerable study. By using a very short gap with a small volume of effective field strength the lag without artificially applied external ionization may be indefinitely long. Laue and Zuber<sup>52</sup> studied these lags down to about  $10^{-3}$  second at normal breakdown voltage and as a function of the intensity of ionization. The lags were found to be purely statistical in time, that is, if the number of lags  $n$  out of  $n_0$  that exceeded  $t$  seconds are plotted against  $t$ , then the curve of  $n/n_0$  plotted against  $t$  is of the form  $n = n_0 e^{-\beta t}$ , where  $\beta p = 1/\tau$  and  $\tau$  is the average time lag. From the plot of  $\log(n_0/n)$  against  $t$  the straight line of slope  $1/\tau = \beta p$  is obtained. Now, as Laue points out,  $\beta$  represents the chance that an electron is liberated by the ionizing agent. In Zuber's case the *volume* of the gas was ionized by  $\gamma$  rays and  $\beta$  depended not only on the number of electrons liberated per unit volume per second but also on the chance that they were liberated in the effective volume of the gap. Thus here  $\beta$  depends on both the ion current and the volume.  $p$  is the chance that one electron will start the discharge. It depends on the overvoltage and on the mechanism active, as shown on page 443 to 447. In Zuber's work the range of the investigation was not very extensive. He established the law and showed that  $\tau$  or  $\beta p$  was dependent on the intensity of illumination.

At the time no lower physical limit to  $\tau$  was looked for. It was

believed that the statistical lag was caused merely by the fact that a single electron had to be liberated at a propitious time and/or spot in the gap to start the discharge, and that  $\beta p = 1/\tau$  marked the chance that this would occur for a given set of conditions. It was taken for granted, however, that there must be a finite time  $\tau$  which comprised the actual time to break down the gap (formative lag) once the electrons were produced with sufficient frequency in the gap to get rid of the statistical lag. This formative lag was believed to be very short, for it was thought that it corresponded to the time taken for the charges to cross the electrode spacing in the high fields. Already relatively early P. O. Pedersen,<sup>41</sup> using Lichtenberg figures, estimated that this time could be of the order of  $10^{-7}$  second.

When in 1928 Loeb<sup>46</sup> and Rogowski<sup>45</sup> independently attempted to salvage the Townsend theory of secondary ionization by means of positive ions by assuming space charges in the gas, Loeb pointed out that the space-charge formation created by the movement of positive ions alone (which was the most powerful one and easiest to invoke) required finite time intervals of the order of  $10^{-5}$  second to develop in a gap of 0.1 cm at 760 mm in air. He stated that a finite limit for the statistical lags of Zuber and Laue should be found in this interval. Within a year the papers of Torok,<sup>42</sup> Beams,<sup>25</sup> Tamm,<sup>44</sup> Rogowski,<sup>45</sup> and others had appeared confirming Pedersen's short time intervals in the spark mechanism. These and the later results of Strigel<sup>59</sup> indicated that these short time lags extended well down to  $10^{-8}$  second but occurred only under conditions of rather high overvoltage (20 per cent or more) and strong illumination, and were shorter the higher the overvoltage.

In consequence Loeb<sup>46</sup> modified his theory to take account of the spark-discharge mechanism in high fields by which high space charges could be built up by single electron movements over short distances, due to the rapid increase in  $\alpha$  with  $X/p$ . Shortly thereafter von Hippel and Franck<sup>47</sup> put forward their theory of the building up of space charges by successive electron avalanches which occur in intervals of  $10^{-8}$  to  $10^{-7}$  second. Similar calculations were made by W. O. Schumann,<sup>48</sup> Sämmer,<sup>49</sup> and Kapzov.<sup>50</sup> Whichever picture of the exact mechanism of formation of this space charge caused by electron movement is taken, and doubtless under different conditions each of the mechanisms comes into play, it is clear that these give rise to formative lags of a different order from those causing space charge by movement of positive ions, i.e.,  $10^{-8}$  in contrast to  $10^{-5}$  second. The preceding analysis has in fact shown that the mechanism of Loeb and Rogowski cannot take place except in very short gaps, while at low pressure that of Franck and von Hippel et al. probably occurs. None of these mechanisms operates at atmospheric pressure and above 3-mm gap length. Since the positive-ion mechanism gives more powerful space charges and requires lower values of  $\alpha$  one would expect

that the formative lags taking  $10^{-5}$  second would occur for low over-voltages.

On the author's suggestion Tilles<sup>53</sup> undertook the problem of studying the shorter lags. To this end he developed an ingenious device for measuring the time lags lying between  $10^{-5}$  and 1 second. The method consisted in measuring with a ballistic galvanometer the constant output current given by a modified vacuum-tube voltmeter between the time of application of the sparking potential and its fall during the spark. Two series were run, one with an impulse wave of short duration, another with an approach voltage of 96 per cent of  $V_s$  and the sudden application of a voltage  $V_0$  which was from 1 to 5 per cent greater than  $V_s$ . Tilles obtained linear curves for  $\log n_0/n$  plotted against  $t$ , as had Zuber at low overvoltages and low intensity of illumination (see Fig. 204, curves *a* and *b*). The slopes of these lines varied in a linear fashion with overvoltage and with the logarithm of the intensity of ultraviolet illumination which was varied by a factor of  $10^5$ . For these statistical lags Tilles found that for static breakdown with 96 per cent approach voltage one may write for Cu spheres 0.952-cm radius and gap length 0.0683 cm at  $V_s = 3820$  volts

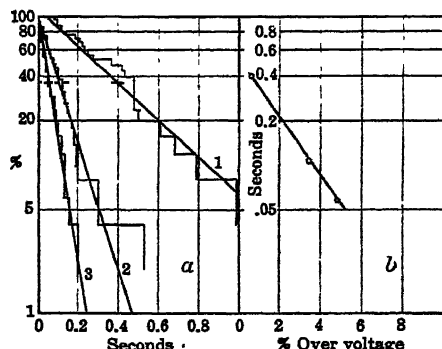


FIG. 204.

$$\tau = 0.0037 e^{-0.89 \frac{\Delta V}{V_s}} 100 I^{-0.76}.$$

Here  $\Delta V/V_s \times 100$  is the per cent overvoltage,  $\Delta V$  being given by  $V_0 - V_s = \Delta V$ ,  $V_0$  being the applied potential, and  $V_s$  that of normal sparking. This law holds from 1 to  $10^{-4}$  second in his gap.  $I$  is the vacuum photoelectric current density measured in the gap in units of  $10^{-12}$  amp/cm<sup>2</sup> from a clean Ni plate. This does not actually correspond to the current per square centimeter from the Cu sphere because of the difference in photoemission from Cu and Ni.  $I$  is, however, *proportional* at constant pressure and approximately constant field strength to the actual number of photoelectrons liberated in the spark gap, and is proportional to the photoelectric current density.

It is therefore possible to apply Tilles' measurements to the interpretation of the statistical time lags given by Laue. Thus one has

$$\frac{1}{\tau} = \beta p = \frac{1}{0.0037} e^{89 \frac{\Delta V}{V}} I^{\frac{3}{4}}.$$



In these experiments  $\beta$  is directly proportional to  $I$ , the current density of photoelectrons.  $p$  contains the chance that one electron suffices and is modified by factors which increase this chance. That the overvoltage should affect  $p$  critically is clear, and that the overvoltage should increase  $p$  very rapidly is more or less to be expected since changes in  $X/p$  strongly affect  $\alpha/p$  and hence secondary electron emission, space charges, etc. The term  $p\beta$  is proportional to  $I$  if one electron can suffice under proper conditions to start a spark. If two electrons simultaneously were required then  $p\beta$  would be expected to vary with  $I^2$ , etc. As in theory  $\beta$  is proportional to  $I$ , it is clear that, since  $\beta p$  is observed to be proportional to  $I^{3/4}$ ,  $\beta p$  must contain in itself

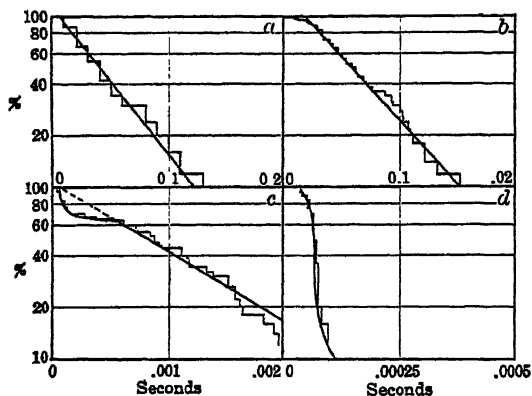


FIG. 205.

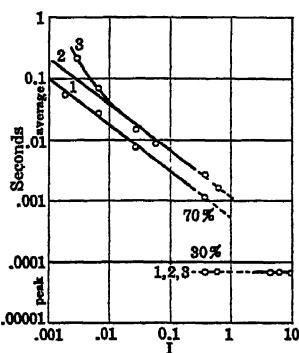


FIG. 206.

other conditions that act apparently to reduce the effectiveness of increasing ultraviolet illumination. Actually  $p$  would have to contain a factor  $(I)^{1/4}$  in itself to give the observed change. Whether this result is spurious, or whether the formation of space charges during the approach voltage period and after or other effects prolongs the time lag by making some of the liberated electrons less effective, cannot be said. With surge impulse breakdown at lower illuminations the value of  $\beta p$  as a  $f(I)$  changes to  $\beta p \propto I$ . In this case one can assume that each electron within the regime designated by the value of  $e^{39(\Delta V/V_s)}$  will produce a spark. Under these conditions, with weak illumination, it is possible that action of an inhibitory sort does not take place.

As the illumination intensity is increased the photocurrent reaches a value such that the curves of  $\log(i_0/i)$  against  $t$  alter their shape in a fashion indicating the existence of a minimum value of  $\tau$ , in the shorter time intervals (see Fig. 205a, b, c, and d). At lower values of  $I$  in this regime only a small percentage of the breakdowns show the effect. At  $I = 5 \times 10^{-13}$  amp/cm<sup>2</sup>, however, 30 per cent of the lags are of a fixed length of about  $10^{-4}$  second and 70 per cent are

statistical. Finally both at 3 and 5 per cent overvoltage at about  $2 \times 10^{-12}$  amp/cm<sup>2</sup> the breakdowns are nearly all of one time  $\tau$ , i.e.,  $10^{-4}$  second; that is, one goes from a statistical lag of decreasing  $\tau$  to a formative lag of  $10^{-4}$  second for the gap used, with sufficiently intense photoelectric emission, *overvoltage being constant* (see Fig. 206). In this region of time lag, as overvoltages increase, the formative lag at  $\tau$  remains the lag, but decreases in value as with increasing  $V$ , the electron avalanches produce the necessary ionization density much more effectively. Thus fewer electron avalanches are needed to produce the same gradient and  $\tau$  decreases. Tilles' lags of  $10^{-4}$  second are not determined by the time taken for positive ions to cross the gap. The time of crossing is much shorter than  $10^{-4}$  second. These time lags must represent the time taken for a series of events, probably the building up of space charges by positive-ion movement and successive electron avalanches, for the path is so short that the electrons do not succeed in making more than a few ionizing impacts in the gap length. Thus the current in the gap takes time to build up. White's<sup>54</sup> results in air in intervals of  $6 \times 10^{-8}$  second show that the lags at the same overvoltage are materially longer for a 1-mm gap than for a 5-mm gap, Fig. 207.

It is certain that the *electron movement* either in one or in several successive avalanches following at short time intervals, will produce a space charge which is *not conditioned by ion movement*, and whose minimum value will depend on the time of electron crossing. One mode of such short time-interval space-charge production has been calculated by Franck and von Hippel.<sup>47, 48</sup> It leads to lags of the order of several times  $10^{-8}$  second. In still higher fields the electrons far short of crossing the gap will produce space charges leading to self-propagating streamers which cause gap breakdown in  $10^{-8}$  second or less. Quantitative measurements in this region were begun by

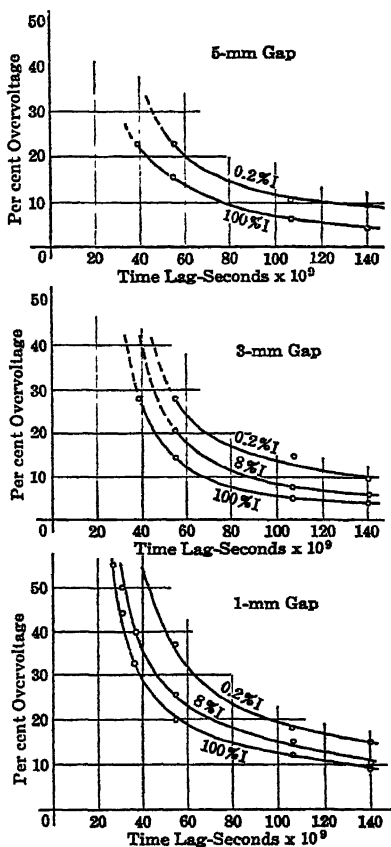


FIG. 207.

H. J. White.<sup>54</sup> White used light from a spark to set off the gap to be studied and by means of the Kerr cell shutter observed the time between the flash of the initiating discharge and the breakdown of his experimental gap. Time lags of a non-statistical sort were observed as a function of gap length, intensity of illumination, and overvoltage. As White worked with very high illumination intensities he found that only small overvoltages of some 14 to 15 per cent were needed to cause formative lags of the order of several times  $10^{-8}$  to  $10^{-7}$  second. The higher the intensity, the lower the overvoltage required. Near  $5 \times 10^{-8}$  second the overvoltages rapidly increased (see Fig. 207). Calculations made by White indicated this time to be that of the order of an electron crossing the gap. White, however, pointed out that the same time intervals were of the order of time taken for the *rapid initial rise of intensity of light emission in the initiating spark source*. Hence the upward bend of overvoltage *versus* time lag curves at about  $5 \times 10^{-8}$  second had to be ascribed to a rapidly decreasing intensity of photoelectric illumination. He, unlike air, and  $\text{CO}_2$  showed a very much higher set of overvoltages (about 30 per cent) for the whole range. This is to be expected because of the low potentials at which He yields appreciable values of  $\alpha$ . At such potentials  $\alpha$  is low and the ionization process is inefficient so that many impacts with atoms are needed to give much multiplication of ions. In short time intervals this requires greatly increased values of  $V$ , in a given gap.

Recently R. R. Wilson<sup>55</sup> has carried White's experiments further, using a source of illumination (quartz Hg arc) which was steady but only  $10^{-5}$  times as strong. Wilson used an approach voltage about equal to the normal sparking potential and suddenly applied an overvoltage. He raised the overvoltage applied in successive steps until a spark could be seen in his optical system, with a given time setting. He found that as overvoltage increased at first an occasional spark was observed when a given overvoltage was applied. He then increased the overvoltage by steps and recorded the percentage of sparks observed when the same overvoltage was repeatedly applied. He plotted this percentage of sparks as a function of overvoltage as seen in Fig. 208B. From these curves he chose, as his overvoltage for a spark in the time interval used, the point at which 50 per cent of the overvoltage applications gave a spark. A series of such curves, shown in Fig. 208B, indicates why this criterion for the value of the overvoltage at a given time was resorted to. He found that corroded electrodes or a decrease in the intensity of illumination produced a decrease in the slope of the curves as shown in Fig. 208C and thus increased the overvoltage chosen for a given time lag. He found that materially higher overvoltages were required with his weak illumination than were observed by White for the same time lags.

Two of his curves for air are given in Fig. 208A with weak and strong illumination. It is seen that Wilson's overvoltages decrease

continually as the lag increases. At about  $1 \times 10^{-8}$  second his overvoltage curves rise relatively steeply. He found, however, *no lower limit to his lags even down to  $10^{-9}$  second if sufficient overvoltage was applied.* For such short time measurements a vacuum switch was required for applying the potential. Wilson also studied breakdown, using a surge impulse with no approach voltage. He points out that with surge voltages, and even with the application of high overvoltages above an approach voltage, the overvoltage values taken from the applied potential lose much significance. This follows since in breakdowns occurring in  $10^{-9}$  second it is possible that the actual voltage applied, owing to the reflection of the surge at the gap electrodes, may be materially higher than the static overvoltage applied. An

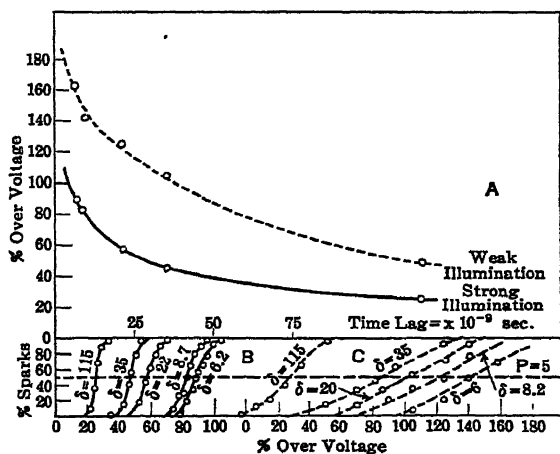


FIG. 208.

indication that this occurs in the present work is seen in the actual observations of breakdowns which take place by the sudden application of surge potentials *under* the normal breakdown voltage of the gap for the time setting. Beams<sup>60</sup> observed similar difficulties in his work. Thus while the overvoltage observed by Wilson in surge impulse breakdown was only some 20 per cent higher than that observed with the approach voltage, it may in reality have been much higher. Wilson also points out that the use of an approach voltage alters the gap in that it builds up a strong gas-intensified photocurrent before the overvoltage is applied. The high electron densities produced by this, however, are all near the anode. With a photoelectric emission of  $10^{-12}$  amp/cm<sup>2</sup> the currents achieved amount to some  $10^{-8}$  amp/cm<sup>2</sup>. In the area of 5 mm<sup>2</sup> where sparking occurs the current is  $10^{-9}$  ampere, giving an equivalent of 10 electrons created in the gap in the  $10^{-9}$  second of observed breakdown. Under these

conditions the chance of breakdown by mid-gap and anode streamers is very probable. In fact, it is just with these conditions that breakdown appears to start from mid gap or the anode.<sup>26, 27</sup> Later studies of Strigel with oscillograph and of Newman<sup>36</sup> with another method confirm White and Wilson's results. Newman shows that the approach voltage does not materially alter the time lag, as will be seen in Part B of this chapter.

It must also be pointed out that in measurements of time lags by the procedures outlined the *definition of time lag varies*. In Wilson's work the lag is that between the application of the overvoltage and the appearance of a light emission in part of the spark gap. In White's work the lag is the time between the illumination of the gap by the auxiliary spark and the first appearance of light emission. In Tilles' work the lag was the time as measured by the linear charging of a condenser from the instant of application of the potential until the spark had so lowered the potential that the condenser ceased charging. It is essential that such differences in interpretation be kept in mind in the discussion of spark lag studies.

In the experiments of White and Wilson the lags are so short that *neither positive ions nor electrons could possibly have crossed the gap in the intervals used*. This is again borne out by a calculation of H. J. White.<sup>54</sup> White showed that if at his observed overvoltage an electron crossed the 5 mm gap used, the number of positive ions left behind by the one electron would be so great that the positive space charge would have produced field distortions preventing the electrons from ever reaching the anode. This condition in the time intervals investigated would lead exactly to the types of field distortion causing Dunnington's mid-gap streamers, which were also in evidence in White's and Wilson's gaps. Thus it is clear that there is no lower limit to the formative lags as regards the crossing time for electrons. This agrees with the mechanism postulated by Loeb.<sup>29</sup> At lower overvoltages and lower pressures it is probable that the electrons do cross the gaps giving other durations of time lags. It is further possible that time lags can be conditioned on the movement of positive ions. Such lags have so far not been observed. Tilles' lags of  $10^{-4}$  second cannot be interpreted in this fashion. More work is required in the region of longer lags extending from  $10^{-7}$  to  $10^{-4}$  second.

#### 16. REFERENCES FOR PART A, CHAPTER X

1. J. S. TOWNSEND, *Nature*, 62, 340, 1900; *Phil. Mag.*, 1, 198, 1901; 3, 557, 1902; 6, 389, 598, 1903; 8, 738, 1904; *Electricity in Gases*, p. 322 ff.
2. F. PASCHEN, *Wied. Ann.*, 37, 69, 1889.
3. J. S. TOWNSEND, *Electricity in Gases*, Oxford, 1915, pp. 327, 380.
4. VARNEY, WHITE, LOEB, and POSIN, *Phys. Rev.*, 48, 818, 1935; see also L. B. LOEB, *Rev. Modern Phys.*, 8, 276, 282, 1936.
5. W. O. SCHEUMANN, *Durchbruchfeldstärke von Gasen*, Springer, Berlin, 1923, pp. 51, 114.

6. J. J. THOMSON, *Conduction of Electricity through Gases*, 3d Edition, Vol. 2, p. 486, Cambridge, 1933.
7. E. MEYER, *Ann. Physik*, 58, 297, 1919.
8. HOLST and OOSTERHUIS, *Phil. Mag.*, 46, 1117, 1923.
9. JAMES TAYLOR, *Phil. Mag.*, 3, 753, 1927; 4, 405, 1927; *Proc. Roy. Soc.*, A 114, 73, 1927.
10. W. S. HUXFORD, *Phys. Rev.*, 55, 75, 1939.
11. F. EHRENKRANTZ, *Phys. Rev.*, 55, 219, 1939.
12. PENNING and ADDINK, *Physica*, 1, 1007, 1934.
13. L. J. NEUMAN, *Proc. Natl. Acad. Sci.*, 15, 259, 1929.
14. D. Q. POSIN, *Phys. Rev.*, 50, 650, 1936.
15. L. B. LOEB, *Rev. Modern Phys.*, 8, 267, 1936.
16. D. H. HALE, *Phys. Rev.*, 55, 815, 1939.
17. R. SCHOEFER, *Z. Physik*, 110, 21, 1938.
18. W. S. HUXFORD, *Phys. Rev.*, 55, 75, 1939.
19. R. W. ENGSTROM, *Phys. Rev.*, 56, 1939.
20. W. E. BOWLS, *Phys. Rev.*, 53, 293, 1938.
21. R. T. STRUTT, *Phil. Trans. Roy. Soc.*, A 193, 377, 1900; H. E. HURST, *Phil. Mag.*, 11, 534, 1900.
22. H. J. WHITE, *Phys. Rev.*, 48, 113, 1935.
23. ROGOWSKI and WALRAFF, *Z. Physik*, 97, 758, 1935.
24. H. RAETHER, *Z. Physik*, 107, 91, 1937.
25. J. W. BEAMS, *J. Franklin Inst.*, 206, 809, 1928.
26. LAWRENCE and DUNNINGTON, *Phys. Rev.*, 35, 396, 1930; F. G. DUNNINGTON, *Phys. Rev.*, 38, 1935, 1931.
27. L. v. HAMOS, *Ann. Physik*, 7, 857, 1930.
28. H. J. WHITE, *Phys. Rev.*, 46, 99, 1934.
29. L. B. LOEB, *Science*, 69, 509, 1929.
30. L. B. LOEB, *Phys. Rev.*, 48, 684, 1935.
31. FLEGLER and RAETHER, *Z. Physik*, 103, 315, 1936.
32. J. SLEPIAN, *Electrical World*, 91, 768, 1928.
33. F. OLLENDORF, *Arch. Elektrotech.*, 26, 193, 1932.
34. A. M. CRAVATH, *Phys. Rev.*, 8, 267, 1935; C. DECHÈNE, *J. Phys.*, 7, 533, 1936.
35. SCHONLAND and COLLENS, *Proc. Roy. Soc.*, A 143, 645, 1934; A 152, 595, 1935; A 164, 132, 1938.
36. ALLIBONE and MEEK, *Proc. Roy. Soc.*, A 166, 97, 1938; A 169, 246, 1938.
37. G. W. TRICHEL, *Phys. Rev.*, 55, 382, 1939.
38. A. F. KIP, *Phys. Rev.*, 55, 549, 1939.
39. FLEGLER and RAETHER, *Z. Physik*, 99, 635, 1936; 103, 315, 1936; H. RAETHER, *Z. Physik*, 96, 567, 1935.
40. LOEB and KIP, *J. App. Phys.*, 10, 142, 1939.
41. P. O. PEDERSEN, *Ann. Physik*, 71, 371, 1923.
42. J. J. TOROK, *Trans. A.I.E.E.*, 47, 177, 1928; 48, 46, 1930.
43. BURROWAY, *Arch. Elektrotech.*, 16, 14, 1926.
44. TAMM, *Arch. Elektrotech.*, 20, 1928.
45. W. ROGOWSKI, *Arch. Elektrotech.*, 20, 99, 1928.
46. L. B. LOEB, *J. Franklin Inst.*, 205, 305, 1928; 210, 15, 1930.
47. FRANCK and VON HIPPEL, *Z. Physik*, 57, 695, 1929.
48. W. O. SCHUMANN, *Z. Tech. Physik*, 11, 58, 132, 195, 1930.
49. J. J. SÄMMER, *Z. Physik*, 81, 490, 1933.
50. N. KAPZOV, *Physik. Zeits. Sowjetunion*, 6, 82, 1934.
51. CRAVATH and LOEB, *Physics*, 6, 125, 1935.
52. K. ZUBER, *Ann. Physik*, 76, 231, 1925; M. VON LAUE, *Ann. Physik*, 76, 261, 1925.
53. A. TILLES, *Phys. Rev.*, 46, 1015, 1934.
54. H. J. WHITE, *Phys. Rev.*, 49, 507, 1936.

55. R. R. WILSON, *Phys. Rev.*, **49**, 1082, 1936.
56. M. NEWMAN, *Phys. Rev.*, **52**, 652, 1937; R. STRIGEL, *Wiss. Veröffentl. Siemens-Werken*, **15**, 1, 1936.
57. TERADA and NAKAYA, *Sci. Papers. Phys. Chem. Inst. Tokyo*, **4**, 129, 1926; **8**, 1, 63, 103, 197, 1928; **10**, 43, 1929.
58. G. W. TRICHEL, *Phys. Rev.*, **54**, 1078, 1938.
59. R. STRIGEL, *Wiss. Veröffentl. Siemens-Konzern*, **11**, 53, 1937.
60. J. W. BEAMS, *J. Franklin Inst.*, **206**, 809, 1926.
61. JONES and GALLOWAY, *Proc. Phys. Soc. London*, **50**, 307, 1938; R. GREGOROVICI, *Bull. Soc. Roumaine Phys.*, **38**, 7, 1937.
62. R. STRIGEL, *Wiss. Veröffentl. Siemens-Werken*, **15**, 13, 1936.
63. O. KLEMPERER, *Z. Physik*, **52**, 650, 1928.
64. F. H. SANDERS, *Phys. Rev.*, **44**, 1020, 1933.
65. H. RAETHER, *Z. Physik*, **110**, 611, 1938.
66. Since the great ion density is concentrated at the anode end of an electron avalanche starting from the cathode, it is clear that such an avalanche cannot be considered as bridging the gap. Thus for the completion of a spark, a return positive streamer must advance from the positive space charge tip at the anode to the cathode. Meek<sup>68</sup> has recently shown, in conformity with these considerations, that when the density of the positive space charge at the end of the avalanche is such as to produce a radial field of the order of magnitude of the imposed field, the streamer will advance. It does this because under these conditions the radial field draws into the streamer channel photoelectrons produced about the tip which would otherwise proceed as avalanches direct to the anode. Hence when  $\delta$  and  $p$  reach such values that these space charges occur, breakdown by streamer formation occurs leading to a new equation for the value of  $V_s$  in conformity with the observation. The existence of such positive streamers has been shown in recent cloud track photographs of Raether.<sup>67</sup> See also the track to the right in Fig. 200 B.
67. H. RAETHER, *Z. Physik*, **112**, 464, 1939.
68. J. M. MEEK. Paper submitted to *Proc. Roy. Soc.*, Sept. 1939.
69. Reference 62, Chap. X.

## PART B. ESSENTIAL TECHNIQUES IN THE STUDY OF SPARK DISCHARGE \*

### 1. INTRODUCTION

The fundamental processes in, and theory of, spark breakdown having been surveyed, it is next of interest to discuss certain aspects of the actual procedures used for the study of spark phenomena. It must be clear, in view of the later improved techniques, that many of the earlier measurements were of necessity crude. Hence in what follows it can be expected that only the more recent procedures should be presented. Various aspects of the problem of spark-breakdown studies will be considered separately.

### 2. THE SPARK GAP; ELECTRODES—SHAPE AND MATERIAL

One may begin such a discussion by considering first the spark gap itself. From the recent findings on the influence of the cathode material and its state on sparking, certain precautions at once become evident which in the past have been largely ignored.† Inasmuch as, in all lower-pressure sparks and in a small measure those at atmospheric pressure, the sparking potential observed depends on the value of the second Townsend coefficient  $\beta$  or  $\gamma$ , this factor merits some consideration. In such sparks where the second coefficient comes from photoionization in the gas it is clear that the electrodes are of no consequence. However, for many studies, particularly for those at low pressures and at atmospheric pressure where the smaller electrode is the cathode, the electrode material and its condition play a most important role.

In general it is very important that the chemical nature of the metal of the electrodes, especially the cathode, be accurately specified in any sparking-potential study. To this end one had best use a pure metal of unique character, such as Al, Zn, Cu, Fe, or Pt of known purity. Brass and other alloys, especially those that are not homogeneous in composition as shown by etch figures, should be avoided. Needless to state, the electrodes should be clean. They should be devoid of films of oil, grease, organic material, *finger prints*, etc., as well as of films of oxide or small specks of dust, oxides or insulating

\* References to Part B of Chapter X will be found on page 470.

† Unless very much to the point as specific instances of procedure, references in support of such general statements as this sentence will not be given. The whole preceding section gives ample basis for much that is said.



particles (see page 498). The question of oxidation is a particularly difficult one to deal with. All metals tend to oxidize in air, including especially Al, Cu, and Fe. They do this to different degrees from monomolecular layers as in Pt to thick layers as in Al. In many techniques for cleaning metals chemically in the presence of air the supposedly clean surfaces are left in a partially oxidized state. This is especially true for  $\text{HNO}_3$ ,  $\text{NH}_4\text{OH}$ , and even  $\text{HCl}$  on Cu. Initial polishing with an abrasive such as chalk or rouge suspended in distilled water followed by careful rinsing with distilled water or pure grain alcohol and outgassing in vacuum at  $400^\circ\text{C}$  or higher is advisable. Clean electrodes could be produced by making the electrode a cathode and sputtering it in an inert gas like A after careful outgassing and heating to  $400^\circ\text{C}$ . Similar surfaces could be prepared by evaporation of appropriate metals in vacuum, or in a few millimeters of inert gas. It is probable, however, that for any given problem the preparation of the electrode will have to be considered individually as the nature of the gas and the conditions of use require.

One fact is certain: the electrodes should be smooth. Rough points, or pits left by previous sparks where heavy currents follow, lead to alterations in sparking potentials due to brush discharge as do bits of oxides of microscopic size. There is a possibility that cathode surfaces of some electrical uniformity and reproducibility can be made by evaporation in the presence of small pressures of an inert gas, e.g., Ni, Fe, Pt, and Pd about 3000 atoms thick in 1–2 mm A or  $\text{N}_2$ . Beeck<sup>1</sup> and his co-workers have, in fact, found surfaces of great catalytic and crystallographic reproducibility and uniformity to be produced under such conditions. This technique may eventually lead to the production of characteristic and reproducible cathode surfaces which will be of immense value in discharge studies.

Aside from the preparation of the electrode surface prior to study, it must be recalled that gases and vapors can materially change its work function after preparation. First, any condensable vapor in the system such as Hg or oil from diffusion pumps will surely condense on the electrode surfaces during periods of evacuation. Hence the work function will be at least in part characteristic of the condensate rather than the metal. It is probable that even at vapor pressures as low as  $10^{-8}$  mm, in some hours' time in vacuum or at low pressures, a monomolecular film of condensable substance will form. Scrupulous care, therefore, must be used to keep the vapor pressure of condensable vapors as low as possible. All gases should be passed very slowly over a long path in liquid air, or through an efficient cooling system, and *traps should always be used between the tube and pumps or system* when the tube is connected to the system. *Once Hg gets into a chamber, nothing short of chemical cleansing will certainly remove it.* One-tenth the normal vapor pressure of  $1.4 \times 10^{-3}$  mm of Hg at  $20^\circ\text{C}$  will materially lower the sparking potential in most gases. Even such

non-volatile metals as Na not only appear in some gases to distil onto the cathode during evacuation but also will form compounds that materially influence the sparking potential of the gas.

Again it must be remembered that *all but the inert gases* either react chemically with most metal surfaces or else they are adsorbed as monomolecular layers. It is probable that even the inert gases themselves may react with metal surfaces when they strike in the ionic state. In the case of  $O_2$  or  $S_2$  oxidation of the surface can be expected. Hence in time even when the gas is dry the cathode will change its character. This is especially to be expected where the  $O^+$  ions are drawn to the cathode and are there neutralized. Oxidation of the cathode by sparking will in general raise the sparking potential. In the presence of  $O_2$  it is doubtful that one ever has a pure Cu, Al, or Mg surface. Surfaces of metallic Al or Mg may be prepared only by sputtering in the presence of an inert gas or evaporation in vacuum. In gases like the halogens  $Cl_2$ ,  $Br_2$ ,  $I_2$ , and halides HCl, or reactive sulfur compounds  $H_2S$  and  $SO_2$ , reactions and changes of the surface make discharge studies highly uncertain and variable in their results.

Again, many of the common electrode materials Cu, Ni, Fe, Pd, and Pt are what is known as surface catalysts. These form adsorbed layers of certain gases on their surfaces which do not follow the gas laws for adsorbed gases.<sup>1,2</sup> It appears that they form pseudo chemical combinations with the gases, in which the gas is in a particularly reactive state. Thus  $H_2$  forms atoms of H on the surface of Pt and likewise  $O_2$  condenses on the surface in a reactive state. The O does not evaporate and cannot be removed except by  $H_2$  or CO or some other substance adsorbed on the surface which can combine with it. Now these layers exert a profound effect on the surface properties of a point. Thus Pt loaded with  $H_2$  gas has a very much reduced work function and a high secondary emission on electron bombardment. Traces of  $SO_2$ ,  $H_2S$ , and even CO "poison" the Pt surface, which becomes highly insensitive.<sup>3</sup> Again the high photoelectric sensitivity of NaH to visible light can be compared to that of pure Na, which is far less sensitive and furnishes us with an idea of the effect of H in combination with a metal.

The recognition of the profound effects of the surface films on secondary emission and on Townsend's second coefficient makes many actions observed in the past understandable. For instance, it is a frequent observation in a discharge tube at pressures of the order of 0.1 mm or less, near the minimum sparking potential, that the unidirectional discharge of an induction coil if often repeated causes the spark to cease.<sup>4</sup> If the terminals are reversed so that the electrode which was the anode acts as cathode the spark will pass readily at first. After repeated sparking the spark will no longer pass but will pass on again reversing the potentials. Curtiss<sup>3</sup> has shown that the old Geiger-Mueller point counter using catalytic metals Cu, Fe, Ni, or Pt

operated only on this principle. The bombardment of the cathode surface with high-speed positive ions denudes the surface of its activating gas film and lowers  $\beta$  or  $\gamma$ . As the potential is just enough to cause a breakdown or a corona from the point, the lowering of  $\gamma$  causes the sparking to cease. After a time the gas film reforms and the point is again capable of sparking. The existence of "hard" and "soft" electrodes of the same metal at atmospheric pressure is clearly pointed out by Campbell<sup>27</sup> in a study of spark plugs. More data on this are also given by the work of Duffendack<sup>28</sup> and his associates.

It is thus seen that the act of sparking with certain surfaces in certain gases alters the surface so that, where  $\beta$  or  $\gamma$  affects sparking, measurements of sparking potential are almost impossible.

It is clear from this that in making breakdown studies in gases it is essential to consider carefully the character and state of the electrode, and the character of the gas both as regards purity and as regards its reaction with the metal surface, when interpreting the sparking-potential data.

As regards the shape of electrodes a great deal can and has been said, much of which will not be repeated here. From Paschen's law it is clear that  $V_s$  is a function of  $p\delta$  through the relation

$$V_s = \int_0^s X_s dx. \quad \text{This means that } V_s \text{ must depend in a measure on}$$

the field strength  $X$  and its distribution in space. Furthermore, it must be clear from the analysis of spark breakdown, at least at higher pressures, that the effect of local values of  $dV/dx = X$ , the field strength, aside from any space charges, is completely determinative as to the mechanism which is favored. Thus probably less than a 10 per cent change in  $X$  near sparking will favor progression by electron avalanche or as a positive streamer. Since with enough molecules present and with low diffusion the breakdown initiates at the point of highest  $X$  when an electron appears at that point as an axial tear, or field distortion, which propagates itself in one form or another, it will be clear that the distribution of  $X$  in space will set the form of the discharge. Once we know the critical fields,  $X$ , for avalanche and streamer formation in each gas under conditions existing, it is clear that if the form of the field as a function of  $x$  is known for a given gap we can predict the mechanism of gap breakdown. The effect of various electrode surfaces on the field distribution in the gap undistorted by space charge is a purely classical problem in electrostatics. Basically such problems present no great theoretical difficulties. The methods of setting up the equations and of the calculations are well known and can be found in any classical treatise on electrostatics. The solution of the equations is usually complicated, time-consuming, and "messy," mathematically speaking. The difficulties are not insuperable if the objective is worth the time required.

For the more complicated electrode arrangements the mathematical calculation can be avoided by the use of cross-sectional models studied electrolytically. By making a cross-sectional model and placing it in a solution of weak electrolyte in a large trough with the appropriate alternating potentials across the terminals the equipotential lines can easily be traced by a probe connected through a telephone receiver. The method can be made much more accurate and significant by using 60-cycle alternating current at, say, 110 volts with a small lamp in series across the terminals with a weak solution and replacing the telephone by a galvanometer (table type) and copper oxide rectifier. In this way the potentials can be measured accurately, for the drop across the solution is then accurately measured as about 30–35 volts on an a-c meter. A scaled high-resistance wire with sliding contact across the electrodes attached to the rectifier galvanometer and probe gives one at once a set of known potentials whose equipotential lines can be picked off at will on the coordinate scale in the bottom of the trough. By measuring the distance on any line between intersections with the equipotential lines one can evaluate the fields along that line as  $dV/dx$ . If needed, three-dimensional models can be studied also.

Certain field distributions have already been calculated for electrode arrangements of specified form. Thus, in Schumann's<sup>5</sup> excellent book on electrical breakdown field strengths in gases, one will find data on spherical electrode gaps of various lengths and sphere radii. Calculations for the point to plane gap are exceedingly onerous and inaccurate without a great deal of time consumption. Confocal paraboloid gaps are easy of calculation. The use of such gaps, however, limits the range of gaps and points investigated. In the use of such gaps in air the worker is warned to look out for changes in the air as a result of chemical action produced by coronas in a confined space, a difficulty encountered by Trichel and Kip in their studies.

Ignorance of the elements of electrostatics has occasionally led to misinterpretations of more intricate combinations of points, spheres, and plates. What is so often neglected is the fact that, when one has electrodes separated by relatively large distances and assumedly isolated, the *electrodes are not isolated* from the surrounding inductive effects to ground and to other objects. The field distortions by these must be taken into account. In addition a conductor near a field *cannot* be left "floating" with any hope of sensible results. The potential will not only be unknown, owing to inductive effects, but will alter with time on account of migrations of ions. With each conductor at a known potential relative to ground through a sufficiently low resistance the "mysteries" of behavior which are so often reported all vanish. In this respect it must not be forgotten that insulating surfaces of glass or otherwise are excellent accumulators of static charges from the ions. These should be removed as far from the electrodes and the gap as possible and adequately screened. Again

leads to the electrodes also seriously distort the fields unless carefully arranged.

Aside from the question of the form of the field, which will vary in an infinitude of fashions as experimental arrangements change, one can make certain statements of a general character concerning the sparking phenomena observed. Actual photographs of sparks under a large variety of conditions have been published by Terada and Nakaya.<sup>25</sup> These very beautiful pictures, though they give no information as to mechanism, are of value in typifying various modes of breakdown. With a uniform field between plane parallel electrodes, obviously the phenomena discussed in the Part A of Chapter X can be expected. The uniformity of the field obtained will, of course, depend on the ratio of the linear dimensions of the electrode to gap length. For a ratio of linear dimensions to gap length of 3 to 1, the field will be uniform to better than 1 per cent for a distance of the order of the gap length *in the center* of the gap. By confining the active region, by ultraviolet illumination, to an area of linear dimension considerably smaller than this, at the center, adequate uniformity can be achieved. Great trouble is encountered at the edges of the plates, however, owing to their finite thickness. For this reason the edges of the circular plates should be gradually curved upwards in a profile which does not seriously distort the field. If this is not done, breakdown will proceed from the edges with their low radius of curvature as if from two smaller electrodes. The profiling of the edges of the electrodes is best done by means of a model study. The electrodes can be spun out of thin metal or turned out of heavy metal. The names of various workers are often ascribed to such profiles. They have been so often developed independently that no name really should be associated with them.

With sphere gaps there is no essential difficulty as long as the spheres have equal radius. For gaps short relative to the radius, in general, no difficulty is encountered and the departure from the plane parallel potentials is not great. Schumann<sup>6</sup> gives data on these gaps. It must be noted, however, that the higher fields will *now be at the electrode surfaces*. This circumstance will facilitate avalanche production at the cathode and streamer production at the anode at higher pressures. As the electrode radius becomes considerably smaller than the gap length the field is highly distorted. Care must be taken to avoid distortion in mid gap by neighboring conductors, walls, or ionic space-charge accumulations. The initiation of a discharge becomes then primarily a function of the fields at or near the electrodes. If the cathode work function is low and the gas is propitious a negative glow discharge (low pressure) or a corona will appear at the cathode. If conditions are otherwise, a positive corona will start at the anode. These have as a rule a more or less definite "onset" potential at which they become self-sustaining, preceded by a region of intermittent discharge. Depending on gases and electrode surface, these "onset "

potentials may be lower for the negative than for the positive electrode, or vice versa. Neither of these is a spark in the true sense. They will be discussed under the mechanisms of the corona discharge. As the potential is raised above the corona point the mid-gap gradient rises. When with space charges from the coronas present the field in mid gap is such that a streamer can propagate from the anode, a spark will occur. In this case it is seen that already the sparking process is a complicated one proceeding in two or more discharge steps. The progress of such breakdown can be seen at low pressures and even atmospheric with small points in a darkened room.

When one electrode is smaller than the other it is clear that the initiation of corona or glow will be facilitated for the electrode of smaller radius of curvature. This may be more significant when the smaller is positive or negative, depending on circumstances. Hence the breakdown process will tend to become markedly unsymmetrical. *Dissimilar electrodes can then have a limited rectifying action.* It can be said, however, as a result of the point to plane corona investigation that, while the discharge may initiate as a corona or glow at the smaller negative electrode, ultimate breakdown will emanate as a streamer propagation from the anode for at least half the gap length. In these discharges it is seen that the ultimate breakdown potentials depend on the fields in the mid-gap region and that these are strongly influenced by space-charge distortions of the field by corona discharge. They must then also depend on the corona current before breakdown. In this region the influence of neighboring objects must be carefully watched. It is also probable that in such cases air currents in the weak field region, as well as the presence of impurities such as  $H_2O$  or  $NO_2$  in air, which are electron traps, must be considered in their influence. In the extreme case of the point to plane discharge the mechanism is now well understood and will be discussed later.

In general, discharge studies with sharp points cease to have any real significance, and measurements with points from a sparking-potential viewpoint are *sloppy* and meaningless. The "*needle*" gap is not of value in potential measurements, for it is impossible in such cases to define the radius of curvature or to make field-strength calculations, especially in the presence of space-charge distortion. Even for small spheres separated by considerable distances the fields are hard to calculate and inadequately known, owing to the effect of supporting leads and space charges. With needles or points of indefinite shape, sharp cones, hemispherically ended rods, etc., the results as regards potential and field strength are not very significant except as empirical data. When accuracy is needed it is best to use confocal paraboloids. Combinations of more than two electrodes need hardly be discussed from the point of view of sparking-potential studies, for reasons obvious from what has preceded.

The gaps may be used in open air where breakdown under existing

conditions must be known. Otherwise the gaps should be in enclosed chambers as far from walls as possible. All gases should be filtered, and insulators should be dry and so arranged that leakage and corona are prevented. Very frequently minute particles of dust, especially lint when moist atmosphere is present, will completely falsify discharge potentials. Dust must be scrupulously avoided<sup>26</sup> in the gas and on electrodes. Non-conducting dust in the gas is ineffective, but it rapidly charges and settles on the plates, giving corona points or starting secondary discharges at the electrode surface; see page 498. This lint or dust gives rise to minute corona currents and thus causes space charges which may distort the gap. A beautiful illustration of this has recently been seen in corona studies in  $\text{CH}_4$ .  $\text{CH}_4$  breaks down, giving  $\text{C}^+$  ions which collect on the needlepoint cathode. They form filaments of carbon which break off when too large and go to the anode, giving anode streamers. The best procedure is to have all gas admitted through a purifying train with sections filled with glass wool. *Note* glass wool as commercially obtained is *not* chemically clean. All glass wool should be soaked overnight in concentrated  $\text{H}_2\text{SO}_4$  with  $\text{K}_2\text{CrO}_4$  dissolved in it. Then it should be thoroughly drained and rinsed in distilled water until clean and dried under cover or in vacuum. It should be handled as little as possible in the process. (*Caution:* Use rubber gloves.)

All odorous insulating materials should be avoided; this applies equally to stopcock greases. Mercury seals should be avoided. A substance which can be *smelled* emits molecules which may pollute the gas. Hard rubber and the various plastics should *not* be used. The only substances so far found satisfactory are glass, quartz, the glazed porcelains, and the steatites, which are not too porous and can be heat treated. All glass surfaces must be adequately shielded to prevent surface-charge accumulation. The glass should be washed with soap and water and with concentrated  $\text{H}_2\text{SO}_4$  with  $\text{K}_2\text{CrO}_4$  dissolved in it, rinsed with distilled water several times, and outgassed if possible at 350–400° C. If quartz windows are used these had best be joined by quartz to Pyrex seals. Greased and waxed joints should be avoided if possible. If necessary the quartz window can be ground to fit on its seat and sealed with some *hard* sealing wax on the *outside*. Metal parts must be rinsed free from organic materials and had best be outgassed if possible by induction furnace in vacuum, or by at least heating to 250–400° C. All metal parts that are machined are certain to have grease and oil on them. These should be washed off by rinsing in  $\text{CCl}_4$  or acetone, then 95 per cent alcohol and distilled water. Ethyl ether may be used but leaves a slight residue.

The electrodes should be mounted as rigidly as possible. Inter-electrode distances should be read through clear fairly plane glass by cathetometer or traveling microscope, preferably by fiducial marks. Interelectrode distance can be varied from outside by electromagnetic

control. The most accurate method is to produce motion by a threaded nut revolving in a rigid slot and actuated by a soft iron lug which extends within a millimeter of the tube walls. This nut works a screw attached to the electrode. The motion of the electrode should be confined to one axis by rigid ways. It is even possible with slight mechanical ingenuity to arrange to polish an electrode surface in vacuum by electromagnetic control.

*All sparking-potential measurements, except for those designed to test breakdown vagaries in some installation in situ, should have provision made to insure adequate ionization in the gap and especially near the cathode or at its surface.* For a-c gaps it is best to illuminate both electrodes with ultraviolet light.

The reason for this is that in the process of any sparking-potential measurement the potential applied is gradually raised and the passage of a spark looked for. Unless at the time when the potential is reached an electron appears *in an appropriate place in the gap* there will be no spark. The potential will then be raised, and the potential at which a spark finally appears may be considerably above the value at which it would have appeared had electrons been present. That is, the statistical time lag must be reduced to a time short compared to the time delay between increments of potential increase.

Failure to note this has reduced the value of countless spark-potential investigations in past years, largely in the applied field. The best procedure is to illuminate the cathode, or in alternating current *both electrodes*, by means of the light from a quartz mercury vapor arc focused on it by a quartz lens.\* Other ultraviolet sources are not steady and are hard to control or reproduce. Another good procedure is to place within 30 to 100 cm a source of radioactive material giving  $\gamma$  radiation. Generally 2-3 mg of radium salt will suffice. One difficulty attends the use of  $\gamma$ -ray secondaries as an ionization source. The ions are not produced as a continuous random current of isolated electrons. They occur fairly densely arranged in a path, at times in critical regions of the gap within  $10^{-8}$  second of each other. This can lead to the type of rare but propitious ionizing sequences giving sparks below the conventional value of  $V_s$  sought. Sparking will therefore

\* Note that the light from a quartz Hg arc produces quantities of  $O_3$  and other irritating if not poisonous gases in its passage through air. It is best to place the arc under a large glass bell jar with a window cut in it just large enough to take out the needed beam. The base of the bell jar can be perforated, and air should be *withdrawn slowly* by aspirator. The beam of light in its passage through the air can be confined in a tube. For long hours of observation in the confined air of a room these precautions are absolutely essential. Serious chronic sinus and respiratory infections follow prolonged irritation of the mucous membranes by ozone. The technique above assures a steady arc and protects both lungs and eyes from the arc and its chemical products. An opaque box heats too much, and a rapid air blast makes the arc unsteady. Light from the quartz arc *unless filtered through glass* is *very dangerous to eyesight*.



sometimes be more erratic than with ultraviolet light. The ultraviolet light is best and can be almost universally used. The radio-active ionization is not of value for very short gaps or gaps of very small active volume. The source that will produce of the order of 1 electron per microsecond in the active volume of the gap is usually entirely adequate.

The effect of the use of such a source is to reduce the fluctuations of the observed sparking potentials from a spread of the order of 5 to 10 per cent to less than 1 per cent and to *reduce* the average value in the order of 1 or 4 per cent in absolute value.<sup>6</sup> *Adequate ionization must be provided in all sparking-potential measurements.*

The light of a *naked condensed spark* during  $10^{-5}$  second or less when focused on an electrode furnishes an exceedingly powerful source of ions. This gives photocurrents of the order of  $10^6$  times those obtained with the quartz arc. It makes possible sequences of electronic events which are otherwise rare and will produce abnormally low values of the sparking potential as conventionally measured. Except for this condition and the reduction of fluctuations the use of ordinary sources of ionization does *not* affect the sparking potential.

### 3. GASEOUS PURITY

It is clear from the earlier chapters that traces of impurity of certain types and in certain gases when present to 1 part in  $10^6$  can materially influence the Townsend coefficients and hence  $V_s$ .<sup>8</sup> It is clear, then, that sparking-potential measurements on a given gas must be carried out with the possible influence of small traces of impurity in mind. For inert gases and those with metastable states, other gases or vapors of ionization potential below the metastable level are *undesirable impurities* in concentrations down to 1 in  $10^6$  or less. Larger concentrations of impurity having inelastic electronic impacts will reduce the average energy of the electrons and hence  $\alpha$ . Again, traces of gases attaching electrons, such as  $O_2$ ,  $SO_2$ , and the halogens, will by trapping free electrons materially alter the sparking potential. Such impurities, formerly called "*electronegative impurities*," are undesirable. To illustrate this, one might recall that in attempting to reduce sparking in a Van de Graaf generator by placing it in a high-pressure chamber it was announced as a *new discovery* that the use of  $CCl_4$  decreased the sparking and nearly doubled the breakdown potential. There was, in fact, *nothing new* in the discovery. It had been well known for more than thirty years that the halogens in small quantities materially raised the sparking potential. Electrons attach at once to  $Cl_2$ , giving  $Cl^-$  and  $Cl$ .  $Cl^-$  requires 4.1 volts to detach the electron. Pure halogens are too reactive and react with metals unless present in traces, in which case they are removed. Hence any gas like  $CCl_4$

which can yield small amounts of  $\text{Cl}_2$  by ionization as needed will act in this fashion, for, in the act of avalanche formation which precedes discharge, Cl is liberated *right in the discharge path*, and electrons are so reduced in number by attachment that breakdown is prevented.

The matter of impurities is exceptionally difficult to cope with. For inorganic gases the average chemical purification procedure will give purities of the order of 1 in  $10^3$  or  $10^4$ . In most gases the *common* impurities are known, and steps can be taken to reduce them. Certain modes of preparation tend to accentuate impurities. Thus, in the preparation of pure  $\text{O}_2$  by the method recommended in atomic-weight determinations of heating  $\text{KClO}_4$ , the  $\text{O}_2$ , from an ionic viewpoint, was highly impure (1 in  $10^5$ , perhaps), owing to the formation of chlorine oxides. Heating  $\text{KMnO}_4$  or fractionation of commercial  $\text{O}_2$  by liquid air gave  $\text{O}_2$  that was ionically pure but probably *chemically* impure, as it may have contained some of the inert gases which in this work were innocuous. Again, for spectroscopic purposes  $\text{N}_2$  is prepared in a satisfactorily pure state by heating  $\text{NaN}_3$ . Since  $\text{NaN}_3$  is made in an organic process known as diazotization it is contaminated with traces of nitrogen-hydrogen compounds which are liberated as  $\text{NH}_3$ ,  $\text{NH}_2$ , and  $\text{NH}$  in the decomposition of  $\text{NaN}_3$  and with ionization of the gas. These are bad for ion-mobility studies. Similarly,  $\text{N}_2$  made from  $\text{NH}_4\text{NO}_3$  is not pure from an ionic viewpoint (see page 343). To prepare pure, *dry*  $\text{Cl}_2$  devoid of  $\text{HCl}$  one must heat  $\text{CuCl}_2$  and keep it from contact with traces of  $\text{H}_2\text{O}$ . These factors must be carefully considered in the production of gases for spark-potential measurements.

Of all substances, the most difficult to obtain in relatively *pure* state are the organic compounds. Most organic reactions take place in such a fashion that several possible reactions proceed simultaneously with almost equal probability. One hundred per cent theoretical reactions are non-existent, and many unexpected impurities must be avoided. In fact, when we consider that in  $1 \text{ cm}^3$  of a gas there are  $2.7 \times 10^{19}$  molecules it is clear that even with the best technique *no really pure gas* exists. Since impurities from the baked-out glass walls and electrodes give at least vapor pressures of  $10^{-5}$  or  $10^{-6}$  mm we can always expect many unknown impurities which even at 1-mm pressure amount to 1 part in  $10^5$  or  $10^6$ .

Finally, in all compound molecular gases (other than simple molecules such as  $\text{N}_2$ ,  $\text{H}_2$ , and  $\text{O}_2$ ), it is clear that after the first ionization avalanches we will get *dissociation products* and *new molecular species* from atomic recombinations. Thus even the purest of such gases change progressively with a series of sparking-potential measurements in the same gas sample. Even the ultraviolet light used will modify the gas.<sup>29</sup>

#### 4. POWER SOURCES AND TECHNIQUES IN SPARKING-POTENTIAL MEASUREMENT

In the early days of spark-discharge investigations the potential sources available were either static machines or more usually batteries of the liquid sort. The batteries were of limited power output and except at very high expense limited in potential output. Hence, for many years, study was limited to shorter gaps and low pressures. The influence of these limitations on advance and research has been illustrated adequately in Chapters VIII and IX. With the development of the diode rectifier, far higher potentials, constant to 1 per cent and limited in power output, began to be available. More recently the gas-filled rectifiers of the Hg or A type which remove space-charge limitations by the introduction of positive ions into the discharge have considerably extended the power available. The subsequent development of the multigrad control tubes and of the saturable-core reactor stabilizers, as well as of high-capacity high-voltage condensers of the pyranol type, has immensely extended the range of perfection and performance of the rectified a-c high-potential sources. By using 500-cycle a-c generators controlled by saturable-core reactor circuits, full wave rectification, heavy chokes, and capacities in the tenths of microfarad to microfarads, high-potential sources have been perfected that successfully give potentials up to the order of 50 to 100 kv for spark breakdown studies. These are independent of line fluctuations and give potentials constant to 1 part in 1000 and probably to 1 part in 10,000 below 30 kv. The design of these for filtered d-c sources is now so conventionalized that details will not here be given. For the later designs of the saturable-core reactor circuits the reader is referred to a paper by A. F. Kip.<sup>9</sup>

In addition to these, the development of high-tension sources, such as the Van de Graaf static generator and the Cockroft and Walton device capable of giving up to  $2 \times 10^6$  volts for nuclear studies, has still further extended the ranges of application.

One of the great drawbacks to high-voltage studies of breakdown in the past has been the difficulty of making accurate measurement of high potentials. For some years the high potentials were measured by the sparking potential of the sphere-gap electrodes in air. This *most unreliable* and imperfect instrument is now almost obsolete except for high frequencies. It is probable that even this can be avoided in the future. The development of high-resistance towers of accurately known value and the use of such towers with microammeter or galvanometer in series have resulted in a precision in potential measurement of the order of 1 part in 1000 or better below 10 kv and about 1 or 2 per cent at 1000 kv. Such towers used to calibrate the static generator voltmeters or static voltmeters of the repulsion type have given us considerable control of the high-potential measurements.

For the application of high-potential surges for short time intervals numerous devices have been developed and used in recent years, for some of which references are here given.<sup>12,\*</sup> The various modifications of the surge impulse generator by which high potentials are developed in charging condensers in parallel and discharging them in series cannot be presented in detail here. They are still somewhat deficient in yielding potential waves of a known steepness of front and in the sharpness of cut-off after the pulse has passed, if shorter intervals than  $10^{-6}$  second are desired. Still, most interesting results have been obtained. One caution must be urged in the interpretation of the actual potentials developed *at the sparking electrodes* or across the gap in such potential impulse waves. Owing to the reflection of the potential pulse at the end of the line across the gap, a *doubling* of potential for short time intervals may result from phase shifts. As a consequence the real impressed potential can be anywhere from 0 to 100 per cent *above* the amplitude of the potential pulse. The significance of this in the quantitative interpretation of the results must be obvious at once. The matter has been discussed by Wilson and Newman rather briefly.<sup>13</sup> Such difficulties may be avoided by the use of matched impedances.

#### 5. THE DETECTION OF BREAKDOWN AND THE PROCEDURE OF BREAKDOWN MEASUREMENTS

The important feature in previous studies of spark breakdown has lain chiefly in the measurement of the potential  $V_b$  at which the breakdown *appeared* to take place under the conditions existing. An item of considerable interest, which, however, is difficult to measure, is the *current* just preceding the breakdown. So far this has not been exhaustively studied, largely because of the difficulty of measuring the enormous current changes in the transition. Allibone and Meek<sup>14</sup> have made some studies of this sort with the oscillograph in long sparks.

The measurement of the potential at the breakdown instant presents no difficulty. It is the last reading of the potential registering meter before the transition. The criterion for breakdown at which this reading is taken, however, is somewhat varied by circumstances.

The breaking of a visible, audible spark with the corresponding sharp drop in potential in some cases and instantaneous rise of current is a relatively simple criterion. And we see in this procedure several ways in which the spark passage is manifest, to wit: (1) optical, light emission; (2) abrupt potential change; (3) abrupt change in current. These three criteria are the conventional modes of detection. For breakdown with considerable change in light emission the visual

\* Considerable discussion of this can be found in the volume of reference 15 on other pages.

criterion is the most convenient. It is used not only in sparking-potential measurement directly but also as a criterion in the time lag studies with the Kerr cell shutter. The potential change can be used in many cases. It is not common, however, except in oscillographic studies.<sup>15</sup> Here the interpretation of the happenings in respect to potential changes as revealed in the record is of considerable interest, and much work of this kind has been done in the few laboratories equipped with the expensive and elaborate Rogowski and DuFour single-sweep high-speed cathode-ray oscillographs. In fact, until the successful development of these instruments in the latter part of the decade 1920-1930 no such studies were possible. Fig 209A, B shows

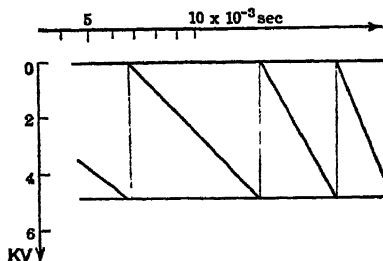


FIG. 209A.

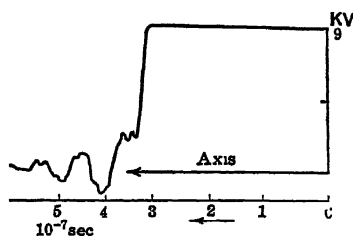


FIG. 209B.

some oscillographs obtained by Strigel and by Rogowski in short-interval surge impulse breakdown. Today there are being placed on the market at reasonable cost cathode-ray oscillographs with single sweep giving better than  $10^{-6}$  second which will aid in the study of many transient phenomena.

Where discharges at low pressure break with relatively small current changes which can be read on the single scales of meters and in which the visually perceptible changes in light intensity are small, it is convenient to use the current changes. Although these different criteria may introduce some difficulties in the interpretation of data involving time lag studies, they are of little difference in their significance in an evaluation of  $V_s$ . In respect to accuracy, the limited range in deflection of the oscillographic record makes the evaluation of the potential as such of little significance except as an orienting magnitude.

The most common procedure in measurement is to proceed with a constant illumination with ultraviolet light and to raise the potential in small increments, pausing in each step from about 5 to 30 seconds to observe whether a spark passes. If no spark passes, then the potential is raised by another increment, and so on. As soon as the first spark is observed the careful investigator will then use smaller increments as he approaches the potential of the first spark. In this way a narrow range in increments of a small order will reveal that in the time

of observation a spark will pass in 50 to 90 per cent of the applications. This is usually taken as fixing the sparking potential. Because in the past the fluctuations in the potential source have given the operator a lack of confidence in his measurements, within a certain potential range, the criteria above have sufficed to fix the potential in his estimation within a certain range of probable error. The occasional sparks which pass at lower potentials have been ascribed to line fluctuations and will not be considered significant.

In the light of what has been said about the mechanism of sparking in Part A, however, such abnormal potentials may have a real significance, for, as was seen, the conventional procedure above in spark-potential measurement is in a sense arbitrary and meaningless. There is a *real* minimum sparking potential or *threshold* in each case set by the condition  $\gamma e^{\alpha s} = 1$ . This is not measured. Above this, *perhaps* as much as 10 per cent or more, lies the *observed conventional sparking potential*  $V_s$ . Between these two a spark may and does pass, but it passes with a given photocurrent the more rarely the nearer the potential applied lies to the threshold. It is quite imperative that the study of the sparking potential be undertaken in a new way. That is, that, with a stabilized source, the potential for a given  $i_0$  be set for a period of hours, and by means of a thyatron circuit and recording counter the number of sparks that pass in a convenient time be counted. The potential should then be raised by an adequate increment and the count should be repeated. Then a plot should be made of the *number of sparks*  $n$ , *per initiating electron*  $n_0$  *in the active part of the gap* as determined from  $i_0$ . In such measurements the photocurrent density should be varied in a known fashion. Such a curve will unquestionably show an exponential variation with potential. It will rise sharply as one approaches the conventional sparking potential and passes beyond it. From the slope of the  $\log n/n_0$  curve against potential  $V$ , an estimate of the threshold value should be obtained. From such a study one will also gain an understanding of the significance and importance of  $V_s$  as actually observed. For a rough evaluation of the sparking potential regime, obviously the value of  $V_s$  will prove useful as it has in the past.

In time lag studies other techniques have been employed. These arise from the necessity of having an initial signal and a breakdown signal to operate the shutter which are sharply defined and electrically convenient. In the investigations of Dunnington<sup>16</sup> and White<sup>17</sup> with the Kerr cell shutter the potential was placed on the gap with constant ultraviolet illumination under such conditions that the statistical time lag was long compared to the time constants of the circuits. Under these conditions the potential across the gap was also across the plates of the Kerr cell,  $K$  of Fig. 210, containing very pure nitrobenzene. This potential renders the nitrobenzene doubly refracting and causes light coming from a source (here the spark gap  $G$ ) which

has passed through a Nicol prism  $N_1$  and is therefore polarized to be partially transmitted through a crossed Nicol  $N_2$  on the far side. Hence as long as the potential is on the Kerr cell the light from  $G$  can be seen. Now, as a spark develops, the light, traveling with the velocity  $c$  in air, passes through  $K$ ,  $N_1$ ,  $N_2$ , until the potential across  $G$  has fallen so low that this fall transmitted over the wires  $W$  has reduced the potential at  $K$  to a value such that the nitrobenzene is no longer doubly refracting. Now as the length of the wires increases,

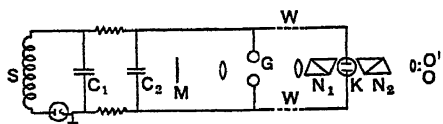


FIG. 210.—Dunnington and White's Arrangement for Visual and Photographic Study of the Initial Stages of Spark Breakdown Using Kerr Cell Shutters.

the potential at  $K$  falls at a later and later time. What is then observed as  $W$  is altered is the continuous emission of light from the instant the spark begins until the potential on  $K$  has fallen to cut-off. As  $W$  is shortened, and with a short distance from  $G$  to  $K$ , earlier stages of the spark can be observed. By placing a mirror  $M$  on the far side of  $G$  from which the light can be brought to a new focus  $O'$ , instead of that at  $O$  for the direct light from  $G$ , one can by changing the distance  $MG$  observe simultaneously light from a later phase of the spark (the direct light) and an earlier phase of the reflected light. By making the path  $GMO'$  sufficiently long compared to  $GO$  and  $W$ , cut-off occurs in  $K$  when the light from earlier and earlier stages of the spark in  $G$  reaches it. At the point where no more light is seen at  $O'$  one knows that the distance  $GMO'$  has been traversed by light in just the time between the emission of the first light and the closing of the shutter.

If the cell were ideal, and the beginning of the sharp fall of potential in the gap caused an equally rapid closing of  $K$ , then the length of the wire path divided by the velocity of the impulse in the wire circuit would give the time elapsed between the fall of potential in the gap, i.e., breakdown, and the closing of the shutter. From the characteristics of the Kerr cell and these measured times it is possible to determine the actual time elapsed between the beginning of the fall of potential in the gap to the effective closing of the shutter. The difference between this time and that for extinction of light along  $GMO'$  gives the time between sharp voltage drop and the first light emission. Hence it is seen that, in these studies, time lags and breakdown can be described in terms of two criteria—sharp voltage drop, and the appearance of light. However, the method does not yield a time lag study. All that the method permits is a study, visual or photographic, of the discharge at *various stages* after breakdown. Hence breakdown as a function of time *after* the sharp drop in voltage can be studied. This study, then, reveals merely the various stages of breakdown in terms of light emission, once the process has started.

Tilles<sup>18</sup> in his measurement of the time lag of sparking used the charge accumulated on a condenser, served by the saturation current from a vacuum tube, to measure the time between the application of potential to the time when the spark appeared. The discharge of the condenser through a ballistic galvanometer divided by the tube current gave the time elapsed. The application of the sparking potential started the charging of the condenser within about  $10^{-5}$  second after application, and the fall of the potential across the gap on sparking terminated the period of charge, as seen in Fig. 211. It was convenient to use, as a preliminary, a potential equal to 96 per cent of  $V_s$ , called the approach voltage. The timing mechanism was operated by the addition of the sparking potential applied, which was the lacking 4 per cent of  $V_s$  plus any overvoltage chosen. Tilles then measured the time lags observed for each overvoltage and plotted them on logarithmic scale. Aside from the fact that he used an exceedingly short gap which made his formative lags long, as stated in Part A of

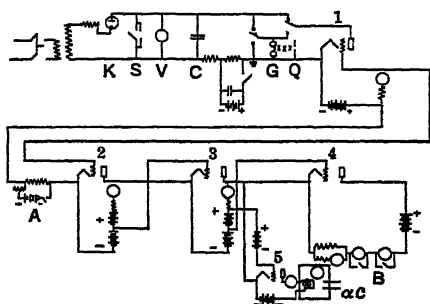


FIG. 211.—Tilles' Arrangement for Measuring Statistical Time Lags of Sparking.

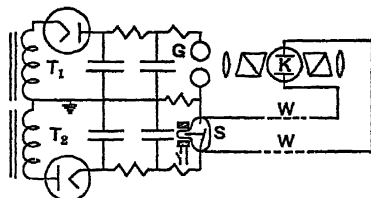


FIG. 212.—Wilson's Arrangement for Studying the Very Short Time Lags of Sparking.

this chapter, the approach voltage must have modified breakdown in his gap, for with 96 per cent of  $V_s$  continually applied there were space-charge accumulations in the gap before  $V_s$  was applied. This must have modified the sparking potential. This was indicated by some measurements made by suddenly applying the whole sparking potential ( $V_s + \text{overvoltage}$ ) at once. In this case the lag phenomena showed a variation with intensity of photoillumination which differed from that in the approach voltage study.

With Kerr cell studies the problem of time lag measurements was complicated by the necessity of having the cell operated to transmission from the *time of application* of the sparking potential to cut-off. Wilson<sup>19</sup> did this as follows. The potential on the gap  $G$  was in two parts, as shown in Fig. 212. The chief potential was given by rectifier set operated by a transformer  $T_1$  continually across the gap. This was a constant *approach* voltage in the neighborhood of  $V_s$  for static





high value of  $i_0$  to initiate the discharge of  $G_2$ . For longer lags this method is excellent if the time for the emission of enough light from  $G_1$  to set off  $G_2$  is *short* compared to the lags studied. Since  $G_1$  takes some  $10^{-8}$  second to reach sufficient intensity to set off  $G_2$ , the method is not applicable to measurement of lags much less than  $2-3 \times 10^{-8}$  second. In Wilson's experiments the true lag from the application of the overvoltage with weak illumination of the cathode was studied. However, the gap had been *prepared* by the development of some space charge as a result of the potential in the approach period. How much the positive space charges in Tilles' and Wilson's studies influenced the breakdown and time lag of the gap cannot be stated. If the *approach* voltage was sufficiently below sparking, the space charges did not play a predominating role.

In a more recent study M. Newman<sup>21</sup> has carried on time lag measurements by a rather unique device. A series of recording meters are so arranged that they respond to the positive surge of the applied voltage, or overvoltage, and to the negative breakdown wave produced by the current in a transmission line. From the known time of travel down the line for the surge impulse, and the point on the line where surge impulse and breakdown wave meet, it is possible to calculate the time lag. This dual wave method eliminates the oscillations and uncertain potentials due to reflection of Wilson's method as well as White's uncertainty in time of breakdown of gap  $G_1$ . Newman finds little difference in the overvoltage-time lag curve for 50 and 98 per cent approach voltages, which indicates that the approach voltages did not seriously disturb the breakdown potential in Wilson's work.

The combined results are shown in Fig. 214. The dotted curves with black triangles are White's curves for weak (1 per cent) ultraviolet illumination, and the open ones for the same work are for Wilson's 100 per cent strong source of ultraviolet light. Agreement with the heavy full curve of Newman with circles and crosses, would be good if correction were made for the  $2 \times 10^{-8}$  second breakdown of  $G_1$ . The curves with the black squares are Wilson's curves for weak illumination, and the curves extrapolated to indefinitely strong illumination are indicated by open squares. It is seen in addition that the difference in definition of time lag does not materially alter the results.

R. Strigel<sup>22</sup> used the cathode-ray oscillograph to study short time

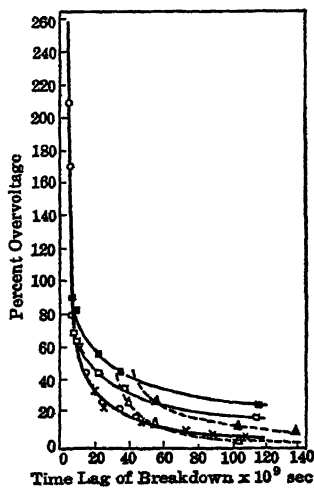


FIG. 214.

lags as a function of overvoltage. Later<sup>24</sup> he used a "Zeit transformer" designed by Steenbeck<sup>23</sup> and himself. This again utilized the charging of a capacity as a time measurement. Strigel's results are not materially different from White's.

## 6. REFERENCES FOR PART B, CHAPTER X

1. BEECK, WHEELER, and SMITH, *Phys. Rev.*, **55**, 601, 1939; SMITH and BEECK, *Phys. Rev.*, **55**, 602, 1939.
2. I. LANGMUIR, *J. Am. Chem. Soc.*, **40**, 1361, 1918.
3. L. F. CURTISS, *Phys. Rev.*, **31**, 1060, 1127, 1928.
4. J. J. THOMSON, *Conduction of Electricity through Gases*, 3d Edition, Vol. 2, pp. 454 ff.
5. W. O. SCHUMANN, *Elektrische Durchbruchfeldstärke von Gasen*, Springer, Berlin, 1923.
6. L. E. REUKEMA, *Proc. Am. Inst. Elec. Eng.*, **47**, 38, 1928; K. MASCH, *Arbeiten aus dem Elektrotech. Inst. der Techn. Hochschule Aachen*, Springer, Berlin, 1931, Vol. IV, p. 87.
7. H. J. WHITE, *Phys. Rev.*, **48**, 113, 1935; ROGOWSKI and WALLRAFF, *Z. Physik*, **97**, 758, 1935.
8. F. M. PENNING, *Phil. Mag.*, **11**, 961, 1931; *Z. Physik*, **46**, 335, 1928; *Konigl. Akad. van Wet. Amsterdam*, **34**, 2, 1931.
9. A. F. KIP, *Rev. Sci. Instruments*, 1940.
10. TUVE, HAFSTAD, HEYDENBERG, and HERB, *Phys. Rev.*, **50**, 504, 1936.
11. J. THOMSON, *Phil. Mag.*, **23**, 6, 1937.
12. T. E. ALLIBONE, *J. Inst. Elec. Eng.*, **81**, 741, 1937.
13. R. STRIGEL, *Wiss. Veröffentl. Siemens-Konzern*, **11**, 52, 1932; R. R. WILSON, *Phys. Rev.*, **49**, 210, 1936; M. NEWMAN, *Phys. Rev.*, **52**, 652, 1937.
14. ALLIBONE and MEEK, *Proc. Roy. Soc.*, **A 166**, 97, 1938.
15. See, for example, volume entitled *Arbeiten aus dem Elektrotechnischen Institut der Technischen Hochschule Aachen*, Julius Springer, 1931, Vol. IV, pp. 75, 85, 193; also R. STRIGEL, *Wiss. Veröffentl. Siemens-Konzern*, **11**, 53, 1932; W. ROGOWSKI, *Arch. Elektrotech.*, **20**, 99, 1928.
16. F. G. DUNNINGTON, *Phys. Rev.*, **35**, 396, 1930; **38**, 1535, 1931.
17. H. J. WHITE, *Phys. Rev.*, **46**, 99, 1934.
18. A. TILLES, *Phys. Rev.*, **46**, 1015, 1934.
19. R. R. WILSON, *Phys. Rev.*, **50**, 1082, 1936.
20. H. J. WHITE, *Phys. Rev.*, **49**, 507, 1936.
21. M. NEWMAN, *Phys. Rev.*, **52**, 652, 1937.
22. R. STRIGEL, *Wiss. Veröffentl. Siemens-Konzern*, **11**, 52, 1932.
23. STEENBECK and STRIGEL, *Arch. Elektrotech.*, **26**, 831, 1932.
24. R. STRIGEL, *Wiss. Veröffentl. Siemens-Werken*, **15**, 1, 1936.
25. TERADA and NAKAYA, *Sci. Papers Instit. Phys. Chem. Research Tokyo*, **4**, 129, 1926; **8**, 1, 63, 103, 197, 1928; **10**, 43, 1929.
26. S. FRANCK, *Z. Physik*, **87**, 323, 1934.
27. N. CAMPBELL, *Phil. Mag.*, **38**, 214, 1919.
28. DUFFENDACK, WOLFE, and RANDOLPH, *Trans. Am. Electrochem. Soc.*, **59**, 181, 1931.
29. R. N. VARNEY, *Phys. Rev.*, **42**, 547, 1932.

## PART C. SPECIAL TYPES OF BREAKDOWN

### 1. INTRODUCTION

Heretofore we have discussed the theory of spark breakdown in gases at atmospheric pressure and somewhat lower, as well as the conditions under which these can be studied. It is now necessary to consider certain types of discharges which do not exactly fall under the category of the original Townsend theory and must be separately studied. These comprise the so-called vacuum spark, the low- and high-pressure corona discharges, including the Geiger counter and the very long sparks as well as a-c sparks. Some of these phenomena are now in a status to be treated in extenso; others, either from lack of information or because the author does not feel himself qualified to discuss them extensively, will be only slightly touched upon.

### 2. VACUUM SPARKS \*

As can be seen from the theory of Townsend, as modified, if the quantity  $p\delta$  becomes vanishingly small, there should be no spark. Interpreted mechanistically, this merely means that, unless gas molecules are present in a space, ionization by collision and hence spark breakdown should not occur. Actually sparks have at all times been observed in vacuum if the potential was high enough. At first this discovery was not seriously regarded, as vacuum technique was not such as to warrant drawing many conclusions. With the development of molecular pumps around 1910, and especially of the mercury vapor jet pump in 1913, pressures of  $10^{-5}$  mm of mercury and less could be achieved. Even at these pressures vacuum sparks could be obtained. Under the direction of R. A. Millikan<sup>1</sup> there had been a series of researches on these sparks which came to a more or less logical conclusion in 1925-28. In this the observations of Lilienfeld<sup>2</sup> on *highly evacuated* X-ray tubes about 1921 also aided, as he observed emission and sparks at sufficiently high potentials which merited further study. It was observed that sparks passed in the best vacua obtainable, which by that time exceeded  $10^{-6}$  to  $10^{-7}$  mm. The sparks passed more readily if the negative electrode was a small point or better still a fine wire. They seemed to emanate from the cathode. They appeared when the field strength on the negative wire surface reached values in excess of  $10^5$  to  $10^6$  volts/cm.

\* References to Section 2, Part C, of Chapter X will be found on page 476.

Millikan, Eyring,<sup>3</sup> and Mackeowen studied these sparks and came to the conclusion that they resulted from intense localized electron emission at the surfaces of electrodes due to the "pulling of electrons out of metals" by the high fields. Since the work function of a metal surface is known, and since this depends in a great measure on the electrostatic image force which is exerted by the conductor on the electron, it seemed plausible that, given sufficiently high electrostatic fields, the potential barrier at the surface would be so lowered that electrons in their thermal motions could escape from the metal. The only difficulty was that the fields required by the value of the work function indicated that the gradients at the metal surface should be more in the order of  $10^8$  volts/cm instead of the  $10^6$  volts/cm observed.

Extensive studies by Millikan and Eyring and Mackeowen and Lauritzen,<sup>3</sup> and also by the staff of the English General Electric Company Research Laboratory under the leadership of Gosling,<sup>5, 6</sup> clarified the situation. This was that the more the wire was flashed in vacuum and the more it was used at a given potential the higher was the applied potential required for sparks. The sparks also occurred only at localized points on the wire,<sup>15</sup> and often spark passage left fine pits on the surface of the wire. All this pointed to the existence of small irregularities on the wire surface at which the field gradients were far higher than those calculated for the wire surface. What then occurred was that in these fields the electrons were able to pour out of the point on the metal. This so raised the local temperature that the gas films at the anode and the metal point vaporized, giving sufficient instantaneous amounts of gas and metal vapor to form a path across which a spark passed. After this the point was destroyed, and some other point requiring in general a higher potential broke down. By judicious choice of wires, and the flashing in vacuum with repeated application of higher and higher potentials, it was possible to reach wire fields of the order of  $10^7$  volts/cm without breakdown.

It was at first believed that the applied external field so reduced the potential barrier of the metal holding the electrons that in their heat agitation they could escape. According to Schottky,<sup>7</sup> for Na this would be  $9 \times 10^7$  volts/cm, and for W  $2.8 \times 10^8$  volts/cm. On this basis the *effect should be* temperature dependent. Up to well above  $1500^\circ\text{C}$  the effect was shown to be independent of temperature.<sup>8, 8</sup> In the period following the introduction of the wave mechanics in 1926, Sommerfeld developed the new electron theory of metals, so that after 1928 the interpretation was open to theoretical treatment by the powerful methods of wave mechanics. At once Houston,<sup>9</sup> Oppenheimer,<sup>10</sup> Nordheim,<sup>11</sup> and Fowler<sup>12</sup> developed the theory to its logical conclusion.

On this treatment the leakage of electrons over the potential barrier at the metal surface by diffraction was considered. When the application of the external field sufficiently lowers the barrier, *all* the elec-

trons, including the degenerate ones, can leak out. The chance of escape at once gives a measure of the current density. It is the larger the greater the lowering of the barrier by the applied field. In this case not only the electrons in the upper edge of the electron band which are subject to thermal agitation can leak over but all the so-called degenerate electrons in the band as well. This then *makes the current largely independent of temperature* at any conveniently realizable temperatures. The equation deduced by Fowler and Nordheim gives the current density  $j$  as

$$j = \frac{e}{2\pi h} \frac{\mu^{1/2}}{(\mu + \phi)\phi^{3/2}} X^2 e^{-\frac{4\pi\phi^{3/2}}{3X}}.$$

Here  $e$  is the electron;  $h$ , the Planck constant;  $\mu$ , the critical temperature of degeneracy in the Fermi distribution, which is

$$\mu = \left(\frac{3n}{\pi}\right)^{2/3} \frac{h^2}{8m};$$

$n$  is the number of free electrons per cubic centimeter;  $m$  is the electron mass;  $\phi$  is the work function;  $X$  is the field strength; and  $K^2 = 8\pi^2 m/h^2$ . In their summarizing article in the *Handbuch der Physik*, Vol. 24, page 441, Sommerfeld and Bethe give a more recent treatment, correcting for the image force field. The equation in amperes per square centimeter for  $\phi$  in volts and  $X$  in volts per centimeter reads

$$j = 1.55 \times 10^{-6} \frac{X^2}{\phi} e^{-\frac{6.8 \times 10^7 \phi^{3/2}}{X}} \psi\left(\frac{3.62 \times 10^{-4} \sqrt{X}}{\phi}\right).$$

Here  $\psi\left(\frac{3.62 \times 10^{-4} \sqrt{X}}{\phi}\right)$  is taken from a table of values and gives the correction for the image force. With the equation of Nordheim and Fowler one can calculate at what value of  $X$  one could expect a detectable current for W with  $\phi = 4.5$  volts. This value is in the neighborhood of  $2-3 \times 10^7$  volts/cm. Actually currents have been observed at fields calculated from the radius of the wire of the order of  $10^5$  to  $10^6$  volts/cm.

This was at once explained by assuming with Schottky<sup>7</sup> that at spots there were small points at which  $X$  was much greater than that computed for a wire. By getting rid of such spots by careful processing, Millikan and Roether got up to fields of  $10^7$  volts/cm before marked emission occurred. Such irregularities have actually been observed on the surface of W wires. To take account of the irregularities, Schottky set  $X = \beta X_m$ , where  $X_m$  is the macroscopically imposed field. Here  $\beta$  is the correction factor coming from the irregularities. If the irregularity is a hemispherical boss on an infinite plane surface

it can be shown that  $\beta = 3$ . If the emitting surface is a second hemispherical boss sitting on the first one, and if it is small compared to the first one,  $\beta = 3^2$ . Thus with submicroscopic irregularities of  $10^{-5}$  to  $10^{-6}$  cm radius one might easily get values of  $\beta = 10$ . This is not unusual and can account for many observations. However, occasional values of  $\beta$  as high as 200 have been reported. This could hardly be correct, for the currents came from only a few spots, and in some cases currents of such a magnitude are observed that it seems hardly likely that such small points as those giving a  $\beta$  of 200 could survive these currents. Therefore, according to Müller,<sup>13</sup> some other factor must be active.

Müller has measured the variation of  $j$  with  $\phi$  for fine points with W and with Ba and Cs. He finds that, contrary to the expectations of the theory, the field emission is *proportional to  $\phi^3$  instead of  $\phi^{3/2}$*  in the exponent. This will at once explain the high values of  $\beta$  required in the experiments of Penning and Mulder,<sup>14</sup> for substituting  $\phi^3$  for  $\phi^{3/2}$  makes the use of values of  $\beta \sim 200$  unnecessary. There is no theoretical reason for this definite empirical fact. The wave-mechanical theory was tested by Müller<sup>13</sup> on the basis of the energy distribution curves of the electrons emitted. These indicate that the observed electrons are the free electrons expected from the wave-mechanical treatment, which is in agreement with the lack of observed temperature dependence. Cs-coated W points gave a measurable field emission at as low as  $10^4$  volts/cm for macroscopically calculated fields. It appears then that the Fowler-Nordheim theory is correct in its broader aspects, but the variation with  $\phi^3$  instead of  $\phi^{3/2}$  in the exponent needs explanation. In any case, however, the general nature of field emission can be said to be understood and calculable, although the constants multiplying into the exponential term cannot be tested accurately by experiment. The currents for any but the highest fields are generally small, but not so small that they are unable to give rise to the vacuum spark. Incidentally, it was on the basis of the vacuum spark that Millikan was inspired to put Sawyer to the task of developing the vacuum spectrograph.

Before leaving the discussion of vacuum sparks and *auto electronic* or *field emission*, a word of caution must be expressed. It has become fashionable in some quarters to assign to auto-electronic emission the electron source necessary to initiate some discharges and to maintain others. Thus, in the arc discharges for the low-boiling-point metals, Mackeown,<sup>16</sup> Compton,<sup>20</sup> Langmuir,<sup>17</sup> Tonks,<sup>18</sup> and Seeliger and Becker<sup>19</sup> have attempted to account for the electrons needed to maintain the arcs on the basis of auto-electronic emission. It is true that the *temperatures of vaporization* of such metals as Cu, Fe, or Hg *cannot permit* of a classically conceived *thermionic emission* sufficient to maintain the arcs. Hence it has become fashionable to invoke field emission at these surfaces, for, over the distance of the mean free paths,

potentials of  $10^5$  to  $10^6$  volts/cm can be *thought of* as acting. However, using the known field emission equations, the auto-electronic currents at such potentials as might exist fall *orders of magnitude short of giving the electronic current densities needed*. In this the theory is just as unsatisfactory as that accounting for such emission on a conventional thermionic basis. In fact, as will later be seen in the discussion of arcs, a thermionic emission of a microscopic type is more likely to be possible than the field emission. In view of the very feeble currents possible from auto-electronic processes, it seems more reasonable to consider the mechanism of electron emission at the cathode of such low-melting-point arcs an unsolved problem than to hide one's ignorance under the glib assumption of auto-electronic emission.

This statement is equally applicable to the suggestion of Flowers<sup>21</sup> that certain low-pressure sparks in swept gaps can be explained by auto-electronic emission. This is especially true when one considers that in this case such sparks have also been observed at somewhat higher potentials from positive point electrodes. In this case Flowers goes so far as to postulate field emission of *positive* ions. Since this type of field emission has never been observed, it seems more logical to attribute both phenomena to the residual gas, which from other lines of evidence in the measurements appears to play a definite role. For real sparks in vacua of  $10^{-7}$  mm or better, auto-electronic emission is unquestionably the causative agent. As long as gas is present the bombardment of the cathode by positive ions, few though they are, may suffice to liberate more gas and cause processes which can lead to a spark.

There are, however, many special cases in which applied fields calculated around points reach  $10^6$  volts/cm. Examples of those may be seen in some impulse breakdowns giving Lichtenberg figures, and in liquids. In these fields the *initiating* electrons leading to later ionization by collision may come from the auto-electronic process. The same might apply to the charged bits of insulating materials on electrodes which lead to self-counting in Geiger counters; see page 499. In the cases mentioned in the preceding paragraphs it is doubtful whether field emission is active. In any case the magnitude of the applied fields can in all such experiments be estimated. Using a maximum value of  $\beta = 10$  one may then calculate the currents to be expected on the Fowler-Nordheim theory. From this one can then definitely decide whether the fields are adequate to give the currents. Unless the Fowler-Nordheim theory is definitely wrong these calculations must suffice and are far more reliable than guesses. In all too many cases the field emission is postulated or assumed as the interpretation without any such calculations.



## 3. REFERENCES FOR SECTION 2, PART C, CHAPTER X

1. MILLIKAN and SHACKELFORD, *Phys. Rev.*, 12, 167, 1918; 15, 239, 1920; G. M. HOBBS, *Phil. Mag.*, 10, 17, 1905.
2. LILIENFELD, *Physik. Z.*, 23, 506, 1922.
3. MILLIKAN and EYRING, *Phys. Rev.*, 27, 51, 1926; EYRING, MACKEOWEN, and MILLIKAN, *Phys. Rev.*, 31, 900, 1928.
4. MILLIKAN and LAURITZEN, *Phys. Rev.*, 33, 598, 1929; *Proc. Natl. Acad. Sci.*, 14, 45, 1928.
5. B. S. GOSLING, *Phil. Mag.*, 1, 609, 1926.
6. STERN, GOSLING, and FOWLER, *Proc. Roy. Soc.*, A 124, 699, 1929.
7. W. SCHOTTKY, *Z. Physik*, 14, 63, 1923.
8. N. A. DE BRUYNE, *Phys. Rev.*, 35, 172, 1930.
9. W. V. HOUSTON, *Z. Physik*, 47, 33, 1928.
10. J. R. OPPENHEIMER, *Phys. Rev.*, 31, 66, 1928.
11. L. NORDHEIM, *Proc. Roy. Soc.*, A 119, 173, 689, 1928; *Physik. Z.*, 30, 177, 1929.
12. FOWLER and NORDHEIM, *Proc. Roy. Soc.*, A 118, 229, 1928.
13. E. W. MÜLLER, *Z. Physik*, 102, 734, 1936.
14. PENNING and MULDER, *Physica*, 2, 724, 1935.
15. WEHNELT and SCHILLING, *Z. Physik*, 98, 286, 1935.
16. S. S. MACKEOWEN, *Phys. Rev.*, 34, 611, 1929.
17. I. LANGMUIR, *Science*, 58, 290, 1923.
18. L. TONKS, *Phys. Rev.*, 46, 278, 1934; 48, 562, 1935.
19. SEELIGER and BECKER, *Ann. Physik*, 24, 609, 1935.
20. K. T. COMPTON, *Phys. Rev.*, 37, 1077, 1931.
21. J. W. FLOWERS, *Phys. Rev.*, 48, 954, 1935.

## 4. SPARKS AT LOW PRESSURES \*

About this region which lies in general below the pressure of the minimum sparking potential, ranging from  $10^{-5}$  mm up to  $10^{-1}$  mm of pressure, very little is known. The rapid increase of the potential  $V_s$  at values of  $p\delta < (p\delta)_m$  has in part militated against studies in this region. Again, the fact that cathode material and state play such an important role in the value of  $V_s$  has on account of the impossibility of control made the results so unreplicable that no progress can be made. However, of recent years interest seems to have revived in this field so that some results have been achieved and some conclusions can be drawn.

The earliest and most extensive study was that of Carr<sup>1</sup> in 1903 in his investigation of the minimum sparking potential. He carried his measurements to fairly high values of  $V_s$  below the minimum value of  $p\delta$  and got curves for the rise of  $V_s$  for potentials below the minimum. Needless to say, the techniques of that day did not take into account the effects of impurity, and one can be sure that his gases and electrodes were contaminated with Hg. He established Paschen's law around the minimum and showed that for a given set of conditions the value of  $V_{sm}$  was constant and that as  $\delta$  was increased the position of the pressure  $p_m$  was shifted to lower values  $p$  such that  $(p\delta)_m$  was con-

\* References for Section 4, Part C, Chapter X, will be found on page 484.

stant. Strutt<sup>2</sup> had shown for  $N_2$  the effect of  $O_2$  on the value of  $V_{sm}$ , and in 1923 Holst and Oosterhuis<sup>3</sup> had shown the effect of cathode material in inert gases. Under the conditions mentioned in Part A of this chapter it is hardly worth while to list values of the minimum in various gases, as these change for traces of impurity, changes in cathode material, and with the degree of cathode bombardment by sparking.

In 1932, after the discovery of Holst and Oosterhuis and the necessity for the use of pure gases, Penning<sup>4</sup> began a study of the inert gases. He found the curve for pure Ne, shown in Fig. 215, using Fe electrodes. When Ne was admixed with small amounts of A ( $\sim 0.002$  per cent), the single minimum of Ne was replaced by a double minimum as shown in Fig. 215. The cause for this is readily seen. At low pressures the small amount of A has no effect, and we observe the usual minimum for pure Ne. As  $p$  increases, the increased number of A

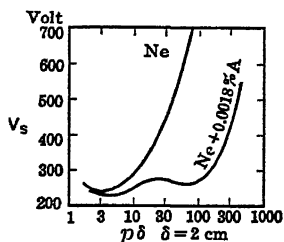


FIG. 215.

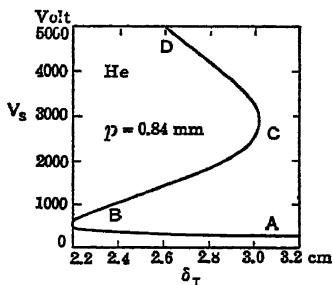


FIG. 216.

atoms which increase in proportion to  $p$  and which are ionized by metastable atoms of Ne give an increase to the value of  $\alpha$  such that a new minimum results. That is, at an adequate total pressure of A it takes a lower potential  $V$  to give a spark than with little A present, owing to the increase in the value of  $\alpha$  by metastable Ne ionizing the A. There are thus two minima, one for Ne and one for A + Ne.

Penning used two tubes of different ratios of gap length to electrode diameter. In these two tubes  $V_{sm}$  occurred at different values of  $p\delta$  (the values of  $[p\delta]_m$  differed by a factor of 3). This appears to be a deviation from Paschen's law. In reality it is not, for Paschen's law can be applied only to a large ratio of electrode diameter to gap length where the conditions in the gap are not altered. In a gap where the gap length  $\delta$  is large compared to the diameter  $D$ , diffusion at these low pressures can alter  $V_{sm}$ . In this case where A was present the diffusion and destruction of metastable atoms of Ne are much larger in the tube of large  $\delta/D$ , so that the tube shows a value of  $(p\delta)_m$  three times as great as with a more normal ratio.

With He the curve gave a peculiar shape indeed. The value of  $V_s$  decreases with  $p\delta$  in the usual fashion from high values of  $p\delta$ . Event-

ally it tends towards a minimum. Then, as in Fig. 216, it slowly increases, reaches a turning point, rapidly increases, requiring larger values of  $p\delta$  at a higher potential. This part of the curve can be obtained only by setting a value of  $V$  in the region studied and varying  $\delta$  until the spark appears. If the value of  $\delta$  were fixed and  $V$  varied, one would get a spark only at the lowest  $V$  and  $\delta$ . At 0.84-mm pressure of He the value of  $V_s$  increases slowly above the minimum to  $\delta = 2.2$  cm. At 2.2 it increases rapidly and then more slowly with increasing  $\delta$  up to 3000 volts and  $\delta = 3$  cm at  $C$  of Fig. 216. Thereafter it increases as  $\delta$  is decreased and ultimately rises sharply. The measurements were made by changing  $\delta$  at a given  $V$ . In the region  $AB$  for  $\delta$  between 2.8 and 2.2 cm the increase ceased. By going to higher voltages and varying  $V$  and  $\delta$ , the parts  $BC$  and  $CD$  could be traced out. It is seen that at the value  $\delta_T$ , Fig. 216, there are three separate values of  $V_s$  of about 300, 1800, 4300 volts, respectively.

The explanation is not especially involved and follows at once from the Compton-Van Voorhis curves. In this region the value of  $V_s$  is in general set by the condition  $\gamma e^{\alpha\delta} = 1$ . As  $X/p$  increases with  $V_s$ ,  $\alpha/p$  at first increases as a  $f(X/p)$ . When, however, the average energy of the electrons is about 3 to 5 times  $E_i$ , the value of  $\alpha$  must fall. This decline was observed by Huxford and Engstrom in  $A$  above  $X/p = 1000$  and by Hale in  $H_2$  at an  $X/p = 1300$ . In the case of He, Compton and Van Voorhis find the peak of the cross-section curve for electron ionization to lie at an electron energy of about 200 volts. The condition for the spark then requires for its realization that  $\gamma e^{\alpha\delta} = 1$ . Assume  $\gamma$  constant, and at a fixed  $p$  let us vary  $\delta$ . As  $\delta$  decreases,  $\alpha$  must increase by increasing  $X/p$  and hence  $X$ . When, however, we get to the peak of the Compton-Van Voorhis curve, an increase in energy of the electrons, and hence an increase in  $X$ , can no longer increase  $\alpha$ . Thus  $\delta$  can no longer be decreased, and we cannot get a spark *under these assumptions below a given value of  $\delta$* . As we continue to increase  $X$  we will find that sparks again pass at larger values of  $\delta$ , for there are two values of  $X$ , one low and one high, at which the ionization probability,  $P_i$ , on the Compton-Van Voorhis curves has the same value. See Loeb Atomic Structure, page 282.

Hence, on the high-voltage side of this curve, as  $\delta$  decreases,  $X$  and  $V_s$  increase, and this would continue indefinitely. However, in this region  $\gamma$  has begun to increase materially, for the positive ions are able to acquire tens of volts of energy and more. Thus as  $\gamma$  increases, even with decreasing  $\alpha$ ,  $\gamma e^{\alpha\delta} = 1$ . At about  $\delta = 3$  cm,  $p \sim 0.76$  mm, and  $V_s = 3000$ , we have  $X = 1000$  volts/cm and a value of  $X/p = 10^6$ . The ionic free path is 0.01 cm; the energy gain of the positive ion per free path is of the order of 10 volts. Hence in this region the positive ions are striking the cathode with 10–30 volts and more. Here  $\gamma$  takes on large values and increases rapidly with  $X$  and  $V_s$ , while  $\alpha$  is decreasing more slowly with  $X$ . Hence the value of  $V_s$  can *again* increase with

decreasing  $\delta$ . Under these conditions the curve for  $V_s$  will continue to rise along more or less conventional lines as  $p\delta$  decreases. In this case we see that, at a given  $p\delta$  in the region between  $\delta = 2.2$  and  $2.8$  cm at  $0.84$  mm pressure of He, there will be three values of  $V_s$ , two caused by the variation of  $\alpha$  with  $X/p$  and one by the rapid rise of  $\gamma$ . Unless  $\delta$  is varied for a given  $V$  in the higher regions, only one point,  $V_s$ , the lowest, will be observed.

One may immediately ask whether this can occur for other gases. Penning found no other gas of those tried that did this. Both A and Ne show peaks in the Compton-Van Voorhis curves at about 130 and 300 volts of electron energy. However, the electron energy distribution in A and in Ne is very different from that in He. Hence it may be that the necessary average energy of the electrons to give a peak for the value of  $\alpha$  does not lie in the range of  $X/p$  encountered near the minimum. Since it is only when the peak for the value of  $\alpha$  occurs for  $p\delta$  at or above the minimum within reasonable potentials that the phenomenon can be observed, it is not strange that it has not been seen. If the peak of the  $\alpha$  curve occurs at values of  $X/p$  for which a spark occurs at larger  $p\delta$  than the minimum, the other sparking potentials cannot readily be observed. In the molecular gases the values of  $X$  and  $V$  required to bring it out are probably so large that it has never been observed. In fact, data on the low-pressure side of  $(p\delta)_m$  are meager; except for the work of Carr there are no data until the more recent work of Cerwin,<sup>5</sup> Neuert<sup>21</sup> and Quinn.<sup>6</sup>

Cerwin and Quinn worked in pure gases and used outgassed electrodes of Ni, except that Quinn used stainless steel with air. Cerwin used air up to 80 kv with  $\delta$  from 2 mm to 10 mm, and Quinn used air,  $\text{CO}_2$ ,  $\text{H}_2$ , and He extending measurements up to 24 kv. Both observers found  $V_s$  to follow more or less an empirical equation,  $V_s = A - B \log p\delta$ , in the straight portion below the minimum. On the basis of Cerwin's measurements, Dempster<sup>18</sup> in 1934 calculated the necessary values of  $\gamma$  to account for sparks at values of  $V_s$  at  $p\delta$  below the minimum. The values are surprisingly high, ( $\gamma = 10 - 100$ ), compared to those of other workers.<sup>19,20</sup> Dempster accounts for these on the basis of points of very low work function which determine the sparking potential while the values of  $\gamma$  observed are averages over a surface.

It was impossible to find data on the first Townsend coefficient at the high values of  $X/p$  utilized. Dempster therefore set up his own theoretical equation for the accumulation of ions, which is equivalent to  $\gamma e^{n\delta} = 1$ . In doing this he proceeded directly from the extension of the Compton-Van Voorhis curve by Buchmann,<sup>19</sup> which applies to electrons of a unique velocity. He apparently ignored the fact that the electrons were gaining energy in a gas and furthermore did not take account of the cumulative character of ionization by collision. The neglect of these factors, which must have been operative even at the lower pressures, results in an *underestimate* of ion multiplication by

electron impact, which is cumulative, therefore throwing the burden of equalization onto the value of the second Townsend coefficient. It is therefore not strange that his computed values of  $\gamma$  should be higher than any previously observed. It is quite essential that measurements of Townsend's  $\alpha$  be carried to high values of  $X/p$  and that these be utilized in the conventional equation to evaluate  $\gamma$ .

Despite these meager data, one may make certain general statements concerning low-pressure sparks. It is seen that the breakdown is roughly set by the criterion  $\gamma e^{\alpha d} = 1$ . Hence the breakdown potential must always depend on the electrical nature of the gas, and we saw the powerful effect of even small traces of impurities in Ne-A mixtures. Thus the minimum and the higher values of  $V_b$  at low  $p$  will always depend on  $\alpha$ . In tubes at very low pressures,  $<0.01$  mm, the character of the gas becomes somewhat doubtful, for adsorbed gases coming from the walls and electrodes, whose nature is unknown, begin to play an important role. Below  $10^{-5}$  mm the gas present is completely indeterminate.

It is seen that again  $\gamma$  plays a very important part in low-pressure sparks. In making this statement we must use the term  $\gamma$  much as we would Townsend's  $\beta$ , that is, as one capable of several interpretations. Primarily at the values of  $X/p$  existing below the minimum,  $(p\delta)_m$ , the mechanism must be a cathode mechanism largely dependent on *secondary liberation by positive-ion bombardment*.<sup>18</sup> As we saw, the minimum usually occurs in the region of  $X/p > 300$  and well up into values of 1000. This corresponds in inert gases to electron energies in the hundreds of volts and in other gases of electron energies well in the tens of volts. Positive-ion energies in He were seen to range from about 2 volts gain per free path to 10 volts, giving positive ions striking the cathode with energies of well up to 5 to 30 volts or more. These have been definitely shown by Oliphant<sup>7</sup> and Penning<sup>7,11</sup> to give notable values of  $\gamma$ . Photoionization in the gas is definitely unlikely. At these electron energies, photon production is not so efficient, as ionization and photon absorption in the rarefied gas at such pressures are most unlikely. What little photoelectric ionization occurs will largely be at the electrodes and will contribute to  $\gamma$ . How the photoelectric component of  $\gamma$  will vary with  $X/p$  and thus with  $V_b$  is difficult to predict. As the work of Bowls and Hale<sup>8</sup> show, peaks may be expected. Photon production decreases as  $X/p$  increases, but more photons reach the cathode. Despite positive-ion energies of the order of 30 volts at low pressures and below  $(p\delta)_m$ , the chances of ionization of the gas by positive impact will be relatively if not vanishingly small. At positive-ion energies approaching 100 volts, if enough molecules are encountered, we can begin to observe some ion production in this action. Despite Penning's<sup>9</sup> statement it will probably *never* play an important role in discharges. Again, at lower  $X/p$ , Penning and Druyvesteyn<sup>9</sup> attempt to explain the great decrease in  $\gamma$  (they esti-

mate it as low as  $10^{-10}$  from sparking in air) as due to the formation of *cluster ions* which produce no secondaries by impact on the cathode. This interpretation is quite faulty. *Ions are not clusters.* Some are simple, small electrochemical complexes. At an  $X/p$  above 20, even these complexes will break up, or better, *they can never form.* How much the complexes would reduce  $\gamma$  is not known. In any case low values of  $\gamma$  are to be expected at low positive ion energies with high pressures where photons are absorbed.

As was seen in the chapter on high-pressure sparks, the mechanism above  $p\delta = 600$  in air depends little on the cathode and most sparking takes place by photoionization in the gas. The studies of Hale in  $H_2$  with Pt and NaH surfaces indicates that at lower  $X/p$  the sparking does *not* depend on a secondary liberation by positive-ion bombardment, but largely on photoelectric processes at the cathode. Hence the phenomenon of secondary electron liberation by positive ions at the cathode appears to be important only in the region of the lower-pressure sparks. When field strengths occur at the cathode surface in excess of  $10^5 - 10^6$  volts/cm, for some metals, sparking may proceed via field currents from small points. Here, despite the low pressure,  $\gamma$  gets to be so large by field emission that the residual gas is completely ionized. Positive-ion bombardment then liberates enough gas from the cathode and the walls to make  $\alpha$  and  $\gamma$  great enough for a spark. Mason<sup>10</sup> has shown that the *electron bombardment of the anode does not liberate enough gas to lead to a spark as might be expected.* Concentration of the discharge at the point can also lead to vaporization and thus the formation of an arc.

As Penning<sup>4</sup> has shown, metastable atoms of a gas  $A$  can materially act to increase  $\alpha$  at low pressures in a gas  $B$  where  $E_{Am} > E_{iB}$ . There are, however, pressures where these effects are an optimum. Below these pressures, diffusion out of the gap and to the anode makes metastable action less important. As elsewhere stated, positive ions are not much less effective as ionizers at the cathode than are metastables.<sup>7</sup> Positive ions can penetrate into the surface and there be neutralized without liberating electrons. Metastables do not penetrate. In many cases positive ions of high speed leave the surface as metastables and thus also produce secondaries. The secondary production at the metal by metastables may be as high as 50 per cent or more, once the metastables reach the surface. On the other hand, metastables diffuse and are lost or destroyed in their diffusion. Practically *all* positive ions reach the cathode. It is therefore doubtful whether at any time metastable atoms serve as the *prime agents* in  $\gamma$ , though at times they are important. On this basis, one could list the possible  $\gamma$  mechanisms and their role in determining  $V_s$  at low pressures. The relative importance is marked by percentages near the minimum and at, say,  $10^{-2}$  mm or less. These are *guesses* based on the author's experience to date.

TABLE XXXV

|   | Near Minimum | Very Low Pressure |
|---|--------------|-------------------|
| Secondary from + ions in gas.....   | None 0       | Few 5%            |
| Secondary from + ions at cathode.....                                       | Some 60%     | Very many 74%     |
| Secondary from photons at cathode ....                                      | Some 24%     | Few 15%           |
| Secondary from photons in gas.....  | Very few 1%  | None 0            |
| Secondary from metastables at cathode..                                     | Few 5%       | Few 5%            |
| Secondary from metastables in gas.....                                      | Some 10% *   | Very few 1%       |
| Secondary from emission of charged insulating particles on the cathode..... | Very few     | Perhaps many      |

\* May go up to 50% with right gases at right pressure.

As to the mechanism of breakdown, practically nothing is known. It must proceed along the lines of the Franck and von Hippel, Schumann, Sämmer, and Kapzov mechanisms. It may show a considerable formative lag compared to the breakdown in overvolted gaps at atmospheric pressure. In a more recent paper Steenbeck <sup>12</sup> gives a plausible theory of the mechanism of breakdown where the gap is long and walls play a role.

One more aspect of the low-pressure discharges are the high velocities of propagation of a glow discharge down a long tube. The phenomenon was first observed by J. J. Thomson <sup>13</sup> in 1893. It was later studied by James <sup>14</sup> and was again observed by Beams <sup>15</sup> in 1926. Beginning in 1930, Beams <sup>16</sup> and later Snoddy, Beams, and Dieterich <sup>17</sup> have studied the phenomenon with revolving mirrors and later with the DuFour oscillograph. When a sharp-wave-front surge of high potential, positive or negative, is applied to the electrode at one end of a discharge tube with air or H<sub>2</sub> at pressures of 0.03 to 15 mm of Hg, the potential wave is propagated down the tube with a very high velocity, in the order of  $10^8$  to  $9 \times 10^9$  or more cm/sec. This is accompanied by luminosity which travels with nearly if not

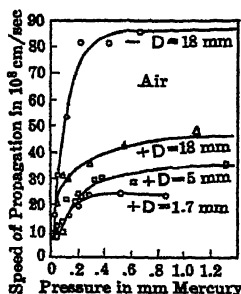


FIG. 217.

the same velocity as the potential wave. On reaching the grounded end of the tube it is reflected and returns to the original sending end with an even higher velocity. Fig. 217 shows the variation of the velocity with pressure and tube diameter in dry air for positive and negative pulses. The velocity in dry air at 0.4 mm increases almost linearly from  $1.7 \times 10^9$  cm/sec at about 73 kv to  $3.7 \times 10^9$  cm/sec at about 175 kv. The maximum currents in the initial wave are very high, ranging from 90 to 200 amperes. The current densities range in the order from 90 to 4000 amp/cm<sup>2</sup>. The potential wave travels down the tube with some attenuation which increases with increas-

ing pressure. For a 194-kv impulse, the attenuation for a 1200-cm tube was such that it reached 180 kv at small pressures, where it fell slowly with increase in pressure and dropped rapidly so that it reached 100 kv at 10-mm pressure. The speed of the returning discharge wave up the tube was much higher and was nearly independent both of sign and of tube diameter. It exceeded slightly the highest limiting wave velocity for the negative pulse and varied very little with sign. For a 132-kv impulse wave it was about  $1 \times 10^{10}$  cm/sec.

It is to be noted that even though this is a low-pressure discharge the propagation is remarkably similar to that observed in lightning discharges. One observes the slow velocities of the leader strokes and the high velocities of the return stroke though the magnitudes at low pressures are not strictly the same. It is clear that in previously ionized plasma the return potential wave has velocities characteristic of an electronic process nearly independent of the various parameters that influence the initial wave. The data are as yet insufficient to formulate a complete theory. It has been suggested by Snoddy, Dieterich, and Beams that the potential pulse is carried by electron ionization, by the rapid movement of electrons, *and* by ionization in advance of the potential pulse by photoionization in the gas. This view is just that advanced by Cravath and Loeb in the explanation of lightning discharge and elaborated in greater detail in the discussion of spark breakdown. What happens in the positive potential pulse is that the enormous field at the cathode starts off an electron avalanche which cumulatively spreads laterally over the whole tube diameter and leaves a positive space charge behind. Into this the photoelectrons pour from the region farther down the tube, ionizing in their turn. In this way the positive potential pulse moves down the tube followed by a luminous pulse with a velocity within 20 per cent of that of the potential pulse. The velocity of formation of the pulse is high, but the initial velocities measured indicate *a definite time to build up the pulse*. At collecting electrodes 110 and 963 cm from the transmitting electrode the potential gradients  $X$  for a 5-mm tube at various pressures were: at 0.4 mm for a positive pulse of 125 kv, 2300 and 2200 volts/cm; at 0.56 mm, 670 and 560 volts/cm; and at 1.3 mm, 420 and 340 volts/cm, respectively. In these,  $X/p$  ranged from  $5 \times 10^4$  to 300. It is possible, of course, that the fronts could have been steeper, but these estimates give a rough idea of the operating conditions.

For the negative pulse the electrons are shot forward and the negative space charge is propagated *ahead* of the potential wave by photoionization. In this case the advance is more rapid. It is a little hard to see how this can be. However, the positive-space-charge field requires for its extension that the electrons travel well inside the tip. Hence they must travel from the point of origin quite a little farther to give the positive tip its necessary field. In the case of the negative wave all that is needed is that the photons be produced ahead in a clear ionizing



region by the gradient. These are unhampered by the positive ions they leave behind, because of the action of the potential in accelerating the negative space charge from the preceding avalanche.

Higher velocities at higher pressures are at first to be expected, since at low pressures the distance required for electron motion between ionizing acts becomes too large. Eventually the pressures must become so high that the inhibiting effects of space charges and the absorption of photons lead to a terminal if not even a diminished velocity. In the ionized plasma, electrons are uniformly present and able to propagate discharge without the delays needed to build up adequate space charges by movement over some paths. Obviously, the higher the imposed surge potential, the faster the wave. Since electron velocities increase about as  $\sqrt{X}$  and the values of  $\alpha$  increase about as the  $\sqrt{X}$  in the region studied, the linear relationship is not surprising. The wall charges on the tubes appear to retard the propagation, although the effect is not very large. If, with increasing data, as Snoddy, Beams, and Dieterich hope, it will become possible to interpret the phenomenon quantitatively, we will be in a fair way to deduce the analogous theory for the high-pressure sparks including lightning.

With these remarks we may leave the subject of the low-pressure sparks for future investigators and turn to the study of the coronas at low and high pressure.

## 5. REFERENCES FOR SECTION 4, PART C, CHAPTER X

1. CARR, *Proc. Roy. Soc.*, A 71, 374, 1903; *Phil. Trans. Roy. Soc.*, 201, 403, 1903.
2. R. J. STRUTT, *Phil. Trans. Roy. Soc.*, 193, 377, 1900.
3. HOLST and OOSTERHUIS, *Phil. Mag.*, 46, 1117, 1923.
4. F. M. PENNING, *Koenigl. Akad. van Wetens. te Amsterdam*, 34, 1305, 1931; *Physica*, 12, 65, 1932.
5. S. S. CERWIN, *Phys. Rev.*, 46, 1054, 1934.
6. R. B. QUINN, *Phys. Rev.*, 55, 482, 1939.
7. F. M. PENNING, *Koenigl. Akad. van Wetens. te Amsterdam*, 31, 14, 1928; 33, 841, 1930; *Physica*, 8, 13, 1928; M. L. E. OLIPHANT, *Proc. Roy. Soc.*, A 124, 228, 1929; OLIPHANT and MOON, *Proc. Roy. Soc.*, A 127, 373, 1930.
8. W. E. BOWLS, *Phys. Rev.*, 53, 293, 1938; D. H. HALE, *Phys. Rev.*, 55, 815, 1939.
9. F. M. PENNING, *Nederland. Tijdschrift v. Natuurkunde*, 2, 33, 1938.
10. R. C. MASON, *Phys. Rev.*, 52, 126, 1937.
11. F. M. PENNING, *Physica*, 8, 13, 1928; *Koenigl. Akad. van Wetens. te Amsterdam*, 31, 14, 1928; 33, 841, 1930.
12. M. STEENBECK, *Wiss. Veröffentl. Siemens-Werke*, 15, 32, 1936.
13. J. J. THOMSON, *Recent Researches*, p. 115, 1893.
14. J. JAMES, *Ann. Physik*, 15, 954, 1904.
15. J. W. BEAMS, *Phys. Rev.*, 28, 475, 1926; 36, 997, 1930.
16. SNODDY, BEAMS, and DIETERICH, *Phys. Rev.*, 50, 469, 1936.
17. SNODDY, DIETERICH, and BEAMS, *Phys. Rev.*, 52, 739, 1937.
18. A. J. DEMPSTER, *Phys. Rev.*, 46, 728, 1934.
19. E. BUEHMANN, *Ann. Physik*, 87, 524, 1928.
20. G. SCHNEIDER, *Ann. Physik*, 11, 382, 1931.
21. H. NEUERT, *Phys. Z.*, 39, 309, 1938.

## 6. THE DISCHARGES FROM POINTS AND WIRES \*

As indicated in Part B of this chapter, when we have two electrodes of different size and well separated the field is concentrated at the electrodes and the mechanisms which are active center in the regions of intense field. Since the fields with appropriate points or wires become sufficiently high for breakdown at these regions long before a spark can propagate across the gas space, we can expect breakdown to proceed in two steps. The first is a breakdown at the electrodes, one or both; and ultimately the second step is a breakdown of the gap as a whole, i.e., a spark. A manifestation of discharge or breakdown at the electrodes is the emission of light, sometimes accompanied by audible noise and by current fluctuations which can be picked up inductively and which manifest themselves in radio interference. The peculiar forms of these localized and partial breakdowns have led to their being characterized by such names as corona and brush discharge and at lower pressures glow discharges.

Thus, as the potential is raised at a point or wire, in the absence of external ionization, there is no appreciable current until one reaches a rather poorly defined potential  $V_s$ , the "starting" potential of the corona or glow. If ionization is present, there is a field-intensified current which near  $V_s$  breaks into a glow or corona having a current some 100 to 1000 times the dark current. In reducing the potential, once the glow has started, one reaches a relatively sharply defined value called the "offset potential" which in reality marks the value of the potential for a self-sustaining corona discharge. It is the potential threshold determined by  $V_s$  at *offset* that we will call the "starting" potential. At potentials ranging from volts at low pressures to hundreds of volts at 760 mm, below  $V_s$ , there is the potential  $V_g$  where pulses of corona start but are not self-sustaining and go out. The region from  $V_g$  to  $V_s$  is called the "*Geiger counter regime*," of which more will be said later. Thereafter, as  $V$  increases beyond  $V_g$  and  $V_s$ , the current increases until, at a potential in some cases many fold higher, the gap as a whole breaks down into a glow or arc at a potential  $V_{sp}$ , the sparking potential.

The terms glow, brush, and corona characterize different visual forms of the phenomena which will be identified with changes in mechanism as the phenomena are studied. At lower pressures the luminosity is general and diffuse over the surface of the electrodes, as one might expect from the high diffusion of electrons at low pressures. This gives the term glow discharge to the manifestation. At atmospheric pressures the luminosity at the negative point or wire is localized at points of small area, while at the positive point it sometimes spreads as a thin film over the high field portions of the conductor. This is termed the corona proper. Under other conditions the luminosity

\* References for Section 6, Part C, Chapter X, will be found on page 513.

extends out into the gap in the form of a brush of diverse geometry. This was originally called the brush discharge.

In what follows we shall first take up the mechanism of the positive and negative wire coronas in concentric cylindrical form at low pressures as the wires permit the study of the fields quite accurately. For the coronas at atmospheric pressure we shall use the point to plane geometry as the tendencies for localization of the discharges in the negative corona to a single spot on the wire would complicate the discussion if a wire were used. In essence there is no fundamental difference in the phenomena using concentric cylinders, confocal paraboloids, or point to plane geometry. The fields in the absence of space charge can readily be computed with concentric cylindrical form. For localized discharges the point to plane or confocal paraboloids must be used, the field in the case of the point to plane geometry being only approximately calculable with any convenience.

**a. The Positive Wire Corona with Concentric Cylinders at Low Pressures.** Let us consider a positive wire of radius  $a$  and a concentric cylindrical cathode of radius  $A$  composed of a metal whose work function is known and constant. For simplicity let us consider the cylindrical condenser of capacity  $C$  thus formed to be of infinite length so that the field is undistorted by the ends and no charges or photons escape. The potential  $+V$  can be applied to the wire  $W$ , the cathode cylinder being grounded. The potential at any point  $r$  cm from the axis of the cylinder in vacuum is then

$$V_r = \int_A^r X dr = \int_A^r -\frac{2q}{r} dr = 2q \log \frac{A}{r}.$$

Here  $q$  is the charge on the condenser given by  $q = CV$ . The capacity of the cylindrical condenser per unit length is  $C = 1/(2 \log A/a)$  if the dielectric constant  $D$  of the gas is neglected. Hence

$$V_r = V \frac{\log (A/r)}{\log (A/a)},$$

and the field at  $r$  cm from the axis is  $X = V/(r \log A/a)$ . It is seen that, if  $r$  and  $a$  are made small,  $X_r$  can become very large.

One may now consider the cylinder filled with a gas at a pressure below 20-mm, but a pressure such that the mean free path of the electrons is still of the order of at least  $A/100$ . The field near the cylinder is relatively weak and at the wire surface is very strong. If, now, an electron is generated in the gas in the cylinder by photon,  $\gamma$  ray, or cosmic ray, then it will move towards the wire  $W$  and at some appropriate distance from  $W$  will begin to ionize by collision. An electron avalanche will then descend upon the wire, creating positive ions and photons in the gas. When the avalanche has reached  $W$ , the positive

space charge, rapidly at first, and later more slowly, will drift to the cylinder  $C$ , while the photons that do not excite or ionize the gas will reach  $C$  with the speed of light.

All the positive ions eventually reach the wall of  $C$ , and a very few of these may produce secondary electrons. However, as the field  $X$  at  $C$  is  $V/(A \log A/a)$ , it is seen that the secondary liberation of electrons by positive ions will be small, i.e.,  $\gamma$  is low. In addition, at the pressures existing, only 1 out of 2 to 20 of these electrons will escape diffusion back to  $C$  in the weak field. On the other hand, practically all the photons, that are not absorbed in the gas and so degraded that they cannot cause electron liberation either in the gas or at  $C$ , will eventually reach  $C$  or liberate an electron in the gas. The photoionization in the gas at low pressures, however, will be relatively small. Hence a fair percentage of the photons for which  $E_\gamma > \phi_s$  will reach the walls of  $C$  and eventually liberate a photoelectron. If a photon is reflected from  $C$ , unless absorbed in the gas, it eventually strikes  $C$  again. For a metal of low  $\phi_s$ , therefore a considerable proportion of the photons can liberate photoelectrons. Hence the  $\eta\theta g$  of Chapter IX can produce an efficient yield of secondary electrons. Greiner<sup>1</sup> has, in fact, shown that the photons produced in a cylindrical system falling onto the walls of a similar one can actually cause the discharge to start. Various estimates have been made as to the efficiency of photoelectron production in such cylinders acting as Geiger counters. The estimates so far made indicate that it takes between  $10^3$  and  $10^4$  photons to produce one photoelectron. In some cases the process may be far more efficient. The number have not been investigated for cylinders that are efficient photoelectric emitters; only the relatively insensitive Geiger counter surfaces have so far been studied. The efficiency, however, is of the order of magnitude of the observed efficiency of photoelectric emission from metals.\*

In addition to the action of photons and positive ions the creation of metastable atoms in the region about  $W$  will yield an important secondary electron production. If these *are not destroyed by foreign atoms or molecules, or by radiation*, they will in general diffuse away from  $W$  and eventually reach  $C$ . There, according to Oliphant,<sup>4</sup> they can liberate electrons more efficiently than positive ions can. If there is in the gas just the optimum number of molecules of class B, whose value of  $E_i$  is less than  $E_m$  of the vehicular gas, then electrons are created by metastables *in the gas*. In this case the metastables do not have to diffuse so far to reach the place of optimum action; each electron liberated is almost certain to be multiplied in the field about  $W$ , for very few electrons can from near  $W$  diffuse back to  $C$  against the field, and the metastables have less losses in number before ionizing. Thus meta-

\* Locher has succeeded in producing photon emitters in Geiger counters which are sensitive to the visible. They have a high background count but appear to be very efficient. These may yield far higher efficiencies than those given.

stables, with their long lives of  $10^{-2}$  second or more, are very effective in liberating electrons and contributing to  $\beta$  or a  $\gamma$  supposed to be due only to positive-ion bombardment. Hence from photon, positive ion, and metastable action we liberate secondary electrons at the cathode or in the gas.

As we raise  $V$  to higher values, the electron avalanches containing more electrons are produced. These avalanches consist of  $\int_r^a \alpha dx$

electrons where  $\alpha = pf(X/p)$ . They contribute a current of  $e(e^{\int_r^a \alpha dx})$  esu per avalanche, and if stimulated from the outside by a number  $n$  of electrons per second the field-intensified current is  $ene^{\int_r^a \alpha dx}$  esu. These avalanches are accompanied by a large number of photons which sooner or later may produce a new photoelectron. This will in due time produce a new avalanche. Hence one avalanche may be followed by another avalanche at some other point, and the current will be larger by a factor  $(1 + l)$ , where  $l$  is the number of secondary avalanches per primary one. If at a potential  $V_i$  a series of fortunate coincidences kept an avalanche coming for each preceding avalanche, then the discharge would be self-maintaining and a constant current independent of externally produced electrons would result. If, however, by chance, in the absence of an external source, one avalanche did not succeed in giving a new photoelectron so timed and placed as to start a new avalanche, the succession would be broken and the current would terminate. Thereafter a new series of avalanches of short duration would occur, started anew by chance ionization imposed from outside and thus capable of being used to count such externally produced electrons. The breaking off of the succession would merely depend on the chance that a photoelectron that could start a new avalanche was *not* created by the last avalanche. The lower  $\int_r^a \alpha dx$ , the less the photon

production and the smaller the chance of a self-sustaining corona. This region of temporary currents due to the partially self-sustaining character of the corona we call the *intermittent corona regime*. It is present in all corona processes and for reasons to be given covers a measurable range of potentials.

When we reach a value of  $V$  such that there is a fair chance of a continued succession of avalanches, we have reached the "*starting*" *potential* of the self-sustaining corona  $V_{sk}$ . This is obviously determined by the Townsend condition  $(\beta/\alpha)e^{\int_r^a \alpha dx} = 1$ , using  $\beta$ , as defined in Chapter IX, in its broadest sense. The condition could also be written  $\gamma e^{\int_r^a \alpha dx} = 1$ , or since *photons* are chiefly active here, it should be

$$\frac{\eta\theta}{\alpha} e^{\int_r^a \alpha dx} = 1.$$

At this potential,  $V_{sg}$ , self-sustaining corona is *likely to predominate* but not with *certainly* as fluctuations can still disturb it. The disturbance is the more likely since, as soon as the self-sustaining corona starts, a space charge of positive ions in transit is formed. This acts to reduce the field at the wire and forces us to increase  $V$  above  $V_{sg}$  to  $V_s$  in order to have the field at the wire sufficient to sustain corona. Thus there is a region of potentials beginning rather indefinitely at  $V_g$  and extending to a higher somewhat less indefinite value  $V_s$  at which the corona sustains itself *despite space charge*. In this at first *occasional* electrons will give a sufficient number of successive self-excited avalanches to register a measurable current. At slightly higher potentials,  $V_{sg}$ , we pass through a region where *each* electron will give a *sustained* series of avalanches long enough to register, but choke themselves off by their own space charge. Finally a region of potentials is reached near  $V_s$  where the chance of break-off is relatively remote.

Now in the region of intermittent corona,  $V_{sg}$  and above, the current pulses  $i$  through a high series resistance  $R$  produce an  $iR$  drop which impressed on the grid of a control circuit can be used to count the current pulses, and thus the frequency of the initiating external electrons from  $\gamma$  rays, etc. Near  $V_g$ , counting may be unreliable, as not *every* electron can start a series of avalanches. Near  $V_s$  each electron starts a series, but the pulse persists so that from  $\gamma$  rays in rapid succession the electrons will not be resolved. The potential regime where counting begins and is unreliable with further potential increase thus gives way to a region in which counting is quite reliable. The range of the reliable counting is increased by the action of the positive space charge which in building up quenches the corona that might otherwise persist. At high enough potentials the *meager* space charge cannot lower the field below the self-sustaining value, and we have above  $V_s$  a steady corona. Owing to diffusion at low pressures this will be of the glow type. The "*plateau*" of self-extinguishing corona where each electron registers is the regime of the *Geiger counter* action. It can be extended by placing a high enough resistance,  $R_s$ , in series with the wire so that the self-sustaining current  $i_s$ , multiplied by  $R_s$ , gives a potential which when subtracted from  $V$ , the applied potential, will reduce the potential of  $W$  below  $V_g$ . The currents  $i_s$  of this character have various values under different conditions but can be reckoned in the order of microamperes as usually studied. Hence if  $R_s \sim 10^9$  ohms the plateau which usually extends over the range of values of the space-charge potential of some 1-3 volts can be extended to 1000 volts. This, however, has the drawback of a long relaxation period, in order to rebuild the potential after the discharge ceases, which makes the counting rate slow. Of this Geiger counter region more will be said later.

Returning now to the condition for self-sustaining corona, we can

quantitatively calculate the effect of space charge and the starting condition for the self-sustaining corona and thereby gain a new insight into the counter and corona action. The analysis to be followed was deduced by Sven Werner<sup>6</sup> in a study of Geiger counter action. An analogous equation based on the same reasoning had been derived in 1914 by Townsend<sup>6</sup> with simplified assumptions. Approximate agreement had convinced Townsend of its essential validity. He then as usual assumed it accurate, and later he and Boulind<sup>7</sup> extended it to very low pressures for estimating ion mobilities. In doing this they carried the equation to conditions where the simple assumptions originally made no longer applied. Thus the peculiar variations of the ion mobility observed by them must be ascribed to an equation which does not apply. Hence once again an equation of the correct form has been applied well beyond its capabilities, leading to data in disagreement with other, more valid observations.

To evaluate the space charge one must apply the breakdown criterion  $\gamma e^{\int_r^a \alpha dx} = 1$  by setting a value of the lower limit  $r$  in the integral. One could assume  $r$  to be the region,  $r_\alpha$ , where  $X/p$  reaches such a value as to make  $\alpha$  finite. This radius is somewhat too large, for what will interest us later is the thickness of the region of intense electron ionization. Owing to the cumulative character of  $e^{\int_r^a \alpha dx}$ , the radius of intense ionization,  $r_u$ , is considerably smaller than,  $r_\alpha$ , that at which  $\alpha$  is first active. The reason for choosing the zone of intense ionization  $r_u$  instead of the zone  $r_\alpha$  where  $\alpha$  is effective will become clear later.<sup>26</sup> In anticipation, however, it may be said that in evaluating the space charge there is a zone of active ionization where the space charge is reduced, owing to electron production, and an important zone outside where space-charge density is constant. It will be useful to use the limit of this zone, which is  $r_u$ , as our limit in integration, so that  $r_u$  will be used in place of  $r_\alpha$ .

Let us then assume that in the region from  $r = a$  to  $r = r_u$  there are  $n$  electron free paths of length  $\lambda$ . And since  $\lambda \propto 1/p$  if  $\lambda_0$  is the free path at 1-mm pressure,  $\lambda = \lambda_0/p$ , where  $p$  is in millimeters of mercury. Whence we have

$$r_u - a = n\lambda = n \frac{\lambda_0}{p}.$$

Now when the applied potential at the positive wire  $V$  is equal to the starting potential  $V_s$  we must assume that the potential at  $r_u$  reaches a critical value  $u$  such that  $\gamma e^{\int_{r_u}^a \alpha dx} = 1$ . Thus, at the potential  $V_s$ ,

$$r_u = \frac{\lambda_0 n}{p} + a,$$

and from the equations for the cylindrical condenser on page 486

$$\begin{aligned} u &= V_s \frac{\log(r_u/a)}{\log(A/a)} = V_s \frac{\log[(\lambda_0 n/p) + a]/a}{\log(A/a)} \\ &= V_s \frac{\log[(\lambda_0 n/ap) + 1]}{\log(A/a)}, \end{aligned}$$

so that

$$u \log \frac{A}{a} = V_s \log \left[ \frac{\lambda_0 n}{ap} + 1 \right].$$

From the constants of the current potential relations at various pressures, as will later be seen, one is able to evaluate  $u$  and  $n$  if  $\lambda_0$  is known. To give an idea of the character of  $u$  and  $n$ , Werner has evaluated the constants for  $H_2$  as follows:  $a = 0.005$  cm,  $A = 0.5$  cm,  $V_s = 650$  volts,  $p = 50$  mm, giving  $n \sim 70$  and  $u \sim 400$  volts.

To calculate the effect of space charge let us proceed as follows. Call  $q$  the number of positive ions per cubic centimeter. This concentration happens to be constant independent of  $r$  beyond the region of intense ionization  $r_u$ , for the following reasons. Let us consider the volume of a concentric shell 1 cm long,  $dr$  thick, at a distance  $r$ . This volume is  $2\pi r dr$ . Now the number of positive ions in transit in any region is inversely proportional to the velocity  $v$ . Hence  $q$  is proportional to  $1/(v2\pi r dr)$ . But  $v$  is directly proportional to  $X_r$ , the field at  $r$ , for the velocity of ions in a gas is  $v = kX_r$ , where  $k$  is the ionic mobility. But  $X_r = V/(r \log A/a)$ , whence

$$q \text{ is proportional to } \frac{r \log(A/a)}{kV2\pi r dr},$$

and hence is independent of  $r$  outside of the region where ionization is taking place. This region is some tens of free paths thick in most cases. In the region from  $a$  to  $r_u$  because of the small volume and the electrons the space charges do not materially affect the fields and hence for simplicity are assumed not to disturb the balance. The space charge outside of this radius  $r_u$  is due to the slowly moving mass of positive ions created in the space, and it acts to reduce the potential  $V$  placed on  $W$ . Now the contribution to the field due to space charge inside a distance  $r$  from  $W$  is per unit length of cylinder

$$\Delta X_r = 4\pi q \frac{\text{Volume inside } r}{\text{Area at } r},$$

as it is only the radial component of the space charge which acts along  $r$ . Hence

$$\Delta X_r = 4\pi q \frac{\pi r^2}{2\pi r} = 2\pi q r.$$



Now  $\Delta X_r = dV/dr = 2\pi qr$ , so that  $V = 2\pi q \int r dr$ . From the wire at  $r = a$  to the cylinder at  $r = A$  the space charge potential, except for the small ionizing region, is

$$V_{aA} = 2\pi q \int_a^A r dr = \pi q(A^2 - a^2).$$

Hence the potential  $V$  is reduced by space charge in the amount  $V_{aA}$  so that

$$V - V_{aA} = V - \pi q(A^2 - a^2).$$

Notice that we have neglected to subtract the space charge within  $r_u$ , which is small only as long as  $r_u$  is small. For large  $r_u$  the equations deduced are inaccurate. The field  $X_r$  is therefore more accurately given by

$$X_r = \frac{V - \pi q(A^2 - a^2)}{r \log(A/a)} - \Delta X_r,$$

when a space charge outside of  $r$  reduces  $X_r$ . Thus we have

$$X_r = \frac{V - \pi q(A^2 - a^2)}{r \log(A/a)} - 2\pi qr.$$

Integrating  $X_r$  from  $r = a$  to  $r = r$ , we find

$$V_r = [V - \pi q(A^2 - a^2)] \frac{\log(r/a)}{\log(A/a)} + \pi q(r^2 - a^2).$$

One may now insert the condition for a self-sustaining corona, which is that  $V_{ru} = u$  at  $r = r_u = \frac{\lambda_0 n}{p} + a$ . Thus we find

$$u = [V - \pi q(A^2 - a^2)] \log \frac{[(\lambda_0 n/ap) + 1]}{\log(A/a)} + \pi q(r_u^2 - a^2).$$

But

$$u \log \frac{A}{a} = V_s \log \left( \frac{\lambda_0 n}{ap} + 1 \right),$$

so that

$$V - V_s = \pi q \left[ (A^2 - a^2) - (r_u^2 - a^2) \frac{\log(A/a)}{\log(r_u/a)} \right].$$

It is next essential to evaluate  $q$ . Now the total current per centimeter length of cylinder at any distance  $r$  is  $i = 2\pi r q v_+$ , where  $v_+$  is the velocity of the positive ions. But

$$v_+ = k_+ X_r = \frac{K}{p} \frac{V}{r \log(A/a)},$$

if we neglect the small correction factors due to space charge. Here  $k_+$  is the ionic mobility at pressure  $p$ ,  $K$  that at 1-mm pressure, and  $V$  is the applied potential. Accordingly we can write

$$i = 2\pi r q \frac{KV}{pr \log(A/a)} = \frac{2\pi q}{\log(A/a)} \frac{VK}{p}$$

and

$$q = \frac{i}{V} \frac{p}{K} \frac{\log(A/a)}{2\pi} = \frac{pi \log(A/a)}{2\pi VK}.$$

Actually this equation is not quite accurate since we have neglected to deduct  $\pi q(A^2 - a^2)$  from  $V$  in  $X$ , and  $2\pi qr$  from the term  $V - \pi q(A^2 - a^2)/r \log(A/a)$  due to field distortions. However, the correction is not serious since the space charge is of the order of some per cent (1-3 per cent) only. The inclusion of all the terms of  $X$ , with field distortion would have made  $q$  a complicated quadratic function of  $i$ . For simplicity, therefore, the approximation is legitimate. Inserting the value of  $q$  into the equation above for  $V - V_s$  we find

$$V(V - V_s) = \frac{\pi \log(A/a) pi}{2\pi K} \left[ (A^2 - a^2) - (r_u^2 - a^2) \frac{\log(A/a)}{\log(r_u/a)} \right].$$

If we neglect  $a$  compared to  $A$  and  $(r_u^2 - a^2)$  compared to  $A^2$ , we find

$$V(V - V_s) = \frac{piA^2}{2K} \log \frac{A}{a}.$$

On analogous considerations, omitting space-charge distortions and neglecting  $a^2$  relative to  $A^2$ , Townsend<sup>6</sup> also found

$$V(V - V_s) = \frac{piA^2}{2K} \log \frac{A}{a}.$$

This equation was early found to hold approximately at higher pressures. When at lower pressures it failed to hold, Townsend ascribed the variation to changes in  $K$ , and this method was used by Townsend and Boulind to evaluate  $K$ . Inasmuch as the equation without corrections cannot be accurate, and since at lower pressures  $r_u$  is much larger than  $a$ , the equation *should* fail. Consequently Boulind's<sup>7</sup> calculations are meaningless, as the equation is no longer accurate. Werner did not evaluate  $q$  accurately, as was done above. He merely wrote  $q = (Cpi)/VK$ , where  $C$  is a constant of proportionality containing the  $\log(A/a)/2\pi$  term of our equation. Werner's equation then reads

$$V(V - V_s) = \frac{\pi C pi}{K} \left[ (A^2 - a^2) - (r_u^2 - a^2) \frac{\log(A/a)}{\log(r_u/a)} \right].$$

The current is 0 at  $V = V_s$ , and above this  $i$  rises as a parabolic func-

tion of  $V$ , for the expression is of the form  $V^2 - VV_s = Bi$ . Let us designate by the letter  $R$  the quantity

$$R = \frac{\pi C p}{KV} \left[ (A^2 - a^2) - (r_u^2 - a^2) \frac{\log(A/a)}{\log(r_u/a)} \right].$$

Then  $V - V_s = iR$ , in which  $R$  has the dimensions of a resistance and expresses the corona gap resistance.

Now  $V_s$  can be determined experimentally by the offset potential, and  $i$  can be measured as a function of  $V$ . Hence we can evaluate  $(V - V_s)/i = R$ , the effective corona resistance, as a function of  $A$ ;  $a$ ; pressure,  $p$ ; and the characteristics of the gas. Again, when  $r_u = A$ , the term in the brackets goes to zero and  $R$  becomes 0, for theoretically we have no space charge then active. From the pressure at which  $R = 0$  and  $r_u = A$  we can solve for  $\lambda_0 n$  from the expression

$$r_u = \frac{\lambda_0 n}{p} + a.$$

If anything is known about the electron free paths, then  $n$  can be evaluated. This is of no great interest, but the evaluation of  $\lambda_0 n$  can at once give us  $r_u$  at any pressure,  $p$ , *provided* that  $\lambda_0 n$  does not change materially with pressure.<sup>28</sup> From  $V_s$ ,  $\lambda_0 n$ ,  $p$ ,  $A$ , and  $a$  we can evaluate  $u$ . With a knowledge of  $r_u$ ,  $a$ ,  $A$ ,  $p$ ,  $V$ , and  $R$  we can calculate  $C$ , assuming the known mobility  $K$  to be the value observed under these conditions. It is seen that, as  $r_u$  approaches  $A$ ,  $V(V - V_s)$  for constant  $C$  and  $K$  begins to decrease. Townsend, in ignorance of this fact, *interpreted the decrease as a real increase in  $K$* . From all these data we can at once calculate the field strength at any point  $r$  from

$$X_r = \frac{V - \pi q(A^2 - a^2)}{r \log(A/a)} + 2\pi q r$$

and compare it with the undistorted field

$$X_r = \frac{V}{r \log(A/a)}.$$

Thus we can derive most of the properties of the corona discharge which are needed for the discussion of the Geiger counter regime if we make measurements of  $i$ ,  $V_s$ , and  $V$ . The resistance  $R$  can be derived from the slope of the  $i - V$  curves above  $V_s$ . Some curves in  $H_2$  at different pressures taken from Werner are shown in Fig. 223. On the other hand, these data tell us little about the actual mechanism. From the knowledge of the field  $X_r$ , we could evaluate  $e \int_{r_u}^a \alpha dx$ , for we can get  $\alpha$  as a function of  $X_r/p$  and thus of  $r$ . With this by setting  $\gamma e \int_{r_u}^a \alpha dx = 1$ , we can evaluate  $\gamma$  or  $\eta\theta/\alpha$ , or whatever quantity we desire. This could and

should be done if really proper control of the cathode cylinder  $C$  and gas properties is to be exercised in the construction of Geiger counters.

As was indicated, the whole operation of the Geiger counter and of the corona depends on the secondary emission from the cathode surface, largely by the action of photons, for without a  $\gamma$  the current could not build beyond that of a single avalanche for each of the electrons from a cosmic ray. Since, however, the value of  $\alpha$  for the gas also enters in, the phenomenon is quite complex.

As concerns gas filling, it is clear that  $\alpha$  will determine the potential in considerable measure. The higher the value of  $X/p$  required for a given value of  $\alpha$ , the higher  $V_s$  may be expected to be. However, it was noted that for proper counter action  $r_u$  must not be too large, otherwise the space-charge action cannot be as positive as it should be.<sup>26</sup> Now, since  $\alpha$  has finite values in inert gases for low  $X/p$ , and *increases slowly*, it is clear that in these gases  $r_u$  at low pressures will be large. Thus space charges at lower pressures will not be effective. For this reason, in order to get an extended Geiger counter regime, *high pressures must be used* with inert gases. This is the case, and in fact in pure inert gases it is necessary to use pressures of nearly 300 mm or more to get counting action.<sup>5</sup> In addition, the presence of metastable atoms keeps potential secondary emission alive for periods of the order  $10^{-2}$  to  $10^{-3}$  second, and care must be used to destroy these before they can diffuse too far beyond  $r_u$ . Here again high pressures are of value. The minimum current  $i_s$  at  $V_s$  is very small, i.e., of the order of  $10^{-9}$  ampere, while  $V_s$  is low,  $\sim 300$  volt at  $p = 535$  mm in Ne-He mixtures.  $R$  is very high, being about  $150 \times 10^6$  ohm. Removal of metastable states by soiling the inert gases with gas molecules destroying metastable states without being ionized is often resorted to and gives good results.

It must be noted that  $R$  the resistance of the counter or corona varies as  $1/K$ . Thus, the lower the mobility,  $K$ , the larger the value of  $R$  the resistance due to space charge. As a consequence, the  $iR$  drop of the corona, once it starts, will be correspondingly larger. Since below  $V_s$  the effective agent in interrupting the corona, aside from chance unfavorable occurrences, is the  $iR$  drop due to space charge, it is clear that the greater  $R$  the larger the natural counting plateau. Hence gases or vapors that reduce  $K$ , other things being equal, have the effect of increasing the plateau for counting. Accordingly, organic vapors like alcohols, acetone, or ether which are not very effective as electron traps do materially lower the mobilities of the positive ions. Probably the best vapors of this sort to use would be the heavier amines, such as propyl amine, which lower the *positive* mobility but do not affect electrons or negative ions. All such gases, however, have the disadvantage of being decomposed by corona discharges, and such counters quickly deteriorate. For example, the life of alcohol vapor counters used for cosmic rays with normal currents is of the order of two months. The heavier the corona currents the worse this deteriora-

tion becomes. Care must be taken in using such vapors to add them to a neutral vehicular gas and not to use them as the gas giving the main pressure, for the vapor-pressure curves of many of these substances are such as to make the counters quite temperature sensitive at ordinary temperatures.

For good counter action one of the best gases is  $H_2$ , which gives a fairly low value of  $V_s$ , has no metastables, and yields a fair plateau since  $i_s$  at  $V_s$  is large. It has also the advantage that it does not react too violently with the pure metal cathodes to alter  $\gamma$ , or  $\eta\theta/\alpha$ , with time by chemical change to give non-conducting films, or to produce reaction products which might give photons after long time intervals (see page 498).

$N_2$  gas is also fairly good. It has a higher threshold than  $H_2$  and gives a lower starting current  $i_s$ , requiring a large external series resistance for a good plateau.  $N_2$  has active forms, (N), and metastable states which reduce its usefulness and tend to make the counter self-exciting. It has the distinct advantage over  $H_2$  of being more effectively ionized by  $\gamma$  and cosmic rays. It also is relatively inert as regards the cathode.

$O_2$  has a very high threshold  $V_s$  but a high  $i_s$ . It is not self-exciting. It is furthermore an electron trap and in the low field regions captures electrons, making negative ions, which is what helps in raising  $V_s$  and is a disadvantage. Its worst drawback is its chemical reactivity which causes a progressive change in the pure metal cathodes with time unless the cathode is thoroughly oxidized to begin with. Air is bad since it combines the disadvantages of  $O_2$  and  $N_2$  and adds to these the creation of complex and varied reaction products.

Some attempts have been made to use organic molecules such as  $C_2H_5OH$  or acetone.<sup>8</sup> These substances are quite chemically unstable and in the corona quickly disintegrate, liberating carbon and other disintegration products which may even give sharp points on the anode wire and spurious discharges. They give a good plateau as they form ions of low mobility, and are reliable in  $\gamma$ -ray and cosmic-ray counters.

There is therefore as yet no thoroughly satisfactory gas, but  $H_2$  and contaminated inert gases at higher pressures appear to give the best results at present.

As regards the cathode surfaces the situation is far worse. These cannot be made so as to have reproducible or even predictable characteristics, and they continually change with use as a result of gaseous reactions, especially if the discharge draws any appreciable current.

For photon counting, surfaces of low work function are desirable. In this connection one immediately thinks of the alkali metals. These have been extensively studied by Werner<sup>5</sup> and actively used by G. L. Locher. Aside from the necessity of keeping them in the dark they have a high natural background count which makes them useless for fine work. As shown by Schulze,<sup>9</sup> this arises from the fact that for large

surface areas the low work function makes *thermionic emission* at room temperatures already so great that the electron liberation from the surface from this cause gives counts in the hundreds per minute. The surfaces are chemically reactive and tend to show bad chemical activation as well as self-excitation which makes counting of rapid events hopeless, unless used with the proper inert gas ( $H_2$ , A, Kr, or Xe). However, they have been used for counting fairly strong photon emission at long wavelengths.

The elements Al and Mg in the *clean and pure unoxidized* state are still too sensitive for ordinary counters. They tend to give spurious counts due to effects of oxides (see page 499) and sensitivity to longer wavelength photons. They therefore tend to self-excitation long after the discharge has died out. Duffendack, Lefschutz, and Slawsky<sup>10</sup> have tried to use clean surfaces of Cu and Fe obtained by sputtering in vacuum. Here again the Cu surfaces appeared to be reactive and are sensitive to photons in the near ultraviolet. Similar results on pure clean outgassed metals heated in vacuum by induction furnace by Henning and Schade<sup>11</sup> showed them to work but in some cases high counts were observed.

Occasionally with fresh unoxidized metal surfaces it was found that the corona continued going off and on regularly after the first corona discharge even in the absence of metastable atoms. These spurious counts due to discharges which either intersperse themselves among the regular externally excited discharges and seriously falsify results or else lead to a continuous periodic counting at the speed at which the discharge circuit permits operation have been a source of considerable annoyance as well as mystery. It was early recognized that with the inert gases using insensitive cathode cylinders some counts were due to the metastable atoms.

Subsequently Bosch,<sup>19</sup> Christoph,<sup>20</sup> and Medicus<sup>21</sup> have ascribed them to the presence of impurities on the cathode. Schade<sup>22</sup> and Kiepenheuer<sup>23</sup> ascribed the action to field emission caused by lowering of the work function by positive ions. They are most frequently observed with dirty electrodes, dirty or soiled glass walls of the containing tube, and dusty gases. They are produced by fingerprint marks on the cathode surface, residues from greases which have been burned off the cathode, and similar agents. They are at times influenced by the use of certain gases, e.g.,  $O_2$  in the tube, which may increase or decrease counts of this character depending on the electrode material and on the gas that is used in the tube subsequently. Bosch,<sup>19</sup> Christoph,<sup>20</sup> and Medicus<sup>21</sup> suspected that on the cathode they were caused by small particles of insulating material which became charged up by the positive ions from the preceding discharge. According to Medicus<sup>21</sup> the effect is decreased by the presence of Hg vapor in the tube.

It was observed that they are definitely produced by an initial dis-

charge. After the *first* discharge the power to produce spurious discharges remains in the tube for some time, but diminishes quasi exponentially with time. The half life of this condition varies from 0.1 second with clean electrodes and pure inert gases giving metastable states to seconds or tens of seconds with soiled electrodes. The magnitude of the effects where metastables do not occur varies over enormous ranges depending on conditions,  $10^6$  or more counts per second to 10 counts. Electrodes thoroughly cleaned by glowing and/or by repeated heavy discharge with properly shielded glass containers, or glass far removed from the unscreened counter apertures do *not* show this phenomenon.

As stated in an interview by G. L. Locher, with properly constructed electrodes, well cleaned, the spurious counts can be ascribed almost entirely to the glass walls. His explanation was that the positive ions reach the clean dry insulating glass walls and are bound there by inductive effects. Conduction currents on the outer surface of the glass walls gradually neutralize the outer bound charges and release the ions inside. These ions eventually give out photons in their subsequent careers and so initiate new discharges. This effect is especially pronounced with counters where split cylinders for admitting photons are used. Locher circumvents this action by covering the outer glass surface with an insulating wax (Superla wax, made by the Shallcross Chemical Company).

A very interesting recent investigation of the self-excitation phenomenon has been made by H. Paetow.<sup>24</sup> Paetow confines himself largely to the action of the electrodes. He studied the action of these activated electrodes by measuring the statistical time lag in overvolted plane parallel gaps. Then he found that with the properly dirty electrodes a single discharge produced conditions such that the statistical time lag for subsequent discharges was much reduced. He plotted the frequency of the subsequent discharges as a function of time of exposure to the initiating discharge for various discharge currents, and as a function of current for various exposures to the initial discharge. Both plots showed a rapid and then slower increase to a saturation count as time of discharge and current increased. After a given discharge the counts fall off rapidly in a quasi exponential fashion to the normal background count in time intervals ranging from tenths of a second to tens of seconds. The initial fall is sharper than an exponential fitted to the later portion of the curve. The effects came from the electrode that had been anode as well as that which had been cathode, though they favored the anode. By using an auxiliary gap so that light from the discharge struck the electrodes of the main gap, the effect could also be produced. The use of quartz in front of the auxiliary discharge destroyed the effect. The removal of traces of impurities by outgassing at high temperatures progressively reduced the counts from  $10^5$  or less to  $10^3$ ,  $10^2$ , and then to about 10. By painting the electrodes with

a dusty brush or dusting MgO powder onto the electrodes, the effect was much increased, prodigious currents being produced. These were identified with the spray electronic emission observed by Güntherschulze from special oxide-coated cathodes of glow-discharge tubes. Coating the cathode with aquadag and then with MgO produced the characteristic emissions observed by Güntherschulze.<sup>25</sup>

The explanation is in part simple. Bits of non-conducting material are charged up on the cathode by positive ions and on the anode and the cathode by *photoelectric* emission by ultraviolet light of *very short wavelength*. Some oxides such as MgO and  $\text{Al}_2\text{O}_3$  do not charge up with the wavelengths from ordinary gases by photo processes. Light from discharges in He and Ne, however, can charge some oxides. He, with its ionization potential at 24 volts is needed for  $\text{Al}_2\text{O}_3$ . The charges on these small particles remain on them until neutralized. This neutralization takes time intervals running into seconds. The presence of these ionized insulating points on the electrodes leads therefore to some process liberating electrons from the cathode for intervals extending over seconds after the discharge has passed.

Paetow postulates a field emission in analogy to Güntherschulze's explanation of the spray electron discharge on cold oxide-coated cathodes. In the latter case a uniform coating of oxide exists and a glow discharge is maintained without ordinary cathode fall, a copious supply of electrons of up to 20 volts energy flowing from the oxide. Güntherschulze, however, finds that a layer of aquadag beneath the  $\text{Al}_2\text{O}_3$  coating is necessary. Whether field emission occurs may be questioned. However, it furnishes a possible mechanism. Unless the fields can be calculated to show that field emission results the explanation cannot be taken as satisfactory or even plausible. Alternative actions must also be considered. For example, across fine bits of insulating materials which are charged by positive-ion bombardment or by photoelectric process and which are lying on an electrode one can expect high fields. If the particles are  $10^{-5}$  cm across and charged to +10 volts on the outside, the fields are of the order of  $10^6$  volts/cm and field emission is not impossible. The field currents would then furnish electrons which initiate new discharges in a Geiger counter and also gradually discharge the particles. Since, however, the dielectric strength of the insulating materials is perhaps less than one that can support  $10^6$  volts/cm the oxide may break down and localized discharges in the dielectric may give the needed electrons. There is also the chance that all these dirty oxides with very short wavelengths behave much as do the phosphorescent zinc sulphides when exposed to light in the visible range. That is, they may reemit the photons absorbed, or longer ones, in the course of time, by much the same processes as have been studied in the zinc sulfides. These photons would of course also trigger off a Geiger counter or an overvolted gap.

It is not clear which of the three processes accounts for the electron



emission from the cathode spots, and probably all are active. Hg vapor reduces the action since it destroys the photons which ionize the oxides. The effect of prolonged heating indicates more probably the destruction of active phosphorescent centers since it is unlikely that at outgassing temperatures the oxides are evaporated or destroyed.

There is an essential difference between the photoionized particles and those charged by positive-ion bombardment. The bombardment charges the *outer* layer of the oxide which is quite readily discharged by subsequent electron bombardment. The photoionization charges the interior as well as the exterior of the oxide grains and thus takes a much longer time to discharge or to reliberate its photons. The ultimate discharge of Al-Al<sub>2</sub>O<sub>3</sub>-Cs<sub>2</sub>O surfaces after charging by positive-ion bombardment shows a high temperature coefficient for discharge, thus indicating that some of the charged particles can discharge by conduction. The dirt particles observed in Paetow's study gave no definite action of this character.

One can then conclude that self-excitation of Geiger counters is largely produced by the accumulation of positive ions on the insulating container walls or the charging of dirt particles on the electrodes by positive ions or photoelectric ionization. As these charges are gradually neutralized either by recombination, phosphorescent action, insulation breakdown, or field emission currents, the metal and glass surfaces emit electrons or photons which ionize the gas and give spurious counts for seconds after an initial discharge.

The avoidance of such annoyances in Geiger counters requires:

1. Adequate screening of insulator surfaces, removal from the proximity of the gap, and/or good external insulation.

2. Extreme cleanliness of the electrode, insured by cleaning before and after mounting, flashing of the filament, and repeated glowing of the metal surfaces and/or cleaning by prolonged heavy discharge under the pump.

3. The use of clean dust-free gases, and the avoidance of He and Ne whose photons are particularly active.

4. The use of metals whose oxides are not prone to give trouble. Al and Mg, unless very carefully cleaned, are not good, since oxides are always present, unless the surfaces are made in vacuum. On the other hand, thicker deposits of CuO do not appear to cause trouble as prepared for cosmic-ray counters. It is either the very highly insulating oxides or those giving phosphorescent compounds activated by extremely short ultra-violet frequencies that cause trouble. It is these actions which have been mis-called chemical effects in reference to spurious counts.

For stable and *relatively insensitive* surfaces which will respond to cosmic-ray,  $\gamma$ , or  $\beta$ -ray ionization and will cut off spurious counts due to few photons of low energy the best surfaces are apparently stable, fairly heavily oxidized surfaces of Cu. These are manufactured in

various ways which amount chiefly to formularies of chemical cookery. The important thing is to get them *uniform*, stable, and reproducible. Needless to say, counters should be made gas tight, and the wire and the cylinder should be clean, smooth, and free from points. The condition or nature of the positive wire plays no role. It can therefore be conditioned by flashing in vacuum. It is hoped that the evaporation of metals in 1–2 mm pressure of inert gases such as A or N<sub>2</sub> giving uniform and oriented reproducible surface films of any metals 1000 to 2000 atoms thick, discovered by Beeck, may eventually lead to cathode surfaces which are more amenable to control. Changes with use, however, cannot be completely avoided.

In the use of these coronas for Geiger counters it is clear that the design for construction must depend on the use and service demanded. Large counters have a large background due to secondary effects but are needed in certain work. For photons large background must be tolerated since sensitive surfaces are paramount. It is thus clear that there is no *general-service* counter. It is also clear that in all counters the design will fall far short of perfection. Many compromises must be made. *Spurious* counts can never be entirely eliminated, and many electrons or  $\gamma$  rays, etc., are not counted. The present-day demand for rapid counting immediately puts on restrictions. Werner has made a fairly good statistical study of the counting rate. He measures the time for the discharge to go out. It is clear that the time required to start the corona and stop it must determine the limit of resolution of the counter. This time,  $t_m$ , is an exponential function of the overvoltage applied,  $V' = V - V_s$ . At  $V_s$ ,  $t_m$  in one case was extrapolated to  $2.5 \times 10^{-7}$  second in H<sub>2</sub>. In going from 0.5 volt to 4 volts in  $V'$  the time changed from  $10^{-6}$  to  $10^{-2}$  second. The probability of the extinction of the discharge as a function of  $V'$  was also determined. In general, aside from the question of the time taken for the discharge to go out, once the potential begins to fall because of space charge (which takes of the order of  $10^{-7}$  to  $10^{-3}$  second, depending on  $V_s$ ), the circuit constants must influence this time. Reducing the capacity reduces the time. Furthermore, conditions leading to self-excitation, excitation by metastable states, and the action of dust will lengthen the time. Too high values of the series resistance used to get a broad plateau will also reduce the counting rate, as this increases the charging time of the circuit after the corona is out as well as the time needed to extinguish the corona. It is necessary to arrive at a suitable balance between these various factors in designing a successful counter so as to count all desired agents and omit all spurious ones.

Before closing this discussion it is of interest to show a few characteristic curves of the positive corona taken from Werner. Fig. 218 shows the current-potential curve for an H<sub>2</sub>-filled tube. The currents are to a logarithmic scale to cover the range of currents. The tube is operated with photons incident on the cylinder from the outside. The

two different curves marked *C* are due to two photocurrents, the lower curve having a photon intensity 29 per cent less than the upper. The lower portions of these curves represent field-intensified photocurrents. The portion marked *B* is the region of rapid increase beyond  $V_s$  where

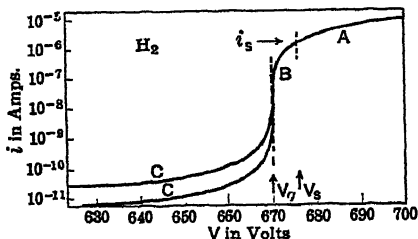


FIG. 218.

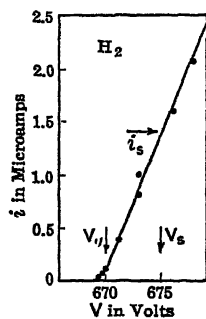


FIG. 219.

photocurrents cease to be due to single avalanches for each photoelectron, but begin to be self-perpetuating, breaking off after a few avalanches owing to space charge. This is the region which marks the rapid rise in counting number with applied potential. The third portion

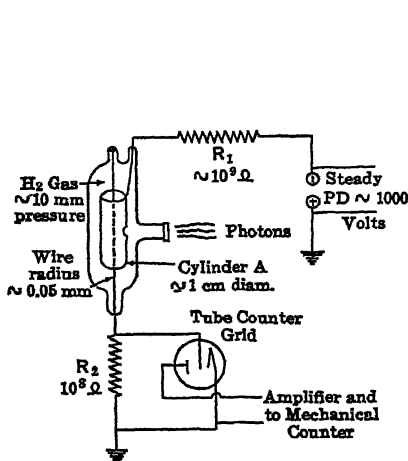


FIG. 220.

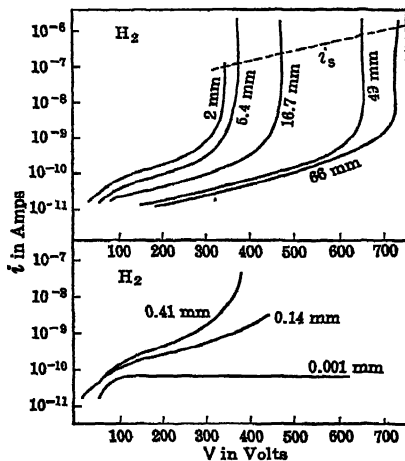


FIG. 221.

*A* is the region of self-sustaining corona. The current  $i_s$  is nearly constant, and the starting potential  $V_s$  is slightly above the break point. It is seen that the region  $V_s$  to  $V_0$  is a very limited region of potential. Fig. 219 gives a detailed picture of the current-potential curve in  $H_2$  with currents plotted to a linear scale in microamperes. The regions

$V_g$  and  $V_s$  are clearly indicated, and the critical current  $i_c$  at  $V_s$  is clearly shown. This current multiplied by  $R_1$ , the series resistance in the Geiger circuit diagram of Fig. 220, gives the applied potential range of the counting plateau in the operated counter, for, when the current rises from a small value to  $i_c$ , as the corona is started, the  $i_c R_1$  drop reduces the applied potential to a value  $\sim V_s$  or below and ensures extinction of the corona. Fig. 221 shows the evolution of the corona curves with change in pressure in the tube. The dashed line by its intercept gives  $i_c$  and  $V_s$ . Beginning with 66 mm of  $H_2$ , the value of  $V_g$  is high and the currents are large.

The thresholds decrease as  $p$  decreases to a minimum at about 2 mm and then again increase. The value of  $V_s$  thus passes through a minimum and then increases as  $p$  decreases further. The last curve at 0.001 mm shows merely a saturation photocurrent slightly increased by ionization by collision.

The curves can be followed to the sparking potential  $V_s$ , with increased potential if desired. The spark occurs in the counters described at currents in the hundreds of microamperes compared to microamperes for  $i_c$  and at about 1.5  $V_s$  to 2  $V_s$ . The lower linear portions of the curves above  $V_g$  at various pressures are shown in Fig. 223. Fig 222 shows the number of counts registered by the counter, by placing an amplifying circuit connected to a mechanical counter across  $R_2$ .

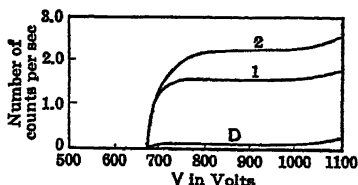


FIG. 222.

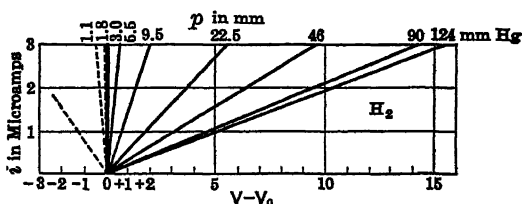


FIG. 223.

The lower curve  $D$  is the natural background count due to  $\alpha$  particles from the walls, cosmic rays, etc.

As the region  $V_g$  at 680 volts is reached the counts are occasional and only the larger successions of avalanches count. At a slightly higher potential almost all photoelectrons produce successions of avalanches that register, and we reach the counting plateau. At the higher potentials the  $i_c R_1$  drop does not succeed in extinguishing the corona completely. That is, after the discharge is out, a metastable atom, a dust-particle discharge, or imprisoned radiation again sets it off. In some cases the tube remains so active that as soon as the discharge is out and the potential recovers a new discharge starts and one has the

Every time the current flows in the system the potential  $iR_2$  biases the input tube of the amplifier and a count is registered. The upper two curves are with two different intensities of photon illumination of the cathode cylinder.

discharge quite periodic with a period determined by capacity, resistance, and other circuit constants. In this case it is probable that  $V$ , the applied potential, is so high that while the voltage drops by  $i_e R_1$  it does not reach  $V_e$  but ends between  $V_e$  and  $V_s$  and rekindles the discharge as soon as the potential is restored. In this region we therefore encounter spurious counts and the tube is useless and unreliable. By removing  $R_1$  and placing a variable condenser across  $R_2$  with a string electrometer we can, as Werner<sup>6</sup> has shown, observe the course of events with weak illumination. The first discharge carries the potential from  $V$  that applied down to  $V_s$ . If before the potential is restored a second photoelectron acts, the potential falls again in small irregular steps to  $V_e$ . The size of the steps depends on the duration of the avalanche succession in the intermittent Geiger regime, before space charge and/or chance breaks off the discharge. In practical operation the capacity is merely that of the counter (5–20 cm), and the resistance  $R_1$  is such that the potential rises nearly to  $V$  after each discharge. In discharge the potential falls at least to  $V_e$  or below, and the corona extinguishes. In the counter discharges the corona discharge, except at very low pressures, is localized fairly closely to the origin of the initiating electrons. That is, they do not usually spread laterally down the length of the wire.

**b. The Negative Wire Corona.** Having now discussed most of the properties of the positive wire low-pressure corona, one may turn to the negative wire corona. Here conditions are materially altered. The cylinder  $C$  is now positive, and the multiple reflection of photons from the walls results in no photoelectrons except in the gas. The many passages through the gas on reflection enhance photoelectric ionization in the cylinder space. Most of this, however, takes place in the large outer volume of low  $X$ , where the electrons are useless. The small surface of  $W$  compared to  $C$  makes the photoelectric liberation from  $W$  smaller than in the case of the positive wire in the ratio  $(a/A)$ . For  $A = 0.5$  cm and  $a = 0.005$  cm, a not unusual case, the ratio is  $10^{-2}$ . Thus  $\eta\theta/\alpha$  and photoelectric ionization in the gas are practically of no influence.

On the other hand, the high field region lies close to the negative wire. In this region positive ions can achieve fairly high energies, especially over the last free path. For in the case of the 0.005-cm corona wire with  $A = 0.5$  cm in  $H_2$ , the value of  $X_a/p$  at the wire surface is of the order of 2000. Here positive ions strike the surface in their last free path with energies of the order of 20 volts. Thus electron liberation by positive-ion impact begins to take on effective values. Hence, once a positive ion is liberated photoelectrically inside  $C$ , there is a chance, albeit not a good one (1 to perhaps 10 per cent), that it will strike the surface and start an outward-moving electron avalanche. This in turn will liberate many positive ions, which in their turn will start new electron avalanches, and so on. If the pressure is low, as in the cases which

we are considering, the diffusion of the outward avalanches<sup>12</sup> spreads the glow over considerable areas of the wire surface and distributes the positive space charge in such a way as to prevent its choking off the corona. It is possible that near onset the corona will tend to localize at points of high  $\gamma$  and may thus like the negative corona at high pressures and the positive corona at all pressures tend to choke itself off by space-charge formation (see page 517). Data, however, are lacking on this point.<sup>13,14</sup> At higher pressures, diffusion does not take place and the localized dense charges quickly succeed in extinguishing the corona.<sup>13,14</sup> The period of extinction lasts until the positive space charge is swept to the wire and the last positive ions rekindle the corona. Thus at high pressures the corona is periodic with a defined frequency determined by the field and the velocity of the positive ions. At the lower pressures, positive-ion velocities are higher, the field extends out farther as the value of  $X/p$  for discharge increases as  $p$  goes down, and the ionization by the electrons is not so intense near the cathode wire as there are not enough molecules in the high field region to be ionized. Thus the chances for heavy space-charge accumulation are less.

It must be borne in mind that, in contrast to the case of the positive wire, where the density of ionization in the avalanche increases up to the surface as a result of the cumulative effect and of the increase in  $\alpha$  with  $X_r$ , it is quite the opposite with the negative wire. Here  $X_r$  is a maximum at  $a$ , and  $\alpha$  is large near  $a$ . On the other hand, the cumulative ionization does not take place effectively for many *ionizing* free paths from the surface of the wire. In that region  $X_r$  is already weak. Thus for the positive corona  $r_u$  was taken as  $n$  electronic free paths in the gas, and for  $H_2$ ,  $n \sim 70$ . This makes  $r_u \sim 0.02$  mm at 20-mm pressure, and  $X_r$  is already one-fourth as great as at the wire surface. Hence, while the ion density should increase exponentially as we leave the wire owing to cumulative ionization,  $X_r$  decreases according to  $1/r$  and  $\alpha$  decreases in the lower range of values of  $X/p$  nearly exponentially with  $X_r$ , so that the ionization rises at first slightly slower than exponentially with  $(r > a)$ , reaches a peak, and drops *very sharply*. This density profile of ionization can be calculated for the *undistorted field only*. In this case the number of ions formed in an electron avalanche for the negative and positive point or wire for the same conditions is the same mathematically, for  $\int_{r_u}^a \alpha dx$  is independent of the sign of the

field. However, in practice there is a marked difference. In the case of the positive point the high field and high electron velocity remove the electrons at once, leaving a space charge of positive ions that enhances the field near the point. With the negative point the electrons move out from a *negative* point, form relatively immobile *positive ions between themselves and the point*, thus weakening the field driving them away, and strengthening the field near the surface. Hence ion production is enhanced near the point but reduced farther out. As a result, there

will probably be in effect less total ion production for the negative wire under similar conditions per electron avalanche. In addition the maximum ion production will be at several ionizing free paths from the negative wire, and hence there will be a definite dark space between wire and the luminous glow. This will constitute what is in essence termed the Crookes dark space in glow discharge, while the glow beyond will correspond to the negative glow. Hence, while the glow is brightest *at the wire in positive wire corona*, there is a definite detachment of the first luminous sheath from the cathode wire surface in the negative corona. This will be more pronounced the lower the pressure.

As is seen, the lateral diffusion of the electron avalanches and some photoionization spread the negative corona over the wire surface at low enough pressures. However as the value of  $\gamma$  is determinative, if this varies over the cathode surface the glow will not be uniformly equally luminous about the wire as it is with the positive corona. It may settle down in patches of enhanced luminosity of greater or less area. At the higher pressures there will appear but a single small patch of corona. At lower pressures, near  $V_s$  there may be only isolated patches of large area. The corona may also show a flickering near onset due to the fact that the positive-ion bombardment temporarily alters  $\gamma$  by denuding the surface of its gas film. The discharge then decreases or goes out in that region to resume again when the surface has recovered. At lower pressures and well beyond the threshold  $V_s$  the glow should be fairly steady and the conditions mentioned do not show.

The current-potential characteristics for the low-pressure negative wire corona near onset have not been studied with modern techniques as intensively as have the positive wire phenomena, as the negative wires do not lend themselves for use as counters. Such studies are now under way in the author's laboratory, but we have no quantitative data at present.

The question of space-charge limitation of the current at once arises. In a gas where the electrons attach to form ions, especially at higher pressures, the negative ions retarded by the positive space charge about the wire can form negative ions. These at higher pressures build up a heavy negative space charge at values of  $r$  well beyond  $r_u$ . The gradient in this region may be such as to cause a new low field region of ionization by collision typified in air by the purple haze of the arc lines. This would correspond to the positive column at low pressures in glow discharge. At somewhat lower pressures the ionization may not occur, but since negative ions have a value of  $K$  about the same as positive ions one could expect the space-charge effect to be about the same. In other gases, however, the electrons being free, with a value of  $K \sim 10^3$  that of positive ions, the *negative* space charge will be negligible. However, there is the positive space charge to consider, which so far has *not* been sufficiently studied. In the high-pressure air corona (760 mm)

it is sufficient and sufficiently localized completely to choke off the discharge and to give a periodic discharge. At lower pressures this will probably no longer occur. The positive space charge is interesting in that it lies inside the region of ionization by collision and helps in setting up this region. It is in part neutralized by the transit (in some places retarded) of the electrons. It is also not entirely destructive, as near to the cathode wire it enhances  $X$  and increases  $\gamma$ . Again, unlike the positive wire corona, it is located in a region of high  $X$  where the accumulation, heavy and concentrated though it is, is being quickly removed. At low pressures it may occur that for this region it is a space-charge sheath of more uniform density than at higher pressures. In any case the space-charge interference at pressures below 1-mm pressure should *not* be so destructive or so strong as with the positive wire corona.

**c. The Starting Potentials of Corona and Pressure.** One aspect of this field of study, the variation of the starting potential of both positive and negative wire or point coronas as a function of gas type and pressure, has been intensively undertaken in more recent years. It was originally started by E. A. Watson<sup>15</sup> and by Townsend's<sup>15</sup> investigations in 1910 to 1914 and has since been carried further by Huxley,<sup>16</sup> Boulind,<sup>7</sup> Bruce,<sup>17</sup> and Penning.<sup>18</sup> Early measurements by Townsend<sup>15</sup> had shown that both coronas have a minimum value of the starting potential  $V_s$ , and this has been confirmed by numerous later observers<sup>6, 7, 16, 17, 18</sup>. This is made theoretically likely from the fact that Townsend<sup>15</sup> had shown that Paschen's law held for the corona discharges. The study of the positive wire corona by Werner<sup>6</sup> as shown in Fig. 221 indicated that as in all such studies where Paschen's law holds one may expect a pressure at which  $V_s$  has a minimum value. In the positive wire corona this appears to occur when the value of  $r_c$  reaches the cathode cylinder  $C$ . At this point Werner has shown that the value of  $R$ , the corona resistance as obtained from the linear starting potential-current curves, takes on a negative slope. These are shown for  $H_2$  in Fig. 223. Here the pressure of 2 mm represents the minimum value  $V_{sm}$ . When this occurs, the glow ceases to lie along the wire *within* the cylinder but lies instead down the wire *extending well beyond the ends of the cylinder*. That is, the discharge needs a greater  $p\delta$  and gets it by increasing  $\delta$ .

Now Huxley<sup>16</sup> observed that in Ne and He the minimum value of  $V_s$ ,  $V_{sm}$  for the negative corona lay at lower values of  $V$  and at slightly lower pressures than  $V_{sm}$  for the positive wire corona under otherwise the same conditions. This is not surprising in view of what has been said concerning the lower space charges occurring in the negative corona when electrons are free as well as the greater effectiveness of  $\gamma$  relative to  $\eta\theta/\alpha$  at low pressures. At higher pressures, however,  $V_s$  for the negative corona appeared to rise above the values of  $V_s$  for the positive corona, instead of following below it as one might expect.



Penning<sup>18</sup> in a masterly study proved that at lower pressures the effect was due to the presence of impurities in the gas. If in Ne we have a gas whose value of  $E_{iA}$ , the ionizing potential, is less than but near  $E_{mNe}$ , the metastable state of Ne, the metastable states begin to exert a very important influence on  $V_s$ , especially as pressure increases and the

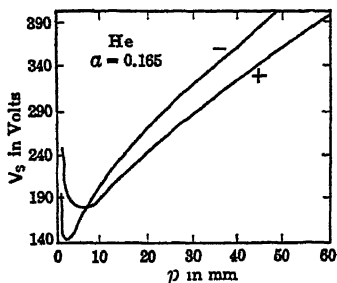


FIG. 224.

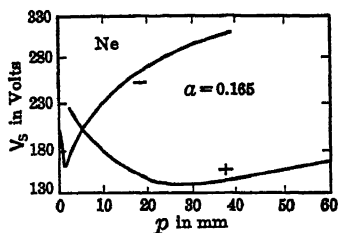


FIG. 225.

pressure of the gas  $A$ , the impurity, becomes appreciable. In this case  $V_s$  for the positive corona is reduced considerably *relative* to  $V_s$  for the negative corona. Both coronas have  $V_s$  reduced, but in the positive corona, for reasons to be given,  $V_s$  is much more reduced. In fact, just as in the case of the plane parallel gap one may observe the *double*

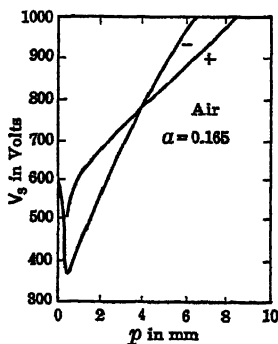


FIG. 226.

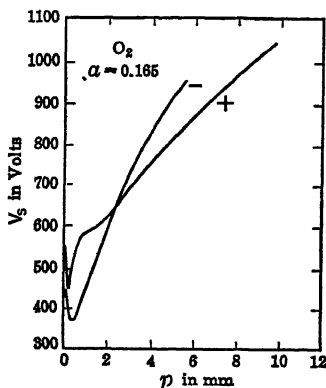


FIG. 227.

*minimum* exhibited by the gap with just the proper quantity of impurity. Curves for the starting potential plotted against pressure in He and in Ne as observed by Huxley<sup>16</sup> are shown in Figs. 224 and 225. In Figs. 226, 227, 228, and 229 are shown Boulind,<sup>7</sup> Huxley, and Bruce's<sup>17</sup> curves for air,  $O_2$ ,  $N_2$ , and  $H_2$ .

Figs. 230 and 231 show the curves of Penning<sup>18</sup> for really pure He

and A. Note that the negative wire curve lies entirely below that for the positive wire. At the end of the run two points were taken after heating the iron electrodes in an induction furnace. The two last points indicated by triangle and circled point after this heat treatment show the negative potential above the positive one. In Fig. 231 the contam-

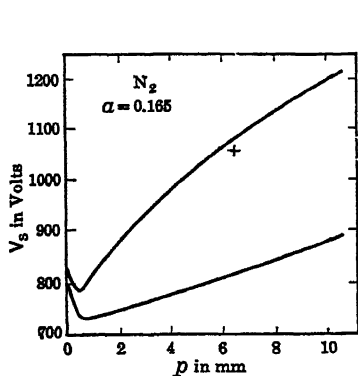


FIG. 228.

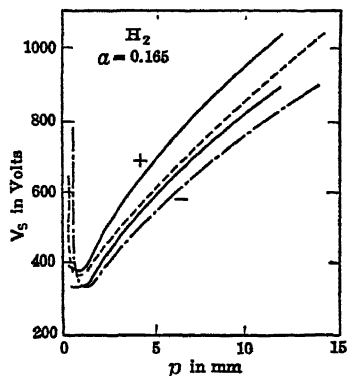


FIG. 229.

ination in A was a small globule of Hg. In both figures the plane parallel electrode results are also represented. In Figs. 232 and 233 the positive and negative wire coronas in pure Ne with different amounts of A as a contaminant are shown for positive and negative wires respectively.

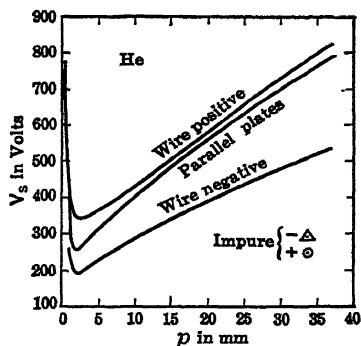


FIG. 230.

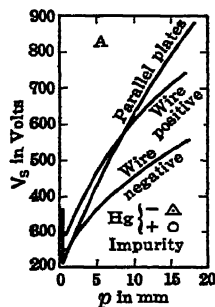


FIG. 231.

If one cared to, one could by comparison of Huxley's<sup>18</sup> curve nearly estimate the percentage of A or analogous impurity that was present in Huxley's Ne, the curves are so similar. Fig. 234 shows a curve in pure Ne and one contaminated with 0.002 per cent A. The dotted curve represents the same contaminated gas irradiated by intense Ne

light. This destroys the Ne metastables and indicates that, even with the inefficient removal of metastables by radiation, the effect is quite

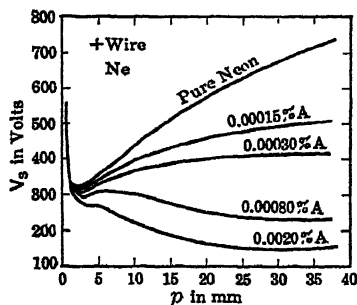


FIG. 232.

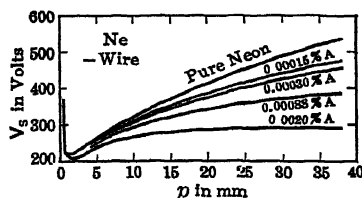


FIG. 233.

pronounced. Analogous results can be obtained by using  $N_2$ , which can destroy Ne metastables without being ionized.

In Fig. 235 is shown the effect of the mercury vapor pressure, in

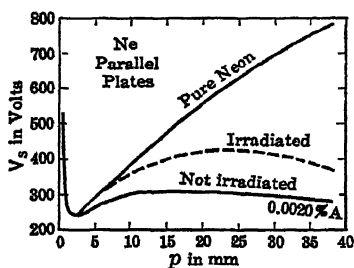


FIG. 234.

terms of temperature, in lowering the observed  $V_s$  in Ne at 21 mm with plane parallel electrodes as observed by Penning.<sup>3</sup> Figs. 236 and 237 show the influence of different percentages of A and Hg on the sparking potential of Ne with plane parallel electrodes.<sup>3</sup> It is seen that Hg is about 10 times as effective as A in Ne. Figs. 238 and 239 give the analogous data for Hg in A and for  $I_2$  in A.<sup>3</sup>

In the latter case, despite the electronegative character of  $I_2$ , the sparking potential is *lowered* by direct ionization of *small amounts*. As soon as  $I_2$  becomes a good electron trap, by being present in any great amount,  $V_s$  rises rapidly.

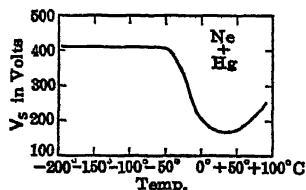


FIG. 235.

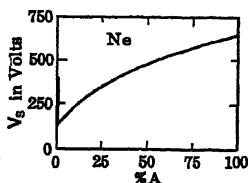


FIG. 236.

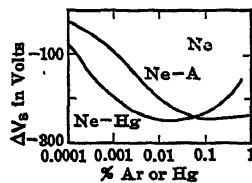


FIG. 237.

Figs. 240 and 241 show the *increase* of  $V_s$ ,  $\Delta V_s$ , for plane parallel electrodes, at different distances  $d$ , for Ne with different amounts of A at 18.4 mm Ne, and Ne-A mixtures at various *pressures* of Ne with 0.0009

per cent A as a function of gap length, produced by irradiating the gas with Ne light.<sup>3</sup> This destroyed the neon metastables. The pressure and percentage variations give us a chance to see where the optimum of destruction of metastables takes place under different conditions. Actual calculations carried out by Penning<sup>3</sup> on the destruction of the metastable states are in rough agreement with the observed maxima. The data on the effect of impurities are introduced at this point inas-

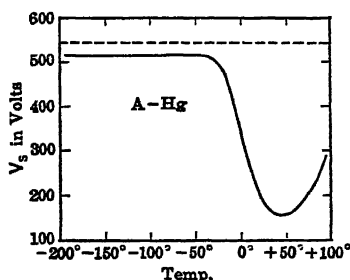


FIG. 238.

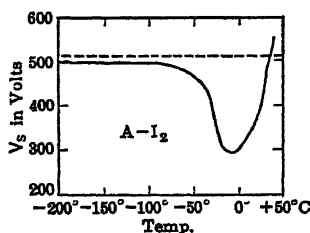


FIG. 239.

much as it is in the study of the coronas that these effects originally came to light, and, since no discussion will be given of  $V_s$  for the glow discharge between plane parallel electrodes, these important data must be included here.

The question of  $V_s$  for positive and negative wires must now be considered analytically in the light of the results just presented. Neglect-

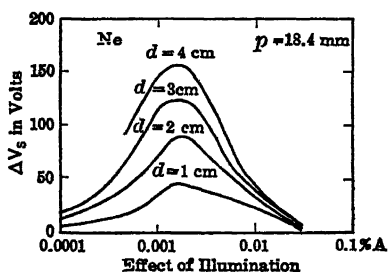


FIG. 240.

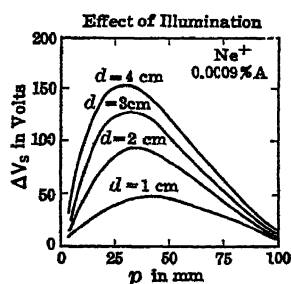


FIG. 241.

ing space charge for the present, we have indubitably for the positive wire at low pressure to set the sparking criterion

$$\frac{\eta \theta g}{\bar{\alpha}} e^{\int_{r_u}^a \frac{ds}{r_u}} = 1,$$

with  $g$  probably unity. Here  $\bar{\alpha}$  is the average value of  $\alpha$  acting. For the negative wire it is certain that the condition at lower pressures will

be  $\gamma e^{\int_{r_u}^{\infty} \alpha dr} = 1$ . Now at low pressures for finer wires  $\gamma$  is sufficiently high so that the value of  $\alpha$  need not be so high in the negative as in the positive case. Thus  $V_s$  might be expected to be lower for the negative corona than for the positive at and around the minimum. In this direction space charges must also militate to increase  $V_s$  for the positive wire above that for the negative wire.

At higher pressures  $\gamma$  should begin to be more nearly commensurate with  $\eta\theta/\alpha$ , since absorption and diffusion to the cathode are only slowly reducing  $\eta\theta$  and the shortened free paths are reducing  $\gamma$  very rapidly above 2-mm pressure. In gases where electrons attach, as in  $O_2$  and air, the negative corona should also begin to encounter increased negative-ion space charges as pressure increases. This is particularly true in  $O_2$  if the electrons get velocities near 1.62 volts before reaching the anode. Again, the action of the corona discharge with  $O_2$  present will change the work function of the cathode by oxidation. This will affect both  $\gamma$  and  $\eta\theta$  but may do so in different measure. At very high pressures (760 mm) where electrons attach the whole mechanism of the coronas change. The space charges throttle off the negative corona and make it periodic;  $\gamma$  is very low. The positive corona no longer depends on  $\eta\theta$  and the cathode but on *photonization in the gas*. Here it is probable that  $V_s$  for the positive point with a streamer-forming mechanism may well be below  $V_s$  for the negative corona. The knowledge with the present data is entirely too uncertain to allow us to prophesy the course of the curves for  $V_s$  for different gases at pressures above 20 mm as a function of  $p$ .

With lower pressures the case is clearer.<sup>2</sup> Here  $\gamma$  for the negative wire is more effective than  $\eta\theta g/\alpha$  is for the positive wire.  $V_s$  near the minimum should be lower for the negative wire and is observed to be so. On the other hand, with gaseous mixtures in which  $E_m$  for the vehicular gas is greater than  $E_i$  for the impurity, the picture is altered. In both cases, metastables are created near the wire and between  $r_u$ , or some distance characterizing the beginning of effective ionization by collision, and  $a$ . These metastable atoms all *diffuse outward*. In the case of the positive wire each electron produced outside of  $r_u$  by such action gives an avalanche of  $e^{\int_{r_u}^a \alpha dr}$  electrons, for loss by diffusion back to the cylindrical cathode is remote.<sup>2,18</sup> On the other hand, for the same ion produced in the negative wire corona the electron is in a weak field region where it does not multiply.<sup>2</sup> The positive ion, it is true, does run into the wire, but only a fraction  $\gamma$  of these will produce an avalanche.<sup>2</sup> Even granted that, for such an avalanche, space charge does not decrease the size of the avalanche, the number of new ions created per metastable with the negative wire is only  $\gamma e^{\int_{r_u}^a \alpha dr}$ . Of course, such metastables as ionize in the cylindrical volume between  $a$  and  $r_u$  will be as effective as in the positive case. Thus, except at very low pressures, where  $r_u$  is large, the negative wire corona will not

have its value of the effective secondary production  $\gamma$  nearly as much influenced as the positive wire corona.<sup>2,18</sup> This is amply borne out by all the careful studies of Penning<sup>18</sup> for various impurities at different concentrations.

The analogous reasoning applies to all impure gases, and it is seen that, as long as gases are pure, *except* for O<sub>2</sub> (which also may not have been pure), the value of  $V_*$  for a negative wire lies below that for a positive wire of the same radius. It is possible in O<sub>2</sub> that O or O<sub>3</sub> formed by the corona discharge may have acted as a different molecular species and thus have yielded the same effect as an impurity.

The percentages of the various constituents of the mixed gas, air, make it doubtful whether we can explain the change in relative positions of  $V_*$  for positive and negative coronas on the basis of metastable states or impurities. Thus one should not accept the statement that  $V_*$  for the negative point should *always remain below that of the positive point*<sup>18</sup> unless there is *impurity* present as a *universal* rule. For pure inert gases the statement of Penning<sup>18</sup> is true and must be true. For molecular gases it appears to be true for N<sub>2</sub> and H<sub>2</sub>, while it does not appear to be true for O<sub>2</sub> and air. The common feature of these two non-conforming gases is that they are electron traps. At 2 mm, however, where crossing of the  $V_*$  curves appears to occur, there is probably little trapping of electrons under ordinary conditions. It must, in any case, be clear that, where the mechanism of corona action can change as radically as it does between 2 mm and 760 mm, crossing of the  $V_*$ - $p$  curves may take place. Since there are also other factors sufficient to cause interchange of the positions of the  $V_*$  curves for positive and negative corona beside impurity, this fact should not be overlooked in trying to account for such reversals. Thus, although in general we have some excellent information regarding low-pressure positive and negative coaxial cylindrical corona discharges, much remains to be learned about the behavior of the negative corona at lower pressures.

## 7. REFERENCES FOR PART C, SECTION 6, CHAPTER X

1. H. GREINER, *Z. Physik*, **81**, 543, 1933.
2. L. B. LOEB, *J. Applied Physics*, **8**, 495, 1937.
3. F. M. PENNING, *Z. Physik*, **46**, 335, 1928; **57**, 723, 1929.
4. M. L. E. OLIPHANT, *Proc. Roy. Soc., A* **124**, 228, 1929.
5. SVEN WERNER, *Z. Physik*, **90**, 356, 1934; **92**, 705, 1934.
6. J. S. TOWNSEND, *Phil. Mag.*, **28**, 83, 1914.
7. H. F. BOULIND, *Phil. Mag.*, **18**, 909, 1934.
8. TROST, *Z. Physik*, **105**, 399, 1937.
9. R. SCHULZE, *Z. Physik*, **90**, 67, 1934.
10. DUFFENDACK, LEFSCHUTZ, and SLAWSKY, *Phys. Rev.*, **52**, 1231, 1938.
11. HENNING and SCHADE, *Z. Physik*, **90**, 597, 1934.
12. H. RAETHER, *Z. Physik*, **107**, 91, 1937.
13. G. W. TRICHEL, *Phys. Rev.*, **54**, 1078, 1938.
14. G. W. TRICHEL, *Phys. Rev.*, **55**, 382, 1939; A. F. KIP, *Phys. Rev.*, **55**, 549, 1939.

15. TOWNSEND and EDMUNDS, *Phil. Mag.*, 27, 789, 1914; J. S. TOWNSEND, *Phil. Mag.*, 28, 83, 1914; *Electricity in Gases*, Oxford, 1915, p. 376 ff.; E. A. WATSON, *Electrician*, Feb. 11, 1910; J. S. TOWNSEND, *Electrician*, 71, 348, 1913.
16. L. G. H. HUXLEY, *Phil. Mag.*, 5, 721, 1928; 10, 185, 1930.
17. J. H. BRUCE, *Phil. Mag.*, 10, 476, 1930.
18. F. M. PENNING, *Phil. Mag.*, 11, 961, 1931.
19. C. BOSCH, *Ann. Physik*, 19, 65, 1934.
20. W. CHRISTOPH, *Ann. Physik*, 20, 145, 1936.
21. G. MEDICUS, *Z. Physik*, 103, 76, 1936.
22. R. SCHADE, *Z. Physik*, 104, 500, 1937.
23. K. O. KIEPENHEUER, *Z. Physik*, 107, 145, 1937.
24. H. PAETOW, *Z. Physik*, 111, 770, 1939.
25. GÜNTHERSCHULZE and BÄR, *Z. Physik*, 106, 668, 1937; A. GÜNTHERSCHULZE, *Z. Physik*, 86, 778, 1933; GÜNTHERSCHULZE and FRICKE, 86, 821, 1933; 96, 551, 1935.
26. This empirical limit applies successfully for counters where  $A \gg a$ . For  $A \sim a$  the lower limit must be  $r_\alpha$ . See BROWN and KIP. Paper submitted to *Phys. Rev.*, Sept. 1939.

#### 8. POSITIVE AND NEGATIVE POINT TO PLANE CORONAS IN AIR AT ATMOSPHERIC PRESSURE \*

As stated in the introduction to Section 6, for reasons soon to become evident, despite the simple field calculations for the concentric cylinders, the high-pressure studies are best considered in terms of the point to plane geometry, owing to the intensive space localization of events. One may open the discussion by a consideration of field conditions and ionization by collision about the point in the point to plane geometry. Both theory and experiment agree in assigning to the geometry and field *about the point* the predominating role in the point to plane gap, and relatively little importance to the plane electrode, provided that the gap is long. While hemispherically capped cylindrical electrodes permit of field calculations, such calculations are tedious and the results are not very accurate. Accurate solutions can be carried out for the fields in the case of confocal paraboloid electrodes.<sup>1</sup> Experimental studies were carried out both with hemispherical and confocal paraboloid arrangements by Kip,<sup>1</sup> and the results indicated that estimates made from the hemispherical points assuming confocal paraboloid geometry would serve under most circumstances for longer gaps.

The values of the ratio of field strength to pressure in the gap near the point as a function of distance from the point are computed and shown in Fig. 242 for 0.03- and 4.7-mm-diameter points for a 6-cm gap at the starting potentials of fields for the positive point corona in air at atmospheric pressure. The reason for the use of the ratio instead of field strength is that this permits at once of the evaluation of Townsend's first coefficient at each point. On this basis it is possible from Sander's<sup>2</sup> and Masch's<sup>3</sup> data for  $\alpha/p$  as a function of  $X/p$  to calculate the values of  $\alpha$  as a function of distance  $x$  from these various points. For the positive point this gives some chance to calculate the number of

\* References for Sections 8 and 9, Part C, Chapter X, will be found on page 535.

ions formed per electron approaching the point, since one may neglect the inhibiting action of the space charge. For the negative point, as we shall see, the decreasing field as  $x$  increases from the point makes the space-charge distortion such that calculations are not very significant except for low ionization. In Fig. 242 the values of Townsend's function  $\alpha$  are also plotted as a function of  $x$  at the existing fields. The areas under these curves for positive corona at onset placed in the exponent for  $\alpha x$  of the expression  $n = e^{\alpha x}$  gives the number of electrons in a single electron avalanche proceeding from outside to a positive point. This for the points used rises continuously from some 10 electrons for the largest point to 10,000 for the smallest point and is the same for negative as well as positive points where space charges do not inhibit. We will here designate as an *electron avalanche* an electron and all the other electrons it creates in the field in its path to or from an electrode. With this background we may now turn to consideration of the negative point corona in air.

a. **Negative Point Corona.** As soon as the field at some spot on the negative point reaches such a value that an incoming positive ion is likely to generate a secondary electron at the cathode (negative point) surface on impact, that electron proceeds outward and ionizes the gas by collision, producing an electron avalanche. In the strong field near the point it will quickly ionize, but the cumulative effect of the avalanche does not become appreciable until the electrons produced have traversed several ionizing free paths away from the point. That is,  $n = e^{\alpha x}$  and thus depends on  $x$  as well as  $\alpha$ . As the avalanche recedes, the fields causing the electrons to ionize weaken for two reasons: first, because of the rapid decline of the field  $X$  as distance  $x$  increases; and second, because the electrons in moving away leave behind them relatively immobile positive ions whose space charge reduces the field. Hence the electrons recede from the point, leaving a cloud of positive ions behind whose density rises nearly exponentially as one recedes from the point and then declines more gradually. Retarded by this space charge, the electrons slow down and attach to molecules of  $O_2$  to make slow negative ions which eventually drift to the positive plate. The field set up between the point surface

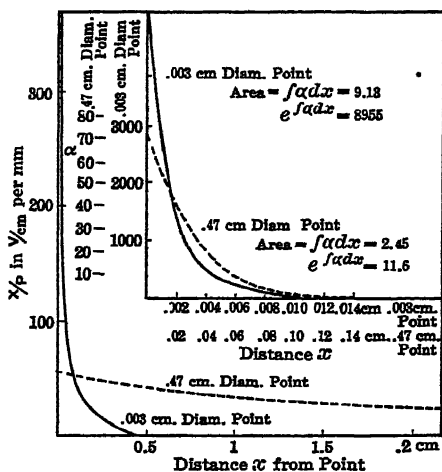


FIG. 242.



and the positive space charge increases the field acting on electrons near the point. Positive ions reach the cathode, more electrons are liberated, and so new avalanches form. These increase the ionization and the space charge near the cathode, decreasing ionization strongly beyond the positive space charge. Meanwhile the positive space charge is slowly moving towards the cathode surface.

As an accompaniment to the ionization a considerable number of atoms are excited to radiation by the electrons. With the high fields some molecules are simultaneously ionized and excited. This is indicated by the presence of the spark spectrum of  $N_2$  and air near the cathode. Such excited atoms emit radiations which are capable of ionizing the gas photoelectrically. Hence with the first avalanche photons causing ionization are emitted in all directions by the discharge. This photoelectric ionization has been directly observed and measured by Greiner,<sup>4</sup> Cravath,<sup>5</sup> and Dechène<sup>6</sup> in corona, while Raether<sup>7,8</sup> and Gorrill<sup>9</sup> have similar evidence from cloud chamber studies. The ions start new avalanches at neighboring spots until the whole region of the point which is capable of emitting electrons by positive-ion impact is carrying out the process noted above. The magnitude of the field required depends on the following considerations. The chance of electron liberation must be such that one of the positive ions created in a given avalanche must liberate a secondary electron at the cathode to perpetuate the avalanches. This with constantly changing fields is thus a rather ill-defined quantity. However, it depends on the work function for secondary electron emission on positive-ion bombardment and on the kinetic energy of the positive ions as well as their ionization potential. It varies from spot to spot on the surface and is lower (secondary emission  $\gamma$  higher) for a gas-coated than for an outgassed surface. It is exceedingly capricious, and so far it has been nearly impossible to control and reproduce the values of this quantity.  $H_2$  enhances the effect under some conditions, as with Pt, Cu, Fe, and Ni electrodes; CO,  $SO_2$ , and  $H_2S$  destroy it.<sup>8b</sup>

The extent of the spread of the avalanches over the surface depends on the extent of the active surface where adequate fields exist. For needle points of 0.03-mm diameter, the whole point is doubtless covered. For larger points the spots vary in size to about 0.2 mm.<sup>10</sup> The spot on a given electrode varies very little in size as the field increases and the current varies. It is not possible to fix the velocity with which the avalanches spread over the point and build up the space charge until that charge chokes off the further growth. Oscillograms to be shown and the time sequence of events indicate that it is very rapid. An avalanche of the size inferred above probably takes some 2 to  $3 \times 10^{-9}$  second. The lateral spread and the building up of successive avalanches must therefore require on the order of some  $10^{-8}$  to  $10^{-7}$  second. In this time the advance of the positive space charge has allowed it to reach the cathode, giving the positive current pulse shown

in the oscillograms of Fig. 243 taken from the work of Trichel.<sup>10</sup> Ionization has practically ceased during this time.

The space charge then clears by being swept into the cathode, and the current declines probably much as shown in the current oscillogram.

When the field has been increased sufficiently by the removal of positive ions, the last ions start new electron avalanches and the process repeats. It is seen that, depending on the strength of the clearing field and the rate of removal of the ions, the potential remaining constant, the process will repeat itself periodically. Thus one can expect to observe the regular current pulses shown in the oscillograms, which resemble closely those of a relaxation oscillator. The periodic discharges have been observed down to values as low as 5000 per second. At applied potentials giving frequencies somewhat below this value the pulses become sporadic and irregular owing to the fields decreasing to such magnitudes that repetition of the pulses periodically is not insured by secondary electron emission by positive-ion bombardment. As the field is gradually increased, the clearing fields speed up the process.

With constant spot size, the frequency and hence the current rise regularly with the potential. These give the linear increase of frequency with current shown in Figs. 244 and 245. It is seen that gap length does not increase the frequency for a given current but the point size does. This is to be expected since, at the starting potential, fields at the point vary very little with gap length, while the smaller points, having smaller active areas, shorter ionizing distance  $x$ , and higher fields, give the same currents by increasing the frequency. As fields increase for the same spot the currents rise linearly, and the oscillograms show that this is accomplished by having the new current impulses start at higher points on the decaying positive-ion space-charge currents. How far up in frequency the regular impulses occur could not be ascertained, as the resolving power of the oscillograph begins to be defective at 200,000 impulses. It may continue until it approaches the time for the lateral spread of the discharge, or what is more likely it will continue until with increasing potentials a second active spot appears. This spot will in general take up the discharge, being a new point where low work function and high field now permit

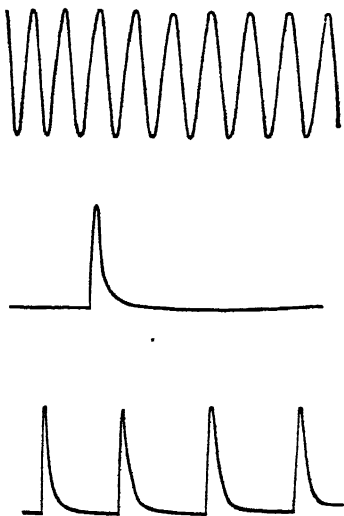


FIG. 243.—Trichel's Oscillograms of Negative Point Corona. Upper curve 8000 cycle timing curve. Lower curve regular corona pulses.

the process to occur, giving the surface of the first spot denuded of its gas film by the positive-ion bombardment time to recover.<sup>13</sup> Once it

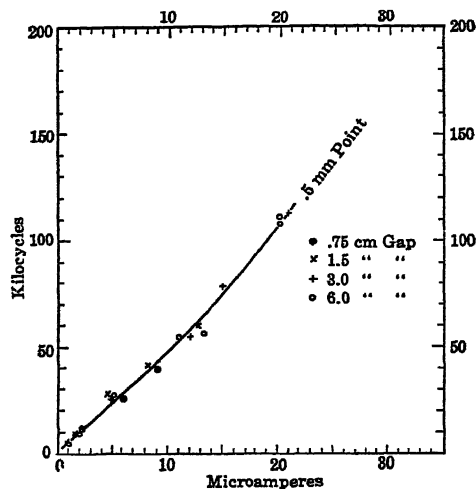


FIG. 244.

has recovered, the first spot takes on its function and the second spot goes out, and so alternation continues. Later several spots may appear.

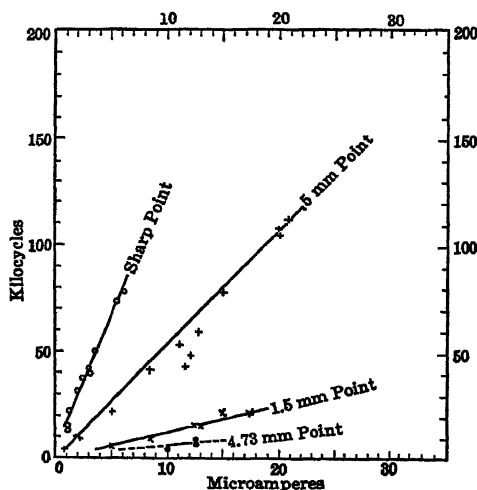


FIG. 245.

This is apparent in Fig. 246, where one sees the glow extending farther and farther into the gap, as the field increases, to the last point where two or three new spots appear at active localities on the needle shank.

These phenomena are all confirmed by the visual observation of the point in discharge by telemicroscope. Such observations are shown in Fig. 247. There one can see the fine dark space at the cathode which appears as a dark ring, akin to a Crookes dark space in glow discharge, due to lack of ionization and excitation in the first few free paths. Beyond this is the bright electric blue glow of the ionization by the avalanches which in the second picture has materially spread out into the gap. Still farther out, in the region where electrons are slowing up, one sees a larger dark space of no appreciable ionization. Beyond this again where the attaching electrons build up a heavy negative space

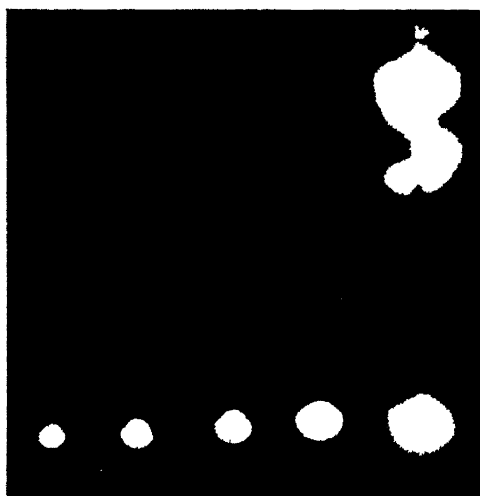


FIG. 246.—Photographs of Negative Point Corona with Increasing Potential. Right showing several spots on one point.

charge one sees the faint purplish haze (arc spectrum of  $N_2$  and  $NO$ ) due to a second weakly ionizing region produced by this accumulation. At higher fields this extends well into the gap, and takes on the characteristic mushroom shape shown which may vary with external conditions and point size. From the scale of the drawing one sees, however, that this is only a small fraction of the 3- to 6-cm gap used. The succession of events just after ionization and during the last of the clearing of the positive space charge is seen in Fig. 248 which schematically shows the density of ions above the axis and the field distortions below. It also shows the appearance of the correlated visual phenomena.

In the rest of the gap the weak fields allow of a considerable accumulation of slowly moving negative ions. The field here is only a few hundred volts per centimeter. At the plate, however, this space charge produces a sharp gradient which becomes more and more pronounced

as current increases. Now it must be clear from all that has preceded that the negative point discharge is a self-extinguishing phenomenon due to field concentration and positive-space-charge accumulation. A breakdown to a spark cannot propagate from the cathode through the space-charge cloud. Since at appropriate fields the negative point corona *does cause breakdown to a spark*, it appears that spark propagation *cannot have proceeded outward from the point*. When the positive

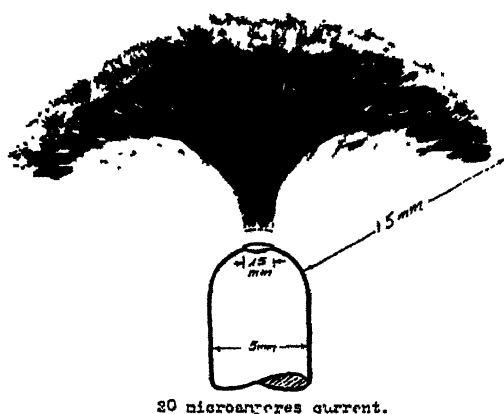
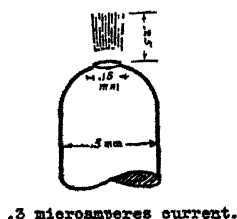


FIG. 247.—Trichel's Very Much Enlarged Sketch of Negative Point Corona. Note Crookes' dark space, negative glow, Faraday dark space, and positive column.

corona is studied it will be seen that, on the other hand, the positive space charge can build out or propagate as a streamer toward the cathode. Hence, it is clear that, when the space charge at the positive plane electrode due to the negative ions reaches an appropriate value, the spark will break by a positive discharge from the anode. This will be discussed later.

**b. Positive Point Corona.** One may now turn to the positive point to plane corona in air. When one places a positive potential on

the point and measures the current as a function of the potential, one at first gets practically no current, unless outside ions from a radioactive source, or from the plate cathode, are liberated in the gap. Under these conditions one gets a weak current proportional to the strength of the outside ionization which is larger than the ion saturation current  $i_0$ .<sup>1</sup> It is termed a *field-intensified ionization current* and represents merely a multiplication of the electrons in the field near the point due

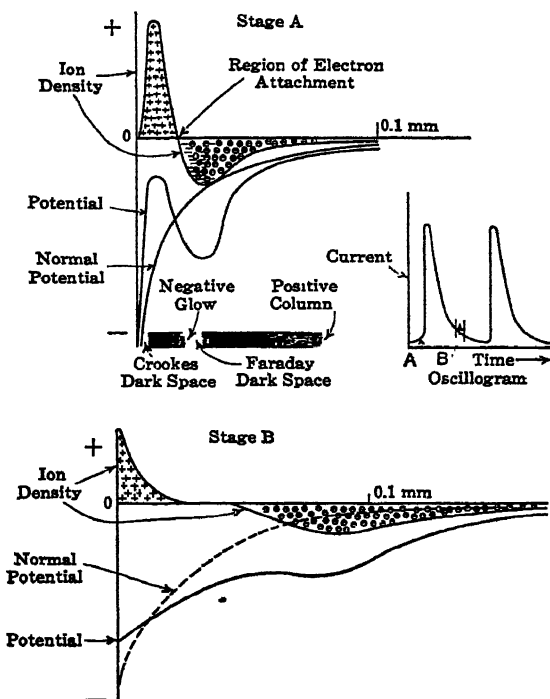


FIG. 248.

to ionization by electron impact. While Townsend's  $\alpha$  has values in regions where the field strength to pressure ratio,  $X/p$ , is greater than 20 in air, the current above does not increase until the ratio  $X/p$  at some ionizing paths from the point reaches a value  $X/p = 90$ . Experiments by Loeb<sup>14</sup> have shown that it is not until negative ions encounter such fields that the negative ion sheds its electron so that it is free to ionize. Experimentally the starting potentials for such coronas are observed only when fields are such that  $X/p = 90$  extends out some tenths of a millimeter from the point.

The current then increases asymptotically with a given  $i_0$  from low values and increases smoothly. This is shown in part A of the curve of

Fig. 249. Above a certain minimum value one reaches a sudden increase of current of considerable magnitude. On the oscillograph this increase is characterized by the appearance of pulses of current lasting perhaps as much as  $10^{-3}$  second which then go out.<sup>12</sup> These, when examined with sufficient amplification, were shown by Trichel<sup>11</sup> to be composed many small and partially resolved bursts of current involving up to about  $10^7$  ions and occurring at frequencies of the order of  $10^5$  per second or more. The region in which these phenomena occur are indicated on part B of Fig. 249. For very fine needle points these increase in number until at what we term the *onset potential* the corona proceeds as a continuous self-sustaining *burst corona*.<sup>11</sup> At this point external ionization is no longer needed. The value of the onset potential  $V_s$  can be accurately located only by raising the potential above  $V_s$  and then reducing it until the current ceases. This *offset potential* corresponds to the value of

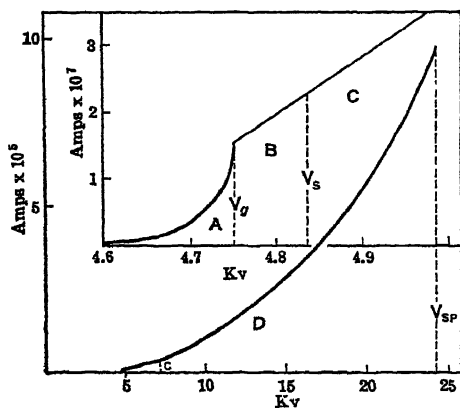


FIG. 249.

$V_s$  at which the pulses of *burst corona* become self-sustaining in the oscillograph, and thus the onset potential can be determined by the offset potential. The onset potential might be found by using an external ion source and noting at what potential the pulses change to a steady burst corona.

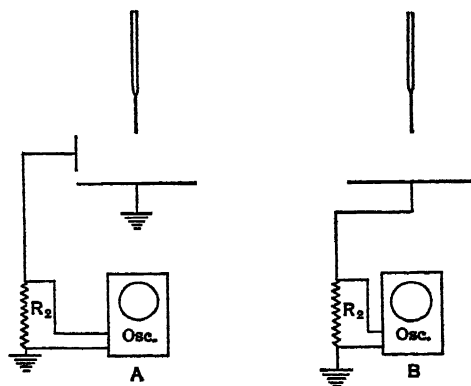
The regime beginning with the first pulses of the burst corona and extending to the onset potential is the regime of *intermittent corona* and is termed the *Geiger counter regime*. It is the region in which each ion created in the gap, when sufficiently spaced in time, produces a burst pulse which lasts for some time and goes out. As the burst pulse current is of the order of tenths of a microampere it can be used to count the advent of ions in the gap, and thus can be utilized to count the number of ionizing particles in the active volume. Geiger<sup>15</sup> and others<sup>16</sup> found that, by placing a high resistance  $R$  in series with the point, the  $iR$  drop due to the burst pulse current lowers the potential of the point below the value of  $V_s$ . Thus the burst pulses are cut off quickly so that the device can be used to count  $\alpha$  and  $\beta$  particles and  $\gamma$  or cosmic rays by the ions created by them in the gap, *if they do not come at too high a frequency*. The effect of the resistance is merely to extend the narrow counting plateau in voltage, so that cut-off becomes more certain and is not limited to the inconveniently small potential range between the beginning of burst pulses and  $V_s$ .

With all but the finest needle points, slightly above the voltage at which intermittent burst pulse corona at  $B$  starts, but well below the onset of the steady burst corona at  $V_s$ , there appear on the oscillograph *inductive kicks* of much larger magnitude than those characterizing burst corona.<sup>12</sup> These may be observed by the arrangement shown in Fig. 250*B*, which is also used for detecting intermittent burst pulses. In some cases isolated kicks of this type may appear; in others, these kicks initiate the burst corona. *After a burst starts, one never observes the kicks.* The oscillograms of the burst corona pulse are shown in Fig. 251 while Fig. 252 shows an inductive kick initiating a burst pulse corona which later cuts itself off owing to space charge weakening the field.

By the proper arrangement of gap geometry and voltage, and the judicious use of electrons from  $\gamma$ -ray ionization, or by means of a gauze over the plate with an appropriate field between it and the plate to regulate the passage of negative ions into the gap as shown in Fig. 253, the inductive kicks

can be made to repeat themselves without leading to a burst corona. The frequency of these kicks can be controlled in a measure by the field applied between gauze and plate. High resistance in series with a point will also cause repeated kicks without burst corona. If one attempts to increase the frequency of inductive kicks beyond a certain value, depending on gap geometry and applied voltage, by increasing the strength of the external ionization, the kicks go over to a more or less continuous burst corona. In general it may be stated that if enough external ionization is provided the burst corona process occurs at all voltages above  $A$ , while if no external ionization exists  $V_s$  marks the beginning of the stable burst corona. At voltages approaching  $V_s$  and above it, the burst-corona process is always initiated by an inductive kick. In addition, kicks never occur during the burst corona process.<sup>11,12</sup>

By shielding the plate with a gauze as shown in Fig. 253, the current to the plate is characterized by neither the irregular burst pulse nor the kick. All that is observed is a smooth pulse of the ion current due to the burst pulse or to the kick. Hence both the fluctuations in the burst corona and the kick registered in the case of the unscreened plate



FIGS. 250*A, B*.—Arrangements of Kip for Detecting Burst Pulses and Inductive Kicks as well as Ion Currents in Corona.



are *inductive effects* due to sudden changes of charge distribution about the point and in the gap.<sup>12</sup> The method shown in Fig. 250B thus measures both the inductive effect and the ion current to the plate. By



FIG. 251.—Oscillograms of Burst Pulse Corona Just above  $V_g$  Taken by Kip. Individual pulses not resolved. Time passage left to right. Duration of pulses  $\sim 10^{-8}$  sec. Asymptotic decline is instrumental.

using a plate placed near to the gap and shielded from ions by a cardboard screen as shown in Fig. 250A, the inductive pulses only, due either to burst pulse or kick, may be observed.<sup>11</sup>

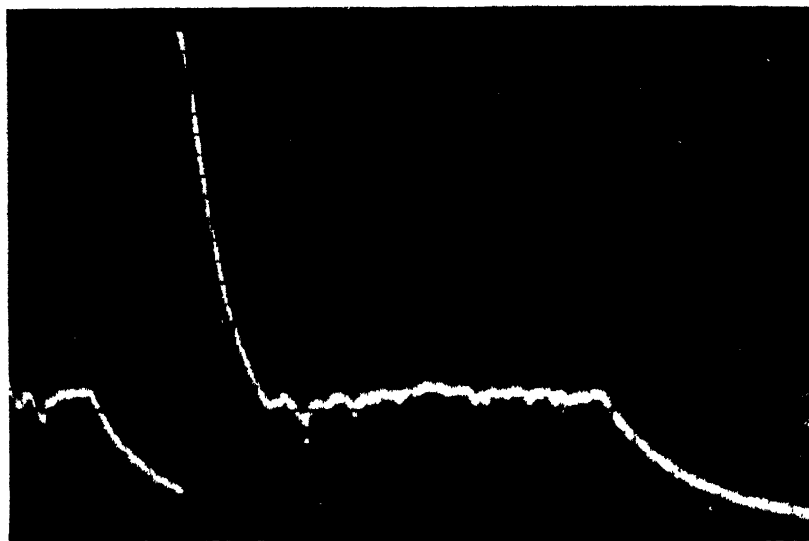


FIG. 252.—Inductive Kick Initiating a Burst Pulse Corona. Time scale left to right. Duration of pulse  $\sim 5 \times 10^{-8}$  sec. Note relative magnitudes of kick and pulses.

Fig. 254 shows the small inductive kick with pick-up as in Fig. 253 but with only *partial screening* of the plate. Here the ion current reaching the plate, and the inductive kick on the plate, are both registered. Complete shielding would eliminate the inductive kick but leave the

ion current pulse. From the time elapsed between the kick and the advent of the center of the current pulse, the time of transit of the ions in the kick from point to plane can be measured. Calibration of the oscillograph deflection and the magnitude and duration of the current pulse enable the number of ions producing the kick to be measured. This number varies from  $10^9$  to  $10^{10}$  ions.

Visual observation of the point with the telemicroscope and with camera reveals at once the difference between burst pulses and the large kick-producing phenomena. The burst corona is always manifested by a brilliant blue glow covering the point and lying very close to it, with maximum intensity *at the point surface*. The kicks are always characterized by streamers from 3 mm to 2 cm in length radiating from the point, and in many cases moving straight towards the plate. These are fine lines of a bright blue color that extend outward from the point and will hereafter be called *streamers*. Fig. 255A shows a photograph of the burst corona; Fig. 255B shows streamers superposed on the bursts. The camera, being sensitive to the near ultraviolet, reveals on longer exposure much more in extent than the eye

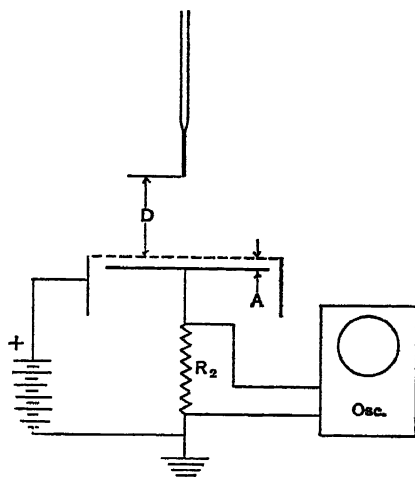


FIG. 253.—Kip's Arrangement for Measuring Ion Current and Velocity of Ions in Streamers in Positive Point Corona.



FIG. 254.—Kip's Oscillograph with Partially Screened Plate. Time scale left to right. Note inductive kick followed by pulse of ion current to plate. Marks below indicate  $10^{-3}$  sec.

sees. On the other hand, no less than 50 streamers can be revealed by the camera while the eye sees individual streamers. The camera indicates a lateral spreading or branching of streamers. The eye does not see this in individual streamers except for the intense ones from

larger points. Cloud track pictures made by Gorrill<sup>9</sup> of the pre-onset streamers definitely indicate them to be branched, accounting for the apparent bulging of the streamers of Fig. 255B, as seen in Fig. 256.

As the potential increases *above onset*, as previously stated, streamers disappear and *only the fluctuating burst corona* is observed. Above onset the current-potential curve rises *linearly* with a slope which is greater the shorter the gap.<sup>1</sup> If the gap is very short the corona does not occur and *a spark breaks at once without corona*.<sup>1</sup> The gap length at which corona is no longer observed corresponds to the length of the pre-onset streamers observed with that point as predicted by Loeb in

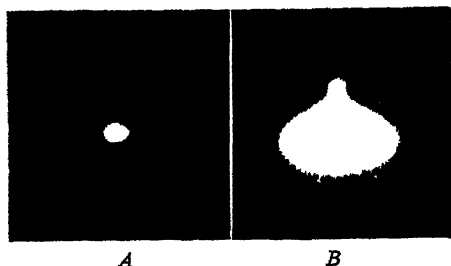


FIG. 255A, B.—Photographs of Positive Point with Burst Pulse Corona (A), and Streamers Superposed on Burst Pulse Corona (B) Taken by Kip.

Kip's first paper.<sup>12</sup> The ratio of potential to current in the linear region corresponds to the *space-charge gap resistance*  $R$ .<sup>1,16</sup> This resistance  $R$  multiplied by the current gives a potential which is equal to the value of the space-charge potential set up by the positive ions crossing the gap. Its value at onset is nearly equal to the width of the Geiger counter region  $B$  of Fig. 249. Hence the Geiger

counter region and its attendant phenomena are in part to be ascribed to the effect of the positive-ion space charge which the burst pulses set up and which obviously inhibit and at lower voltages choke off the burst corona in this region.

As the potential is increased beyond onset, the glow on the point spreads continuously over larger areas of the point, quite in contrast to the glow on the negative point corona.<sup>11</sup> With increasing potentials the linear relation between current and potential ceases and current increases rapidly with applied potential.<sup>1</sup> Eventually the current and potential reach such a value that a *spark* ensues. Just before this point is reached, oscillograph, visual, and camera observation *again shows the presence of streamers*.<sup>12</sup> For small points these streamers can be observed to lengthen with increasing potential, and shortly thereafter the spark occurs.<sup>12</sup> With large points the reappearance of streamers is followed so quickly by the spark that these streamers can be observed only by placing a high resistance in series with the point. The increase in length of the streamers from 6 mm to 1 cm has been measured as a function of potential. In a 6-cm gap with 0.05-mm point the breakdown followed after the streamers had reached a length of 1.1 cm. Visual observation at this stage indicates that breakdown occurs when one decaying streamer path is reached by a new streamer

before it is extinct. The successive streamers follow down old streamer channels. If on striking the cathode such streamers make an efficient cathode spot, a rearrangement of space charges at once results in a spark. That the old extinct streamer channels are thus utilized is indicated if one shoots a stream of air parallel to the plate.<sup>11</sup> The extinct channels move sufficiently slowly near the plate to be diverted by an air blast. As the rapidly propagating new streamers reignite an old deflected path, the revived path shows the deflection of the old channel. The *streamers* are not visibly deflected by air blasts.

Observation of the point in air enclosed in a Pyrex glass tube in the dark shows that as the potential rises a great deal of ultraviolet light is present. The glass glows brilliantly, as does the cathode surface. Studies with the screen over the plate show a considerable photoelectric emission from the cathode plate *if the gap is not too large*. There is some diffuse general photoionization of the gas, but this is far less than the photoemission of the plate for a 3-cm gap. Fig. 249 shows the characteristic course of a current-potential curve. Region *A* is that of the field-intensified ionization current; *B* represents the Geiger counter regime, and  $V_s$ , the onset potential. Region *C* represents the linear region of the current-potential curve; in region *D* Ohm's law ceases to hold and  $V_{sp}$  is the sparking potential. With this description we are able to analyze the mechanism active in the light of our analysis of the field at the points at onset.

At low fields all one observes is the avalanche formation and ion multiplication by factors of the order of 10 in the region near the point at which  $X/p$  exceeds 90 resulting from electrons detached from ions. As the field increases and the avalanches become greater the electrons formed are quickly drawn into the point, leaving the positive space charge behind. Once this has occurred, the photoelectrons produced in the gas outward from the point by the first avalanche send electrons into the point. Since the field distortion produced by the space charge of the first avalanche has an axis normal to the point, the maximum field distortion will lie along such an axis. The field at the tip of the avalanche will be increased above that at the point surface. The photoelectrons coming in along the axis will be favored by the axial field, where  $\alpha$  is higher. The ionization produced by the next electron moving into the point along its axis gives a second avalanche. The electrons from this avalanche rapidly move up the space-charge channel to the point. This action can readily be demonstrated by the potential changes induced on the electrode in position of Fig. 250*A* in streamer formation when a high resistance is in series with the point and the pick-up electrode is placed level with the point, for the streamers reduce the point potential to a value where the field reverses at the pick-up electrode. As a result of the second avalanche, the space charge along the axis of the first avalanche is increased and extended radially from the point. The field at the tip of the space charge is still further

increased. Hence the ionization proceeds outward from the tip at the velocity of electron travel *or higher*, increasing the field and producing more space charge along the axis. This succession of avalanches along an axis constitutes a *burst* or an *incipient streamer*. In a uniform potential gradient, or field, of sufficient magnitude, this process would continue right across the gap. In the radial field of the point, however, the field strength rapidly decreases, and presently the tip of the burst or streamer finds itself in a region where the potential gradient is so low that even with its enhanced field it can no longer propagate. That is, a burst or streamer can form and proceed only as long as the potential gradient is adequate. To *start* a burst or a streamer probably requires *a much higher field* than to *continue the propagation of a well-developed burst or streamer*. Hence the occurrence and length of bursts and streamers depend on the field distribution about the point.

In a clear gap the length of the streamer varies with the applied potential, as one might expect. If the field is reduced by the diffused positive space charge of a preceding streamer, near but ahead of the point, bursts *cannot develop into streamers*. The propagation of bursts or streamers is also inhibited by other effects. First self-repulsion and diffusion of the positive ions tend to broaden the streamer channel and weaken the space charge. This movement is slow since positive ions have a low mobility. Thus in the  $10^{-8}$  second of streamer formation the movement of the ions is negligible. In addition, the positive-ion channel as a whole tends to move radially from the point towards the plate with a velocity of  $10^5$  cm/sec, near the point, down to a velocity of  $10^3$  cm/sec near the plate. There is also some broadening of the channel due to the lateral diffusion of the electrons with high thermal energies. The average radius is  $\bar{y} = \sqrt{2Dt}$ , where  $D$  is the coefficient of diffusion and  $t$  is the time of travel. In the short travel and high fields at points,  $t$  is short and broadening is small. This accounts for the strongly directive character of the streamer axis. The electrons of later avalanches moving up the space charge probably do not diffuse much, owing to the conservative action of the positive-space-charge channel.

Again the photoelectrons are produced in the gas all about the axis of the streamer in diminishing numbers as one recedes from the axis. Near the tip of the burst or streamer the number is greatest, but many electrons are produced at points such that lines drawn from them to the tip make an angle with the axis. This can lead to the formation of a crooked streamer if only one electron is produced. If more are produced and are equally successful in ionizing, then the streamer branches. If the fields are high enough such branches may develop for a considerable distance. Since, however, they expand the tip at the beginning, they tend to shorten the length of the branched streamer, especially early in the branching process. Hence it is not strange to find branching taking place *conspicuously only in high field regions*.

such as in overvolted plane parallel gaps and *near the point* in point to plane gaps. Where, as in a plane parallel gap, the field is highly directive, branches in general trend towards the cathode. In the corona this tendency is less noticeable. Hence aside from propagation into low field regions, streamer propagation is inhibited by electron and ion diffusion, divergence of incoming avalanches, and actual branching. Fig. 256 shows branching in a cloud track picture of a streamer taken by Gorrill.<sup>9</sup>

The diagram of Fig. 257 shows the potential distribution in a gap and the effect of space charge on the development of bursts or streamers schematically. From the character of this action we at once understand the positive point to plane corona mechanism.

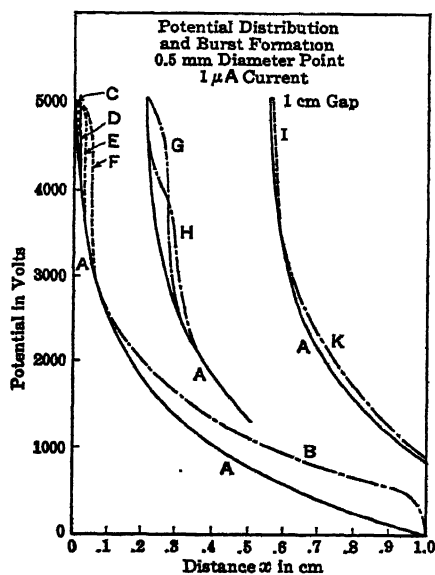


FIG. 257.—A, Undistorted field. B, Distortion by ionic space charge. C, D, E, F, Field at point after 1, 2, 10, 100 avalanches. G, H, K, Subsequent career of distortions at point. I, Beginning of a new pulse.



FIG. 256.—Cloud Track Picture of Pre-onset Streamers Taken by Gorrill Showing Branching. Expansion after streamer causes diffuse picture. Probably no more than two streamers are present here.

Given an adequate field, the first ion starts an avalanche which quickly develops into a burst. At low fields this propagates only to the extent of creating a *burst* streamer of some  $10^6$  to  $10^7$  electrons. This takes some  $10^{-8}$  to  $10^{-7}$  second. It then ceases, and its micro area of electrode is inhibited from starting a new burst for some  $10^{-5}$  second or more, while the space charge is being swept away from the point. In the meantime, photoelectrons created to each side of the axis of the burst as far away as  $10^{-2}$  mm crash into the positive point, at clear places, giving other avalanches that propagate new bursts. These in  $10^{-5}$  to  $10^{-8}$  second spread all over the regions of the point surface where the field is adequate. Before the  $10^{-3}$  second needed for clearing out the first burst has elapsed, the many

offspring bursts ranging in size from avalanches of  $10^2$  to bursts of  $10^7$  ions have built up a positive space charge outward in the gap. This is large enough to *lower the field at the point surface to such a value that bursts can no longer form*. Thus the *burst pulse in the Geiger regime below onset* is merely a series of bursts extinguished by their own space charge.

In  $10^{-3}$  second or more the gap is clear of all positive space charge and a *new* burst pulse can start. The duration of the pulses is irregular; some are long and others short. The appearance of burst pulses depends on the presence of initiating negative ions or electrons in the gap which reach the point. There can thus be no regularity as regards size or frequency of such burst pulses, and we have the intermittent burst pulse corona of the Geiger regime. For small points the fields are so confined that the avalanches can lead only to burst formation, and bursts never can develop into long streamers.

As the potential on the points is increased, the space-charge accumulation must be larger and larger in order to choke off the bursts and to give the burst pulses. Eventually a potential  $V_s$  is reached where the space charge no longer suffices to choke off the bursts and we have merely the fluctuating burst corona of Trichel.<sup>11</sup> This is composed of bursts and avalanches random in time, space, and size, occurring in the order of  $10^5$  to  $10^6$  or more per second and comprising from  $10^2$  to  $10^8$  ions. As the field increases still further, these bursts extend over larger areas of surface and farther out into the gap, as seen in Fig. 258. Eventually the fields become so high (300 to 500 per cent above onset) that space charges in the gap *cease to inhibit* streamer growth and adequate fields even for fine points extend so much farther into the gap that the bursts can develop into streamers.

The careful measurement of the potential of the first appearance of bursts with confocal paraboloid electrodes permits of an evaluation of the minimum fields for burst formation at the electrode. If the space charges are measured for a given corona current, one could at once predict the value of  $V_s$  and the width of the Geiger regime.

With larger points the high fields extend farther into the gap. Under these conditions the growth of bursts out into the gap is to be expected and streamers will form. Streamers propagate further into the gap the larger the radius of the point and the higher the potential applied. Data at present are not sufficiently complete to permit us to determine the minimum field for the development of a burst and its propagation as a streamer. It is possible that this will be found shortly. It is clear, however, that, once a streamer or burst pulse has propagated with its  $10^9$  to  $10^{10}$  ions, the gap is fouled by a space charge of positive ions. In its propagation the streamer may have initiated a burst pulse such as shown in Fig. 252. In general it will do so. It is possible that the space-charge distortion of a streamer may even be great enough to choke off a burst, and in fact at the *onset of streamer*

*propagation* but few of these initiate bursts. If the burst pulse is short lived it may not appear against the background of the inductive disturbances set up by the streamer.

If, after the streamer has died out and its space charge is removed from the gap, a timely ion, or secondary electron from a  $\gamma$  ray or elsewhere, arrives at the point, a new streamer may start out. By choosing a gap length such that after each streamer the space charge is removed, a *series* of streamer kicks or pulses can be obtained. This can be accomplished by judicious  $\gamma$ -ray ionization, by getting photoelectric ions from the plate by means of a screen and auxiliary field, or

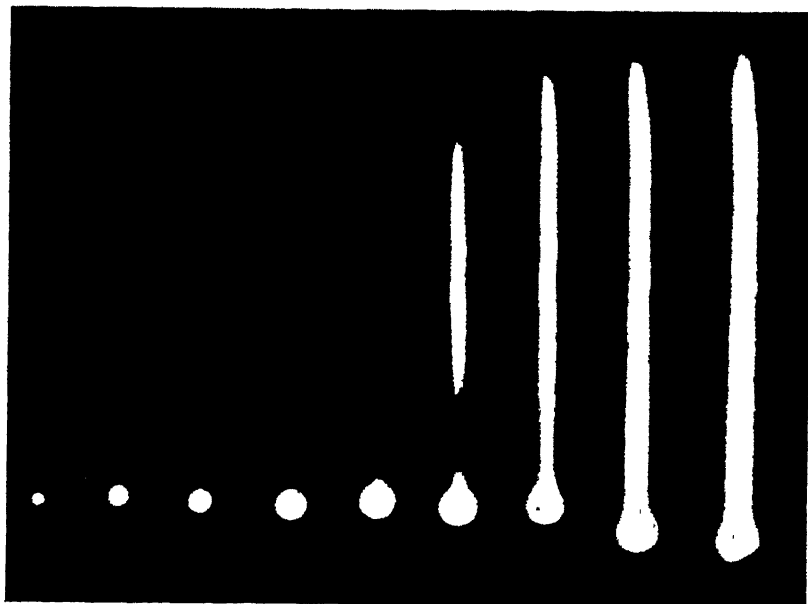


FIG. 258.—Kip's Photograph of Positive Point Corona above Onset,  $V_s$ , as Potential Increases. Note the spread of the burst pulses over the needle as current increases.

by the use of a *high* resistance in series with the point which so reduces the potential of the point that the new streamer or burst corona cannot start before the gap is cleared. By varying the field between screen and plate so that the photoelectric ions from the plate arrive at the point in shorter and shorter time intervals, the time between streamers can be reduced until the interval begins to be less than that to clear the field. At this stage the streamers cease to repeat. If the  $\gamma$ -ray source is made so intense that there is not time enough for space-charge clearance between streamers, the streamers go over to burst corona.



As the potential increases beyond the streamer potential threshold, the burst corona pulses are more likely to follow a streamer and they increase relative to the streamers, ending finally in continuous burst corona. Thus the *potential range of pre-onset streamer production is quite limited*. This fact coupled with the late introduction of the oscillograph into corona studies is primarily responsible for the very recent discovery of streamers.\*

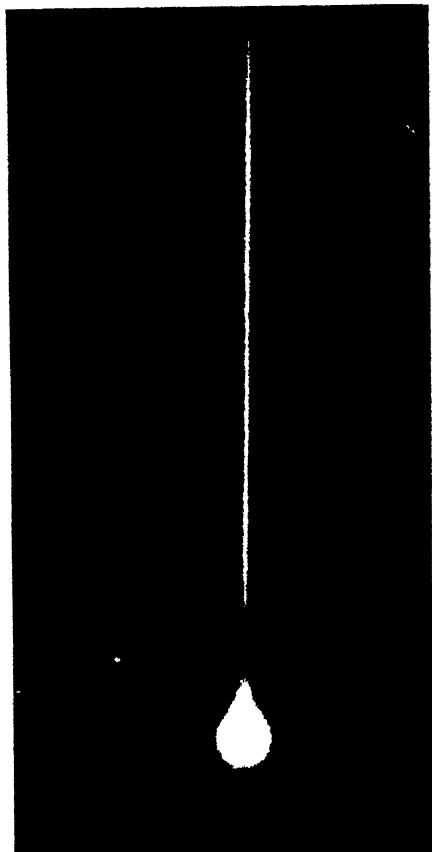


FIG. 259.—Kip's Photograph of Positive Point Corona at Point Where Breakdown Streamers Are Just Beginning to Show Beyond Burst Pulse Glow.

For a 0.5-mm point and a 4-cm gap, burst pulses,  $V_g$ , begin at some 4900 volts. By 5100 volts one has already passed through the region of Geiger counter action, streamers, and burst pulses and into the continuous fluctuating burst corona,  $V_s$ . An increase of some 3900 more volts takes one past the linear space-charge-controlled burst corona. In this region the field at the point is kept nearly constant owing to the effect of the positive ions from the burst corona. Hence bursts do not propagate far outward, and current increases only by the lateral areal spread of the bursts over the point surface. It is this condition which permits of the constant resistance of the gap. As potential increases, the current increases in direct proportion. The resistance for confocal paraboloids, where fields are known, is then a linear function of the gap length, as Kip showed.<sup>1</sup>

On further increase of potential the space charge is swept out more and more rapidly. There is far less space charge about the point, and the resistance decreases with increasing potential. Hence the current

\* Many years ago M. Toepler<sup>18</sup> and J. Zeleny<sup>17</sup> in a study of a corona actually observed streamers. The streamers were designated brush discharges, and not recognized in their relation to the burst corona.

increases more rapidly than linearly with the potential. This increase continues for a very long range of potentials from 10,000 volts up to nearly 30,000 volts. Where this takes place the burst corona glow extends farther and farther into the gap as shown in the photographs of Fig. 258. Eventually the field is high enough at some distance from the point so that the bursts again begin to grow into streamers. Incipient streamers are shown in Fig. 259 just beyond the glow. Then in a very short range of potentials streamers begin to propagate across the gap. For one needle point of 0.05-mm diameter with a 6-cm gap the streamers were 6 mm long at 23 kv and 11 mm long at 30 kv. Thereafter, with little potential increase, they began to cross the gap. Visually this crossing *appears* to result from new streamers that catch up with old streamer channels and so revive them and propagate across the gap. Fig. 260 shows a number of such streamers taken with camera using an exposure time of 5 seconds. When one of these streamers succeeds in creating a good source of secondary electrons at the cathode plate a spark or an arc results.

The breakdown or sparking mechanism in the positive point to plane corona discharge is easily seen in the case of spark breakdown at the potential of streamer production *below* burst corona onset *when the gap is short*. If for instance in a long gap a given point at a certain potential gives a 1-cm streamer, then in a 1-cm gap at about that potential there is no corona. The gap at once breaks down in the form of a spark, and corona is not observed. In this case the *pre-onset*

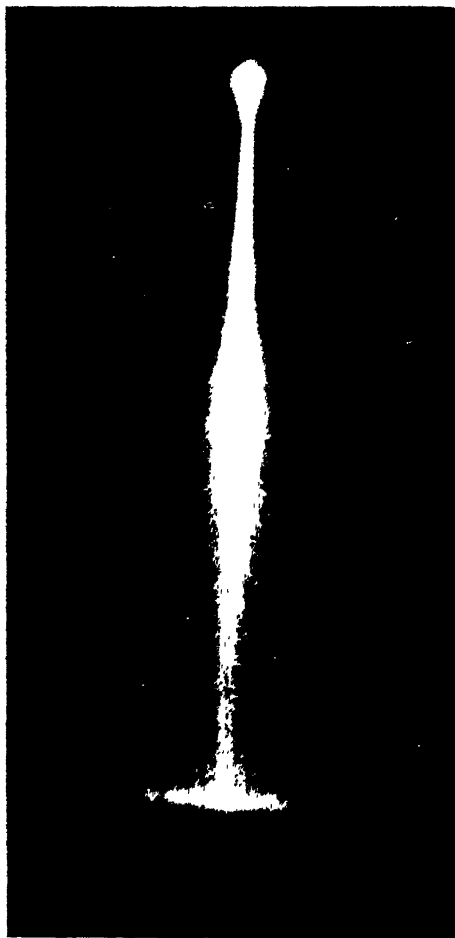


FIG. 260.—Kip's Photograph of Breakdown Streamers in Positive Point Corona. Many streamers are shown crossing to cathode below.

*streamers cross the gap* and, striking the cathode, start the breakdown mechanism. Here the cleared gap field is *high enough across the whole gap to allow streamers* to propagate across, once the point potential is high enough to initiate a streamer. It is seen that in this instance we are approaching closely to the conditions existing in a plane parallel-plate gap. This analysis, then, it is seen, brings us nearer to an understanding of ordinary spark breakdown at atmospheric pressure.

As regards the phenomena in other gases, not enough data are at hand to date to permit of discussion. The fluctuating positive burst corona occurs in air and  $H_2$  but *not* in pure  $N_2$ .<sup>11</sup> It is futile to speculate too much. Electron-attaching gases should influence the negative coronas more than the positive since they introduce larger space charges. However, they increase  $V_s$  for both coronas since they require a break-up of negative ions to yield electrons. The influence of the gas characteristics should also be more important in the negative corona than in the positive, for it influences not only  $\alpha$  but also  $\gamma$ . Probably two of the most important items in these discharges are the photo-electrical properties and the absorption coefficients of the gases. About these in the regions of photoelectrically active wavelengths little is known in molecular gases. It is also clear that for shorter gaps at least the photoelectric emissive properties of the plane play a role, and it may be that electron attachment will also be of some importance in influencing the rekindling of positive burst corona at or just above onset. With this material we can leave the coronas, having indicated the general mechanism and the future problems.

## 9. THE EFFECT OF TEMPERATURE ON SPARKING POTENTIALS

It has been generally noted that Paschen's law governs at least roughly practically all spark-breakdown phenomena. The only place where the law may in part fail is where space-charge accumulations play a predominating role.<sup>19</sup> The discussion of Paschen's law and its derivation indicate that the essential significance of  $p\delta$  in sparking lies in the number of molecules per cubic centimeter, or better, per centimeter length of electron path in the field direction, that are encountered in the gap. This number, as with all applications of Avogadro's law, *depends primarily on gas density* and not on pressure alone. In all discussion of sparking the temperature has been assumed constant and essentially either  $273^\circ K$  or in the neighborhood of  $295^\circ K$ . Actually sparking has largely been investigated at these temperatures. However, what studies have been made in the past indicate that Paschen's law holds in regard to temperature under usual conditions. Hence we should really have inserted  $\rho\delta$  for  $p\delta$  in the Paschen's law equation, where  $\rho$  is the gas density. Hence where temperature is varied the value of  $V_s$  is a function of  $\rho\delta$ . Since density varies as  $\rho = \rho_0(273/T)$ , the equivalent pressure must change in proportion to

273/ $T$ . Thus as long as the density  $\rho$  is constant  $V_s$  is independent of  $T$ . This question has been investigated experimentally by SNOW,<sup>20</sup> BOUTY,<sup>21</sup> EARHEART,<sup>22</sup> WHITEHEAD,<sup>23</sup> and BOWKER.<sup>24</sup> The correction for change of temperature from  $T_1$  to  $T_2$  at constant pressure can be easily made by shifting the curves for  $V_s$  as plotted against  $p_1\delta$  at  $T_1$  to a new set of values of  $p\delta$ ,  $p_2\delta$ , at  $T_2$  by altering  $p_1$  to  $p_2$  at  $T_2$  by the relation  $p_2 = p_1(T_1/T_2)$ , keeping  $\delta$  constant. Then, by plotting  $V_s$  as read off from the curve at  $T_1$  and  $p_1\delta$ , and replotting it at a value  $p_2\delta = p_1(T_1/T_2)\delta$ , one has the curve for  $V_s$  at  $T_2$  as a function of  $p\delta$ . Approximate empirical expressions for changing  $V_s$  at  $T_1$  to that at  $T_2$  are not desirable since the procedure above is accurate and simple.

It is clear that where space-charge formation largely determines  $V_s$ , as in long sparks there may well be deviations, but they will not be serious. Again it is clear that at temperatures where  $\gamma$  may be materially influenced by the cleansing or alteration of the metal surface by heat we can expect changes dependent on  $\gamma$ .<sup>25</sup> Finally, where the cathode begins to emit thermionically, the value of  $V_s$  may not obey Paschen's law on this account. Some studies were made of the influence of temperature in its action on the a-c sparking potential of spark-plug gaps<sup>26</sup> such as used in operating internal-combustion engines. In this engine  $\delta$  is fixed and  $p$  and  $T$  are given by the adiabatic compression, so that no difficulty is encountered in predicting the sparking potential, if the curve  $V_s$  as a  $F(p\delta)$  is known at a standard temperature and pressure. In the range of temperatures studied,  $V_s$  was on the nearly linear portion of the  $V_s$ -curve. As a result  $V_s$  was found to vary as  $\rho$  or inversely as the absolute temperature at constant pressure.

#### 10. REFERENCES FOR SECTIONS 8 AND 9, PART C, CHAPTER X

1. A. F. KIP, *Phys. Rev.*, **54**, 139, 1938.
2. F. G. SANDERS, *Phys. Rev.*, **44**, 1020, 1936.
3. K. MASCH, *Arch. Elektrotech.*, **26**, 589, 1933.
4. H. GREINER, *Z. Physik*, **81**, 543, 1933.
5. A. M. CRAVATH, *Phys. Rev.*, **8**, 267, 1935.
6. C. DECHÈNE, *J. phys.*, **7**, 533, 1936; H. RAETHER, *Z. Physik*, **110**, 611, 1938.
7. H. RAETHER, *Z. Physik*, **107**, 91, 1937.
8. H. RAETHER, *Z. Physik*, **96**, 567, 1935; FLEGLER and RAETHER, *Z. Physik*, **99**, 635, 1936; **103**, 315, 1936.
9. S. GORRILL, thesis in preparation, California, 1939.
10. G. W. TRICHEL, *Phys. Rev.*, **54**, 1078, 1938.
11. G. W. TRICHEL, *Phys. Rev.*, **55**, 382, 1939.
12. A. F. KIP, *Phys. Rev.*, **55**, 549, 1939.
13. L. F. CURTISS, *Phys. Rev.*, **31**, 1066, 1127, 1928.
14. L. B. LOEB, *Phys. Rev.*, **48**, 684, 1935.
15. GEIGER and MÜLLER, *Physik. Z.*, **29**, 839, 1928.
16. SVEN WERNER, *Z. Physik*, **90**, 384, 1934; **92**, 705, 1934.
17. J. ZELENY, *Phys. Rev.*, **3**, 69, 1914; *J. Franklin Inst.*, **218**, 685, 1934.
18. M. TOEFLER, *Ann. Physik*, **2**, 50, 1900.
19. L. B. LOEB, *Rev. Modern Phys.*, **8**, 276, 1936.
20. H. W. SNOW, *Phil. Trans. Roy. Soc.*, **124**, 230, 1894.

21. E. BOUTY, *Compt. rend.*, **137**, 741, 1903.
22. F. EARHEART, *Phys. Rev.*, **29**, 293, 1909; **31**, 652, 1910.
23. WHITEHEAD and FITCH, *Proc. Am. Inst. Elec. Eng.*, **32**, 1313, 1913.
24. BOWKER, *Proc. Phys. Soc. London*, **43**, 96, 1931.
25. F. EERENKRANTZ, *Phys. Rev.*, **55**, 219, 1939.
26. LOEB and SILLSBEE, Fifth Annual Report, National Advisory Committee for Aeronautics, U. S. Government Printing Office, 1919.

# 11. SPARKING PHENOMENA FOR VERY LONG GAPS AND HIGH PRESSURES \*

The mechanism of the ordinary spark at atmospheric pressure and moderate gap lengths has been discussed in extenso in Part A of this chapter. It was there shown that probably at least two procedures were possible. Of these, one seemed to predominate for the longer gaps, to wit, the breakdown by streamer formation. This was due to the fact that for large distances the values of  $e^{ax}$  became so large that space-charge distortions of great magnitude favored positive streamer development and propagation. Once this condition exists, the axial field distortion along a streamer produces a field of such magnitude that the breakdown proceeds of itself provided only that the general field gradient is high enough to permit of streamer propagation. Since this field is distinctly less than that needed to start breakdown and streamer formation in air at atmospheric pressure, the *average* gradient for spark breakdown with long gaps falls below that under those conditions. Hence while a sparking potential of 30,000 volts/cm holds in air at 760 mm for a 1- to 2-cm gap,  $X/p \sim 40$ , the sparks such as one observes in lightning appear to take place for *average* gradients of 10,000 volts/cm and  $X/p \sim 14$  or less. It is, of course, impossible to study such long discharges in uniform fields, so that most studies have been made with gaps giving unsymmetrical fields. In such cases the streamer formation, except for highly overvolted gaps, proceeds rather slowly, and considerable space charges may accumulate as a result of corona before the field distortion permits of complete propagation across the gap as a leader stroke ending in breakdown.

The many observations of Allibone and Meek<sup>1</sup> with moving-film camera show the almost infinite variety of such breakdowns. Into the final picture in these cases, we must, furthermore, bring the question of the circuit constants and characteristics. There is no question but that circuit resistance is of a paramount importance in determining the course of the ultimate breakdown. The high resistance has been shown by Allibone and Meek<sup>1</sup> to lead to "stepping" in propagation. That is, the point with high resistance in series starts a breakdown which can proceed only a certain distance before the potential is lowered to such a point that further advance is no longer possible. This necessitates a pause while the field at the point builds up again. Then a new burst

\* References for Section 11, Part C, Chap. X, will be found on page 558.

of discharge down the old ionized path at a very high speed furnishes the necessary energy for the next advance, and so on. This effect is also clearly seen in lightning discharge and in the many fine oscillograms of Rogowski<sup>2</sup> and his co-workers. The question of oscillations in discharge also depends on such constants. The final course of all discharges, and in shorter gaps even the initial steps, also depend on the cathode work function. Thus, once a streamer has propagated across the gap, the possibility and the magnitude of a return stroke or discharge up to the ionized path are conditioned by the ease of formation of a cathode spot. If the current supply is adequate and the resistance is low, once the conducting path is established, the current may increase along the path to a point where it begins to vaporize the electrode. In this case the air arc is changed to a metal-vapor arc of much higher current capacity and lower potential gradient.

The development of an arc and the later career of a spark are nicely shown in the studies of Lawrence and Dunnington<sup>3,4</sup> with a Kerr cell shutter. With ample power and a 1-cm gap it was noted that the gap was bridged in some  $10^{-8}$  second. Thereafter the spark grew in intensity, and within  $10^{-7}$  second the spark lines of Zn were observed to appear, starting from the cathode, which was of brass. These lines propagated outward up the ionized path at the ionic velocity of some  $10^4$  cm/sec. These Zn lines were *very much broadened*. The Doppler effect to be expected from atoms even under the most optimistic guesses as to atomic velocities ( $\sim 10^4 - 10^5$  cm/sec) could not account for such a broadening. Zn, however, is very subject to broadening by intense electrical fields, through the Stark effect. But since the potential gradient in the spark path which was initially 30,000 volts/cm had dropped to a few thousand volts in  $10^{-7}$  second, as shown by many oscillographic studies, the Stark-effect broadening of Zn which corresponded to fields of the order of  $10^5$  volts/cm could not be ascribed to the imposed potential gradients. The only fields capable of causing such broadening in the spark channel were the fields due to the ionized atoms and molecules. If an excited Zn atom is within  $10^{-8}$  cm of a positive ion, the field acting is of the order of  $1.44 \times 10^5$  volts/cm.

From the broadening of the Zn lines, Dunnington<sup>3,4</sup> was able to estimate that fully 30 per cent of the atoms in the spark channel of some 0.02-cm breadth were ionized. Thus, in this case, within some  $10^{-7}$  second of breakdown, fully one-third of the molecules and atoms in the path had been ionized. The ionization at first was direct and by single electron impact, but in later stages the electrons ionized many of the excited atoms, producing excited atomic and molecular ions by successive impacts. These emit the so-called spark lines in place of the arc lines, which are due to excited neutral configurations. Hence the intensely blue color of the spark in contrast to the purple haze of the arc spectrum. The energy liberated in this time is enormous. Leaving out the kinetic energy of the molecules in the spark gap

entirely, one can estimate that, if the average energy of ionization and excitation in the volume of the path of  $1.2 \times 10^{-3} \text{ cm}^3$  is 15 volts, then  $0.9 \times 10^{19} \times 1.2 \times 10^{-3}$  molecules are ionized, giving an energy  $2.6 \times 10^5$  ergs used in ionization alone. This amounts to  $0.63 \times 10^{-2}$  calorie, which would suffice to raise the temperature of the gas to about  $2 \times 10^7$  degrees centigrade. In addition it must be realized that the energy has also gone to excitation in probably an equal measure. Finally during the later stages of the spark the  $10^{19}$  positive ions are each being given an energy of the order of 0.03 volt between free paths, and the positive ions in their motion are thus contributing energy to the gas molecules at an approximate rate of 12 calories per second in their  $10^9$  impacts with them. Thus in the later stages of the spark an enormous energy is being liberated as light, potential energy, and heat in a very confined space. Since the process is adiabatic, one can expect a sudden pressure wave of considerable steepness of front and high energy to propagate outward. This furnishes the exasperating noise of the spark and is largely responsible for the detonating action of a spark on explosive mixtures. The action is borne out by the observations of Campbell on the ignition by sparks.<sup>5</sup>

It is, in fact, this enormous energy expenditure in a small volume of gas, after the gap has broken down, that has led to the concept of a "temperature" breakdown mechanism.<sup>6</sup> The theory promulgated on the basis of this consideration gained some popularity, largely among engineers, when it was first promulgated. It is thus necessary to say a word about the temperature concept in this connection.

Physically, absolute temperature  $T$  is defined as the quantity which multiplied into the gas constant  $R$  represents the value of a certain average of the kinetic energy of agitation of the molecules of a gas *at equilibrium*. Thus kinetic theory, thermodynamics, and statistical mechanics teach us that a large assemblage of elastic spherically conceived molecules when isolated and left to themselves for a sufficient time will come to *equilibrium* with a given energy distribution, in which the number of molecules in each energy state is distributed about a *probable velocity*  $\alpha$  in the form of a function known as the Maxwell-Boltzmann distribution law. Now this probable velocity is related to the absolute temperature of the assemblage  $T$  by the simple relation  $\frac{1}{2}m\alpha^2 = kT$ , where  $m$  is the molecular mass and  $k$  is the gas constant per mole  $R_A$  divided by the Avogadro number; see page 644. It is to be noted, then, that we can speak of temperature only when the gas assemblage has reached, or very nearly reached, equilibrium. Actually, however, in electrical fields the electrons do not reach an equilibrium as they are gaining and losing energy continually from an outside agent. They frequently gain a *steady state* in which gain and loss are equal. In this case, depending on conditions, the distribution of energy among the electrons or molecules is likely to be very different both in form and value from that of the ambient gas molecules, and the gas molecules

subject to an intense bombardment of positive ions in themselves may also have a peculiar distribution. While the average energy, or most probable velocity, can be ascertained, these will in general have very different relative values in different cases. Hence the square root of the average of the squared velocities will not be related in the familiar fashion to the most probable velocity, and it will depend on a purely arbitrary definition in each case as to what we choose as the *temperature*. For convenience in some cases we take the average energy in such a distribution and equate it to  $\frac{3}{2}RT$ , thus *defining an arbitrary analog to absolute temperature in each case*. Hence one does hear of the "electron temperature" or the "positive-ion temperature" in a plasma. This, however, is a very loose but convenient way of describing the average energy instead of using ergs or equivalent electron volts. But in the steady states the term temperature, crude as it is, is much more justified than it is in the rapidly altering transient spark.

At the outset of breakdown, during the first  $10^{-8}$  second while the electron avalanches are blazing a trail between the electrodes, the *kinetic energy of the gas molecules and even of the positive ions is quite low*. True, the *potential energy* of the ions and excited molecules is rapidly increasing, but this is *not* temperature. The electrons owing to their low inertia are moving very rapidly (energy of the order of 6 volts) and have an "effective temperature" of some  $50,000^{\circ}$  K. This energy *is being expended in ionizing and does not go to kinetic energy of the molecules*. It is only in time intervals of the order of  $10^{-6}$  second, in which the positive ions have been moving long enough to put some  $1 \times 10^{-5}$  calorie into energy of agitation of gas molecules and the molecular energy has increased by this mechanism to  $50,000^{\circ}$  K. *assuming equilibrium, that one can speak of an enhanced temperature*. In this same time the energy from the recombination of ions and electrons and the decay of excited states will also have been degraded to heat in some measure and we remotely begin to *approach* a "temperature." Hence, given time enough in a breakdown process, the error is to some extent to be condoned. In liquid and solid *slightly* conductive dielectrics the currents by means of the  $i^2R$  heating have been assumed to produce a localized heating and vaporization which is very effective in causing breakdown. Recent work of von Hippel<sup>41</sup> has made one even question some of the supposedly authentic cases of such breakdown. In this case the process is truly a thermal one to the point where the gas bubbles form, and one might speak of a "temperature breakdown." The *passage of the spark in the vapor, however, is not a thermal process*. As was seen in Part A, the true mechanism of breakdown is a complex ionization mechanism that relatively late in the process of producing breakdown *results in the production of a very high localized temperature*. Thus the *breakdown process was the cause, not the result, of the heating*.

As has been seen the end phase of the spark-breakdown process, once the cathode spot forms and a return stroke occurs, must depend



on the circuit conditions. Thus, whether a glow, an arc, or a damped or an oscillatory spark occurs, discharging the electrodes, is immaterial to our definition. We have now carried the complicated mechanism up to the point where the conducting path is formed and seen it terminate in a highly ionized luminous and ultimately very hot localized path in air.

In discussing the behavior of such a channel it must be clearly emphasized that while its properties are not mysterious the conventional conditions of gross macroscopic thermodynamics do not apply until after time intervals appropriate to millions of successive impacts. It is clear that the physics to be applied is the physics of the microscopic and electronic, atomic world in appropriate time intervals. It is not surprising that other attempts to interpret the micro happenings on macroscopic principles should also fail. An excellent illustration is seen in some of the attempts to measure the "temperatures" in sparks by band spectral analysis, as well as in some of the attempts to determine the *larger-scale electrical potential gradients down the channel* of arcs from the Stark-effect broadening of lines. The error in the latter attempts must be pointed out, for they appear to be perpetuated and repeated in subsequent papers. Certain very beautiful and careful studies of potential gradients in arcs by means of Stark effect were undertaken by Nagaoka and Suguira.<sup>7</sup> These studies at once indicated varying electrical potential gradients (fields) down the arc path which when integrated gave potentials across the electrodes orders of magnitudes above those applied. What was actually observed was the Stark-effect broadening of certain metallic lines by the fields of the neighboring ions in the gas.<sup>8</sup> From these data, proper information as to the density of ionization in arc channels can be obtained. The misinterpretation of the data of Nagaoka and Suguira has, however, been perpetuated to such an extent in the literature of the arc problem as seriously to complicate the interpretation of the arc mechanism. It is for this reason that the warning is issued at this point. Thus again it is seen that we must first complete the microscopic analysis before we turn to the macroscopic interpretation.

Before closing the topic of very long sparks in air it is perhaps worth while to give a few data as to the magnitudes and mechanisms involved in the dangerous but fascinating phenomena of the longest known sparks, the lightning discharge.

## 12. THE LIGHTNING DISCHARGE

The atmosphere near the earth has in general a *normal potential gradient*, due to a positive charge in the atmosphere relative to the earth, which averages around 100 volts/meter. When thunderclouds consisting of charged water droplets, created by either a spray electrification, an inductive charging in the earth's field, or from ionic cur-

rents in the earth's field, pass overhead, the sign of the potential gradient may reverse, indicating a negative charge on the bottom of the cloud. Usually a typical heat thunderstorm cloud traveling with the wind in the upper atmosphere has a negative charge in the front, or leading basal portion, followed by a positive charge in the neighborhood of the scud cloud, where the first large raindrops fall and the earth wind currents reverse. These drops are also positively charged. Following this portion of the cloud base the charge is again negative. Sounding balloons launched by Simpson and Scarse,<sup>9</sup> however, showed a concentration of positive charge at the top of the cloud with the predominating negative base. In the region of the positive base of the cloud a higher negative charge exists above it with a greater density of positive charge above that. This is shown in Fig. 261. There are, of course, many variants of the usual or typical thundershower cloud, for which the reader is referred to the beautiful paper by Simpson and Scarse.<sup>9</sup> During the later phases of the heat thundercloud, the rain from the negative base as the cloud recedes is negative.

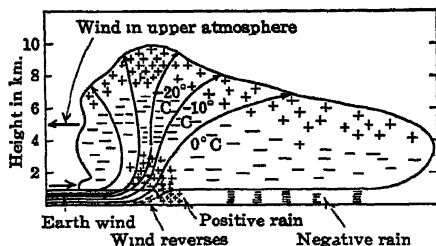


FIG. 261.—Charge Distribution in "Typical" Thunder Storm Cloud. After work of Simpson and Scarse.

Simpson and Scarse<sup>9</sup> have measured the potential gradients at the ground and find them never to exceed 300 volts/cm except immediately and momentarily after a lightning flash. The cloud bases ranged between 1 and 2 km above the ground. It appeared that there were occasionally high gradients in the clouds, but these either produced sparking in their apparatus so that no record was obtained or else they were not recorded. From this fact, Simpson concludes that the high gradients leading to lightning discharges are either concentrated in localized regions, or else materialize very rapidly, so that they were not recorded by his mechanism except as a spark.

When such regions occur and the potential gradients are built up, one can obtain from recorded measurements of lightning discharge the following data.<sup>10,22</sup> The height of the cloud bases studied ranged from 180 to 1200 meters. The discharges recorded lasted in general from  $5 \times 10^{-6}$  to  $4.0 \times 10^{-4}$  second, 50 per cent of the lightning discharges lasting beyond  $3.0 \times 10^{-5}$  second.<sup>11</sup> This was the time for the cloud to discharge itself. The gradients *near the earth* before discharge were 270,000 volts/meter, or 2700 volts/cm. This may be compared to the static sparking potential in air for gaps about 9.4 meters long, which is 4400 volts/cm. This places the total potential differences between earth and cloud for lightning strokes of 272 and 555 meters length as of

the order of  $10^9$  to  $2 \times 10^8$  volts. The currents, of course, varied widely, but at their peaks they attained values ranging from 10,000 to 500,000 amperes. The quantity of electricity that passed varied from 1 to 20 coulombs on heavy strokes, but strokes with as low as 0.1 coulomb have been recorded. Recent measurements of strokes by Holzer and Workman<sup>12</sup> for discharges from a 2.4-km high cloud have given from 20 to 200 coulombs of quantity transferred. Similar quantities have recently been reported by McEachron.<sup>35</sup> The energy involved amounts to 3 to 100 kw-hr per stroke. The power obviously is very high. Most of the strokes are impulsive, but highly damped oscillatory discharges are observed. In some cases as many as 10 to 40 strokes will follow the same ionized path as it drifts along in the wind. The discharges have been known to *volatilize* No. 12 copper wire occasionally. Usually they melt these wires and volatilize No. 14 copper wire. In the former case the current required is 500,000 amperes for  $5.0 \times 10^{-5}$  second or 100,000 amperes for  $1 \times 10^{-3}$  second with the charge varying from 50 to 20 coulombs. The No. 14 wire requires 300,000 amperes for a  $5 \times 10^{-5}$  second current to volatilize it.

The data above were taken from a lecture by the late F. W. Peek, Jr.<sup>10</sup> He states his belief that a large majority of the strokes came from negatively charged clouds. A similar view is taken by Schonland and Collens.<sup>13</sup> This question is somewhat controversial at present and must not be accepted as settled. However, in South African thunderstorms Schonland and associates have definitely recorded 70 flashes with 300 strokes to ground, both photographically and with oscillograph, and in each case the changes in field point to the discharge from a negative cloud. It must be noted that it is very difficult to be able positively to identify the polarity of a given distant observed stroke owing to the multiplicity of discharges occurring. Nevertheless, the possibility of the correctness of these conclusions must be considered. On the other hand, Jensen,<sup>20</sup> Lutkin,<sup>20</sup> and also Norinder<sup>20</sup> observe some 20–50 per cent of the strokes to be positive. The evidence from the signs of the charges picked up on power systems and towers, which is overwhelmingly negative, is not conclusive, for the greater facility of *positive streamer propagation from conducting structures* would tend to make the negative charge caught appear to be a negative stroke from the cloud when in reality it is a positive discharge from the conductor. That is, given equal numbers of positive and negatively charged clouds the majority of the strokes registered will be from the negatively charged clouds as the positive breakdown streamers propagate more readily from conductors positively charged by induction.

Despite the fact that since the time of Benjamin Franklin the electrical nature of the lightning discharge has been known, practically no advance was made in the understanding of the mechanism until the researches of Schonland<sup>13</sup> and his associates using the Boys camera started in 1934. Since that time the progress has been rapid. The first

step in picturing the mechanism resulted from considerations of Schonland<sup>11</sup> based on his results and the work of Cravath and Loeb.<sup>14</sup> A subsequent paper by Meek<sup>36</sup> furnished the missing elements needed in the analysis and has led to a fairly complete semi-quantitative outline of the process. Before discussing this it is necessary to present a few observational facts.

The Boys camera is a high-speed camera using a revolving lens. Thus the picture of the progress of the lightning stroke from earth to ground can be photographed in point of time, so that various phases of the sequence of the events can be studied at leisure.

The discharges observed by Schonland<sup>11</sup> were all discharges from the cloud (assumed negative) to the ground. The discharge was observed to advance from the cloud base to the ground at an *average* rate of about  $2 \times 10^7$  cm/sec. As it advanced towards the ground it showed some lateral branching in a downward direction of widely varying amounts. When quite near the ground the advancing tip was usually met by one or more upward moving branches. The downward stroke, or *leader stroke*, was relatively faint. When leader stroke and ground streamers met, the very bright *return*, or *main stroke*, proceeded upward along the old leader channel with high intensity and *very* great speed. This *return*, or *main*, stroke was sometimes followed by successive discharges down the old ionized channel such that in some cases 10 to 40 successive strokes have been observed down a channel. These successive strokes are separated by considerable intervals of time of the order of 0.03 second. In the return stroke as it moved up the leader-stroke channel at velocities of the order of  $10^{10}$

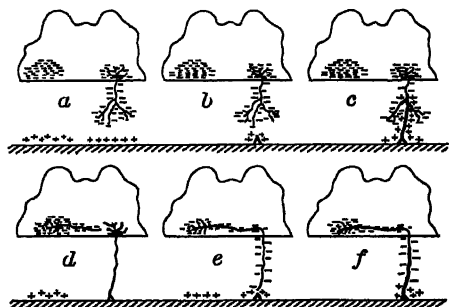


FIG. 262.—Progress of a Typical Lightning Discharge from Negative Cloud to Ground According to Schonland.

cm/sec the discharge re-excited the branches and in so doing diminished both in intensity and in speed. A sketch of the progress of a lightning discharge as pictured by Schonland is shown in Fig. 262.

Stranger than the return stroke, however, was the character of the leader stroke. For while its *average* speed of advance was  $2 \times 10^7$  cm/sec it actually advanced in steps which proceeded at a velocity of some  $2 \times 10^9$  cm/sec for 10 meters, or 50 microseconds to each step. After such an advance the leader then stopped and later again advanced at the speed above mentioned. The duration of the steps had the peculiarity of being *remarkably uniform*, all observed leader stroke steps lying between 30 and 80 microseconds in duration. Thus, while the average

velocity of advance of the leader stroke was  $10^7$  cm/sec, the actual velocity was more nearly  $2 \times 10^9$  cm/sec, but taken in steps giving an *average* velocity of  $2 \times 10^7$  cm/sec. At other times what Schonland called a *dart* leader was observed to travel from cloud to ground down an established leader channel at  $2 \times 10^8$  cm/sec which sometimes became stepped as it approached the ground. The study of long sparks in air (all less than 10 meters long) by Allibone and Meek<sup>1</sup> using a camera with moving film showed in general the same characteristic behavior as lightning except that the stepping of the leader stroke could never be observed unless resistance was placed in series with the spark.

The explanation of the mechanism did not follow at once. Cravath and Loeb<sup>14</sup> in a paper showed that the observed velocities of the stepped leader and main strokes were far in excess of those to be expected of electrons on any assumption of the potential gradients present. They postulated that the stroke of high speed must advance through *preionized air*, the channel being formed by ionization of the region by pre-existing ions acting under a potential wave. It was assumed by them that these pre-existing ions might be the natural ions existing in air. Loeb<sup>15</sup> later stated that the ions could be furnished by photoelectric ionization in advance of the tip on the basis of Cravath's<sup>37</sup> proof of ionization in air produced by a corona discharge. In the meanwhile, on the basis of his extensive data, Schonland<sup>11</sup> postulated that the mechanism must proceed about as follows.

When the discharge starts it begins as a *negative pilot streamer* invisible in the photographs which advances from the cloud into virgin air at a speed of  $2 \times 10^7$  cm/sec—a velocity which is about the velocity of electron avalanche advance in a field of 30,000 volts/cm or at an  $X/p$  of 40. Schonland<sup>11</sup> then postulated that for some reason a *new* discharge propagated from the cloud down the preionized channel left by the pilot streamer at  $2 \times 10^9$  cm/sec until it reached the tip of advance of the pilot streamer. The pilot streamer then advanced for some 50 microseconds more before it again was caught by the stepped leader. On the basis of reasonable assumptions as to ion densities in the pilot streamer and in the stepped leader channels, Schonland was able to calculate velocities of the stepped leader and return strokes in agreement with those observed, using the concept suggested by Cravath and Loeb. The reason for the stepping and its remarkable uniformity irrespective of the great diversity in cloud characteristics was not clear, however. It is here that Meek<sup>38</sup> supplied the missing link by introducing the effect of the recombination of ions on the resistance of a leader channel.

The reasoning is as follows: When suddenly at the cloud base in a given locality potential gradients due to charged cloud elements arise, having values in the order of those at which air breaks down under static sparking conditions (see page 536), viz., 30,000 volts/cm, an

electron avalanche caused by one free electron starts producing the stressed condition described on page 426. This sets up a breakdown mechanism which allows the pilot streamer to advance into virgin air by photoionization at the constant rate of about  $2 \times 10^7$  cm/sec. How far such a streamer would advance in the existing potential gradient plus that caused by axial distortion before it loses its energy by dissipation cannot be foretold. It is reasonable, however, that, to maintain such an advancing pilot streamer, the average gradient must have a certain value and the streamer tip must be nourished by a certain minimum current  $i$ .

Now it is clear that such a streamer tip must have a minimum potential gradient  $X$ , and in addition it must have a certain channel radius  $r$ . If we have a current maintained by a flow down a channel advancing with a velocity  $v$ , Rudenberg<sup>38</sup> has estimated this current  $i$  in relation to  $X$ ,  $v$ , and  $r$ . The equation given by Rudenberg is incorrect owing to a careless blunder in definition but is correctly used by Schonland<sup>11</sup> and a similar expression is given by Jehle.<sup>39</sup> The expression reads  $i = (Xvr)/2$  esu, where  $X$  is in esu,  $v$  in centimeters per second and  $r$  is in centimeters. Now the work of Raether<sup>18</sup> enables one to compute  $r$  as  $r$  is caused by the diffusion of the electrons of the tip in the 50 microseconds of streamer tip advance, if we assume, as is natural, that at the tip  $X = 30,000$  volts/cm. Raether's equation reads  $r = \sqrt{2Dt}$ . With  $D = 500$  at an  $X/p = 40$  for electrons and  $t = 50$  microseconds,  $r = 0.23$  cm. We will use the more convenient figure of 0.3 cm which is nearly enough correct. From this value of  $r$  we at once calculate the current needed for the advance of the streamer as 0.1 amp.

From this fact we can calculate the ion density in the pilot streamer channel as  $(i/e)(1/\pi r^2 v)$ , where  $e$  is the electron. The density of ions in the streamer channel tip is thus  $1.1 \times 10^{11}$  ions/cm<sup>3</sup>. This density might be visible to the eye, but densities of the order of  $10^{12}$  ions/cm<sup>3</sup> in the single corona streamers, which are visible, cannot be photographed individually by a fast camera. Hence the streamer tip cannot be photographed in the Boys camera, which appears to be the case.

Now it is clear that while there are  $10^{11}$  ions in the pilot streamer tip the number at the cloud end of the channel has decreased by recombination during the 50 microseconds of pilot advance. The number  $N$  out of  $N_0$  ions remaining in the channel after 50 microseconds may be computed at once from the equation  $N = N_0/(1 + N_0\alpha t)$ . Here  $\alpha$  can be taken from Sayer's<sup>40</sup> data as  $2 \times 10^{-6}$ . This makes  $N = 10^{10}$  ions/cm<sup>3</sup> at the cloud end of the channel after 10-meter advance of the tip. It should be pointed out that  $10^{11} \times 2 \times 10^{-6} \times 50 \times 10^{-6} \sim 10$ , which is greater than the 1 in the denominator. Hence for practical purposes with  $10^{10}$  or more ions/cm<sup>3</sup> the value of  $N$  is *nearly independent* of  $N_0$  so that we shall see that for a given  $\alpha$  the value  $N$  in discharge channels is substantially constant. This is the circumstance which accounts for the uniformity of stepping.

Now after the 10-meter advance of the pilot streamer tip in 50 microseconds we can calculate the specific resistance of the resultant cloud end of the pilot streamer channel with its  $10^{10}$  ions/cm<sup>3</sup>. For the specific resistance of the channel,

$$R_s = R \frac{d}{A} = \frac{V}{i} \frac{d}{A} = \frac{1}{NeK},$$

where  $K$  is the electronic mobility. This is roughly  $K = (e/2m)/(\lambda/c)$ , where  $\lambda$  is the electronic free path ( $\sim 5 \times 10^{-5}$  cm),  $m$  is its mass, and  $c$  is its velocity of random thermal motion at the end of 50 microseconds (about  $10^7$  cm/sec). Thus

$$R_s = \frac{2mc}{Ne^2\lambda} = \frac{1.3 \times 10^{15}}{N} \text{ ohms} \times \text{cm}.$$

Hence  $R_s = 4.6 \times 10^5$  ohms  $\times$  cm at the cloud end of the pilot streamer after 50 microseconds. Since we postulated a current at the tip of 0.1 ampere the  $iR$  drop across 1 cm at the *cloud end* of the pilot streamer rises to  $4.6 \times 10^4$  volts/cm. This gradient, however, is quite enough to *start a new discharge down a preionized path*. That is, the stepped leader results from the propagation of a new discharge down the preionized pilot streamer channel as a result of the voltage drop produced by the resistance resulting from the loss of ions by recombination. The new discharge then starts down the pilot streamer channel and it is necessary to determine whether the velocity observed by Schonland is reasonable.

In order that the stepped leader may be photographed, the density of ions in the stepped leader tip must be of the order  $10^{14}$  to  $10^{15}$  ions/cm<sup>3</sup>. We must therefore consider the conditions existing when a potential pulse is multiplying the  $10^{10}$  ions/cm<sup>3</sup> at the cloud end, or the  $10^{11}$  ions/cm<sup>3</sup> at the tip of the pilot streamer, to the  $10^{14}$  ions/cm<sup>3</sup> existing in the tip of the advancing stepped leader. To understand the propagation of the stepped leader with  $10^{14}$  ions/cm<sup>3</sup> down the channel with  $10^{10}$  ions/cm<sup>3</sup> at a speed of  $2 \times 10^9$  cm/sec with the individual electrons moving roughly  $2 \times 10^7$  cm/sec, we must reason as follows. The essential fact is that each electron must advance a distance  $x$  in the field of strength  $X$  to multiply each of the  $10^{10}$  electrons by  $10^4$  to give  $10^{14}$  ions/cm<sup>3</sup>. While this is happening the front of the ionizing pulse has advanced  $d$  cm at  $2 \times 10^9$  cm/sec. Hence we have

$$e^{\int_0^{x_a} \alpha dx} = 10^4 \text{ or } \int_0^{x_a} \alpha dx = 9.2, \text{ with } \alpha \text{ a function of } x. \text{ The time.}$$

taken for this advance is  $t$  seconds. Then if the electron velocity is  $v = 2 \times 10^7$  cm/sec, and the advance of the leader tip is  $u = 2 \times 10^9$  cm/sec,  $v = x_a/t$  and  $u = d/t$  so that  $x_a/v = d/u$  or  $x_a = (v/u)d =$

$(d/100)$ . Thus  $\int_0^{\frac{2d}{u}} \alpha dx = 9.2$ . However,  $\alpha$  is a function of the field strength  $X$  caused by the tip. This field depends on the potential of the tip of the leader, which for convenience is assumed to be that of a hemispherically capped cylinder. Such a cylinder of charge has a field  $X$  at a distance  $x$  cm from the tip given by  $X = (rV/x^2)$ , with  $V$  the tip potential, where  $r$  is the radius of tip and cylinder, in this case 0.3 cm. It may now be postulated that the field at  $d$  cm from the advancing tip of the leader,  $(r + d)$  cm from the center of the tip, must be 30,000 volts/cm, that needed to propagate a discharge in the advancing point. Under these conditions  $30,000 = rV/(d + r)^2$ , whence the tip potential is  $V = 30,000 (d + r)^2/r$ . So that  $X = 3 \times 10^4 (d + r)^2/x^2$ . Now in the region  $x_a$  long, from  $x_1 = d + r$ , to  $x_2 = (1 + v/u)d + r$  the  $\int_{x_1}^{x_2} \alpha dx$  must equal 9.2. We can now plot  $X$  as a function of  $x$  for various assumed values of  $d$ . Then we may from Sander's data of  $\alpha$  as a  $f(X)$  plot  $\alpha$  as a function of  $x$  for various values of  $d$ . The area under the  $\alpha - x$  curve from  $x_1$  to  $x_2$  for various values of  $d$  may then be computed for each value of  $d$ . The value of  $d$  at which  $\int_{d+r}^{(1+\frac{v}{u})d+r} \alpha dx = 9.2$

will give the value of  $d$  needed. Analysis shows this to be at  $d = 0.8$  cm under the conditions assumed. From this value of  $d$  the tip potential is found to be  $V = 3 \times 10^4 (0.8 + 0.3)^2/0.3 = 1.2 \times 10^5$  volts, which is not excessively high. This makes the velocity seem reasonable. The reasoning given is that initially developed by Schonland<sup>11</sup> using the Cravath-Loeb<sup>14</sup> mechanism but differs from that in his calculations owing to the fact that we know more precisely the density of ions at the time the stepped leader begins to move. The velocity  $u$  of the stepped leader will be the greater the smaller the multiplication of the ions needed, i.e., the greater the initial ionization. Hence in its progress down the pilot streamer the stepped leader will increase in speed.

When the end of the advance of the pilot streamer is reached the stepped leader can advance only with the speed of the electron avalanches. This rate may be increased slightly by the higher field at the tip of the leader but not materially. The stepped leader thus stops while the pilot streamer then forges ahead. This trail of  $10^{14}$  ions/cm<sup>3</sup> left in the wake of the stepped leader, in the meanwhile, gradually decays. At the end of 50 microseconds while the pilot streamer advances 10 meters further, recombination has reduced these ions down the path of the first step to nearly  $10^{10}$  ions/cm<sup>3</sup>. Thus, at the cloud end first, and later farther down, the  $iR$  drop starts a new potential wave down the preionized channel. Hence a new stepped process travels the 20 meters from the cloud to the end of the advance of the pilot streamer and stops there, to be photographed as step 2.



Accordingly, at intervals of 50 microseconds there will be a new discharge passing down the pilot channel. If the cloud to ground path is long enough so that the last stepped tip has not reached the pilot streamer in 50 microseconds there may be two such steps under way at one time. Since the speed of the step is  $2 \times 10^9$  cm/sec, the length of path for this to occur must be  $50 \times 10^{-6} \times 2 \times 10^9 = 1 \times 10^5$  cm or 1 km. If the discharge path is less than 10 meters long the *step will not develop* since the resistance  $R_s$  cannot drop to a low enough value in less than 50 microseconds. Thus, unless resistance is placed in series with such a gap, stepping will not be observed in conformity to the work of Allibone and Meek.

With the approach of the stepped leader to the ground, the fields set up are sufficient to start a positive streamer propagation upward. Once the two join, or once the gradient at the ground end begins to act on the ionized path of the stepped leader or pilot streamer, a *return* potential wave travels up the channel at high speed. Since in the ground end of the stepped leader the value of  $N$  is about  $10^{14}$  or more ions/cm<sup>3</sup>, the velocity  $u$  of the return stroke will be very high. The value of the ionization density achieved will depend on the gradients set up and will transcend by orders of magnitude those in the step process. Thus the brilliant portion of the flash is that of the *main* or *return* stroke where  $N_0$  may reach  $10^{19}$  or more. As the return stroke proceeds up the channel,  $N$  is decreasingly great, and the main or return stroke moves more and more slowly as it proceeds. The relatively low resistance of the ground compared to that of the cloud is the reason for this far higher main stroke proceeding upward.

After the main stroke several later discharges propagate down the old channel. These propagate from the cloud to the ground. They are no longer stepped and are called by Schonland *dart* leaders. They travel from the cloud to the ground at an average speed of  $2 \times 10^8$  cm/sec. If the time between dart and the preceding main stroke is long the dart may be stepped as it approaches the ground. The dart leader is started by a new increase of potential gradient between the upper end of the previous channel at ground potential and the cloud. In the 0.03 second between successive *darts* the value of  $N$  is about  $2 \times 10^7$  ions/cm<sup>3</sup>, so that the rate of advance is now much slower in the dart leader. The return stroke from ground then completes the dart picture. In this period the channel radius increases by diffusion so that later strokes may have channels of the order of 1-5 cm diameter.

From what has been given we can estimate the potential difference between cloud and ground. With a cloud 2 km above the ground, two steps will be advancing down the channel. Hence the potential gradient along the channel of 2-km length is  $2 \int_0^{10^8} R_s dx$ , where  $R_s$  is the specific resistance of any section  $x$  cm from the tip of the leader. The

time since the tip of the leader passed  $x$  is  $t = x/u$ , and  $R_s = \frac{4.6 \times 10^{15}}{N}$ , whence  $R_s = 4.6 \times 10^{15} \frac{\left(1 + N_0 \alpha \frac{x}{u}\right)}{N_0}$  ohms  $\times$  cm. The current  $i = 0.1$  ampere. Hence the cloud potential is

$$\begin{aligned} V_c &= 2 \times 0.1 \int_0^{10^8} \frac{4.6 \times 10^{15}}{N_0} \left(1 + N_0 \alpha \frac{x}{u}\right) dx \\ &= 9.2 \times 10^{14} \left(\frac{10^8}{N_0} + 5 \times 10^{-6}\right) \text{ volts.} \end{aligned}$$

With  $N_0 = 10^{14}$ ,  $V_c = 4.0 \times 10^9$  volts, this is changed only 1 per cent if  $N_0 = 10^{12}$ .

That the mechanisms are in their general character correctly assumed is made likely by the studies of Snoddy, Dieterich, and Beams<sup>19</sup> on the propagation of discharges down long tubes at low pressures. Both positive and negative discharges propagate down evacuated tubes with velocities comparable to those observed in lightning. Although the pressures are different and tube walls impair the propagation (see page 482), the mechanisms are sufficiently similar to be highly suggestive.

The author would like to point out, however, that the theory of Schonland<sup>11</sup> and of Meek<sup>26</sup> is evolved only for the negative strokes. That positive strokes occur cannot be questioned, and in some cases it is estimated that perhaps 50 per cent of the strokes are positive. The character of the positive stroke mechanism has already amply been discussed in terms of the streamer formation. Since that mechanism is favored in spark propagation it should appear frequently in lightning. The conditions of the initiation of lightning discharges are obscure. If, however, small oppositely charged cloud masses drift past each other the instantaneous fields can reach the values of 30,000 to 60,000 volts/cm required to initiate positive streamers or negative avalanches which are then self-propagating at average gradients of 2700 volts/cm or more. It is probably the mechanism of charged cloud formation and storm development that determines the sign arrangement in clouds and leads to negative or positive strokes to ground. It is therefore probably not a question as to the most efficient or likely electrical mode of breakdown propagation which determines the sense of the propagation observed in different localities and storms. It is much more likely the mechanics of the storm cloud formation, which may be a local affair, that determines the sign arrangements and hence the rather discordant observations as to the direction of propagation. This general view of the recent status of knowledge concerning the longest sparks in air suffices to close the discussion of the mechanism of static spark breakdown in air.

### 13. SPARK BREAKDOWN WITH ALTERNATING CURRENT

The discussion of this involved subject can add little to a book on fundamental processes. It is clear that alternating potentials complicate the picture by reversing electrodes, where these are dissimilar, and by launching field-distorting space charges of positive and negative ions, which, owing to differences in mobilities of electrons and ions and diffusion, will accumulate in complicated ways. The diversity of electrode shapes and the changes produced by changes of frequency make lengthy discussion in a text of this scope hardly worth while.

However, one may consider a sphere gap of not too great a length and briefly observe what happens to the sparking potential as the frequency is varied. If the gas is one like air, where electrons attach, the case will be somewhat different, but not vastly so, from that in which electrons remain free. In regarding such a gap it again must be remembered that ultraviolet illumination of at least one electrode is essential for good or consistent measurement. In this case either electrode will serve. It is probably better to illuminate both electrodes or provide a source of radioactive ionization if the ultraviolet light is inconvenient. The influence of ultraviolet light on alternating potential studies is nicely illustrated by Reukema,<sup>21</sup> whose use of ultraviolet light reduced the observed average sparking potential 3.5 per cent.

Assuming that electrons are in the gap and near both electrodes, consider now a 60-cycle alternating current. Near  $V_s$ , but below it, the ions and electrons are accelerated from the instantaneous cathode sphere beginning with the rise of negative potential. As the potential rises to 28,000 volts across a 1-cm gap with relatively large electrodes, the electrons cross the gap nearly as fast as liberated, for the time of crossing is of the order of  $10^{-7}$  second. The negative ions formed during periods of lower field cross at the maximum field in some  $2 \times 10^{-5}$  second but are being continually produced. As the field declines, there are then positive and negative ions and electrons over the whole gap, which are withdrawn during the reversal of the field. With both electrodes illuminated, electrons at high fields and ions at the lower fields will always be present in the gap. At the peaks, however, the electrons will be ionizing by collision, and thus positive and negative ions will be created in the gaps. As the fields decline these will gradually be swept out. In this sweeping the electrons will first be removed and then the negative ions with their lower mobility will follow. Finally, if the gap is short and the fields are high, the slower positive ions will disappear. For longer gaps where the ions cannot cross during the quarter cycle it is clear that a residue of positive ions will remain in the gap. These will gradually build up a space charge. This action is in all cases enhanced by the diffusion of ions, for while diffusion is slow at atmospheric pressure there is a finite diffusive displacement of the ion mass in both directions from a given moving ion front as shown in Chapter IV.

Hence the reverse cycle *will never* recall all the ions or electrons of a given sign that have moved out into the gap. With low frequencies and more uniform fields, except for the lateral escape of ions, the conditions for spark breakdown should not materially differ from the static breakdown. It is possible because of spark lag effects that the value of  $V_s$  with alternating current under these conditions could be slightly higher than the corresponding case for static breakdown. This follows since the potential active is the *peak value* which lasts but a very short time, such that statistical time lags can require that the lower potentials present in the more extensive portion of the cycle be raised to  $V_s$  before the spark breaks. This is clearly indicated in Reukema's relatively large lowering of the value of  $V_s$  on illumination.

For longer gaps, however, space-charge accumulations will certainly make a lowering possible. As the frequency is increased to the time of crossing of the ions across the gap during the interval of the high voltage, the matter changes radically. Reukema<sup>21</sup> found that for 6.25-cm-diameter spheres with gap lengths ranging from 0.25 to 2.5 cm the sparking potential began to be lowered below that at 60 cycles when frequencies of 20,000 cycles per second were achieved. At 0.25 cm the potential was about 7000 volts effective (peak value  $\sim 10,000$  volts), so that  $X \sim 28,000$  volts/cm. The mobility of positive ions is about 1.6 cm/sec, hence the ions at the peak voltage have a velocity of 45,000 cm/sec and cross the 0.25 cm in  $1.2 \times 10^{-6}$  second. However, positive ions are being formed when  $X \sim 15,000$  volts/cm and is falling rapidly. Here again the ions can cross the gap. But for a 2.5-cm gap the ions created in the later parts of the cycle cannot get across. The ions will have been generated pretty well across the gap near the electrode, which was the anode on the declining wave. When the potential has fallen to zero they will be near the electrode that is to be the anode in the approaching cycle. They will then be driven across the gap to their place of origin just as the potential begins to reach high values. Thus *they form an enhancing positive-space-charge field for ionization by the electrons* from the temporary cathode. In this way ionization by collision at the cathode will be facilitated. When the frequency goes up still further the space charges at the cathode will be increasingly greater and with an enhanced  $\alpha$  at the cathode breakdown must occur at a lower value of  $V$  than before. Increasing the frequency will make the space charge greater and greater, causing a progressive lowering of the value of  $V_s$  as much as 17 per cent for the 2.5-cm gap. Reukema found for the gaps used that there was a progressive lowering of  $V_s$  with increasing frequency from about 20,000 to 60,000 cycles. At greater frequencies the lowering approached a limiting value, which remained constant up to 425,000 cycles. This indicates that, while between 20,000 and 60,000 cycles the space charge was increasing, it in turn gradually reached some limiting effective value. It may be suspected that the limitation is set by the lateral loss of ions out of the gap, for the

lack of further change in  $V_s$  with increasing rate of accumulation of ions in the gap, can signify only a loss process driving positive ions out of the gap. The variation of  $V_s$  with frequency for sphere gap in air as found by Reukema between 60 and 425,000 cycles is shown in Fig. 263, the potentials being *effective*, i.e. nearly rms values.

When frequencies begin to approach the time of transit of electrons across the gaps, we may expect another change in  $V_s$  with frequency resulting in a possible further lowering. In this case, during the peak of each cycle, electrons are created which are not removed and thus in part survive in the gap. Hence cumulative ionization by electrons builds up, and at each cycle the number of initial electrons increases, so that during the high field period more and more electrons are ready to initiate new avalanches. Thus the ionization builds up over many

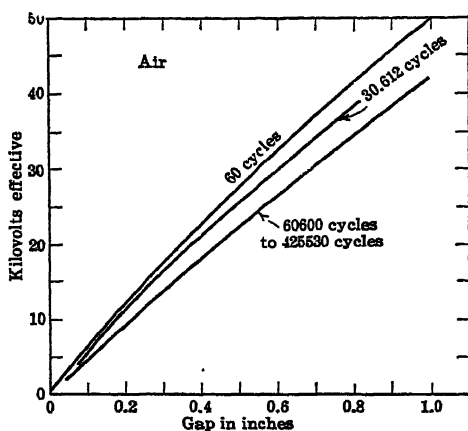


FIG. 263.

cycles and the gas becomes conducting with a sufficient number of cycles, once the peak of the applied voltage exceeds a value such that the field strength  $X$  at the existing pressure gives Townsend's  $\alpha$  finite values. The sparking potential for very high frequencies would then be expected again to decrease to yield values of  $X$  or  $X/p$  where electrons are of the order just to be able to ionize by collision. For most gaps these frequencies must be *very* high. Actually, fields may have to be

*somewhat higher* than those to give an  $X/p$  needed to make  $\alpha$  finite, as, in the short time intervals allowed by the frequencies of  $10^7$  to  $10^8$  cycles, the electrons may not have a chance to reach their terminal energy. This becomes clear from the following data: For a 1-cm gap the electron velocities at ordinary sparking potentials are of the order of  $2 \times 10^7$  cm/sec. Hence electrons would be expected to cross the gap in  $5 \times 10^{-8}$  second. If the frequency is of the order of  $2 \times 10^8$  cycles per second there is a fair chance of an accumulation of electrons in the gap. During the time of the peak the electrons will have made at most some 10 to 100 impacts with molecules and thus will not be in a steady state. It must also be pointed out that at such frequencies the positive ions are relatively fixed in space while the electrons follow the field so that the positive space charge cannot be ignored. The way in which multiplication takes place, then, depends on the positive-space-charge distribution as well as on the imposed field.

It is clear that the multiplication of electrons by the high-frequency field will not continue indefinitely, for eventually space charges build up such gradients that self-repulsion and diffusion to the walls and electrodes, accompanied by recombination on the walls and in the gas as well as flow to the electrodes, where present, will balance the rate of ion production.

This is precisely what happens in the so-called *electrodeless* discharge where flow to the electrodes is obviated. Here a bulb containing a gas is placed in the intense high-frequency-field region within an induction-furnace coil or a Tesla coil. The electrostatic fields about a solenoidal coil with high frequency in some regions are quite intense.<sup>27</sup> There is in addition the magnetic field of the solenoid.<sup>28</sup> The static field inside a glass vessel filled with a gas or vapor at low pressure placed within the coil is reduced in some measure by the conductivity of the glass at high frequency.<sup>26</sup> It now appears probable that electrons that find themselves free in such a gas will *begin* to ionize during the high electrostatic peaks.<sup>25,31,32</sup> Once electrons are present, the magnetic field also acts, and thus both from the magnetic and the electrostatic fields the electrons acquire energies sufficient to ionize by collision.<sup>25,26,27,28,32</sup> During the low-field periods the ions and electrons recombine very little. Thus those electrons that are not driven to walls, or electrodes if present, by electrostatic fields will remain for the next high-field cycle. The charges then multiply and accumulate over many cycles.

The *electrostatic action is needed to start the affair*,<sup>32</sup> but once electrons are moving the magnetic fields appear to predominate in the electrodeless case.<sup>32</sup> The reason for this is clear, for while the electrical fields drive the electrons to the walls the magnetic forces drive the electrons in circuital paths about the field lines,  $H$ , within the bulb at various distances  $r$ . Hence, since as we shall see the effectiveness at lower frequencies depends on the possible length of the electron paths before annihilation, the magnetic field in which electronic paths may be indefinitely long have the advantage. Thus the most intense effect, in the absence of electrodes, is the *ring discharge* concentric with the coil.<sup>25,26,32</sup> The inner longitudinal ionization along the axis which is static is less intense. As a result of electrical and magnetic field action, electrons and positive ions accumulate continuously. Eventually the electron diffusion to the walls produces a negative wall potential; positive ions flow to the walls and neutralize the electrons there, thus establishing equilibrium between production and destruction of charge. The mechanism of the wall currents will be discussed at length in Chapter XI. Where electrodes are present inside, the charges of course are mostly removed as ion currents to these. The ionization in this case is largely electrostatic.<sup>32</sup> The theory for the electrodeless ring discharge has been worked out on a magnetic basis by J. J. Thomson.<sup>23</sup> It will be presented in outline in what follows. The theory for the electrostatic

action has as yet not been worked out. In a general way, J. Thomson <sup>22</sup> has indicated the solution, but this is not complete enough to merit presentation at present.

In the case of the magnetic field the situation as given by J. J. Thomson <sup>23</sup> is as follows: If the amplitude of the magnetic field produced by the solenoid is  $H_0$ , and  $H$  the field varies as  $H = H_0 \sin 2\pi Nt$ , it can be shown that the equation governing the discharge is

$$\frac{q^2 + (2\pi N\lambda_0)^2}{2\pi N\lambda_0} = \frac{reH_0}{m}.$$

Here  $q$  is given by the expression  $eV_i = \frac{1}{2}mq^2$ , such that  $q$  is the velocity of an electron with energy equal to the ionizing potential  $V_i$  of the gas. The quantity  $r$  is the radial distance of the electron, or discharge section considered, from the axis of the tube. In this effect the time  $t$  in the expression for  $H$  must represent the time for an electron to acquire the velocity  $q$ . In this time the electron has traversed a distance

$$\frac{rH_0e}{4\pi Nm} (1 - \cos 2\pi Nt).$$

This distance must be less than the distance  $\lambda_1$  required for the electron to attach to a molecule, recombine, or be lost to a wall, i.e., the time to become inactive. If we chose a path  $\lambda_0$  which is less than  $\lambda_1$  but which varies inversely as  $p$  the gas pressure, the *active mean free life* path, we can arrive at the equation above. Except at higher pressures in very active gases  $\lambda_0$  will be quite long, especially if attachment to ion formation is unlikely. The expression

$$\frac{q^2 + (2\pi N\lambda_0)^2}{2\pi N\lambda_0} = \frac{reH_0}{m}$$

has its left side very large when  $2\pi N\lambda_0$  is very large and also when  $2\pi N\lambda_0$  is very small. It has a minimum value when  $q = 2\pi N\lambda_0$ , or when in one cycle  $qT = 2\pi\lambda_0$ ,  $N = 1/T$ , that is, when the free existence path of the electron used as radius describes the distance traversed in one period. Since  $\lambda_0$  is proportional to  $1/p$  there will be a value at which  $reH_0/m$  is a minimum at a different pressure for each gas ( $q$ ) at each frequency. This has been found to be correct in a rough fashion by J. J. Thomson. Thus even here we have a *minimum potential equivalent to the minimum in the  $V_s - p\delta$  curve for sparks*. At high pressures,  $\lambda_0$  will be small,  $2\pi N\lambda_0$  will be small, compared with  $q$ , and we will have

$$H_0r \propto \frac{q^2}{2\pi N\lambda_0}$$

which varies directly as the pressure. At very low pressures  $2\pi N\lambda_0$  will be large compared to  $q$  and  $rH_0 \propto 2\pi N\lambda_0$  or to  $1/p$ . Thus  $H$  will pass

through a minimum at a certain value of the pressure, for a given  $r$ . Since the passage of this discharge depends on  $rH_0$  at a given pressure, the electrons at the outer surface of the bulb will be the first to ionize. In this case the electron loss and  $\lambda_0$  will in a large measure depend on lateral diffusion to the walls. The discharge at lower values of  $H_0$ , when it appears, will be at the largest  $r$ , i.e., the periphery of the bulb containing the gas. The discharge forms a ring about the inner circumference of the bulb which accounts for the name ring discharge. As  $H_0$  increases, the ionization and excitation will proceed inward. The color of the discharge will obviously change with  $r$ , as the relative intensity of spectral lines depends on the energy distribution of the electrons, those lines of lowest  $E_e$  being excited on the inner portions of the ring.

The theory holds only so long as the gas currents are so small that the magnetic fields due to ion currents in the gas can be neglected relative to  $H_0$ . Since the magnetic fields due to the gas currents are of the opposite sign compared to those in the solenoid, the field  $H$  in the center of the bulb may be zero. By placing a sealed bulb at the optimum pressure in a larger one in which the pressure can be varied the following sequence is observed. At high pressure in the outside bulb the inner bulb glows brightly. As the pressure in the outer bulb reaches the optimum pressure, the glow in the inner bulb extinguishes while the outer bulb lights up brilliantly. As the pressure goes down below the optimum in the outer bulb, the inner bulb again lights up. In passing through the range of pressures in the outer bulb there is a point at which, while the outer bulb glows slightly, the inner bulb is extinguished. This point corresponds to a maximum *current* in the outer bulb with, however, less luminosity. High excitation, as can be expected from the energy distribution laws and from Hale's observations on Townsend's second coefficient  $\beta$ , may not correspond to maximum ionization in the gas. The demonstration is thus very striking.

The electrodeless ring discharge enables a number of investigations of fundamental electrical properties of gases to be made which are otherwise impossible. One of these is the effect of a beam of ultraviolet light passing through quartz such that the photons can *excite* but *not* ionize the gas. In this case the beam went through the bulb from tubes at both ends so that no photoelectrons were produced. It was observed that, if  $H_0$  was not great enough to produce a discharge at a given pressure but was near such a value, the beam of light brought forth a ring discharge. The effect occurs in air,  $H_2$ , He, A,  $O_2$ ,  $N_2$ ,  $CO_2$ , I, and Hg. It is probable that in J. J. Thomson's studies some of these gases were not perfectly free from Hg so that the metastable action could have been expected. The effect of illumination was due to excitation of the molecules or atoms by the ultraviolet from any source. There was no indication that it was produced by *selective* resonance excitation. For example, light from an  $H_2$  discharge in quartz did not produce an abnormal amount of luminosity in  $H_2$ . Ionization in these



gases by the ultraviolet light of wavelength  $> 1200 \text{ \AA}$  could not be detected.

The effect of traces of impurity on the discharges can also be studied to advantage in such tubes, especially in the different zones of excitation. Thomson demonstrated the effects of even small traces of sulfur in this fashion. The ring discharge is also of value in studying the chemical and other after-effects producing the afterglows. In some cases there are metastable states, which, in the absence of metal electrodes, persist for a long time. In others they appear to be chemical substances which can be condensed by liquid air and kept in an activated state by low temperature, thus proving their chemical character. The appearance of the glow on the glass surface, if liquid air was applied to the walls to condense the gases, indicates that these glows are due to different active chemical compounds which are evaporated at different temperatures and react on warming. There is thus no question but that these glows are in some measure produced by chemical interactions and not by excited and metastable states, for these cannot be condensed and frozen. Since such reactions as ensue emit visible light in detectable quantities, and doubtless ultraviolet light as well, the reason for some of the mysterious effects observed in Geiger counters, such as spurious counts and self-excitation which may last for some time after the tube is first used, becomes clear (see also page 498). Gases like  $\text{O}_2$ ,  $\text{N}_2$ ,  $\text{N}_2\text{O}$ , and  $\text{NO}$  produce quite strong effects of this nature.

The study of the sparking potential between electrodes with frequency above  $10^6$  cycles appears not to have been carried out so systematically as in Reukema's work at lower frequencies. One of the difficulties lies in the fact that large electrode distances are needed so that the time of crossing of the plates can be such as to compare with the conveniently attainable frequencies of oscillation. It is difficult to get controllable frequencies of sufficient energy much above  $3 \times 10^8$  cycles. With electron velocities of  $5 \times 10^7 \text{ cm/sec}$  the frequencies for reasonably spaced electrodes 1–3 cm must be of the order of magnitude of  $10^8$  cycles. However, a great deal of study has been devoted, in more recent years, to the behavior of the *electrostatically* initiated high-frequency discharge in view of a controversy as to the mechanism of the electrodeless discharges in gases. Initially, as indicated for the ring discharge, J. J. Thomson<sup>23</sup> suggested that the ring discharge was of a *magnetic* character. Townsend<sup>27</sup> and his collaborators contended that the electrical intensity was nearly 30 times as large as the magnetic intensity in the coils. Hence they ascribed the ring discharge to an electrical effect and not to the magnetic action. MacKinnon,<sup>28</sup> Knipp,<sup>25</sup> Smith, Lynch, and Hilberry,<sup>28</sup> Esclangon,<sup>24</sup> and Brasefield<sup>30</sup> have as a result of many diverse and ingenious experiments succeeded in showing that both actions occur in the electrodeless effect as stated earlier. The ring discharge which is brightest is largely magnetic but requires for its

initiation the electrostatic effect to form initiatory electrons. The inner and fainter discharge, however, is purely static. There are bright static discharges when the electrodes are placed on the glass, but the high-frequency conductivity of the *glass* container reduces the electrostatic action and complicates the results. The longer magnetic paths at higher pressures, in the absence of electrodes, makes the ring discharge and magnetic effect easier to produce.

To study the other static phenomena, large electrode distances, *large* electrodes, pure gases, and very high frequencies should be used.<sup>32</sup> Probably the most outstanding work in this direction is due to J. Thomson.<sup>32</sup> Before discussing this work one should state that the earlier work was done by Gutton<sup>33, 34</sup> and his associates on the values of starting potentials as a function of frequency. They worked with rather improper electrodes, wires or plates, with rather important

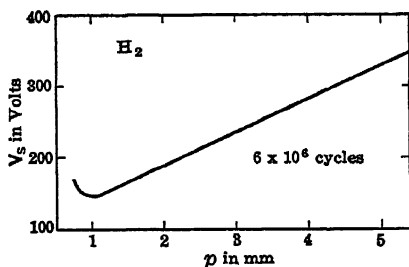


FIG. 264.

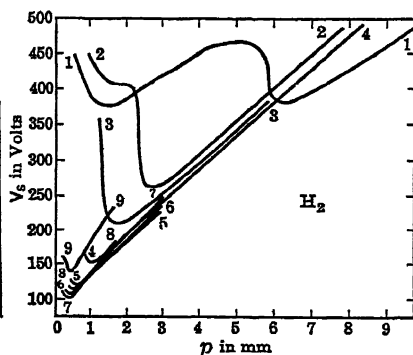


FIG. 265.

effects of the tube walls. Since their results are largely corroborated and extended to cover larger ranges by J. Thomson they will not be given.

The experiments of J. Thomson<sup>32</sup> were made on pure mercury-free gases with proper electrodes. He compared low-frequency and static curves with curves up to frequencies as high as 10<sup>8</sup> cycles per second. In the later work, electrodes of 8-cm diameter separated by 2.58 cm were used, with pure, Hg-free H<sub>2</sub> gas. It was found that the peak value of  $V_s$  followed a typical Paschen curve, of which Fig. 264 at about  $6 \times 10^6$  cycles shows an example. The particular feature is the linearity of the curve at moderately high frequencies beyond  $V_{sm}$ . This curve is accurately given by an equation  $V_s = A + Bp$ , where  $A$  appears particularly sensitive to *purity of the gas* and is a function of frequency,  $\nu$ ,  $A = f(\nu)$ . The beginnings of the curves at various frequencies near the minimum are shown in Fig. 265. Curves 1, 2, 3, 4, 5, 6, 7, 8, 9 correspond to 1.8, 2.8, 3.73, 6.33, 15.6, 49.5, 65.4, 77.1, and 99

million cycles, respectively. The constant  $A$  decreases with frequency at first from 121 for curve 2 to 77, and then rises again in curves 8 and 9.  $B$  is constant in curves 2 to 5 and then gradually rises from  $(1/2.58) B = 18$  to 31.4.  $V_{sm}$  decreases from 260 for curve 2 to 99 for curve 7 and then rises again to 138. The minimum pressure likewise falls from  $p_m = 2.6$  mm for curve 1 to a minimum of 0.3 at curve 7, and rises to 0.36 for curve 9. These curves are in general similar to those of C. and H. Gutton using  $H_2$  with parallel-plate external electrodes. The double minimum at higher pressures is real and was observed by Gill and Donaldson.<sup>27</sup> It is possible that this is a wall effect due to distances of finite travel at longer times. For static breakdown in similarly pure  $H_2$  an approximate equation of the form  $V_s = 320 + 33.3 p \delta$  applies.

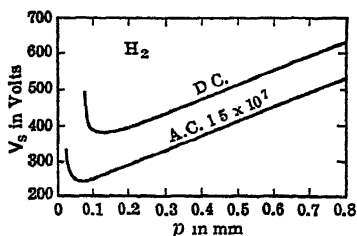


FIG. 266.

Fig. 266 shows curves comparing high-frequency and static breakdown under the same conditions. It is seen that  $A$  is less at higher frequencies and  $B$  is also smaller. The behavior of the value of  $V_s$  with frequency depicted is what one would, a priori, expect to observe. It is also consistent with the observations of Reukema. J. Thomson<sup>32</sup> sketches a theory of the discharge which is in general plausible

and probably correct, but it is not sufficiently complete or detailed to warrant discussion at this time. Thomson's work is an outstanding land mark in these studies, and it is to be hoped that more data of this type will eventually become available in other gases and higher pressures.

Aside from the glow discharge and the arc, this completes all the essential forms of discharge studied except the very short spark. The latter is in essence not very different from the lower-pressure sparks. The breakdown requires time for the building up of space charges. The work of Hobbs on these led to the discovery of field emission. The short sparks, though interesting, do not merit extended discussion at this point. Thus, although a survey of the data on the short spark would doubtless be worth while, a book of this scope must be kept within reasonable bounds, and this subject will not be treated.

#### 14. REFERENCES FOR SECTIONS 11 TO 13, PART C, CHAPTER X

1. ALLIBONE and MEEK, *Proc. Roy. Soc.*, A 166, 97, 1938; A 169, 24, 6, 1939.
2. W. ROGOWSKI, and students, *Arbeiten aus dem Elektrotech. Institut. der Tech. Hochsch. Aachen*, Vol. IV, Springer, Berlin, 1929-30.
3. LAWRENCE and DUNNINGTON, *Phys. Rev.*, 35, 396, 1930.
4. F. G. DUNNINGTON, *Phys. Rev.*, 38, 1535, 1931.
5. CAMPBELL and PATTERSON, *Proc. Phys. Soc. London*, 31, 168, 227, 1919.
6. J. SLEPIAN, *Elec. World*, 91, 768, 1928.
7. NAGAOKA and SUGIURA, *Jap. J. Phys.*, 3, 45, 1924.

8. LOEB, HILLEBRAND, WHITE, VARNEY, and MILLER, *Phys. Rev.*, **49**, 703, 1936.
9. SIMPSON and SCARSE, *Proc. Roy. Soc.*, **A 161**, 309, 1937.
10. These data are scattered through a voluminous literature. The author is indebted to a compilation of the data given by F. W. PEEK, JR., in the mimeograph of a lecture delivered at the University of California in March, 1933. Some of these data are also found in articles to be cited.
11. B. F. J. SCHONLAND, *Proc. Roy. Soc.*, **A 164**, 132, 1938.
12. WOREMAN and HOLZER, *Phys. Rev.*, **55**, 598, 1939.
13. SCHONLAND and COLLENS, *Proc. Roy. Soc.*, **A 143**, 654, 1934; **A 152**, 595, 1935.
14. CRAVATH and LOEB, *Physics*, **6**, 125, 1935.
15. L. B. LOEB, *Rev. Modern Phys.*, **8**, 267, 1936.
16. B. F. J. SCHONLAND, *Phil. Mag.*, **23**, 503, 1937.
17. F. OLLENDORF, *Arch. Elektrotech.*, **27**, 169, 1933.
18. H. RAETHER, *Z. Physik*, **107**, 91, 1937.
19. SNODDY, DIETERICH, and BEAMS, *Phys. Rev.*, **52**, 739, 1937.
20. J. C. JENSEN, *J. Franklin Inst.*, **216**, 707, 1933; H. NORINDER, *Proc. Phys. Soc. London*, **49**, 364, 1937; F. E. LUTKIN, *Proc. Roy. Soc.*, **A 171**, 285, 1939.
21. L. E. REUKEMA, *Trans. Am. Inst. Elect. Eng.*, **47**, 38, 1928.
22. W. T. WORMELL, *Proc. Roy. Soc.*, **168**, S97, 1938.
23. J. J. THOMSON, *Conduction of Electricity through Gases*, 3d Edition, Cambridge Press, 1933, Vol. 2, p. 431 ff.; *Phil. Mag.*, **32**, 321, 445, 1891; **4**, 1128, 1927; *Proc. Phys. Soc. London*, **40**, 79, 1928.
24. ESCLANGON, *Ann. Physik*, **1**, 276, 1934.
25. C. T. KNIPP, *Phys. Rev.*, **37**, 756, 1931.
26. MACKINNON, *Phil. Mag.*, **8**, 605, 1929.
27. TOWNSEND and DONALDSON, *Phil. Mag.*, **5**, 178, 1928.
28. SMITH, LYNCH and HILBERRY, *Phys. Rev.*, **37**, 1091, 1931.
29. G. D. YARNALD, *Phil. Mag.*, **13**, 1179, 1932.
30. C. J. BRASEFIELD, *Phys. Rev.*, **37**, 82, 1931.
31. G. KIRCHNER, *Ann. Physik*, **57**, 287, 1925; **7**, 798, 1930.
32. J. THOMSON, *Phil. Mag.*, **10**, 280, 1930; **18**, 696, 1934; **23**, 1, 1937.
33. GUTTON, MITRA, and YLOSTALO, *Compt. rend.*, **176**, 1871, 1923; **178**, 476, 1924.
34. C. and H. GUTTON, *Compt. rend.*, **186**, 303, 1928.
35. K. B. MCEACHRON, *J. Franklin Inst.*, **227**, 149, 1939.
36. J. M. MEEK, *Phys. Rev.*, **55**, 972, 1939.
37. A. M. CRAVATH, *Phys. Rev.*, **47**, 254, 1935.
38. K. RUDENBERG, *Wiss. Veröffentl. Siemens-Konzern*, **9**, Part 1, 1930.
39. H. JEHLE, *Z. Physik*, **82**, 784, 1933.
40. J. SAYERS, *Proc. Roy. Soc.*, **A 169**, 83, 1938.
41. MERRILL and VON HIPPEL, *Phys. Rev.*, **55**, 1122, 1939.

## CHAPTER XI

### THE ARC AND GLOW DISCHARGE

In a book on fundamental processes in electrical discharge through gases it is proper that some space should be devoted to a summary of such processes as are active in the most widely used industrially of the various discharge types, the arc and glow discharges. Each of the discharges is sufficiently broad to merit a book of its own. Probably more papers have been published on various aspects of the glow discharge than on all the other discharge phenomena combined. Under such conditions it must be clear that in a chapter of a book such as this the treatment cannot be more than superficial. Again the author makes no pretenses as to authoritative knowledge in this field. While he is competent to discuss the fundamental processes, neither he nor his students have worked either on arcs or glow discharges. However, in view of the fact that some information on these phenomena is needed to complete the book and that no recent summary of these discharges is available in a convenient form in English, this chapter is written.

#### *A. THE GLOW DISCHARGE \**

##### **1. THE GLOW DISCHARGE AS A FUNCTION OF PRESSURE**

One may begin the discussion of the glow discharge by describing the transitions observed when a tube filled with a gas at 760 mm, air for example, is gradually evacuated while an adequate high potential from a d-c source is applied across two plane electrodes at the end of the tube. The usual case is to consider a tube whose length is ten to twenty or more times its diameter, with disc electrodes of diameter about two-thirds to three-fourths the diameter of the tube. An induction coil gives nearly unidirectional surges of high potential, as the potential on the "break" is usually much higher than on the "make" of the contact. For purposes of demonstration it is exceedingly convenient compared to variable high-potential d-c sources.

Let us consider an induction coil placed across two plane electrodes separated by some 50 cm in a tube of some 3-cm diameter, and start with the tube filled with air at atmospheric pressure. If then we proceed to exhaust the tube the sequence of events will be as follows. At

\* References for Part A of Chapter XI will be found on page 602.

first sparks will jump the safety gap of the induction coil outside of the tube. As the pressure reaches a value such that  $p\delta$  gives a  $V$ , equal to the potential given by the induction coil a spark will jump inside the tube. Probably as soon as  $p$  is low enough for a spark it will be observed that the spark is no longer the bright, intense narrow *bluish* spark one usually expects but that it has a more pinkish lavender color, characteristic of air, and that though the path is zigzagged its channel is wide and diffuse. This results from the increased velocity and thus amplitude of diffusion of the electron avalanches at the lower pressure. In the neighborhood of 1-cm pressure, even in air, the zigzag spark disappears and the tube is filled by a uniform glow of a pinkish purple color in air extending down the whole length of the tube, except near the electrodes. Thus diffusion results in quite a uniform discharge condition, the charges arriving at the walls acting to confine the mass of glowing gas to a fairly uniform distribution except for a few millimeters from the walls, or less. The first two stages described above are shown in Figs. 267*A* and *B* for air at 100 and 20 mm pressure. The negative electrode called the cathode is clearly indicated by the letter *C*. If now we replaced the intermittent discharge of the induction coil by a steady d-c potential and by means of a surge gave enough added potential to the direct current to cause a spark between the electrodes, the spark would go over to a continuous and steady glow discharge whose further evolution with pressure may be studied. Fig. 267*C* shows the tube just as it begins to be filled with the uniform glow at about 5-mm pressure. At about 5 mm a definite electric blue glow will be seen on the cathode, *C*, separated by a slightly darker patch, *FDS*, between the cathode and the broad diffuse column that is quite luminous. The latter column, *P*, called the *positive* column, is the source of the luminosity in all the luminous discharge signs. The dark space designated by *FDS* was discovered by Michael Faraday and is called after him the Faraday or sometimes the second dark space. It fades out at lower pressures and becomes lost in the end of the *striated* positive column when the latter is observed. At still lower pressure more structure appears as seen at about 1 mm in Fig. 267*D*. At the cathode surface in air there appears an orange glow called the *cathode glow*, *CG*. Very near to it is a new dark space extending to 1 mm from the cathode called the *Crookes dark space* *CDS* by the English and the *Hittorf dark space* by the Germans. Then comes a whitish blue luminous cloud (in air) called the *negative glow*, *NG*, which lies between the Crookes, *CDS*, and *Faraday dark space* *FDS*. Beyond the Faraday dark space lies the positive column *P*. Right at the anode there is sometimes seen a reddish or orange glow, *AG*, called the *anode glow*. The positive column in air is a brilliant reddish purple which at lower pressures tends towards a salmon pink.

On further reduction of pressure the elements remain the same, except that the Crookes dark space extends outward in the measure

that pressure decreases. The negative glow grows in length and prominence, and the Faraday dark space dwindles in definition. At 0.1-mm pressure in air the structure mentioned is perhaps the most prominent, as shown in Fig. 267E. Under these conditions the Crookes dark space is about 1 cm wide. The negative glow is about

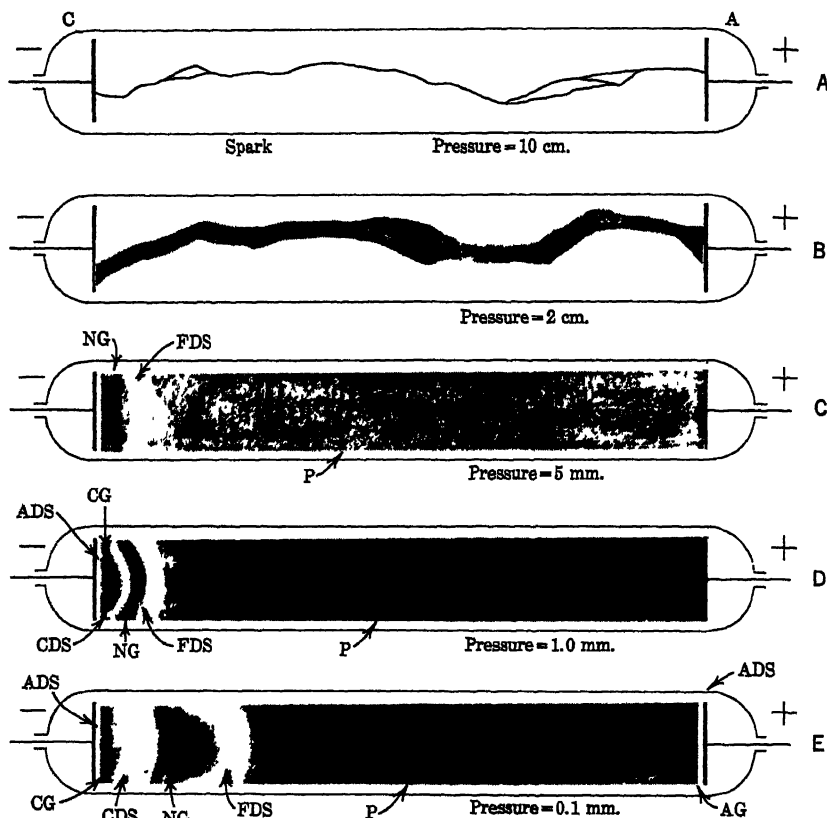


FIG. 267.

2 to 3 cm long. The cathode and anode glows are prominent, while the positive column is beginning to get fainter. At somewhat below this pressure the walls near the cathode and even near the anode begin to show a greenish fluorescence which is characteristic of X-ray tubes. Sometimes with the appearance of the fluorescence bluish streamers are seen to emanate from the cathode towards regions of fluorescence. The fluorescence is caused by the impact of fast electrons, cathode rays, on the walls. Intense ultraviolet light will cause some glasses such as Pyrex to glow.

Below these pressures, say 0.01 mm, the Crookes dark space nearly fills the tube. The cathode glow fades. The positive column is gone, and the negative glow at the anode end of the tube plus the brilliant fluorescence on the walls is all the luminosity observed. The faint bluish cathode-ray streamers can be seen if looked for with care. This is the X-ray emissive stage studied by Roentgen when he observed the first evidences of X-rays.

## 2. CERTAIN CHARACTERISTIC STRUCTURAL FEATURES OF THE GLOW DISCHARGE

In pure He, Ne, and the other inert gases at the right pressures a very fine and very dark space is observed between the cathode and the cathode glow. It has been called the *Aston dark space ADS* in honor of its discoverer. It probably occurs in all *pure gases* but is usually too fine to be observed as it would be 0.1 as thick in molecular gases as in inert gases.<sup>6</sup>

Under many conditions, but usually in mixed or impure gases and perhaps in some pure ones, between 0.01- and 1-mm pressure, the discharge in the positive column has a *beaded* appearance. This is known as the *striated* discharge, and the beads are known as *striations*. At 0.05 mm the discharge would appear as in Fig. 268*A* while at 0.5 mm the appearance would be as shown in Fig. 268*B*. In some cases the striations move down the tube. The moving striations, however, are different in mechanism and character from the fixed ones. They may occur in pure gases and are presumably due to electrical plasma oscillations. There need not always be a glow at the anode, and it may only partially cover the anode.

*The cathode glow at lower currents will not cover the whole cathode, but as the current increases it will cover the cathode. As long as the cathode is not covered by glow we find the potential across the tube constant as current increases. Once the glow covers the cathode, the further current increase requires increase in potential across the tube. This is an exceedingly important feature of the glow discharge. As long as the potential is constant the potential across the Crookes dark space is constant and we speak of the normal cathode fall of potential. Once the electrode is covered with glow we find that the added potential goes to increasing the fall of potential across the Crookes dark space and we speak of the abnormal cathode fall of potential. The cathode glow appears to be associated with positive ions, for we find that a perforated cathode will have the glow passing back through the perforations and showing somewhat the same color as that shown by the fast positive ions constituting the canal rays. This identity in color is not always observed.*

*The positive column is not a vital feature of the glow discharge, though for utilitarian purposes it is important. It really consists of a conducting and luminous path for the discharge from the end of the*



Faraday dark space to the anode. As the anode is brought nearer the cathode, the positive column merely shortens in length and *the potential to maintain the discharge falls by the amount of potential fall in the section of the column removed*. Thus the cathode can be brought so close to the anode that the positive column is virtually absent without altering conditions appreciably. If they are brought closer together the potential will have to be increased to maintain the discharge, since then the necessary operating mechanisms near the cathode are confined in so short a length that increased ionization by electron impact ( $\alpha$ ) and secondary emission at the cathode ( $\gamma$ ) are required, which can occur only at higher fields. Another factor that is essential to increase the prominence of the positive column is the confining action of the tube walls. If the discharge operates in a *large spherical enclosure, the positive column virtually disappears*. In this case the discharge and ionization diffuse over the whole volume, and the density of excited atoms becomes relatively low. It seems as if the Faraday dark space is spread over the whole distance from negative glow to the anode. It is probably because of the large area open to current flow that ionization and its accompanying excitation are relatively less dense. At the anode, however, if this is small the concentration of field and current produces an accentuated anode glow. It is sometimes said that the walls are necessary for a positive column. Perhaps this is in a measure correct, for the walls confine the discharge and as we shall see play an important part in the energy and electrical balance. Except for providing a source of loss of carriers and concentrating light emission it is doubtful whether they are essential.

One more word must be said concerning dark spaces, those of Aston, Crookes, and Faraday. Except for the Aston dark space, these are never really dark, and it is probable that even that of Aston is not dark. They represent regions of *relatively less excitation and ionization* than the regions of glow. There are ionization and excitation in both the Crookes and Faraday dark spaces. In the Aston dark space there may also be some excited ions and atoms, although excitation and ionization may not occur in that region. The negative glow may at times be quite sharply defined, and in mixed gases it may be observed that the light from gases of higher excitation potentials predominates at the cathode side.

From what has been said it must be clear that the character of the discharge as regards the intensities and dispositions of its dark spaces and glows must depend upon the character of the gas, the pressure, the current density, the nature of the cathode material, and the shape and dispositions of the container and electrodes. With adequate potentials and long narrow tubes the cathode and anode portions can be reduced to relatively limited regions, and the intensities and varied colors of the positive column may be used for various purposes. The greatest variety of colors can be produced in the columns, ranging

from the brilliant reds of neon, through the purples and salmon pinks of air, the grays of  $\text{CO}_2$  and  $\text{O}_2$ , to the blues of A and Hg and the golden yellow of Na. However, the colors of the A-Hg, Ne-Hg, Ne-Na, and Ne signs so often seen in advertising display are not all positive column colors. The wide variety of colors seen from the creams, yellows, greens, fluorescent blues, purples, and whites are all produced by appropriate absorption glasses.

### 3. POTENTIAL, FIELD STRENGTH, AND DENSITY DISTRIBUTIONS IN A CONVENTIONAL GLOW DISCHARGE

The principal visual phenomena having been described, it will next pay to study the electrical characteristics of the glow discharge. To

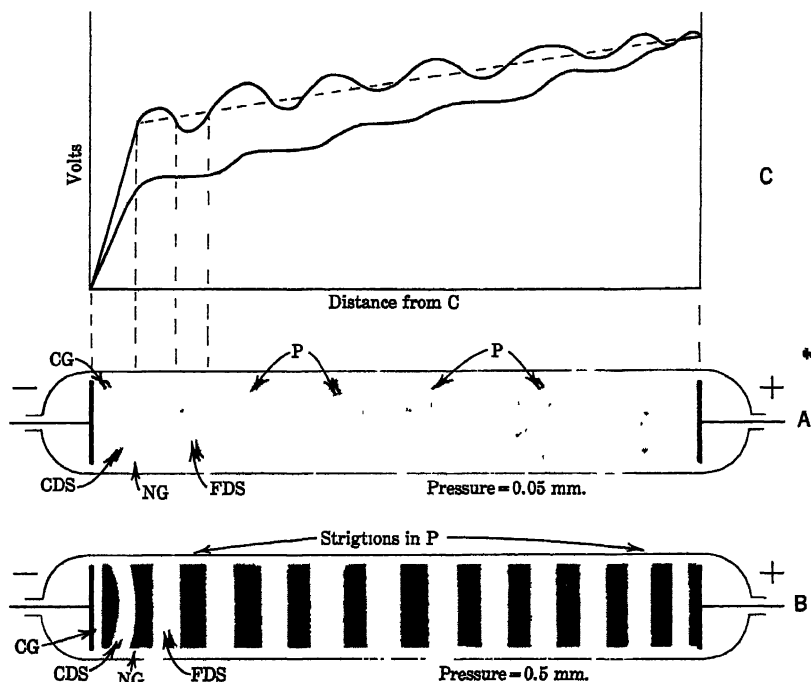


FIG. 268.

this end one might consider a tube such as mentioned in the introduction at some tenths of a millimeter of pressure, for instance with A. We may then correlate the intensities of light emitted, the potential distribution, the field strength, the net and the positive and negative space-charge densities at various points in the discharge. These are shown properly labeled for the unstriated discharge in Fig. 269 and for the striated discharge in Fig. 268C.

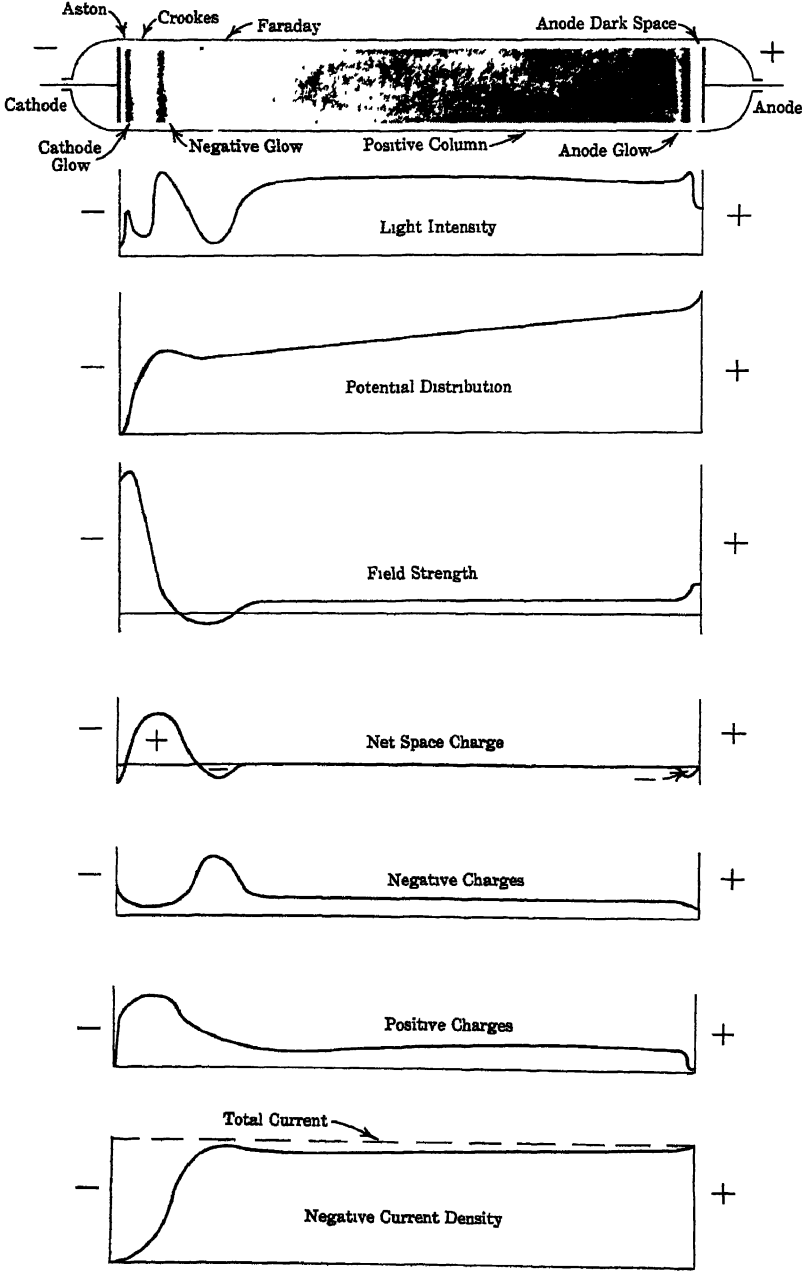


FIG. 269.

From these plots it is clearly seen that close to the cathode there is a small negative space charge due to low-velocity electrons of secondary origin at the cathode. This causes the potential to rise slowly at first well inside the Aston dark space, where that space occurs. Next to this there is a very heavy space charge of positive ions moving inward towards the cathode. These permeate the Crookes dark space and produce a powerful potential drop and hence a high field strength on the cathode side of the negative glow. As the negative glow is approached, more and more electrons appear and the positive-ion space charge diminishes. As a result the potential reaches a maximum or at least a plateau in the negative glow. It is possible that the electrons actually predominate slightly on the anode side of the negative glow, giving a small drop in potential. Thus the field gradient may be zero on the far side of the negative glow and in the Faraday dark space, or even slightly negative. Beyond this on the anode side of the Faraday dark space the potential again rises to take on a constant practically linear slope in the positive column. In this region the field strength increases somewhat sharply and thereafter remains constant. The electron and positive-ion densities in the column are practically equal. At the anode again there are a small decrease in electron density due to electron removal, and a sharper drop in the positive-ion densities due to the repulsive effect of the anode. Hence there is a slight increase in field strength in this region due to the net electronic charge. There is also a slight dark space next the anode at lower pressures representing a distance of about the last ionizing free path.

#### 4. MEASUREMENTS OF FIELD STRENGTHS

The field-strength measurements have been made in various discharges, in diverse ways, in a variety of gases, under different conditions. Some measurements have been made by means of the probe studies discussed in Chapter V.<sup>1,2,3</sup> Other studies have been made by means of the Stark-effect<sup>4</sup> broadening of spectral lines. While in general the values yielded by this method have not diverged too widely from those found by other methods, too much reliance cannot be placed on such results unless ion densities are less than  $10^{10}$  ions per  $\text{cm}^3$ . The most interesting method is that evolved by J. J. Thomson and used by Aston. In this, Aston<sup>4</sup> measured the transverse deflection of a fine pencil of fast cathode rays by the field of the glow discharge due to the field gradients as the cathode rays crossed the discharge tube. With the help of these methods we have a fairly good idea of field strengths and the potential distribution in the glow discharge.

## 5. GENERAL MECHANISM OF THE GLOW DISCHARGE

As a result of these data we are now in a position to discuss in qualitative outline the salient characteristics of the mechanism operating in the glow discharge. With this outline before us we then will be able in detail and in some points quantitatively to discuss in turn the various portions of the discharge. Since the discharge is a *steady-state self-sustaining discharge* we may at once apply the condition for a self-sustaining discharge  $(1 + 1/\gamma) = e^{\int_0^d \alpha dx}$ , discussed in the last chapter. For it is clear that there must be a mechanism present by which, in the active region of the discharge, the  $\gamma$  secondary electrons liberated per positive ion from the cathode must in ionization by collision in some essential distance  $d$  produce enough new electrons in the gas to maintain the discharge current at its constant value.

This condition at once indicates that the cathode region is the seat of vital activity and that there must be an important distance or length  $d$  from this in which the primary action takes place. It also indicates that we must at once consider not only the values of  $\alpha$ , but also the nature and values of the secondary electron-producing mechanism which is active and which was designated as  $\gamma$  in the equation above. The field distribution at once shows us that, close to the cathode, in the Crookes or cathode dark space, there is an exceptionally high electrical field which extends out to the edge of the negative glow and thus has a critical length of  $d$ . It is obviously this region in which the principal action occurs and to which the equation  $(1 + 1/\gamma) = e^{\int_0^d \alpha dx}$  must apply.

Now, from the potential gradients observed, as well as the relatively low pressures active, we can see that positive ions must strike the cathode surface with considerable energy. The values of the potentials in this space run from 50 to 400 volts across distances of 0.1 to 1 cm at pressures from 1 mm to 0.1 mm. This makes  $X$  of the order of 500 volts/cm and  $X/p$  from 500 on up. We can therefore be sure that the secondary mechanism will involve as an important feature, if not the prime feature, the liberation of electrons by positive-ion bombardment (see Chapter IX). This circumstance will be borne out by the fact that the current in this region is largely carried by positive ions. There is no doubt from what we have learned from Chapter X that the photoelectric action of the high-energy photons on the cathode will also furnish some secondary electrons. That the *photoelectric effect is small compared to positive-ion impact in secondary electron liberation* is indicated by the fact that the current and the other characteristics of the discharge are little altered if the cathode is an exceedingly fine wire gauze, instead of a solid plate. The use of the fine wire gauze, transmitting photons, reduces the photoelectric effect at the cathode to a small fraction while all the positive ions still

strike the wires. At the *lowest pressures* it is *possible* that the positive ions occasionally produce electrons by impact with gas molecules (see Chapter IX). However, the probability of this process is so small that it is not likely at low pressures to contribute much to secondary electron production. There is also the probability that in some gases metastables may lead to a secondary emission from the cathode. Here again the positive ions have the advantage because *they all strike the cathode* and are little removed by recombination, while metastables must *diffuse* to the cathode and can be destroyed by various agents before arrival.

The ingenious idea that the positive-ion space charge acting as a uniform ionic layer one free path long will give fields at the cathode of  $10^6$  volts/cm and *thus cause field current emission* instead of  $\gamma$  is *not to be taken seriously*. The mobility of the positive ions, the random distribution in space as they approach the surface, etc., make such a picture ridiculous, unless one wishes to dodge under the sophistry that the electrical image force of a positive ion at a molecular diameter is the origin of the field current. This action is made unlikely by the fact that  $\text{He}^+$  "pulls" electrons out of W while  $\text{Cs}^+$  does not, although the *image forces are the same* in both cases. The whole process by which positive ions liberate electrons at the cathode is a problem which should be open to wave-mechanical treatment and must so be solved. All theories such as local heating, photoeffect from neutralization, etc., are naïve. The ionic image force does, of course, affect the potential barrier and allow an electron to escape more easily. In addition the energy, kinetic and potential, of positive ions and the energy of neutralization are available to aid the process. That the character of the interaction is complex has been shown by Oliphant and Moon, and Arnot's dual accommodation coefficients for negative-ion formation indicate no simple interpretation as seen in Chapter IX.<sup>79</sup> There is thus little doubt but that the electron liberation by positive-ion bombardment liberates by all odds the greater proportion of the secondary electrons. We are thus justified in using the equation above with  $\gamma$  interpreted in its original sense.

Hence we can imagine the Crookes dark space as representing a region of positive space charge, due to positive ions created between the cathode *C* and the negative glow, as well as largely in the negative glow, from which the positive ions crash into the cathode with considerable energy. The studies of the energy balance at the cathode, as we shall later see, indicate in fact that the energy given to the cathode is practically equal to the positive-ion current multiplied by the potential drop across the Crookes dark space. While the mechanism of this transfer is somewhat complex, the fact that the energy is delivered to the cathode suggests that there should be ample secondary electron liberation as a result.

The secondary electrons emerge from the cathode on the whole,

with low energies. Hence before they achieve their velocities from the field they produce a *small* negative space-charge accumulation, which is never very large. In gases where the cathode fall of potential across the dark space is small, as in the inert gases, and when electrons gain energies over many free paths, it can happen that at low pressures the electrons can proceed for visible distances before they gain energy enough to excite the gas. This would account for the Aston dark space, for between the cathode and the distance to gain the exciting energy there will be no light emission. In gases such as  $N_2$  where the gain of energy is not so easy much higher values of the potential are needed and the dark space cannot be perceived by the eye.<sup>6</sup> A very pretty experiment of Holst and Oosterhuis<sup>8</sup> in Ne, under just the proper conditions, shows a series of dark and light spaces, the potential between the layers being close to 21.5 volts, the ionizing potential of Ne.

The cathode glow as a whole, however, cannot really be accounted for by ionization and excitation after the Aston dark space, although as Engel and Steenbeck<sup>9</sup> point out we would expect a maximum intensity of light emission right near but not at the cathode in the region where the electrons have just the exciting energy. As the electrons proceed beyond this point they gain energy and become more efficient at ionizing and less efficient at exciting. Thus one might expect the *maximum light emission from the excitation by secondary electrons to lie near the cathode*. It is probable that *the secondary electrons are too few at this point to give much light, and it is not until they begin to slow up again after ionizing cumulatively in the Crookes dark space* that we would expect the intense light emission seen in the negative glow. Furthermore, the spectra of light observed in the cathode glow do not bear out the theory of the first excitation by electrons, for the color and distribution are vastly different from those in the positive column or negative glow in most cases which are known to be produced by electron impact.

It is quite probable that the cathode glow results from things happening to the positive ions as they are being neutralized at the cathode. Little is known about the processes occurring at metal surfaces in the act of neutralization of positive ions and secondary emission. Oliphant has shown that the process results in a considerable neutralization to excited states at the cathode, including a copious formation of metastable atoms where these can form, as seen in Chapter IX.<sup>79</sup> It is thus safer to assume that the negative glow is due largely to what happens to positive ions at the cathode rather than what *excitation is produced by the few secondary electrons liberated*.

We see, therefore, that what happens in the Crookes dark space is a speeding up of the secondary electrons from the cathode to a point where  $P_1$  may be small, together with some cumulative ionization by collision by these in the region of declining field when  $P_1$  is large, while the newly created positive ions and the many from the negative glow

are being drawn to the cathode with nearly constant velocity. The constant velocity is due to a nearly uniform field in the dark space, as will be seen. Thus, in the Crookes dark space in the cathode fall of potential there must be *some* light emission, albeit relatively feeble compared to that in other parts of the discharge, both because of the high electron energies and the relatively few of these present. As the potential gradient in the positive charge of the dark space towards the negative glow becomes less, the electrons cease to gain energy and begin to lose energy in atomic or molecular collisions and eventually to ionization. Hence near the cathode edge of the negative glow these electrons reach velocities where they excite. Furthermore, the electrons produced by ionization by collision on the anode side of the Crookes dark space, which begin to be very numerous owing to the cumulative ionization, travel much shorter distances than  $d$  in the field and so both have smaller energies and ionize and excite very effectively.

Hence in what appear *visually as very short distances* we begin to get a marked increase in the visual intensity of the light. This forms the *cathode edge* of the negative glow. Photometrically the increase in intensity is much more gradual than that giving the visual impression, so that as we should expect from the wide range of electron energies the negative glow is really rather diffusely defined. Since many of the electrons exciting and ionizing in the negative glow have energies in the tens of volts, gathered in crossing the Crookes dark space (cathode fall of potential), it is not surprising to see that the spectrum of the negative glow contains many spark lines and represents higher states of excitation of the atoms and molecules present, especially at its cathode boundary—hence the bluish cast of the light which differentiates the negative glow from the positive column. Furthermore, the cathode side of the glow encounters the impacts of the faster electrons so that spectroscopically the lines of higher excitation and those due to gases of higher  $E_i$  in a mixed gas should be more prominent on that side of the glow. This is actually observed spectroscopically by placing the slit of the spectroscope parallel to the tube axis when viewing the discharge.<sup>10</sup>

As a result of the heavy and efficient ionization of the gas in the negative glow, the anode end contains many free and relatively slow electrons. This builds up a strong negative space charge which lowers the field. Since on the other hand many of the electrons ionizing in the region of the negative glow retain a good deal of their energy, these added to the slower electrons may even give a slight negative space-charge gradient. Beyond this point the impressed field produces a slight increase of potential, and in the Faraday dark space, which belongs to this region of increased gradient, the electrons on the anode end of the negative space charge again begin to gain energy. This they do over the whole Faraday dark space. As they regain the



ionizing and exciting energy they again cause light emission on the cathode end of the positive column. From here on, in the unstriated discharge, these new electrons move towards the anode in a fairly uniform potential gradient. This is such that the creation of new electrons and positive ions is nearly constant over the length of the column. Inasmuch as the gradient is weak but produces ionization and a maximum of excitation there is generally a production of more ions and electrons than needed to carry the discharge. Some very few ions and electrons in this fairly dense *plasma*, of  $10^7$  to  $10^{10}$  ions/cm<sup>3</sup>, recombine. Most of the excess electrons and ions, however, diffuse to the walls and there recombine. As a matter of fact, the electrons in the column have average energies of 1 to 10 volts. Under these conditions they diffuse very rapidly and give the tube walls a negative charge relative to the plasma. The wall potential of some 1–4 volts then draws positive ions to the walls (ambipolar diffusion), and these on reaching the walls neutralize the electron charge fairly readily. Thus the walls play an important part in preventing electron diffusion and dispersion and in removing excess charge production along the column.

The very large spread of electron energies produced by the statistical fluctuations of exciting and ionizing impacts in the negative glow results in a considerably greater diffusion of the anode end of the negative glow and the cathode end of the positive column. Hence the light emission at the two borders of the Faraday dark space changes much more gradually, making this dark space far less clearly defined at lower pressures than the Crookes dark space. In the latter the initial secondary electrons and their progeny emanating from the cathode have very much more uniformly distributed energies, leading to a fairly sharply defined cathode edge of the negative glow.

It might be expected that, in the center of the negative space charge in the negative glow, where the electron energies are low, there would be a considerable recombination of electrons and positive ions. Thus it was believed that the spectrum of the negative glow would show a considerable intensity of the *continuous recombination spectrum*. Owing to the fact that the electrons in this region have less energy than those in the positive column, recombination should be larger in the glow. This is so, but *in no case does the recombination spectrum predominate over the line emission*. At high ion or electron densities of the order of  $10^{10}$  per cm<sup>3</sup> one can expect definite indications of a recombination spectrum. Thus even in the negative glow the ion loss is largely by diffusion to the walls and recombination at the walls.

At the anode there will be a fairly high electron energy in the plasma of the positive column. The positive ions are being forced away from the anode, and thus in the absence of the positive ions the electron space charge will produce a slight but sharp rise in potential in going towards the anode. The reason why the electrons do not all

fall into the anode at once is that they have a high average energy, and diffusion reduces the velocity of drift in the field. In the last free paths towards the anode the electrons in the enhanced field may gain enough energy to excite more freely than in the positive column and so may cause the excitation of the anode glow.

It was observed in very pure Ne by Holst and Oosterhuis<sup>8</sup> that under some conditions at lower pressures a succession of dark spaces of the Aston type could be observed, followed by glows which were very sharply delineated. Probe measurements showed that the length of the dark spaces corresponded to a potential drop of just 21.5 volts in each case, which is the ionization potential. It was then believed that in analogy the striated discharge is merely a repetition of the Faraday dark space, or an analogous region, over which electrons gain the ionizing potential, preceded by regions of intense ionization and excitation. Hence, owing to uniformity in starting from the cathode and the sharpness of the Crookes dark space, the alternation of dark spaces and glows continued up to the anode. If this is true, then the more conditions lead to a uniform procedure, with less diffusive actions operative, the more clearly stratified the discharge. Now low pressures aid diffusion and increase the relative spread of electron energies. Metastable atoms also move quite independently of any field regions and by their ionizing or exciting action can act to diffuse the glow and make space-charge distributions more uniform. If these are removed by impurities the striations should appear. *Pure gases should show no striations.* This appears to be true.<sup>11</sup> On this basis Compton, Turner, and McCurdy<sup>2</sup> ascribe to metastable atoms the destruction of striations in the pure inert gases. It appears that the *pure* inert gases show no striations, whereas *other gases sometimes show them*.<sup>11</sup> Air will sometimes show them and sometimes not. They are always more sharply defined and regular at higher pressures. It is the belief of Compton, Turner, and McCurdy that, where impurities, destroying metastables, are present, the striations can appear. Thus they found that pure Hg gave no striations but H<sub>2</sub> mixed with Hg did. On the other hand, He up to 10<sup>8</sup> times the concentrations of H<sub>2</sub> in Hg gave no striations. In the luminous portions with H<sub>2</sub>, atomic H was observed, which obviously was produced by metastable Hg but proves nothing. However, as striations do or do not appear in mixed gases like air the explanation appropriate for Compton, Turner, and McCurdy's case<sup>2,12</sup> is not universally applicable. It is the author's opinion that, though the striations, as indicated by probe measurements, are in a sense recapitulations of negative glow and Faraday dark space produced by some regularity, the mechanism of their appearance and absence is completely obscure. He is of the opinion that conditions at the tube walls may be of some importance. The striations so far discussed, however, are *only the stationary striations*. The moving striations present another problem entirely and appear to be associated with the so-called plasma oscilla-

tions. It is not impossible that the appearance of fixed striations themselves is caused by nodes and loops set up by invisible plasma oscillations.

## 6. THE CROOKES DARK SPACE AND THE CATHODE FALL OF POTENTIAL

It is clear from what was said above that the crux of the mechanism of the glow discharge lies in the Crookes dark space. It was seen that  $\gamma$  and  $\alpha$  which act to maintain the discharge are determined by the field strength  $X$  in this region. It was also seen that this field strength depends largely on the potential drop across the region, and that this drop was characteristic of electrode and gas. It was also observed that the potential across the tube and hence across the dark space appeared to be constant as long as one was in the region of the "normal cathode fall of potential" and the glow did not cover the whole cathode. Once the cathode is covered by the glow, the potential rises with increasing current, and this rise is mainly in the cathode fall. We will first confine ourselves to the normal cathode-fall conditions, and as the theory is deduced we will understand the reasons for the normal and abnormal falls and their interrelation.

Now if we disregard fine structure, such as the Aston dark space and the small cathode electron space charge, we will find some striking general relations of an approximate but significant sort. The cathode fall of potential is caused by the space charge of positive ions largely produced beyond the apparently sharply defined cathode seam of the negative glow. At or near this point the electronic space charge begins effectively to annihilate the positive space charge so that the field is nearly zero. Observations have shown that the *visual width* of the Crookes dark space is quite definite and characteristic of the combination of gas and cathode material. The width  $d$  of this dark space varies inversely as the gas density<sup>13</sup> and hence as the gaseous pressure, i.e.,  $pd = c$ , or  $pd = k$  if temperature is constant.  $d$  appears, despite the illusory character of the sharpness of the transition, to be closely the same as the width of the region of the sharp fall in potential as revealed by probe and other studies. It is clear that this distance represents the number of electronic free paths required to permit the secondary electrons from the cathode to produce enough electrons by ionization to maintain discharge.

This distance  $d$ , even though the visual edge of the glow used to measure it is not physically very significant, thus represents a most important parameter in the operation of the glow. We shall use it in quantitative study later. The reason why a knowledge of the *exact value of  $d$*  is not too important is that the anode end marks a point in a slightly ill-defined region of *low field strength*. In view of the rather indefinite character of the edge of the dark space, and the small differences in the measurements of the potential fall, various workers have

defined the length of  $d$  and the corresponding potential fall differently. Stark,<sup>15</sup> Gelhof,<sup>16</sup> and Rottgardt<sup>17</sup> use the cathode edge of the negative glow. But probe measurements here are not accurate. Skinner<sup>19</sup> extends it to the potential minimum in the glow, as does Holm.<sup>20</sup> Warburg<sup>21</sup> used the edge of the negative glow next the Faraday dark space. This was also used by Schaufelberger.<sup>18</sup> Güntherschulze,<sup>22</sup> proposed defining the potential fall in terms of the minimum potential found as anode approaches the cathode in a tube with mobile electrodes. The cathode edge of the glow, however, is good enough. The diversity of definitions leads to varied values of the cathode fall  $V_c$ . For purposes of calculation, extrapolation of the field strength to zero field, as we shall see, probably gives suitable values. A series of values taken from Steenbeck<sup>23</sup> give  $d$  at 1-mm pressure, or  $K$ , for various combinations of electrodes and gases, as in Table XXXVI.

TABLE XXXVI

$K$ , LENGTH IN MILLIMETERS OF THE NORMAL CATHODE DARK SPACE  $d$  AT 1-MM PRESSURE

| Material | Air   | O <sub>2</sub> | N <sub>2</sub> | H <sub>2</sub> | He    | Ne    | A     | Hg   |
|----------|-------|----------------|----------------|----------------|-------|-------|-------|------|
| Cu       | 0.23  | .....          | .....          | 0.8            | ..... | ..... | ..... | 0.6  |
| Mg       | ..... | 0.25           | 0.35           | 0.61           | 1.45  | ..... | ..... |      |
| Zn       | ..... | .....          | .....          | 0.8            |       |       |       |      |
| Hg       | ..... | .....          | .....          | 0.9            |       |       |       |      |
| Al       | 0.25  | 0.24           | 0.31           | 0.72           | 1.32  | 0.64  | 0.29  | 0.33 |
| C        | ..... | .....          | .....          | 0.9            | ..... | ..... | ..... | 0.69 |
| Fe       | 0.52  | 0.31           | 0.42           | 0.9            | 1.30  | 0.72  | 0.33  | 0.34 |
| Ni       | ..... | .....          | .....          | 0.9            | ..... | ..... | ..... | 0.4  |
| Pt       | ..... | .....          | .....          | 1.0            |       |       |       |      |

The value of  $d$  as measured for the normal cathode fall, expressed as the number of *molecular free paths*, for Al and Fe cathodes in different gases, is shown in Table XXXVII.

TABLE XXXVII

|                       | He   | Ne   | A     | H <sub>2</sub> | N <sub>2</sub> | O <sub>2</sub> |
|-----------------------|------|------|-------|----------------|----------------|----------------|
| $\lambda \times 10^5$ | 1.8  | 1.26 | 0.635 | 1.12           | 0.519          | 0.647          |
| $N_{Al}$              | 96.5 | 66.3 | 59.1  | 85.3           | 77.5           | 48.3           |
| $N_{Fe}$              | 121  | 75.5 | 73.9  | 107            | 107            | 63.2           |

It is worth noting that  $d$  in a gas depends on the mean free path of the gas for electrons, or perhaps more probably on the free path for ionization by collision. It is largest in He and next in H<sub>2</sub> while N<sub>2</sub> and A do

not differ much. It is low in  $O_2$  because of the very inelastic impacts of electrons in  $O_2$ . It is also probable that the mobility of the positive ions may exert some influence, as this determines the space-charge density. As regards cathode material, it is clear that the lower the work function, and thus the larger  $\gamma$ , the shorter will be  $d$ . The influence, however, is not very pronounced. It must also be realized that the lower  $V_c$  the cathode fall the longer will be  $d$ , since low  $V_c$  makes  $\alpha$  low. This is nicely shown in terms of the number of molecular mean free paths in the gases for the Al electrodes. For the Fe electrodes the rule does not seem to hold. It is possible that the agreement shown is purely fortuitous, as the electronic and ionizing mean free paths are not necessarily related at all to the molecular free paths at these velocities.

Measurements have further revealed that the fall of potential across  $d$  is characteristic for each electrode and cathode combination. In other words, in order that the glow shall be self-maintaining there is a critical potential, the normal cathode fall  $V_c$ , which is required by any combination of gas and cathode materials in order that in the distance  $d$  the condition  $(1 + 1/\gamma) = e^{\int_0^d \alpha dx}$  shall be fulfilled. This fall of potential is independent of pressure, and sample values taken from a table given by v. Engel and Steenbeck<sup>24, 25, 26</sup> are shown in Table XXXIX. These values are largely illustrative. They are in most cases measured to the edge of the negative glow, except values marked with a question mark, where the measurement goes to the anode side of the negative glow. A more complete table of values using other criteria as to the cathode fall (see page 575) is given by Bär.<sup>23</sup> From what has been said about  $\alpha$  and  $\gamma$ , in Chapters VIII and IX, it is hardly necessary to remind the reader that one cannot place too much significance as constants on the values from such measurements. Gaseous purity and the cathode condition make the results hard to reproduce accurately in any case, and in addition  $\gamma$  may change with time in the discharge. Various measurements in the literature are also bound to vary, depending on the choice of the length of the cathode drop, as shown on page 575. The choice of the edge of the cathode glow is perhaps not so good as somewhat within the glow, since the positive space charge is hardly reduced to zero at the edge. The cathode drop, however, cannot extend as far as the anode side of the negative glow. Table XXXVIII, taken from Bär,<sup>23</sup>

TABLE XXXVIII

RELATION BETWEEN CATHODE DROP  $V_0$  AND WORK FUNCTION  $\phi$ 

|        | Mg  | Al  | Be  | Ni    | Zn  | Cu  | Pt  | Ag  | Fe  |
|--------|-----|-----|-----|-------|-----|-----|-----|-----|-----|
| $V_0$  | 247 | 302 | 339 | 353   | 372 | 375 | 425 | 428 | 363 |
| $\phi$ | 2.7 | 3.0 | 3.7 | ..... | 3.4 | 4.0 | 4.4 | 4.1 | 3.7 |

indicates the relation of cathode work function to the normal cathode fall in a single gas; it shows that there is some parallelism between the two, as one might expect.

TABLE XXXIX  
NORMAL CATHODE FALL IN VOLTS

| Cathode Material | Air   | O <sub>2</sub> | N <sub>2</sub> | H <sub>2</sub> | He    | Ne    | A     | Hg   | Cl <sub>2</sub> |
|------------------|-------|----------------|----------------|----------------|-------|-------|-------|------|-----------------|
| Na .....         | 200   | .....          | 178?           | 185?           | 80?   | 75    |       |      |                 |
| K.....           | 180   | .....          | 170?           | 94             | 59    | 68    | 64    |      |                 |
| Cu.....          | 370   | .....          | 208            | 214            | 177?  | 220   | 130   | 447  |                 |
| Ag.....          | 280   | .....          | 233            | 216            | 162   | 150   | 130   | 318  |                 |
| Mg.....          | 224   | 310?           | 188            | 153            | 125   | 94?   | 119   |      |                 |
| Ca.....          | ..... | .....          | 157            | .....          | 86    | 86    | 93    |      |                 |
| Ba.....          | ..... | .....          | 157            | .....          | 86    | ..... | 93    |      |                 |
| Zn.....          | 277   | 354            | 216            | 184            | 143   | ..... | 119   |      |                 |
| Hg.....          | ..... | .....          | 226            | 337            | 143   | ..... |       | 340  |                 |
| Al.....          | 229   | 311?           | 180            | 170            | 140?  | 120   | 100   | 245  | 280?            |
| C.....           | ..... | .....          | .....          | 280            | ..... | ..... |       | 475  |                 |
| Sn.....          | 266   | .....          | 216            | 226            | ..... | ..... | 124   |      |                 |
| W.....           | ..... | .....          | .....          | .....          | ..... | 125   | ..... | 305  |                 |
| Fe.....          | 269   | 290            | 215            | 250            | 150   | 150   | 165   | 298  |                 |
| Ni.....          | 226   | .....          | 197            | 211            | 158   | 140   | 131   | 275  |                 |
| Pt.....          | 277   | 364?           | 216            | 276            | 165?  | 152?  | 131   | 340? | 275?            |

It is seen that, the lower the work function, or the higher  $\gamma$ , the lower  $V_c$ . Again, as might be expected,  $V_c$  is lower for the inert gases, and for the gases He, Ne, and A, despite their higher ionizing potentials. That the higher-atomic-weight atoms such as Hg with low  $E_i$  should have higher values of  $V_c$  than Ne or A is perhaps to be ascribed to the higher values of  $\gamma$  which one can expect from the less massive positive ions, having higher velocities. It may also depend on the low values of  $E_i$  for Hg. Thus the lowest cathode falls can be expected in the gases He, Ne, and A with alkali atom cathodes. Güntherschulze<sup>27</sup> tried the variation of  $V_c$  as a function of the percentage of gas in binary mixtures. Results for Hg and A and Hg and H<sub>2</sub> mixtures are shown in Fig. 270. Complicated results were found in many cases. Hg and A follow a simple law; Hg and H<sub>2</sub> follow a complex curve. He and Ne produced a lowering of  $V_c$  with 32 per cent Ne. In the case of Hg and O<sub>2</sub>, the smallest traces of O<sub>2</sub> rapidly increased  $V_c$  to a value higher than for pure Hg or pure O<sub>2</sub>. At 70 per cent O<sub>2</sub> the curve fell sharply to the

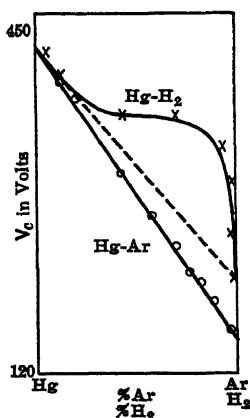


FIG. 270.

normal value for  $O_2$  at 100 per cent  $O_2$ . What such results indicate is not clear. The value of  $V_c$  depends on both  $\gamma$  and  $\alpha$ , so that until more data on these are available speculation is futile.

Table XL for normal current density,  $j$ , divided by pressure squared in  $10^{-6}$  amp/cm<sup>2</sup>  $\times$  mm<sup>2</sup>, as given by Engel and Steenbeck,<sup>24</sup> completes the data on the normal cathode fall.

TABLE XL

NORMAL CURRENT DENSITY,  $j$ , DIVIDED BY PRESSURE SQUARED,  $p^2$ , IN  $10^{-6}$  AMPERE/CENTIMETER<sup>2</sup>  $\times$  MILLIMETER<sup>2</sup> AT ROOM TEMPERATURE

| Material | Air   | O <sub>2</sub> | N <sub>2</sub>         | H <sub>2</sub> | He    | Ne    | A     | Hg    |
|----------|-------|----------------|------------------------|----------------|-------|-------|-------|-------|
| Cu       | 240   | .....          | .....                  | 64             | ..... | ..... | ..... | 15    |
| Mg       | ..... | .....          | .....                  | .....          | 3     | 5     | 20    | ..... |
| Zn       | ..... | .....          | .....                  | 80             | ..... | ..... | ..... | ..... |
| Al       | 330   | .....          | .....                  | 90             | ..... | ..... | ..... | 4     |
| Fe       | ..... | .....          | 400                    | 72             | 2.2   | 6     | 160   | 8     |
| Ni       | ..... | .....          | About the same as iron | .....          | ..... | ..... | ..... | ..... |
| Pt       | ..... | 550            | 380                    | 90             | 5     | 18    | 150   | ..... |

Aston,<sup>4</sup> using the method of the cathode-ray exploratory beam, has measured the strength of the field in the Crookes dark space, and he finds it to decrease linearly from the cathode to the edge of the negative glow as shown in Fig. 271. There are some doubts about the accuracy of this measurement, for it is certain that the transition at the negative glow should be more gradual. Close to the cathode again the negative space charge must cause a rounding off and perhaps a small decrease. However, these changes are small and extend over very limited regions compared

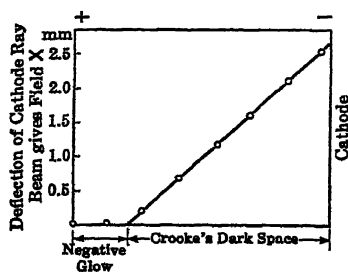


FIG. 271.

to  $d$ . The greatest deviation occurs at the distance  $d$  from the cathode. As the field is weak here, the contribution by ionization by collision is small in calculations, so that the error made by assuming a linear decline in the field is negligible. In fact, most observers with widely differing methods agree to a general linear decline of the field strength in the cathode dark space.

What this assumption means physically can be seen at once. For convenience choose the origin at the cathode. Let us measure distances  $x$  towards the anode up to the point  $d$  which represents the end of the cathode fall. One may at once write that the potential  $V$  at the earthed cathode is 0, and that at the negative glow, where  $x = d$ , it has

the characteristic value  $V_c$  of the cathode fall. Aston's measurements have shown that very near the cathode the field strength has a value  $X_c$  and that this value falls linearly, virtually, to 0 at  $x = d$ . This can be expressed by writing that  $X = C(d - x)$ , where  $C$  is a constant to be evaluated. Now the potential  $V$  at any point  $x$  is given by

$$V = \int_0^x dV = \int_0^x X dx = C \int_0^x (d - x) dx.$$

Thus  $V = C(xd - x^2/2)$ . Since  $V = V_c$  at  $x = d$ ,

$$V_c = C \frac{d^2}{2}, \text{ so that } C = \frac{2V_c}{d^2} \text{ and } V = V_c \left( \frac{2x}{d} - \frac{x^2}{d^2} \right),$$

which rises from 0 at  $x = 0$  to a vertex  $V_c$  at  $x = d$ . The evaluation of  $C$  permits us at once to write

$$X = C(d - x) = \frac{2V_c}{d^2} (d - x).$$

If we designate by  $X_c$  the field at the cathode,  $x = 0$ , then  $X_c = 2V_c d/d^2 = 2V_c/d$ , or  $V_c = X_c d/2$ . We can thus write

$$X = X_c \frac{(d - x)}{d}.$$

Finally the equation of Poisson says that

$$\frac{dX}{dx} = \frac{d^2 V}{dx^2} = 4\pi\rho = \frac{X_c}{d} = \frac{2V_c}{d^2} = \text{constant}.$$

Hence this leads one to conclude that the density of space charge  $\rho$  is constant in the dark space and is given in value by  $\rho = V_c/2\pi d^2 = X_c/4\pi d = \text{constant}$ . The physical implications of this constancy are not clear. It is obvious that positive ions are being created in a small but increasing measure from the cathode towards  $d$  by the  $\gamma$  secondary electrons per incident positive ion. This number is in general relatively small until the cumulative ionization in the last ionizing paths before the negative glow both change  $dV/dx$  and produce the large mass of ions. Thus, since the positive ions start in a great measure within a distance perhaps  $0.1 d$  to  $0.2 d$  in length, their velocity in the cathode field and their number are relatively constant, making  $\rho$  constant. If, however, there is much ionization in the dark space, then J. J. Thomson shows that Aston's law requires the rate of ionization to be constant throughout the dark space. If this is correct it can be shown that the current  $i$  is related to  $d$  and to  $V$  by the relation,

$$V^{3/4} = \pi^2 \sqrt{\frac{M}{2e}} i d^2,$$



which is like the ordinary space-charge equation but has different constants. Here  $e$  is the electron and  $M$  is the mass of the positive ions. There is again no physical reason why this should be so.

Probably, since Aston's law has been checked in but a few instances and holds only approximately, the regions where it has been tested are those where ionization in the dark space is negligible. It seems unlikely that the second criterion of Thomson required to fulfill Aston's law would apply exactly. It could apply approximately, since, while the  $\gamma(i/e)$  electrons from the cathode ionize cumulatively, as  $dV/dx$  decreases  $\alpha$  decreases, and *in part* of the region at least the decrease in  $\alpha$  is also exponential. Thus the rate of ion production could be more or less constant until the last free paths before the negative glow, where the deceleration of the electrons by impacts reduces their energy so that  $P_+$  becomes high and cumulative ionization results in a sharp edge to the negative glow. In fact, using an approximation to the exponential equation for  $\alpha/p$  as a  $f(X/p)$ , v. Engel and Steenbeck<sup>29</sup> show that the linear fall of potential is consistent with the existing equations for the phenomena and gives better than qualitative agreement with observation.

If one assumes the linear fall of potential in the dark space to hold even approximately, one can at once proceed to a very interesting analysis of the mechanism of the glow discharge. In what follows, the treatment given by v. Engel and Steenbeck<sup>30</sup> will be used even though, as will be seen, it has some defects and probably applies to a few cases only. The derivation originally was initiated by a paper by Compton and Morse<sup>31</sup> on the general condition for the normal cathode fall of potential based on a principle of maximum economy of operation. Later extensions permitting of a further development of the theory were due to Steenbeck<sup>32</sup> and to Rogowski.<sup>33</sup> Seeliger<sup>34</sup> had previously applied the criterion of a self-sustaining discharge enunciated by Holst and Oosterhuis<sup>35</sup> in connection with spark discharge. Finally, von Hippel<sup>36</sup> had brought all the elements of these various papers together, in order to see if from them one could not derive the laws of the glow discharge for the normal cathode fall. With the aid of Compton and Morse's<sup>31</sup> principle he formulated the expression for the form of the potential variation with distance,  $x$ , from the cathode, as the linear fall of potential was not then accepted. The law was exponential instead of parabolic, as here assumed from empirical data. On the basis of the resulting relations he was able to verify the theory by predicting the nature of the variation of the important parameters of the glow discharge in agreement with observation. The treatment of this problem as given by von Engel and Steenbeck<sup>30</sup> appears to be a solution of the problem of far greater simplicity and of sufficient accuracy which results from the assumption of the linear cathode fall. It will accordingly be given, following their outline of procedure.

One may begin the analysis by assuming from observation that the

field  $X_x$  at any point  $x$  distant from the cathode is given by the expression

$$X_x = X_c \left( 1 - \frac{x}{d} \right) \quad (1)$$

already deduced. It is next clear that the number of secondary electrons liberated from the cathode per positive-ion impact is at once given by the ratio,  $\gamma = j_0^-/j_0^+$ , of the electron current density  $j_0^-$  at the cathode, to  $j_0^+$ , that for the positive ions striking the cathode. The total current density  $j$  is then  $j = j_0^+ + j_0^-$ , and since  $j_0^-/j_0^+ = \gamma$  we have

$$j = j_0^+(1 + \gamma) \quad (2)$$

But  $j_0^+ = \rho_0^+ v_0^+$ , and, since  $\rho$  is constant,  $\rho_0^+$  can be computed from  $4\pi\rho = dX/dx$ , as seen on page 579. Hence  $\rho = (1/4\pi)(dX/dx)$ , and from equation 1,  $dX/dx = X_c/d$ , whence

$$\rho_0 = \frac{1}{4\pi} \frac{X_c}{d}. \quad (3)$$

Now the velocity of the positive ions is closely given by the expression  $v_0^+ = k_+ X_c$ , where  $k_+$  is the positive ion mobility. At very low pressures this is no longer true and one must use the equation of Compton for  $k_+$  at very low pressures or the values of Hershey for  $k_+$  at intermediate pressures. With this equation

$$j_0^+ = \frac{1}{4\pi} \frac{X_c}{d} k_+ X_c \quad \text{so that} \quad j = \frac{X_c^2 k_+}{4\pi d} (1 + \gamma). \quad (4)$$

Since the cathode fall of potential is  $V_c = \int_0^d X dx$ , the value of  $V_c = X_c d/2$ , so that equation 4 becomes

$$j = \frac{V_c^2 k_+ (1 + \gamma)}{\pi d^3}. \quad (5)$$

The Holst and Oosterhuis<sup>35</sup>-Seeliger<sup>34</sup> condition for a stable discharge can be written in its more exact form as

$$\left( 1 + \frac{1}{\gamma} \right) = e^{\int_0^d \alpha dx}, \quad (6)$$

if we assume that the secondary mechanism is largely electron liberation by positive-ion impact. At this point Steenbeck, von Hippel and practically all others assume the form of the function  $\alpha/p = f(X/p)$  to be that *empirical* expression of Townsend discussed at length on page 367. The equation reads

$$\frac{\alpha}{p} = A e^{-Bp/X}. \quad (7)$$

This equation, while it gives an S-shaped curve analogous to that observed for  $\alpha$ , is not only theoretically but also *physically wrong*, for all but a limited range of values of  $X/p$ . The difference between this equation and the experimental equations for  $\alpha/p = f(X/p)$  in  $N_2$  gas is shown in Fig. 183. The curve is too sharp. However, in the absence of more accurate equations, in the limited region of  $X/p$  here required, we can use this approximation as a purely empirical expression. It is convenient but only fortuitously useful for some gases.<sup>7a</sup> A more accurate equation of the empirical sort will give analogous results. As the work involved is too extensive for a place in this book the original assumption as to  $\alpha/p = f(X/p)$  of Townsend will be used. From equations 6 and 7 one thus has

$$\log \left( 1 + \frac{1}{\gamma} \right) = \int_0^d \alpha dx = A p \int_0^d e^{-\frac{B p}{X_e [1 - (x/d)]}} dx \quad (8)$$

Through substitution this equation becomes

$$\log \left( 1 + \frac{1}{\gamma} \right) = A B p^2 \frac{d}{X_e} \int_{y=0}^{y=\frac{X_e}{B p}} e^{-\frac{1}{y}} dy = A p d \frac{1}{\frac{X_e}{B p}} S \left( \frac{X_e}{B p} \right). \quad (9)$$

The integrals  $\int_0^x e^{-\frac{1}{y}} dy = S(x)$  can be found from tables. One may now replace  $X_e$  in equation 9 by setting  $X_e = 2 V_e/d$ , so that we have

$$\log \left( 1 + \frac{1}{\gamma} \right) = A (p d)^2 \frac{B}{2 V_e} S \left( \frac{2 V_e}{p d B} \right). \quad (10)$$

By solving equation 5,  $j = \frac{V_e^2 k_+}{\pi d^3} (1 + \gamma)$ , for  $d$ , and substituting in equation 10, one finds that

$$1 = \frac{(C_1 V_e)^{1/4}}{(C_2 j)^{1/4}} S [(C_1 V_e)(C_2 j)]^{1/4}. \quad (11)$$

Here

$$C_1 = \frac{2A}{B \log(1 + 1/\gamma)}. \quad (12)$$

and

$$C_2 = \frac{4\pi \log(1 + 1/\gamma)}{A B^2 (p k_+)(1 + \gamma)} \frac{1}{p^2}. \quad (13)$$

$C_1$  is a reciprocal potential, and  $C_2$  is a reciprocal current density. Thus we have a dimensionless characteristic equation for all gases and

cathodes. Using it, v. Engel and Steenbeck<sup>57</sup> calculate the relation between  $C_1 V_e$  and  $C_2(j/p^2)$  and obtain the curve shown in Fig. 272.

This diagram may be used as follows: Assume a large cathode surface  $f$  with a current  $i$ ; then  $j = i/f$ , where  $i$  is the current. Assume an Al cathode of 10 cm<sup>2</sup> area with  $i = 30$  milliamperes at 10-mm pressure in A. For this  $\gamma$  is by direct measurement  $1.2 \times 10^{-1}$  and  $k_+$  at 1-mm pressure is  $1 \times 10^3$  cm/sec per volt/cm or  $3 \times 10^5$  in cm/sec per esu/cm. For A,  $A$  is  $13.6 \text{ cm}^{-1} \times \text{mm}^{-1}$ ;  $B = 235$  volt/cm  $\times$  mm Hg or  $0.783$  esu/cm  $\times$  mm Hg;  $j = 3 \times 10^{-3}$  amp/cm<sup>2</sup> =  $9 \times 10^6$  esu/cm<sup>2</sup>. This gives  $C_2 j = 89$ . From the plot,  $C_1 V_e = 14.5$ . This gives

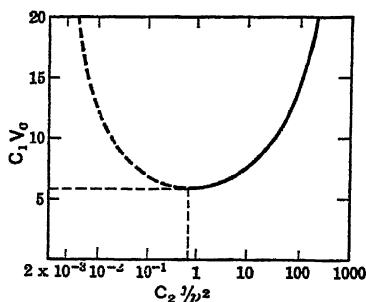


FIG. 272.

$$V_e = \frac{14.5}{2A} B \log \left( 1 + \frac{1}{\gamma} \right) = 0.93 \text{ esu} = 279 \text{ volts.}$$

Experimentally under these conditions the observed value is  $265 \pm 25$  volts, which is a good agreement.

This agreement is, in fact, exceptionally and probably fortuitously good, when one considers the approximation made in the value of  $\alpha$  and the linear cathode field.\*

One may now consider a more important aspect of the equation. If the current of 30 milliamperes is reduced, then  $C_1 V_e$  falls down the right-hand branch of the curve until  $C_2 j = 0.67$ , at which point  $i = 0.22$  milliampere. At this point  $C_1 V_e$  is 115 volts and is a minimum. According to the equation we would then expect the value of  $V_e$  to rise as  $j$  and  $i$  still further decrease, as indicated by the curve. However, this does not happen in practice since, by reducing the area  $f$ ,  $i$  can decrease, maintaining  $j$  constant at the minimum value. If it were possible to anchor the discharge over the whole surface  $f$  so that  $j$  decreased with  $i$ ,  $V_e$  would have to increase. Since we cannot anchor the discharge,  $i$  decreases and with it  $f$ , so that  $j$  remains constant, maintaining a constant  $V_e$  as indicated by the dashed line. Thus in the normal cathode fall  $V_e$  is constant and  $i$  increases proportionally to the area covered, keeping current density  $j$  constant up to the value of  $i$  at which the whole surface is covered with the glow. From then on, we reach the region of abnormal cathode fall of potential, with an ascending characteristic, and  $V_e$  increases.

\* In a very recent article Druyvesteyn<sup>78</sup> put this theory to an extensive experimental test in several gases. His results show that the assumptions made result in poor agreement except for a very limited range of data. This should not surprise one in view of the assumptions made.

At the other end of the curve,  $V_c$  does not remain constant as  $i$  decreases indefinitely; for, when the diameter of the cathode glow reaches values of the order of  $d$ , lateral diffusion of electrons, of which we have not taken account, alters the problem. Here  $V_c$  must be increased to make up for this loss, so that  $V_c$  rises as  $i$  decreases below this point.

The physical interpretation of this behavior is quite clear. In order that the space charge be maintained at such a value that  $j$  and  $\alpha$  have the values appropriate to a self-sustaining discharge at  $(1 + 1/\gamma) = e^{\int_0^d \alpha dx}$ , the current density  $j$  must not fall below a certain minimum value, as otherwise the space charge becomes too low. This is the value at the bottom of the curve. If the current density does fall below this value, then  $V_c$  and hence the potential across the discharge must be increased to increase both  $\alpha$  and  $\gamma$ . Since practically the discharge cannot be held over all the area  $f$  of the cathode, reduction of the current  $i$  decreases  $f$  rather than  $V_c$ .

The reason for the discharge not being held to the whole surface is simple. Any inequality in  $\gamma$  over different points in the surface gives a greater current to that point. This locally increases the space charge and hence the emission above the average value. Hence the current density locally increases, and if the density elsewhere remains constant  $i$  increases. If there is any resistance  $R$  in the circuit the increase of  $i$  lowers the potential by an amount  $iR$  so that the discharge goes out at the points of lower  $\gamma$  and concentrates so as to give a constant  $j$  and maintain  $V_c$  constant. If we start to *increase the current density*,  $j$ , beyond the minimum value of  $j$ , then the space-charge density increases. This disturbs the field strength and may change both  $V_c$  and  $d$ ; for  $\rho = V_c/(2\pi d^2)$ , or better we have

$$j = \frac{V_c^2 k_+ (1 + \gamma)}{\pi d^3}.$$

Hence an increase in  $j$  must mean either an increase in  $V_c$ , a decrease in  $d$ , or both. Now whether  $V_c$  increases or  $d$  decreases must depend on the condition for stability  $(1 + 1/\gamma) = e^{\int_0^d \alpha dx}$  and on the form of  $\alpha$  as a function of  $x$ . The functions assumed in this case result in *both an increase in  $V_c$  and a decrease in  $d$  over that in the normal fall to maintain the discharge*. Thus  $V_c$  rises again.

For the normal cathode fall the equations simplify somewhat so that

$$V_{cn} = 3.0 \frac{B}{A} \log \left( 1 + \frac{1}{\gamma} \right) \text{ volts,}$$

and

$$j_n = 5.92 \times 10^{-14} \frac{AB^2(k_+ p)(1 + \gamma)}{\log(1 + 1/\gamma)} p^2 \text{ amp/cm}^2,$$

when the values of  $A$  and  $B$  as well as  $k_+$  are in  $\text{cm}^{-1} \times \text{mm}^{-1}$ ,  $\text{volt/cm} \times \text{mm}$ , and  $k_+$  is in  $\text{cm/sec per volt/cm}$ . The value of  $d$  for the normal cathode fall is then

$$d_n = 0.82 \frac{\log(1 + 1/\gamma)}{A} \frac{1}{p}.$$

With these data we may leave the mechanism in the dark space and turn to the positive column.

## 7. THE POSITIVE COLUMN

As was stated in the introductory discussion, the positive column is not a vital element in the mechanism of the glow. It acts virtually like a continuous conducting gaseous element, of constant resistance per unit length, connecting the Faraday dark space to the anode. To this end it was pointed out that the fall of potential was linear in the column, which means that  $dV/dx = X_1$  is constant. As a consequence there can be no space charge of either sign predominating as one moves along the tube axis, so that positive and negative carrier *densities* are closely equal. The light emission and charge densities as measured are quite constant over the length of the column, indicating great uniformity in ionization and excitation. Both positive and negative carrier currents are constant in magnitude down the column, and thus as many electrons or positive ions enter one side of a transverse section of column as leave by the other. The section as a whole, therefore, gains or loses no charge by the current-induced flow of charges along the axis. Since the electrons have a higher velocity than the positive ions, the electron current is greater than the positive-ion current.

On the other hand, there is no uniformity among the electrons in the section. They have an energy distribution as a result of the action of the field superposed on their thermal energy. At *low current densities*, as stated in Chapter V, their energy distribution will *not* be Maxwellian. At higher current densities as usually observed, i.e., with densities of the order of  $10^8$  electrons per  $\text{cm}^3$ , in the small gradients in the column, the energy distribution is again nearly Maxwellian. The positive ions have a much lower energy than the electrons and, probably, also a Maxwellian energy, distribution whose average is somewhat higher than the ambient temperature of the space. As a result of their high energy, the electrons will diffuse in all directions. Since the uniformity of axial flow indicates that axial diffusion is compensated down the column, the only diffusive flow which one must consider is the radial flow towards the tube walls. It is clear that some electrons and ions will recombine in the gas space. However, below  $10^{10}$  ions/ $\text{cm}^3$  the loss from this action can be neglected.

On the other hand, the diffusive flow of electrons to the walls must be seriously considered as a possible source of loss of carriers, for the

following reasons. With their high energy or "temperature,"  $T_e$ , the electrons will diffuse rapidly in a radial direction and thus will accumulate on the walls. Unless the walls are quite conducting, however, there will be little flow of electrons through the glass or down the walls. Hence the electrons will diffuse to the walls, charging them up to a negative potential, which is just able to repel the faster electrons in the distribution. This at once sets up a positive radial potential gradient, outward from the axis of the tube to the walls. As a result the

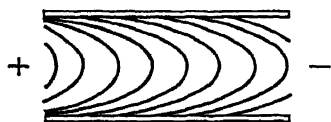


FIG. 273.

equipotential surfaces in the positive column, which in the absence of the wall potential would be planes normal to the axis of the column, become curved surfaces of revolution about the axis whose cross-section contours are indicated in Fig. 273. The field close to the wall

then has a very strong component normal to the wall compared to the externally imposed axial gradient.

As a result of this field, positive ions will be drawn to the wall and will there, by three-body impacts, quickly be neutralized. As a result of the field produced by the electron diffusion to the walls, and the consequent dragging in of positive ions, we have in a sense a *new type of diffusive action characteristic of plasma* which Seeliger<sup>38</sup> terms *ambipolar diffusion*. Thus, as a result of ambipolar diffusion and wall recombination, as well as by some little volume recombination, charges are being removed from the sections of positive column which must be replenished. They are replenished by ionization in the positive column, and the fields along the axis of the positive column must be high enough to replenish this loss and maintain the conducting state. It is seen that under these conditions interesting relations between axial potential gradients and other characteristics of the column must exist. The first one to work out these relationships was Schottky,<sup>39</sup> who developed a rough theory. This theory was later much developed by Tonks and Langmuir,<sup>40</sup> at lower pressures, and subsequently by R. Holm<sup>41</sup> and by Seeliger and Hirschert,<sup>42</sup> Seeliger,<sup>42</sup> and Druyvesteyn.<sup>44,45</sup> It is here presented in essence as developed by v. Engel and Steenbeck,<sup>46</sup> inasmuch as their presentation is condensed and especially clear.

For simplicity we will consider only pressures such that the electron free path  $\lambda$  is much smaller than the tube radius  $R$ . We will also consider that the loss of electrons and ions by diffusion is so nearly the same that we can assume that the concentrations of positive ions  $N_+$  and electrons  $N_-$  are essentially the same and equal to a value  $N$ . Under conditions of this sort we must consider what the ambipolar diffusion coefficient is, so that we may apply it where needed. Now the electrons in a sense *drag* the positive ions with them in their diffusion, in view of the fields produced. We can therefore write that the

average positive-ion velocity  $\bar{v}_+$  is equal to the average negative-ion velocity  $\bar{v}_-$  such that  $\bar{v}_+ = \bar{v}_- = v$ , the average velocity of the ions. Hence as in Chapter IV we can write

$$N_+ \bar{v}_+ = -D_+ \frac{dN_+}{dx} + N_+ k_+ X,$$

where  $X$  is the field acting and  $x$  is the direction of the concentration gradient causing diffusion. The above equation is merely the well-known diffusion equation of Chapter IV. For the negative ion we have

$$N_- \bar{v}_- = -D_- \frac{dN_-}{dx} - N_- k_- X.$$

Setting  $N_+ = N_- = N$ , and eliminating  $X$  from the two equations above, we can write

$$\bar{v} = \frac{D_+ k_- + D_- k_+}{k_+ + k_-} \frac{1}{N} \frac{dN}{dx}.$$

However, since we define

$$N \bar{v} = D_a \frac{dN}{dx},$$

for unit area, where  $D_a$  is the *ambipolar coefficient of diffusion*, we have at once

$$D_a = \frac{D_+ k_- + D_- k_+}{k_+ + k_-}.$$

Again, as seen in Chapter IV, we set  $k_+/D_+ = k_-/D_- = Ne/P = Ne/R_1 T = e/kT$ , where  $k = R_1/N$ , the Boltzmann constant. If one inserts this expression for  $k_-$  into  $D_a$ , and remembers that  $T_e = T_-$  for electrons is much greater than  $T_+$  and that  $k_e = k_- \gg k_+$ , one can write

$$D_a = D_+ \frac{T_e}{T_+} = D_- \frac{k_+}{k_e} = D_- \frac{k_+}{k_-}.$$

One may next consider a cylindrical zone  $dr$  thick, along the radial direction  $r$ , measured from the axis of a plasma confined in a tube of radius  $R$ . Into unit length of this radial shell an ambipolar diffusion of coefficient  $D_a$  is taking place towards the walls. At the distance  $r$  the number diffusing in unit time is

$$\left( \frac{dn}{dt} \right)_r = -2\pi r D_a \left( \frac{dN}{dr} \right)_r.$$

At the surface distant  $r + dr$ , the number diffusing outward is

$$\left( \frac{dn}{dt} \right)_{r+dr} = -2\pi(r + dr) D_a \left( \frac{dN}{dr} \right)_{r+dr}.$$



The net rate of loss of ions due to diffusion in this cylindrical volume  $dV$  is at once the difference of the two quantities, viz.:

$$d\nu = 2\pi r D_a \left( \frac{dN}{dr} \right)_r - 2\pi(r + dr) D_a \left( \frac{dN}{dr} \right)_{r+dr}.$$

Neglecting higher-order terms,

$$d\nu = 2\pi D_a \left[ r \frac{d^2 N}{dr^2} + \frac{dN}{dr} \right] dr,$$

analogous to the differential equation for the radial flow of heat in a cylinder. Let us call  $z$  the ionizing frequency, viz., the number of times per second that an electron in its random heat motion gets the ionizing energy and is able to ionize. Then, in order to maintain the conductivity of the column,  $d\nu$  must be equal to the rate of production of ions by collision of electrons. Hence  $d\nu = 2\pi r dr N z$ , where  $N$  is the number of electrons per cubic centimeter. This at once leads to the differential equation for the radial diffusion in the form

$$\frac{d^2 N}{dr^2} + \frac{1}{r} \frac{dN}{dr} + \frac{z}{D_a} N = 0.$$

If we set  $r = \sqrt{D_a/z} x$ , we find

$$\frac{d^2 N}{dx^2} + \frac{1}{x} \frac{dN}{dx} + N = 0,$$

which on integration yields a Bessel function  $J$  of the zero order  $J_0$ ,

$$N = N_0 J_0(x) = N_0 J_0 \left( r \sqrt{\frac{z}{D_a}} \right).$$

This is represented by the curve of Fig. 274 as a function of  $x$ . The number  $N_0$  is the concentration at the axis of the column, at  $r = 0$ .

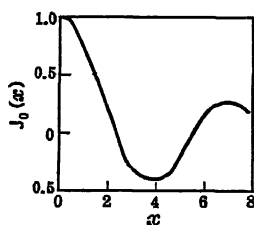


FIG. 274.

In view of the creation of ions in the operation and the establishment of the balance we can expect  $D_a$ ,  $z$ , and  $N_0$  to be functionally related, and will thus have to seek other relations to complete the picture. This is borne out by the fact that if they were independent then we would get meaningless negative values of  $N_0$  beyond a certain value of  $x$ . The largest possible value of  $x$  is thus limited at the point  $r = R$  to a numerical value 2.405, at which  $x$  takes on negative values. The concentration at the wall  $N_R$  must then take on such values that the diffusion from  $N_0$  at the axis, to  $N_R$  at the wall, carries away all ions newly created in the cylindrical section of the column of unit length. The gradient will be the greater

the smaller  $D_a$ , i.e., the higher the pressure, and at high pressures  $N_R/N_0$  can become indefinitely small. Thus at  $r = R$  the value of  $x$  must approach closely to  $x_R = 2.405$ , the first zero value of the Bessel function. This allows one to write approximately

$$x_R = \sqrt{\frac{z}{D_a}} R = 2.405.$$

If we put this relation into our expression for diffusion, we obtain the concentration of ions  $N_r$  at any distance  $r$  from the axis as

$$N_r = N_0 J_0 \left( 2.405 \frac{r}{R} \right).$$

We may now express  $D_a$  and  $z$  as functions of the "electron temperature." From this, and from the condition  $R\sqrt{z/D_a} = 2.405$ , we can evaluate the electron temperature, i.e., the average electron energy defined by assuming a Maxwellian energy distribution. In so doing we must be careful of the definition of electron temperature as used by different writers, which was pointed out by Druyvesteyn,<sup>45</sup> who has attempted to test the theory quantitatively. Tonks and Langmuir and thereafter American workers use as the electron temperature the definition  $eV = \frac{1}{2}m\alpha^2 = kT_e$ , where  $\alpha$  is the most probable velocity, in which 1 electron volt is equal to 11,600° K. Other workers use the more correct definition of electron temperature  $eV_0 = \frac{1}{2}mC^2 = \frac{3}{2}kT_e$ , where  $C$  is the root mean square velocity and  $k$  is the Boltzmann constant. Here we shall use the Langmuir and Tonks definition of temperature.

Now it was shown that for the ambipolar diffusion we can write, approximately,

$$D_a = \frac{D-k_+}{k_-} = \frac{k}{e} k_+ T_-,$$

where  $k$  is the Boltzmann constant and  $k_+$  is the positive ion mobility. As further shown on page 368, we can set  $z$  approximately equal to

$$z = \frac{600a}{e\sqrt{\pi}} m p \alpha^3 e^{-\frac{eV_i}{kT_e}} \left( \frac{1}{2} \frac{eV_i}{kT_e} \right),$$

when the energy of ionization  $eV_i$  is large compared to the probable electron energy.  $a$  is a constant of proportionality;  $m$  and  $e$  are the electronic mass and charge, and  $\alpha$  is the probable thermal velocity at  $T_e$ , to wit,  $\frac{1}{2}m\alpha^2 = kT_e$ . This at once allows us to combine the expressions for  $D_a$  and  $z$  as

$$\frac{1}{\sqrt{\frac{eV_i}{kT_e}}} e^{-\frac{eV_i}{kT_e}} = \frac{600\sqrt{2}\sqrt{e}}{(2.405)^2\sqrt{\pi}\sqrt{m}} \frac{a\sqrt{V_i}}{k_+p} p^2 R^2 = 1.16 \times 10^7 c^2 p^2 R^2.$$

In this equation  $R$  is in centimeters,  $p$  in millimeters of mercury,  $V_i$  is in volts, with  $k_+$  in cm/sec per volt/cm  $\times$  mm. The constant  $c$  is then given by  $c^2 = (a\sqrt{V_i})/(k_+p)$ , and is a gas-dependent characteristic evaluated for a few gases by v. Engel and Steenbeck in the table below.

| Gas | He                   | Ne                   | A                    | Hg                   | N <sub>2</sub>       | H <sub>2</sub>        |
|-----|----------------------|----------------------|----------------------|----------------------|----------------------|-----------------------|
| $c$ | $3.9 \times 10^{-3}$ | $5.9 \times 10^{-3}$ | $5.3 \times 10^{-2}$ | $1.1 \times 10^{-1}$ | $3.5 \times 10^{-2}$ | $1.35 \times 10^{-2}$ |

It is seen that  $V_i/T_e$  is a unique function of  $cpR$ . As a result one can plot a curve of  $T_e/V_i$  as a function of  $cpR$ , following v. Engel and Steenbeck, as shown in Fig. 275A.

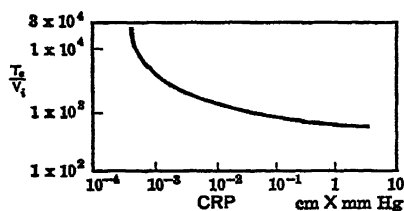


FIG. 275A.

From such a curve, given  $V_i$ , the ionizing potential,  $c$ ,  $p$ , and  $R$ , we can evaluate  $T_e$ . Thus, for instance, for  $R = 1$  cm with Ne at 1-mm pressure, we have  $cpR = 5.9 \times 10^{-3}$ , which gives  $T_e/V_i = 1.58 \times 10^3$ . From this the electron temperature  $T_e$  is  $34,000^\circ$  K. The agreement between observation and theory for Ne and A is remarkably satisfactory. These

conditions hold only as long as the current density is large enough so that  $D_e$  can be applied but not so high that the ionization takes place by much ionization in successive steps. The theory for  $z$  contains only the probabilities of ionization by single electron impacts.

If we wish to calculate the potential gradient, or field strength  $X_i$ , along the axis, needed to maintain the current against diffusion, we proceed as follows. If the electron on the average loses a fraction  $f$  of its energy in an impact with a molecule, the energy lost in an impact against gas molecules thought of as at rest (see page 200) is  $f(m/2)v^2$ , where  $v$  is the electron velocity. The number of impacts per cubic centimeter per second is given by

$$dz = \frac{v}{\lambda_e} dN_e = \frac{4N_e}{\sqrt{\pi}\lambda_e} \frac{v^3}{\alpha^3} e^{-\frac{v^2}{\alpha^2}} dv; \text{ see page 367.}$$

Whence the rate of energy transfer for electrons of velocity between  $v$  and  $v + dv$  per cubic centimeter per second is

$$d\left(\frac{dE}{dt}\right) = \frac{2mfN_e}{\sqrt{\pi}\lambda_e} \frac{v^5}{\alpha^3} e^{-\frac{v^2}{\alpha^2}} dv.$$

For electrons of all velocities in 1 cm<sup>3</sup> this yields, on integration,

$$\frac{dE}{dt} = \frac{2mfN_e\alpha^3}{\sqrt{\pi}\lambda_e}.$$

In a steady state the electrons must regain this energy from the field.

Hence we must write  $dE/dt = evX_i$ , if the electrons move a distance  $v$  in unit time in a field  $X_i$  with the charge  $e$ . From the simple basic mobility equation of page 178,

$$v = \frac{e}{m\alpha} \lambda_e X_i.$$

Inserting the value of  $v$  in the equation above, we find

$$\alpha = \sqrt[3]{\frac{\pi}{4}} \sqrt{\frac{e}{m}} \sqrt{X_i \lambda_e} \frac{1}{\sqrt[4]{f}}.$$

This also gives the electron velocity as

$$v = \frac{\sqrt[4]{2}}{\sqrt[3]{\pi}} \sqrt{\frac{e}{m}} \sqrt[4]{f} \sqrt{X_i \lambda} \text{ (see page 368),}$$

which is not seriously different from the Compton equation on page 186. The electron temperature defined by  $\frac{1}{2}m\alpha^2 = kT_e$  then is given by

$$T_e = \frac{\sqrt[4]{\pi}}{2\sqrt{2}} \frac{e}{k} \frac{X_i \lambda_e}{\sqrt[4]{f}}.$$

In all this work at the high charge densities we are justified in using the Maxwellian distribution law. This was not used before, since in Chapters IV and V, at low densities, the Maxwellian distribution must be replaced by that of Druyvesteyn. From the equation above, one may at once derive  $X_i$  from  $T_e$ , in the column, as

$$X_i = \frac{2\sqrt{2}}{\sqrt[4]{\pi}} \frac{\sqrt[4]{f} k T_e}{\lambda_e e} = 1.83 \times 10^{-4} \frac{\sqrt[4]{f}}{\lambda_e} T_e,$$

in volts per centimeter. This gives

$$\frac{X_i}{p} = 1.83 \times 10^{-4} \frac{\sqrt[4]{f}}{\lambda_e p} T_e \text{ volts/cm} \times \text{mm Hg}.$$

Since  $T_e$  is a function of  $Rp$ , one can at once write that  $X_i/p = f(Rp)$ . The value of the elasticity of impact, i.e., the fractional energy loss by collision,  $f$ , is not the simple quantity which was encountered in the previous work, for it involves energy loss to ionization and excitation as well. Up to 4 electron volts energy, v. Engel and Steenbeck recommend the values of  $f$  determined experimentally from the later electron velocity and electron energy measurements of Bailey<sup>47</sup> and of Brose and Sayman<sup>48</sup> using the Townsend methods on purified gases. At higher energies the inelastic excitation losses must be included. This is done in an approximate fashion by v. Engel and Steenbeck as

follows. Call  $Z$  the ratio of exciting to ionizing impacts. For Ne, data of Penning and Teves give the following values for  $Z$  as a  $f(X/p)$ :

TABLE XLI

| $X/p$ | 5  | 10 | 20  | 30  |
|-------|----|----|-----|-----|
| $Z$   | 30 | 9  | 2.7 | 1.5 |

If this is known, then we proceed as follows. If  $z$  ions are formed per second per electron, then the energy loss is  $ze(V_i + ZV_e)$ , where  $V_e$  is the energy of excitation. In this time the electron makes  $\bar{v}/\lambda_e$  impacts, where  $\bar{v}$  is the average energy of excitation. Hence it loses

$$\frac{ze(V_i + ZV_e)\lambda_e}{\bar{v}} \text{ per impact.}$$

Since its average energy is  $\frac{3}{2}kT_e$ , it loses the fraction

$$f_{in} = \frac{2ze(V_i + ZV_e)\lambda_e}{3\bar{v}kT_e} = 200p\lambda_e a(V_i + ZV_e) \frac{eV_i}{kT_e} e^{-\frac{eV_i}{kT_e}}.$$

The loss to elastic collisions is  $f_{el} = 2m/M \sim 1 \times 10^{-3} (1/M_1)$ , where  $M_1$  is the molecular weight. These must be added to  $f_{in}$ . Hence  $f = f_{in} + f_{el}$ , so that this must be used to calculate  $X_1/p$ . For the case where  $f_{in} \gg f_{el}$  we can include  $f_{in}$  in the equation for  $X_1/p$  and we obtain, on eliminating  $z$ , by substitution, setting  $z = (1/R^2)(T_e/p)$ ,

$$\frac{X_1}{p} \sim \frac{1}{R} \sqrt{\frac{T_e}{p}} \sqrt{V_i + ZV_e} \sqrt{\frac{1}{p}} \sqrt{\frac{1}{T_e^3}} T_e.$$

This makes  $X_1$  for constant  $Z$  at lower  $X/p$  vary as  $X_1 \sim (1/R) (T_e)^{3/4}$  and with  $T_e$  nearly constant this gives  $X_1 \sim 1/R$ . This was observed by Claude to be approximately true in a limited range in Ne. At lower  $Rp$  the value of  $X_1$  increases more rapidly than  $1/R$ , owing to the increase in  $T_e$ . At high pressures  $f_{el} \gg f_{in}$ , and therefore  $f$  is nearly constant, as well as  $T_e$ . Under these conditions  $X_1$  is merely proportional to  $p$ .

One must next calculate the concentration gradient  $N_R/N_0$ . In each second there pass through the cross section of the column, with a current  $i$ ,  $n = i/e$  electrons. Each electron produces in 1 cm  $z/v$ , electrons where  $v$  is the velocity of the electrons in the field direction. Thus across the whole cross section per second and per unit length there is created a total of  $\nu = (i/e)(z/v)$  new ion pairs. This must equal the number of ions that by diffusion reach the walls per unit length of column per second. If the concentration of ions is  $N$  and they move with

a mean thermal velocity  $\bar{v}$  the number striking 1 cm<sup>2</sup>/sec is by kinetic theory  $N\bar{v}/4$ . At the wall where  $r = R$ ,  $N = N_R$ , so that

$$\nu = \frac{N_R \bar{v}}{4} 2\pi R \text{ per cm length of wall per second.}$$

This at once gives

$$N_R = \frac{2zi}{eR\pi v\bar{v}}.$$

The value of  $\bar{v}$  is not clear, since actually it is the *average velocity of ions and electrons*. It must at once be calculable from the ambipolar diffusion coefficient by means of the simple kinetic-theory definition of the coefficient of diffusion  $D_a = (\frac{1}{3}) \bar{v}\lambda$ , where  $\lambda$  is the average mean free path of the *electrons and ions*. This also presents some difficulty, since these are not the same. Let us assume some average and eliminate  $\bar{v}$  from the equation for  $N_R$  in the form of

$$N_R = \frac{2zi\lambda}{3eD_a R\pi v}.$$

Again we may proceed to evaluate  $N_0$  as follows. The current  $i$  is equal to the integral of the drift velocity of the ions in the field, times the electron, times the integral of all the ion concentrations  $N_r$  in the volumes  $2\pi r dr \times 1$  at various distances  $r$  from the axis,  $r = 0$  to the wall at  $r = R$ . Thus

$$i = 2\pi e v \int_0^R N_r r dr = 2\pi e v N_0 \int_0^R J_0 \left( \sqrt{\frac{z}{D_a}} r \right) r dr.$$

Since  $\sqrt{z/D_a} = 2.4/R$ , we have

$$i = 2\pi e v N_0 \int_0^R r J_0 \left( \frac{2.4r}{R} \right) dr.$$

Calling  $x = 2.4 r/R$ , we have

$$i = \frac{2\pi e v N_0 R^2}{(2.4)^2} \int_{x=0}^{x=2.4} x J_0(x) dx.$$

The integral has the value 1.25, whence  $i = 1.36 e v N_0 R^2$ , and  $N_0 = i/(1.36 e v R^2)$ . This at once gives us  $N_R/N_0$  as

$$\frac{N_R}{N_0} = \frac{2zi\lambda \times 1.36 e v R^2}{3eD_a \pi R v i} = \frac{2.72 z \lambda R}{3\pi D_a}.$$

Since  $\sqrt{z/D_a} = (2.405/R)$ , we have at once  $N_R/N_0 = 1.66 \lambda/R$ . The indefinite value of  $\lambda$  is not very serious, since the value of  $\lambda_e$  and  $\lambda_i$  for

electrons and ions, does not on the average differ by more than a factor of 5.

The radial potential gradients can readily be solved for in the case of the ambipolar diffusion, since assuming a common drift velocity  $v$  and equality of ion and electron concentrations greatly simplifies the complicated equations of Chapter VII. As we have assumed  $N_+ = N_- = N$  and  $v_+ = v_- = v$ , the concentration gradients may also be assumed nearly equal  $dN_+/dx = dN_-/dx = dN/dx$ . We may then write the equations of page 587 as

$$N = -\frac{D_+}{N} \frac{dN}{dx} + k_+ X_z = -\frac{D_-}{N} \frac{dN}{dx} - k_- X_z.$$

Solving these equations for  $X$ , one has

$$X_z = \frac{1}{N} \frac{dN}{dx} \frac{D_+ - D_-}{k_+ + k_-}.$$

Since  $D_- \gg D_+$  and  $k_- \gg k_+$ , we can write

$$X_z = -\frac{1}{N} \frac{dN}{dx} \frac{D_-}{k_-}.$$

Therefore we can write

$$X_z dx = -\frac{k}{e} T_e \frac{dN}{N},$$

which on integration between points where the potential is  $V_1$  and  $V_2$  and concentrations are  $N_1$  and  $N_2$  at once yields

$$V_2 - V_1 = -\frac{k}{e} T_e \log \frac{N_2}{N_1}.$$

If  $V_2 = V_R$  and  $N_2 = N_R$  at the walls, while  $V_1 = V_0$  and  $N_1 = N_0$  at the axis, we have at once

$$V_R - V_0 = -\frac{kT_e}{e} \log \frac{N_R}{N_0} = -\frac{kT_e}{e} \log \left( 1.66 \frac{\lambda}{R} \right).$$

It is seen that, if  $V_R$  and  $V_0$  are known, we can, knowing  $T_e$ , evaluate  $\lambda$ , or better  $N_R/N_0$ . Thus although the equations hold only approximately, on the basis of the crude assumptions made, still the agreements within the limits of pressure, radius, and current densities allowed by the theory are quite satisfactory. Hence the mechanism of the positive column is fairly well understood.

It is perhaps worth while to note a few facts concerning the positive column which, though open to computation from the above data, are not at once obvious. v. Engel and Steenbeck give the normal potential gradient in the positive column for some gases as follows in terms of  $X_1/p$  in volts/cm  $\times$  mm:

TABLE XLII

| Gas   | O <sub>2</sub> | N <sub>2</sub> | H <sub>2</sub> | H <sub>2</sub> O | He     | Ne                   | A                    |
|-------|----------------|----------------|----------------|------------------|--------|----------------------|----------------------|
| $X/p$ | 13.1           | 8.25           | 2.23           | 50               | < 0.12 | < $2 \times 10^{-3}$ | < $2 \times 10^{-3}$ |

As orienting magnitudes one might give the following data from Bär<sup>51</sup>:

TABLE XLIII

| Gas                    | Hg   | He   | H <sub>2</sub> | N <sub>2</sub> |
|------------------------|------|------|----------------|----------------|
| Pressure (mm).....     | 9.2  | 8.0  | 8.0            | 8.0            |
| Diam. 2R (mm).....     | 24   | 25   | 15             | 15             |
| $i$ in ma.....         | 0.35 | 0.52 | 1.0            | 1.5            |
| $X_1$ in volts/cm..... | 14.8 | 22.7 | 117.0          | 156.8          |

The gradient is especially large for the halogens. These form stable negative ions, and electrons attach readily. Hence high values of  $X/p$  are needed to get enough ionization by impact before electrons attach. On the other hand, diffusion is much less and hence less ionization is needed in the column. In general,  $X_1/p$  decreases as  $Rp$  increases, and the curves are hyperbola-like and of the form of the curve in Fig. 275B taken from v. Engel and Steenbeck. As  $i$  increases, the values of  $X_1/p$  decrease.

The energy radiated in light by the positive column is small, compared to the total energy consumed by the current. It obviously varies with  $X/p$ , for it depends on electron energy.

Ångström years ago measured the energy radiated with a bolometer and estimated that for N<sub>2</sub> the fraction of energy radiated was in the neighborhood of 7.4 per cent. The greater proportion of energy expenditure, however, is *not* in the column. Measurements of heating in the column are difficult. From the power expenditure per centimeter length of column, i.e., from  $Xi$ , the energy consumed in ionization, excitation, and heating can be estimated. The energy expended in creating ions is largely liberated as heat *at the walls*, while the *frictional* loss of the positive-ion current, and of electrons in elastic impacts, goes to raising the temperature of the gas.<sup>70</sup> The energy of the electrons spent in inelastic impacts of excitation, that do not lead to ionization in successive impacts, largely go to external radiation or to heat. In the molecular gases the chance for degradation of such energy to heat is greater than in the

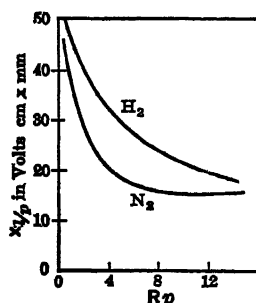


FIG. 275B.



atomic gases. The heat liberation at the walls may well exceed that in the gas.<sup>71</sup>

Rather discordant estimates of temperature increase in the gas of the column exist. Wood<sup>53</sup> found in  $N_2$  from 0.3 to 3 mm at 5 milliamperes a rise in temperature of  $75^\circ C$ , which is reasonable. In  $O_2$ , Lilienfeld<sup>54</sup> found in a 1.3-cm tube, at 16–92 milliamperes, tube temperatures from  $165$  to  $215^\circ C$ . Geiger<sup>55</sup> verified the results of Wood at low currents, but found in tubes of 3- to 4-cm diameter, with 1 to 2 amperes of current, temperatures of  $1200^\circ C$ . Using the Doppler effect in  $H_2$ , Gehrke and Lau<sup>56</sup> found, for a 1-cm tube and 50 milliamperes, a molecular temperature of  $50^\circ C$  and as low as  $-82^\circ C$  to  $-120^\circ C$  when the tube was in liquid air. Recent measurements in an  $N_2$  discharge using band spectra have been made by Hamada<sup>72</sup> with analogous results. This at least gives the order of magnitude of the effects observed, and it is seen that, except in the more arclike currents in the tenths of amperes or more, the gas temperatures are low.

## 8. THE ANODE FALL OF POTENTIAL

One may now turn to the anode fall of potential. The anode, accepting the electrons of the column and accelerating the positive ions, closes the circuit of the glow discharge. There appears to be some controversy, and thus more uncertainty, concerning the conditions at the anode than in any other part. Thus, for instance, the real existence of a normal and abnormal anode fall has not been decided. If the anode is too small relative to the column, a comparatively complicated situation appears in which a larger glow, of appropriate surface, about the anode, seems to replace the anode itself. If the surface is large there is no particular change. Occasionally patches are observed on the anode that are particularly active. These appear to be regions of gas evolution, or else of easily vaporizing substances, which furnish denser localized gas paths and concentrate the discharge in regions on the surface. The anode phenomena are particularly difficult to observe and measure, as the potential fall is at best small and is very subject to disturbance both by traces of gaseous impurities and dirty anode surfaces.

The situation may be pictured as follows. The electrons have a relatively high energy of agitation in the positive column, at least in the order of 2–8 volts. With such energies, as shown in Chapter V, they diffuse rapidly, and the imposed potential gradients in the positive column cannot control their motion by giving them a high drift velocity. Thus a negative space charge will tend to build up at the anode. In addition, the positive ions are being drawn away from the region of the anode to furnish the small but important positive-ion current. Since the space charges of electrons and positive ions are about equal, the high electron drift velocity compared to the positive-

ion drift velocity makes the current of positive ions at most some percentage of the electron current. However, the positive ions move down the tube, and, since in the sections of the column the new positive ions created just compensate the loss to radial diffusion, there must be *near the anode an increased rate of ion production to furnish the axial positive-ion current*, plus the loss to radial diffusion. This production requires an enhanced field at the anode, and this comes about through dearth of positive ions plus the electron space charge. There must therefore be, over a region of length  $d_A$ , a potential  $V_A$ , the anode potential fall, required to create the necessary positive ions.

This consideration can lead us to an approximate theory which predicts that  $V_A$  must be of the order of the ionization potential. There is no indication, however, that there should be an abnormal and a normal anode fall. As a result of the enhanced field, the increased ionization, just in front of the anode, should call for an accompanying increase in excitation. Thus where the anode has the same area as the column the increased density of excited atoms or molecules must cause an enhanced light emission. If  $V_A$  is somewhat larger than  $E_i$ , and the pressure is low, this light emission would be more intense at a portion of  $d_A$  remote from the anode, where the potential drop was about equal to  $E_e$  for excitation. This would account for the anode dark space. Where the anode area is small, then the intense field region of space charge would extend out into the gas and the anode would be surrounded by a considerable area of glow. From what has been said of its mechanism, the anode fall of potential need never be very high, as long as we deal with free electrons. In the case of the halogens, the problem is complicated by the fact that many more positive ions are needed, since the negative component of the current is in a good measure carried by negative ions instead of electrons. Hence because of the high negative-ion space charge and the need for many positive ions it must not surprise one to see the anode fall of potential in the halogens in some cases rising to values of 1000 volts. Low pressures will increase the anode fall, since the efficiency of ionization at low potential gradients cannot suffice to maintain the positive ions. The larger diffusion coefficient at lower pressures then also gives a higher space charge. Thus the anode fall is observed to increase in magnitude and extent as pressure decreases.

The measurements on the anode fall, preceding the Langmuir<sup>57</sup> studies on probes, are probably of little value. Thus whereas older probe methods at the anode in Hg gave about 7 volts anode<sup>55</sup> fall, Langmuir probes gave 2-3 volts, and estimates of  $V_a$ , measuring the energy liberation as heat at the anode as  $E = i(V_a + \phi_a)$ , gave 3 volts.<sup>58,59</sup> In the equation above, for the energy liberation,  $i$  is the total current which at the anode is electronic, and  $i\phi_a$  is the energy gain due to absorption of electrons. It is the surface work function of the anode. Probe measurements of a modern sort have been made and

compared with heating methods on the inert gas Ne by Penning.<sup>60</sup> Penning found three types of anode fall. In one, there was no anode glow and fall was negligible. In this  $E = i\phi_a$ . In the case that the increased pressure called forth the anode glow  $E = i(V_a + \phi_a)$ , with  $V_a = 21.5$  volts, the ionizing potential of Ne. At pressures and currents where the hemispherical red glow appeared at the anode,  $V_a$  was 2–3 volts less than 21.5 volts. In one of the experiments described by Penning, the pressure  $p$  was changed from  $\sim 0$  to 20 mm with 2 milliamperes of current. Below 2-mm pressure,  $E = \phi_a \sim 5$  volts. Above this  $E = 26.5$  volts or 23.5 volts. For  $H_2$ , Bramley,<sup>61</sup> using Langmuir probes under varied conditions, found that  $V_a$  was equal to 15 volts and ran down to 5 in the striated discharge. Güntherschulze,<sup>58</sup> with heating methods, found 16.7 volts, the ionization potential. In  $N_2$ , de Groot from heating experiments found 26 volts, while Güntherschulze<sup>58</sup> found 16.5, which is near the ionizing potential. It is seen that the results are not consistent, possibly as a result of impurities, and partly owing to differences in experimental conditions which change the fall.

## 9. THE ENERGY BALANCE AT THE CATHODE

Before closing, a word or two must be added about the energy balance at the cathode. Since  $V_a$  is the highest potential difference in the discharge, since it is concentrated in a limited range (some 100 molecular free paths), and since the current in this region is largely carried by positive ions, the major proportion of the energy expenditure and heat production must occur in this portion of the discharge. Thus it is at the cathode that we may expect the greatest heating. Now experiments of various sorts have shown that between 30 and 85 per cent of the energy  $V_a i$ , given by the cathode fall to the positive ions, is liberated as heat at the cathode.<sup>62,63</sup> That is, the cathode seems to consume some 30 to 85 per cent of the energy given the positive ions. This caused some concern, for the positive ions make from 50 to 150 impacts with gas molecules in  $d$ . However, much of the high field is concentrated at the cathode, so that in the last ten free paths the positive ions gain a good fraction of their energy, which will in a good measure be given up to the cathode.

Again, the gas *molecules* that are heated by impact of the ions have some persistence of velocity, and a not important fraction of their energy is *directed towards* the cathode. Finally, under most circumstances,  $d$  is small compared to the distance of the walls from the cathode, and much of the heat engendered in the gas space by positive-ion impact (the gas temperature in  $d$  must be very high) will by conduction go to the cathode, since the distance to it is less than to the walls. In addition each positive ion adds its heat of ionization to the cathode, except for those that lose some of this energy to secondary

electron production or to radiation.<sup>64</sup> Since these losses are small ( $\gamma$  and light emission in cathode glow are small), this contributes a considerable amount of added energy to the cathode.

For instance, almost all the positive ions in He give 26 volts to the cathode, while the total cathode fall with an Al cathode is of the order of 140 volts. If, now,  $d = 1.3$  mm, and the pressure is 10 mm, while the walls of the tube are 10 mm distant, it is not surprising that some 70 per cent of the energy from this 140 volts should appear at the cathode, for this would comprise 98 volts of energy measured at the cathode, of which 25 volts, coming from the neutralization of He, has not been deducted. Thus in such a case really only 73 volts, or 52 per cent of the heat from the cathode fall, reaches the cathode by direct impact of positive ions, and by direct conduction from a small, compact, and intensely hot layer of gas at its surface. The problem is exceedingly complex. It has been studied very much in detail in arcs where the heating of the cathode is vital to the arc operation. Compton, as shown on page 612, has considered this much in detail, accounting for radiation and conductive losses and for loss by reflection of positive ions from the surface. The problem is not acute for the cathode of the glow discharge.

## 10. SPUTTERING AT THE CATHODE

Another important phenomenon in discharge tubes is *sputtering*. If one observes the glass around the cathode of a discharge tube that has been run a long while, one will observe that it has been blackened. This is due to *cathodic sputtering*. The atomic ions of the gas come crashing into the cathode and tear off atoms and groups of atoms of cathode material. These go to the walls of the tube. The mass  $m$  sputtered in unit time is empirically given by the relation  $m = a(V_c - K_0)$ , where  $a$  and  $K_0$  are constants and  $V_c$  is the cathode fall of potential. The value of  $K_0$  for most materials ranges from 400 to 600 volts and is thus well above the *normal* cathode fall  $V_c$ . For  $V_c = 1000$ ,  $m$  is proportional to the current and is nearly equal to the amount of metal deposited by  $i$  in a voltameter. Thus, whenever the current density is increased by covering the cathode with glow, giving the abnormal cathode drop at high  $V_c$ , sputtering may occur. The sputtered metal carries with it to the wall and occludes the *gas* in the tube.

In neon signs it was a serious problem to have electrodes which would give continuous operation and intense light, but which would not sputter and thus remove the neon and make the tube go "black." The French engineer Claude obtained the patents on neon signs on the basis of the *empirical* discovery that, by increasing electrode area for small-diameter tubes, he could get the *normal* cathode fall and yet a high current density (i.e., luminosity) in the positive column with little sputtering. The question was fought over in the courts for some years. Patent limitation was circumvented in one case by using small

electrodes, beyond the patent limitations of Claude, and an abnormal cathode drop, by decreasing  $V_c$ , the cathode fall, below the sputtering potential by using Cs near and on the electrodes. Cs reduces the cathode fall even more than Na does and is sputtered to the walls. It can be retrieved by merely heating the tube, thus restoring the gas. Hence by means of a low cathode fall in an abnormal glow the current density is high and the sputtering is reduced.

The sputtering as stated depends on the cathode. It is also the greater the heavier the bombarding gas ions. Güntherschulze<sup>66</sup> showed further that the sputtered mass  $m$  was governed by the relation  $mpD = \text{constant} = C$ , where  $p$  is the pressure and  $D$  the plate distance between anode and cathode. The pressure appears since the molecular mean free path is inversely proportional to the pressure, and this influ-

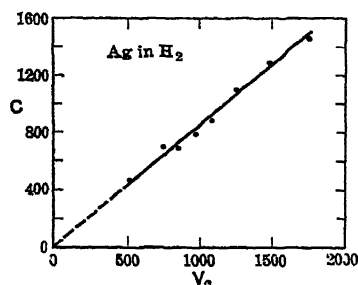


FIG. 276.

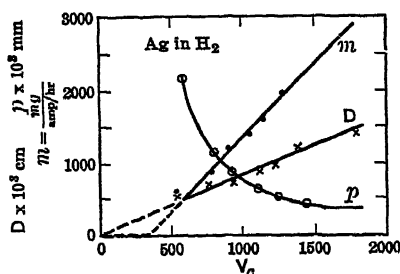


FIG. 277.

ences the diffusion of the sputtered metal atoms from the cathode. The value of  $C$  is directly proportional to the cathode fall of potential  $V_c$  as shown in Fig. 276. Fig. 277 shows the variation of  $m$ ,  $p$ , and  $D$  for Ag in  $H_2$  as a function of  $V_c$ . Both these are taken from Güntherschulze.<sup>66</sup>

The mechanism of sputtering is little understood. It obviously depends on the impact of positive ions on the cathode, in which the sputtered metal is thrown off in considerable measure, largely in the atomic and uncharged form at lower ion energies. There is some evidence that larger aggregates are present at the higher potentials  $V_c$ . Kingdon and Langmuir have promulgated a theory to explain their results.<sup>66</sup> It is possible that this is a manifestation of the localized cathode surface "heating" by positive-ion bombardment, a micro-process to be discussed under the low-melting point metal arcs. According to Von Hippel,<sup>67</sup> while for low  $V_c$  the atoms are probably uncharged and pick up ions in the discharge as they leave the region of cathode fall, the atoms above  $V_c = 550$  volts appear to be predominately positively charged. There is evidence that the gases like He, which are absorbed by, or can enter into, the cathode material, sputter less efficiently than those atoms that do not do so. In some cases abnormally heavy sputtering is due to chemical interactions of the gas with the

surface.<sup>65</sup> Table XLIV gives the mass of sputtered metal in  $H_2$  in a discharge of  $V_c = 850$  volts in  $10^{-6}$  gram per ampere-second as reported by Güntherschulze.<sup>66,68</sup>

TABLE XLIV

| Mg  | Ta  | Cr  | Al | Cd  | Mn | Mo | Co | W  | Ni | Fe | Sn | C   | Cu | Zn | Pb  | Au  | Ag  |
|-----|-----|-----|----|-----|----|----|----|----|----|----|----|-----|----|----|-----|-----|-----|
| 2.5 | 4.5 | 7.5 | 8  | 8.9 | 11 | 16 | 16 | 16 | 18 | 19 | 55 | 73? | 84 | 95 | 110 | 130 | 205 |

### 11. HOLLOW CATHODES

The operation of hollow cathodes also offers a rather interesting example of the fundamental principles. Instead of a large tubular cylindrical cathode open towards the positive column, such as is often used, consider two plane parallel-plate cathodes, well separated and parallel to the axis of the tube. Each cathode has its inner surface covered by the dark space and negative glow. The faster electrons from the dark space will penetrate the glow and approach the glow of the cathode opposite. Here they will be decelerated, and, except for collisions with energy loss, they will reverse their paths and re-penetrate their own glow, ionizing at that point. As the two surfaces approach each other, so that the outer sides of the glows touch each other, the number of the fast electrons that bat back and forth from one glow to the other increases materially. In this fashion all the energy of the faster electron swarms in the cathode fall are *efficiently* used in creating new positive ions. Thus the efficiency of ion production is increased for the same cathode fall and the current rises. This is shown in Fig. 278 taken from v. Engel and Steenbeck, where the pressure  $p$  in millimeters times the distance  $x$  between the plates is plotted against the current density over pressure squared  $j/p^2$  in amperes/cm<sup>2</sup>  $\times$  mm<sup>2</sup> at two values of  $V_c$  with iron cathodes in  $H_2$ . It is seen that when  $px$  is large the cathodes act independently, but as the negative glows approach,  $j/p^2$  increases sharply.

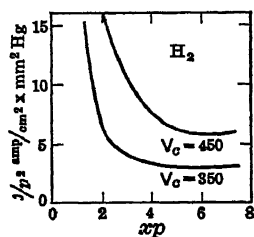


FIG. 278.

### 12. PLASMA OSCILLATIONS

Perhaps a word should be said in closing about another quality of the positive column. It has a nice balance of space charges of electrons and ions, so bound together as to lead to ambipolar diffusion. Since the electronic carriers have a far lower inertia than the binding positive charge, this medium of charges must respond fairly rapidly to changes

in electrical intensity. In consequence the ionized mass of gas in the positive column, termed *plasma* by Langmuir, is capable of transmitting potential waves. The matter is discussed by Thomson,<sup>73</sup> who shows that two types of waves may be expected—waves of a phase velocity depending primarily on the average electronic energy of agitation  $\eta mC^2/2$ ; waves depending on the average ionic energy, which is near that due to the molecular energy of agitation,  $MC^2/2$ . The lower limit to the frequency,  $p/2\pi$ , of the *electronic energy wave* which can be transmitted is given by  $\sqrt{e^2N_0/\pi m}$ , which is the frequency of the glow vibrating as a whole. Here  $e$  and  $m$  are the charge and mass of the electron, and  $N_0$  is the electron density. This gives frequencies for gases, between the values of  $N_0 = 10^8$  and  $5.5 \times 10^9$ , of  $9 \times 10^7$  to  $6.6 \times 10^8$  cycles/sec. The wave velocity of the positive ionic wave is always greater than the root mean square velocity of agitation  $C$ , and it does not exceed  $\sqrt{\eta C^2 + (m/M)C^2}$ . The critical frequency in this case is  $\sqrt{e^2N_0/\pi M}$ , where  $M$  is the ionic mass. This frequency is distinctly lower. It is seen not only that such oscillations can be transmitted, but also that the plasma can, under appropriate conditions, become the *seat of oscillations*, if energy is supplied. These oscillations were first discovered by Penning.<sup>74</sup> This stimulated Tonks and Langmuir,<sup>75</sup> Tonks,<sup>76</sup> and later the Guttons<sup>77</sup> to study the field. The presence of oscillations has been proved and their characteristics studied. If these frequencies are very high they can readily pass unnoticed. If, however, we measure the average conditions in a discharge by means of probes we may discover that groups of electrons have a far higher energy than average conditions warrant. Thus in low-pressure mercury discharges Langmuir in 1928 discovered electrons of 10 volts and more of energy where they should not have been observed. Among other explanations, the possibility of plasma oscillations was suggested. Consequent to Penning's<sup>74</sup> work, Tonks<sup>75,76</sup> discovered the presence of such oscillations and studied their properties. This behavior of the glow discharge must therefore not be lost sight of in the interpretation of the results of probe measurements.

With this incomplete and rapid survey, in which it is hoped that an indication of the operation of fundamental processes in the glow discharge has been given, we may leave the subject.

### 13. REFERENCES FOR PART A, CHAPTER XI

1. W. H. WESTPHAL, *Verhandl. deut. physik. Ges.*, **12**, 245, 1910; **14**, 223, 1912.
2. W. H. MCCURDY, *Phil. Mag.*, **48**, 898, 1924; COMPTON, TURNER, and MCCURDY, *Phys. Rev.*, **24**, 597, 1924.
3. A. SCHAUFELBERGER, *Ann. Physik*, **73**, 21, 1923.
4. F. W. ASTON, *Proc. Roy. Soc.*, **84**, 526, 1911; J. J. THOMSON, *Conduction of Electricity through Gases*, 2nd Edition, p. 532.
5. E. BROSE, *Ann. Physik*, **58**, 731, 1919.
6. A. GÜNTHERSCHULZE, *Z. Physik*, **33**, 810, 1925.

7. J. J. THOMSON, *Conduction of Electricity through Gases*, 3d Edition, Cambridge Press, Cambridge, 1933, Vol. 2, p. 296.
8. HOLST and OOSTERHUIS, *Physica*, 1, 78, 1921; *Phil. Mag.*, 46, 1117, 1923.
9. v. ENGEL and STEENBECK, *Elektrische Gasentladungen*, Springer, Berlin, 1934, p. 62.
10. R. SEELIGER, *Ann. Physik*, 59, 613, 1919; SEELIGER and POMMERING, *Ann. Physik*, 59, 589, 1919; R. SEELIGER, *Physik. Z.*, 25, 56, 1924.
11. G. GELHOF, *Verhandl. physik. Ges.*, 14, 960, 1912; P. NEUBERT, *Physik. Z.*, 15, 430, 1914.
12. McCURDY and DALTON, *Phys. Rev.*, 27, 163, 1920.
13. A. GÜNTHERSCHULZE, *Z. Physik*, 20, 1, 1923; 30, 175, 1925; 34, 549, 1925.
14. N. HEHL, *Physik. Z.*, 3, 547, 1903.
15. J. STARK, *Elektrizität in Gasen*, p. 169.
16. G. GELHOF, *Ann. Physik*, 24, 553, 1907.
17. K. ROTTGARDT, *Ann. Physik*, 33, 1161, 1910.
18. A. SCHAUFELBERGER, *Ann. Physik*, 73, 21, 1923.
19. C. A. SKINNER, *Phys. Rev.*, 5, 483; 6, 158, 1915.
20. R. HOLM, *Physik. Z.*, 17, 407, 1916.
21. E. WARBURG, *Wied. Ann.*, 40, 1, 1890.
22. A. GÜNTHERSCHULZE, *Z. Physik*, 28, 129, 1924; 30, 175, 1924.
23. R. BAR, GEIGER and SCHEEL, *Handbuch der Physik*, Vol. 14, p. 203, Springer, Berlin, 1927.
24. v. ENGEL and STEENBECK, reference 9, p. 103.
25. M. STEENBECK, MÜLLER-POUILLET, *Lehrbuch der Physik*, Vol. IV, p. 3, Vieweg and Sohn, Braunschweig, 1933.
26. R. SEELIGER, *Physik der Gasentladungen*, 2nd Edition, Barth, Leipzig, 1934.
27. A. GÜNTHERSCHULZE, *Z. Physik*, 21, 50, 1924.
28. J. J. THOMSON, *Rays of Positive Electricity*, 2nd Edition, p. 112, also *Conduction of Electricity through Gases*, 3d Edition, Vol. 2, p. 300.
29. v. ENGEL and STEENBECK, reference 9, p. 78.
30. v. ENGEL and STEENBECK, reference 9, p. 71.
31. COMPTON and MORSE, *Phys. Rev.*, 30, 305, 1927.
32. M. STEENBECK, *Z. Physik*, 76, 1, 1932.
33. W. ROGOWSKI, *Arch. Elektrotech.*, 24, 688, 1930; 27, 523, 1933; *Z. Physik*, 25, 551, 1931; 82, 473, 1933.
34. R. SEELIGER, *Naturwissenschaften*, 16, 665, 1928.
35. HOLST and OOSTERHUIS, *Phil. Mag.*, 46, 1117, 1923.
36. A. VON HIPPEL, *Z. Physik*, 76, 1, 1932.
37. v. ENGEL and STEENBECK, reference 9, p. 73.
38. R. SEELIGER, *Physik. Z.*, 15, 777, 1914.
39. W. SCHOTTKY, *Physik. Z.*, 25, 342, 635, 1924; SCHOTTKY and ISSENDORF, *Z. Physik*, 31, 163, 1925.
40. TONKS and LANGMUIR, *Phys. Rev.*, 34, 877, 1929.
41. R. HOLM, *Z. Physik*, 75, 171, 1932.
42. K. SEELIGER, *Physik. Z.*, 33, 273, 313, 1932.
43. SEELIGER and HIRCHERT, *Ann. Physik*, 11, 817, 1931.
44. M. J. DRUYVESTEYN, *Physik. Z.*, 33, 822, 1932.
45. M. J. DRUYVESTEYN, *Z. Physik*, 81, 571, 1933.
46. v. ENGEL and STEENBECK, reference 9, p. 82 ff.
47. V. A. BAILEY, *Phil. Mag.*, 13, 993, 1932.
48. BROSE and SAYMAN, *Ann. Physik*, 5, 797, 1930.
49. PENNING and TEVES, *Physica*, 9, 87, 1929.
50. G. CLAUDE, *Compt. rend.*, 157, 432, 1913; 158, 479, 692, 1914.
51. R. BAR, *Handbuch der Physik*, p. 269.
52. K. ÅNGSTRÖM, *Ann. Physik*, 48, 493, 1893.
53. R. W. WOOD, *Ann. Physik*, 59, 238, 1896.



54. J. LILIENTHAL, *Verhandl. deut. physik. Ges.*, **8**, 182, 1906.
55. R. GEIGER, *Ann. Physik*, **22**, 973, 1907.
56. GEHRKE and LAU, *Physik. Z.*, **21**, 634, 1920; *Ann. Physik*, **65**, 564, 1921; **67**, 388, 1922; **74**, 574, 1924.
57. I. LANGMUIR, *J. Franklin Inst.*, **196**, 751, 1923; see also Chapter V.
58. A. GÜNTHERSCHULZE, *Z. Physik*, **37**, 868, 1926.
59. W. DE GROOT, *Physica*, **5**, 121, 234, 1925.
60. F. M. PENNING, *Physica*, **4**, 380, 1924; **5**, 217, 1925.
61. A. BRAMLEY, *Phys. Rev.*, **26**, 794, 1925.
62. R. HODGSON, *Phil. Mag.*, **25**, 453, 1913; **26**, 911, 1913.
63. A. GÜNTHERSCHULZE, *Z. Physik*, **15**, 8, 1923; **23**, 334, 1924; **33**, 810, 1925.
64. HOLST and OOSTERHUIS, *Physica*, **4**, 375, 1924; A. GÜNTHERSCHULZE, *Z. Physik*, **31**, 507, 1925.
65. A. GÜNTHERSCHULZE, *Z. Physik*, **38**, 575, 1926.
66. KINGDON and LANGMUIR, *Phys. Rev.*, **22**, 148, 357, 1923.
67. A. VON HIPPEL, *Ann. Physik*, **80**, 672, 1926.
69. v. ENGEL and STEENBECK, reference 9, p. 115.
70. K. SOMMERMEYER, *Ann. Physik*, **28**, 240, 1937.
71. B. J. KLARFELD, *Tech. Phys. U. S. S. R.*, **4**, 44, 1937.
72. T. HAMADA, *Elect. Tech. J. Japan*, **1**, 57, 1937.
73. J. J. THOMSON, *Conduction of Electricity through Gases*, 3d Edition, Vol. 2, p. 353.
74. F. M. PENNING, *Nature*, **118**, 301, 1926; *Physica*, **6**, 241, 1926.
75. TONKS and LANGMUIR, *Phys. Rev.*, **33**, 195, 980, 1929.
76. L. TONKS, *Phys. Rev.*, **37**, 1459, 1931.
77. H. GUTTON, *Ann. phys.*, **13**, 62, 1930; C. GUTTON, *Ann. phys.*, **14**, 5, 1930.
78. M. J. DRUYVESTEYN, *Physica*, **5**, 875, 1938.
79. R. A. SMITH, *Proc. Roy. Soc.*, **A 168**, 19, 1938.

## PART B. THE ARC DISCHARGE.\*

### 1. THE DEFINITION OF AN ARC

Although the electrical arc was discovered in the form of the carbon arc by Davy in 1808 to 1810, shortly after the discovery of the voltaic pile, its mechanism is less understood quantitatively than the glow discharge. This is to be ascribed in a measure to the extreme temperatures yielded and to the exceedingly small scale of the critical regions, such as the cathode fall of potential.

The arc discharge is characterized and distinguished from other types of discharge by its exceptionally low cathode fall of potential and its high current densities. Its cathode falls run about one-tenth or less of those in the glow discharge, and arc currents are measured in the order of amperes to thousands of amperes per square centimeter, in place of tens of microamperes per square centimeter.

The difference in behavior can be accounted for readily in terms of a basic difference in mechanism. In the arc the meager secondary electron liberation due to a  $\gamma$ , requiring a high cathode fall which characterizes the glow, is replaced by an exceedingly copious electron emission necessitating only a low cathode drop but in contrast requiring a high current density. Although, according to numerous workers,<sup>1,2,3</sup> several mechanisms may be active in the case of the arc, the author is inclined to agree with J. J. Thomson,<sup>4</sup> Hagenbach,<sup>5</sup> Nottingham,<sup>6</sup> and others in their belief that the primary mechanism at the cathode of the arc is *thermionic* in nature. Through intense concentration of current, enough heat is poured into localized areas to raise the electrode temperature, locally, to the point of *some sort of thermionic emission*, in sufficient strength so as to maintain the discharge.

While in the arcs of refractory metals and substances this mode of operation is generally accepted, there is doubt in many minds about the arcs of the low-boiling-point metals from Hg on up to Fe. As will later be seen, if one is willing to redefine the concept of temperature to apply to the microscale of occurrences which take place at the cathode under some conditions, it is probable that one may be able to *define an arc as a discharge whose cathode mechanism depends largely on thermionic emission*. Until the acceptance of this idea becomes more universal we will define the arc in terms of its low cathode fall and large current density.

\* References for Part B, Chapter XI, will be found on page 639.

Arcs exist either at high and low pressure, usually at high pressures, and in the ambient gases or in the vapor of their own volatilized electrodes. They are *initiated* either by a spark or glow discharge, or a contact between two electrodes that are separated. As the contact breaks, the heavy current through the electrodes fuses and vaporizes the last small point of contact, leaving a metal vapor discharge which can change to an arc, if the external resistance is low. The process is called "drawing out an arc." This is a very important factor in high-voltage switching in industry, and the problem of suppressing the power arc is not yet satisfactorily solved. If the arc is drawn out too far, the convection currents due to the rising heated vapor may *blow* it out. In fact, from what has gone before, it is seen that for an arc to be created the current density at the striking point must be such as to raise the cathode to a sufficient temperature to maintain the current.

## 2. THE TRANSITION FROM A GLOW TO AN ARC

Perhaps one of the best illustrations of the difference in characteristics of glows and arcs is to describe the transition from a glow to an arc discharge. Let us assume a glow discharge tube, having the cathode of a thin refractory metal, so thermally isolated that it will readily be heated by the discharge current. The gas may be neon, or nitrogen, or any desirable gas at some millimeters of pressure. By means of an induction coil one may start a glow discharge and measure the current-potential characteristics. At very small currents the discharge starts from the cathode in a small point whose dimensions are comparable with the dark space in length. This discharge is in the region of *normal* cathode fall, and we might expect the potential  $V$  across the tube to remain constant as current increased and hence as the glow area increases. However, once the glow spot reaches dimensions comparable with  $d$ , the dark space, the cathode fall increases above  $V_c$ . The reason for this is that with too small an area of glow serious electron loss by lateral diffusion of electrons cannot be prevented. Hence, to make up for this,  $\alpha$  and  $\gamma$  must increase. Thus when the linear dimensions of the glow in the region of normal cathode drop become comparable with or less than  $d$  we enter a new regime, that of the *subnormal voltage drop*, where  $V$  rises as  $i$  decreases. Thus at very low currents one begins with the cathode fall above  $V_c$ , a tube potential  $V$  above  $V_n$ , and a small current  $i$ . When the spot area becomes large enough  $V$  will have fallen to the normal value  $V_n$  and will remain constant while  $i$  increases proportionally to glow area. This is the region of the *normal cathode fall*, and the course of the curve is illustrated in Fig. 279. At the point where the glow covers the cathode the potential rises and we enter the region of *abnormal cathode fall*. This rise in potential continues with increasing current for a considerable range. Eventually it will be observed that the cathode begins to show signs

of heating as a consequence of the current flow. This heating arises from the energy concentration at the cathode and its heat insulation. When the cathode begins to be *nearly white hot* the potential will cease rising as current increases. It will reach a maximum and then will rapidly drop as the current increases. Eventually it will reach the steady low value characteristic of the region of the arc discharge.

At the point where the potential sensibly ceases to rise with rising current, according to the equations for the glow discharge we know that we are supplementing the secondary electrons, determined by the quantity  $\gamma$ , by electrons liberated thermionically from the cathode. In the region beyond the peak the current is distinctly aided by thermionic emission, and the region of negative slope ( $dV/di$  negative) is one in which both  $\gamma$  and thermionic emission are active. At higher currents still,  $\gamma$  becomes of no influence and the whole discharge economy goes over to the more efficient mechanism of the arc. In fact, Druyvesteyn<sup>7</sup> observed at the peak of the curve in Ne that the W cathode temperature was 2000° K.

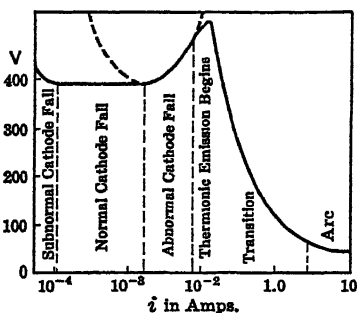


FIG. 279.

The transition can be computed from the theory of the glow discharge. The theory as developed by v. Engel and Steenbeck<sup>8</sup> will be given, as it is quite complete and very clear. The constant  $\gamma$  of secondary electron emission due to positive-ion impact must now be replaced by a quantity  $\gamma'$ , which gives the number of electrons, *thermionic and secondary by bombardment*, liberated per positive ion at the cathode. Thus we can at once write  $\gamma' = (i_-/i_+) = (i - i_+)/i_+$ , if the currents are measured at the cathode surface as on page 581. Here,  $i$  is the total current, and  $i_-$  and  $i_+$  are the electron and ion currents. The total electron current at the cathode is, then,  $i_- = \gamma i_+ + i_t$ , where  $i_t$  is the current due to thermionic emission,  $i_t = a A T^2 e^{-b/T}$ , from Richardson's equation for thermionic emission,  $T$  being the temperature of the cathode and  $a$  the area of the cathode. The total current is then

$$i = i_- + i_+ = i_+(1 + \gamma) + i_t.$$

From this we can evaluate  $\gamma'$  as

$$\gamma' = \gamma + \frac{1 + \gamma}{(i/i_t) - 1}.$$

If now  $T$  is known and  $\gamma$  is not changed by heating, we can calculate the various new quantities, following the procedure of page 582. An approximation to  $T$  as a function of  $i$  can be had by roughly setting the

energy transfer to the cathode as  $iV_c$  and equating this to the radiant-energy emission. Assuming a black-body radiation we can set  $iV_c = \sigma T^4$ , with  $\sigma = 5.7 \times 10^{-12}$  watt/cm<sup>2</sup> × degree<sup>4</sup>. This enables us to get  $\gamma'$  as a function of  $iV_c$ , and  $\gamma$ , if the constants  $a$ ,  $A$ , and  $b$  are known. From the equations on page 582, correcting for the effect of temperature on the gas density, one can then get an approximate expression for  $V_c$  as a function of  $i$ . Using 2000° K as the average uniform temperature of gas, v. Engel and Steenbeck<sup>8</sup> were able to compute the dashed curve of Fig. 280 from known constants and compare it with the

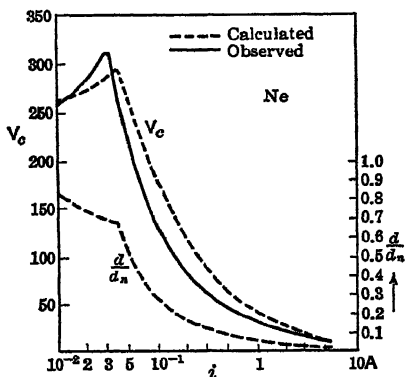


FIG. 280.

observed full curve. Despite the inaccuracies in the assumptions as to heat transfer to the cathode and the neglect of the "grayness" of the radiative emitter, the agreement is striking. From this relation one can also evaluate the length of the cathode fall  $d$  as compared to the normal cathode fall. The value of  $d/d_n$ , the ratio of  $d$  to  $d_n$  for the normal fall, is shown in Fig. 280. It is important to note that, as the effect of  $\gamma$  dwindles in importance, compared to the thermionic contribution, the length  $d$  needed to give the necessary ionization to

maintain the discharge becomes much less, i.e.,  $d/d_n$  decreases. As to the ultimate values of  $d$  for the arc, more will be said at a later point.

### 3. CHARACTERISTIC POTENTIAL CURVE OF AN ARC

Owing to the high temperatures in arcs, potential measurements are very unsatisfactory. Attempts have been made by probes,<sup>8,9</sup> by falling electrodes passing through the arc, by Stark-effect studies,<sup>10</sup> and by high-frequency conductivity measurements to determine the characteristics of the cathode fall.<sup>42</sup> Actually, Stark-effect studies are meaningless because of the high ion densities and resulting interionic fields. It was pointed out by Loeb, Hillebrand, White, Varney, and Miller<sup>11</sup> that Nagaoka's<sup>10</sup> measurements of gradients in arcs by Stark effect, if integrated over the length of the arc, gave potential differences many times greater than the actual applied potentials. However, it has been possible to obtain approximate values of the potentials in arcs. Temperatures can be obtained from band-spectral studies<sup>12</sup> and from the velocity of sound in arc channels,<sup>13</sup> as well as by the radiation.

The ranges of  $\alpha$  particles in arcs also yield estimates of the temperature.<sup>30</sup> A generalized potential distribution curve typical of the

refractory metal arc of 1-cm length is shown in Fig. 281. The length of the cathode and anode falls of potential cannot be drawn to scale along the arc axis. They occur in distances of only a few electron free paths, perhaps less than 10, which at atmospheric pressure and arc temperature are of the order of  $10^{-3}$  to  $10^{-2}$  cm. The magnitude of the potential drop at the cathode in truly hot arcs is of the order of only one to two times the ionizing potential of the vapor. At the anode the fall may be somewhat greater than the cathode fall, depending on the anode material and temperature. The positive column has in general a small potential gradient, and the ratio  $X_1/p$  for the arc column is small compared to the glow column. The drop varies very much with the gas, or vapor, and with the temperature which can be maintained in the column. It is, in some cases, hardly enough to sustain much ionization by collision by electrons. This is especially true where the heat furnished by the motion of carriers in the field and chemical reactions can maintain a temperature requisite for thermal ionization following Saha's equation.

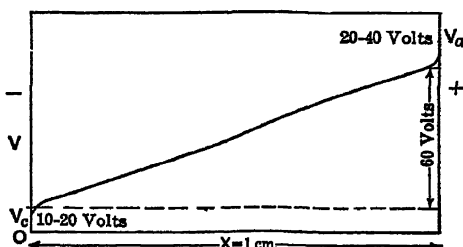


FIG. 281.

#### 4. THE CATHODE FALL IN AN ARC

One may study the problem of the cathode fall of potential as follows. Let us assume that the current is maintained by the action of the incoming positive ions in falling through the cathode fall  $V_c$  and giving enough energy to the electrode to maintain it at a thermionically emitting temperature. This necessitates a minimum positive current density,  $j_+$ . As a result of the heating there is a thermionic electron emission from the metal. This emission must be such as to maintain the positive space charge by producing positive ions through collision within a distance  $d$ , in the cathode fall  $V_c$ . Owing to the very small values of  $d$  and  $V_c$  we cannot assume that any one electron ionizes much more than once or twice, and in some arcs it takes two successive electron impacts on a molecule to give an ion. Probably many electrons never ionize. Hence the short cathode drop and the low energies, with the small excitation and ionization probabilities, mean that many electrons are needed to make one positive ion. Hence the arc must have high current densities, and the electron current at the cathode may be considerably larger than the positive-ion current. Thus the number of electrons emitted from the cathode and created by ionization per second, which enter the positive column, may be anywhere from one to

ten or more times the positive-ion current. The excess of electrons, despite their high velocity relative to positive ions, cannot be too great since the positive-ion space charge must be able to build up to considerable values. Thus we can expect to find  $j_-$  larger than  $j_+$ , but not very much so for an economical arc. Earlier estimates, such as those of Compton<sup>14</sup> in 1923, of 50 to 1 are probably too high. The electrons with their high mobility therefore do not contribute to much of the space charge, and we have a positive-ion space charge at the cathode. This space charge at once limits the current of positive ions flowing to the cathode.

Thus we can apply the equation for the positive-space-charge-limited current of page 319 to the calculation of the positive-ion current density. This equation reads

$$j_+ = \frac{1}{9\pi} \sqrt{\frac{2e}{M}} \frac{V^{3/2}}{d^2}.$$

Now in this equation,  $M$  is the mass of the ions, and  $V$  and  $d$  are the corresponding potentials across the cathode fall, and the length of the fall.<sup>14</sup> For  $N_2$  gas at atmospheric pressure one may calculate the value of  $j_+$ , assuming  $d$  equal to the mean free path of  $N_2$  molecules in the gas at 2000–3000° K, which is about  $6 \times 10^{-6}$  cm, and assuming  $V$  as equal to the ionizing potential of  $N_2$ , which is 15.8 volts. This calculation probably underestimates both  $d$  and  $V_c$ . It yields, however, a positive ion current density of some 180 amp/cm<sup>2</sup>. If the electron current density,  $j_-$ , is some 2 to 10 times larger than the ion current, the total current density  $j = j_- + j_+$  would be of the order of 400–2000 amp/cm<sup>2</sup>. In  $N_2$  the observed values of  $j$  lie within these limits of order of magnitude. It is seen from this that, in principle,  $V_c$  and  $d$  are small. Since  $V_c$  as actually measured is never very much larger than  $E_i$  for the gas (not more than twice), and may be less, it is seen that  $d$  cannot be very much more than 2 to 4 mean free paths, *unless* the ratio of  $j/j_+$  is much greater than the ratio of 2 to 10 assumed.

In the case of the Hg and Cu arcs, at atmospheric pressure, larger current densities are observed (up to  $3 \times 10^3$  amp/cm<sup>2</sup>), and in vacuum up to  $10^4$  amp/cm<sup>2</sup>. In this case the electron emission must be prodigious, and ionization by multiple impact does occur. Here then the positive-ion current would be required to be but a small fraction (5 per cent) of the electron current. In the case of the Hg arc, Lamar and Compton<sup>15</sup> estimate on the basis of probe theory that  $i_+/i_- = 1/400$ , which, corrected for random velocities, etc., should be more nearly  $1/40$ . This gives the value of  $d$  for Hg  $< 1.8 \times 10^{-4}$  cm. It is to be noted that, even with such large values of  $d$ , the *electron free path is several times longer and its ionizing free path for single-impact ionization may be 10 d or more*. Ionization by successive electron impacts is here quite certain. v. Engel and Steenbeck<sup>16</sup> assume, on

the contrary, that  $d$  must be one-third to one-fourth of the value of the free path used above. This they explain as being due to an increase in gas pressure in the cathode region, as a result of the momentum transfer of positive ions to the vapor molecules. That such pressures might and do exist in some cases there can be no doubt. In the vacuum Hg vapor arc the pressure in the cathode region has been demonstrated.<sup>17, 18, 19, 20, 21, 22</sup> How much it will alter the mean free path is not known. However, as will later be shown, it is highly questionable that the terms "temperature" and "pressure" as commonly understood can logically be applied to processes taking place on the microscopic scale of  $10^{-5}$  cm and in  $10^{-5}$  second.

Assuming the positive-ion space charge, one can, by substituting the ionic mass for the electronic mass in the second equation of page 319, evaluate the field strength at the cathode. This equation reads,

$$X_c = \frac{dV}{dx} = 4 \sqrt{\pi j_+} \sqrt{\frac{M_+}{2e}} \sqrt[4]{V_c}.$$

If we now insert the value of  $j_+$  just deduced into the equation,  $X_c$  becomes  $X_c = \frac{4}{3} V_c/d$ . This makes  $X_c$  in air at atmospheric pressure, assuming  $V_c = E_i$  and  $d = \lambda_e$ , about  $3 \times 10^5$  volts/cm. For Hg, Lamar and Compton<sup>15</sup> find  $7.76 \times 10^5$  volts/cm. Extending this to the case of the Cu arc, v. Engel and Steenbeck,<sup>23</sup> assuming a smaller value of  $\lambda_e$ , envisage field strengths of the order  $10^6$  volts/cm. It is on calculations of this sort that one gets fields which may suffice to cause *autoelectronic* emission from the surfaces in the case of the Cu and Hg arcs. Such emission *might* occur if we could be sure of such field strengths. Whether *it would suffice to produce electron current densities of the order of  $10^4$  amps/cm<sup>2</sup>*, however, is another matter. Whether the values of  $V_c$  computed above are correct or not, it appears not unlikely that the positive space charge gives values of  $X_c$  of the order of  $10^4$  to  $10^5$  volts/cm.

Some guesses can be made as to the ratio of electron to ion current from the energy balance at the cathode. The energy given up to the cathode per unit time is the positive-ion current times  $V_c$  plus the same current times  $E_i$ , the energy of neutralization. Some of this energy may be removed by reflection of the neutralized positive ions, possibly 1 to 30 per cent. The cathode loses the energy of evaporation of the electrons needed to neutralize the positive ions in those cases where the positive ions leave the surface as neutral atoms. In computing such a heat balance, v. Engel and Steenbeck<sup>23</sup> count this energy as a loss to *all* positive ions. This loss amounts to  $i_+ \phi_e$ . The energy transfer by positive ions is on this basis  $E = i_+(V_c + E_i - \phi_e)$ . The energy losses of the cathode are the heat of evaporation of the electrons  $i_- \phi_e$ , plus losses to radiation, to evaporation of cathode material,



and to conduction. Assuming that  $i_- \phi_e \gg E_i$ , where  $E_i$  is the energy lost to other processes, one can then write

$$i_- \phi_e = i_+(V_c + E_i - \phi_e).$$

If we do this we have the maximum value of  $i_-/i_+$  given by

$$\left(\frac{i_-}{i_+}\right)_m = \frac{V_c + E_i - \phi_e}{\phi_e}.$$

In the case of the carbon arc in air, v. Engel and Steenbeck set  $V_c = E_i = 15.8$  volts, and  $\phi_e = 4.5$  volts, making  $(i_-/i_+)_m$  about 5. For the Cu cathode using  $E_i = 7.7$  and  $\phi_e = 4.3$ , v. Engel and Steenbeck find  $(i_-/i_+)_m = 2.5$ . Using Nottingham's data for the Cu arc in air,  $V_c = 20.5$ , which makes  $i_-/i_+ = 8.5$  for the Cu arc. Compton<sup>24</sup> made an elaborate study of the real losses for the Hg arc and determined the various possible values of  $i_-/i = f$ , ( $i = i_- + i_+$ , whence the ratio  $i_+/i = 1 - f$ ). He used the value of  $V_c = 10$  volts and  $V_i = 10.4$  volts. He considered  $\phi_e = 4.5$  volts, unless it is much reduced by the action of the field, in which case he deducted a value  $\phi_-$ . Probably it is safest to assume  $\phi_e = 4.5$  volts, although Compton calculates  $f$  for various values of  $\phi_-$ .  $R$  is the radiation loss which, according to Güntherschulze,<sup>25</sup> is 0.04 volt. The energy,  $E$ , lost by evaporation can be as much as 2.21 volts. However, experiments indicate no *direct evaporation*, but an apparent evaporation due to an accommodation coefficient  $a \sim 0.9$  (see later). Hence a value of  $E = 0$  is not seriously in error. The cooling by conduction through the cathode  $C$  is 2.68 volts, according to Güntherschulze, while that by gaseous conduction is zero. The energy lost in giving the electrons their energy of thermal agitation,  $\bar{V}_-$ , is 1.5 by probe measurements. A fraction,  $F$ , of the energy given up to the molecules by electron impact, that does not go to ionization, returns to the cathode. It lies between 0.5 for radiation and 1.0 for metastables, etc. Neglecting the field lowering of the work function, and evaporation, but assuming that  $a = 0.9$  and that  $F = 0.9$ , one finds  $f$  equal to 0.90, so that  $i^+/i = 1 - 0.9 = 0.1$ . This seems quite a reasonable ratio. Altering the various assumptions within reasonable limits, however, Compton is able to get values of  $f$  ranging from 0.64 to 0.99.

Hence it is seen how utterly fallible the method is. Proper probe measurements, could they be carried out, might give us the ratios of electron and ion densities from which  $i_-$  and  $i_+$  can be inferred. Unfortunately probes cannot be used in the small cathode layer. This whole calculation becomes even more doubtful if we remember that there is no such thing as a solid metal surface, of a stable sort, acting in the Cu arc. In the micro volume of impacting positive ions it is impossible, in the confused vaporizing mass at the metal surface, to

give values to the work function, accommodation coefficient, etc., derived from clean, relatively cool surfaces. Hence one must hesitate still further to say too much about the energy balance.

## 5. CATHODE TEMPERATURE

The question as to the cathode temperature existing cannot be theoretically solved, owing to inadequate data. For the carbon arc in  $N_2$ , the temperature  $T_c$  has been estimated as very close to  $3600^\circ C$  by radiation and from band-spectra measurements. This allows current densities of electron emission, from the thermionic equation, of 500 to 800 amp/cm<sup>2</sup>, with a  $\phi_c$  of 4.5 volts. With the Cu and Hg arcs, temperature estimates, all the way from 100 to  $2360^\circ K$  and even 300,000 K have been made,<sup>9, 20, 21, 26, 27, 28, 29</sup> indicating that the *conditions are not amenable to ready interpretation in terms of temperature*. Estimates have been made on the basis of radiated energy, assuming a continuous emitter either pyrometrically<sup>29</sup> or otherwise, by the amount of evaporation of substance and by the momentum of the evaporated vapor atoms.<sup>20, 21</sup> When such discordant results appear on the basis of classical evidence, we must realize *that we are not dealing with a classical situation*. The word *temperature in the ordinary sense is probably meaningless at these cathodes*. If the lower estimates, given in books and papers, of temperatures below  $2000^\circ K$  are correct, thermionic emission currents of 10<sup>3</sup> amp/cm<sup>2</sup> cannot be generated.

## 6. POTENTIAL-FALL MEASUREMENTS WITH PROBES

More adequate data on the fall of potential than those given by v. Engel and Steenbeck come from the measurements of Nottingham and later of Mason.<sup>9</sup> Data as to the fall in the positive column can be had by maintaining  $j$  constant and lengthening the arc. The increase in  $V$ ,  $\Delta V$ , is ascribed to the fall in the column, and the gradient is taken as  $\Delta V/\Delta l = X_l$ . If the lengthening of the arc did not change  $X_l$ , owing to changed cooling conditions the method would be good, as it is for the positive column of a glow discharge. It gives approximate values. The falls can also be estimated by measuring the *conductivity* of the arc plasma by a high-frequency current. The method is discussed later.

Let us return now to the results of Nottingham and Mason with probes. Nottingham<sup>6</sup> used a swinging probe and measured the potential as a function of the distance from the cathode. His value for a 6-mm Cu arc at 6 amperes is shown in Fig. 282. There it is seen that  $V_c = 20.5$  volts, which is the second ionizing potential of Hg. The anode fall of potential was between 7 and 8 volts. The field gradient in the positive column was 47 volts/cm. The current density was of the order of 3000 amp/cm<sup>2</sup>. In the positive column the electron ener-

gies were  $2.3 \pm 0.1$  volts, near the cathode, and  $2.7 \pm 0.1$  near the anode. This *average energy* should permit of some ionization by electron impact. However, at these current densities, cumulative ionization

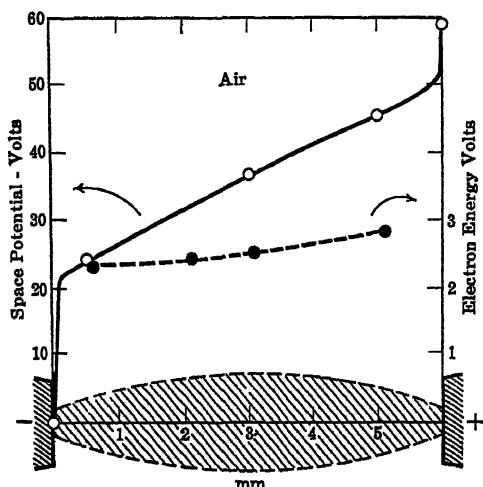


FIG. 282.

will suffice to give the current. The fact that the arc burns at the double ionizing potential may mean that at the high electron densities Cu is doubly ionized. This more than doubles  $E_i$  as well as  $V_c$ . Mason,<sup>9</sup> however, finds that the probe method requires careful interpretation in the high-temperature, high-pressure arc. In the C arc he shows that Nottingham's value of  $V_c$  is too low and his value of  $V_a$  is too high. Mason's careful study of probe characteristics in arcs leads to the curve of Fig. 283 for the C arc at 3 and 6 amperes. This makes the cathode fall something over 10 volts and the anode fall of the order of 20 volts. The current density in the positive column is about  $20 \text{ amp/cm}^2$ , the gradient  $X_i$  is 33 volts/cm, and the ion density is about  $10^{14}$ . Other information on  $X_i$  in this arc is given by Hörmann.<sup>41</sup> In the column the temperature was taken as  $6000^\circ \text{K}$ .

At this point it is profitless to discuss the cathode mechanism further. In what follows, the anode conditions and positive column will be discussed. Subsequently certain classical and useful data on the behavior of arcs consequent on their properties will be presented. After this it will be appropriate to discuss in a more thorough fashion the question of the low-melting-point metal arc and briefly the low-voltage arc in Hg.

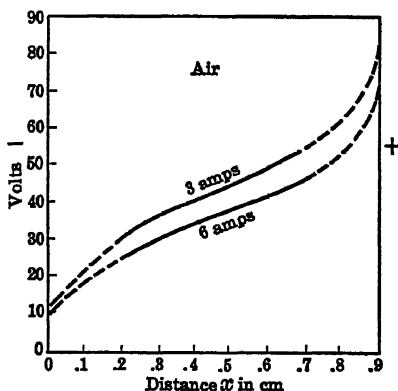


FIG. 283.

## 7. THE ANODE FALL

What happens at the anode is again not clear, owing to lack of data. Into the anode there flows the very high electron current, which must needs give a heavy negative space charge, partly because of its enormous density of current and partly because of its temperature. Furthermore, the anode itself, which is often as hot as if not hotter than the cathode, must also be a thermionic emitter. Electrons leave the anode in this process, but the field pulls them back. They must, however, add to the negative space charge *near* the anode. In fact, where the anode is cooler the anode fall, according to Hagenbach,<sup>31</sup> is less than where the anode is very hot. In the arc column the electron temperature is about one-third to one-half that in the glow discharge, and perhaps less. Thus the space charges could well be less, except for the enormous electron densities. In any case, at the anode, there must be an adequate supply of positive ions to keep the positive-ion current in the column going. Owing to their low mobility these ions will influence the electron space charge even if present in small numbers compared to the electrons. Indications are that the anode temperatures are equal to or even in excess of the cathode temperatures, e.g., in the C arc  $T_a = 4000^\circ \text{K}$  and  $T_c = 3600^\circ \text{K}$ . In a measure, chemical reactions such as oxidation may increase the anode temperature, as seems to be the case for C. The values of the anode fall are not easy to obtain, but appear to be as large, and in fact larger than the cathode fall. The Stark-effect studies show *smaller field strengths at the anode*, but again these data may merely be an indication of lower ion densities. Assuming lower fields at the anode, then the greater anode fall must extend further into the gap. This may or may not be correct.

It is stated by v. Engel and Steenbeck<sup>32</sup> that the energy balance at the anode should be less complicated and hence the results more capable of exact interpretation than those at the cathode. Remembering the fallibility of all such calculations, as indicated by Compton,<sup>24</sup> one may indicate how to compute the balance. Here the energy losses are to conduction, evaporation, and radiation, while there may be a gain of energy from chemical action. If we call the quantity  $g$  the emissivity of the anode relative to a black body, the radiation loss is then  $g\sigma T^4$  per  $\text{cm}^2$  approximately. The anode gains the electron energy  $j_-(V_{an})$ , and the energy  $j_-\phi_s$ , from the heat of condensation of the electrons. As a result one may roughly write

$$g\sigma T^4 = j_-(V_{an} + \phi_s),$$

neglecting loss of energy by evaporation, which may *not* be small in this case, as there is no pumping action of incident positive ions which nearly equal in number the normally evaporated atoms. Hence we can compute  $V_{an}$  as

$$V_{an} = \frac{g\sigma T^4}{j_-} - \phi_s, \text{ with } g \sim 0.75.$$

For C with  $j_- = 80$  amp/cm<sup>2</sup>, this gives, at  $T_{an} = 4100^\circ$ ,  $V_{an} = 10.5$  volts. If one includes conduction and evaporation, the first term is increased and the value  $V_{an}$  approaches more nearly the observed value, which is twice as great. In the anode fall the electrons must pick up the energy to ionize and thus furnish the needed positive ions to maintain the arc. Thus at the cathode one obtains the needed electrons and by ionization by collision in an extended  $d_{an}$  one obtains the positive ions needed to carry the current. Hence we find the anode fall  $V_A > V_K$ , the cathode fall. Thus we find not only a greater potential fall at the anode but also a greater anode temperature. This, in the C arc, is  $4200^\circ$  K, and up to 120 amp/cm<sup>2</sup> is independent of current. Increasing the current merely enlarges the anode spot. *The temperature depends on the anode material.* Studies of the vapor pressure curves of C and anode temperature variations with pressure indicate that the anode temperature is the boiling point of the anode material. The melting point of C is  $280^\circ$  below its boiling point. Thus the surface of the anode is molten and boiling. It furnishes a stream of vapor of low ionizing potential to operate the arc. At 22 atmospheres the brightness of the C arc increases 18 fold, and its temperature is  $5890^\circ$  K.

In Mg, Al, and Zn in air, the anode temperature is very much greater than the melting temperature. This is due to the formation of oxide layers. If  $N_2$  is used as the gas, the oxides do not form and the anode temperature is much lower. Water-cooled anodes still permit arcs to operate. This merely means that the arc is no longer a metal arc but an arc in the gas used. Thus, while high temperatures of the anode are not essential for maintenance of arcs, the character of the arc, its characteristics, and its economy are much influenced by the anode. Where the anode material has a low work function compared to the ambient gas it will prefer to volatilize the anode material. At the anode, the potential drops must also suffice to ionize the vapor and to heat the anode.

### 8. THE POSITIVE COLUMN

Concerning the positive column, much can be speculated, but little is known. At atmospheric pressure, diffusion is small, the column is self-contained, without walls. The electrons have on the average very much lower energies (temperatures) than in the glow discharge. This decreases the ambipolar diffusion. *The potential gradients down the column are higher than in the glow discharge.* On the other hand, the gradients,  $X_1/p$ , per unit pressure are *very much smaller*. For values see page 614 and reference 41 for the C arc. Measured electron temperatures in the column lie around 1-3 electron volts. These are large enough to cause ionization by collision at single impact of many of the chemical reaction products in the column, such as NO, CO, CN, though possibly not of the gases like  $H_2$ ,  $N_2$ ,  $O_2$ , C, He, Ne, and A themselves. These reaction product molecules show themselves to be

present in large numbers, in the excited states, in band spectra observed in the column. The presence of impurities such as Na in impregnated C electrodes materially lowers the gradients and the column temperatures. The electron densities in many cases are such as to permit of ionization by successive electron impact especially at higher current densities. Electron densities of the order of  $10^{13}$ – $10^{14}$  electrons/cm<sup>3</sup> are not uncommon. The effect of increasing current, and hence current density, is uniformly to reduce the potential gradient in the positive column. This points strongly to ionization by successive impacts and analogous phenomena, in increasing amount, as current densities increase.

In view of the large excess of electrons, much of the energy transfer from the field to the gas molecules must take place through electron impacts. While the elastic loss per impact against molecules is small, the electron impacts are very numerous. In addition, excitation to vibration, and electronic excitation of the gas by electrons, are possible and these processes will degrade to heat sooner or later. The positive ions, of course, are efficient in transferring energy, but are not great enough in number to do as much as they do at the cathode. The gas temperatures in the column are high, and in fact much higher in some cases than at the electrodes, as indicated by studies from line <sup>33</sup> and band spectra <sup>12</sup> and from the velocity of sound. The C arc has temperatures as high as 6000° K, as given by Ornstein <sup>12</sup> and his collaborators from spectra, and Mannkopf from line spectra.<sup>33</sup> Analogous values come from v. Engel and Steenbeck's measurements of density with  $\alpha$  particles.<sup>30</sup> The values in Table XLV, taken from studies of the velocity of sound by Suits,<sup>13</sup> are significant and in agreement with the results from spectra.

TABLE XLV  
TEMPERATURES IN COLUMN OF CARBON ARC

|                       |         |                              |                   |
|-----------------------|---------|------------------------------|-------------------|
| Cored C. . . . .      | 5500° K | W 6-mm electrodes . . . .    | 5950° K           |
| NaCl cored C. . . . . | 4740° K | Fe-Fe welding arc. . . . .   | 6020° K           |
| Al cored C. . . . .   | 6160° K | Cu arc. . . . .              | 4100 $\pm$ 300° K |
| W cored C. . . . .    | 6220° K | Independent of current . . . | 30 $\pm$ 6 amp    |

On this basis it has been stated repeatedly that the ionization in the arc column is a "temperature ionization."<sup>12</sup> In fact, in further pursuing this viewpoint, Slepian <sup>34</sup> has proposed a temperature theory of the arc mechanism. Because more esthetic taste and emotion than common sense has gone into the subsequent discussion of this proposal, it is essential to consider carefully what is meant by "temperature ionization."

Saha,<sup>35</sup> considering a gas at a high temperature *in equilibrium*, has shown that, as a result of the kinetic energy of agitation of the atoms in the Maxwellian velocity distribution, those atoms whose energy in the *translational* motion exceeds the ionizing or exciting potential will cause ionization or excitation. The rate of ionization and recombination depends on the

collision frequency and the cross sections for ionization as well as on the energy distribution and recombination. At equilibrium as many ions recombine per second as ionize, and the equilibrium concentration of ions can be computed from  $E_i$ ,  $T$ , and universal constants. On this basis Saha has worked out his famous equation for the density of ionization  $N_i$  relative to the total density  $N_0$  of atoms. This reads:

$$\log_{10} \frac{N_i^2}{N_0} = -5040 \frac{V_i}{T} + \frac{3}{2} \log_{10} T + 15.385,$$

where  $T$  is the absolute temperature and  $V_i$  is the ionizing potential in volts. Since the equation represents an equilibrium condition the nature of the processes does not enter in. It is proper, however, to ask whether the ionization proceeds by impacts among the atoms or by electron impact, for it is obvious that, once electrons are present, these also cause ionization, and in considering the process in detail we must take into account a complicated set of reactions which can be worked out at equilibrium on the basis of the principle of detailed balancing.

At the enormously high temperatures of the arc columns it is clear that the ion densities should be calculable on Saha's theory from the temperature *if there is equilibrium*. Now Ornstein<sup>12</sup> in his very careful and detailed study has considered the conditions in the positive column of an arc and finds that far from the electrodes the excitation and ionization of the molecules of lower  $E_i$  and  $E_a$  are probably the direct result of the thermal collisions of the atoms and molecules, as anticipated by the Saha equation. To this condition the term "*temperature ionization*" has been applied. Mannkopf, on the basis of studies of line and band spectra in arcs, does not entirely agree with Ornstein. He concludes that in a very rough fashion the Saha theory is applicable.<sup>33</sup> Other data may be found in papers by Witte<sup>40</sup> and Hörmann.<sup>41</sup> What Ornstein's conclusion signifies is *merely that the rate of gain of energy of the electrons from the low fields is so small that in general their energy distribution is not sensibly different from the Maxwellian*, while their *average* energy may be a *bit* above that required by the temperature  $T$  of the gas. They are thus able to ionize in proportion to the fraction of their number with adequate energy and their cross section for ionization. Since the electrons are few in number compared to atoms such ionization processes are rare. However, owing to the overwhelming preponderance of atoms and molecules in equilibrium at nearly the same high temperature relative to charged carriers, *the greater proportion of the excited and ionized atoms or molecules will be produced by collisions between neutral configurations and not electrons even though the atomic cross sections are smaller*.

That ionization, in the arc probably proceeds *via* collisions of atoms and atoms, instead of by electrons and atoms, no one questions. Where the trouble arises lies in the confusion, not only in the readers'

minds but all too often in the writers' minds, as to exactly the relation of the temperature ionization to the arc mechanism as a whole. For it is implied by statements that "temperature ionization" *maintains the arc*. This is in no sense the case, for the *electrical energy is only put into the column via electrons and ions and thus these are responsible for producing ionisation and maintaining the column*. The only difference between the glow and arc columns lies in the fact that *the electrons in the glow ionize by impact directly*, whereas in the arc *they ionize indirectly by raising the temperature of the column*.

In order to understand this, let us consider a section of positive column far from the electrodes. There enters the cathode end a heavy current density of electrons, generated largely at the cathode and flowing through it to the anode. There enters its anode end a small current density of positive ions which leave the cathode end, on their way to the cathode. The electrons move rapidly, the positive ions slowly. At any instant there are in the section *approximately equal numbers of free electrons and ions*. These remain *constant* in number in transit, as a net result of processes to be discussed, and together give the arc current. These electrons and ions pick up energy in traversing the potential gradient along the positive column and give this energy up in impacts of various sorts to the atoms and molecules of the gas. Thus *the gas atoms and molecules offer a resistance to the passage of these charged carriers*, and produce heat as a result, just as, in a metal, the resistance offered by the atom lattice to the electrons takes up the electrical energy,  $i^2R$ , furnished the electrons, as heat. This heat transfer to the column, in a stable column, must just balance the radial and axial heat loss by radiation and conduction produced by various mechanisms. Thus *the temperature of the column is maintained by electrical work put in by the current of ions and electrons*. Unless the chemical reactions also augment the heat input to the column it must clearly be understood that *the energy comes solely from the movement of electrons and ions along the column in the axial field  $X_1$* . Now in addition to loss of heat by radiation and conduction in the ambient gas, *energy and charges are lost out of the section of column by radial ambipolar diffusion and recombination*. Small though the numbers diffusing are at atmospheric pressure, the energy transfer by these and diffusing excited atoms is not very small. Hence, while the *axial* currents of ions and electrons entering and leaving the section are equal, there is a steady radial loss of charges from the column, as in wall currents in the glow discharge as well as loss by recombination. We could assume that this loss of carriers in the glow discharge was made good by the *ionization by electron impact of the electrons*, in the gradient of the column. In fact, this assumption enabled us quantitatively to relate wall currents, charge densities, and axial potential gradient. Now what "*temperature ionisation*," when properly used, means, is just that the electron energies are so low and densities are so high in the arc column that



they do a little ionization directly, or in successive impacts. Thus most of the ionization of gas molecules of  $E_i < 10$  volts is *not accomplished directly by electron impact, but indirectly by energy furnished by electrons to the molecules of the gas*. That is, the electrons and ions create a high temperature, e.g., high kinetic energy of the gas molecules, and these produce the needed new ions indirectly. Why this detail of mechanism, which is so relatively unimportant in the arc economy, should be so insisted upon as important and receive such prominence that it leads to confusion and misunderstanding in the minds of students and others, the author cannot understand. Perhaps the fact that human beings like comfortable *catch words*, that enable them to avoid thinking any more than necessary, furnishes the clue to this overemphasis.

There is, however, a very definite value to the proof of a semi-equilibrium state, such as Ornstein<sup>12</sup> has given, and even more to the proper use of the Saha<sup>25</sup> equation. First, the data enable the spectroscopists to know how far they can go in interpreting their spectral studies as regards temperature measurement and transition probabilities. Secondly, it permits us to infer at once from the temperature the densities of positive ions and electrons in any section of the column to which the law applies, provided that  $E_i$  for the gas is known. Ornstein has shown that one cannot in all probability apply it where  $E_i > 10$  volts, i.e., to the inert-gas arcs. He has shown that it certainly does not hold very near the cathode or the anode nor in the lower-pressure arcs, i.e., below about 7-cm pressure. For other restrictions see Mannkopf.<sup>23</sup>

Having now seen what is meant by the much-abused term, one may put it to use. For instance, Suits<sup>13</sup> in a Cu arc found  $T = 4000^\circ \text{K}$  in the column. From the atom density of  $N_0 = 1.8 \times 10^{18}/\text{cm}^3$  at  $4000^\circ$  and a value of  $E_i$ , one should from Saha's equation evaluate  $N_i$ . Unfortunately in a Cu arc  $E_i$  is not known for a composite gas showing  $\text{N}_2$  bands and Cu lines. However, from  $T$ , assuming the electrons in equilibrium, which is not quite correct as Ornstein<sup>12</sup> points out, we can estimate the electron mobility  $k_e$  as shown in Chapter V. From the mobility and the potential gradient  $X_i$  in the arc column, obtained by means of drawing out the arc for the same current and measuring the increase in applied potential, one can estimate  $N_i$  from the current by  $j = N_i e X_i k_e$ . Hence if  $X_i$ ,  $j$ , and  $k_e$  are known, we can calculate  $N_i$ . Again the method of measuring  $X_i = \Delta V/\Delta \epsilon$  by drawing out the arc is not particularly good. In a uniform column of the glow discharge this procedure is accurate, but lengthening the open air arc column changes cooling and hence also  $V$ . From such a calculation, however, Suits found the total ion concentration  $N_i = 0.6 \times 10^{12}/\text{cm}^3$ , which makes  $N_i/N_0 = 0.3 \times 10^{-6}$ , with  $N_0$  the number of molecules of  $\text{N}_2$  per  $\text{cm}^3$ . Now the arc has a strong  $\text{N}_2$  band spectrum with Cu lines superposed. Hence the gas is  $\text{N}_2$  with some small amount of Cu vapor. That is,

there are  $N_0 N_2$  molecules, and  $N_{0\text{Cu}}$  Cu atoms, with  $N_i = N_{iN_2} + N_{i\text{Cu}}$ , i.e., composed of  $N_{iN_2} N_2^+$  ions and  $N_{i\text{Cu}} \text{Cu}^+$  ions. Since Cu has an ionization potential of 7.7 volts while  $N_2 = 15.9$ , one can calculate the value of  $N_{i\text{Cu}}/N_{0\text{Cu}}$  in the Saha equation from  $E_{i\text{Cu}}$  and  $T$ . One can also compute  $N_{iN_2}/N_0$  at  $T$  from  $E_{iN_2}$ . From these data with the observed value of  $N_i$  and the known value of  $N_0$ , setting  $N_i = N_{i\text{Cu}} + N_{iN_2}$ , we can compute  $N_{0\text{Cu}}$ ,  $N_{iN_2}$ , and  $N_{i\text{Cu}}$ . This gives a value of  $N_{0\text{Cu}}$  equivalent to  $7.5 \times 10^{-7}$  atmosphere of Cu vapor or  $5.7 \times 10^{-4}$  mm pressure.  $N_{i\text{Cu}}$  is found to be  $0.97 N_i$ , and  $N_{iN_2}$  is  $0.03 N_i$ .

This calculation may not be exactly correct, but it is nicely illustrative of how the Saha equation can be used. If the ratio  $N_i/N_0$  calculated from  $k_s$  and  $X_i$  is inserted into the Saha equation one could solve for  $E_{i\text{eff}}$ , the "effective" ionization potential of the arc, which is rather meaningless, but perhaps a useful empirical constant if the value of  $E_{i\text{eff}}$  does not change with  $j$ . The value of  $E_{i\text{eff}}$  thus calculated was 12.3 volts in Suits' case, which is not far off from a value of 11 calculated by v. Engel and Steenbeck<sup>36</sup> in a similar arc. These values lie between  $E_{iN_2}$  and  $E_{i\text{Cu}}$ . Analogously, v. Engel and Steenbeck consider an arc in air of  $R = 0.25$  cm, at 2 amp,  $X_i = 28$  volt/cm,  $T_0 = 4600^\circ \pm 350^\circ$  K,  $k_s = 1.8 \times 10^4 \sqrt{T/273}$ . This gives  $N_i = 3 \times 10^{13}$  electrons/cm<sup>3</sup>. If  $E_{iN_2}$  is used in Saha's equation,  $N = 4 \times 10^{11}$  electrons. If we use  $E_{iN_0} = 11$  volts, in Saha's equation this gives the observed value of  $N_i = 3 \times 10^{13}$  at  $T = 4650^\circ$  K. As was seen in the case of Cu, however, the problem is involved and the agreement is one of order of magnitude only.

The rate of loss of ions from the column by ambipolar diffusion and the energy loss by radiation and conduction have not been worked out. Horst and Ornstein<sup>13</sup> give the fraction of total energy input radiated from the positive column alone; for the C arc they are as follows:

TABLE XLVI

|                        |       |        |        |
|------------------------|-------|--------|--------|
| Current.....           | 5 amp | 10 amp | 14 amp |
| Per cent radiated..... | 0.8   | 1.4    | 3.0    |

The radiation is *small*, owing to the fact that the emission of the light proceeds only from the lines of atomic or band spectra, which are narrow with large non-radiating gaps between. Since these are assumed in thermal equilibrium they should emit as black-body radiators. For a continuous spectrum as at the electrodes in C the radiation is propor-

tional to  $\int_0^\infty E_\lambda d\lambda$ , while with a line or band spectrum it is proportional to  $\sum_{\lambda_1}^{\lambda_2} E_\lambda \delta\lambda$ , which is much less.

The large energy loss is by means of heat conduction, in the kinetic-theory sense, at high temperature, with, however, a very effective transfer by means of excited higher vibrational and rotational states as well as of metastable states and ions. The core of the arc, i.e., the true column, is thus surrounded by a considerable mantle of hot gas. For all arc columns in free gas spaces convection plays a very important role in the cooling. The air convection currents in the horizontal arc deflect the center of the column upward and tend to draw it out or lengthen it. If violent enough, the upward currents may draw the arc out to such a length that it cannot maintain itself at the existing potential and hence it will blow out. It is the convection currents which especially interfere with measurements of  $dV/dl = X_i$  by lengthening the column.

There is obviously a transport of positive ions from anode to cathode. In the vacuum Hg arc this transport is of considerable magnitude. Hence in operating such arcs a means must be provided for the Hg transported to the cathode to return to the anode. The transport of material and vaporization produces peculiar effects at the electrodes. In the C arc the anode has a crater developed, as if the C vaporized more rapidly from the hotter axial core of the C. It is in this region of the crater that the high values of  $T_{an}$  are observed. At the cathode, the arc tends to form the electrode into a cone. At the surface of the cone in some cases globules of molten C can be observed to form. The reason for this shape is obscure.

## 9. EXPERIMENTAL DATA

The d-c arc has been studied by numerous workers. The most exhaustive early study was made by Mrs. H. Ayrton,<sup>37</sup> who evolved the following experimental empirically expressed relation for various arcs, which has been subsequently amply checked. It relates the potential  $V$ , the arc length  $l$ , and the current  $i$  in the form

$$V = \alpha + \beta l + \frac{\gamma + \delta l}{i},$$

where  $\alpha$ ,  $\beta$ ,  $\gamma$ , and  $\delta$  are constants.

Obviously this equation can have no claim to great precision since the length of the arc is somewhat indefinite. In many arcs the electrodes are cupped at the positive end and conical at the negative end. Usually the crater edge is used in measuring. If instead we use the crater pit, Rasch claims that  $\gamma$  drops out. In general, the 4 constant equation gives the best results. If we plot  $V_i$  against  $i$ , it is seen that

$$V_i = (\alpha + \beta l)i + (\gamma + \delta l),$$

which is linear. Such straight lines are actually observed.

The values of the constants are given in Table XLVII.

TABLE XLVII  
AYRTON CONSTANTS FOR AIR

| Electrode Material | $\alpha$ | $\beta$ | $\gamma$ | $\delta$ | Remarks                               |
|--------------------|----------|---------|----------|----------|---------------------------------------|
| Carbon.....        | 38.9     | 2.0     | 16.6     | 10.54    | Cooled electrode                      |
|                    | 39.6     | 1.7     | 15.5     | 11.5     |                                       |
|                    | 45.8     | 3.33    | 35.7     | 19.3     |                                       |
|                    | 38.5     | 2.15    | 56.0     | 6.1      |                                       |
| Silver.....        | 50.0     | 15.8    | 9.0      | 32.0     | 4.5 amp taken in 1 sec                |
|                    | 19.01    | 11.30   | 14.19    | 3.64     |                                       |
| Copper.....        | 15.24    | 10.69   | 21.38    | 3.02     | Cooled electrodes<br>16-mm electrodes |
|                    | 26.61    | 2.22    | 32.44    | 18.65    |                                       |
| Iron.....          | 15.01    | 9.44    | 15.73    | 2.52     |                                       |
|                    |          |         |          |          |                                       |

AYRTON CONSTANTS IN DIFFERENT GASES (CARBON ARC)

|                | Stagnant Air | Moving Air | A    | CO <sub>2</sub> | N <sub>2</sub> |
|----------------|--------------|------------|------|-----------------|----------------|
| $\alpha$ ..... | 35.7         | 44.1       | 24.8 | 44.5            | 48.2           |
| $\beta$ .....  | 3.0          | 2.6        | 0.9  | 1.7             | 2.6            |
| $\gamma$ ..... | 114.6        | 17.8       | 10.2 | 18.2            | 23.3           |
| $\delta$ ..... | 1.8          | 1.8        | 0.0  | 8.7             | 5.3            |

VARIATION OF AYRTON CONSTANTS WITH PRESSURE (CARBON ARC IN AIR)

| $p$ in mm | $\alpha$ | $\beta$ | $\gamma$ | $\delta$ |
|-----------|----------|---------|----------|----------|
| 740       | 38.5     | 2.15    | 56       | 6.1      |
| 200       | 35.5     | 1.84    | 39       | 8.2      |
| 50        | 33.7     | 1.22    | 30       | 10.6     |
| 5         | 27.5     | 1.2     | 0        | 16.0     |

The following values for anode and cathode fall are given by the Ayrtton equation.

$$\text{Anode: } V_a = \frac{4\alpha}{5} + \frac{\gamma}{i} \quad \text{Cathode: } V_k = \frac{\alpha}{5} + \frac{\gamma}{i}$$

The gradient in the column is  $X = \beta + (\delta/i)$ . The  $\beta$  of this equation is shown by Hörmann <sup>41</sup> to be too large.

Nottingham has developed an empirical formula for the metal arc which reads

$$V = A + Bi^{-n},$$

which has  $n$  determined by  $n = 2.62 \times 10^{-4} T_B$ , where  $T_B$  is the boiling point of the metal. This may be a significant equation, although its validity has recently been seriously questioned by Suits.<sup>39</sup>

## 10. NEGATIVE CHARACTERISTIC AND OSCILLATIONS

The fact that the arc has a negative characteristic has certain consequences as regards stability. Let  $R$  be the resistance of the rest of the circuit and  $i$  the current, while  $E'$  is the emf of the current supply system. Then, if  $\alpha + \beta l = a$  and  $\gamma + \delta l = b$ , two constants in the Ayrton equation, we have

$$E' = Ri + a + \frac{b}{i}.$$

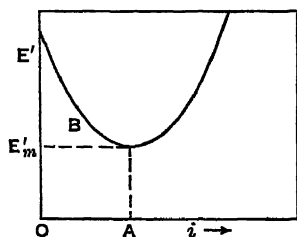


FIG. 284

Thus the graph of the relation is a hyperbola. This has a minimum  $E'$  at a value

$$E'_m = 2\sqrt{bR} + a$$

as shown in Fig. 284. The region B to the left of A is unstable. To study this, suppose that the current is changed from  $i_0$  to  $i_0 + x$  and that there is self-induction in the circuit. Then, replacing  $a + b/i$  by the more general  $F(i)$ , we can write

$$E' - L \frac{dx}{dt} = R(i_0 + x) + F(i_0 + x),$$

and, for small values of  $x$ ,

$$-L \frac{dx}{dt} = x[R + F'(i_0)],$$

where  $F'(i_0) = (dF/di)_{i_0}$ . Hence

$$x = Ce^{-\frac{t}{L}(R+F'(i_0))}.$$

If  $R + F'(i_0)$  is negative, as at B in the figure,  $x$  will increase with  $t$  and the current will be unstable. At A in the curve the quantity is 0, and to the right of A it is positive. Thus, for stability, the current must be greater than that at A, that is, greater than  $\sqrt{b/R}$ .

If  $F(i) = a + b/i$ , the value of  $i_m = \sqrt{b/R}$  and  $E_m = 2\sqrt{bR} + a$ , so that the arc will go out if the resistance,  $R$ , is greater than that given by the solution of

$$E_m = 2\sqrt{bR} + a \quad \text{or} \quad R_m = \frac{(E_m - a^2)}{4b}.$$

Hence for every  $E$  there is an external circuit value of  $R$  which, if exceeded, will extinguish the arc. This is given by

$$\frac{(E - a)^2}{4b} = R.$$

The same sort of conclusion can be arrived at by a graphical analysis which can be found in almost any article dealing with arcs. Introduction of the Ayrton constants gives

$$i_m = \sqrt{\frac{\gamma + \delta l}{R}}, \quad R_m = \frac{\gamma + \delta l}{i^2}, \quad l_m = \frac{i^2 R}{\delta} - \gamma.$$

The negative characteristic property of the arc can be used to produce electrical oscillations.

Assume that the inductance in the leads is so great that the current  $I$  is constant. Place a capacity  $C$  in series with the resistance  $R$  in the parallel branch  $B$  as in Fig. 285. Call the arc current  $x$ , and let that through the branch  $CR$ , or  $B$ , be  $y$ . Then at any instant  $I = x + y$ , where  $x$  and  $y$  are the components in the arc branch  $A$  and the condenser branch  $B$  respectively.

Let  $C$  be the capacity of the condenser and  $L$  the inductance of the circuit. If then  $E_0$  is the potential across the arc terminals, Kirchhoff's second law gives us

$$E_0 = L \frac{dy}{dx} + Ry + \frac{Q}{C}.$$

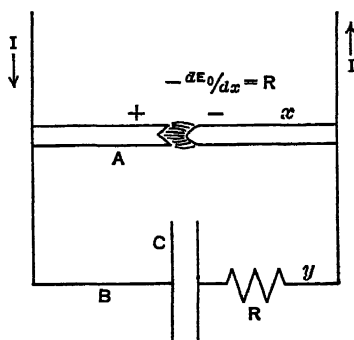


FIG. 285.—Circuit of the Singing Arc.

Now,  $dE_0/dt = (dE_0/dx) (dx/dt)$ ; but  $x + y = \text{constant} = I$ , and, differentiating,  $-dx = dy$ , so that  $dE_0/dt = - (dE_0/dx) (dy/dt)$ . Thus

$$- \frac{dE_0}{dx} \frac{dy}{dt} = L \frac{d^2y}{dt^2} + R \frac{dy}{dt} + \frac{y}{C}.$$

If now  $dE_0/dx$ , which is negative and is dimensionally a resistance, is chosen numerically equal to  $R$ ,  $-dE_0/dx = R$ , then

$$R \frac{dy}{dt} = L \frac{d^2y}{dt^2} + R \frac{dy}{dt} + \frac{y}{C},$$

so that

$$L \frac{d^2y}{dt^2} + \frac{y}{C} = 0.$$

Thus the negative resistance of the arc neutralizes the damping resistance  $R$  of the circuit.

The solution of this equation leads to an undamped oscillation. This is precisely one of the properties of a negative resistance. That is, the effective negative resistance of the arc annihilates the ohmic resistance of the line.

That the equation must lead to an undamped oscillation can be seen at once from the analogy to the well-known mechanical relation

$$m \frac{d^2x}{dt^2} = -kx, \quad x = A \sin t \sqrt{\frac{k}{m}}, \quad T = 2\pi \sqrt{\frac{m}{k}},$$

$$L \frac{d^2y}{dt^2} = -\frac{y}{C}, \quad y = A \sin \frac{t}{\sqrt{LC}}, \quad T = 2\pi \sqrt{LC}.$$

Under these conditions, the arc may emit an audible note, and is called a singing arc. This is *not* to be confused with the *hissing arc*, to be discussed later.

## 11. THE ARC RESISTANCE

The fact that the arc has a resistance makes it desirable to evaluate the resistance  $R_a$ . This can be measured by means of a high-frequency potential method, assuming no phase lag as shown by Duddell<sup>42</sup> and extended by Simon.<sup>43</sup> Then, if the current and potential are measured between two electrodes in the arc plasma, the resistance can be found. The high-frequency current can be measured by a thermogalvanometer, and the impressed potential can be compared with that across a variable resistance. Duddell, using 11-mm C electrodes, spaced 6 mm apart, with a direct current of 9.91 amperes and 100,000 cycles found a resistance  $R_a$  of 3.81 ohms. The potential drop  $E$  across the electrodes was 49.8 volts. Then, since  $E = V_a + iR_a$ , we have  $V_a = E - iR_a$ , and in the above case  $V_a = 12$  volts.

This potential is called the *counter emf of the arc*.

The resistance  $R_a$  for cored carbons varies with the current  $I$ , as

$$R = \frac{33.5}{I} + \frac{42}{I^2},$$

while  $V_a$  is constant.

In some combinations of cathodes and anodes we find  $V_a$  negative. This is especially the case if the anode is what is known in German as "Effect Kohle," a special type of carbon.

By means of probes we can apportion parts of  $V_a$  to the anode and cathode, as Hagenbach<sup>41</sup> has shown. Thus  $V_{aa} = E_a - iR_{aa}$  at the

anode, and  $V_{aK} = E_K - iR_{aK}$  at the cathode. Hence the fall in potential can be broken up into three regions as follows:

$$E = V_{aa} + iR_{aa} + V_{aK} + iR_{aK} + iR_{al},$$

in which  $R_{al}$  is the resistance of the column.

Thus, with ordinary carbons, we have, for example,

$$\begin{array}{lll} V_{aa} = 16.7. & iR_{aa} = 21.2. & E_a = 37.9. \\ V_{aK} = -6.1. & iR_{aK} = 13.2. & E_K = 7.2. \\ iR_{al} = +5.6 \times 0.76. & & \end{array}$$

The total  $E$  by addition is 67.8. The observed value is 68.6. This work was initiated by Hagenbach and Wehrli.<sup>31</sup>

In the case of cored carbons the reality of these potential drops can be seen. At the cathode, where the gradient is less, the atoms emitting are the core materials Na, Ca, etc., of low  $V_i$ . At the anode, where higher fields exist,  $N_2$  and CO lines are seen. Note that  $V_{aK}$  is negative, that is, the counter emf assists the current. At the anode it is positive and larger. These falls are due to thermionic space charges. At the cathode, electrons facilitate the current. At the anode, the thermionically emitted electrons *increase* the space charge and thus increase the anode fall, according to Hagenbach. This opposes the flow of current. Where the anode temperature is low and where the positive-ion creation from the anode is larger, relative to the thermionic electron emission,  $V_{aa}$  is small. The counter emf and  $V_{aa}$  both rise in magnitude with temperature.

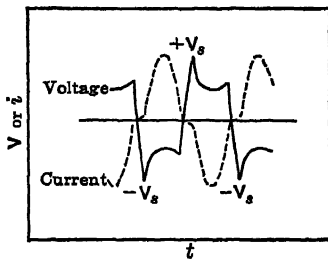


FIG. 286.

In general the a-c arcs will not be discussed in this book, but one or two points might be brought forward. An oscillogram of current and potential is given in Fig. 286.

The negative characteristic is clearly seen in the fall of  $V$  as  $i$  rises, and vice versa. It is seen that the arc goes out as the current passes through zero, and does not rekindle again until  $V$  reaches the striking potential  $V_s$ . This rekindling voltage increases with

1. Increasing arc length  $l$ .
2. Increasing external resistance.
3. Reduction in frequency.
4. All temperature-reducing factors.

This is clear, as it merely indicates that the rekindling process is a sort of spark mechanism, whose potential  $V_s$  depends on the conduc-



tivity of the old arc path, and the means for speedy breakdown. As a result of the difference in current and potential curves, an area is cut out in the  $V - i$  plane. That is, there is an actual a-c arc "hysteresis"

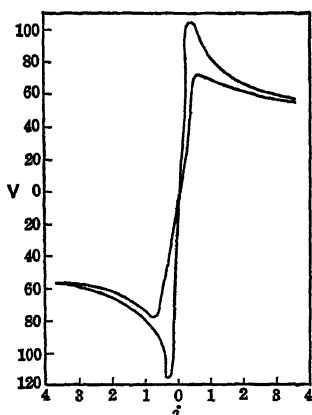


FIG. 287.

loop. This is shown in Fig. 287. The area represents power expenditure, to reignite, and thus to keep the arc going. Self-induction increases the sinusoidal nature of the arc and makes the periods of extinction shorter.

H. T. Simon<sup>44</sup> has worked out a complete theory of the a-c arc the main features of which are sustained by experiment. There is no place for it in this book.

## 12. OTHER ARC PROPERTIES

Before considering the theory of the arc, mention may be made of two more arc phenomena.

If we make the arc length too short for a given potential, we have the unpleasant hissing arc. This is due to oscillations in the vapor mass of the arc. It appears to be due to an excessive evaporation or ebullition at the anode at the high current density required by a short path and high potential. A cloud of vapor at the anode cools the arc and reduces the fall of potential at the anode so that the current increases. As soon as the current exceeds the value fixed by the stability conditions, it drops back and the cycle repeats. As the process is periodic, or better intermittent and of high frequency, we have the unpleasant sound produced by the pulsating vapor emission. It appears to occur above 70 amp/cm<sup>2</sup> with the C arc and is usually heard on first striking the arc.

Since an arc represents a current, we would expect it to be affected by a magnetic field. With the proper arrangement of field and current, the arc will rotate about a line as an axis. Poulson used the effect of a magnetic field in causing an arc to move so that it extinguished itself, in order to create undamped high-frequency oscillations for radio communication, before the development of the three-electrode tube. Today many of the large magnets built for high power Poulson arcs are being used in the construction of cyclotrons for the production of high-energy particles.

Finally, it is clear from the asymmetry of conditions at the cathode and anode of the arc, which has large current-carrying capacity, that conditions favoring the maintenance of such an asymmetry in one direction will impede arc formation in one direction and assist it in the other. Hence, in an arc with electrodes of different metals, or with

one electrode well cooled and the other not, etc., when alternating current is impressed, the arc will kindle for one polarity only on the electrodes. Hence, the arc *can be used as a rectifier for alternating current*.

Wide use is made of this for commercial rectification. Hg against a metal like W, in Hg vapor, will make a perfectly rectifying arc up to 3000 volts. This preference for one-way passage of an arc was also used in generating high-frequency alternating current in the days before the three-electrode tube. In this a condenser was charged to the rekindling potential of a rectifying arc by a d-c generator. This generator could not continuously furnish a current  $i_{\min}$  to maintain the arc, but the discharge current of the condenser was sufficient. Thus the arc, once struck, would burn until the condenser discharge had proceeded to a certain point. Then the arc would go out, and if the capacity,  $C$ , was charged to the rekindling voltage in a time sufficiently short it would reignite. Hence, depending upon the capacity  $C$ , upon the resistance of the generator circuit, and upon the striking voltage,  $V_s$ , of the arc, a series of unidirectional d-c surge impulses could be given to a tuned circuit, which would keep it in periodic sustained, and hence only slightly damped, oscillation.

### 13. THE CATHODE MECHANISM OF THE LOW-BOILING-POINT METAL-VAPOR ARCS

One may return now to the troublesome question of the cathode mechanism of the low-boiling-point metal arc. As was seen, the evidence in the case of the arcs for refractory metals is such that the thermionic theory of the cathode action is at once admitted. With the other metals the problem becomes more difficult. There is no doubt that the boiling point of Hg and Cu, etc., at 357°, 2300° C respectively, is well below the temperature of effective thermionic emission leading to electron current densities  $j \sim 3000$  to 4000 amp./cm<sup>2</sup>. These currents would require temperatures between 3000° and 4000° K, unless the high temperatures and fields materially lowered the thermionic work functions, which is doubtful. Now on *macroscopic* physical principles it is quite impossible to expect temperatures of the electrode surfaces in excess of 3000° K, when the substance boils at anywhere from 600 to 3300° K.

In view of this difficulty Langmuir<sup>1</sup> in 1923 and later Mackeown<sup>2</sup> proposed that the so-called *autoelectronic* emission, more properly termed *field emission* (see page 473), could supply electrons for the arc without the appeal to high temperatures. Many other workers have embraced the theory and have attempted to justify it in one way or another.<sup>3, 24, 45, 46</sup> This concept appeared the more plausible since the apparent temperatures, as evaluated at that time, at the hot spot surfaces of these cathodes appeared not to be far from the boiling points. Now it is true that, if we assume that the normal cathode fall is of the observed order, of 10 to 20 volts, and exists over distances of one or two

mean free paths from the cathode, say  $10^{-5}$  to  $10^{-4}$  cm, we get fields between  $10^5$  and  $10^6$  volts/cm caused by positive space charges at the cathode. Such fields can be augmented, as shown on page 474, by the action of small points on the surface to a value, at a maximum, of the order of ten times that calculated from applied potentials or space charge,  $\beta \sim 10$ . In order that this may be so, the irregularities at which the emission takes place must be very small indeed and hence incapable of giving very large currents (see page 474). The enhanced temperature would alter the field emission very little, but the field might lower the potential barrier slightly. On the basis of these data one may calculate the current *density* to be expected from such a micro-point,  $\beta = 10$ , and with  $X_c = 10^6$  volts/cm. For Cu one might set  $\phi_*$  at 3 volts, which is doubtless much too low even with the field acting. With these data inserted into the equation of Fowler and Nordheim, we have

$$j = 6.2 \times 10^{-6} \frac{\mu^{1/2} \beta^2 X_c^2}{(\mu + \phi_*) \sqrt{\phi_*}} e^{-\frac{6.8 \times 10^7 \phi_*^{3/2}}{\beta X_c}}$$

for Cu  $\mu = 7$  volts. Hence

$$j = 9.5 \times 10^{-6} \times 10^{14} e^{-35.3} = 9.5 \times 10^8 \times 4.6 \times 10^{-16} \\ = 4.4 \times 10^{-7} \text{ amp/cm}^2.$$

It is clear that the field currents, computed in this fashion, *would not account for the observed current densities of electron emission in the arc by many orders of magnitude.* On the other hand, the work of Penning and Mulder<sup>47</sup> and of Müller<sup>48</sup> indicates that the reasonable value of  $\beta$  used above may be too low. That is, on cold wire surfaces or points, *field emission currents* have been *assumedly* observed at fields of  $10^5$  volts/cm. These far transcended the values computed on this equation with  $\beta \sim 10$ . In fact, Penning and Mulder assigned values of  $\beta$  of the order of 200. The nature of these currents is not known. They were undoubtedly induced by fields at low pressures, and  $\phi_*$  may have been very low. As they *do not fit into the accepted theory of field emission* it is conceivable that they present a new phenomenon. Did such conditions as observed by Penning *exist at the arc cathode*, one could draw the obvious conclusion but the current densities even then would be relatively low. Unless, then,  $\phi_*$  is exceptionally low at the arc cathode, classical field current emission does not suffice. If  $\phi_*$  were very low, thermionic emission could also account for the currents. If then the observations of Penning and Mulder apply to arc cathodes, and an empirical equation is used, it is possible that one might agree with v. Engel and Steenbeck that some sort of field emission was possible. Theoretically, and within the experience of careful workers, the field-emission theory seems substantiated, and it is hard to reconcile field emission with the currents in arcs, much as these would facilitate the explanation.

On the other hand, it is doubtful in the author's mind whether it is necessary to postulate field emission in any case. Let us consider the Cu arc with a current of  $3000 \text{ amp/cm}^2$ . If but 3.3 per cent of the current (an exceptionally low estimate) is carried by positive ions, we have a current density of positive ions of  $100 \text{ amp/cm}^2$ . The cathode fall according to Nottingham is 20 volts. The energy imparted to  $1 \text{ cm}^2$  of surface in 1 sec is then 2000 joules, which gives 480 calories, neglecting losses and heat of neutralization. The specific heat of Cu is about  $0.1$  in this region. Thus 1 gram of copper would be raised to  $4800^\circ \text{C}$  in 1 second. If one remembers that heat flows slowly, the impact energy of these ions would not penetrate very rapidly, and one would have a sharp gradient of temperature at the surface. If one regard a layer of Cu  $10^{-5} \text{ cm}$  thick (about 500 atoms) and of  $1 \text{ cm}^2$  area, the mass of Cu is  $9 \times 10^{-5} \text{ gram}$ . With the influx of energy this layer would be heated to  $4000^\circ$  in  $7.5 \times 10^{-5} \text{ second}$ . A layer 50 atoms thick or about  $10^{-6} \text{ cm}$  would be raised to a thermionic emission temperature in  $7.5 \times 10^{-6} \text{ sec}$ .

With such a rate of transfer one can well raise the question as to what one means by temperature. It is clear that, in layers 50 atoms deep, in  $10^{-5} \text{ second}$ , with the rate of energy influx, one cannot speak of *thermal equilibrium*, nor is it probably correct to treat the surface layers as a macroscopic metal surface. Again the current is borne by  $1.25 \times 10^{22}$  ions striking a square centimeter of surface per second. Assuming the distance between atoms on the surface as  $2 \times 10^{-8} \text{ cm}$ , the area per atom is  $4 \times 10^{-16} \text{ cm}^2$ , so that on the average  $2.5 \times 10^{15}$  atoms form a monomolecular layer, and in  $2 \times 10^{-7} \text{ second}$  enough positive ions strike to yield a monomolecular layer of atoms over the surface.

Experiments on the momentum of the evaporated Cu vapor and the force on the cathode, by Tanberg,<sup>20</sup> indicate that all the evaporating Cu atoms measured by loss of weight from a Cu arc, plus most of the incoming ions, leave the cathode as neutral atoms with a velocity equivalent to a temperature of at least  $4100^\circ \text{K}$ . It is then quite legitimate to ask *whether one can properly speak of temperature* in the welter of incoming ions, outgoing atoms, and rapidly moving surface atoms in an atmosphere of gas. It even is more legitimate to ask whether the classical work functions assigned to an orderly and relatively cool surface, the macroscopic laws of heat conduction, and the macroscopic mechanism of evaporation in the confusing mass of ions and atoms can sensibly be applied to the active microvolumes at the cathode surface. It is clear that there is a welter of fast incoming and reflected ions and "hot" atoms at high pressure, whose condition is changing rapidly, such as have not been treated wave mechanically or otherwise. What is the work function and hence thermionic or field emission in such a state? It is not inconceivable that in the intense ionic force fields, with high energies, plus the imposed space charge

gradient, escape of electrons may be greatly facilitated. Whether this is called field emission or thermionic emission is again a purely academic question. Hence, irrespective of classically conceived temperatures, or field emissions, we actually often observe an enhanced emission of electrons adequate to explain the arc currents, from conditions which we have never before encountered.

The idea that our ignorance of the physics of the microprocesses is responsible for the difficulty in explaining the low-melting-point metal arcs receives support in many ways. In the Sloan X-ray tube the 1-mm thick Cu target was bombarded with currents of near  $10^{-2}$  ampere of electrons at  $10^6$  volts. It was water cooled on the inside. Yet the outer surface clearly showed that it had been raised to its melting point and flowed freely under the impact of the electron beam. This indicates the effect of rapid superficial energy transfer to a surface. Another indication lies in the many experiments made by Stolt,<sup>49,50</sup> Ramberg,<sup>45</sup> and others with rapidly rotating Cu discs as cathodes. In these, despite the presence of a rapidly moving cold cathode, the great rate of energy transfer to the surface raised its temperature to a point where it could furnish adequate electrons. The point of impact of the positive ions on the Cu indicates a peculiar pitting, which can either represent a loss of Cu (probably not owing to the low rates of evaporation), or else a fusion, vaporization, and flowing to the boundaries under the pressure impact of the positive ions. Calculations have been made on the temperature by Güntherschulze<sup>50</sup> and by Stolt.<sup>49</sup>

The great rate of energy transfer should have as its consequence a considerable evaporation of the metal. This should be very prominent in the Hg arc, especially if, as classically suggested, boiling takes place, preventing the formation of a macroscopically considered hot spot, which is assumed too cool to emit thermions. At first, results seemed to point to such an evaporative loss in measurements of Schaefer<sup>17</sup> and Güntherschulze.<sup>18</sup> The work of v. Issendorf<sup>19</sup> and later of Tanberg<sup>20</sup> and Kobel<sup>21</sup> shows the *net* evaporation to be relatively small. For Hg, Kobel finds about  $2 \times 10^{-5}$  gram/amp sec. With a current density of about 1900 amp/cm<sup>2</sup> the rate was  $3.25 \times 10^{-2}$  gram/cm<sup>2</sup> sec.

In attempting to calculate the temperature of the Hg in the hot spot, Compton<sup>24</sup> estimated a greater rate of evaporation, since, as he points out, many of the evaporating atoms are ionized and return to the cathode as ions. Thus he assumed that  $W = W_0 + 0.00209(1 - f)j$ . Here the 0.00209 is the electrochemical equivalent of Hg, and  $f$  is the fraction of the current carried by positive ions. From the well-known kinetic-theory equation relating vapor pressure to rate of evaporation and temperature,<sup>68</sup>  $p = 4W \sqrt{kT/3M}$ , one can get a series of values of  $p$  and  $T$  which would satisfy the equation. Assuming that the loss of Hg measured by Kobel<sup>21</sup> gave  $W_0$  and that the ordinary vapor pressure law for Hg holds at the hot spot, then we can uniquely fix the value of  $T$ . Depending on the value of  $f$  chosen, between  $f = 0.95$  and  $f = 0.8$ , the

temperature was on this assumption shown to lie between  $16^{\circ}\text{C}$  and  $202^{\circ}\text{C}$ . For the two values of  $f$ , Compton then estimated the length of the cathode fall  $d$  and compared it with the free path of the electrons at that temperature. At  $f = 0.95$ ,  $T = 167^{\circ}\text{C}$ ,  $p = 5.4\text{ mm}$ , the value of  $\lambda = 3.3 \times 10^{-4}\text{ cm}$ ,  $d = 3.9 \times 10^{-5}\text{ cm}$ ; at  $f = 0.8$ ,  $T = 202$ ,  $p = 19.6\text{ mm}$ ,  $\lambda = 8.4 \times 10^{-5}\text{ cm}$ ,  $d = 1.9 \times 10^{-5}\text{ cm}$ . Here we see that  $d$  is much less than  $\lambda$  and still less than the ordinary ionizing free path, unless the atoms have a very much larger cross section for excitation and ionization than for collision under ordinary circumstances. Compton, however, showed that by successive impacts the ionization could be accounted for adequately and used these data to support the theory of ionization by successive impact, which seems plausible. It is not certain, however, in view of what has been said before, that Compton's reasoning as to the *temperature of the hot spot has any significance* at all. This will become evident when we consider the momentum given the cathode.

The question of the temperature of the cathode spot becomes confused when the values of the rate of evaporation are related to the mechanical forces observed on the cathode spot. Early experiments by Schaefer<sup>17</sup> and Güntherschulze<sup>18</sup> giving larger amounts of evaporation than those of Tanberg<sup>20</sup> on the Cu arc, and Kobel<sup>21</sup> on the Hg arc, were shown by v. Issendorf<sup>19</sup> to have been falsified by spraying, or sputtering, of the metal vapor as the hot spot moved over the surface. This motion in the case of the Hg arc seems to be due to the heat penetrating the surface and raising the pressure above the boiling point in areas of sufficient size to cause local explosions, which blow the surface up and shift the discharge to a new unheated point. The values of the rate of evaporation of Tanberg and Kobel are, however, consistent and probably correct.

Now both Kobel and Tanberg *observed considerable pressures on the Hg or Cu, cathode*, which were confirmed by Tonks.<sup>22</sup> These were ascribed to the momentum of the "evaporating" atoms. By measuring the rate of evaporation and the force, or momentum per unit time, imparted by the occurrences at the cathode spot to the cathode, or to the vapor stream, both observers obtained concordant estimates of the *average velocity* of the "reflected or evaporating" Hg and Cu atoms. These were exceedingly high, indicating temperatures of  $300,000^{\circ}\text{K}$  for Cu to  $2 \times 10^6 - 12 \times 10^6^{\circ}\text{K}$  for Hg, or atomic energies of the order of 48 volts for Cu and 200–1200 volts for Hg. This interpretation of the data fitted in very nicely with the concept of an exceedingly high "temperature" of the cathode surface. In fact, it indicated a fantastically optimistic estimate of the temperature, when one tries to evolve a thermionic theory, for the energy of the atoms exceeds that of the incoming ions. However, Compton<sup>24</sup> correctly pointed out that there was a more plausible alternative interpretation. This was that with the large number of impacting positive ions, of some 10 volts

energy, a certain fraction in the order of per cent were reflected, or re-emitted as neutral atoms of Hg of very high energy. Such reflection had been observed by Compton and Van Voorhis with He, Ne, and A.<sup>51, 52, 53</sup> These could furnish the momentum observed and would not indicate a high vapor temperature. To understand this consideration we must look at the quantitative data. Kobel's value of the apparent, or net, rate of evaporation amounts to  $(1.7 \times 10^{-5})/200 \times 6 \times 10^{23} j$  atoms of Hg per  $\text{cm}^2 = 5 \times 10^{16} j$  atoms/ $\text{cm}^2 \times \text{sec}$ . On the other hand, the number of positive ions striking the surface is  $6.3 \times 10^{18} j^+ = 6.3 \times 10^{18} j (1 - f)$ , where  $f$  is the fraction of the current borne by electrons. We have in general chosen  $f$  as roughly 0.9 in these arcs, so that we have  $6.3 \times 10^{17} j$  positive ions striking the surface, with roughly 10 volts energy/ $\text{cm}^2/\text{sec}$ , of which only  $5 \times 10^{16} j$  appear to evaporate as a net loss in weight of the cathode. However, the fact that the cathode loses weight at the rate  $5 \times 10^{16} j$  atoms/sec, while the cathode is gaining by deposition about  $6.3 \times 10^{17} j$  atoms by ion deposition, means that, *for 1 atom evaporating as a net loss, roughly 11 atoms actually evaporate*. Thus the *measured* loss of weight yields  $5 \times 10^{16} j$ , while the real loss is  $5 \times 10^{16} j + 6.3 \times 10^{18} j (1 - f)$ . Thus all the *velocities* reported by Tanberg and Kobel must be divided roughly by 11, and more correctly multiplied by

$$\frac{5 \times 10^{16}}{5 \times 10^{16} + 6.3 \times 10^{18}(1 - f)},$$

and the computed energies must be divided by roughly  $(11)^2 = 121$ , or be multiplied by  $\left[ \frac{5}{5 + 6.3 \times 10^2(1 - f)} \right]^2$ . These yield *average* temperatures of 16,000 – 95,000° K, or 1.6 to 9.5 volts energy, spread over *all the "evaporating" atoms*.

Studies of the impact of ions on surfaces have shown that not all the ions striking remain on the surface. A considerable number rebound as *neutral atoms*, but with considerable of their initial energy. Compton and Van Voorhis<sup>54</sup> had measured this quantity indirectly for He, Ne, and A ions and called the accommodation coefficient  $a$  the fraction of the incident ion energy given up to the cathode. Lamar<sup>52, 55</sup> later directly measured  $a$  for He and found it to be about 0.5. These measurements were made in low-voltage low-pressure arcs. In these  $j$  is not high and the fraction of current carried by electrons  $f$  is relatively low,  $\sim 0.5$ , which is not true for the Hg arc.

Assuming that in the case of these positive Hg ions in the arc an accommodation coefficient was active, Compton,<sup>54</sup> on the basis of simple considerations, has shown that these fast recoiling neutral atoms give momentum to the cathode and depart with a high velocity lying between their initial energy and zero. If the accommodation coeffi-

cient  $a$ , the fraction of the energy of the ions given to the cathode, is less than unity, we can reason as follows:

TABLE XLVIII

|   |  |
|---|--|
| 1. Positive-ion current at cathode                              | $= j(1 - f)$ amp.                      |
| 2. Mass of positive ions striking cathode/sec                   | $= 0.00209j(1 - f)$ g.                 |
| 3. Number of positive ions striking/sec                         | $= 0.63 \times 10^{18}j(1 - f)$ .      |
| 4. Kinetic energy of positive ion (10 volts)                    | $= 1.59 \times 10^{-11}$ erg.          |
| 5. Total kinetic energy of ions striking/sec                    | $= 1 \times 10^8 j(1 - f)$ erg.        |
| 6. Total kinetic energy of neutralized ions leaving cathode/sec | $= 1 \times 10^8 j(1 - f)(1 - a)$ erg. |
| 7. Total momentum of neutralized ions leaving cathode/sec       | $= 647j(1 - f)\sqrt{1 - a}$ dyne.      |

The pressure on the cathode spot is given by equation 7 if the atoms leave the surface normally. If they leave in random directions, as was the case for He, then we must use just one-half the quantity in equation 7. Hence  $p = 0.33j(1 - f)\sqrt{1 - a}$ , gram  $\text{cm}^{-2}$ . From the average pressure of Kobel, which was 5.75 cm Hg or 78.2 g  $\text{cm}^{-2}$  at a spot where  $j = 1912$  amp/ $\text{cm}^2$ , the following results may be computed:

TABLE XLIX

|                           |       |      |      |      |      |
|---------------------------|-------|------|------|------|------|
| $f$ .....                 | 0.5   | 0.6  | 0.7  | 0.8  | 0.9  |
| $a_{\text{normal}}$ ..... | 0.985 | 0.98 | 0.96 | 0.90 | 0.62 |
| $a_{\text{random}}$ ..... | 0.95  | 0.92 | 0.84 | 0.60 |      |

It is seen that we must make  $f$  small if  $a$  is to be large. This means that either a much smaller proportion of the current is carried by electrons,  $j^+$  must be large, or else to get the very large momentum transfer observed *a must be small*. In fact, the value of  $a$  is so low for random reflection that Compton does not give it if we assume that  $f = 0.9$  as we have done in this chapter.

The significance of this fact must not be lost. This means that with reasonable assumptions as to the fraction of current borne by electrons we must assume that *almost every positive ion incident on the cathode plus a few more atoms "evaporate" or are reflected with a high energy*. Now, just previously, Compton,<sup>24</sup> on the basis of the observed mass evaporation rate alone, had estimated the "temperature" of the cathode spot. This estimate *was legitimate if the atoms largely come off with thermal energies*. However, *reasonable values of  $f$  cannot be had unless  $a$  is very low*, because of the high values of the observed pressure. The required values of  $f$ , and hence of  $a$ , definitely indicate that "evaporation" in the classical sense cannot be assumed in order to compute the "temperature" of the cathode spot, and that a considerable fraction of the Hg atoms lost from the cathode have energies in the order of volts.

This very important fact brings us once again to the conclusion already suggested. That is that, under the unusual conditions at the cathode spot, it ceases even to be an academic question whether we



can speak of evaporation, reflection, and an accommodation coefficient in the classically accepted meaning of the terms. The same applies to the use of the terms *thermionic* and *field emission* as classically defined. We are faced with a new physical situation, or even a new physical state, when we deal with enormous energies put into small volumes of matter in exceedingly short time intervals. It behooves physicists and engineers to cease quibbling about inapplicable catchwords and terminology and to concentrate their efforts to evolve a new physics of the microvolume with high rates of energy input. With this statement we may leave the subject of the mechanism of the low-boiling-point metal arc and turn to another arc problem whose solution is in a more satisfactory state.

#### 14. THE LOW-VOLTAGE ARC

Before closing the section on arcs it is inspiring to consider the mechanism of a once baffling phenomenon which is now fairly satisfactorily solved. This is the question of the low-pressure, low-voltage arc. The low-voltage arc came into prominence between 1915 and 1917, when it was observed that these arcs would operate on high currents with total potentials across their electrodes of less than the ionizing potential of the gas.<sup>54, 55, 56, 57, 58</sup> Arcs operating in Hg as low as 4.9 volts were known before 1917. Since then 2 volts have been reported for Cd arcs and 1.8 volts for Hg arcs.<sup>60, 61</sup> An arc in He started above 19.8 volts, its first excitation potential, was reduced down to 8 volts before it went out.<sup>59</sup> It was at first assumed that the potential difference in such arcs must be as great as, or greater than,  $E_i$  for the gas. This belief, in fact, aided in the confusion as to the value of the ionizing potential of Hg, during the period before the Bohr interpretation of spectra triumphed; for the 4.9-volt Hg arc pointed to a value of  $E_i$  for Hg of 4.9 volts until properly interpreted by Van der Bijl.<sup>57</sup>

With high current densities, it was suggested by Van der Bijl<sup>57, 58</sup> that excited atoms could be ionized by successive impacts so that arcs could operate below  $E_i$ .<sup>62</sup> The possibility that this would occur became greater when metastable states were recognized. When arcs using hot cathodes were observed to burn below  $E_i$  the problem again became acute.<sup>60, 61</sup> This was particularly so when Holst and Oosterhuis showed that these arcs operated in the absence of any oscillations.<sup>66</sup>

If a source of electrons from a heated cathode is provided, either oxide coated or otherwise, from which ample electron currents can be drawn, then the arcs will operate well below the excitation potentials at the values indicated above. This fact baffled the physicists for some time until Compton and Eckart<sup>65</sup> in 1925 made probe measurements in the low-voltage arc between an oxide-coated tungsten wire  $W$  and an anode of Ni with A gas. The distribution of potential was quite peculiar, as shown in the diagram of Fig. 288. It is there seen that in front of, and in fact all around, the cathode there is a positive space

charge close to 11.7 volts, the excitation potential of A. If contact potentials are corrected for, it may well be above 11.6 volts. Thus with successive ionization in heavy currents the gas could be maintained in conducting state.

The cause for the space-charge accumulation is readily explained in that the electrons, being mobile and having a large area of anode to collect on, are removed, leaving behind a considerable space charge of positive ions which cannot be removed as rapidly in the existing fields. Thus the space charge builds up so that the space potential is 11.7 volts to the cathode at zero. The *average* electron energy is seen to be relatively high in the high-field regions, and the electron densities in the high-field region are quite high for such low pressures, i.e., of the

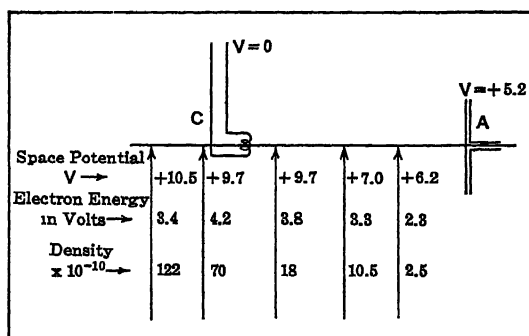


FIG. 288.

order of  $10^{12}$  electrons/cm<sup>3</sup>. From the electron energies observed one can expect excitation and ionization by cumulative impacts.

There was one serious difficulty, however, which will become clearer when we regard some later measurements made by Druyvesteyn.<sup>67</sup> Druyvesteyn<sup>67</sup> used A and Ne gas with a W cathode, a BaO-coated cathode, or an indirectly heated BaO cathode, and a fine W probe of 100 to 50 microns diameter, quartz insulated. His cathodes were of Ni. Contact potentials were large. The results of his measurements in A and in Ne are shown in the curves of Fig. 289 plotted in millimeters from the cathode at 0 potential. The scale on the extreme left and the full curve give the space potential, not corrected for contact potentials; the dashed curves give the electron concentration with the scale on the right; the dot-dashed curves give the average electron energy with the inner scale on the left. The excitation potential of the 1 S state of A is 11.7 volts, and that of the 2 p state of Ne is 18.5 volts. Now it is seen that the electrons which have left the cathode can get the excitation energy of either A or Ne in virtue of the positive-ion space charge, which, when corrected for contact potentials, is adequate. Those electrons that escape ionizing will lose 5.5, or 12.2, volts in bucking the

decelerating positive space charge after leaving the peak and reaching the anode. Those electrons with the 0.1 volt or so of energy left them after exciting an A atom, just beyond the peak of the potential curve, *have no chance of reaching the anode*. These electrons should thus accumulate and build up a neutralizing electron space charge. Thus the arc should extinguish itself. There must be some way in which this difficulty is overcome.

Holst proposed that the electron could be captured by an ion, but not radiate, and in a second encounter with an electron could give that electron its energy so that the second electron could get to the cathode. Calculation by Druyvesteyn<sup>67</sup> showed that this occurrence was too rare to count appreciably. It is also possible that an electron could get energy by many impacts with fast atoms. This again is an unlikely

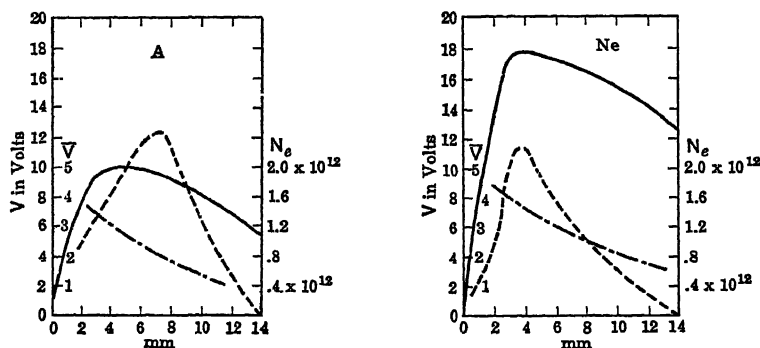


FIG. 289.

process. If the metastable atoms gave the electrons their energy by inelastic impacts of the second class, see Loeb *Atomic Structure*, page 319, then we could get the energy to carry the electrons to the anode. But this would remove all the metastable atoms so vital to the operation of the arc.

The solution proposed by Druyvesteyn, however, is exceedingly simple. There are *plenty of high-energy electrons in the gas that do not ionize*. If these give some of their energy in Coulomb-force encounters to the slow electrons that have just ceased exciting, then these electrons can both proceed to the anode against the 4.5 and 5.2 volts retarding potentials in A and Ne. An analysis of the exchange of electron energy shows that the collision cross section for the transfer of adequate energy from a fast to a slow electron is of the order of  $\sigma_e = 2.8 \times 10^{-16} \text{ cm}^2$ , i.e., that of an ordinary kinetic-theory collision cross section with an atom. Thus, if  $\sigma_e$  is this cross section and there are  $C_1$  slow electrons of velocity  $v_1$  and  $C_2$  fast electrons of velocity  $v_2$  per  $\text{cm}^2$  with  $v_2 \gg v_1$ , the number of transfer encounters per second will be  $N_e = C_1 C_2 v_2 \sigma_e$ . One may compare this with the kinetic-theory collisions between the  $C_1$

slow electrons of velocity  $v_1$  and the  $C_a$  atoms of A or Ne, per  $\text{cm}^3$  of gas. If  $\sigma_a$  is the Ramsauer collision cross section, then  $N_a = C_a C_1 v_1 \sigma_a$ . From this we can evaluate the relation between  $N_a$  and  $N_e$ . If  $C_2 = 2 \times 10^{12}$ , and the pressure is 6 mm, as in one of the experiments, then  $N_a = 3 \times 10^4 N_e$ . This means that the slow electron gets the energy to go to the anode once in  $3 \times 10^4$  impacts with atoms. The region of the potential peak where these exchanges occur is about 3 mm wide. In crossing such a space at 6-mm pressure with the existing fall of potential across 3 mm only, the electron will make  $1.2 \times 10^3$  collisions with atoms. It is seen that this is only  $1/25$  of the number of collisions needed before the electrons gain energy enough to get to the anode. In the weak-field region at the potential peak this gives ample opportunity for the electrons to get the energy.

To understand how the low-voltage arc operates on this point of view we may with Druyvesteyn consider a specific case. Take, for example, an electron in a low-voltage arc in A operating at 7.0 volts. The excitation potential of A is 11.7 volts. The peak of the potential curve will be in the neighborhood of 11.7 volts. This is true in the case above, where the space potentials, which are lower, have not been corrected for contact potential. It loses its 11.7 volts and starts with 0.1 volt energy. It needs  $11.7 - 7 = 4.7$  volts to reach the anode. After roughly  $3 \times 10^4$  collisions with atoms at 6-mm pressure in the peak it interacts with an 11.7-volt electron and gets its 4.7 volts. Both electrons then reach the anode. This is nicely corroborated by means of the probe studies. The energy distribution of the electrons is Maxwellian. The potentials given in Fig. 289 must be corrected for the contact potentials involved. These were high in the case of the W, W + BaO cathodes and the Ni anode. The real peak of the A curve was at 12 volts, which is very close to 11.7. In Ne the true potential was 19 volts, which is close to the value 18.5 expected. The concentrations of  $2.5 \times 10^{12}$  electrons/ $\text{cm}^3$  at the peak are in excellent agreement with the predictions of the theory and with Compton and Eckart's measurements.

It is thus seen that here at least one of the baffling arc discharge problems has been quite satisfactorily solved by recourse to a study of the fundamental processes in the conduction of electricity through gases.

## 15. REFERENCES FOR PART B, CHAPTER XI

1. I. LANGMUIR, *Science*, **58**, 290, 1923; *Gen. Elec. Rev.*, **26**, 731, 1923.
2. S. S. MACKBOWN, *Phys. Rev.*, **34**, 611, 1929.
3. v. ENGEL and STEENBECK, *Elektrische Gasentladungen*, Springer, 1934, Vol. 2, p. 134 ff.
4. J. J. THOMSON, *Conduction of Electricity through Gases*, Cambridge Press, Cambridge, 3d Edition, 1933, Vol. 2, pp. 596 ff.
5. A. HAGENBACH, GEIGER and SCHEEL, *Handbuch der Physik*, Julius Springer, Berlin, 1927, Vol. XIV, Chapter 6, p. 342 ff.

6. W. B. NOTTINGHAM, *J. Franklin Inst.*, 206, 43, 1928; 208, 191, 1929.
7. M. J. DRUYVESTEYN, *Z. Physik*, 73, 727, 1932.
8. v. ENGEL and STEENBECK, reference 3, Sec. 53, p. 119.
9. R. C. MASON, *Phys. Rev.*, 51, 28, 1937.
10. NAGAOKA and SUGUIRA, *Jap. J. Phys.*, 3, 45, 1924.
11. LOEB, HILLEBRAND, WHITE, VARNEY and MILLER, *Phys. Rev.*, 49, 703, 1936.
12. L. S. ORNSTEIN, *Physica*, 1, 797, 1934; *Litt.*, p. 817.
13. G. G. SUITS, *Physics*, 6, 190, 315, 1935.
14. K. T. COMPTON, *Phys. Rev.*, 21, 266, 1923; SLEPIAN and HAVERSTICK, *Phys. Rev.*, 33, 52, 1929.
15. LAMAR and COMPTON, *Phys. Rev.*, 37, 1069, 1931.
16. v. ENGEL and STEENBECK, reference 3, p. 132.
17. SCHAEFER, dissertation, Darmstadt, 1910.
18. A. GÜNTHERSCHULZE, *Z. Physik*, 11, 74, 1922.
19. J. v. ISSENDORF, *Physik. Z.*, 29, 857, 1928.
20. R. TANBERG, *Phys. Rev.*, 35, 1080, 1930.
21. E. KOBEL, *Phys. Rev.*, 35, 1636, 1930.
22. L. TONKS, *Phys. Rev.*, 50, 226, 1936.
23. v. ENGEL and STEENBECK, reference 3, p. 134 ff.
24. K. T. COMPTON, *Phys. Rev.*, 37, 1077, 1931.
25. A. GÜNTHERSCHULZE, *Z. Physik*, 31, 508, 1925.
26. J. STARK, *Physik. Z.*, 5, 51, 750, 1904.
27. COMPTON and LAMAR, *Science*, 71, 517, 1930; *Phys. Rev.*, 37, 1069, 1931.
28. R. SEELIGER, *Physik. Z.*, 27, 37, 1926.
29. *Brown & Boveri Review*, 16, 61, 1929.
30. v. ENGEL and STEENBECK, *Wiss. Veröffentlich. Siemens-Konzern*, 10, 156, 1931; 12, 87, 1933.
31. HAGENBACH, PERCY and WEHRLI, *Z. Physik*, 20, 96, 1923; 26, 23, 1924; also reference 5, p. 342.
32. v. ENGEL and STEENBECK, reference 3, p. 137 ff.
33. R. MANNEKOFF, *Z. Physik*, 86, 161, 1933.
34. J. SLEPIAN, *Phys. Rev.*, 26, 407, 1926.
35. M. N. SAHA, *Phil. Mag.*, 40, 472, 809, 1920; *Proc. Roy. Soc.*, A 99, 135, 1921; M. N. and N. K. SAHA, *Treatise on Modern Physics*, India Press, Allahabad, 1934, Vol. I, p. 632.
36. v. ENGEL and STEENBECK, reference 3, p. 143.
37. H. AYRTON, *The Electric Arc*, The Electrician Publishing and Printing Co.
38. W. B. NOTTINGHAM, *J. Am. Inst. Elec. Eng.*, 42, 12, 1923.
39. C. G. SUITS, *Phys. Rev.*, 46, 252, 1934.
40. H. WITTE, *Z. Physik*, 88, 415, 1934.
41. H. HÖRMANN, *Z. Physik*, 97, 539, 1935.
42. DUDELL, *Electrician*, 46, 269, 1900; 51, 902, 1903.
43. H. T. SIMON, *Physik. Z.*, 7, 433, 1906.
44. H. T. SIMON, *Physik. Z.*, 6, 297, 1905.
45. W. RAMBERG, *Ann. Physik*, 12, 314, 1932.
46. BECKEN and SOMMERMEYER, *Z. Physik*, 102, 551, 1936.
47. PENNING and MULDER, *Physica*, 7, 724, 1935.
48. E. W. MÜLLER, *Z. Physik*, 102, 734, 1936.
49. H. STOLT, *Ann. Physik*, 74, 80, 1924; *Z. Physik*, 26, 95, 1924; 31, 240, 1925.
50. A. GÜNTHERSCHULZE, *Z. Physik*, 28, 235, 1924.
51. VAN VOORHIS and COMPTON, *Phys. Rev.*, 37, 1596, 1931.
52. E. S. LAMAR, *Phys. Rev.*, 37, 842, 1931; 43, 169, 1933.
53. COMPTON and LAMAR, *Phys. Rev.*, 44, 338, 1933.
54. J. C. MCLENNAN, *Proc. Roy. Soc.*, A 91, 485, 1915; A 92, 305, 1916.
55. T. C. HEBB, *Phys. Rev.*, 9, 372, 1917; 11, 170, 1918; 12, 482, 1918.
56. J. T. TATE, *Phys. Rev.*, 7, 686, 1916.

57. H. J. VAN DER BIJL, *Phys. Rev.*, 9, 173, 1917.
58. H. J. VAN DER BIJL, *Phys. Rev.*, 10, 548, 1917.
59. COMPTON, LILLY, and OLMSTEAD, *Phys. Rev.*, 16, 282, 1920.
60. T. C. HEBB, *Phys. Rev.*, 16, 375, 1920.
61. Y. T. YAO, *Phys. Rev.*, 21, 1, 1923.
62. R. A. MILLIKAN, *Phys. Rev.*, 9, 378, 1917.
63. F. KANNENSTINE, *Astrophys. J.*, 55, 355, 1922.
64. BÄR, LAUE and MEYER, *Z. Physik*, 20, 83, 1923.
65. COMPTON and ECKART, *Phys. Rev.*, 25, 139, 1925.
66. HOLST and OOSTERHUIS, *Physica*, 4, 42, 1924.
67. M. J. DRUYVESTEYN, *Z. Physik*, 64, 782, 1930.
68. L. B. LOEB, *Kinetic Theory of Gases*, 2nd Edition, McGraw-Hill, New York, 1934, p. 106.



## APPENDIX I

### 1. THE KINETIC NATURE OF A GAS

**a. The Pressure of a Gas.** It is necessary that one review a few fundamental facts concerning the kinetic nature of a gas.

The atomic theory of matter, together with a study of the mechanical equivalent of heat and the evolution of the law of conservation of energy between 1800 and 1850, led to the conclusion that the gaseous state could be described in terms of a vast assemblage of minute atoms or molecules moving freely in space in a chaotic fashion with their own proper heat motions. Thus it is not strange that in 1845 Joule should have shown correctly that the pressure of a gas  $p$  is due to the momentum contributed by the myriad of atomic or molecular encounters with the surface of the containing vessel in unit time. The expression which he derived reads  $pv = \frac{1}{3}nmC^2 = R_vT$ . Here  $C$  is a special average value of the molecular velocity,  $m$  is the mass of the molecule,  $n$  is the number of molecules in the volume  $v$ , and  $R_v$  is the ideal gas constant for this volume, while  $p$  is the pressure and  $T$  is the absolute temperature. Dividing through by  $v$ , one has

$$p = \frac{1}{3} N m C^2 = \frac{R_v}{v} T = R_1 T.$$

Here  $N = n/v$ , the number of molecules per unit volume, hereafter referred to as the Loschmidt number, and  $R_1$  is the ideal gas constant per cubic centimeter.  $N = 2.69 \times 10^{19}$  molecules/cm<sup>3</sup> at 0° C and 760 mm pressure. If the other quantities are in cgs units,  $p$  is in dynes per square centimeter.

It is frequently advantageous to speak of a mole of gas. This is a mass of gas equal to the molecular weight expressed in grams. Since the mass of gas used is in proportion to the mass of the molecules, and since equal volumes of gases have equal numbers of molecules, then as the masses of 1 cm<sup>3</sup> of different gases, i.e., their densities, under standard conditions are in proportion to the molecular weights, the volumes of a mole of different gases will all be equal. The volumes are experimentally equal to 22,414 cm<sup>3</sup>. This is called the molar volume. Thus, according to Avogadro's rule, a mole of any gas has the same number of molecules: to wit,  $2.69 \times 10^{19} \times 22,414 = 6.023 \times 10^{23}$  molecules at 0° C and 760 mm. The value of the gas constant for a mole is  $R_A =$



$22,414 R_1 = 8.3 \times 10^7$  ergs per degree C or 1.988 calories per degree. Since  $\frac{1}{2}NmC^2 = R_1T$ ,  $\frac{1}{2}N_A mC^2 = R_A T$ , and the kinetic energy of the mole of gas  $\frac{1}{2}N_A mC^2 = \frac{3}{2}R_A T$ . Hence the average kinetic energy of the  $6.02 \times 10^{23}$  gas molecules at a temperature  $T$  is  $\frac{3}{2}R_A T$ . The average energy of 1 molecule is then

$$\frac{1}{2} mC^2 = \frac{3}{2} \frac{R_A}{N_A} T = \frac{3}{2} kT.$$

Here  $R_A/N_A = k$  is the gas constant per molecule. It is named after Boltzmann the *Boltzmann constant*. It is of frequent occurrence in equations involving gaseous discharges.

The average molecular velocity  $C$  is given at once by  $p = \frac{1}{3}NmC^2 = R_1T$ . Since the density of the gas is  $Nm = \rho$ , we have  $C = \sqrt{3p/\rho}$ .  $C$  is independent of the variation of  $p$ , for  $p/\rho$  is a constant at any given temperature. Since

$$C = \sqrt{\frac{3R_1T}{Nm}} = \sqrt{\frac{3kT}{m}},$$

it is seen that  $C$  is proportional to  $\sqrt{T}$  and to  $1/\sqrt{m}$ . The more massive a molecule the slower its speed, and the higher the temperature the greater the molecular speed. Since  $v$  the velocity of sound is approximately given  $v = \sqrt{\gamma p/\rho}$ , where  $\gamma$  is the ratio of the specific heats which varies from 1.66 for atomic gases to nearly 1.1 for complex molecules, it is seen that the molecules travel slightly faster than the compressional sound wave which they transmit. The speed is about that of a low-velocity rifle bullet. The value for  $H_2$  molecules at  $0^\circ C$  is  $1.84 \times 10^5$  cm/sec, and for  $O_2$  molecules it is  $4.61 \times 10^4$  cm/sec. Any other velocities can be derived from these by means of the laws cited above. As the electronic mass is closely  $1/1836$  that of the H atom the electronic velocity is about 60.6 times that of the  $H_2$  molecule.

**b. Molecular Free Paths.** Now while molecules are very small, having radii of the order of  $1.5 \times 10^{-8}$  cm for the outer electronic shells of smaller configurations, they are not indefinitely small. Hence collisions between them are not unexpected. The shapes of molecules have been suggested by the form of the outer electronic shells or levels, and while these are not spherically symmetrical, being more ellipsoids than spheres, it is a great mathematical convenience to treat them as equivalent elastic spheres of diameter  $\sigma$ . In kinetic theory in general it is more convenient to use the diameters  $\sigma$  than the radii  $r$ , since in impact the *molecular centers* approach each other to within  $\sigma$  cm. When an electron encounters an atom the approach at impact is more nearly  $r$  as the electronic radius is  $\sim 10^{-13}$  cm.

The paths of molecules between impacts are straight lines until the molecules are very nearly  $\sigma$  cm apart.\* If the gas is near its condensation temperature, or far from being a perfect or ideal gas, the mutual attractions of molecules bend the paths so that they are curved over appreciable distances. In liquids the paths are no longer straight at all. As temperature increases and the molecules move more rapidly the deviations from rectilinear paths become less. At low pressures the paths are straight over long stretches. The curvatures of the paths due to attractions between molecules have the effect of making collisions more frequent. As temperature increases and paths straighten the molecules *collide* less frequently and the paths increase in length. This increase has been taken as a decrease in molecular diameter with increase in energy. Actually  $\sigma$  remains nearly constant, but the *apparent*  $\sigma$  inferred from free paths does decrease as  $T$  increases.

If the pressure is about 0.01 mm the free paths begin to approach a centimeter in length, and, in vessels of finite size, collisions of molecules with the walls will not be uncommon. At atmospheric pressure, however, the tremendous numbers of molecules make the chance of a molecule  $A$  in the interior of the gas colliding with the walls practically zero. Hence in the body of a gas the molecule  $A$  in question is surrounded by a highly irregular surface produced by describing a radius  $\sigma$  about each other molecule from which  $A$ 's center is excluded in impact. Hence, no matter in what direction  $A$  moves, it will after a path  $l_1$  collide with some other molecule and be deflected. After another path  $l_2$ ,  $A$  will again collide with a molecule, and so on. It is clear that the value of  $l$ , the length of one particular free path, is among other factors dependent on the direction the molecule chances to take. If, however, a large number of paths are observed in a given gas at a constant density it will be seen that  $l$  has an average value  $L$  called the mean or *average free path*. Its value depends somewhat on its velocity relative to the other molecules and is given by Maxwell, correcting for relative velocities and energy distribution among molecules, as  $L = 1/(\pi\sqrt{2}\sigma^2N)$ . Here  $\sigma$  is the molecular diameter and  $N$  is the Loschmidt number. Actually Tait has shown that a small correction of 5 per cent must be added to Maxwell's average value because of an inexact averaging procedure used by Maxwell. However, the errors in kinetic theory based on the average free path concept as applied in analysis are probably greater than this error and so render the correction of doubtful value. It is thus customary to use the frequently quoted Maxwell mean free path without correction.

It is at once seen that since  $N$  depends on the density  $\rho$  of the gas

\* It is true that the molecules are subject to attraction in the earth's gravitational field. The force is so small that the paths are very little curved. The technique of molecular beams has developed so far that Stern and Estermann have succeeded in measuring the deflection for Cs atoms in vacuum. It is about 0.3 mm in 2 meters.

and as  $\sigma$  is constant  $L \propto 1/\rho$ , so that at constant temperature  $L \propto 1/p$ , where  $p$  is the pressure. Hence

$$L = L_0 \frac{\rho_0}{\rho} = L_0 \left( \frac{760}{p} \right)_T,$$

where  $L_0$  is the mean free path at the standard density  $\rho_0$ , or at 760 mm and constant temperature  $0^\circ \text{C}$ . As  $\sigma$  is of the order of  $2 \times 10^{-8} \text{ cm}$  while  $N$  is of the order of  $3 \times 10^{19}$ , at  $0^\circ$  and 760 mm,  $L_0$  will be of the order of  $2 \times 10^{-5} \text{ cm}$ . In  $\text{H}_2$ ,  $L_0 = 1.83 \times 10^{-5} \text{ cm}$ ; in  $\text{He}$  it is  $2.8 \times 10^{-5}$ ; in  $\text{N}_2$  it is  $0.944 \times 10^{-5} \text{ cm}$ ; in  $\text{A}$ ,  $1 \times 10^{-5}$ ; in  $\text{Cl}_2$  it is  $0.457 \times 10^{-5}$ ; and in  $\text{CO}_2$  it is  $0.629 \times 10^{-5} \text{ cm}$ . The average velocity  $\bar{c}$  divided by the mean free path  $L$  gives the *collision frequency*,  $z = \bar{c}/L = \pi\sqrt{2}\sigma^2 N\bar{c}$ , a very useful concept.

If an electron were a point charge moving at a speed  $\sqrt{3680}$  times the fastest molecule,  $\text{H}_2$ , the expression for  $L$  would become  $L_e = 4\sqrt{2} L$ , where  $L_e$  is the electron free path and  $L$  is that of the molecule. The factor 4 comes from the fact that the collision radius of an electron and molecule is, on the assumptions made,  $\sigma/2$  and not  $\sigma$ , the molecular diameter. The  $\sqrt{2}$  comes from the fact that the molecules are relatively at rest compared to the electron, and the relative velocity factor  $\sqrt{2}$  drops out. Hence

$$L_e = 4\sqrt{2}L = \frac{1}{\pi N \sigma_e^2},$$

where  $\sigma_e = \sigma/2$ . Actually, electrons in virtue of their electrical field and deBroglie wavelength do *not interact as point charges with molecules*. Fast electrons go fairly close to molecules without deflection, while slow electrons are badly diffracted about. Of this more will be said when we have discussed the distribution of molecular free paths.

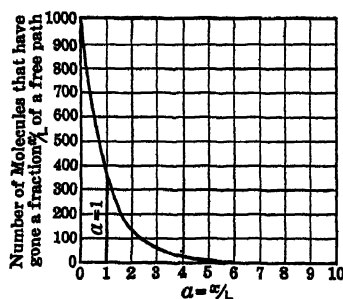


FIG. 290.

It was observed that, owing to the irregularity of the surrounding molecular surface presented to any molecule  $A$  at a given instant, the value of the free path  $l$  that was to be executed depended entirely on the direction of its next motion, i.e., to chance. It turns out that the result of this purely chance value of a given free path leads to a very definite prediction as to how many molecules  $n$  out of  $n_0$  molecules starting free paths at a given instant will traverse a distance  $x$  without

impact. The law deduced is that  $n = n_0 e^{-x/L}$ , where  $L$  is the mean free path. This can be plotted with  $n$  as ordinates and  $x$  as abscissas as in Fig. 290. At  $x = 0$ , the curve starts with  $n = n_0$  and declines thereafter monotonously and exponentially to 0 as  $x = \infty$ . There is thus *no*

grouping of free paths about any value; the longer the path, the less likely it is. The average value of the molecular free path  $L$  is today best determined experimentally from the coefficient of viscosity of a gas through the relation  $\eta = 0.499 \rho \bar{c} L$ , with  $\bar{c}$  the average velocity and  $\rho$  the density. It is seen that the value of  $n/n_0$  at which  $x = L$  is  $n/n_0 = 1/e = 1/2.7183 = 0.366$ ; that is, but 37 per cent of the molecules have not collided after a distance  $x$  equal to the average path  $L$ . The ratio  $n/n_0$  in general is the *chance* that a molecule has of traversing a distance  $x$  without impact. This chance is  $e^{-x/L}$ , the value of  $L$  being a scale factor determined by the conditions under which the molecule finds itself. The number of molecules  $dn$  colliding between  $x$  and  $x + dx$  is then given by

$$dn = - \frac{n_0}{L} e^{-x/L} dx.$$

When plotted in terms of  $x/L$ , it is seen that

$$dn = - n_0 e^{-x/L} \frac{dx}{L}$$

is also an exponential function of  $x/L$  and that the number  $dn$  depends on  $n_0$  and on the width of the interval  $dx$  (i.e., between  $x$  and  $x + dx$ ) compared to  $L$ .

As stated, owing to the nature of the electron, its interaction radius at various velocities is not the value  $4\sqrt{2}L$  expected from simple kinetic theory. Fortunately, the detection of electrons is a very simple matter, and it is possible to measure the number of electrons out of an initial number  $n_0$  that have *not* collided with molecules so as to suffer serious deflections or energy exchange after traversing a given distance in the gas. From this it is at once easy to infer the "*absorbing*" or deflecting *area of cross section  $q$  of the gas molecules for an electron*. That is, from the mean free path or survival equation  $n = n_0 e^{-x/L_0}$ , since

$L_0 = 1/\pi\sigma_e^2 N = \frac{1}{Qp}$  we can write  $n = n_0 e^{-qx} = n_0 e^{-qN_1 x}$ . Here  $n$  is the number of electrons undeflected after  $x$  centimeters,  $n_0$  is the initial number starting,  $p$  is the pressure in millimeters, and  $N_1$  is the number of molecules in  $1 \text{ cm}^3$  at 1 mm pressure, while  $Q = qN_1$  expresses the "*absorbing*" or deflecting cross section of *all* the  $N_1$  atoms in the cubic centimeter of gas at 1 mm pressure and  $q = \pi\sigma_e^2$  is the deflecting cross section of a *single* atom for an electron. This at once gives us the value of  $\sigma_e$ , for by measuring  $n$  and  $n_0$  as a function of  $x$  and  $p$  we get  $Q$  and hence  $q$ .

The discovery of the variable scattering behavior for electrons at low electron energies must be credited to Akesson and later to Ramsauer and Mayer who worked with Lenard. Ramsauer's pioneer measurements and the later ones of Ramsauer and Kollath have been carried to such perfection that we today speak of the electron free

paths as *Ramsauer free paths*. Other workers who have made notable contributions in this field are Brode<sup>2</sup> and his pupil Normand. The data, as given in Ramsauer and Brode's summaries,<sup>1,2</sup> are now generally accepted as correct. The Ramsauer free paths have been computed from wave-mechanical considerations and agree accurately with the observed paths where satisfactory atomic force fields are available for the calculation.

In general, the *free paths*  $L_e$  are not given in the published curves of current literature but instead either  $q$ , or  $Q$  at 1 mm pressure, are plotted against the electron energy in volts. Such a set of curves for some gases is given in Fig. 291 *A, B, C, D*. The kinetic-theory cross sections calculated from  $L_e = 4\sqrt{2}L$  from classical kinetic-theory values of  $L$  are indicated at the sides of the diagram as  $A_{KT}$ ,  $N_{KT}$ . It is seen that the Ramsauer cross sections are of the same order of magnitude as  $4\sqrt{2}L$  but vary in some cases over wide ranges with electron energy. It is striking how in atoms and molecules with similar electronic configurations the curves have similar shapes. Thus A, Kr, Xe,  $N_2$  and CO are strikingly similar, while  $H_2$  and He and Zn, Cd and Hg are similar and have similar electronic dispositions. The alkalis Na, K, etc., are also similar in their curves. The effect of this variable cross section on the discharge phenomena is of great importance. For simplicity in earlier work  $L_e$  was chosen as constant. Actually the variation of  $L_e$  with energy causes profound changes in the distribution of electron energy in gases and in excitation and ionization processes. The importance of the variation cannot today be ignored.

It is seen at once that in the case of ions or electrons in an electrical field in a gas the distribution of free paths must be of considerable importance, for the rate of gain of energy in the field depends upon the length of the path during which these particles are subject to free action of the field between impacts. Thus long free paths will favor energy gain. If the gain in energy were a linear function of the path, and if free paths were independent of energy, then after *very* many free paths electrons would show a nearly uniform energy equal to the gain per mean free path times the number of paths, with only the fluctuations due to chance differences over the last few paths. But if only a few paths are executed or if energy gain is not proportional to the free path and if the free path is a function of energy it is clear that the free-path distribution will cause a large spread in the energies, ionizing possibilities, and mobilities of the electrons or ions. As was seen, the Ramsauer free paths of electrons make this action highly probable.

When the variation of the atomic or molecular free paths with pressure was discussed, nothing was said about the variation of  $L$  with temperature (average energy), aside from the effect of temperature on the density  $\rho$ . It is essential, however, to point out that, when one

<sup>1</sup> Ramsauer and Kollath, *Handbuch der Physik*, XX, 11/2, 243, 1933.

<sup>2</sup> R. B. Brode, *Rev. Modern Phys.*, 5, 257, 1933.

considers the small molecular energies corresponding to ordinary temperatures in gases (i.e., 0.03 to 0.1 volt), the high energies involved in the *deformation* of the outer electronic shells of molecules (tens of volts) indicate that, as far as the deformation of the electron shells in impact is concerned,  $\sigma$  the molecular diameter for collision should vary

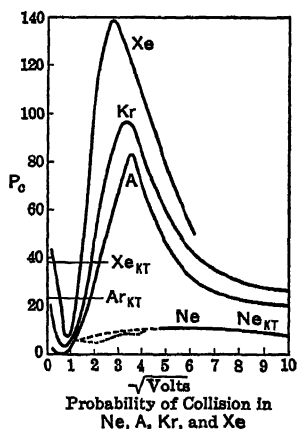


FIG. 291A.

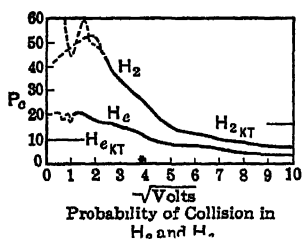


FIG. 291B.

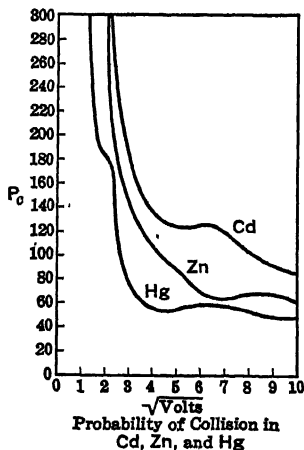


FIG. 291C.

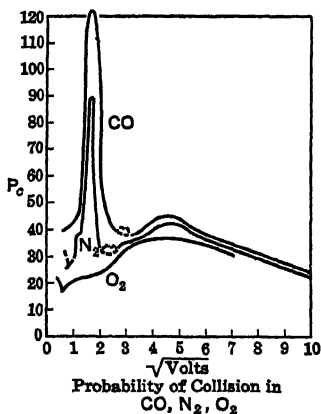


FIG. 291D.

very little with temperature. This general lack of deformability is not, of course, applicable to loosely bound atoms in readily dissociated molecules where vibrations at room temperatures change the molecular size appreciably. It can, however, in general be said to apply to most common gases, and  $\sigma$  should be constant for most common tempera-

tures. As stated,  $L$  for gases is evaluated from the coefficient of viscosity  $\eta$ . Now since the coefficient of viscosity

$$\eta = 0.499\rho\bar{c}L = \frac{0.499\rho\bar{c}}{\pi\sqrt{2}N\sigma^2} = \frac{0.499m\bar{c}}{\pi\sqrt{2}\sigma^2},$$

it should only change proportionally with the  $\sqrt{T}$  since  $m$  and  $\sigma$  are constant. Actually, it is observed to change faster than proportional to  $\sqrt{T}$  in fact, in some gases at certain temperatures reaching nearly direct proportionality with  $T$ . It is *certain* that the *molecular diameters do not change by this amount*.

This phenomenon is easily explained when we realize that  $\sigma$  as evaluated from  $L$  and  $\eta$  does not represent the distance of repulsion in molecular impact, due to electronic shells, but that it represents an *effective collision radius modified by attractive forces* as well as repulsive forces. That is, molecules like atoms exert attractive forces of the character of  $f = +a/r^m$ , with  $m = 6$  and repulsive forces of the approximate form  $f = -b/r^n$  with  $n$  varying from 9 to 14. Now the attractive forces are appreciable at some distances from the molecules. Thus a molecule flying past another along its initially straight trajectory is deflected toward the other molecule as it approaches. Its path is the more curved the more slowly it moves. Hence, if the original path would have carried the molecules apart without an impact, the curvature would produce an impact. Accordingly, the "*apparent*" or *effective collision radius*  $\sigma_1$  which is measured would contain not only the real repulsive force diameter  $\sigma$  but the additional portion due to the deviation of the molecule from its straight path. As temperature goes up, with a constant force law acting, the deviation of the path decreases and the molecule has a longer free path. Thus care must be used in attempting to infer the ionic or atomic diameter from data which evaluate the mean free path. Failure to do so in the study of ions has led to much waste of effort.

**c. Distribution of Velocities.** One may now turn to the question of the distribution of velocities or energies among the molecules. The velocities  $C$  which one evaluates from  $p = \frac{1}{2}NmC^2 = R_1T$  represent the *square root of the averaged square of the velocities*. Since squaring emphasizes higher velocities, this special velocity is greater than the average velocity if all molecules do not have the same speed. One must thus inquire into the distribution of velocities among the molecules: For it is clear from dynamics that molecules in an assemblage undergoing elastic collisions among themselves will not long retain equal velocities as a consequence of such impacts between molecules supposed spherical. This follows at once if one regards a special case, that of two spherical molecules  $A$  and  $B$  of equal masses, moving at right angles with each other, with equal speeds  $v$ ,  $A$  striking  $B$  centrally. As a result,  $B$  will move with a velocity  $\sqrt{2}v$  at an angle of  $45^\circ$  with

the original velocities while  $A$  will be at rest. Hence, in this special single impact, two molecules of equal speed have been altered to one molecule of 0 speed and one of  $\sqrt{2}$  times its initial speed. Thus velocity is distributed as a result of the impact, while the energy remains constant at  $E = \frac{1}{2}m_A v_A^2 + \frac{1}{2}m_B v_B^2 = \frac{1}{2}m_A 0 + \frac{1}{2}m_B (\sqrt{2} v_B)^2 = m_A v_A^2$  with  $v_A = v_B$ , and  $m_A = m_B$ .

When one has a vast assemblage of molecules of this sort and starts them off each with a velocity  $v$  and an energy  $\frac{1}{2}mv^2$ , after very few collisions each of the molecules will have a different velocity, with the average energy, however, still  $\frac{1}{2}mv^2$  per molecule. If one waits long enough, it is clear that the molecules must so distribute the velocities among themselves that at each instant as many molecules leave one velocity group by collisions as enter it by other collisions. One then has a *steady state* or *equilibrium* distribution of velocities among the molecules, which is characteristic only of the average energy and masses of the molecule. Since the energy is constant and independent of mass and varies only with the temperature, we then have an *equilibrium* energy distribution dependent only on the absolute temperature. If one assumes equilibrium with spherical elastic molecules present in large numbers, Boltzmann has shown that one and only one characteristic distribution exists. The form of this law is invariant with temperature, its distribution about the average or most probable value being the same and only the average value being displaced with temperature. A similar law was earlier deduced by J. C. Maxwell for a statistical assemblage such as molecules were assumed to represent. The law of energy distribution is, therefore, called the Maxwell-Boltzmann distribution law, and the distribution the Maxwellian distribution.

It is to be noted that the law is an *equilibrium* condition only, and its form depends on this circumstance. Hence in *non-equilibrium* processes, such as *heat conduction, diffusion, and viscosity*, and in the case of ions or electrons in electrical fields in gases, especially in discharges, the distribution is *not* Maxwellian. Since temperature is associated with a special average energy in a Maxwellian distribution, the average energies of non-equilibrium distributions are not strictly speaking to be associated with the word temperature. Since the average kinetic energy of a single molecule is associated with temperature in a Maxwellian distribution, we speak of the "temperature" of an electron or molecule in this sense. In non-equilibrium processes, it is *not accurate* to speak of "temperatures" of electrons or molecules, although the term is often applied to these in discharges as in a loose fashion expressing the average energy of the particles. Thus a gas in an oven in equilibrium at an elevated temperature may be ionized. This is spoken of as "temperature ionization" and represents the degree of ionization on a Maxwellian energy distribution. It is seriously incorrect to speak of a "temperature ionization" in *most discharges* since the process is not an equilibrium process.



The Maxwell-Boltzmann distribution law can be written as

$$N_{dc} = \frac{4Nc^2}{\alpha^3\sqrt{\pi}} e^{-\frac{c^2}{\alpha^2}} dc = \frac{4}{\sqrt{\pi}} N \frac{c^-}{\alpha^2} e^{-\frac{c^2}{\alpha^2}} \frac{dc}{\alpha} = \frac{4}{\sqrt{\pi}} N x^2 e^{-x^2} dx, \text{ if } x = \frac{c}{\alpha}. \quad (1)$$

$N_{dc}$  is the number out of  $N$  molecules that have a speed between  $c$  and  $c + dc$  irrespective of direction in space.  $N_{dc}/N$  is the chance of a velocity between  $c$  and  $c + dc$ . It depends on  $dc/\alpha = dx$  and the value of the ratio  $c/\alpha$ . By choosing  $dc/\alpha = dx = 1$ , one has the form of the curve at once by plotting  $N_{dc}/N$  as a function of  $x$  as shown in Fig. 292.

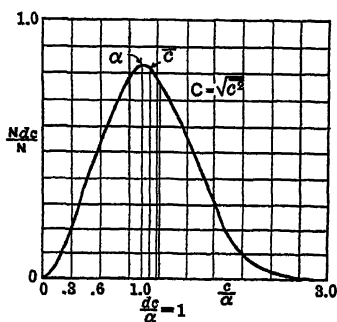


FIG. 292.

It is seen at once that the curve is an asymmetrical bell-shaped one with a slightly greater area on the side of the large values of  $x$  relative to the peak at  $x = 1$  and  $c = \alpha$  than on the side of lower values of  $x$ . The constant  $\alpha$  is found, by differentiation of the function and equating to 0, to be the abscissa of the peak of the curve at  $x = 1$  and  $c = \alpha$ ; it is called the *most probable velocity* and is obviously related to the absolute temperature through the energy. The asymmetry of the curve makes the average velocity

$\bar{c}$  lie to the right of the most probable velocity, and  $C$ , the square root of the mean of the squared velocities, lies still further to the right of  $\alpha$  beyond  $c$ . The values are related as follows:

$$\begin{aligned} \bar{c} &= \frac{2}{\sqrt{\pi}} \alpha, & \bar{c} &= 1.128\alpha, & C &= \sqrt{\frac{3}{2}} \alpha \\ C &= 1.224\alpha, & \bar{c} &= \sqrt{\frac{8}{3\pi}} C, & \bar{c} &= 0.922C. \end{aligned}$$

Thus since  $C$  evaluated from  $C = \sqrt{3p/\rho} = \sqrt{3kT/m}$ , and since  $C = \sqrt{\frac{2}{3}} \alpha$ ,  $\alpha = \sqrt{2kT/m}$ ,  $\frac{1}{2}m\alpha^2 = kT$ . Thus  $kT$  is the *most probable kinetic energy* of a molecule, and  $\frac{3}{2}kT = \frac{1}{2}mC^2$  is the *average energy*. Hence the distribution law can also be written as

$$N_{dc} = 4\pi N \left( \frac{m}{2\pi kT} \right)^{3/2} c^2 e^{-\frac{mc^2}{2kT}} dc. \quad (2)$$

Owing to complications in printing fractional exponents, many authors use a form in which  $h = \frac{1}{2}kT$  replaces the  $\frac{1}{2}kT$ . Hence the form

$$N_{dc} = 4\pi N \left( \frac{hm}{\pi} \right)^{3/2} e^{-hmc^2} c^2 dc \quad (3)$$

is often found. Since the kinetic energy is  $\frac{1}{2}mc^2$ , by multiplying top and bottom of all fractions in equation 2 by  $m/2$  and converting the differential  $dc$  into the energy differential  $dE$ , one has the equation in the energy form

$$N_{dE} = \frac{2N\sqrt{E}}{\pi^{1/2}(kT)^{3/2}} e^{-\frac{E}{kT}} dE, \quad (4)$$

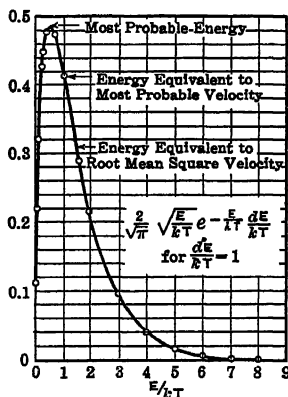


FIG. 293A.

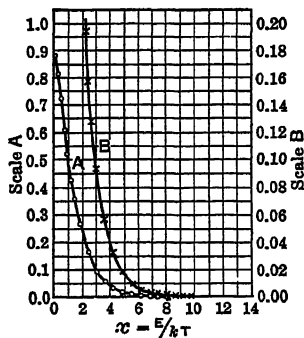


FIG. 293B.

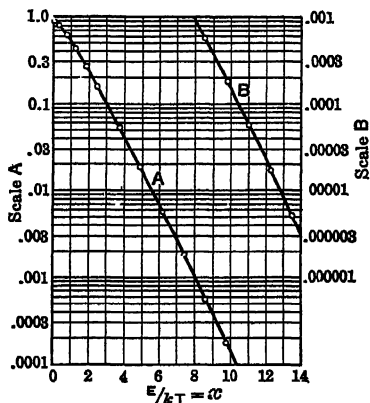


FIG. 293C.

which is shown in Fig. 293A together with its integral from different values of  $E$  to  $\infty$  in Figs. 293 B and C.

It is also of use to know not only how many molecules out of  $N$  have a velocity between  $c$  and  $c + dc$ , but also how many have a particular value of the velocity  $c$  having  $x$ ,  $y$ , and  $z$  components  $u$ ,  $v$ , and  $w$  ending between  $u$  and  $u + du$ ,  $v$  and  $v + dv$ ,  $w$  and  $w + dw$ , i.e., how many molecules of velocity  $c$  directed along a vector of components

$u$ ,  $v$ , and  $w$  that ends in a small velocity element  $du dv dw$ . Such an equation is of importance in all problems involving emission of molecules, evaporation, and thermionic emission where direction is of importance. This is expressed as

$$N_{vvv}(du dv dw) = \frac{N}{\alpha^3 \pi^{3/2}} e^{-\frac{u^2 + v^2 + w^2}{\alpha^2}} du dv dw. \quad (5)$$

Plotted against  $x$  where  $x^2 = c^2/\alpha^2 = (u^2 + v^2 + w^2)/\alpha^2$ , it takes the form shown in Fig. 294.

It is next of interest to plot the law in the energy form for three different temperatures,  $T_1$ ,  $T_2$ , and  $T_3$ , increasing in the order named, as shown in Fig. 295. The areas under the curves are constant, but the *probable energies* are displaced to the right in proportion to the absolute temperature,  $T$ . It is at once seen that the spread of velocities or energies increases as  $T$  increases. If one chooses a value of  $E$  as

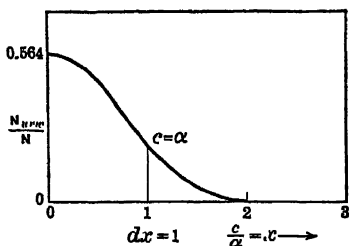


FIG. 294.

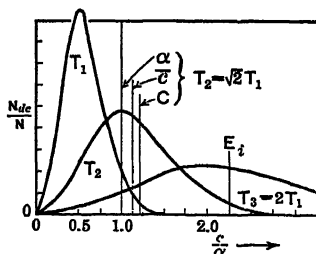


FIG. 295.

a critical energy,  $E_i$ , at which a molecule can escape from a surface against the potential energy, or at which an electron can be torn out of an atom, one will see that the area to the right of  $E_i$  increases rapidly as  $T$  increases. Fig. 296 shows the integral of the curves  $T_1$  and  $T_2$  of Fig. 295. That is, it gives as ordinates the areas to the right of values of  $c/\alpha$  plotted as abscissas, i.e., it gives the fraction of the molecules having an energy in excess of different values of  $E_i$  as given by  $c/\alpha$ . If then we plot the number of evaporating or ionized particles as a function of  $T$ , the curve will start asymptotically and rise exponentially as  $T$  increases. This is characteristic of vapor-pressure, thermionic-emission, and ionization-function curves. Such a curve is seen in Fig. 297 for vapor pressure as a function of temperature.

Boltzmann generalized the distribution law to include the probability  $W$  of finding molecules in a given state of potential energy  $E_p$  when in a medium surrounded by molecules of kinetic energy expressed

by  $kT$ . The resultant equation is  $W = A e^{-\frac{E_p}{kT}} d\tau$ . Here  $A$  is a constant of the distribution law depending on  $E_p$  and the average energy as well

as geometrical parameters, while  $d\tau$  is an element of volume in the potential field which limits the region where  $E_p$  obtains. This probability multiplied by the number of molecules per unit volume gives the number of molecules in the energy regime in question. In many

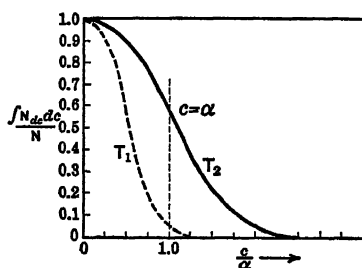


FIG. 296.

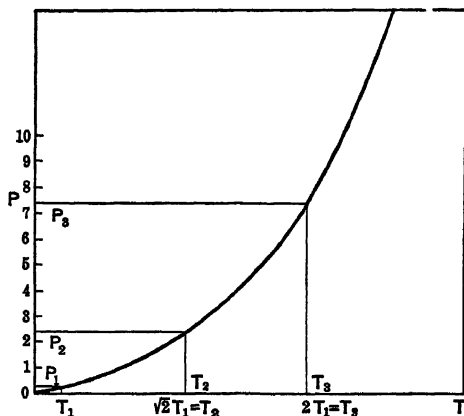


FIG. 297.

cases the constant  $A$  is eliminated, as we are interested in the relative numbers of molecules in two different states characterized by  $E_{p1}$  and  $E_{p2}$ .

# APPENDIX II

## CRITICAL POTENTIALS IN VOLTS

| Element | Atomic Number | First Exciting Potential | Metastable State       | Ionization Potential   | Second Ionization Potential |
|---------|---------------|--------------------------|------------------------|------------------------|-----------------------------|
| He..... | 2             | 19.75                    | { 19.73 }<br>{ 20.55 } | 24.48                  | 54.16                       |
| Ne..... | 10            | 16.60                    | .                      | 21.47                  |                             |
| Ar..... | 18            | 11.57                    | .....                  | { 15.69 }<br>{ 15.86 } |                             |
| Kr..... | 36            | 9.9                      | .....                  | 13.3                   |                             |
| Xe..... | 54            | 8.3                      | .....                  | 11.5                   |                             |
| H.....  | 1             | 10.15                    | .....                  | 13.54                  |                             |
| Li..... | 3             | 1.84                     | .....                  | 5.37                   |                             |
| Na..... | 11            | 2.09                     | .....                  | 5.12                   |                             |
| K.....  | 19            | 1.60                     | .....                  | 4.32                   |                             |
| Rb..... | 37            | 1.55                     | .....                  | 4.16                   |                             |
| Cs..... | 55            | 1.38                     | .....                  | 3.88                   |                             |
| Mg..... | 12            | 2.70                     | .....                  | 7.61                   |                             |
| Ca..... | 20            | 1.89                     | .....                  | 6.08                   |                             |
| Hg..... | 80            | 4.89<br>(2537Å)          | { 4.67 }<br>{ 7.69 }   | 10.39<br>.....         | 18.97                       |

| Gas                                 | Excitation<br>1st Vib. | First Excitation Potential |                   | State  | Ionization Potential |       | Dissociation Potential            |
|-------------------------------------|------------------------|----------------------------|-------------------|--|----------------------|-------|-----------------------------------|
|                                     |                        | Calc.                      | Obs.              |  | Calc.                | Obs.  |                                   |
| H <sub>2</sub> .....                |                        | 11.15                      | 11.5              | $^1\Sigma_g^+ \rightarrow \frac{1}{2}^3\Sigma_u^-$                                 | 15.37                | 15.37 | 4.36                              |
| N <sub>2</sub> .....                | 1 <                    | 6.14<br>8.50               | 6.1 ± 0.5<br>9.25 | $^1\Sigma_g^+ \rightarrow ^3\Sigma_g^+$<br>$^1\Sigma_g^+ \rightarrow ^1\Pi$        | 15.51                | 15.65 | 11.6                              |
| O <sub>2</sub> .....                | 1.62                   | 6.09                       | 7.9<br>1.62       | $^3\Sigma_g^- \rightarrow ^3\Sigma_u^-$<br>$^3\Sigma_g^- \rightarrow ^1\Sigma_g^+$ | 12.2                 | 12.5  | { 7.05 }<br>{ 6.5 } ?<br>{ 5.75 } |
| NO.....                             |                        |                            | 5.44              |  |                      | 9.5   | 5.3                               |
| CO.....                             |                        | 6.00                       | 6.0               | $^1\Sigma^+ \rightarrow ^3\Pi$   |                      | 14.1  | 9.6                               |
| CO <sub>2</sub> .....               |                        | 10.0                       |                   |  |                      | 14.4  | 5.5 ?                             |
| H <sub>2</sub> O.....               |                        | 7.6                        |                   |  |                      | 12.7  |                                   |
| Cl <sub>2</sub> .....               |                        |                            |                   |  | 13.2                 |       | 2.47                              |
| Br <sub>2</sub> .....               |                        |                            |                   |  | 12.8                 |       | { 1.96 }<br>{ 2.00 } ?            |
| I <sub>2</sub> .....                |                        | 1.93                       | 2.3               | $^1\Sigma_g^+ \rightarrow 0_g^+$   | 10.1                 |       | { 1.53 }<br>{ 1.50 } ?            |
| NH <sub>3</sub> .....               |                        |                            |                   |  | 11.1                 |       |                                   |
| HCl.....                            |                        |                            |                   |  | 13.75                |       |                                   |
| HBr.....                            |                        |                            |                   |  | 13.25                |       |                                   |
| HI.....                             |                        |                            |                   |  | 12.75                |       |                                   |
| CH <sub>4</sub> .....               |                        |                            |                   |  |                      | 14.5  |                                   |
| C <sub>2</sub> H <sub>2</sub> ..... |                        |                            |                   |  | 11.35                | 11.2  |                                   |
| C <sub>2</sub> H <sub>4</sub> ..... |                        |                            |                   |  | 10.41                | 12.2  |                                   |
| CH <sub>3</sub> Cl.....             |                        |                            |                   |  | 11.2                 | 10.7  |                                   |

### APPENDIX III

For aid in computation it is convenient to have at hand a table of fundamental physical constants. Such a *self-consistent* table was prepared in 1929 by R. T. Birge. It was published in Volume I of the *Reviews of Modern Physics*. Since the table was published some important revisions in the units have been made. In particular, the recent change in the experimental value of the charge on the electron has made the table somewhat inaccurate. The state of our present knowledge of the fundamental units has unfortunately become distinctly less satisfactory than it was in 1929, owing to later, more accurate measurements of many sorts, which have introduced mutual inconsistencies in the assumed established relations of the various units. Hence at present no one has attempted to derive a new and *consistent* table of fundamental data conforming to the new value of the electronic charge. However, for the purposes of many computations the accuracy of the 1929 data will suffice. Thus despite the recent changes in the accepted value of the electronic charge the following table is included for the convenience of the reader, as it is the only *consistent* set of data at present available.

Table a. Principal Constants and Ratios

|  |   |
|--|---|
| Velocity of light.....   | $c = (2.99796 \pm 0.00004) \times 10^{10} \text{ cm} \cdot \text{sec}^{-1}$               |
| Gravitation constant.....                                      | $G = (6.664 \pm 0.002) \times 10^{-8} \text{ dyne} \cdot \text{cm}^2 \cdot \text{g}^{-2}$ |
| Liter.....   | $l = 1000.027 \pm 0.001 \text{ cm}^3$   |
| Volume of perfect gas ( $0^\circ \text{ C}$ , $A_n$ ) $v_n =$  | $(22.4141 \pm 0.0008) \times 10^3 \text{ cm}^3 \cdot \text{mole}^{-1}$                    |
|  | $R_n = 22.4135 \pm 0.0008 \text{ liter} \cdot \text{mole}^{-1}$                           |
| Volume of perfect gas ( $0^\circ \text{ C}$ , $A_{45}$ ) $R =$ | $22.4146 \pm 0.0008 \text{ liter} \cdot \text{mole}^{-1}$                                 |
| International ohm ( $=p \text{ abs-ohm}$ ) $p =$               | $1.00051 \pm 0.00002$   |
| International amp ( $=q \text{ abs-amp}$ ) $q =$               | $0.99995 \pm 0.00005$   |
| Atomic weights   |   |
| O (oxygen) = 16.0000 (definition)                              | Ag (silver) = $107.880 \pm 0.001$   |
| H (hydrogen) = $1.00777 \pm 0.00002$                           | I (iodine) = $126.932 \pm 0.002$  |
| He (helium) = $4.0022 \pm 0.0004$                              | C (carbon) = $12.003 \pm 0.001$   |
| N (nitrogen) = $14.0083 \pm 0.0008$                            | Ca (calcium) = $40.075 \pm 0.005$   |
| Normal atmosphere.....   | $A_n = (1.013249 \pm 0.000003) \times 10^6 \text{ dyne} \cdot \text{cm}^{-2}$             |
| $45^\circ$ atmosphere.....                                     | $A_{45} = (1.013199 \pm 0.000003) \times 10^6 \text{ dyne} \cdot \text{cm}^{-2}$          |
| Ice point (absolute scale).....                                | $T_0 = 273.18 \pm 0.03^\circ \text{ K}$   |
| Mechanical equivalent of heat.. $J_{15} =$                     | $4.1852 \pm 0.0006 \text{ abs-joule} \cdot \text{cal}_{15}^{-1}$                          |
|  | $J_{20} = 4.1813 \pm 0.0006 \text{ abs-joule} \cdot \text{cal}_{20}^{-1}$                 |
| Electrical equivalent of heat.. $J'_{15} =$                    | $4.1835 \pm 0.0007 \text{ int-joule} \cdot \text{cal}_{15}^{-1}$                          |
|  | $J'_{20} = 4.1796 \pm 0.0007 \text{ int-joule} \cdot \text{cal}_{20}^{-1}$                |
| Faraday constant.....  | $F = 96494 \pm 5 \text{ int-coul} \cdot \text{g-equiv}^{-1}$                              |
|  | $= 96489 \pm 7 \text{ abs-coul} \cdot \text{g-equiv}^{-1}$                                |
|  | $= 9648.9 \pm 0.7 \text{ abs-cm-unit} \cdot \text{g-equiv}^{-1}$                          |
|  | $Fc = (2.8927_0 \pm 0.0002) \times 10^{14} \text{ abs-es-unit} \cdot \text{g-equiv}^{-1}$ |

|  |  |
|--|--|
| Electronic charge .....                          | $e = (4.770 \pm 0.005) \times 10^{-10}$ abs-es-units                           |
|  | $e/c = (1.5910_8 \pm 0.0016) \times 10^{-20}$ abs-em-units                     |
| Specific electronic charge (spectroscopic) ..... | $e/m = (1.761 \pm 0.001) \times 10^7$ abs-em-unit $\cdot$ g $^{-1}$            |
|  | $(e/m)c = (5.279_{41} \pm 0.003) \times 10^{17}$ abs-es-unit $\cdot$ g $^{-1}$ |
| Specific electronic charge (deflection) .....    | $e/m = (1.769 \pm 0.002) \times 10^7$ abs-em-unit $\cdot$ g $^{-1}$            |
|  | $(e/m)c = (5.303_{39} \pm 0.006) \times 10^{17}$ abs-es-unit $\cdot$ g $^{-1}$ |
| Planck constant .....                            | $h = (6.547 \pm 0.008) \times 10^{-27}$ erg $\cdot$ sec                        |

Table b. Additional Quantities Evaluated or Used in Connection with Table a

|   |  |
|---|--|
| Ratio of <i>es</i> to <i>em</i> units (direct). $c' = (2.9971 \pm 0.0001) \times 10^{10}$ cm $^{1/2}$ $\cdot$ sec $^{-1/2}$ $\cdot$ int $\Omega^{-1/2}$ | $= (2.9979 \pm 0.0001) \times 10^{10}$ cm $\cdot$ sec $^{-1}$              |
| Ratio of <i>es</i> to <i>em</i> units (indirect)  | $c' = c = (2.99796 \pm 0.00004) \times 10^{10}$ cm $\cdot$ sec $^{-1}$     |
| Acceleration of gravity (45°) ... $g_{45} = 980.616$ cm $\cdot$ sec $^{-2}$   |  |
| Mean density of earth .....   | $\delta = 5.522 \pm 0.002$ g $\cdot$ cm $^{-3}$                            |
| Maximum density of water ... $\delta_m = 0.999973 \pm 0.000001$ g $\cdot$ cm $^{-3}$  |  |
| Acceleration of gravity (normal) $g_n = 980.665$ cm $\cdot$ sec $^{-2}$   |  |
| Density of oxygen gas (0° C, $A_{45}$ ) ... $L = 1.428965 \pm 0.000030$ g $\cdot$ liter $^{-1}$   |  |
| Factor converting oxygen (0° C, $A_{45}$ )  |  |
| to ideal gas .....  | $1 - \alpha = 1.000927 \pm 0.000030$                                       |
| International coulomb (= $q$ abs-coul) .....  | $q = 0.99995 \pm 0.00005$  |
| International henry (= $p$ abs-henry) .....   | $p = 1.00051 \pm 0.00002$  |
| International volt (= $pq$ abs-volt) $pq = 1.00046 \pm 0.00005$   |  |
| International joule (= $pq^2$ abs-joule) .....  | $pq^2 = 1.00041 \pm 0.00010$   |
| International gauss (= $q$ abs-gauss)   |  |
| Density of nitrogen (0° C, $A_{45}$ ) ... $L = 1.25046 \pm 0.000045$ g $\cdot$ liter $^{-1}$  |  |
| Factor converting nitrogen (0° C, $A_{45}$ )  |  |
| to ideal gas .....  | $1 - \alpha = 1.00043 \pm 0.00002$   |
| Specific gravity of Hg (0° C, $A_n$ )   |  |
| referred to air-free water at maximum density .....   | $\rho_n = 13.59546 \pm 0.00003$  |
| Density of Hg (0° C, $A_n$ ) .....  | $D_n = 13.59509 \pm 0.00003$ g $\cdot$ cm $^{-3}$                          |
| Electrochemical equivalent of silver .....  | $E_{Ag} = (1.11800 \pm 0.00005) \times 10^{-3}$ g $\cdot$ int-coul $^{-1}$ |
|   | $= (1.11805 \pm 0.00007) \times 10^{-3}$ g $\cdot$ abs-coul $^{-1}$        |
| Arbitrary calcite grating space (18° C.) .....  | $d_{18}'' = 3.0294 \times 10^{-8}$ cm                                      |
| Density of calcite (20° C.) .....   | $\rho = 2.7102 \pm 0.0004$ g $\cdot$ cm $^{-3}$                            |
| Structural constant of calcite (20° C.) .....   | $\phi(\beta) = 1.09630 \pm 0.00007$  |
| Rydberg constant for hydrogen. $R_H = 109677.759 \pm 0.05$ cm $^{-1}$   |  |
| Rydberg constant for ionized helium .....   | $R_{He} = 109722.403 \pm 0.05$ cm $^{-1}$                                  |

Wave-length of red Cd line

(15° C.,  $A_n$ ) . . . . .  $\lambda(\text{Cd}) = 6438.4696 \text{ I.A. (definition of I.A. unit)}$ 

Rydberg constant for infinite

mass . . . . .  $R_\infty = 109737.42 \pm 0.06 \text{ cm}^{-1}$  $R_\infty c = (3.28988 \pm 0.00004) \times 10^{15} \text{ sec}^{-1}$  $R_\infty$  (indirect)  $= 2\pi^2 e^5 / h^3 c^2 (e/m)_{sp} = 10974 \pm 170 \text{ cm}^{-1}$  $R_\infty c$  (indirect)  $= (3.290_{08} \pm 0.005) \times 10^{15} \text{ sec}^{-1}$  $e/m$  (spectroscopic, indirect) $e/m = 2\pi^2 e^5 / h^3 c^2 R_\infty = (1.7611_2 \pm 0.0025) \times 10^7 \text{ abs-em-unit} \cdot \text{g}^{-1}$ 

True grating space of calcite

(20° C.) . . . . .  $d'_{20} = (3.0283 \pm 0.0010) \times 10^{-8} \text{ cm}$ 

Effective grating space of calcite

(20° C.) . . . . .  $d_{20} = (3.0279 \pm 0.0010) \times 10^{-8} \text{ cm}$ Avogadro's number . . . . .  $N_0 = Fc/e = (6.064_{36} \pm 0.006) \times 10^{23} \text{ mole}^{-1}$ Gas constant per mole  $R_0 = \nu_n A_n / T_0 = (8.3136_0 \pm 0.0010) \times 10^7 \text{ erg} \cdot \text{deg}^{-1} \cdot \text{mole}^{-1}$  $R_0' = R_0 / (J_{15} \times 10^7) = 1.9864_3 \pm 0.0004 \text{ cal}_{15} \cdot \text{deg}^{-1} \cdot \text{mole}^{-1}$  $R_0'' = R_0 / (A_n \times 1000.027) = (8.2046_4 \pm 0.0009) \times 10^{-2}$ liter · atmos · deg<sup>-1</sup> · mole<sup>-1</sup> $R_0''' = R_0 / A_n = \nu_n / T_0 = 82.048_8 \pm 0.009 \text{ cm}^3 \cdot \text{atmos} \cdot \text{deg}^{-1} \cdot \text{mole}^{-1}$ Boltzmann constant . . . . .  $k = R_0 / N_0 = (1.3708_9 \pm 0.0014) \times 10^{-16} \text{ erg} \cdot \text{deg}^{-1}$ 

Second radiation constant (ex-

perimental) . . . . .  $c_2 = 1.432 \pm 0.003 \text{ cm} \cdot \text{deg}$ 

Second radiation constant (in-

direct) . . . . .  $c_2 = hc/k = 1.4317_4 \pm 0.0006 \text{ cm} \cdot \text{deg}$ 

Stefan-Boltzmann constant (ex-

perimental) . . . . .  $\sigma = (5.735 \pm 0.011) \times 10^{-5} \text{ erg} \cdot \text{cm}^{-2} \cdot \text{deg}^{-4} \cdot \text{sec}^{-1}$ 

Stefan-Boltzmann constant (in-

direct) . . . . .  $\sigma = 2\pi^5 k^4 / 15c^2 h^3 = (5.713_9 \pm 0.006) \times 10^{-5} \text{ erg} \cdot \text{cm}^{-2} \cdot \text{deg}^{-4} \cdot \text{sec}^{-1}$ 

Radiation density constant (ex-

perimental) . . . . .  $a = 4\sigma/c = (7.651_8 \pm 0.015) \times 10^{-15} \text{ erg} \cdot \text{cm}^{-3} \cdot \text{deg}^{-4}$ 

Radiation density constant (in-

direct) . . . . .  $a = 8\pi^5 k^4 / 15c^3 h^3 = (7.623_7 \pm 0.007) \times 10^{-15} \text{ erg} \cdot \text{cm}^{-3} \cdot \text{deg}^{-4}$



Table c. Miscellaneous Derived Constants

|   |  |
|---|--|
| Mass of electron (spectroscopic).....                   | $\frac{e}{c(e/m)_{sp}} = (9.035_{10} \pm 0.010) \times 10^{-28} \text{ g}$                                       |
| Mass of electron (deflection).....                      | $m_0 = \frac{e}{c(e/m)_{defl}} = (8.994_{25} \pm 0.014) \times 10^{-28} \text{ g}$                               |
| Atomic weight of electron (spectroscopic).....          | $m = F/(e/m)_{sp} = (5.479_{22} \pm 0.003) \times 10^{-4}$   |
| Atomic weight of electron (deflection).....             | $m = F/(e/m)_{defl} = (5.454_{44} \pm 0.006) \times 10^{-4}$   |
| Mass of atom of unit atomic weight.....                 | $M_0 = 1/N_0 = (1.6489_6 \pm 0.0016) \times 10^{-24} \text{ g}$  |
| Mass of hydrogen atom.....                              | $M_H = H/N_0 = (1.6617_6 \pm 0.0017) \times 10^{-24} \text{ g}$  |
| Atoms per gram of hydrogen.....                         | $1/M_H = (6.017_{61} \pm 0.0006) \times 10^{23} \text{ g}^{-1}$  |
| Mass of proton.....                                     | $M_p = (H - m)/N_0 = (1.6608_9 \pm 0.0017) \times 10^{-24} \text{ g}$  |
| Mass of $\alpha$ -particle.....                         | $M_\alpha = (He - 2m)/N_0 = (6.597_{74} \pm 0.007) \times 10^{-24} \text{ g}$                                    |
| Charge in electrolysis of 1 g hydrogen.....             | $e/M_H = F/H = 9574.51 \pm 0.7 \text{ abs-em-units} \cdot \text{g}^{-1}$   |
| Specific charge of proton.....                          | $e/M_p = F/(H - m) = 9579.73 \pm 0.7 \text{ abs-em-units} \cdot \text{g}^{-1}$                                   |
| Specific charge of $\alpha$ -particle.....              | $2e/M_\alpha = 2F/(He - 2m) = 4823.11 \pm 0.6 \text{ abs-em-units} \cdot \text{g}^{-1}$                          |
| Ratio mass H atom to mass electron (spectroscopic)..... | $\frac{(e/m)_{sp}}{e/M_H} = 1839.48 \pm 1$   |
| Ratio mass H atom to mass electron (deflection).....    | $\frac{(e/m)_{defl}}{e/M_H} = 1847.41 \pm 2$   |
| Ratio mass proton to mass electron (spectroscopic)..... | $= 1839.26 - 1 = 1838.26 \pm 1$  |
| Ratio mass proton to mass electron (deflection).....    | $= 1847.61 - 1 = 1846.61 \pm 2$  |
| Energy associated with unit wave-number.....            | $e/\nu' = hc = (1.9627_{60} \pm 0.0025) \times 10^{-16} \text{ erg} \cdot \text{cm}$                             |
| Potential associated with unit frequency.....           | $V/\nu = h/e = (1.3725_{14} \pm 0.0005) \times 10^{-17} \text{ erg} \cdot \text{sec} \cdot \text{cs-unit}^{-1}$  |
| Frequency associated with unit potential.....           | $\nu/V = e/h = (7.2857_7 \pm 0.0027) \times 10^{16} \text{ cs-unit} \cdot \text{erg}^{-1} \cdot \text{sec}^{-1}$ |
| Wave-number associated with 1 abs-volt.....             | $\nu/V'' = e \cdot 10^8/hc = (2.4302_6 \pm 0.0009) \times 10^{14} \text{ sec}^{-1} \cdot \text{abs-volt}^{-1}$   |
| Wave-length associated with 1 abs-volt.....             | $\lambda_0 = \lambda/V'' = hc^2/e = 8106.31 \pm 3 \text{ cm}^{-1} \cdot \text{abs-volt}^{-1}$                    |
| Energy of 1-abs-volt-electron.....                      | $h\nu/V'' = e \cdot 10^8/c = (1.5910_6 \pm 0.0016) \times 10^{-12} \text{ erg}$                                  |
| Speed of 1-abs-volt-electron (spectroscopic).....       | $v_0 = [2 \cdot 10^8(e/m)_{sp}]^{1/2} = (5.9346_1 \pm 0.0017) \times 10^7 \text{ cm} \cdot \text{sec}^{-1}$      |
| Speed of 1-abs-volt-electron (deflection).....          | $v_0 = [2 \cdot 10^8(e/m)_{defl}]^{1/2} = (5.9481_1 \pm 0.0034) \times 10^7 \text{ cm} \cdot \text{sec}^{-1}$    |

Table c. Miscellaneous Derived Constants—(Continued)

|  |   |
|--|---|
| Fine structure constant.....   | $\alpha = 2\pi e^2/hc = (7.2834 \pm 0.006) \times 10^{-3}$  |
| Reciprocal of fine structure constant.....   | $1/\alpha = 137.294 \pm 0.11$   |
| Square of fine structure constant.....   | $\alpha^2 = (5.3053 \pm 0.008) \times 10^{-5}$  |
| Bohr unit of angular momentum.....   | $\hbar/2\pi = (1.04196 \pm 0.0013) \times 10^{-27} \text{ erg} \cdot \text{sec}$<br>$e^2/c = a\hbar/2\pi = (7.58946 \pm 0.015) \times 10^{-30} \text{ es-unit}^2 \cdot \text{sec} \cdot \text{cm}^{-1}$ |
| Magnetic moment of 1 Bohr magneton (spectroscopic).....  | $\mu_1 = (\hbar/4\pi)(e/m)_{sp} = (0.917470 \pm 0.0013) \times 10^{-20} \text{ erg} \cdot \text{gauss}^{-1}$  |
| Magnetic moment of 1 Bohr magneton (deflection).....   | $\mu_1 = (\hbar/4\pi)(e/m)_{defl} = (0.921688 \pm 0.0016) \times 10^{-20} \text{ erg} \cdot \text{gauss}^{-1}$  |
| Ratio Bohr magneton to Bohr mechanical unit (spectroscopic).....                                 | $\frac{\mu_1}{\hbar/2\pi} = \frac{1}{2} \left( \frac{e}{m} \right)_{sp} = 0.8805 \pm 0.0005 \times 10^7 \text{ gauss}^{-1} \cdot \text{sec}^{-1}$   |
| Ratio Bohr magneton to Bohr mechanical unit (deflection).....                                    | $\frac{\mu_1}{\hbar/2\pi} = \frac{1}{2} \left( \frac{e}{m} \right)_{defl} = (0.8845) \pm 0.0010 \times 10^7 \text{ gauss}^{-1} \cdot \text{sec}^{-1}$   |
| Magnetic moment per mole for one Bohr magneton per molecule (spectroscopic).....                 | $\mu_1 N_0 = 5563.87 \pm 10 \text{ erg} \cdot \text{gauss}^{-1} \cdot \text{mole}^{-1}$   |
| Same (deflection).....   | $\mu_1 N_0 = 5589.14 \pm 11 \text{ erg} \cdot \text{gauss}^{-1} \cdot \text{mole}^{-1}$   |
| Zeeman displacement per gauss.....   | $\frac{\Delta\nu'}{H} = \frac{(e/m)_{sp}}{4\pi} = (4.67488 \pm 0.003) \times 10^{-5} \text{ cm}^{-1} \cdot \text{gauss}^{-1}$   |
| Band spectra constant connecting wave-number and moment of inertia, $I$ . $\hbar/8\pi^2 c$ ..... | $\hbar/8\pi^2 c = (27.6583 \pm 0.04) \times 10^{-40} \text{ g} \cdot \text{cm}$   |
| Same, connecting frequency and $I$ .....   | $\hbar/8\pi^2 = (8.29187 \pm 0.011) \times 10^{-29} \text{ erg} \cdot \text{sec}$   |
| Same, connecting ergs and $I$ .....  | $\hbar^2/8\pi^2 = (5.42886 \pm 0.014) \times 10^{-55} \text{ erg}^2 \cdot \text{sec}^2$   |
| Atomic specific heat constant.....   | $c_2/c = \hbar/k = (4.77573 \pm 0.0019) \times 10^{-11} \text{ sec} \cdot \text{deg}$   |
| Rotational specific heat constant.....   | $\sigma IT = \hbar^2/8\pi^2 k = (39.5971 \pm 0.06) \times 10^{-40} \text{ g} \cdot \text{cm}^2 \cdot \text{deg}$  |
| Reduced mass of H atom.....  | $\mu_H = R_H(m_0)_{sp}/R_\infty = (9.03019 \pm 0.010) \times 10^{-28} \text{ g}$  |
| Schroedinger constant for H atom.....  | $8\pi^2 \mu_H/\hbar^2 = (1.66342 \pm 0.003) \times 10^{27} \text{ g} \cdot \text{erg}^{-2} \cdot \text{sec}^{-2}$   |
| Schroedinger constant for electron.....  | $8\pi^2(m_0)_{sp}/\hbar^2 = (1.66438 \pm 0.003) \times 10^{27} \text{ g} \cdot \text{erg}^{-2} \cdot \text{sec}^{-2}$   |
| Ionization potential for H atom.....   | $R_H/v_0 = 13.5290 \pm 0.005 \text{ abs-volt}$  |
| Ionization potential for He <sup>+</sup> .....   | $4R_{He}/v_0 = 54.1417 \pm 0.020 \text{ abs-volt}$  |
| Separation of nucleus and electron in normal H atom, using experimental value of $R_H$ .....     | $a_0 = \frac{\alpha(1 - \alpha^2)^{1/2}}{4\pi R_H} = (0.528468 \pm 0.0004) \times 10^{-8} \text{ cm}$   |

Table c. Miscellaneous Derived Constants—(Continued)

|  |   |
|--|---|
| Same, using calculated value of $R_H$ .....  | $\frac{h^2(1-\alpha^2)^{1/2}}{4\pi^2\mu_H} = (0.5284_{31} \pm 0.0005) \times 10^{-8}$   |
| Radius of Bohr orbit in normal H, referred to center of mass,<br>using experimental $R_\infty$ ..... | $\frac{\alpha(1-\alpha^2)^{1/2}}{4\pi R_\infty} = (0.5281_{30} \pm 0.0004) \times 10^{-8}$ cm   |
| Same, using calculated $R_\infty$ .....  | $a_0' = \frac{h^2 c(e/m)_{sp}(1-\alpha^2)^{1/2}}{4\pi^2 e^2} = (0.5281_{34} \pm 0.0005) \times 10^{-8}$ cm  |
| Speed of electron in normal H orbit, referred to nucleus.....  | $v_0' = \alpha c = (2.18361 \pm 0.0017) \times 10^8$ cm·sec <sup>-1</sup>   |
| Same, referred to center of mass, using experimental $R_H$ and $R_\infty$ .....                      | $v_0 = \alpha c R_H / R_\infty = (2.1824_3 \pm 0.0017) \times 10^8$ cm·sec <sup>-1</sup>  |
| General spectroscopic doublet constant.....  | $R_\infty \alpha^2 = 5.821_{71} \pm 0.009$ cm <sup>-1</sup>   |
| Hydrogen doublet constant.....   | $\Delta\nu_H = R_H \alpha^2 / 16 = 0.3636_{50} \pm 0.0006$ cm <sup>-1</sup>   |
| Dispersion constant.....   | $\frac{e^2/2\pi m_0}{8\pi c^4} = \frac{ec(e/m)_{sp}/2\pi}{8\pi c^4} = (4.007_{97} \pm 0.005) \times 10^7$ cm <sup>3</sup> ·sec <sup>-2</sup>  |
| X-ray scattering coefficient.....  | $\frac{8\pi e^4}{3m_0^2 c^4} = \frac{3c^2}{3m_0^2 c^4} = (6.576_{91} \pm 0.015) \times 10^{-28}$ cm <sup>2</sup>  |
| Compton shift at 90° (spectroscopic).....  | $\frac{h}{m_0 c} = \frac{h}{m} \left( \frac{e}{m} \right)_{sp} = (0.024170_1 \pm 0.000016) \times 10^{-8}$ cm   |
| Compton shift at 90° (deflection).....   | $\frac{h}{m_0 c} = \left( \frac{e}{m} \right)_{defl} = (0.02428_{93} \pm 0.00003) \times 10^{-8}$ cm  |
| Wave mechanics $\lambda$ of 1-abs-volt-electron (spectroscopic).....                                 | $\frac{h}{m_0(v_0)_{sp}} = (12.210_0 \pm 0.006) \times 10^{-8}$ cm  |
| Loschmidt number (0° C., $A_n$ ).....  | $n_0 = N_0/v_n = (2.705_{50} \pm 0.003) \times 10^{19}$ cm <sup>-3</sup>  |
| Wien's displacement constant (indirect).....   | $A = c_2/4.9651 = 0.28836_1 \pm 0.00011$ cm·deg   |
| First radiation constant.....  | $c_1 = 8\pi h c = (4.932_{98} \pm 0.006) \times 10^{-16}$ erg·cm<br>or $hc^2 = (0.5884_{30} \pm 0.0008) \times 10^{-9}$ erg·cm <sup>2</sup> ·sec <sup>-1</sup><br>or $2\pi hc^2 = (3.697_{30} \pm 0.005) \times 10^{-5}$ erg·cm <sup>2</sup> ·sec <sup>-1</sup> |
| Energy per mole for 1-abs-volt-electron per molecule.....  | $\frac{F \text{ (abs. coul per gram equiv.)}}{J_{15} \text{ (abs. joules per cal.)}} = 23054.8 \pm 4$ cal <sub>15</sub> ·mole <sup>-1</sup>   |
| Translational energy of molecule at 0° C.....  | $E_0 = 3kT_0/2 = (5.617_{40} \pm 0.006) \times 10^{-14}$ erg  |
| Translational energy per degree.....   | $e_0 = E_0/T_0 = 3k/2 = (2.0563_3 \pm 0.0021) \times 10^{-16}$ erg·deg <sup>-1</sup>  |

# AUTHOR INDEX

## A

ADDINK, C. C. J., 348, 369, 414, 449  
 AITKEN, J., 46  
 AKESSON, N., 647  
 ALEXIEVSKY, A. P., 85  
 ALLEN, H. W., 196, 199, 231, 370  
 ALLIBONE, T. E., 404, 407, 435, 441, 449,  
 463, 470, 536, 544, 548, 558  
 ALLIS, W. P., 194, 196, 199, 202, 210, 211,  
 221, 228, 231, 295, 363  
 ÅNGSTRÖM, K., 603  
 ARENDT, P., 149, 160  
 ARNOT, F. L., 301, 303, 304  
 ASHELEY, M. F., 49, 50  
 ASTON, F. W., 564, 567, 573, 579, 580, 602  
 ATKINSON, R. d'A., 369  
 AYERS, T. L. R., 343, 346, 355, 369, 395,  
 406  
 AYRTON, H., 622, 640

## B

BAERWALD, H., 189, 199  
 v. BAHR, E., 375, 406  
 BAILEY, V. A., 35, 50, 196, 198, 230, 268,  
 275, 279, 282, 283, 304, 313, 315, 335,  
 342, 369, 591, 603  
 BALLANTINE, R. J., 251, 257  
 BÄR, R., 514, 603, 641  
 BARTELS, H., 150, 160  
 BARTON, F. A., 304  
 BEAMS, J. W., 442, 447, 449, 450, 482,  
 483, 484, 549, 559  
 BECKER, O., 474, 476, 640  
 BECKETT, C., 303, 304  
 BEECK, O., 376, 377, 383, 384, 406, 452,  
 470, 501  
 BÉLÁR, M., 443, 450  
 BENADE, J. M., 369  
 BETHE, H., 473  
 BIRGE, R. T., 658  
 BLACKWOOD, O., 51  
 BLANC, A., 43, 50, 51

BLOCH, E., 294, 295, 297, 304  
 BLODGETT, K. B., 160, 256  
 BOECKNER, C., 150, 153, 160, 256  
 BOHR, N., 149, 362, 375, 406, 636  
 BOLTZMANN, L., 44, 79, 109, 179, 185,  
 320, 322, 587, 589, 644, 651, 654  
 BOSCH, C., 497, 514  
 BOULIND, H. F., 348, 369, 490, 493, 507,  
 508, 513  
 BOUTY, E., 535, 536  
 BOWKER, H. C., 535, 536  
 BOWLS, W. E., 338, 343, 350, 353-357,  
 369, 392, 393, 395, 406, 416, 418, 449,  
 480, 484  
 BOYLAN, R. K., 50, 148, 160  
 BRADBURY, N. E., 2, 5, 11, 14, 16, 23, 26,  
 30, 31, 34, 35, 40-42, 49, 50, 97, 127,  
 131, 139, 159, 160, 177, 178, 181, 182,  
 187, 189, 194, 196, 198, 213, 229, 230,  
 252, 268, 276, 288, 291, 294, 295, 297,  
 298, 302, 304, 312-315, 317, 335, 343,  
 364, 369, 370  
 BRAGG, W. H., 102, 139, 160  
 BRAMLEY, A., 598, 604  
 BRASEFIELD, C. J., 556, 559  
 BRATA, L., 20, 31, 38, 39, 48-51, 64, 69,  
 77  
 BRODE, R. B., 379, 406, 409, 648  
 BROSE, H. L., 180, 181, 198, 199, 275,  
 280, 292, 304, 313, 335, 591, 602, 603  
 BROWN, W. L., 257  
 BRUCE, J. H., 369, 507, 508, 514  
 BUCHMANN, E., 479, 484  
 BURAWOY, O., 449

## C

CAMPBELL, N., 454, 470, 538, 559  
 CARR, W. R., 476, 479, 484  
 CASHMAN, R. J., 407  
 CERWIN, S. S., 479, 484  
 CHAPMAN, S., 6, 30, 37, 50, 68, 160  
 CHATTOCK, A. P., 28, 31  
 CHENAULT, R. L., 154, 160, 335

CHILD, C. D., 335  
 CHOW, C. T., 257  
 CHRISTOPH, W., 497, 514  
 CLAUDE, G., 592, 599, 600, 603  
 COCKROFT, J. D., 462  
 COLE, W. C., 406  
 COLLENS, H., 404, 407, 440, 441, 449, 542, 559  
 COMPTON, K. T., 65, 71-73, 77, 78, 85, 182, 183, 187-190, 197-199, 201, 202, 211, 213, 215, 231, 256, 279, 317, 320, 324, 335, 362, 363, 364, 368, 369, 474, 476, 478, 479, 573, 580, 591, 599, 603, 610-612, 615, 633-636, 639-641  
 CONDON, E. U., 44  
 COOK, L., 307, 309  
 COOK, W. R., 62, 68, 69-71, 83, 85  
 COOLIDGE, W. D., 91, 92, 97  
 COULOMB, C. A., 103, 107, 113, 115, 116, 638  
 COWAN, H. MC. N., 257  
 CRAVATH, A. M., 24, 31, 104, 106, 183, 186, 199, 209, 210, 213, 231, 268, 272-279, 281, 282, 291, 292, 304, 312, 335, 383, 384, 404, 406, 430, 440, 449, 483, 516, 535, 543, 547, 559  
 CROOKES, W., 368, 426, 506, 519, 561, 563, 564, 567-574  
 CUNNINGHAM, E., 83  
 CURTISS, L. F., 398, 403, 407, 453, 470, 535

## D

DALTON, J., 162, 603  
 DARROW, K. K., 234, 256  
 DAVIES, A. C., 375, 406  
 DAVIS, B., 362, 369  
 DAVY, H., 605  
 DAVYDOV, B., 215, 221, 225, 231  
 DE BRUYNE, N. A., 476  
 DEBYE, P., 44  
 DECHÈNE, C., 383, 384, 404, 406, 430, 449, 516, 535  
 DEMPSTER, A. J., 49, 479, 484  
 DESACHY, G. P., 50, 148, 160  
 DEUTSCH, W., 149, 160  
 DIDLAUKIS, A. P., 209, 213, 231  
 DIETERICH, I. R., 482, 483, 484, 549, 559  
 DITTMER, A. F., 257  
 DONALDSON, R. H., 558, 559  
 DOPPLER, J. C., 596

DRUYVESTYEN, M. J., 52, 173, 194, 195, 197, 199, 203, 209, 210, 212-216, 221, 226, 229, 230, 231, 233, 234, 246, 249, 252, 256, 257, 279, 295, 362, 363, 369, 480, 583, 586, 589, 591, 603, 604, 607, 637-41  
 DUDELL, W., 626, 640  
 DUFFENDACK, O. S., 470, 497, 513  
 DUFOUR, A., 464, 482  
 DUNNINGTON, F. G., 435, 440, 448, 449, 465, 470, 537, 558  
 DUSAULT, L., 49  
 DYK, K., 50

## E

EARHEART, R. F., 535, 536  
 ECKART, C. H., 256, 636, 639, 641  
 EDLEFSEN, N. E., 335  
 EDMUNDS, P. J., 514  
 EHRENKRANTZ, F., 357, 369, 374, 381, 406, 415, 418, 419, 449, 536  
 EINARSSON, A. W., 50  
 EINSTEIN, A., 109, 110, 172, 174, 176, 312  
 EMMELÉUS, K. G., 231, 249, 251, 257, 298, 300, 365, 368, 370  
 V. ENGEL, A., 234, 238, 244, 367, 470, 482, 484, 570, 576, 578, 580, 583, 586, 590, 591, 594, 595, 601, 603, 604, 608, 610, 611, 613, 615, 617, 621, 630, 639, 640  
 ENGSTROM, R. W., 350, 370, 400, 401, 407, 417, 449, 478  
 EPSTEIN, P. S., 320, 335  
 ERIKSON, H. A., 2, 5, 7, 30, 36, 38, 40, 42, 50, 51, 93, 121, 122, 159, 160  
 ESCLANGON, F., 556, 559  
 ESTERMANN, I., 645  
 EVANS, R. D., 74  
 EYRING, O. C., 472, 476

## F

FARADAY, M., 110, 167, 228, 561, 562, 564, 567, 571-573, 585  
 FERMI, E., 202, 221, 473  
 FINNEY, G. A., 74  
 FITCH, T., 536  
 FIZEAU, H. L., 19  
 FLEGLER, E., 428, 431, 432, 440, 449, 535  
 FLOWERS, J. W., 475, 476  
 FONTELL, N., 20, 31, 40, 171, 176  
 FOOTE, P. D., 154, 160, 335

FOURIER, J. B. J., 163, 176  
 FOWLER, R. H., 107, 375, 406, 472, 473, 476, 630  
 FOX, G. W., 257  
 FRANCK, J., 2, 8, 11, 30, 34, 36, 43, 51, 168, 176, 178, 181, 188, 189, 198, 200, 202, 258, 259, 285, 297, 304, 360-362, 367, 375, 376, 406, 439, 442, 445, 449, 470, 482  
 FRANKLIN, B., 542  
 FRICKE, H., 514  
 FRY, P. C., 320, 335

## G

GALLOWAY, W. R., 414, 450  
 GARDNER, M. E., 41, 50, 97, 98, 100-102, 106, 112, 114, 118, 120-124, 131, 133, 134, 136, 137, 138, 139, 146, 147, 159, 406  
 GEHRKE, H., 596, 604  
 GEIGER, R., 384, 398, 402, 403, 453, 471, 475, 485, 487, 489, 490, 494, 495, 499, 500, 501, 503, 504, 522, 527, 530, 532, 535, 603, 604, 639  
 GEISSLER, H., 208  
 GELHOF, G., 575, 603  
 GILL, E. W. B., 342, 362, 369  
 GLOCKER, G., 298  
 GORRILL, S., 384, 407, 435, 516, 526, 529, 535  
 GOSLING, B. S., 472, 476  
 GREEVES, F. D., 251, 257  
 GREGOROVICI, R., 414, 450  
 GREINER, H., 383, 384, 403, 407, 487, 513, 516, 535  
 GRINDLEY, G. C., 2, 5, 11, 14, 30, 34, 40, 49, 50, 51  
 DE GROOT, W., 598, 604  
 GÜNTHERSCHULZE, A., 256, 499, 514, 575, 577, 598, 600-604, 612, 632, 640  
 GUTTON, C. AND H., 557, 558, 559, 602, 604

## H

HAFSTAD, L. R., 470  
 HAGENBACH, A., 605, 615, 626, 627, 639, 640  
 HAINES, W. B., 51

HALE, D. H., 338, 343, 355, 356, 357, 365, 369, 370, 375, 392, 395, 406, 418, 419, 420, 449, 478, 480, 481, 484  
 HAMADA, T., 596, 604  
 VON HAMOS, L., 431, 440, 449  
 HAMSHERE, J. L., 20, 31, 40  
 HARKNESS, R. W., 304  
 HARPER, W. R., 105, 107, 110-112, 119, 127-130, 148, 160  
 HARRIES, W., 189, 199, 203, 231  
 HARRINGTON, M. C., 256  
 HASELFOOT, C. E., 169, 176  
 HASELTINE, W. R., 72, 257, 307, 407  
 HASSÉ, H. R., 59, 62, 66, 68-71, 81, 83, 85  
 HAUPT, C. R., 201  
 HAVERSTICK, E. J., 640  
 HAYNER, L., 151, 160  
 HEBB, T. C., 640, 641  
 HEHL, N., 603  
 HENDERSON, G. H., 375, 406  
 HENDREN, L. L., 93, 159  
 HENNING, E., 497, 513  
 HERB, M. H., 470  
 HERSHEY, A. V., 26, 27, 31, 33, 34, 49, 65, 72-74, 77, 83, 85  
 HERTZ, G., 173, 176, 202-204, 206, 210, 231, 311, 317, 335, 360, 361, 363, 367  
 HEYDENBERG, N., 470  
 HIGLEY, E. A., 123  
 HILBERRY, N. F., 556, 559  
 HILLEBRAND, W. F., 558, 608  
 VON HIPPEL, A., 406, 439, 442, 445, 449, 482, 539, 559, 580, 581, 600, 603, 604  
 HIRCHERT, R., 586, 603  
 HOBBS, G. M., 558  
 HODGSON, R., 604  
 HOGNESS, T. R., 285, 304  
 HOLM, R., 367, 575, 586, 603  
 HOLST, G., 343, 369, 370, 381-383, 406, 415, 423, 449, 477, 484, 570, 573, 580, 603, 604, 636, 638, 641  
 HOLZER, R. E., 542, 559  
 HOOPER, W. J., 375, 406  
 HÖRMANN, H., 614, 618, 623, 640  
 HORTON, W. F., 375, 406  
 HOUSTON, W. V., 476  
 HULL, A. W., 325  
 HURST, H. E., 342, 369, 417, 449  
 HUXFORD, W. S., 350, 370, 400, 407, 449, 478  
 HUXLEY, L. G. H., 348, 369, 507-509, 514

## I

- ISRAEL, H., 160  
 ISSENDORFF, J. V., 256, 603, 632, 633, 640

## J

- JACKSON, W. J., 382, 406  
 JAEGER, J. C., 198  
 JAFFÉ, G., 102, 132, 139-142, 144, 160  
 JAMES, J., 482, 484  
 JEANS, J. H., 67  
 JEHLE, H., 545, 559  
 JEN, G. K., 294, 304  
 JENSEN, J. C., 542, 559  
 JOELBAUER, A., 360, 369  
 JOFFÉ, A., 106  
 JOHNSTON, J. E. McF., 251, 257  
 JONES, F. L., 257, 384, 414, 450  
 JOULE, J. P., 643

## K

- KALLMAN, H., 48, 49, 69, 70, 149, 160, 170, 377  
 KANNENSTINE, F., 641  
 KAPLAN, J., 355, 370  
 KAPZOV, N., 442, 449, 482  
 KAUFMANN, W., 37, 50  
 KECK, P., 335  
 KELLY, H. C., 230  
 KELVIN, LORD, 118  
 KENNEDY, D., 50  
 KENTY, C., 131, 150, 151, 155, 160, 253, 257, 383, 406  
 KIEPENHEUER, K. O., 497, 514  
 KILLIAN, T. J., 256  
 KINGDON, K. H., 325, 327, 335, 600, 604  
 KIP, A. F., 50, 407, 441, 449, 455, 462, 470, 514, 526, 535  
 KIRCHNER, G., 559  
 KIRCHSTEIN, B., 376, 406  
 KLARFELD, B. J., 604  
 KLEEMAN, R. D., 139, 160  
 KLEMPERER, O., 348, 370, 407, 450  
 KNIPP, C. T., 556, 559  
 KOBEL, E., 633, 635, 640  
 KOLLATH, R., 229, 647, 648  
 KOVARICK, A. F., 12, 34, 36, 49, 50, 258-265, 304  
 KRAUS, P., 159  
 KREUSLER, H., 369

- KRUITHOFF, A. A., 215, 231, 317, 335, 350, 351, 358, 363, 369, 392, 393, 400, 401, 407  
 KUNSMAN, C. N., 10, 26, 69, 74, 161, 319

## L

- LAMAR, E. S., 194, 199, 202, 210, 211, 221, 228-231, 295, 610, 611, 634, 640  
 LANDALE, S. E. A., 257  
 LANGEVIN, P., 14, 30, 37-39, 45, 48, 50, 52-55, 62, 65-67, 69-71, 73, 78, 80, 81, 84, 85, 87, 94, 96, 102-110, 112-114, 120-122, 125-129, 144, 148, 159, 170, 175, 178, 183, 262  
 LANGMUIR, I., 160, 209, 232, 247, 255, 256, 312, 317, 319-325, 335, 363, 470, 474, 586, 589, 597, 598, 600, 602-604, 629, 639  
 LAPORTE, M., 19, 30  
 LAU, E., 596, 604  
 V. LAUE, M., 440-443, 449, 641  
 LAURITZEN, C. C., 472, 476  
 LAWRENCE, E. O., 74, 201, 335, 449, 537, 559  
 LENARD, P., 52, 55, 335, 647  
 LENNARD-JONES, J. E., 37, 68  
 LIEFSCHUTZ, H., 497, 513  
 LILIENTELD, J., 471, 476, 596, 604  
 LILLY, E. G., 641  
 LITTLE, E. M., 154, 160  
 LOCHER, G. L., 487, 496, 498  
 LOEB, L. B., 5, 11, 12, 14, 23, 24, 26, 30, 31, 33-35, 37, 38, 40, 43, 44, 48-52, 54, 59, 60, 62, 85, 97, 98, 106, 107, 117, 126, 131, 144, 150, 153, 159, 160, 176-179, 181-184, 188, 189, 198-201, 252, 257-259, 262, 264-268, 272, 282, 287, 294, 304, 312, 314, 315, 328, 335, 343, 348, 353, 363, 369, 375-378, 383, 386, 404, 406, 407, 421, 422, 428, 429, 439, 440, 442, 448, 449, 478, 483, 513, 521, 535, 536, 543, 559, 608, 638, 640, 641  
 LOEB, L. L., 176  
 LORENTZ, H. A., 202, 211, 213, 231  
 LOSCHMIDT, J., 643, 645  
 LOZIER, W. W., 298, 304  
 LUHR, O., 39, 40, 41, 50, 97, 100, 102, 131, 133, 137, 143, 146, 147, 159, 160  
 LUNN, E. G., 285, 304  
 LUNT, R. W., 231, 365, 368, 370

LUSE, H. F., 24, 31, 273, 304  
 LUTKIN, F. E., 542, 559  
 LYNCH, W. A., 556

## M

MACKINNON, K. A., 556, 559  
 MCCALLUM, S. P., 220, 350, 363, 369  
 MCCLELLAND, J. A., 86, 93, 159  
 MCCLUNG, R. K., 93, 123, 159  
 MCCURDY, W. H., 573, 602, 603  
 MCEACHRON, K. B., 542, 559  
 MCGEE, J. D., 198  
 MCGREGOR, E. J. R., 249-251, 257  
 MCLELLAND, J. A., 50  
 MCLENNAN, J. C., 640  
 MÄCHLER, W., 124, 126, 127, 159  
 MACKEOWN, S. S., 472, 474, 476, 629, 639  
 MAHONEY, J. J., 50  
 MAIER-LEIBNITZ, H., 201, 216, 227, 231, 363  
 MAJORANA, E., 69  
 MANNKOFF, R., 617, 618, 640  
 MARSHALL, L. C., 93, 97, 100, 102, 106, 123, 131, 133, 143, 159  
 MASCH, K., 341, 343, 345, 346, 350, 354, 369, 470, 514, 535  
 MASON, R. C., 481, 484, 613, 614, 640  
 MASSEY, H. S. W., 69, 85, 291, 294, 296, 297, 304  
 MATHUR, L. S., 369  
 MAXWELL, J. C., 61, 71, 79, 153, 177, 184, 192, 193, 194, 197, 201, 202, 209, 210, 212-215, 221, 225, 226, 229, 233-236, 240, 246, 247, 249, 251, 253, 256, 322, 362, 365, 366-368, 585, 589, 591, 617, 618, 639, 645, 651  
 MAYER, H. F., 38, 43, 50, 85, 647  
 MEDICUS, G., 497, 514  
 MEEK, C. A., 365, 368, 449  
 MEEK, J. M., 231, 370, 404, 407, 435, 441, 450, 463, 470, 536, 543, 544, 548, 549, 559  
 MEITNER, L., 51  
 MEYER, E., 412, 449, 641  
 MIE, G., 94  
 MILLER, F. C., 559, 608  
 MILLIGAN, J. C., 304  
 MILLIKAN, R. A., 49, 51, 83, 85, 167, 471, 472-474, 476, 641  
 MITCHELL, J. H., 20, 31, 33, 41, 49, 51, 71, 73, 77, 85

MITRA, S. K., 559  
 MOHLER, F. L., 131, 143, 150, 151, 153-157, 159, 160, 256, 335  
 MOHR, C., 69, 85  
 MONTGOMERY, E., 257  
 MOON, P. B., 382, 395, 484, 569  
 MOONEY, M., 267  
 MOREAU-HANOT, M., 160  
 MORSE, P. M., 154, 160, 194, 199, 202, 210, 211, 221, 228-231, 256, 295, 580, 603  
 MOTT, N. F., 69  
 MOTT-SMITH, H. M., 160, 232, 247, 256  
 MOULIN, M., 139-141, 160  
 MOUZON, J. C., 376, 406  
 MULDER, J. G. W., 474, 476, 535, 630, 640  
 MULLER, E. W., 474, 476, 535, 603, 630, 640  
 MULLIKAN, R. S., 355, 369

## N

NAGAOKA, H., 504, 558, 608, 640  
 NAKAYA, U., 450, 456, 470  
 NEUBERT, D., 603  
 NEUMAN, L. J., 379, 381, 406, 407, 449  
 NEVIN T. E., 51  
 NEWMAN, M., 440, 448, 450, 469, 470  
 NIELSEN, R. A., 23, 26, 31, 35, 50, 177, 178, 181, 187, 189, 192, 194-197, 198, 213, 230, 231, 252, 313, 315, 335, 364, 370  
 NOLAN, J. J., 51, 160  
 NOLAN, P. J., 50, 148, 160  
 NORDHEIM, L., 472, 473, 476, 630  
 NORDMEYER, M., 376, 406  
 NORINDER, H., 542, 559  
 NORMAND, C. E., 190, 191, 199, 229  
 NOTTINGHAM, W. B., 201, 231, 605, 612-614, 623, 631, 640

## O

O'BROLCHAIN, C., 148  
 OHM, G. S., 527  
 OLDENBURG, O., 304  
 OLIPHANT, M. L. E., 382, 395, 406, 407, 480, 484, 513, 569  
 OLLENDORF, F., 429, 449, 559  
 OLMSTEAD, P. S., 641



ONSAGER, L., 130, 160

OOSTERHUIS, E., 369, 381-383, 406, 415,  
449, 477, 484, 570, 573, 580, 603, 604,  
636, 641

OPPENHEIMER, J. R., 153, 160, 472, 476

ORNSTEIN, L. S., 618, 620, 640

## P

PAAVOLA, M., 341, 343, 345, 348, 350,  
369, 386, 392, 407

PAETOW, H., 498-500, 514

PARTZSCH, A., 314, 335

PASCHEN, F., 410, 448, 476, 477, 507, 508,  
534, 557

PATTERSON, C. C., 558

PAULING, L., 69

PAUTHENIER, M., 160

PAVLOW, V. J., 375, 406

PEARCE, A. F., 20, 31, 50

PEDERSEN, P. O., 440, 442, 449

PEEK, W. F., 542, 559

PENNING, F. M., 203, 220, 231, 257, 317,  
335, 343, 348-351, 356, 358, 363, 369,  
382, 385, 393-395, 398, 400, 406, 407,  
414, 449, 470, 474, 476, 477, 479, 480,  
481, 484, 507, 510, 511, 513, 514, 592,  
598, 602-604, 630, 640

PERCY, R., 640

PHILLIPS, P., 36, 38, 43, 50, 121, 160

PIDDUCK, B. F., 79, 85, 182, 198, 202, 211,  
231, 342, 362, 369

PLANCK, M., 473

PLIMPTON, S. J., 94, 106, 108, 121, 123,  
131, 159

POHL, R., 304

POLLOCK, J. A., 45, 50

POMMERING, E., 603

POSIN, D. Q., 343, 345, 346-348, 353, 354,  
369, 406, 407, 448, 449

POULSON, W., 628

POWELL, C. F., 2, 14, 18, 19, 20, 30, 31,  
34, 35, 39, 40, 48-50, 69, 73, 77, 82, 85

PRESS, R., 303, 304

PRZIBRAM, K., 1, 33, 43, 49-52, 85

## Q

QUINN, R. B., 479, 484

## R

RAETHER, H., 384, 404, 407, 427, 432,  
434, 440, 441, 449, 450, 473, 513, 516,  
535, 545, 558

RAMBERG, W., 632, 640

RAMIEN, H., 189, 191, 199, 231

RAMSAUER, C., 180, 184, 185, 188, 190,  
194, 197, 198, 201, 203, 212, 213, 216,  
229, 281, 295, 362, 636, 647, 648

RANDALL, R. H., 157

RANDOLPH, D. W., 470

RATNER, S., 30, 31, 258, 304

REGNAULT, V., 93

REICHRUDEL, E., 257

REUKEMA, L. E., 470, 550-552, 556, 558,  
559

RICHARDSON, O. W., 104, 105, 107, 114,  
116, 160

RIDLER, K. W., 20, 31, 33, 41, 49, 51, 71,  
73, 77, 85

RIECKE, E., 94, 159

ROGOWSKI, W., 343, 345, 383, 407, 421,  
422, 439, 442, 449, 464, 470, 537, 558,  
580, 603

ROHMANN, H., 149, 160

ROSEN, B., 48, 49, 69, 70, 149, 160, 170,  
377

ROSTAGNI, A., 335, 376, 377, 406

ROTTGARDT, K., 575, 603

RUDENBERG, K., 545, 559

RUMELIN, G., 93, 96, 105, 106, 123, 131,  
159

RUTHERFORD, E., 2, 7, 11, 20, 26, 30, 36,  
51, 86, 93, 97, 105, 121, 159, 178, 181,  
258, 259, 262, 264, 267

## S

SAHA, M. N., 369, 609, 617, 618, 620, 621,  
640

SAHA, N. K., 640

SALLES, E., 176

SÄMMER, J. J., 439, 442, 449, 482

SANDERS, F. G., 338, 339, 341-346, 348,  
365, 369, 375, 386, 392, 406, 450, 514,  
535

SAWYER, R. A., 474

SAYERS, J., 93, 100, 122-124, 127, 131,  
147, 160, 559

SAYMAN, E. H., 181, 199, 591, 603

SCARSE, F. J., 541, 559

SCHADE, R., 497, 513, 514

SCHAEFER, B., 632, 633, 640  
 SCHAUFELBERGER, A., 575, 602, 603  
 SCHEEL, K., 1, 49, 603, 639  
 SCHEMEL, J., 141, 142, 160  
 SCHILLING, H., 36, 50, 476  
 SCHNEIDER, G., 382, 407, 484  
 SCHOEFER, R., 369, 407, 417, 449  
 SCHONLAND, B. F. G., 404, 407, 440, 441, 449, 542-545, 547-549, 559  
 SCHOTTKY, W., 256, 320, 335, 472, 473, 476, 586, 603  
 SCHULZE, R., 496, 513  
 SCHUMANN, W. O., 412, 439, 442, 448, 449, 455, 456, 470, 482  
 SEELIGER, R., 256, 474, 476, 580, 586, 603, 640  
 SEEMAN, H., 334, 335  
 SEILER, R., 201, 231  
 SERBER, R., 109  
 SHACKELFORD, B. E., 476  
 SHAW, P. E., 85  
 SHEPPARD, P. A., 50  
 SILLSBEE, F. B., 536  
 SIMON, H. T., 626, 628, 640  
 SIMPSON, C. G., 541, 559  
 SKINNER, C. A., 575, 603  
 SKINKER, M. F., 198  
 SLAWSKY, M. M., 497, 513  
 SLEPIAN, J., 429, 440, 449, 558, 617, 640  
 SLOANE, R. H., 250, 251, 257, 304, 632  
 SMIT, J. A., 196, 198, 221, 222, 230, 231, 362, 363, 370  
 SMITH, A. E., 407  
 SMITH, P. T., 201, 364, 365, 367, 370, 556  
 SMITH, R. A., 294, 297, 298, 303, 304, 470, 559, 604  
 v. SMOLUCHOWSKI, M., 110  
 SNODDY, L. B., 482-484, 549, 559  
 SNOW, H. W., 535  
 SOMMERFELD, A., 107, 111, 112, 472, 473, 604  
 SOMMERMEYER, K., 640  
 SPIWAK, G., 257  
 SPONER, H., 201, 203, 231  
 STARK, J., 537, 540, 575, 603, 608, 640  
 STARR, L. H., 30  
 STEENBECK, M., 234, 238, 244, 367, 470, 482, 484, 570, 575, 576, 578, 580, 581, 583, 586, 590, 591, 594, 595, 601, 603, 604, 608, 610, 611, 613, 615, 617, 621, 630, 639, 640

STERN, O., 476 645  
 STOKES, G., 83, 84  
 STOLETOW, A., 335, 369  
 STOLT, H., 460, 632  
 STRAEHLER, H., 256  
 STRIGEL, R., 440, 442, 448, 450, 464, 469, 470  
 STRUTT, R. T., 417, 449, 477, 484  
 STUECKELBERG, E. C. G., 154, 160  
 SUGUIRA, Y., 540, 558, 640  
 SUITS, G. G., 620, 621, 624, 640  
 SUTHERLAND, W., 36, 37, 52, 53, 58, 59, 85  
 SUTTON, R. M., 376, 383, 384, 406

## T

TAIT, P. G., 645  
 TAMM, R., 442, 449  
 TANBERG, R., 633, 634, 640  
 TATE, J. T., 298, 304, 370, 406, 640  
 TATEL, H., 286, 287, 304  
 TAYLOR, J., 383, 406, 449  
 TERADA, T., 450, 456, 470  
 TESLA, N., 553  
 TEVES, M. C., 592, 603  
 THIRKILL, H., 121, 160  
 THOMSON, J., 554, 557, 559  
 THOMSON, J. J., 1, 2, 30, 33, 35, 37, 46, 49, 50, 59, 60, 62, 85, 86, 93, 104, 106, 107, 108, 111-114, 116, 119-122, 124-131, 144, 149, 159, 160, 167, 178, 261, 267, 268, 272, 282, 296, 304, 305, 311, 312, 314, 317, 328, 333, 335, 353, 375, 376, 377, 406, 449, 482, 484, 553-558, 559, 567, 579, 580, 602-605, 639  
 TILLES, A., 440, 443, 445, 448, 449, 467, 470  
 TIZARD, H. T., 31, 179, 198, 271, 275, 276, 280, 281, 286, 304, 313, 335, 369, 406  
 TODD, W., 26, 31  
 TOEPLER, M., 535  
 TONKS, L., 209, 228, 231, 255, 257, 363, 474, 586, 589, 602, 603, 604, 633, 640  
 TOROK, J. J., 442, 449  
 TORRESON, O. W., 45, 50, 160  
 TOWNSEND, J. S., 2, 26, 31, 49, 74, 75, 86, 93, 159, 161, 163-165, 167-169, 176-182, 190, 192, 193, 195-197, 202, 209, 210, 214, 215, 217, 219, 220, 228-232, 235, 268, 270, 271, 275, 276, 278, 280,

- 281, 286, 304, 313, 315, 334-340, 342-346, 348, 350, 353-355, 358-363, 365, 367, 369-372, 374, 377, 381, 383, 386, 402, 405-407, 409, 411, 412, 416, 423, 448, 451, 453, 460, 471, 479, 480, 488, 490, 493, 494, 507, 513, 514, 515, 521, 559, 581, 582, 591
- TRICHEL, G. W., 407, 441, 449, 450, 455, 513, 517, 522, 530, 535
- TROST, A., 513
- TURNER, L. A., 573
- TUVE, M. A., 470
- TUXEN, O., 296, 304
- TYNDALL, A. M., 2, 5, 11, 14, 19, 20, 29, 30, 31, 34, 35, 38, 40, 43, 48-51, 69, 73, 77, 82, 85, 107
- U
- UYTERHOEVEN, W. V., 253, 256
- V
- VAN DE GRAAF, R. J., 19, 31, 460, 462
- VAN DER BIJL, H. J., 641
- VAN DER WAALS, J. D., 67, 68, 78, 81, 82
- VAN GORCUM, A. H., 249, 251, 257
- VAN VOORHIS, C. C., 478, 634, 640
- VARLEY, C. F., 314, 335
- VARNEY, R. N., 11, 20, 30, 34, 40, 49, 50, 173, 176, 328, 335, 348, 369, 376, 377, 383, 384, 386, 406, 407, 421, 448, 470, 559, 608
- VON SCHWEIDLER, E., 369
- W
- WAHLIN, H. B., 35, 50, 51, 178, 182, 188, 198, 252, 265, 266, 267, 285-287, 304
- WAIT, G. R., 47, 51, 160
- WALRAFF, A., 421, 449, 470
- WALTON, E. D., 462
- WARBURG, E., 575, 603
- WATSON E. A., 507, 514
- WAYLAND, N., 377, 406
- WEBB, H. W., 157
- WEHNELT, A., 476
- WEHRLI, M., 627, 640
- WELLISCH, E. M., 35, 49, 51, 52, 53, 58, 59, 85, 105, 259, 260, 265, 266, 304
- WERNER, S., 407, 490, 491, 494, 501, 504, 507, 513, 535
- WESTPHAL, W. H., 168, 176, 602
- WHEELER, A., 470
- WHIPPLE, E. J. W., 148, 160
- WHITE, H. J., 198, 348, 369, 386, 407, 421, 427, 431, 432, 435, 440, 446, 448, 449, 465, 468-470, 559, 608
- WHITEHEAD, J. B., 535, 536
- WIGAND, A., 50
- WILSON, C. T. R., 46, 100, 268
- WILSON, R. R., 428, 440, 446, 447, 448, 450, 467-470
- WITTE, H., 618, 640
- WOLFE, H. C., 470
- WOOD, R. W., 596, 603
- WOOLSEY, R. E., 314, 335
- WORKMAN, E. J., 542, 559
- WORMELL, W. T., 559
- Y
- YAO, Y. T., 641
- YARNALD, G. D., 559
- YEN, KIA-LOK, 49, 294, 304
- YLOSTALO, V., 559
- YOUNG, L. A., 312, 317, 335
- Z
- ZELENY, J., 2, 3, 4, 12, 14, 30, 34, 38, 40, 165, 176, 535
- ZUBER, K., 440-443, 449

## SUBJECT INDEX

Numbers in **bold-faced type** represent pages where the title is either discussed *in extenso* or else mentioned in some important connection. Other numbers give pages where the subject is mentioned.

- Abnormal cathode fall in glow discharge, 563, 583, 606
- Abnormal cathode fall of potential explained, 583
- Absolute values of ionic mobility, 5, 11, 18, 22, 23, 25, 28, 33, 64, 69, 70, 76
- Absorbing cross sections, for electron ionization and excitation, 195, 201, 216, 227, 363, 364, 367, 478, 479, 570, 634
  - in molecular or electronic collisions, 647
- Accommodation coefficient for positive ions, 254, 301, 634, 635
  - in probe studies, 254
  - of arc cathodes for positive ions, 634, 635
- Active spot size in negative point to plane corona, 516
- Active spots, multiple, in negative point to plane corona, 519
- Adsorbed gases in sparking potential measurements, 453
- Aging effects with ions, 40, 147
- Aging of ions and recombination, 147
- Air, Ayrton constants for, 623
  - Chapman's curves with Erikson's air-blast method in, 6, 40
  - characteristic sparking curve of, 411
  - columnar ionization and recombination in, 141, 142
  - diffusion constant in, 165
  - electrical shutter methods, for, 19
  - electron attachment in, 259, 260, 263, 267, 271, 274, 275, 278
  - electron mobility in, 181, 191
  - first Townsend coefficient for, 340, 342, 344, 361, 366
  - fluctuating burst corona in, 534
  - free electrons in, 263
  - groups of ions in, 48
  - initial recombination in, 94, 121, 123, 137, 138
  - ionization by collision in, 340; *see also* Townsend's first coefficient
  - ionization current in, 339
  - Langevin and intermediate large ions in, 46, 47
  - length of normal cathode dark space, 575
  - low-pressure sparking in, 479
  - methods of measurement of coefficient for recombination involving, 93
  - minimum starting potential of corona in, 508
  - mobilities in gaseous mixtures in, 42, 43, 55
  - normal cathode fall of potential in, 577
  - normal current density divided by pressure squared, 578
  - potential fall in arc in, 614
  - preferential recombination in, 127, 128
  - probability of electron attachment in, 271, 275, 279, 280
  - spark breakdown with alternating current in, 553
  - speed of propagation of spark in, 428, 431, 434-439, 448, 482
  - values of coefficient of recombination in, 147
  - variation of mobility of negative ions with pressure in, 35, 259, 260
  - volume recombination of ions in, 124

- Air-blast method, 3, 5, 92, 164  
  for coefficient of recombination, 92  
  for evaluating coefficient of diffusion, 164  
  of Erikson for ionic mobilities, 5  
  of Zeleny for ionic mobilities, 3, 4, 5  
Air-blast methods, 3, 4, 102, 164  
  deficiencies of, 7  
Alkali metals in Geiger counters, 496  
Allen's electron mobilities, 197  
 $\alpha$ , coefficient of recombination, definition of, 88; *see also* Recombination coefficient  
  methods of measurement for, 91  
 $\alpha/p$  as  $f(X/p)$ , 342  
  Compton's theoretical treatment of, 362  
  decline in, at high fields, 351, 357, 370, 478  
  Druyvesteyn's first attempt at theory of, 209  
  Druyvesteyn's theory for Ne, 220, 363  
  effect of, on space-charge formation, 390  
  v. Engel and Steenbeck's theory of, 367  
  evaluation by theory of Emmeléus, Lunt and Meek, 366  
  Holm's theory for, 365  
  simple correct approximate theory for, 363  
  theoretical evaluation of, 209, 220, 358, 362, 363, 366, 367, 370  
  Townsend's theoretical evaluation of, 358  
  Townsend's theory in glow discharge, 581  
 $\alpha$  particle, ionization and recombination, 139  
  ranges, temperature in arcs from, 608, 617  
A-c arc, oscillogram of, 627  
  theory of, 628  
A-c method of determining distribution law with probes, 249  
A-c mobility measurement, Franck modification of, 11  
  Rutherford method, 7  
A-c spark potential measurements, need for illumination of both electrodes in, 459  
Alternating potentials, spark breakdown with, 550  
Alternative processes to ionization by positive ions in gas, 377; *see also* Townsend's  
  second coefficient, alternatives to  $\beta$   
Ambipolar diffusion, 586, 589, 616, 619, 621  
  in arc columns, 616, 619, 621  
  in glow discharge columns, 586, 589  
Anode fall of potential, 333, 596, 597, 615, 623, 627  
  in arcs, 615, 623, 627  
  in glow discharge, 596, 597  
  values of, 598  
  with ion currents in a gas, 333  
Anode glow, 561, 562, 596, 597  
  ionization in, 597  
Anode of arcs, electron space charge at, 615  
  energy balance at, 615  
Anode streamers in spark breakdown, 431  
Anode temperature of arcs, 615, 616, 617, 629  
Anomalous sparking potentials in He near minimum, 477  
Apparent molecular collision radius, 650  
Approach voltage, effect of, in time lag studies, 443, 444, 446, 467, 469  
Arc, a-c, 627, 628  
  and glow discharge, 560  
  anode fall of potential in, 615, 623, 627  
  anode temperature in, 615, 616, 617, 629  
  Ayrton constants in, 622, 625

- Arc, cathode fall in, 605, 609, 623, 627, 630  
  energy balance at, 611, 634  
  field emission at, 611, 629, 636  
  cathode temperature in, 613, 615, 616, 626, 632, 635  
  characteristic potential curves of, 608, 614  
  chemical reactions in, 615, 616, 617  
  column, densities of ions in, 617, 620  
    diffusion in, 616, 619, 621  
    electron densities in, 155, 157, 617, 620  
    energy losses in, 622  
    equilibrium in, 618  
    fraction of energy radiated by, 621  
    ionization by electron impact in, 616, 620  
    mechanism of, 619  
    potential fall in, by lengthening of arc, 613, 620  
     $X_i/p$ , low values characteristic of, 609, 616  
  counter emf of, 626  
  current densities in, 605, 609, 610, 631  
  definition of, 605  
  discharge, 605  
  effect of impregnation of carbon with salts on, 617  
  energy balance at anodes of, 615  
  evaporation at cathodes of, 612, 632, 634  
  experimental data in, 622  
  extinction of, by convection currents, 606, 622  
  extinguishing resistance for, 625  
  field strengths, at cathodes of, 611, 623, 627, 631  
    in positive columns of, 609, 613, 614, 616, 620, 621, 623, 627  
  fraction of current carried by positive ions in, 610, 612, 631, 634, 635  
  frequency of oscillation in, 626  
  hissing, 626, 628  
  hysteresis curve of, 628  
  in magnetic fields, 628  
  initiation of, 606  
  ion deposition at cathode of, 631, 634  
  ion transport in, 622  
  ionization in, by successive electron impacts, 610, 620, 636  
  length of cathode fall in, 609, 610, 623, 630  
  low boiling point, and field emission, 474, 629, 636  
    cathode mechanism in, 629  
  low-voltage, 636  
    contact potentials in, 637  
    oscillations not needed in, 636  
    potential distribution in, 637, 638  
    probe measurements in, 637  
  measurement of potentials in, with probes, 613  
  metal, cathode temperatures from rate of evaporation of, 632, 635  
    cooled cathode in, 632  
    Nottingham equation for, 623  
    pitting of cathodes in, 632  
  microprocesses in cathode emission in, 605, 613, 631, 632, 636  
  momentum of evaporated metal vapor in, 631, 632, 633, 634, 635  
  negative characteristic of, and oscillations, 624  
  negative resistance in, 625, 627  
  positive column of, 616; *see also* arc column  
  positive ion space charge limited current in, 610  
  potential fall in, by Stark effect, 608, 615

- Arc, potential fall in column of, by lengthening, 613, 620  
     Poulson, 628  
     rectifying action of, 628  
     rekindling voltage of, 627  
     resistance by high-frequency a c, 626  
     temperature from radiation, band spectra, velocity of sound and ranges of alpha particles, 608  
     temperature ionization in, 609, 617, 620  
     temperatures in, 608, 610, 613, 614, 615, 616, 617, 629, 631  
     thermionic emission in, 605, 607, 629, 636  
     transition of glow discharge to an, 606  
     use of probes in study of cathode fall in, 612  
     value of cathode fall in, 609, 610, 623, 627, 630  
     vapor pressures, partial in, from temperature ionization, 621
- Argon, 33, 38, 49, 63, 64, 67, 70, 73, 75, 76, 78, 82, 158, 193, 194, 195, 196, 197, 230, 289, 297, 343, 349, 350, 399, 400, 414, 509, 511, 575, 577, 578, 623, 638, 649, 656  
     absolute values of mobilities in, 33, 64, 70, 82  
     arcs, potential distribution in low-voltage, 638  
     Ayrton constants for, 623  
     distribution of electron energies in, 196, 230  
     electron affinity of, 297  
     electron mobility in, 193, 194, 195, 196, 197  
     electronic recombination in, 158  
     first Townsend coefficient of, 343, 349, 350  
     ionization potential of, 656  
     length of normal cathode dark space in, 575  
     mean values of first Townsend coefficient for, 349  
     minimum sparking potential of, 414  
     minimum starting potential of corona in, 509, 511  
     mobilities, ionic, at low pressures and high fields in, 73, 75, 76, 78  
         of ions in, 33, 49, 63, 64, 67, 70, 82  
         value of, in, 70  
     normal cathode fall in, 577  
     normal current density divided by pressure squared, 578  
     Ramsauer free paths in, 649  
     second Townsend coefficient in, 399, 400  
     structure of and electron attachment, 289  
     values of coefficient of recombination in, table of, 158  
     variation of mobility with mass and dielectric constant in, 38
- Arnot process of negative ion formation, 298
- Aston dark space, 563, 564, 570, 573
- Atom deposition in arcs by current, 631, 634
- Atomic fields cause Stark effect in sparks and arcs, 537, 540, 608
- Atomic negative ions, formation of, 297
- Atomic structure and electron attachment, 288
- Atoms, and molecules, ionization by collision due to, in arc columns, 618  
     electron affinities of, 297  
     hot, ionization by, 377, 618
- Attachment, electron, *see* Electron attachment; Negative ions, formation of.
- Autoelectronic emission, *see* Field emission.
- Avalanche, *see* Electron avalanche.
- Average electronic random velocity, 179; *see also* Electron energy distribution laws.
- Average energies, of atoms evaporating from metal arc cathodes, 633, 634  
     of electrons, *see* Electron energy distribution law.
- Average free path, molecular, 645
- Average electron free paths, *see* Mean free path, electron.

- Average number of electron impacts for attachment, 261; *see also* Electron attachment, probability of.
- Average velocities, different values of, for molecules, 652
- Average velocity of lightning discharge, 543
- Avogadro number, 644
- Ayrton constants in arcs, 622, 625
- Background counts in Geiger counters, 496, 500, 503
- Bailey's method for measurement of probability of electron attachment, 268
- Balanced space charge detector, 326
- Band spectra, temperatures in arcs from, 609, 617
- $\beta$ , Townsend's, *see* Townsend's  $\beta$ .
- Blanc's law, 43
- deviations from, 44
- Bloch-Bradbury theory of electron attachment in  $O_2$ , 294
- Bohr theory and electron recombination, 149, 158
- Boltzmann constant, 644
- Boltzmann's law for probability of an energy state, 654
- Bowls' studies, of first Townsend coefficient in Hg-free  $N_2$ , 354
- of second Townsend coefficient on Hg-free surfaces, 392
- Boys camera studies of lightning discharge, 543
- Bradbury and Nielsen's values of electron mobilities, 190
- Bradbury-Nielsen shutter method of mobility measurement, 23
- Bradbury's form of Compton equation for electron mobility, 187
- Bradbury's method for measurement of attachment probability, 276
- Bradbury's modification of Tyndall and Grindley method, 14
- Branching, in spark discharge, 433
- of streamers in positive point corona, 529
- Breakdown, detection of, in sparking potential studies, 463
- special types of, 471
- Break-up of cluster ion, 33, 35, 45, 52, 56, 58, 71, 258, 265, 481
- Brownian particles attracting each other, Harper theory for motion of, 111
- Sommerfeld theory for motion of, 108
- Brush discharge, 485, 525, 532
- Burst pulse corona of Trichel, 522, 526, 528
- mechanism of, 528
- Capture cross sections for electrons, by atoms, radiative, 298
- by ions, *see* Electron recombination.
- by molecules, *see* Electron attachment, probability of.
- Cathode, cooled, in metal arcs, 632
- coverage of, and normal or abnormal fall of potential, 563
- dark space, 568; *see also* Crookes dark space.
- deposition of ions at, by arc current, 631, 634
- emission and microprocesses in arcs, 605, 613, 631, 632, 636
- energy balance at, in arc discharge, 611, 612, 634, 635
- in glow discharge, 598
- fall in arc, 605, 609, 623, 627
- length of, 609, 610, 623, 630, 633
- values of, 609, 610, 623, 627, 630
- fall of potential, abnormal and normal, 563, 583, 607
- and Crookes dark space, 575
- and sputtering, 599
- equation for, 583
- explanation of normal and abnormal, 583
- in gaseous mixtures, 577
- length of normal, 568, 608



- Cathode, fall of potential, linear character of normal, 578  
    subnormal, 584, 606  
    normal and abnormal in glow discharge, 584, 606  
    theory of normal, 579, 584  
    values of normal, 577  
    values of width of normal, 575, 585  
    with ions current in gas, 333  
glow, 561, 562, 570, 583  
    nature of, 570  
    spread of, over cathode, 583  
material and sparking potential, 349, 381, 400, 403, 407, 414, 415, 419, 420, 450,  
    451-454, 474, 478, 479-482  
mechanism,  
    in glow discharge, 568, 581  
    in corona, 483, 504, 516  
    in low-pressure sparks, table of, 482  
    of arc, 605, 610, 629  
    of low-boiling-point metal vapor arc, 629  
mechanisms known to be active, in discharge, table of, 403, 482  
of arc, evaporation at, 612, 632, 634, 635  
    field strengths at, 611, 623, 627, 631  
of arcs, no thermal equilibrium at, 631  
of low-melting-point metal arc, field emission at, 611, 629, 636  
of metal arc, pitting of, 632  
photoelectric processes at, 253, 311, 379, 380, 395, 396, 398, 402, 403, 430, 480, 482,  
    486, 502, 504, 512, 527, 531, 568  
-ray beam, measurement of field strength by, 567  
secondary mechanisms known to be active at, in discharge, 403  
spot, efficient, needed for gap breakdown, 426, 537  
sputtering, 599  
    and life of glow discharge tubes, 599  
surface and sparking potential, 349, 381, 400, 403, 407, 414, 415, 419, 420, 450,  
    451-454, 474, 478-482  
surfaces in Geiger counters, 496, 500  
temperature in arcs, 613, 615, 616, 629, 632, 635  
Cathodes, hollow, in glow discharge, 601  
Chance of electron attachment, *see* Electron attachment, probability of.  
Change of charge, and ionic mobilities, 36, 40, 41, 48, 63, 71, 84, 147, 169  
    and recombination, 147  
    ionic, 36, 40, 41, 48, 71, 147, 169  
Characteristic, negative, of arcs and oscillations, 624  
Characteristic curve, for potential fall in an arc, 608, 614  
    for potentials and fields in glow discharge, 566  
    for spark discharge, 412  
    for transition from glow to arc, 607  
Charge, density distribution in glow discharge, 565  
    distribution in typical thunderstorm cloud, 451  
    ionic, and mobility, 48, 49, 63, 83, 84, 170  
Charges, acquired by suspended particles in gases, 148  
    multiple, on ions, 36, 40, 41, 48, 63, 71, 84, 147, 169  
Chattock, electrical wind method of mobility measurement, 28  
Chemical effects in electrodeless discharge and self-excitation in Geiger counters, 497,  
    556  
Chemical reaction products in arc column, 618  
Chemical reactions in arcs, 615, 616, 617  
Child's equation for space-charge-limited current, 319  
Circuit resistance and breakdown of long gaps, 536

- Cleaning of electrodes for spark potential measurements, 452
- Cloud chamber studies of time lags in spark breakdown, 428, 431, 440
- Clouds, polarity of, in lightning discharge, 542
- Cluster ion, 33, 35, 40, 43, 45, 52, 56, 58, 71, 258, 265, 481  
break-up of, 259, 265
- Coefficient, of diffusion, ambipolar, 162, 586, 589  
measurement of, 164, 168  
ratio of, to mobility, 166, 179  
values of, 165  
variation with mass, pressure, and temperature, 175, 176  
of electron recombination, values of, 150, 155, 158  
of recombination, 88; *see also* Recombination coefficient.  
of electron ionization in a gas, *see* Townsend's first coefficient.  
of secondary liberation of ions, *see* Townsend's second coefficient.  
of viscosity, 647, 650
- Collision frequency of electrons, 261, 367, 590
- Colors of glow discharge, 565
- Column, of arc, *see* Arc column; Positive column.  
positive, of glow discharge, *see* Positive column; Glow discharge.
- Columnar ionization and recombination, 87, 139, 142, 144
- Columnar recombination, effect of electrical field on, 142
- Collision, cross section, for electron energy exchange, 639  
cross sections of molecules for electrons, 180, 181, 194, 196, 201, 213, 229, 336,  
647, 648; *see also* Ramsauer free paths; Electron free paths  
frequency, electronic, 261, 367, 590  
ionization by, by electrons in a gas, 336; *see also* Townsend's first coefficient.
- Commutator, Loeb, for high potentials, 97
- Complex ions, 38, 41, 43, 47, 48
- Compton, equation for electron mobility, 186
- Compton's theory, of  $\alpha/p$  as a  $f(X/p)$ , 362  
of electron mobilities, 182  
of "evaporation" of atoms from cathodes in metal arcs, 635
- Compton-Van Voorhis curves, 201, 364, 367, 370, 478, 479; *see also* Ionization,  
efficiency of.
- Concentration gradient of ions in radial direction in glow discharges, 593
- Concentric cylindrical condensers, field and potential distribution in, 486
- Condition for a self-sustaining discharge and sparking threshold, 423; *see also*  
Criterion for self-sustaining discharge.
- Constants, physical, table of, 658
- Contact potentials, in low-voltage arcs, 637  
in probe studies, 254
- Convection currents, extinction of arcs by, 606, 622
- Conventional sparking potential, 423, 432, 465  
definition of, 432
- Corona, burst pulse, of Trichel, 522, 528  
discharge, 384, 485, 486, 504, 507, 514, 520  
action of metastables in, 487, 495, 501, 510-513  
and ionization by positive ions in a gas, 384, 527-531  
and streamer formation, 431, 523, 525, 526, 528, 532, 533  
at low pressures, cumulative ionization in, 490, 512  
effect of gaseous impurities on starting potentials of, 509  
intermittent regime in, 488, 522  
minimum starting potentials in, 503, 507  
negative, 504, 507, 514  
at low pressure, 504  
secondary mechanisms in, 504  
theory of starting potentials of, 512

- Corona, discharge, negative, localization of discharge at point, in corona studies, 514
  - point, at atmospheric pressure, 515
  - positive, 486, 507, 520; *see also* Geiger counter.
  - and negative point to plane in air at atmospheric pressure, 514
  - Ohm's law in, 494, 502, 526, 532
  - point in air at atmospheric pressure, 520
  - wire, at low pressures, 486; *see also* Geiger counter
- pre-onset streamers in, 525, 526, 532
- spark breakdown in, 407, 450, 526, 527, 534
- starting potentials of, and pressure, 507, 513
- zones of effective ionization as defined by Werner and Townsend, 490, 512, 514
- resistance, effective, 494, 526, 532
- Cosmic-ray counters, best surfaces for, 500
- Counter emf of arc, 626
- Counts, spurious, in Geiger counters, 497
- Cravath-Loeb mechanism for rapid propagation of lightning discharge, 440, 483, 544, 547
- Cravath's energy distribution laws, 209, 213
- Cravath's measurement of electron attachment, 273
- Criterion for self-sustaining discharge, 423, 432, 478, 480, 488, 490, 505, 514, 515, 568, 581, 584, 605, 607, 609
- Crookes dark space, 519, 520, 561, 562, 563, 564, 568, 574, 578
  - and cathode fall of potential, 574
  - in negative point to plane corona, 519, 520
  - length of, 568, 574
  - linear fall of potential in, 578
  - positive space charge in, 566, 569
  - potential across, in abnormal and normal cathode fall, 563
- Cross sections, collision or absorbing, 647; *see also* Ramsauer free paths.
- Cumulative ionization at points in point to plane corona, 515
- Current, densities in arcs, 605, 609, 610, 631
  - density divided by pressure squared in normal glow discharges, 578, 585
  - geometrically conditioned saturation, 307
  - in arcs, fraction of, carried by positive ions, 610, 612, 631, 634, 635
  - ionic or electronic lack of saturation in, 309, 314, 315, 333, 338
  - potential curve in a gas with X-ray ionization, 333
  - potential equation in Geiger counters, 493
  - pulse, frequencies in negative point to plane corona, 517
    - time of formation of, 516
  - pulses in Geiger counters, 489
  - space-charge-limited, 237, 317, 319, 320, 323, 325, 610
    - due to positive ions, 237, 320, 610
    - effect of positive ions on, 325
    - equations for, 319
    - in vacuum, 317
    - with cylindrical electrodes, 323
    - with finite velocity of electron emission, 321
- Currents, anomalous in field emission, 474
  - in gases in field below ionization, 305
  - ion, lack of saturation in, 309, 314, 315, 333, 338
  - photoelectric, of low density in gases, 310
    - or thermionic, of low density in gases, Thomson theory for, 312
  - thermionic, 317
    - with volume ionization and positive and negative ions in a gas, 328
- Cylindrical electrode systems, space-charge-limited currents in, 323
- Cylindrical probe, 238, 243, 244, 248, 255

- Dark spaces of Aston, Crookes, and Faraday, darkness of, 564  
Dart leaders in lightning discharge, 548  
Davydov's law for electron energy distribution, 221, 225  
Debye effect in ionic mobilities in mixtures, 44  
Deficiencies, of air-blast method of measuring, diffusion, 165  
    mobilities, 6  
    recombination, 93  
of Bradbury-Nielsen shutter method for mobilities, 25  
of early measurements on recombination coefficients, 93, 94, 95, 101, 102, 197, 198, 214, 228  
of electrical wind method of mobility measurement, 30  
of four-gauze method of mobility measurement, 23  
of Franck modification of Rutherford method for mobilities, 13  
of Rutherford a-c method of measuring mobilities, 11  
of spark potential method for Townsend coefficients, 348, 400, 417  
of Townsend magnetic deflection method for mobilities, 28, 75, 76, 228  
of Townsend measurements for electron energies, 180, 181, 189  
of Tyndall and Grindley method for ionic mobilities, 18  
Definition, of a spark, 408  
    of an arc, 605  
    of coefficient of diffusion  $D$ , 163  
    of coefficient of recombination  $\alpha$ , 88  
    of first Townsend coefficient  $\alpha$ , 339  
    of mean free path  $L$ , 644  
    of mobility  $k$ , and mobility constant  $K$ , 2, 33, 35  
    of probability of attachment,  $h$ , of electrons to molecules, 261  
    of second Townsend coefficient  $\beta$ , 372, 385  
    of Townsend factor  $\eta$ , giving average electron energy, 180  
Density, of electrons, *see* Electron densities.  
    of gas and sparking potential, 535  
    of ions, in arcs, 155, 157, 617, 620  
        in glow discharge columns, 585, 594  
        in spark channels, 537  
Detachment of electrons, *see* Electron detachment.  
Diameters, molecular, 644  
Didlauskis' energy distribution law, 209  
Dielectric constant, and ionic forces, 57, 62, 65, 68, 82  
    from ionic mobilities, 82  
    variation of ionic mobility with, 37, 59, 62, 63, 65, 68, 82  
Difficulty in study of known ions, 48  
Diffusion, ambipolar, 586, 589, 616, 619, 621  
    and columnar recombination, 140  
    and electron attachment in recombination, 111, 126  
    and initial recombination, 135  
    and theory of recombination, 103, 104, 107, 111, 126, 128, 140  
    and velocity of agitation, 162, 167, 175, 179, 202, 313, 314, 353, 402, 596, 615  
    coefficient, definition of, 162  
        evaluation of, by air-blast method, 164  
        from mobility, 166  
    of ions, values of, 165  
    variation with mass, pressure, and temperature, 175  
early measurements of, 165  
effect of, on mobility studies, 4, 5, 7, 42, 171  
Einstein theory of, 174  
electron, *see* Electron diffusion.  
in discharge and conduction phenomena, 170  
in electron avalanches, 427, 528

- Diffusion, in evaluation of first Townsend coefficient, 353  
  in glow discharge tubes, 572, 586  
  in streamer formation, 528  
  ion, rate of, 161, 165, 238  
  ion loss by, relative to recombination, 157  
  loss by, in recombination studies, 100, 103  
  loss of photoelectrons to cathode as a  $f(X/p)$  in  $N_2$ , 402  
  ratio of mobility to, 166, 168, 170, 180, 587  
    by Townsend method, 168  
    theory of, 166  
  velocities, molecular, distribution law for, 239, 248, 653  
Disappearance method of studying recombination, 90  
Discharge, arc, 605  
  and glow, 560  
  criterion for stable self-sustaining, 423, 432, 478, 480, 488, 490, 505, 514, 515, 568, 581, 584, 605, 607, 609  
  disruptive in gases, 408  
  electrodeless, 553  
    ring, 553, 556  
  from points and wires, 485  
  initiated by field emission, 475  
  lightning, 540  
    data on, 541  
    theory for, 544  
  low-pressure, velocity of propagation down long tubes in, 482  
  phenomena, diffusion in, 170  
  radio interference by, 485  
  secondary mechanisms known to be active in, 402, 482; *see also* Townsend's second coefficient.  
  spark, characteristic curve for, 412  
  temperature ionization in, 538, 609, 617, 620, 651  
  ultra-high-frequency, characteristic curves for, 557  
Disruptive discharge in gases, 408  
Dissociation, and electron capture, 298  
  in electron attachment, 283, 285, 286, 287, 288  
Distance needed for electrons to gain terminal energy, 77, 184, 351, 370  
Distribution, of charges in typical thunderstorm cloud, 541  
  of electron energies and probe theory, 232  
  of electron energies in a gas in an electrical field, 200, *see also* Electron energy distribution.  
  of energies and electron temperature, 239; *see also* Electron temperature.  
  of free paths, 646  
  of molecular velocities, 650  
  of potential, and charges in a glow discharge, 566  
    in arcs, 609, 614, 627  
    in conduction currents, in a gas, 333  
    in low-voltage arcs, 637, 638  
    in negative and positive coronas, 494, 521, 529  
    in space-charge-limited currents, 317  
Distribution law, determination of, by probe measurements, 246, 249  
  by using a-c on probes, 249  
  Druyvesteyn probe method for, 247  
  Druyvesteyn's, with Ramsauer free paths, 184, 194, 196, 213, 229, 366, 648  
  for directed velocities, 239, 248, 653  
  for electron energies, 194, 196, 208, 209, 210, 212, 213, 219, 221, 224, 225, 226, 227, 228, 229, 240, 247, 249, 366, 648  
  forms of, 652

- Distribution law, Maxwell's, energy form of, 653  
for electrons, 179, 183, 194, 196, 202, 210, 214, 221, 225, 233, 235, 240, 246, 249, 256, 322, 365, 367, 538, 585, 617, 639, 651  
of Druyvesteyn and of Maxwell, 194  
of Morse, Allis, and Lamar, *see* Druyvesteyn distribution law
- Doppler effect, and temperature in positive column, 596  
in spark lines on breakdown, 537
- Double minimum in spark potential studies with small amounts of impurities, 477
- Drawing out of arcs, 606
- Drift velocity, electron, 177, 179, 184, 186, 190, 196, 213, 219, 229, 261, 267, 275, 277, 311, 364, 368, 591, 620; *see also* Electron mobilities.  
terminal, 184  
ionic, *see* Ionic mobilities.
- Druyvesteyn's derivation of electron energy distribution law, 203, 215, 216  
Druyvesteyn's distribution law, 194, 196, 208, 210, 212, 225, 229, 240, 366  
Druyvesteyn's first attempt at theory of first Townsend coefficient, 209, 363  
Druyvesteyn's procedure for obtaining distribution law by probes, 247  
Druyvesteyn's theory, of  $\alpha/p$  as a  $f(X/p)$  in Ne, 220, 363  
of low-voltage arc, 638
- Dunnington and White's arrangements for Kerr cell spark studies, 466
- Earth's electrical field, 540  
Earth's potential gradient, 540
- "Effective" ionization potentials in arcs, 621
- Einstein equations for velocity of diffusion, 174
- Elastic electron impacts, fractional energy loss in, 126, 183, 187, 189, 191, 200, 204, 210, 211, 362, 590, 596
- Electric field, below ionization, currents in, 305  
distribution of electron energies in gases in, 200; *see also* Electron energy distribution.  
gain of electron energy in, 179, 183, 184, 200, 204, 359, 591
- Electrical quantities involved in lightning discharges, 542
- Electrical shutter, methods of mobility measurement, 19, 20, 22, 190  
mobility measurement of electrons, 190
- Electrical wind method of mobility measurement, 28
- Electrode material, and cathode sputtering, 600  
and sparking potential, 349, 381, 400, 403, 407, 414, 415, 419, 420, 450, 452-454, 478, 479-482,
- Electrode shape and spark potential measurements, 454
- Electrode temperature of low-boiling-point metal vapor arcs, 629, 631, 633, 635, 636
- Electrodeless discharge, 553  
aided by photo excitation of gas, 555  
electrostatic effects needed to start, 553, 556
- Electrodeless ring discharge, 553  
effect of impurities studied by, 556  
Thomson theory of, 553, 556
- Electrodes, avoidance of dirt on, in spark potential measurements, 451  
avoidance of Hg and condensable vapors on, in spark potential measurements, 452  
cleaning of, for spark potential measurements, 452  
dissimilar, rectifying action in breakdown, 457  
effect of insulating specks on, in discharges, 499  
evaporated or sputtered for sparking studies, 452  
gas films on, in spark potential measurements, 453  
oxidation of, in spark potential measurements, 452, 453  
point, spark potential measurement by, are meaningless, 457  
shape and material of, in study of sparks, 451  
unequal, in spark gap lead to stepwise breakdown, 456

- Electrolytic study of fields about gaps on models, 455
- Electron, approximate energy in electrical field, 184
- cross section of, for ionization and excitation, 175, 201, 216, 227, 231, 363, 364, 367, 370, 478, 479, 570, 634
    - for radiative capture, 298
  - distance to gain terminal energy in field for, 184
  - Maxwell's distribution law for, 179, 183, 194, 196, 202, 210, 214, 221, 225, 233, 235, 240, 246, 249, 256, 322, 365, 367, 538, 585, 617, 639, 645, 651
  - number of, striking unit surface per second in a gas, 240, 313, 593
  - only one required for a spark, 424
  - Ramsauer cross section or free path for, *see* Electron free paths.
  - random or thermal velocities of, 126, 153, 179, 183, 235, 236, 238, 239, 248, 261, 268, 312, 364, 367, 590, 653; *see also* Electron energy distribution; Electron temperature.
  - secondary production, at cathode in discharges, 403, 482
    - by metastable atoms, 253, 348, 352, 379, 401, 403, 404, 477, 487, 495, 501, 508, 509, 510, 511, 512, 569, 573
    - at surfaces, 253, 379, 401, 403, 404, 481, 482, 508-512, 569
    - by photoelectric process at cathode, 253, 311, 379, 380, 395, 396, 398, 402, 403, 431, 482, 483, 487, 502, 504, 512, 527, 531, 568
    - by photoionization in gas, 379, 383, 384, 403, 404, 428, 430, 433, 434, 482, 512, 516, 528, 529, 544, 547
    - by positive ion bombardment, 378, 382, 396, 397, 398, 399, 403, 478, 479, 480, 482, 504, 512, 568, 581, 607
  - thermionic emission of, at cathode of glow discharge, 607
- Electron affinities of elements, 297
- Electron attachment, and atomic or molecular structure, 289
- and electron energy, 126, 132, 135, 259, 266, 268, 271, 275, 278, 290, 293, 294, 298
  - and energy dissipation, 290
  - and inelastic impacts, 279
  - and interpretation of ion mobility curves at low pressure, 263, 267
  - and recombination, 126, 132
  - dissociation in, 283, 285, 286, 287, 288
  - in air, 278, 281
  - in Cl<sub>2</sub>, 285
  - in CO, 283
  - in CO<sub>2</sub>, 287
  - in HCl, 286
  - in H<sub>2</sub>O, 288
  - in H<sub>2</sub>S, 287
  - in NH<sub>3</sub>, 282
  - in NO, 284
  - in N<sub>2</sub>O, 286
  - in O<sub>2</sub>, 280
    - Bloch-Bradbury theory of, 294
    - energy and character of, 291
  - in SO<sub>2</sub>, 287
  - more accurate evaluation of, 267
  - pressure dependence of, 275, 279, 284, 288
  - probability of, 126, 132, 259, 261, 266, 268, 271, 275, 278, 290, 293, 294, 298
    - Bailey's method, 268
    - Bradbury's method, 276
    - Cravath's method, 274
    - defined, 261
    - energy dependence of, *see* Electron attachment and electron energy
    - Loeb's method, 264, 268
  - processes of, 290, 291

- Electron attachment, table of, 289
  - values of probability of, 267, 268, 271, 275, 278, 288
- Electron avalanche, at points at atmospheric pressure, 515, 529
  - diffusion in, 427, 525
  - in low-pressure negative wire corona, 505, 512
  - in low-pressure positive wire corona, 488
  - in negative wire corona, 515
  - in positive wire corona, 515, 527
  - in spark discharge at higher pressures, 426, 427, 433, 435, 450
  - production in Geiger counters, 488
  - propagation and photoionization in a gas, 428, 430, 516, 527, 528, 529
  - simultaneous in gap, 428, 431
  - space-charge distortions by, in spark breakdown, 429
  - succession in Geiger counters, 488
  - velocity of, in field, 427, 428, 434, 445-448, 469, 482-484, 516, 528, 529, 543-548
  - width of, 427, 528
- Electron bombardment of surfaces, gas liberation by, 481
- Electron capture, by dissociation of molecules, 282, 298
  - by radiative process, 290, 298
- Electron collision frequency, 261, 367, 590
- Electron densities, in arc columns, 155, 157, 617, 620
  - in glow discharge columns, 585, 594
  - in low-voltage arcs, 637, 638, 654
  - in spark channels, 537
- Electron detachment, 266, 275, 278, 291, 294, 295, 428, 521, 527
  - energy of, 294
  - in high fields, 428, 521, 527
- Electron diffusion, at anode of arcs, 615
  - at electrodes, loss by, 202, 240, 242, 313, 314, 353, 401, 402, 596, 615
  - in a field in a gas, 202, 203, 240, 242, 311, 313, 314, 316, 353, 402, 596, 615
  - in anode glow, 567, 596
  - in arc column, 616, 619, 621
  - in avalanches, 427, 528
  - in cathode glow, 567, 570
  - in evaluation of first Townsend coefficient, 353
  - in positive column, 586, 595
  - in positive glow discharge column, 586, 589
  - in positive streamers in corona, 528
  - variation of ratio to mobility with energy, 180
- Electron drift velocity, 177, 179, 184, 186, 190, 196, 213, 219, 229, 261, 267, 275, 277,  
311, 364, 368, 591, 620
  - terminal, 184
- Electron emission, *see* Electron, secondary production.
  - thermionic, 317, 318, 320, 447, 605, 607, 629, 636
  - equation for, 320
- Electron energy, and Townsend's  $\eta$ , 179
  - distribution, 194, 196, 208, 209, 210, 212, 213, 219, 221, 224, 225, 226, 227, 228,  
229, 240, 247, 249, 366, 648
  - and electron temperature, 239
  - and inelastic impacts, 215, 221, 228, 230
  - and plasma oscillations, 602
  - and probe theory, 232, 246, 249
  - and Ramsauer free paths, 184, 194, 196, 213, 229, 366, 648
  - Druyvesteyn's derivation of, 203, 215, 216
  - law, of Cravath, 209, 213
    - of Davydov, 221, 225
    - of Didlauskis, 209



- Electron energy, distribution, law, of Druyvesteyn, 208, 219  
  of Morse, Allis and Lamar, 212, 216  
  of Smit, 225, 228  
  of Townsend, 210  
  measurement of, 232  
  with inelastic impacts, 215, 221, 228, 230  
evaluated by ratio of  $k/D$ , 180  
exchange, collision cross section for, 639  
gains in electrical fields, 179, 183, 184, 200, 204, 359, 591  
in attachment studies from inert gases, 279  
loss in impact and electron mobilities, 188; *see also* Electron impact, elastic.  
volt equivalent for, 183
- Electron equivalent of positive ion in space-charge detector, 327
- Electron filter, introduction of, in study of attachment, 272  
  Loeb, 23, 189, 272, 273, 277, 292
- Electron free paths, 126, 178, 180, 184, 185, 188, 190, 194, 196, 197, 201, 203, 212,  
  213, 216, 229, 260, 261, 262, 359, 360, 367, 368, 490, 591, 592, 611, 639,  
  646, 647, 648  
  and attachment, 281  
  and energy distribution laws, 194, 196, 213, 229, 366, 648  
  and mobilities, 181, 188, 196, 201, 213, 229  
  classical value of, 646  
  in arcs, 611  
  of Ramsauer, 178, 180, 184, 188, 190, 194, 196, 201, 202, 203, 213, 216, 229, 281,  
  295, 362, 639, 646, 647, 648
- Electron impact, elastic, fractional energy loss in, 126, 183, 187, 189, 191, 200, 204,  
  210, 211, 362, 590, 592  
  in He, number of relative to inelastic, 228  
  inelastic, and attachment, 280  
  with excitation and ionization, 175, 195, 201, 215, 216, 221, 227, 231, 363, 364,  
  367, 370, 478, 479, 634  
  ionization by, in arc columns, 616, 620  
  successive, ionization in arcs by, 610, 620, 636
- Electron ionization, *see* Ionization.
- Electron mobilities, 177, 179, 184, 186, 190, 194, 196, 213, 219, 229, 261, 267, 275,  
  277, 311, 315, 364, 368, 591, 620  
  and Maxwell's law, 194  
  at atmospheric pressures, 181  
  by magnetic deflection, and errors due to energy distribution, 229  
  by Townsend deflection method and energy distribution, 229  
  by Townsend magnetic deflection method, 26, 179, 229  
  early measurements of, 178  
  equations for, 179, 186, 187, 219  
  from photoelectric currents, 277, 315  
  of Bradbury and Nielsen, 190  
  results of, Bradbury and Nielsen method, 190-195  
  Loeb with a-c method, 181  
  photoelectric current method, 277, 315  
  Townsend method, 179  
  test of equations for, 188-199  
  theory, of Allen for, 197, 226  
  of Compton for, 182-186  
  as modified by Bradbury, 187  
  of Druyvesteyn for, 219  
  of Loeb for, 182  
  simple, for, 178-180  
  Townsend's factor  $\eta$  in, 179

- Electron mobilities, when excitation and ionization occur, 193
  - with inelastic impacts to excitation and ionization, 192-198, 215, 219, 221, 228, 230
- Electron recombination, 87, 144, 149, 150, 158, 572
  - in glow discharge, 572
  - preferential, 86, 144, 150
  - theory of, 158
  - values of coefficient for, 150, 155, 158
  - volume, ion loss by, compared to wall currents, 157
- Electron space charges, 615
- Electron temperature, 155, 157, 211, 229, 230, 234, 235, 239, 240, 367, 368, 539, 586, 587, 589, 590, 591, 618-621, 651
  - and energy distribution, 196, 213, 214, 228-230, 239
  - in sparks, 539
  - measurement of, by probes, 240
- Electron volts, 183
- Electronegative gases, 258
- Electronegative impurities, effect of, on sparking potentials, 460, 509-512
- Electrons, "pulling" out of metals, 472; *see also* Field emission.
  - ratio of elastic to inelastic impacts for, in He, 228
- Electrostatic effect needed to initiate electrodeless discharge, 553, 556
- Elementary theory of ionic mobility, 54
- Emf, counter, of arcs, 626
- Emission, thermionic, 317, 605, 607, 629, 636
- Emmeléus, Lunt, and Meek, theoretical values of  $\alpha/p$  as  $f(X/p)$  of, 366
- Emmeléus' theory for  $\alpha/p$  as  $f(X/p)$ , 363
- Energies of atoms "evaporating" from metal arc cathodes, 633, 634
- Energy, balance, at anodes of arcs, 615
  - at arc cathodes, 611, 635
  - at cathode, in glow discharge, 598
- dissipation in electron attachment, 290
- distribution, among negative ions formed from positive ions, 303
  - integrals of, 653
  - law as a function of temperature, 655
  - law of Maxwell, 179, 183, 194, 196, 202, 210, 214, 221, 225, 233, 235, 240, 246, 249, 256, 322, 365, 367, 385, 538, 617, 639, 651
  - of electrons, *see* Electron energy distribution.
- form of distribution law, 653
- fraction of, radiated as light from glow discharge column, 595
  - radiated by arc column, 621
- gain of electrons in electrical field, 179, 183, 184, 200, 204, 359, 590, 591
- liberation, at anode, evaluation of anode fall from, 597
  - at arc cathodes and temperature, 631
  - in spark breakdown, 538
- loss, relative elastic and inelastic in He, 228
- loss of electrons on impact, 126, 185, 187, 189, 191, 200, 204, 210, 211, 362, 590, 592; *see also* Electron impact, elastic; Inelastic electron impacts.
- losses in arc column, 622
- most probable, 653
- of electron attachment in  $O_2$ , 291
- of electron detachment, 294
- of electrons and probability of attachment, 126, 132, 135, 259, 266, 268, 271, 275, 278, 290, 293, 294, 298
- probability of a given state, 654
- v. Engel and Steenbeck's theoretical approximation to Townsend's equation for  $\alpha/p$ , 367
  - theory of glow discharge, 581

- Equilibrium, and spark "temperature," 538  
  concentration, evaluation of recombination coefficient by, 93, 123  
  concentration of ions in recombination, 91  
  gaseous and temperature, 229, 230, 538, 617, 619, 651  
  in arc columns, 618
- Erikson air-blast method, 5
- Essential techniques in study of spark discharge, 451
- Evaporation, at cathodes of arcs, 612, 632, 634  
  rate of, and "temperature" of metal arcs, 632, 635
- Excitation potentials, 194, 195, 200, 227, 359, 636, 639, 654, 656; *see also* Ionization and excitation potentials.
- Excitation probabilities, 201, 216, 227, 231, 363, 570, *see also* Ionization and excitation potentials.
- Experimental data on ionic mobilities, 32
- Experimental test of volume recombination theory, 120
- Experimentally observed sparking potential, 423, 425, 432, 465; *see also* Sparking potential threshold.
- Extinction of arcs by convection currents, 606, 622
- Extinguishing resistance for arcs, 625
- f*, fractional electron energy loss on impact, 126, 183, 187, 189, 191, 195, 200, 204, 210, 211, 362, 590, 592
- Faraday dark space, 561, 562, 564, 571  
  in negative point to plane corona, 519, 520  
  mechanism of, 271
- Field, about point with confocal paraboloid geometry, 515  
  about points at corona potentials, 515  
  and potential distribution, in concentric cylindrical condensers, 486  
  in glow discharge, 565  
  in negative point to plane corona, 521  
  in positive point to plane corona, 529  
  at cathodes of arcs, 611, 623, 627, 631  
  causing Stark effects in arcs and sparks is atomic, 537, 540, 608, 615  
  distortion, axial, by electron avalanche at spark breakdown, 430  
  distortion in spark gap by charged insulators and neighboring conductors, 455  
  distribution in ion current in a gas, 331  
  distributions about electrodes determined from model studied electrolytically, 455  
  electric, effect on columnar recombination, 141  
  of earth, 540
- emission, 472, 473, 474, 475, 481, 499, 569, 611, 629, 636  
  and vacuum sparks, 472  
  at arc cathodes, 474, 611, 629, 636  
  currents anomalous of Penning and Müller, 474  
  currents from cathodes in glow discharges, 569  
  fields in, Schottky theory of, 473  
  from oxide specks on electrodes, 499  
  in low-pressure discharges, 481  
  in low-pressure sparks in swept gaps, 475  
  in special discharges, 475  
  studies of Müller, 474  
  wave-mechanical theories of, 473
- energy gain of electrons from, 179, 183, 184, 200, 204, 359, 590, 591
- for sparking in long gaps, 530
- in arcs, and sparks from Stark effect, 537, 540, 608, 615
- in glow discharge, measurement of, by cathode-ray beam, 567
- in long gaps, not uniform, 536
- longitudinal, in positive column of glow discharge, 590

- Field, in pilot streamer and stepped leader tips, 546, 547  
 in positive columns of arcs, 609, 613, 614, 616, 620, 621, 623, 627  
 in space-charge-limited currents, 319  
 intensified ionization current, 503, 521, 527  
 measurement of, in glow discharge, 567  
 to pressure ratio,  $X/p$ , in ion studies, 338
- Filter, electron, of Loeb, 23, 189, 272, 273, 277, 292
- First Townsend coefficient, *see* Townsend's first coefficient.
- Fluctuating burst pulse corona of Trichel, 522, 526, 528
- Force laws, and ionic mobilities, 36, 44, 58, 59, 62, 63, 65, 67, 68, 69, 70, 81, 82, 83  
 molecular, 650
- Forces between ions and molecules, 36, 44, 56, 57, 58, 62, 65, 67, 68, 69, 81, 82, 83
- Formation, of negative atomic ions, 296  
 of negative ions, 258; *see also* Electron attachment; Negative ions.
- Formative time lags, and spark breakdown, 427, 428, 440, 444, 445, 446, 447, 469, 482, 483, 517, 529  
 in short gaps, 444
- Fraction, of current carried by positive ions in arcs, 610, 612, 631, 632, 634, 635  
 $f$ , of energy lost by electrons in molecular impact, 126, 183, 187, 189, 191, 195, 200, 204, 210, 211, 362, 590, 592
- Franck's modification of the a-c method, 11, 13, 259, 264  
 deficiency of, 13
- Franck's theory of ionization by positive ions, 375
- Free electron gases, 258, 267, 289, 297
- Free paths, electron, *see* Electron free paths.  
 ionic, 55, 56, 58, 60, 64, 77, 83, 84, 359, 383, 370  
 molecular, 644  
   distribution of, 646  
   of Maxwell and Tait, 645  
   temperature variation of, 650
- Frequency, dependence of a-c spark breakdown, 550  
 of oscillations in arcs, 626  
 very high, spark breakdown with, 557
- Fundamental physical constants, table of, 658
- $\gamma$ , alternative second Townsend coefficient, number electrons per positive ion liberated  
 at cathode, may include photon and metastable action as well as positive ion impacts, 253, 378, 379, 380, 382, 395, 396, 397, 398, 399, 400, 401, 403, 404, 431, 478, 479, 480, 482, 483, 487, 504, 512, 516, 531, 568, 581, 607  
 anomalous high values of, at high  $X/p$ , 479  
 as a function of  $X/p$ , 392-400, 401  
 at high,  $X/p$ , 480  
 caused by metastable atom impact, 253, 379, 401, 403, 404, 481, 482  
 caused by photoeffect at cathode, 253, 380, 395, 396, 397, 398, 401, 403, 431, 483, 487, 527, 531, 568  
 caused by positive ion impact at cathode, 378, 382, 396, 397, 398, 399, 403, 478, 479, 482, 504, 512, 568, 581, 607  
 effect of, on minimum sparking potential, 414, 415, 477, 478; *see also* Minimum sparking potential.  
 evaluation of, from sparking potential, 349, 400, 414, 415, 416, 419, 420, 479  
 evaluation of sparking potential from, 416, 417, 418, 419, 420  
 falsified, by dirt on cathode after discharge, 403, 498, 499  
   by space charges, 348, 386  
 in discharges, summary of nature of, 403, 482  
 in glow discharge, 568, 581-585, 607  
 in low-pressure sparks, 412, 413, 414, 415, 417-420, 451-454, 476-482  
 in negative point to plane corona, 516

- $\gamma$ , in negative wire coronas at low pressure, 504, 512
  - value of, in A for Ba surface, 400
  - in A for Cs-Ag-O and Ni-Cs surfaces, 399
  - in  $H_2$  for NaH surface, 397, 398
  - in  $H_2$  for Pt surface, 397, 399
  - in  $N_2$  for NaH surface, 394
  - in  $N_2$  for Pt surface, 394
  - in Ne and Ne-A mixtures for Cu surface, 394
- $\gamma$ ,  $\beta$ , or cosmic-ray counters, best surfaces for, 500
- Gaps, long, 536
- Gardner's method for coefficient of recombination, 98
- Gas, constant per mole, ideal, 644
  - kinetic nature of, 643
  - liberation by electron bombardment, 481
  - pressure of, 643
    - effect of, on photoelectric emission, 311
    - on secondary electron emission, 311, 401, 402
- Gaseous purity, and ionic mobilities, 7, 33, 38, 40, 41, 43, 47, 71
  - and recombination coefficient, 93, 101, 137, 138, 143-147
  - and striations in glow discharge, 573
  - and value of first Townsend coefficient, 343, 348, 351, 352, 354, 355, 357, 358, 415, 460-462, 477-479, 507-512
  - effect of impurities on starting potentials of low-pressure corona discharge, 509-512
  - effect of traces of impurity in electrodeless ring discharge, 555
  - effect of traces of impurity on sparking potential, 418, 460
  - in spark potential measurements, 460
  - nature of action of impurities on first Townsend coefficient, 343, 348, 351, 354, 355-358, 476-479, 507-514
- Gases, action of different, in Geiger counters, 495
  - adsorbed on electrodes in spark potential measurements, 453
  - electronegative, 258
  - free electron, 258, 267, 289, 297
  - ionization currents in, in fields below ionization by electron impact, 305
  - mixtures of, cathode fall of potential in, 577
    - ion mobilities in, 42
  - modification of purity in, by sparks in sparking potential measurements, 461
  - photoelectric currents of low density in, 311
- Geiger counter, avoidance of self-excitation in, 500
  - background count in, 496, 500, 503
  - best cathode surfaces for  $\gamma$ ,  $\beta$ , or cosmic-ray counts, 500
  - cathode surfaces in, 496, 500
  - current-potential equation for, 493
  - different gases in, 495-497, 500
  - electron avalanche production in, 488
  - limitations of, 501
  - limits of effective ionization in, 490, 514
  - metastable atom action in, 487, 495, 501
  - photoelectric effects in, 487, 502
  - plateau in, 489, 495, 496, 501, 503
  - pulses, of current in, 489
  - regime, 485, 489, 502, 503, 522, 530
  - resistance in, 494, 495, 501, 503; *see also* Geiger counter, space-charge effects in.
  - resistance of external circuit in, 489, 495, 501, 503, 504
  - space-charge effects in, 489, 490, 493, 497, 522, 526
  - spurious counts in, 497
  - starting potentials in, 488, 493, 494, 501, 507
  - thermionic emission in, 497

- Geiger counter, time constants for, 501, 504  
Geometrically conditioned saturation current, 307  
Glassware, cleaning of, for spark potential and other measurements, 458  
Glow and arc discharge, 560  
Glow discharge, 485, 560  
    abnormal cathode fall in, 563, 583, 606  
    anode glow in, 561, 562, 596  
    as a function of pressure, 560  
    Aston dark space in, 563, 564, 570, 573  
    cathode fall of potential in, 563, 566, 567, 568, 569, 570, 571, 574-585, 598, 599, 601, 606  
    cathode glow in, 561, 562, 570, 583  
    characteristic structural features of, 563  
    colors in, 565  
    Crookes dark space in, 561, 562, 563, 564, 568, 574, 585; *see also* Glow discharge, cathode fall of potential in.  
    electron densities in, 585, 594  
    energy balance at cathode in, 598  
    Faraday dark space in, 561, 562, 564, 566, 571, 572, 573  
    field emission at cathode in, 569  
    ionization near anode required in, 597  
    measurement of field strengths in, 567  
    mechanism of, 568, 579-594  
    negative glow in, 561, 562, 564, 566, 571, 572, 573  
    normal cathode fall in, 563, 577, 583, 585, 606  
        values of potential and width of, 575, 577, 585  
    photoelectric effect at cathode in, 568  
    positive column in, 561, 562, 563, 564, 572, 585-596  
    potential, field strength and density distributions in, 565  
    radial ion concentration gradients in, 593  
    recombination in, 572  
    secondary mechanisms at cathode of, 568, 569  
    spread of glow over cathode, explained, 583  
    striated, 561, 563, 565, 573  
    striations in, origin of, 573  
    subnormal, normal and abnormal, cathode falls in, 584, 606  
    subnormal cathode fall of potential in, 584, 606  
    thermionic emission from cathode in, 607  
    transition from, to arc, 606  
    tubes, life of, and cathode sputtering, 599  
    wall currents in positive column of, 572, 586  
    wall potentials in, 572, 586, 594  
Glow transition to arc, characteristic curve of transition for, 607  
Groups of ions, 40, 41, 42, 43, 45, 47  
  
H<sub>2</sub>, current densities in, with hollow cathode, 601  
    diffusion of ions in, 165  
    electron mobilities in, 189, 190, 316  
    first Townsend coefficient in, 355, 356, 666  
    formation of negative ions in, 267, 289, 301, 303  
    high-frequency a-c sparks in, 557  
    high-pressure corona in, 534  
    in Geiger counters, 496  
    ionic mobility in, 38, 40, 70, 76  
    normal cathode fall of potential in glow discharge in, 575, 577  
    photoelectric currents in, 316  
    positive column, gradient in, 595

- $H_2$ , Ramsauer free paths in, 181, 649  
  recombination coefficient in, 147  
  second Townsend coefficient in, 396, 397, 398, 399  
  sparking potentials in, 419, 479  
  sputtering in, 600  
  starting potentials for negative and positive low-pressure corona in, 509  
Hale's studies of the first Townsend coefficient in pure Hg-free  $H_2$ , 357  
Harper theory, of Brownian particles attracting each other, 110  
  of recombination, 110, 127  
Hassé and Cook theory of ionic mobilities, 68  
He, 22, 23, 33, 36, 37, 49, 64, 65, 67, 68, 70, 73, 75, 76, 82, 188, 192, 194, 195, 196,  
  197, 227, 228, 289, 297, 327, 336, 365, 477, 478, 479, 508, 509, 575, 577, 578,  
  656  
  absolute values of mobilities in, 33, 64, 70, 82  
  distribution of electron energies in, 196, 227, 228, 330  
  effect of positive ions in space-charge-limited current in, 327  
  electron affinity of, 297  
  electron mobility in, 188, 192, 194, 195, 196, 197  
  first Townsend coefficient in, 365  
  ionization potential of, 656  
  length of normal cathode dark space in, 575  
  low-pressure sparks in, 477, 478, 479  
  minimum starting potential of corona in, 508, 509  
  mobilities in, at low pressures and high fields, 73, 75, 76  
  mobilities of ions in, 33, 49, 64, 65, 67, 68, 70, 82  
  table of, 70  
  normal cathode fall in, 577  
  normal current density divided by pressure squared in, 578  
  structure of, and electron attachment, 289  
  temperature variation of mobility in, 36, 37  
  Tyndall, Powell four-gauze method, in, 22, 23  
Hershey, mobility measurements of, at high  $X/p$ , 73  
  theory of ionic mobility of, at high  $X/p$ , 79  
Hertz derivation of electron energies in gases in fields, 203  
Hg, *see* Mercury.  
High frequencies, spark breakdown with, 552  
  ultra, spark breakdown with, 557  
High-frequency, a-c measurements of arc resistance, 626  
Hissing arc, 626, 628  
Hittorf dark space, 561; *see also* Crookes dark space.  
Hollow cathodes in glow discharge, 601  
Holm's theory for evaluating  $\alpha/p$  as  $f(X/p)$ , 365  
Hot spot in low-boiling-point metal arcs, temperature of, by evaporation rate, 633, 635  
Hump effect in electron filters, 273, 292  
Hysteresis curve of arc, 628  
  
Illumination, intensity of, and time lag of sparking, 441, 443, 445, 447  
  of cathode, method of, in evaluation of first Townsend coefficient, 348, 350  
Impacts, elastic, fractional energy loss in, 126, 183, 187, 189, 191, 200, 204, 210, 211,  
  362, 590, 592  
  inelastic, and energy distribution, 215, 221, 228, 230  
  of second class, 255, 638  
Impurities, *see* Gaseous purity.  
Inductive kicks in positive point to plane corona, 523  
Inelastic electron impacts, and attachment, 280  
  and electron mobilities, 193-197, 215, 219, 221, 228, 230  
  and energy distribution, 215, 219, 221, 228, 230

- Inelastic electron impacts, in He, number of, relative to elastic, 228
  - of second class, 255, 638
  - with excitation and ionization, 195, 201, 215, 216, 221, 227, 363, 364, 367, 370, 478, 479, 634
- Inert gases, in Geiger counters, 495
  - use of, for determining electron energies in attachment studies, 279
- Inhibiting action of space charge on discharge, 424, 448, 512, 517, 520, 529, 530
- Inhibiting effect of space charge, in negative corona, 512, 517, 520
  - in positive point corona, 526, 527, 530, 532, 533, 534
  - in spark propagation, 424, 448, 485
- Initial recombination, 87, 105, 131, 144
  - discovery of, 105
- Instability criterion for a spark gap, 423
- Intense photoelectric currents, effect of, on Townsend's coefficients, 348, 350, 386
- Intermediate large ions, 45
- Intermittent corona regime, 488, 522
- Interpenetrating fields and ionic mobilities, 13, 20, 22
- Ion, small, theory of, 53, 58
- Ion bombardment of cathode, secondary liberation of electrons by, 378, 382, 396, 397, 398, 399, 403, 478, 479, 482, 504, 512, 568, 581, 607
- Ion cluster, 33, 35, 40, 43, 45, 52, 56, 58, 71, 258, 265, 481
  - break-up of, 35, 259, 265
  - stability criterion for, 58
  - statistical, 45
- Ion currents, in a gas, 329
  - field strength distribution in, 331
  - potential distribution in, 333
  - lack of saturation in, 309, 314, 315, 333, 338
  - with volume ionization and positive and negative ions in a gas, 328
- Ion densities, 155, 157, 537, 545, 585, 594, 617, 620, *see also* Electron densities.
  - in arc columns, 155, 157, 617, 620
  - in glow discharge column, 585, 594
  - in pilot streamer, 545
  - in spark channels, 537
- Ion formation, negative, by positive ion impact on surfaces, 298
- Ion loss by recombination in gaseous ion currents, 329
- Ion mobility curves, low pressure, interpreted by electron attachment, 263, 267
- Ion size and mobility equations, 83
- Ion spectrum, 47
- Ion transport in arcs, 622
- Ionic and atomic radii, 56, 58, 64, 82
- Ionic charge and mobility, 48, 63, 84
- Ionic diffusion, rate of, 165, 238; *see also* Ambipolar diffusion.
- Ionic drift velocity, 54; *see also* Ionic mobilities.
- Ionic free paths, 55, 56, 58, 59, 60, 64, 77, 83, 84, 359, 370, 385
- Ionic forces and dielectric constant, 57, 62, 65, 68, 82
- Ionic mobilities, 1-83
  - absolute values of, 5, 18, 22, 33, 69, 70, 76
  - agreement between theory and experiment, 63-65, 69-71, 76, 81-83
  - and change of charge, 36, 40, 41, 48, 71, 84
  - and charge, 49, 63, 83, 84, 170
  - and density, 34, 35, 36, 56, 63, 65
  - and dielectric constant, 37, 59, 62, 63, 65, 68, 82
  - and field strength, 32, 63, 71, 73, 76, 80, 259
  - and force laws, 36, 44, 57, 58, 59, 62, 63, 65, 67, 68, 69, 70, 81, 82, 83
  - and mass of ion, 37, 55, 59, 63, 64
  - and mean free path, 55, 56, 58, 83, 84



- Ionic mobilities, and molecular mass, 37, 55, 59, 60, 63, 64, 65, 72, 73, 76, 80, 84  
and nature of attractive force action, 36, 44, 59, 62, 63, 65, 67, 68, 69, 70, 81, 82, 83  
and pressure, 34, 35, 36, 63, 65  
and Stokes' law, 83  
and temperature, 36, 37, 55, 63, 80, 81  
and terminal velocities, 77  
and van der Waals forces, 67, 82  
as function of time, 33, 34, 38, 39, 40, 47, 48  
at high  $X/p$ , 33, 71, 73, 76, 80, 259  
deficiencies, in air-blast method, 7  
    in Bradbury-Nielsen method, 25  
    in electrical wind method of measurement of, 30  
    in four-gauze method, 23  
    Rutherford a-c method, 11, 13  
    in Townsend magnetic deflection method, 28, 75-77  
    in Tyndall and Grindley method, 18  
definition of, 2  
dielectric constant from, 82  
effect of diffusion on evaluation of, 4, 42, 57, 171  
experimental data on, 32  
from corona currents, 490, 493, 494  
in gaseous mixtures, 42  
in ion currents in a gas, 329  
measured, by air-blast methods, 3  
    by Bradbury modification of Tyndall and Grindley method, 14  
    by Bradbury-Nielsen method, 23  
    by Chattock electrical wind method, 28  
    by electrical shutters, 19  
    by Franck modification of a-c method, 11  
    by Hershey at high  $X/p$  with Townsend deflection method, 74  
    by Rutherford a-c method, 7  
    by sinusoidal alternating potential, 9  
    by study of corona currents, 490, 493, 494  
    by Townsend magnetic deflection method, 26, 74, 179  
    by Tyndall and Powell four gauze method, 20  
measurement of, 1  
of known ions, 34, 36, 38, 39, 40, 41, 42, 43, 48, 64, 69, 70, 76, 82  
positive and negative, difference in, 38  
positive in Crookes dark space, 581  
summary of methods of measurement of, 2  
theory of, 52  
    Compton for high  $X/p$ , 72, 76, 77  
        modified by Loeb, 73, 78  
    elementary, 54  
    Hassé and Cook, 68  
    Hershey at high  $X/p$ , 80  
    Langevin, complete, 65  
        small ion, 60-63  
        solid elastic, 55, 84, 178  
    Loeb and Thomson, 59, 60  
    more exact, 65  
    simple, 54  
    wave-mechanical, 69, 71  
variation with mass and dielectric constant, 37  
Ionic recombination, *see* Recombination  
Ionic resistance, definition of, 42  
Ionic temperature at high  $X/p$ , 79

- Ionization, and excitation, effect of on electron mobilities, 192**  
and excitation potentials, 149, 150, 194, 195, 200, 227, 252, 359, 364, 508, 509, 510, 555, 570, 571, 573, 598, 636, 638, 654, 656  
and excitation probabilities, 195, 201, 216, 227, 362, 363, 364, 367, 370, 478, 479, 634  
by collision by electrons, in a gas, 336; *see also* Townsend's first coefficient  
experimental procedure in study of, 337  
in arc columns caused by atoms and molecules, 618  
by electron impact in arc columns, 616, 620  
by fast atoms, 377, 618  
by fast positive ions, 375  
by positive ion impact, coefficient of, 372; *see also* Townsend's second coefficient; Townsend's  $\beta$ .  
in gases, 370, 371, 372, 374-377, 381-385, 391, 392, 393-406, 407, 414, 448, 480, 569 (other evidence on this comes from data on spark, and corona where  $\gamma$  and photoionization in the gas are active; *see*, 413, 414, 415-416, 426-432, 440, 448, 476-479, 480, 527-531)  
alternatives to, 377  
problem of, 374  
on cathodes, *see*  $\gamma$  caused by positive ion impact at cathode; Electron, secondary production, by positive ion bombardment.  
by positive ions in a gas, and positive corona discharge, 384  
falsified by secondaries from walls, 375  
in glow discharge, 569  
probability of, at sparking potentials, 370, 383  
Townsend's study of, 384  
Townsend's theory of, 370, 372, 384  
with space-charge distortion, 343, 383  
by successive electron impact in arcs, 610, 620  
cumulative, in positive and negative point to plane coronas at atmospheric pressure, 515  
current, field intensified, 503, 521, 527  
in gases in fields below ionization by electron impact, 305  
efficiencies for ionization by positive ions in a gas, 370, 376, 383; *see also* Townsend's  $\beta$ , Townsend's second coefficient; Ionization by positive ion impact in gases.  
efficiency of, 201, 216, 227, 362, 364, 367, 370, 478, 479, 556, 634  
frequency of, 368, 588  
in anode glow, 597  
in gas, photoelectric, secondary electron production by, 379, 383, 384, 403, 404, 430, 433, 434, 482, 483, 512, 516, 528, 529, 544, 547  
limits of effective, in Geiger counters, 490, 514  
potential, Townsend's early evaluation of, 359  
potentials, 194, 195, 200, 227, 359, 364, 636, 638, 654, 656  
effective, in arcs, 621  
probabilities, 195, 201, 216, 227, 363, 364, 367, 370, 478, 479, 570, 634; *see also* Electron, cross section of, for ionization and excitation.  
pulse in negative point to plane corona, time of formation of, 516  
temperature, 609, 617, 620, 621, 651  
in arcs, 609, 617, 620, 621  
in discharges, 651  
**Ionized filament across gap needed for spark, 425**  
**Ionized volume and recombination coefficient, 89, 100, 123, 131-135, 138, 143**  
**Ionizing energy liberated at cathode in glow discharge, 599**  
**Ionizing frequency of electrons, 368, 588**  
**Ions, aging of, 40, 147**  
and molecules, forces between, 36, 44, 56, 65, 67, 68, 69, 73, 81, 82, 83

- Ions, atomic negative, formation of, 296  
complex, 38, 39, 40, 41, 42, 43, 48, 56, 71, 137, 138, 147  
difficulty in study of known, 48  
diffusion of, 161  
disappearance of, by recombination, 90  
equilibrium concentration of with recombination, 91  
fraction of current carried by positive, in arcs, 610, 612, 631, 632, 634, 635  
groups of, 47  
in gap, need for, in all spark potential measurements, 459  
Langevin and intermediate large, 45  
large, charges acquired by, 148  
    coefficient of recombination for, 148  
multiple charges on, 36, 40, 41, 48, 63, 71, 84, 147, 169  
negative, *see* Negative ions.  
number,  $\alpha$ , of, made by one electron in 1 cm advance in field direction in a gas, 341; *see also* Townsend's first coefficient; Townsend's  $\beta$ ; Ionization by positive ions in a gas.  
number of, striking unit surface per second, 238, 313, 593  
positive and negative, difference in mobility of, 38  
    effect of, on space-charge-limited electron current, 325  
radial concentration gradient of, in glow discharges, 593  
radioactive, 48  
recombination of, 86  
space-charge-limited currents for positive, 238, 610  
values of coefficient of diffusion for, 165
- Jaffé theory of columnar recombination, 139
- Kallmann and Rosen effect in ionic mobilities, 36, 40, 41, 48, 63, 71, 84, 147, 169
- Kaufmann's law, 37
- Kerr cell, 427, 431, 440, 445, 446, 447, 464, 465, 468, 537  
    circuits used in spark studies, 465-470  
    detection of spark breakdown by, 464  
    studies of later phases of sparks, 537  
    studies of spark breakdown, 438, 439, 444-448, 450, 464  
    studies of time lags of sparks, 444-448
- Kinetic nature of a gas, 643
- Langevin and intermediate ions, 45
- Langevin's method for coefficient of recombination, 95
- Langevin's mobility equation, 37, 55, 59, 62, 65, 73, 78  
    exact theory of, 65, 73  
    small ion type of, 37, 62  
    solid elastic type of, 55, 178
- Langevin's mobility theory, experimental test of, 63
- Langevin's recombination theory, 103  
    correction factor  $\epsilon$  for, 104  
    error in, 107  
    holds for preferential recombination, 125
- Leader stroke in lightning discharge, 543
- Length of cathode fall, in arcs, 633, 609, 610, 623, 630, 633  
    in glow discharge, 568, 608
- Light, energy of radiation of, from positive column, 595  
    from column of arcs, 621
- Lightning discharge, 540  
    average velocity of, 543

- Lightning discharge, dart leaders in, 548  
  data on, 541  
  duration of, 541  
  electrical quantities involved in, 542  
  gradients due to, at earth, 541  
  leader stroke in, 543  
  mechanism of, 543  
  metal melted by, 542  
  necessity of pre-ionized channels for high velocities in, 544  
  path, recombination in, 545  
    resistance in, 546  
  photoionization in gas required for, 544  
  polarity, and positive streamer formation, 542  
    of clouds in, 542  
  positive strokes in, 549  
  progress of a typical, 543  
  quantitative data on pilot streamer in, 545  
  return or main stroke in, 543  
  Schonland's observations of, 543  
  stepped leader strokes in, 543  
  studies with Boys camera in, 543  
  successive strokes in, 543  
  theory of, mechanism of, 544  
    stepping in, 544  
  tip fields in stepped leader in, 547  
  total potential in, 542  
    calculated, 549  
  velocity of return stroke in, 543  
Loeb's commutator for high potentials, 97  
Loeb's electron filter, 23, 189, 272, 273, 277, 292  
Loeb's electron mobility studies at atmospheric pressures, 187, 188, 189  
Loeb's empirical extension of Kaufmann's law of ionic mobilities, 37  
Loeb's evaluation of absolute ionic mobilities, 5, 34  
Loeb's first mobility measurements on known ions as a function of age, 34, 40, 69  
Loeb's picture of mechanism of spark discharge at higher pressures, 325, 423, 426-440  
Loeb's proof of the stability of ions in high fields, 32, 266  
Loeb's studies, of electron attachment, 259, 260, 264, 265, 267, 282  
  of ion mobilities in mixtures, 38, 43  
Loeb's theory, of electron mobility, 182  
  of positive point to plane corona in air at atmospheric pressure, 527  
Loeb's value of correction factor,  $\epsilon$ , in recombination, 118  
Loeb-Thompson mobility equation, 37, 50, 59, 60-62  
Long sparks, absence of stepping, reason for, 548  
Loschmidt number, 643, 645  
Low-boiling-point metal vapor arcs, cathode mechanism in, 629  
  field emission at cathode of, 474, 611, 629, 636  
Low pressure discharges, velocity of propagation down long tubes in, 482  
Low-pressure sparks, 476  
Low-voltage arc, 636  
  contact potentials in, 637  
  Druyvesteyn theory of, 638  
  electron densities in, 637, 638, 654  
  potential distribution in, 637, 638  
Lusk's test of electron filters, 272  
  
Magnetic deflection method for mobilities, 26, 74, 179, 229  
  effect of energy distribution on, 229

- Magnetic field, in electrodeless ring discharge, 553, 554, 556  
on arc, effects of, 629
- Maier-Leibnitz curves, 201, 216, 227, 231, 363, 570; *see also* Ionization and excitation probabilities.
- Main stroke in lightning discharge, 543
- Masch's measurements of first Townsend coefficient in air, 341, 343, 345, 346
- Mass, of ions and coefficient of recombination, 119, 122, 131, 138, 146, 147  
variation of diffusion coefficient with, 176  
variation of mobility with, 37, 55, 59, 63, 64  
variation of molecular velocity with, 644
- Material of electrodes in a spark gap, 451
- Maxwell distribution law, forms of, 652
- Maxwell energy distribution law, 183, 184, 196, 202, 214, 221, 225, 233, 235, 240, 249, 256, 322, 365, 367, 538, 585, 617, 639, 651
- Maxwell free path, 645
- Maxwell law and electron mobilities, 194; *see also* Electron mobilities.
- Mean free path, electron, 126, 178, 180, 184, 185, 188, 190, 194, 196, 197, 201, 203, 212, 213, 216, 229, 260, 261, 262, 359, 360, 366, 367, 368, 490, 591, 592, 611, 639, 646, 647, 648; *see also* Electron free paths of Ramsauer.  
classical values for, 646  
ionic, 55, 56, 58, 59, 60, 64, 77, 83, 84, 359, 370, 383  
molecular, 645  
evaluation of, 647, 650  
variation of, with pressure and density, 646  
width of cathode fall in terms of, 575
- Measurement, of coefficient of recombination,  $\alpha$ , 91  
of ionic mobilities, 1
- Mechanism, of glow discharge, 568  
of lightning discharge, 543  
of spark breakdown, 426, 433  
of the arc column, 619  
of volume recombination, 114
- Mercury, 38, 39, 42, 71, 147, 157, 158, 159, 250, 298, 299, 300, 302, 303, 348, 354, 355, 392-394, 414, 452, 649  
effect of, on ion mobilities, 71  
on second Townsend coefficient, 392-394  
formation of negative atomic ions in, 298, 299, 300, 302, 303  
minimum sparking potential of, 414  
Ramsauer free paths in, 649  
value of coefficient of electron recombination in, 158
- Mercury arc, electron energy distribution in, by a-c probes, 250  
recombination of electrons in, 157, 158, 159  
rectifying action of, 629
- Mercury-free surfaces and Townsend's second coefficient, 392-399
- Mercury vapor, avoidance of, in spark potential studies, 348, 354, 355, 393-399, 414, 415, 452, 477, 479-481, 507-513  
effect of, on first Townsend coefficient, 348, 354, 355  
on second Townsend coefficient, 392-399
- Metal arcs, Nottingham equation for, 623
- Metals for use in a spark gap, 451
- Metastable atoms, action of, 253, 348, 352, 379, 401, 403, 404, 477, 481, 487, 495, 501, 508, 509, 510, 511, 512, 569, 573  
at cathodes in glow discharge, 569  
at surfaces, 253; *see also* action of, on second Townsend coefficient; Electron, secondary production by metastable atoms.  
in coronas, 487, 495, 501, 510  
in Geiger counters, 487, 495, 501

- Metastable atoms, action of, in low-pressure discharges, 476-482, 508-512  
  in striated glow discharges, 573  
  on first Townsend coefficient, 351-353, 355, 477, 481, 482, 508-512  
  on second Townsend coefficient, 253, 379, 401, 403, 404, 481, 482, 508-512, 569  
  destruction of, by radiation in Ne, 510  
  disturbance of probe measurements by, 253
- Methods of measurement of  $\alpha$ , 91
- Microprocesses, in arcs and cathode emission, 605, 613, 631, 632, 636  
  in spark phenomena, 540
- Midgap streamers in spark breakdown, 431, 436, 440, 448
- Minimum, double, with impurities in spark potential studies, 477
- Minimum sparking distance, 413, 414
- Minimum sparking potential, 413, 414, 419, 420, 476, 477, 478, 479, 480, 503, 507, 554, 558  
  in corona, 503, 507  
  in electrodeless ring discharge, 554  
  in He, anomalous, 477  
  in ultra-high-frequency discharges, 558  
  sparking below, 476  
  values for, 414
- Mixtures, gaseous, mobilities in, 42  
  of  $O_2$  and  $N_2$ , probability of attachment in, 276, 281
- Mobilities, and diffusion coefficients, ratios between, at high  $X/p$ , 180  
  Townsend method for, 168  
  relation between, 166, 168, 170, 180, 587  
  electronic, *see* Electron mobilities.  
  ionic, *see* Ionic mobilities.
- Mobility constant, 35
- Mobility curves at low pressures and electron attachment, 263, 267
- Mobility equations over an extended range of ion size, 83
- Mobility spectrum, 41
- Mobility studies, effect of diffusion on, 171
- Molar volume, 643
- Molecular collision radius, apparent, 650
- Molecular diameter, 644
- Molecular force laws, 650
- Molecular free paths, 645  
  evaluation of, 647, 650  
  temperature variation of, 650  
  variation of, with pressure and density, 646  
  width of cathode fall in terms of, 575
- Molecular structure and electron attachment, 288
- Molecular velocities, distribution of, 651  
  various averages for, 652
- Molecular velocity, 644  
  mass variation of, 644  
  temperature variation of, 644
- Momentum of evaporated metal vapor from arc cathodes, 631, 632, 634, 635
- Morse, Allis, and Lamar derivation of electron energy distribution, 211; *see also*  
  Druyvesteyn distribution law
- Most probable velocity, 652
- Motion of Brownian particles attracting each other in a gas, 108, 111
- Multiple charged ions, 36, 40, 41, 48, 63, 71, 84, 147, 169
- $N_2$ , effect of  $X/p$  on secondary electron liberation in, 402  
  electron affinity for, 297  
  electron mobilities in, 188, 190, 316

- $N_2$ , first Townsend coefficient in, 346, 347, 354, 356  
formation of negative ions in, 267, 289, 301, 303  
high-pressure corona in, 534  
in Geiger counters, 496  
ionic mobility in, 33, 36, 64, 70, 76  
normal cathode fall of potential in glow discharge in, 575, 577  
photoelectric currents in, 315  
positive column gradient in, 595  
Ramsauer free paths in, 649  
recombination coefficients in, 147  
second Townsend coefficient in, 393, 394  
sparking potentials in, 417, 418  
starting potentials for negative and positive low-pressure corona in, 509
- Na, effect of, on first Townsend coefficient in  $N_2$  and  $H_2$ , 357, 358  
on second Townsend coefficient in A,  $H_2$ , and  $N_2$ , 393, 394, 396, 397, 398, 402, 415, 419, 420
- Nature of probe measurement, 236
- Ne, 38, 63, 192, 194, 195, 196, 197, 209, 214, 220, 349, 350, 351, 477-479, 480, 508, 510-512, 565, 570, 573, 575, 577, 608, 638  
Aston dark space in, 570, 573  
electron affinity for, 297  
electron energy distribution in, 196, 214, 215  
electron mobilities in, 192, 194, 195, 197  
low-pressure sparks in, 477-479, 480, 510-512  
low-voltage arc in, 608, 638  
minimum sparking potential in, 414  
mobilities of ions in, 38, 49, 63, 64, 67, 82  
normal cathode fall in, 575, 577  
Ramsauer free paths in, 649  
starting potentials of corona as function of pressure in, 508-512  
values of first Townsend coefficient in, 209, 220, 349, 350, 351, 352
- Needle gap breakdown measurements meaningless, 457
- Negative characteristics of arcs and oscillations, 624
- Negative glow, 519, 520, 561, 562, 564, 566, 571, 572, 573  
cause of, 571  
in negative point to plane corona, 519, 520
- Negative ions, atomic, formation of, 296  
detachment of electrons from, 266, 275, 278, 291, 294, 428, 521, 527  
at high fields, 428, 521, 527  
formation of, 258, 259, 265, 267, 271, 275, 278, 296, 298  
by positive ion impact, on gas films, 303  
energy distribution for, 303  
on surfaces, 298-304  
probability of, 301  
Thomson theory of, 126, 132, 135, 261-265, 268, 274, 277  
value of probability of, 261, 262, 264, 267, 268, 271, 275, 278-288  
Wellisch theory of, 259, 265  
initiation of sparks by, 428  
mobility curves, at low pressures, 35, 259, 264, 267  
interpreted by electron attachment, 264
- Negative point to plane corona, active spot size in, 516  
at atmospheric pressure, 514-519  
Crookes dark space in, 519, 520  
current pulse frequencies in, 517  
glow discharge like structure of, 519, 520  
multiple spots in, 519  
photoionization in, 516

- Negative point to plane corona, time of formation of pulse in, 516
- Negative potential, space charge trough, trapping of positive ions by, 328
- Negative potential trough, in space-charge-limited currents, 321, 328
- Negative resistance in arcs, 625, 627
- Negative wire corona, at low pressure, 504-506
  - cumulative ionization in, 505, 572
  - secondary cathode mechanism in, 504
  - theory of starting potentials of, 512
- Newman's arrangement for studies of time lags in sparking, 469
- Newman's studies of time lags of sparking, 448, 469
- Noise of sparks, origin of, 538
- Nottingham equation for metal arcs, 623
- Normal cathode fall of potential, 563, 568, 575, 577, 579, 583, 584, 607, 608
  - length of, 568, 575, 585, 608
  - linear character of, 578
  - theory of, 579, 583, 584
  - values of, 577
- Normal current density divided by pressure squared in glow discharges, 578, 585
- Number, of electron collisions to gain terminal energy, 185
  - of electrons attaching in distance,  $x$ , 262
  - of initiating electrons per spark, 465
  - of ions,  $\alpha$ , per electron per cm. path in field direction in a gas, 341; *see also* Townsend's first coefficient.
    - $\beta$ , created per cm. path in field by positive ions, 372; *see also* Townsend's second coefficient.
  - striking unit surface per second, 238, 313, 593
- O<sub>2</sub>, 41, 55, 56, 90, 91, 97, 102, 117, 120, 121, 122, 123, 125, 127, 142, 144, 145, 146, 147, 180, 181, 189, 191, 274, 275, 278, 279, 280, 289, 290, 291, 293, 295, 297, 301, 302, 303, 315, 461, 496, 508, 513, 575, 577, 578, 649, 656
  - aging effects with ions in, 41
  - columnar ionization and recombination in, 142
  - detachment of negative ions in, 293
  - direct electron attachment in, 290, 291
  - electron affinity of, 297
  - electron attachment in, 274, 275, 278
  - electron free paths in, 181
  - electron mobilities in, 180, 189, 191
  - in Geiger counters, 496
  - ionization potential of, 656
  - length of normal cathode dark space in, 575
  - methods of measurement of, recombination in, 97, 102
  - mobilities of ions in, 55, 56
  - normal cathode fall in, 577
  - normal current density divided by pressure squared in, 578
  - photoelectric current in, 315
  - preferential recombination in, 125, 127
  - probability of electron attachment in, 275, 279, 280, 295
  - probability of negative ion formation in, 301, 302, 303
  - pure, preparation of, 41, 461
  - Ramsauer free paths in, 649
  - recombination of ions in, 90, 91
  - starting potential of corona in, 508, 513
  - structure of, and electron attachment, 289
  - values of the coefficient of recombination in, 146, 147
    - table of, 144, 145
  - volume recombination of ions in, 117, 120, 121, 122, 123



- Offset potential, in corona and brush discharges, 485, 494, 501, 504, 522, 527  
  in positive point to plane corona, 522, 527
- Ohm's law in positive corona discharge, 494, 502, 526, 532
- Onset potential for corona and brush discharges, 485, 494, 507, 522; *see also* Offset potential.
- Organic vapors in Geiger counters, 495, 496
- Oscillations, and negative characteristics of arcs, 624  
  by arcs, 628  
  frequencies of, in arcs, 626  
  not needed in low-voltage arcs, 636  
  of a-c arc, 627  
  plasma, 601
- Oscillograms, of bursts and kicks in positive point to plane corona, 524  
  of current pulses in negative point to plane corona, 517
- Overvoltage, effect of, on spark breakdown, 427, 431, 433, 443, 445, 447, 448
- Overvolted gap defined, 433
- Oxide specks on electrodes, self-counting by, 499
- Ozone, danger from, in use of ultraviolet sources in ion studies, 459
- Paschen's law, 410, 411, 412, 454, 477, 534  
  and space-charge-conditioned sparks, 412  
  apparent breakdown of, with improper electrodes, 477
- Penetration of fields through gauzes in mobility measurements, 13, 20, 22
- Photoelectric activation of oxide specks on electrodes, 499
- Photoelectric current, density, effect of, on sparking potential, 348, 372, 386-391  
  421-423, 432, 443, 444, 445, 446, 459, 460  
  in vacuum, 310, 315  
  of low densities in gases, 310, 277
- Photoelectric effects, at cathode, 253, 311, 379, 380, 382, 383, 395, 396, 398, 402, 403,  
  431, 482, 483, 487, 502, 504, 512, 527, 531, 568  
  effects of gas pressure and  $X/p$  on, 311-317, 402  
  in glow discharge, 568  
  in low-pressure discharge, 482  
  at electrodes, disturbance of probe studies by, 253  
  in negative wire corona at low pressures, 504, 512
- Photoelectric excitation and electrodeless ring discharge, 555
- Photoelectric ionization, in gas, and electron avalanche propagation, 428  
  at high  $X/p$ , 480  
  in discharge, 379, 383, 384, 403, 404, 428, 430, 433, 434, 480, 482, 483, 487, 502,  
  512, 516, 528, 529, 544, 547  
  in high-pressure positive corona, 384, 512  
  in lightning discharge, 544  
  in negative point to plane corona, 516  
  in Geiger counters, 487, 502  
  in propagation of high-velocity discharges at low pressures, 483  
  needed at both electrodes in a-c spark breakdown measurement, 550
- Photoelectric peaks in second Townsend coefficient, 393-400, 419
- Photoelectric saturation current in studies of ionization by collision, 311-317, 339
- Photographs of spark breakdown, 434-440
- Photon production accompanying ionization, 379; *see also* Photoelectric ionization  
  in gas in discharge.
- Physical constants, table of, 658
- Pilot streamer, current in, 545  
  in lightning discharge, quantitative character of, 545  
  ion density in, 545  
  radius of, 545  
  tip field of, 545

- Pitting of cathodes in metal arcs, 632
- Plane parallel spark gaps, uniformity of field in, 456
- Plane probe, large, 238, 242
- Plasma, 234, 236, 242, 243, 251, 252, 255, 429, 563, 572, 586, 589, 601, 616, 619, 621
  - ambipolar diffusion in, 586, 589, 616, 619, 621
  - disturbance of, by probes, 252
  - in glow discharge, 572
  - in spark breakdown avalanches, 429
  - oscillations, 255, 563, 573, 601
    - and moving striations in glow discharge, 563, 573
    - and probe measurements, 255
  - potential, 236, 242, 243, 251, 255
- Plateau in Geiger counter action, 489, 495, 496, 501, 503
- Points, discharges from, 485
- Poisson's equation, 318, 329, 387, 579, 581
- Polarity of clouds in lightning discharge, 542
- Polarizability and mobility, 38, 56, 64, 82
- Positive column, 519, 520, 561, 562, 563, 564, 565, 572, 573, 585, 586, 590, 593, 595,  
609, 613, 614, 616, 620, 621, 623, 627
  - in arcs, 609, 613, 614, 616, 620, 621, 623, 627
  - in glow discharge, colors in, 565
    - fraction of energy of, radiated as light, 595
    - longitudinal field strength in, 590
    - potential distribution in, 586
    - radial ion concentration gradients in, 593
    - relation of, to tube walls, 564
    - striated, origin of, 573
    - temperatures in, 596
  - in negative point to plane corona, 519, 520
- Positive corona, 486, 507, 520
  - and negative, point to plane in air at atmospheric pressure, 514
  - at low pressure, cumulative ionization in, 490
  - branching of streamers in, 529
  - burst pulse of Trichel in, 522, 526, 528
  - effect of impurities on starting potentials of, 509
  - "effective" resistance in, 494, 502, 522, 526, 532
  - intermittent regime in, 488, 522
  - metastable action in, 487, 495, 501, 510
  - minimum starting potentials in, 503, 507
  - Ohm's law in, 494, 502, 526, 532
  - photoionization in gas in, 384, 512, 527-529
  - point to plane, at atmospheric pressure, 520
  - pre-onset streamers in, 525, 526
  - spread of glow over point, 531
  - starting potential of, as function of pressure, 507
  - streamer formation in, 431, 523, 525, 526, 528, 532, 533
  - wire at low pressures, 486; *see also* Geiger counter
  - zones of active ionization in, 490, 512, 514
- Positive ions, accommodation coefficient of, 301, 634, 635
  - at arc cathodes, 634, 635
  - charging of oxide specks by, on cathodes, 499
  - disturbance of probe measurements by, 253
  - effect of, on space-charge-limited electron current, 325
  - equivalent of electrons in space-charge detector, 327
  - fraction of current carried by, in arcs, 610, 612, 631, 632, 634, 635
  - ionization in a gas by, alternatives to, 253, 377, 378, 379, 380, 382, 395, 396, 397,  
398, 399, 400, 401, 403, 404, 431, 478, 479, 480, 482, 483, 487, 504, 512,  
516, 531, 568, 581, 607

- Positive ions, ionization in a gas by, by impact, 370, 371, 372, 374-377, 381-385, 391, 392, 393-406, 407, 414, 448, 480, 569 (other evidence comes from data on spark and corona where  $\gamma$  and photoionization in the gas are active, 413, 414, 415-416, 426-432, 440, 448, 476-479, 480, 527-531)  
    in glow discharge, 569  
    probability of, at sparking potentials, 370, 383  
    studies falsified by secondary electron emission from surfaces, 375  
    Townsend theory for, 370, 372, 384  
mobility of, in Crookes dark space, 581  
movement of, space charges due to, in a-c breakdown, 551  
negative ion formation by impact of, 298  
probabilities of conversion to negative ions, 302  
secondary electrons from bombardment of cathode by, 378, 382, 396, 397, 398, 399, 403, 478, 479, 480, 482, 504, 512, 568, 581, 607  
secondary electrons from bombardment of cathode in glow discharge, 568, 581  
slow, resonance character of ionization by, 376  
space-charge detector, 326  
space-charge-limited current, equations for, 237, 320, 610  
temperature in sparks, 539  
trapped in negative potential space-charge trough, 328
- Positive point to plane corona, burst pulse process of Trichel in, 522, 526, 528  
gaps, potential distribution in, 529  
in air at atmospheric pressure, 520  
in other gases, 534  
inductive kicks in, 523  
offset potential in, 522, 527  
oscillograms of bursts and kicks in, 524  
pre-onset streamers in, 532, 533  
resistance of, 526, 532  
spark breakdown criterion in, 534  
spark breakdown in, 526, 527, 533, 534  
streamer formation in, mechanism of, 528  
streamers in, 431, 523, 525, 526, 528, 532, 533
- Positive probes and plasma potential, 243
- Positive space charge in Crookes dark space, 566, 569
- Positive space-charge-limited current, 238, 610
- Positive strokes in lightning discharge, 549
- Positive wire corona with concentric cylinders at low pressures, 486; *see also* Geiger counter; Positive corona.
- Potential, alternating, spark breakdown with, 550  
anode fall of, 333, 596, 597, 615, 623, 627  
    in arcs, 615, 623, 627  
cathode fall of, *see* Cathode fall of potential.  
differences in lightning discharge, 542  
distribution, in arc, 609, 614, 627  
    in glow discharge, 565  
    in low-pressure positive corona, 493  
    in low-voltage arc, 637, 638  
    in negative point to plane corona, 515, 521  
    in positive column, 586  
    in positive point to plane corona, 529, 515  
    with ion currents in a gas, 333  
energy state, probability of, 654  
excitation and ionization, 149, 150, 194, 195, 200, 227, 252, 359, 508, 509, 510, 555, 570, 571, 573, 598, 636, 638, 654, 656  
fall, in arc columns measured by lengthening arc, 613, 620  
    in arcs and Stark effect, 608, 615

- Potential, fall, measurements with probes in arcs, 613
  - gradient at the earth's surface, 540
  - gradients in thunderstorm clouds, 541
  - normal and abnormal cathode fall of, 563, 568, 575, 577, 579, 583, 584, 607, 608
  - space or plasma, 242, 251
  - total, calculated, for lightning discharge, 549
  - wall, 241, 572, 586, 594
- Poulson, arc, 628
- Power sources in sparking potential measurement, 462
- Pre-breakdown streamers in positive point to plane corona, 532, 533
- Preferential electron recombination, 144, 150
- Preferential recombination, 87, 125-131, 144
- Pre-onset streamer production in positive point corona, 525, 526, 532, 533
- Pressure, dependence of electron attachment, 275, 279, 284, 288
  - high, and very long gaps, sparking in, 536
  - lowering and streamer branching in spark breakdown, 435
  - of a gas, 643
  - recombination at very low, 130
  - variation of, coefficient of volume recombination, 120
    - diffusion coefficients, 175
    - glow discharge, 560
    - ionic mobility, 34, 35, 36, 56, 63, 65
- Probable velocity, the most, 652
- Probability, of a given potential energy state, 654
  - of conversion of positive to negative ions, 302
  - of electron attachment, 126, 132, 259, 261, 266, 268, 271, 275, 278, 290, 293, 294, 298
    - and electron energies, 126, 132, 135, 259, 266, 268, 271, 275, 278, 290, 293, 294, 298
  - by Bailey's method, 268
  - by Bradbury's method, 276
  - by Cravath's method, 274
  - by Loeb's method, 264, 268
  - in mixtures of  $O_2$  and  $N_2$ , 276, 281
  - in  $O_2$  with inelastic impacts, 280
  - more accurate evaluation of, 267
  - values of, 267, 268, 271, 275, 278-288
  - of ionization and excitation, 195, 201, 216, 227, 231, 362, 363, 364, 367, 370, 478, 479, 570, 634
  - of negative ion formation at surfaces by positive ion impact, 301
- Probe, cylindrical, 238, 243, 244, 248, 255
  - disturbance of, by metastables, positive ions and photons, 253
- Druyvesteyn method for determining distribution law by, 247
- in cathode fall of arcs, 612
- measurements, affected by accommodation coefficient, 254
  - and contact potentials, 254
  - and determination of distribution law, 246
  - and plasma oscillations, 255, 602
  - in low-voltage arcs, 637
  - nature of, 236
  - of electron temperature, 240
  - of potential fall in arcs, 613
  - sources of error in, 251
- plane, large, theory of, 238, 242
  - thickness of space charge sheath in, 238
- positive and plasma potential, 243
- spherical, 238, 243, 244, 255

- Probe, strongly negative, 237  
  theory and use of, 232  
  theory of, 237  
  use of, in electron recombination studies, 155, 157  
  use of a-c to determine distribution law, 249
- Purity, gaseous, *see* Gaseous purity.
- Quantities, electrical, involved in lightning discharges, 542
- Quartz Hg arcs, cautions in use of, 459
- Radiation, temperatures in arcs from, 608
- Radiative capture of electrons, 291, 294, 297, 298
- Radioactive ions, mobility of, 48
- Ramsauer collision cross sections, *see* Ramsauer free paths.
- Ramsauer free paths, 126, 178, 180, 184, 185, 188, 190, 194, 196, 197, 201, 203, 213, 216, 229, 260, 261, 262, 359, 360, 367, 368, 490, 591, 592, 611, 639, 646, 647, 648  
  and energy distribution laws, 184, 194, 196, 213, 229, 366, 648  
  by magnetic deflection, 181
- Rate of disappearance method for coefficient of recombination, 90, 94, 99, 123
- Rate of electron attachment, 262
- Rate of growth method for coefficient of recombination, 91, 93, 99, 123
- Recombination, columnar, 139  
  electron, *see* Electron recombination.  
  evaluation of Thomson-Richardson correction factor,  $e$ , 116  
  in glow discharge, 572  
  in ion currents in a gas, 328  
  initial, 105, 131  
    discovery of, 105  
  ionic, and stepping in lightning discharge, 545  
  of ions, 86  
  preferential, 125  
    electron, 144, 150  
  types of, 86, 144  
  volume, calculation of coefficient of, 119  
    experimental test of theory of, 120  
    mechanism of, 114, 115  
    Sayer's and Gardner's evaluation of, 123  
    table of values of, 147
- Recombination coefficient, 88  
   $\alpha$ , summary of methods of measurement of, 92  
  and aging of ions, 147  
  and  $\alpha$ -particle ionization, 93, 102, 139  
  and change of charge, 146, 147  
  and character of process, 87, 101  
  and columnar ionization, 139  
  and diffusion, ion loss by, 157, 328, 572, 589  
  and electron attachment, 126, 132, 134, 144  
  and gaseous purity, 101, 139, 146, 147  
  and ionized volume, 89, 100, 123, 132, 143  
  and mass of ions, 119, 122, 131, 147  
  and sphere of active attraction in, 107, 111, 113, 116, 120, 125, 128, 132, 144, 145  
  and  $X$ - or  $\beta$ -ray ionization, 132  
  at very low pressures, 130  
  by equilibrium concentration, 91, 123  
  by Gardner's method, 98, 120  
  by Langevin's method, 95

- Recombination coefficient, by rate of disappearance method, 90, 94, 99, 123  
by rate of growth method, 91, 93, 99, 123  
by rotating shutter, 97, 98, 110, 120-124  
calculation of volume, 119  
change of, with time, 131, 137, 138, 146, 147  
from earlier studies, 101  
in ion currents in a gas, 329  
of large ions, 148  
table of, values for, 144, 147  
temperature and pressure variation of, 119, 120, 124, 125, 126, 127, 130, 138, 142, 144, 145, 159  
theories, of Harper and Sommerfeld, comparison of, 111  
theory of, diffusion, 103, 104, 107, 111, 126, 128  
of electron, 158  
of Harper, for volume and preferential, 110, 111, 127, 128-130  
of Jaffé for columnar, 139-142  
of Langevin, error in, 107  
for volume, 103, 121, 125, 126  
of Loeb, for extended pressure range and at low pressures, 126, 127, 130  
for initial, 131  
for volume, 117, 118  
of Mohler for evaluating, 151  
of Richardson for factor,  $\epsilon$ , 104, 112, 116  
of Sommerfeld for Brownian movement of ions, 108, 111  
of Thomson, first, for volume, 113, 129  
for volume, 107, 112, 116, 118, 119, 129  
over extended pressure range, 127, 129  
time intervals of, measurement of, 101  
values of, and their interpretation, 143  
variation of, over extended pressure range, 124, 126, 127, 129  
Recombination spectrum in glow discharge, 572  
Rectifying action, of arcs, 628  
of dissimilar electrodes in spark breakdown, 457  
Reflection of ions at cathodes in arcs, 634, 635  
Rekindling voltage of arc, 627  
Relaxation oscillator-like pulses in negative point to plane corona, 517  
Resistance, effective, of corona, 494, 526, 532  
in positive point to plane corona, 526, 532  
ionic, 42  
negative, in arcs, 625, 627  
of arcs by high frequency a-c, 626  
of Geiger counters, 494, 495, 501, 503  
of lightning discharge path, 546  
positive corona discharge at low pressures, 494, 495, 501, 503  
to extinguish arcs, 625  
Resonance character of ionization by slow positive ions, 376  
Return stroke, in lightning discharge, 543  
velocity of, in lightning discharge, 543  
Richard-Thomson correction factor,  $\epsilon$ , in recombination, 104, 116  
Root mean square velocity, 652  
Rutherford a-c method, 7, 11, 181, 259, 264, 267  
deficiencies of, 11  
for electron mobilities, 181  
Saha's equation of thermal ionization in arcs, 609, 617, 620  
Sander's measurements of first Townsend coefficient in air, 344  
Saturable core reactors in control of generators in spark potential studies, 462

- Saturation, current, geometrically conditioned, 307  
photoelectric, in a gas, 313  
lack of, in ionization studies, 309, 314, 315, 333, 338  
thermionic emission current, 320
- Schonland's observations of lightning discharges, 543
- Schottky's theory of fields active in field emission, 473
- Second Townsend coefficient, *see* Townsend's second coefficient.
- Secondary electron liberation at cathode, 403, 482; *see also* Townsend's Second Coefficient
- Secondary emission, false, from charged non-conductors on cathode, in discharge, 403, 405  
on positive ion bombardment, spurious high values of, 479
- Secondary mechanisms, active at cathode in glow discharge, 568, 581  
active in discharge, 402  
in low-pressure sparks, table of, 482
- Self-excitation, avoidance of, in Geiger counters, 500  
in Geiger counters, 497  
and chemical effects, 497, 556
- Self-sustaining discharge, and condition for sparking threshold, 422, 423  
in glow discharge, criterion for, 568
- Sheath, space charge, 234, 237
- Sloane and McGregor's determination of distribution law with probes, 249
- Small ion theory, 37, 53, 58-65
- Smit derivation for energy distribution among electrons, 221
- Smith curves for efficiencies of ionization, 201, 364, 370, 478, 479
- Sodium, effect of, on first Townsend coefficient in  $N_2$  and  $H_2$ , 357, 358  
on second Townsend coefficient in A,  $H_2$ , and  $N_2$ , 393, 394, 396, 397, 398, 402, 414, 415, 419, 420  
on sparking potentials in  $N_2$ ,  $H_2$ , and A, 414, 415, 419, 420
- Solid elastic ionic mobility equation, 55
- Sommerfeld treatment for Brownian particles attracting each other, 108, 110
- Space charge, accumulations and low-pressure breakdown, 482
- detector, 326  
electron equivalent of an ion in, 327  
distortion and ionization by positive ions, 343, 383  
due to electron accumulations in high-frequency a-c breakdown, 557  
due to positive ion movement in a-c spark breakdown, 551-552  
effects, in evaluation of first Townsend coefficient, 348, 386, 387, 390  
in evaluation of second Townsend coefficient, 372, 386, 390, 391, 403, 405  
in Geiger counter action, 489, 490, 493, 497, 522  
in negative wire corona, 505  
in negative point to plane corona, 516  
in positive point to plane corona, 526, 527, 530, 533, 534  
in spark breakdown, 343, 348, 371, 383, 390, 391, 403, 404, 407, 427, 429, 431, 440, 441, 442, 445, 448, 450, 520, 526, 527, 530, 533, 534, 550-558  
and time lags, 441, 442, 448  
by electron avalanche, 427, 450  
with overvolted gaps, 448  
in spark gaps by electron avalanches, 429
- electron, at anode of arcs, 615
- fields, magnitudes of, produced by strong photoionization, 391
- formation and variation of  $\alpha/p$  as  $f(X/p)$ , 390
- formation in a-c spark breakdown, 550
- gap resistance in positive corona, 526
- induced discharges in long gaps, 403, 405, 407
- inhibiting action of, 424, 485, 512, 517, 520, 529  
on negative corona, 512, 517, 520

- Space charge, inhibiting effects of, on sparks, 424, 448, 485  
    on streamer formation, 529  
    positive, in Crookes dark space, 566, 569, 578-582  
    sheath, 234, 237
- Space-charge-limited current, 237, 317, 319, 320, 323, 325, 610  
    equation, derivation of, 318  
    equations for, 319  
    field strength in, 319  
    for cylindrical electrodes, 323  
    for electrons emitted with finite velocity, 321  
    in arcs, positive, 610  
    in vacuum, 317  
    negative potential trough in, 321, 328
- Space-charge-limited electron current, effect of positive ions on, 325
- Space potential in plasma by probe studies, 242, 251
- Spark (sparks), definition of, 408  
    branched, 433  
    low-pressure, table of, cathode mechanisms in, 483  
    mechanism of, 407, 426, 450  
    number of electrons to initiate, 421, 424, 465  
    origin of noise in, 538  
    vacuum, 471  
    zigzag, nature of long, 433
- Spark breakdown, a-c, and space-charge formation, 550  
    as a function of frequency, 550  
    at very high frequencies, 557  
    and alternating potentials, 550  
    and formative time lags, 427  
    and negative point to plane corona, 520  
    and space charges, 343, 348, 371, 383, 390, 391, 403, 404, 407, 427, 429, 431, 440, 441, 442, 445, 448, 450, 550; *see also* Corona discharge, spark breakdown in.  
    and value of space charges in avalanches, 407, 427, 448, 450  
    anode streamers in, 431  
    at low pressures, effects of impurities, pressures, and illumination on, 511  
        mechanisms in, 482  
    criterion in positive point corona, 534  
    current measurement in, 463  
    decrease of pressure, effect of, on time lags in, 438  
        favors branching in, 435  
    detected, by current changes, 464  
        by light emission, 464  
        by potential changes, 464  
    d-c, compared to ultra-high-frequency breakdown, 538  
    Doppler effect in, 537  
    effect of overvoltage on, 427, 431, 433, 443, 445, 447, 448  
    energy liberation in, 538  
    further consideration of mechanism of, 433  
    in corona discharge, 526, 527, 533, 534  
    later phases of, 537  
        by Kerr cell shutters, 537  
    measurements, procedure in, 463  
    need of ionized path across gap for, 425  
    observation with Kerr cell by, 427, 431, 440, 445, 446, 447, 464, 465, 468, 537  
    occurs in steps for unsymmetrical electrodes, 485  
    of a gap and sparking threshold, 425  
    photographs of, 434-440  
    proper procedure of observation of, 464



- Spark breakdown, role of cathode spot in, 537
  - simultaneous electron avalanches in, 428
- Stark effect in, 537
- statistical time lags in, 441, 443, 447
- streamer formation in, 407, 430, 433, 438, 440, 448, 450
- study of, ideal, 465
- summary of development of theory of, 440
- temperature theory of, 538
- time lag of, 428, 431, 434-436, 438, 439, 440, 441-448, 469, 482, 485, 542, 544-548
  - by Kerr cell shutter, 434-436, 438, 439, 440, 441-448, 469
  - by cloud track pictures, 428, 431, 424-436, 440
- Spark channels, ion density in, 537
  - micro processes in, 540
- Spark discharge, branching in, 433
  - characteristic curve for, 412
  - essential techniques in, 451
- Spark gap, cautions about interference by surface charges on insulators and neighboring conductors, 455
  - electrodes, shape and material, 451
    - unequal, lead to steps in breakdown, 456
  - field distribution in, studied by electrolytic models, 455
  - instability criterion for, 407, 423, 425, 432, 450, 465
  - long, stepping in breakdown of, 536
  - need for dry, clean, dust-free gases in, 458
  - overvolted, defined, 433
  - plane parallel, profiling of edges in, 456
  - uniformity of field in, 456
- Spark propagation, at low pressures, photoionization in, 483
  - in long tubes at low pressures, high velocity of, 482
- Spark studies, Kerr cell circuits used in, 465, 469
- Spark transition, lower threshold for, 407, 423, 425, 432, 450, 465
- Sparkling, at low pressures, 476
  - and increase in  $\gamma$  at high  $X/p$ , 479
  - below conventional sparking potential, 432
  - criterion of Townsend, 374, 407, 409, 416, 420, 423, 425, 432, 450, 465
  - experimental test for, 416
  - influence of initial current, 420
  - electrical fields in, not revealed by Stark effect, 537, 540
  - in low-pressure swept gaps and field emission, 475
  - in very long gaps at high pressures, 536
  - number of initiating electrons per spark in, 421, 424, 465
  - theory of, 408
  - time lag of, and intensity of illumination, 441, 443, 445, 447
- Sparkling distance, minimum, 413
- Sparkling potential, and cathode surface, 349, 381, 400, 403, 407, 414, 415, 419, 420, 450, 451, 452-454, 478, 479-482
  - and gas density, 535
  - as influenced by photoelectric current density, 348, 372, 386-391, 403, 405, 421, 423, 432, 443, 444, 445, 446, 459, 460
  - below minimum, 477
  - conventional, 423, 432, 465
  - effect of electronegative impurities on, 460, 476-479, 510-512
  - effect of temperature on, 534
  - evaluation of, by Townsend's coefficients, 348, 351, 399, 400, 415, 416-420, 479,
  - experimental or observed, 423, 432, 465
  - falsified by reflection at electrodes for surge impulse breakdown, 447
  - gradients for long gaps, 536

- Sparkling potential, in positive point corona, 526  
measurements, adsorbed gas films on electrodes in, 453  
avoidance of dirt on electrodes in, 451  
cautions in use of ultraviolet light in, 459  
cleaning of glass ware in, 458  
effect of intense ultraviolet illumination in, 420-423, 432, 433, 441, 445, 460  
electrode configuration in, 454  
need for electrons in gap in, 459  
oxidation of cathode in, 452, 453  
power sources in, 462  
require illumination of cathode with d c and both electrodes with a c, 459, 550  
minimum, 413  
no unique value for, 425, 465  
shows double minimum with impurities, 477  
studies, avoidance of Hg and condensable vapors in, 452  
detection of breakdown in, 463  
gaseous purity in, 460  
limiting concentrations of impurities in, 460, 461  
of Cerwin and Quinn below minimum, 479  
production of impurities in, by sparks, 461  
with point electrodes meaningless, 457  
threshold, 407, 423, 425, 432, 433, 450, 463, 465  
triple value of, near minimum in He, 477
- Sparkling threshold, and condition for a self-sustaining discharge, 423  
and gap breakdown, 425
- Sphere of active attraction in recombination, Thomson's, 107, 111, 113, 116, 120, 125, 128, 132, 144, 145
- Spherical probe, 238, 243, 244, 255
- Spurious counts in Geiger counters, 497
- Sputtered metals, for cathodes in spark potential studies, 456  
in Geiger counters, 497
- Sputtering at cathode, 599
- Stability criterion for ionic cluster, 58
- Stark effect, 537, 540, 567, 608, 615  
and potential fall in arcs, 608, 615  
field strength measurements from, 567  
in spark breakdown, 537, 540
- Starting potential, for corona, brush or glow discharges, 485, 493, 501, 509, 513  
in corona, effect of gaseous impurities on, 509  
minimum, 503, 507  
in Geiger counters, 488, 493, 494, 501, 507  
of coronas, action of metastable atoms in, 510  
and pressure, 507, 513  
of low-pressure discharges, effects of impurities, pressure, and illumination on, 511  
of negative wire coronas, theory of, 512  
of point to plane coronas, cumulative ionization at, 515  
field strengths at, 515
- Statistical time lags, circuits of Tilles and Wilson, 467  
in spark breakdown, 441, 443, 447
- Stepped leader, strokes in lightning discharge, 543  
tip field strengths in, 547
- Stepping, and recombination in lightning discharge, 545  
in breakdown of long gaps, 536, 548  
in long sparks, reason for absence of, 548  
theory of, in lightning discharge, 544  
uniformity of, in lightning discharges, 543
- Streamers, branching in, in positive corona, 529

- Streamers, formation of, in corona breakdown, 431, 426, 533, 534  
  in positive point corona, mechanism of, 528  
  in spark breakdown, 430, 433, 438, 440, 448, 450  
  in positive point corona, control of, 531  
  in positive point to plane corona, 431, 523, 525, 526, 528, 532, 533  
  pilot, nature of, in lightning discharge, 545  
  pre-onset in corona discharge, 525, 526, 532  
  propagation of, and observed polarity of lightning discharge, 542  
Striated glow discharge, 561, 563, 565, 573  
  origin of, 573  
Striations in glow discharge, moving, 563, 573  
Subnormal cathode fall of potential, 584, 606  
  
Table of physical constants, 658  
Tait free path, 645  
Taylor's theory of photoelectric ionization, 383  
Temperature, and gaseous equilibrium, 651  
  and thermal ionization or excitation curve, 655  
  effect of, on distribution law, 655  
  electron, 155, 157, 211, 229, 230, 234, 235, 239, 240, 367, 368, 539, 586, 587, 589,  
    590, 591, 618-621, 651  
  definition of, 230, 239, 538, 651, 652  
  in arcs, 608, 610, 613, 614, 615, 616, 617, 629, 631  
    anode, 615, 616, 617, 629  
    cathode, 613, 615, 616, 629, 632, 635  
      by rate of evaporation, 632, 633, 634, 635  
      for low-melting-point metals cannot be measured by evaporation, 635  
      from radiation, band spectra, velocity of sound, and ranges of  $\alpha$  particles, 608, 617  
  in glow discharge, cathode, 598, 606-608  
    column, 596  
  ionization, in arcs, 609, 617, 620  
    in discharges, 651  
    vapor pressures in arcs from, 621  
  theory of breakdown, in liquids, 539  
    in sparks, 538  
  theory of thermal ionization in arcs, 617, 621, 635, 651  
  variation, of coefficient, of diffusion, 175  
    of recombination, 119, 120, 121, 125, 130, 131, 137, 138, 145  
    of volume recombination, 120  
    of field emission, 472  
    of ionic mobility, 36, 37, 55, 63, 80, 81  
    of molecular free paths, 650  
    of molecular velocity, 644  
    of sparking potentials, 534  
Terminal energy of electrons in field, 185  
Terminal velocity of electrons, 184  
Theory, of air-blast mobility methods, 3, 6  
  of Allen, for electron velocities in a gas, 229  
  of a-c arc, 628  
  of a-c mobility measurements, 9, 10, 12, 14, 17  
  of ambipolar diffusion, 587  
  of arc oscillations, 624  
  of arcs, by temperature ionization, 617  
  of attachment of electrons in  $O_2$ - $N_2$  mixtures, 281  
  of Bailey for study of electron attachment, 269  
  of Bloch and Bradbury for electron attachment in  $O_2$ , 295  
  of Brode and Loeb for photoelectric liberation of electrons at cathode, 379

- Theory, of cathode fall, in arcs, 611  
  in glow discharge, 581  
of cathode mechanisms in low-pressure discharges, 481  
of characteristic curve for spark discharge, 412  
of cluster ion, 56  
of Compton, for cathode temperatures from rate of evaporation, 632, 635  
  for electron energies in a gas, 202, 362  
  for electron mobilities, 183  
  for "evaporation" of atoms from cathodes of metal arcs, 635  
of Cravath, and Bradbury for study of attachment with electron filters, 274, 277  
  for electron energy distribution, 209  
of current pulses in negative point to plane corona, 517  
of Didlaukis for electron energy distribution, 209  
of Druyvesteyn, for electron energy distribution in a gas, 205  
  for electron mobilities with inelastic impacts, 219  
  for energy distributions of electrons, with inelastic impacts, 215  
  for ionization by electron impact in Ne, 215, 219, 363  
  for low-voltage arc, 638  
  for obtaining distribution law from probe studies, 247  
of effect of space charge on second Townsend coefficient, 386  
of Einstein for diffusion of particles, 174  
of electrical wind method of mobility measurement, 29  
of electron mobilities, elementary, 178  
of electron recombination, basic, 158  
Emmeléus, for ionization by electrons in a gas, 365  
  for measuring distribution law by a c on probes, 249  
of energy balance at arc cathodes, 611  
of v. Engel and Steenbeck for ionization by electrons in a gas, 367  
of evaluation of electron attachment from a-c mobility measurements, 264  
of field and potential distribution in cylindrical condensers, 486  
of field emission, 473  
of forces between ions and molecules, 57  
of Fowler and Nordheim of field emission, 473  
of Gardner, method for recombination of ions, 99  
of geometrically conditioned saturation current, 307  
of Harper, for Brownian particles attracting each other in a gas, 111  
  for recombination of ions, 127  
of Hershey for mobilities of ions at high  $X/p$ , 78  
of Hertz for electron movements in a field in a gas, 203  
of high-velocity propagation of low-pressure discharges down tubes, 483  
of influence of photocurrent from cathode on sparking potential, 422  
of initial recombination, 133  
of ionic diffusion, 162  
of ionic mobilities, 52, 54  
  at high  $X/p$ , 72, 73, 78, 79  
  elementary, 55  
  Hassé and Cook's using force centers, 68  
  in gaseous mixtures, 43  
  mass variation in, 37  
  temperature variation in, 37  
  wave-mechanical, 71  
of Jaffé for columnar recombination, 139  
of Kingdon for positive ion space-charge detector, 325  
of Langevin, for ionic mobilities, 55, 65  
  for recombination of ions, 103  
  method for recombination of ions, 95  
of linear normal cathode fall of potential, 579

- Theory, of Loeb for transition from volume to preferential recombination as a  $f(p)$ , 126
- of magnetic deflection mobility measurements of Townsend, 27, 75, 229
  - of Massey and Smith for formation of atomic negative ions, 297
  - of mechanism, of ionic recombination, 115
    - of lightning discharge, 544
  - of minimum sparking potential, 414
  - of mobility measurements by electrical shutters, 22, 25
  - of Mohler for evaluating electron recombination coefficient, 152, 155
  - of Mooney for electron attachment by a-c mobility studies, 267
  - of Morse, Allis, and Lamar for electron energy distribution in a gas, 211
  - of normal cathode fall of potential, 581, 584
  - of positive point to plane corona of Loeb, 527
  - of potential gradients down positive column in glow discharge, 590
  - of probes, 237
  - of radial ionic concentration gradients in positive column, 593
  - of ratio between diffusion and mobility coefficients of ions, 166
  - of recombination, Langevin's, 103
    - simple, 89
  - of Schottky for electrical fields, in field emission, 473
  - of self-sustaining discharge and sparking threshold, 423
  - of small ion, 59
  - of Smit for energy distributions of electrons, 221
  - of Sommerfeld and Bethe of field emission, 473
  - of Sommerfeld for Brownian particles attracting each other in a gas, 109
  - of space-charge-limited currents in vacuum, 318, 320, 321
  - of spark breakdown, summary of development, of, 440
  - of spark mechanism, 407, 427, 450
  - of spurious counts and self-counting in Geiger counters of Paetow and Locher, 498
  - of starting potentials of negative wire low pressure corona, 512
  - of temperature breakdown of sparks, 538
  - of Thomson and Townsend for ion currents with electron liberation by positive ion bombardment at cathode, 378
  - of Thomson, for conduction currents in a gas with volume ionization, 329
    - for electrodeless ring discharge, 553
    - for electron attachment, 261
    - for photoelectric currents in gases, 313
    - for volume recombination, 112
      - first, 113
  - of Townsend, for air-blast measurement for ionic diffusion, 164
    - for corona action, 490, 493
    - for direct measurement of ratio  $k/D$ , 168
    - for electron energies in a gas, 210
    - for ionization, by collision, 339, 341
      - by positive ions in a gas, 373
    - for mechanism of ionization, by collision in a gas, 358
      - by positive ions in a gas, 383, 407
    - for spark, 374, 409
  - of transition of glow to an arc, 607
  - of Wellisch for negative ion formation, 260
  - of Werner for Geiger counters, 490
- Thermal ionization in arcs, 604, 617, 620
- Thermionic currents in vacuum, 317
- Thermionic emission, 318, 320, 497, 605, 607, 629, 636
- equation for, 320
  - from cathode in glow discharge, 607
  - in arcs, 605, 607, 629, 636
  - of metals in Geiger counters, 497

- Thermionic equation, derivation of, 318
- Thomson-Bohr theory of ionization by positive ions, 375
- Thomson-Loeb theory of ionic mobilities, 37, 59, 61, 62
- Thomson-Richardson correction factor  $\epsilon$  in volume recombination, 104, 105, 114, 116-119, 125, 131
- Thomson's derivation of equation for photocurrents in a gas, 312
- Thomson's method of field strength measurement with cathode-ray beam, 567
- Thomson's sphere of active attraction, 107, 111, 112, 113, 116, 120, 125, 128, 132, 144, 145
- compared to that of Sommerfeld and Harper, 111
- Thomson's theory, for electrodeless ring discharge, 553, 556
- for ion currents in a gas under X-ray ionization, 329
- for ionization currents in gases, 328
- for negative ion formation, 261, 265, 268, 274, 277
- for photoelectric currents in a gas, 313
- for secondary electron emission by positive ion impact on cathode, 377
- for volume recombination, 112-119, 121-124, 126, 129, 144, 145, 147
- first attempt at, 113, 129
- Threshold of sparking, 407, 423, 425, 433, 450, 463, 465
- Thunderstorm cloud, distribution of charges in, 541
- potential gradients in, 541
- Tilles' arrangement for study of statistical time lags in sparks, 467
- Tilles' measurements of time lags of sparks, 443, 467
- Time constants for Geiger counters, 501, 504
- Time lags, and intensity of illumination, 441, 443, 445, 447, 459, 469
- and overvolted gaps, 427, 431, 443-448, 469
- and spark breakdown at lower pressures, 438
- definition of, in different studies, 449
- effect of approach voltage in, 443, 444, 446, 469
- formative, 444, 447
- in spark breakdown, by Kerr cell studies, 427, 431, 440, 445, 446, 467-470
- statistical, 441-444, 447
- of spark breakdown, 441, 467
- of sparks, by Newman, 448, 469
- circuits used by White, Wilson, and Tilles in, 467, 468
- studies of Tilles, 443
- Townsend and Boulind's measurements of ionic mobilities from corona currents, 490, 493, 494
- Townsend's air-blast method for coefficient of diffusion, 164
- Townsend's  $\alpha$ , for ionization by collision in a gas, 219, 339, 341, 342; *see also* Townsend's first coefficient
- Townsend's  $\beta$ , 371, 372-374, 378, 381, 382, 385, 386, 391, 392, 393, 394, 395, 396, 397, 398, 399, 400, 401, 403, 404, 405, 426, 451, 478, 479, 480, 482, 504, 516, 568, 581, 607; *see also* Townsend's second coefficient.
- alternative interpretations of, 377, 379, 381, 383, 385, 391-399, 401, 403, 405, 410, 415, 429, 450, 482, 504, 516, 561, 568, 581, 607
- evaluation of, from sparking potentials, 348, 351, 399, 400, 415, 416-420, 479
- Townsend's early evaluation of ionization potentials, 359
- Townsend's electron energies, and mobilities on Allen's theory, 197
- Townsend's energy distribution law, 210
- Townsend's equation for  $\alpha/p$  as a  $f(X/p)$ , 358, 359, 367, 370, 581
- in glow discharge, 581
- Townsend's evaluation of electron energies in gases, 179, 186, 193, 214, 229, 235, 268, 269, 271, 315
- Townsend's experimental study of ionization by positive ions in a gas, 384
- Townsend's factor  $\eta$ , 179, 186, 193, 214, 229, 235, 268, 269, 271, 365
- in electron mobilities, 179

- Townsend's factor  $\eta$ , values of, 180
- Townsend's first coefficient, 219, 220, 334, 339, 341-344, 344-347, 348, 350, 351, 355, 358, 361, 362-364, 366, 367, 370, 371, 386, 387, 390, 399, 400, 407, 415, 416, 420, 478, 479
- as a  $f(X/p)$ , 342, 344, 345, 346, 347, 351, 354, 355, 358, 359, 361, 362, 364, 366, 367, 370, 371
- curves, abrupt termination of, at low  $X/p$ , 371, 407
- decline in values of, at high  $X/p$ , 351, 357, 370, 478
- effect of Na in  $H_2$  and  $N_2$  on 357, 358
- effect of Hg vapor on, 348, 354, 355
- evaluation of, from sparking potential, 348, 399, 400, 415, 416-420, 479
- illumination of cathode, method of, in evaluating, 348, 350
- in air at low  $X/p$ , 345
- in  $N_2$ , empirical expressions for, 347
- in  $N_2$ ,  $\alpha/p$  as a  $f(X/p)$ , 346, 356
- pure Hg-free, 354
- influence of gaseous purity on, 343, 348, 351, 352, 354-358, 415, 418, 460-462, 478, 481, 508-513
- influence of space-charge effects on, 348, 386-390
- mechanism of action of impurities on, 351, 354, 355, 357, 358, 478, 481, 509, 513
- theoretical evaluation of, 220, 358, 359, 362, 363, 366, 367, 370
- theory, of Compton for, 362
- of Druyvesteyn for, in Ne, 220, 363
- of Emmeléus, Lunt and Meek for, 365
- of v. Engel and Steenbeck for, at high  $X/p$ , 367
- of Holm for, 365
- of Townsend for, 359-362, 367, 370
- of simple, correct approximate for, 363
- values for, from theory of Emmeléus, Lunt, and Meek, 366
- in A, 349
- in A, at high  $X/p$ , 351
- in  $H_2$ , 355-357
- in Hg-contaminated air, 345
- in  $N_2$  contaminated with Hg, 345-347
- in  $N_2$ , Hg-free, 354, 356
- in Ne, 349
- tables of, 343, 346, 349, 356
- Townsend's magnetic deflection method for mobilities, 26, 74, 179, 229, 271, 275
- applied to positive ion mobilities, 74
- effect of energy distribution on, 229
- Townsend's method of evaluating  $k/D$ , 168-170, 179
- Townsend's second coefficient, 371, 372, 378, 381, 382, 386, 391-399, 400, 401, 403, 404, 405, 407, 426, 451, 478, 479, 480, 482, 504, 516, 568, 581, 607
- alternatives to  $\beta$ , 377, 379, 381, 383, 385, 391-399, 401, 403, 405, 407, 410, 415, 429, 450, 482, 504, 516, 561, 581, 607
- and ionization by positive ions in a gas, 370, 372, 374-377, 381, 383, 385, 407
- and secondary liberation of electrons, by photoelectric effect on cathode, 253, 311, 379, 380, 395, 396, 398, 402, 403, 431, 482, 483, 487, 502, 504, 512, 527, 531, 568
- by photoelectric ionization in the gas, 379, 383, 384, 403, 404, 428, 430, 433, 482, 483, 512, 516, 528, 529, 544, 547
- by metastable atoms, at cathode, 253, 379, 401, 403, 404, 481, 482, 508-512, 569
- in gas, 253, 348, 352, 401, 403, 404, 477, 487, 495, 501, 508, 510, 511, 512, 569, 573
- by positive ion impact on cathode, 378, 382, 390, 397, 398, 399, 403, 478, 479, 480, 482, 504, 512, 568, 581, 607

- Townsend's second coefficient, and spark potential measurements, 451
  - anomalous high values of at high  $X/p$ , 479
  - cannot be due to ionization by positive ions in gas, 370, 374-377, 383, 384, 385, 403, 407, 450
  - data on interpretation of, 381
  - defined, 372, 385
  - effect of Hg and Na on, 392, 393, 394, 396, 397
  - evaluation of, from sparking potential, 348, 351, 399, 400, 415-420, 479
  - falsified by space charges, 372, 386, 391, 403, 405, 421, 432
  - for Ba surfaces in A, 400
  - for Cu surfaces in Ne and Ne-A mixtures, 393
  - for Na surfaces in  $N_2$ , 394
  - for NaH surfaces in  $H_2$ , 396
  - for Pt Surfaces in  $H_2$ , 395
  - for Pt surfaces in  $N_2$ , 394
  - from glow discharge, 568, 581, 607
  - in A with Cs-Ag-O and Ni-Cs cathodes, 399
  - in low-pressure sparks, table of active mechanisms, 482
  - in negative point to plane corona, 516
  - in negative wire corona, 504
  - increase in at high  $X/p$  and low-pressure sparks, 478
  - interpretation of, on Pt and Na surfaces, 397
  - photoelectric peaks from surfaces in, 394, 397
  - values of, for Pt and NaH surfaces in  $H_2$ , 398
    - in  $N_2$  and  $H_2$ , 392-400
    - on Hg-free surfaces, 392
  - variation of, with  $X/p$ , 401
- Townsend's sparking criterion, 374, 409, 416, 420, 423, 425
  - experimental test for, 416
  - influence of initial current, 420
- Townsend's sparking equation not intended for transient phenomenon, 421
- Townsend's studies on ionization by collision in gases, 336
- Townsend's theoretical evaluation of  $\alpha/p$  as a  $f(X/p)$ , 358, 359, 367, 370, 581
- Townsend's theory, of first Townsend coefficient, inadequate, 360, 368, 370
  - of ionization, by electron impact applied to ionization by positive ions, 370, 383
  - by positive ions, 372
  - of low-pressure corona, 490, 493
- Trichel or burst pulse corona, 522, 526, 528
- Trough, negative potential, in space-charge-limited currents, 321, 328
- Tyndall and Grindley method of mobility measurement, 14; *see also* Ionic mobilities
- Tyndall and Powell data on ionic mobilities, 64
- Tyndall and Powell four-gauze method of mobility measurement, 14, 20; *see also* Ionic mobilities.
- Types of recombination, 86, 144, 145
- Ultra-high-frequency discharges, characteristic curves for, 558
  - minimum potentials in, 558
- Ultraviolet illumination of cathode and sparking potential, 348, 372, 386-391, 403, 405, 420-423, 432, 441, 443, 444, 445, 446, 459, 460
- Ultraviolet light, disturbance of probe measurements by, 253
  - precautions in use of, 459
- Vacuum, photoelectric currents, 310, 315
  - sparks, 471
    - effect of temperature on, 472



- Values, of coefficient of recombination and their interpretation, 143  
  of mobilities on theory and experiment, 64, 69, 70
- van der Waals forces and mobilities, 67, 82
- Vapor-pressure curve and temperature, 655
- Vapor pressures, partial, in arcs from temperature ionization, 621
- Variation of molecular free paths with pressure and density, 646
- Velocities, directed, distribution law for, 653  
  electronic, average, 179, 186, 193, 214, 229, 235, 268, 269, 271, 365; *see also*  
    Electron energy distribution; Electron temperature.  
  drift, *see* Electron mobilities.  
  random or thermal, *see* Electron energy distribution; Electron temperature.
- \*ionic, *see* Ionic mobilities.
- molecular, 644  
  average, 652  
  different averages for, 652  
  distribution of, 650  
  most probable, average and root mean square, 652  
  variation of, with mass and temperature, 644
- of electron avalanches in fields, 427, 428, 434, 441, 445-448, 469, 482, 516, 528, 529, 543-548
- of evaporating atoms at arc cathodes, 612, 632, 633, 634, 635
- of lightning discharge, and preionized paths, 544  
  average, 543
- of propagation of low-pressure discharges down long tubes, 482
- of return strokes in lightning discharge, 543
- Velocity of sound, 644  
  temperatures in arcs from, 609, 617
- Viscosity, coefficient of, 647, 650
- Volume, ionization with positive and negative ions in a gas, 328  
  recombination, 87, 120, 144, 328  
  in ion currents in a gas, 328
- Wall currents, 157, 241, 586  
  in glow discharge, 157, 586  
  in positive column of glow discharge, 586
- Wall potentials, 241, 571, 586, 594  
  in glow discharges, 572, 586, 594
- Wall recombination, 144, 241
- Walls, effect of, on positive column, 564
- Wave-mechanical theory of ionic mobility, 69
- Wellisch theory of negative ion formation, 259, 265
- Werner and Townsend's zones of effective ionization in coronas, 490, 512, 514
- Werner's theory of Geiger counter action, 490
- White's arrangement for Kerr cell studies of spark discharge, 466, 468
- White's time lag studies with intense illumination, 445
- Wilson's arrangement for Kerr cell studies of spark lag, 467
- Wilson's time lag studies of sparking, 446
- Wires, discharges from, 485
- Work function, and field emission, 473, 474, 629  
  according to Müller, 474  
  in arcs, 629  
  and sparking potential, 382; *see also* Sparking potential and cathode surface.  
  of cathode and secondary emission, 382, 395, 403; *see also* Townsend's second coefficient.  
  of metals and use in Geiger counters, 496

- $X/p$ , for sparks in very long gaps, 536
  - in ion studies, 32, 71, 72, 73, 76-83, 338
- $X_i/p$ , low values of, characteristic of arc columns, 609, 616
  - values of, in arc columns, 591, 592
- X-ray ionization, and recombination, 132
  - currents in a gas, 328
- Zeleny air-blast method, 3
- Zuber and Laue's discovery of statistical time lags in spark breakdown, 441







